



Kyoji Sassa · Paolo Canuti · Yueping Yin *Editors*

Landslide Science for a Safer Geoenvironment

Volume 1

The International Programme on Landslides (IPL)



 Springer

Landslide Science for a Safer Geoenvironment

Kyoji Sassa • Paolo Canuti • Yueping Yin
Editors

Landslide Science for a Safer Geoenvironment

Volume 1: The International Programme
on Landslides (IPL)

 Springer



Editors

Kyoji Sassa
UNITWIN Headquarters Building
Kyoto University Uji-Campus
Uji, Kyoto, Japan

Paolo Canuti
ICL - International Consortium on Landslides
Florence, Italy

Yueping Yin
Center of Geo-Hazards Emergency Technology, MLR
Beijing, China

ISBN 978-3-319-04998-4 ISBN 978-3-319-04999-1 (eBook)
DOI 10.1007/978-3-319-04999-1
Springer Cham Heidelberg New York Dordrecht London

Library of Congress Control Number: 2014938096

© Springer International Publishing Switzerland 2014

This work is subject to copyright. All rights are reserved by the Publisher, whether the whole or part of the material is concerned, specifically the rights of translation, reprinting, reuse of illustrations, recitation, broadcasting, reproduction on microfilms or in any other physical way, and transmission or information storage and retrieval, electronic adaptation, computer software, or by similar or dissimilar methodology now known or hereafter developed. Exempted from this legal reservation are brief excerpts in connection with reviews or scholarly analysis or material supplied specifically for the purpose of being entered and executed on a computer system, for exclusive use by the purchaser of the work. Duplication of this publication or parts thereof is permitted only under the provisions of the Copyright Law of the Publisher's location, in its current version, and permission for use must always be obtained from Springer. Permissions for use may be obtained through RightsLink at the Copyright Clearance Center. Violations are liable to prosecution under the respective Copyright Law.

The use of general descriptive names, registered names, trademarks, service marks, etc. in this publication does not imply, even in the absence of a specific statement, that such names are exempt from the relevant protective laws and regulations and therefore free for general use.

While the advice and information in this book are believed to be true and accurate at the date of publication, neither the authors nor the editors nor the publisher can accept any legal responsibility for any errors or omissions that may be made. The publisher makes no warranty, express or implied, with respect to the material contained herein.

Cover Illustration: The Loess landslide, 100 m long, 70 m wide, with a volume of 180,000 m³, occurred in Dongxiang town, Gansu Province, China, in March 2011. The landslide destroyed major roads and tens of houses, but 760 people were evacuated successfully due to early warning.

Printed on acid-free paper

Springer is part of Springer Science+Business Media (www.springer.com)

Foreword for *International Consortium on Landslides*



United Nations
Educational, Scientific and
Cultural Organization

Organisation
des Nations Unies
pour l'éducation,
la science et la culture

Organización
de las Naciones Unidas
para la Educación,
la Ciencia y la Cultura

Организация
Объединенных Наций по
вопросам образования,
науки и культуры

منظمة الأمم المتحدة
للتربية والعلم والثقافة

联合国教育、
科学及文化组织

More than 200 million people are affected every year by natural hazards, and the impact is deepening—especially in developing countries, where they can set back healthy growth for years. Globally, an estimated one trillion United States dollars have been lost in the last decade alone.

We may not be able to stop disasters, but we can reduce their risks and their consequences. Mitigating the effects of natural hazards requires education, training, and capacity building at all levels. Fundamentally, it calls for new thinking—to move from reaction after disasters to action before.

Landslides are important in this regard, given the tragic loss of life and the economic disruption they cause. More than ever, we need to address landslides in ways that are integrated and coordinated internationally. This is the goal guiding the *International Consortium on Landslides* and its International Programme on Landslides, focusing on research, education, and capacity building in landslide risk reduction, working with international, governmental, and non-governmental actors.

Associated with the *International Consortium on Landslides*, UNESCO has accompanied the International Programme on Landslides from its inception, as an innovative initiative for cooperative research and capacity building in landslide risk mitigation. In the same spirit, UNESCO and Kyoto University established a University Twinning and Networking Cooperation Programme on landslide risk mitigation for society and the environment in March 2003, in order to deepen cooperation in this vital area.

This publication is an essential tool for both organizations and individuals to deepen understanding of landslide phenomena and to reduce their risks. Drawing on latest scientific developments, this volume presents a range of initiatives under way across the world and puts forward recommendations on risk mitigation. At a time when the consequences of climate change are deepening, this work provides a benchmark reference to strengthen the resilience of societies under pressure. I wish to thank all participants in the *International Consortium on Landslides* and all involved in this important work. Let me highlight especially Professor Kyoji Sassa, Chairperson of the

Consortium, for his tireless efforts. In this spirit, I look forward to further strengthening UNESCO's cooperation with the *International Consortium on Landslides*.



A handwritten signature in blue ink that reads "Irina Bokova". The signature is written in a cursive, flowing style.

Ms. Irina Bokova
Director-General of UNESCO

Foreword

Landslide, floods, drought, wildfire, storms, tsunami, earthquakes, and other types of natural hazards are increasingly affecting the world. For the first time in history the world has experienced 3 consecutive years (2010–2012) where annual economic losses have exceeded \$100 billion due to an enormous increase in exposure of industrial assets and private property to extreme disaster events. During the period of 2000–2012, 2.9 billion people were affected by disasters, economic damage is equivalent of USD 1.7 trillion, and 1.2 million people were killed by disasters.¹

The Global Assessment Report (GAR), a regular publication by the United Nations on disaster risk levels, trends, and analysis of the underlying causes, found that most of the small-scale recurrent disasters such as landslides are not effectively accounted for by authorities. The same report also found that while landslides and other recurrent natural hazards are responsible for only a small proportion of global disaster mortality, they account for a very significant proportion of damage to public assets, such as health and educational facilities and infrastructure, as well as to the livelihoods, houses, and assets of low-income groups.

Extensive risk associated with localized, mainly weather-related hazards with short return periods. These highly localized yet frequent hazards include surface water and flash flooding, landslides, fires, and both agricultural and hydrological drought. They are exacerbated by badly managed urban development, environment degradation, and poverty.²

The *Hyogo Framework for Action 2005–2015: Building the Resilience of Nations and Communities to Disasters (HFA)*, adopted at the 2nd World Conference on Disaster Reduction (WCDR, Kobe, Hyogo, Japan, in January 2005), represents the most comprehensive action-oriented policy guidance in universal understanding of disasters induced by vulnerability to natural hazards and reflects a solid commitment to implementation of an effective disaster reduction agenda. In order to ensure effective implementation of HFA at all levels, tangible and coordinated activities must be carried out. Since 2005, we have seen many activities and initiatives developed to implement HFA in various areas. As a concrete activity in the area of landslide risk reduction, the International Programme on Landslides has maintained the momentum created in 2005 through organizing the two World Landslide Forums in 2008 in Tokyo and in 2011 in Rome, being led by the International Consortium on Landslides. It is my great pleasure to see the valuable development for the last 8 years.

There is a growing evidence of the need for a strong science basis to understand the causes and impacts of landslides as well as the most effective measures to reduce landslide risk. This book includes a number of substantive articles on landslide risk reduction. Applying science into practice is one of the key words for the global endeavour. I expect this book as well as the Third World Landslide Forum to make a substantive contribution for that purpose in the area

¹ Disasters refers to drought, earthquake (seismic activity), epidemic, extreme temperature, flood, insect infestation, mass movement (dry and wet), storm, volcano, and wildfire/Data source: EM-DAT: The OFDA/CRED International Disaster Database/Data version: 12 March 2013 - v12.07.

² Global Assessment Report on Disaster Risk Reduction 2013: http://www.preventionweb.net/english/hyogo/gar/2013/en/home/GAR_2013/GAR_2013_2.html

of landslide risk reduction by the promotion of exchange of experience and achievements in science and facilitating discussion on sustainable disaster risk management.

Recognizing that disaster reduction needs interdisciplinary and multi-sectoral action, we build on partnerships and take a global approach to disaster reduction. Therefore, we welcome better cooperation between government authorities and the international community including scientific community that play a critical role in helping people make life-changing decisions about where and how they live before the disaster strikes, in particular high-risk urban areas.

Once the ten-year mark has been passed in 2015, the world will have a new disaster risk reduction framework. Consultations on elements for the post-2015 framework (“HFA2”) are currently ongoing. Multi-stakeholders, including academic and scientific institutions, are encouraged to be engaged in the ongoing consultation towards HFA2, which is expected to be adopted at the Third World Conference on Disaster Risk Reduction in March 2015 in Sendai, Japan.

Scientist, international, and regional institutions have a responsibility to assist with the tools, knowledge, and capacity to understand their risk and take the most effective measures to reduce them. The knowledge on landslides is a key part of the equation and the work and outcome of The Third World Landslide Forum in June 2014 in Beijing will be important contribution to these efforts and ongoing consultation towards 2015. UNISDR is fully behind the community of practice working on landslide risk.



A handwritten signature in black ink, appearing to read 'Margareta Wahlström'.

Ms. Margareta Wahlström
Special Representative of the UN Secretary-
General for Disaster Risk Reduction, Chief
of UNISDR

Preface: Landslide Science for a Safer Geoenvironment

The Third World Landslide Forum (WLF3) was held at the China National Convention Center, Beijing, China, on 2–6 June 2014. WLF is the triennial conference of the International Consortium on Landslides (ICL) and the International Programme on Landslides (IPL).

ICL (The International Consortium on Landslides) launched at the Kyoto Symposium in January 2002 is an international non-governmental and non-profit scientific organization promoting landslide research and capacity building for the benefit of society and the environment. Major activities of the ICL are the publication of a bimonthly full-colour journal “Landslides: Journal of the International Consortium on Landslides”, the International Programme on Landslides including IPL Projects in many countries/regions, and the Triennial World Landslide Forum and promotion of ICL regional and thematic networks and the World Centres of Excellence on Landslide Risk Reduction (WCoE). All activities involve cooperation by ICL-supporting organizations and other various stakeholders (national and local governments, civil society, and private sectors) contributing to landslide risk reduction.

The IPL is a programme of the ICL. It is developed in partnership with ICL-supporting organizations. The programme is managed by the IPL Global Promotion Committee including ICL and ICL-supporting organizations: the United Nations Educational, Scientific and Cultural Organization (UNESCO), the World Meteorological Organization (WMO), the Food and Agriculture Organization of the United Nations (FAO), the United Nations International Strategy for Disaster Risk Reduction (UNISDR), the United Nations University (UNU), the International Council for Science (ICSU), the World Federation of Engineering Organizations (WFEO), and the International Union of Geological Sciences (IUGS). The IPL contributes to the United Nations International Strategy for Disaster Reduction.

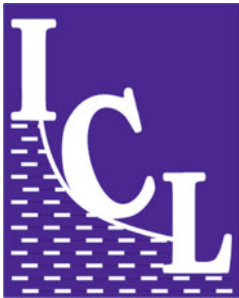
ICL-IPL invites relevant organizations and programmers to promote Landslide Science for a Safer Geoenvironment.

The International Consortium on Landslides (ICL)

- ICL was established by adopting its statutes in January 2002. The headquarters was registered as a legal body under the Japanese law for non-profit-making organizations (NPO) in the Kyoto Prefectural Government, Japan, in August 2002.
- ICL established the UNITWIN (University Twinning and Networking) Cooperation Programme on Landslide Risk Mitigation for Society and the Environment with UNESCO and Kyoto University in March 2003. The UNITWIN Headquarters Building was constructed by ICL and Kyoto University at the Kyoto University Uji Campus in September 2004. The programme was developed to promote landslide and water-related disaster risk management for society and the environment in November 2010.
- ICL founded “*Landslides*”: *Journal of the International Consortium on Landslides* in 2004. It was established as a quarterly journal published by Springer Verlag. It was approved as an ISI journal in 2005 and moved to a bimonthly journal from Vol. 10 in 2013.
- ICL founded the International Programme on Landslides (IPL) in partnership with seven global stakeholders by adopting the 2006 Tokyo Action Plan. It exchanged MoU to

promote IPL with the United Nations Educational, Scientific and Cultural Organization (UNESCO), the World Meteorological Organization (WMO), the Food and Agricultural Organization of the United Nations (FAO), the United Nations International Strategy for Disaster Reduction (UNISDR), the United Nations University (UNU), the International Council for Science (ICSU), and the World Federation of Engineering Organizations (WFEO) in 2006.

- The IPL Global Promotion Committee (IPL-GPC) was established following the 2006 Tokyo Action Plan to manage IPL activities including IPL projects, the World Landslide Forum (WLF) every 3 years, and the World Centres of Excellence for Landslide Risk Reduction (WCoEs) to be identified at WLFs.
- ICL headquarters in Kyoto, Japan, was approved as a scientific research organization (No. 94307) which can receive scientific grants from the Ministry of Education, Culture, Sports, Science and Technology (MEXT), Japan, in March 2007 and registered in the cross-ministerial research and development management system of all ministries of Japan in May 2008.
- ICL was approved as an NGO having operational relations with UNESCO in April 2007. It was reclassified as an NGO with consultative partnership with UNESCO in March 2012.
- ICL-IPL organized the First World Landslide Forum (WLF1) at the United Nations University, Tokyo, in November 2008.
- ICL-IPL organized the Second World Landslide Forum (WLF2) at the Food and Agriculture Organization of the United Nations, Rome, in October 2011.
- ICL-IPL is organizing the Third World Landslide Forum (WLF3) at the China National Convention Center, Beijing, in June 2014.
- ICL-IPL will organize the Fourth World Landslide Forum (WLF4) in Ljubljana, Slovenia, in May 29–June 2, 2017.



The symbol of ICL was designed as below.

I is a symbol of cultural heritage at landslide risk

C symbolizes the moving landslide mass

L is a symbol of retaining wall to stop landslides for its risk reduction.

The greatest discussion on C whether the Consortium should stand still or might be inclined during dynamic motion.

The International Programme on Landslides (IPL)

- The United Nations World Conference on Disaster Reduction was held on 18–22 January 2005 in Kobe, Japan. At this conference, the ICL proposed the organization of a thematic session to develop the IPL within the WCDR, and it was approved by the United Nations Secretariat for the International Strategy for Disaster Risk Reduction. With financial support from the Cabinet Office of Japan, the Ministry of Education, Culture, Sports, Science and Technology of the Government of Japan (MEXT), and the Disaster Prevention Research Institute of Kyoto University, the thematic conference Session 3.8 “New International Initiatives for Research and Risk Mitigation of Floods (IFI) and Landslides (IPL)” was organized together with ICL-supporting organizations and also the flood group.
- The thematic session 3.8 was opened with the addresses by Koichiro Matsuura (Director-General of UNESCO), Michel Jarraud (Secretary-General of WMO), and others. The session was chaired by Hans van Ginkel (Rector of UNU). The ICL proposed a **Letter of**

- Intent** to promote further joint global activities in disaster reduction and risk prevention through “Strengthening research and learning on ‘Earth system risk analysis and sustainable disaster management’ within the framework of the ‘United Nations International Strategy for Disaster Reduction’ (ISDR)”. This Letter of Intent was agreed and signed by heads of seven global stakeholders of UNESCO, WMO, FAO, UNISDR, UNU, ICSU, and WFEO.
- Based on this Letter of Intent, ICL, UNESCO, WMO, FAO, UNISDR, UNEP, UNU, and Kyoto University jointly organized the Round Table Discussion (RTD) “Strengthening research and learning on earth system risk analysis and sustainable disaster management within UN-ISDR as regards landslides—towards a dynamic global network of International Programme on Landslides (IPL)” on 18–20 January 2006 at Elizabeth Rose Hall of the United Nations University, Tokyo, Japan. The RTD was cosponsored by Japanese and international governmental and non-governmental organizations. The 2006 Tokyo Action Plan was adopted as the result of RTD.
 - The 2006 Tokyo Action Plan decided to develop the International Programme on Landslides (IPL) which is managed by IPL Global Promotion Committee. It is formed by ICL member organizations, ICL-supporting organizations which have exchanged the Memorandum of Understanding with ICL to promote ICL, and organizations which provide Subvention to IPL.
 - The ICL exchanged the Memoranda of Understanding with each of seven global stakeholders: UNESCO, WMO, FAO, UNISDR, UNU, ICSU, and WFEO to promote the 2006 Tokyo Action Plan within 2006. Then, IPL was formally launched as a programme of the ICL in partnership with ICL-supporting organizations aiming at organizing work in response to the ICL goals.
 - The logo of IPL in Fig.1 is a simple design of ICL and ICL-supporting organizations which have exchanged MOU with ICL to promote ICL-IPL.



Fig. 1 Logo of the International Programme on Landslides (IPL)

The World Landslide Forum

The First World Landslide Forum: Implementing the 2006 Tokyo Action Plan on the International Programme on Landslides (IPL)

WLF1 was organized at the United Nations University, Tokyo, in November 2008. It was a global cross-cutting information and cooperation platform for all types of organizations from academia, United Nations, governments, private sectors, and individuals that are contributing to landslide research and education and who are willing to strengthen landslide and other related earth system risk reduction.

- Plenary sessions were (1) Open forum “Progress of IPL Activities”, (2) Plenary symposium “Global Landslide Risk Reduction”: A special Report and four keynote lectures, (3) Public Forum on “Protection of Society and Cultural and Natural Heritage, (4) “Landslides for Children”, (5) High-level panel discussion “Landslides in Global Change—How to mitigate risk? Toward the Second World Landslide Forum in 2011”.
- Parallel sessions were (1) A look from space, (2) Case Studies and National Experiences, (3) Catastrophic slides and avalanches, (4) Climate change and slope instability, (5) Landslides threatening heritage sites, (6) Economic and Social Impact of Landslides, (7) Education, Capacity Building and Public Awareness for Disaster Reduction, (8) Environmental Impact of Landslides, (9) Landslides in General, (10) Landslides and multi-hazards, (11) Mapping: inventories, susceptibility, hazard and risk, (12) Monitoring, prediction and early warning, (13) Policy and Institutional framework for Disaster Reduction, (14) Rainfall, debris flows, and wildfires, (15) Landslide Disaster Mitigation Engineering Measures, (16) Watershed and Forest Management for Risk Reduction, (17) Landslides in Dam Reservoirs.
- One full-colour book—Landslides-Disaster Risk Reduction—including all papers in plenary sessions and introduction of all parallel sessions was published, two monocolour proceedings for full papers were accepted for parallel sessions, and papers accepted for poster papers were printed and also are uploaded in the ICL web in full colour.
- 430 people from 48 countries and several other international organizations participated (175 from Japan, and 255 from abroad).

The Second World Landslide Forum: Putting Science into Practice

WLF2 was organized at the Headquarters of the Food and Agriculture Organization of the United Nations (FAO) on 3–9 October 2011. It was jointly organized by the IPL Global Promotion Committee (ICL, UNESCO, WMO, FAO, UNISDR, UNU, ICSU, WFEO) and two ICL members in Italy: the Italian Institute for Environmental Protection and Research (ISPRA) and the Earth Science Department of the University of Florence with support from the Government of Italy and many Italian landslide-related organizations.

- 864 people from 63 countries and several international organizations participated. Attendance was larger than expected, and twice the attendance at the First World Landslide Forum 2008 in Tokyo.
- 25 Technical sessions were held, and 465 full papers were submitted. All accepted papers were edited in seven full-colour volumes titled as “**Landslide Science and Practice**” as below.
 - Vol. 1 Landslide inventory and susceptibility and hazard zoning
 - Vol. 2 Early warning, instrumentation and monitoring
 - Vol. 3 Spatial analysis and modelling
 - Vol. 4 Global environmental change (420 pages)
 - Vol. 5 Complex environment (520 pages)
 - Vol. 6 Risk assessment, management and mitigation (430 pages)
 - Vol. 7 Social and Economic Impact and Policies (430 pages)

The Third World Landslide Forum: Landslide Risk Mitigation Toward a Safer Environment

WLF3 will be organized on 2–6 June 2014 in Beijing, China.

Three full-colour volumes (Vol. 1–Vol. 3) will be published by Springer, titled as Landslide Science for a Safer Geoenvironment. 303 papers will be published in three full color volumes. One monocolour proceedings which contains 123 full papers and an abstract volume will be published by the Chinese Organizing Committee. Volume 1 includes Plenary lectures, and selected papers from the side events. Volume 2 includes papers accepted in sessions for methods of landslide studies. Volume 3 includes papers accepted for methods of landslide studies. Front matters include two Forewords from Ms. Irena Bokova, Director-General of UNESCO and Ms. Margareta Wahlström, Special Representative of the UN Secretary General for Disaster Risk Reduction, Chief of UNISDR, and Preface by Kyoji Sassa (Executive Director), Paolo Canuti (President) and Yueping Yin (Incoming President) of ICL. Back matters include “Landslide Technology and Engineering in Support of Landslide Science” and “ICL Structure”.

Plenary sessions are:

1. High-Level Panel Discussion toward a Safer Geoenvironment
2. Plenary Lectures “Progress in Landslide Science”
 - Runqiu HUANG: Progress in Large-Scale Landslide Studies in China
 - Farrokh NADIM: Progress in Living with landslide risk in Europe
 - Rex BAUM: Progress in Regional landslide hazard assessment
 - Kyoji SASSA: Progress in Landslide Dynamics
3. Round Table Discussion “Major achievement in WLF3 and development toward WLF4”

Parallel sessions are:

Special Sessions

A1 International Programme on Landslides, A2 Thematic and Regional Networks on Landslides, A3 Policy, Legislation and Guidelines on Landslides, A4 Climate & Landuse Change Impacts on Landslides, A5 Recognition and Mechanics of Landslide, A6 General Landslide Studies

Sessions for Methods of Landslide Studies

B1 Physical Modeling and Material Testing, B2 Application of Numerical Modeling Techniques to Landslides, B3 Remote Sensing Techniques for Landslide Mapping and Monitoring, B4 Hazard Mapping, B5 Monitoring, Prediction and Warning of Landslides, B6 Risk Assessment, B7 Remedial Measures & Prevention Works, B8 Risk Reduction Strategy, B9 Inventory and Database

Sessions for Targeted Landslides

C1 Debris Flows, C2 Rock-Slope Instability and Failure, C3 Earthquake-Induced Landslides, C4 Rain-Induced Landslides, C5 Landslides in Cultural/Natural Heritage Sites, C6 Urban Landslides, C7 Landslides in Cold Regions, C8 Landslide in Coastal and Submarine Environments, C9 Natural Dams and Landslides in Reservoirs

Side Events

D1 Student Session, D2 Landslide Teaching tools, D3 Dialogues on Country Landslide Issues

Other ICL-IPL Activities

Other ICL-IPL activities include (1) IPL Projects, (2) ICL Regional and thematic networks, (3) World Centre of Excellence on Landslide Risk Reduction, (4) ICL Landslide Teaching Tools.

Landslides: Journal of the International Consortium on Landslides

The ICL decided to create a new international journal on landslides “Landslides: Journal of the International Consortium on Landslides” at the First Board of Representatives of ICL held at the UNESCO Headquarters, Paris on 19-21 November 2002. The ICL planned to publish full color journal presenting full color photos and colored maps & figures to attract policy makers, government officers and citizens as well as scientists and engineers in many fields.

The first issue of the journal *Landslides* was published from Springer Verlag in April 2004 as the core project of the International Programme on Landslides (IPL). This journal was the first full-colour scientific journal without a full-colour printing fee. The field of landslides is very wide in the related basic science fields. Common information source which all readers may understand is a full-colour photo of landslides. Landslide researchers from geology, geomorphology, geotechnology, geophysics, and landslide dynamics may obtain various aspects of information from the colour photos. The journal “Landslides” aims to promote landslide research and investigation in the developing countries as well as in developed countries. Published papers of most international journals are shared by researchers in the developed countries. *Landslides* have made the following five categories to promote contribution from developing countries and young researchers.

Within these categories, “Original articles” will deal with the frontiers of landslide science and technology. “Recent landslides” will accept recent landslide reports from developing countries where many landslide disasters will occur and “Technical note” will accept case studies of landslides in the less reported countries. “ICL-IPL activities” will report for international information dissemination and cooperation. As a central tool of the global landslide community, the journal is planned to provide different functions.

1. Original paper (6–12 pages): original research and investigation results.
2. Review paper (6–12 pages): review of current research and development of technology in a thematic area of landslides.
3. Recent landslide (less than 6 pages): reports of recent landslides including location (latitude/longitude), plan, section, geology, volume, movement, mechanism, and associated disasters.
4. Technical note (less than 6 pages): research notes, review notes, case studies, progress of technology, and best practice in monitoring, testing, investigation, and mitigation measures.
5. ICL-IPL activities: progress of IPL projects and ICL committee activities.



Fig. 2 Cover of “Landslides”, Vol.11, No.2, 2014

“Landslides” have published 513 articles in 42 issues in Volume 1–Volume 10 since 2004. Volumes 1–9 were 4 issues per year. The total pages in Vol. 9 were 569 pages containing 47 papers. Vol. 10 from 2013 was 6 issues per year. The total pages in Vol. 10 are 851 pages containing 68 papers. Figure 2 presents the front and back cover of Vol.11, No.2, 2014. The design of the cover is the same from the founding issue in 2004.

“Landslides” was identified as an SCI journal by Thomson Reuters in 2005. The impact factor was 2.216 in the 2011 Journal Citation Report, and it was 2.093 in 2012 Journal Citation Report. This journal is the core activity of ICL-IPL to share information on scientific and technological development and to develop “Landslide Science” toward a Safer Geoenvironment.

IPL Projects

IPL Projects are proposed by one or more ICL members or by IPL-Global Promotion Committee (IPL-GPC) by submitting the [IPL project proposal form](#) by 30 March every year. Proposal form will be evaluated by IPL Evaluation Committee. The proposer or a member of the project is requested to orally explain the project in the IPL-GPC which will be organized together with the Board of Representatives (BOR) of ICL each year. IPL-GPC will decide the approval of proposed project based on the evaluation committee report, oral presentation, and discussion. Each IPL Project leader with ongoing status is requested to submit an annual report of the project by 30 March each year.

The IPL project may authorize the leader and the accepted project by the IPL Global Promotion Committee. The project, leaders, and the annual report are uploaded in IPL WEB <http://www.iplhq.org/>. The progress and the research results are invited to contribute to **Landslides: Journal of the International Consortium on Landslides**. The achievements of IPL Projects are evaluated every 3 years. Three successful IPL projects will be identified at the World Landslide Forum. The leaders will receive US\$3,000 per project together with a certificate.

ICL Regional and Thematic Networks

Establishment of ICL networks was proposed at the 10th Session of Board of Representatives of ICL held at the headquarters of the Food and Agriculture Organization of the United Nations (FAO) in Rome, Italy, on 5 October 2011. The networks were approved at the 10th anniversary meeting of ICL held on 17–20 January 2012 in Kyoto, Japan. The regional and thematic networks are platforms for cooperation within ICL member organizations and non-ICL member organizations in each region and each thematic field.

Current networks are:

ICL Regional Networks

- (1) Adriatic-Balkan Network, (2) Latin America Network, (3) North-East Asia Network, (4) South-East Asian Network for Landslide Risk Management

ICL Thematic Networks

- (1) Landslides Risk Management Network, (2) Capacity Development Network, (3) Landslides in Cold Regions Network, (4) Landslides and Cultural & Natural Heritage Network, (5) Landslide Monitoring and Warning Network

World Centre of Excellence on Landslide Risk Reduction

The Global Promotion Committee (GPC) of the International Programme on Landslides (IPL) will identify World Centres of Excellence on Landslide Risk Reduction at the World Landslide Forum organized every 3 years within eligible organizations, such as universities,

institutes, NGOs, government ministries, and local governments, contributing to “Risk Reduction for Landslides and Related Earth System Disasters”. An independent Panel of Experts, set up by the Global Promotion Committee of International Programme on Landslides (IPL-GPC), endorses the WCoEs.

Objectives of WCoE:

To strengthen the International Programme on Landslides (IPL) and IPL Global Promotion Committee

To create “A Global Network of entities contributing to landslide risk reduction”; and

To improve the global recognition of “Landslide Risk Reduction” and its social-economic relevance, and entities contributing to this field

Twelve World Centres of Excellence (WCoEs) 2008–2011 were identified at the First World Landslide Forum in November 2008 at UNU in Tokyo, Japan. Fifteen WCoEs for 2011–2014 were identified at the Second World Landslide Forum in October 2011 at FAO, Rome, Italy. New WCoEs for 2014–2017 will be identified and announced at WLF3. WCoEs are cores of ICL regional and thematic networks.

ICL Landslide Teaching Tools

ICL Landslide Teaching Tools aim to provide various teaching materials to ICL members and other landslide institutions and entities for their efforts to educate university students, local government officers, people in non-governmental organizations, and local communities. Tools include text including figures and full-colour photos, PDFs of published papers, guidelines and laws, and PPTs for lectures.

Copyright and Responsibility for Each Teaching Tool

ICL called for contributions and compiled the accepted teaching tools. Copyright and responsibility for the content of each tool lie with its contributing organization. Each tool may be updated by the contributing organization.

The Teaching Toolbox contains five parts:

1. Mapping and Site Prediction
2. Monitoring and Early warning
3. Testing and Numerical Simulation
4. Risk Management and Others
5. Country Practices and Case Studies

The Teaching Toolbox contains three types of tools:

1. The first type are TXT-tools consisting of original texts with figures.
2. The second type are PDF-tools consisting of already published reference papers, manuals, guidelines, laws, codes, and others. They are on the accompanying CD as pdf files.
3. The third type are PPT-tools consisting of Powerpoint[®] files made for lectures. They are on the accompanying CD as ppt files.

ICL invites landslide research organizations and their experts to jointly develop effective and practical Landslide Teaching Tools. The copyright and the updating responsibility belong to the contributing organization.

A Call for ICL-IPL Partners

The International Consortium on Landslides (ICL) and partners of the International Programme on Landslides (IPL), including the United Nations Educational, Scientific and Cultural Organization (UNESCO), the World Meteorological Organization (WMO), the Food

and Agricultural Organization of the United Nations (FAO), the United Nations Office for Disaster Risk Reduction (UNISDR), the United Nations University (UNU), the International Council for Science (ICSU), the World Federation of Engineering Organizations (WFEO), and the International Union of Geological Sciences (IUGS), invite related international programmes and initiatives from natural sciences (earth sciences and water sciences), engineering sciences, human and social sciences, and governmental and non-governmental programmes to promote science and technology and their applications for landslide risk mitigation and to support this initiative by joining the International Networking and Partnerships aimed at enhancing capacities, in particular in the developing world, to reduce risk and vulnerabilities and build resilience related with landslides, and contribute to a safer Geoenvironment in support of UNISDR.

The “Third World Conference on Disaster Risk Reduction of the United Nations (3rd WCDRR)” will be organized in Sendai, Japan, on 14–18 March 2015, succeeding the 2nd WCDR (Kobe, 18–22 January 2005). ICL-IPL is examining an activity for 3rd WCDRR to enhance partnerships and agree with relevant organizations and programmes on ICL-IPL SENDAI PARTNERSHIPS 2015–2024 for Landslide Disaster Risk Reduction for a Safer Geoenvironment.

Kyoji Sassa
Executive Director of ICL



Paolo Canuti
President of ICL



Yueping Yin
Incoming President of ICL



ICL-IPL Secretariat

ICL office: The International Consortium on Landslides
138-1 Tanaka Asukai-cho, Sakyo-ku, Kyoto 606-8226, Japan
IPL office: UNESCO-KU-ICL UNITWIN Headquarters
Kyoto University Uji Campus, Uji Kyoto 611-0011, Japan
Email: secretariat@iclhq.org
URL: <http://icl-iplhq.org/> and <http://www.iplhq.org/>

List of Editors

Editors

Kyoji Sassa
International Consortium on Landslides
Kyoto, Japan

Yueping Yin
Center of Geo-Hazards Emergency Technology, MLR
Beijing, China

Paolo Canuti
International Consortium on Landslides
Florence, Italy

Associate Editors

Eileen and Mauri McSaveney
GNS Science,
Lower Hutt, New Zealand

Lynn Highland
U.S. Geological Survey
Denver, Colorado, USA

Vol.1 Part Editors

Part 2
Matjaž Mikoš
University of Ljubljana,
Ljubljana, Slovenia

Part 4
Sálvano Briceño
International Consortium on Landslides
Kyoto, Japan

Part 6
Luciano Picarelli
Seconda Univ. di Napoli
Aversa, Italy

Part 8
Bin He
Nanjing Institute of Geography & Limnology, CAS
Nanjing, China

Part 3
Snjezana Mihalić Arbanas
University of Zagreb
Zagreb, Croatia

Part 5
Vit Vilimek
Charles University
Prague, Czech Republic

Part 7
Peter Bobrowsky
Geological Survey of Canada
Ottawa, Ontario, Canada

Vol.2 Part Editors

Part 1
Binod Tiwari
California State University, Fullerton
Fullerton, California, USA

Part 3
Vern Singhroy
Canada Centre for Remote Sensing
Ottawa, Ontario, Canada

Part 5
Željko Arbanas
University of Rijeka
Rijeka, Croatia

Part 2
Marc-Andre Brideau
BGC Engineering Inc.
Vancouver, British Columbia, Canada

Part 4
Rex Baum
U.S. Geological Survey
Denver, Colorado, USA

Part 6
Huabin Wang
Huazhong University of Science and Technology
Wuhan, Hubei, China

Part 7
Sebastian Fischer
Technische Universität Darmstadt
Darmstadt, Germany

Part 9
Snježana Mihalić Arbanas
University of Zagreb
Zagreb, Croatia

Vol.3 Part Editors

Part 1
Giovanni Crosta
Università degli Studi di Milano Bicocca
Milano, Italy

Ko-Fei Liu
National Taiwan University
Taipei, Taiwan

Part 3
Kazuo Konagai
Yokohama University
Tokyo, Japan

Fawu Wang
Shimane University
Matsue, Shimane, Japan

Part 5
Jan Vlcko
Comenius University, Bratislava
Bratislava, Slovakia

Part 7
Ying Guo
Northeast Forestry University
Harbin, China

Part 9
Alexander Strom
JSC "Hydroproject Institute"
Moscow, Russian Federation

Part 8
Farrokh Nadim
International Centre for Geohazards at NGI
Oslo, Norway

Part 2
Jan Klimeš
Institute of Rock Structure and Mechanics, CAS
Praha, Czech Republic

Part 4
Binod Tiwari
California State University, Fullerton
Fullerton, California, USA

Part 6
José Chacón
University of Granada
Granada, Spain

Part 8
Michael Strasser
ETH Zurich
Zurich, Switzerland

Contents

Activities of the International Programme on Landslides (IPL): IPL Projects and World Centres of Excellence on Landslide Risk Reduction (WCoE) xxvii
Matjaž Mikoš and Snježana Mihalić Arbanas

Part I Plenary Lectures

Plenary: Progress of Living with Landslide Risk in Europe 3
Farrokh Nadim, Bjørn Kalsnes, and Anders Solheim

Plenary: Progress in Regional Landslide Hazard Assessment—Examples from the USA 21
Rex L. Baum, William H. Schulz, Dianne L. Brien, William J. Burns, Mark E. Reid, and Jonathan W. Godt

Plenary: Progress in Landslide Dynamics 37
Kyoji Sassa, Bin He, Khang Dang, Osamu Nagai, and Kaoru Takara

Part II International Programme on Landslides

Introduction: International Programme on Landslides—IPL 71
Matjaž Mikoš, Badoui Rouhban, Irasema Alcántara-Ayala, and Xiaochun Li

IPL Project 181: Study of Slow Moving Landslide Umka Near Belgrade, Serbia 75
Biljana Abolmasov, Svetozar Milenković, Branko Jelisavac, Uroš Đurić, and Miloš Marjanović

Efforts in Landslide Risk Reduction in Asia 81
N.M.S.I. Arambepola and Senaka Basnayake

Study of Landslides in Flysch Deposits of North Istria, Croatia: Landslide Data Collection and Recent Landslide Occurrences 89
Željko Arbanas, Sanja Dugonjić Jovančević, Martina Vivoda, and Snježana Mihalić Arbanas

“Report a Landslide” A Website to Engage the Public in Identifying Geologic Hazards 95
Rex L. Baum, Lynn M. Highland, Peter T. Lyttle, Jeremy M. Fee, Eric M. Martinez, and Lisa A. Wald

Discrete Boundary Shear Strength of a Landslide at High Rainfall Precipitation Zone in Sri Lanka 101
A.A. Virajh Dias, S.B.S. Abayakoon, and R.K. Bhandari

Glacial Lake Outburst Floods (GLOFs) Database Project 107
Adam Emmer, Vít Vilímek, and Jan Klimeš

Towards Landslide Instrumentation and Monitoring in Teziutlán, Puebla, Mexico	113
Ricardo Garnica-Peña, Leobardo Domínguez-Morales, and Irasema Alcántara-Ayala	
Synoptic Pan-European Landslide Susceptibility Assessment: The ELSUS 1000 v1 Map	117
Andreas Günther, Javier Hervás, Miet Van Den Eeckhaut, Jean-Philippe Malet, and Paola Reichenbach	
Landslide Risk in South-East Nigeria: Important Facilities Under Serious Threat	123
Ogbonnaya Igwe	
Assessing Landslide Frequency for Landform Hazard Zoning Purposes	129
Gabriel Legorreta Paulín, José Lugo Hubp, and José Fernando Aceves Quesada	
Comparison of Soil Modulus E_{50} of Residual Soil Slope Failures in Two Different Rainfall Zones	135
M.A.S.N. Mallawarachchi, E.M.T.M. Ekanayake, S.S.I. Kodagoda, and A.A. Virajh Dias	
WCoE: Mechanisms of Landslides in Over-Consolidated Clays and Flysch and IPL-151 Project: Soil Matrix Suction in Active Landslides in Flysch—The Slano Blato Landslide Case	143
Matjaž Mikoš, Jošt Sodnik, Ana Petkovšek, Matej Maček, and Bojan Majes	
Slope Data Acquisition Along Highways in Sabah State for Hazard Assessment and Mapping	149
Shabri Shaharom, Che Hassandi Abdullah, and Roslan Majid	
Climate-Change Impacts on Embankments and Slope Stability in Permafrost Regions of Bei'an-Heihe Highway	155
Wei Shan, Ying Guo, Chengcheng Zhang, Zhaoguang Hu, Hua Jiang, and Chunjiao Wang	
International Summer School on Rockslides and Related Phenomena in the Kokomeran River Valley, Tien Shan, Kyrgyzstan: IPL-106-2 Project and WCoE	161
Alexander Strom and Kanatbek Abdrakhmatov	
Rainfall Intensity and Duration for Debris Flow Triggering in Peninsular Malaysia	167
Suhaimi Jamaludin, Che Hassandi Abdullah, and Norhidayu Kasim	
Part III Thematic and Regional Networks on Landslides	
Introduction: Thematic and Regional Networks on Landslides	175
Snježana Mihalić Arbanas, Kaoru Takara, N.M.S.I. Arambepola, and Renato Eugenio de Lima	
The ICL Latin American Network: Past Activities and Challenges Ahead	181
Irasema Alcántara-Ayala, Raúl Carreño, Guillermo Ávila, and Aníbal Godoy	
A South-East Asian Network for Landslide Risk Management for Regional Collaboration	187
N.M.S.I. Arambepola	
Landslide Monitoring Techniques Database	193
Matej Maček, Ana Petkovšek, Bojan Majes, and Matjaž Mikoš	

Landslide Knowledge Exchange Through the Regional Cooperation in the Adriatic-Balkan Region	199
Željko Arbanas, Snježana Mihalić Arbanas, Martina Vivoda, Kristina Martinović, and Sanja Bernat	
Part IV Policy, Legislation and Guidelines on Landslides	
Introduction: Policy, Legislation and Guidelines on Landslides	209
Salvano Briceno	
Disaster Risk Reduction and Sustainable Development	211
Mark Pelling, Reid Basher, Joern Birkmann, Susan Cutter, Bina Desai, S.H.M. Fakhruddin, Ferruccio Ferrugini, Tom Mitchell, Tony Oliver-Smith, John Rees, and Kuniyoshi Takeuchi	
Economic Impact Assessment of Landslide Events	217
Mike G. Winter, Derek Palmer, Jonathan Sharpe, Barbara Shearer, Clare Harmer, David Peeling, and Trevor Bradbury	
A Safety Guideline for Hill-Site Development of Penang, Malaysia: Challenges and a Way Forward	223
See-Sew Gue	
Guidelines and Initiatives in the Aftermath of Highland Towers Landmark Landslide	229
Abdullah Che Hassandi	
Part V Climate and Land-Use Change Impacts on Landslides	
Introduction: Climate and Land-Use Change Impacts on Landslides	239
Vít Vilímek and Mike Winter	
Modelling the Influence of Tree Removal on Embankment Slope Hydrology	241
Kevin Briggs, Joel Smethurst, and William Powrie	
Age and Reactivations of Catastrophic Complex Flow-Like Landslides in the Flysch Carpathians (Czech Republic/Slovakia)	247
Tomáš Pánek, Veronika Smolková, Jan Hradecký, Ivo Baroň, and Karel Šilhán	
Antecedent Precipitation as a Potential Proxy for Landslide Incidence in South West United Kingdom	253
Catherine Pennington, Tom Dijkstra, Murray Lark, Claire Dashwood, Anna Harrison, and Katy Freeborough	
Natural Hazards in the Cordillera Blanca of Peru During the Time of Global Climate Change	261
Vít Vilímek, Jan Klimeš, Adam Emmer, and Jan Novotný	
Land-Use Change and Shallow Landsliding: A Case History from the Apennine Mountains, Italy	267
Janusz Wasowski, Marina Dipalma Lagreca, and Caterina Lamanna	
Applicability of Relative Weights Derived for Nuwara Eliya and Badulla Regions to the Areas with Different Terrain and Climatological Characteristics	273
Kumari M. Weerasinghe, P.H.E. Dulanjalee, H.K.D.W.M.I.U.K. Hapuhinna, and Hasali Hemasinghe	

Landslide Hazard and Risk in a Changing Climate	281
Mike G. Winter and Barbara Shearer	
Validation of a Simulation Chain to Assess Climate Change Impact on Precipitation Induced Landslides	287
Alessandra L. Zollo, Guido Rianna, Paola Mercogliano, Paolo Tommasi, and Luca Comegna	
Part VI Recognition and Mechanics of Landslides	
Introduction: Recognition and Mechanics of Landslides	295
L. Picarelli and B. Abolmasov	
Mechanism and Dynamics of Umka Landslide, Belgrade, Serbia	297
Biljana Abolmasov, Svetozar Milenković, Branko Jelisavac, Uroš Đurić, and Miloš Marjanović	
Shear Strength Recovery of Clayey Soils Following Discontinuation of Shear at a Residual State	303
Deepak R. Bhat, Netra P. Bhandary, and Ryuichi Yatabe	
Landslides on a Cretaceous Fluvial Sediment	309
Peter Redshaw, Max Barton, and Caroline Stuver	
Prediction Method of the Onset of Landslides Based on the Stress-Dilatancy Relation Against Shallow Landslides	315
Katsuo Sasahara, Kazuya Itoh, and Naoki Sakai	
Part VII General Landslide Studies	
Introduction: General Landslide Studies	323
Peter Bobrowsky, Yueping Yin, and Alexander Strom	
Early Warning Systems and Time Series Modelling: A New Challenge for Landslide Risk Prevention	325
Emmanuelle Klein, Cristina Occhiena, Alicia Durenne, Yves Gueniffey, and Marina Pirulli	
Slope Stability Analysis at Bloemendhal Open Dump Site in Sri Lanka	333
Udeni P. Nawagamuwa and W.H.R.S. Dayarathne	
Slope Dynamic Geomorphology of the Mailuu-Suu Area, Aspects of Long-Term Prediction	339
Yuri Aleshin and Isakbek Torgoev	
An Overview of Rock Avalanche-Substrate Interactions	345
Anja Dufresne	
Landslide Susceptibility of Kavaja, Albania	351
Olger Jaupaj, Olivier Lateltin, and Mentor Lamaj	
Recent Extreme Rainfall-Induced Landslides and Government Countermeasures in Korea	357
Su-Gon Lee and Stephen R. Hencher	
How the Stabilizing Effect of Vegetation on a Slope Changes Over Time: A Review	363
Wei Meng, Thom Bogaard, and Rens van Beek	

Analysis of a Deep-Seated Landslide in the Phan Me Coal Mining Dump Site, Thai Nguyen Province, Vietnam	373
Do Minh Duc, Nguyen Manh Hieu, Kyoji Sassa, Eisaku Hamasaki Khang Dang, and Toyohiko Miyagi	
Geological Complexities of Rawana Landslide, Sirmaur District, Himachal	379
D.K. Chadha	
Highways Vs. Landslides and Their Consequences in Himalaya	389
Kishor Kumar, Lalita Jangpangi, and S. Gangopadhyay	
Characteristics of Landslides from Sigou Gorge to Lagan Gorge in the Upper Reaches of Yellow River	397
Zhiqiang Yin, Xiaoguang Qin, and Wuji Zhao	
Evaluation on Effect for the Prevention and Control Against the Landslide Disasters in the Three Gorges Reservoir Area	407
Yong Zhang, Sheng-wei Shi, Jun Song, and Ying-jian Cheng	
Fiber Optic Strain Monitoring and Evaluation of a Slow-Moving Landslide Near Ashcroft, British Columbia, Canada	415
David Huntley, Peter Bobrowsky, Zhang Qing, Wendy Sladen, Chris Bunce, Tom Edwards, Michael Hendry, Derek Martin, and Eddie Choi	
Landslides Susceptibility of Chittagong City, Bangladesh and Development of Landslides Early Warning System	423
Reshad Md. Ekram Ali, Lloyd Warren Tunbridge, Rajinder Kumar Bhasin, Salma Akter, Md. Mahmood Hossain Khan, and Mohammad Zohir Uddin	
Part VIII Side Events	
Introduction: Session D1-D4—Side Events of World Landslide Forum	431
Bin He and Kyoji Sassa	
Detection of Active Landslide Zone from Aerial Photograph Interpretation and Field Survey in Central Provinces of Vietnam	435
Hong Luong Le, Toyohiko Miyagi, Shinro Abe, Eisaku Hamasaki, and Van Tien Dinh	
Numerical Assessment of Shallow Landslide Using the Distributed Hydrological–Geotechnical Model in a Large Scale	443
Pingping Luo, Apip, Kaoru Takara, Bin He, Weili Duan, and Maochuan Hu	
Stability Analysis of a High Slope Along a Loess Plateau Based on Field Investigation and Numerical Analysis	451
Zongyuan Ma, Hongjian Liao, Chunming Ning, and Zhigang Feng	
The Simulation of a Deep Large-Scale Landslide Near Aratozawa Dam Using a 3.0 MPa Undrained Dynamic Loading Ring Shear Apparatus	459
Hendy Setiawan, Kyoji Sassa, Kaoru Takara, Toyohiko Miyagi, Hiroshi Fukuoka, and Bin He	
Study on Strength and Deformation Behavior of Loess Slope Supported by Micropiles	467
Chenglin Tian, Hongjian Liao, Yonggang Peng, Dongrui Hao, and Jianbing Peng	
The Influence of Countermeasure on Debris Flow Hazards with Numerical Simulation	473
Ying-Hsin Wu and Ko-Fei Liu	

Simulation of a Rapid and Long-Travelling Landslide Using 2D-RAPID and LS-RAPID 3D Models	479
Bin He, Kyoji Sassa, Osamu Nagai, and Kaoru Takara	
Landslide Technology and Engineering in Support of Landslide Science	485
Kyoji Sassa	



Activities of the International Programme on Landslides (IPL): IPL Projects and World Centres of Excellence on Landslide Risk Reduction (WCoE)

Matjaž Mikoš and Snježana Mihalić Arbanas

Part of the International Programme on Landslides (IPL) are also two important activities: the IPL projects and the World Centres of Excellence on Landslide Risk Reduction (WCoE). This introductory chapter to the Volume 1 of the Proceedings of the World Landslide Forum 3 is a short summary of the above-mentioned activities of the ICL members between the WLF2 in Rome 2011 and WLF3 in Beijing 2014. In this period altogether 53 IPL projects were active or are still ongoing. Each year new projects of the ICL members are proposed and approved. At the WLF2 in Rome 2011, 15 WCoEs were approved for the period 2011–2014, and new ones will be approved at the WLF3 in Beijing 2014 for the period 2014–2017.

IPL Programme

The International Programme on Landslides (IPL) is a programme of the International Consortium on Landslides (ICL) that was established in Kyoto, Japan, in January 2002. The IPL contributes to the United Nations International Strategy for Disaster Reduction.

The IPL was initiated by the 2006 Tokyo Action Plan and was developed in partnership with the ICL-supporting organizations (UNESCO, WMO, FAO, UNISDR, UNU, ICSU, WFEO, IUGS) aiming at achieving the ICL goals. The IPL is managed by the IPL Global Promotion Committee (IPL-GPC). More detailed description of the ICL and IPL is given in the Preface to this Volume 1 (Sassa et al. 2014) or elsewhere (Sassa 2012).

The most successful ICL/IPL project so far and also widely accepted in the landslide community is the journal *Landslides*—for its achievements and impact refer to Sassa et al. (2009) and Mikos (2011).

Overview of IPL Projects

An IPL project can be annually proposed by any active ICL member. Each project proposal is screened and evaluated/ranked by the IPL Evaluation Committee. The evaluation of the proposed projects is the basis for the decision during the annual meeting of the Board of Representatives (BOR). Casagli et al. (2009) prepared for the WLF1 in Tokyo in 2009 overview of over 60 IPL projects conducted in the period 2002–2008.

M. Mikoš
University of Ljubljana, Faculty of Civil and Geodetic Engineering,
Jamova c. 2, SI-1000 Ljubljana, Slovenia
e-mail: matjaz.mikos@fgg.uni-lj.si

S.M. Arbanas
University of Zagreb, Faculty of Mining, Geology and Petroleum
Engineering, Pierottijeva 6, HR-10000 Zagreb, Croatia
e-mail: smihalic@rgn.hr

Each project proposal must deal with at least one of the following main project fields:

- (1) Technology development:
 - A. Monitoring and early warning
 - B. Hazard mapping, vulnerability, and risk assessment
- (2) Targeted landslides—mechanisms and impacts:
 - A. Catastrophic landslides
 - B. Landslides threatening heritage sites
 - C. Landslide hazard risk management in urban areas
- (3) Capacity building:
 - A. Enhancing human and institutional capacities
 - B. Collating and disseminating information/knowledge
- (4) Mitigation, preparedness, and recovery:
 - A. Mitigation
 - B. Preparedness
 - C. Recovery

During the period between the two World Landslides Forums (WLF2 in Rome 2011 and WLF3 in Beijing 2014), i.e. in the period 2011–2013, altogether 53 IPL projects were active (see Table 1). The countries being actively involved into IPL projects are shown on the world map in Fig. 1. It follows a short description of each of the active IPL projects in the period 2011–2013 (ongoing and completed ones). For the older IPL projects please refer to the paper Casagli et al. (2009).

IPL-112 Project

Project Title: Landslide mapping and risk mitigation planning in Thailand

Country: Thailand

Leader: Saowanee Prachansri

Period: 2002/2008–

Status: ongoing

Main Project Fields: technology development; hazard mapping; vulnerability; and risk assessment

Objectives: to assess and map landslide susceptible areas in 204 sub-basins in Thailand that are planned for development or that have been developed, in addition to zone landslide risk areas, design and conduct prevention, and/or mitigation measures in landslide risk areas.

Study area: Critical potential landslide areas subject to development or already developed in 204 sub-basins in Thailand.

IPL-132 Project

Project Title: Research on vegetation protection system for highway soil slope in seasonal frozen regions

Country: China, Japan

Leader: Wei Shan, Fawu Wang

Period: 2008–

Status: ongoing

Main Project Fields: mitigation; preparedness technology

Objectives: This study aims to establish a comprehensive vegetation protection system for highway soil slope in seasonal frozen regions. The system will be of benefit to regional environment green along the highway, and the highway slope stabilization.

Study area: A major highway in China's Heilongjiang Province, Kiamusze to Harbin of Tong-San Expressway.

Table 1 The chronological overview of the IPL projects active in the period 2011–2013

IPL Project	Project title	Country/ Organization	Project leader	Period	Status
IPL-101-2	Landslides monitoring and slope stability at selected historic sites in Slovakia	Slovakia	Jan Vlcko	2002/2008–	Ongoing
IPL-101-3	The geomorphological instability of the Buddha niches and surrounding cliff in Bamiyan valley (Central Afghanistan)	Italy	Claudio Margottini	2002/2008–	Ongoing
IPL-105	Early warning of landslides	Japan	Kyoji Sassa	2005–	Ongoing
IPL-106-1	Landslide museum in Civita di Bagnoregio	Italy	Claudio Margottini	2006/ 2008–2013	Completed
IPL-106-2	International summer school on rockslides and related phenomena in the Kokomerren River Valley, Tien Shan, Kyrgyzstan	Russia	Alexander Strom	2008–	Ongoing
IPL-112	Landslide mapping and risk mitigation planning in Thailand	Thailand	Saowanee Prachansri	2002/2008–	Ongoing
IPL-132	Research on vegetation protection system for highway soil slope in seasonal frozen regions	China, Japan	Wei Shan, Fawu Wang	2006/2008–	Ongoing
IPL 134	Large-scale rockslides in coarse-bedded carbonate rocks in the Apennines (Italy), Caucasus (Russia) and Zagros (Iran): evaluation of possible triggers and hazard assessment	Russia	Alexander Strom	2007–2011	Completed
IPL-138	Long run out and catastrophic landslides study: Yigong Landslide, Tibet China	China	Yin Yueping	2008–2011	Completed
IPL-139	Development of low-cost early warning system of slope instability for civilian use	Japan	Ikuo Towhata, Taro Uchimura	2008–	Ongoing
IPL-140	Landslide and multi-geohazards mapping for community empowerment in Indonesia	Indonesia	Dwikorita Karnawati	2008–2011	Completed
IPL-141	Geo-risks management for Third World Countries— Mapping and assessment of risky geo-factors for land use (e.g. in Ethiopia)	Czech Republic	Jiří Zvelebil	2008–	Ongoing
IPL-142	Seismic landslide hazards mapping in Sichuan	China	Yuepin Yin	2009–2011	Completed
IPL-143	Evaluation of sensitivity of the combined hydrological model (dynamic) for landslide susceptibility risk mapping in Sri Lanka	Sri Lanka	A. A. Virajh Dias	2008–2012	Completed
IPL-144	SafeLand—Living with landslide risk in Europe: Assessment, effects of global change, and risk management strategies	Norway	Bjørn Kalsnes	2009–2012	Completed
IPL-145	Preparation of landslide risk map in Taleghan Area-Iran	Iran	S. H. Tabatabaei	2009–2011	Completed
IPL-146	Spatial monitoring of joint influence of an atmospheric precipitation and seismic motions on formation of landslides in Uzbekistan (Central Asia)	Uzbekistan	Rustam Niyazov	2010–2012	Completed
IPL-147	Study on debris flow controlling factors and triggering mechanism in Peninsular Malaysia	Malaysia	Che Hassandi Abdullah	2010–2011	Completed
IPL-149	Canadian Landslide Best Practice Manual	Canada	Peter Bobrowsky	2010–	Ongoing
IPL-150	Capacity building and the impact of climate-driven changes on regional landslide distribution, frequency and scale of catastrophe	Nigeria	Ogbonnaya Igwe	2010–	Ongoing
IPL-151	Soil matrix suction in active landslides in flysch—the Slano Blato landslide case	Slovenia	Bojan Majes	2010–	Ongoing
IPL-153	Landslide hazard zonation in Kharkov region of Ukraine using GIS	Ukraine	Oleksandr M. Trofymchuk	2010–2013	Completed
IPL-154	Development of a methodology for risk assessment of the earthquake-induced landslides	Japan	D. Higaki	2010–2013	Completed
IPL-155	Determination of soil parameters of subsurface to be used in slope stability analysis in two different precipitation zones of Sri Lanka	Sri Lanka	A. A. Virajh Dias	2010–	Ongoing
IPL-156	Best practices for early warning of landslides in a changing climate scenarios	Thailand	N.M.S.I. Arambepola	2009–2012	Completed

(continued)

Table 1 (continued)

IPL Project	Project title	Country/ Organization	Project leader	Period	Status
IPL-157	Dynamics of subaerial and submarine megaslides	Japan	Kyoji Sassa	2010–	Ongoing
IPL-158	Development of community-based landslide early warning system	Indonesia	Teuku Faisal Fathani	2009–2013	Completed
IPL-159	Development of education program for sustainable development in landslide vulnerable area through student community service	Indonesia	Dwikorita Karnawati	2009–2013	Completed
IPL-160	Landslides and floods under extreme weather condition and resilient society	Japan	Hiroshi Fukuoka	2009–	Ongoing
IPL-161	Risk identification and land-use planning for disaster mitigation of landslides and floods in Croatia	Japan	Hideaki Marui	2009–	Ongoing
IPL-162	Tier-based harmonized approach for landslide susceptibility mapping over Europe	Italy	Javier Hervás	2007–2012	Completed
IPL-163	Mechanical-mathematical modeling and monitoring for landslide processes	Russia	Svalova Valentina	2009–2013	Completed
IPL-165	Development of community-based landslide hazard mapping for landslide risk reduction at the village scale in Java, Indonesia	Indonesia	Dwikorita Karnawati	2010–2013	Completed
IPL-167	The effect of freezing-thawing on the stability of ancient landslide of North-Black highway	China	Wei Shan	2009–	Ongoing
IPL-168	Engaging U.S. citizens in Landslide Science through the website, “Did You See It? Report a Landslide”	USA	Rex Baum	2010–2013	Completed
IPL-169	Landslide hazard and risk assessment in Geysir Valley (Kamchatka)	Russia	Oleg V. Zerkal	2010–2012	Completed
IPL-170	Landslide susceptibility and landslide hazard zonation in volcanic terrains using Geographic Information System (GIS): A case study in the Río Chiquito-barranca Del Muerto watershed; Pico de Orizaba volcano, México	Mexico	Gabriel Legorreta Paulín	2010–2013	Completed
IPL-171	Study of the geotechnical characteristics of an unstable urban area of Barranquilla (Colombia) severely affected for slope instabilities and soil volume changes	Colombia	Guillermo Ávila	2010–2013	Completed
IPL-172	Documentation, Training and Capacity Building for Landslides Risk Management	India	Surya Parkash	2011–	Ongoing
IPL-173	Croatian Virtual Landslide Data Center	Croatia	Snježana Mihalić Arbanas	2011–	Ongoing
IPL-175	Development of landslide risk assessment technology and education in Vietnam and other areas in the Greater Mekong Sub-region	Japan, Vietnam	Kyoji Sassa, Nguen Xuan Khang	2012–	Ongoing
IPL-176	Slope Data Acquisition along Highways in Sabah State for hazard assessment and mapping	Malaysia	Che Hassandi Abdullah	2012–2013	Completed
IPL-177	Study on geological disasters focusing on landslides in and around Tegucigalpa City, Honduras	Honduras	Aníbal Godoy	2012–2013	Completed
IPL-179	Database of Glacial Lake Outburst Floods (GLOFs)	Czech Republic	Adam Emmer, Vit Vilfemek	2012–	Ongoing
IPL-180	Introducing Community-based Early Warning System for Landslide Hazard Management in Cox’s Bazaar Municipality, Bangladesh	Thailand	N.M.S.I. Arambepola	2011–2012	Ongoing
IPL-181	Study of slow moving landslide Umka near Belgrade, Serbia	Serbia	Biljana Abolmasov	2012–	Ongoing
IPL-182	Characterization of landslides mechanisms and impacts as a tool to fast risk analysis of landslides related disasters in Brazil	Brazil	Renato Eugenio de Lima	2012–	Ongoing
IPL-183	Landslides in West Africa: impacts, mechanism and management	Nigeria	Igwe Ogbonnaya	2012–	Ongoing
IPL-184	Study of landslides in flysch deposits of North Istria, Croatia: sliding mechanisms, geotechnical properties, landslide modeling and landslide susceptibility	Croatia	Željko Arbanas	2012–	Ongoing

(continued)

Table 1 (continued)

IPL Project	Project title	Country/ Organization	Project leader	Period	Status
IPL-185	Landslide hazards assessment and modeling sediment yield of landslides using Geographic Information System (GIS): A case study in the Río El Estero on the SW flank of Pico de Orizaba volcano, Puebla-Veracruz, Mexico	Mexico	Gabriel Legorreta Paulín	2013–	Ongoing
IPL-186	Rock-fall hazard assessment and monitoring in the archaeological site of Petra, Jordan	Italy	Claudio Margottini	2013–	Ongoing
IPL-187	Design and Validation of an Early Warning System for Landslides—DeVEL	Germany	Rolf Katzenbach	2013–	Ongoing
IPL-188	Study of slow moving landslide Potoška planina (Karavanke Mountain, NW Slovenia)	Slovenia	Marko Komac	2013–	Ongoing

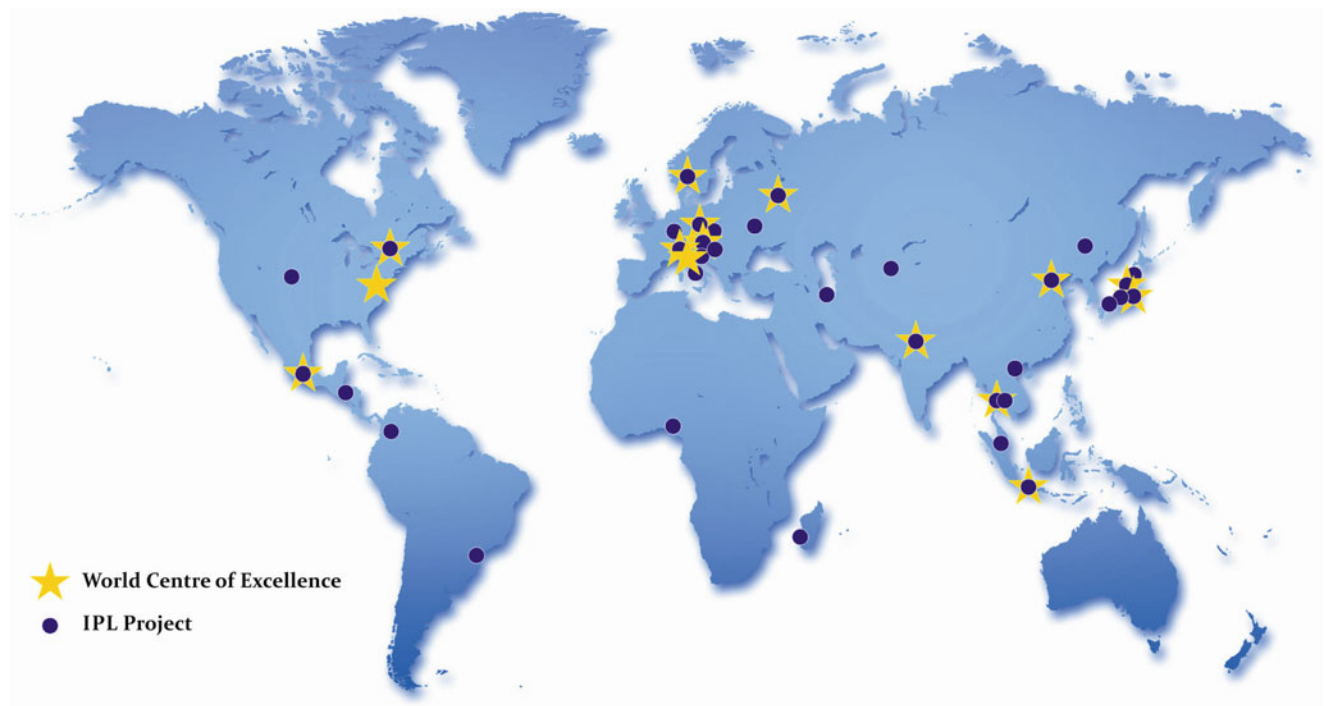


Fig. 1 Worldwide distribution of the IPL projects being active in the period 2011–2013 with the distribution of ICL World Centres of Excellence (WCoE) for the period 2011–2014

IPL-134 Project

Project Title: Large-scale rockslides in coarse-bedded carbonate rocks in the Apennines (Italy), Caucasus (Russia) and Zagros (Iran): evaluation of possible triggers and hazard assessment

Country: Russia

Leader: Alexander Strom

Period: 2007–2011

Status: completed

Main Project Fields: study of bedrock landslides mechanisms; landslide hazard assessment

Objectives: Revealing of mechanisms and possible triggers of large-scale bedrock landslides in coarse-bedded carbonate rocks folded in large box folds by comparative analysis of case studies from different regions.

Study area: Dagestan (Eastern part of the Great Caucasus, Russia), Zagros, including the Seimareh landslide area (Iran), Apennines (Italy).

IPL-138 Project**Project Title:** Long run-out and catastrophic landslides study: Yigong Landslide, Tibet China**Country:** China**Leader:** Yin Yueping**Period:** 2008–2011**Status:** completed**Main Project Fields:** catastrophic landslides**Objectives:** To find out the relationship between the global warming and catastrophic landslide. To study the metrology of mapping and investigating of catastrophic landslide. To develop the technique of RS in the catastrophic landslide mapping and monitoring. To assess the run-out with wind tunnel test and the risk of a certain catastrophic landslide. To clarify the mechanism of the catastrophic landslide.**Study area:** On Egong landslide in Tibet, China. Several other catastrophic landslides are considered together to form the whole idea of the same kind landslide.**IPL-139 Project****Project Title:** Development of low-cost early warning system of slope instability for civilian use**Country:** Japan**Leader:** Ikuo Towhata, Taro Ichimura**Period:** 2008–**Status:** ongoing**Main Project Fields:** monitoring and early warning**Objectives:** A simple and low-cost early warning system will be developed, and its applicability and effectiveness will be tested at slopes with failure risk in Japan and some other countries. The system should work with batteries for several (ideally, five or more) years, transfer real-time data via wireless network, and be low-cost and simple so that non-expert residents in risk area can handle it easily even in developing countries.**Study area:** Urban and mountainous areas in Japan, and some countries in Asia.**IPL-140 Project****Project Title:** Landslide and multi-geohazards mapping for community empowerment in Indonesia**Country:** Indonesia**Leader:** Dwikorita Karnawati**Period:** 2008–2011**Status:** completed**Main Project Fields:** mitigation (conducted in conjunction with IPL Project no. IPL158 and IPL 159)**Objectives:** This research was intended to provide landslide and multi-geohazard maps to support the development of landslide early warning system and community empowerment with respect to landslide and earthquake disaster risk reduction programme in Indonesia. Rapid site investigation and assessment were also conducted in this study to support the rehabilitation/reconstruction of the disaster areas.**Study area:** Yogyakarta and Central Java, Indonesia.

IPL-141 Project

Project Title: Geo-risks management for Third World Countries—Mapping and assessment of risky geo-factors for Land Use (e.g. in Ethiopia)

Country: Czech Republic

Leader: Jiří Zvelebil

Period: 2008–

Status: ongoing

Main Project Fields: engineering geological mapping; non-linear modelling of risky processes; information dissemination

Objectives: Improvement of methodology for rugged, hard accessible terrains with satellite imagery broad use; to gain experience under different geologic-climatic conditions.

Study area: Ethiopia: Jemma River basin, Gibe River basin; Czech Republic: NW Bohemia—Sandstone areas.

IPL-142 Project

Project Title: Seismic landslide hazards mapping in Sichuan

Country: China

Leader: Yuepin Yin

Period: 2008–2012

Status: completed

Main Project Fields: hazard mapping, vulnerability, and risk assessment

Objectives: Developing a method for a quick hazard mapping of earthquake-triggered landslides. A factor selection and stability judgment programme will be developed and a rough run-out assessment method will be introduced into this method.

Study area: Niujuangou, Yingxiu, Wenchuan, Sichuan, China. The epicentre area.

IPL-144 Project

Project Title: SafeLand—Living with landslide risk in Europe: Assessment, effects of global change, and risk management strategies.

Country: Norway

Leader: Bjørn Kalsnes

Period: 2009–2012

Status: completed

Main Project Fields: landslide risk assessment

Objectives: Providing policymakers, public administrators, researchers, scientists, educators, and other stakeholders with improved harmonized framework and methodology for the assessment and quantification of landslide risk in Europe's regions. Evaluating the changes in risk pattern caused by climate change, human activity, and policy changes. Providing guidelines for choosing the most appropriate risk management strategies, including risk mitigation and prevention measures.

Study area: Europe (12 countries), India, China.

IPL-145 Project

Project Title: Preparation of landslide risk map in Taleghan Area-Iran

Country: Iran

Leader: S. H. Tabatabaei

Period: 2009–2011

Status: completed

Main Project Fields: database; hazard and risk assessment; societal application

Objectives: The main aims of this project are to identify effective parameters on landslide occurrence and preparation of landslide risk map in order to reduce landslide risk in Taleghan area. The study can help to formulate a master plan and technique which can be adapted for other places with a similar environment and catastrophic events.

Study area: The study area covers about 932 Sq. Km. Civil works development such as dam building and road construction has posed a serious threat to ground stability.

IPL-146 Project

Project Title: Spatial monitoring of joint influence of an atmospheric precipitation and seismic motions on formation of landslides in Uzbekistan (Central Asia)

Country: Uzbekistan

Leader: Rustam Niyazov

Period: 2011–2012

Status: completed

Main Project Fields: technology development; monitoring and early warning; hazard mapping, vulnerability, and risk assessment

Objectives: Increasing reliability and timeliness of the precautionary information about threat of landslide processes. Project tasks include analyses of successful and unsuccessful cases of the warning of landslide hazard, influence of climate change on activation of landslides, and comparison of time of landslides occurrence (1958–2012) with time of influence of deep-focal (230km) and long (1.5–2.5min) earthquakes in Pamir Hindu Kush (Afghanistan) zone.

Study area: Mountain and foothill territories of north-east and south-west regions of Uzbekistan.

IPL-147 Project

Project Title: Study on debris flow controlling factors and triggering mechanism in Peninsular Malaysia

Country: Malaysia

Leader: Che Hassandi Abdulah

Period: 2010–2011

Status: completed

Main Project Fields: technology development; monitoring and early warning; hazard mapping, vulnerability, and risk assessment

Objectives: Developing preliminary rainfall threshold criteria for occurrence of debris flow in Peninsular Malaysia. Conducting case study of hazard zonation of debris flows on a chosen site and preparing a preliminary guideline for hazard mapping.

Study area: Eight sites in Peninsular Malaysia have been chosen which are Kuala Lumpur-Karak Highway, Kuala Kubu Baru-Gap Road, Simpang Pulai-Cameron Highland Road, Gap-Fraser Hill Road, Lojing-Gua Musang Road, Karak Highway, Gunung Tempurung, and Gunung Pulai.

IPL-149 Project

Project Title: Canadian Landslide Best Practice Manual

Country: Canada

Leader: Peter Bobrowsky

Period: 2010–

Status: ongoing

Main Project Fields: engineering geology; geotechnics; landslide mapping; monitoring and analysis; landslide hazard interpretation

Objectives: The Geological Survey of Canada is coordinating the compilation and publication of a multi-authored guidelines document for technical landslide studies in Canada. The 11-chapter volume will highlight successful best practices for identifying, monitoring, mapping, analysing, and managing slope stability hazards.

Study area: All of Canada.

IPL-150 Project

Project Title: Capacity building and the impact of climate-driven changes on regional landslide distribution, frequency and scale of catastrophe

Country: Nigeria

Leader: Ogbonnaya Igwe

Period: 2010–

Status: ongoing

Main Project Fields: capacity building; landslide investigation; risk assessment

Objectives: One of the major objectives is (1) to increase the capacity of Africans to respond to landslide hazard and risk. It is also aimed (2) to determine the actual processes that lead to the initiation of landslides using a slope stability model, (3) to determine the mechanism of the moving mass using a new ring shear apparatus that simulates the mobility of landslides, and (4) to generate data that could be used for a future landslide susceptibility map.

Study area: Nigeria, Cameroon, and Uganda.

IPL-151 Project

Project Title: Soil matrix suction in active landslides in flysch—the Slano Blato landslide case

Country: Slovenia

Leader: Bojan Majes

Period: 2010–

Status: ongoing

Main Project Fields: monitoring and early warning; mechanisms and impacts; large landslides; mitigation, preparedness, and recovery

Objectives: Comparing continuous measurements of soil matrix suction in an active landslide (of the order up to 50kPa) with measurements of matrix suction in highly weathered and progressively disintegrating flysch rock the landslide is fed from. Designing of an early warning system for the deep-seated Slano Blato landslide in W Slovenia, based on soil matrix suction measurements and online landslide displacement measurements.

Study area: The active Slano Blato landslide in W Slovenia.

IPL-153 Project

Project Title: Landslide protection structures and their development in the Autonomous Republic of the Crimea, Ukraine

Country: Ukraine

Leader: Oleksandr M. Trofymchuk

Period: 2010–2013

Status: completed

Main Project Fields: capacity building

Objectives: Collecting and structuring of the information about landslide protection structures. Collecting and structuring of the information about landslide protection measures. Developing of the structure of the target database of landslide protection structures and landslide protection measures.

Study area: Autonomous Republic of the Crimea and Carpathian Mountains region, Ukraine.

IPL-154 Project

Project Title: Development of a methodology for risk assessment of the earthquake-induced landslides

Country: Japan

Leader: Daisuke Higaki

Period: 2010–2013

Status: completed

Main Project Fields: hazard mapping, vulnerability, and risk assessment; catastrophic landslides; preparedness

Objectives: Clarifying the mechanism of the earthquake-induced landslides on the basis of surveying types, dimensions, distributions, and run-out distances of the landslides and analysing relations to the seismicity and geology. Making up of appropriate technical guidelines for risk assessment of earthquake-induced landslides.

Study area: Asian-Pacific Region (especially in Asian Orogenic Zone).

IPL-155 Project

Project Title: Determination of soil parameters of subsurface to be used in slope stability analysis in two different precipitation zones of Sri Lanka

Country: Sri Lanka

Leader: A A Virajh Dias

Period: 2010–

Status: ongoing

Main Project Fields: hazard mapping, vulnerability, and risk assessment

Objectives: Determination of critical and other important in situ soil parameters for various soil types that are present in two different precipitation zones in Sri Lanka and comparison of the same.

Study area: Heavily precipitated zone in wet zone with annual average rainfall above 4000mm: Watawala, Nawalapitiya. Wet zone with annual average rainfall between 2,500 and 3,000 mm: Haldummulla, Haputale, Ratnapura, Kalawana.

IPL-156 Project

Project Title: Best practices for early warning of landslides in a changing climate scenarios

Country: Thailand

Leader: N.M.S.I. Arambepola

Period: 2009–2012

Status: completed

Main Project Fields: monitoring and early warning; capacity building

Objectives: Developing and disseminating good practices in early warning of landslides in participating countries. Forming joint working groups among the professionals from participating countries to research and analyse the critical factors responsible for slope destabilization under different conditions. Introducing and developing existing and new concepts pertaining to precipitation threshold values for landslides in different geological materials. Providing input to local and regional multi-hazard platforms for early warning and identifying suitable mitigation measures in areas that require immediate attention.

Study area: Asian Region: Bangladesh, Bhutan, People's Republic of China, India, Indonesia, Nepal, Philippines, Sri Lanka, Thailand, and Vietnam.

IPL-157 Project

Project Title: Dynamics of subaerial and submarine megaslides

Country: Japan

Leader: Kyoji Sassa

Period: 2010–

Status: ongoing

Main Project Fields: technology development; monitoring and early warning, vulnerability and risk assessment; catastrophic landslides; coastal and marine landslides; preparedness and mitigation.

Objectives: Mega landslides of 100–1000m in depth, greater than 10 million m³ in volume, cause a great effect either on land, coastal, or under water. Megaslides may trigger

Tsunami, or form landslide dams which may fail and cause great debris flows or floods as well as causing direct damages. So far dynamics of such megaslides has not been studied. This project will develop a super high stress ring shear apparatus of 10 MPa for 100–1,000m deep landslides. The ring shear test results are combined to the Multibeam Swath Bathymetry, InSAR, GPS on-land and seafloor investigation, combined with 50 Centrifuge model experiment for landslide triggered tsunami, and computer simulation. It aims to establish Dynamics of Subaerial and Submarine megaslides which may provide reliable risk analysis of ongoing and also potential megaslides over the world.

Study area: Japan, Pakistan, Uzbekistan, Norway, Italy, Central Asia, Mediterranean Sea, Vietnam.

IPL-158 Project

Project Title: Development of community-based landslide early warning system

Country: Indonesia

Leader: Teuku Faisal Fathani

Period: 2010–2013

Status: completed

Main Project Fields: monitoring and early warning

Objectives: Community empowerment with respect to community-based disaster risk reduction in landslide vulnerable area, by integrating technical and social networks of landslide early warning system.

Study area: Central Java Province and West Sumatera Province, Indonesia.

IPL-159 Project

Project Title: Development of education program for sustainable development in landslide vulnerable area through Student Community Service

Country: Indonesia

Leader: Dwikorita Karnawati

Period: 2010–2013

Status: completed

Main Project Fields: capacity building

Objectives: Capacity building of students as the future leaders/decision makers/researchers for sustainable development through enhancement of learning programme in higher education, which provides opportunity for the students to a) implement their knowledge and skill for landslide mitigation and risk reduction and b) develop the ethical values and spirit of sustainable development with respect to landslide risk reduction (development of various hearth skill such as adaptability, flexibility, tolerance, team working, and empathy through community empowerment activities for landslide risk reduction).

Study area: Java and Sumatera, Indonesia.

IPL-160 Project

Project Title: Landslides and floods under extreme weather condition and resilient society

Country: Japan

Leader: Hiroshi Fukuoka

Period: 2009–

Status: ongoing

Main Project Fields: monitoring and early warning; hazard mapping, vulnerability, and risk assessment; catastrophic landslides; capacity building

Objectives: Developing interdisciplinary research and promoting capacity building activities on landslides and floods in Asia and Africa countries. Extreme weather conditions are closely related to ongoing climate change.

Study area: Asia and Africa.

IPL-161 Project

Project Title: Risk identification and land-use planning for disaster mitigation of landslides and floods in Croatia

Country: Japan

Leader: Hideaki Marui

Period: 2009–

Status: ongoing

Main Project Fields: monitoring and early warning, hazard mapping, vulnerability, and risk assessment; catastrophic landslides, landslides threatening sites with high societal value; enhancing human and institutional capacities and collating and disseminating of information and knowledge; preparedness and mitigation

Objectives: Contributing to the development of land-use planning in order to reduce disasters caused by landslides and floods through the basic scientific study of mechanism, risk identification, and the practical study of land-use planning. Zoning technology of “Integrated landslide/flood hazard map” and formulation methodology of “land-use guidelines” are developed for nation-wide application in Croatia.

Study area: Croatia; to be applied to the whole Adriatic and Balkan Region in future.

IPL-162 Project

Project Title: Tier-based harmonized approach for landslide susceptibility mapping over Europe

Country: Italy

Leader: Javier Hervás

Period: 2007–2012

Status: completed

Main Project Fields: hazard mapping

Objectives: Producing a landslide susceptibility map of Europe using datasets available for the whole of Europe and a common approach. The results will allow identifying priority areas where more detailed landslide susceptibility mapping is required. For this purpose, suggestions towards a common quantitative methodology will be made.

Study area: Europe (European Union and neighbouring countries).

IPL-163 Project

Project Title: Mechanical-mathematical modeling and monitoring for landslide processes

Country: Russia

Leader: Valentina Svalova

Period: 2009–2013

Status: completed

Main Project Fields: monitoring and early warning; landslides threatening heritage sites

Objectives: Elaboration of mechanical-mathematical model for landslide process on the base of Navier–Stokes equation. Investigation of triggering mechanism for landslide processes. Promotion of monitoring systems. Geophysical background research in earthquake areas. Alarm and early warning systems elaboration.

Study area: Moscow landslides, Russian landslides.

IPL-165 Project

Project Title: Development of community-based landslide hazard mapping for landslide risk reduction at the village scale in Java, Indonesia

Country: Indonesia

Leader: Dwikorita Karnawati

Period: 2010–2013

Status: completed

Main Project Fields: mitigation

Objectives: Providing a simple, practical, and communicative landslide hazard map, developed through community participation.

Study area: Karanganyar Regency (Gempolan Village and Plosorejo Village of Kerjo District, in Karanganyar Regency Central Java).

IPL-167 Project

Project Title: Landslides mechanism and the subgrade stability controlling measures in Island Permafrost Area

Country: China

Leader: Wei Shan

Period: 2010–

Status: ongoing

Main Project Fields: mitigation, preparedness, and recovery

Objectives: Under the permafrost, landslides and other complex geological conditions investigation, design, construction, and monitoring technical of the targeted Expressway expansion project.

Study area: The Bei-Hei Expressway Extension Project K160–K182 Section.

IPL-168 Project

Project Title: Engaging U.S. citizens in Landslide Science through the website, “Did You See It? Report a Landslide”

Country: USA

Leader: Rex Baum

Period: 2010–2013

Status: completed

Main Project Fields: enhancing human and institutional capacities; collating and disseminating information/knowledge

Objectives: Educating Americans about the landslide hazards they face and to build better inventories of landslides through citizen participation. This project will try to make it as easy as possible for the public to report their observations of landslides on a website. The information gathered through the website can be used to classify the landslides and damage, as well as provide information to scientists about the location, time, speed, and size of the landslides. The website that is being developed will display summary maps showing locations of recent landslides, as well as graphs showing simple statistics derived from the collected data, such as number of landslide reports, cumulative losses, or number of landslides by type.

Study area: All of the USA.

IPL-169 Project

Project Title: Landslide hazard and risk assessment in Geysir Valley (Kamchatka, Russia)

Country: Russia

Leader: Oleg V. Zerkal

Period: 2009–2012

Status: completed

Main Project Fields: landslides threatening heritage sites

Objectives: Slope stability analysis, slope hazard mapping, research of landslide process mechanics, and risk assessment.

Study area: Geysir Valley, Kamchatka, Russia.

IPL-170 Project

Project Title: Landslide susceptibility and landslide hazard zonation in volcanic terrains using Geographic Information System (GIS): A case study in the Río Chiquito-barranca Del Muerto watershed; Pico de Orizaba volcano, México

Country: Mexico

Leader: Gabriel Legorreta Paulín

Period: 2010–2013

Status: completed

Main Project Fields: hazard mapping, vulnerability, and risk assessment

Objectives: Preparing a landslide inventory map and landslide susceptibility zonation for the study area in GIS. Evaluating the performance of GIS-based slope stability models to select the model that meets criteria for scientific accuracy, technical accessibility, and applicability. Developing a method (protocol) for hazard assessment of potentially unstable landforms with the designated mapping methodology for volcanic terrains.

Study area: Río Chiquito-barranca Del Muerto watershed at Pico de Orizaba volcano, México.

IPL-171 Project

Project Title: Study of the geotechnical characteristics of an unstable urban area of Barranquilla (Colombia) severely affected for slope instabilities and soil volume changes

Country: Colombia

Leader: Guillermo Ávila

Period: 2010–2013

Status: completed

Main Project Fields: catastrophic landslides

Objectives: Studying the mechanical and mineralogical characteristics of the soils in an urban area landslide and evaluating the effects of those characteristics in the instability problems and severe volume changes that are observed. Analysing and understanding the effects of moisture and suction changes in the microfabric and the related effects in the macro-structural behaviour. Proposing remedial actions to reduce the magnitude and rates of the instabilities.

Study area: Mountain area of Barranquilla City, located in the North part of Colombia, near the Caribbean Sea, covering a study area of about 60,000 m².

IPL-172 Project

Project Title: Documentation, training, and capacity building for landslides risk management

Country: India

Leader: Surya Parkash

Period: 2011–

Status: ongoing

Main Project Fields: enhancing human and institutional capacity

Objectives: Documenting case studies on catastrophic landslides. Preparing a digital web-based bibliography on landslides. Organizing trainings for enhancing capacity on landslides risk management. Establishing mechanism for collection, compilation, and analysis of landslides database. Disseminating information/knowledge/experience to end users.

Study area: Mainly implemented in different parts of India but may be extended for adjoining countries like Bhutan and Nepal.

IPL-173 Project

Project Title: Croatian Virtual Landslide Data Center (CiViLdc)

Country: Croatia

Leader: Snježana Mihalić Arbanas

Period: 2011–

Status: ongoing

Main Project Fields: collating and disseminating information/knowledge

Objectives: Introducing systematic collection of data about landslides in Croatia in the form of a database aimed at dissemination of information to wider society, primarily to public and governmental entities. Specific objectives are as follows: a) Development of a web-based landslide database; b) Collection of data about past and present landslides in Croatia;

and c) Organization of presentations of Croatian virtual data center to governmental entities so as public offering.

Study area: All of Croatia.

IPL-175 Project

Project Title: Development of landslide risk assessment technology and education in Vietnam and other areas in the Greater Mekong Sub-region

Country: Japan, Viet Nam

Leader: Kyoji Sassa, Doan Minh Tam

Period: 2012–

Status: ongoing

Main Project Fields: hazard mapping, vulnerability, and risk assessment

Objectives: Contributing to landslide disaster reduction along main transport arteries and on residential areas through study on effective application of new technology on forecast, monitoring, and treatment of landslides in Vietnam and other areas in the Greater Mekong Sub-region in close cooperation with Japanese universities and also ICL. The following targets are expected: a) Development of landslide risk assessment technology suitable for the targeted areas in Vietnam; b) Capacity development for research on landslide risk identification and hazard mapping; and c) Social application over the regions.

Study area: Vietnam, Japan, countries in the Greater Mekong Sub-region (e.g. Laos and Myanmar).

IPL-176 Project

Project Title: Slope data acquisition along highways in Sabah State for hazard assessment and mapping

Country: Malaysia

Leader: Che Hassandi Abdullah

Period: 2012–2013

Status: completed

Main Project Fields: monitoring and early warning; hazard mapping, vulnerability, and risk assessment

Objectives: Establishing spatial and non-spatial database for slope assessment and mapping. Producing hazard and risk mapping. Providing a “decision support system” for slope maintenance programme. Identifying potential problematic area.

Study area: The approved man-made slopes situated along the selected 22 Federal routes in the State of Sabah, Malaysia.

IPL-177 Project

Project Title: Study on geological disasters focusing on landslides in and around Tegucigalpa City, Honduras

Country: Honduras

Leader: Aníbal Godoy

Period: 2012–2013

Status: completed

Main Project Fields: enhancing human and institutional capacities

Objectives: Capacity building on landslide inventory and hazard mapping in and around the Tegucigalpa City, supported and cooperated by JICA Experts. The outline of the project is as follows: a) constructing landslide database on landslide in and around Tegucigalpa, capital city of Honduras; b) landslide interpretation using stereo viewer at workshop associated with field researching; c) guidance for judgment of danger of landslides for making hazard mapping using AHP methodology; and d) description and total evaluation on landslides and related factors (natural and social) using GIS technology.

Study area: UPI and Tegucigalpa city and surroundings, Honduras.

IPL-179 Project**Project Title:** Database of glacial lake outburst floods (GLOFs)**Country:** Czech Republic**Leader:** Adam Emmer, Vit Vilímek**Period:** 2012–**Status:** ongoing**Main Project Fields:** vulnerability and risk assessment; collating and disseminating information/knowledge**Objectives:** Creating broadly available overview of GLOFs and providing basic information about them. This database can show some regional differences as well. Understanding them can help us to create an optimal regional method of GLOF hazard assessment.**Study area:** Online database including information about GLOFs appearing all over the world in the past 150 years. Verification of methods and field experiences in the mountain range of Cordillera Blanca (Peru).**IPL-180 Project****Project Title:** Introducing community-based early warning system for landslide hazard management in Cox's Bazaar Municipality, Bangladesh**Country:** Thailand**Leader:** N.M.S.I. Arambepola**Period:** 2011–2012**Status:** completed**Main Project Fields:** monitoring and early warning; landslide hazard and risk management in urban areas; enhancing human and institutional capacities**Objectives:** Facilitating the preparation of landslide inventory and landslide hazard zonation maps for the city. Development of precipitation thresholds. Establishment of community level early warning system. Creating community awareness on landslide preparedness and mitigation measures.**Study area:** The Municipality of Cox's Bazaar covers an area of 21 km². It is located between 21024' and 21036' north latitudes and between 91059' and 92008' east longitudes. It is bounded by Chittagong district on the north, Bay of Bengal on the south, Bandarban district, Arakan (Myanmar), and the Naf River on the east, and the Bay of Bengal on the west. According to the population census 2001, the total population of Cox's Bazaar Municipality is 51918.**IPL-181 Project****Project Title:** Study of slow moving landslide Umka near Belgrade, Serbia**Country:** Serbia**Leader:** Biljana Abolmasov**Period:** 2012–**Status:** ongoing**Main Project Fields:** monitoring and early warning**Objectives:** Continual monitoring of the proposed case study area by combining different monitoring techniques. Aiding decision-making and mitigation measures design for this particular case study.**Study area:** The study area is located at the right bank of Sava River, on the meandering apex, crossing the landslide Umka, near the City of Belgrade, Serbia.

IPL-182 Project

Project Title: Characterization of landslides mechanisms and impacts as a tool to fast risk analysis of landslides related disasters in Brazil

Country: Brazil

Leader: Renato Eugenio de Lima

Period: 2012–

Status: ongoing

Main Project Fields: hazard mapping, vulnerability, and risk assessment; landslide hazard risk management in urban areas; preparedness.

Objectives: To study the Brazilian disasters related to landslides. Mapping the distribution of types of mass movements all around Brazil. Classifying the most destructive landslides in Brazil. Offering scientific knowledge to facilitate the preparation and response of landslide disasters. Developing and improving methodologies for rapid landslide analysis useful in disasters.

Study area: The project aims to evaluate all the most prone landslide areas in Brazil and is planned to develop detailed studies in the States of Paraná, Rio de Janeiro, and Santa Catarina.

IPL-183 Project

Project Title: Landslides in West Africa: impacts, mechanism, and management

Country: Nigeria

Leader: Igwe Ogbonnaya

Period: 2012–

Status: ongoing

Main Project Fields: monitoring and early warning; hazard mapping, vulnerability, and risk assessment; landslide hazard and risk management in urban areas; enhancing human and institutional capacities; preparedness

Objectives: Studying the impacts and mechanisms of West African landslides in West Africa. Mapping the distribution and types of mass movements all around the sub-region. Developing a landslide inventory using aerial photograph interpretation, satellite data, and fieldwork, including historical data surveying and analyses. Classifying catastrophic landslides in West Africa. Promoting research and education geared towards facilitating the preparedness and response to landslide events. Improving and installing early warning systems at vulnerable locations in the region.

Study area: Region of West Africa.

IPL-184 Project

Project Title: Study of landslides in flysch deposits of North Istria, Croatia: sliding mechanisms, geotechnical properties, landslide modeling, and landslide susceptibility

Country: Croatia

Leader: Željko Arbanas

Period: 2012–

Status: ongoing

Main Project Fields: hazard mapping, vulnerability, and risk assessment; collating and disseminating information/knowledge; preparedness; mitigation

Objectives: Study of triggering factors and landslides mechanisms of instabilities in flysch formations in North Istria, Croatia. Laboratory analyses of soil materials from flysch deposits using ring shear apparatus. Modelling of typical instabilities in flysch deposits: back analyses. Identification of conditions that caused landslides in flysch deposits. Recommendations for landslides susceptibility and hazard mapping in flysch areas.

Study area: Flysch Paleogene Basin in the North part of the Istria Peninsula, Croatia.

IPL-185 Project

Project Title: Landslide hazards assessment and modeling sediment yield of landslides using Geographic Information System (GIS): A case study in the Río El Estado on the SW flank of Pico de Orizaba volcano, Puebla-Veracruz, Mexico

Country: Mexico

Leader: Gabriel Legorreta Paulín

Period: 2013–

Status: ongoing

Main Project Fields: hazard mapping, vulnerability, and risk assessment

Objectives: Preparing a landslide inventory map for the study area in GIS. Preparing a hazard map for the study area in GIS. Estimating the potential total material delivered to the main stream drainage channel by all landslides in the catchment.

Study area: Río El Estado watershed at Pico de Orizaba volcano, México.

IPL-186 Project

Project Title: Rock-fall hazard assessment and monitoring in the archaeological site of Petra, Jordan

Country: Italy

Leader: Claudio Margottini

Period: 2013–

Status: ongoing

Main Project Fields: monitoring and early warning; hazard mapping; landslides threatening heritage sites; enhancing human and institutional capacities; preparedness; mitigation

Objectives: Identifying potential detectable unstable areas in the Siq and other sites by means of field engineering geological techniques. Carrying out long-term monitoring of selected unstable Siq slope portions, by means of a set of monitoring methods (from remote to field) to define the most suitable and reliable techniques for different geomorphological settings. Providing guidelines for sustainable landslide mitigation and management for the entire park. Improving knowledge of local authorities for the identification of unstable areas, monitoring of the site, and design and implementation, following international standards, of landslide mitigation works/strategies (e.g. monitoring, field analysis).

Study area: Archaeological Park of Petra, Jordan.

IPL-187 Project

Project Title: Design and validation of an early warning system for landslides—DeVEL

Country: Germany

Leader: Rolf Katzenbach

Period: 2013–

Status: ongoing

Main Project Fields: monitoring and early warning; catastrophic landslides; enhancing human and institutional capacities; collating and disseminating information/knowledge; preparedness

Objectives: Designing and validating an early warning system which can give information on the risk of expectable landslides, especially in areas of former mining activities. To achieve a reliable early warning system (EWS), sensor and observation technology has to be connected with the modelling of the processes which occur during landslides and immediately prior to them.

Study area: Germany, Switzerland.

IPL-188 Project

Project Title: Study of slow moving landslide Potoška planina (Karavanke Mountain, NW Slovenia)

Country: Slovenia

Leader: Marko Komac

Period: 2013–

Status: ongoing

Main Project Fields: monitoring and early warning; catastrophic landslides; collating and disseminating information/knowledge; preparedness; mitigation; recovery

Objectives: Continual monitoring of the site Potoška planina where GPS and radar interferometry (PSI) measurements are already installed; combining these with different in situ monitoring techniques. Improving our understanding of the causes of ground failure and assessing the dynamics of the landslide for the purpose of mitigation measures design.

Study area: The landslide at Potoška Mt. (~1300 m a.s.l, NW Slovenia), located above settlement Koroška Bela with approximately 2,000 inhabitants, public infrastructure, and heavy (steel) industry.

Overview of the World Centres of Excellence on Landslide Risk Reduction 2011–2014

Objectives of WCoE are threefold, i.e. to:

- Strengthen the International Programme on Landslides (IPL) and the IPL Global Promotion Committee (IPL-GPC);
- Create “A Global Network of entities contributing to landslide risk reduction”; and
- Improve the global recognition of “Landslide Risk Reduction” and its social-economic relevance, and entities contributing to this field.

The WCoE candidates are Governmental and non-governmental entities such as universities, agencies, and other institutions, and their subsidiary entities (faculties, departments, centres, divisions, or others) which meet the following two conditions:

- Contributing to “Risk Reduction for Landslides and Related Earth System Disasters”;
- Willing to support IPL intellectually, practically, and financially by either joining ICL or contributing to IPL-GPC and promote “landslide research and risk reduction” on a regional and/or global scale in a mutually beneficial manner.

The application of World Centre of Excellence in Landslide Risk Reduction for the period 2011–2014 was called on December 3, 2010. The received applications were evaluated by the before-mentioned objectives and criteria and furthermore identified through the following steps of screenings: eligibility examination by ICL Secretariat; technical evaluation by the IPL Evaluation Committee; and evaluation from wider scope and endorsement by the Independent Panel of Experts consisting of five members from UNESCO, UNU, ICSU, a Landslide expert, and a Disaster Reduction expert. Finally, the recommended 15 candidates for the World Centre of Excellence (WCoE) in Landslide Risk Reduction 2011–2014 were reported and approved by the IPL-Global Promotion Committee at its 6th Session, and inaugurated on the opening ceremony of the Second World Landslide Forum held in Rome on October 3, 2011.

During the period between the two World Landslide Forums (WLF2 in Rome 2011 and WLF3 in Beijing 2014) altogether 15 WCoEs were active (Table 2). The countries having an active WCoE are shown in Fig. 1. It follows a short presentation of each of the WCoE 2011–2014 in an alphabetical order of WCoE’s country.

Table 2 An alphabetical overview of the 15 World Centres of Excellence, inaugurated at the World Landslide Forum 2 in Rome in October 2011 for the period 2011–2014

Nr.	WCoE title	WCoE leader	Country	Institution
1.	Canadian Landslide Loss Risk Reduction Strategy and Implementation	Peter Bobrowsky	Canada	Geological Survey of Canada, Earth Sciences Sector, Natural Resources Canada, Ottawa, Ontario
2.	Risk Assessment and Disaster Mitigation Code for Long Run-out Landslides	Yueping Yin	China	China Geological Survey (CGS), Beijing
3.	Scientific research for landslide risk analysis and international education for mitigation and preparedness	Vit Vilímek	Czech Republic	Faculty of Science, Charles University, Prague
4.	Training, Research and Documentation on Landslides Risk Management	Surya Parkash	India	National Institute of Disaster Management (NIDM), New Delhi
5.	Development of Community-based and Most Adaptive Technology for Landslide Risk Reduction	Dwikorita Karnawati	Indonesia	Universitas Gadjah Mada, Yogyakarta
6.	Research on landslide risk management harmonisation in support to European Union policy making	Javier Hervás	Italy	Institute for Environment and Sustainability, Joint Research Centre (JCR), European Commission, Ispra
7.	Advanced Technologies for Landslides	Nicola Casagli, Filippo Catani	Italy	Department of Earth Science, University of Florence, Florence
8.	Development of a methodology for risk reduction of earthquake-induced landslides	Keizo Ugai	Japan	The Japan Landslide Society (JLS), Tokyo
9.	Risk identification and land-use planning for disaster mitigation of landslides	Hideaki Marui	Japan	Research Institute for Natural Hazards and Disaster Recovery, Niigata University, Niigata
10.	Landslide monitoring and community based early warning systems	Irasema Alcántara-Ayala	Mexico	National Autonomous University of Mexico (UNAM), Mexico
11.	Research on mitigation of landslide risk and training of specialists	Farrokh Nadim	Norway	International Centre for Geohazards (ICG), Oslo
12.	Annual Summer School on Rockslides and Related Phenomena in Kyrgyzstan	Alexander Strom	Russia and Kyrgyz Republic	Institute of Geosphere Dynamics (IGD) of Russian Academy of Sciences (RAS), Moscow and Institute of Seismology, National Academy of Sciences, Bishkek
13.	Mechanisms of landslides in over-consolidated clays and flysch	Bojan Majes, Ana Petkovšek	Slovenia	Faculty of Civil and Geodetic Engineering, University of Ljubljana (UL FGG), Ljubljana
14.	Promoting knowledge, innovations and institutions with South–South focus through a regional network of Landslide Risk Reduction	N.S.M.I. Arambepola	Thailand	Asian Disaster Preparedness Center (ADCP), Bangkok
15.	Scientific Research for Landslide Hazard Analysis	Peter Lyttle	USA	U.S. Geological Survey Landslide Programme, Reston, Virginia

1. WCoE “Canadian Landslide Loss Risk Reduction Strategy and implementation”

Country: Canada

Institution: Geological Survey of Canada, Earth Sciences Sector, Natural Resources Canada, Ottawa, Ontario

Leader: Peter Bobrowsky

Activity scale/targeted region: National/Canada.

Objectives: The Geological Survey of Canada is coordinating a multi-partner effort to publish a series of technical best practice guidelines for engineers, geologists, geotechnical experts, and other professionals dealing with mitigating the impact of landslide hazards in Canada. A companion non-technical landslide guideline for the Canadian public and other non-professionals is also being produced. Aims are to reduce landslide losses.

2. WCoE “Risk Assessment and Disaster Mitigation Code for Long Run-out Landslides”

Country: China

Institution: China Geological Survey (CGS), Beijing

Leader: Yueping Yin

Activity scale/targeted region: National/China and Regional/Southeast Asia and East Asia.

Objectives: Starting research on Risk Management of Long Run-out Landslides. Developing a visualized real-time monitoring system. Developing a method for estimation of run-out distances under China conditions. Finishing the Risk assessment guidebook for long run-out landslides. Mending the landslide risk mitigation code. Sharing experiences with some East and Southeast Asia countries.

3. WCoE “Scientific research for landslide risk analysis and international education for mitigation and preparedness”

Country: Czech Republic

Institution: Faculty of Science, Charles University, Prague

Leader: Vit Vilímek

Activity scale/targeted region: Global/Target regions: Intercontinental (South America, Africa, Europe), Regional (Central Andes, East African Rift, Central Europe), and National (various localities in Bohemian Massif and Western Carpathians).

Objectives: Strengthening the International Programme on Landslides (IPL) through landslide process analysis with regard to landscape evolution; evaluation of mass movements in overall hazard and risk assessment in connection with environmental changes (including climatic ones). Creating a network among entities contributing to landslide risk reduction (South America, Africa, and Europe). Establishing the bottom-up local Disaster Management Units in those regions.

4. WCoE “Training, research and documentation on landslides risk management”

Country: India

Institution: National Institute of Disaster Management (NIDM), New Delhi

Leader: Surya Parkash

Activity scale/targeted region: National and Regional.

Objectives: Training on landslide hazard zonation mapping, risk assessment, development of early warning system for landslides, and preventive and remedial measures for landslides risk reduction. Networking, linkage, and coordination of organizations, individuals, and resources for mainstreaming landslide risk management. Integrating landslide risk management with focus on multi-hazard perspective, developmental process, public safety, and protection/conservation of resources and environment. Research on community-based landslides risk management and development of suitable guidelines for landslides management at community level. Documentation of good and bad practices with respect to landslides management in hills.

5. WCoE “Development of community-based and most adaptive technology for landslide risk reduction”

Country: Indonesia

Institution: Universitas Gadjah Mada, Yogyakarta

Leader: Dwikorita Karnawati

Activity scale/targeted region: Intercontinental, Regional, and Local.

Objectives: Community empowerment with respect to community-based disaster risk reduction in landslide vulnerable area by integrating technical and social networks of landslide early warning system. Implementation of student community service programme to support community-based landslide disaster risk reduction.

6. WCoE “Research on landslide risk management harmonisation in support to European Union policy making”

Country: Italy

Institution: Institute for Environment and Sustainability, Joint Research Centre (JRC), European Commission, Ispra

Leader: Javier Hervás

Activity scale/targeted region: Continental/Europe.

Objectives: The main objective is to develop guidelines, procedures, and models for the generation of harmonized landslide databases and susceptibility and hazard zonation maps in support to European Union (EU) policymaking, including legislation and policy actions. In order to meet these objectives we will continue our current research on these topics in collaboration with the European Landslide Expert Group members, and Geological Surveys, research institutes, and universities in Europe.

7. WCoE “Advanced technologies for landslides”

Country: Italy

Institution: Department of Earth Science, University of Florence, Florence

Leader: Nicola Casagli, Filippo Catani

Activity scale and targeted region: Global.

Objectives: Further developing advanced technologies with special emphasis on remote sensing for the assessment and mitigation of landslide risk. In particular the project will focus on the development of Earth Observation (EO) methods useful for applications on landslides such as a) remote sensing technologies for landslide detection, monitoring and rapid mapping; b) coupling of short-term weather forecasting with geotechnical modelling for shallow landslide prediction; and c) evaluation and development of reliable procedures and technologies for early warning.

8. WCoE “Development of a methodology for risk reduction of earthquake-induced landslides”

Country: Japan

Institution: The Japan Landslide Society (JLS), Tokyo

Leader: Keizo Ugai

Activity scale and targeted region: National/Japan and Regional.

Objectives: Clarifying the mechanism of the earthquake-induced landslides on the basis of investigating types, dimensions, distributions, and run-out distances of the landslides and analysing relations to the seismicity and geology. Making up appropriate technical guidelines including a methodology for risk reduction of the earthquake-induced landslides, applied to high-risk areas in the world.

9. WCoE “Risk identification and land-use planning for disaster mitigation of landslides”

Country: Japan

Institution: Research Institute for Natural Hazards and Disaster Recovery, Niigata University, Niigata

Leader: Hideaki Marui

Activity scale/targeted region: Global and Intercontinental.

Objectives: Developing land-use planning methodology in order to reduce landslide disasters through the basic scientific study of mechanism as well as risk identification on landslide occurrence and the practical study of land-use planning. Appropriate landslide hazard maps and land-use guidelines will be formulated for the targeting regions and countries.

10. WCoE “Landslide monitoring and community based early warning systems”

Country: Mexico

Institution: National Autonomous University of Mexico (UNAM), Mexico City

Leader: Irasema Alcántara-Ayala

Activity scale and targeted region: National/Mexico.

Objectives: Evaluating the impact of landsliding in Mexico. Instrumentation and monitoring of a hillside in a vulnerable community, situated in the province of Puebla (Teziutlán municipality), which has been severely damaged by landslides in the last years. Developing a community-based warning system for Teziutlán that can be used for other areas affected by landslides.

11. WCoE “Research on mitigation of landslide risk and training of specialists”

Country: Norway

Institution: International Centre for Geohazards (ICG) at Norwegian Geotechnical Institute (NGI), Oslo

Leader: Farrokh Nadim

Activity scale and targeted region: Global.

Objectives: Develop appropriate methods for the assessment of landslide hazards and risk and web-based tools for the evaluation of the impact of major landslides. Develop methodologies to assist decision makers in dealing with landslide risk management. Coordinate an EU project related to effects of global change on landslide risk in Europe and adaptation strategies. Education and training of international postgraduate students and specialists.

12. WCoE “Annual Summer School on Rockslides and Related Phenomena in Kyrgyzstan”

Country: Russia and Kyrgyz Republic

Institution: Institute of Geosphere Dynamics (IGD) of Russian Academy of Sciences (RAS), Moscow, and Institute of Seismology, National Academy of Sciences, Bishkek

Leader: Alexander Strom

Activity scale/targeted region: Global.

Objectives: Organization of annual training course for students and young landslide researchers, focused on the morphologies of large-scale bedrock landslides and rock avalanches and on the internal structure of their deposits.

13. WCoE “Mechanisms of landslides in over-consolidated clays and flysch”

Country: Slovenia

Institution: Faculty of Civil and Geodetic Engineering, University of Ljubljana, Ljubljana (UL FGG)

Leader: Bojan Majes, Ana Petkovšek

Activity scale and targeted region: National/Slovenia.

Objectives: Determining the role of suction and viscosity in flysch landslide dynamics. Using detailed field monitoring data on weathering factors, and field and laboratory data on soil characteristics (water content, suction, viscosity at different shear rate), new functional relationship between water content, shear stress, and suction for flysch landslides will be developed.

14. WCoE “Promoting knowledge, innovations and institutions with South-South focus through a regional network of Landslide Risk Reduction”

Country: Thailand

Institution: Asian Disaster Preparedness Center (ADCP), Bangkok

Leader: N.S.M.I. Arambepola

Activity scale and targeted region: Regional/Asia.

Objectives: Promoting good practices for early warning for landslide prone areas in a changing climate scenario to save lives and property. Specific objectives are a) promoting the concept of landslide monitoring and early warning in countries in Asia through the activities of the network; b) presenting methodologies pertaining to establishing precipitation threshold values for landslides in different geological materials through pilot initiatives in partner countries; c) providing inputs to local and regional multi-hazard platforms for early warning; d) facilitating a dialogue among landslide risk reduction practitioners,

policymakers, academia, and disaster management community through organization of networking events for enhancement of knowledge on Landslide Risk Reduction among all existing network partners (around 16 different universities, research institutions, and government agencies in Southeast and South Asia); and e) supporting learning opportunities for partners in higher education.

15. WCoE “Scientific Research for Landslide Hazard Analysis”

Country: USA

Institution: U.S. Geological Survey Landslide Programme, Reston, Virginia

Leader: Peter Lyttle

Activity scale and targeted region: Global and Intercontinental.

Objectives: Performing analysis and development of landslide, rock-fall, and debris-flow models and real events, using rainfall thresholds, real-time monitoring, field analysis for the United States, and in cooperation with other nations. Multi Hazards Demonstration Project (MHDP) for California, USA, using landslide science to improve resilience of communities to natural disasters including earthquakes, tsunamis, wildfires, landslides, floods, and coastal erosion. Hazard assessments, susceptibility, and warning for Post-wildfire Debris Flow Hazards in the United States. Cooperating for emergency response and analysis of earthquake-induced landslides, which have included Haiti, China, Pakistan, and others, and which will be continued in the future as needed.

Acknowledgments

The first author would like to thank members of the IPL Evaluation Committee for their valuable assessment of the submitted IPL proposals and the WCoE proposals in the past period, especially to (in alphabetical order): Željko Arbanas, Irasema Alcántara-Ayala, Peter Bobrowsky, Wolfgang Eder, Teuku Faisal Fathani, Hiroshi Fukuoka, Dwikorita Karnawati, Hideaki Marui, Alexander Strom, Vit Vilímek, Jan Vlcko, and Fawu Wang. Both authors would like to thank for the technical support to the ICL Secretariat in Kyoto and especially to Kyoji Sassa, ICL Executive Director.

References

- Casagli N, Falorni G, Tofani V (2009) Projects of international programme on landslides. In: Sassa K, Canuti P (eds) *Landslides—disaster risk reduction*. Springer, Berlin, pp 15–28. ISBN 978-3-540-69966-8
- Mikoš M (2011) *Landslides*: a state-of-the art on the current position in the landslide research community. *Landslides* 8(4):541–551
- Sassa K (2012) ICL strategic plan 2012–2021—to create a safer geo-environment. *Landslides* 9(2):155–164
- Sassa K, Canuti P, Yin YP (2014) Landslide science for a safer geoenvironment. In: Sassa K (ed) *Proceedings of the third world landslide forum*. Springer, Berlin, pp 1–11 (this volume)
- Sassa K, Tsuchiya S, Ugai K, Wakai A, Uchimura T, (2009) Landslides: a review of achievement in the first 5 years (2004–2009). *Landslides* 6(4): 275–286

Part I

Plenary Lectures



Plenary: Progress of Living with Landslide Risk in Europe

Farrokh Nadim, Bjørn Kalsnes, and Anders Solheim

Abstract

The need to protect people and property with a changing pattern of landslide hazard and risk caused by climate change and changes in demography, and the reality for societies in Europe to live with the risk associated with natural hazards, were the motives for the research project “SafeLand” on landslide risk in Europe.

One of the main aims of the SafeLand project was to produce practical tools and guidelines for stakeholders and end-users of various backgrounds. These products are a mixture of state-of-the-art practices and the results of new and innovative research. The main achievements and products of SafeLand were:

- Various guidelines related to landslide triggering processes and run-out modelling.
- Development and testing of several empirical methods for predicting the characteristics of threshold rainfall events for triggering of precipitation-induced landslides, and development of an empirical model for assessing the changes in landslide frequency (hazard) as a function of changes in the demography and population density.
- Guidelines for landslide susceptibility, hazard and risk assessment and zoning.
- New methodologies for physical and societal vulnerability assessment for different categories of elements at risk.
- Identification of landslide hazard and risk hotspots for Europe.
- Different regional and local climate model simulations over selected regions of Europe at spatial resolutions of 10×10 km and 3.8×3.8 km.
- Guidelines for use of remote sensing techniques, monitoring and early warning systems.
- Development of a prototype web-based “toolbox” of innovative and technically appropriate prevention and mitigation measures.
- Case histories of well-documented landslides.

F. Nadim (✉)

International Centre for Geohazards, Norwegian Geotechnical Institute, P.O. Box 3930 Ullevaal Stadion, 0806 Oslo, Norway
e-mail: farrokh.nadim@ngi.no

B. Kalsnes

Soil Slides and Georisk, Norwegian Geotechnical Institute, P.O. Box 3930 Ullevaal Stadion, 0806 Oslo, Norway
e-mail: bjorn.kalsnes@ngi.no

A. Solheim

Natural Hazards, Norwegian Geotechnical Institute, P.O. Box 3930 Ullevaal Stadion, 0806 Oslo, Norway
e-mail: anders.solheim@ngi.no

- Research on stakeholder workshops and participatory processes to involve the population exposed to landslide risk in the decision-making process for choosing the most appropriate risk mitigation measure(s).
- Estimates of changes in landslide hazard and spatial distribution of population at risk in Europe due to climate change, changes in land use, and demographic changes in the twenty-first century.

The results of the SafeLand project have provided educators, researchers, stakeholders and authorities with state-of-the-art knowledge and improved access to a landslide risk management system for increased safety and cost-effectiveness. The SafeLand project deliverables are expected to help provide the basis for future European directives in relation to natural hazards. All the deliverables of the SafeLand project can be downloaded from the project web site <http://safeland-fp7.eu>

Keywords

Landslide • Risk management • Early warning systems • Stakeholder participatory processes

Background

Because of climate change and the changes in demography, land use, exposure and vulnerability, the spatial pattern of landslide risk in Europe is gradually changing. The effects of global change on the evolution of landslide risk are schematically shown on Fig. 1.

The changing pattern of landslide hazard and risk requires a proactive risk management strategy. In areas with high population density, protection works often cannot be built because of economic or environmental constraints, and it is not always possible to evacuate people because of societal reasons. There are many initiatives at national and local level in various European countries to improve landslide risk management. This paper focuses on a recent multi-national European project named “SafeLand” that addressed these issues. The changing pattern of landslide hazard and risk, the need to protect people and property, the expected climate change, the reality for society in Europe to live with hazard and risk and the need to manage risk were the reasons for initiating the project “SafeLand: Living with landslide risk in Europe: Assessment, effects of global change, and risk management strategies”.

SafeLand was a large, integrating research project with total budget of 8.75 million Euros under the European Commission’s 7th Framework Programme (FP7). It was coordinated by the International Centre for Geohazards (ICG) at Norwegian Geotechnical Institute (NGI), involved 27 partners from 12 European countries, and had international collaborators and advisers from China, India, USA, Japan and Hong Kong. SafeLand also had 25 End-Users from 11 countries. The European partners in SafeLand are listed in Table 1. In addition to the partners listed in Table 1, SafeLand had an International Advisory Board comprised of Dr. Peter Lytle from USGS, Professor Hideaki Marui from

Niigata University in Japan and Dr. H.N. Wong, of Geotechnical Engineering Office of Hong Kong.

The SafeLand project had three main objectives (1) To provide policy-makers, public administrators, researchers, scientists, educators and other stakeholders with improved harmonized framework and methodology for the assessment and quantification of landslide risk in Europe’s regions; (2) To evaluate the changes in risk pattern caused by climate change, human activity and policy changes; and (3) To provide guidelines for choosing the most appropriate risk management strategies, including risk mitigation and prevention measures. To achieve these objectives and address the multitude of challenges in landslide risk assessment and management, six research areas with specific objectives were defined in SafeLand:

1. Landslide triggers and run-out
2. Quantitative risk assessment
3. Global change scenarios
4. Monitoring technology
5. Risk management
6. Database of landslide case studies

The work done in these research areas are described in the project deliverables that can be downloaded from the project web site <http://safeland-fp7.eu>

Policy Context of the SafeLand Project

The SafeLand project responded to a number of European and international policies. In Europe, SafeLand supported the EU Thematic Strategy for Soil Protection (Commission of the European Communities 2006a) and the associated Proposal for a Soil Framework Directive (Commission of the European Communities 2006b). The EU Thematic

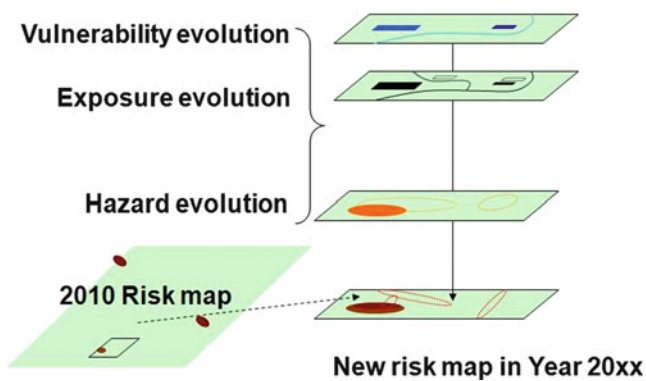


Fig. 1 Schematic diagram: Evolution of landslide risk caused by changes in vulnerability, frequency of landslides (hazard) and exposure of elements at risk

Strategy considers landslides as one of the main soil threats in Europe, and prompts for identification of areas at risk to landslides in EU Member States using common methodologies, as well as for risk reduction measures. On the other hand, according to the Commission's Communication entitled "A community approach on the prevention of natural and man-made disasters" (Commission of the European Communities 2009), a better understanding of disasters such as landslides is prerequisite for developing efficient prevention measures. This requires e.g. inventories of information on disasters and developing of guidelines on hazard and risk mapping. These are important objectives of the SafeLand project. The communication further states that outcomes of the Seventh Framework Programme for Research and Technological Development should be directly implemented in European prevention approaches.

At the global level, SafeLand supported the UN International Strategy for Disaster Reduction (UNISDR). UNISDR aims at building disaster resilient communities by promoting increased awareness of the importance of disaster reduction as an integral component of sustainable development, with the goal of reducing human, social, economic and environmental losses due to natural hazards and related technological and environmental disasters. These disaster reduction efforts are guided by "The Hyogo Framework for Action (HFA) 2005–2015: Building the resilience of Nations and Communities to Disasters", to which 168 governments agreed in Hyogo, Kobe, Japan. The plan encourages local authorities to identify landslide risk and vulnerabilities, establish hazard maps and put in place effective monitoring systems. It also recommends implementing protective engineering works, urban planning strategies, environmental management and community preparedness. The landslide hazard and exposure mapping procedures developed in SafeLand have already been applied in UNISDR's Global assessment reports on disaster risk reduction in 2011 and 2013 to assess the landslide risk in Indonesia and El Salvador, respectively.

Table 1 List of organisations in the SafeLand consortium

No.	Partner name	Country
1.	International Centre for Geohazards	Norway
2.	Universitat Politècnica de Catalunya	Spain
3.	A.M.R.A. s.c.a.r.l.	Italy
4.	Bureau de recherches géologiques et minières	France
5.	Università degli Studi di Firenze	Italy
6.	International Institute for Applied Systems Analysis	Austria
7.	Joint Research Centre	Italy
8.	Fundación Agustín de Betancourt	Spain
9.	Aristotle University of Thessaloniki	Greece
10.	Università degli Studi di Milano—Bicocca	Italy
11.	Max-Planck-Gesellschaft zur Förderung der Wissenschaften e.V.	Germany
12.	Centro Euro-Mediterraneo per i Cambiamenti Climatici s.c.a.r.l.	Italy
13.	Studio Geotecnico Italiano S.r.l.	Italy
14.	University of Salerno	Italy
15.	International Institute for Geo-information Science and Earth Observation—United Nations University (ITC-UNU)	Netherlands
16.	Eidgenössische Technische Hochschule Zurich	Switzerland
17.	Université de Lausanne	Switzerland
18.	C.S.G. S.r.l. Centro Servizi di Geoingegneria	Italy
19.	Centre National de la Recherche Scientifique	France
20.	King's College London	United Kingdom
21.	Geologische Bundesanstalt (Geological Survey of Austria)	Austria
22.	Ecole Polytechnique Fédérale de Lausanne	Switzerland
23.	TRL Limited	UK
24.	Geological Institute of Romania	Romania
25.	Geological Survey of Slovenia	Slovenia
26.	Risques & Développement	France
27.	Central Recherche S.A.	France

IIT-Roorkee (India) and Chengdu University of Technology (China) participated as subcontractors to, respectively, ICG and ITC-UNU

Reducing loss of life and property from natural and human-induced disasters, including landslides, is one of the objectives of GEOSS, the Global Earth Observation System of Systems (2005–2015), currently constructed by the Group on Earth Observations (GEO).

The need for risk management strategies is further acknowledged by the Intergovernmental Panel on Climate Change (IPCC) who predicts an increase of the mean temperature as

well as a change in rainfall patterns in the future, leading to potential increased instability of slopes especially in mountain and permafrost areas. In many global change scenarios, it is expected that more people will be exposed to landslide hazard. Therefore IPCC recently published a special report on “Managing the Risks of Extreme Events and Disasters to Advance Climate Change Adaptation”.

In Europe, there is a general lack of legislative tools to reduce the risk posed by natural hazards, partly because of the risk complexity of the risk governance aspect. A notable exception to this judicial gap is the Floods Directive adopted by the European Commission in 2007. Member states have been asked to do flood risk assessment and develop maps to support flood risk management plans. This only constitutes a first step towards enhanced assessment and mapping methodologies for natural hazard risks, with a second stage planning effort foreseen in 2021.

SafeLand has developed the tools for landslide hazard and risk assessment and mapping at various scales. These tools will be available to end-users and their consultants when such assessment becomes a requirement through a national law or an EC Directive.

Quantification of Landslide Hazard

Overview of Existing Procedures

A first and necessary step towards the harmonization and development of new procedures was the review of the actual official practices at European level, as applied by geological surveys, administration offices and decision makers (hazard and risk assessment procedures, regulations and codes) (Corominas et al. 2012). The compilation of this information is useful for people managing landslide risk, practitioners interested in the currently applied procedures in their country or region, and researchers and scientists investigating the current state of the art. It also serves as a basis for detecting inconsistencies between methodologies and gaps of knowledge before dealing with new procedures and recommendations. The reported countries and territories were Andorra, Austria, France, Italy (selected river basins from southern, central and northern Italy), Norway, Romania, Spain (Catalonia), Switzerland and United Kingdom. The comparison of the various methodologies used in Europe indicated discrepancy in terminology, diversity of criteria for addressing the different landslide mechanisms, lack in considering the effect of hazard amplification due to the spatial superposition of different types of instabilities, as well as of the synergistic action of other natural phenomena (i.e. earthquake) where applicable. Lack of well-established quantitative risk assessment methods for landslides, especially in

comparison with landslide hazard and susceptibility assessment methods, is outlined in SafeLand deliverable D2.1.

For the harmonization of the methodologies and outputs for susceptibility, hazard and risk, some important points are the following: All relevant information and documents should be accessible to the experts and to the public. Digitization of the maps will make them available online, allowing their reproducibility and, more importantly, the possibility of being updated. The methodologies for the assessment of the susceptibility and hazard should be transparent and reproducible. The use of step-by-step analytical or weighted factors techniques, in order to minimize the uncertainties that relate to judgmental approaches and the homogenization of hazard matrices are recommended. So far, there is significant disparity among them, in particular with respect to the hazard parameters, levels and thresholds used. Depending on the mapping scale and given that the quantitative information in probabilistic terms offers an objective insight to hazards and risks, when feasible, it is necessary to work on quantitative methodologies in order to minimize the uncertainties that derive from expert judgments and qualitative considerations.

Triggering of Precipitation-Induced Landslides and Their Run-Out

As mentioned earlier, one of the main goal of SafeLand was to assess the impact of climate change on landslide hazard in Europe. To achieve this goal, considerable work was done on developing models for the prediction of precipitation-induced landslides. Part of this research focused on the statistical and empirical models for triggering of landslides, an essential input for most landslide early warning systems. The empirical models developed in SafeLand built on the datasets collected in the following sites: Barcelonnette in France; La Frasse in Switzerland; Satriano, Verzino and Sarno in Italy; and south-eastern and western regions of Norway. The results showed that the initial moisture conditions, essentially governed by precedent precipitations, must be accounted for the evaluation of the triggering conditions. In many cases, the contribution of snow melt can be significant. Hydraulic conductivity and thickness of soil covers can have a strong influence on the features of triggering weather events. The thresholds for landslide triggering are affected by long-term precipitations in areas that are covered by deep deposits of fine-grained soils, while they are controlled by short-term precipitations in areas with shallower deposits of coarse-grained soils. Concerning thresholds of landslides in rocks, freeze-thaw effects should be accurately taken into account.

Another part of SafeLand research examined the landslide run-out models that are suitable for hazard assessment.

A correct evaluation of the hazard zone requires the knowledge of the terrain surface that can be run over by the landslide mass. Another useful output of the run-out models is the velocity of the landslide body, a fundamental parameter for assessing the vulnerability of exposed elements (and consequent risk), and designing structural defence systems. The relevant SafeLand deliverables provide a comprehensive review of both analytical and empirical models, including available software, which could be used to solve the problem; and summarise the available methods for analysis of triggering and run-out with indication of advantages and limits of every one.

Landslides Triggered by Anthropogenic Factors

One of the main objective of SafeLand was to improve our knowledge about the impact of human activities on increasing or decreasing the landslide hazard. Landslides are triggered by both natural and human-induced changes in the environment. Human-induced landslides may result from changes in slope caused by terracing for agriculture, cut-and-fill construction for highways, construction activity, mining operations, rapid draw-down of dams, changes in land cover such as deforestation, and changes in irrigation or surface runoff. For example, Fig. 2 shows the seasonal distribution of large clay slides in Norway during an 80-year period and the proportion that were triggered by human activity.

Development of an innovation empirical model for assessing the changes in landslide frequency (hazard) as a function of changes in the demography and population density was one of the main achievements of SafeLand. This empirical model and illustrative case histories of human-induced landslides are described in SafeLand deliverable D1.6.

Experiences in China and India

To take advantage of similar experiences outside Europe, a workshop was organised in the Chengdu University of Technology in April 2010, with the aim to assess the state of art of landslide hazard and risk assessment in the P.R. of China. For achieving this objective, Chinese experts in landslide hazard and risk assessment were invited to give presentations and write a chapter for a report, which formed one of the SafeLand deliverables. This deliverable was also published as a book in China and included chapters on: Landslide hazards in China: an overview; Landslide inventory mapping in China; Remote sensing applications for landslide research in China; Medium and large scale landslide hazard assessment in China; Methods for local scale hazard assessment; Landslide early warning and monitoring; Earthquake-induced landslides; The case of Wenchuan earthquake.

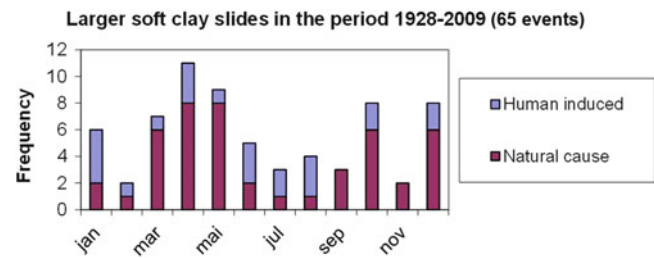


Fig. 2 Seasonal distribution (by month) of large clay slides in Norway during 1928–2009

The researchers in IIT-Roorkee produced a similar report for SafeLand, providing an overview of landslide hazard and risk assessment methodologies in India.

Landslide Databases

Given the importance of the quality of input data for the landslide risk assessment, attention was also drawn to landslide databases. The issues related to these include inventory maps and are linked with alphanumeric information, which allow quantitative landslide hazard and risk assessment on the condition that they contain information on the location of landslide phenomena, typology, history, state of activity, magnitude or size, failure mechanisms, causal factors and the damage caused. The SafeLand studies made a detailed review of existing national landslide databases in Europe together with a number of regional databases. These investigations showed that no national (or regional) landslide database in Europe contains all the information required for doing quantitative risk assessment (QRA). The SafeLand studies proposed improvements for delineating areas at risk in agreement with the EU Soil Thematic Strategy and its associated Proposal for a Soil Framework Directive, and for achieving interoperability and harmonisation in agreement with INSPIRE Directive (as defined in INSPIRE Thematic Working Group Natural Risk Zones, 2011, version 1.9; 29/04/2011), launched by the European Union. This report was based on the analysis of replies to a detailed questionnaire sent out to the competent persons and organisations in each country, and a review of literature, websites and main European legislation on the subject. The relevant conclusions can be found in detail in Safeland deliverable D2.3 and in Van Den Eeckhaut and Hervás (2012). As currently no harmonised landslide databases are available throughout Europe, suggestions for overcoming the variability concerning language, structure, format and accessibility are also given at the same deliverable (with mention to the INSPIRE Directive and the preliminary data specifications of Natural Risk Zones, including landslides, as well as recommendations by the European Landslide Expert Group). Thus, the work performed in SafeLand may serve as

a platform for the construction of databases for the storage of spatial data that are made available and maintained at the most appropriate level. This would make it possible to combine the information from different sources across the Community in a consistent way and share them among several users and applications.

Recommended Practice for Hazard and Risk Zonation

An important part of the work done in SafeLand was providing recommendations for the quantitative assessment of landslide susceptibility, hazard, vulnerability and risk, as well as zoning. Procedures for verification and validation of the results were also recommended. The recommended methodologies mainly focus on approaches for the quantitative assessment and zoning of landslide susceptibility, hazard and risk at different scales, which were summarized from recently published research work. Guidelines on how to proceed from susceptibility to hazard, a topic that is seldom addressed, are provided. Specific methodologies developed during the SafeLand project were incorporated into the guidelines. They mainly consist in new procedures for calculating quantitative vulnerability, based on fragility curves and for different landslide mechanisms (Mavrouli and Corominas 2012; Fotopoulou and Pitilakis 2012; Smith et al. 2012). Furthermore, a selection of the best-suited procedures for verification of the models and validation of the results are presented. The proposed procedures are categorised according to the landslide type and the working scale (site specific, local, regional and national). Particularly important and innovative aspects of the work done in SafeLand was the evaluation of the probability of occurrence of different landslide types with certain characteristics, the specific consideration of the elements at risk (persons, buildings, infrastructures. . .) and their spatio-temporal probability of exposure, which could be directly incorporated in the quantitative risk assessment (QRA) analysis. The respective document (SafeLand deliverable D2.4) is addressed to scientists and practicing engineers, geologists and other landslide experts.

Vulnerability to Landslides

Vulnerability assessment to landslides is a complex process that must consider multiple dimensions and aspects of vulnerability, including both physical and socio-economic factors. Physical vulnerability is a function of the intensity and magnitude of the landslide hazard as well as of the resistance levels of the exposed elements. However, the vulnerability of a society and its resilience are also related to factors such as demography, preparedness levels, memory of past events, and institutional and non-institutional abilities

for handling natural hazards. Physical models are particularly useful for estimating direct impacts (physical damages, consequences) to landslides, while socio-economic models are used (and developed) for indirect and intangible losses, i. e. losses due to medium and long-term effects of the hazard event mainly of social and economic nature. SafeLand research attempted to establish both physical and socio-economic vulnerability models related to landslides.

Regarding physical vulnerability, SafeLand research dealt with the proposition and quantification of efficient methodologies for assessing the physical vulnerability of various elements at risk to different landslide hazards using the concept of probabilistic fragility functions or indexes, and appropriate definition of relevant damage states (SafeLand deliverable D2.5). An attempt to distinguish between different types of landslides and affected assets (buildings, persons and infrastructures) was made. The applicability of the developed methodologies depends on few general parameters such as the landslide type, the typology and classification of the exposed elements, the analysis scale and the triggering mechanism (intense rainfall, earthquake). The main landslide movement types considered were rockfalls, debris flows and slow moving landslides. Four different analysis scales were considered: small (1:100,000), medium (1:25,000), large (1:5,000) and detailed/site-specific (1:2,000), requiring different criteria to identify the elements at risk. Finally, various landslide intensity parameters were considered (e.g. permanent displacement, landslide velocity, volume of the landslide deposit, impact force, kinetic energy, etc.) depending on the landslide type, the element at risk and the scale of analysis. Representative applications of the proposed physical vulnerability assessment models are provided in SafeLand deliverable D2.7. Additionally, the investigation of the physical vulnerability of roadways with respect to the damage caused by debris flows was also carried out. Based on a questionnaire, empirically-based fragility curves were derived, relating flow volume to damage probabilities for three different damage states (Smith et al. 2012).

Regarding social and economic vulnerability, the SafeLand research focused on the development of an indicator-based methodology to assess the social vulnerability levels. The indicators represent the underlying factors which influence a community's ability to deal with, and recover from the damage associated with landslides. The proposed method includes indicators which represent the demographic, economic and social characteristics, as well as indicators representing the degree of preparedness and recovery capacity. The purpose of the indicators is to set priorities, serve as background for action, raise awareness, analyse trends and empower risk management (SafeLand deliverable D2.6). The proposed methodology was tested for six locations in Europe, two in Norway and one each in Greece, Andorra, France and Romania. The purpose of the

case studies was to compare the vulnerability levels and to test and possibly improve the proposed approach (Eidsvåg et al. 2012).

Tools and Guidelines for Landslide Risk Management

One of the main aims of the SafeLand project was to produce practical tools and guidelines for stakeholders and end-users of various backgrounds. These products are a mixture of state-of-the-art practices and the results of new and innovative research. Some of the main products of SafeLand relevant for landslide risk stakeholders and end-users are presented below.

Quantitative Risk Assessment

In Europe, there is a need for developing efficient and reliable tools on which support land use planning decisions, civil protection plans and mitigation measures to manage landslide risk. Either susceptibility maps showing the existing or potential unstable areas or hazard maps that further include the affected areas and the temporal probability of occurrence, or risk maps that additionally incorporate the severity of the consequences may be used to this end. Although the first two map types are the most common so far, latest global tendencies are shifting towards the consideration of credible risk scenarios in which location, nature and evaluation of damages can be fully analysed. Furthermore, zoning schemes tend to use quantified susceptibility, hazard and risk assessments, meaning that qualitative descriptive rankings (i.e. low to high) are replaced by the annual probability (or frequency) of a given event of a given magnitude/intensity and its consequences in numbers (financial, population of the affected exposed elements etc.).

As mentioned earlier, the SafeLand project developed recommendations for landslide susceptibility, hazard and risk assessment and zoning, to be used for the quantitative assessment of the landslide hazard, vulnerability and risk, as well as for the verification and validation of the results (SafeLand Deliverable 2.4: Guidelines for landslide susceptibility, hazard and risk assessment and zoning). The recommended methodologies mainly focus on approaches for the quantitative assessment and zoning of landslide susceptibility, hazard and risk at different scales. The proposed procedures are categorised according to the landslide type and the working scale (site specific, local, regional and national). Particularly important and innovative aspects have been the evaluation of the probability of occurrence of different landslide types with certain characteristics, the specific consideration of the elements at risk (persons, buildings, infrastructures...) and their spatio-temporal

probability in order to be directly incorporated in the quantitative risk assessment (QRA).

For demonstration of the given guidelines, examples of the quantitative risk assessment QRA for different types of landslides, at different scales and for various exposed elements (buildings and people) were done in SafeLand. In every case study, the risk was expressed using a variety of metrics. Different landslide types such as deep-seated landslides, debris slides, hyper-concentrated flow, and rockfalls were studied at scales varying from site-specific to regional. The innovative aspects involved the use of remote sensing data and the incorporation of the vulnerability in quantitative terms. Especially the latter has been rarely considered in other methodologies.

Another important activity in SafeLand was the development of toolboxes (set of precompiled computer routines) that can be used by stakeholders, practitioners and other interested parties for the quantitative evaluation of the key components that are involved into the landslide zoning and risk calculation (hazard, vulnerability of the exposed elements. . .). Three toolboxes were prepared based on deterministic or probabilistic approaches for the quantification of the risk parameters. The tools serve for quantitative vulnerability and risk assessment of buildings and protection galleries exposed to rockfalls.

Standards for validation of both hazard and risk assessment models were proposed for the quantification of the reliability of the assessment (accounting for data vagueness and uncertainties, “limited” knowledge on the physics of the processes and taking into account the issue of the “mapping unit”, independently of the scale), as well as the quantification of the validity of the assessment (considering validation/evaluation of the maps, robustness and accuracy of the predicting systems and output types).

Given that for landslides, QRA procedures are not as well established as for earthquakes and river floods, much of the work in SafeLand was focused on improvement and development of tools for landslide zoning and the provision of a framework for quantitative risk assessment. Within this framework the main activities were realized with reference to: (i) the integration and regionalization of the information (in particular using modern data gathering techniques such as ground-based terrestrial laser scanner, digital photogrammetry, and remote sensing techniques such as DInSAR); (ii) the improvement and development of procedures for quantifying landslide susceptibility, frequency and intensity at different scales and (iii) the improvement and development procedures for QRA at different scales; (iv) validation of QRA schemes and zoning maps; and (v) QRA analysis at hotspots in Europe.

The achievements of activities (i), (ii), (iii) and (v) concerning the use of modern technologies and the development of procedures for the landslide hazard and risk (with emphasis on frequency and intensity assessment) are presented in SafeLand deliverable D2.11. The deliverable

presents examples of QRA for different types of landslides, at different scales and for various exposed elements (buildings and people). For every case-study, the risk is expressed using a variety of risk metrics. Different landslide types such as deep-seated landslides, debris slides, hyper-concentrated flows, and rockfalls are studied at scales varying from site-specific to regional are considered in the case studies. The innovative aspects involve the use of remote sensing data and the incorporation of vulnerability in quantitative terms. Especially the latter has been rarely considered so far by other methodologies.

Another SafeLand contribution to QRA for landslides was the improvement and development of toolboxes (set of precompiled computer routines) that can be used by stakeholders, practitioners and other interested parties for the quantitative evaluation of the key components that are involved into the landslide zoning and risk calculation (hazard, vulnerability of the exposed elements...). Three toolboxes were prepared based on deterministic or probabilistic approaches for the quantification of the risk parameters. The tools serve for (i) rockfall quantitative vulnerability of buildings (ii) rockfall quantitative risk assessment for protection galleries and (iii) rockfall quantitative risk assessment. A presentation of them is given in D2.9.

With respect to the activity (iv), standards for validation of both hazard and risk assessment models are proposed for the quantification of the reliability of the assessment (accounting for data vagueness and uncertainties, “limited” knowledge on the physics of the processes and taking into account the issue of the “mapping unit”, independently of the scale), as well as the quantification of the validity of the assessment (considering validation/evaluation of the maps, robustness and accuracy of the predicting systems and output types). The compilation of the proposed methodologies is presented in SafeLand deliverable D2.8.

Toolbox of Risk Mitigation Measures

SafeLand researchers provided a compendium of tested and innovative structural and non-structural (including insurance) mitigation measures for different landslide types (SafeLand deliverable D5.1: Compendium of tested and innovative structural, non-structural and risk-transfer mitigation measures for different landslide types). This compendium is the basis of a user-friendly web-based toolbox that can help experts and other users identify appropriate technologies for protecting people and property against landslides. The compendium and toolbox are based on a classification of measures depending on whether they reduce the hazard (for example, a retaining wall), reduce vulnerability (for example, strengthening structures) or reduce exposure (for example, relocating homes). Each measure includes a “fact sheet” that describes the measure, gives

guidance on its design, schematic details, practical examples and references. The fact sheets also include a subjective rating of the applicability of the specific mitigation measure in relation to the descriptors used for classifying landslides. The web-based toolbox includes the following features: data management, user forum, help function, report generation function and the ranking of the mitigation measures as they apply to a particular landslide context. The toolbox and the compendium are described in more detail in the “Dissemination” section of this paper.

Stakeholder Involvement and Decision Making Process

Increasingly public interventions to reduce the risk of landslides and other hazards are moving from “expert” decisions to include the public and other stakeholders in the decision process. Indeed, EU legislation, most notably the Water Framework Directive, is requiring public officials to consult stakeholders in the allocation of public funds for risk mitigation. The SafeLand project developed and tested a public communication and participatory process for mitigating the risks of landslide in the highly at-risk community of Nocera Inferiore in southern Italy (SafeLand deliverable D5.7: Design and testing: a risk communication strategy and a deliberative process for choosing a set of mitigation and prevention measures). The pilot study demonstrated the potential and challenges of public participation in decisions characterized by high personal stakes and intricate technical, economic and social considerations. It should prove useful in informing similar processes, as stakeholders in Europe increasingly demand a voice in choosing landslide mitigation measures.

The research for the design and testing of a participatory process was structured in four parts (1) a case study analysis with a literature review and semi-structured interviews, (2) a public questionnaire, (3) six meetings with selected residents, and (4) communication activities, including a website, videos, an online discussion group, press releases and contacts with local media. Figure 3 shows the flow chart for the stakeholder process that was run in SafeLand.

In case study at Nocera Inferiore, the selected resident group agreed on fundamental priorities, i.e. the improvement of the warning system, the implementation of an integrated system of monitoring and active (usually non-structural) risk mitigation measures. Much more debate was devoted to the relocation of residents from the most endangered areas and/or the need to build passive structural works, especially on private properties. The results show that it is feasible to organize an expert-informed participatory process that respects and builds on conflicting citizen perspectives and interests, and demonstrates spheres of policy consensus as well as policy dissent.

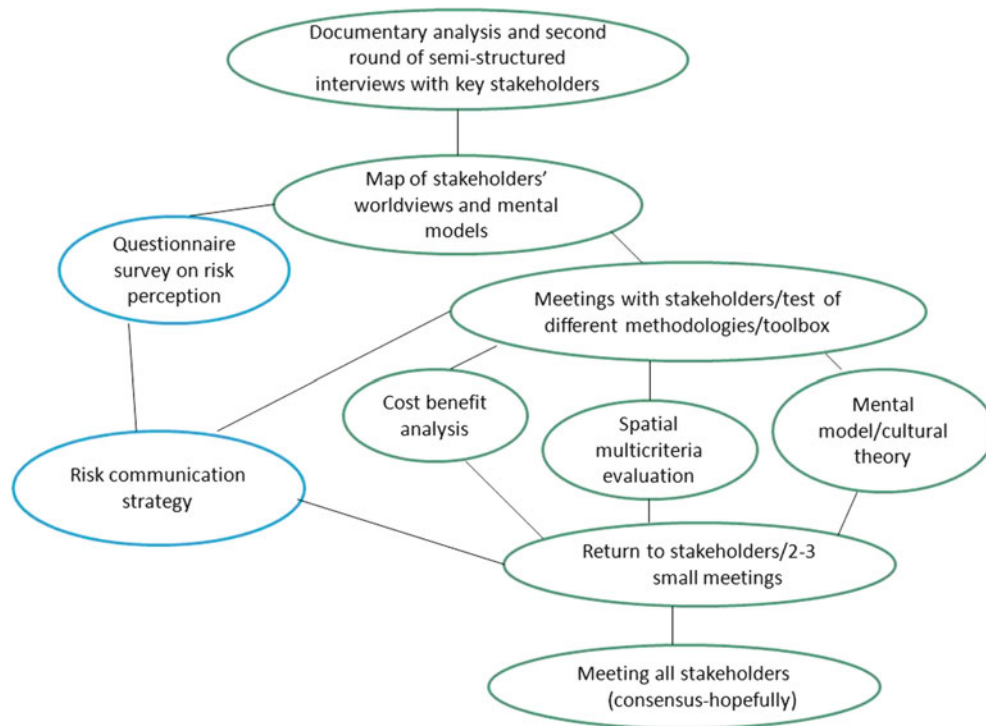


Fig. 3 Flow chart of stakeholder process developed in SafeLand

European Landslide Risk Hotspots

The public and media focus on landslide hazard and risk in Europe is greatly increased in the immediate aftermath of catastrophes such as the widespread flooding and landsliding in Switzerland and Austria in summer 2005, Messina (Italy) in autumn 2009, or the events in Madeira in January 2010 and southern Italy in February 2010, despite the fact that numerous landslides occur all over Europe every year. Experts know to a certain degree which parts of the continent are most exposed to landslide hazard. Nevertheless, neither the geographical location of previous landslide events nor knowledge of locations with high landslide hazard necessarily point out the areas with highest landslide risk. In addition, landslides often occur unexpectedly and the decisions on where investments should be made to manage and mitigate future events are based on the need to demonstrate action and political will. The goal of this study was to undertake a uniform and objective analysis of landslide hazard and risk for Europe.

Two independent models, an expert-based or heuristic model (denoted the ICG model) and a statistical model based logistic regression (denoted the JRC model), were developed to assess the landslide hazard. Both models were based on applying an appropriate combination of the parameters representing susceptibility factors (slope, lithology, soil moisture, vegetation cover, etc.) and triggering factors (extreme precipitation and seismicity). The weights of different susceptibility and triggering factors are calibrated

to the information available in landslide inventories and physical processes. The analysis is based on uniform gridded data for Europe with a pixel resolution of roughly $30\text{ m} \times 30\text{ m}$. The results obtained with the ICG model for rainfall-induced landslides in Europe are shown on Fig. 4. The landslide hazard “hotspots” are also marked on the figure.

A validation of the two hazard models by partner organizations in Scotland, Italy and Romania showed good agreement for shallow landslides and rockfalls, but the hazard models fail to cover areas with slow moving landslides. In general, the results from the two models agree well pointing out the same countries with the highest total and relative area exposed to landslides. Landslide risk was quantified by counting the number of exposed people and exposed kilometres of roads and railways in each country. This process was repeated for both models. The results showed the highest relative exposure to landslides in small alpine countries such as Lichtenstein. In terms of total values on national level, Italy scores highest in both the extent of exposed area and number of exposed population. Again results agree between the two models, but differences between the models are higher for the risk than for the hazard results. The analysis gives a good overview of the landslide hazard and risk hotspots in Europe and allows a simple ranking of areas where mitigation measures might be most effective. These outcomes are described in detail in SafeLand deliverable D2.10.

A database of case histories of well-documented landslides, including several “hotspots” of European

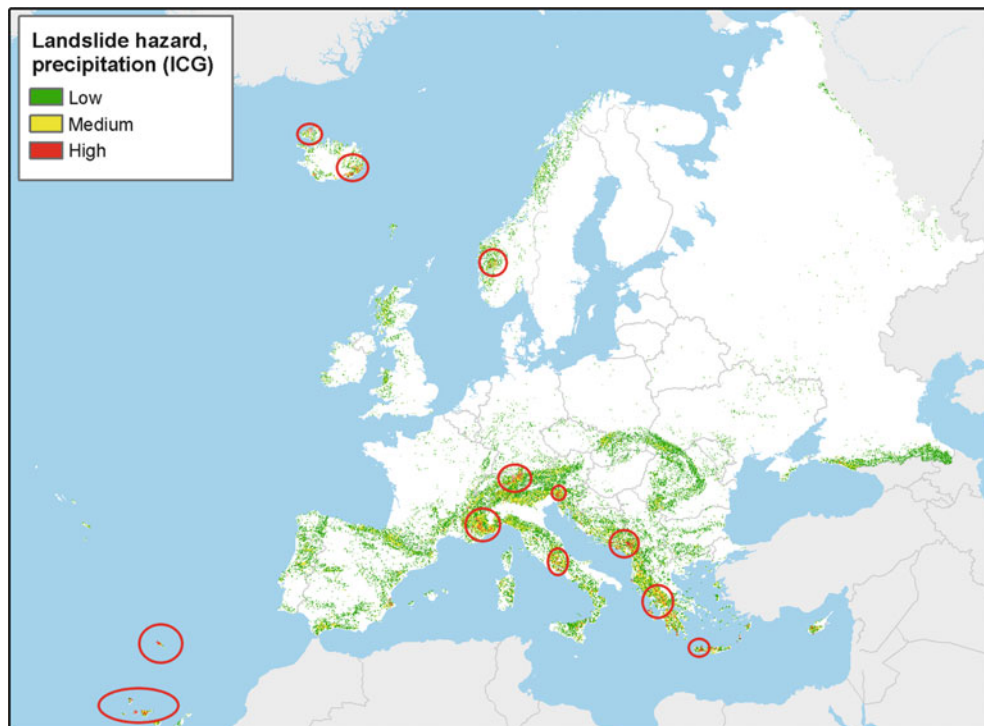


Fig. 4 Hazard map for precipitation-triggered landslides in Europe. *Red ellipses* show possible hotspots with very high hazard

landslides, was developed in SafeLand. Data for close to 50 potential case study sites were compiled and summarised. Most of the case study sites are located in Europe (Italy, France, Norway, Switzerland, Austria, Andorra, and Romania); but they also include one site in Canada and one in India. Almost every type of landslide and every type of movement is represented among these sites. Figure 5 provides an overview of the case studies in the SafeLand database.

Global Change Scenarios

A major research task in SafeLand was to assess the effects of global change on landslide risk in Europe. This required developing climate change scenarios for selected regions in Europe, considering alternative scenarios for human activity and demographic changes at various scales, and assessing the landslide risk evolution in selected “hotspots” areas in Europe.

At the European scale, the regional climate model simulations from EU FP6 ENSEMBLES project ($25 \times 25 \text{ km}^2$ resolution over Europe) were used to perform an extreme value analysis for trends in heavy precipitation events (SafeLand deliverable D3.1). Summer and winter were examined separately to identify seasonal characteristics in the patterns of changes for the period 1961–2099.

The large-scale pattern of heavy precipitation changes appears to be consistent across the simulations (eight

regional models). In winter, the simulations agree particularly well on the positive changes in heavy precipitation over the northern and central European landmasses. Inconsistencies are mainly found in regions where regional features play a large role. This is in particular the case in the mountainous regions or at the foothills of the mountains. In summer, most model agree on an increase in heavy precipitation events over Scandinavia and a decrease over southern Europe. The largest inconsistencies among models are found in the transition zone across central Europe, which separates areas with positive trends in the North and areas with negative trends in the South.

In parallel to this analysis of extreme precipitation events patterns, “Expected changes in climate-driven landslide activity (magnitude, frequency) in Europe in the next 100 years” have been studied (SafeLand deliverable D3.7). Figure 6 shows the spatial distribution of the European population exposed to landslides in 2010 and the positive or negative trends in exposure until 2090.

The European-scale analysis of present and future landslide hazard and risk required many simplifications. The main difficulty was to find homogenous datasets that cover all of Europe with the same accuracy. This is even more challenging when the datasets have to cover future predictions. The climate model results used in the study were based on a physical climate model and have a reasonable level of uncertainties in the future predictions. On the other hand, land cover and population datasets are secondary products based on climate simulations and economical

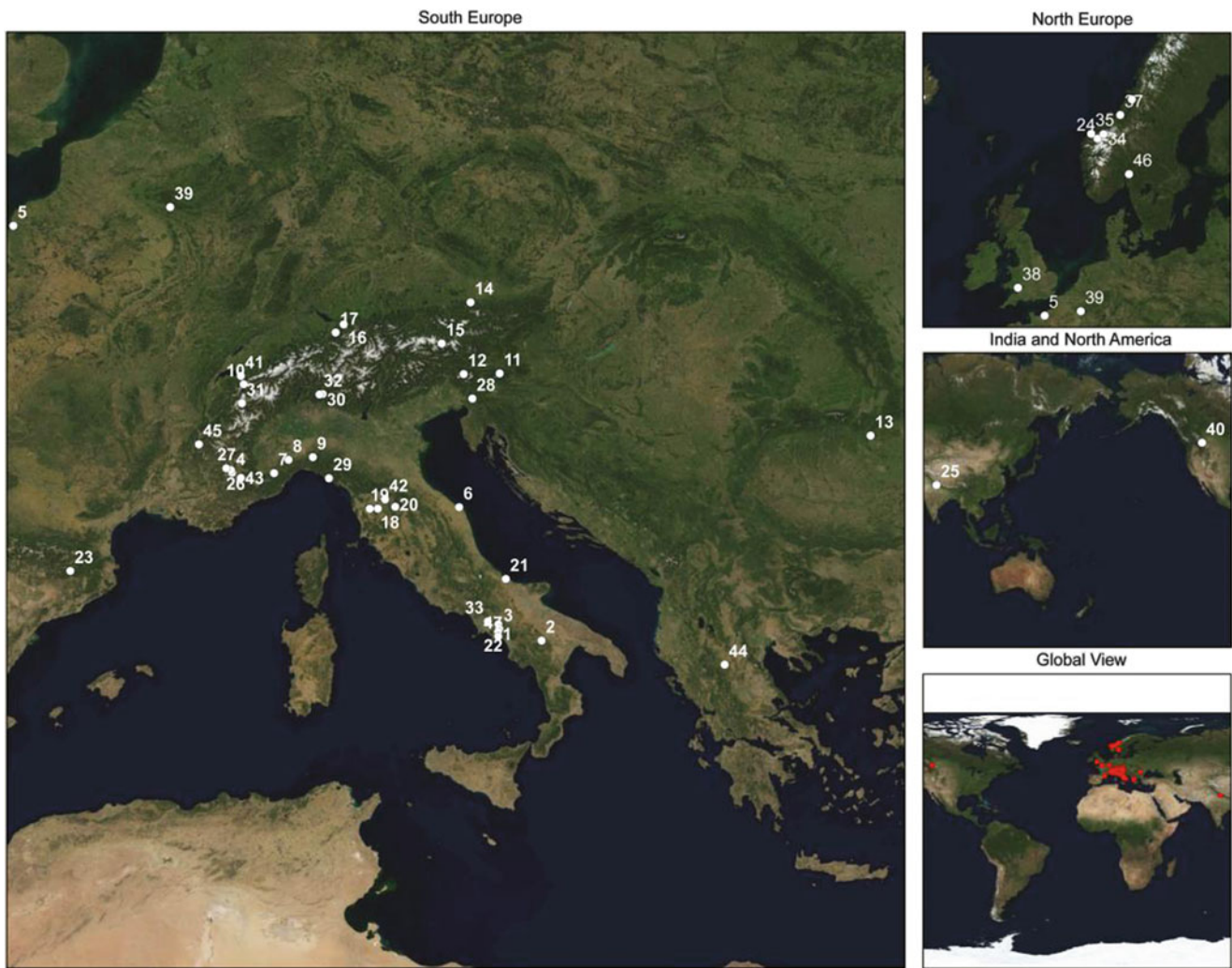


Fig. 5 Map of the collected case study sites in the SafeLand database

modelling, which naturally include more assumptions and simplifications in the process and are far more uncertain. In this context, the predicted changes in landslide hazard and risk in Europe, although certainly indicative, have to be investigated and used with care. The main changes in landslide risk at European scale are mainly due to changes in population pattern in Europe.

Nevertheless, the results from this study are useful for a prognosis of the landslide hazard and risk in next 80 years in Europe. In total, the change affects about 0.7 % of the total European population. This increase has to be seen in comparison to other climate change imposed challenges for the next 80 years (e.g. flooding, drought). Ten countries can still expect some significant changes of more than 2 % increase in exposed population. Most of these countries have significant challenges to cope with the landslide risk already today.

Landslide hazard threatens today about 4 % of the European citizens. The mitigation of these problems is a significant challenge already today and should be continued with

all available efforts. The slight increase expected for the next 80 years will not change this situation significantly. If all mitigation efforts against landslides that are necessary today are implemented, Europe will be very well prepared for the expected future changes in landslide hazard and risk.

For the case study sites at local scale, climate simulations were downscaled to a $3.8 \times 3.8 \text{ km}^2$ resolution on four selected sites in Europe (Nedre Romerike, Southern Norway; Pizzo d’Alvano, Campania, Italy; Barcelonnette, French Alps; Telega, Romania) for the time period 1951–2050, employing the A1B emission scenario (SafeLand deliverable D3.3). The usage of the model output data for simulations on an even more refined grid is expected to improve the ability to simulate even localised heavy precipitation events in regions where rain-induced landslides occur on a regular basis.

- In the area of Nedre Romerike strong increases of temperature are projected especially in winter, while a general increase of precipitation is expected in winter, with a

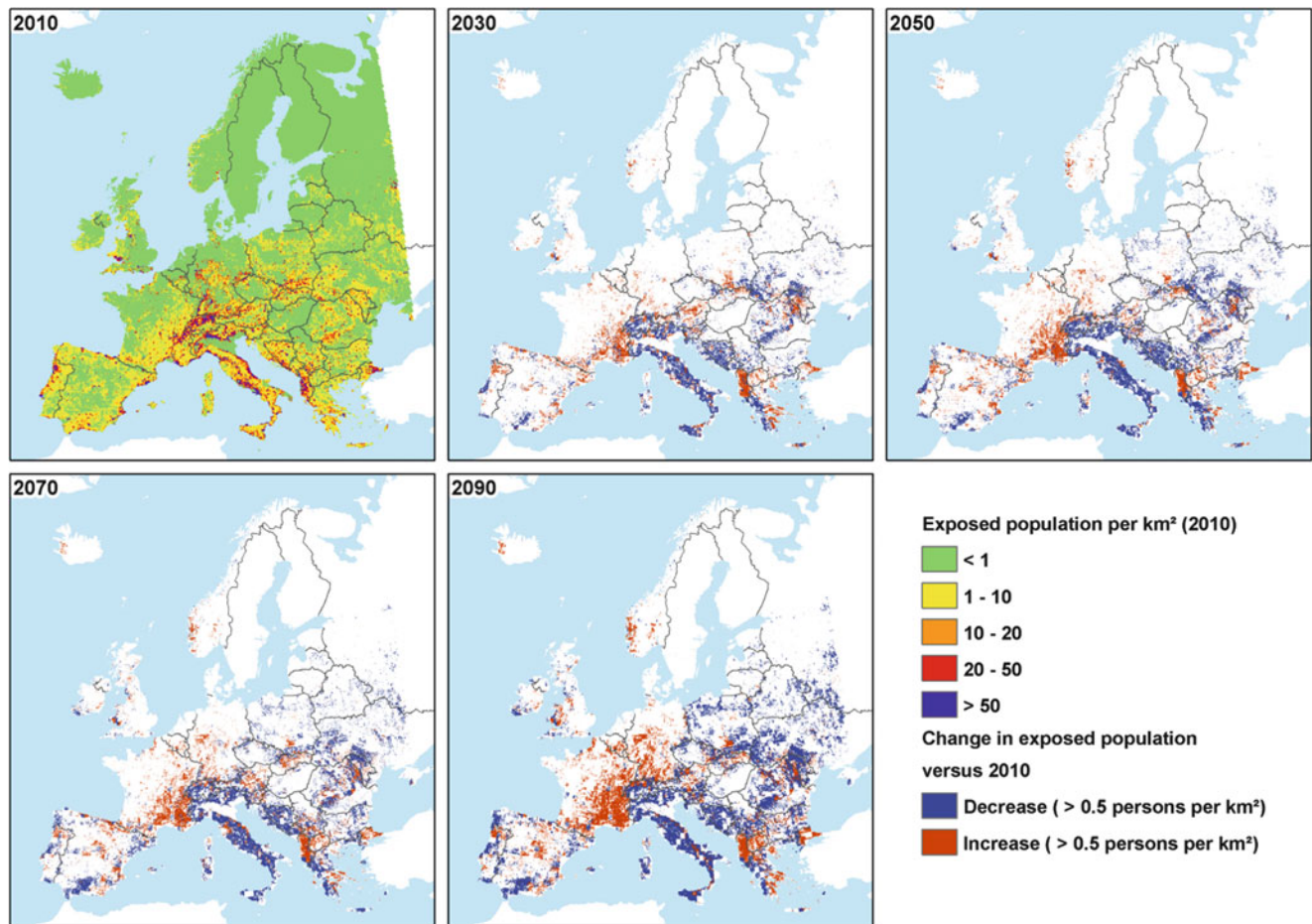


Fig. 6 Exposed population in 2010 and the positive or negative change until 2090. Changes are mostly due to changes in the population density in Europe

general increase of extreme events, which is most, pronounced in the western part of the domain.

- In the area of Pizzo d'Alvano, an increase of temperature is also projected, even if less evident than the previous case. In winter, strong increases of precipitation (with strong extreme events) are expected in the area of Pizzo d'Alvano. In summer slight reductions are expected for the average monthly precipitation over the whole domain, which is in contrast to a projected increase in daily precipitation extremes in the Pizzo d'Alvano region and along the western coast line.
- In the area of Barcelonnette, significant increase of temperature, up to 3 °C, is expected in the future. The increase will be especially pronounced in winter months. An increase of precipitation is expected in small sub-domains throughout the year, with slight changes of extreme events on the whole domain.
- In the area of Telega, a general increase of temperature of about 1.5 °C is expected over the whole domain, for both summer and winter. In winter an increase of precipitation is expected, while a general significant reduction is

expected in summer; an increase of extreme events is expected in winter and summer in the north of the domain with the magnitude of the changes being higher in winter.

The impact of climate change on landslide hazard was assessed on the three focused areas: Pizzo d'Alvano for Southern Italy, Barcelonnette for the Alps and Nedre Romerike for Southern Norway (SafeLand deliverable D3.8). Even if these sites present different contexts in view of landslides causes (climates, size of landslides), the analyses show that climate change is likely to induce similar trends in landslide activities. Based on the IPCC A1B scenario and on the resulting climate change scenarios at local scale, the different models predict an increase in landslide activities. This change would materialize either as an increase in the frequencies of landslides or as an increase in surface area of the potentially unstable areas.

The results differ from the predictions provided by larger scale models. These differences might be explained by the finer calibration processes used for local scale analysis and also to the finer climate model used, which, for example, take into account the influence of topography on climate (mostly

on precipitation). Therefore, if large-scale models are useful to determine where landslide activities will vary relatively to the other regions, the different kinds of local scale models are necessary for urban planners and all local authorities to estimate what would be the future risks in their communes or valley, with for some of the models, spatial information. However, these models require precise data, not only for calibration but also for prediction, and so climate models should be adapted to such resolutions, like in this study.

In parallel to the climate scenarios, human activity and demography scenarios were developed on the Norwegian and the French sites (SafeLand deliverables D3.5 and D3.6). When they exist, prospective data were used. Unfortunately, data are sparse, rarely geo-referenced and not always adapted to the local context. However, this lack of information can be partially compensated by the analysis of past and present trends. Satisfactory data have been collected for the Barcelonnette site and have allowed the elaboration of demography scenarios at local level by 2030. The land-use change scenario by 2100 has been studied. Acknowledging significant uncertainties, the demographic forecasts can be extended from 2030 to 2100. Demographic scenarios have been partially developed for the Nedre Romerike site (Norway).

Three studies of landslide risk assessment have been performed on French, Norwegian and Scottish sites (SafeLand deliverable D3.9). The results seem to show a similar trend: an increase of landslide risk, which is more-or-less significant depending on the considered sites. Due to a high level of uncertainties on population and traffic evolution scenarios, precautions need to be taken when interpreting and using the results.

Remote Sensing Technologies and Early Warning Systems

Remote Sensing for Landslide Detection, Monitoring and Rapid Mapping

One of the main research areas of SafeLand was exploring the use of modern remote sensing technologies for landslide detection, monitoring and rapid mapping. The objectives of the research in this were:

- Define and validate a common methodology for detection, rapid mapping, characterization and monitoring of landslides at regional and catchment scales using advanced remote sensing techniques;
- Define and validate a common methodology for the rapid creation and updating of landslide inventories and hazard maps at regional/catchment scale using advanced remote sensing techniques;

- Prepare user-oriented guidelines for the incorporation of advanced within integrated risk management processes and best practices.

These objectives were achieved through the following steps:

1. Overview of recent and emerging ground based techniques for landslide analysis.
2. Overview of recent and emerging remote sensing technologies for landslide analysis.
3. Set up of a questionnaire on landslide monitoring methods (have been prepared).
4. Set up of questionnaire on remote sensing technologies (have been prepared).
5. Description on the use of ground based, airborne and spaceborne techniques in SafeLand case studies.
6. Evaluation of ground based, airborne and space-borne techniques based on the literature review, on the aforementioned questionnaires and on SafeLand case studies.

As an example, Fig. 7 shows the application of Permanent Scatterers Interferometric Synthetic Aperture Radar (PS-InSAR) to monitoring of slope movements on the South flank of Mount Etna.

Early Warning Systems for Landslides

A people-centred Early Warning System (EWS) comprises five key elements (1) knowledge of the risks; (2) monitoring, analysis and forecasting of the hazards; (3) operational centre; (4) communication or dissemination of alerts and warnings; and (5) local capabilities to respond to the warnings received. In this context, SafeLand addressed the technical and practical issues related to monitoring and early warning for landslides for different landslide types, scales and risk management steps, and identified the best technologies available in the context of both hazard assessment and design of early warning systems (SafeLand deliverable D4.8: Guidelines for landslide monitoring and early warning systems in Europe—Design and required technology). The targets for this work were end-users and it aimed to facilitate the decision process for stakeholders by providing guidelines based on a synoptic view of existing monitoring methodologies and early-warning strategies and their applicability for different landslide types, scales and risk management steps. The guidelines include several comprehensive checklists and toolboxes to support informed decisions. One of the main objectives in this work was to merge experience and expert judgment and therefore to create synergies on EC-level towards guidelines for early warning and to make these results available to end-users and local stakeholders.

A key element in a modern EWS is the use of remote sensing techniques. Guidelines for use of remote sensing technologies were developed for end-users and stakeholders

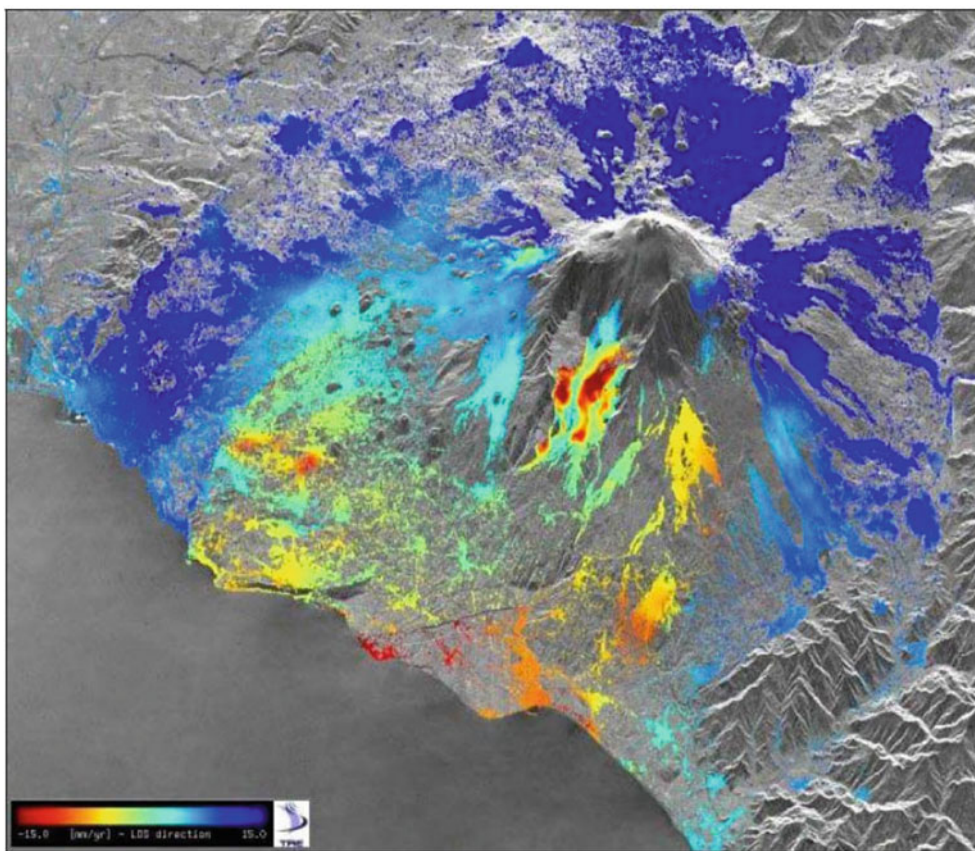


Fig. 7 Example of PS-InSAR analysis at large scale: ground deformation due to active faults in the South flank of Mount Etna (Italy)

(SafeLand deliverable D4.4: Guidelines for the selection of appropriate remote sensing technologies for monitoring different types of landslides). These guidelines may be used for selecting the remote sensing technologies that are most suitable to detect/characterize/map/monitor the landslide process at hand. Combining the technological features of each remote sensing method, the possible geomorphological features of the landslides (e.g. typology, displacement velocities and observational scales) and risk management strategies, the guidelines can be used to initially constrain the choice of methods to a few techniques that seem most feasible for the landslide process at hand. Before final decisions on the methods to be used are taken, further information and expertise will typically be required (Nadim and Intriery 2011).

Dissemination of Project Results

The aim of the dissemination activities in the SafeLand project was to inform the scientific community and stakeholders of the activities carried out within the project. To achieve this aim, the dissemination and exploitation of the results and the management of intellectual property were

done on two fronts: first, the internal exchange amongst the project partners (internal dissemination) and, second, the distribution of final results to end-users (external dissemination). Specifically, three different tasks were developed: Task 1: Dissemination activities through the web portal of the Project; Task 2: Educational activities; and Task 3: Dissemination to decision-makers, professionals and scientists.

The SafeLand web site (<http://www.safeland-fp7.eu>) was set up in the first phase of the project together with an Extranet page for internal use. The web site provides information about the project, the objectives of the research carried out and the consortium partners. Moreover, by the end of the project, all the obtained results collected in project deliverables have been made available on the web page.

Regarding Task 2, collaboration and know-how exchange were carried out via key educational activities such as “LAndslide Risk Assessment and Mitigation” (LARAM) International School and Mountain Risk Project. The LARAM School, organized by the University of Salerno (Italy), is held annually and is aimed at 40 Ph.D. students selected every year from those working on landslide-related topics in the fields of Civil Engineering, Environmental Engineering, Engineering Geology or Natural Geography. The main objectives of LARAM are to develop high-

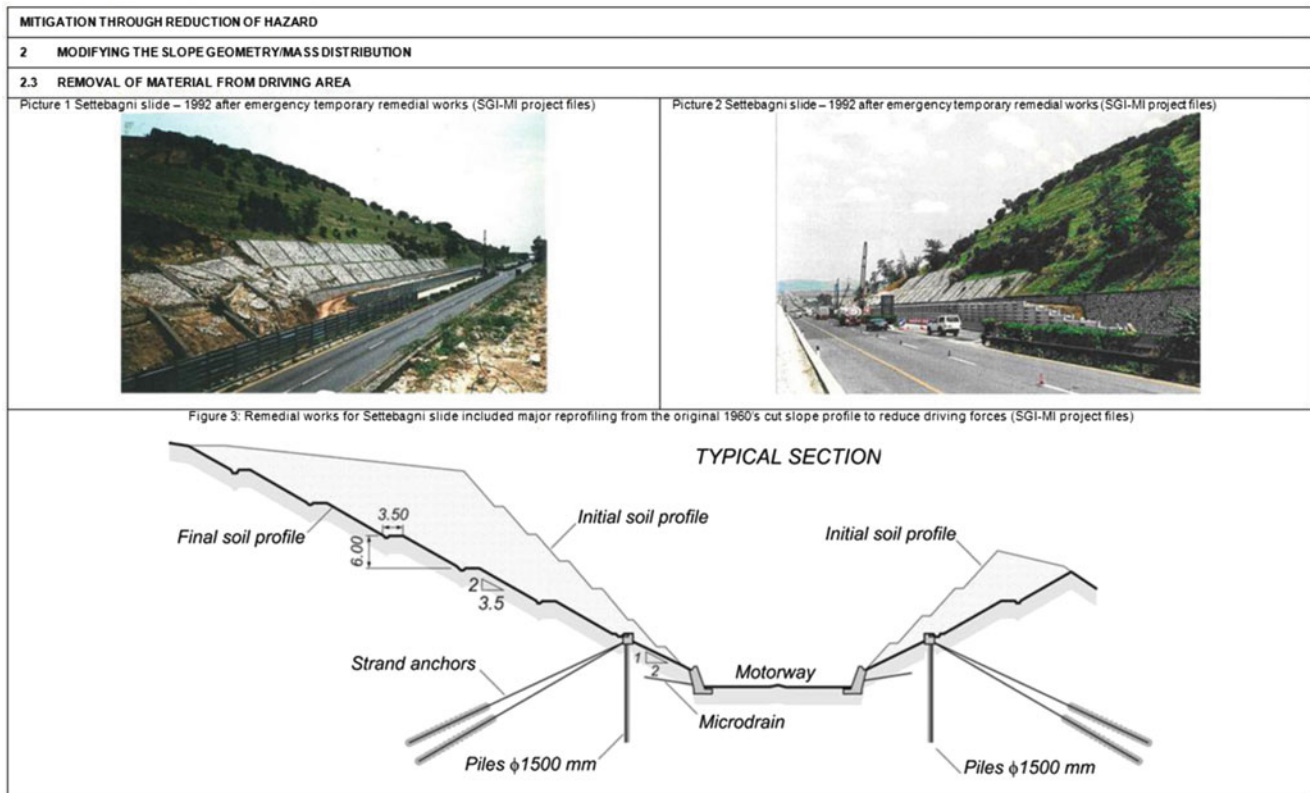


Fig. 9 Typical information provided in the compendium mitigation measures for landslides

Journals are under development to present the results of each Work Area of the Project. A series of SafeLand related papers were also presented at the Second World Landslide Forum (WLF, Rome October 2011), aimed at gathering scientists, stakeholders, policy makers and industry members dealing with the management of landslide risk, including a special session dedicated to the Project.

At the end of the Project, a special session on “Effects of global change on spatial and temporal patterns of landslide risk” was organized during the EGU General Assembly 2012 (22–27 April 2012, Vienna, Austria), to present the results of SafeLand project.

Regarding the dissemination of SafeLand results to decision-makers and professionals, as mentioned earlier, a toolbox for mitigation measures was implemented to assist and to guide the user in the choice of the most appropriate mitigation measures for potential landslides situations. The toolbox assists the user with the following: identifying the type of ground movement expected; assessing the level of hazard associated with the ground movements; evaluating the consequences of the ground movement; evaluating the risk class and determining the need for mitigation; and for selecting the most appropriate mitigation approaches to use, and comparing them. The toolbox contains default implementation criteria and “scores” for each mitigation and preventing measure. The user can, at any time, introduce

his own “scores” and “weights” for each of the mitigation measures. In term of non-structural measures, only early working systems are included at this time. The other non-structural measures refer to the stakeholder process for risk management for their evaluation and ranking. Figure 8 shows typical panels in the web-based toolbox.

The aforementioned toolbox uses the information provided in a compendium of tested and innovative structural, non-structural and risk-transfer mitigation measures for different landslide types. This compendium was prepared as one of the main SafeLand deliverables for landslide risk management. The compendium includes a categorization system for the different structural mitigation and prevention measures. About 60 structural measures were documented and evaluated. The description of these measures in the compendium includes guidance on the applicability and effectiveness of each mitigation measure for different types of landslides; information on the maturity of the technology, ranging from “prototype development” to “obsolete”; information on current design methods, their maturity and associated uncertainties; and comparative (qualitative) information on costs. The measures were evaluated for different types of ground movements and slides. Each measure was then ranked with “scores” and placed into an applicability matrix that was used later in the toolbox. Figure 9 shows a typical page of the compendium.

Social Impact

The results of the SafeLand project are expected to have impact on the protection and safety of population and material property in Europe at several levels: technology will be improved, more reliable landslide susceptibility, hazard and risk maps will be made available and public awareness will be put on the agenda in a systematic manner. Dialogue and understanding among scientists and experts will be made more natural and early warning systems will be ready for implementation. Stakeholders and authorities will have improved access to a risk management system for increased safety and cost-effectiveness. The project deliverables are expected to help provide the basis for future European directives in relation to natural hazards.

The project brought together leading European research centres and technologically advanced SMEs with highly developed experience in their specialized fields, such as GIS, remote sensing, modelling, risk assessment and management and decision-support, to allow a leap forward in pre-disaster planning and mitigation in Europe and worldwide.

The SafeLand project, in co-ordination with the JRC-chaired European Landslide Working Group (“the Landslide Group”) will provide Member States with a common methodology for the first identification of areas at risk to landslide threat.

Examples of specific impacts of SafeLand are:

- The inventory (synthesis) of landslide “hotspots” in Europe will be a significant contribution to a proposal for a Soil Framework Directive that asks Member States to identify areas at risk to landslides on the basis of a common methodology. Identifying sensitive areas and/or contexts in Europe where changes in landslide frequency may be expected will constitute a roadmap for actions required and level of urgency for improving safety and reducing risk associated with landslides.
- The guidelines for landslide susceptibility, hazard and risk assessment will contribute not only to the development of the common risk assessment methodology but also to systematic quantification of landslide risk. QRA outputs will provide guidance to stakeholders in where to direct research and development efforts and to allocate resources where uncertainties need to be reduced or where cost-effectiveness can be increased.
- The methodology for landslide risk assessment due to both climate change and anthropogenic changes at the European level will help policy-setters and decision-makers to optimize the urban development and infrastructure planning.

SafeLand has already started to have some impact through its dissemination activities. The achievements of

the project were presented to PhD candidates working on landslide-related issues at the LARAM School since 2009, and special sessions at the LARAM Workshop in Salerno in September 2010 and at the Mountain Risks Conference in Florence in November 2010 were dedicated to SafeLand. The methodology developed in SafeLand for large-scale landslide hazard and risk mapping is used in the Global Assessment Reports of UNISDR (GAR09, GAR11 and GAR13) to estimate the number of people affected by landslides world-wide.

Concluding Remarks

The research done in SafeLand clearly demonstrates that risk and vulnerability assessment for landslides, or any other natural hazard a society is facing, requires expertise from different disciplines. Modern risk and vulnerability assessment activities require looking beyond the borderlines of single disciplines or single sectors. However, inter-disciplinary research is not an easy task. Policy and decision makers could provide incentives for inter-disciplinary studies, for example by allocating funds through research programmes and calls specifically asking for inter-disciplinary research.

A proactive approach to landslide risk mitigation is far more effective than a reactive approach. However, decision makers and authorities do not always have the necessary information to invest in natural hazard risk reduction measures. Furthermore, such investments must compete with many other societal needs. Improved communication between decision makers and scientists and experts is essential in setting the priorities for a society. This requires an effort both from the decision makers and from the scientific community.

Acknowledgments The project “SafeLand—Living with landslide risk in Europe: Assessment, effects of global change, and risk management strategies” was supported by European Commission’s 7th Framework Programme through Grant Agreement No. 226479. Their support is gratefully acknowledged. The authors also wish to thank the efforts and contributions of their 100+ colleagues in the SafeLand consortium, as well as the SafeLand collaboration partners IIT-Roorkee in India and Chengdu Technical University in China, representatives of the SafeLand End-Users group and members of the SafeLand International Advisory Board.

References

- Commission of the European Communities (2006a) Thematic strategy for soil protection. COM(2006)231 final, Brussels, 22 September 2006, p 12
- Commission of the European Communities (2006b) Proposal for a Directive of the European Parliament and of the Council establishing a framework for the protection of soil and amending

- Directive 2004/35/EC. COM(2006)232 final, Brussels, 22 September 2006, p 30
- Commission of the European Communities (2009) A community approach on the prevention of natural and man-made disasters. COM(2009)82 final, Brussels, 23 February 2009, p 9
- Corominas J, Mavrouli O, Santo A, Di Crescenzo G, Ulrich T, Sedan Miegemolle O, Malet J-P, Remaître A, Narasimhan H, Maftai R, Filipciuc CT, Van Den Eeckhaut M, Hervás J, Smith J, Winter M, Tofani V, Casagli N, Crosta GB, Agliardi F, Frattini P, Cascini L, Ferlisi S, Faber MH (2012) Comparison of landslide hazard and risk assessment practices in Europe. European Geosciences Union (EGU) General Assembly, Vienna, Austria, 22–27 April 2012
- Eidsvig U, McLean A, Vangelsten BV, Kalsnes B, Ciurean RL, Argyroudis S, Winter M, Corominas J, Mavrouli OC, Fotopoulou S, Pitilakis K, Baills A, Malet JP (2012) Socio-economic vulnerability to natural hazards—proposal for an indicator-based model. European Geosciences Union (EGU) General Assembly, Vienna, Austria, 22–27 April 2012
- Fotopoulou S, Pitilakis K (2012) Vulnerability assessment of RC buildings subjected to seismically triggered slow moving earth slides: an analytical approach. *Landslides*. doi:10.1007/s10346-012-0345-5
- IPCC Report (2012) “Managing the risks of extreme events and disasters to advance climate change adaptation”. <http://ipcc-wg2.gov/SREX/report>
- Mavrouli O, Corominas J (2012) Vulnerability of simple reinforced concrete buildings to damage by rockfalls. *Landslides* 7:169–180. doi:10.1007/s10346-010-0200-5
- Nadim F and Intriери E (2011) Early warning systems for landslides: challenges and new monitoring technologies. In: Keynote paper, 5th Canadian conference on geotechnique and natural hazard, Kelowna, BC, Canada, 15–17 May 2011
- SafeLand deliverables. <http://www.safeland-fp7.eu/results/Documents>
- Smith JT, Winter MG, Fotopoulou S, Pitilakis K, Mavrouli OC, Corominas J, Argyroudis S (2012) The physical vulnerability of roads to debris flow: an expert judgement approach. In: Proceedings of ISL-NASL 2012, 11th international and 2nd North American symposium on landslides, Banff, AB, Canada, 3–8 June
- UNISDR’s Global assessment reports. <http://www.unisdr.org/we/inform/publications/19846>
- Van Den Eeckhaut M, Hervás J (2012) State of the art of national landslide databases in Europe and their potential for assessing susceptibility, hazard and risk. *Geomorphology* 139–140:545–558. doi:10.1016/j.geomorph.2011.12.006



Plenary: Progress in Regional Landslide Hazard Assessment—Examples from the USA

Rex L. Baum, William H. Schulz, Dianne L. Brien, William J. Burns, Mark E. Reid, and Jonathan W. Godt

Abstract

Landslide hazard assessment at local and regional scales contributes to mitigation of landslides in developing and densely populated areas by providing information for (1) land development and redevelopment plans and regulations, (2) emergency preparedness plans, and (3) economic analysis to (a) set priorities for engineered mitigation projects and (b) define areas of similar levels of hazard for insurance purposes. US Geological Survey (USGS) research on landslide hazard assessment has explored a range of methods that can be used to estimate temporal and spatial landslide potential and probability for various scales and purposes. Cases taken primarily from our work in the U.S. Pacific Northwest illustrate and compare a sampling of methods, approaches, and progress. For example, landform mapping using high-resolution topographic data resulted in identification of about four times more landslides in Seattle, Washington, than previous efforts using aerial photography. Susceptibility classes based on the landforms captured 93 % of all historical landslides (all types) throughout the city. A deterministic model for rainfall infiltration and shallow landslide initiation, TRIGRS, was able to identify locations of 92 % of historical shallow landslides in southwest Seattle. The potentially unstable areas identified by TRIGRS occupied only 26 % of the slope areas steeper than 20°. Addition of an unsaturated infiltration model to TRIGRS expands the applicability of the model to areas of highly permeable soils. Replacement of the single cell, 1D factor of safety with a simple 3D method of columns improves accuracy of factor of safety predictions for both saturated and unsaturated infiltration models. A 3D deterministic model for large, deep landslides, SCOOPS, combined with a three-dimensional model for groundwater flow, successfully predicted instability in steep areas of permeable outwash sand and topographic reentrants. These locations are consistent with locations of large, deep, historically active landslides. For an area in Seattle, a composite of the three maps illustrates how maps produced by different approaches might be combined to assess overall landslide potential. Examples

R.L. Baum (✉) • W.H. Schulz • J.W. Godt
U.S. Geological Survey, Geologic Hazards Science Center, Denver,
CO 80225-0046, USA
e-mail: baum@usgs.gov; wschulz@usgs.gov; jgodt@usgs.gov

D.L. Brien • M.E. Reid
U.S. Geological Survey, Volcano Science Center, Menlo Park,
CA 94025, USA
e-mail: dbrien@usgs.gov; mreid@usgs.gov

W.J. Burns
Oregon Department of Geology and Mineral Industries, Portland,
OR 97232, USA
e-mail: bill.burns@dogami.state.or.us

from Oregon, USA, illustrate how landform mapping and deterministic analysis for shallow landslide potential have been adapted into standardized methods for efficiently producing detailed landslide inventory and shallow landslide susceptibility maps that have consistent content and format statewide.

Keywords

Landslide susceptibility • Landslide probability • Deterministic models • LiDAR • Landform mapping

Introduction

Landslides cause untold human misery, with annual fatalities estimated in the thousands worldwide (Kirschbaum et al. 2010; Petley 2012) and annual losses estimated in the billions of dollars (Dai et al. 2002). Efforts to estimate the probability of landslides have resulted in gradual improvements in methods and results over the last five decades. Several authors have published overviews of the state of the art of landslide hazard zonation and related topics at various times (Varnes 1984; Soeters and van Westen 1996; Aleotti and Chowdury 1999; Guzzetti et al. 1999; Dai et al. 2002; van Westen et al. 2006). This paper illustrates our progress on regional landslide hazard assessment during the last decade with selected case studies from work in the U.S Pacific Northwest. We conclude by discussing some of the outstanding issues for ongoing and future research.

Background

Much of the recent progress in landslide hazard assessment has been made possible by recent advancements in technology and availability of digital data. Progress also has resulted from application of scientific advancements in earth science and other fields to landslide problems. After a brief review of the history of landslide hazard assessment, along with a survey of techniques described in the literature, we highlight a few examples of recent progress and developments in regional landslide hazard assessment in the USA. The examples help to illustrate (1) the contributions of recent technological advancements to improved topographic data, (2) the contribution of improved models to analytical results, (3) progress in methods for evaluating or validating model results, and (4) the contribution of standardized methods to rapid production and distribution of landslide maps. This includes mapping in rapid response mode—post-disaster assessments for major landslide events.

Landslide hazard assessment aims to answer questions about where and when landslides will occur, how often they

will happen, how large they will be, and how fast and far they will travel. In general, the goal is to assess the (numerical) probability of landslide occurrence or impact (Dai et al. 2002). Regional hazard assessments commonly focus on the questions of location and timing (where and when) with secondary emphasis on frequency (how often), size (how large), and travel distance or inundation area (how far).

The term “regional” has been associated with map scales ranging from 1:100,000–1:500,000 (Soeters and van Westen 1996). For purposes of this paper, we include methods that could be applied at medium scales (1:25,000–100,000) as well, because recent advancements in computer hardware, Geographic Information Systems (GIS), and digital spatial data have made it possible to apply more detailed analysis over larger areas, somewhat reducing the distinction between regional- and medium-scale assessments. Thus, for purposes in this paper, regional refers to methods of landslide hazard assessment that can be applied to areas ranging from tens to thousands of square kilometers.

History

Mapping of landslides and landslide-susceptible areas has been performed since the 1930s or earlier (Varnes 1981). Early efforts were generally local and sporadic. Concerted efforts, mainly by government organizations in various parts of the world, to delineate and zone or rank hazardous areas began to accelerate in the late 1960s. Examples of computer-assisted assessments of landslide hazard began to appear in the early 1970s (Varnes 1984). Most regional landslide hazard assessments published before 1980 were map-based assessments of landslide susceptibility that relied on either cartographic analysis of geology and terrain features or numerical rating of contributing factors (Varnes 1984). Landslide susceptibility usually refers to an assessment of the long-term, qualitative (or relative) probability of landslides, whereas landslide hazard usually refers to a quantitative estimate of probability of landslide occurrence or impact (Soeters and van Westen 1996; Dai et al. 2002).

These studies relied heavily on expert judgment and some combination of field studies and air photo interpretation. For example, in the USA, federal and state agencies developed relative-slope-stability maps at various scales in the 1970s for several major urban areas (Brabb et al. 1972; Miller 1973; Artim 1976). These maps were based on simplified geologic data and topographic slope, generally at scales of 1:30,000–1:125,000, and lacked the currently desired level of detail for managing land use by cities and counties.

By the mid-1990s, improvements in computer hardware and software as well as improvements in satellite remote sensing enabled a number of advancements. GIS methods had advanced to the point that they could be used profitably in analysis of landslide susceptibility and hazard. Concurrently, four distinct, and now commonly recognized approaches for landslide hazard assessment developed: landslide inventory-based probabilistic, statistical, deterministic, and heuristic (Soeters and van Westen 1996). For example, an innovative debris-flow hazard assessment took advantage of GIS technology and statistical methods to calculate debris-flow probability including runout zones (Ellen et al. 1993). Numerous examples of weight of evidence (Harp and Noble 1993; Suzen and Doyuran 2003; van Westen et al. 2003), bivariate (Brabb et al. 1972) and multivariate statistical models (Carrara 1983; Carrara et al. 1991, 1999; Chung et al. 1995) applied to landslide hazard assessment appeared. Satellite remote sensing improved both in terms of spatial resolution and spectral resolution to the point that it could be used to delineate the extent of landslides induced by major regional storms or major earthquakes (Soeters and van Westen 1996). Nevertheless, vertical aerial photography remained the preferred type of imagery for mapping landslides to develop landslide inventories. A number of GIS-based deterministic models (Montgomery and Dietrich 1994; Wu and Sidle 1995; van Westen and Terlien 1996; Borga et al. 1998; Pack et al. 1998) also emerged in the literature. Methods of using landslide inventories to check accuracy of landslide susceptibility and hazard assessments also began to be devised (Carrara et al. 1991; Montgomery et al. 1998). The terms landslide hazard and landslide susceptibility were commonly used interchangeably and despite the technical advances, most maps published by the mid 1990s depicted landslide susceptibility, rather than hazard (Soeters and van Westen 1996).

Steadily increasing numbers of regional- and medium-scale landslide hazard assessments have appeared in the literature since the mid-1990s. Further advancements in science and technology have paved the way for progress in regional landslide hazard assessment in recent years. These advancements include improvements in satellite (InSAR, high-resolution optical) imagery and airborne remote

sensing (primarily the airborne laser scanning technology known as Light Detection and Ranging, LiDAR) (Schulz 2004, 2007; Burns and Madin 2009; Roering et al. 2009), as well as platforms for obtaining and visualizing the imagery, such as Google Earth. New methods and existing methods from other fields were applied, such as, artificial neural networks (ANN) (Lee et al. 2003; Lu and Rosenbaum 2003; Falaschi et al. 2009), and logistic regression and other new statistical models (Dai and Lee 2003; Ohlmacher and Davis 2003; Van den Eeckhaut et al. 2006; Felicísimo et al. 2013). Along with these changes have come improvements in methods for validating landslide hazard maps (Chung and Fabbri 2003; Van Den Eeckhaut et al. 2006). Coe et al. (2004a) introduced a method for estimating landslide probability based on historical records. New deterministic models have emerged for assessing large deep landslides (Miller 1995; Reid et al. 2000, 2001, 2010; Franciss 2004; Xie et al. 2004; Brien and Reid 2007, 2008) and shallow rainfall induced landslides (Crosta and Frattini 2003; Savage et al. 2003; Frattini et al. 2004; van Beek and van Asch 2004; Baum et al. 2008, 2010, 2012; Salciarini et al. 2008; Simoni et al. 2008). Technology advances have also made possible more rapid assessments for areas where few data exist (Coe et al. 2004b; Harp et al. 2009). New types of assessments have also been developed, including event-based seismic landslide hazard assessments (Jibson et al. 2000), and post-fire probabilistic debris-flow hazard assessments (Cannon et al. 2010). Models of ground motion are beginning to be applied to analysis of seismic landslides (Harp et al. 2012). Tools originally developed for assessing hazards from volcanic debris flows (Schilling 1998) have been adapted to mapping potential inundation areas for smaller debris flows and rock avalanches (Berti and Simoni 2007; Griswold and Iverson 2008; Magirl et al. 2010).

Throughout the 1990s and before, the main audience for landslide hazard assessments was primarily land-use planners and engineers. Hazard assessments were used so that high-density residential and commercial development or redevelopment of areas with high potential for landslides could be avoided or regulated. More recently, municipal governments and other users have recognized the value of landslide susceptibility and landslide hazard assessments in emergency preparedness planning, landslide early warning, and setting priorities for engineered mitigation of landslide prone-areas (Coe et al. 2004a). Knowing where landslides are likely to occur frequently helps in selecting evacuation routes, placing equipment in preparation for removing debris after a storm, and targeting warnings of potential landslides. Some recent efforts have focused on developing hazard maps for insurance purposes (Godt et al. 2012).

Examples of Progress in Regional Hazard Assessment

As too many examples of recent progress in regional landslide hazard assessment exist in the literature to be cited here, we highlight USGS research that utilized improved spatial data and technology. The improvements in technology have allowed us to develop applications of new statistical methods to landslide susceptibility mapping, improved physically based models, improved methods of evaluation, and standardization of procedures for conducting assessments over large areas or in rapid response mode. In the following sections, we present case studies from our work in the Pacific Northwest of the USA that illustrate progress in some of these areas. Specifically, we present examples of advancements derived from improved spatial data and visualization methods (Schulz 2007), improved deterministic models (Brien and Reid 2007, 2008; Godt et al. 2008a, b; Baum et al. 2010, 2012), improved methods of evaluation (Chung and Fabbri 2003; Van den Eeckhaut et al. 2006), composite hazard assessments, and standardization of methods for rapid assessments (Burns and Madin 2009; Burns et al. 2012).

Seattle Case Study

Baum et al. (2005) described in considerable detail the then ongoing USGS regional assessment of landslide hazard for Seattle, Washington, USA (Fig. 1). In the sections that follow, we highlight some further advancements from that work and combine some of the assessments to illustrate the concept of a composite assessment of landslide potential. Using a common field area, we demonstrate a geomorphic approach based on high-resolution topography and two deterministic methods for separately assessing shallow and deep landslides. The composite integrates results from the three different models to give an overview of the combined potential for all types of landslides that commonly occur in the area.

Geomorphic Assessment of Landslides with LiDAR

The advent of high-resolution remotely sensed topographic data has revolutionized mapping of landslides and landslide features for inventory and susceptibility purposes. As part of our assessment of landslide hazard for the Seattle area, Schulz (2004, 2007) developed and tested a methodology for mapping landslide features using LiDAR data over the entire city of Seattle (217 km²). These studies used a LiDAR-derived DEM with 1.8 m resolution, and a raw point density of ground returns of about 1 per m², with vertical errors of about 30 cm, except in densely vegetated

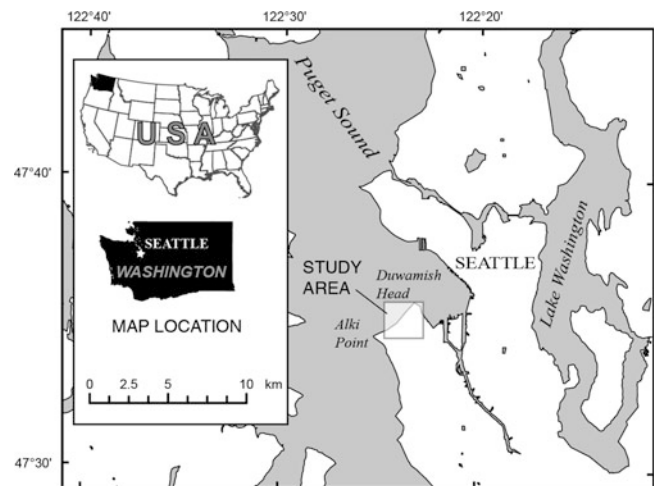


Fig. 1 Map showing Seattle, WA, USA study area

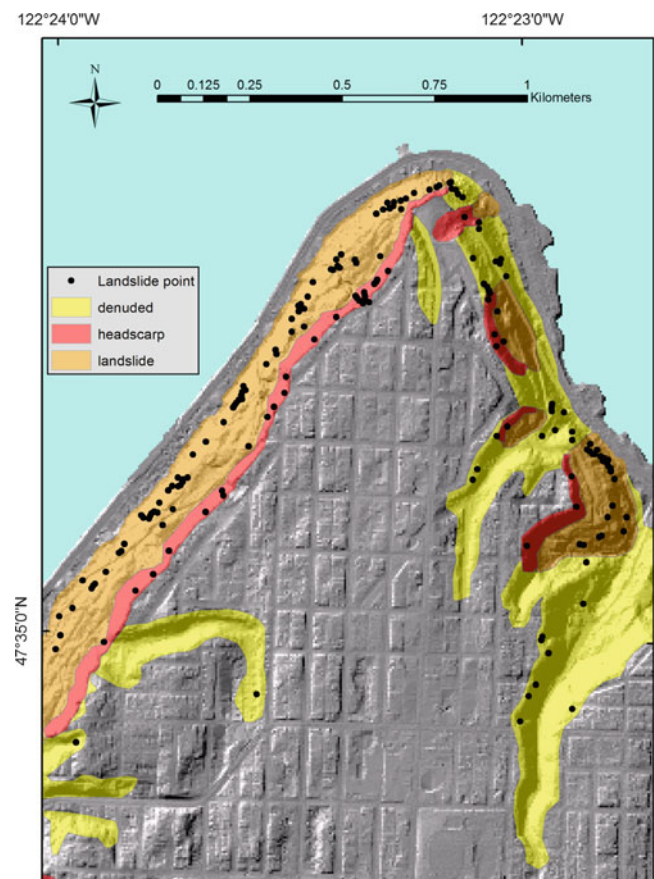


Fig. 2 Map showing landslide-derived landforms identified by Schulz (2004, 2007) using LiDAR imagery for the area shown in Fig. 1

areas, where vertical errors were locally as much as 5 m (Haneberg 2008).

Schulz (2004, 2007) used LiDAR-derived imagery to map landforms in Seattle created mainly by landslide activity. The landforms identified were: (1) landslide deposits, (2) head scarps, and (3) denuded slopes (Fig. 2). These

landforms in all cases truncate the glacially sculpted upland surface. Denuded slopes were defined as slopes that formed by erosion and mass wasting following deglaciation, but which lacked discernible deposits of individual landslides. Denuded slopes, therefore, were mapped where the glacial upland surface is truncated, but where landslides could not be identified. Field observations indicate that denuded slope areas probably lack discernible landslides because many Seattle landslides are too small and thin to be resolved by LiDAR and their deposits have often been removed or modified by erosion, other mass wasting, and human activity.

Using a GIS, landform mapping was performed with LiDAR-derived imagery including shaded relief, slope, and topographic contour maps, as well as almost 400 topographic profiles. These maps and profiles were visually evaluated for topographic characteristics indicative of landslides, such as scarps, hummocky topography, convex and concave slope areas, midslope terraces, and offset drainages. Maps were evaluated at scales ranging from 1:30,000 to 1:2,000; mapping was generally performed at 1:5,000. Mapped landforms were evaluated in the field and the maps were revised based on field observations, although very little revision was necessary.

The total number of landslides mapped using LiDAR was about four times that of previously published maps produced using aerial photographs, and the LiDAR-mapped landslides included all shallow and deep landslides depicted in those maps. In addition, 93 % of historical landslides recorded in the Seattle landslide database (Laprade et al. 2000) are within the boundaries of the LiDAR-mapped landslides. Landslides were consistently identified using the LiDAR imagery if they had landslide-related topographic features that were at least 30 m long and local relief of a few meters. Wait's map (2001) was most applicable for comparison to results of the LiDAR study (Schulz 2004, 2007) and used 1:2,000–1:2,500-scale black-and-white, color, and color-infrared aerial photographs taken during March 1974, June 1986 and 1991, and September 1995 and 1997. Evaluation of Wait's map (2001), which identified the most landslides of previous efforts, indicated that aerial photographs were instrumental for identifying recent individual landslides; therefore, aerial photographs appear to be more effective than LiDAR in the Seattle area for discerning boundaries of recently active landslides within landslide complexes. The resolution of the LiDAR data (1.8 m) appeared to be inadequate to resolve many landslide boundaries within landslide complexes. However, LiDAR was much more effective for identifying presumably older landslides and the boundaries of complexes in which recently active landslides occurred (Schulz 2004).

Schulz (2007) found that historical landslides were concentrated within the mapped landslide-derived

landforms, and appeared to generally be located on the steepest parts of slopes. The mapped landforms (landslides, head scarps, and denuded slopes) were created by the temporally integrated influence of many individual landslide events. The landslide, head scarp, and denuded slope landforms cover 4.6 %, 1.2 %, and 9.5 % of Seattle's land area, respectively. The spatial distribution of mapped landforms and 1,308 historical landslides within the Seattle city limits show that historical landslide activity has been concentrated on the mapped landforms, but most of the landslide activity that created the landforms was prehistoric. Thus, the spatial densities of historical landslides within the mapped landforms (122/km², head scarps; 42.8/km² landslides; 23.7/km², denuded slopes), were essentially equivalent to the relative susceptibilities of the landforms to historical and presumably future landsliding. The susceptibilities are relative in that they are only meaningful when compared between landforms or landslides with different characteristics in Seattle.

As with many other landslide inventories, the Seattle landslide inventories constructed using LiDAR, aerial photography, and other means omit many areas prone to landsliding because they exclude excavated landslide scars. Denuded slopes appear to primarily consist of coalescing landslide scars and disrupted, thin landslide deposits. Over 37 % of historical landslides in Seattle occur on LiDAR-mapped denuded slopes, (23 % on head scarps and 33 % on landslides) thus denuded slopes should be considered in regional evaluations of landslide susceptibility even though they have the lowest susceptibility of the three landforms.

By comparing landforms and historical landslide locations with geologic mapping, Schulz (2007) identified no strong relations between stratigraphy and landslide occurrence, regardless of type; however, landslide characteristics and slope morphology appeared to be related to stratigraphic conditions. Human activity was a contributing factor in about 80 % of historical Seattle landslides (Laprade et al. 2000). The distribution of mapped landforms and human-caused landslides suggests the probable characteristics of future human-caused landslides on each of the landforms. The distribution of mapped landforms and historical landslides indicates that erosion of slope-toes by surface water has been a necessary condition for causing Seattle landslides. Through construction of seawalls and related structures, human activity has largely arrested this erosion, which implies that landslide activity will decrease with time as hillsides naturally stabilize. However, landslide activity in Seattle is likely to continue for the foreseeable future.

Assessment of Shallow Landslides Using a Physically Based Model

Godt et al. (2008a) described the results from an application of a distributed, transient infiltration–slope-stability model

for an 18 km² area of southwestern Seattle. They used the USGS model TRIGRS: Transient Rainfall Infiltration and Grid-based Regional Slope-stability analysis (Savage et al. 2003; Baum et al. 2008, 2010) that combines an infinite slope-stability calculation with an analytic, one-dimensional solution for pore-pressure diffusion in a soil layer of finite depth in response to time-varying rainfall. The transient solution for pore-pressure response can be superposed on any steady-state groundwater-flow field that is consistent with model assumptions. Applied over digital topography, the model computes a factor of safety, F , for each grid cell at any time during a rainstorm. Input variables may vary from cell to cell, and the rainfall rate can vary in both space and time. For Seattle, topographic slope derived from a LiDAR-based 3-m digital elevation model (resampled from the 1.8-m data) (DEM) and hourly rainfall intensities were used as model inputs. Maps of soil and water-table depths derived from geotechnical borings and a model for observed, systematic variation of colluvium and groundwater depth in relation to specific landforms and the seepage face of the regional aquifer (Schulz et al. 2008) constrained initial and boundary conditions for the model. Material strength and hydraulic properties used in the model were determined from field and laboratory measurements (Godt and McKenna 2008), and a tension-saturated initial condition was assumed. Because the equations of groundwater flow are explicitly solved with respect to time, the results from TRIGRS simulations can be portrayed quantitatively to assess the potential landslide hazard based on changing rainfall conditions.

Factor of safety results (Fig. 3) were evaluated by comparing the locations of 212 historical shallow landslides (a subset of the historical landslide database used by Schulz 2007) with the area mapped as having a factor of safety less than 1.2. An effective landslide hazard map maximizes the number of historical landslide locations included in a hazard class while minimizing the total area mapped in that class (Chung and Fabbri 2003). In a comparison of shallow landslide locations with the results of the hazard map, Godt et al. (2008a) determined that the most susceptible class ($F < 1.0$) includes only 8.4 % of the area steeper than 20° and contains 26 % of the historical landslides. A cutoff of 20° was selected because nearly all historical shallow landslides have occurred on slopes steeper than 20°. For the entire study area, the TRIGRS map captures almost 92 % of the historical landslides but only identifies 26 % of the area with slope angles greater than 20° as potentially unstable during realistic rainfall conditions for Seattle. Effectiveness ratios, defined as the ratio of the percentage of historical landslides to the percentage of the mapped area in each class, range from 3.0 to 7.5, indicating that each class has discriminatory power (Chung and Fabbri 2003). To capture the same

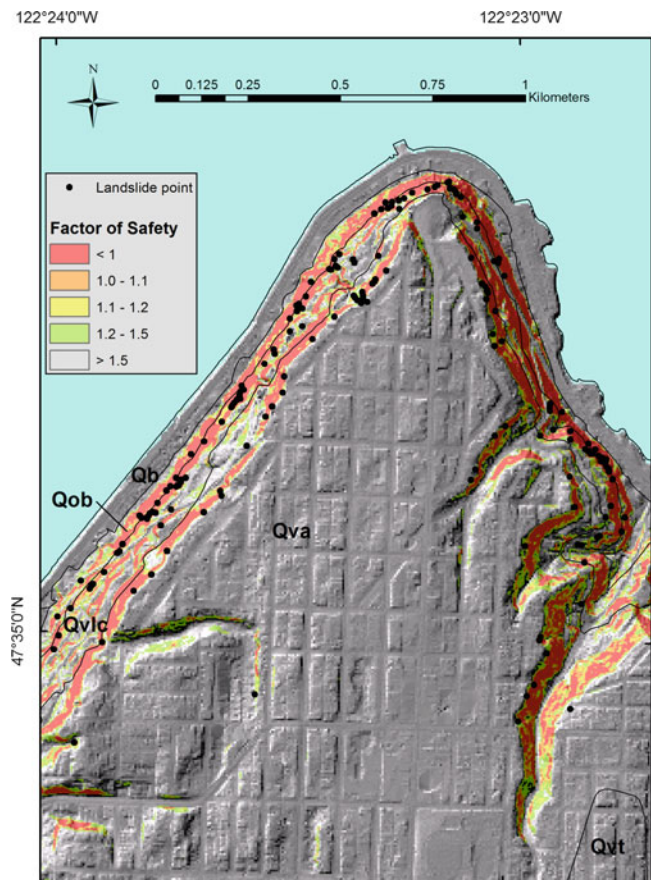


Fig. 3 Map showing part of Godt et al.'s (2008a) factor of safety results for southwest Seattle, computed using the TRIGRS model. Black points indicate locations of historical landslides (center of head scarp, Coe et al. 2004a). The predicted factor of safety is at the end of a simulation of a 28-h rainfall event (17–18 January 1986) that induced many shallow landslides. This simulation used the saturated, finite-depth infiltration solution (Savage et al. 2003; Baum et al. 2008, 2010) and is based on Fig. 14 of Godt et al. (2008a). Geologic contacts are shown as gray lines. Interpretations of geologic unit symbols are Qb—beach deposits, Qvt—Vashon till, Qva—advance outwash deposits of the Vashon Drift, Qvlc—Lawton Clay Member of the Vashon Drift, Qob—Olympia beds (interbedded sand, clayey silt and silty clay)

percentage of historical landslides (92 %) using only topographic slope would require all areas with slope angles greater than 20° to be considered susceptible. Thus, the main discriminatory power of the model, as applied in southwestern Seattle, is its ability to exclude nonsusceptible steep (>20°) hillslope areas from the susceptible classes. This is the result of both the spatially variable input (colluvium thickness and initial water-table depth) and the modeling approach.

Recent advancements with the TRIGRS model include an unsaturated infiltration module (Savage et al. 2004; Baum et al. 2008, 2010), a module for analyzing 3D slope stability (Baum et al. 2012), and progress on methods for specifying

model parameters using sensitivity analyses (Gioia et al. 2013) and using a probabilistic framework (Raia et al. 2013). Figure 4 compares results for the Mukilteo study area north of Seattle using the original 1D saturated infiltration model, the 1D unsaturated infiltration module, and the saturated and unsaturated infiltration models combined with a simple method of columns for 3D slope stability. Landslide polygons depicted in Fig. 4 include the source area and deposit of each shallow landslide that occurred during the winter of 1996–1997 and provide a more complete indication of unstable areas for comparing model results than the landslide points available for southwest Seattle (Fig. 3). Analysis using the Receiver Operating Characteristics (ROC) analysis (Swets 1988; Fawcett 2006), which recently has become widely used (Van den Eeckhaut et al. 2006; Falaschi et al. 2009), indicates lower false positive rates achieved by the 1D unsaturated model compared to the 1D saturated, and improvements of the simple 3D analysis compared to the 1D infinite-slope analysis (greater true positive rate with slight or no reduction in false positive rate). In the case shown, the 3D saturated model predicts a greater fraction of the historical landslides than the unsaturated model, at the expense of higher rate of false positives.

Assessment of Large Landslides with the 3D Slope-Stability Model, SCOOPS

In Seattle, deep-seated landslides on bluffs along Puget Sound have historically caused extensive damage to land and structures. These large landslides are controlled by three-dimensional (3D) variations in material strength and pore-water pressures. The 3D effects of groundwater, geology, and landslide geometry greatly complicate analysis of large, deep landslides when compared to small, shallow slides. Although the infinite slope analysis has been applied successfully to shallow landslides, especially where the landslides are close to the size of the DEM grid cells, infinite slope analysis is generally inadequate for large deep landslides. USGS researchers have developed a computer program, SCOOPS (Reid et al. 2000), to assess the slope stability of a digital landscape, as represented by a DEM. SCOOPS has been used to assess the relative stability of volcanic edifices (Reid et al. 2000, 2001, 2010) as well as other settings where large landslides might occur (Brien and Reid 2007, 2008). SCOOPS calculates slope stability by extending conventional two-dimensional (2D) limit-equilibrium analysis to three dimensions (3D) using a method of columns. SCOOPS systematically searches a digital landscape and computes the stability of millions of potential landslides encompassing a wide range of depths and volumes that potentially affect different parts of the DEM, thereby allowing determination of the minimum factor of safety at each DEM cell.

Brien and Reid (2007, 2008) assessed the slope stability of part of southwestern Seattle using SCOOPS coupled with a 3D groundwater flow model (MODFLOW-2000, Harbaugh et al. 2000). The availability of high- (3-m-) resolution digital topography, detailed geologic mapping (1: 12,000 scale, Troost et al. 2005), and a compilation of subsurface exploration logs were used to build 3D models of geology, groundwater, and slope stability. In order to assess the relative stability of coastal bluffs for potential large deep-seated landslides, digital topography (represented by a DEM) was combined with 3D interpretations of geologic mapping and published strength values for the geologic units. The 3D geologic model (Fig. 5) consists of four layers derived from the mapped geologic units. The influence of 3D pore pressures was incorporated based on the results of a 3D groundwater flow model using MODFLOW-2000, calibrated with measured groundwater levels.

The geology of the Seattle area consists of a layer of permeable glacial outwash sand overlying less permeable glacial lacustrine silty clay (Troost et al. 2005). Incorporation of these layers as hydrogeologic units in a 3D groundwater model reproduced an elevated water table above the less permeable units. This water table produces elevated pore pressures in the uppermost hydrogeologic unit, hence a destabilizing factor. The simulated 3D pore-pressure distribution from average rainy season and extreme rainy season recharge scenarios were then used to quantify the stability of the coastal bluffs in SCOOPS. Figure 6 shows factor of safety results for three potential scenarios: (a) moderately large potential landslides (3,000–30,000 m³) with average rainy season recharge, (b) moderately large potential landslides with extreme rainy season recharge, and (c) very large potential landslides (30,000–300,000 m³) with extreme rainy season recharge. The analyses indicate that the least stable areas (low values of *F*, Fig. 6) are steep portions of the uppermost geologic unit, a permeable sand (Q_{va}, see Fig. 5). The elevated pore pressures in this geologic unit produce a destabilizing factor and low factors of safety compared to steep areas in other geologic units. This result is consistent with historical observations of the location of deep-seated landslides. Regions predicted to be least stable include the areas in or adjacent to three mapped historically active deep-seated landslides. Groundwater flow also converges in coastal reentrants, resulting in elevated pore pressures and destabilization of slopes in reentrant regions. As expected, areas of low factor of safety expand with extreme rainy season conditions. Factor of safety greatly decreases in the topographic re-entrants where groundwater flow is concentrated due to topographic convergence. The results of the 3D analyses differ significantly from a slope map or results from one-dimensional (1D) analyses of shallow landslide potential (Fig. 3).

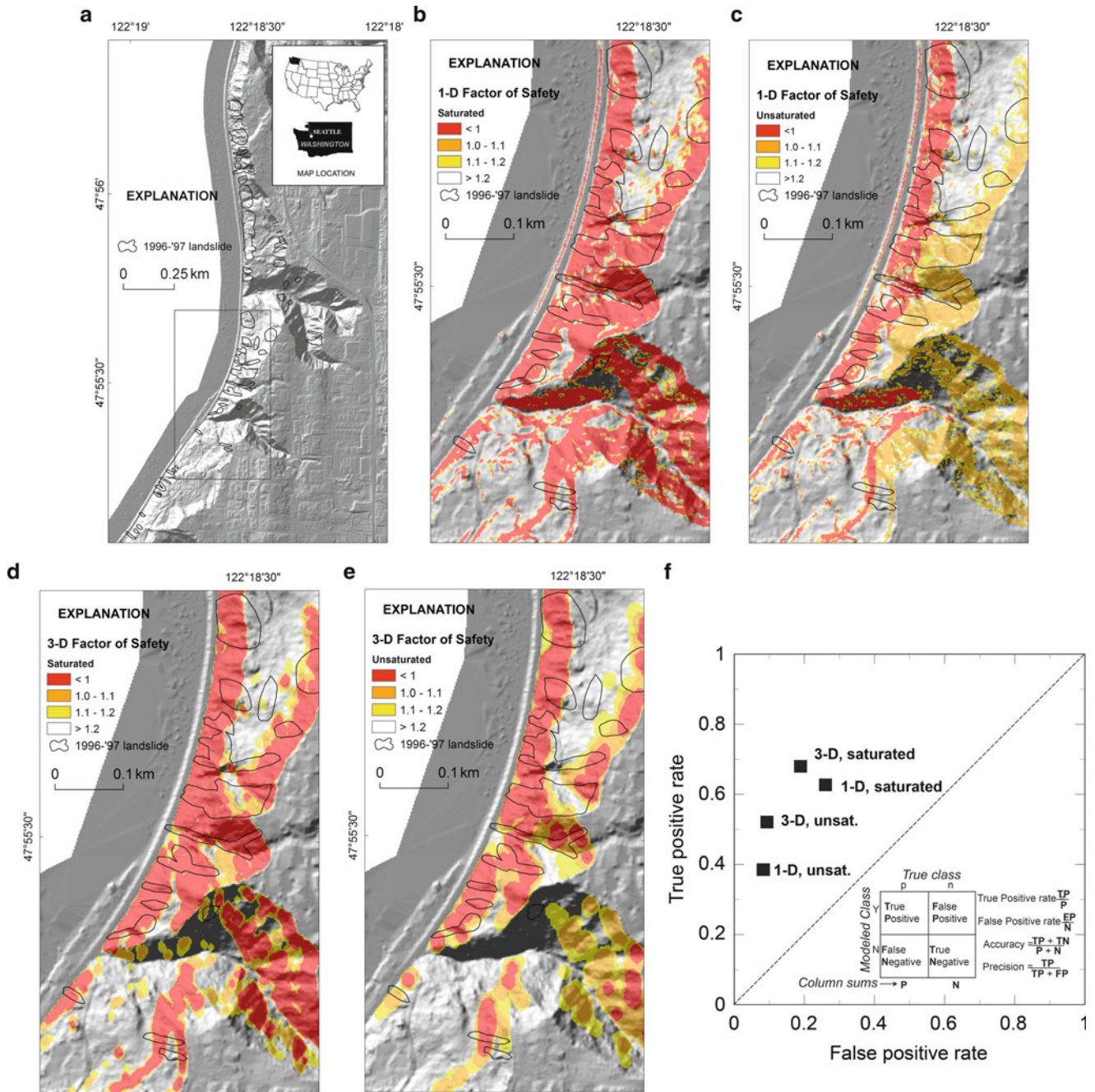


Fig. 4 Maps and diagrams showing factor of safety computed using the TRIGRS model for the Mukilteo study area, about 15 km north of Seattle. (a) Location and outlines (scarp and deposit) of 1996–1997 shallow landslides. Rectangle indicates area shown in (b–e). Factor of safety results for (b) saturated infiltration and 1D infinite-slope analysis (Godt et al. 2008b), (c) unsaturated infiltration and 1D infinite-slope

analysis (Baum et al. 2010), (d) saturated infiltration and simplified 3D limit-equilibrium slope stability analysis, (e) unsaturated infiltration and simplified 3D limit-equilibrium slope stability analysis (Baum et al. 2012) are (f) compared for performance using a Receiver-Operating Characteristics (ROC) plot. A perfect prediction would plot at the upper left corner of the ROC plot

Composite Landslide Assessment

One of the advantages of using different approaches to assess landslide hazard is the ability to make a composite map showing all hazardous areas identified by the different approaches. A composite or ensemble map can reduce the

uncertainty about where landslides might happen by combining the results of different analyses that address the potential for specific types of landslides. Some technical challenges exist in combining the results of different mapping approaches to create a defensible composite (i.e.,

a map created using an objective, reproducible, and quantitatively rigorous method). To combine the two factor of safety maps, (Figs. 3 and 6), which have continuous values, with the geomorphologically based map of landslide-derived landforms, (Fig. 2), we arbitrarily assigned factor of safety

values to each landform type (head scarps, 0.99; landslide deposits, 1.099; and denuded slopes, 1.199) based on relative density of historical landslides in each. We then assigned the lowest factor of safety (corresponding to the highest susceptibility) among the three input maps to the composite map.

Figure 7 shows a composite map that combines the areas identified by the geomorphological approach (Schulz 2007), the analysis for shallow landslide potential (Godt et al. 2008a), and the analysis for deep landslide potential (Brien and Reid 2008). This map displays the highest susceptibility level identified at each grid cell by the component maps to show the “worst” case. Whereas the map includes many areas that would be included on a slope map, it also includes some susceptible areas of low slope and areas of medium landslide susceptibility are quite different than would be predicted based on slope alone. Such a map can be used as an initial screening tool to identify areas that have high, moderate, or low composite landslide potential, without being specific about the particular landslide type. This assumes that the high, moderate, and low potential areas on the three component maps are equivalent. Equivalent classes might be established, for example, by setting the boundaries for high, medium, and low on the factor of safety maps equal to densities of corresponding landslide types on the landform map.

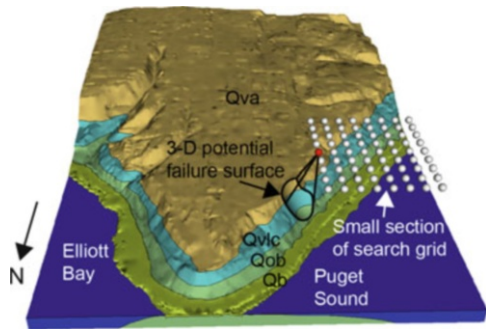


Fig. 5 Perspective view, looking south, of the topography in the southwestern Seattle study area (Fig. 1) with an example of a potential failure removed. The view shows the 3D geologic model, and one layer of a small section of a coarse-resolution search grid used in SCOOPS. Geology is a 3D interpretation (Brien and Reid 2007, 2008) of the geologic map by Troost et al. (2005). Topography is from the City of Seattle 3-m DEM (2000, written commun.) (after Brien and Reid 2008, Fig. 5). Interpretations of geologic unit symbols are Qb—beach deposits, Qvt—Vashon till, Qva—advance outwash deposits of the Vashon Drift, Qvlc—Lawton Clay Member of the Vashon Drift, Qob—Olympia beds (interbedded sand, clayey silt and silty clay)

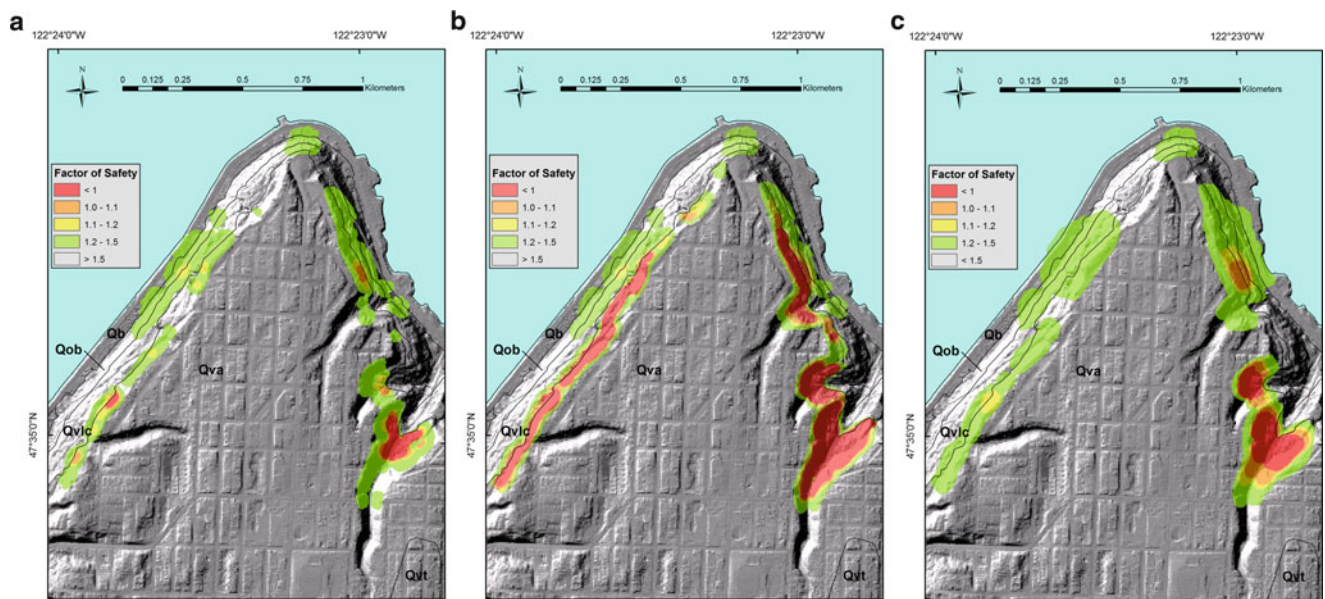


Fig. 6 Map images showing factor of safety (F), computed using the slope-stability model SCOOPS, for 3D critical surfaces with associated volumes between 3,000 and 300,000 m³. A critical surface is the potential failure with the lowest F at each digital elevation model cell. F is indicated by color. Results are shown for (a) moderately large potential landslides (3,000–30,000 m³) with average rainy season recharge, and (b) moderately large potential landslides with extreme

rainy season recharge, and (c) very large potential landslides (30,000–300,000 m³) with extreme rainy season recharge. Geologic contacts are shown as gray lines. Interpretations of geologic unit symbols are Qb—beach deposits, Qvt—Vashon till, Qva—advance outwash deposits of the Vashon Drift, Qvlc—Lawton Clay Member of the Vashon Drift, Qob—Olympia beds (interbedded sand, clayey silt and silty clay) [modified from Brien and Reid (2008), Fig. 8]

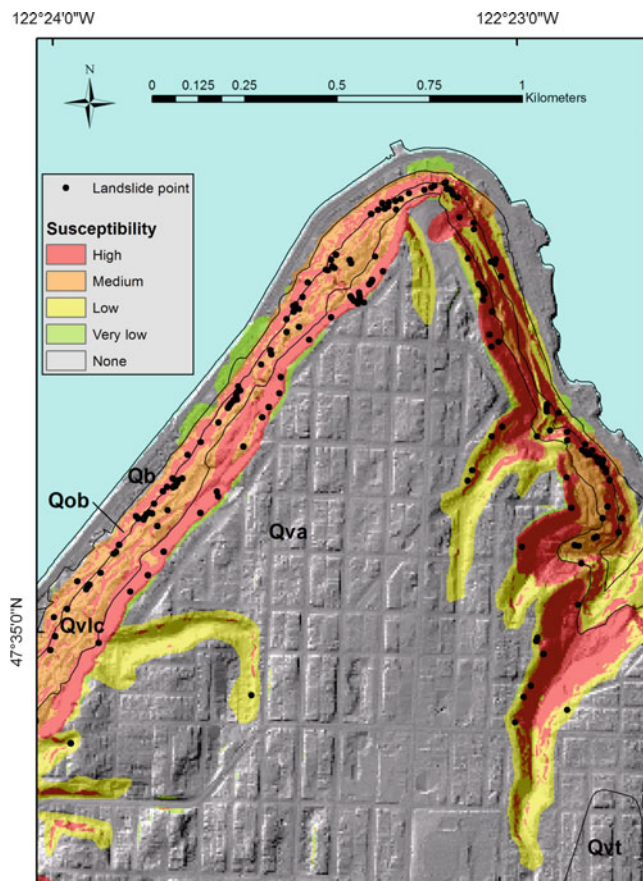


Fig. 7 Composite landslide susceptibility map showing worst susceptibility class (high, medium, low) for each pixel based on results shown in Figs. 2, 3, and 6b. Geologic contacts are shown as gray lines. Interpretations of geologic unit symbols are Qb—beach deposits, Qvt—Vashon till, Qva—advance outwash deposits of the Vashon Drift, Qvlc—Lawton Clay Member of the Vashon Drift, Qob—Olympia beds (interbedded sand, clayey silt and silty clay)

Relating the landforms and the factor of safety to historical landslide density might allow a more rigorous assignment of factor of safety to the landforms. We did not attempt this for the map shown in Fig. 7, due to the different extent of areas considered in each analysis. Taking this idea a step further, the landslide density could be used to estimate landslide probability by adding a temporal frequency corresponding to computed values of factor of safety for shallow (Fig. 3) and deep landslides (Fig. 6) respectively and within each landform type (Fig. 2). A composite map depicting maximum landslide probability drawn from the three analyses (shallow landslides, deep landslides, and landslide landforms) would present a somewhat different picture than Fig. 7, because it would explicitly consider the lower frequency of large, deep landslides. In other words, the weight given to each of the three maps in defining the composite would be different.

Standardized Methods and Rapid Assessments

Improvements in technology for remote sensing, increasingly rapid dissemination of remotely sensed spatial data, and GIS have made it possible to standardize methods for rapidly conducting regional landslide hazard assessments. For example, Cannon et al. (2010) developed tools for assessing the potential for debris flows in previously burned areas. These assessments can be completed in a matter of days after containment of a wildfire. Similarly, Harp et al. (2009) devised methods for rapidly assessing potential for future precipitation-induced landslides after a major storm. Their method makes use of a landslide inventory for a single event (i.e., the major storm) to calibrate a factor of safety model; this has been accomplished even in developing areas (Honduras, Micronesia) where few or no geotechnical data are available. In 2005, the Oregon Department of Geology and Mineral Industries (DOGAMI) began a collaborative landslide research program with the USGS Landslide Hazards Program to identify and understand landslide hazards in Oregon, USA. A major result of this collaboration has been development of standard procedures (protocols) for landslide mapping and susceptibility analysis. These procedures made it possible to map large areas in Oregon uniformly.

Oregon Landslide Mapping Protocol

Landslides are one of the most widespread, frequent, and damaging natural hazards in the state of Oregon (Burns and Madin 2009). To create a consistent landslide inventory for Oregon as a starting point for assessing landslide hazard, DOGAMI developed a protocol for mapping recent and prehistoric landslides using LiDAR imagery (Burns and Madin 2009). Encouraged by the findings of Schulz (2004, 2007), a pilot project area was selected in western Oregon to compare remote sensing data/images for effectiveness (Burns 2007). Data considered in the study included 30-m SRTM, 10-m USGS DEM, 7-m City of Portland DEM, 1-m LiDAR DEM, and stereo color aerial photography. Two key findings from this pilot study were: the use of 1-m LiDAR data (1) resulted in identification of 3–200 times the number of landslides found with the other data sets, consistent with findings in Seattle (Schulz 2004, 2007), and (2) greatly improved the accuracy of the spatial extent of the landslides thus identified. Consequently, LiDAR-derived digital elevation models were selected as the base from which to create the landslide inventories throughout Oregon. The inventory includes all landslides, distinguished by type and recency, that can be identified using the LiDAR imagery, as well as any landslides known from previous inventories. Creating the protocol and its associated map template and geodatabase has somewhat streamlined mapping and publication of landslide inventory data. Following a standard

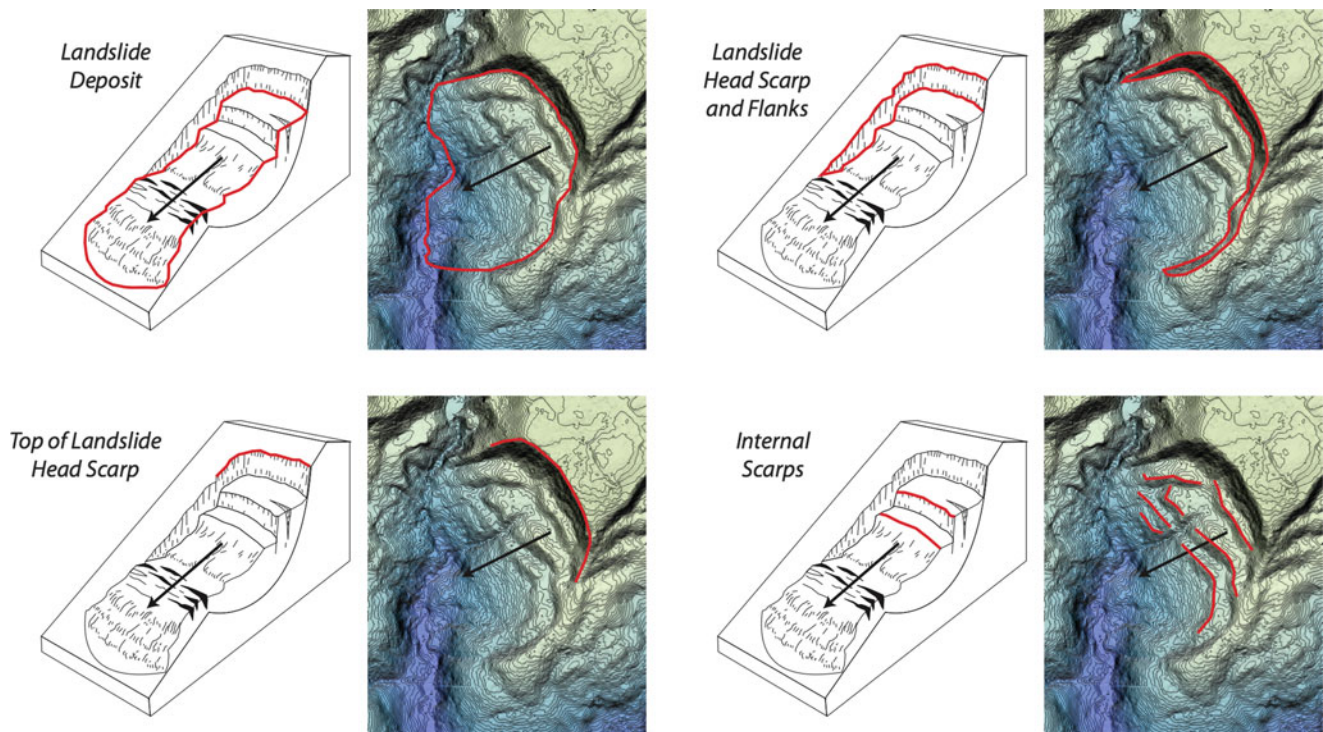


Fig. 8 Block diagrams and map views showing the four kinds of landslide features that are routinely identified and mapped using the Oregon landslide mapping protocol [after Burns and Madin (2009), Fig. 12]

procedure reduces time required to map the landslides and record the attributes by eliminating the need for the mapper to experiment with visualization techniques or decide what attributes to map. Nevertheless, successful adaptation of the protocol requires a mapper with a reasonable level of expertise on the topic and time to represent all the features. Using the map template and referencing the protocol (Burns and Madin 2009) similarly simplifies the effort needed to prepare the map for publication.

The inventory mapping protocol prescribes procedures for base data acquisition and visualization, mapping landslide features and recording attributes in GIS, field checking, a map template for displaying results, and outlines limitations and recommended use of the landslide inventory data produced by the process (Burns and Madin 2009). The method relies on use of several types of base data: a 1-m DEM derived from LiDAR data with point density averaging 1 m^{-2} or better, a slope map derived from LiDAR data, orthorectified aerial photo of similar age to the LiDAR data, previous landslide inventories or other data on landslides within the proposed mapping area, and a geologic map. Through trial and error, Burns and Madin (2009) determined optimal procedures for visualizing the data to accurately identify landslides and map landslide features, such as, head scarps and internal scarps (Fig. 8). These features are useful in assessing confidence of landslide identification, and scarp height is useful in estimating minimum landslide

depth. They also developed a geodatabase template for acquiring landslide attribute data, including classification, dimensions and other quantitative data, confidence of interpretation, and geologic unit. Thus, the protocol includes not only recommended procedures for mapping landslides using LiDAR data, but also specific guidance on setting up the GIS geodatabase necessary for mapping and recording tabular data about each landslide. The final product is a map and database of landslide deposits and features at a scale of 1:8,000, tiled by quarters of USGS 7.5-min quadrangles (Fig. 9).

Oregon Shallow Landslide Susceptibility Protocol

In addition to the landslide inventory mapping protocol, DOGAMI developed a standardized procedure for developing shallow-landslide susceptibility maps. The shallow-landslide susceptibility map protocol combines an inventory of existing landslides, as described previously (Burns and Madin 2009) with hazard zones derived from a Factor of Safety map and buffers (Burns et al. 2012). This protocol also includes a map template for producing a standardized shallow-landslide susceptibility map at a scale of 1:8,000. For purposes of this protocol, DOGAMI defined 4.6 m as the depth boundary between shallow and deep landslides. Like the protocol for mapping landslides described in previous paragraphs, the protocol includes not only recommended procedures for mapping susceptibility to shallow landslides

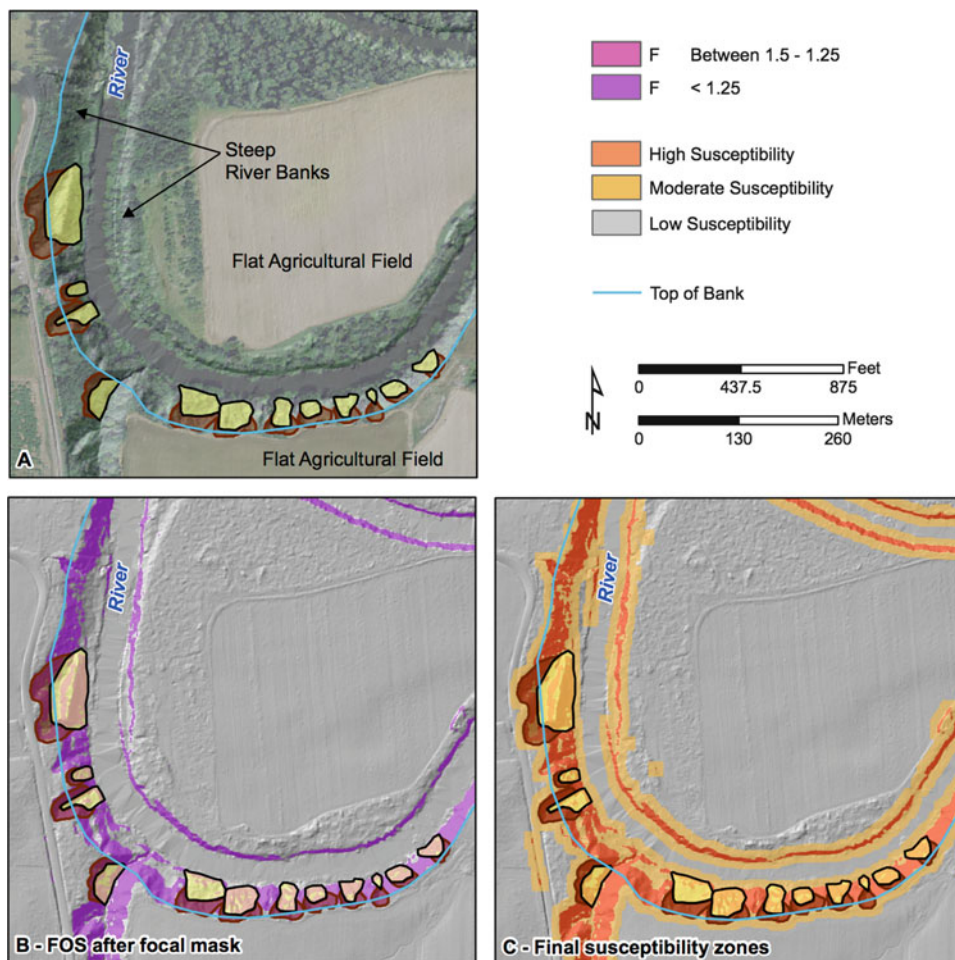


Fig. 10 Sample maps illustrating head-scarp and Factor of Safety, F , buffer components (Table 1) of Oregon’s shallow landslide susceptibility protocol. (a) Landslide inventory (landslide deposits shown as yellow polygons and head scarps shown as red polygons) displaying the

top of head scarps above the top of the locally steep slope (riverbank) area. (b) F zone map filtered to remove artifacts from low-relief features. (c) Filtered F zone map with head scarp and F buffers added [modified from Burns et al. (2012), Fig. 21]

and other properties of the subsurface that affect slope stability. Surrogates for these factors, such as geological or soils map units, vegetation type, and others too numerous to list, that are commonly used in statistically based regional assessments are likewise subject to uncertainty due to transitional or obscure contacts, with unknown subsurface geometry, and sometimes subtle or subjective differences between map units. Effects of land use and land-use changes, as well as temporal climate variability, likewise introduce uncertainty into hazard assessments. As a result of these sources of uncertainty, probabilistic frameworks are commonly needed to couch the results of hazard assessments. Regardless of expected advances in probabilistic analysis, which will surely help, major future progress in landslide hazard assessment will in large measure depend on progress in reducing data uncertainty.

Despite the difficulties imposed by data uncertainty, technological advancements have enabled significant progress. High-resolution topographic data, particularly when used in combination with high-resolution optical imagery, can contribute to greatly improved mapping and identification of landslide deposits and features as demonstrated by recent work (Schulz 2004, 2007; Burns 2007; Burns and Madin 2009; Roering et al. 2009). This is encouraging because high-quality landslide inventories are the backbone of regional and medium-scale landslide hazard assessments (Harp et al. 2011) and besides topography and optical imagery, few other data that are needed to specify landslide susceptibility or slope stability model parameters exist in many areas of the world.

Improvements to deterministic models, such as those demonstrated here, are contributing to progress in

regional landslide hazard assessment by making better use of those data that are available and making better estimates of potential landslide volume (Brien and Reid 2007, 2008). As GIS-based models of slope stability continue to improve and become integrated with models for debris flow and debris avalanche runout (Schilling 1998; Griswold and Iverson 2008), they can contribute to better estimates of downslope areas potentially impacted by landslides. Recent and ongoing research to improve models for predicting or mapping soil or colluvial depth is also expected to contribute to more accurate assessments of shallow landslide hazard (Dietrich et al. 1995; Roering 2008; Schulz et al. 2008; Pelletier and Rasmussen 2009; Catani et al. 2010; Ho et al. 2012). Ongoing work in model parameterization using sensitivity and probabilistic approaches combined with analysis of one or more historical landslide events is showing promise as a way to calibrate deterministic models (Gioia et al. 2013; Raia et al. 2013). These developments can make deterministic models useful in a wider range of settings, because even in many highly developed countries, few relevant data are available for most areas and spatial distribution of important factors is rarely known in sufficient detail.

Data and model uncertainty will always exist even as models improve and technological advancements make it possible to reduce uncertainty in certain types of spatial data. Nevertheless, if the current momentum of technological advancement and landslide hazard research continues unabated throughout the next decade, we can look forward to considerable progress in understanding and modeling where, when, and how often landslides are likely to occur. We can also expect advances in predicting their volumes and extents and being able to apply that knowledge to regional assessments of landslide hazard.

Acknowledgments Jeff Coe and Kevin Schmidt (both USGS) provided constructive reviews of the manuscript.

Disclaimer Any use of trade, product, or firm names in this publication is for descriptive purposes only and does not imply endorsement by the U.S. Government.

References

- Aleotti P, Chowdury R (1999) Landslide hazard assessment: summary review and new perspectives. *Bull Eng Geol Env* 58:21–44
- Artim ER (1976) Slope stability map of Thurston County, Washington. Geologic Map GM-15, Division of Geology and Earth Resources, Washington Department of Natural Resources, Olympia, WA, USA, 1:125,000
- Baum RL, Coe JA, Godt JW, Harp EL, Reid ME, Savage WZ, Schulz WH, Brien DL, Chleborad AF, McKenna JP, Michael JA (2005) Regional landslide-hazard assessment for Seattle, Washington, USA. *Landslides* 2(4):266–279. doi:10.1007/s10346-005-0023-y
- Baum RL, Savage WZ, Godt JW (2008) TRIGRS—A FORTRAN program for transient rainfall infiltration and grid-based regional slope-stability analysis, version 2.0. US Geological Survey Open-File Rep 2008-1159. <http://pubs.er.usgs.gov/publication/ofr20081159>
- Baum RL, Godt JW, Savage WZ (2010) Estimating the timing and location of shallow rainfall-induced landslides using a model for transient, unsaturated infiltration. *J Geophys Res* 115:F03013. doi:10.1029/2009JF001321
- Baum RL, Godt JW, Coe JA, Reid ME (2012) Assessment of shallow landslide potential using 1-D and 3-D slope stability analysis. In: Eberhardt E, Froese C, Turner AK, Leroueil S (eds) *Landslides and engineered slopes: protecting society through improved understanding*. Taylor & Francis, London, pp 1667–1672
- Berti M, Simoni A (2007) Prediction of debris flow inundation areas using empirical mobility relationships. *Geomorphology* 90 (1–2):144–161
- Borga M, Fontana GD, Ros DD, Marchi L (1998) Shallow landslide hazard assessment using a physically based model and digital elevation data. *Environ Geol* 35(2–3):81–88. doi:10.1007/s002540050295
- Brabb EE, Pampeyan EH, Bonilla MG (1972) Landslide susceptibility in San Mateo County, California. US Geological Survey Miscellaneous Field Studies Map 360, 1:24,000
- Brien DL, Reid ME (2007) Modeling 3-D slope stability of coastal bluffs using 3-D ground-water flow, southwestern Seattle, Washington. US Geological Survey Scientific Investigations Report 2007-5092. <http://pubs.usgs.gov/sir/2007/5092/>
- Brien DL, Reid ME (2008) Assessing deep-seated landslide susceptibility using 3-D groundwater and slope-stability analyses, southwestern Seattle, Washington. In: Baum RL, Godt JW, Highland LM (eds) *Engineering geology and landslides of the Seattle, Washington, area*, vol 20, Geological Society of America reviews in engineering geology. Geological Society of America, Boulder, pp 83–101. doi:10.1130/2008.4020(05)
- Burns WJ (2007) Comparison of remote sensing data-sets for the establishment of a landslide mapping protocol in Oregon. Conference presentations, 1st North American landslide conference, AEG Special Publication 23, Vail, CO
- Burns WJ, Madin IP (2009) Protocol for inventory mapping of landslide deposits from light detection and ranging (LiDAR) imagery. Oregon Department of Geology and Mineral Industries Special Paper 42
- Burns WJ, Madin IP, Mickelson KA (2012) Protocol for shallow landslide susceptibility mapping. Oregon Department of Geology and Mineral Industries Special Paper 45
- Cannon SH, Gartner JE, Rupert MG, Michael JA, Rea AH, Parrett C (2010) Predicting the probability and volume of postwildfire debris flows in the intermountain western United States. *Bull Geol Soc Am* 122(1–2):127–144
- Carrara A (1983) Multivariate models for landslide hazard evaluation. *Math Geol* 15(3):403–426
- Carrara A, Cardinali M, Detti R, Guzzetti F, Pasqui V, Reichenbach P (1991) GIS techniques and statistical models in evaluating landslide hazard. *Earth Surf Process Landforms* 16:427–445
- Carrara A, Guzzetti F, Cardinali M, Reichenbach P (1999) Use of GIS technology in the prediction and monitoring of landslide hazard. *Nat Hazards* 20:117–135. doi:10.1023/A:1008097111310
- Catani F, Segoni S, Falorni G (2010) An empirical geomorphology-based approach to the spatial prediction of soil thickness at catchment scale. *Water Resour Res* 46, W05508. doi:10.1029/2008WR007450

- Chung CF, Fabbri AG (2003) Validation of spatial prediction models for landslide hazard mapping. *Nat Hazards* 30:451–472. doi:[10.1023/B:NHAZ.0000007172.62651.2b](https://doi.org/10.1023/B:NHAZ.0000007172.62651.2b)
- Chung CJ, Fabbri A, van Westen CJ (1995) Multivariate regression analysis for landslide hazard zonation. In: Carrara A, Guzetti F (eds) *Geographical information systems in assessing natural hazards*. Kluwer Publications, Dordrecht, pp 107–133
- Coe JA, Michael JA, Crovelli RA, Savage WZ, Laprade WT, Nashem WD (2004a) Probabilistic assessment of precipitation-triggered landslides using historical records of landslide occurrence, Seattle, Washington. *Environ Eng Geosci* 10(2):103–122
- Coe JA, Godt JW, Baum RL, Bucknam RC, Michael JA (2004b) Landslide susceptibility from topography in Guatemala. In: Lacerda WA et al (eds) *Landslides, evaluation and stabilization*. Proceedings of the 9th international symposium on landslides, vol 1. Rio de Janeiro, pp 69–79
- Crosta GB, Frattini R (2003) Distributed modeling of shallow landslides triggered by intense rainfall. *Nat Hazards Earth Syst Sci* 3:81–93
- Dai FC, Lee CF (2003) A spatiotemporal probabilistic modelling of storm induced shallow landsliding using aerial photographs and logistic regression. *Earth Surf Process Landforms* 28(5):527–545
- Dai FC, Lee CF, Ngai YY (2002) Landslide risk assessment and management: an overview. *Eng Geol* 64(1):65–87
- Dietrich WE, Reiss R, Hsu M-L, Montgomery DR (1995) A process-based model for colluvial soil depth and shallow landsliding using digital elevation data. *Hydrol Process* 9:383–400. doi:[10.1002/hyp.3360090311](https://doi.org/10.1002/hyp.3360090311)
- Ellen SD, Mark RK, Cannon SH, Knifong DL (1993) Map of debris-flow hazard in the Honolulu District of Oahu, Hawaii. US Geological Survey Open-File Report, pp 93–213, 1:30,000
- Falaschi F, Giacomelli F, Federici PR, Puccinelli A, D’Amato Avanzi G, Pochini A, Ribolini A (2009) Logistic regression versus artificial neural networks: landslide susceptibility evaluation in a sample area of the Serchio River valley, Italy. *Nat Hazards* 50:551–569. doi:[10.1007/s11069-009-9356-5](https://doi.org/10.1007/s11069-009-9356-5)
- Fawcett T (2006) An introduction to ROC analysis. *Pattern Recognit Lett* 27:861–874
- Felicitísimo ÁM, Cuartero A, Remondo J, Quirós E (2013) Mapping landslide susceptibility with logistic regression, multiple adaptive regression splines, classification and regression trees, and maximum entropy methods: a comparative study. *Landslides* 10(2):175–189
- Franciss FO (2004) Landslide hazard assessment on hilly terrain. In: Lacerda WA, Ehrlich M, Fontoura SAB, Sayão ASF (eds) *Landslides—evaluation and stabilization*. Proceedings of the 9th international symposium on landslides, vol 1. Balkema, Rio de Janeiro, Brazil, pp 143–150
- Frattini P, Crosta GB, Fusi N, Dal Negro P (2004) Shallow landslides in pyroclastic soils, a distributed modeling approach for hazard assessment. *Eng Geol* 73(3–4):277–295. doi:[10.1016/j.enggeo.2004.01.009](https://doi.org/10.1016/j.enggeo.2004.01.009)
- Gioia E, Speranza G, Ferretti M, Marincioni F, Godt JW, Baum RL (2013) Rainfall induced shallow landslide forecasting in large areas: application of the TRIGRS model over a broad area of post-orogenic Quaternary sediments (Abstract). *Geol Soc Am Abs Prog* 45(7):775
- Godt JW, McKenna JP (2008) Numerical modeling of rainfall thresholds for shallow landsliding in the Seattle, Washington, area. In: Baum RL, Godt JW, Highland LM (eds) *Engineering geology and landslides of the Seattle, Washington, area*, vol 20, Geological Society of America reviews in engineering geology. Geological Society of America, Boulder, CO, pp 121–135. doi:[10.1130/2008.4020\(07\)](https://doi.org/10.1130/2008.4020(07))
- Godt JW, Schulz WH, Baum RL, Savage WZ (2008a) Modeling rainfall conditions for shallow landsliding in Seattle, Washington. In: Baum RL, Godt JW, Highland LM (eds) *Engineering geology and landslides of the Seattle, Washington, area*, vol 20, Geological Society of America reviews in engineering geology. Geological Society of America, Boulder, CO, pp 137–152. doi:[10.1130/2008.4020\(08\)](https://doi.org/10.1130/2008.4020(08))
- Godt JW, Baum RL, Savage WZ, Salciarini D, Schulz WH, Harp EL (2008b) Transient deterministic shallow landslide modeling: requirements for susceptibility and hazard assessments in a GIS framework. *Eng Geol* 102:214–226. doi:[10.1016/j.enggeo.2008.03.019](https://doi.org/10.1016/j.enggeo.2008.03.019)
- Godt JW, Coe JA, Baum RL, Highland LM, Keaton JR, Roth RJ Jr (2012) Prototype landslide hazard map of the conterminous United States. In: Eberhardt E, Froese C, Turner AK, Leroueil S (eds) *Landslides and engineered slopes: protecting society through improved understanding*. Taylor & Francis Group, London, pp 245–250
- Griswold JP, Iverson RM (2008) Mobility statistics and automated hazard mapping for debris flows and rock avalanches. US Geological Survey Scientific Investigations Report: 2007-5276
- Guzzetti F, Carrara A, Cardinali M, Reichenbach P (1999) Landslide hazard evaluation: a review of current techniques and their application in a multi-scale study, Central Italy. *Geomorphology* 31(1–4):181–216. doi:[10.1016/S0169-555X\(99\)00078-1](https://doi.org/10.1016/S0169-555X(99)00078-1)
- Haneberg WC (2008) Elevation errors in a LiDAR digital elevation model of West Seattle and their effects on slope stability calculations. In: Baum RL, Godt JW, Highland LM (eds) *Engineering geology and landslides of the Seattle, Washington, area*, vol 20, Geological Society of America reviews in engineering geology. Geological Society of America, Boulder, CO, pp 55–65. doi:[10.1130/2008.4020\(03\)](https://doi.org/10.1130/2008.4020(03))
- Harbaugh AW, Banta ER, Hill MC, McDonald MG (2000) MODFLOW-2000, the US Geological Survey modular groundwater model—user guide to modularization concepts and the ground-water flow process. US Geological Survey Open-File Report 00-92
- Harp EL, Noble MA (1993) An engineering rock classification to evaluate seismic rock-fall susceptibility and its application to the Wasatch Front. *Bull Assoc Eng Geol* 30:293–319
- Harp EL, Michael JA, Laprade WT (2006) Shallow-landslide hazard map of Seattle, Washington. US Geological Survey Open-File Report 2006-1139. <http://pubs.usgs.gov/of/2006/1139/>
- Harp EL, Michael JA, Laprade WT (2008) Shallow landslide hazard map of Seattle, Washington. In: Baum RL, Godt JW, Highland LM (eds) *Engineering geology and landslides of the Seattle, Washington, area*, vol 20, Geological Society of America reviews in engineering geology. Geological Society of America, Boulder, CO, pp 67–82. doi:[10.1130/2008.4020\(04\)](https://doi.org/10.1130/2008.4020(04))
- Harp EL, Reid ME, McKenna JP, Michael JA (2009) Mapping of hazard from rainfall-triggered landslides in developing countries: examples from Honduras and Micronesia. *Eng Geol* 104:295–311
- Harp EL, Keefer DK, Sato HP, Yagi H (2011) Landslide inventories: the essential part of seismic landslide hazard analyses. *Eng Geol*. doi:[10.1016/j.enggeo.2010.06.013](https://doi.org/10.1016/j.enggeo.2010.06.013)
- Harp EL, Hartzell SH, Jibson RW, Ramirez-Guzman L (2012) Relation of landslides triggered by the Kiholo Bay earthquake and modeled ground motion. In: Eberhardt E, Froese C, Turner AK, Leroueil S (eds) *Landslides and engineered slopes: protecting society through improved understanding*. CRC, London, pp 507–510
- Ho J-Y, Lee KT, Chang TC, Wang Z-Y, Liao Y-H (2012) Influences of spatial distribution of soil thickness on shallow landslide prediction. *Eng Geol* 124:38–46
- Jibson RW, Harp EL, Michael JA (2000) A method for producing digital probabilistic seismic landslide hazard maps. *Eng Geol* 58:271–289
- Kirschbaum DB, Adler R, Hong Y, Hill S, Lerner-Lam AL (2010) A global landslide catalog for hazard applications—method, results and limitations. *Nat Hazards* 52(3):561–575

- Laprade WT, Kirkland TE, Nashem WD, Robertson CA (2000). Seattle landslide study. Shannon & Wilson, Inc. Internal Report W-7992 - 01. 164 pp. http://www.seattle.gov/dpd/cms/groups/pan/@pan/documents/web_informational/dpdp025740.pdf
- Lee S, Ryu J-H, Min K, Won J-S (2003) Landslide susceptibility analysis using GIS and artificial neural network. *Earth Surf Process Landforms* 28(12):1361–1376
- Lu P, Rosenbaum MS (2003) Artificial neural networks and grey systems for the prediction of slope stability. *Nat Hazards* 30(3):383–398
- Magirl CS, Griffiths PG, Webb RH (2010) Analyzing debris flows with the statistically calibrated empirical model LAHARZ in southeastern Arizona, USA. *Geomorphology* 119:111–124
- Miller RD (1973) Map showing relative slope stability in part of west-central King County, Washington. US Geological Survey Miscellaneous Investigations Series Map, I-852-A, 1:48,000
- Miller DJ (1995) Coupling GIS with physical models to assess deep-seated landslide hazards. *Environ Eng Geosci* 1(3):263–276
- Montgomery DR, Dietrich WE (1994) A physically based model for the topographic control on shallow landsliding. *Water Resour Res* 30(4):1153–1171. doi:10.1029/93WR02979
- Montgomery DR, Sullivan K, Greenberg HM (1998) Regional test of a model for shallow landsliding. *Hydrol Process* 12(6):943–955. doi:10.1002/(SICI)1099-1085(199805)12:6:943:AID-HYP664.3.CO;2-Z
- Ohlmacher GC, Davis JC (2003) Using multiple logistic regression and GIS technology to predict landslide hazard in northeast Kansas, USA. *Eng Geol* 69(3–4):331–343
- Pack RT, Tarboton DG, Goodwin CN (1998) The SINMAP approach to terrain stability mapping. In: Proceedings of the 8th international congress of the international association of engineering geology and the environment, Vancouver, British Columbia, Canada, September 21–25, vol 2. AA Balkema, Rotterdam, pp 1157–1165
- Pelletier JD, Rasmussen C (2009) Geomorphically based predictive mapping of soil thickness in upland watersheds. *Water Resour Res* 45, W09417. doi:10.1029/2008WR007319
- Petley D (2012) Global patterns of loss of life from landslides. *Geology* 40(10):927–930
- Raia S, Alvioli M, Rossi M, Baum RL, Godt JW, Guzzetti F (2013) Improving predictive power of physically based rainfall-induced shallow landslide models: A probabilistic approach. *Geosci Model Dev Discuss* 6:1367–1426. doi:10.5194/gmdd-6-1367-2013
- Reid ME, Christian SB, Brien DL (2000) Gravitational stability of three-dimensional stratovolcano edifices. *J Geophys Res* 105(B3):6043–6056. doi:10.1029/1999JB900310
- Reid ME, Sisson TW, Brien DL (2001) Volcano collapse promoted by hydrothermal alteration and edifice shape, Mount Rainier, Washington. *Geology* 29(9):779–782
- Reid ME, Brien DL, Waythomas CF (2010) Preliminary slope-stability analysis of Augustine Volcano. In: Power JA, Coombs ML, Freymueller JT (eds) The 2006 Eruption of Augustine Volcano, Alaska, US Geological Survey Professional Paper 1769, pp 321–332. http://pubs.usgs.gov/pp/1769/chapters/p1769_chapter14.pdf
- Roering JJ (2008) How well can hillslope evolution models “explain” topography? Simulating soil transport and production with high-resolution topographic data. *Geol Soc Am Bull* 120(9/10):1248–1262. doi:10.1130/B26283.1
- Roering JJ, Stimely LL, Mackey BH, Schmidt DA (2009) Using DInSAR, airborne LiDAR, and archival air photos to quantify landsliding and sediment transport. *Geophys Res Lett* 36(19). doi:10.1029/2009GL040374
- Salciarini D, Godt JW, Savage WZ, Baum RL, Conversini P (2008) Modeling landslide recurrence in Seattle, Washington, USA. *Eng Geol* 102(3–4):227–237. doi:10.1016/j.EngGeo.2008.03.013
- Savage WZ, Godt JW, Baum RL (2003) A model for spatially and temporally distributed shallow landslide initiation by rainfall infiltration. In: Rickenmann D, Chen C (eds) Debris-flow hazards mitigation: mechanics, prediction, and assessment. Mill Press, Rotterdam, pp 179–187
- Savage WZ, Godt JW, Baum RL (2004) Modeling time-dependent aerial slope stability. In: Lacerda WA, Erlich M, Fontoura SAB, Sayao ASF (eds) Landslides—evaluation and stabilization. Proceedings of the 9th international symposium on landslides, vol 1. Balkema, London, pp 23–36
- Schilling S P (1998) LAHARZ: GIS programs for automated mapping of lahar-inundation hazard zones. US Geological Survey Open-File Report 98-638
- Schulz WH (2004) Landslides mapped using LiDAR imagery, Seattle, Washington. US Geological Survey Open-File Report 2004-1396
- Schulz WH (2007) Landslide hazards revealed by LiDAR imagery, Seattle, Washington. *Eng Geol* 89(1–2):67–87
- Schulz WH, Lidke DJ, Godt JW (2008) Modeling the spatial distribution of landslide-prone colluvium and shallow groundwater on hillslopes of Seattle, WA. *Earth Surf Process Landforms* 33:123–141
- Simoni S, Zanotti F, Bertoldi G, Rigon R (2008) Modelling the probability of occurrence of shallow landslides and channelized debris flows using GEOtop-FS. *Hydrol Process* 22(4):532–545. doi:10.1002/hyp.6886
- Soeters R, van Westen CJ (1996) Slope instability recognition, analysis, and zonation. In: Turner AK, Schuster RL (eds) Landslides, investigation and mitigation. Transportation Research Board Special Report 247. National Research Council, Washington, DC, pp 129–177
- Suzen ML, Doyuran V (2003) A comparison of the GIS based landslide susceptibility assessment methods: multivariate versus bivariate. *Environ Geol*. doi:10.1007/s00254-003-0917-8
- Swets J (1988) Measuring the accuracy of diagnostic systems. *Science* 240:1285–1293
- Troost KG, Booth DB, Wisher AP, Shimmel SA (2005) The geologic map of Seattle—A progress report. US Geological Survey Open-file Report 2005-1252
- van Beek LPH, van Asch TWJ (2004) Regional assessment of the effects of land-use change on landslide hazard by means of physically based modeling. *Nat Hazards* 31:289–304
- Van den Eeckhaut M, Vanwalleggem T, Poesen J, Govers G, Verstraeten G, Vandekerckhove L (2006) Prediction of landslide susceptibility using rare events logistic regression: a case-study in the Flemish Ardennes (Belgium). *Geomorphology* 76:392–410
- van Westen CJ, Terlien MTJ (1996) An approach towards deterministic landslide hazard analysis in GIS: a case study from Manizales (Colombia). *Earth Surf Process Landforms* 21(9):853–868
- van Westen CJ, Rengers N, Soeters R (2003) Use of geomorphological information in indirect landslide susceptibility assessment. *Nat Hazards* 30(3):399–419
- van Westen CJ, van Asch TWJ, Soeters R (2006) Landslide hazard and risk zonation—why is it still so difficult? *Bull Eng Geol Env* 65:167–184. doi:10.1007/s10064-005-0023-0
- Varnes DJ (1981) The principles and practice of landslide hazard zonation. *Bull Int Assoc Eng Geol* 23:13–14
- Varnes DJ (1984) Landslide hazard zonation: a review of principles and practice. UNESCO, Paris, 60 pp
- Wait TC (2001) Characteristics of deep-seated landslides in Seattle, Washington. M.S. thesis, Colorado School of Mines, Golden, CO
- Wu W, Sidle RC (1995) A distributed slope stability model for steep forested hillslopes. *Water Resour Res* 31:2097–2110
- Xie M, Esaki T, Zhou G (2004) GIS-based probabilistic mapping of landslide hazard using a three-dimensional deterministic model. *Nat Hazards* 33:265–282



Plenary: Progress in Landslide Dynamics

Kyoji Sassa, Bin He, Khang Dang, Osamu Nagai, and Kaoru Takara

Abstract

Landslide Dynamics is a relatively new field in Landslide Science. Reliable scientific knowledge to assess the motion of landslides including hazard area, speed and depth is needed to reduce human loss from landslides. However, the initiation and motion of landslides is not easy to explain quantitatively because of pore-pressure generation during initiation and motion, and continuing changes in grain size, grain shape and water content of the involved soils in the shear zone. An apparatus has been developed to physically simulate the formation of sliding surfaces and the post-failure motion of the involved soils under realistic stresses. It can simulate pore-pressure increase due to rain water infiltration and dynamic loading due to earthquakes in the field, and can monitor pore-pressure generation, and mobilized shear resistance together with shear displacement. The apparatus has evolved from the model DPRI-1 in 1984 through DPRI-2, 3, 4, 5, 6, to the model ICL-1 in 2011 and ICL-2 in 2013. This apparatus which is called the landslide ring-shear simulator is now in use in foreign countries. This paper presents the progress of the landslide ring-shear simulator and its application to earthquake-induced landslides, the 2006 Leyte landslide killing over 1,000 people, the 1792 Unzen Mayuyama landslide killing 15,000 people, and a hypothetical Senoumi (Stone flower sea) submarine megaslide using a cored sample from 190 m below the sea floor. A new integrated computer model (LS-RAPID) simulating the initiation and motion using soil parameters obtained from the landslide ring-shear simulator has been developed in parallel with the development of landslide ring-shear simulator. LS-RAPID was applied to the three earthquake-induced landslide cases mentioned above. The simulations included two triggering factors: pore-

K. Sassa (✉) • O. Nagai
International Consortium on Landslides, Sakyou-ku, Kyoto 606-8226, Japan
e-mail: sassa@iclhq.org; nagai@iclhq.org

B. He
Key Laboratory of Watershed Geographic Sciences, Nanjing Institute of Geography and Limnology, Chinese Academy of Sciences, Nanjing 21008, China
e-mail: hebin@niglas.ac.cn

K. Dang
International Consortium on Landslides, Sakyou-ku, Kyoto 606-8226, Japan
Department of Civil and Earth Resources Engineering, Graduate School of Engineering, Kyoto University, Kyoto, Japan
e-mail: khangdq@gmail.com

K. Takara
Disaster Prevention Research Institute (DPRI), Kyoto University,
Uji 611-0011, Japan
e-mail: takara.kaoru.7v@kyoto-u.ac.jp

water pressure and three-component seismic waves. The combination of landslide ring-shear simulator and integrated landslide simulation model provides a new tool for landslide hazard assessment.

Keywords

Landslide dynamics • Ring shear apparatus • Landslide simulation • Computer model

Introduction

Slope-stability analysis is to study whether a slope fails or not, and is the main tool for the study of landslide initiation. *Landslide dynamics* is to study landslide mobility after failure. The former study focuses on the design of engineered slopes including embankments and earth dams, and also the prevention of occurrence of landslides. The latter study focuses on landslide hazard and risk assessment to identify the hazard level, area exposed to hazard and landslide velocity if the landslide were to occur. These data are necessary for early warning, evacuation and land-use planning to reduce human loss. The necessary geotechnical parameters and deformation in testing for each study are different. Slope-stability analyses need the peak shear resistance at failure and the mobilized shear deformation/displacement is usually of the order of a few mm or cm before the failure, although this depends on the sample size. On the other hand, landslide dynamics needs the steady-state shear resistance mobilized during post-failure motion. Results of basic geotechnical tests such as the triaxial test and direct shear tests are used in slope stability, while the results from physical simulation tests (i.e. undrained dynamic-loading ring-shear test) reproducing the sliding surface and post-failure motion are used in landslide dynamics. The comparison is shown in Table 1.

The science of slope-stability analysis advanced much earlier than landslide dynamics. Many people are killed by landslides especially in the developing countries due to urbanization and extensive regional development. Expensive landslide prevention works are difficult in developed countries as well as in the developing countries within limited budgets. The most effective and economical way to reduce human loss from landslides is landslide-hazard assessment and disaster preparedness including early warning, evacuation and land-use planning. A limited displacement and/or a low speed of motion may cause failure of structures but not be dangerous for humans. A high-speed, long-runout and wide-spreading motion may cause a great disaster. The significance of landslide dynamics is becoming more important.

Development of Landslide dynamics needs a tool to measure the mobilized geotechnical parameters after the

formation of a sliding surface—the post-failure strength reduction to its value at steady-state motion. It also needs an integrated computer model to simulate both the initiation and the motion of the landslide within the same programme using the geotechnical parameters mobilized in the landslide motion. This contribution summarises three decades of development of our tools for measuring dynamic geotechnical parameters (namely the landslide ring-shear simulator) and our development of a computer simulation from the initiation to the motion. It focuses on the research and technological developments which have been implemented in the Disaster Prevention Research Institute (DPRI), Kyoto University, Japan and the International Consortium on Landslides since 1984.

The Landslide Ring-Shear Simulator

Aim and Concept of the Landslide Ring-Shear Simulator

The formation of a sliding surface is not a simple phenomenon. Strain is not defined in the shear zone. Grains of soil in the shear zone are crushed or broken. Size and shapes of grains in the shear zone are changed. Those changes necessarily affect pore-water pressure due to volume change in the shear zone. The extent of changes is different for different soils such as volcanic or sedimentary, angular or round, hard or soft minerals. The confining stress level much affects the behaviour of grain crushing in the shear zone. It is difficult to infer a reliable general principle for all the cases of concern.

The basic concept of the landslide ring-shear simulator (Fig. 1) is to reproduce the stresses due to gravity, seismic force or pore pressure on soils taken from the field and to observe what happens; fail or not fail, excess pore-water pressure generated or not generated in the initiation, failure, and post-failure processes, and how much shear resistance is mobilized in the whole process.

Figure. 2 illustrates the landslide initiation mechanism due to increase of pore-water pressure in deep and shallow slides. The upper figure shows the soil column with a unit length along the bottom of a soil (weathered rock) layer, or more precisely, a landslide-susceptible layer. The weight of

Table 1 Slope stability and landslide dynamics

Necessary items for both analysis	Slope stability	Landslide dynamics
Objectives of analysis	Design of engineered slopes and prevention of landslide occurrence	Landslide-risk assessment for early warning, evacuation or land-use planning
Necessary parameters	Shear strength parameters (Shear resistance at failure)	Steady-state shear resistance during post-failure motion
Necessary deformation in testing	Order of mm to cm until failure	Order of m in shear displacement
Difference from the initial state of grain size/shape/structure	The initial state is mostly kept	The initial state is completely lost
Testing methods	Element tests such as triaxial tests and direct shear tests	Physical simulation test to reproduce sliding surface and post-failure motion (i.e.: Landslide ring-shear simulator)
Application of measured data	Slope-stability analysis	Numerical simulation of landslide motion
Basic science/analysis	Soil mechanics—stability analysis	Soil dynamics—landslide dynamics

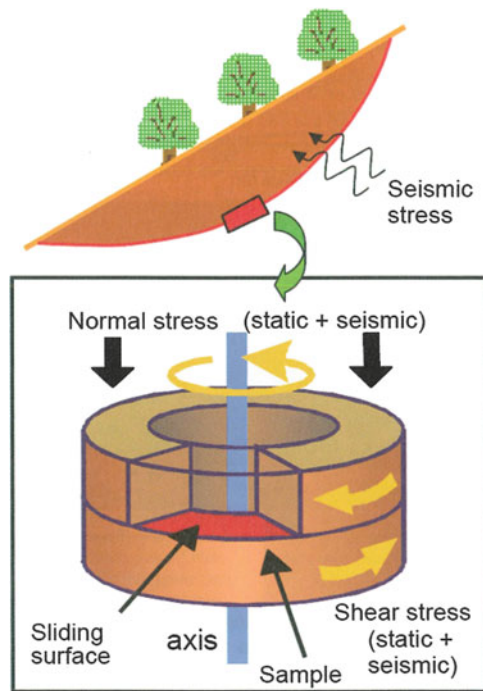


Fig. 1 Concept of landslide ring-shear simulator

the soil column is expressed as $m \times g$ in Fig. 2. where, m is a mass of the soil column, and g is gravity.

If no ground-water table exists within the soil column, that is, zero pore-water pressure is acting, the initial stress at the bottom on this column is plotted as “I” in the stress-path figure of normal stress and shear stress.

Normal stress at I is $\sigma_0 = mg \cdot \cos\theta$, Shear stress at I is $\tau_0 = mg \cdot \sin\theta$.

Note:

1. The initial stress point is located on the line with an inclination of angle θ .
2. The distance between the origin and the stress point I presents $m \times g$ (= the weight of soil column).

When ground-water level increases, pore-water pressure u increases. The stress moves toward to the left. When the stress reaches the failure line, shear failure will occur at the stress at

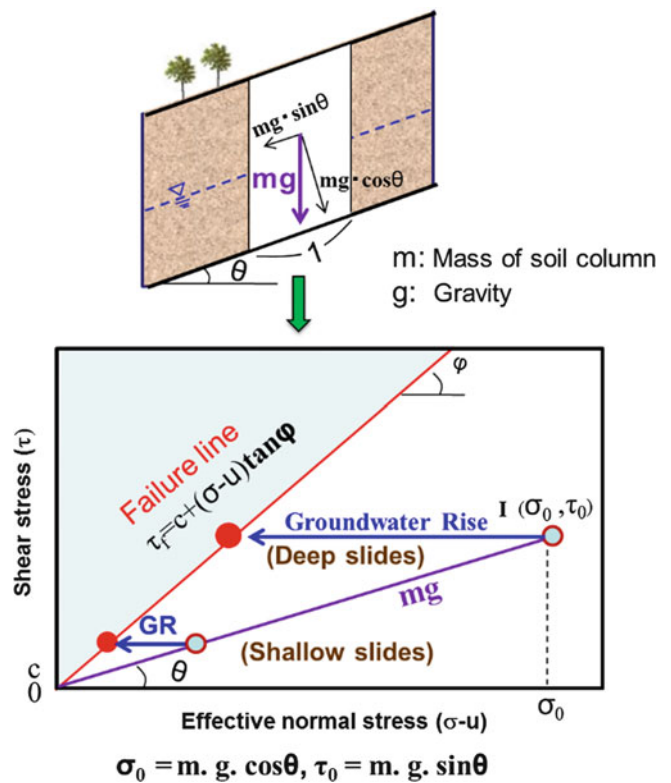


Fig. 2 Initiation by ground water rise (pore-pressure increase)

failure (shown as red circle along the failure line). Deeper slides need a greater pore-pressure rise as seen in the Fig. 2.

$$\tau_f = c + \sigma \cdot \tan\phi \tag{1}$$

Figure 3 presents the loaded stress in the slope (a: left figure) and the stress path during earthquakes (b: right figure). The initial stress acting on the bottom of the landslide-susceptible layer ($m g$) is plotted as A_0 (if no pore pressure is acting, it is the same as I in Fig. 2). When an earthquake occurs and a cyclic seismic load is applied, the loaded stress is expressed by $k \cdot m g$, where k is seismic coefficient which is the ratio of seismic acceleration (a) and gravity (g), namely $k = a/g$.

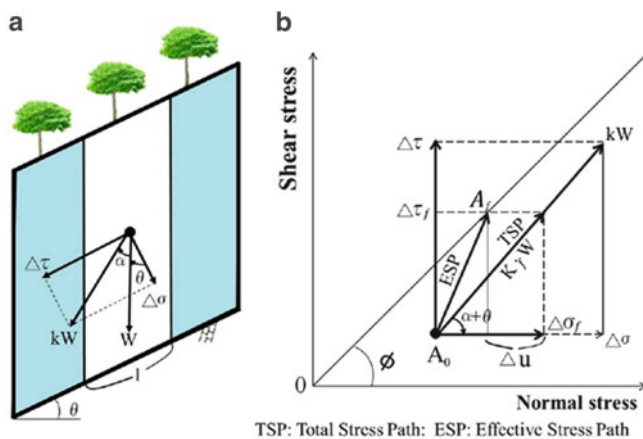


Fig. 3 Initiation by seismic loading during earthquakes. (a) Loading stresses in the slope, (b) Stress paths during earthquakes

When expressing the direction of seismic force as α from vertical direction, the direction of the seismic stress increment in the stress diagram (b) is expressed as $(\alpha + \theta)$.

The effective stress path during an earthquake is not in the same direction as the total stress path.

Figure 3 illustrates the case where the initial stress + the seismic stress reach the failure line.

When pore-water pressure is generated during seismic loading, the effective stress path shifts from A_0 to A_f .

When the seismic stress reaches or even crosses the failure line, the difference between shear stress and shear resistance is used to accelerate the soil column. Each time period when stress crosses over the failure line is short. If post-failure shear-strength reduction does not occur, the shear displacement will be very limited and stabilized after termination of the earthquake. However, if shear resistance is much decreased after failure, rapid motion will occur due to the difference between applied shear stress and mobilized shear resistance on the sliding surface. The landslide ring-shear simulator (undrained dynamic-loading ring-shear apparatus) can reproduce the post-failure motion, measure the pore-water pressure generated in the shear zone and the resulting shear resistance during motion including that under steady state conditions.

Development of the Dynamic-Loading Ring-Shear Apparatus Series (from DPRI-1 to ICL-2)

Sassa and colleagues of the Disaster Prevention Research Institute (DPRI), Kyoto University and the International Consortium on Landslides (ICL) have developed a series of dynamic-loading ring-shear apparatus from DPRI-1 (initial version, 1984), DPRI-2, DPRI-3, DPRI-4, DPRI-5, DPRI-6, DPRI-7, ICL-1 and ICL-2 (the latest version, 2013). To reproduce most earthquake-induced landslides it is necessary to maintain a undrained condition in the soil

sample. Pore-water pressure is very important in the mechanism of the long runout landslides. Maintaining an undrained condition and measuring pore-water pressure accurately are difficult to achieve. Models DPRI-1 and DPRI-2 could not create the undrained condition although rapid shearing could be produced. Model DPRI-3 was an intermediate version from the initial model to the developed version of the apparatus. Model DPRI-4 was a trial version, and models DPRI-5 and DPRI-6 were produced at the same time after obtaining a special budget to mitigate earthquake disasters soon after the Hyogoken Nambu Earthquake in 1995. These two apparatus are developed versions of an undrained dynamic-loading ring-shear apparatus having the features of undrained condition, pore-water pressure monitoring near the sliding surface, and dynamic loading (regular cyclic or filtered real seismic record). These two apparatus succeeded reproducing sliding-surface formation and measuring post-failure motion in rain- and earthquake-induced landslides. Sassa planned to test large-scale landslides and aimed to test under 2 MPa (DPRI-5) and 3 MPa (DPRI-6). However, these devices failed to reach this intended high stress state in a stable manner and also failed to maintain an undrained condition under this high stress state. For these reasons sensors were changed to smaller capacities. They successfully tested up to 500 kPa (with one successful test to 630 kPa in Fig. 12 in DPRI-5). The latest models ICL-1 and ICL-2 use a different loading system, successfully allowing higher normal stress and maintaining an undrained condition up to 1 MPa (ICL-1) and 3 MPa (ICL-2).

The aim of models DPRI-1 to DPRI-7 was scientific research to achieve high-precision results for science. The aim of models ICL-1 and ICL-2 is for practical use, less expensive to manufacture, lower-cost maintenance, and the capability to be maintained abroad. Both apparatus were developed to donate to developing countries, one to Croatia and the other to Vietnam.

We introduce the initial apparatus DPRI-1, the intermediate DPRI-3, one of the developed stage (DPRI-6, the largest model), and the latest and most advanced model ICL-2 using three figures of the structures (Figs. 4, 5 and 6) and two tables of characteristics (Table 2) and sealing structures for maintaining undrained condition (Table 3). Figure 4 presents the structure of models DPRI-1 and DPRI-3. The initial model (DPRI-1 in the upper figure of Fig. 4) aimed to reproduce the shear zone of debris flows. The concept was to use a circular device to represent an endless flume. Loading stress is achieved with a motorcycle inner tube. This was not an undrained condition. A water container was attached outside the shear box. Sponge rubber was pasted in the gap between upper and lower shear boxes as shown in Table 3. Water could move freely through the edge.

The DPRI-3 structure is presented in the lower figure of Fig. 4. It has a loading frame similar to a triaxial test

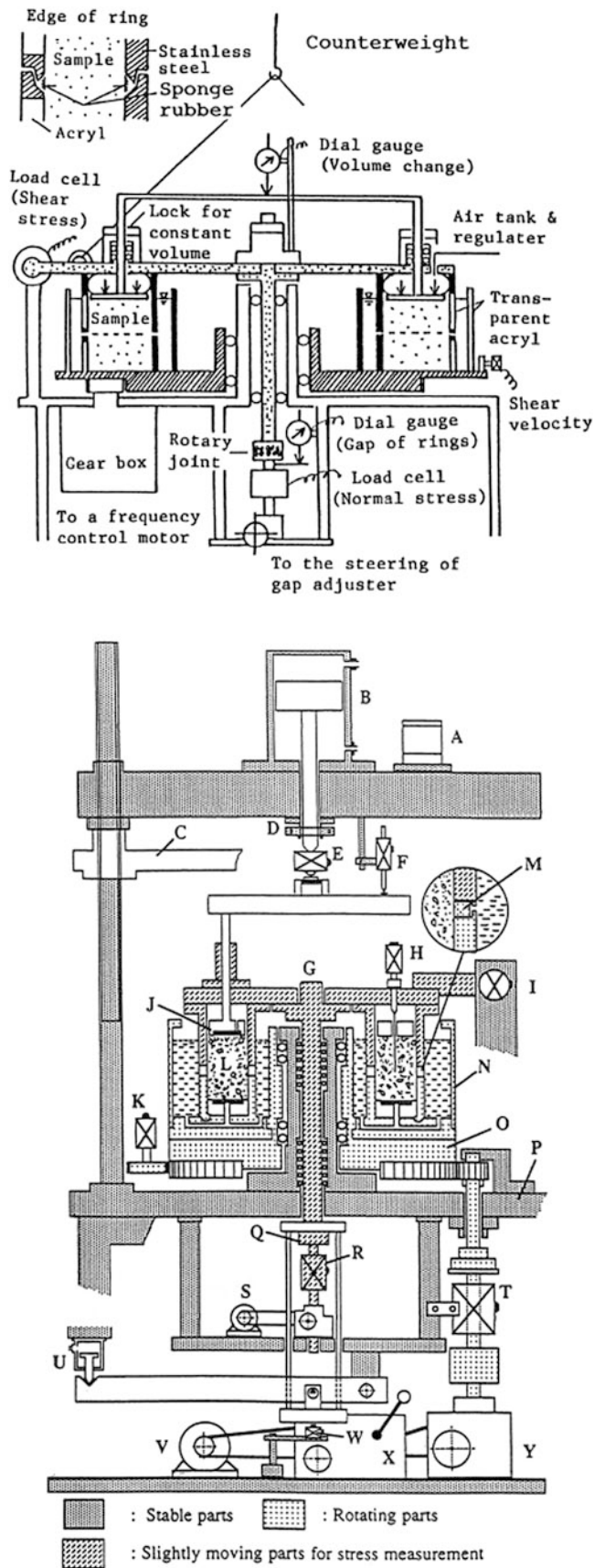


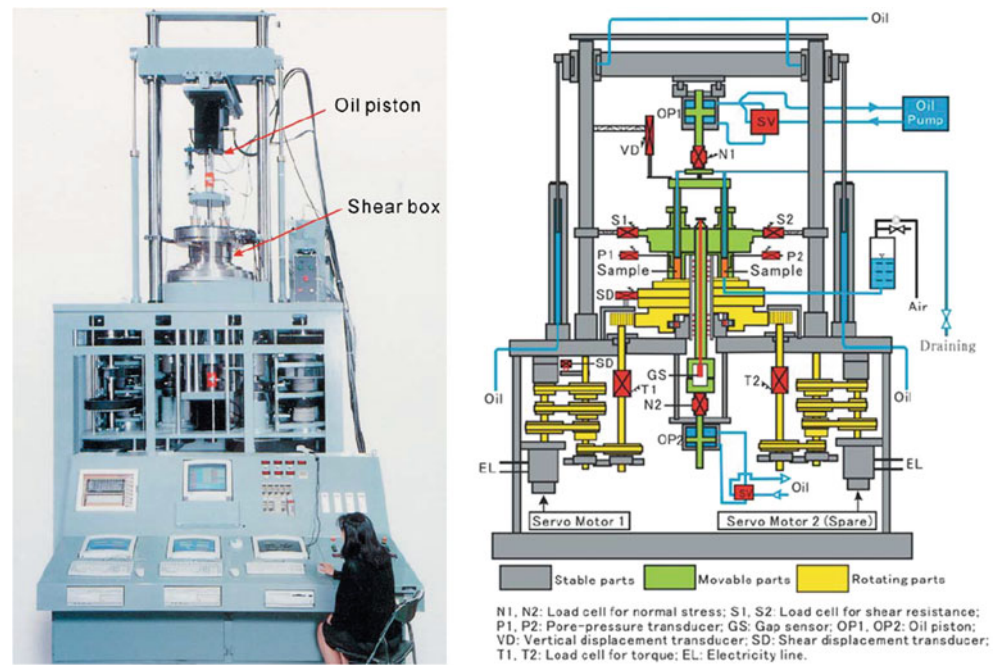
Fig. 4 I The initial stage of apparatus of DPRI-1 and the intermediate apparatus of DPRI-3

apparatus. Normal stress is loaded by air-servo valve and compressor. Initially, the undrained condition was not kept. A water bath was attached outside the shear box as seen in Fig. 4. Pore-water pressure was measured by inserting a needle (covered by porous cup) through the top cap connecting to a pore-pressure sensor. Pore-water pressure monitoring was unsuccessful. The area exposed to the pore water was too small to push the diaphragm of the pore pressure sensor. The sensitivity was insufficient and the needle was deformed by the shear displacement. The mechanism of model DPRI-3 was improved. The DPRI-3 (final) in Table 3 presented the eventual mechanism to measure pore-water pressure and to keep the undrained condition. To increase the contact stress between the rubber and upper shear box, the top of the rubber edge was changed from flat to stepped, thus reducing the contact area. The area exposed to water pressure was much increased by installing a metal filter around the whole circumference of the upper and outer shear box. A smaller diaphragm pore-pressure sensor was also used. This system dispensed with the water container, but still could not produce a perfect undrained condition.

In January 1995, the Kobe earthquake occurred and 36 persons were killed by a rapid landslide. The mobility of the landslide was one of a debris flow, however, there was no rain at all during this very dry season and no water present in a very small river at the toe of the slope. A landslide study was needed to investigate this mechanism and to mitigate future landslide disasters. Funding to develop an advanced undrained dynamic-loading ring-shear apparatus was obtained. Then, we developed two apparatus (a large shear box (25–35 cm) and a smaller one (12–18 cm)). We aimed to produce a high stress of 2–3 MPa. To create this capacity, DPRI-6 has two stress- and speed-control servo-motors (37 kW) and DPRI-5 has a 37 kW motor plus an oil piston to give additional shear load around peak failure strength. Both attempts failed to produce such a high shear force. We could not maintain the undrained state at such high stresses, and also we could not control the normal stress at such a high level. This was caused by several reasons: at high load, the tall poles of the frame were extended, and the horizontal beam to load normal stress was deformed. The deformation was elastic, and when sudden stress change occurs, the servo-control system could not work properly due to the oscillation.

We had great difficulty reproducing stresses and shear failure with crushable sand grains at such high stress levels. The structure and the photo of DPRI-6 are shown in Fig. 5. One advancement was a vertical positioning bar (shown in red in Fig. 5 right) passing through the central axis. The bar was fixed to the loading plate and moved together with the upper shear box. The displacement of the bottom of the vertical positioning bar was measured by a gap sensor connected to the stable base, namely the lower shear box. The gap between the upper shear box and the lower shear box was measured by a gap sensor with a precision of 1/

Fig. 5 The developed stage of apparatus of DPRI-6. Models DPRI-5 and DPRI-7 are the basically same system though the shear-box size, the maximum velocity and the loaded maximum stresses are different



1,000 mm. However, it was unsuccessful in avoiding oscillation in the gap servo-control system at a level of MPa.

Figure 6 presents the latest model undrained dynamic-loading ring-shear apparatus which has been developed to simulate megaslides up to 3 MPa, and planned to be donated to Vietnam in 2014. The ease of maintenance in Vietnam was a major consideration in the design. A photograph of the main apparatus is presented in the left top (a). Figure b presents the mechanical structure of model ICL-2. The greatest difference between (ICL-1 and ICL-2) and (DPRI-3 and DPRI-6) is the system for loading normal stress. Models DPRI-3 and DPRI-6 have a long loading frame consisting of two long vertical pillars and one horizontal beam. The frame is extended and compressed in pillars and deformed in beam during changes in loaded stress due to cyclic and seismic loading and sudden stress changes when grains or soil structures fail due to high normal or shear stress. This sometimes disturbs the function of the servo-control system and an oscillation occurs. To minimize the effect of extension/compression and deformation, the loading frame is removed in the ICL series. The basic concept returns to the DPRI-1 loading system without the loading frame. In DPRI-1, an air tube pressed to the sample and the loading cap which was restrained by the central axis. The loading normal stress is provided by a tensile stress along the central axis. Models ICL-1 and ICL-2 achieve this via a loading piston in place of an air tube. Figure 6b, d shows the structure and the servo-control system of ICL-2. Oil pressure within the loading piston is controlled by servo-valve (SV) using the feedback signal from the load cell (N) measuring the normal stress. When a testing programme

has been selected and a control signal given for monotonic stress, cyclic or seismic stress loading, oil is pumped into the loading piston, loading the normal stress by pulling on the central axis. The normal stress acting on the sliding surface (upward) is retained by the central axis (downward), and this load is measured by the vertical load cell (N). In this system, the role of the two long pillars used in models DPRI-5, 6, and 7 was replaced by one short central axis column and the role of the long horizontal beam is replaced by the loading piston. Deformation of this system is much smaller than in the frame loading system. This structure enables stable servo-stress-control. The minimum deformation during cyclic and seismic loading and possible sudden stress change due to grain crushing on sands has enabled maintenance of an undrained state up to 3 MPa during tests.

Another difference between the DPRI series apparatus (DPRI-5, 6, 7) and the ICL series is the rubber edge which has a critical role for sealing. Rubber edges of all DPRI series apparatus were glued to the shear box. A constant thickness of glue is impossible to achieve and the height of the upper surfaces of the rubber edges of the inner ring and the outer ring must be the equal to maintain an undrained condition. Hence after a new rubber edge had been glued to the shear box, it had to be machined by a skilled technician. In the ICL series, the rubber edges are fixed without glue as is illustrated in Table 3 (ICL-2). This shape (grey color) of rubber edge is processed from a constant-thickness rubber plate. A number of rubber edges of this shape can be commercially purchased in reasonable cost. The rubber edge is simply placed on the lower ring. Then the rubber edge is pressed by a Teflon ring holder, and this holder is pressed in

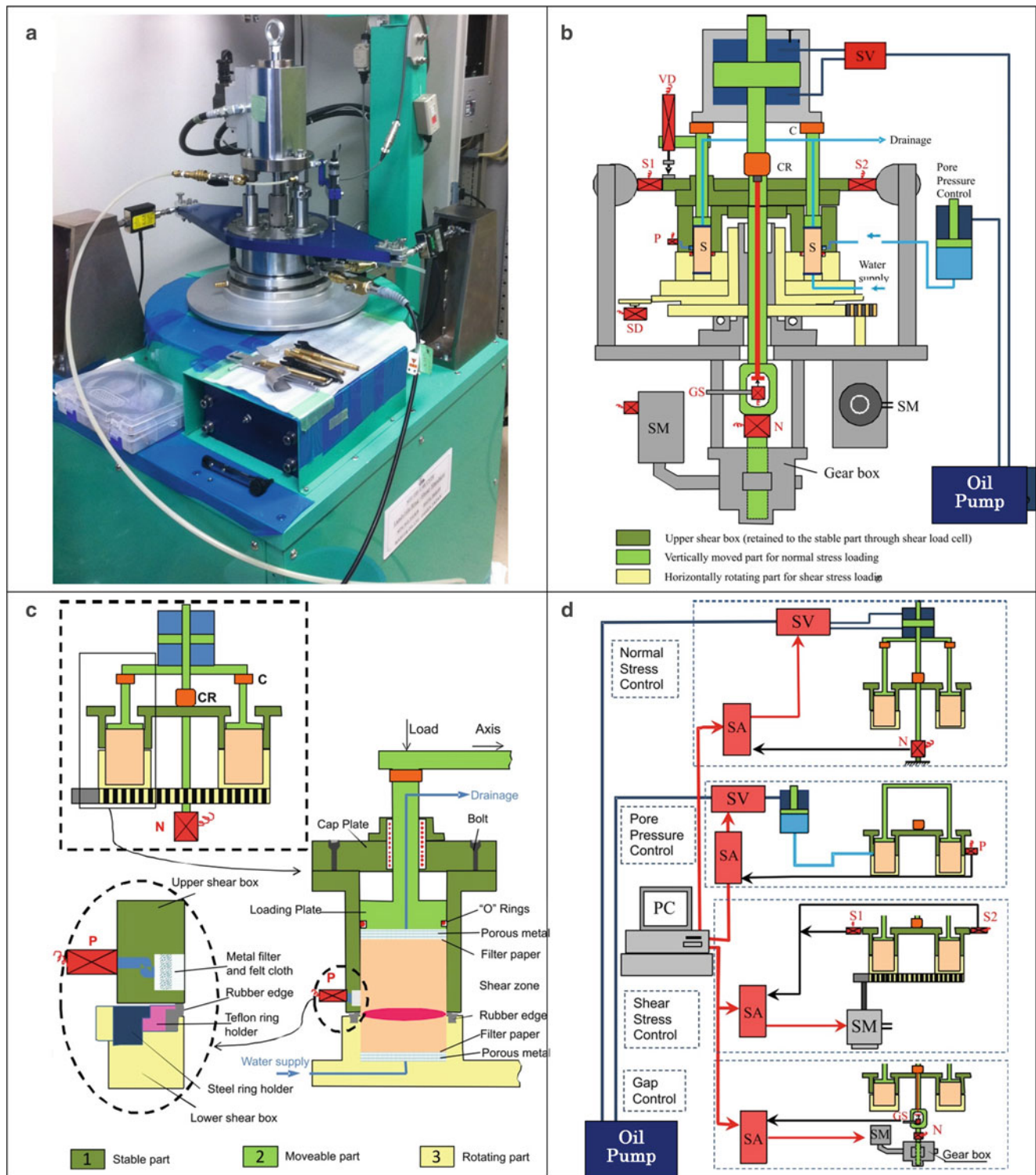


Fig. 6 The most updated and practical apparatus of ICL-2. ICL-1 and ICL-2 are developed for use and maintenance in foreign countries. (a) Photograph of the main apparatus, (b) Mechanical structure of the main apparatus, (c) Close-up view of the shear box and the undrained sealing

and pore pressure monitoring, (d) Servo-control systems for normal stress and pore pressure through servo-valves (SV) and servo-control systems for shear stress and gap through servo-motors (SM)

turn by a steel ring holder fixed by a set of screws No glue or specialist machining are needed. The Teflon ring holder was designed for the high stress of ICL-2 (3 MPa). Because the

rubber edge used in DPRI-6 was deformed outwards due to a high lateral stress, it could not maintain undrained state. To prevent such deformation in the ICL series, a Teflon ring

Table 2 Characteristics of each stage of the ring shear apparatus (DPRI-1, 3, 6 and ICL-2)

Type	Characteristics
DPRI-1	<ul style="list-style-type: none"> • Aim: to reproduce debris-flow motion under a certain normal stress within a rotational channel • Target: Debris flows frequently occurred in Volcano Usu, Volcano Sakurajima and others in Japan • Normal stress Maximum normal stress: 40 kPa Loading system: Rubber tube by air compressor and regulator which was installed between the loading plate and the top cap of the upper shear box (no loading frame) Monitoring: one load cell by automatic side-friction canceling • Shear stress Shear box: 300–480 mm in diameter and transparent acrylic shear box Loading system: Speed- control motor Maximum shear speed in the center of shear box: 100 cm/s • Gap control, undrained condition, and pore pressure monitoring Gap control system: Manual gap control by measuring the position change of the upper loading plate Sealing of sample leakage: Silicon rubber Undrained condition: Not possible No pore pressure measurement • Major reports: Sassa (1984) in 4th ISL and Sassa 1988 in 5th ISL, Lausanne
DPRI-3	<ul style="list-style-type: none"> • Aim: to reproduce earthquake-induced landslides. • Target: Ontake landslide triggered by the 1984 Naganoken-Seibu earthquake in Japan. • Normal stress Maximum normal stress: 500 kPa Loading system: Loading piston with air servo-valve, compressor and loading frame to support piston Monitoring: two load cells, one for loading pressure, another for side friction within the shear box • Shear stress Shear box: 210–310 mm in size with a transparent acrylic outer ring Loading system: Stress-control and speed-control motor Maximum shear speed in the center of shear box: 37 cm/s • Gap control, undrained condition, and pore-pressure monitoring Sealing of water leakage: Polychloroprene (®Neoprene) rubber edge passed on the lower ring (Rubber hardness Index, 45°JIS) Gap control: Servo-gap control system by measuring the position change of the upper loading plate and adjusting by servo-motor (Extension of central axis was neglected) Undrained condition and pore-water pressure monitoring: It was improved from 6th ISL in Christchurch 1992–1994 Successful undrained condition: 400 kPa Pore pressure was monitored by a needle inserted close to the shear zone in 1992. It was monitored from the gutter (4 × 4 mm) along the whole circumference of the upper-outer shear box 2 mm above the gap in 1994 Major reports: Sassa (1992) in 6th ISL and 7th ICL in 1996
DPRI-6	<ul style="list-style-type: none"> • Aim: to develop landslide ring-shear simulator • Target: Nikawa landslide killing 34 persons. Triggered by the 1995 Hyogoken-Nambu earthquake • Normal stress Maximum normal stress: designed for 3,000 kPa. However, normal stress servo-control system does not function well. Tests were conducted to 750 kPa by changing the normal stress load cell Normal stress loading system: Loading piston by oil servo-valve and oil-pressure pump and loading frame to support piston Monitoring: two load cells: one for loading pressure, the other for side friction within the shear box • Shear stress Shear box: 250–350 mm in size with non-transparent outer and inner rings of stainless steel. Maximum shear speed in the center of shear box: 224 cm/s • Gap control, undrained condition, and pore-pressure monitoring Rubber edge in the gap: Polychloroprene rubber with Rubber hardness Index, 45° JIS Gap control: Piston with oil servo-valve and oil pressure pump by measuring the position change of the upper loading plate. To avoid the effect of extension of central axis, a displacement guide was installed within the central axis Successful undrained condition: 550 kPa Pore pressure is monitored along the entire circumference of the upper-outer shear box 2 mm above the gap (same with DPRI-3) • Major reports: Sassa et al. 2004 in Landslides, Vol.1, No.1
ICL-2	<ul style="list-style-type: none"> • Aim: to develop a landslide ring-shear simulator for mega-slides (3 MPa normal stress) and able to be maintained in a developing country • Targets: 1792 Unzen Mayuyama landslide killing 14,528 persons and submarine mega-landslides including a 30 km wide and 20 km long possible landslide trace in Senoumi, Suruga Bay in Japan • Normal stress Maximum normal stress: 3 MPa Normal-stress loading system: Loading piston by oil servo-valve and oil pressure pump which is retained by the central axis (no loading frame) Monitoring: One load cell with automatic side-friction canceling

(continued)

Table 2 (continued)

Type	Characteristics
	<ul style="list-style-type: none"> • Shear stress Shear box: 100–142 mm in diameter with non-transparent outer and inner rings of stainless steel Shear speed in the center of shear box: up to 50 cm/s • Gap control, undrained condition, and pore-pressure monitoring Rubber edge in the gap: Polychloroprene rubber with Rubber hardness Index, 90°JIS Gap control: Mechanical jack driven by a servo-control motor with feed-back signal of gap sensor for the position change of the upper loading plate. (to avoid the effect of extension of central axis, a displacement guide is installed within the central axis) Successful undrained condition: 3 MPa Pore pressure is monitored along the whole circumference of the upper-outer shear box 2 mm above the gap <p>Major reports: Contributed to Landslides in 2013 and this paper</p>

horizontally supports the rubber edge. The height of the rubber edge is gradually reduced by wear during experiments. If the steel ring holder were to touch the upper ring, it would mobilize a large shear resistance and damage the upper ring. The Teflon ring is softer than steel and has low friction, and so it causes no damage. However, when wear allows the Teflon ring to touch the upper ring, it can be noticed that it is time to change rubber edge.

Models ICL-1 and ICL-2 have been developed for practical use for landslide risk assessment in other countries including developing countries. Model ICL-1 is small, light-weight and transportable, and capable of testing up to 1 MPa at low shearing speed (5.4 cm/s). Model ICL-2 was designed for up to 3 MPa and up to 50 cm/s. Both apparatuses are commercially available as practical testing machines (although careful handling is needed). Apparatus ICL-1 was donated to Croatia and it is currently working in the laboratory of the Faculty of Civil Engineering, University of Rijeka. Apparatus ICL-2 is planned to be donated to the Institute of Transport Science and Technology (ITST) of the Ministry of Transport, Vietnam.

Application of the Landslide Ring-Shear Simulator

The undrained dynamic-loading ring-shear apparatus (landslide ring-shear simulator) of the developed stage of ring-shear apparatus (DPRI-5 and 6) were applied to many cases and reported in Sassa et al. (2004, 2005, 2010 and others). Two test results using DPRI-5 are introduced here.

Initiation and Motion of Landslides Triggered by Earthquakes (Higashi-Takezawa Landslide)

Figure 7 presents the Higashi Takezawa landslide triggered by the 2004 Mid-Niigata Prefecture earthquake (M 6.8). The landslide occurred within a previous landslide mass as illustrated in the figure. The sliding surface was formed at the contact between a siltstone layer and a sand layer. We tested two samples taken from the siltstone and the sand

layer. We performed a cyclic loading test and also a seismic loading test using the nearest seismic record. The test results were reported in Sassa et al. (2005). Figure 8 shows the time series data (a) and the stress path (b) of the seismic loading test on sands taken from the landslide. The green color line in Fig. 8a is normal stress. The wave form of normal stress can reproduce the calculated normal stress from the monitored seismic record. The red color line in Fig. 8a presents shear stress. The shear stress cannot exceed the failure line, so the shear stress over the shear strength is cut off. The blue color line shows the pore pressure generated in the sample. It was increased during seismic loading and also in the progress of shear displacement, reaching a level very close to the normal stress. Therefore, the steady-state shear resistance was very low as shown in the red effective stress path (ESP) in Fig. 8b. Accordingly, the apparent friction angle (calculated from the ratio between the mobilized shear resistance and the total normal stress) was only 2.5°. The blue color line in Fig. 8b is the total stress path (TSP). Cyclic loading tests were conducted on silts taken from the silt layer (Sassa et al. 2005). No pore-water pressure was generated during cyclic loading tests for silts and limited motion occurred only while the loaded stress was over the failure line, but stopped immediately the loading stopped. We concluded that the sliding surface probably formed at the base of the sand layer, and not at the top of the siltstone layer.

Application to Landslide-Induced Debris Flows

Another example of the application of the landslide ring-shear simulator is for the 2003 Minamata debris-flow disaster. A landslide occurred on a mountain slope and the landslide mass moved onto a torrent deposit. A sliding surface was created within the torrent deposit and the enlarged mass including the initial landslide mass plus the scraped torrent deposit flowed along the torrent and killed 15 people in a village constructed on an alluvial fan.

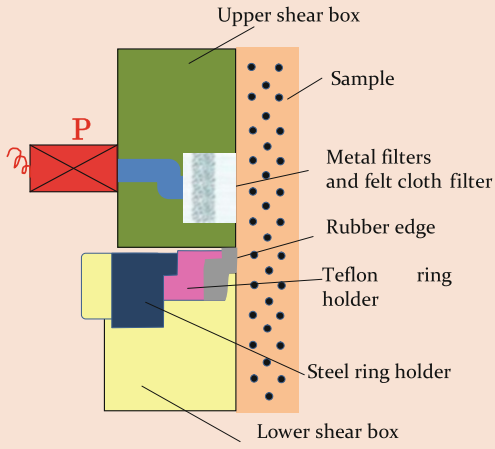
Figure 9 explains the model of the landslide-triggered debris flow (Sassa et al. 1997). The stress on the base of the soil column is presented in Fig. 9b. The initial stress at the base of the torrent deposit is expressed by the point “A”.

Table 3 Progress of the sealing of the gap

Type	Section of Sealing	Notes
DPRI-1		<ul style="list-style-type: none"> • Sponge rubber was pasted on the upper edge • Samples were glass beads and coarse sands • Drained condition
DPRI-3 (initial)		<ul style="list-style-type: none"> • Square shape of the polychloroprene rubber edge (Rubber Hardness Index is 45° JIS) was pasted onto the lower ring • Incomplete undrained condition • Water bath is set outside of the shear box • Unsuccessful pore-pressure measuring
DPRI-3 (final)		<ul style="list-style-type: none"> • Stair shape of the polychloroprene rubber edge (Rubber Hardness Index is 45° JIS) was pasted onto the lower ring • Successful undrained condition up to 400 kPa under 0.1 Hz cyclic test • Successful pore-pressure measuring through the gutter along the whole circumference in the upper ring
DPRI-6		<p>Stair shape of the polychloroprene rubber edge (Rubber Hardness Index is 45° JIS) is pasted onto the lower ring</p> <p>After rubber edge is pasted, the upper surface of inner and outer rubber edges needs to be processed by a lathe or file to ensure that the rubber surface is everywhere the same height</p> <p>Successful undrained condition up to 550 kPa under realistic seismic wave loading</p> <p>Successful pore-pressure measuring through the gutter along the entire circumference in the upper ring</p>

(continued)

Table 3 (continued)

Type	Section of Sealing	Notes
ICL-2		<p>The polychloroprene rubber edge (grey) (Rubber Hardness Index is 90°JIS) was pressed by a polytetrafluoroethylene (teflon) ring holder (pink) which was pressed by a stainless steel ring holder. No glue was used. The rubber edge was simply placed and pressed. Successful undrained condition up to 3,000 kPa. Successful pore-pressure measuring up to 3,000 kPa.</p>

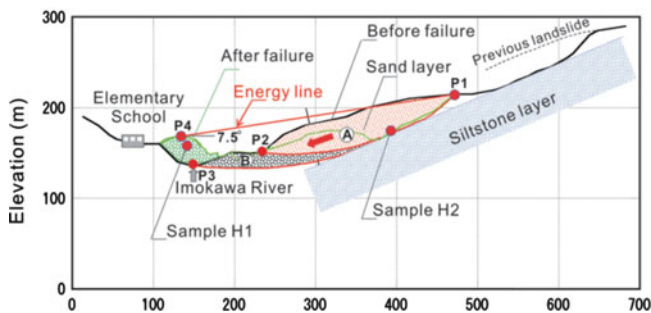


Fig. 7 The Higashi-Takezawa landslide induced by the 2004 Mid-Niigata Prefecture earthquake (M 6.8)

If no excess pore pressure is generated during rapid loading by a moving landslide mass, the stress point moves to point C by adding the static stress (ΔW) to the initial stress. In addition, by adding the dynamic stress (F_d) to the static stress, the total stress moves to point B. Therefore, the stress path in the actual field case tends to move from point A to point B. However, when the stress path reaches the failure

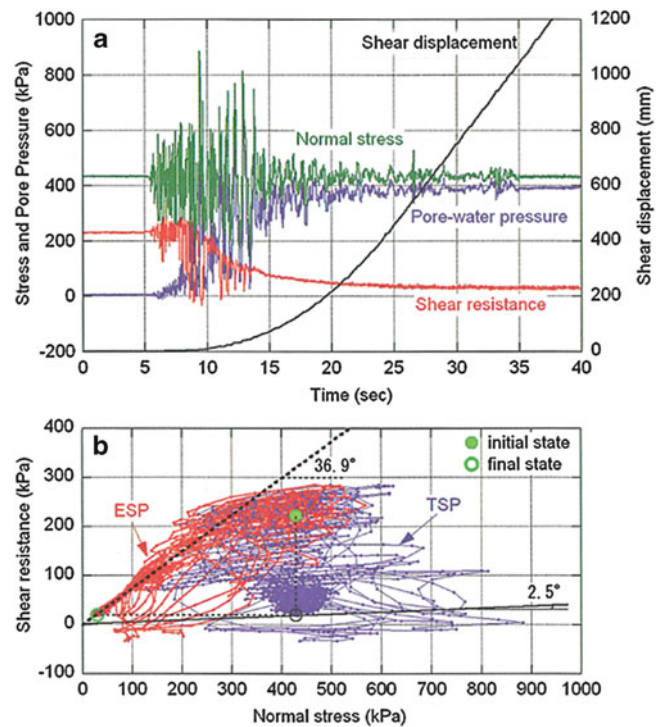


Fig. 8 The result of the seismic loading ring shear test by DPRI-6 for sands taken from the landslide

line, it moves along the failure line as seen in Fig. 9b, because the stress path cannot exceed the failure line. At the point where the dynamic stress reduces to zero, the total stress moves back to the stress point C, namely the sum of W_0 and ΔW . Denoting the angle of thrust during the collision with the torrent deposit as α and the dynamic stress as F_d , using a dynamic coefficient $k_d = (F_d/\Delta W)$, the dynamic shear stress and normal stress are expressed as:

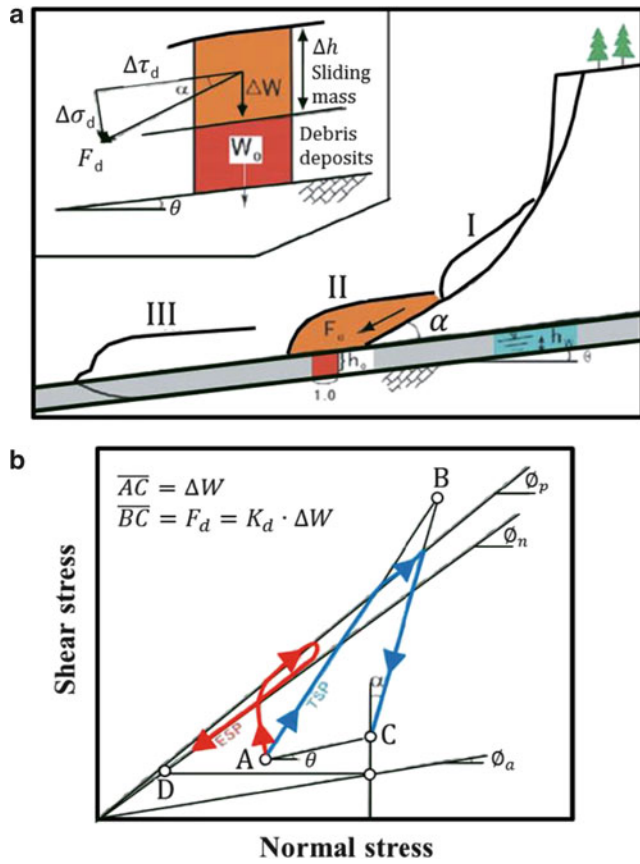


Fig. 9 Thematic figure of the landslide-induced debris flow (Sassa et al. 1997). (a) Illustration of the model; (b) stress path of the torrent deposit during loading. α : angle of thrust between the slope and the torrent bed; F_d : dynamic stress; k_d : dynamic coefficient ($F_d/\Delta W$)

$$F_d \cos \alpha = \tau_d, F_d \sin \alpha = \sigma_d \quad (2)$$

The stress path from A to B to C is the total-stress path (TSP) in the case where no pore pressure is generated. However, excess pore pressure is likely to be generated during loading and also during shearing after failure. In this case, the effective-stress path (ESP) will deviate from the total-stress path (TSP) as a curved line from A to D.

When the landslide mass moves from a steep slope to a gentle slope, the angle α is great, but when the landslide mass (i.e., the debris flow) travels along the torrent, the angle α is zero. Figure 10 presents the test result simulating the case of the landslide (debris) mass moving onto the torrent deposits. The gradient of the torrent bed was 15° , the depth of the torrent deposit was 2–4 m, and the dynamic coefficient was 0.9. Because of rapid loading by the fast-moving slide mass (more than 10 m/s), the test was carried out under undrained conditions similar to the seismic loading test. A sliding surface was formed inside the torrent deposits which were composed of reworked andesitic lava or tuff breccia.

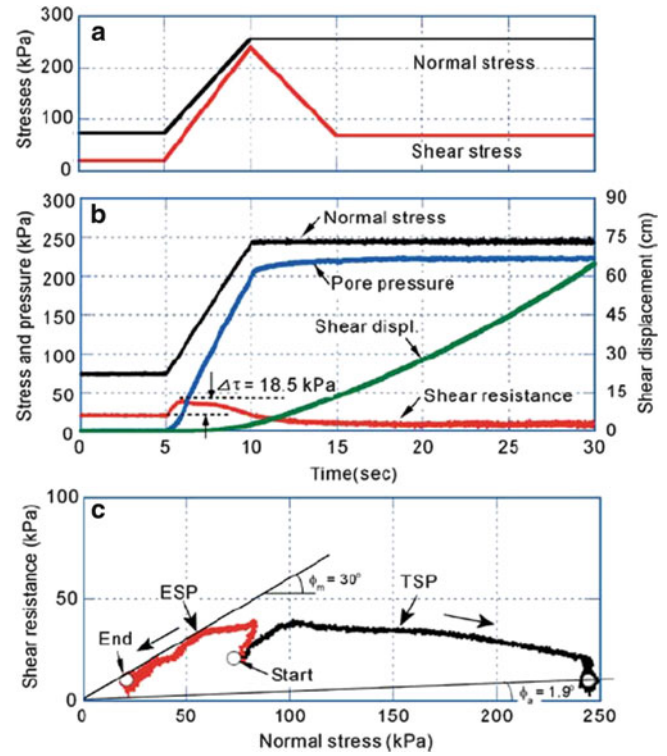


Fig. 10 Test result simulating the torrent deposit scraped by undrained loading of a moving landslide mass ($B_D = 0.89$). (a) Control signal for normal stress and shear stress simulating the undrained loading on the torrent deposit, (b) Monitored loaded normal stress, generated pore pressure, mobilized shear resistance and shear displacement during undrained loading, (c) Monitored total stress path (black) and effective stress path (red) during undrained loading

The test result of this landslide ring-shear simulator visualized that the torrent deposit must shear and move together with the original slide mass. Only 18.5 kPa was necessary as an additional shear stress to cause shear failure. The mobilized apparent friction angle was only 1.9° in this rapid and undrained loading condition as seen in the stress path (Sassa et al. 2004).

Development of a Numerical Simulation Using Measured Parameters

Theory of the Integrated Simulation Model

The basic concept of this simulation is explained in Fig. 11. A vertical imaginary column is considered within a moving landslide mass. The forces acting on the column are (1) self-weight of the column (W), (2) seismic forces (vertical seismic force F_v , horizontal x–y direction seismic forces F_x and F_y), (3) lateral pressure acting on the side walls (P), (4) shear resistance acting at the base (R), (5) the normal stress acting at the base (N) given by the stable ground as a reaction

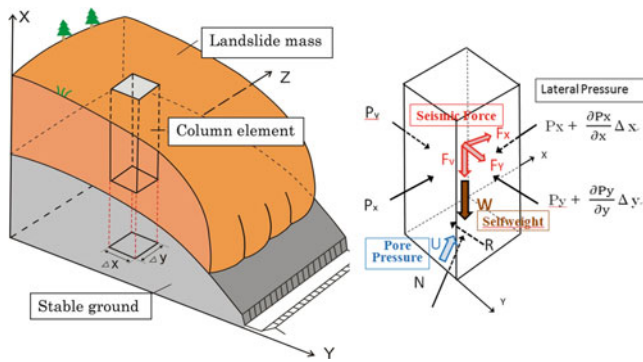


Fig. 11 Concept of landslide simulation model (Sassa et al. 2010)

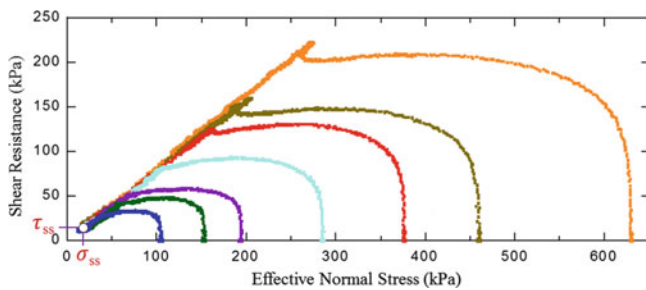


Fig. 12 Steady-state shear resistance under different normal stresses ($B_D = 0.95-0.96$) from Okada et al. (2000)

against the normal component of the self-weight, (6) pore pressure acting at the base (U).

The landslide mass (m) will be accelerated by a force (a) given by the sum of these forces: driving force (self-weight + seismic forces) + lateral pressure + shear resistance

$$am = W_p + \left(\partial P_x / \partial x \cdot \Delta x + \partial P_y / \partial y \cdot \Delta y \right) + R \quad (3)$$

Here, R includes the effects of forces of N and U in Fig. 11 and works in the upward direction of the maximum slope line before motion and in the opposite direction of landslide movement during motion.

The slope angle varies depending on the position of the column within landslide mass. All stresses and displacements are projected to the horizontal plane and calculated on the plane (Sassa 1988).

Effect of Soil Depth in the Landslide Mass on the Steady-State Shear Resistance

The most important factor in predicting the motion of landslides is the steady-state shear resistance. The term “Steady State” is defined as the stress state at the failure surface in which shear displacement will proceed without any change of stress. Steady-state shear resistance is affected by pore-pressure generation in the shear zone. The Nikawa landslide was triggered in the Osaka formation by the 1995 Hyogoken Nanbu earthquake. It killed 34 people in

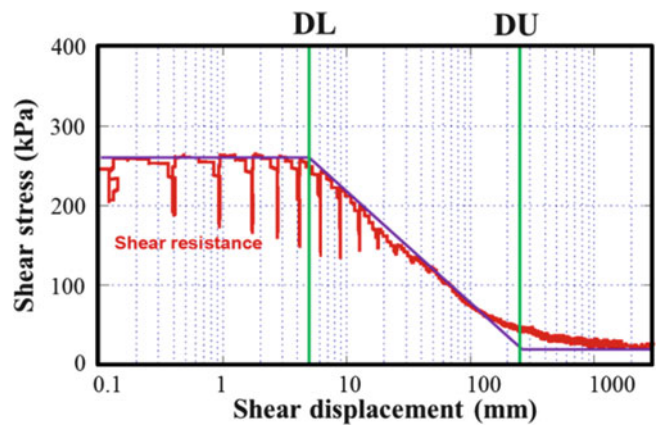


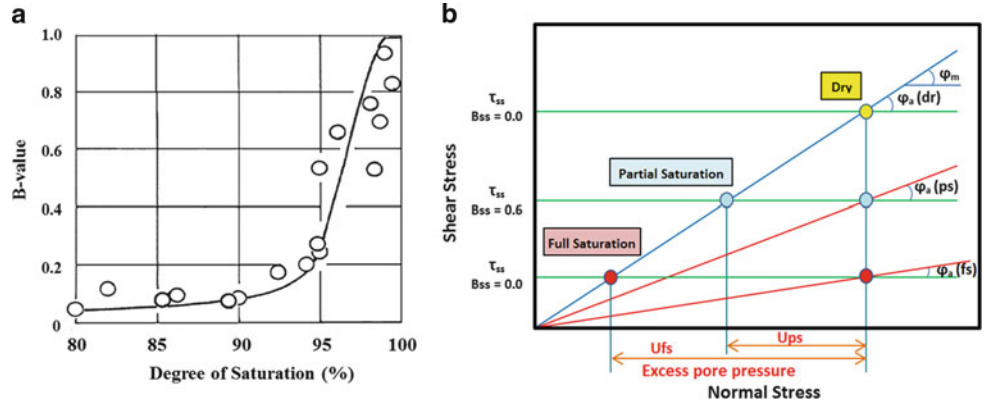
Fig. 13 Shear-resistance reduction after failure to steady state ($B_D = 0.98$)

Nishinomiya city, Hyogo Prefecture, Japan. Figure 12 presents test results for weathered granitic soils taken from the Osaka formation (Okada et al. 2000). All soils with different normal stresses reached the same steady-state shear resistance (τ_{ss}) in the undrained ring-shear test. The steady state without any further stress change is interpreted as meaning that there is a certain critical normal stress for each soil below which no grain crushing and volume reduction will occur. The critical normal stress for steady state for this soil is σ_{ss} . Initial stresses varied from 110 to 630 kPa. All of the effective stress paths in these undrained monotonic ring-shear tests reached the same failure line and followed down the failure line due to the pore-pressure generation and were stopped upon reaching steady state (σ_{ss}, τ_{ss}). The depth of the landslide mass changes in the process of movement across different ground topography. The total normal stress acting on the sliding surface changes, but the mobilized steady state shear resistance is constant. This relationship was used in the new integrated computer simulation model (LS-RAPID) simulating the initiation and the motion of landslides (Sassa et al. 2010).

Shear Resistance Reduction After Failure to the Steady State

Figure 13 is the result of a cyclic loading ring-shear test on Tertiary-age sand in which a rapid landslide (the Higashi Takezawa landslide shown in Fig. 7) is triggered by the 2004 Mid-Niigata earthquake. The shear resistance started to decrease after a shear displacement (DL) of 5 mm at the peak shear strength. The landslide initiation process continues until the point DL. After DL, the shear resistance continued to decrease until it reached a steady state after some hundred millimetres of displacement. This relationship of reduction in shear resistance is approximated by a straight line (the purple line in the figure). In this case, the initiation of steady state appears to be at DU (240 mm).

Fig. 14 Effect of saturation on the steady-state shear resistance. (a) Effect of degree of saturation on the pore-pressure parameter B-value (ratio of generated pore pressure for confining pressure increment by undrained triaxial test. Sassa 1988); (b) Conceptual figure of steady-state shear resistance at different soil saturation levels



Modelling of both process of landslide initiation and motion was difficult in a single model. Therefore, the slope-stability analysis dealt with the initiation of landsliding until failure, while landslide runout analysis dealt the landslide motion. There was no method able to model both the initiation and motion in a single integrated model. The undrained ring-shear test enables modeling of both the initiation and the motion in the following approximation (Sassa et al. 2007).

Stage 1 (before failure)

$$\text{for } D < DL : \tan \phi_a = \tan \phi_p, c = c_p, \gamma_u = \gamma_u \quad (4)$$

Stage 2 (steady state)

$$\text{for } D > DL : \tan \phi_a = \tan \phi_{a(ss)}, c = 0, \gamma_u = 0 \quad (5)$$

Stage 3 (transient state)

for $DL \leq D \leq DU$:

$$\tan \phi_a = \tan \phi_p - \frac{\log D - \log DL}{\log DU - \log DL} (\tan \phi_p - \tan \phi_{a(ss)})$$

$$c = c_p \left(1 - \frac{\log D - \log DL}{\log DU - \log DL} \right)$$

$$\gamma_u = \gamma_u \frac{\log DU - \log D}{\log DU - \log DL} \quad (6)$$

Effect of Saturation on Steady-State Shear Resistance

Pore water pressure generation is affected by the degree of saturation. The relationship between pore-water pressure parameter $B = \Delta u / \Delta \sigma_3$ and the degree of saturation (Sr) can be measured in triaxial tests. Figure 14a is the relationship between the B-value and the degree of saturation and was obtained by isotropic triaxial compression tests on the torrent deposits in the 1984 Ontake debris avalanche at

different degree of saturation (Sassa 1988). The sliding surfaces in the landslide and the ring-shear test are both direct shear state. However, the B value in the triaxial compression state and $B_D (= \Delta u / \Delta \sigma)$ in the direct shear state are the same in isotropic soils. This relationship is a reference for the effect of saturation on the steady-state shear resistance. The steady-state shear resistance is changed by the degree of saturation of the soil. We measure the fully saturated steady-state shear resistance from the undrained, fully saturated ring-shear test (namely the point of “full saturation” in Fig. 14b).

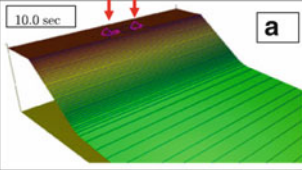
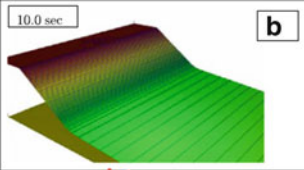
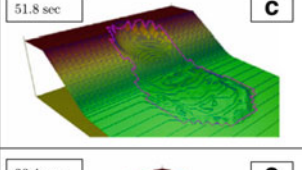
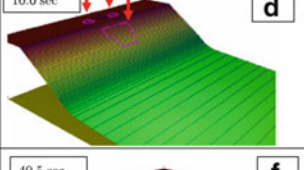
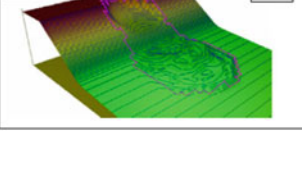
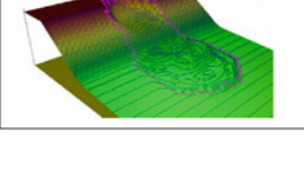
If field conditions are dry, the steady-state shear resistance of the mobilized dry soil layer will be the point “Dry” just above the acting total normal stress shown in Fig. 14b. We use a parameter of pore-pressure generation rate B_{ss} which is very similar to pore-pressure parameter B, although B is defined in the undrained isotropic compression triaxial test while B_{ss} is defined in the undrained ring-shear test. In Fig. 14b, we denote the steady-state shear resistance at full saturation as τ_{ss} ($B_{ss} = 1.0$) and the dry steady state as τ_{ss} ($B_{ss} = 0.0$). If the proportion of pore-pressure generation is 60 % of the full saturation, the steady state is denoted as τ_{ss} ($B_{ss} = 0.6$). As found in this figure, the apparent friction angle ϕ_a (dr) = ϕ_m in the dry state. ϕ_a (fs) at full saturation is the lowest, ϕ_a (ps) at partial saturation has an intermediate value.

Application of LS-RAPID Simulation to a Simple Slope Condition and the 2006 Leyte Landslide

Application of LS-RAPID to a Simple Slope

The performance of the initiation process of LS-RAPID was examined by applying it to a simple imaginary slope and comparing the results with safety factors obtained from some conventional limit equilibrium slope stability analyses: (1) Fellenius, (2) Bishop simplified, (3) Janbu simplified, (4) Spenser, and (5) Morgenstern–Price methods. The imaginary slope which is composed of three slope parts: flat

Fig. 15 Landslide initiation in LS-RAPID and Slope Stability Analysis (Sassa et al. 2010). Values of parameters: $\tan \phi_p = 0.8$, $C_p = 50$ kPa, $\tau_{ss} = 50$ kPa, $k = 0.5$, $B_{ss} = 0.99$, $\tan \phi_m = 0.60$, $\alpha = 0$. Each mesh size = 10 m, each contour interval = 2 m, simulated area = 350×440 m. *1 Fellenius, *2 Bishop simplified, *3 Janbu simplified, *4 Spencer, *5 Morgenstern-Price

PP ratio r_u	Landslide simulation RAPID		Slope stability analysis				
	DL=10mm, DU=1000mm	DL=2000mm, DU=5000mm	Fel. (*1)	Bisp (*2)	Jan (*3)	Spn (*4)	M&P (*5)
0.4	 a	 b	1.545	1.443	1.381	1.433	1.431
0.5	 c	 d	1.351	1.207	1.151	1.200	1.199
0.6	 e	 f	1.155	0.973	0.923	0.970	0.970

ground at the top, a steep slope in the middle and a gentle slope at the bottom. The area of simulation is 350 m wide and 440 m long, the size of mesh is 10 m, the maximum vertical landslide depth is 40.53 m, the total landslide volume is 231,300 m³. The imaginary landslide body was created in the form of an ellipsoid.

The initiation process due to pore pressure increase was examined by inputting three pore-pressure ratios; $r_u = 0.4, 0.5, 0.6$. The characteristic of LS-RAPID is the expression of strength reduction during deformation and progressive failure, while the limit-equilibrium slope-stability analyses assume that the whole landslide sliding surface fails at once.

A relatively strong slope was considered which could be failed by a high pore-pressure ratio supplied from the bed rock. The values of $\tan \phi_p = 0.8$, $c_p = 50$ kPa, $\tau_{ss} = 50$ kPa, $k = 0.5$, $B_{ss} = 0.99$, $\tan \phi_m = 0.60$ were given to the entire simulation area. As the parameters of the shear-resistance reduction, the shear displacement at the start of reduction DL was given as 10 mm, and the shear displacement when steady-state shear resistance DU was reached was given as 1,000 mm. Local failure and shear-strength reduction starts first at a mesh (site) where the shear displacement first reaches DL = 10 mm, then it may develop to a progressive failure.

In order to compare this simulation result to the safety factors by the limit-equilibrium slope stability analysis such as Fellenius, Bishop, Janbu, Spencer, Morgenstern-Price, enough large shear displacement minimizing the effect of progressive failure was chosen to be 2 m instead of 10 mm for DL, and 5 m for DU, respectively. The large shear displacement DL is effective to restrain the effect of shear-resistance reduction and the progressive failure in the initiation process. The simulation results are shown in the form of 3D perspective views in Fig. 15. The contour line is 2.0 m

pitch. The red color line shows the area of the moving landslide mass. The red color appears when/where the velocity at a mesh exceeds 0.5 m/s.

DL = 10 mm, DL = 1,000 mm

In the case of $r_u = 0.4$ in Fig. 15a, only two small areas at the top of the slope showed slight movement and two red colored circles were observed, but no further progressive failure appeared.

For $r_u = 0.5$ and 0.6, rapid landslide motion appeared as shown in Fig. 15c, e.

DL = 2,000 mm, DU = 5,000 mm

No motion appeared for $r_u = 0.4$, limited deformation appeared for an instant in the case of $r_u = 0.5$ as shown Fig. 15b, d. A rapid landslide occurred for $r_u = 0.6$ (Fig. 15f). The border of landslide initiation is between $r_u = 0.4$ and 0.5 for smaller DL-DU, and it is between 0.5 and 0.6 for larger DL-DU.

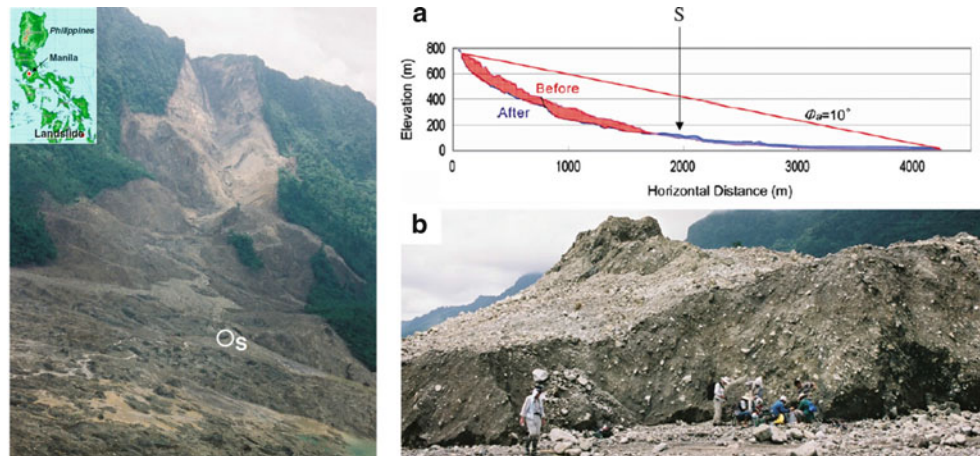
Time

Simulation stops when a zero velocity appears for all meshes. Time in the figure shows the time from the start to the end of motion. Ten seconds for A, B, D is a pre-determined minimum calculation time, because the initial velocity is zero, and some calculation is necessary to know if movement will start or not.

Safety Factors

For the central section of this landslide mass 2D slope stability analyses were implemented using the stability analysis software “Slide V5” by Rocscience Inc. The same peak shear strength parameters and the same pore pressure ratio ($\tan \phi_p = 0.8$, $c_p = 50$ kPa, $r_u = 0.4, 0.5, 0.6$) were used in

Fig. 16 Photo and section of the 2006 Leyte landslide. *Left:* The front view of the Leyte landslide on 17 February 2006 and sampling point S; *Right:* The central longitudinal section of landslide (a) and the sampling point S at the bottom of flow mound (b)



all stability analysis methods. The calculated safety factors for 1: Fellenius, 2: Bishop simplified, 3: Janbu simplified, 4: Spenser, 5: Morgenstern–Price are shown in the right column of Fig. 15. The onset of landslide motion, namely the unit safety factor ($FS = 1.0$) appears when the value of r_u is between 0.5 and 0.6 for four models. For the Fellenius method, the factor of safety becomes unity ($FS = 1.0$) when the value of r_u is between 0.6 and 0.7. Therefore, the border of stability is same with the border by LS-RAPID in the case of long shear displacement (2 m) until the start of shear-strength reduction except in the Fellenius method. The difference between LS-RAPID and the limit equilibrium slope stability analysis comes mainly from LS-RAPID's consideration of local shear and progressive failure vs. the overall shear of the whole landslide body at once. The differences between the three dimensional analysis (LS-RAPID) and the two dimensional analysis cannot be examined in this way.

Application of LS-RAPID to the 2006 Leyte Landslide

A rapid and long-traveling landslide occurred on 17 February 2006 in the southern part of Leyte Island, Philippines. The landslide caused 154 confirmed fatalities and 990 people missing in the debris. The International Consortium on Landslides (ICL) and the Philippine Institute of Volcanology and Seismology (PHIVOLCS) jointly investigated the landslide on the ground and from a helicopter. Figure 16 is a frontal view of the landslide taken by K. Sassa from a helicopter. A planar surface of hard rock is seen at the left side of the head scarp. Other parts of the slope seem to be weathered volcanoclastic rocks or debris. The landslide mass moved from the slope and deposited on the flat area. Many flow-mounds or hummocky structures were found. The features of this landslide were reported by Catane et al. (2007).

The longitudinal section of the central line of the landslide (Fig. 16a) was surveyed by a non-mirror total station and a ground-based laser scanner in the field and compared with a SRTM (Shuttle Radar Topography Mission) map before the landslide which was implemented by H. Fukuoka, a member of the team and colleagues from Philippines. The red-color part shows the initial landslide mass while the blue-color part presents the displaced landslide debris after deposition. The length of landslide from the head scar to the toe of the deposition was around 4 km. The inclination connecting the top of the initial landslide and the toe of the displaced landslide deposit is approximately 10° , which indicates the average apparent friction angle mobilized during the whole travel distance. The value is much smaller than the usual friction angle of debris (sandy gravel) of $30\text{--}40^\circ$. Therefore, it suggests that high excess pore-water pressure was generated during motion. Figure 16b shows a flow mound that travelled from the initial slope to this flat area without much disturbance. Movement without much disturbance is possible when the shear resistance on the sliding surface became very low; thus, movement of the material is like that of a sled.

The material of the flow mound is volcanoclastic debris, including sand and gravel. We observed the material in the source area from the surface and by hand-scoop excavation in the valley-side slope after the landslide. It consisted of volcanoclastic debris or strongly weathered volcanoclastic rocks. It is regarded to be the same material (either disturbed or intact) as observed in the flow mound shown in Fig. 16b. Therefore, we took a sample of about 100 kg from the base of the flow mound shown in the point “S” in the section of Fig. 16a and the photo of Fig. 16b. The location is in the center of travel course and just below the source area. Then, we transported the material to Kyoto, Japan.

A dynamic-loading ring-shear test was conducted as follows. The sample was set in the shear box (250 mm inside diameter, 350 mm outside diameter) of apparatus DPRI-6,

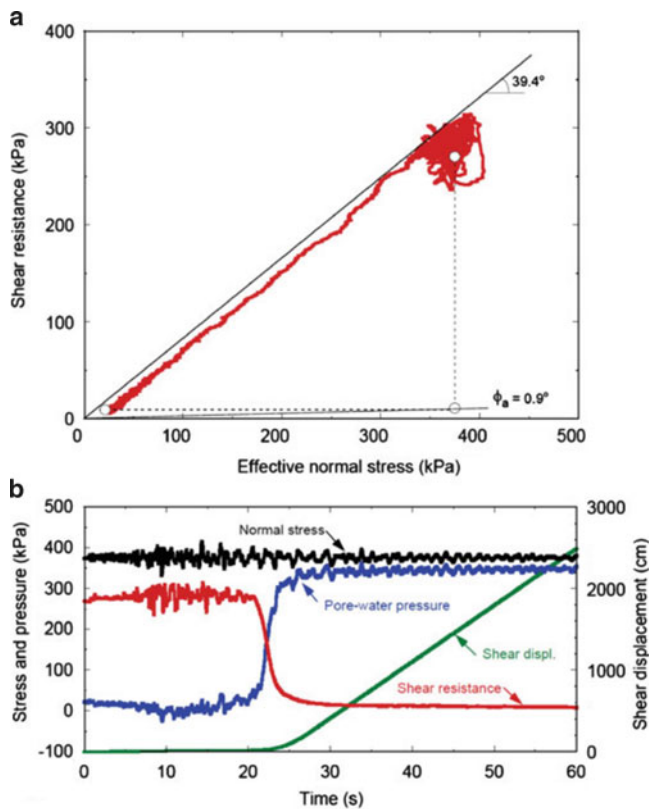


Fig. 17 Test result of the ring shear test of the sample taken from flow mound ($B_D = 0.98$). (a): Stress path. (b): time series data of stresses, pore pressure, shear resistance and shear displacement

and fully saturated ($B_D = 0.98$). The stress acting on the sliding surface of the deepest part (around 120–200 m) is very high. However, because of the capacity of this apparatus DPRI-6 (ICL-2 was not yet developed in 2006): the sliding surface was assumed for the test to be 35 m deep and at an inclination of 25° . The unit weight of the soil was assumed to be 20 kN/m^3 . In the preliminary test to increase pore-water pressure until failure, the failure line of this material was obtained. It has a friction angle of 39.4° and almost zero cohesion. In the simulation test of a rain- and earthquake-induced landslide, the normal stress corresponding to that of 5 m lower than the critical ground-water level (i.e., further 5 m rise of ground-water level shall trigger the landslide) was first loaded on the sample. Then, the shear stress due to the self-weight of the soil layer was loaded. It is the stress point shown by the white circle in Fig. 17a. Using the three components of seismic record observed at Massin (PHIVOLCS, Code number: MSLP, Latitude: 10.1340, Longitude: 124.8590, Elevation: 50.0), normal stress and shear stress acting on the shear surface of 35 m deep with 25° inclination on the direction of the Leyte landslide were calculated so that the peak seismic stress may correspond to the range of seismic acceleration of 60–200 gal which was estimated from the seismic record, attenuation by the

hypocentral distance, amplification by the contract between the base rock and the volcanoclastic debris and the focusing effect of the mountain ridge (Sassa et al. 2010).

Figure 17a presents the stress path of the test. The effective stress path showed a complicate stress path like a cloud. The stress path reached the failure line repeatedly. Therefore, this small seismic stress failed the soil structure and grains during the period of stress reaching the failure line. It generated a pore-water pressure (blue color line) due to grain crushing and volume reduction, and it was accelerated in progress of shear displacement (green color line). Namely sliding-surface liquefaction occurred. The value reached a very small steady-state stress (red color line). This process is presented in the time series data around the failure in Fig. 17b. The mobilized apparent friction coefficient defined by steady-state shear resistance divided by the total normal stress was 0.016 (0.9°).

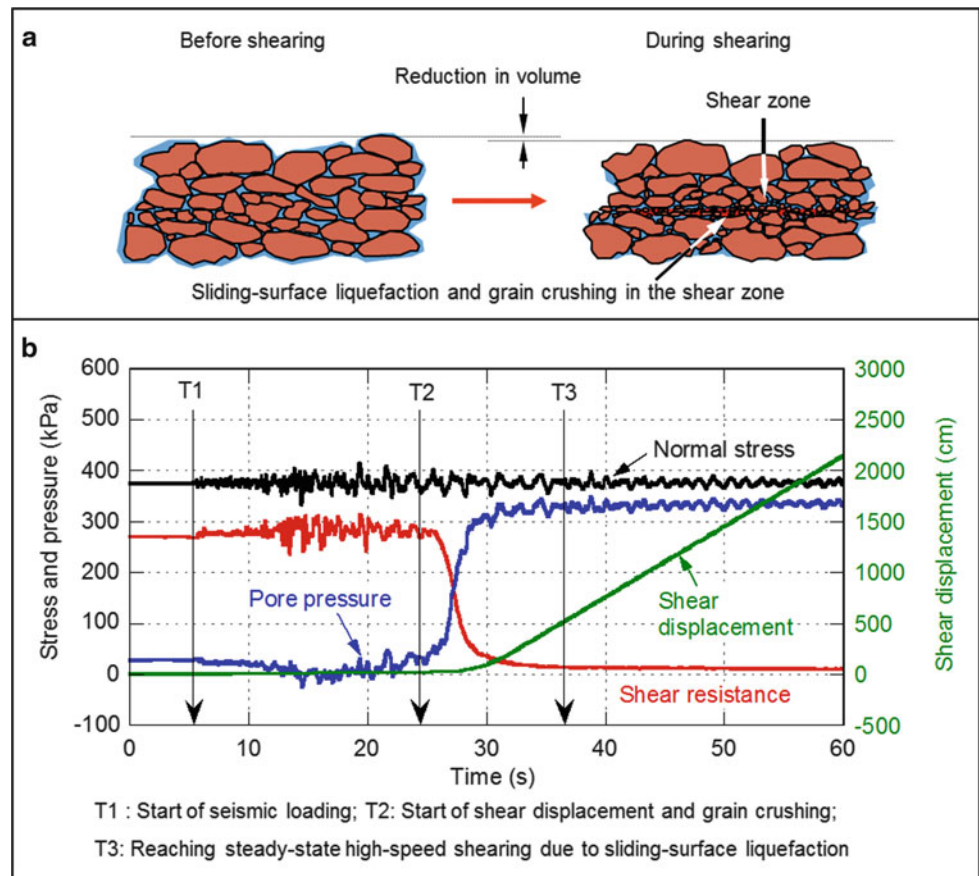
Explanation of Sliding-Surface Liquefaction in This Test Result

The sliding-surface liquefaction is a key finding in the progress of landslide dynamics. It was reported in Sassa (1996, 2000), Sassa et al. (1996). The test result of Fig. 17 presents one of the best examples of “Sliding Surface Liquefaction”. It is here explained in Fig. 18a, b.

Grains in the shear zone are crushed during shearing under a normal stress greater than a critical normal stress at steady state (σ_{ss}). The soil structure failed and was subjected to volume reduction. In the fully saturated undrained state, a high pore pressure was generated by a minimum reduction of volume. Then, both of the effective stress and the mobilized shear resistance were reduced. T1 in b figure is the onset of seismic loading. Immediately pore pressure started to decrease. It is interpreted that a dilatancy occurred which is a characteristic of dense materials. T2 in b figure is the start of post-failure shear displacement. The pore pressure was progressively increased to close to the normal stress and then kept constant. The difference between normal stress and pore-water pressure corresponds to the normal stress at steady state (σ_{ss}). T3 in b is the start of steady-state high-speed motion, namely rapid landslide motion. The mobilized shear resistance at this stage is the steady-state shear resistance (τ_{ss}). A rapid motion was reproduced in this simulation test.

The most important parameter for landslide motion was the steady-state shear resistance (τ_{ss}). The steady-state shear strength was very low (less than 10 kPa in Fig. 17). The testing condition was full saturation ($B_D = 0.98$) and the loading stress corresponded to 35 m deep (much shallower) and the sample used may be more weathered than that in the deep landslide body. So we selected $\tau_{ss} = 40 \text{ kPa}$ as a practical value for this landslide. Various combinations of values of factors can be considered. It was not easy, but we

Fig. 18 The explanation of the sliding surface liquefaction using the test of Fig. 17. (a) Illustration of the sliding-surface liquefaction, (b) Monitored pore pressure generation and mobilized shear resistance during the sliding surface-liquefaction in the undrained seismic-loading ring shear test on the sample taken from the 2006 Leyte landslide (Sassa et al. 2010)



assumed the following: The landslide was deep and the material seemed to be intact in the source area as seen in Fig. 16. Then, we estimated that the peak friction and peak cohesion before motion in the source area should be high ($\tan\phi_p = 0.9$, $c_p = 100\text{--}300$ kPa); the part of the head scarp shown in Fig. 16 would be not saturated because it was close to the ridge, probably there was less ground water to generate excess pore-water pressure. A value of $B_{ss} = 0.1\text{--}0.2$ was assigned in this area; the middle part was probably more saturated ($B_{ss} = 0.4\text{--}0.6$) and the lower part in the paddy fields on the flat area was probably well saturated ($B_{ss} = 0.9\text{--}0.97$); The landslide body was stiff in the top, and moderate in the middle and much disturbed in the lower part and on the flat area (lateral pressure ratio $k = 0.2\text{--}0.7$); The shear displacement of shear strength reduction was estimated as $DL = 100$ mm, $DU = 1,000$ mm referring to the test of Fig. 17.

In the trial simulation, no landslide occurred when the pore-pressure ratios were $r_u = 0.10$ and 0.15 . However, the case of $r_u = 0.16$ caused a rapid landslide. Namely $r_u = 0.16$ (the ground-water depth was equal to about 30 % of the depth of landslide mass) was the critical value to trigger a landslide without an earthquake. Then, various magnitudes of seismic shaking using the wave

forms of EW, NS, and UD recorded at Maasin, Leyte were given in addition to a pore pressure ratio of 0.15. The threshold to create a rapid landslide was between $K_{EW} = 0.11$ and 0.12 . We used $K_{EW} = 0.12$. Using the ratio of magnitudes of seismic records of EW, NS and UD, $K_{NS} = K_{UD} = 0.061$ were given. The seismic shaking of three directions of EW, NS and UD were applied in this simulation. Unstable deposits three meters thick were assumed in the alluvial deposit area.

Blue dots shown in Fig. 19a are the unstable soil deposits (initial landslide body) in the source area and also the unstable deposits in the alluvial flat area. A series of simulated positions of the landslide are presented in Fig. 19. Each step of a–e is explained as follows.

- r_u rises to 0.15 and earthquake starts but no motion.
- Continued earthquake loading ($\text{Max } K_{EW} = 0.12, K_{NS} = K_{UD} = 0.061$) triggers a small local failure as presented in red color mesh,
- An entire landslide block is formed and moving,
- The top of the landslide mass goes on to the alluvial deposits,
- Deposition at the end of landslide motion.

The travel distance and the major part of the landslide distribution were well reproduced (Sassa et al. 2007).

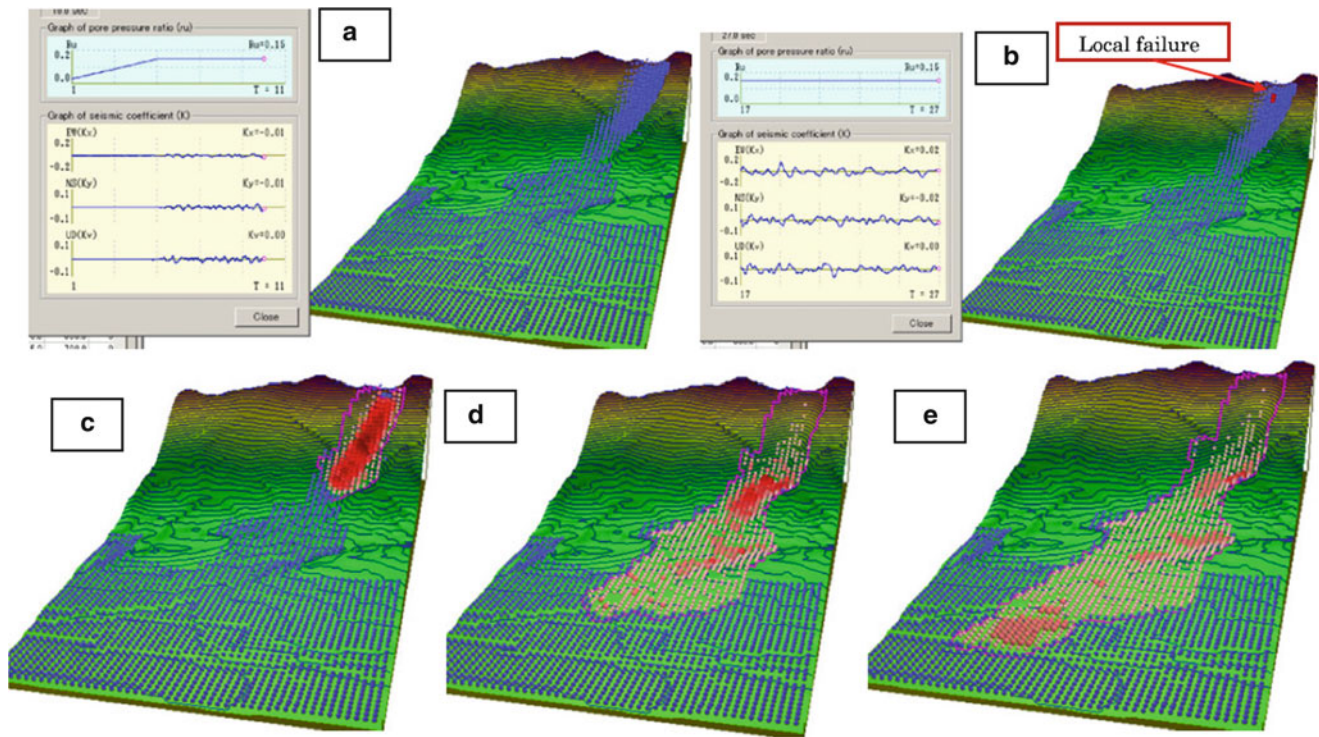


Fig. 19 Simulation result of the Leyte landslide. Pore pressure ratio due to ground water: $r_u = 0.15$; Seismic coefficient by the earthquake: $K_{EW} = 0.12$, $K_{NS} = K_{UD} = 0.061$; Mesh size is 40 m. Area is $1,960 \times 3,760$ m. Contour line is each 20 m. Three meter unstable deposits was assumed in the whole alluvial area. (a) Simulation result after 11 sec from loading the triggering factors. The upper-left figure

shows pore pressure ratio, and the lower-left figure presents seismic loading. The right figure shows distribution of unstable soil mass without motion, (b) Simulation result after 27 sec, starting a local failure, (c–e) Simulation results showing the motion of landslide from the source area to the deposit

Latest Progress of Landslide Dynamics

Study of Dynamics of Submarine Megaslides

Figure 20 presents the onland and submarine topography in Suruga Bay, Japan, where the Philippine Sea Plate subducts under SW Japan. A distinctive depression known as Senoumi (Sea of stone flower). Senoumi forms a step on the western side of the Suruga Bay with a gully. The section A-A' passing through this gully is shown in the lower figure of Fig. 20. The slopes in the steep parts of the head scarp and toe in the section A-A' are $8\text{--}12^\circ$. The shape of the Senoumi feature differs from those of most landslides as the exit to the Suruga Trough is very narrow relative to the width of the Senoumi depression. If Senoumi had formed by a blockslide, the mass could not move out through this narrow exit. However, it is possible to form such a shape if the landslide mass almost liquefies after failure and moves/flows down-slope with very low shear resistance while the landslide enlarges retrogressively. The landslide is very large compared to terrestrial landslides. However, the sizes of submarine landslides are known to range very widely (Locat and

Lee 2008, and others). Due to downward erosion rivers are well developed on land, and therefore, the width of a single slope between rivers can not be so wide. However, the development of rivers is minimal beneath the sea. So a unit of slope can be very wide. It is one of the main reasons for the large size of submarine landslides. A detailed explanation on Senoumi is reported in Sassa et al. (2012). We introduce the application of the undrained dynamic-loading ring-shear apparatus to Senoumi, to define a mechanism for a possible submarine landslide.

The application of the undrained dynamic-loading ring-shear apparatus to study the mechanism of submarine landslides attracted the Integrated Ocean Drilling Program (IODP) researchers. Sassa and colleagues applied to use a submarine sample recovered from the inferred base of a large paleo-landslide in the Nankai Trough cored at Site C0018 during Integrated Ocean Drilling (IODP) Expedition 333 in December 2010 (Strasser et al. 2012). The recovered section (0–315 m below sea bottom) records ~ 1 Ma of submarine landsliding history in this active tectonic setting. Six mass-transport deposits (MTDs) with thickness up to 60 m were identified in the drill cores. Fig. 21 summarizes location of MTDs, dominant lithology in the stratigraphic

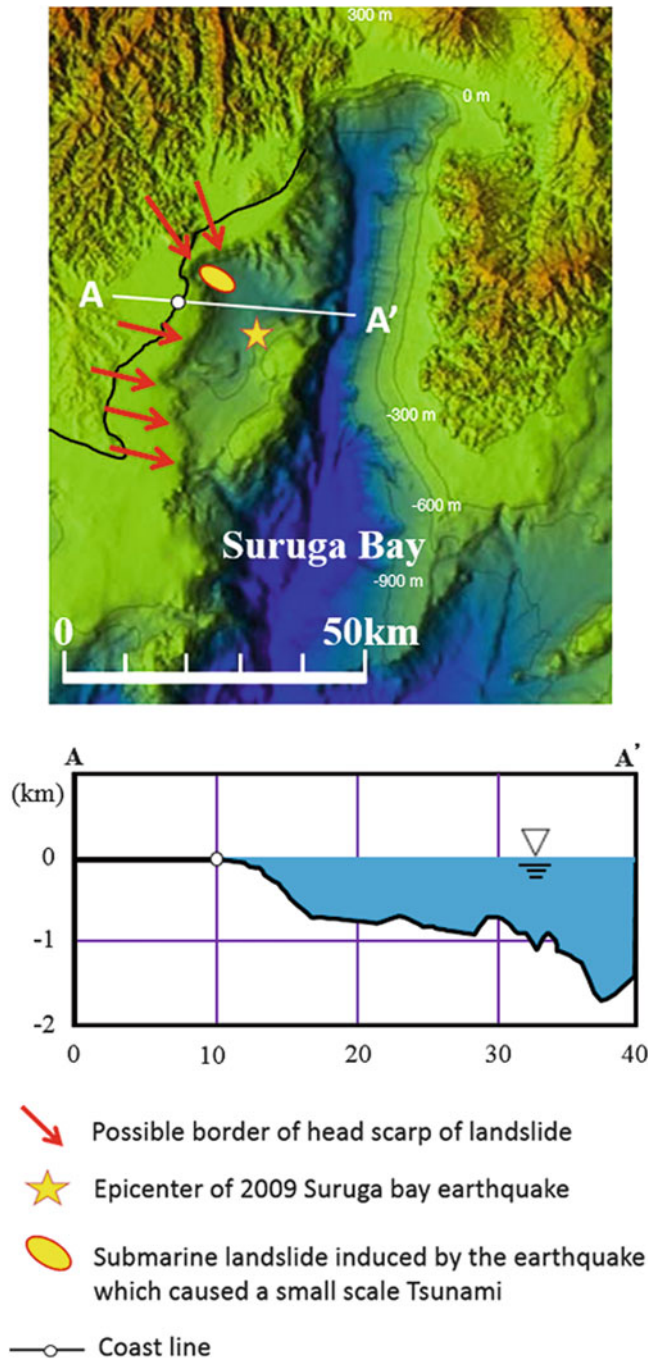


Fig. 20 A possible megaslide in the Suruga Bay in Japan

column and structural geological observations (Strasser et al. 2012). A volcanic-ash layer inferred to be the base of the MTD 6 was used as the test sample in this study. A section photo of this part and also a microscope image are included in Fig. 21. This ash layer correlates to the “Pink” volcanic ash sourced from the Kyushu island, Japan and is dated to 0.99–1.05 Ma (Hayashida et al. 1996). Comparable volcanic-ash layers as cored at IODP C0018 drill site are

likely to have been deposited also in Suruga Bay, where no deep-drill hole is available as yet. We therefore tested a sample taken from this fine-grained volcanic ash layer at the base of the landslides (MTD) drilled at IODP Site C0018 as an analog material for potential Suruga Bay sliding surfaces using Ring-shear apparatus ICL-1.

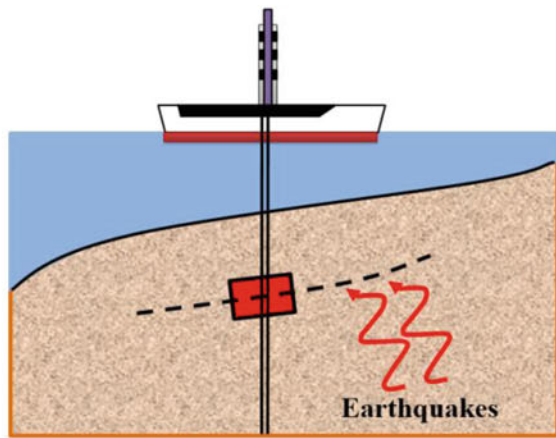
The effective unit weight of soils in the sea water is expressed by the difference between the unit weight of saturated soil and the unit weight of sea water. The total unit weight of soils in the submarine layer was assumed to be 18.6 kN/m^3 from C0018 drilling data (Expedition 333 Scientists 2012). The unit weight of sea water was 10.1 kN/m^3 from the average sea water density ($1,026 \text{ kg/m}^3$). The normal stress of 1,000 kPa (the maximum capacity of ICL-1) corresponds to a burial depth of 117 m. The thickness of the largest landslide deposit from Site C0018 (MTD 6) is 60 m, but the sample depth is 189 m below sea bottom (Fig. 21). A depth of landslide in Senoumi Bay was estimated to be 200–600 m from current sea bottom. We selected 1,000 kPa for the loaded normal stress since it is the upper limit of ICL-1. The angle of the slope is given by \tan^{-1} (initial stress/initial normal stress due to gravity). The angle of the steeper slopes in section A-A' of Fig. 20 is $8\text{--}12^\circ$. Thus, 160 kPa was assumed as the initial shear stress, which corresponds to a slope of $\tan^{-1}(160/1,000) = 9.09^\circ$.

The procedure of the test was as follows: (1) a necessary amount of sample was saturated with de-aired water and left in a vacuum cell for one night to remove air bubbles; (2) the sample box was filled with de-aired water; (3) the fully saturated sample was placed in the de-aired water in the shear box; (4) de-aired water was circulated for a while; (5) the B_D value ($\Delta u/\Delta\sigma$) was measured and confirmed to be greater than 0.95; (6) the normal stress was increased to 1,000 kPa and the shear stress was increased to 160 kPa, both under drained conditions to create the initial stress state of the soil under gravitational loading; (7) a dynamic shear stress was applied using the predetermined program (either cyclic stress or seismic stress using the 2011 Tohoku Earthquake wave form).

The Tohoku earthquake is an example of the wave form of a megaquake which has two main shocks, and a long duration of shaking. We examined whether this Tohoku earthquake waveform could produce a rapid landslide motion in a gently dipping sea floor where a shear surface is formed either in volcanic ash or in Neogene silty sand. Various factors of testing conditions such as earthquake wave, loading stress, loading time were examined prior to beginning the undrained ring-shear test.

Examination of Testing Conditions

On 11 March 2011, a great earthquake occurred offshore of the Tohoku Region of Japan. Seismic acceleration from some hundreds to a few thousands gal were recorded at



Drilling by the Drilling Vessel Chikyu of the Japan Agency for Marine-Earth Science and Technology at Coo18 along the Nankai Trough as the Integrated Ocean Drilling Program (IODP) Expedition 333.

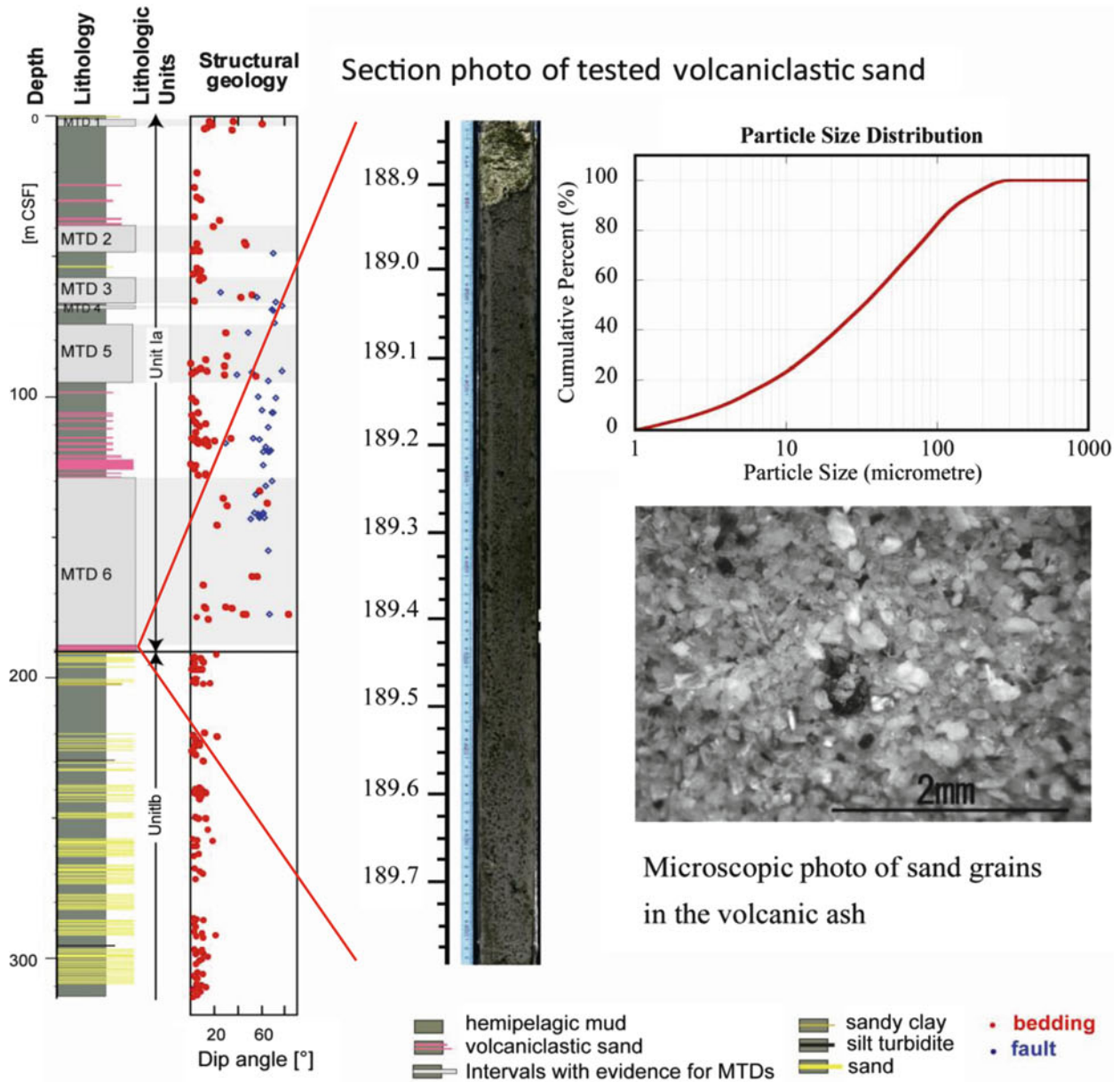


Fig. 21 Sampling of soils of submarine landslides and drilled core

monitoring stations in the Tohoku Region. The largest measured earthquake acceleration (2,933 gal as the resultant acceleration of EW, NS, and UD components and 2,699 gal as a single component) was recorded at station MYG004 at Tsukidate in Miyagi Prefecture, 176 km west of the epicenter. Since mega earthquakes similar to the 2011 Tohoku earthquake have occurred in the past, and likely will occur in the future, the Cabinet Office of the Government of Japan is examining the risk of such a mega earthquake in the Suruga trough (Cabinet Office 2011, 2012). The seismic record of the NS component of MYG004 was used for the ring-shear test as an example of mega-earthquake loading.

Examination of Loading Shear Stress

We examined the testing plan of seismic loading ring shear test based on the results of a cyclic loading test (Sassa et al. 2012). Initial normal stress and shear stress was decided to be the same as used in the cyclic loading test, namely 1,000 and 160 kPa, which corresponds to the normal stress and shear stress due to gravity on a slope of 9.09° . According to the cyclic loading test, an additional 400 kPa of shear stress may fail the sample. So we used 0.3 times the MYG004 NS acceleration record as the maximum acceleration (810 gal) in this ring-shear test. The same value was recorded in FKS009 in Ono of Fukushima Prefecture (217 km from the epicenter).

Examination of Loading Duration

The cyclic loading tests of 0.1 Hz were successful for this sample in ICL-1. The servo-shear stress control motor (400 W) cannot reproduce the high-frequency loading using the recorded data of the 2011 Tohoku earthquake. Preliminary tests were conducted to investigate the time required to reproduce the seismic wave form of MYG004 by increasing the shaking time by factors of 10, 20, and 30. We found that a 30-fold increase in time scale could reproduce shear stress changes similar to the recorded wave form. The ring-shear test is conducted under undrained conditions, and so pore pressure is unaffected by time because no pore-pressure dissipation occurs. The same stress path can be obtained in a 30-times longer test as would be obtained in a real-time test. The comparison of the monotonic (corresponding to 0.0 Hz) undrained shear stress loading test and 0.2, 0.4, and 1.0 Hz cyclic undrained shear stress loading test presented almost the same relationship between stress and shear displacement and also almost the same stress path between the curve of monotonic loading test and the curve connecting peak values of the cyclic loading test (Trandafir and Sassa 2005). Then, the test was conducted in the 30-times longer time period.

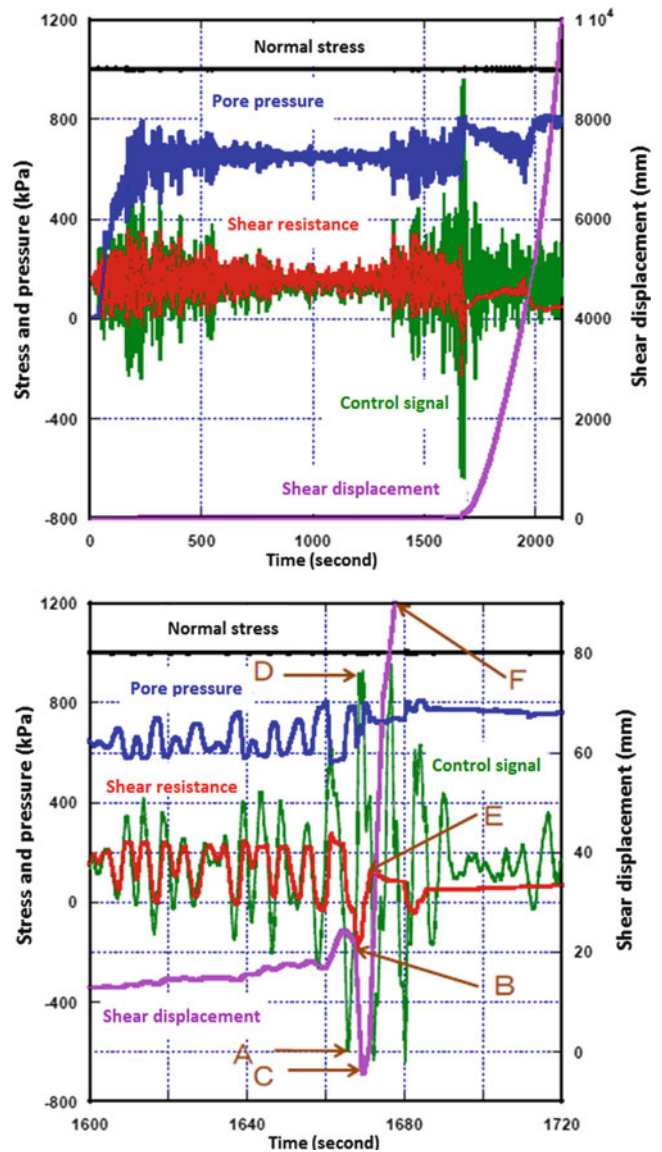
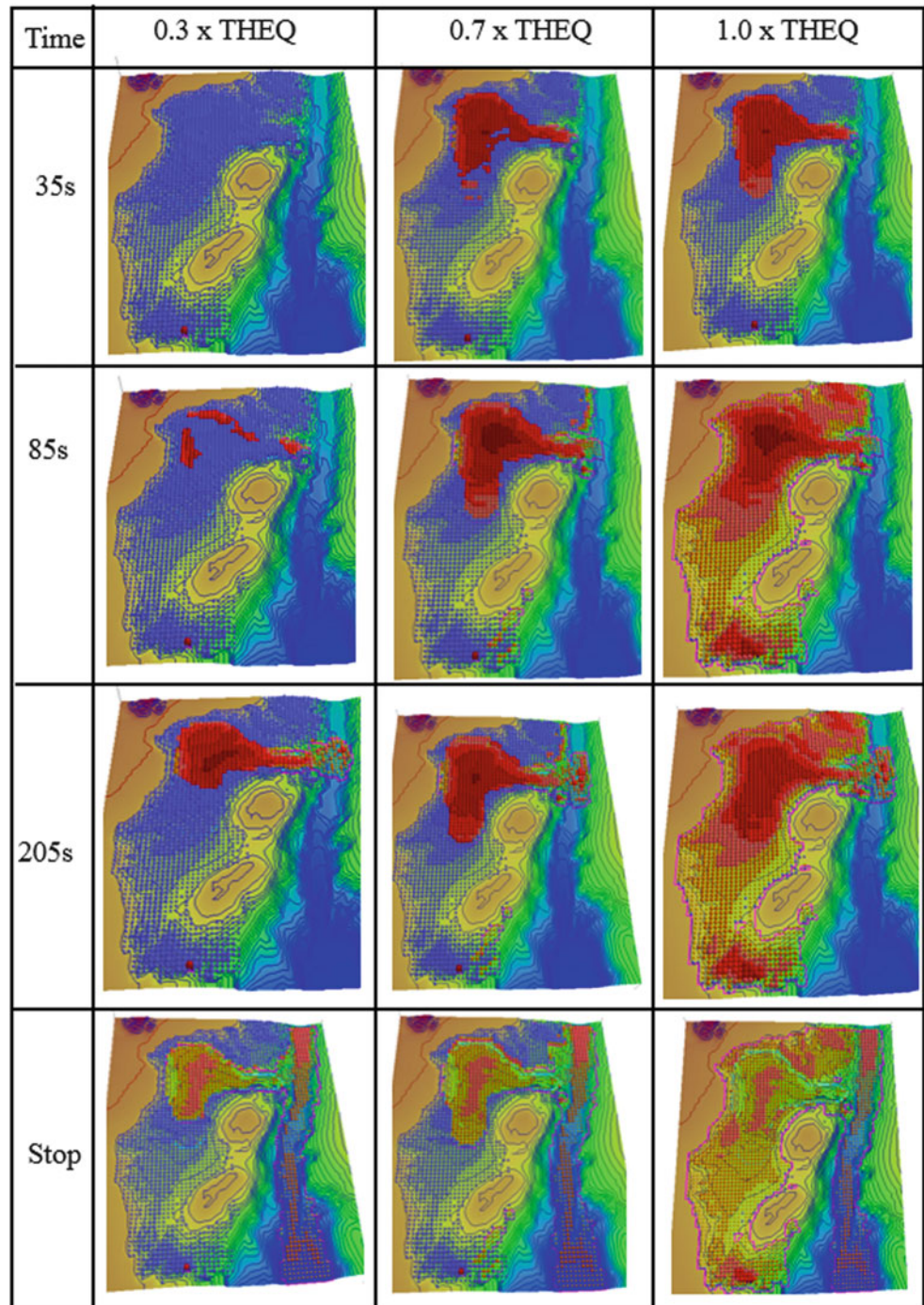


Fig. 22 Test result of seismic loading test on drilled core using the 2011 Tohoku earthquake wave form. The *upper figure* is the time-series data during the seismic loading test. The *lower figure* is the enlarged part of the failure and the start of rapid landslide motion. *Black line* is normal stress, *red line* is the monitored shear resistance during loading, *blue line* is the monitored generated pore pressure during loading, *green line* is control signal for shear stress which is the wave form of the 2011 Tohoku earthquake, but 0.3 times lower acceleration

Figure 22 presents the ring-shear simulation test for the behavior of a submarine slope including a volcanic ash layer subjected to the 0.3 times the largest acceleration history of the Tohoku earthquake.

When the first shock of the seismic loading started, a high pore pressure was soon generated. The mobilized shear stress is smaller than the control signal (loaded shear stress). It means the failure occurred. However, the shear

Fig. 23 Simulation result (LA-RAPID) of the Suruga Bay landslide



displacement was closely below DU (initiation of steady state), then, a rapid motion did not occur. When the second shock arrived, the sample failed before the peak of the second shock and shear strength reduction and rapid landslide motion started, probably the shear displacement exceeded DU. In the lower figure, a negative shear stress failed the soil at the point A, and a large shear displacement started from the point B. When the peak acceleration D arrived, very rapid shear displacement occurred from C to

F under a reduced shear resistance of E and later steady state shear resistance. Here, negative shear displacement means the landslide mass above the sliding surface moved upslope (namely the bed rock below the sliding surface moved downward). This can occur in seismic loading. This ring-shear test simulated experimentally the submarine slope including the volcanic ash layer and showed that it could fail even on a very gentle slope if a very large earthquake were to strike the area.

In order to examine the hypothesis that the Senoumi depression was formed by a submarine megaslide, we applied the new integrated computer simulation model (LS-RAPID) to this case. We input all of the soil properties including key parameters of steady-state shear strength, the critical shear displacements of DU and DL, friction angles at the peak and during motion and others (Sassa et al. 2012). We input all of three components of the MYG004 2011 Tohoku Earthquake acceleration wave form as an example of a very strong earthquake in Japan. The record at MYG004 was the greatest in this earthquake. Recorded accelerations differ between recording stations even at almost the same distance from an epicenter such as 2,933 gal for 176 km at MYG004, 810 gal for 217 km at FKS009. We input the wave form of MYG004, but amplitudes of acceleration multiplied by 1.0, 0.7, 0.4, and 0.3 times, and the excess pore pressure ratio $r_u = 0.3$ in the central and deep area along the A-A' line of the Senoumi depression (Fig. 20) as another triggering factor into the computer simulation LS-RAPID.

The simulation results for IODP volcanic ash using 0.3 times, 0.7 times and 1.0 times MYG004 seismic record is shown in Fig. 23. Blue balls represent soil columns stable or less than 0.5 m/s moving velocity. Red balls show columns with values greater than 0.5 m/s velocity.

In Fig. 23, Time = 35 s presents the situation soon after the first shock. A very small local failure was caused in the bottom of the figure by the first shock of $0.3 \times \text{THEQ}$ (2011 Tohoku Earthquake acceleration). The deep central part subjected to $r_u = 0.3$ failed by $1.0 \times \text{THEQ}$. $0.7 \times \text{THEQ}$ case is in between.

Time = 85 s presents the situation after the second shock. The whole Senoumi area was failed by $1.0 \times \text{THEQ}$. But local failures around the central depression zone only occurred in $0.3 \times \text{THEQ}$.

Time = 205 s presents the further movement of the initiated landslide mass into the Suruga trough.

The final figure (STOP) presents the deposition after the movement of all meshes was terminated.

This result presents that the whole Senoumi area could be formed by a single strong earthquake. An alternative interpretation is that a strong earthquake moved a central part of the Senoumi depression eastwards. Then, a series of subsequent backward development of landslides together with shallow landslides and submarine erosion could create the current whole Senoumi depression.

The ring-shear-simulation tests reproduced the situation of the central part along A-A' line by $0.3 \times \text{THEQ}$. This part failed in $0.3 \times \text{THEQ}$ also in this simulation. Both results agree. The ring-shear test and the computer simulation result gave a reasonable interpretation of the formation of the central part of the Senoumi depression feature.

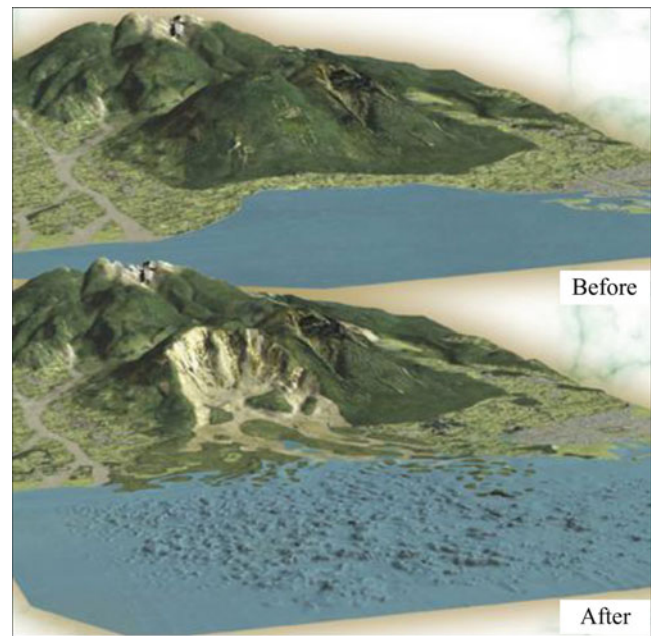


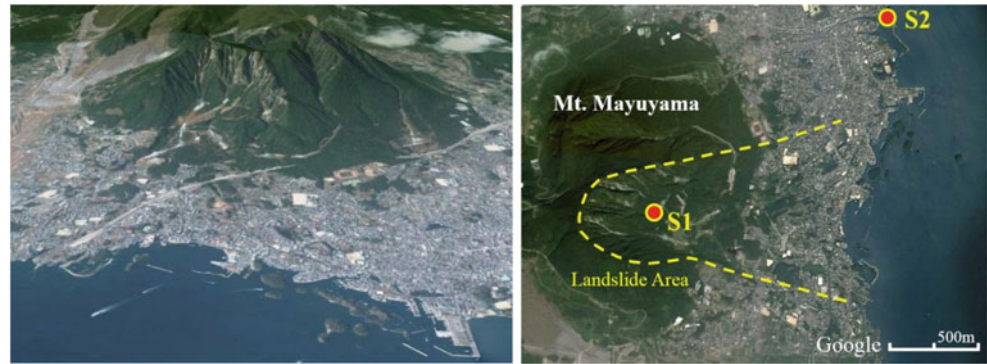
Fig. 24 The 1792 Mayuyama landslide before and after the event (Estimated by the Unzen Restoration Office 2003)

Application of ICL-2 and LS-RAPID to the 1792 Unzen Mayuyama Landslides

The 1792 Unzen Mayuyama megaslide is the largest landslide disaster and also the largest historical volcanic disaster in Japan. This landslide killed a total of 15,153 people, 10,139 people in the Shimabara area, many other people were killed on the opposite banks by the landslide-induced Tsunami wave; 4,653 people in the Kumamoto Prefecture, 343 people in Amakusa Island and 18 people in other areas (Usami 1996). Figure 24 presents a 3D view of the Unzen Mayuyama landslide area before and after the event. It is taken from the cover of Japanese leaflet published by the Unzen Restoration Office of the Ministry of Land, Infrastructure and Transport of Japan (2003) based on a topographic survey and analysis of available sources. The ground surface before the landslide was estimated from paintings of Unzen-Mayuyama from the top of Shimabara castle and others by the Unzen Restoration Office of Japan (2002) referring to Inoue K (1999, 2000). The bed-rock surface in the source area in the upper slope was drawn from the current topography and the location of the bed-rock surface of the lower area was estimated from drilled bore holes.

Figure 25 presents the current images of the Unzen Mayuyama landslide (from Google Earth) and the location of sampling points S1 for the landslide source area. S2 location was selected outside of the landslide moving area to eliminate the effect of the displaced landslide mass. S2

Fig. 25 The present 1972 Mayuyama landslide and the sampling point



sample was tested to represent the soils in the deposition area before the event.

We conducted many tests on sample S1. We introduce one of the basic tests (Fig. 26) which was to trigger the landslide only by increasing pore-water pressure. Firstly the sample was saturated (B_D value was 0.98). Then, it was consolidated to 3.0 MPa normal stress and 1.5 MPa shear stress in the drained condition. This initial stress corresponds to a slope of $\arctan(1.5/3.0) = 26.5^\circ$ which was the initial average slope. Then, pore-water pressure was gradually increased at a rate of $\Delta u = 1$ kPa/s. Failure occurred at pore-water pressure of 1.2 MPa, that is, a pore-water pressure ratio $r_u = 1.2/3.0 = 0.4$. The friction angle at failure was 39.4° .

Figure 26 presents the results of this pore-pressure control test on Sample 1. The value of pore pressure is automatically controlled by the servo-control system using the feedback signal from pore pressure sensor shown in Fig. 6d. The stress path moved to left direction as pore pressure increased until it reached the failure line. Then, the line dropped until the steady-state shear resistance was reached ($\tau_{ss} = 113$ kPa). The real effective stress acting on the sliding surface should be on the failure line after failure. So the pore pressure acting on the sliding surface and the pore pressure monitored by the pore-pressure sensor are different in the pore pressure control test. The time-series data of this test are shown in Fig. 26b. Pore pressure is steadily increased at a predetermined rate ($\Delta u = 1$ kPa/s). At 1,220 s after the start of the test, shear displacement initiated, and simultaneously the shear resistance dropped and the pore pressure increased slightly. But the pore-pressure value was returned to the predetermined rate by the servo-control system. The tentative pore-pressure rise at the time of failure (Fig. 26b, c) suggested a volume reduction due to grain crushing. Thereafter, the shear resistance was maintained at a certain value shown in Fig. 26c. Pore pressure generated in the shear zone due to gain crushing in the shear zone should have dissipated. However, the shear resistance exponentially decreased to the steady state from 1,320 to 113 kPa. During this period, the shear displacement increased from 1.5 to 4.5 m. A pore-pressure controlled test is basically a drained

test because pore water can move in or out of the shear box, as volume reduction due to grain crushing proceeds. A finite width of a less permeable silty layer formed by grain crushing can cause a difference between the pore-pressure value monitored by the pore-water pressure sensor and the pore pressure amongst the fine particles of the shear zone. That is, a high excess pore pressure builds up within the less permeable shear zone, while pore-water pressure outside maintains the value controlled by the pore-pressure servo-control system through the permeable sand sample beyond the shear zone. For comparison, the undrained monotonic shear-control test and the pore-pressure control test were conducted under the same normal stress (3 Mpa). Photos of shear zones in both tests are shown in Fig. 27.

This test result shows that this landslide mass could move rapidly even if it were triggered by a slow rate of pore-water rise during rain.

Another implemented test was a seismic loading ring-shear test to simulate initiation of the Mayuyama landslide by the combined effect of pore-water pressure and earthquake shaking. The Unzen Mayuyama landslide was triggered by a nearby earthquake; its magnitude has been estimated to be $M = 6.4 \pm 0.2$ (Usami 1996). Usami notes that the seismic intensity of this earthquake at Shimabara was around “V-VI.” The Unzen Restoration Office estimated that the seismic intensity which triggered the Mayuyama landslide was VII because more than 30 % houses were destroyed in the Shimabara area. The exact seismic acceleration is not known, but it may have been around 400 cm/s^2 or greater.

The Japanese seismic intensities (Usami 1996) are:

V: $80\text{--}250 \text{ cm/s}^2$ (where walls and fences are cracked and Japanese gravestones fall down)

VI: $250\text{--}400 \text{ cm/s}^2$ (where less than 30 % of Japanese wooden houses are destroyed)

VII: More than 400 cm/s^2 (where more than 30 % houses are destroyed, landslides are triggered and faults rupture the ground surface).

This earthquake was not recorded on a seismograph. We investigated recent landslide cases in Japan to find a similar

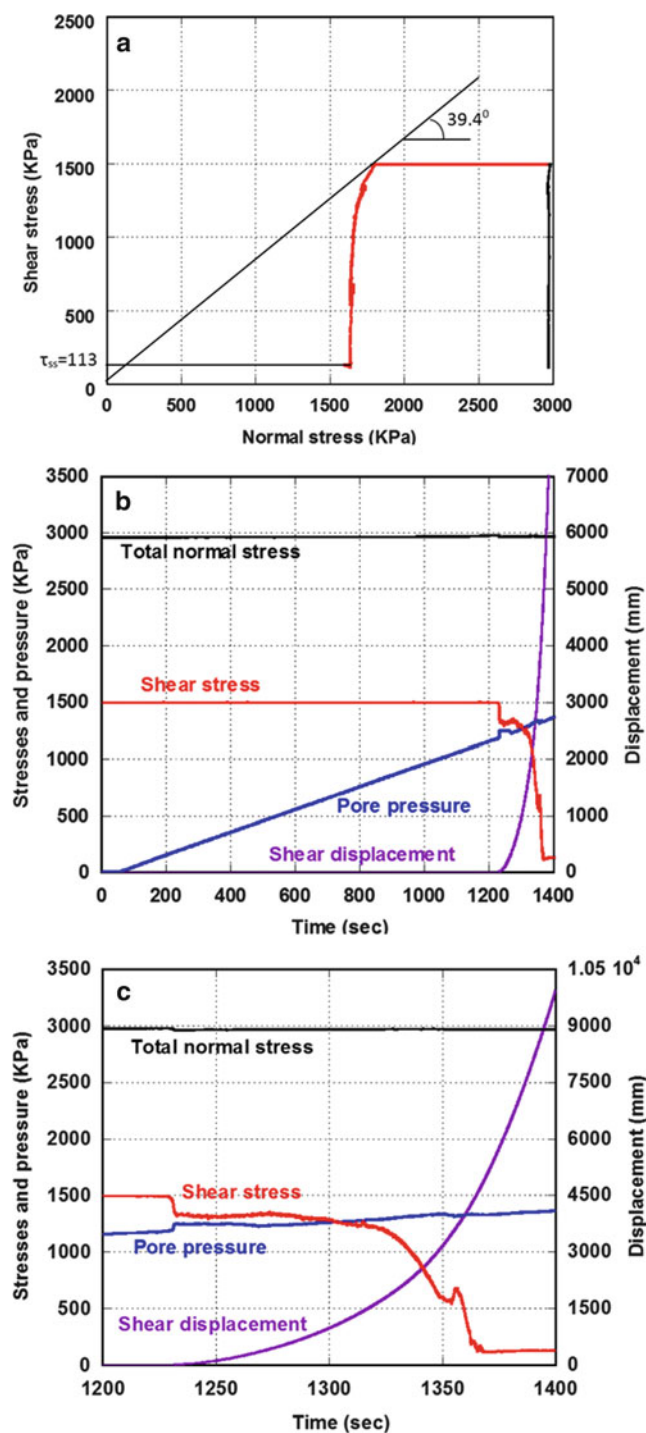


Fig. 26 Ring shear test result simulating the failure due to pore-pressure increase ($B_D:0.98$) (a) Stress path, (b) Time-series data of monitored stresses, (c) Time-series data around the failure

earthquake record that could be used in landslide simulation. The 2008 Iwate-Miyagi Nairiku Earthquake ($M = 7.2$) triggered the Aratozawa landslide (67 million cubic meters) in

Miyagi Prefecture. The maximum recorded acceleration was 739.9 cm/s^2 at MYG004 (National Research Institute for Earth Science and Disaster, Prevention (NIED)). It would be similar to the earthquake which triggered the 1792 Unzen Mayuyama landslide and both earthquakes triggered megaslides. We used the Iwate-Miyagi earthquake wave form recorded in Miyagi Prefecture (MYG004) in the ring-shear test and the numerical simulation.

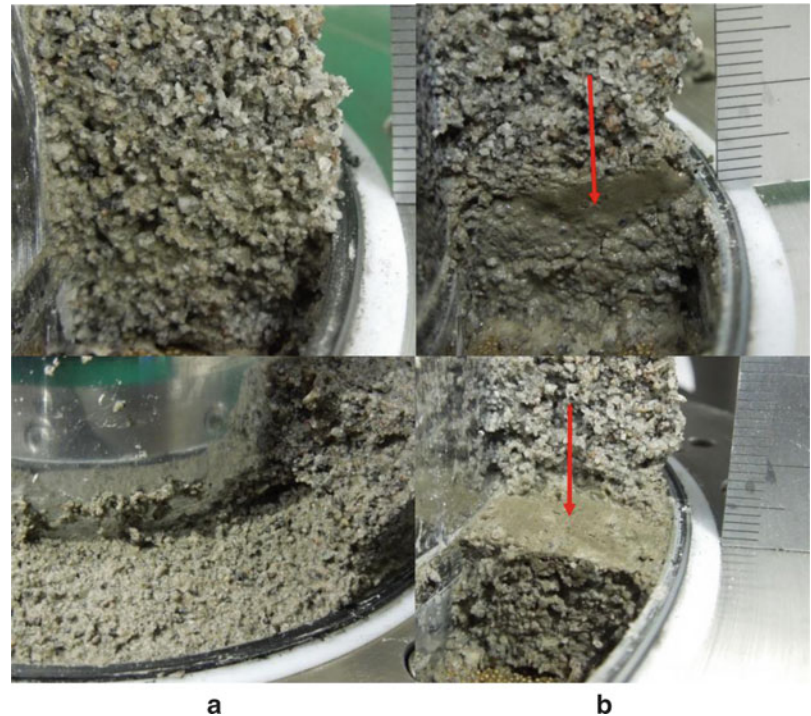
The adopted procedure of the ring shear test for this landslide was as follows.

Initially, the sample (S1) was saturated ($B_D = 0.94$) and consolidated to 3 MPa normal stress and 1.5 MPa shear stress. That is, the corresponding slope angle was $\arctan(1.5/3.0) = 26.6^\circ$. Then, pore-water pressure was increased up to 800 kPa (pore-water pressure ratio $r_u = 800/3,000 = 0.27$) as the initial slope condition (although the exact value was not known, but it must be smaller than 0.4). A preparatory test in Fig. 26 showed that $r_u = 1.2/3.0 = 0.4$ was the critical pore water pressure which caused a landslide without an earthquake. As stated above, the earthquake which triggered the 1792 Unzen-Mayuyama landslide was estimated to be $M = 6.4 \pm 0.2$ with a Japanese Seismic intensity between VI (25–400 cm/s^2) and VII (more than 400 cm/s^2) during the earthquake. The maximum shaking was probably more than 400 cm/s^2 .

The maximum recorded seismic acceleration record of the 2008 Iwate-Miyagi earthquake was 739.9 cm/s^2 which caused the Aratozawa landslide. We loaded the NS component 2008 Iwate-Miyagi earthquake record (maximum acceleration 739.9 cm/s^2) at MYG004 as the additional shear stress. For precise pore-pressure monitoring as well as servo-stress control, a five-times slower speed of seismic acceleration record was applied. The test result is shown in Fig. 28a, b. Figure 28a presents the stress path and Fig. 28b presents the time series data. The green line in the time-series data is the control signal. The maximum value is 2,469 kPa ($1,500 + 969 \text{ kPa}$) and the minimum value is 369 kPa ($1,500 - 1,131$). The loaded acceleration is calculated from the ratio of acceleration (a) and gravity (g): $a/g = 969/1,500$ for positive acceleration or $a/g = -1,131/1,500$ for negative acceleration. The acceleration corresponds to $(969/1,500) \times 980 = +633 \text{ cm/s}^2$ and $(-1,131/1,500) \times 980 = -739 \text{ cm/s}^2$. The control signal for shear stress given to the ring shear apparatus exactly corresponded to the monitored acceleration record.

As the figure shows, failure occurred around 1,825 kPa, at $a/g = (1,825 - 1,500)/1,500 = 0.22$, the necessary acceleration at failure was 216 cm/s^2 . This test result suggested that around 1/3 smaller earthquake shaking (around $216/633 = 0.34$) than the Iwate-Miyagi earthquake could cause failure or the landslide could be triggered under a slope

Fig. 27 Observation of shear zones in an undrained test and in a pore pressure control test (drained) test Total normal stress: 3 MPa. (a) Photo of sample after the undrained monotonic shear stress control test. Any clear grain-crushing shear zone was not observed (B_D : 0.95). (b) Photo of the sample after the pore-pressure control test (B_D : 0.99). A grain-crushing silty shear zone was clearly observed (red arrow)



condition with a pore pressure ratio of 0.27. The steady-state shear strength was 157 kPa. The friction angle was 41.0° , slightly higher than that of the pore-pressure control test in Fig. 26 (39.4°).

LS-RAPID was applied to the 1792 Unzen Mayuyama landslide. The simulation used the geotechnical parameters obtained in the ring-shear test on S1 and S2 and the earthquake record of the 2008 Iwate-Miyagi earthquake at MYG004. The parameters used were the following:

1. Steady-state shear resistance: 120 kPa in the landslide source area (deep soil layer), while 40–80 kPa in the landslide moving area (shallower soil layer) from the test results of normal stresses of 370 kPa, 1,020 kPa, 1,980 kPa (Sassa et al. 2014).
2. Friction angle during motion: 40° .
3. Peak friction angle: 42.0° . The maximum angle was 41.2° in this series of tests. However, the angle under field conditions can be greater.
4. Critical shear displacement for start of strength reduction (DL) and the start of steady state (DU) were 6 mm and 90 mm from cyclic, monotonic and dynamic tests (Sassa et al. 2014).
5. Pore-pressure generation rate B_{ss} is 0.7–0.9 in the source area, and 0.99 under the sea (completely saturated). Outside of the landslide it was 0.2 as the ground was assumed to be unsaturated.
6. Lateral pressure ratio $k = 0.7$ -0.9. We assumed 0.9 in the coastal area and under water. Outside of landslide was 0.4 assuming the ground was not saturated.
7. Unit weight of soils: 19.5 kN/m^3 .

The unit weight of soils at Unzen was not measured. To estimate it, we consolidated the sample (S1) in the ring-shear apparatus in a saturated condition. The consolidation stress, sample height, dry unit weight and saturated unit weight were measured (Sassa et al. 2014). The saturated unit weight can reach 21 kN/m^3 at 3 MPa, but the dry unit weight was 19 kN/m^3 at 3 MPa. Smaller values can exist in shallower area. We used one value for the whole area. We assumed this value to be 19.5 kN/m^3 .

The simulation results are presented in Fig. 29.

At 11 s, the pore water pressure reached 0.21 and the earthquake started, but no motion appeared.

At 17 s, the main shock of earthquake attached the area and the failure occurred within the slope. Failure started from the middle of slope.

At 26 s, the earthquake has almost terminated. The whole landslide mass was formed during the earthquake shaking.

At 64 s, the landslide mass continued to move after the earthquake and entered into the sea.

At 226 s, the landslide mass stopped to move and deposited.

The deposition area was compared with the figure made by topographic survey including the submarine state by the Unzen Restoration office (2002) (bottom-right of Fig. 29). Both landslide hazard areas are very similar. The section of line A in the right-bottom figure and the EW section (almost same with line A) of computer simulation were compared. Both travel distances from the headscarp of the initial landslide to the toe of the displaced landslide mass were also very close (about 6.0–6.5 km).

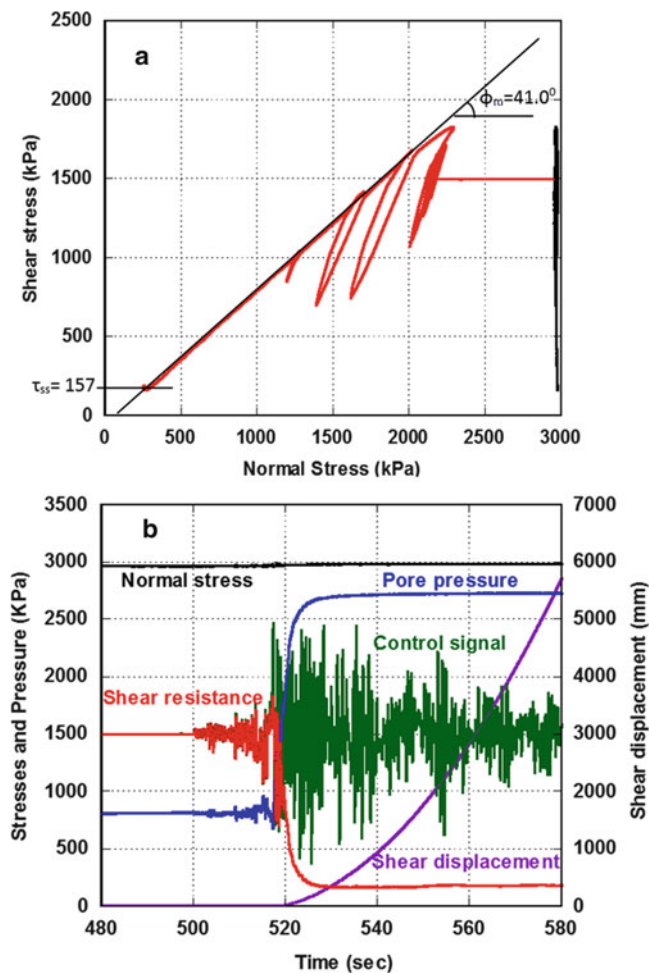


Fig. 28 Undrained ring shear test result simulating the failure due to pore pressure plus seismic loading using the 2008 Iwate Miyagi earthquake (BD: 0.94). (a) Stress path, (b) Time series data of monitored stresses, pore pressure and shear displacement as well as control signal

Significance and Difficulties in Social Implementation of the Landslide Dynamics

The World Landslide Forum (WLF) is a platform for scientists, engineers, practitioners and policy makers who are involved in landslide disaster risk reduction. It is not only a scientific and technical symposium. Please allow us to add the significance in the social implementation of the landslide dynamics and the difficulties to be solved as the background of this study.

The subtitle of WLF2 was “Putting Science into Practice”, the subtitle of WLF3 is “Landslide Risk Mitigation toward a Safer Geoenvironment”. Putting Science into Practice toward a Safer Geoenvironment is one of major objectives of WLF. The social implementation of the landslide dynamics is very important for this target. Sassa and his colleagues have focused on the development of landslide

dynamics for its social implementation for landslide risk reduction as well as the basic science. The mechanism and dynamics of sliding-surface formation within a slope and its post-failure motion are not easy to explain and understand. Even strain is not defined in the shear zone. The material in the shear zone changes before the motion and during the motion in terms of grain-size distribution (components of sands, silts, clays) and grain shape (angular, round). In addition, pore-pressure generation in the shear zone increases the difficulty of application of any universal theoretical analysis.

The most simple and practical method used for landslide risk assessment is to physically simulate the initiation and the motion of landslide by reproducing all of the stresses (gravity, pore-water pressure, seismic stress) on a sample taken from the field under a stress level the same as or similar to the field rather than a theoretical approach based on material science.

Among many soil mechanical tests, the ring-shear apparatus is one able to produce a sliding surface within a soil mass. Most ring-shear apparatus (Bishop et al. 1971; Bromhead 1979; Sadrekrimi and Olson 2009) can shear samples at a certain speed. However, natural phenomena are controlled by the applied stress and stress-control apparatus are necessary to physical simulate natural sliding phenomenon. Then, efforts have been made to reproduce seismic stress loading by earthquakes, pore-pressure increase during rainwater infiltration, and dynamic loading on torrent deposits.

Another important factor necessary for understanding landslide triggering and landslide dynamics is to measure pore-water pressure generated in the shear zone and the shear resistance mobilized on the shear surface during motion. Ring shear apparatus have a gap between the lower shear box and the upper shear box (Bishop et al. 1971; Sassa et al. 2004 and others). Undrained conditions must be kept to measure pore-water pressure in the shear zone during motion (Maximum 5.4 cm/s (ICL-1) to 300 cm/s (DPRI-7) at the center of the sample) by preventing any leakage of water from the moving gap. Pore water pressure is desirable to be measured within or near the shear zone for understanding the mobilized shear resistance. Great effort has gone into solving these two tasks (Table 3 and the servo gap control system in Fig. 6).

We believe that the current undrained dynamic loading ring-shear apparatus (landslide ring-shear apparatus) has been developed from a scientific tool to a practical tool for landslide risk assessment. However, further effort was needed to shift it from being a practical tool within Japan to being an internationally practical tool. Maintenance of the apparatus must be convenient, practical and inexpensive. A new programme known as the Science and Technology Research Partnership for Sustainable Development Program

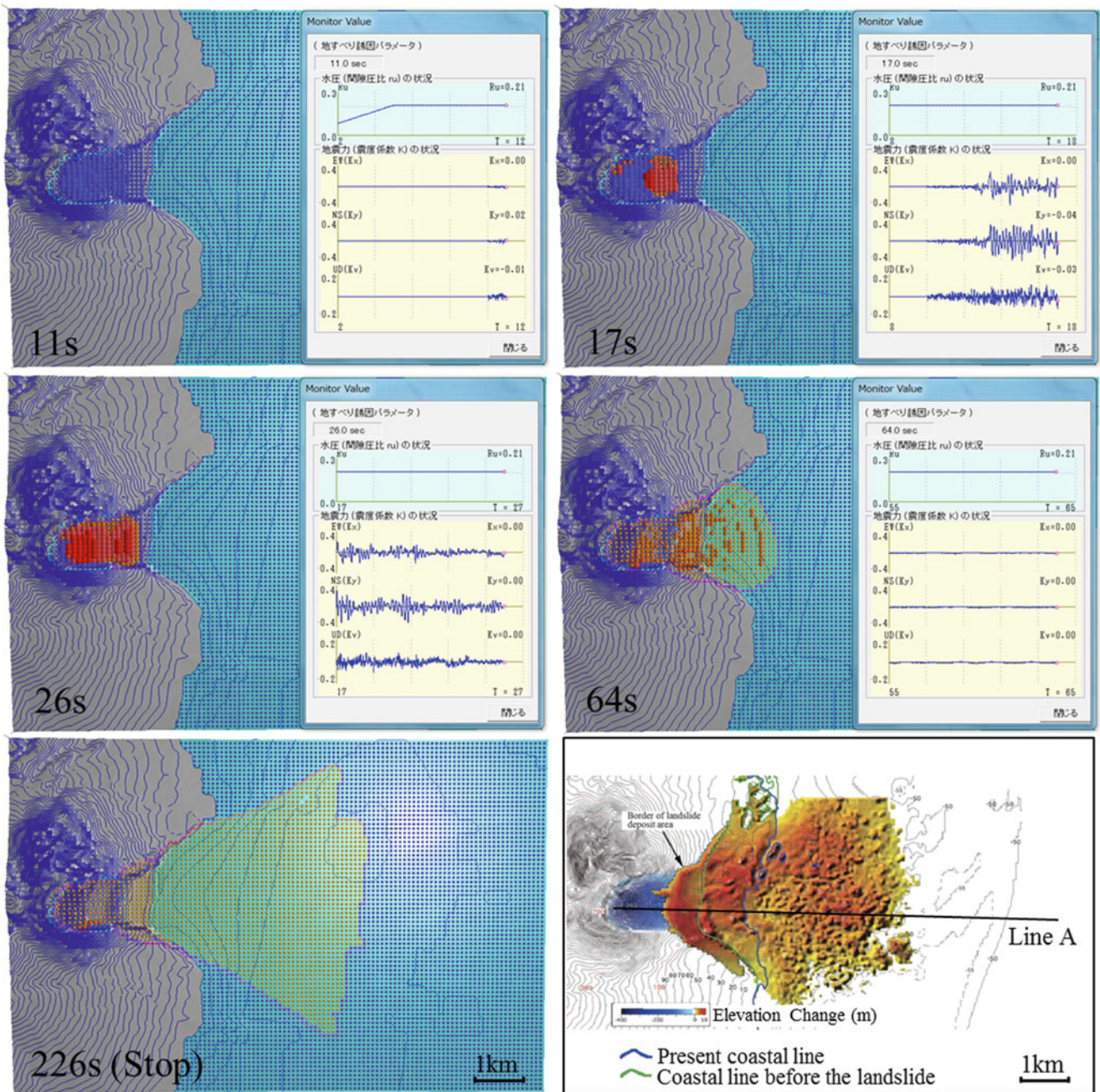


Fig. 29 Simulation result and topographic survey in the plan. Red color balls represent moving mass, while blue balls represent stable mass

(SATREPS) of Japan has started since 2009 in cooperation with the Ministry of Education, Culture, Sports, Science and Technology (MEXT) and the Ministry of Foreign Affairs (MOFA) of Japan. The aim of this programme is to promote the application of Japanese science and technology to sustainable development in developing countries. ICL has obtained funding for two projects (for Croatia and for Vietnam). During these projects, ICL has developed two types of undrained dynamic-loading ring-shear apparatus (ICL-1 for Croatia and ICL-2 for Vietnam). Those two

apparatus were developed for use abroad by minimizing maintenance costs. ICL-1 was donated to Croatia in 2012 and it is well used at the University of Rijeka. The landslide ring-shear simulator is now an international practical tool as well as a scientific tool for landslide science.

The computer simulation for the initiation and the motion (LS-RAPID) has been developed from a scientific research code (initially Sassa 1988) to a user-friendly software used abroad (Sassa et al. 2010) and further improvement through a SATREPS project. The English manuals for

the undrained ring-shear apparatus (Ostic et al. 2013a, b) and the computer simulation (LS-RAPID) (Sassa et al. 2013) were made as part of ICL Landslide Teaching Tools (He et al. 2013, 2014). These manuals are available from <http://icl.iplhq.org/>.

Conclusion

1. A reliable and practical technology is needed to reduce landslide-disaster risk by assessing landslide initiation and motion including landslide velocity, moving area and area at landslide risk, and depth of soils.
2. Analyses of initiation and motion of landslide phenomena are complicated because of pore-pressure generation and changes of grain size, grain shape and water content of the involved soils in the shear zone due to grain crushing and mobilization.
3. Sassa and others together with the Disaster Prevention Research Institute, Kyoto University, and the International Consortium on Landslides have developed a series of ring-shear apparatus models from DPRI-1 to DPRI-7, ICL-1 and ICL-2.
4. The later series of apparatus developed after the 1995 Hyogoken Nambu earthquake can reproduce the sliding-surface formation and post-failure motion by cyclic loading/seismic loading and pore pressure increase within the apparatus.
5. The latest apparatus (ICL-1 and ICL-2 developed by SATREPS projects) increased undrained capacity from 500–630 kPa to 1 MPa (ICL-1) and 3 MPa (ICL-2) by changing the loading structure.
6. The purpose of SATREPS projects is that scientific research and technology developed in Japan can be applied for social implementation in developing countries, namely “Putting Science into Practice”
7. ICL-1 and ICL-2 were much improved from the previous DPRI series in manufacturing cost and maintenance in foreign countries. Improvements include the undrained sealing in the gap between the upper stable shear box and the lower rotatable shear box.
8. Key parameters in landslide dynamics including the steady-state shear resistance (τ_{ss}) and the critical shear displacement (D_L , D_U) and triggering factors of pore-water pressure and seismic records/waves are input to the integrated computer simulation model (LS-RAPID) simulating the initiation and the motion of the landslide. The simulation result can present the initiation from a local failure to formation of a landslide mass through progressive failure; and then present the initial motion of the landslide mass, entrainment of substrate deposits on the lower slopes and deposition with the cessation of motion.
9. Landslide dynamics is a scientific tool, but it is developing into a practical tool for landslide-disaster

reduction in developed and developing countries alike with support from relevant institutions and colleagues.

Acknowledgments The series of undrained dynamic-loading ring-shear apparatus have been supported by various funds from the Ministry of Education, Culture, Sports, Science and Technology of Japan (MEXT). The latest development of ring-shear apparatus models ICL-1 and ICL-2 and accompanied research have been financially supported by the Science and Technology Research Partnership for Sustainable Development Program (SATREPS) of Japan which are financed by the Japan Science and Technology Agency (JST) and the Japan International Cooperation Agency (JICA). Both are projects of the International Programme on Landslides (IPL): IPL-161 Risk identification and land-use planning for disaster mitigation of landslides and floods in Croatia and IPL-175: Development of landslide-risk assessment technology and education in Vietnam and other areas in the Greater Mekong Sub-region. We have obtained much support from ICL and ICL supporting organizations through these two projects. Development of LS-RAPID and currently developing “ICL Landslide Teaching Tools” which is an international joint activity are very important elements for the development of Landslide Dynamics as practical tools. Prof. Zeljiko Arabanas of Lijeka University, Croatian leader of the landslide group in IPL-161 and the user of ICL-1 donated to Croatia, is appreciated for his discussion on this paper. The promotion of these IPL projects by colleagues from ICL and ICL supporting members is very much appreciated.

References

- Bishop AW, Green GE, Garga VK, Andersen A, Brown JD (1971) A new ring-shear apparatus and its application to the measurement of residual strength. *Geotechnique* 21(1):273–328
- Bromhead EN (1979) A simple ring-shear apparatus. *Ground Eng* 12(5):40–44
- Cabinet Office of the Government of Japan (Committee on megaquake model in Nankai Trough) (2011) Intermediate report of the study team for the Mega-quake model in Nankai trough. http://www.bousai.go.jp/jishin/chubou/nankai_trough/chukan_matome.pdf
- Cabinet office of the Government of Japan (Committee on Megaquake Model in Nankai Trough) (2012) The tsunami-fault model in the 2011 off the Pacific Coast of 2011 Tohoku Earthquake, Reference No. 1 of the 12th meeting of Megaquake Model in Nankai Trough. http://www.bousai.go.jp/jishin/chubou/nankai_trough/12/sub_1.pdf
- Catane SG, Cabria HB, Tomarong CP, Saturay RM, Zarco MA, Pioquinto WC (2007) Catastrophic rockslide-debris avalanche at St. Bernard, Southern Leyte, Philippines. *Landslides* 4(1):85–90
- Expedition 333 Scientists (2012) Site C0018. In: Henry P, Kanamatsu T, Moe K, and the Expedition 333 Scientists (eds) *Proc. IODP, 333: Tokyo (Integrated Ocean Drilling Program Management International, Inc.)*. doi:10.2204/iodp.proc.333.103.2012
- Hayashida A, Kamata H, Danhara T (1996) Correlation of widespread tephra deposits based on paleomagnetic directions: link between a volcanic field and sedimentary sequences in Japan. *Quat Int* 34–36:89–98
- He B, Sassa K, Ostic M, Takara K, Yamashiki Y (2013) Effects of parameters in landslide simulation model LS-RAPID on the dynamic behaviour of earthquake-induced rapid landslides. In: Margottini C, Canuti P, Sassa K (eds) *Landslide science and practice*. Springer, Berlin, pp 119–125
- He B, Sassa K, McSaveney M, Nagai O (2014) Development of ICL landslide teaching tools. *Landslides* 11:153–159

- Inoue K (1999) Shimabara-Shigatusaku Earthquake and topographic changes by Shimabara catastrophe. *J Jpn Soc Erosion Control Eng* 52(4):45–54
- Inoue K (2000) Shimabara-Shigatusaku earthquake and topographic change by Shimabara Catastrophe in 1792. *Geographical Reports of Tokyo Metropolitan University*, No. 35:59–69
- Locat J, Lee H (2008) Submarine mass movement and their consequences: an over view. In: Sassa K, Canuti P (eds) *Landslides—disaster risk reduction*. Springer, New York, pp 115–142
- Okada Y, Sassa K, Fukuoka H (2000) Liquefaction and the steady state of weathered granite sands obtained by undrained ring shear tests: a fundamental study on the mechanism of liquidized landslides. *J Nat Disaster Sci* 22(2):75–85
- Ostic M, Sassa K, Ljutic K, Vivoda M, He B, Takara K (2013a) PDF-tool 3.081-1.1 manual for ICL-1—a transportable ring shear apparatus. ICL landslide teaching tools, p.362 and pdf (46 pages) in the attached CD
- Ostic M, Sassa K, He B, Takara K, Yamashiki Y (2013b) Portable ring shear apparatus and its application. In: Canuti P, Sassa K (eds) *Margottini. Landslide science and practice*, Springer, Berlin, pp 365–369
- Sadrekarami A, Olson SM (2009) A new ring shear device to measure the large displacement shearing behavior of sands. *Geotech Test J* 32(3):197–208
- Sassa K (1984) The mechanism starting liquefied landslides and debris flows. In: *Proceedings of 4th international symposium on landslides*, vol 2. pp 349–354
- Sassa K (1988) Geotechnical model for the motion of landslides. *Special Lecture of 5th international symposium on landslides, Landslides, Balkema*, vol 1. pp 37–55
- Sassa K (1992) Access to the dynamics of landslides during earthquakes by a new cyclic loading high-speed ring-shear apparatus. In: *6th International symposium on landslides, Landslides, Balkema*, vol 3. pp 1919–1937
- Sassa K (1996) Prediction of earthquake induced landslides. In: *Proceedings of 7th international symposium on landslides. A.A. Balkema, Trondheim*, 17–21 June, vol 1. pp 115–132
- Sassa K (2000) Mechanism of flows in granular soils. In: *Proceedings of GeoEng2000, Melbourne*, vol 1. pp 1671–1702
- Sassa K, Fukuoka H, Scarascia-Mugnozza G, Evans S (1996) Earthquake-induced landslides: distribution, motion and mechanisms. *Soils and Foundations, Special Issue for the Great Hanshin Earthquake Disaster*, pp 53–64
- Sassa K, Fukuoka H, Wang FW (1997) Mechanism and risk assessment of landslide-triggered-debris flows: lesson from the 1996.12.6 Otari debris flow disaster, Nagano, Japan. In: Cruden DM, Fell R (eds) *Landslide risk assessment, proceedings of the international workshop on landslide risk assessment*. Honolulu, 19–21 February, pp 347–356
- Sassa K, Fukuoka H, Wang G, Ishikawa N (2004) Undrained dynamic-loading ring-shear apparatus and its application to landslide dynamics. *Landslides* 1(1):7–19
- Sassa K, Fukuoka H, Wang FW, Wang GH (2005) Dynamic properties of earthquake-induced large-scale rapid landslides within past landslide mass. *Landslides* 2(2):125–134
- Sassa K, Fukuoka H, Wang FW, Wang GH (2007) Landslides induced by a combined effects of earthquake and rainfall. In: Sassa K, Fukuoka H, Wang F, Wang G (eds) *Progress in landslide science*. Springer, Berlin, pp 311–325
- Sassa K, Nagai O, Solidum R, Yamazaki Y, Ohta H (2010) An integrated model simulating the initiation and motion of earthquake and rain induced rapid landslides and its application to the 2006 Leyte landslide. *Landslides* 7(3):219–236
- Sassa K, He B, Miyagi T, Strasser M, Konagai K, Ostic M, Setiawan H, Takara K, Nagai O, Yamashiki Y, Tutumi S (2012) A hypothesis of the Senoumi submarine megaslide in Suruga Bay in Japan—based on the undrained dynamic-loading ring-shear tests and computer simulation. *Landslides* 9(4):439–455
- Sassa K, Nagai O, He B, Gradiski K (2013) PDF-tool 3.081-1.2 manual for the LS-RAPID software. ICL landslide teaching tools, p 363, 43 pages (pdf) in the attached CD
- Sassa K, Dang KQ, He B, Takara K, Inoue K, Nagai O (2014). Development of a new high-stress undrained ring shear apparatus and its application to the 1792 Unzen-Mayuyama megaslide in Japan. (contributed to landslides in 2013)
- Strasser M, Henry P, Kanamatsu T, Thu M, Moore G, IODP Expedition Scientists et al (2012) Scientific drilling of mass-transport deposits in the Nankai accretionary wedge: first result of from IODP Expedition 333. In: Yamada Y et al (eds) *Submarine mass movements and their consequences*, vol 31, *Advances in natural and technological hazards research*. Springer, New York, pp 671–681
- Trandafir A, Sassa K (2005) Seismic triggering of catastrophic failures on shear surfaces in saturated cohesionless soils. *Can Geotech J* 42:229–251
- Unzen Restoration Office of the Ministry of Land, Infrastructure and Transport of Japan (2003) *The Catastrophe in Shimabara -1791-92 eruption of Unzen-Fugendake and the sector collapse of Mayuyama*. A Japanese leaflet (44 pages)
- Unzen Restoraton Office of the Ministry of Land, Infrastructure and Trasnport of Japan (2002) *The Catastrophe in Shimabara -1791-92 eruption of Unzen-Fugendake and the sector collapse of Mayuyama*. An English leaflet (23 pages)
- Usami T (1996) *Materials for comprehensive list of destructive earthquakes in Japan*. University of Tokyo Press, Tokyo

Part II

International Programme on Landslides



Introduction: International Programme on Landslides—IPL

Matjaž Mikoš, Badoui Rouhban, Irasema Alcántara-Ayala, and Xiaochun Li

Abstract

This is a short introduction to the Special Session A1 *International Programme on Landslides—IPL* dedicated to the IPL projects and to the World Centres of Excellence (WCoE) in Landslide Risk Reduction, and their activities in the period between the WLF2 in Rome (2011) and the WLF3 in Beijing (2014) (Sassa et al. *Landslides* 9(2):285–297, 2012).

Keywords

International Consortium on Landslides • International cooperation • International Programme on Landslides • Landslide research • Landslide risk reduction, World Centres of Excellence

This is a short introduction to the Special Session A1 *International Programme on Landslides—IPL* dedicated to the IPL projects and to the World Centres of Excellence (WCoE) in Landslide Risk Reduction, and their activities in the period between the WLF2 in Rome (2011) and the WLF3 in Beijing (2014) (Sassa et al. 2012).

The IPL is a programme of the ICL. It is developed in partnership with ICL supporting organizations aiming at organizing work in response to the ICL goals. The programme is managed by the IPL Global Promotion

Committee (IPL-GPC) including ICL and the following ICL supporting organizations: the United Nations Educational, Scientific and Cultural Organization (UNESCO), the World Meteorological Organization (WMO), the Food and Agriculture Organization of the United Nations (FAO), the United Nations International Strategy for Disaster Risk Reduction (UNISDR), the United Nations University (UNU), the International Council for Science (ICSU), the World Federation of Engineering Organizations (WFEO) and the International Union of Geological Sciences (IUGS).

The World Centres of Excellence (WCoE) on Landslide Risk Reduction are identified every three years on the occasion of the World Landslide Forum with the aim of: (i) strengthening IPL and IPL-GPC; (ii) creating “A Global Network of entities contributing to landslide risk reduction”; (iii) improving the global recognition of “Landslide Risk Reduction” and its social-economic relevance, and entities contributing to this field.

The IPL projects and the WCoEs on Landslide Risk Reduction were an important part of the ICL/IPL activities in the first decade of the ICL, and these two forms of international cooperation remain a vital part of the ICL Strategic Plan 2012-2021 (Sassa 2012) that is oriented towards creation of a safer geoenvironment.

M. Mikoš (✉)

Faculty of Civil and Geodetic Engineering, University of Ljubljana, Jamova c. 2, SI-1000, Ljubljana, Slovenia
e-mail: matjaz.mikos@fgg.uni-lj.si

B. Rouhban

Section for Disaster Reduction, UNESCO & IPL Advisor of the International Consortium on Landslides, 138-1 Tanaka Asukai-cho, Sakyo-ku, Kyoto 606-8226, Japan

I. Alcántara-Ayala

Instituto de Geografía, Universidad Nacional Autónoma de México, Circuito Exterior s/n., Mexico, Mexico

X. Li

Department of Hydrogeology and Environmental Geology, China Geological Survey, 45 FuWai Street, Beijing 100037, China

The Session A1 titled “International Programme on Landslides—IPL” was the first session in a row of 3 parallel sessions at the World Landslide Forum WLF3 (Sassa 2013a):

- A. Special Sessions (8 sessions);
- B. Sessions for Methods of Landslide Studies (10 sessions);
- C. Sessions for Targeted Landslides (9 sessions);
- D. Side events (5 sessions).

Altogether, 346 full papers were received by October 31, 2013 for the WLF3 (Sassa 2013b). The editors of the Session A1 received numerous abstracts about the activities of WCoEs and IPL projects. For the Session A1, finally, 16 full papers were reviewed, revised by the authors, and finally accepted for publication in this volume of the WLF3 proceedings. In this short introduction to the WLF3 Session A1, a short summary of each of the accepted full papers is presented—the list runs alphabetically according to the paper’s first author family name.

Abolmasov et al. (2014) report on the on-going IPL-181 project “Study of slow moving landslide Umka near Belgrade, Serbia” that started in 2012. The landslide Umka is located on the right banks of the Sava River, active for several decades (slow moving) and with the volume of 14 million m³. The Project is lead by the University of Belgrade, Faculty of Mining and Geology and supported by the Highway Institute Belgrade. The paper describes the past investigations in the landslide area, and the proposed activities within the project.

Arambepola and Basnayake (2014) report on the efforts in landslide risk reduction in Asia, undertaken in recent years by the Asian Disaster Preparedness Centre (ADCP). Using their expertise from the terminated IPL-156 project “Best Practices for Early Warning of Landslides in a Changing Climate Scenarios”, the ADCP initiated the new IPL-180 project “Introducing Community-based Early Warning System for Landslide Hazard Management in Cox’s Bazaar Municipality, Bangladesh” aiming at developing a city-level landslide hazard risk-management strategy in Bangladesh so that other vulnerable cities in Asia will be able to replicate effective practices for reducing future losses.

Arbanas et al. (2014) report on the activities of the on-going IPL-184 project “Study of landslides in flysch deposits of North Istria, Croatia: sliding mechanisms, geotechnical properties, landslide modelling, and landslide susceptibility” that started in 2012. The paper describes the background of the project, introduces the project area covering about 550 km² with the volume of recent landslides exceeding 0.5 million m³, and the project structure. The first project activities encompassed supplementation of the existing landslide database, field investigations of recent and existing landslides in North Istria, Croatia, and soil sampling for laboratory testing. The paper also presents methods used for landslide susceptibility and landslide hazard assessment.

Baum et al. (2014) report on the activities undertaken by the USGS Landslide Hazards Program on a web-based landslide reporting system that was included into the terminated IPL-168 project “Engaging U.S. citizens in Landslide Science through the website, “Did You See It? Report a Landslide”.

Dias et al (2014) report on the on-going IPL-155 project “Determination of Soil Parameters of Subsurface to be used in Slope Stability Analysis in Two Different Precipitation Zones of Sri Lanka” that started in 2010. The paper focuses on the importance of the determination of discrete boundary shear strength of soils as an important parameter when assessing slope (landslide) stability and designing mitigation works. Using the deep-seated Watawala Earthslide (width 65 m, length 530 m, depth 9–28 m) in the Sri Lanka’s zone of high precipitation totals (average annual rainfall >5,000 mm) as a case study, the paper reports on the field and laboratory investigations undertaken on this slide.

Emmer et al. (2014) report on the on-going IPL-179 project “Database of Glacial Lake Outburst Floods (GLOFs)” that started in 2012. The main goal of this project is the creation of a widely available online database of GLOFs that have occurred worldwide since the end of the “Little Ice Age”. The paper describes the project background and the current status of the project, presenting research institutions involved into the project and introducing the database that is available on-line.

Garnica-Peña et al. (2014) report on the activities of the World Centre of Excellence WCoE “Landslide monitoring and community based early warning systems” undertaken by the National Autonomous University of Mexico (UNAM), aiming at the implementation of a community-based early warning system, in which the participation of the local population will be essential. The paper introduces the design, instrumentation and monitoring system developed for an unstable slope situated in one of the most affected areas of Teziutlán, Puebla, Mexico.

Günther et al. (2014) report on the synoptic pan-European landslide susceptibility assessment that produced the first version of the 1 km grid size European Landslide Susceptibility Map (ELSUS 1000 v1), covering the EU and neighbouring countries. This work was done within the framework of the on-going IPL-162 project “Tier-based harmonised approach for landslide susceptibility mapping over Europe”, and of the Council of Europe’s EUR-OPA project “Pan-European and nation-wide landslide susceptibility assessment”, coordinated by the European Centre on Geomorphological Hazards (CERG).

Igwe (2014) reports on the on-going IPL-150 project “Capacity building and the impact of climate-driven changes on regional landslide distribution, frequency and scale of catastrophe”. The focus of the paper is on landslide risk in South-East Nigeria, where important facilities, such as

electricity, communication and water projects located on hilly terrains, are under serious threat due to landsliding and associated earth movements. The IPL-150 project investigated the extent of vulnerability and found that while the slopes are fairly stable in the short-term, sustained and unchecked excavation could be a major factor in eventual collapses in the investigated region with high annual rainfall and complex stratigraphy that contains some potentially liquefiable lithologic units.

Legerreta Paulín et al. (2014) report on the on-going IPL-170 project “Landslide susceptibility and landslide hazard zonation in volcanic terrains using Geographic Information System (GIS): A case study in the Río Chiquito-barranca Del Muerto watershed; Pico de Orizaba volcano, México”, aiming at conducting a multi-temporal landslide inventory, analyzing the distribution of landslides, and characterizing landforms that are prone to slope instability by using Geographic Information Systems (GIS). The project is conducted by the Institute of Geography at the National Autonomous University of Mexico (UNAM). The paper introduces the study area and discusses the first results of the landslide mapping and landslide hazard zonation for varied landforms in unstable sedimentary and volcanic terrains.

Mallawarachchi et al. (2014) report on the on-going IPL-155 project “Determination of soil parameters of subsurface to be used in slope stability analysis in two different precipitation zones of Sri Lanka”. The paper compares soil modules of residual soil slope failures in two precipitation zones in Sri Lanka with different annual rainfalls. This was an experimental study to formulate a relationship between the potential slope failures quantify shear strength characteristics of soils which could be easily discussed on scenarios of the first time occurrence failures and repetitive failures in residual soil formation.

Mikoš et al. (2014) report on the activities of the World Centre of Excellence WCoE “Mechanisms of landslides in over-consolidated clays and flysch” undertaken by the Faculty of Civil and Geodetic Engineering, University of Ljubljana (UL FGG). Furthermore, the paper reports on the on-going IPL-151 project on “Soil matrix suction in active landslides in flysch—the Slano Blato landslide case” that aims at comparing continuous measurements of soil matrix suction in an active landslide (i.e. the Slano blato landslide in W Slovenia) with the measurements of matrix suction in highly weathered and progressively disintegrating flysch rocks the landslide is fed from.

Shaharom et al. (2014) report on the on-going IPL-176 project “Slope Data Acquisition along Highways in Sabah State for hazard assessment and mapping” that started in 2012. The project was focused on the slope data acquisition as the first step towards the Malaysian highway slope maintenance program; an important part of which is the prioritization

of slopes to be repaired based on the damage and public safety involved. The paper discusses the problems involved in the slope database preparation.

Shan et al. (2014) report on the on-going-IPL-167 project “Landslides Mechanism and the Subgrade Stability Controlling Measures in Island Permafrost Area”. The focus of the paper is the stability of the embankments and slopes close to the Expressway from Bei’an to Heihe in Northeast China. Based on the annual average temperature data from 1954 to 2011, the relationship between the annual average temperature change and the permafrost distribution are analyzed. The embankment and slope stability and mass movement events were studied on the basis of ground temperature data, moisture data, and surface and landslide deformation monitoring data from 2009 to 2012 in the Bei’an to Heihe Expressway.

Strom and Abdrakhmatov (2014) report on the activities of the on-going IPL-106-2 project “International Summer School on Rockslides and Related Phenomena in the Kokomeran River Valley, Tien Shan, Kyrgyzstan”. The summer school was successfully carried out since 2006 with more than 50 students and young landslide researchers from 17 countries. They have been introduced to rockslides and rock avalanches of different morphological types, some of which have formed deeply eroded rockslide dams that allow study of their internal structure, as well as evidence of inundation and of catastrophic outburst floods, and impressive manifestations of recent tectonic phenomena in the studied area.

Suhaimi et al. (2014) report on the activities of the terminated IPL-147 project “Study on Debris Flow Controlling Factors and Triggering Mechanism in Peninsular Malaysia”. The paper focused on rainfall intensity and duration as triggering factor for debris flows in Peninsular Malaysia. They have studied 4 debris-flow cases, and the study results show that the relationship between rainfall patterns (intensity, duration) and the occurrence of debris flows is similar to that elsewhere in the world.

The corresponding editors of this Session A1 would like to thank all the reviewers who have reviewed the papers submitted to this special session. The session was improved by thoughtful proof-editing of Eileen McSaveney and Mauri McSaveney; their editorial work is fully appreciated.

References

- Abolmasov B, Milenković S, Jelisavac B, Đurić U, Marjanović M (2014) IPL Project 181 – Study of slow moving landslide Umka near Belgrade, Serbia. In: Sassa K (ed) *Landslide science for a safer geo-environment*, vol 1: International program on landslides. Springer, Heidelberg
- Arambepola NMSI, Basnayake S (2014) Efforts in landslide risk reduction in Asia. In: Sassa K (ed) *Landslide science for a safer geo-environment*, vol 1: International program on landslides. Springer, Heidelberg

- Arbanas Ž, Dugonjić Jovančević S, Vivoda V, Mihalić Arbanas S (2014) Study of landslides in flysch deposits of North Istria, Croatia: Landslide data collection and recent landslide occurrences. In: Sassa K (ed) *Landslide science for a safer geo-environment*, vol 1: International program on landslides. Springer, Heidelberg
- Baum RL, Highland LM, Lyttle PT, Fee JM, Martinez EM, Wald LA (2014) "Report a landslide" A website to engage the public in identifying geologic hazards. In: Sassa K (ed) *Landslide science for a safer geo-environment*, vol 1: International program on landslides. Springer, Heidelberg
- Dias Virajh AA, Abayakoon SBS, Bhandari RK (2014) Discrete boundary shear strength of a landslide at high rainfall precipitation zone in Sri Lanka. In: Sassa K (ed) *Landslide science for a safer geo-environment*, vol 1: International program on landslides. Springer, Heidelberg
- Emmer A, Vilímek V, Klimeš J (2014) Glacial lake outburst floods (GLOFs) database project. In: Sassa K (ed) *Landslide science for a safer geo-environment*, vol 1: International program on landslides. Springer, Heidelberg
- Garnica-Peña R, Domínguez-Morales L, Alcántara-Ayala I (2014) Towards landslide instrumentation and monitoring in Teziutlán, Puebla, Mexico. In: Sassa K (ed) *Landslide science for a safer geo-environment*, vol 1: International program on landslides. Springer, Heidelberg
- Günther A, Hervás J, Van Den Eeckhaut M, Malet J-P, Reichenbach P (2014) Synoptic pan-European landslide susceptibility assessment: the ELSUS 1000 v1 map. In: Sassa K (ed) *Landslide science for a safer geo-environment*, vol 1: International program on landslides. Springer, Heidelberg
- Igwe O (2014) Landslide risk in South-East Nigeria: important facilities under serious threat. In: Sassa K (ed) *Landslide science for a safer geo-environment*, vol 1: International program on landslides. Springer, Heidelberg
- Legorreta Paulín G, Lugo Hubp JL, Aceves Quesada JF (2014) Assessing landslide frequency for landform hazard zoning purposes. In: Sassa K (ed) *Landslide science for a safer geo-environment*, vol 1: International program on landslides. Springer, Heidelberg
- Mallawarachchi MASN, Ekanayake EMTM, Kodagoda SSI, Virajh Dias AA (2014) Comparison of soil moduli E50 of residual soil slope failures in two different rainfall precipitation zones. In: Sassa K (ed) *Landslide science for a safer geo-environment*, vol 1: International program on landslides. Springer, Heidelberg
- Mikoš M, Sodnik J, Petkovšek A, Maček M, Majes B (2014) WCoE: mechanisms of landslides in over-consolidated clays and flysch & IPL-151 Project: soil matrix suction in active landslides in flysch – the Slano Blato landslide case. In: Sassa K (ed) *Landslide science for a safer geo-environment*, vol 1: International program on landslides. Springer, Heidelberg
- Sassa K (2012) ICL strategic plan 2012–2021 – To create a safer geo-environment. *Landslides* 9(2):155–164
- Sassa K (2013a) World Landslide Forum 3. *Landslides* 10(1):111–117. doi:[10.1007/s10346-013-0381-9](https://doi.org/10.1007/s10346-013-0381-9)
- Sassa K (2013b) World Landslide Forum 3. *Landslides* 10:843–851. doi:[10.1007/s10346-013-0450-0](https://doi.org/10.1007/s10346-013-0450-0)
- Sassa K, Canuti P, Margottini C, Yin Y (2012) The Second World Landslide Forum, Rome, 2011 and the Third World Landslide Forum, Beijing, 2014. *Landslides* 9(2):285–297
- Shaharom S, Abdullah C, Majid R (2014) Slope data acquisition along Highways in Sabah State for hazard assessment and mapping. In: Sassa K (ed) *Landslide science for a safer geo-environment*, vol 1: International program on landslides. Springer, Heidelberg
- Shan W, Guo Y, Zhang C, Hu Z, Jiang H, Wang C (2014) The impact of climate change on the stability of embankment and slope of Bei'an Highway in Permafrost Regions. In: Sassa K (ed) *Landslide science for a safer geo-environment*, vol 1: International program on landslides. Springer, Heidelberg
- Strom A, Abdrakhmatov K (2014) International summer school on rockslides and related phenomena in the Kokomeren River Valley, Tien Shan, Kyrgyzstan: IPL-106-2 Project and WCoE. In: Sassa K (ed) *Landslide science for a safer geo-environment*, vol 1: International program on landslides. Springer, Heidelberg
- Suhaimi J, Che Hassandi A, Norhidayu K (2014) Rainfall intensity and duration for debris flow triggering in Peninsular Malaysia. In: Sassa K (ed) *Landslide science for a safer geo-environment*, vol 1: International program on landslides. Springer, Heidelberg



IPL Project 181: Study of Slow Moving Landslide Umka Near Belgrade, Serbia

Biljana Abolmasov, Svetozar Milenković, Branko Jelisavac, Uroš Đurić, and Miloš Marjanović

Abstract

Serbia is well known for numerous landslide phenomena. Landslides are particularly notable for the valley walls of the rivers Sava and Danube and their respective tributaries. They have in common the fact that they all originated in complexes of Neogene sediments made of different lithological elements, and most often clays, sands, and marls with pronounced zones of weathering up to approx. 20 m deep. Landslides on the right banks of the Sava and Danube have deep sliding surfaces, formed on the contact of the weathered zone and unaltered clay and marl sediments. The basic trigger of the processes, apart from the precipitation, is prolonged erosion of the right banks of the Sava and Danube rivers. Most of the landslides are active or suspended, where periods between reactivation phases could be several years long. The IPL-181 Project started in November 2012. The study area is located on the right bank of Sava River, 25 km southwest of Belgrade, Serbia. The project focused on review and analysis of previous detailed site investigations and field instrumentation, analysis of aerial photo and orthophoto images, and analysis of monitoring results. Project beneficiaries will be the local community, and local and regional authorities. Here we present results of the 1st year of proposed project targets—a review and analysis of previous field investigations performed by Project participants.

Keywords

Serbia • Slow-moving landslide • IPL Project

B. Abolmasov (✉) • U. Đurić • M. Marjanović
Faculty of Mining and Geology, University of Belgrade, Đušina 7,
11000 Belgrade, Serbia
e-mail: biljana@rgf.bg.ac.rs; djuric@rgf.bg.ac.rs;
milos.marjanovic@rgf.rs

S. Milenković
Geomonitoring Team, Juriša Gagarina 111, 11070 Belgrade, Serbia
e-mail: tozony@gmail.com

B. Jelisavac
The Highway Institute, Kumodraška 257, 11000 Belgrade, Serbia
e-mail: jelisavac.branko@gmail.com

Introduction

Republic of Serbia on the Balkan Peninsula in southeast Europe covers an area of 88,361 km² and has a population of 7,181,505 (<http://stat.gov.rs>) (Fig. 1). Because of its complex geological history, terrain composition, and morphological and climate characteristics, 15 % of Serbia is affected by landslides (active, suspended and dormant), (Dragičević et al. 2011). The majority of landslides in Serbia are formed in Tertiary and Quaternary sediments. Tertiary sediments in Serbia are prevalent in the areas of the Pannonia basin and its northerly rim, and include the remains of isolated lake basins in the central region south of the Sava and Danube rivers. Around 18 % of Serbia is mantled by Neogene sediment complexes where clays, marls, soft limestones, sands and gravels prevail in a great variety of spatial ratios. In terrains



Fig. 1 Geographical location of Republic of Serbia on the Balkan Peninsula (Source: Google Earth 2013)

composed of the Tertiary complexes, more than 25 % of the territory is affected by landslides (Abolmasov 2010).

Especially interesting are the areas of outer Belgrade and the slopes of the right banks of the Sava and Danube, which are known for their instability. Luković (1951), Vujančić et al. (1981, 1984), Lokin et al. (1988) and Rokić et al. (1998), Rokić and Vujančić (2002) have all written about this phenomenon. The basic cause of this instability is the complex geological and morphological evolution of the terrain, further influenced by development of intensive anthropogenic activity, so that many dormant landslides have been reactivated, but many new ones have become active as well. According to the latest landslide inventory from 2010, which included the inner area of the General Plan of Belgrade and covers an area of 437 km² (1/3 of the total area of the city), over 30 % of the territory is composed of active and suspended landslides (Lokin et al. 2010).

The initiative to collaborate with the International Consortium on Landslides was started in September 2009 when Prof. K. Sassa and Prof. H. Marui from ICL, representative of JICA for Croatia Mr H. Komiyama and colleagues from the University of Zagreb, Faculty for Mining, Geology and Petroleum Engineering, Prof. S. Mihalić Arbanas and M. Krkač completed a 3-day visit to Serbia. In collaboration with colleagues from The Highway Institute, some characteristic landslides on Belgrade territory were visited (Umka, Karaburma, Vinča), landslides on the Belgrade–Niš motorway (Begaljičko brdo and Ražanj), and the landslide Mramor near Niš.

The Faculty of Mining and Geology of the University of Belgrade became a member of ICL in 2011, and a member of the ICL Adria-Balkan Network in 2012 (Mihalić-Arbanas

et al. 2013). In March 2012, Faculty of Mining and Geology and The Highway Institute applied for an IPL project and during the 7th Session of IPL-GPC in Paris in 2012, a joint project number 181 was approved. It was entitled “Study of Slow Moving Landslide Umka near Belgrade Serbia”.

This paper contains interim results obtained during less than a year of the conducted project, as described in the project plan and program.

Project Description

The landslides of Umka and Duboko are located 25 km south–west of Belgrade and have been investigated in detail for a long number of years. As a result, extensive geotechnical documentation was collected, with publication of a great number of papers in the last 30 years. The greatest amount of research was conducted in order to prepare technical documentation for various phases of design and planning of the E-76 and E-763 motorways, whose routes cross the landslides of Umka and Duboko. To lesser extent, research was done for the purpose of urbanization of the settlement of Umka. The last phase of research for the level of the preliminary design for the E-763 motorway was completed in 2005, and no further research has been conducted since then; no remedial measures were taken and the motorway was not built. Automatic GNSS monitoring was introduced in March 2010 in the body of the Umka landslide as part of the TR36009 project supported by the Ministry of Education, Science and Technological Development of the Republic of Serbia. Movement, fluctuations of levels of the Sava river, as well as hydro-meteorological parameters (type and intensity of precipitation, temperature regimens etc.) have been monitored daily since then. Umka landslide is located on the territory of Belgrade Municipality of Čukarica, in the right meander of the Sava River (Fig. 2). The landslide surface is 1.8 km² and its volume is 14,000,000 m³; it is classified as a slow active landslide.

The basic objective of the “Study of slow moving landslide Umka near Belgrade, Serbia” project was to analyze, correlate and synthesize data obtained from various phases of investigation after 30 years of research. Apart from this, the analysis of data received from monitoring conducted during certain phases of research would be compared with data from automated GNSS monitoring during later years. Synthesis of research results would help define the mechanism and dynamics of movement of this large active slow landslide, with the objective of proposing adequate remedial measures. Project results would also help in better understanding other landslides found on the right banks of the Sava and Danube rivers.

During numerous investigations various research methods were used for research and monitoring. The project

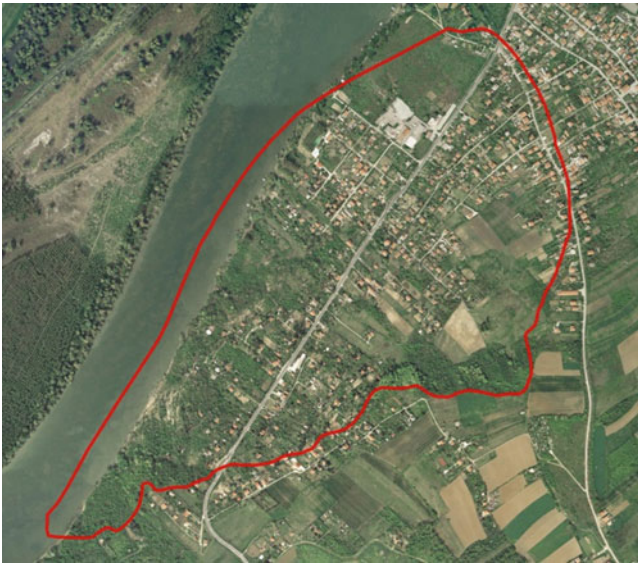


Fig. 2 Landslide Umka (Source: Google Earth 2013)

will be focused on: (1) analysis of previous detailed site investigations and field instrumentation from 1990–2005, (2) analysis of aerial photo and orthophoto images from 1960–2010 and (3) analysis of automated GNSS monitoring results from 2010 up to the end of the Project. Analysis of precipitation and levels of the Sava River will be included.

The following activities are planned while conducting the project:

- Review and organization of existing results
- Analysis of previous detailed site investigation and monitoring results
- Analysis of aerial photo and orthophoto images
- Analysis of the precipitation regime and Sava river levels
- Analysis of GNSS monitoring results
- Compilation and analysis of all results and proposal of remedial measures

After certain activities, it was planned to prepare partial reports, and to prepare a comprehensive report at the end. Preparation of a paper for the Landslide journal was also foreseen. Deliverables and time frames are as follow:

- Compilation of results of previous field instrumentation and site investigation up to 2005 (end of 1st year)
- Compilation of remote sensing data up to 2010 (end of month 18)
- Compilation of precipitation data and Sava river levels up to end of Project (end of month 30)
- Compilation of GNSS monitoring results (end of month 30)
- Final report (end of 3rd year)

The Project is organized by the University of Belgrade, Faculty of Mining and Geology and The Highway Institute Belgrade. University and Institute staff are providing all necessary documentation for Project finalization. Additional

equipment will be necessary for some field instrumentation (automated rain-gauge station and an additional GNSS receiver). Maintenance of equipment will be organized by both institutions. The total budget requirement is 40,000 USD and Project duration will be 3 years. Project Leader is Associate Professor Biljana Abolmasov from University of Belgrade, Faculty of Mining and Geology. Core members of the Project are: Svetozar Milenković, MSc, Branko Jelisavac, MSc, Uroš Djurić, PhD student, and Miloš Marjanović, PhD researcher.

Results

Project IPL 181—“Study of slow moving landslide Umka near Belgrade, Serbia” was approved in November 2012. Review and organization of existing results was conducted for 9 months afterwards, as per the Project Plan. Extensive archive documentation was collected from The Highway Institute, as well as papers on the Umka and Duboko landslides published for international and local scientific conferences. The Umka and Duboko landslides were subjects of papers by Vujanić et al. (1981, 1984, 1995), Ćorić et al. (1994, 1996), Dangić et al. (1997) and Jelisavac et al. (2006).

Formats of the available documentation differ, with some of the older reports in hard-copy/paper form, while some of the newer reports are in digital format. The results of field investigations and laboratory testing conducted during different phases are available in original format, with interpretations necessary for specific levels of geotechnical reports. Table 1 gives an overview of all research conducted from 1978 to 2005 at the Umka and Duboko landslides, including the name of the company conducting the research and purpose of the research, together with a note on documentation availability. It was important for conducting this Project to have documentation available in any format, and especially the documentation that was not produced as a compilation of previous research, but produced from different site investigations carried out for that purpose. Out of eight different reports or documentation pre-dating 1980, two were not available in any format (1 and 2). In order to produce documentation listed under numbers 4 and 7, no research was carried out, but the reports were produced based on existing research results from previous years. Most extensive field investigations and instrumentation, as well as laboratory testing, were conducted during 1992 and 2005 as needed for the preliminary design of motorway E-763 (5 and 8) for both landslides.

Table 2 presents the overview of the type and extent of investigations conducted for locations on the Umka and Duboko landslides during 1992 and 2005. It can be seen that most extensive investigations were conducted in 1992.

Table 1 Overview of the available documentation for the Umka landslide

No.	Title of reports/documentation (Serbian)	Title of reports/documentation (English)	Year	Site investigations	Availability
1	Geotehničke podloge za izradu projekta autoputa Beograd-Obrenovac na deonici Ostružnica-Umka km 9 + 000 do 16 + 711	Geotechnical documentation for Belgrade-Obrenovac motorway project design, section Ostružnica-Umka km 9 + 000 to 16 + 711	1978	Yes	No
2	Geotehnički uslovi izgradnje autoputa Beograd-Obrenovac preko klizišta Umka i Duboko km 17 + 000 do 21 + 000	Geotechnical conditions for construction Beograd-Obrenovac motorway over Umka and Duboko landslides, section km 17 + 000 to 21 + 000	1980	Yes	No
3	Katastar klizišta i nestabilnih padina na teritoriji opštine Čukarica	Inventory of landslides and marginally stable slopes of Municipality Čukarica territory	1984	Yes	Yes
4	Idejni projekat uređenja reke Save na potezu od Umke do Bariča u sklopu izgradnje autoputa E-76, Knjige 1–4	Preliminary design of Sava river regulation from Umka to Barič within motorway E-76, Book 1–4	1990	No	Yes
5	Geotehnička istraživanja u zoni klizišta Umka i Duboko za nivo Idejnog projekta autoputa E-76 Beograd-Obrenovac km 15 + 500 do 19 + 750	Geotechnical Investigations of landslides Umka and Duboko—Preliminary design of Highway E-76, Belgrade-Obrenovac, section km 15 + 500 to 19 + 750	1992	Yes	Yes
6	Inženjerskogeološka istraživanja terena za nivo izmene i dopune DUP-a naselja Umka	Engineering geological investigation for Detail Urban Plan of settlement of Umka	1992	Yes	Yes
7	Geotehnički elaborat o uslovima sanacije klizišta na putu Beograd-Obrenovac (kod klizišta Umka) i Glavni projekat sanacije	Geotechnical conditions of remedial measures works for landslide Umka on the Belgrade-Obrenovac road—Main design report	1996	No	Yes
8	Idejni projekat autoputa E763 (Beograd-Ljig-Požega), sektor 1, Beograd-Ljig, Beograd (Ostružnica)—Umka	Preliminary design of Highway E-763 (Beograd-Ljig-Požega), Section 1: Beograd-Ljig, Beograd (Ostružnica)—Umka	2005	Yes	Yes

Table 2 Type and scope of investigations conducted on the Umka and Duboko landslides

Type of investigations	Used reports/documentation	
	Geotechnical investigations of landslides Umka and Duboko—Preliminary design of Highway E-76, Belgrade-Obrenovac km 15 + 500 to 19 + 750 (1992)	Preliminary design of Highway E-763 (Belgrade-Ljig-Požega), Section 1: Belgrade-Ljig, Belgrade (Ostružnica)—Umka (2005)
Engineering geological mapping	Detailed engineering geological mapping of both landslides, cca 7 km ² , scale 1:1,000	Detailed engineering geological mapping of both landslides, cca 7 km ² , scale 1:1,000
Drilling of boreholes	25 boreholes and logging of cores, total 621 m	62 boreholes and logging of cores, total 1,200 m
Shafts	4 shafts and logging total depth 78 m	–
SPT	3 tests—total depths 20 m	–
Inclinometers	10—installation and monitoring—total 300 m	33—installation and monitoring—total 770 m
Piezometers	16—installation and reading piezometers up to depths of 27 m—total 430 m	–
Geodetic bench marks	65 geodetic bench marks	–
ERT	2 km profiles	–
Echo sounding of Sava river	Echo sounding of Sava riverbed—50 profiles	–
Laboratory testing	400 samples for determination/classification tests and 50 samples for stress–strain tests	66—samples for determination/classification tests and for stress–strain tests
Palaeontology sampling	30 samples for stratigraphy/palaeontology analysis	–
Geochemical sampling	30 samples for mineralogy/geochemical analysis	–
Chemical sampling	20 samples of groundwater and Sava river	–
Trial pits	4 trial pits, total 10 m depth	–

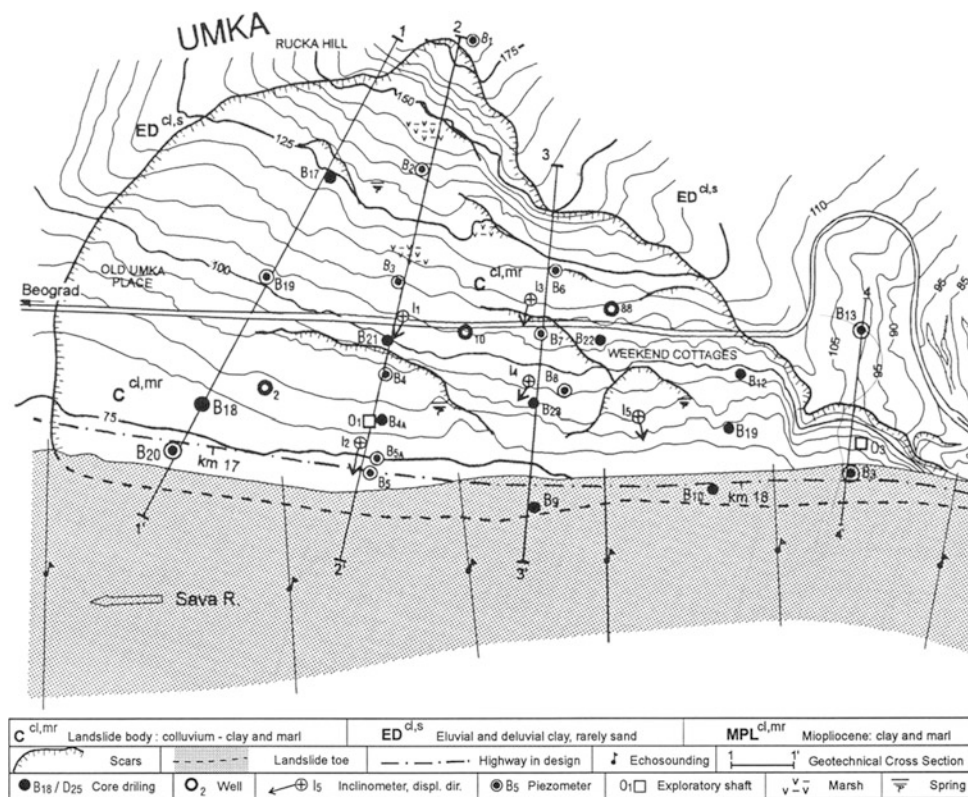


Fig. 3 Engineering geological map of the Umka landslide [scan from Ćorić et al. (1996)]

Documentation was available in printed-paper version, and so it was necessary to digitalize the maps and cross-sections of the terrain, and establish unique databases of laboratory and other measurements and observations. Documentation from 2005 was processed in AutoCad format, but was also available partly in printed and partly in electronic versions. Scanning, digitalization and referencing of all spatial data is currently underway, as is the development of the database of laboratory and other results from field observations, as well as the correlation of research results from both sets of documentation. All published papers from last 30 years have also been collected and scanned. For example, the scan of an engineering geological map resulting from the investigations from the year 1992 is shown in Fig. 3.

Conclusion

First research results from the IPL-181 project after almost a year of project work are presented in the paper. Data on available geotechnical reports as well as data published in expert and scientific papers in the last 30 years about the Umka landslide near Belgrade have been collected. The analysis, correlation and synthesis of a large volume of data are currently being performed. All data will be scanned and geo-referenced, and database

will be built. It is planned to collect all available geodetic and remote sensing data, based on which the landslide dynamics will be analyzed after the 1st year of project activity. Data from the installed automated GNSS receiver, precipitation and Sava river levels will be followed in parallel to these activities. Three years after the start of the project, analysis and synthesis of all data, it will be possible to propose adequate remedial measures for the Umka landslide.

Acknowledgments The IPL-181 Project would have not been possible without support from Republic Geodetic Authority and Republic Hydrometeorological Service of Serbia. The research was supported by the Ministry of Education, Science and Technology of the Republic of Serbia Project No TR 36009.

References

- Abolmasov B (2010) Landslide types and processes in Serbia. In: Abstract proceedings of 1st workshop of the project "Risk identification and land-use planning for disaster mitigation of landslides and floods in Croatia", Dubrovnik, Croatia, 22–24 November 2010. p 40.
- Ćorić S, Božinović D, Vujanić V, Jotić M, Jelisavac B (1994) Slope instability analysis in Neogene clays and marls. In: Oliveira R, Rodrigues LF, Coelho AG, Cunha AP (eds) Proceedings of 7th

- international IAEG congress, vol 3, Lisboa, Portugal, 5–9 September 1994. Balkema, Rotterdam, pp 1759–1770
- Ćorić S, Božinović D, Vujanović V, Jotić M, Jelisavac B (1996) Geotechnical characteristics of old landslides in Belgrade area. In: Senneset K (ed) Proceedings of the 7th international symposium on landslides, vol 2, Trondheim, Norway, 17–21 June 1996. Balkema, Rotterdam, pp 689–694
- Dangić A, Vujanović V, Josipović J, Jotić M, Jelisavac B (1997) Geochemical and geotechnical study of complex landslide in vicinity of Belgrade, Yugoslavia. In: Marinos P, Koukis GC, Tsiambaos GC, Stournaras GC (eds) Proceedings of the international symposium on engineering geology and environment, vol 1, Athens, Greece, 23–27 June 1997. Balkema, Rotterdam, pp 581–566
- Dragičević S, Filipović D, Kostadinov S, Ristić R, Novković I, Živković N, Anđelković G, Abolmasov B, Šećerov V, Đurđić S (2011) Natural hazard assessment for land-use planning in Serbia. *Int J Env Res* 5(2):371–380
- Jelisavac B, Milenković S, Vujanović V, Mitrović P (2006) Geotechnical investigations and repair of the landslide Umka – Duboko on the route of motorway E-763 Belgrade–South Adriatic. International Workshop-Prague-Geotechnical Days, Prague, 2006
- Lokin P, Sunarić D, Cvetković T (1988) Landslides in neogene sediments on the right Danube bank, Yugoslavia. In: Ch Bonnard (ed) Proceedings of the 5th international symposium on landslides, vol 1, Lausanne, 10–15 July 1988. Balkema, Rotterdam, pp 213–217
- Lokin P, Pavlović R, Trivić B (2010) Projekat istraživanja terena za izradu katastra klizišta područja Generalnog urbanističkog plana područja Beograda. J.P. Direkcija za građevinsko zemljište grada Beograda. Unpublished material (in Serbian)
- Luković TM (1951) Važniji tipovi naših klizišta i mogućnosti njihovog saniranja. *Geološki Vesnik Savezne uprave za geološka istraživanja*, Knjiga IX, Beograd, pp 275–310 (in Serbian)
- Mihalić-Arbanas S, Arbanas Ž, Abolmasov B, Mikoš M, Komac M (2013) The ICL Adriatic-Balkan Network: analysis of current state and planned activities. *Landslides* 10:103–109. doi:10.1007/s10346-012-0364-2
- Rokić Lj, Vujanović V (2002) A contribution on the study of landslide origins in Neogene sediments of Danube river coastal area. In: Rybar J, Stemberk J, Wagner P (eds) Proceedings of the 1st European conference on landslides, Prague, Czech Republic, 24–26 June 2002. Balkema, Rotterdam, pp 291–298
- Rokić Lj, Vujanović V, Jotić M (1998) Forecast of the landslide development processes based on the study of erosion processes of rivers in the plains. In: Moore D, Hungr O (eds) Proceedings of 8th international IAEG congress, vol 3, Vancouver, Canada, 21–25 September 1998. Balkema, Rotterdam, pp 1485–1491
- Vujanović V, Livada N, Jotić M, Gojković S, Ivković J, Božinović D, Sunarić D, Šutić J (1981) Klizište “Duboko” na Savi kod Beograda. *Zbornik radova Simpozijuma istraživanje I sanacija klizišta*, Bled 1981, Knjiga 1, pp 119–134 (in Serbian)
- Vujanović V, Livada N, Božinović D (1984) On an old landslide in neogene clays on the right bank of the Sava near Belgrade. In: Proceedings of 4th international symposium on landslides, vol 2, Toronto, pp 227–233
- Vujanović V, Jotić M, Jelisavac B, Božinović D, Ćorić S (1995) Sinteza rezultata gotehničkih istraživanja klizišta na Savi: Umka i Duboko. *Zbornik radova Drugog simpozijuma Istraživanje i sanacija klizišta*, 6–9 juni 1995, Donji Milanovac, pp 335–351 (in Serbian)



Efforts in Landslide Risk Reduction in Asia

N.M.S.I. Arambepola and Senaka Basnayake

Abstract

Mountain areas are highly vulnerable to the adverse impacts of landslide disasters, which have been observed to be increasing over the recent years. Many of the related problems and challenges are associated with social, economic and environmental issues. The use of early warning systems (EWS) for natural hazards such as floods and typhoons has advanced fairly rapidly over the recent past and successful use of such systems has helped save lives in affected areas. However, the use of early warning systems for alerting people to landslide hazards is lacking. In order to promote such efforts in the Asian Region and to share experience with good practices in landslide early warning systems, the Asian Disaster Preparedness Centre (ADPC) has undertaken landslide early warning-related interventions in a few countries and this has been reported under “IPL-156—Best Practices for Early Warning of Landslides in a Changing Climate Scenario”.

Recently, devastating landslide events have been reported in several cities in Asia located within mountain districts, in both their fringe towns and urban centers. Most of the urban centers are strategically located and play a major role in boosting investment and economic activities for the respective countries. Forecasted adverse climatic trends and climate variations are increasingly making such landslide-prone land in urban built-up areas more insecure for living. In recent years, many landslide events have occurred in hilly district cities of Bangladesh such as Chittagong, Cox’s Bazar, and Tecknaf. The pilot project IPL 180 aims at developing a city-level landslide hazard risk-management strategy in Bangladesh so that other vulnerable cities in Asia will be able to replicate effective practices for reducing future losses. In addition, the paper looks at various other landslide-risk reduction pilot initiatives undertaken in Asia by ADPC.

Keywords

Landslide early warning • Community based disaster risk management

Introduction

As the population increases and societies become more complex, landslides result in greater economic and societal losses. The impacts of landslides are predicted to rise in the

future unless proper attention is given at early stages to responding to, preparing for and mitigating their adverse impacts. Increasing human activities in mountain areas can add to the existing vulnerability of communities, and so it is also advisable to regulate development in hilly areas. One way to influence the process is to work with local government authorities closely to enhance their capacity, as they are the institutions responsible for land-use planning and controlling building. Further, it is useful to explore possibilities for mainstreaming the process of risk-sensitive

N.M.S.I. Arambepola (✉) • S. Basnayake
Asian Disaster Preparedness Center, 24th Floor, SM Tower, 979/69,
Phayathai, Bangkok 10400, Thailand
e-mail: arambepola@adpc.net; senaka_basnayake@adpc.net

planning and development control within the local government set-up. The Asian Disaster Preparedness Center (ADPC) has been engaged in building landslide risk management capacity in the partner countries in Asia for more than a decade. The limited number of interventions in landslide mitigation and preparedness in Asia was the rationale behind the initiation of this program. Currently, ADPC is facilitating a network of 16 different agencies, universities, and research institutions in more than 11 countries to advocate for good practices in landslide-risk management. The key objective of the Asian Program for Regional Capacity Enhancement for Landslide Impact Mitigation (RECLAIM-II), implemented by the Asian Disaster Preparedness Centre (ADPC) in Thailand is building landslide-risk management capacity in the partner countries in Asia. The program, which has been funded by the Royal Norwegian Government, received technical assistance from the Norwegian Geotechnical Institute (NGI) in implementing project activities in target countries.

Developing a Local-Government-Level Framework for Landslide-Risk Management

A convenient way to avoid future landslide disasters is to minimize construction on hilly slopes. This is rarely socially acceptable or economically feasible in the present context. The mountain areas are rapidly being developed in many countries in Asia due to the opportunities for tourism, living, recreation, agriculture, and livestock farming. At times communities tend to undertake construction on dangerous slopes while paying little attention to slope stability, as there are few options to build houses in safe areas, as shown in Fig. 1. In addition, hilly areas usually are favored for hydro-power industry, and development of water retention facilities for irrigation, etc.

But often risk information is not used in designing such development projects. In most cases, detailed risk assessment data are not available for designers during the design stage of such projects. Another problem is that developers of such projects do not allocate sufficient funds for detailed investigations when designing such projects. They also do not have a good understanding of the fact that most landslides or potential failures can be predicted if proper investigations are carried out in time, and that such predicted potential failures can be mitigated with good engineering measures. The main thrust of the framework suggested for landslide-risk reduction is to use risk information in development planning and controls on building, considering the proneness of the areas to landslide hazards. This framework also fosters guidelines for development activities on hill slopes to be directed to safer areas, in a manner that such activities will not create new risk or aggravate existing level of risk.



Fig. 1 Vulnerable locations in a built-up area

Approaches for Increasing the Effectiveness of Landslide Early Warning Mechanisms

In many cases, when the resources for expensive mitigation measures are not available, the next best approach will be to promote preparedness measures. Hence in the local government strategy for landslide risk reduction, it is essential to include measures for promoting preparedness for sustainable development and reduction of human losses. In the same way, early warning measures, which have advanced considerably, have served as effective methods in the case of natural hazards such as cyclones and floods, although they are yet to be popular in the case of landslides (NBRO 1994).

More importantly, effective use of early warning in the case of floods and cyclones has developed at the local level, and has proven effective in reducing the human losses considerably. Because there are many stakeholders involved in the process of providing early warning to communities from the time of prediction and information generation up to the community response, a study was undertaken to assess system gaps in the case of landslide early warning in a few selected countries by ADPC (Subbiah and Fakhruddin 2008).

Typically, as shown in Fig. 2, the total early warning system can be divided into three sub-systems: the detection sub-system (which deals with monitoring, detection, data assessment, data analysis, prediction), the management sub-system (which deals with risk assessment, interpretation and communication), and the response sub-system (which deals with the identification of local level elements at risk, preparedness, response and evacuation). The study has shown that gaps exist at all three sub-systems, but more at the management and response sub-systems. Hence it became essential to demonstrate ways to address the gaps at those two levels. A pilot study was undertaken in Bangladesh in

EW System Structure



Fig. 2 Early warning system structure

promoting community-based landslide early warning based on two landslide-prone municipalities to come up with an appropriate framework at the local level. The structure of the early warning system and results of the gap assessment are given in Fig. 3.

Processes for Promoting Community-Based Landslide Risk Reduction Mechanisms for the Most Vulnerable Communities

In recent years, more than 300 people have been killed in landslides in districts such as Chittagong and Cox's Bazar during the period of 2007–2012 (ADPC 2012). The project initiated with the assistance of Comprehensive Disaster Management Program (CDMP) of Bangladesh, which is being funded by a multi-donor consortium headed by UNDP, is considered as a major step by Bangladesh authorities for promoting city-level landslide disaster risk management. In the process, several stakeholders such as city officials, landslide professionals, disaster management practitioners and vulnerable communities living in landslide-prone areas became actively involved in activities that have advocated for landslide hazard early warning, effective local level response mechanisms and increased preparedness measures.

City Level Meetings and Workshops

Several city-level workshops were organized in order to educate the elected officials and other stakeholders. These included the Mayor and elected councilors, city officials, officials from other government agencies such as the local meteorological department and local government engineering departments, and NGOs such as the Red Crescent Society. In these training workshops, subjects such as the factors causing landslides, triggering mechanisms, and issues related to land-use planning, and controls on building were introduced to participants. The project created a landslide hazard map at a 1:10,000 scale for municipalities of Cox's

Bazar and Tecknaf, and the most vulnerable communities within the two cities were identified by the participants of the training workshops. During the workshops, a consensus was reached that the municipality would take the lead role in the implementation of the project, with the technical guidance of the project team. It was also discussed how the elected commissioners could act as change agents to help implement project activities.

The local government councilors selected volunteers and community facilitators in each selected community, with the help of other stakeholders and community members. These volunteers and community facilitators were trained to undertake community-level hazard mapping, identification of most critical risk areas, ways of communicating early warnings and evacuating communities to safe areas, and to act as change agents for undertaking overall landslide risk reduction measures within their communities. They were also assigned the duty of leading the response process in case of the occurrence of indicators of potential new landslides within the community area (Asian Disaster Management News 2008).

Orientation and Training Program for Volunteers and Community Facilitators

The training material included information on community-based disaster risk reduction, the ways to mobilize a vulnerable community, training in community-level landslide hazard risk mapping, vulnerability assessment, and early warning system operations (ADPC 2011). They were also provided an orientation at the site by the project team. During the training, a general outline of causative factors, trigger mechanisms, hazard and vulnerability mapping and identification of critical risk-prone slopes were provided, using simple explanations. In addition, there was a focus on the basic components of the early warning systems, such as vigilance with respect to critical slopes, monitoring the slopes to identify early indicators of landslides, warning dissemination and communication, response planning, and evacuation. During the training, other types of hazards common in the community were also discussed and stock-taking on all vulnerable members within the community was undertaken.

Each community volunteer has been made responsible for a particular section of the community in implementation of the early warning system and response plan (Fig. 4).

Community Risk Assessment

After receiving the training, the volunteers facilitated a community risk assessment in each vulnerable community with their respective community members (Abarquez and Murshed 2008). A community risk map indicating critical

Gap assessment

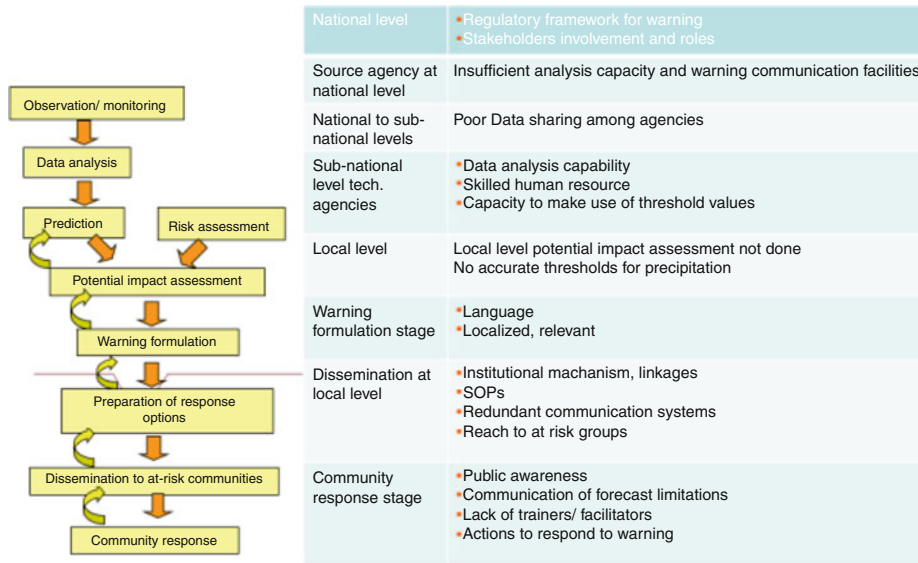


Fig. 3 Structure of early warning systems (EWS) and assessment of gaps



Fig. 4 Community-level meetings facilitated by volunteers, to validate vital information for executing response plans

slopes is shown in Fig. 5. The objectives of the risk and resource mapping exercise are as follows:

- Understand the behavior of monsoon season weather and arrange for extra vigilance during monsoon periods.
- Identify vulnerable segments of community groups (elderly people, disabled people, pregnant women, vulnerable houses, infrastructure etc.) and their locations within the community.
- Identify critical slopes and potential and current landslide locations that need constant monitoring during rainy periods to identify possible early indications of landslides.

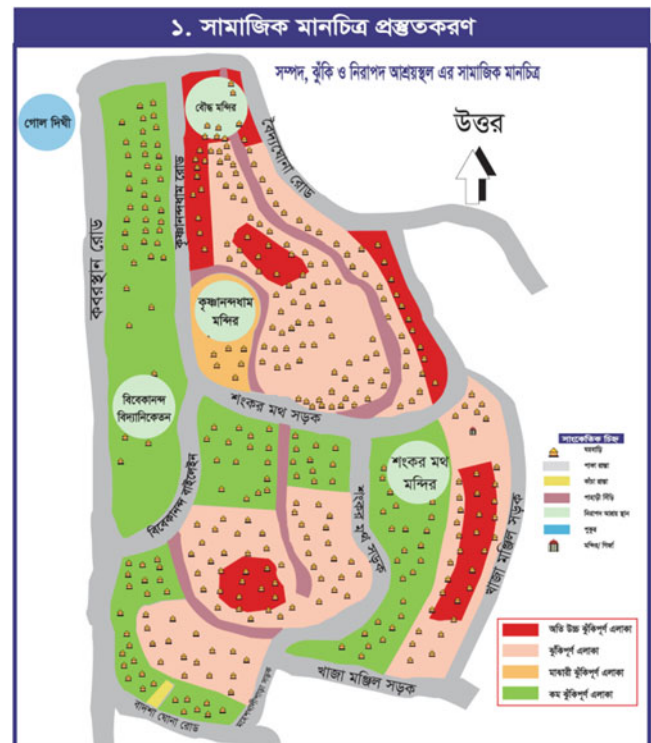
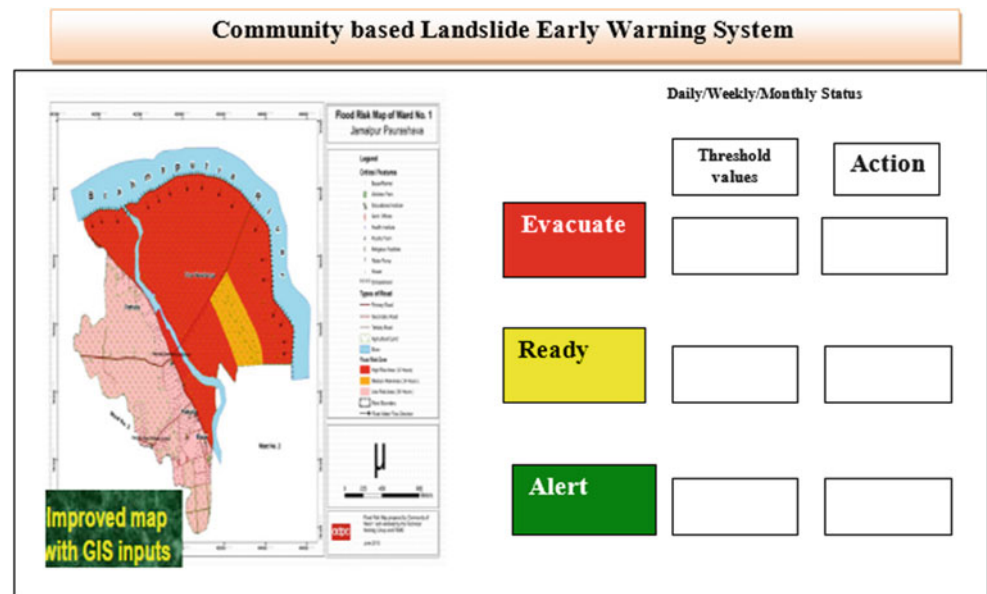


Fig. 5 Community risk map indicating critical slopes

- Identification of evacuation routes within the community in the event of landslides.
- Assess the manpower and community-level resources available to obtain external support when and where necessary.

Fig. 6 Community-based landslide EWS design



Hazard Assessment and Risk Profiling

The most important aspect of an early warning system is to monitor the hazard level and understand how, when and where the potential hazard event will have the potential to severely affect a community. In the traditional scenario, precipitation monitoring and recording is being carried out by the meteorological department and local met office located within the municipality area. To complement the existing efforts to disseminate early warning messages, risk profiling has been carried out from the community level to the municipality level. It has helped in developing risk scenarios for the entire municipality. It helped the municipality officials to understand how community-driven efforts can supplement the existing mechanisms. For example, Cox's Bazar is vulnerable to cyclones, floods and landslides and usually any one or all types of hazards can occur simultaneously in any of the communities. Hence the municipality should have a good idea about the multiple natures of hazards, their potential areas of occurrence and preparedness measures that need to be undertaken to suit all types of hazards. If a hazard turns into a disaster, they should know effective ways to respond to multiple hazards. This approach helped municipality, government agencies and other designated response agencies and non-governmental organizations to make their response more effective in times of emergencies.

Early Warning and Monitoring System Development

After conducting the community risk assessment, an early warning and monitoring system has been developed. A sample community-based landslide early warning system design is shown in Fig. 6. All possible interventions were identified through this activity, and roles and responsibilities have been assigned to respective parties. The local institutions that can be helpful in providing early warning, methods of dissemination to the community, and community-level social dynamics that need to be aligned with external agencies for effective dissemination have been identified. The possible early warning mechanisms for each community have been discussed with the municipality to facilitate effective implementation during monsoon periods.

Development of Decision Support System at the City Level

One of the noticeable factors for failures in the past was the limited capacity of the city to develop a decision support system for responding to multiple types of emergencies. Most of the time, the use of the decision support system or analysis takes place at the national level, which invariably takes time to reach the local level. Even if information is

sent to municipalities, since it has not been generated at an appropriate resolution, local governments cannot use such information for risk reduction interventions. To minimize the information gaps and transmission costs, as well as improve the reaction time, there is a need to enhance the capacity of city level officials to develop a decision support system at the local level. If the city is prone to multiple hazards, including landslides, and if the risk assessment shows a high vulnerability, the city should have the capacity to use the decision support system that would assist the city to prepare for and respond to such multiple events. The same information can be used for land-use planning and control for appropriate construction or to improve community resilience. The training workshops were held to train municipality-level stakeholders in using such decision support systems for future disaster risk reduction.

Installation of Rain Gauges at the Community Level and a Display System

A scientific study was carried out by the project to develop the rainfall threshold values for landslide triggers. To maximize the use of rainfall data and established thresholds, rain gauges have been installed in various vulnerable locations in the selected communities. A sample rain gauge indicating alert, warning and evacuation levels using a color code is shown in Fig. 7 (ADPC 2007). Volunteers and community-based facilitators have been trained to collect the rainfall data on an hourly basis and convey the information to municipality and local meteorological department offices during monsoon periods through an SMS text messaging service. In addition, the information will be conveyed directly to community volunteers and facilitators. The information collected by volunteers and facilitators at each of the rain gauge stations would also be displayed in the community using a display board. The display boards have been installed in strategic locations within the municipality.

Collection and Processing of Rain Gauge Data at the Municipality Level

The early warning system components have been discussed with the city and local meteorological department office as an effective tool in preparing for and response to future events. The community-based operations have been streamlined to complement existing planning. The information collected at the national level would be sent to the local meteorological department offices. Municipalities would closely work with the local meteorological department office, which will provide a summarized outlook covering meteorological and atmospheric predictions on a daily basis to the municipality. The municipality will also share the information received from the community with the local

A three step alerting system developed

নিরাপদস্থানে প্রস্থান করুন	২৪ ঘণ্টায় ২০০ মি.মি. বৃষ্টিপাত ও চলমান
নিরাপদস্থানে প্রস্থানের প্রস্তুতি নিন	২৪ ঘণ্টায় ১০০ মি.মি. বৃষ্টিপাত ও চলমান
সতর্ক থাকুন	২৪ ঘণ্টায় ৭৫ মি.মি. বৃষ্টিপাত ও চলমান



"Alert" - 75 mm rainfall for 24 hours- Increase vigilance and observe appearance of any symptoms of slope destabilization on critical slopes.

"Get ready for evacuation" to safer location from high risk locations on 100 mm rainfall for 24 hours

"Evacuation" - 200 mm rainfall for 24 hours -Warning for evacuation to safer places.

Fig. 7 Sample rain gauge where alert, warning and evacuation levels are indicated using a color code

meteorology office. The municipality will use both sets of data for issuing alert messages to the community and finally, after reaching the precipitation threshold, to issue evacuation orders. A cluster-based "Risk communication strategy" and evacuation plan is shown in Fig. 8. The municipality also uses a display system for direct information dissemination to community-level volunteers and facilitators. In continuation of the community-based early warning systems, the project has facilitated community-level simulations and mock drills to ensure better response capacity.

Towards a Long-Term Landslide Risk Management Strategy

Landslide hazard zonation maps, the development of precipitation thresholds, the establishment of community-level early warning systems and interventions for creating community awareness of landslide preparedness and mitigation are measures that have been used in promoting city-level risk management. The project also demonstrated ways of regulating development using the decision support systems. The response planning and community-based disaster risk reduction interventions helped in strengthening the capacity of the city dwellers to respond, manage and implement the landslide risk management plans effectively.

The work done under the project had become a good starting point for developing a national strategy for landslide risk reduction in Bangladesh. At the end of the project, a national-level workshop with the participation of stakeholders and representatives of urban local governments was organized to present the outcome of the activities and to discuss the strategy for long-term landslide risk management in Bangladesh.

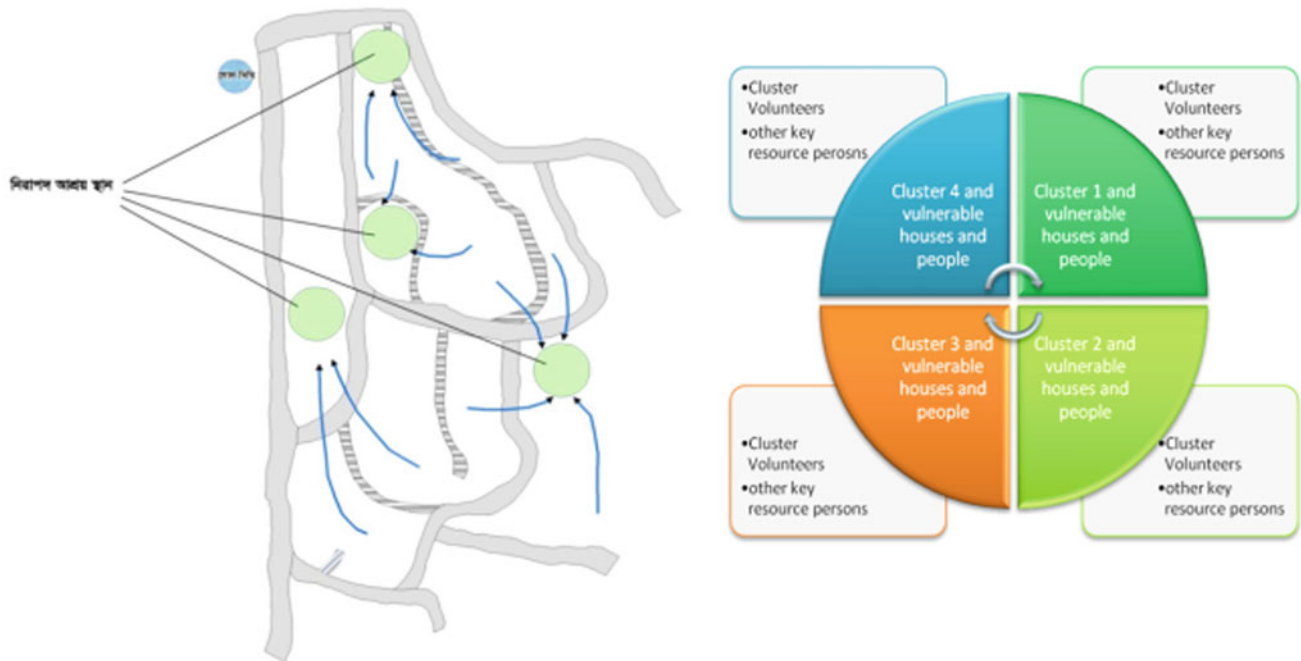


Fig. 8 Cluster-based “Risk communication strategy” and evacuation plan

Conclusion

It has been observed that the urban local authorities involved in planning human settlements and development, as well as service sectors such as water, power and road development authorities, do not give adequate attention to landslide problems for a variety of reasons. Therefore, the project felt that a more effective approach for reducing the impact from landslide events on communities in the future would be to create awareness of the issues related to landslide risk management by local authorities. Subsequently the development of a long-term strategy for landslide risk management was helped by discussion of the issues and solutions in a comprehensive manner. The information products at the local level should serve as decision support systems for local governments to undertake disaster risk reduction. When the resources are not adequate for long-term mitigation interventions, it is also appropriate to have improved preparedness measures. One of the ways to improve the early warning operations is to develop local level early warning systems and improve the response capacity at the community and local government levels. It is important also to conduct warning audits in key areas such as communication and coordination, warning reception, local hazard monitoring, local warning dissemination, preparedness and administrative compliance.

Acknowledgments The authors gratefully acknowledge the contributions made by the Comprehensive Disaster Management Program of Bangladesh Government in helping ADPC to undertake a pilot project to demonstrate the effectiveness of local level actions for effective landslide risk management. The authors wish to note the contributions made by Prof. Maksud Kamal and faculty members of the Dhaka University, ADPC staff involved in the project and staff from local governments in successful implementation of the program. The contributions made by the Norwegian Government in supporting the implementation of the Asian Program for Regional Capacity Enhancement for Landslide Impact Mitigation (RECLAIM) by ADPC in the region since 2004 and technical assistance by the Norwegian Geotechnical Institute for implementing the program are also acknowledged and greatly appreciated.

References

- Abarquez I, Murshed Z (2008) Community based disaster risk management. Field practitioner’s handbook. ADPC
- ADPC (2007) Safer cities 18: The Boy Who Cried, ‘Wolf’ or Why a Community-based Alert System is a good Idea
- ADPC (2011) CBDRR regional training participants workbook
- ADPC (2012) Report on establishment of early warning mechanisms within the identified high risk areas in Bangladesh
- Asian Disaster Management News (2008) ADPC, May–August 2008
- Case study: Community Based landslide Early warning system development in Cox’s Bazar and Teknaf Municipalities in Bangladesh
- Complexities in Landslide Forecasting (1994) LHMP document no. 24. National Building Research Organization, Sri Lanka
- Subbiah AR, Fakhruddin SHM (2008) Community based long lead-early warning and response. Asian Disaster Management News



Study of Landslides in Flysch Deposits of North Istria, Croatia: Landslide Data Collection and Recent Landslide Occurrences

Željko Arbanas, Sanja Dugonjić Jovančević, Martina Vivoda, and Snježana Mihalić Arbanas

Abstract

The northeastern part of the Istrian Peninsula in Croatia is built of Palaeogene flysch deposits, in which instability is common and where a large number of landslides, with significant consequences, have been recorded. Study of landslides in flysch deposits of North Istria will be conducted as one of the main activities of ongoing IPL-184 Project. It includes analyses and recognition of sliding mechanisms to use in landslide modelling and to determine landslide susceptibility and hazard in flysch rock mass deposits. Several landslide types, mechanisms and conditions occur in the study area. The majority of studied landslides occurred during the spring and winter. Generally, the landslides are of rotational and translational sliding type, and rarely rock falls and debris flows. Local roads and rarely other structures and facilities suffered major damage as a consequence of the landslides. Landslide inventories, as well as landslide susceptibility maps, have never been carried out in the study area. Today's knowledge about landslides in this area is based on investigations of individual landslides and partial scientific research. After the project started, some of the activities from all stages of the project have been initiated. The proposed first stage of the project includes supplementation of the existing database, and field investigations of recent and existing landslides in the study area, as well as soil sampling for laboratory testing. Moreover, the methods used for landslide susceptibility and landslide hazard assessment are presented. This paper presents the current state of investigations and research in the initial stage of the IPL-184 Project.

Keywords

Landslide • Flysch • Data collection • Landslide mechanism

Ž. Arbanas (✉) • S. Dugonjić Jovančević • M. Vivoda
Faculty of Civil Engineering, Geotechnical Department, University of Rijeka, Radmile Matejčić 3, Rijeka 51000, Croatia
e-mail: zeljko.arbanas@gradri.uniri.hr; sanja.dugonjic@gradri.uniri.hr; martina.vivoda@gradri.uniri.hr

S. Mihalić Arbanas
Faculty of Mining Geology and Petroleum Engineering, Geotechnical Department for Geology and Geological Engineering, University of Zagreb, Pierottijeva 6, Zagreb 10000, Croatia
e-mail: smihalic@rgn.hr

Introduction

The northeastern part of the Istrian Peninsula has a long history of landslide occurrences and many papers have described instability phenomena there. Benac (1994), in his doctoral thesis, described landslides in the Plomin area on the east coast of the Istrian peninsula; Mlinar et al. (1995) described the Raspadalnica landslide near the city of Buzet; Arbanas et al. (1999) described small landslides which are frequent in this area; Arbanas et al. (2006) described debris flows at the foot of the Čićarija Mountain range; and Arbanas et al. (2010) described mechanisms of the translational Brus landslide. Different authors wrote

papers regarding rock mass strength aspects (Arbanas et al. 2006, 2007, 2010; Benac et al. 2009). A review of research results on recent landslides that occurred in the central and northern parts of the Istrian Peninsula over the past 35 years is presented in Dugonjić Jovančević and Arbanas (2012). Just a few papers present landslide hazard assessments in the area (Mihalić et al. 2011; Dugonjić Jovančević et al. 2014).

In terms of geology, the Istrian Peninsula, situated in the northwestern part of the Adriatic Sea, is formed in flysch rock mass deposits called Gray Istria due to the gray colour of the exposed flysch rock mass. The Istrian Peninsula can generally be divided into three geological units: the Red Istria area in the southern and southwestern part of the peninsula has carbonate rocks covered by red-coloured deposits of Mediterranean soil, or so called terra rossa; the White Istria area, which includes the Čićarija Mountain range and part of the Učka Mountains, has white carbonate rocks visible at the surface; and the Gray Istria area in the central part of the peninsula has Palaeogene flysch deposits (Arbanas et al. 2011).

In typical areas, the flysch bedrock is covered by Quaternary deposits, except in isolated areas where there is more erosion (Dugonjić Jovančević and Arbanas 2012).

The total area included in the study area of this IPL-184 Project covers about 550 km², and the volume of recent landslides exceeds 500,000 m³.

IPL-184 Project: Study of Landslides in Flysch Deposits of North Istria, Croatia: Sliding Mechanisms, Geotechnical Properties, Landslide Modelling and Landslide Susceptibility

The expected duration of the IPL-184 Project is four years, and it includes three senior researchers and six young researchers. The main objectives of the Project are: study of triggering factors and landslides mechanisms of instabilities in flysch formations in North Istria, Croatia; laboratory analyses of soil materials from the flysch deposits using ring shear apparatus; modelling of typical instabilities in flysch deposits: back analyses; identification of conditions which cause landslides in flysch deposits and recommendations for landslides susceptibility and hazard mapping in flysch areas.

The Project activities are listed in Table 1. The first stage consists of data collection; field investigations of existing landslides in the study area and soil sampling for laboratory testing. During the second stage of the project the main activities will be laboratory testing of soil samples and establishment of landslide numerical models based on back analyses and laboratory testing results. The third stage includes spatial analyses of the geotechnical model, spatial

Table 1 Plan of working phases, their duration and expected results for the IPL-184 project

Working phases	Expected results	Time frame
First phase: data collection, field investigations	Field database establishment	12 months
Second phase: laboratory testing, numerical modelling	Geotechnical properties database	12 months
Third phase: spatial analyses	Landslide susceptibility maps, landslide hazard maps for pilot area	10 months
Fourth stage: deterministic landslide analyses	Recommendations for landslide susceptibility and hazard maps preparation in the flysch area of North Istria	8 months
Fifth stage: investigation presentation	Presentation of results to the local authorities in the study area	6 months

analyses of the existing landslide distribution (landslide inventory) and landslide susceptibility and hazard mapping in a pilot area inside the study zone, based on the results of previous investigations.

In the fourth stage, a systematic particular deterministic analysis of landslides susceptibility based on 3D stability analyses will be carried out for the pilot area. Based on the results obtained in the third and fourth stages, recommendations for landslide susceptibility and hazard mapping in the flysch area of North Istria will be prepared. Even during following stages, all the activities from earlier phases will be continued until the end of the project.

In the fifth stage, recommendations will be presented to the local authorities in the study area: the County of Istria, and the cities of Buzet, Pazin and Buje, as well as other municipalities located in study area, as helpful measures for future urban planning.

The expected benefits of the Project are multiple: for society (through implementation of the project's results in physical planning); for local authorities (through better understanding of conditions for land-use planning); for companies that maintain facilities such as roads and pipelines (through identifying landslide hazards for existing and new facilities); and for scientists (through new knowledge of landslide behaviour in flysch deposits).

Supplementation of the Existing Database

The creation of the landslide database for the study area (Fig. 1) began in 2008 at the Department of Hydrotechnics and Geotechnics, Faculty of Civil Engineering, University of Rijeka, using existing documentation collected from the

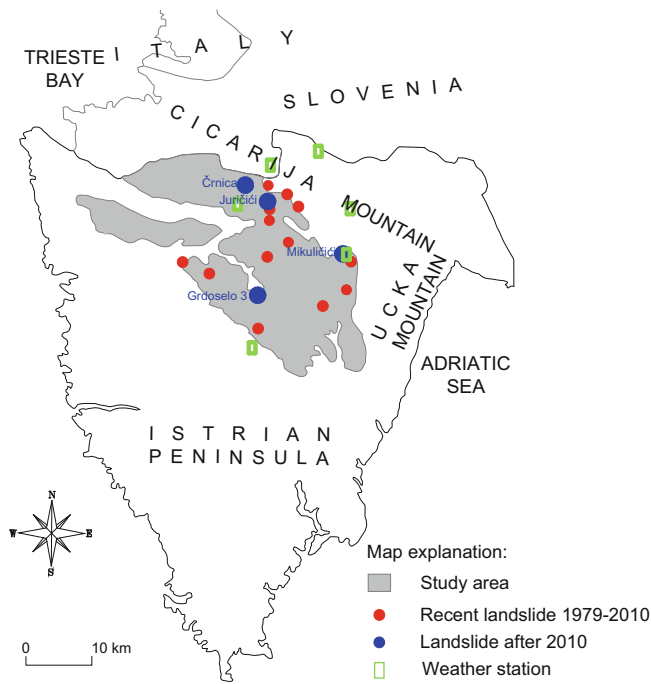


Fig. 1 Map of the Istrian Peninsula with the location of the study area and documented landslides

department's archives and from the archives of the Istrian County Roads Office and the Civil Engineering Institute of Croatia (Dugonjić Jovančević and Arbanas 2012). These documents included geological and geotechnical data from geotechnical field studies for remediation works on landslides. Figure 1 shows the locations of recent landslides documented from 1979 to 2010 for previous research (Dugonjić Jovančević and Arbanas 2012) and landslides documented after 2010 in the first stage of the current IPL-184 Project. Many landslides that occurred in this period are not documented in this paper because they cannot be substantiated. They will be included in the landslide inventory map for the study area which is planned to be done in the third phase of the project.

The database for the studied landslides contains basic information about their location, type, dimensions and time of occurrence, as well as other data from geological and geotechnical studies, laboratory test reports, and remediation designs, as shown in Table 2.

It was observed that landslides on flysch slopes have multiple styles and retrogressive distribution (Cruden and Varnes 1996). Landslides in the area generally cover relatively small slope areas (Arbanas et al. 2007, 2011; Dugonjić Jovančević and Arbanas 2012). In most cases, the slides are rotational, while other types of instability are rare (Arbanas

et al. 2010; Mihalić et al. 2011; Dugonjić Jovančević and Arbanas 2012). The sliding surface usually forms inside the weathered flysch rock mass, between the cover and the fresh bedrock. Instabilities initially develop through the weathering of superficial flysch deposits exposed to atmospheric activity and unfavourable hydrological conditions. Weathering of the flysch rock mass, and processes of erosion and accumulation of the weathered material, which form potentially unstable deposits, are very significant causal factors for landslide initiation in the area. Weathering grades from the cover surface to the flysch bedrock are shown on a profile in the study area (Fig. 2).

Because of the different grades of weathering (ISRM 1985), the strength parameters of soils in the landslide bodies show considerable variation. The strength properties of the flysch bedrock were difficult to assess due to disturbance of the flysch rock mass during the sampling, while the tested samples were collected from different parts of the landslide body, although rarely from the surface of rupture. Different test methods were employed, using different direct shear apparatus, ring shear apparatus and triaxial apparatus.

The volumes of the investigated slope instabilities vary from 700 to 175,000 m³; the average slope angle is between 15 and 30 %, and the thickness of superficial deposits varies from 0.5 to 11 m (Table 2). An overview of the documented landslide dimensions, based on the Multilingual Landslide Glossary (WP/WLI 1993) is shown in Table 3. By analyzing the sliding causes and triggering factors it was concluded that almost all landslides in the study area were initiated by a rise in groundwater level caused by rainfall, and consequently by a decrease of effective strength caused by increasing pore pressure (Dugonjić Jovančević and Arbanas 2012; Arbanas et al. 2011; Dugonjić Jovančević et al. 2014). It is clear that the landslides occurred after long rainy periods, while short-term rainfalls have significant influence on erosion.

Recent Landslide Occurrences 2010–2013

The Grdoselo 3 Landslide occurred in autumn 2011 (Fig. 3a). It is located on a local road on which two more landslides (Grdoselo 1, 2) occurred in the past. The natural slope balance was disturbed and hydrogeological conditions changed during road construction. A large amount of water was flowing on the slope and infiltrating into the road embankment. Infiltration continued until the flysch rock mass was reached and then the groundwater level rose.

The Grdoselo 3 Landslide was caused by a combination of heavy rainfall and human activity that significantly

Table 2 Database of recent landslides in the study area

Location	Time of occurrence	Type of instability	Estimated volume (m ³)	Average slope angle (%)	Cover thickness (m)	Triggering factor
Krbavčiči	January 1979	Rotational I	59,000	15–20	0.5–10.0	Rainfall
Krbavčiči 1	January 1979	Translational I	176,000	15–20	1.0–10.0	Rainfall
Staraj	Spring 1993	Rotational I	1,900	10–30	3.5–4.0	Rainfall
Krušvari	Spring 1993	Rotational I	68,500	14	1.5–9.0	Rainfall/human
Raspadalica 1	1992	Translational I	900	50–70	1.5–3.5	Rainfall
Raspadalica 4	1994	Rotational I	4,100	50–70	2.5–5.5	Rainfall
Čiritež	1995	Rotational I	37,000	14	5.0–10.0	Rainfall
Raspadalica 2	1995	Rotational I	2,900	55–70	2.5–6.5	Rainfall
Raspadalica 5	1995–1999	Rotational I	13,400	50–70	4.0–11.0	Rainfall
Grdoselo 1	Winter 2002	Rotational I	1,800	25	0.5–6.5	Rainfall/human
Grdoselo 2	Winter 2002	Rotational I	2,300	25	0.5–5.5	Rainfall/human
Krbavčiči-reactivated	January 2003	Debris/earth flow	35,000	15–30	0.5–10.0	Rainfall/human
Ivančiči	Spring 2004	Fall	1,500	15–30	1.0–3.6	Rainfall
Vidaci	Winter 2004	Fall	1,400	35–55	1.0–2.5	Rainfall
Drazej	January 2005	Rotational I	9,800	30	4.5–8.0	Rainfall/human
Brus	Spring 2005	Translational I	35,000	15	0.5–1.5	Rainfall
Marinci	Spring 2006	Rotational I	1,800	30	8.0–8.5	Rainfall/human
Juradi	November 2010	Translational I	47,000	10–25	6.0–11.0	Rainfall/human
Kaldir	Winter 2010	Rotational I	2,000	22–30	7.0–9.0	Rainfall
Grdoselo 3	Spring 2011	Rotational/translational I	6,400	42–68	3.8–4.0	Rainfall
Mikuličiči	Autumn 2011	Rotational I	700	50–76	4.8–4.8	Rainfall
Juričiči	November 2012	Rotational I	1,700	57–85	3.0	Rainfall/human

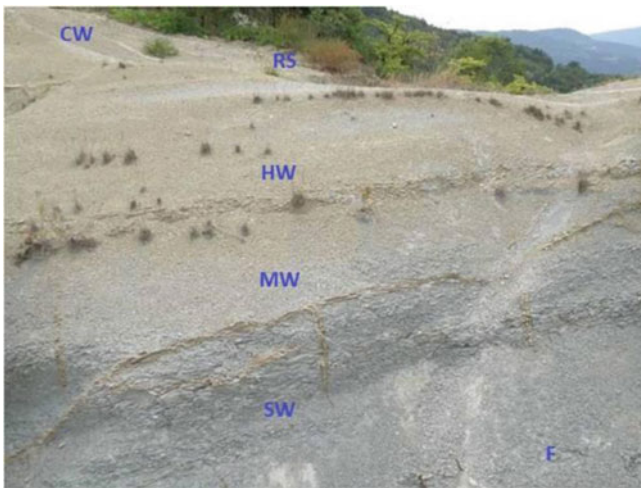


Fig. 2 Weathering profile in flysch rock mass (ISRM 1985): *F* fresh, *SW* slightly weathered, *MW* moderately weathered, *HW* highly weathered, *CW* completely weathered, *RS* residual soil

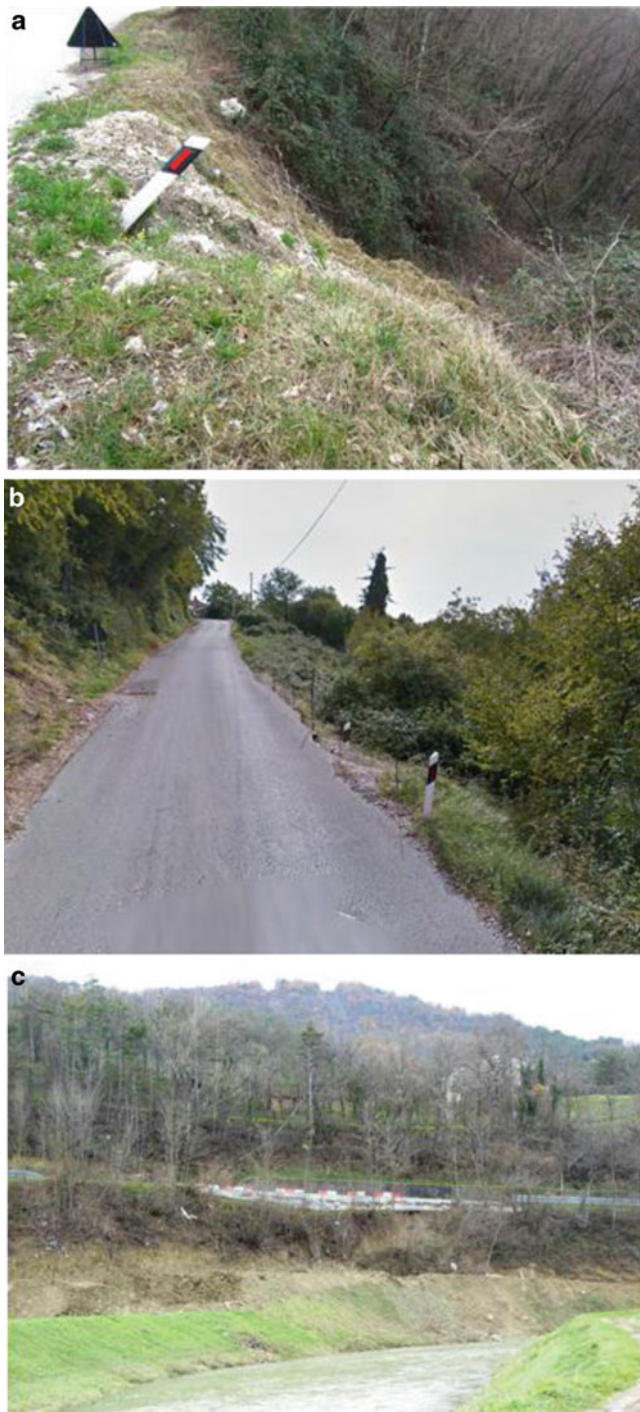
changed slope geometry. Field investigations were conducted in autumn 2011 and consisted of engineering geological mapping, borehole drilling and laboratory testing. The sliding surface was located at the contact between the superficial slope deposits and flysch bedrock. This is a translational type of landslide, and its boundaries were determined from a 35 m long subsidence of the pavement and accumulation of material in the toe.

The Mikuličiči Landslide occurred on the local Lupoglav–Vranja road, and damaged 15 m of the road embankment (Fig. 3b). The average inclination of the slope was approximately 33° in the lower part of the slope to 52° on the slope above the road.

Field investigations were carried out and a geological cross-section was prepared. The geological profile includes embankment fill, colluvium deposits and flysch rock mass in the bedrock and limestone on the top of the slope above the road. Undisturbed heterogeneous flysch rock mass is classified in C, D and E groups, with a Geological Strength Index

Table 3 Dimensions of landslides in the study area

Dim. (m)	Krbavčići (1979)	Krušvari (1993)	Krbavčići (2003)	Dražej (2005)	Brus (2005)	Marinci (2006)	Juradi (2010)	Mikuličići (2011)	Grdoselo 3 (2011)	Juričići (2012)
L	242	115	140	48	208	23	63	31	106	13
L _d	240	80	137	45	142	21	55	31	106	12
L _r	220	115	130	25	142	20	60	13	80	13
W _d	55	145	40	50	37	15	150	25	40	55
W _r	45	85	50	49	37	14.5	145	25	42	55
D _d	10.0	4.5	6	4	8–10	2	8	2	2	2.5
D _r	12.5	7	10	8	10	8.5	11	2	2.5	2.5

**Fig. 3** Photographs taken after sliding: (a) The Grdoselo 3 landslide, (b) the Mikuličići landslide and (c) the Juričići landslide

(GSI) of between 40 and 20 (Marinos and Hoek 2001). The remedial works design proposed a cantilever retaining wall 5.5 m high at the road edge founded in the bedrock and boring a drain system across the road up to limestone.

Excavation of a wastewater trench in the toe of the slope, in combination with period of heavy rainfalls, caused the Juričići Landslide in November 2012 (Fig. 3c). At that time 35 m of local road was damaged, and during the rainy spring of 2013, the width of the landslide enlarged another 30 m and the landslide head scarp damaged the road. The Juričići Landslide is a shallow rotational landslide, which involved 3 m of the clayey cover deposits, together with the road embankment, bringing material down the slope into the landslide toe. Further landslide widening potentially could have occurred due to small hydrodynamic or geometry changes in the slope, so emergency remedial work needed to be done. Construction of a gabion wall at the road edge, 71 m in length and founded on concrete piles, is still in progress (Autumn 2013).

Conclusions

Conditions that predispose flysch slopes to future landslides include the presence of clayey superficial deposits over the flysch bedrock on a slope with suitable inclination and kinematic conditions for sliding. Admission of water into the slope, with the inclination of the almost-impermeable flysch bedrock either retaining the groundwater at a location or promoting groundwater flow close to the slope inclination, and conditions in which the slope is exposed to a sufficiently long, continuous period of rainfall are main triggering factors for the activation of landslides on the flysch slopes of Gray Istria.

According to the well-known and widely applied principle “The past and the present are keys to the future” (Varnes 1984; Carrara et al. 1995), it is assumed that new landslide occurrences on the flysch slopes of Istria will appear in morphological, geological, hydrogeological and geotechnical conditions that are similar to the conditions associated with recent landslide occurrences (Dugonjić et al. 2008; Dugonjić Jovančević and Arbanas 2012). This is an important assumption for the future landslide susceptibility and landslide hazard analyses planned for the coming phases of the IPL-184 Project.

References

- Arbanas Ž, Benac Č, Jardas B (1999) Small landslides on the flysch of Istria. In: Proceedings of the 3rd conference of Slovenian geotechnical society, SloGeD, Ljubljana, pp 81–88
- Arbanas Ž, Benac Č, Jurak V (2006) Causes of debris flow formation in flysch area of North Istria, Croatia. In: Lorenzini G, Brebbia CA, Emmanouloudis DE (eds) Monitoring, simulation, prevention and remediation of dense and debris flows. WIT Trans Ecol Environ 90: 283–292
- Arbanas Ž, Grošič M, Goršič D, Griparić B (2007) Landslides remedial works on small roads of Istria. In: Raus B (ed) Proceedings of the 4th Croatian roads congress. Croatian Road Society-Via Vita, Zagreb, p 38
- Arbanas Ž, Mihalić S, Grošič M, Dugonjić S, Vivoda M (2010) Brus landslide, translational block sliding in flysch rock mass. In: Proceedings of the European rock mechanics symposium: rock mechanics in civil and environmental engineering. CRC Press/Balkema, London, pp 635–638
- Arbanas Ž, Dugonjić S, Benac Č (2011) Causes of small scale landslides in flysch deposits of Istria, Croatia. In: Proceedings of the 2nd world landslides forum, Rome, 3–9 October 2011, pp 221–226
- Benac Č (1994) Engineering-geological characteristics of the coastal belt and Rijeka Bay offshore. Dissertation, Faculty of Mine Geology and Petroleum, University of Zagreb
- Benac Č, Dugonjić S, Arbanas Ž, Oštrić M, Jurak V (2009) The origin of instability phenomena along the Karst-Flysch contacts. In: ISRM international symposium rock engineering in difficult ground conditions: Soft Rock i Karst, Cavtat, Croatia. CRC Press, Boca Raton, pp 757–761
- Carrara A, Cardinali M, Guzzetti F, Reichenbach P (1995) GIS-based techniques for mapping landslide hazard. In: Carrara A, Guzzetti F (eds) GIS in assessing natural hazards. Kluwer, Dordrecht, pp 135–177
- Cruden DM, Varnes DJ (1996) Landslide types and processes. In: Turner AK, Shuster RL (eds) Landslides: investigation and mitigation, transportation research board special report 247. National Academy Press, WA, pp 36–75
- Dugonjić Jovančević S, Arbanas Ž (2012) Recent landslides on the Istrian Peninsula, Croatia. Nat Hazards 62(3):1323–1338
- Dugonjić Jovančević S, Nagai O, Sassa K, Arbanas Ž (2014) Deterministic landslide susceptibility analyses using LS-Rapid software. In: Proceedings of the 1st regional symposium in the Adriatic-Balkan Region with the 3rd Workshop of the Japanese-Croatian Project: landslide and flood hazard assessment, Zagreb, Croatia (in press)
- Dugonjić S, Arbanas Ž, Benac Č (2008) Assessment of landslide hazard on flysch slopes. In: Proceedings of the 5th conference of Slovenian geotechnical society, 12–14 June 2008, Nova Gorica, Slovenia, pp 263–272
- ISRM, Commission on Standardization of Laboratory and Field Test (1985) Suggested methods for determining point load strength. Int J Rock Mech Min Sci Geomech Abstr 22(2):51–60
- Marinos P, Hoek E (2001) Estimating the geotechnical properties of heterogeneous rock masses such as flysch. Bull Eng Geol Environ 60:85–92
- Mihalić S, Krkač M, Arbanas Ž, Dugonjić S (2011) Analysis of sliding hazard in wider area of Brus landslide. In: Proceedings of the 15th European conference on soil mechanics and geotechnical engineering: geotechnics of hard soils – Weak Rocks, 11–15 September 2011, Athens, Greece, pp 1377–1382
- Mlinar Ž (1995) Station D-3: landslide Lupoglav. Excursion tutorial of 1st Croatian Geological Congress, Opatija, Croatia, pp 162–171
- Varnes DJ (1984) IAEG commission on landslides and other mass-movements – landslide hazard zonation: a review of principles and practice. UNESCO Press, Paris, pp 1–63
- WP/WLI (International Geotechnical Societies' Unesco Working Party On World Landslide Inventory) (1993) Multilingual landslide glossary. The Canadian Geotechnical Society, BiTech Publisher Ltd, Richmond, Canada



“Report a Landslide” A Website to Engage the Public in Identifying Geologic Hazards

Rex L. Baum, Lynn M. Highland, Peter T. Lyttle, Jeremy M. Fee, Eric M. Martinez, and Lisa A. Wald

Abstract

Direct observation by people is the most practical way of identifying, locating, and describing most damaging landslides. In an effort to increase public awareness of landslide hazards and encourage public participation in collecting basic data about landslides, the USGS recently launched a website called “Report a landslide.” The website is modeled in part after the highly successful USGS website “Did you feel it?” which has been used for several years to gather data from the public about intensity of felt earthquakes. The new “Report a landslide” website encourages visitors to report where and when they observed a landslide and to classify the landslide by movement type. Interested users also can report information about damage and casualties, dimensions, and simple geological observations, and can submit photographs of the landslide. Once a user submits a report, the location of the reported landslide appears on a map, and the location is linked to a summary of submitted data. Photos are reviewed prior to posting on the event page. By adding existing USGS data from historical landslides and promoting the website in the wake of large, regional landslide events, we hope to generate widespread awareness and interest in the website. The “Report a landslide” site has great potential for eventually creating a nationwide source of basic landslide data.

Keywords

Internet • Citizen science • Landslide inventory

Introduction

In recent years a growing number of scientific endeavours have turned to the public to facilitate collecting or processing data due to the widespread availability of

personal computers and mobile devices (smartphones and tablets) with access to the Internet. Observations that can be made by untrained persons can contribute to collection or analysis of valuable data on a wide range of natural phenomena. Such efforts are often referred to as “citizen science” or “crowd sourcing” and serve to increase public awareness of and interest in science and scientific issues that affect society as well as contributing to scientific research (Graham et al. 2011). Websites or mobile applications for citizen science have been developed for diverse subject areas in the natural sciences including phenology (Enquist et al. 2012); invasive species (Graham et al. 2011); image interpretation for tropical cyclone intensity, space weather, and astronomy applications (Graham et al. 2011; Hennon 2012); environmental monitoring through repeat digital photography (Graham et al. 2011); earthquake intensity (Wald and

R.L. Baum (✉) • L.M. Highland • J.M. Fee • E.M. Martinez • L.A. Wald
U.S. Geological Survey, Geologic Hazards Science Center, Box 25026
DFC M.S. 966, Denver, CO 80225-0046, USA
e-mail: baum@usgs.gov; highland@usgs.gov; jmfee@usgs.gov;
emartinez@usgs.gov; lisa@usgs.gov

P.T. Lyttle
U.S. Geological Survey, 12201 Sunrise Valley Drive, M.S. 908,
Reston, VA 20192, USA
e-mail: plyttle@usgs.gov

Dewey 2005; Atkinson and Wald 2007) and landslides (<http://www.bgs.ac.uk/landslides/reportForm.html>). In May 2009 the USGS Landslide Hazards Program began work on a web-based landslide reporting system (Highland et al. 2009), known as “Report a landslide”. The project subsequently became included in the International Program on Landslides (IPL) as project IPL-168 (<http://iplhq.org/category/iplhq/ipl-ongoing-project/>).

The objectives of this project are to educate Americans about the landslide hazards they face and to build more complete inventories of landslides through citizen participation. This project strives to make it as easy as possible for the public to report their observations of landslides on a website. The information gathered through the website can be used to classify the landslides and damage, as well as provide information to scientists about the location, time, speed, and size of the landslides. The website displays summary maps showing locations of recently reported landslides, as well as graphs showing simple statistics derived from the collected data, such as number of landslide reports and cumulative losses for a particular landslide.

An initial, working version of the website and database went online in June 2012 and was subsequently announced with a news release (<http://landslides.usgs.gov/dysi/form.php>). Several minor coding improvements were implemented in autumn 2012 to make the website compatible with all commonly used web browsers. The on-line questionnaire allows users to submit reports of landslides, including location, timing, description, damages, and photographs. Summary results, except photographs, are available on the “Report a landslide” website shortly after submitting a report. Photographs are reviewed to confirm that they are appropriate for public viewing before posting to the website.

Methods and Approach

Database Schema

Development of “Report a landslide” began with review of landslide report forms that had been developed by others (Cruden and Varnes 1996; Godt 1999; Hofmeister 2000; Laprade et al. 2000; Washington Division of Geology and Earth Resources 2013). Although each report form or database schema that we examined differed in detail, basic kinds of information requested or included were similar: location, date and time, size, damage and casualties, and name and contact information of the person reporting the slide. In addition, many forms asked for landslide type, slope angle, and speed. Some forms asked for one or more of the following: geological setting, certainty, land use, suspected cause, activity level, slope height, and dollar losses.

Our analysis of the existing report forms and their underlying data structure guided our development of a plan for the “Report a landslide” database. Our desire to characterize location, timing, types, and impacts of future landslides helped determine priorities. Landslide location, date of first observation, type of movement, and an identification (ID) number constitute the core of the database. Additional fields, as well as additional reports on the same landslide, are keyed to the ID number. The additional fields contain observations that might be more difficult or time-consuming for most observers including size, speed, activity, damage, casualties, contact information, comments, and photographs.

Questionnaire Design

A questionnaire of critical information for landslide identification was developed. Particular care was taken to prepare questions that could be answered by untrained observers. This was accomplished by selecting a minimum number of questions, phrasing the questions so that they could be interpreted easily, and by providing lists of possible answers. Where needed, tools are provided to help answer the questions. We avoided use of technical terms wherever possible and presented diagrams and photographs to help explain concepts, such as landslide type. Calendar tools simplify date inputs and menus present possible answers for most questions. Three different methods are available for entering landslide location.

Landslide location tools allow for use of text, graphical, and automated methods. (1) A map interface allows the user to type in an address or location name. The map zooms to the location and a marker appears showing the address location in the geodatabase. The user can then drag the marker to the exact landslide location on the large-scale base map or satellite image (Fig. 1). Alternately, a user can (2) enter latitude and longitude obtained by a handheld global positioning system (GPS) receiver or (3) a user on-site with a tablet or laptop with GPS capability can allow the device to automatically set the location. Regardless of method used, “Report a landslide” will display a marker at the reported landslide location.

By prioritizing the information we wanted to obtain (as described in the previous section), certain questions were designated as mandatory. Anyone wanting to submit a report must indicate, at a minimum, the location and time of observation. Users must also classify the landslide according to one of eight movement types: fall, flow, topple, rotational slide, translational slide, spread, avalanche, or unknown (Varnes 1978; Cruden and Varnes 1996). Diagrams and pictures are provided to help identify each landslide type. All remaining questions are optional. The option of declaring movement type as “unknown,” removes any



Fig. 1 Example of using the map tool to locate a landslide. The user can refine the location by clicking and dragging the blue pointer

Table 1 Sample damage report

Type	Damaged	Destroyed
Cars and trucks	2	2
Railroad cars		
Single family houses		
Multi-family houses		
Non-residential buildings		
Street or highway lanes	4	
Railway lines	1	
Bridges		
Pipelines	1	
Above-ground utilities		
Dams		
Forest or grassland acres	2	11
Agricultural land acres		
Type	Injured	Killed
Persons injured or killed	1	

Numbers represent reported damages for a hypothetical landslide crossing a major transportation corridor. The questionnaire asks, “Was anything damaged or destroyed? Report the number in applicable boxes, with Number Damaged/Number Destroyed. There is no need to enter zeros”

impediments to users who either lack the necessary information or confidence to classify the movement type.

The damage section of the report presents the user with a table of asset types (structures, infrastructure, vehicles, etc.)

Table 2 Questions and possible answers about landslide activity, speed, and dimensions

Questions	Answer choices
When did the landslide occur?	Date and time
How long was the landslide moving?	Time in units ranging from seconds to years.
Recurrence rate	Once, Sporadic, Continuous, Episodic, Other
What word best describes its sound?	Silent, Popping or cracking, Rumbling, Unknown, Other—See Comments
What was its speed?	<1 cm/y to >5 m/s
How long was it from top to bottom?	<30 cm to >3 km
How wide was the source area (i.e. area where the landslide started)?	<30 cm to >3 km
How deep was the source area (i.e. area where the landslide started)?	<30 cm to >30 m
How wide was the deposit?	<30 cm to >3 km
How deep was the deposit?	<30 cm to >30 m

Possible answers are presented in pull-down menus. Calendar and time tools are used to ensure that date and time information are entered in correct format (Note: English units are used for speed and dimensions on the website)

Table 3 Questions and possible answers about landslide materials

Questions	Answer choices
What words best describe the material that moved?	Bedrock, Coarse (Gravel, cobble and boulder-sized), Fine (Sand, silt and clay-sized), Mixture of coarse and fine, Unknown/Other
What words best describe the consistency of the deposit?	Liquid, Solid-Wet, Solid-Dry, Rubble, Unknown/Other

Possible answers are presented in pull-down menus

that can be affected by landslide activity (Table 1). The user can enter the number of each type damaged or totally destroyed. The table also contains entries for the number of people either injured or killed and a field for estimated monetary value of losses. We anticipate that as damage data accumulate in the database, rough lower-bound estimates of monetary losses can be computed by combining statistical data about replacement value of lost or damaged assets with totals in the database.

The landslide details section invites the user to answer questions about the landslide event, setting, prior conditions, speed, dimensions, and character of the landslide (Tables 2, 3, and 4). Users have the opportunity to provide details about the landslide event: exact time of occurrence (if known), how long the movement lasted, and the recurrence rate (Table 2). Landslide speed estimates may be reported according to the logarithmic scale proposed by Cruden and Varnes (1996). Dimensions (length, width and depth) of the source area and deposit may similarly be reported on a logarithmic scale (Table 2). We chose logarithmic scales

Table 4 Questions and possible answers about landslide conditions

Questions	Answer choices
What was the general setting? Please select all that apply	Open slope, side-slope of steep canyon, Gully or ravine, Housing development, Mine or quarry, Canal or waterway, Forest, Burned hillside, Coastal or river bluff, Unknown/Other
Was the ground that moved natural or previously modified by human activity?	Natural, Cut, Fill, Embankment, Graded (Cut and fill), Unknown/Other
Which words best describe the condition of trees along its path?	Standing upright, Leaning Uphill, Leaning downhill, Leaning all directions, Fallen, No trees, Scar height on trunk, Mud-coating height on trunk, Unknown/Other
Which words best describe the conditions immediately prior?	Average weather, Unusually dry weather, Unusually wet weather, Short intense rainfall, Prolonged moderate rainfall, Snowmelt, wave erosion, Stream erosion, construction, Earthquake, Unknown/other

Possible answers are presented in pull-down menus if a single answer is desired or as a series of check boxes if multiple answers are acceptable

for speed and dimensions because such estimates are well within the capability of most people and do not require the use of any specialized measuring tools or equipment. Users with more detailed information can enter those data into the comment section at the end of the report. Users may also enter descriptive information about the texture and consistency of the landslide material (Table 3), pre-landslide conditions (rain, earthquake, etc.), and details about the disposition of trees on the slide and the topographic setting of the slide (Table 4). In addition to providing additional information needed to classify and characterize landslides reported by the public, checking some of the descriptive and loss data for internal consistency or consistency with external data may help to assess the quality and accuracy of reports. For example, a reported landslide with a high number of casualties that cannot be corroborated by subsequent news media reports would be suspect.

The final section invites the user to leave written questions or comments along with his or her name and minimal contact information (telephone or e-mail). Reasons for requesting the person's name and contact information are twofold. First, some users have questions or want contact to help them identify a local authority that can come and look at the site. Second, experience with felt earthquake reports has shown that people tend to report more accurately if their name is associated with their report.

Acknowledging the User

Many users expect something in exchange for their time and sharing their information. "Report a landslide" acknowledges users by displaying a summary of their landslide report on the website. A marker appears on the map showing their landslide location. The marker is linked to an entry in a summary table on the event page with the landslide type, date, and location name. The list is also linked to summary tables of the report details, including photographs submitted with the landslide report (Fig. 2). To avoid the possibility of displaying inappropriate content, written user comments are not displayed, and photographic images and captions are reviewed by a USGS employee before posting on the event page (Fig. 2).

Review Process

The "Report a landslide" questionnaire went through several stages of review before it could be made public. Draft versions of the questionnaire, map, and report pages (including a full working prototype of the website) were reviewed by colleagues at the USGS and at state geological surveys and other agencies for technical content and for usability. Federal officials also reviewed the project to ensure that it was in compliance with federal laws that govern collection of data from the public.

Results

The reports we have received have come from a wide range of locations, 13 states, and two foreign countries. About half of the reports have contained damage data. Also about 70 % of reports contained dimensions or other descriptive data. Nearly all included written comments.

Usage of the "Report a landslide" website to date has been rather limited. The USGS Office of Communications has made efforts to promote the site, and a few landslide-inducing rainstorms have occurred since the site launched in June 2012. Additionally, widespread regional landslide events of the type that focus major media and public attention on landslides have not occurred and we suspect that efforts to draw attention to the project will progress slowly until such events occur.

Despite the limited number of reports as of July 2013, the website provides a consistent platform for reporting landslides and is capable of providing useful information for people affected by or interested in landslide events.

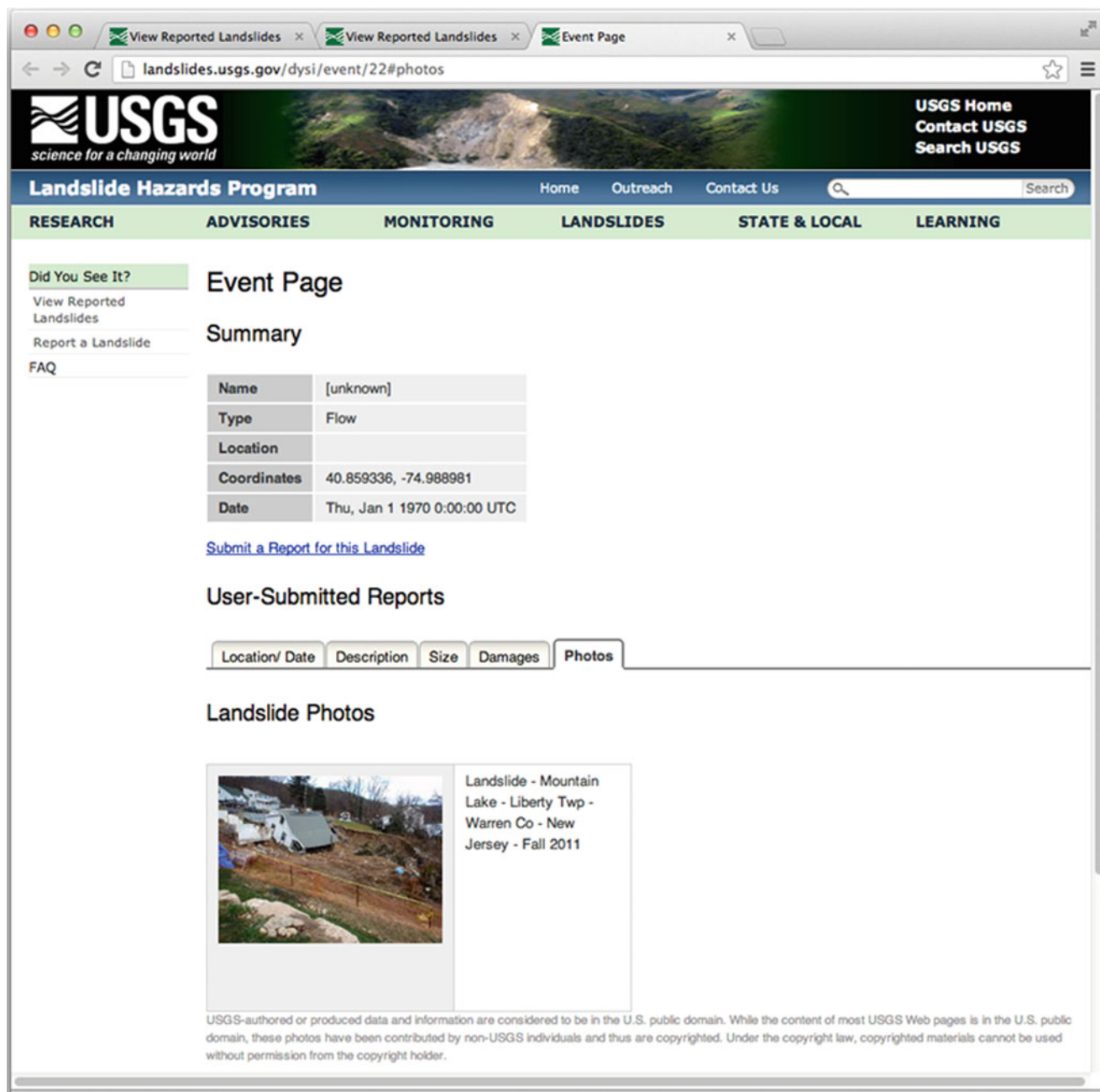


Fig. 2 Sample event page illustrating a user-submitted landslide report. Date shown in the table is the browser’s default value for null; the event date is unknown more precisely than fall 2011

Discussion

The “Report a landslide” website provides a convenient interface for reporting landslides (<http://landslides.usgs.gov/dysi/form.php>). The site is designed to make reporting as rapid and simple as possible so that persons without specialized training can contribute useful observations. During coming months we plan to experiment with loading

USGS data from historical landslide events into the database to help the site become a source of useful data in the near term and thereby encourage more people to contribute. We are also exploring ways to cooperate with the states on collecting these data. It is our hope that “Report a landslide” will serve to increase public awareness of landslides and the hazards they pose. In the long term we expect that it will prove to be a useful means of collecting basic data about landslides as they occur. We would be particularly pleased if

the website helps to collect more precise data about when landslides occur. Such information would be useful in developing or validating rainfall threshold models.

Acknowledgments Nathaniel Cockrell and Arianne Dean (USGS student interns) coded an early working prototype of the website. USGS colleagues Jeff Coe, Sue Cannon, Bill Schulz, David Wald, as well as Bill Burns (Oregon Department of Geology and Mineral Industries) and Tim Walsh, Washington Division of Geology and Earth Resources) provided useful suggestions about the website. Francis Ashland and Joe Gartner provided constructive reviews of this paper.

References

- Atkinson GM, Wald DJ (2007) "Did You Feel It?" Intensity data: a surprisingly good measure of earthquake ground motion. *Seis Res Lett* 78:362–368
- Cruden D, Varnes DJ (1996) Landslide types and processes in landslides investigation and mitigation. In: Turner AK, Schuster RL (eds) Transportation research board special report 247. National Academy Press, Washington, DC, pp 178–230. ISBN: 0-309-06208-X
- Enquist CAF, Rosemartin A, Schwartz MD (2012) Identifying and prioritizing geological data products and tools. *Eos Trans Am Geophys Union* 93(37):356
- Godt JW (1999) Maps showing locations of damaging landslides caused by El Niño rainstorms, winter season 1997–98, San Francisco Bay region, California. US miscellaneous field studies maps MF-2325.
- Graham EA, Henderson S, Schloss A (2011) Using mobile phones to engage citizen scientists in research. *Eos Trans Am Geophys Union* 92(38):313–315
- Hennon CC (2012) Citizen scientists analyzing tropical cyclone intensities. *Eos Trans Am Geophys Union* 93(40):385–387
- Highland LM, Baum RL, Cannon SH, Cockrell NJ, Dean AM, Lyttle P (2009) "Did you see it?" A website to collect reports of landslide occurrence in the United States from the public and practitioners. *Geol Soc Am Abstr Progr* 41(7):254
- Hofmeister RJ (2000) Slope failures in Oregon. GIS inventory for three 1996/97 storm events: Oregon Department of Geology and Mineral Industries Special Paper 34. 20 p (1 compact disc)
- Laprade WT, Nashem WD, Robertson CA, Kirkland TE (2000) Seattle landslide study. Shannon & Wilson Inc., Seattle, WA. http://www.seattle.gov/dpd/cms/groups/pan/@pan/documents/web_informational/dpdp025740.pdf (prepared for Seattle Public Utilities, Seattle, Washington, 164 p. and map folio)
- Varnes DJ (1978) Slope movement types and processes. In: Schuster RL, Krizek RJ (eds) Special Report 176—landslides analysis and control. Transportation Research Board National Research Council, Washington, DC, pp 11–33
- Wald DJ, Dewey JW (2005) Did you feel it?: citizens contribute to earthquake science. U.S. Geological Survey Fact Sheet 2005-3016. 4 p
- Washington Division of Geology and Earth Resources (2013) http://www.dnr.wa.gov/ResearchScience/HowTo/GeologyEarthSciences/Pages/report_a_landslide.aspx. Last Accessed 11 Jul 2013



Discrete Boundary Shear Strength of a Landslide at High Rainfall Precipitation Zone in Sri Lanka

A.A. Virajh Dias, S.B.S. Abayakoon, and R.K. Bhandari

Abstract

Boundary shear strength of a landslide is an important parameter for stability evaluation, prediction and remedial designs. A comprehensive study for the determination of shear strength parameters within and at close proximity of the shear zone at Watawala Earthslide, which is located at a high rainfall precipitation zone in Sri Lanka, was carried out. Triaxial tests were conducted to observe the peak and ultimate relations between the shear stress, s' and the effective mean normal stress, t' . Even though there is a considerable scatter of data, the coefficient of regression is above 0.91 and the linear regression gave effective angle of internal friction 33.50° – 29.82° (peak) and 30.28° – 31.12° (ultimate state). The effective cohesion is 5.99 – 7.72 kPa (peak) and 0.91 – 13.77 kPa (ultimate). Loss of strength due to extensive movements is indicated by in-situ Direct Shear Tests results which have an average effective cohesion, C' , of 2.84 – 4.74 kPa and effective angle of internal friction, ϕ' , of 11.42° – 18.14° . In addition, the laboratory Ring Shear test results give residual angle of internal friction, ϕ_r' , of 9.48° and effective cohesion, c_r' , of 0.0 kPa. On the other hand, the laboratory values direct shear tests give residual internal friction angle, ϕ_r' , between 13.06° and 16.43° and effective cohesion, c_r' , of 0.334 kPa to 3.75 kPa. Thus, strength parameters are highly variable even at the shear zone, probably reflecting a different history of clay mineral weathering and alteration.

Keywords

Watawala Earthslide • Direct shear test • Effective angle of internal friction • Effective cohesion

Introduction

Most of the Sri Lankan landslides investigated to date are mainly associated with high intensity rainfall, colluvium deposits, residual soils and saturated soil-rock composites. Since, reactivation of repetitive slides is highly dependent on shear strength at discrete boundaries, study on evaluation of parameters of such a landslide would amount to understand the sensitivity of high rainfall. According to the recent case studies, the Watawala Landslide is one of the premier examples to demonstrate the importance of evaluation of discrete boundary shear strength characteristics of soils in high rainfall precipitation zones in Sri Lanka. It is presently stabilized by dewatering and was considered as the most sensitive landslide in the 1990s (Fig. 1).

A.A.V. Dias (✉)
Central Engineering Consultancy Bureau, Centre for Research &
Development, Colombo 7, Sri Lanka
e-mail: aavirajhd@yahoo.com

S.B.S. Abayakoon
University of Peradeniya, Peradeniya, Sri Lanka
e-mail: sarathabayakoon@gmail.com

R.K. Bhandari
Landslide Hazard Mapping Project (UNDP/UNCHS) 1990–1996,
National Building Research Organisation, Colombo 5, Sri Lanka
e-mail: rajmee@yahoo.com



1992 : Tragic incident due to the Watawala Landslide.



1993: Reactivation with high intensity of rainfall.



1998–2013: After implementation of permanent remedial measures.

Fig. 1 Case Study—the Watawala Landslide, Sri Lanka. 1992: Tragic incident due to the Watawala Landslide, 1993: Reactivation with high intensity of rainfall, 1998–2013: After implementation of permanent remedial measures

Geologically, in Sri Lanka, formation of parent rocks dates back to Precambrian age of rock history (Cooray 1994). The basement rock is defined as moderately weathered Charnokitic Gneiss underlying various cross bedded rocks. In most repetitive landslides, slope surface features are bound by well-defined discrete boundary shears that are highly distinct and unique in many ways. The landslide movement at Watawala is somewhat difficult to predict considering its overall morphology, activation mechanism and some locations where the subsidence was of a very high order. Since the movement rates varied a great deal within the slide mass, up thrust shears bring on message of landslide motion and its dynamics. The landslide was 65 m wide and 530 m long. The depth of slide varies from 9 m to 28 m. One of the major railway track lines of the country goes across the slide, almost bisecting it in the longitudinal direction. The annual average rainfall in Watawala area generally exceeds 5,000 mm and hence, soil under various geological conditions, is saturated. The deposits mainly consist of residual soils and the uppermost layer of the soil consists of a highly altered soil rock mixture with a relatively high permeability in comparison with the underlying soils.

Displacement History

The Watawala Landslide is one of the examples to highlight the importance of evaluation of in-situ shear strength under various boundary conditions. A landslide often indicates very large number of macro and micro features which if studied in detailed, would enhance our understanding of initiation, development and growth (Dias 1997). This means that failure is defined with the contents of slide initiation, rotation and eventual transforming mechanism into well-defined cracks oblique to the boundary shears, at its maturity. The failure boundary and associated slope surface features in its crown, middle and toe regions reflect displacement history from its first occurrence and some of the representative physical features are shown in Figs. 2 and 3. These observations often direct our attention towards the assessment of shear strength of the discrete boundary, which is scientifically defined as residual state of soil behaviour. The soil mass generally contains soils of yellow-brown or red-brown Clayey Silty Sand or Silty Sand. Moving and transported soil contains boulder/rock fragments and colluvium. Fine particles of weathered mica forms the shining luster on the intact boundary face as in the photo “a” of Fig. 3. These observations were made in about 2–3 m deep open excavation trenches. Observation at boundary explains its long history of slow moving slide by forming different state of in-situ shears (Dias 1997).

The observations of movements associated with discrete boundary surface achieved an accuracy expected for the overall assessment of slope stability. In this content, four inclinometers and six piezometers were installed down the slope near the middle of the slide including two vibrating wire piezometers for the overall monitoring work. All inclinometers measured movements across the shear zones identified at, or close to, the soil overburden/bedrock surface.

Strength Determination

In-Situ Test Approach

Shear strength of a pre-determined shear plane of a landslide is an important parameter for the evaluation. An undisturbed soil sample taken from the shear zone of a landslide always produce reliable results. In case of Watawala, due to the extensive system of instrumentation, it was possible to identify the sliding surface with great accuracy. In this particular study, the amount of rock fragments present in the samples generally increased with depth until the basal boundary of the landslide. Number of 300 mm × 300 mm × 300 mm block samples were collected across the boundary.

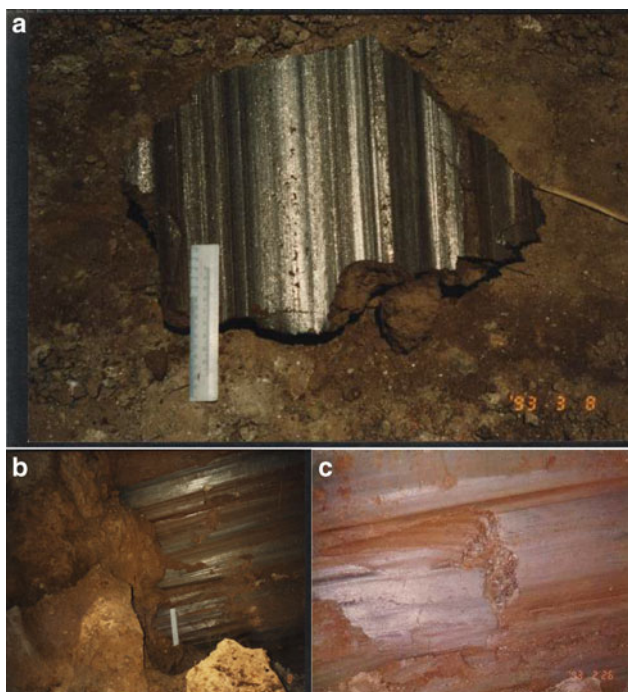


Fig. 2 Closed up pictures (a, b and c) of discrete boundary shears (Dias 1997) (Note: Shining lustre and high degree of particle orientation in the direction of sliding shows that the earthslide has already been subjected to larger displacements)

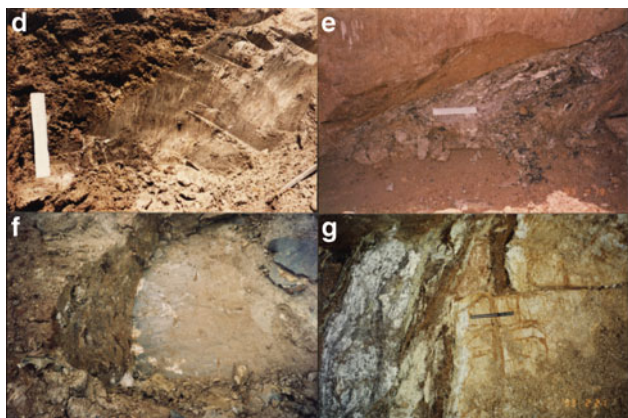


Fig. 3 Observations on (d, e, f and g) macro featuring discrete boundary shears

A reliable estimation of shear strength parameters corresponding to movements of very large order was the essential requirement for the assessment and design of permanent control measures. Therefore an attempt was made with a large (300 mm high by 300 mm in diameter) cylindrical type in-situ shear box apparatus in order to test the natural shear strength of discrete surface which was observed in the field (Fig. 4). The reliability of results was doubtful initially, because of certain difficulties at its



Fig. 4 Field direct shear testing equipment and installation work before testing

Table 1 In-situ direct shear test results (Dias 1997) at the Watawala Earthslide

Test condition	Test depth	Effective cohesion (kPa)	Effective friction angle (Deg)
Series 1	1.5–2.0 m	4.4	18.10
Series 2	2.3–2.5 m	4.7	14.42
Series 3	2.3–2.5 m	3.9	11.42
Series 4	2.3–2.5 m	2.9	16.34



Fig. 5 Observation of uniformity of plane of failure (h and i) after the test (Note: The visual characteristics of slip surface and the past movement history of landslide provide an ample evidence of residual conditions)

development stage due to incapability of controlling of the rate of shearing during the test.

The Watawala Earthside developed into a formidable repetitive slide over the period of several decades on visually seen discrete slide boundaries. However, it is worth to note that once the results are analysed (Table 1) it is seen that in-situ direct shear tests results at the discrete boundary are fairly consistent and have an average effective cohesion, C' , of 2.84–4.74 kPa and effective angle of internal friction, ϕ' , of 11.42° to 18.10° which are more realistic in comparison with results of back analysis of stability (Rajaratnam and Bhandari 1994, Bhandari and Dias 1996) (Fig. 5).

Intensive field and laboratory testing on undisturbed samples extracted from the shear zones conclusively established that the residual strength properties obtained on samples from shear zones were significantly different from

Table 2 Summary of triaxial test data of samples collected from three different samples and depths at site

BH No.	Depth (m)	Specific gravity	Liquid limit (%)	Plastic limit (%)	Peak s' (kPa)	Peak t' (kPa)	Ultimate s' (kPa)	Ultimate t' (kPa)	Volumetric behavior
Triaxial test results (1.00–2.00 m depth)									
UDS-1 BH 03	1.20–1.90	2.75	73	46.6	113.5	83	64.9	33.4	D
					134.1	80.1	107.9	54.2	MD
					173.3	85.1	173.3	85.1	C
					290.2	171.7	265.2	146.7	C
UDS-1 BH 04	1.20–2.00	2.65	50	29.5	95.2	67.7	95.2	67.7	C
					136.5	86.5	136.5	86.5	C
					226.9	141.7	226.9	141.7	C
					333.1	214.6	333.1	214.6	C
UDS-1 BHA1	1.29–1.89	2.57	34.5	25.5	86.8	50.8	117	64	D
					114.3	83.3	161.7	108.7	D
					136	91	200.1	127.1	D
Triaxial test results (4.00–5.00 m depth)									
UDS-2 BH3	4.00–4.65	2.64	38.8	28.3	152.5	123.5	147.7	118.7	MD
					141.2	87.7	129.8	76.3	MD
					225.0	136.8	201.3	113.1	MD
					301.5	184.5	285.8	167.8	C
UDS-1 BH 01	4.72–5.09	2.66	56.7	35.1	113.1	91.1	76.4	54.4	D
					201.4	131.4	182.6	112.6	MD
					352.7	230.7	304.6	182.6	D
UDS-2 BH4	4.5–4.85	2.75	47.1	31.0	75.6	45.6	75.6	45.6	C
					134.3	79.3	134.3	79.3	C
					334.9	216.4	312.0	193.5	C
UDS-2 BHA1	4.50–5.10	2.82	73.5	44.9	160.5	97.5	173.7	84.7	D
					109.5	74.5	133.5	76.5	D
Triaxial test results (8.53–9.73 m depth)									
UDS-2 BH1	9.28–9.73	2.76	57.0	31.3	100.9	70.9	69.1	39.1	D
					142.3	87.3	77.2	22.2	D
					227.5	139.5	164.2	76.2	D
					312.4	194.4	233.1	115.1	MD
UDS-3 BHA1	8.53–9.13	2.58	50.8	31.9	167.4	117.4	267.3	166.3	D
					173.2	90.2	221.2	111.6	D
					226.4	120.4	296.8	149.8	D

those obtained by testing soil samples from within the body of the slide, outside the shear zones.

Laboratory Test Approach

Triaxial shear tests were conducted for number of undisturbed soil samples, which were recovered during extensive drilling operations. There were four number of borehole locations selected along the centre of the longitudinal axis of the landslide and samples were taken for the determination of effective shear strength parameters.

Nine 60 mm diameter tube samples and three 74 mm diameter tube samples were tested under drained conditions at the Soil Mechanics Laboratory, University of Peradeniya. The summary of results giving peak and ultimate strengths of each layer depths are given in Table 2. The rate of

shearing in these tests was controlled so that at any given stage of shearing the excess pore pressure at the bottom of the specimen is limited to within 10 % of the effective cell pressure. Number of undisturbed soil samples collected and tested to represent the properties of deposited material (colluviums) within the sliding mass.

Top layer, 1.20–2.00 m usually contains newly transported soil subjected to number of repetitive shearing stages. The ultimate and peak values of s' and t' have been correlated with the linear regression curve to interpret the effective angle of internal friction and the effective cohesion. The peak and ultimate relations between the shear stress, t' and the effective mean normal stress, s' are also presented in Fig. 6 (1.2–2.0 m) and Fig. 7 (4.00–4.51 m). Even though, there is considerable scatter of data the coefficient of variation is above 0.96 in both cases. The significant loss of cohesion at ultimate stage is noted with the above

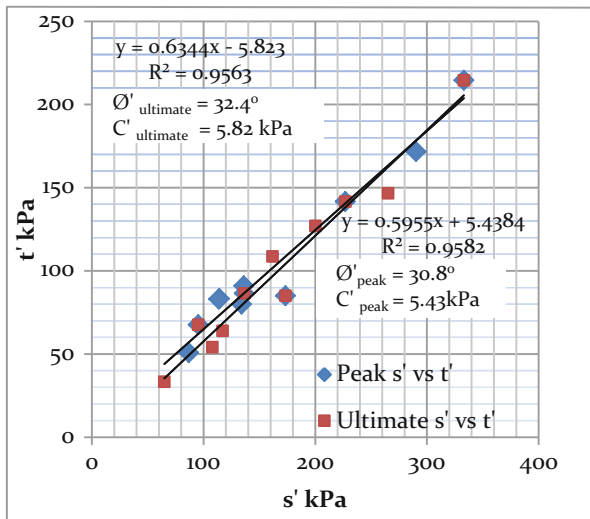


Fig. 6 Relationship between s' and t' (peak and ultimate) relationship at the depth of 1.2–2.0 m

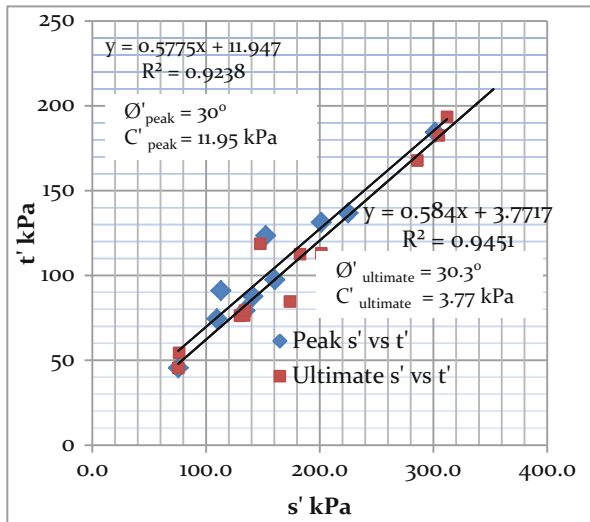


Fig. 7 Relationship between s' and t' (peak and ultimate) relationship at the depth of 4.0–4.51 m

results. In addition, the volumetric behaviour of samples was calculated and those are varied from compressive (C) to mildly dilative (MD) dilative (D) as shown in the Table 2.

The third group of samples represented the soil depth at 8.53–9.73 m as shown in the Table 3.

Laboratory Direct Shear and Ring Shear Test on Discrete Boundary Samples

For the determination of saturated, effective shear strength of discrete boundary samples, the standard drained Direct Shear Apparatus and the Ring Shear Apparatus at the

Table 3 Effective shear strength parameters at the depth of 4.0–4.51 m

Test condition	Effective cohesion (kPa)	Effective friction angle (deg)	R squared value (liner regression)
Peak	13.9	30.32	0.942
Ultimate	6.78	29.82	0.917

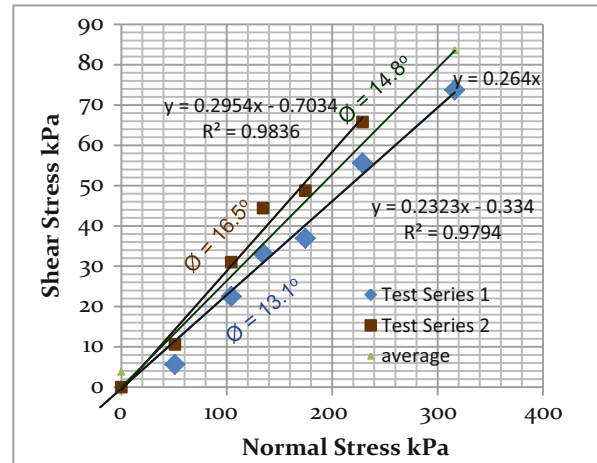


Fig. 8 Relationship between shear and normal stresses of direct shear tests

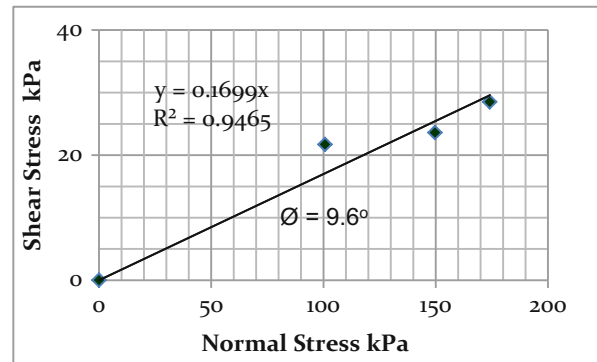


Fig. 9 Relationship between shear and normal stresses of ring shear tests (Dias 1998)

Department of Civil Engineering, University of Warwick have been used. (Report, Dias and Petley 1993) The laboratory direct shear results (residual) have a wide range of values as shown in Fig. 8. Results of ring shear tests (residual) are presented in Fig. 9. It is to be noted that compared to the triaxial test, main advantage is small sample size and facility to orient the pre-determined plane exactly with the plane of failure during installation. There were two series of samples selected for the interpretation of residual shear strength. The average residual strength parameters were

$c_r' = 0.0$ kPa, $\phi_r' = 14.8^\circ$ and these values are closer in-situ direct shear results as given in Fig. 8.

The residual value interpreted from the Ring Shear Test of $\phi_r' = 9.6^\circ$ at this site is much lower than the residual direct shear strength parameter of $\phi_r' = 14.8^\circ$ measured at the laboratory or 11.42° , 14.42° , 16.34° and 18.10° measured at in-situ test within the same geologic formation. Therefore, the residual strength parameters for the discrete boundary shear formation are variable, probably reflecting a different history of clay mineral weathering and alteration. It transpire that shear strength parameters found by testing samples containing actual slip surface provided shear strength values most appropriate for use in stability analysis of a repetitive landslides.

Conclusions

It is essential that the soil samples for obtaining shear strength characteristics and residual shear strength for stability analysis of a landslide are taken from the shear zone of the landslide and not from the general overburden. The shear zone can be reached for soil sampling by open excavations at boundaries or located through inclinometers observations in active landslides. Triaxial shear test on sliding mass interpreted in terms of effective stress indicated variations of effective angle of internal friction and loss of cohesion due to large displacements on the boundary shears. It was possible to explain the kinetics of the repetitive Watawala earthslide based on such testing. Residual strength parameters did cover a wide range of values within the same geologic formation, probably reflecting the degree of weathering and alteration of the clay minerals within the shear zone.

It is important to conclude that reliable assessment of the stability or otherwise of a natural slide, is possible only by scientific elucidation of its mechanism in terms of failure geometry, depth of basal boundary, piezometric pressures and the reliability of the shear strength

parameters. The Watawala Earthslide provides a valued example of shear strength characteristics of a high rainfall precipitation zone in Sri Lanka.

Acknowledgments This paper forms an integral part of the IPL-155 Project on “Determination of Soil Parameters of Subsurface to be used in Slope Stability Analysis in Two Different Precipitation Zones of Sri Lanka” being implemented by the Centre for Research & Development, Central Engineering Consultancy Bureau (CECB) of the Ministry of Irrigation and Water Resources Management, Sri Lanka. Some of the work described in this paper was done as a part of the Landslide Hazard Mapping Project implemented by the government of Sri Lanka, executed by the UNCHS (Habitat) and funded by the UNDP during 1990–1996. Therefore, the author gratefully acknowledges the National Building Research Organisation, University of Peradeniya, Sri Lanka, and University of Warwick, England in this connectivity. The views expressed in the paper are however those of the authors only. Our grateful thanks are due to Eng. N. Rupasinghe, Chairman and Eng. K.L.S. Sahabandu, General Manager, Central Engineering Consultancy Bureau for the permission and encouragements.

References

- Bhandari RK, Dias AAV (1996) Rain triggered slope movement as indicators of landslide dynamics. In: Proceedings of 7th international symposium on landslides, Trondheim, Norway, 17-21 June 1996. Balkema, Leiden, pp 1515–1520
- Cooray PG (1994) Geological factors affecting landslides in Sri Lanka. In: Proceedings of national symposium of landslides in Sri Lanka, Colombo, pp 15–22
- Dias AAV (1997) Stability attribute on discrete boundary shear strength of an earthslide-lessons from the Watawala Earthslide, Sri Lanka. In: 3rd Young geotechnical engineer conference on geotechnical engineers in Asia; 2000 and beyond, Singapore, 14–16, Vol 1. pp 627–638
- Dias AAV (1998) Chartered design review report. Institution of Engineers Sri Lanka (IESL), Sri Lanka, Appendix 2, pp 15, 43, 44
- Dias AAV, Petley DJ (1993) Report on advance training of laboratory testing of landslide investigation work. UNDP Fellowship 1993, Department of Civil Engineering, University of Warwick, England
- Rajaratnam K, Bhandari RK (1994) Back analysis of the Watawala Earthslide in terms of effective stress. In: Proceedings of national symposium of landslides in Sri Lanka, Colombo, pp 113–118



Glacial Lake Outburst Floods (GLOFs) Database Project

Adam Emmer, Vít Vilímek, and Jan Klimeš

Abstract

Due to global climate change and ongoing deglaciation, research on Glacial Lake Outburst Floods (GLOFs) is of great importance. The idea of a glacial lake outburst floods database project arose from our effort to identify regional specifics of these events in our region of research interest—the highest Peruvian mountain range, Cordillera Blanca. The project is designed under the International Programme on Landslides (IPL) for 3 years (2013–2015) and then we suppose it will be continued. The main goal of this project is the creation of a widely available online database of GLOFs that have occurred worldwide since the end of the “Little Ice Age”. An important step will be the initiation of international cooperation between individual scientific departments. We would like to complete and share information about each event, such as probable cause, flood volume, and socioeconomic impacts downstream. Our preliminary results showed important regional differences in the representation and proportion of various causes in different high mountainous regions worldwide. The most frequent causes are various types of dynamic slope movements into lakes (icefalls, rockfalls or other landslides). This cause is dominant in all of the studied regions. On the other hand, some causes are regionally specific—e.g., dam failure following a large earthquake was recorded in only one region, the Cordillera Blanca. Taking these differences into account is a crucial step in creating an optimal regionally focused method of GLOF hazard assessment.

Keywords

Outburst flood • GLOF • Database • IPL Project • International cooperation

A. Emmer (✉) • V. Vilímek
Faculty of Science, Department of Physical Geography and
Geocology, Charles University in Prague, Albertov 6, 128 43 Prague
2, Czech Republic
e-mail: aemmer@seznam.cz; vit.vilimek@natur.cuni.cz

J. Klimeš
Institute of Rock Structure and Mechanics, Academy of Sciences of the
Czech Republic, V Holešovičkách 41, 182 09 Prague 8, Czech
Republic
e-mail: jklimes@centrum.cz

Introduction

The phenomenon of glacial lake outburst floods (GLOFs) is highly important in this period of global climate change, which especially affects glacierized areas, and the effects of GLOFs represent a significant threat for an increasing number of inhabitants (see example in Fig. 1).

Glacier retreat in the majority of high mountains worldwide has led to the formation and evolution of all types of new, potentially hazardous glacial lakes (moraine-dammed, bedrock-dammed or ice-dammed lakes). These young glacial lakes are generally susceptible to dam failure or overflow—in other words they are prone to produce glacial lake outburst floods (Costa and Schuster 1988). The question of



Fig. 1 Example of a failed moraine dam at Lake Milluacocha (Cordillera Blanca, Peru). An outburst flood following dam failure occurred on 6th November 1952 and fortunately caused only minor damage in a valley

GLOF occurrence from specific lakes is a highly complex one and is interconnected with different types of natural hazards (especially with various types of slope movements, strong earthquakes and intense rainfalls; Clague and Evans 2000).

The increasing number of reported GLOFs comes hand-in-hand with the rising number of glacial lakes formed through deglaciation (e.g., Yamada 1998; Reynolds 2003; Emmer and Cochachin 2013).

Detailed knowledge about each event and also complex knowledge about GLOFs in a regional and wider context is an important precondition for reliable hazard assessment and effective hazard and vulnerability mitigation in the framework of GLOF risk management. The collection and provision of complex knowledge about regional specifics and patterns that is usable in hazard assessment is one of the main reasons why the project “Glacial lake outburst floods (GLOFs) database” was established under the International Programme on Landslides (IPL) in 2013. The GLOFs database is widely available online at <http://www.glofs-database.com>. With our collaborating partners from different research departments worldwide, we collected information about more than five hundred GLOFs that have occurred since the end of the last significant glacier advance (Little Ice Age).

Data and Methodology

The database of glacial lake outburst floods is based mainly on three important data sources: (1) published reports, scientific papers and monographs; (2) unpublished research reports from archives and libraries; and (3) communication with a variety of national agencies, services, authorities and scientific departments worldwide. The GLOFs database is focused only on the events which occurred since the end of

Little Ice Age (large paleo-floods are excluded) and includes three groups of characteristics for each event—information about the lake (lake type, coordinates, location), information about the flood (probable trigger, flood volume, debris-flow occurrence), and information about socio-economic impacts (fatalities or missing people, affected sectors). The database also includes “additional info” for unclassifiable data.

Project Background

Previous Studies

Catastrophic glacial lake outburst floods have been reported in glacierized mountainous areas all over the world. Probably the most complex overview of GLOFs was gathered in the Magister thesis of S. Würmli from the University of Zürich, which summarized about 500 GLOFs worldwide (the majority of them from ice-dammed lakes; Würmli 2012). However, these data have yet to be published. Another overview of more than 130 GLOFs from moraine-dammed lakes, together with their basic characteristics, was provided in the Bachelor’s thesis of Emmer (2011) from Charles University in Prague. Also O’Connor et al. (2001) published a comprehensive list of GLOFs from moraine-dammed lakes. This report summarised and gave information on more than 80 events worldwide, with additional information in some cases, such as change in lake level, discharged volume and maximum (peak) discharge. Another regional overview of GLOFs, e.g., from Central Asia, was presented by Yamada (1998), and later by Ives et al. (2010), from Cordillera Blanca in Peru by Lliboutry et al. (1977) and later by Zapata (2002), and from British Columbia in Canada by Clague and Evans (2000). Regional databases, such as the Swiss database of alpine glacier hazards (<http://www.glacierhazards.ch>), European Glaciorisk Project (<http://glaciorisk.grenoble.cemagref.fr>), or the inventory system of the effects of disasters (<http://desinventar.com>), also play an important role.

Our field experiences and data analysis with GLOFs are based especially on research in the most heavily glacierized tropical range in the world—the Cordillera Blanca in Peru. Our initial studies were focused on various types of natural hazards, especially on slope movements (e.g., Vilímek et al. 2000; Klimeš et al. 2009) and neotectonics (e.g., Vilímek and Zapata 1998). Our later and present work deals also with GLOFs (Vilímek et al. 2005; Emmer and Vilímek 2013).

Reasons and Objectives

We had several reasons for initiating the GLOFs database project. Firstly, even if GLOFs are studied in various regions

Table 1 Research institutions and their representatives cooperating on the GLOFs database project (in addition to Charles University in Prague; Czech Republic) by September 2013

Scientific department	Location	Representatives
University of Zürich, Department of Geography	Zürich, Switzerland	Ch. Huggel; Y. Schaub; S. Würmli
BOKU University of Natural Resources and Life Sciences	Vienna, Austria	M. Mergili
Institute of Rock Structure and Mechanics	Prague, Czech Republic	J. Klimeš
Autoridad Nacional del Agua	Huaráz, Peru	A. Cochachin; M.L. Zapata
Instituto Boliviano de la Montaña	La Paz, Bolivia	D. Hoffmann
University of Oregon	Eugene, USA	M. Carey
University of Texas	Austin, USA	R. Chisolm; M. Somos

worldwide, so far no overall broadly available summary of these events has been made (with the exception of the Magister thesis of Würmli (2012)). Comprehensive analysis of such an available database will bring new and also more reliable information useful for hazard assessment, vulnerability mitigation and risk analysis. Secondly, database preparation encourages international cooperation between various scientific departments, possibly producing highly valuable scientific results (see the section on International cooperation). Lastly, there is a virtual space for sharing GLOF “news”, not only with the scientific community but also with a broader group of the interested public.

Current State

Project Foundation

The project entitled “Glacial lake outburst floods (GLOFs) database” was approved at the Board of Representatives of ICL (International Consortium on Landslides) in Paris 2012 and officially started in 2013. The project is carried out under the International Programme on Landslides (IPL) as IPL Project No. 179 (for detailed info please visit IPL webpage about the ongoing projects: <http://iplhq.org/category/iplhq/ipl-ongoing-project/>). This project is officially led by Adam Emmer (Project leader) and Vít Vilímek (Core member of the project) from Charles University in Prague (Czech Republic) and is designed for the period 2013–2015, where each year of the project has its own defined objectives (Vilímek et al. 2013). After 2015 we suppose its long-term continuation as a part of multilateral departmental cooperation.

International Cooperation

The creation of the GLOFs database project enabled the establishment of international cooperation between scientific departments worldwide. It can also be considered as an unofficial platform for information and data exchange which will stress the importance of this scientific topic

with regard to ongoing climate change. Since the official introduction of the database project at *Foro Internacional Glaciares: Retos de la investigación servicio de la sociedad en el marco del cambio climático*, which took place in Huaráz (Peru) between 1st and 3rd July 2013, seven scientific departments from three continents (South America, North America and Europe) have agreed to take part in the project (Table 1). At present, the GLOFs database project is still in the initial stages and is open for new partnerships, especially from regions yet to be represented such as Central Asia, Scandinavia or the New Zealand Southern Alps. Bilateral or multilateral teams could be created and sharing experiences from field work in various regions would increase the efficiency of the ongoing research.

Database Webpage

The GLOFs database website <http://www.glofs-database.org> was established in 2013 as one of the main outputs of the first year of the project. The main content is concentrated in the “database” section. This section outlines all of the GLOFs, which may be classified according to the location, (various mountain ranges worldwide), lake type (moraine-dammed, ice-dammed or bedrock-dammed) or probable trigger (ice-fall/snow avalanche, rockfall/landslide, earthquake, intense rainfall, flood wave from a lake situated upstream, buried ice melting, blocking of underground outflow channel(s), dam self-destruction, unknown trigger). Filtered results may be sorted alphabetically or chronologically, by probable trigger, lake type or location.

Future Perspectives

Filling of the Database

The main objective for the next year of the project is to enter the collected data into the database website. This activity is very time consuming (officially it was planned to take place during the second year of the project, 2014). All of the

summarised data need to be systematically checked, collected from various data sources and, if possible, compared. The next step then is to fill in the standard form, including the above-mentioned three groups of characteristics (characteristics related to the lake, characteristics related to the flood, characteristics related to the socioeconomic impacts and additional information). The last step is to upload the data to the database website and ensure the proper citation of all data sources used.

Data Analysis

The GLOFs database is expected to provide data and information utilizable for various purposes, starting with the analysis of GLOF causes in different regions and ending with flood modelling, hazard assessment or risk management. All of the presented data are widely available for public use. With respect to the structure of the data gathered in the GLOFs database, we expect several possibilities for future application.

Regional differences of GLOF characteristics have already been mentioned in our recent publications (e.g., Emmer and Cochachin 2013; Vilímek et al. 2013). In this work, we analysed the representation of various causes and temporal aspect of GLOFs from moraine-dammed lakes in three regions—Cordillera Blanca of Peru, the North American Cordillera and Central Asia. Our investigation showed that the most frequent cause (from the cases with known probable cause) in all of the studied regions was ice/snow avalanches into the lake producing a displacement wave, nevertheless representation of other causes is regionally specific. In Central Asia the cause of ice/snow avalanche is followed by dam self-destruction (dam failure without any evident dynamic trigger). In the North American Cordillera the cause that is significantly represented is heavy rainfalls and in Cordillera Blanca rockfalls or landslides into the lake and earthquakes. Temporal analysis showed that most of the GLOFs in the North American Cordillera and Central Asia occurred almost exclusively in the summer, while in the Cordillera Blanca GLOFs occurred year-round, with the wet season dominating. These conclusions were subsequently used in the analysis of the suitability of various GLOF hazard assessment methods for use on the regional scale of the Cordillera Blanca mountain range (Emmer and Vilímek 2013).

Conclusions

The GLOFs database was created in early 2013 under the International Programme on Landslides (IPL Project No. 179) and its first official international presentation took place during the international conference in Peru (beginning of July 2013) focused on the influence of climate

change on all aspects of mountain glaciation of the Andes (*Foro Internacional Glaciare: Retos de la investigación servicio de la sociedad en el marco del cambio climático*). The inclusion of the research on GLOFs into the International Programme on Landslides reflects the fact that glacial lake outburst floods are often closely connected with various types of slope movements; either from the point of view of the trigger (e.g., icefalls, rockfalls, landslides) or due the fact that the flood usually converts quickly into debris flows. Currently, seven scientific institutions from three continents (South America, North America and Europe) have agreed to take part in the project. The data will be gathered both from published and unpublished reports and will be available for public use. All of the original sources are cited. Such a worldwide database enables the scientific community to solve specific tasks resulting from the complexity of GLOFs, and regional specifics can also be established. It is generally agreed that the sensitivity of high mountain environments reflects climate change, and glacial retreat in glaciated areas worldwide brings several scientific tasks connected with the destabilization of slopes, permafrost degradation and enhanced natural hazards. The newly established platform on GLOFs may help to strengthen international cooperation and data utilization.

Acknowledgments The authors would like to thank the Grant Agency of Czech Republic (P 209/11/1000) and Grant Agency of Charles University (Project GAUK No. 70 413) for their financial support.

References

- Clague JJ, Evans SG (2000) A review of catastrophic drainage of moraine-dammed lakes in British Columbia. *Quat Sci Rev* 19:1763–1783
- Costa JE, Schuster RL (1988) The formation and failure of natural dams. *Geol Soc Am Bull* 100:1054–1068
- DesInventar (2013) Disasters Inventory System, version 2011.056 Online. <http://online.desinventar.org>. Last Accessed 12 Sep 2013
- Emmer A (2011) Analysis of causes and mechanisms of GLOFs from moraine-dammed lakes (in Czech). Bachelor thesis, Charles University in Prague, Prague, Czech Republic
- Emmer A, Cochachin A (2013) Causes and mechanisms of moraine-dammed lake failures in the Cordillera Blanca, North American Cordillera and Himalaya. *AUC Geographica* 48(2):5–15
- Emmer A, Vilímek V (2013) Review article: lake and breach hazard assessment for moraine-dammed lakes: an example from Cordillera Blanca (Peru). *Nat Hazards Earth Syst Sci* 13(6):1551–1565
- Glacierhazards.ch (2013) Glacier hazards. <http://www.glacierhazards.ch/>. Last Accessed 11 Sep 2013
- Glaciorisk (2013) European Glaciorisk Project. <http://www.nimbus.it/glaciorisk/GlacierList.asp?vista=rischio&IdTipoRischio=8>. Last Accessed 11 Sep 2013
- Ives JD, Shrestha BR, Mool PK (2010) Formation of glacial lakes in the Hindu Kush-Himalayas and GLOF risk assessment. International Centre for Integrated Mountain Development (ICIMOD), Kathmandu, 56 p. ISBN: 978 92 9115 137 0

- Klimeš J, Vilímek V, Omelka M (2009) Implications of geomorphological research for recent and prehistoric avalanches and related hazards at Huascarán, Peru. *Nat Hazards* 50(1):193–209
- Lliboutry L, Morales BA, Pautre A, Schneider B (1977) Glaciological problems set by the control of dangerous lakes in Cordillera Blanca, Peru. I. Historical failures of moranic dams, their causes and prevention. *J Glaciol* 18(79):239–254
- O'Connor JE, Hardison JH, Costa JE (2001) Debris flows from failures of Neoglacial-age moraine dams in the Three Sisters and Mount Jefferson Wilderness areas, Oregon. US Geological Survey, Reston (Virginia), 93p. ISBN: 0-607-96719-6
- Reynolds JM (2003) Development of glacial hazard and risk minimization protocols in rural environments. Methods of glacial hazard assessment and management in the Cordillera Blanca, Peru. Reynolds Geo-Sciences Ltd., Flintshire (UK), 72 p
- Vilímek V, Zapata ML (1998) Geomorphological response of neotectonic activity along the Cordillera Blanca fault zone, Peru. In: Kalvoda J, Rosenfeld CL (eds) *Geomorphological hazards in high mountain areas*. Kluwer Academic Publishers, London, 314 p. ISBN: 0-7923-4961-X
- Vilímek V, Zapata ML, Stemberk J (2000) Slope movements in Callejón de Huaylas, Peru. *Acta Univ Carol Geogr Suppl* 35:39–51
- Vilímek V, Zapata ML, Klimeš J, Patzelt Z, Santillán N (2005) Influence of glacial retreat on natural hazards of the Palcacocha Lake area, Peru. *Landslides* 2:107–115
- Vilímek V, Emmer A, Huggel C, Schaub Y, Würmli S (2013) Database of glacial lake outburst floods (GLOFs) – IPL Project No. 179. *Landslides*. doi: [10.1007/s10346-013-0448-7](https://doi.org/10.1007/s10346-013-0448-7)
- Würmli S (2012) Ausbruchsmechanismen von hochalpinen Seen – ein weltweites Inventar. Magister thesis, University of Zürich, Zürich, Switzerland
- Yamada T (1998) Glacier lake and its outburst flood in the Nepal Himalaya. Japanese Society of Snow and Ice, Tokyo, 96p. ISSN: 1344-1205
- Zapata ML (2002) La dinámica glaciaria en lagunas de la Cordillera Blanca. *Acta Montana A Geodynam* 19(123): 37–60



Towards Landslide Instrumentation and Monitoring in Teziutlán, Puebla, Mexico

Ricardo Garnica-Peña, Leobardo Domínguez-Morales,
and Irasema Alcántara-Ayala

Abstract

Early warning systems have become very important for disaster risk reduction, and in different parts of the world landslide monitoring has contributed to disaster prevention in the last few years. In Mexico, there are two major institutions in charge of landslide monitoring: the National Centre for Disaster Prevention (CENAPRED) and the National Autonomous University of Mexico (UNAM). Based on the expertise of both institutions, slope instrumentation and monitoring has been set up in the municipality of Teziutlán, Puebla, Mexico. The municipality of Teziutlán has been severely affected by landslides for more than five decades. Special attention has been given to this type of hazard after an event in 1999. Extreme precipitation triggered hundreds of landslides in the region and more than a hundred people died in a single event. Lithologic units of the area comprise non-consolidated volcanic deposits, which are highly susceptible to landslides during the rainy season. The final aim of this research is the implementation of a community-based early warning system, in which the participation of the local population will be essential. In this paper, we introduce the design, instrumentation and monitoring system developed for an unstable slope situated in one of the most affected areas of Teziutlán.

Keywords

Community-based early warning system • Landslide • Monitoring • Instrumentation

Introduction

Disasters associated with landslides have caused severe damage in Mexico. They have taken place particularly in states such as Puebla, Chiapas, Guerrero and Oaxaca, which

are also characterized by a high degree of marginalization of the population living in mountainous areas. These events have been specially analyzed for the Sierra Norte de Puebla for various disciplines, both physical and human (Alcántara 2004; Lugo et al. 2005; Alcántara et al. 2006; Capra et al. 2007).

The present study is focused on the early stages of a project involving instrumentation, monitoring and early warning. The research was conducted in the city of Teziutlán, state of Puebla, which was affected in 1999 by a series of landslides causing more than a hundred casualties. This project has involved several steps, including site selection, instrumentation, and real-time monitoring controlled by the Institute of Geography of the National Autonomous University of Mexico (UNAM). This article is a brief description of the development of each stage and the preliminary results of hillslope monitoring.

R. Garnica-Peña (✉) • I. Alcántara-Ayala
Universidad Nacional Autónoma de México, Instituto de Geografía,
Circuito Exterior s/n, Mexico, Mexico
e-mail: garnica@igg.unam.mx; irasema@igg.unam.mx

L. Domínguez-Morales
Centro Nacional de Prevención de Desastres, Delfín Madrigal, No. 665.
Col. Pedregal de Santo Domingo, Delegación Coyoacán CP 04360,
Mexico
e-mail: ldm@cenapred.unam.mx

Study Area

Teziutlán City is situated in the northern sector of the state of Puebla called Sierra Norte de Puebla (Fig. 1), a mountain range composed of Cretaceous rocks and deposits derived from the volcanic activity of the Caldera de los Humeros. A significant part of the city of Teziutlán was built over a large amount of pyroclastic material. These materials are very susceptible to landsliding triggered by rainfall. As such, during the rainy season, particularly in the months of September and October, mass movement processes commonly take place, as witnessed in 1999, 2005 and 2013.

This city has had very substantial urban growth from the 1950s, a product of the mining industry that attracted the nearby population. This has involved the occupation of unstable slopes by the population. In October 1999 a landslide swept away several homes in the La Aurora neighborhood, which is situated in the SE of the city. Not surprisingly, many of the new settlements developed on volcanic pyroclastic deposits are susceptible to instability (Fig. 2).

The site chosen for this research study is in the north of the city, the San Andrés borough, composed of approximately 40 homes. This settlement was established on a hillside on which a slide took place in 2003, 2 years before the construction of the housing development (Fig. 3).

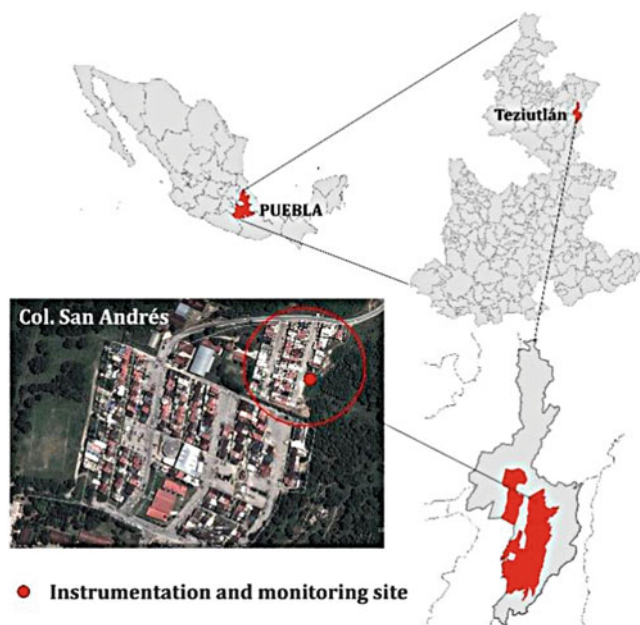


Fig. 1 Location of the landslide monitoring site, San Andrés borough, Teziutlán, Puebla



Fig. 2 Settlements on steep slopes and unstable susceptible volcanic soils



Fig. 3 Slope monitoring site, San Andrés borough

Site Location, Instrumentation and Monitoring

Site Definition

To select the monitoring site it was necessary to assess the hillslopes around the town, aided by the civil protection authorities who knew those places that have had problems due to the instability of the slopes. Afterwards, it was decided to carry out the project implementation and monitoring in the San Andrés borough because of the benefits provided by telecommunications, as well as their location and unstable slopes.

Once the site was selected, several tests and a detailed topographic survey of the study area were carried out (Fig. 4). One set of tests was to determine the resistance of the hillslope-forming materials, and therefore it was also possible to establish the depth of a possible sliding surface. These tests showed that the failure surface is located close to a 6 m depth (Fig. 5).



Fig. 4 Topographic survey on the San Andrés's slope



Fig. 6 Piezometer installed on the slope. A 60 m wire connects the piezometers to the automated-registry system



Fig. 5 Using a penetrometer to determine the depth of the possible failure

Instrumentation

Implementation began with the calibration of different equipment to be installed: piezometers (Fig. 6), tensiometers, a weather station and an extensometer. This was carried out in the facilities of the National Center for Disaster Prevention, with the support of its research staff. Once the calibration was carried out, installation of equipment took place at the selected site. This process took place over a period of about 6 months (Fig. 7); the equipment was installed at different depths based on the data obtained from the dynamic penetrometer (Fig. 8).

The establishment of the monitoring booth was completed with the support of the municipal authorities. The next step was the installation of a weather station by personnel of the Centre for Atmospheric Sciences of UNAM (Fig. 9). It was also necessary to establish telecommunication networks in order to transfer the data from the field to the National Center for Disaster Prevention and to the University facilities. For this purpose it was possible to



Fig. 7 Installation of the equipment

get support from the Center for Public Safety of the State of Puebla, located in the city of Teziutlán. This network center virtually runs 365 days a year without connectivity problems. In this way information is received from both the

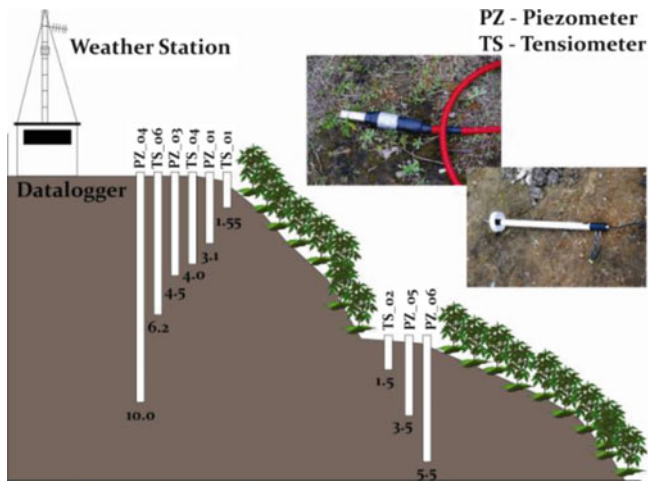


Fig. 8 Scheme of the monitoring equipment location

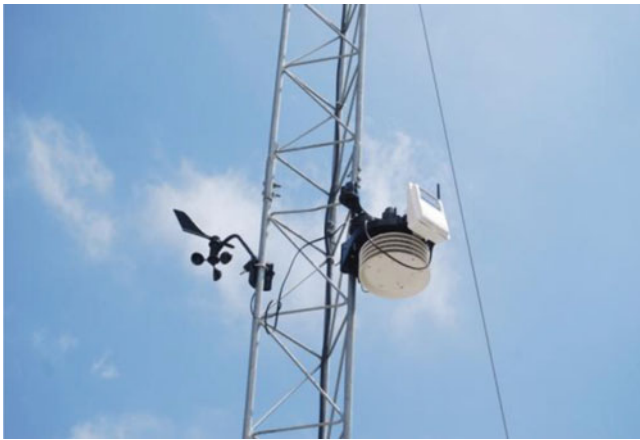


Fig. 9 Meteorological station located on the monitoring site. Rainfall is monitored at 5 min intervals

weather station as well as the instrumentation set up in the slope (Figs. 10 and 11).

Results and Conclusions

So far the station has been running for just over a year, so analysis of data results is thus still under way. Some of the problems faced so far have been linked to the registration of the information due to connectivity problems. The Public Safety Center of Teziutlán city, on which the instrumentation booth is dependent, sometimes has telecommunications network problems which interfere with the recording of data.

The final goal of the instrumentation and monitoring is to create an early warning system that would have the support and participation of the population. The system needs to be integrated into the local strategies for disaster risk reduction based on the engagement of people as main actors of the process.



Fig. 10 Monitoring system inside of the booth

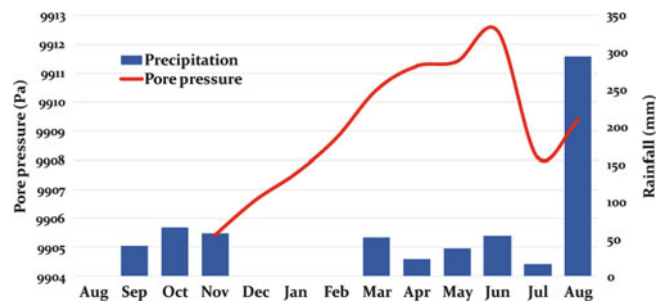


Fig. 11 Data registry from a tensiometer located at 4.5 m depth, August, 2011 to September, 2013

It is important therefore to continue supporting these kinds of projects in Mexico. Recent landslide disasters triggered by rainfall from hurricanes Ingrid and Manuel in September 2013 have proved the urgency of instrumentation and monitoring of unstable slopes, as well as the development of hazard and risk maps useful to both authorities and communities.

Acknowledgements Thanks are due to CONACYT for financial support for the Project 156242: MISTLI.

References

- Alcántara I (2004) Hazard assessment of rainfall-induced landsliding in Mexico. *Geomorphology* 61(1–2):19–40
- Alcántara I, Esteban O, Parrot J (2006) Landsliding related to land-cover change: A diachronic analysis of hillslope instability distribution in the Sierra Norte, Puebla, Mexico. *Catena* 65(2):152–165
- Capra L, Lugo-Hubp J, Zamorano Orozco JJ (2007) La importancia de la geología en el estudio de los procesos de remoción en masa: el caso de Totomoxtla, Sierra Norte de Puebla, México. *Boletín de la Sociedad Geológica Mexicana* 48(2):205–214
- Lugo HJ, Capra L, Zamorano JJ, Inbar M, Alcántara I (2005) Los procesos de remoción en masa en la Sierra Norte de Puebla, octubre de 1999, causas y efectos. *Revista Mexicana de Ciencias Geológicas* 22(2):212–228



Synoptic Pan-European Landslide Susceptibility Assessment: The ELSUS 1000 v1 Map

Andreas Günther, Javier Hervás, Miet Van Den Eeckhaut, Jean-Philippe Malet, and Paola Reichenbach

Abstract

In order to identify areas in Europe susceptible to landslides in the context of the EU Soil Thematic Strategy and the associated Proposal for a Soil Framework Directive, a harmonised approach encompassing geographically-nested susceptibility assessments (“Tiers”) and, where possible, the use of comparable datasets as input criteria for susceptibility modelling was devised. The first version of the 1 km grid size European Landslide Susceptibility Map (ELSUS 1000 v1), covering the EU and neighbouring countries, is derived from “Tier 1” assessment. The mapping approach employed includes first a climate-physiographic regionalisation of the study area. For each region, a spatial multi-criteria evaluation model is established to evaluate landslide susceptibility using commonly available pan-European datasets on slope angle, lithology and land cover, which are considered as the main conditioning factors for all types of landslides at this scale. Factor weights are assigned through pairwise comparisons using analytical hierarchy processes for each region, while region-specific factor class weights are initially established by computing landslide frequency ratios using more than 102,000 landslide locations across Europe. For each model region, a pixel-based susceptibility index is calculated by linear summation of conditioning factor weights and factor class weights. Each index map is then evaluated and classified into five susceptibility levels using true positive ratio breaks derived from receiver operating characteristics curves obtained with the landslide inventory. Finally, the region-specific classified susceptibility maps are spatially combined into the synoptic

A. Günther (✉)
Federal Institute for Geosciences and Natural Resources (BGR),
Stilleweg 2, 30655 Hannover, Germany
e-mail: Andreas.Guenther@bgr.de

J. Hervás
Institute for Environment and Sustainability, Joint Research Centre
(JRC), European Commission, 21027 Ispra, Italy
e-mail: javier.hervas@jrc.ec.europa.eu

M. Van Den Eeckhaut
ARCADIS, 1000 Brussels, Belgium
e-mail: miet.vandeneeckhaut@gmail.com

J.-P. Malet
Institut de Physique du Globe de Strasbourg, CNRS, University of
Strasbourg, 67084 Strasbourg, France
e-mail: jeanphilippe.malet@unistra.fr

P. Reichenbach
Research Institute for Hydrogeological Protection (CNR-IRPI),
National Research Council, 06128 Perugia, Italy
e-mail: Paola.Reichenbach@irpi.cnr.it

ELSUS 1000 v1 map. The map is available from the European Soil Data Centre (ESDAC), hosted by the Joint Research Centre, together with ancillary datasets, including a reliability evaluation of the susceptibility map. Further work is in progress to improve the accuracy of the map, mainly by integrating into the assessment a new pan-European lithological dataset and further landslide locations for areas not represented in the current inventory.

Keywords

Landslides • Soil thematic strategy • Landslide susceptibility assessment • ELSUS 1000 • Europe

Introduction

Small-scale, harmonised assessment of landslide susceptibility over the territory covered by EU member states and adjacent countries is needed to identify areas at risk of landslides, as required by the UE Thematic Strategy for Soil Protection (EC 2006a) and the associated proposal for a Soil Framework Directive (EC 2006b).

Following recommendations by the European Soil Bureau Network for common criteria to evaluate soil threats, including landslides, and geographically-nested (“Tier”-based) approaches (Eckelmann et al. 2006), the European Landslide Expert Group promoted by the Joint Research Centre (JRC Ispra) proposed specifications for landslide susceptibility zoning, including pan-European thematic datasets and common approaches for the various “Tiers” (Hervás et al. 2007). Specific datasets for landslide conditioning factors and approaches for susceptibility assessment for “Tier 1” (continental- or nation-wide, heuristic) and “Tier 2” (nation-wide, statistical) were further presented by Günther et al. (2008, 2013a) and Hervás et al. (2010).

In this work, we outline the “Tier 1” spatial multi-criteria evaluation approach used to produce the first version of the European Landslide Susceptibility Map (ELSUS 1000 v1). Unlike other approaches for landslide susceptibility mapping at a European scale (e.g. Van Den Eeckhaut et al. 2012; Jaedicke et al. 2013) or global scale (e.g. Nadim et al. 2006; Hong et al. 2007), our method includes a prior subdivision of the study area into climate-physiographic modelling regions and accounts for a large number of landslide locations for susceptibility modelling and evaluation of the resulting map.

Materials and Methods

Regionalisation of the Study Area

The European Landslide Susceptibility Map ELSUS 1000 v1 is prepared by first differentiating the study area (27 EU member states and neighbouring countries) into seven

climate-physiographic model zones (0 to 6) by combining climate regions according to the Köppen-Geiger classification (Peel et al. 2007) and physiographic regions (mountain/plain) based on Nordregio (2004), and adding a 1 km-wide zone inland from coastlines to account for specific conditions for coastal landslides (Günther et al. 2014, Fig. 1).

Susceptibility Criteria

Three main geo-environmental criteria (landslide conditioning factors) derived from common pan-European datasets were selected for susceptibility evaluation, as specified for a “Tier 1” assessment (Hervás et al. 2007, 2010; Günther et al. 2008, 2013a, b, 2014; Malet et al. 2013, 2014). They include terrain gradient (slope angle) from the EU27 DEM (Reuter 2009), shallow subsurface lithology from the Soil Geographical Database of Europe 1:1 M (Panagos et al. 2012), and land cover from the ESA’s GlobCover (<http://ionia1.esrin.esa.int>). These criteria are chosen because they reflect basic terrain conditions related to susceptibility to all kinds of landslides. The three criteria are classified and further aggregated (Table 1) using information on the distribution of more than 102,000 landslides provided by national or regional mapping agencies or collected by the Joint Research Centre (JRC) and Federal Institute of Geosciences and Natural Resources (BGR).

Spatial Multi-criteria Evaluation

The susceptibility analysis is carried out individually for each model zone using a 1 km × 1 km pixel as the terrain unit at a scale of 1:1 Million.

Since the collected landslide inventory must be considered incomplete and heterogeneous throughout the model zones, quantitative data-driven (statistical) susceptibility modelling techniques are difficult to apply. A semi-quantitative, index-based heuristic assessment scheme is thus employed, consisting of a spatial multi-criteria evaluation technique. In this evaluation technique, first the weights

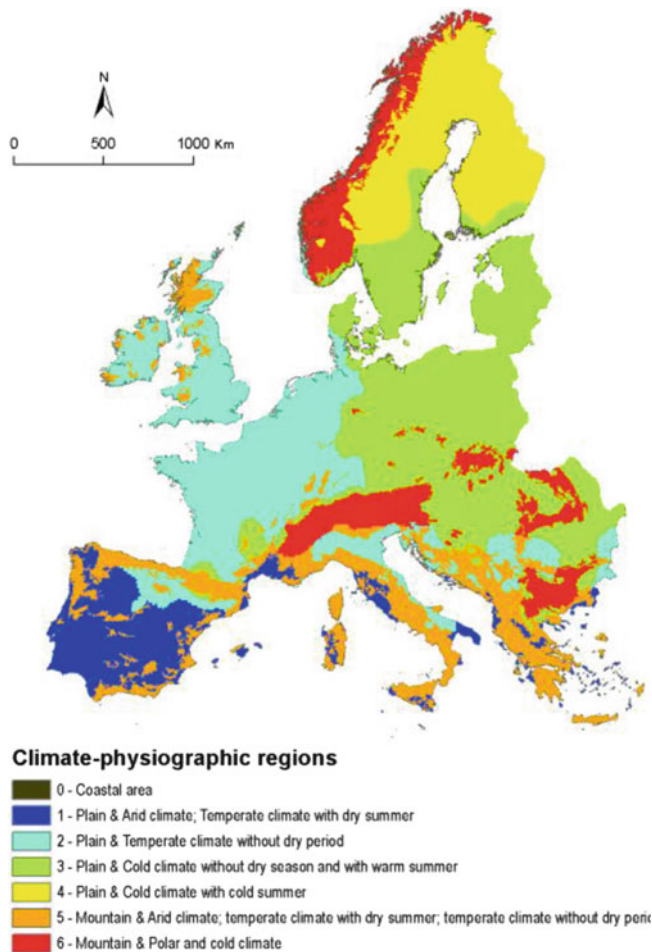


Fig. 1 Climate-physiographic regions used for separate landslide susceptibility modelling (from Günther et al. 2014)

of the hierarchically ordered criteria, or parameters (in the succession slope angle, lithology, and land cover) are assigned through pairwise comparisons using analytical hierarchical processes (Saaty 1980). For the three different physiographic settings (i.e. “coastal areas” 0, “plains” 1-4, and “mountains” 5-6), different pairwise comparisons are established, resulting in different criteria weights (Table 1). For the “coastal areas”, the land cover criterion is discarded, since no evidence was found that it exerts a significant control on landslide susceptibility at the given analysis scale and terrain unit size. It should also be noted in this context that ELSUS 1000 v1 has great limitations for correct assignment of coastal landslide susceptibility because the criteria datasets used have mismatching coastlines.

The second step in the applied spatial multi-criteria evaluation is the assignment of parameter class weights, which are allocated directly. For this, landslide frequency ratios (*FR*) of the criteria classes are computed for each model region using:

$$FR = \frac{LS_{ji}/LS}{A_{ji}/A} \quad (1)$$

where LS_{ji} is the number of pixels affected by landslides in class i of criterion (parameter) j , LS is the total number of pixels affected by landslides, A_{ji} is the number of pixels of class i of criterion j , and A is the total number of pixels of a model zone. The normalized frequency ratio values serve as the initial starting points for the assignment of parameter class weights. They are further modified by expert knowledge to obtain the final parameter class weights listed in Table 1, considering regional and class-specific bias in the landslide inventory, and the regional quality of the criteria data (especially related to lithology).

The pixel-specific landslide susceptibility index (*LSI*) is then determined by a weighted linear summation of the criteria- and criteria-class weights (Voogd 1983) with

$$LSI = \sum_{j=1}^{n=3} w_j \times x_{ji} \quad (2)$$

where w_j is the weight of criterion j and x_{ji} is the weight of class i in criterion j .

Landslide Susceptibility Classification and Evaluation

The zone-specific continuous pixel landslide susceptibility index values are classified into susceptibility levels using true positive ratio breaks deduced from analysis of receiver operating characteristics (ROC) curves obtained with the landslide inventory (Günther et al. 2014). For this instance, four susceptibility levels (“high”, “moderate”, “low”, and “very low”) are used for the “plain” model zones (1-4) to respect the overall lower landslide intensity when compared to “mountains” and “coasts” (5-6, 0), where five levels (“very high”, “high”, “moderate”, “low”, and “very low”) are used. The four susceptibility classes in the “plain” model zones (from “high” to “very low”) are defined by occupancy of 50 %, 25 %, 15 %, and 10 % of the landslide-affected pixels in each zone; the five levels in “mountains” and “coasts” (from “very high” to “very low”) render 50 %, 25 %, 15 %, 7 %, and 3 % of the landslide-affected pixels, respectively.

The compound classified ELSUS 1000 v1 map (Fig. 2) is derived by spatial merging of the zone-specific classified susceptibility maps. The five susceptibility levels of the map (“very high”, “high”, “moderate”, “low”, and “very low”) occupy 6 %, 12 %, 13 %, 17 %, and 53 % of the analysed area and contain 20 %, 30 %, 22 %, 15 %, and 13 % of the landslide-affected terrain elements, respectively.

Table 1 Criteria class weights and analytical hierarchical processes-derived criteria weights (in brackets) used for susceptibility analysis for the seven climate-physiographic zones (Z0–Z6)

Slope angle (°)	Z0 (0.75)	Z1 (0.64)	Z2 (0.64)	Z3 (0.64)	Z4 (0.64)	Z5 (0.58)	Z6 (0.58)
0	0.030	0.049	0.021	0.006	0.012	0.081	0.089
1–3	0.049	0.050	0.057	0.028	0.023	0.095	0.101
4–6	0.085	0.095	0.117	0.078	0.055	0.108	0.101
7–10	0.110	0.140	0.154	0.119	0.075	0.122	0.102
11–15	0.121	0.151	0.163	0.160	0.195	0.128	0.116
16–20	0.153	0.189	0.174	0.188	0.202	0.135	0.140
21–30	0.217	0.169	0.158	0.217	0.236	0.155	0.161
31–90	0.237	0.156	0.154	0.204	0.202	0.176	0.189
Lithology	Z0 (0.25)	Z1 (0.26)	Z2 (0.26)	Z3 (0.26)	Z4 (0.26)	Z5 (0.28)	Z6 (0.28)
Alluvium/Colluvium	0.140	0.115	0.066	0.044	0.342	0.066	0.100
Glaciofluvial materials	0.106	0.104	0.127	0.031	0.158	0.118	0.055
Calcareous rocks	0.058	0.093	0.057	0.100		0.085	0.115
Marls	0.009	0.022	0.137	0.127		0.047	0.160
Clayey materials	0.170	0.120	0.137	0.055	0.092	0.114	0.085
Sandy materials	0.085	0.091	0.046	0.012	0.197	0.095	0.165
Sandstone/Flysch/ Molasse	0.063	0.109	0.153	0.064	0.066	0.114	0.070
Loamy/Silty materials	0.182	0.104	0.040	0.075		0.026	0.015
Detrital formations	0.009	0.005	0.014	0.111		0.039	
Crystalline rocks	0.053	0.010	0.051	0.080		0.071	0.070
Schists	0.087	0.005	0.023	0.177		0.060	0.150
Volcanic rocks	0.037	0.219	0.082	0.118	0.000	0.118	0.010
Other/Organic	0.002	0.002	0.066	0.005	0.145	0.047	0.005
Land cover	Z0	Z1 (0.10)	Z2 (0.10)	Z3 (0.10)	Z4 (0.10)	Z5 (0.13)	Z6 (0.13)
Cropland	–	0.285	0.102	0.107	0.024	0.143	0.143
Open forest	–	0.085	0.153	0.156	0.134	0.119	0.304
Closed forest	–	0.103	0.129	0.162	0.147	0.107	0.232
Shrub	–	0.044	0.027	0.071	0.024	0.036	0.036
Pasture/Meadow	–	0.044	0.259	0.164	0.152	0.238	0.107
Bare	–	0.156	0.071	0.176	0.367	0.119	0.071
Artificial	–	0.285	0.259	0.164	0.152	0.238	0.107

ELSUS 1000 v1 is evaluated on an administrative terrain unit level basis (Eurostat NUTS 3 regions). The resulting confidence level map (Fig. 3) provides reliability information on NUTS 3 units where sufficient landslide information is available to rank ELSUS 1000 v1 as having “good”, “moderate” or “poor” confidence. 38 % of the area covered by the map cannot be evaluated in this respect due to missing landslide information.

Accessibility to ELSUS 1000 v1

The map, accompanied by explanatory metadata, can be downloaded in raster (ESRI GRID) format from the European Soil Data Centre (ESDAC, Panagos et al. 2012) through the European Soil Portal (<http://eusoils.jrc.ec.europa.eu/library/themes/Landslides/#ELSUS>).

Additional downloadable datasets include the confidence level map of ELSUS 1000 v1, a NUTS 3-aggregated map of ELSUS, which was used by ESPON to outline NUTS 3 units with landslide hazard (ESPON 2013), and the climate-physiographic regions, classified slope angle, soil parent material (lithology proxy) and land cover datasets used for landslide susceptibility modelling.

Conclusions

The method used to identify landslide priority areas in Europe for EU soil protection policies can be considered more robust than previously developed approaches, mainly because it uses distributed landslide data and different susceptibility weights can be estimated using spatial multi-criteria evaluation for the same criteria classes depending on their climate-physiographic setting (Günther et al. 2014).

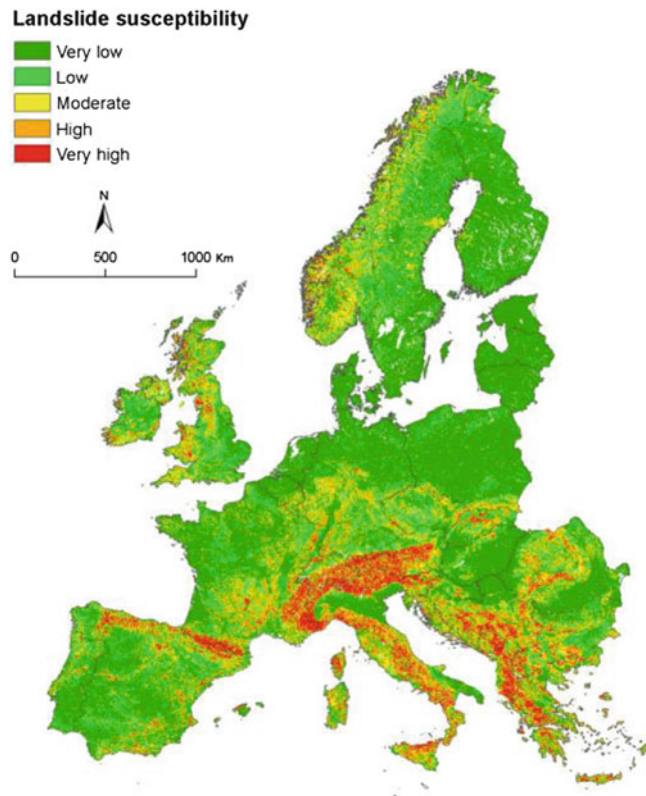


Fig. 2 Classified European landslide susceptibility map (ELSUS 1000 v1) (from Günther et al. 2014)

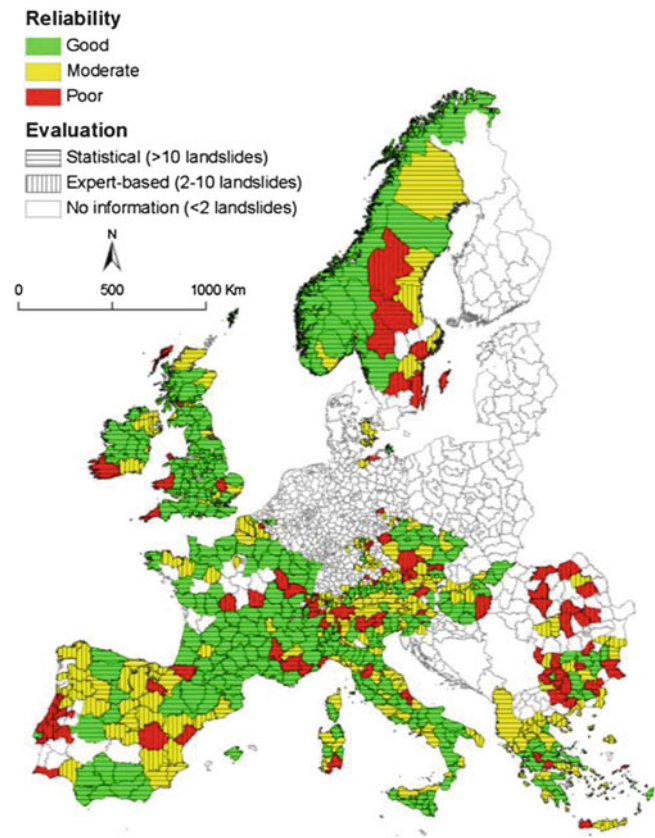


Fig. 3 NUTS 3 territorial units-referenced reliability map of ELSUS 1000 v1 (updated from Günther et al. 2014)

However, as shown by the confidence level map at NUTS 3 territorial unit level, the first version of ELSUS 1000 has some constraints on correctly assessing landslide susceptibility in regions where landslide data was not provided or are scarce, and also because the soil parent material dataset used in the model does not ideally represent the lithology susceptibility criterion.

Work is in progress to further evaluate, validate and eventually improve the accuracy of the map by using a new harmonised lithological dataset derived from the International Hydrogeological Map of Europe at 1:1,500,000 scale (IHME 1500, Gilbrich et al. 2001) in the assessment and by collecting additional landslide inventory data in some regions. In addition, it is envisaged that landslide susceptibility will be evaluated separately for major landslide types in countries where the necessary landslide information can be provided.

Acknowledgements This work has been carried out in the framework of the Joint Research Centre-coordinated European Landslide Expert Group's support to the EU Soil Thematic Strategy. It also forms part of the International Programme on Landslides project IPL-162 "Tier-based harmonised approach for landslide susceptibility mapping over Europe" and of the Council of Europe's EUR-OPA project "Pan-European and nation-wide landslide susceptibility assessment", coordinated by the European Centre on Geomorphological Hazards (CERG).

We are grateful for the support of the following institutions and persons providing basic information on landslides from their national or regional databases: Albanian Geological Survey (AGS, M. Jusufati) Geologische Bundesanstalt, Austria (GBA, N. Tilch), British Geological Survey (BGS, C. Dashwood), Environment, Nature and Energy Department, Flemish Government, Belgium (LNE, L. Vandekerckhove), Czech Geological Survey (CGS, D. Čápová), Bureau de Recherches Géologiques et Minières, France (BRGM, G. Grandjean), Sächsisches Landesamt für Umwelt, Landwirtschaft und Geologie, Germany (LfULG, P. Dommaschk), Bayerisches Landesamt für Umwelt (LFU, A. von Poschinger and T. Gallemann), Landesamt für Umwelt, Naturschutz und Geologie MV (LUNG, K. Schütze), Institute of Geology and Mineral Exploration, Greece (IGME, E. Poyiadji), Hungarian Office for Mining and Geology (BMFH, T. Oszvald), Geological Survey of Ireland (GSI, R.

Creighton), Instituto de Geografia e Ordenamento do Território, University of Lisbon, Portugal (IGOT, J.L. Zêzere), Geological Survey of Norway (NGU, T. Oppikofer and R. Hermanns), Swedish Geotechnical Institute (SGL, M. Öberg and C. Cederbom), and Federal Office for the Environment, Switzerland (FOEN/BAFU, H. Raetzo and B. Loup).

We also thank P. Panagos and M. Van Liedekerke (JRC Ispra, Italy) for publishing the maps on ESDAC.

References

- EC (2006a) Thematic Strategy for Soil Protection. Communication from the Commission to the Council, the European Parliament, the European Economic and Social Committee and the Committee of the Regions. COM(2006)231 final. Commission of the European Communities, Brussels, Belgium. 12p.
- EC (2006b) Proposal for a Directive of the European Parliament and of the Council establishing a framework for the protection of soil and amending Directive 2004/35/EC. COM(2006)232 final. Commission of the European Communities, Brussels, Belgium. 30p.
- Eckelmann W, Baritz R, Bialousz S, Bielek P, Carré F, Houšková B, Jones RJA, Kibblewhite MG, Kozak J, Le Bas C, Tóth G, Tóth T, Várallyay G, Yli Halla M, Zupan M (2006) Common criteria for risk area identification according to soil threats. European Soil Bureau Research Report No. 20, EUR 22185 EN. Office for Official Publications of the European Communities, Luxembourg, 94p.
- ESPON (2013) Territorial Dynamics in Europe – Natural Hazards and Climate Change in European Regions. Territorial Observation No. 7. ESPON, Luxembourg, 27p.
- Gilbrich WH, Krampe K, Winter P (2001) Internationale Hydrogeologische Karte von Europa 1:1.500.000. Bemerkungen zum Inhalt und Stand der Bearbeitung. Hydrologie und Wasserbewirtschaftung 45(3):122–125
- Günther A, Reichenbach P, Hervás J (2008) Approaches for delineating areas susceptible to landslides in the framework of the European Soil Thematic Strategy. In: Proceedings of the first World Landslide Forum, Tokyo, 18–21 November 2008. pp 235–238
- Günther A, Reichenbach P, Malet J-P, Van Den Eeckhaut M, Hervás J, Dashwood C, Guzzetti F (2013a) Tier-based approaches for landslide susceptibility assessment in Europe. *Landslides* 10 (5):529–546
- Günther A, Van Den Eeckhaut M, Reichenbach P, Hervás J, Malet J-P, Foster C, Guzzetti F (2013b) New developments in harmonized landslide susceptibility mapping over Europe in the framework of the European soil thematic strategy. In: Margottini C, Canuti P, Sassa K (eds) *Landslides science and practice*, vol 1. Springer, Heidelberg, pp 297–301
- Günther A, Van Den Eeckhaut M, Malet J-P, Reichenbach P, Hervás J (2014) Climate-physiographically differentiated pan-European landslide susceptibility assessment using spatial multi-criteria evaluation and transnational landslide information. *Geomorphology* (in press)
- Hervás J, Günther A, Reichenbach P, Chacón J, Pasuto A, Malet J-P, Trigila A, Hobbs P, Maquaire O, Tagliavini F, Poyiadji E, Guerrieri L, Montanarella L (2007) Recommendations on a common approach for mapping areas at risk of landslides in Europe. In: Hervás J (ed) *Guidelines for mapping areas at risk of landslides in Europe*. JRC Report EUR 23093 EN. Office for Official Publications of the European Communities, Luxembourg, pp 45–49
- Hervás J, Günther A, Reichenbach P, Malet J-P, Van Den Eeckhaut M (2010) Harmonised approaches for landslide susceptibility mapping in Europe. In: Malet J-P, Glade T, Casagli N (eds) *Proceedings of the international conference on mountain risks: bringing science to society*, Florence, Italy, 24–26 November 2010. CERGI Editions, Strasbourg, pp 501–505
- Hong Y, Adler R, Huffman G (2007) Use of satellite remote sensing data in the mapping of global landslide susceptibility. *Nat Hazards* 43:245–256
- Jaedicke C, Van Den Eeckhaut M, Nadim F, Hervás J, Kalsnes B, Vangelsten BV, Smith JT, Tofani V, Ciurean R, Winter MG, Sverdrup-Thygeson K, Syre E, Smebye H (2013) Identification of landslide hazard and risk ‘hotspots’ in Europe. *Bull Eng Geol Environ*. doi:10.1007/s10064-013-0541-0
- Malet J-P, Puissant A, Mathieu A, Van Den Eeckhaut M, Fressard M (2013) Integrating spatial multi-criteria evaluation and expert knowledge for country-scale landslide susceptibility analysis: application to France. In: Margottini C, Canuti P, Sassa K (eds) *Landslides science and practice*, vol 1. Springer, Heidelberg, pp 303–311
- Malet J-P, Puissant A, Mathieu A, Van Den Eeckhaut M, Fressard M (2014) Landslide susceptibility assessment at 1:1M scale for France. *Geomorphology*: 15p (under review)
- Nadim F, Kjekstad O, Peduzzi P, Herold C, Jaedicke C (2006) Global landslide and avalanche hotspots. *Landslides* 3(2):159–173
- Nordregio (2004) Mountain areas in Europe, analysis of mountain areas in EU member states, acceding and other European countries. Report 2004.1. Nordic Centre for Spatial Development, Stockholm, Sweden, 271p
- Panagos P, Van Liedekerke M, Jones A, Montanarella L (2012) European Soil Data Centre: response to European policy support and public data requirements. *Land Use Pol* 29(2):329–338
- Peel MC, Finlayson BL, McMahon TA (2007) Updated world map of the Köppen-Geiger climate classification. *Hydrol Earth Syst Sci* 11 (5):1633–1644
- Reuter H (2009) A Europe-wide digital elevation model based on SRTM and Russian topographic contours. Data set and documentation for the contract 2007-4500049350. BGR, Hannover, Germany
- Saaty TL (1980) *The analytic hierarchy process*. McGraw Hill, New York, 287p
- Van Den Eeckhaut M, Hervás J, Jaedicke C, Malet J-P, Montanarella L, Nadim F (2012) Statistical modelling of Europe-wide landslide susceptibility using limited landslide inventory data. *Landslides* 9 (3):357–369
- Voogd H (1983) *Multi-criteria evaluation for urban and regional planning*. Pion, London, 367p



Landslide Risk in South-East Nigeria: Important Facilities Under Serious Threat

Ogbonnaya Igwe

Abstract

Important facilities in the South-East part of Nigeria have increasingly been subjected to high levels of vulnerability to landslides and associated earth movements because of elevated mining and excavation activities related to construction and demographic reasons. The stability of electricity, communication and water projects located on hilly terrains has been undermined by the indiscriminate excavation trends of unscrupulous construction firms and poor citizens who are more interested in food than safety. The IPL-150 project investigated the extent of vulnerability and found that while the slopes are fairly stable in the short-term, sustained and unchecked excavation at the sites could be a major factor in an eventual collapse in this region where high annual rainfall and complex stratigraphy that contains some potentially liquefiable lithologic units are always the difference between stable facilities and fatalities. In this paper, a new concept of delayed liquefaction is proposed to explain the behavior of the soils: the trend of pore pressure development and the magnitude of excess pore-water pressure at the residual state are constant regardless of initial stress level. The contrast between the behavior of these slope-materials and readily-liquefiable sands are discussed. The paper also describes a procedure for estimating the critical stress that may trigger instability in the slopes, and based on the work done, a general failure mechanism is proposed.

Keywords

Excavation • Facilities • Fatalities • Landslides • Liquefaction

Introduction

For greater efficiency in distribution and management, contractors often site electrical (Fig. 1), communication and water facilities (Fig. 2) on hilly parts of the country. These hills initially appear to be stable as they are underlain most by lateritic units often used in road construction because of their good engineering properties. Ironically, it is the good engineering properties of the laterites that motivate the poor rural dwellers to sabotage the stability of the

slopes by excavating them for money. Sometimes however, excavation is carried out during construction by firms and entrepreneurs without proper stability evaluations. These situations have reduced the stability of the slopes and increased the risk and hazard posed to people who use or live near the hills.

In addition to hydraulic projects, housing settlements are often located on these local hills in the study area (Fig. 3). With lateral support now undermined, high intensity rainfall could induce slope movements that endanger the facilities. Corominas (2001) reported that high intensity and short duration rains trigger mainly debris flows and shallow slides developed in colluviums and weathered rocks; noting that while rainfall threshold of about 190 mm in 24 h initiates can initiate limited failures more than 300 mm in 24–48 h could

O. Igwe (✉)
Department of Geology, University of Nigeria, Nsukka, Enugu State,
Nigeria
e-mail: igwejames@hotmail.com



Fig. 1 Electrical facility on a hill near Nsukka, South-East Nigeria



Fig. 2 A hydraulic project in the University of Nigeria



Fig. 3 A residential zone on a vulnerable hillside in Nsukka

produce widespread shallow landslides. High initial soil moisture conditions induce fast increase in pore-water pressure that result in a decrease in the safety factor of the slope which increases the likelihood of slope failure (Mukhlisin and Taha 2012). Evaluating the effect of rainwater infiltration and hence the trend of pore pressure generation in slopes

is important in the analysis of rainfall-induced slope failures. The added weight of water and its lubricating effects are potential factors in the development of sliding surfaces. Infiltration capacity is influenced by intensity and duration of rainfall, soil texture, slope angle, nature of vegetative cover.

To minimize the potential effects of landslides, in-depth understanding of the processes that govern slope behavior and adoption of adequate landslide prevention strategy and measures for landslide hazard mitigation are a necessity. Better results could be achieved through careful analytical studies of the characteristics of landslide prone areas and the provision of useful information regarding possible future phenomena. Although the research also studied present and original geometry of slope, geological cross-section and position of water table only the shear strength parameters are emphasized in this paper. Shear strength parameters and the behavior of the materials when stressed are indispensable in slope stability analysis. Because failure would result in traffic disruption, loss of lives and property, a critical evaluation of the stability of slopes hosting these public utilities is necessary. The investigation involved field work, examination of aerial photograph, satellite images and laboratory analysis. The geology of the area and geotechnical properties of the slope soils were assessed to determine the possible failure mechanisms and major sliding processes.

Apparatus and Procedure

The fifth version of the ring shear devices (Fig. 4) at Disaster Prevention Research Institute, Kyoto University, Japan was used in the research. The apparatus is capable of sustaining complete undrained loading throughout the test; and was designed to eliminate some difficulties commonly encountered while studying the mechanism of landslide motion. Because of its ability to measure large displacement of specimen, the ring-shear apparatus is suitable for the investigation of the residual shear resistance mobilized along the sliding surface at large shear displacements in landslides (Sassa et al. 2003; Wang and Sassa 2002, 2003).

The ring-shear apparatus was developed with the aim of reproducing the formation of a shear zone and the resulting motion along the zone. To ensure an accurate determination of the total normal stress acting on a given soil specimen this particular ring shear apparatus was designed to measure the friction between the soil specimen and the sidewalls of the upper shear box. The inner and outer diameters of the shear box are 12 cm and 18 cm, respectively. The shear area is 141.37 cm². The maximum height of the specimen in the shear box is 11.5 cm while the ratio of the maximum height to the width is 3.83. The maximum normal stress that can be applied is 2,000 kPa while the maximum shearing velocity is



Fig. 4 The ring shear apparatus

10 cm/s. The authors think the shear box is deep enough to allow the development of a definite and easily recognizable shear zone within the soil specimen which has the advantage of limiting or eliminating the possibility of measuring the shear resistance between soil specimen and the loading platen or the bottom of the shear box. A computer-controlled servo-motor supplies the shear load. Because the servo-motors can be switched to either constant torque or constant velocity modes it is possible to run stress-controlled and strain-controlled tests.

Oven dried specimens were placed in the shear box and saturated with water. The specimens were placed in the oven for at least 24 h and were removed from the oven 1 h before the commencement of testing. Sassa (1998) introduced a parameter, the B_D parameter, for assessing the degree of saturation of samples in the ring shear apparatus. The B_D parameter is the ratio of change in pore pressure and change in normal stress ($\Delta u/\Delta\sigma$) over a specified period of time. Obtaining the B_D involved a two-phased consolidation process of first applying a normal stress of 49 kPa in drained condition on a sample and increasing the normal stress to 98 kPa in undrained condition when the value of vertical displacement becomes constant. The resultant increase in pore pressure (from zero to a certain monitored value), Δu , divided by the corresponding increase in normal stress (from 49 kPa to 98 kPa), $\Delta\sigma$, is the B_D . To achieve a high B_D value of nearly 1.0 (full or complete saturation) carbon dioxide was first introduced into the samples after which, de-aired water was introduced. All samples were normally consolidated and thereafter, shearing was performed by slow incremental loading of shear stress. Initial shear stress of zero was assumed in the series of tests. The ring shear apparatus was chosen for this study because when investigating landslides, the shearing behavior of slope materials (especially if the material is liquefiable) at large displacements becomes an important consideration for risk

reduction (Wang and Sassa 2003; Sassa et al. 2004; Igwe 2012, 2013; Igwe et al. 2007, 2012). The undrained, large-displacement strength known as the critical state shear strength is determined from laboratory shear devices and aids interpretation of in-situ measurements and field case histories. Although there are many devices used to measure the shearing behavior of sands, it is only the ring shear apparatus that can shear a soil to unlimited displacement; and does that without creating serious disparities in stress and strain distribution. One of the aims of the present research was to investigate the dominant factors initiating the transformation of slide to dangerous flow movements. The ring shear was therefore chosen for adequate evaluation of the soils' behavior at small and large displacements (of at least 10 m). The ring shear device at Kyoto University, Japan has additional capabilities that include (1) rotating principal stresses to simulate field conditions; (2) maintaining constant cross-sectional area as shearing progresses; (3) sustaining complete undrained or constant volume condition for the duration of test and (4) accurate application and measurement of stresses and pore-water pressure.

Results and Interpretation

Samples from the sites of interest were tested at various normal stresses, relative density and saturation conditions. The specimens tested in undrained conditions showed a unique strain-softening behavior distinguished by an initial steady rise in pore pressure as shear stress increased; a second stage of deformation where the specimens experienced a little 'delay' in pore pressure generation; and a final stage of relatively rapid and continuous build-up of excess pore pressure to significant values that correspond to liquefaction (Fig. 5). The stress paths of the specimens are illustrated in Fig. 6, and show that although the samples did not exhibit quick, rapid and sudden rise in pore pressure from the outset of the tests, they neither underwent significant dilation associated with stable materials, instead strain-softened while developing high excess pore-water pressure. To understand this unique behavior, it is necessary to introduce the concept of 'delayed' liquefaction, which is readily distinguished from the outright liquefaction phenomenon associated with clean sands. The specimens under consideration contain high percentage of fines and may be the main reason for the slow-liquefying behavior. This concept may explain why the hills still appear stable even with the advancing excavation.

It is important to note that the slope materials are liquefiable and that when the requisite conditions of stress and pore pressure are satisfied, liquefaction may be initiated. Unfortunately, this may happen at great cost to human and

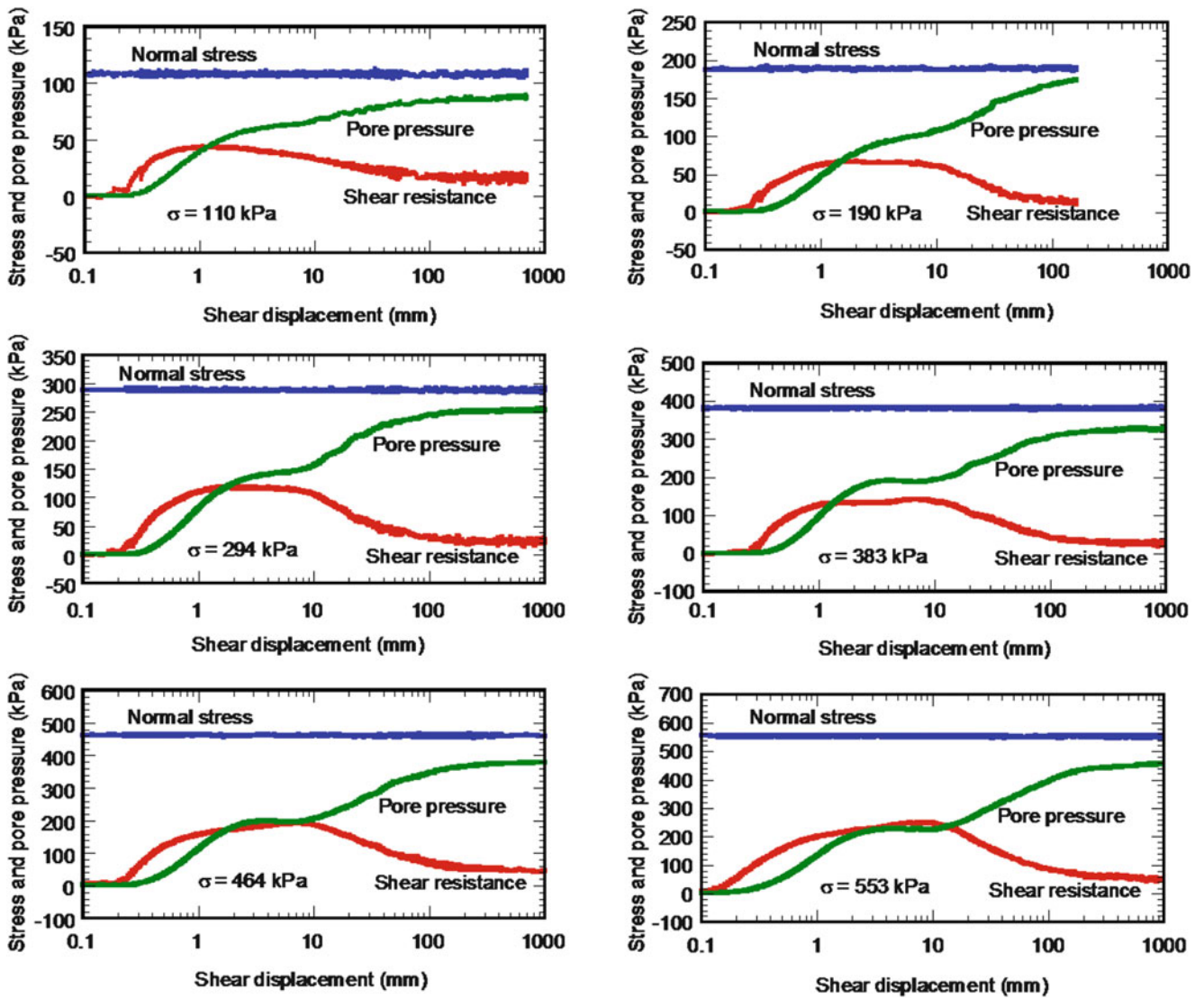


Fig. 5 Undrained shear behavior of the specimens at different normal stresses

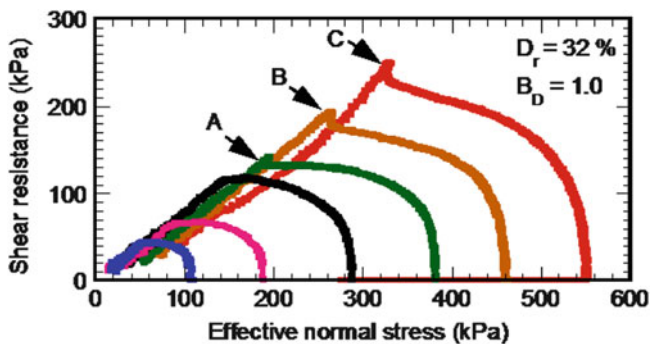


Fig. 6 The stress paths at varying normal stresses

public resources. Any leakage in the water project (Fig. 2) will abruptly elevate pore-water pressure which may trigger unprecedented catastrophe because of its location within the

University Campus where work, research, learning and residential buildings are also located. Making matters a bit scary is the observation that at all the effective normal stresses applied during the tests, the residual strength of the specimens reached low values (Fig. 6).

It can be seen in Fig. 6 that although slight peaks (points A, B, C) began to appear at higher normal stress level of 383 kPa, 464 kPa, and 553 kPa, there was no considerable change in the residual strength. The results also show that the trend of pore pressure is stress dependent, and that it seems there are some critical levels of normal stresses controlling pore pressure trend, and hence soil behavior at low, medium and high stresses (Fig. 5).

The soil deformation pattern at normal stresses of 110 and 190 kPa are similar. In the same vein, the pattern at 294 and 383 kPa are similar. This is also true at 464 and 553 kPa.

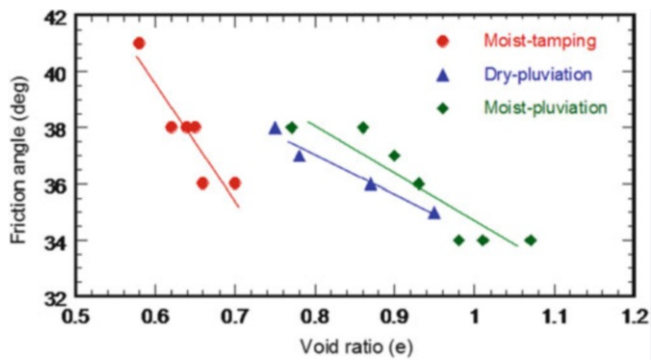


Fig. 7 Relationship among void ratio, friction angle and method of sample preparation

Understanding the critical stress levels beyond which the soil behaviour changes may be a key step to reliable evaluation of the stability of slopes and in designing preventive measures. When such values are incorporated into numerical or stability models, an effective risk assessment will be the result. The specimens were also tested under different sample preparation methods to understand their influence on the shear strength of the slope materials. It was found that the different methods produced large differences in void ratio but only slightly different strength values. Samples prepared with moist-tamping method had the lowest void ratio, while those prepared by moist-pluviation resulted in the highest; the dry-pluviation method led to intermediate value (Fig. 7). Despite these differences there is only a slight difference in the values of friction angle. Stronger interlocks at the contacts between particles inevitably produce stronger resistance to shearing stress. Since one of the most important mechanisms in the deformation of granular materials is the relative sliding between particles, it seems reasonable that stronger interlocking will resist such sliding better, and in effect, deform less than the weaker interlocking between the particles comprising poorly graded specimens. The specimens whose particles witness comparatively more deformation are more likely to yield higher values of excess pore pressure than the ones in which particle deformation is less. However, the results show that different sample preparation method do not give rise to considerable differences in interlocking forces at the particle contacts.

The International Strategy for Disaster Reduction (UNISDR 2009) regarded exposure, hazard and vulnerability as principal components of risk: Risk = vulnerability * hazard * exposure.

Questions on the people's perception of the risk posed by landslides produced instructive responses (Table 1). 12 % of respondents considered landslides high risk, 45 % said landslides posed medium risk, 18 % regarded them as low risk, while 25 % said they did not know how much risk landslides represented. Of those who considered landslides

Table 1 Risk-perception of people at the vulnerable area

Risk perception	Percentage	Social status	Annual salary (USD)
High risk	12	Private and public workers	>20,000
Medium risk	45	Same	Same
Low risk	18	Same	Same
Don't know	25	Same	Same

high risk, only 32 % said they were willing to relocate while 68 % said they would not. In the group of those who considered it medium and low risk only 23 % were willing to move to new places. Of the percentage willing to move in all the categories, 77 % said they were moving because they had to, while others would move because they had found new apartments at safer locations. In the group not willing to move, 46 % said they would live on the slopes to protect their ancestral heritage, 38 % said they would not move because they could not afford a new house, while others said they would not move under any circumstance. This research found that unavailability of housing at safer places, poverty and socio-cultural belief account for the high exposure to landslide hazard. Even in some places where the foundation of houses have been seriously damaged by erosion, the people still refused to move; preferring instead to 'live and die in their ancestors lands'.

Conclusions

A series of tests under varying conditions of void ratio, saturation and sample preparation method was used to study the behavior of slope materials upon which important electrical, communication and hydraulic projects are located.

A new concept of delayed liquefaction is proposed for proper evaluation of the materials' behavior. During interpretation of the data, threshold values of normal stress that appeared to influence the behavior of the materials were observed.

Based on the interpretation of the tests and the insight gained from the new concepts, the following conclusions can be drawn: (1) the slope materials are liquefiable, although not as readily liquefiable as clean or poorly graded sands (2) The materials exhibit relatively slow development of excess pore pressure but eventually generate high values that correspond to liquefaction (3) This delay in pore pressure generation is the major reason some of the slopes are still standing despite excavation activities (4) A leakage on the water facility will lead to abrupt rise in pore pressure and may hasten the destabilization of the slope. High excess pore pressure is a condition for liquefaction and flow failures which may be catastrophic because of the location of the facility (5) Critical or threshold normal stress levels appear to control the behavior of

the materials. The knowledge of these threshold values can add reliability and efficiency in slope stability assessment.

Finally, the research found that unavailability of housing at safer places, poverty and socio-cultural belief account for the high exposure to landslide risk. However, people's perception of the hazard and socio-cultural beliefs, which culminate in their unwillingness to relocate even if safer places were to become available, may be obstacles to future hazard reduction programs.

Acknowledgements The research was carried out under the International Program on Landslides Project 150. Professor Kyoji Sassa, the Executive Director of the International Consortium on Landslides, and Hiroshi Fukuoka of the Research Centre on Landslides, Kyoto University, Japan were supportive of the project. My post-graduate students are acknowledged for their vital roles in the project.

References

- Corominas J (2001) Landslides and climate. In: Bromhead E, Dixon N, Iben ML (eds) 8th International symposium on landslides, vol 4. Balkema, Cardiff, pp 1–33
- Global Assessment Report on Disaster Risk Reduction (2009) UNISDR, 207 pp
- Igwe O (2012) ICL/IPL regional activities in West Africa. *Landslides* 9:433–437
- Igwe O (2013) ICL/IPL activities in West Africa: landslide risk assessment and hazard mapping approach. *Landslides* 10:515–521
- Igwe O, Sassa K, Wang FW (2007) The influence of grading on the shear strength of loose sands in stress-controlled ring shear tests. *Landslides* 4(1):43–51
- Igwe O, Fukuoka H, Sassa K (2012) The effect of relative density and confining stress on shear properties of sands with varying grading. *Geotech Geol Eng* 30:1207–1229
- Mukhlisin M, Taha MR (2012) Numerical model of antecedent rainfall effect on slope stability at a hillslope of weathered granitic soil formation. *J Geol Soc India* 79(5):525–531
- Sassa K (1998) Recent urban landslide disasters in Japan and their mechanisms. In: Proceedings of the 2nd international conference on environmental management, vol 1. Balkema, Rotterdam, pp 47–58
- Sassa K, Wang G, Fukuoka H (2003) Performing undrained shear tests on saturated sands in a new intelligent-type of ring shear apparatus. *Geotech Test J* 26(3):257–265
- Sassa K, Wang G, Fukuoka H, Wang FW, Ochiai T, Sugiyama M, Sekiguchi T (2004) Landslide risk evaluation and hazard mapping for rapid and long-travel landslides in urban development areas. *Landslides* 1(3):221–235
- Wang G, Sassa K (2002) Post-failure mobility of saturated sands in undrained load-controlled ring shear tests. *Can Geotech J* 39:821–837
- Wang G, Sassa K (2003) Pore-pressure generation and movement of rainfall-induced landslides: Effects of grain size and fine particle content. *Eng Geol* 69:109–125



Assessing Landslide Frequency for Landform Hazard Zoning Purposes

Gabriel Legorreta Paulín, José Lugo Hubp, and José Fernando Aceves Quesada

Abstract

This work provides an overview of the on-going research project (Grant PAPIIT, no. IB100412-RR180412 and IPL project #170) from the Institute of Geography at the National Autonomous University of Mexico (UNAM). The project seeks to conduct a multi-temporal landslide inventory, analyze the distribution of landslides, and characterize landforms that are prone to slope instability by using Geographic Information Systems (GIS). The study area is the Río Chiquito-Barranca del Muerto watershed that covers 111 km² and lies on the south-western flank of Pico de Orizaba volcano. The watershed was studied using aerial photographs, fieldwork, and adaptation of the Landslide Hazard Zonation Protocol of the Washington State Department of Natural Resources, USA. A total of 571 gravitational features were recognized, of six types: shallow landslides, debris-avalanche, deep-seated landslides, debris flows, earthflows, and rock falls. This analysis divided the watershed into 12 mass-wasting landforms on which gravitational processes occur: inner gorges, headwalls, active scarps of deep-seated landslides, meanders, plains, three types of hillslopes classified by their gradient (low, moderate, and high), rockfalls, non-rule-identified inner gorges, non-rule-identified headwalls, and non-rule-identified converging hillslopes. For each landform the landslide area rate and the landslide frequency rate were calculated, as well as the overall hazard rating. The slope-stability hazard rating has a range that goes from low to very high. The overall hazard rating for this watershed was very high.

Keywords

GIS • Landslide inventory map • Landslide hazard map • Pico de Orizaba volcano

G. Legorreta Paulín (✉)
Laboratorio de Análisis Geo-espacial, Instituto de Geografía,
Universidad Nacional Autónoma de México, Circuito Exterior, Ciudad
Universitaria, Coyoacán 04510, Mexico
e-mail: legorretag@igg.unam.mx

J. Lugo Hubp • J.F. Aceves Quesada
Departamento de Geografía Física, Instituto de Geografía, Universidad
Nacional Autónoma de México, Circuito Exterior, Ciudad
Universitaria, Coyoacán 04510, Mexico
e-mail: lugoh@igg.unam.mx; acevesquesada.fernando@gmail.com

Introduction

Worldwide, landslide inventory maps and related geodatabases are the preliminary step toward assessment of susceptibility, hazard, and risk (Castellanos Abella and Van Westen 2008; Hervás and Bobrowsky 2009; Guzzetti et al. 2012; Legorreta et al. 2013). In Mexico, efforts to achieve this have used Geographic Information Systems (GIS) and remote sensing (Capra and Lugo-Hubp 2006; García-Palomo et al. 2006; Pérez-Gutiérrez 2007; Secretaría de Protección Civil 2010). Despite these efforts, there are few landslide inventory maps and landslide hazard maps that systematically record the type, abundance, distribution, and

hazard within any region of Mexico. This is the case for Pico de Orizaba volcano, the highest mountain in Mexico (5,675 m a.s.l.), which is affected by continuous gravitational processes because of the long-term weathering of its rock and high seasonal rainfall. This stratovolcano creates a potentially hazardous situation for 500,000 people living within a radius of 27 km of the volcano. On the southwestern flank of Pico de Orizaba, the Río Chiquito-Barranca del Muerto watershed threatens towns such as Córdoba, Orizaba, Río Blanco, Nogales, and Ciudad Mendoza, with a total population of 360,000 people, due to the coalescence of up-stream landslides that have increased the destructive power of debris flows. The Río Chiquito-Barranca del Muerto watershed was selected as a case study. The main goal of this mass wasting project is to provide standardized methods for conducting landslide inventories and producing landslide hazard zonation maps for various landforms to support governmental authorities for hazard mitigation and landscape planning in Mexico. During this study, 571 landslides, covering 0.350 km², were mapped from aerial photos, GIS thematic layers (such as elevation, slope, hill shade, aspect map, and geology map) and field verification.

Derivation of landform units used classification of morphometric parameters, expert knowledge, field verification, and the Landslide Hazard Zonation (LHZ) Protocol of the Washington State Department of Natural Resources (DNR), Forest Practices Division (Dikau et al. 1995; Washington State Department of Natural Resources (DNR), Forest Practices Division 2006; Evans 2012). This analysis divides the watershed into 12 mass wasting landforms that are assigned slope stability hazard ratings from low to very high. Mapped landforms include some of the high-hazard units defined in the Washington State Forest Practices Rules. For each landform the landslide area rate and the landslide frequency rate were calculated, as well as the overall hazard rating for the watershed. The overall hazard rating for the study area was found to be very high.

Background

The landslide mapping and hazard mapping are important in assessment of the potential hazard situation for people and property. Worldwide, the mapping has been addressed by multi-temporal inventories (Washington State Department of Natural Resources (DNR), Forest Practices Division 2006; Hervás and Bobrowsky 2009; Blahut et al. 2010) and modeling landslide hazards by analysis of landslide distribution in landforms units (Iwahashi et al. 2001; Washington State Department of Natural Resources (DNR), Forest Practices Division 2006; Evans 2012; Jasiewicz and Stepinski 2013). For example, in the early 1990s geologists of the Washington State Department of Natural Resources,

Forest Practices Division, USA, conducted multi-temporal landslide inventories and produced landform hazard maps to assist Washington State's forest practices. The method is embedded in a well defined protocol (Washington State Department of Natural Resources (DNR), Forest Practices Division 2006).

In Mexico, numerous GIS-based applications have been used to represent and assess landforms and slope stability through heuristic, statistical, or deterministic approaches (Bocco 1983; Tapia-Varela and López-Blanco 2002; Bolongaro-Crevenna et al. 2005; Capra and Lugo-Hubp 2006; Pérez-Gutiérrez 2007; Secretaría de Protección Civil 2010). These studies include concepts and explanations of landslide and geomorphologic landforms classification, trigger mechanisms, criteria, considerations, and analysis for landslide hazard reconnaissance.

In the study area, most of the research has focused on the volcanic history of Pico de Orizaba volcano to establish the possible mechanisms and eruptive styles that explain the present morphology of the landscape and the potential hazard from volcanic events and flank collapse (Siebe et al. 1992; Carrasco-Núñez et al. 1993, 2006; Carrasco-Núñez and Rose 1995; De la Cruz-Reyna and Carrasco-Núñez 2002; Macías 2005). Based on previous geological studies, computer simulations, GIS, and remote sensing, maps have been created to show the risk of movement of catastrophic voluminous lahars along stream systems of Pico de Orizaba (Hubbard 2001; Sheridan et al. 2001; Concha-Dimas et al. 2005; Hubbard et al. 2007). A multi-temporal inventory map and a landslide susceptibility map were created by using and comparing Multiple Logistic Regression (MLR) and a cartographic/hydrologic model (Stability Index Mapping: SINMAP) (Legorreta et al. 2013). In spite of this effort, there are few landslide inventory maps or geo-datasets, and scant standardized landslide hazard mapping based on landforms along the stream systems of Pico de Orizaba volcano.

Study Area

The Río Chiquito-Barranca del Muerto watershed covers 111 km² and lies within Veracruz and Puebla states, Mexico. The watershed is characterized by hilly and steep terrain with elevations from 1,340 to 5,600 m a.s.l. and slopes between 3° (inner valleys of relatively flat plains) and 61° (mountainous terrain). It is a tributary of the Río Blanco, which flows into the Gulf of Mexico (Fig. 1).

The watershed is on the southwestern flank of Pico de Orizaba volcano, which is located in the Mexican Volcanic Belt physiographic province. The Mexican Volcanic Belt is an active volcanic chain that extends 1,000 km from west to east across central-southern Mexico, from the Pacific Ocean

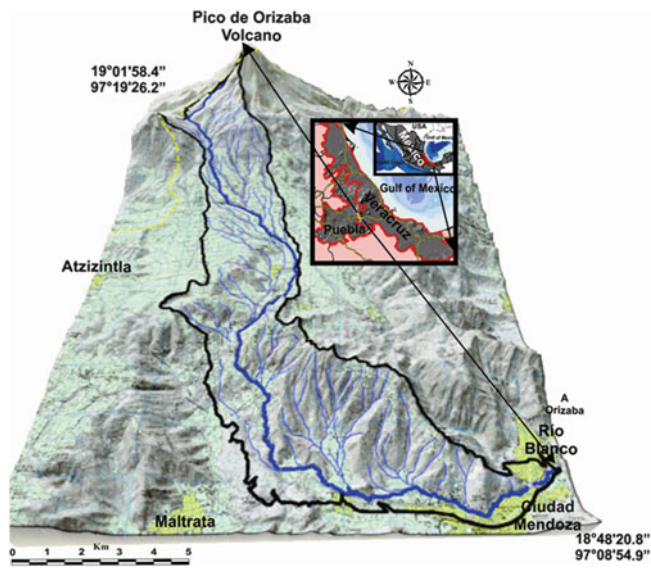


Fig. 1 Location of the study area

to the Gulf of Mexico. The study area is prone to landslides due to its large area of collapsible weathered or disjointed volcano-clastic material at high altitudes and under high seasonal rainfall. In the study area, the climate is Tundra at >4,400 m a.s.l., Subtropical semi-cold at 3,000–4,400 m a.s.l., and Subtropical temperate, sub-humid and Tropical semi-warm, humid at <3,000 m a.s.l. (García 2004). The mean annual precipitation is 1,000–1,100 mm/year at >4,000 m a.s.l. and 927 mm/year at <1,500 m a.s.l. (Palacios et al. 1999), with most falling as rain during seasonal storms in the wet season between May and November. Cretaceous sedimentary rock constitutes about 29.7 % of the total area in the watershed and has been covered by Tertiary and Quaternary lavas, pyroclastic flows, fall deposits, and alluvium. The Tertiary rocks and deposits cover 60.3 % of the watershed area, while the area covered by Quaternary and alluvium is 2.4 % and 7.6 %, respectively (Fig. 2).

Methods

The method encompasses three main stages of analysis to assess landslide susceptibility: Stage 1 builds a historic landslide inventory map. Background information was collected to provide context and to generally characterize landslide processes within the watershed. Background information includes geology, land use, climate and hydrology maps. All paper maps were converted to raster format, geo-referenced, and incorporated as GIS layers.

Within the GIS layers, characteristics such as catchment area, stream length, stream patterns, stream orders, and drainage density were generated from GIS analysis and incorporated as background information. The background information also included orthophotos at 1:10,000, as well

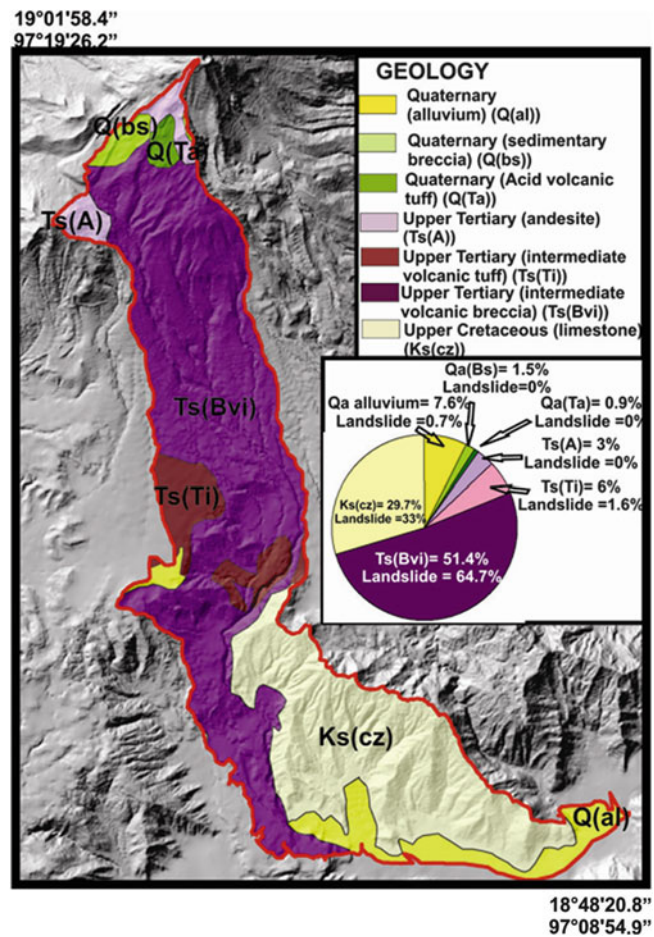


Fig. 2 Distribution and spatial proportions of geologic rocks and deposits

as a 10 m digital elevation model (DEM) and its derived slope angles, slope curvatures, and contributing areas.

By retrieval and on-off switching of the layers in the GIS system, a base map was created to assist in the digitizing of landslides. Landslides were identified by photo-interpretation and field checking. Two sets of aerial photographs were used: one from 1994 at a scale of 1:20,000 and the other from 2008 at a scale of 1:10,000. Fieldwork was conducted three times a year from 2009 to 2012 along the main river and some tributary rivers. The amount of field verification was 37 %, which enhances confidence in the landslide assessment.

In the second stage, specific landforms that exist across the study area were defined by rules adopted by the Washington Forest Practices Protocol to address landslide hazards (Washington State Department of Natural Resources (DNR), Forest Practices Division 2006). These landforms are called rule-identified landforms (inner gorges, bedrock hollows, convergent headwalls, outer edges of meanders, and active scarps of deep-seated landslides). Their differentiation is based on slope gradient and shape, lithology, landslide density and sensitivity to forest practices. The aerial photos, the

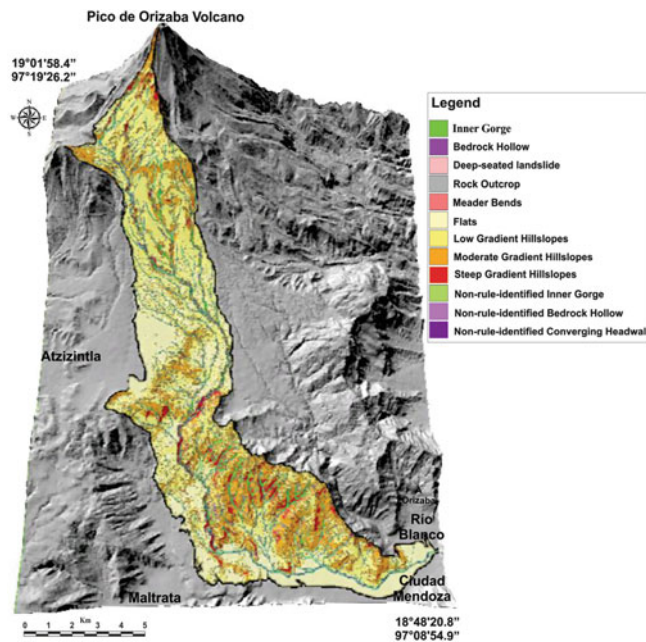


Fig. 3 Landform distribution in the Rio Chiquito-Barranca del Muerto watershed

landslide inventory, and GIS layers were also used to identify other areas that do not meet the rule-identified landform definitions. These areas are called non-rule-identified landforms (such as non-rule-identified inner gorges and bedrock hollows, steep-gradient hillslopes, moderate-gradient hillslopes, and low-gradient hillslopes). Both rule- and non-rule-identified landforms were entered into GIS as part of a landform polygon feature.

The third stage determined the landslide area and the landslide frequency rate for each landform, as well as the overall hazard ratings for the watershed. For both rule- and non-rule-identified landforms a semi-quantitative overall hazard rating is derived from values that correspond to the number and area of landslides within each landform, normalized for a period of time spanned by the aerial photographs used, and to the area of each landform. These values are referred to as the landslide area rate and the landslide frequency rate. After the quantitative rates of landsliding were determined, each was assigned a Low, Moderate, High, or Very High hazard rating. The landslide area rate and landslide frequency rate values were then entered into a matrix in order to determine the overall hazard rating to be assigned to the landforms.

Results

During assessment of the Río Chiquito-Barranca del Muerto watershed, a representative sample of 571 mass-wasting features was inventoried. Six types of mass wasting process

Table 1 Landforms landslide hazard rating

Name of landform	Landform slope stability hazard rating	Slope of land-form	Area (ha)	No. landslides
Inner gorges	Very high	>70 %	236.3	105
Bedrock hollows	Very high	>70 %	4.9	1
Active scarps of deep-seated landslides	Very high	>50 %	1.3	19
Rock outcrops	Very high	30–145 %	28.3	31
Meander bends/overbank dep./surge plain	Very high	30–70 %	12.5	16
Flats	Low	<10 %	2,194.1	14
Low gradient hillslopes	Low	11–40 %	4,449.9	82
Moderate gradient hillslopes	High	41–70 %	2,802	147
Steep gradient hillslopes	High	>70 %	488.6	23
Non-rule Identify inner gorges	Very high	30–70 %	887.3	123
Non-rule-identify bedrock hollow	Very high	<70 %	3.6	2
Non-rule-identify converging headwall	Very high	<70 %	3.6	8
Totals			11,112.4	571

were identified in the watershed. Of the landslides identified, 46.6 % were mapped as shallow undifferentiated failures, 26 % were debris flows, 15.2 % were debris slides, 1.7 % were deep-seated landslides, 1 % were earthflows, and 9.5 % were debris rock topples and falls. Of the 571 inventoried landslide features, 93 % were identified as definitive, 6.3 % as probable, and 0.70 % as questionable. Also, the GIS overlay of geology versus landslide inventory shows that almost two-thirds of the mapped landslides are in volcanic rock or deposits, and the rest are in weathered sedimentary rocks and deposits. Twelve landforms derived from physical attributes of the landscape were mapped. They are intended for use in predicting areas within the watershed that pose hazards for mass wasting (see Fig. 3 and Table 1).

Conclusions

This paper briefly introduces and reviews the implementation of a method for landslide mapping and landslide hazard zonation for varied landforms in unstable sedimentary and volcanic terrains. The study at Rio Chiquito-Barranca del Muerto is an attempt to adapt and produce the prototype for a standardized method for future

landslide studies in Mexico. The method is achieved by adapting the Washington State, DNR Forest Practices Protocol for the standardization and integration of thematic layers and their related geo-database in a GIS-based system to obtain a landslide inventory map and a map of landslide hazard zonation for various landforms.

The GIS overlay of landforms versus landslide inventory shows that landforms differ in their pattern of resistance to erosion processes and in the type of mass movement; these differences are due to their specific geologic and geomorphometric properties. It was found that almost 40 % of the landslides had developed along inner gorges and non-rule-identified inner gorges, which cover only 10 % of the study area. In these two landforms shallow undifferentiated landslides, debris flow, and debris landslides are the predominant mass wasting processes. Both landforms are more prone to landslides in the middle and lower portion of the watershed, where there are steep slopes, loose volcanic ash, pyroclastic flow deposits, and volcano-clastic and sedimentary material. This finding is important in understanding the long-term evolution of the stream system on the southwestern flank of Pico de Orizaba, and may prove useful in the quantification, assessment, and modeling of landslides that occur continually in volcanic terrains.

We emphasize the fact that the study is the first prototype in Mexico to develop a GIS methodology for a systematic landslide mapping and landslide hazard zonation for various landforms. Hence, it is subject to being adapted, modified, and improved. Future research should involve the calibration of the Washington State, DNR Forest Practices method to other Mexican watersheds.

We acknowledge the technical limitation of the landslide inventory, whose quality depends on the experience and skill of the researchers, and the reliability of available information, including the aerial photographs, for identifying the landslides and the complexity of the study area. Regardless of the limitations, the authors foresee the landslide inventory and the landslide hazard zonation using landforms of Rio Chiquito-Barranca del Muerto as an integrated method to handle and support prognostic studies of slope instability. By directly addressing the landslide inventory and hazard mapping issues, local authorities in Mexico will benefit with regard to landslide hazard mitigation and planning.

Acknowledgements The authors thank authorities from the Washington State Department of Natural Resources (DNR) Geology & Earth Resources Division and the Geo-Spatial Analysis Laboratory from the Institute of Geography, UNAM for their approval and help. This research was supported by the Programa de Apoyo a Proyectos de Investigación e Innovación Tecnológica (PAPIIT), UNAM Grant no. IB100412-RR180412, the International Program on Landslides (IPL).

References

- Blahut J, Van Westen CJ, Sterlacchini S (2010) Analysis of landslide inventories for accurate prediction of debris-flow source areas. *Geomorphology* 119(1–2):36–51
- Bocco VG (1983) La Zonalidad Geomorfológica de la región comprendida en la carta Querétaro 1:250,000. En la: Memoria del IX Congreso Nacional de Geografía
- Bologaro-Crevenna A, Torres-Rodríguez V, Sorani V, Frame D, Ortiz MA (2005) Geomorphometric analysis for characterizing landforms in Morelos State, Mexico. *Geomorphology* 67:407–422
- Capra L, Lugo-Hubp J (2006) Fenómenos de remoción en masa en el poblado de Zapotitlán de Méndez, Puebla: relación entre litología y tipo de movimiento. *Rev Mex Cienc Geol* 20(2):95–106
- Carrasco-Núñez G, Rose IW (1995) Eruption of a major Holocene pyroclastic flow at Citlaltépetl volcano (Pico de Orizaba), México, 8.5–9.0 ka. *J Volcanol Geotherm Res* 69(3/4):197–215
- Carrasco-Núñez G, Vallance JW, Rose WI (1993) A voluminous avalanche-induced lahar from Citlaltépetl volcano, Mexico: implications for hazard assessment. *J Volcanol Geotherm Res* 59 (1/2):35–46
- Carrasco-Núñez G, Díaz-Castellón R, Siebert L, Hubbard B, Sheridan MF, Rodríguez SR (2006) Multiple edifice-collapse events in the Eastern Mexican Volcanic belt: the role of sloping substrate and implications for hazard assessment. *J Volcanol Geotherm Res* 158:151–176. doi:10.1016/j.jvolgeores.2006.04.025#_blank
- Castellanos Abella EA, Van Westen CJ (2008) Qualitative landslide susceptibility assessment by multicriteria analysis: a case study from San Antonio del Sur, Guantánamo, Cuba. *Geomorphology* 94:453–466
- Concha-Dimas A, Cerca M, Rodríguez-Elizarrarás S, Watters RJ (2005) Geomorphological evidence of the influence of pre-existing basement structure on emplacement and deformation of volcanic edifices at the Cofre de Perote-Pico de Orizaba chain and implications for avalanche generation. *Geomorphology* 72:19–39
- De la Cruz-Reyna S, Carrasco-Núñez G (2002) Probabilistic hazard analysis of Citlaltépetl (Pico de Orizaba) Volcano, eastern Mexican Volcanic belt. *J Volcanol Geotherm Res* 113:307–318
- Dikau R, Brabb EE, Mark RK, Pike RJ (1995) Morphometric landform analysis of New Mexico. *Z Geomorphol Suppl Bd* 101:109–126
- Evans IS (2012) Geomorphometry and landform mapping: what is a landform? *Geomorphology* 137(1):94–106
- García E (2004) Modificaciones al sistema de clasificación climatic de Köppen. Serie Libros #6, Instituto de Geografía, UNAM, 90 p
- García-Palomo A, Carlos-Valerio V, López-Miguel C, Galván-García A, Concha-Dimas A (2006) Landslide inventory map of Guadalupe Range, north of the Mexico Basin. *Bol Soc Geol Mex* 58 (2):195–204
- Guzzetti F, Mondini AC, Cardinali M, Fiorucci F, Santangelo M, Chang KT (2012) Landslide inventory maps: new tools for an old problem. *Earth Sci Rev* 112:42–66
- Hervás J, Bobrowsky P (2009) Mapping: inventories, susceptibility, hazard and risk. In: Sassa K, Canuti P (eds) *Landslides—disaster risk reduction*. Springer, Berlin, pp 321–349. ISBN 978-3-540-69966-8
- Hubbard BE (2001) Volcanic hazard mapping using aircraft, satellite and digital topographic data: Pico de Orizaba (Citlaltépetl), México. Thesis, Department of Geology, SUNY, Buffalo
- Hubbard BE, Sheridan MF, Carrasco-Núñez G, Díaz-Castellón R, Rodríguez S (2007) Comparative lahar hazard mapping at Volcan Citlaltépetl, Mexico using SRTM, ASTER and DTED-1 digital topography. *J Volcanol Geotherm Res* 160(1):99–124

- Iwahashi J, Watanabe S, Furuya T (2001) Landform analysis of slope movements using DEM in Higashikubiki area, Japan. *Comput Geosci* 27(7):851–865
- Jasiewicz J, Stepinski T (2013) Geomorphons—a new approach to classification of landforms. *Geomorphology* 182:147–156
- Legorreta PG, Bursik M, Ramirez-Herrera MT, Lugo-Hubp J, Zamorano Orozco JJ, Alcantara-Ayala I et al (2013) Chapter 19: Landslide inventory and susceptibility mapping in the Rio Chiquito-Barranca Del Muerto Watershed, Pico de Orizaba Volcano, Mexico. In: Sassa K (ed) *Landslides: global risk preparedness*. Springer, Heidelberg, pp 285–295
- Macías JL (2005) Geología e historia eruptiva de algunos de los grandes volcanes activos de México. *Boletín de la Sociedad Geológica Mexicana. Volumen Conmemorativo del Centenario Temas Selectos de la Geología Mexicana LVII(3)*: 379–424
- Palacios D, Parrilla G, Zamorano JJ (1999) Paraglacial and postglacial debris flows on little ice age terminal moraine: Jamapa Glacier, Pico de Orizaba (Mexico). *Geomorphology* 28:95–118
- Pérez-Gutiérrez R (2007) Análisis de la vulnerabilidad por los deslizamientos en masa, caso: Tlacuitlapa, Guerrero. *Bol Soc Geol Mex* 59(2):171–181
- Secretaría de Protección Civil (2010) Atlas de peligros geológicos e hidrometeorológicos del estado de Veracruz. Comp.: Ignacio Mora González; Wendy Morales Barrera, Sergio Rodríguez Elizarrarás. Xalapa: Secretaría de Protección Civil del estado de Veracruz: Universidad Veracruzana: UNAM. 1V
- Sheridan MF, Carrasco-Núñez G, Hubbard BE, Siebe C, Rodríguez-Elizarraraz S (2001) Mapa de peligros del Volcan Citlaltépetl (Pico de Orizaba). *Inst Geog, Univ Nac Autonoma Mexico*, 1:250,000 scale
- Siebe C, Komorowski JC, Sheridan MF (1992) Morphology and emplacement collapse of an unusual debris avalanche deposit at Jocotitlán Volcano, Central Mexico. *Bull Volcanol* 54:573–589
- Tapia-Varela G, López-Blanco J (2002) Mapeo geomorfológico analítico de la porción central de la Cuenca de México a escala 1:100,000. *Rev Mex Cienc Geol* 19(1):50–65
- Washington State Department of Natural Resources (DNR), Forest Practices Division, (2006) Landslide hazard zonation (LHZ) mapping protocol, version 2.0. Accessed at http://www.dnr.wa.gov/BusinessPermits/Topics/LandslideHazardZonation/Pages/fp_lhz_review.aspx



Comparison of Soil Modulus E_{50} of Residual Soil Slope Failures in Two Different Rainfall Zones

M.A.S.N. Mallawarachchi, E.M.T.M. Ekanayake, S.S.I. Kodagoda, and A.A. Virajh Dias

Abstract

Occurrence of slope failures and landslides in the hilly areas of Sri Lanka poses a threat to lives and frequently makes the roads impassable and thus development process of the country is hindered. The characteristics of slopes, saturation and shear strength of soils are the main parameters associated with rainfall-induced slope failures, and these parameters are directly affected by the different precipitation in prolonged periods of time. In most instances a landslide trigger due to extensive soil saturations and is a function of soil integrity, hydraulic conductivity, density, void content, shear strength and boundary conditions. Two soil samples can have the same dry density but different structures, like loose or dense, and thus have different soil modulus. Water content also impacts soil modulus. At low water contents the water binds the particles, increases the stress and suction between the particles and leads to a high soil modulus. This is especially apparent when considering the stiffness of dried clay. Slope stability analysis enables the identification of risky areas, but the lack of knowledge in terms of variability against the saturations and elastic deformations of subsurface soil is another hindrance in interpretation of instability potential in natural slopes.

Keywords

Soil modules • Rain induced failures • Precipitation

Introduction

In limit equilibrium analysis the relative deformations along the rupture surface are usually ignored but it's a common fact that deformities are highly significant at the failure. Evaluation of stability of natural slopes using the deterministic approach depends on various extrinsic and intrinsic variables for calculation of the factor of safety. Stability of residual soil formations under prolong period of saturation has been the subject of various landslide studies in the recent past, with emphasis placed on evaluation of stability. Since, the subsoil properties and patterns of failures are highly dependent on soil saturation and shear strength, a study on evaluation of inter-related parameters of two different precipitation regions would yield to understand shear strain behavior of soils that can be adopted in each region. The project team has undertaken several sample analysis, shear

M.A.S.N. Mallawarachchi (✉)
CECB Laboratory Services, Central Engineering Consultancy Bureau
(CECB), No.11, Jawatta Road, Colombo 05, Sri Lanka
e-mail: shanikanm@gmail.com

E.M.T.M. Ekanayake
CECB Laboratory Services, Central Engineering Consultancy Bureau
(CECB), Colombo 05, Sri Lanka
e-mail: thushari_e@yahoo.com

S.S.I. Kodagoda • A.A.V. Dias
Centre for Research and Development (CRD), Central Engineering
Consultancy Bureau (CECB), Colombo 07, Sri Lanka
e-mail: sudheerai@gmail.com; aavirajhd@yahoo.com

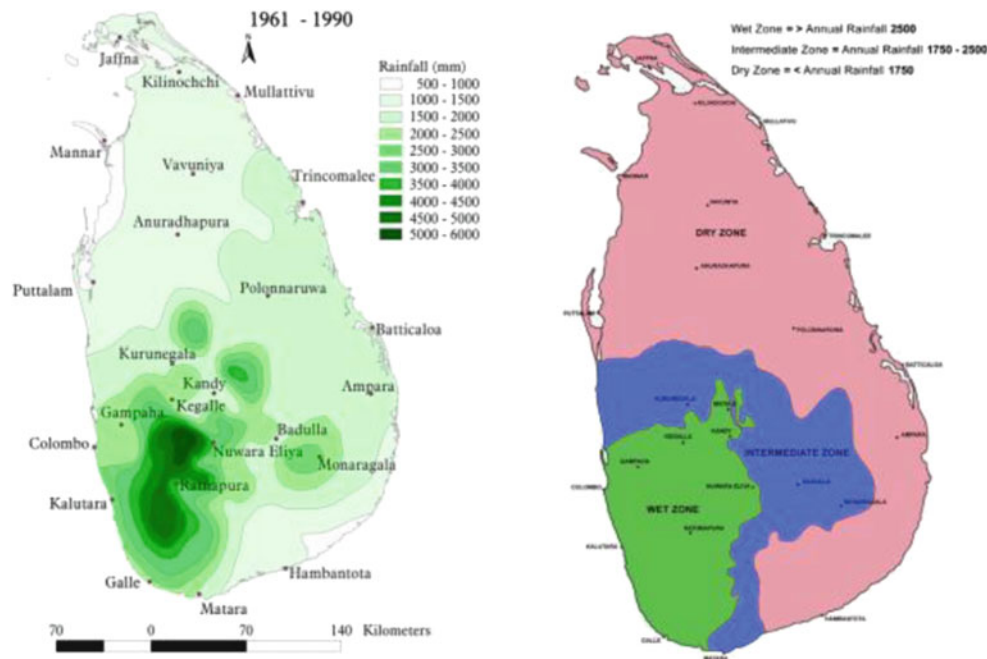


Fig. 1 Average annual rainfall for the period 1961–1990

strength variables and landslide records in selected two rainfall precipitation areas and has obtained various compatibilities under high saturation effects in residual soil.

Rainfall in Sri Lanka

Lying in the equatorial and tropical zone, Sri Lanka is influenced by the monsoons, allowing two distinct main seasons: wet and dry, with two inter-monsoonal seasons.

The first is from mid-May to October, when winds originate in the Southwest, bringing moisture from the Indian Ocean. When these winds encounter the slopes of the Central Highlands, they unload heavy rains on the mountain slopes and the southwestern sector of the island. Some of the windward slopes receive up to 2,500 mm of rain per month (Fig. 1), but the leeward slopes in the East and Northeast receive little rain. The second season occurs in October and November, the inter-monsoonal months. During this season, periodic squalls occur and sometimes tropical cyclones bring overcast skies and rains to the southwest, northeast, and eastern parts of the island. During Northeast monsoonal rains which normally occur from December to March, monsoon winds come from the northeast, bringing moisture from the Bay of Bengal. The northeastern slopes of the mountains may be inundated with up to 1,250 mm of rain during these months. The inter-monsoonal period occurs from March until mid-May, with light, variable winds and evening thundershowers.

Landslides and Rainfall Precipitations

Heavy rain is the main cause for landslide activation in hilly areas of Sri Lanka. There is no record of landslides occurring during the dry season or under any seismicity in Sri Lankan history. Geology, hydro-geology, rainfall precipitation and ground slope are natural causes, while improper land use practices and man-made activities also account for landslide activation. The National Building Research Organisation (NBRO) has conducted studies in many districts that are highly vulnerable to landslides, namely in Kandy, Matale, Nuwara-Eliya, Badulla, Kalutara, Ratnapura, Kegalle, Galle and Matara districts (Bandara 2012). After recent heavy rains, 300 landslide-prone areas were identified in these districts, including, Gampaha and Colombo. Gampaha and Colombo districts have been subjected to precipitation of 2,500 mm similar to Kandy during last few decades. Both areas usually contain residual and lateritic form of soils.

In the late 1980s when information was scanty, the landslide-triggering threshold was placed at 200 mm of rainfall in a 72 h period, provided rain in the area continued (Bhandari et al. 1992). This is mainly because of the preliminary loss of matrix suction, intensive rate of water penetration as well as percolation of rainwater and lack of slope protection ingredients in the event of heavy rains.

Study the conditional probability of landslide occurrences as a ratio of rainfall intensity of the month of the landslide

Table 1 Selected areas for the study—study phase 1

Precipitation zones of study	Area, district	Average annual rainfall in mm
Zone 1	Watawala, Kahagalle, Koslanda/Nuwara Eliya District	4,000–5,500
Zone 2	Kandy/Kandy District, Colombo/District Colombo	2,500–3,000

event and average monthly rainfall of the place against to average monthly rainfall intensity (Bhandari and Dias 1996) was conducted during the 1990s. The criterion worked only partially, in case of reactivation of recent, seasonally active landslides. A relationship of rainfall records of a very large number of landslides shows that 24 h-rainfall associated with a landslide event was generally 2–23 times higher than average daily rainfall (Bhandari and Dias 1996). This was reasonably accurate if the average annual rainfall exceeds more than 3,000 mm in the wet zone of the country.

Methodology: Phase 1

The main objective of the study phase 1 of the research was to determine residual soil moduli and shear strength of two different rainfall precipitation zones. The selected two precipitation zones (Table 1) were:

- Heavy rainfall precipitation zone in wet zone with annual average rainfall above 4,500 mm.
- Moderate rainfall precipitation zone in wet zone with annual average rainfall between 2,500–3,000 mm.

Newly excavated residual soil slopes in the moderate precipitation zone found in Akuregoda, Colombo for the study as in Fig. 2.

In the study, the following comparisons were made:

- Comparison of laboratory and in-situ parameters including cohesion, friction angle and elastic parameters E_{50}
- Determination of other critical soil parameters such as cohesion and angle of internal friction in both regions
- Comparison of values obtained in the study phase 1 as outlined above.

Sampling of Soil

Open-pit excavations were made, recovering large undisturbed soil samples from selected locations at Zone 1; Akuregoda (Fig. 2) and Zone 2; Nuwara Eliya (Fig. 3). Few samples were collected from boundary of old landslides namely Watawala Landslide (in Zone 1), Koslanda Landslide (Zone 1) and potential landslide areas along the road leading to Bandarawela to Nuwara Eliya. Undisturbed soil



Fig. 2 Deep earth cutting sections in residual soils at Zone 2; Akuregoda, Colombo District

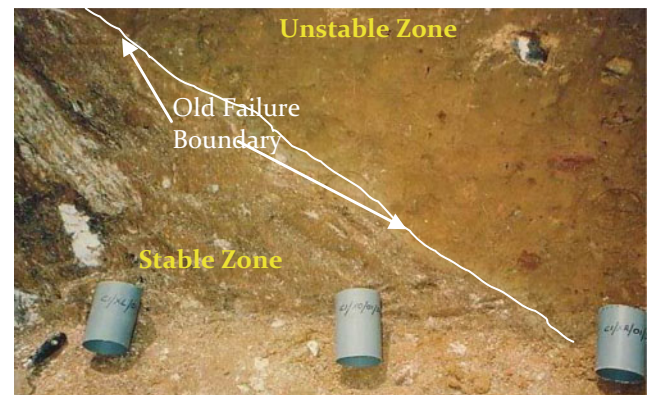


Fig. 3 Identification of stable and unstable zones at site from the deep excavation pits



Fig. 4 Intact soil was obtained by high quality manual sampling method; Zone 1; Nuwara Eliya District

samples taken from the stable and unstable zones closer to the discrete boundary shears of a landslide always produce reliable results. Collection of samples is the most important task during this study (Fig. 4).

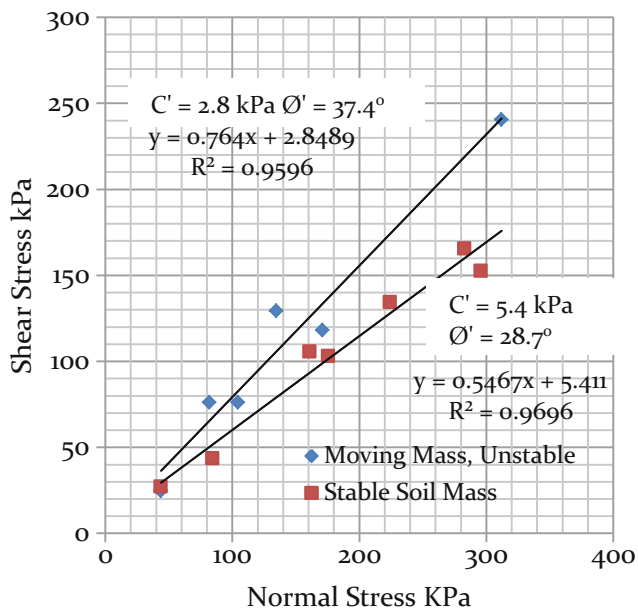


Fig. 5 Shear strength properties interpreted from a standard drained direct shear test in Zone 1

Determination of E_{50} , C' , ϕ' of Residual Soils

All sample locations consisted of common overburden soil type namely, residual soils or Silty Sand (SM) of USC (unified soil classification). The study extended to investigate shear-strength characteristics; effective cohesion intercept C' and effective angle of internal friction ϕ' , which associate rainfall-induced slope failures. Residual soils are usually slightly cohesive. In residual soils, grain-size distribution has a significant influence on internal friction and percentage of clay, silts and sand particles could drastically change the properties exhibited by the sample. Drained or undrained triaxial shear and drained direct shear test (Fig. 5) are generally regarded as the most appropriate laboratory tests to determine shear strength characteristics of soils. Elastic soil modulus, E_{50} , may be estimated from empirical correlations, laboratory test results on undisturbed specimens and results of field tests. The effective strength parameters interpreted from drained direct shear test in shear zone samples but in two different layers are shown in Fig. 5.

If the soil has been subjected to stress in the past due to various deformities, loading and unloading, it will impact the modulus. Therefore, elastic module may create different views on old landslide deposits. An over-consolidated soil will generally have a higher modulus than the same normally-consolidated soil. In this study, a series of triaxial tests were performed on UDS samples to determine the effective shear strength parameters and the secant modulus E_{50} . The interpretation and evaluation of E_{50} using standard saturated consolidated undrained triaxial compression test

for the samples collected from the rainfall precipitation Zone 1 and Zone 2 are shown in Table 2.

Comparison of Results in Different Precipitation Zones

Near the ground surface, residual soils lack texture or traces of the parent rock and consist of brown to red and yellow, high plasticity silts. At a slightly greater depth, the residual soils transition to in-situ weathered and highly decomposed rock are typically dark brown, black and dusky red, low plasticity or non-plastic silts. However, there were some samples with liquid limits greater than 50, and the plasticity index was such that they are plotted below the A-line on the Casagrande plasticity chart. According to the Unified Soil Classification System (USCS) in ASTM D2487, these soils have the abbreviated descriptor MH and SM. Slopes with thick soil layers and slope angle between 15° and 45° have been found to have a greater preponderance for landsliding with maximum tendency of hill slope of angle 26° – 35° to the horizontal (Bandara 2012). It is noted that most of the hilly regions are predominantly covered with residual form of soil and some old depositions of colluvium. Therefore, recent study indicates some similarities among the effective shear-strength parameters of overburdened soils.

In case of slope stability, movements are associated with the deformation of the soil mass essentially under its own weight. Soil with closely packed particles tends to have a higher modulus. This can be determined by looking at the soil's dry density or porosity (void ratio). Most soils exhibit a nonlinear behavior soon after application of shear stress as in Fig. 6. It is assumed that the disturbance is equivalent to an accumulation of shear strain, the tests consist of a repetition of compression and an alternation of compression due to stage load consolidated undrained triaxial test.

The test results as plotted in Fig. 7, shows that E_{50} increases with effective confining pressure. However, the paper compares E_{50} of the residual soil if the effective confining pressure reached 100kPa or 120 kPa in Table 2.

However, two soil samples can have the same dry density but different structures, loose or dense, and thus have different moduli (Briaud 2001). Water content also impacts modulus. At low water contents the water binds the particles, increases the stress and suction between the particles and leads to a high soil modulus. This is especially apparent when considering the stiffness of dried clay. However, this does not hold true for coarse-grained soils. If water content rises too much, the particles are pushed apart and the modulus is reduced. If the soil has been subjected to stress in the past, it will impact the modulus. An over-consolidated soil will generally have a higher modulus than the same normally-consolidated soil (Briaud 2001). No observations

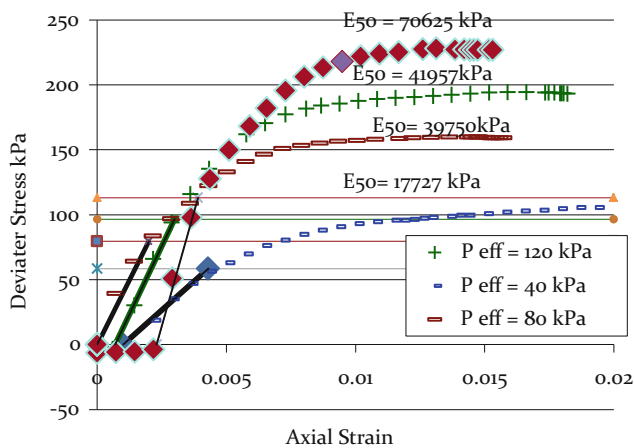


Fig. 6 Determination of E_{50} in a standard undrained triaxial test

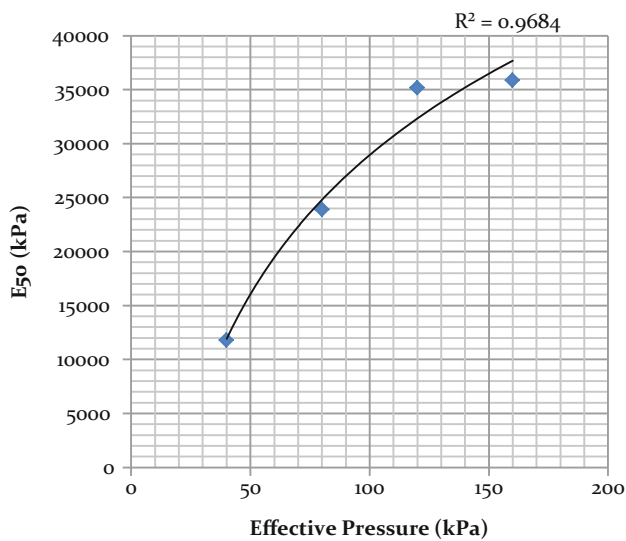


Fig. 7 Relationship of effective confining pressure and soil module E_{50}

were made on residual soils with over-consolidated characteristics similar to cohesive soils. For different soil, samples of residual formations have been used for experimental study by different precipitation zones as in Table 3.

Conclusion

The comparison of soil modulus E_{50} of residual soil slope failures in two different rainfall precipitation zones is an experimental study to formulate a relationship between the potential slope failures quantify shear strength characteristics of soils which could be easily discussed on scenarios of the first time occurrence failures and repetitive failures in residual soil formation. However, the number of soil samples tested in this phase

Table 3 Slope failures in two different precipitation zones along the road section

Zone 1: Balangoda to Bandarawela	39,286	0.838	09 nos of slope failures identified
Zone 1: Koslanda Landslide	41,957	0.810	One major landslide across the road
Zone 1: Gampola to Nuwara Eliya	35,182	0.937	07 number of slope identified
Zone 1: Watawala Landslide	10,714	1.15	One major landslide across the rail road
Zone 2: Colombo and sub regions	56,900	0.788	Newly formed earth cutting
	25,723	0.640	Newly formed earth cutting
	11,909	1.348	Newly formed earth cutting

of study might not be sufficient to demonstrate the above relationship effectively.

The study on evaluation of E_{50} (secant modulus) is an experiment setup to understand the behavior of residual soils under changing stress conditions at site due to various reasons such as prolong period of rainfall precipitations, movement of soils, unloading effects and re-loading effect caused by deposition. The results do not conclude a strong interdependence of e_o and E_{50} with the shear strength characteristics due to a small sample represented in this study. Therefore, it is advised to explore more sample representation in a detail study before the comparison or evaluation of the interdependence of sub coefficients of soils. One of the difficulties faced during the experimental study was to apply the evaluation of degree of landslide density considering a special boundary (area wise) to the selected sample when comparing prior to evaluation of parametric results which could have influence the final results. Therefore, further tests are recommended with more representations of soil samples and also widening the range of test parameters to verify the interdependence capacity of soil parameters and to make it applicable over a wide range of actual failures of residual soils under prolong period of saturation.

Acknowledgments This paper forms part of the IPL-155 project “Determination of Soil Parameters of Subsurface to be used in Slope Stability Analysis in Two Different Precipitation Zones of Sri Lanka” being implemented by the Centre for Research & Development, Central Engineering Consultancy Bureau (CECB) of the Ministry of Irrigation and Water Resources Management. It is published with their permission. The views expressed in the paper are however those of the authors only. Our grateful thanks go to Eng. N Rupasinghe, Chairman Central Engineering Consultancy Bureau and Eng. K L S Sahabandu, General Manager for permission and encouragement.

References

- Bandara RMS (2012) Seventy landslide-prone areas identified; Sunday Observer; 18th November 2012. Reported by S Mohammed NAALIR
- Bhandari RK, Jeyatharan K, Raviskanthan A (1992) Dynamics of rockfalls in Sri Lanka and landslide hazards. In: Proceeding of the international conference on case histories in geotechnical engineering, St. Louis
- Briaud J (2001) Introduction to Soil Moduli, Geotechnical News, June 2001. BiTech Publishers, Richmond, BC
- international symposium on landslides, 17-21 June 1996, Balkema, Trondheim, Norway, pp 1515–1520



WCoE: Mechanisms of Landslides in Over-Consolidated Clays and Flysch and IPL-151 Project: Soil Matrix Suction in Active Landslides in Flysch—The Slano Blato Landslide Case

Matjaž Mikoš, Jošt Sodnik, Ana Petkovšek, Matej Maček, and Bojan Majes

Abstract

The Faculty of Civil and Geodetic Engineering of the University of Ljubljana (UL FGG), Slovenia, Europe, was voted in 2011 at the 2nd World Landslide Forum in Rome, Italy to be one of the 14 new World Centres of Excellence (WCoE) in Landslide Disaster Reduction for the period 2011 to 2014. This successful nomination followed the period 2009–2011, in which UL FGG successfully fulfilled the role as one of the WCoEs for the first time. The title of the activities of the WCoE was selected to be “Mechanisms of landslides in over-consolidated clays and flysch”.

Among the activities of the WCoE at UL FGG we can name the active IPL-151 project on “Soil matrix suction in active landslides in flysch—the Slano Blato landslide case”, as well as activities to establish two ICL networks, the regional one “Adriatic-Balkan Network—ABC” and the thematic one “Landslide Monitoring and Warning Thematic Network—LaMaWaTheN”. In the paper the international activities of the WCoE at UL FGG are elaborated, as well as other international and national activities and projects in which the WCoE has been involved in the field of landslide mitigation and landslide risk reduction.

Keywords

Debris flows • Flysch • Landslides • Risk mitigation • Soil suction • WCoE

Introduction

Faculty of Civil and Geodetic Engineering (FGG) is one of 26 faculties and academies of the University of Ljubljana (UL; in Latin: *Universitas Labacensis*) which is the oldest

M. Mikoš (✉) • A. Petkovšek • M. Maček • B. Majes
Faculty of Civil and Geodetic Engineering, University of Ljubljana,
Jamova c. 2, 1000 Ljubljana, Slovenia
e-mail: matjaz.mikos@fgg.uni-lj.si; ana.petkovsek@fgg.uni-lj.si;
matej.macek@fgg.uni-lj.si; bojan.majes@fgg.uni-lj.si

J. Sodnik
Faculty of Civil and Geodetic Engineering, University of Ljubljana,
Jamova c. 2, 1000 Ljubljana, Slovenia

Water Management Company Kranj, Mirka Vadnova 5, 4000 Kranj,
Slovenia
e-mail: jost.sodnik@vgp-kranj.si

university in Slovenia (established in 1919; with roots in Jesuit-led higher education in seventeenth century and as *Écoles centrales* in the period 1810–1813 during French-ruled Illyrian provinces). It is also the largest (with close to 50,000 full-time and part-time students in 2013) and the internationally best ranked (top 500 in ARWU 2012; #60 in Europe and #168 in the world in Webometrics 2013) university in Slovenia.

The UL FGG was voted in 2008 at the First World Landslide Forum in Tokyo, Japan to be one of the World Centres of Excellence (WCoE) in Landslide Disaster Reduction for the period 2008 to 2011. The title of the activities of the WCoE was selected to be “Mechanisms of landslides in over-consolidated clays and flysch”. We have introduced the UL FGG, its history in the field of landslide research and mitigation, and planned activities as WCoE in an article published in the journal *Landslides* under the topic ICL/IPL

Activities (Mikoš et al. 2009). In 2010, we started a 3-year IPL-151 Project “Soil matrix suction in active landslides in flysch—the Slano Blato landslide case”.

We have reported our activities as a WCoE in November 2011 at the second World Landslide Forum in Rome, Italy (Sodnik et al. 2011). Our contribution to the “Landslides of the world” photo contest won First place in the category Landslide from above. At the second World Landslide Forum in Rome, Italy, the UL FGG was re-elected to be one of the 14 new World Centres of Excellence (WCoE) in Landslide Disaster Reduction for the period 2011 to 2014.

As a part of the activities to celebrate ICL’s 10th Anniversary, a strategic document for the second decade called the ICL Strategic Plan 2012–2021, with the motto “to create a safer geo-environment”, was adopted in Kyoto in January 2012 (Sassa 2012). An important part of this document was a clear ICL dedication to broaden the scope and societal impact in a thematic, institutional, and geographic manner. Thus, thematic and regional networks for landslide risk reduction were recognized to be important forms of ICL activities in the decade to come. The UL FGG soon took active part in these activities.

Fields of Activities at UL FGG as WCoE 2011–2014

The UL FGG activities as World Centre of Excellence since 2011 can be divided into three fields:

- Collaboration in the ICL newly established regional and thematic networks,
- Research work in the field of landslide research,
- Collaboration in the ICL and IPL organizational activities; such as support of the journal *Landslides* (Mikoš 2011b; not discussed in this paper).

The ICL Adriatic-Balkan Regional Network

The general objective of the ‘Adriatic-Balkan Network on Landslides’ is advancing landslide science and its practical application in the region for the benefit of society and the environment. Specific objectives are: (1) to set up a scientific and legislative background for regional cooperation; (2) regional unification of information about landslides and landslide research at national levels; and (3) development of landslide science by capacity building at a regional level and practical applications of outcomes to societies in the region (Mihalić Arbanas et al. 2012a, b).

As part of the network activities, the 1st Regional Symposium on Landslides in the Adriatic-Balkan Region was organized in March 6–9, 2013 in Zagreb, Croatia, with participants from the region and Japan. The UL FGG was

represented in the International Scientific Committee, and the proceedings of the symposium are planned to be available until the end of 2013. More details on the network can be found in a paper published in the journal *Landslides* under the topic ICL/IPL Activities (Mihalić Arbanas et al. 2013).

The ICL Landslide Monitoring and Warning Thematic Network

The ICL Landslide Monitoring and Warning Thematic Network is a joint effort of ten ICL member organizations and two ICL supporters from eight countries; five of them are active ICL World Centers of Excellence in Landslide Risk Reduction in the period 2011–2014. The UL FGG was the initiation institution that proposed this network, and is also coordinating its activities, together with the Croatian Landslide Group (Prof. Arbanas) and the Forestry and Forest Product Research Institute, Tsukuba, Japan (Prof. Ochiai). The general objective of this thematic network is to compare experiences in the field of landslide monitoring and existing/installed (early) warning systems for active landslides in different regions of the world (Mikoš 2012).

At UL FGG we started in 2013 to put together a broad database on different techniques used for landslide monitoring with as detailed as possible descriptions of different landslides used as case studies. On such a basis we will develop a web questionnaire to be filled in on-line by landslide experts, to gain a broad knowledge of the expertise available in the world on the topic of landslide monitoring. More details on the network can be found in a paper published in the journal *Landslides* under the topic ICL/IPL Activities (Mikoš 2012).

IPL-151 Project “Soil Matrix Suction in Active Landslides in flysch: The Slano Blato Landslide Case”

The Slano Blato landslide is one of the largest and the most active landslides in Slovenia. In dry periods the landslide behaves as a group of several slow moving landslides, while in wet periods it moves mainly as a viscous earth flow, with the occurrence of rapid mudflows that endanger Lokavec Village. To protect the village a series of shafts were constructed in the upper part of the landslide (Pulko et al. 2013).

In 2007 the positive effect of matrix suction on shear strength of clayey soil was observed by Petkovšek (2006). Later it was decided to use matrix suction observations as an indicator of landslide stability. This was one of the main research fields of the IPL-151 project; the other was detection of flysch degradation using suction measurements.

After the first 2 years it was observed that, when suction drops below an anticipated threshold, some mass movements were observed at Slano Blato landslide. However, the main landslide body remained virtually unmoved (Petkovšek et al. 2009, 2013).

To better understand soil behaviour at Slano Blato landslide, a series of laboratory tests were performed in 2011 and 2012. A simple shear apparatus was modified for suction control and the water retention curves at different vertical loads were measured. Later a series of shear creep tests at different vertical loads, matrix suctions and constant shear stress ratios were performed using the same apparatus.

Based on measurements of the water retention curves, it was concluded that there is only one soil water retention curve in relation to degree of saturation—suction and that volume deformations are important for the calculation of water movement in clayey soils. For water movement calculations a 1D numerical model was made and back analysis of water movements for period 2007–2012 was performed. To obtain meaningful results, the evaporation from the surface was reduced to 1/3 of potential evaporation. This reduction may be a result of a thin layer of coarse grains (debris) that has accumulated on the landslide surface.

During the shear creep tests, significant excess pore pressures were generated during instantaneous shear loading. The excess pore pressure changed effective stresses in the specimen and the initial shear deformations, and also caused scatter in the measured creep rate. This prevented any conclusions regarding the shear creep rate—suction—total stress relations. However, the measured creep deformations as measured at Slano Blato landslide were at least ten times smaller. Later it was found that landslide movements could be explained more reasonably by loss of stability ($F = 0.99$), due to the increased pore pressure during low suction conditions (i.e., winter) and that small movements are the result of acting viscous forces.

The project results were part of a PhD thesis (Maček 2012) and were presented at several conferences (Maček et al. 2012a, b). The project also initiated scientific cooperation with the Institute for Geotechnical Engineering at the ETH Zurich (Prof. Springman) at the master student level that resulted in the field work at the Slano Blato landslide and several contributions to the annual conference of the European Geosciences Union (Askarinejad et al. 2013a, b, c).

National Research Program “Hydrotechnics, Hydraulics and Geotechnics” (2009–2013)”

Mid-term research programs are one of the main research policy forms in Slovenia to financially support basic research. In this specific research program, four chairs from the UL FGG cooperate with the Institute for Hydraulic

Research IHR (Ljubljana). Among the many topics covered, landslide research is an important topic. Though the landslides in Slovenia can also be earthquake-induced (Mikoš et al. 2012a), the central focus was on rainfall-induced landslides.

Stogovce Landslide

In September 2010 a heavy 4-day rainfall, totaling 300–520 mm of rain, caused large floods and triggered numerous new and old landslides in the Vipava River valley. One of them, the Stogovce landslide, which is located in the vicinity of Slano Blato landslide, destroyed a local road, 15 ha of forests and electricity for a water supply station for nearby villages (Petkovšek et al. 2011).

The Stogovce landslide is located approximately 200 m below the overthrust zone of Mesozoic carbonate rock on Eocene flysch. The slopes were covered with a maximum 10 m thick layer of limestone debris colluvium, which slipped along the flysch bedrock. The unstable masses present serious potential risk if they transform into a fast-moving debris flow. The debris flow could damage Slokarji village, as well as the infrastructure in the Vipava River valley. Such events were already reported in the past. The soils from Stogovce landslide also have similar characteristics to soils from Stože landslide, where a debris flow destroyed Log pod Mangartom village (Petkovšek et al. 2011). A retention barrier for possible moved masses was made at Stogovce landslide, together with its monitoring. The solution is different to that for Stože landslide, where a debris-flow breaker was constructed (Mikoš and Kryžanowski 2011) and most endanger houses were moved. The relocation of the local population produced tensions between them and geotechnical experts (Mikoš 2011a).

To monitor the movements of the landslides, six automatic GPS and gyroscopic sensors were designed and installed for 24/7 observations. The gyroscopic sensors would allow detection of position in the event of large movements in which the GPS antenna could be covered by the debris.

Mathematical Modelling of Debris Flows

In Slovenia, DEM5 and DEM12.5 data are publicly available. The aim of our basic research was to assess the usefulness of this public topographic data for debris flow-modeling (using Flo-2D model) and to compare this data to LiDAR-derived data (Sodnik et al. 2011) (Fig. 1).

The morphological accuracy of these datasets is questionable because of their development methods and their low morphologic resolution. A better solution is LiDAR-derived

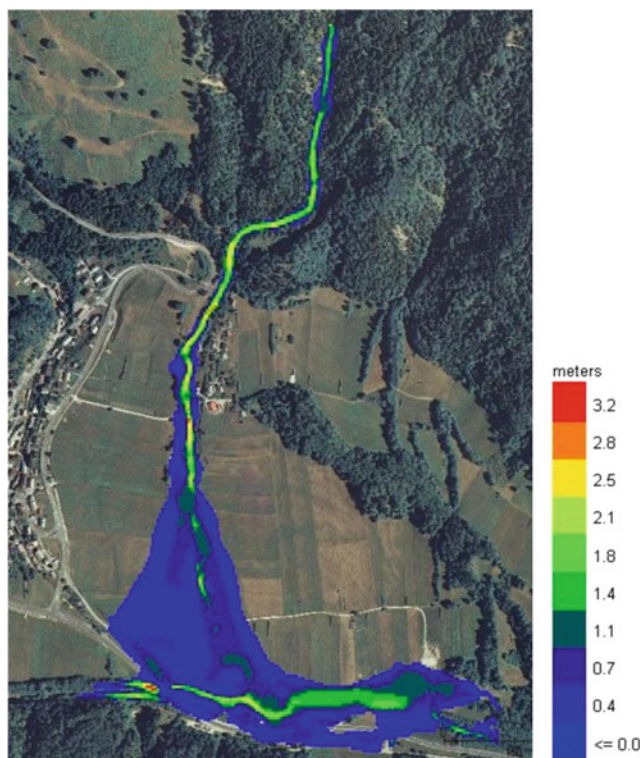


Fig. 1 Maximum debris-flow depths (in m) on the Suhelj torrential fan. The numerical 2D model Flo-2D used numerical grid 5×5 m: debris-flow ($C_v = 0.42$) $Q_{\max} = 34 \text{ m}^3/\text{s}$, and flash flood $Q_{100} = 24 \text{ m}^3/\text{s}$

data with higher resolutions and multiple options for further improvements using different methods and algorithms. The results with LiDAR data are more accurate; the torrent channel is better expressed (Sodnik et al. 2012a, b). One downside of LiDAR data is its high price, which prevents wider usage of more precise data. Another downside is the much longer computational times of the model. More precise data means a more irregular surface of the computational grid, which results in the need for shorter computational steps to ensure numerical stability. We proposed new methods for LiDAR-derived DEM improvements. With modified data, computational times were much shorter and results were even more precise than with non-modified DEMs.

Torrent Check Dams as Debris-Flow Sources

Large dams represent a threat should they collapse. In Slovenia large dams are covered by legislation and there are assessments of the spatial consequences of their failure. Since Slovenia is an alpine country, numerous torrent structures were built in the last century. All these structures are considered in legislation as easy or less demanding

structures with regard to their construction, and no risk assessment is required when planning and building them. In Slovenia, there are over one thousand torrent structures (such as check dams), but no hazard assessment exists for them in case of their failure.

Within the framework of the research project “Earth- and concrete dams of the strategic importance in the Republic of Slovenia (2011–2012)”, we proposed a procedure for qualitative evaluation of the hazard rate due to failure of torrent check dams. The procedure was tested for a chain of torrent check dams in the Suhelj torrent fan in NW Slovenia. Case study of the Suhelj torrent shows that also smaller torrent structures can represent a considering threat and that such structures should also be considered using methods comparable to those for large dams. The results of mathematical modeling of potential debris flows on the fan using a two-dimensional numerical model (Flo2D) confirm that a potential debris flow initiated by a failure of check dams in this torrent truly impose a hazard to the torrent fan area.

Alpine Space EU Project PARAMount (2009–2012)

The European research project called PARAMount (“imProved Accessibility: Reliability and security of Alpine transport infrastructure related to mountainous hazards in a changing climate”; 2009–2012) covered selected natural hazards (avalanches, rock falls, and debris flows) and their impact on traffic routes. For debris flows, the field activities in Slovenia were conducted in two test regions (Mikoš et al. 2012b, c; Sodnik and Mikoš 2012a, b, c).

The densely populated Koroška Bela torrent fan is in the Jesenice Municipality (debris flows, historical debris-flow event in 1789); here debris flows triggered in the active landslide source in the hinterland of the fan could potentially endanger the regional road R2-452 between Žirovnica and Jesenice ($>6,000$ vehicles/day) and the railway connection between Ljubljana and Jesenice (68 trains/day in 2008). We applied the Flo2D model to determine the run-out zones in order to establish a debris-flow hazard map (Fig. 2).

In the Bohinjska Soteska gorge along the Sava Bohinjka River, debris flows caused road and railway interruptions during heavy rains in 2007. Here debris flows during thunderstorms occasionally interrupt the railway track from Jesenice to Nova Gorica (44 trains/day) and the parallel main state road R1-209 between Bled to Bohinjska Bistrica ($\sim 4,000$ vehicles/day). We assessed the area of influence of debris-flows based on geological survey and debris flow susceptibility maps. We applied the TopRunDF model to determine the run-out zones in order to establish a preliminary debris-flow hazard map (Fig. 3).

Fig. 2 Debris-flow hazard map for the Koroška Bela torrent fan determined by a 2D mathematical modeling of debris flows (from the PARAMount project final report)

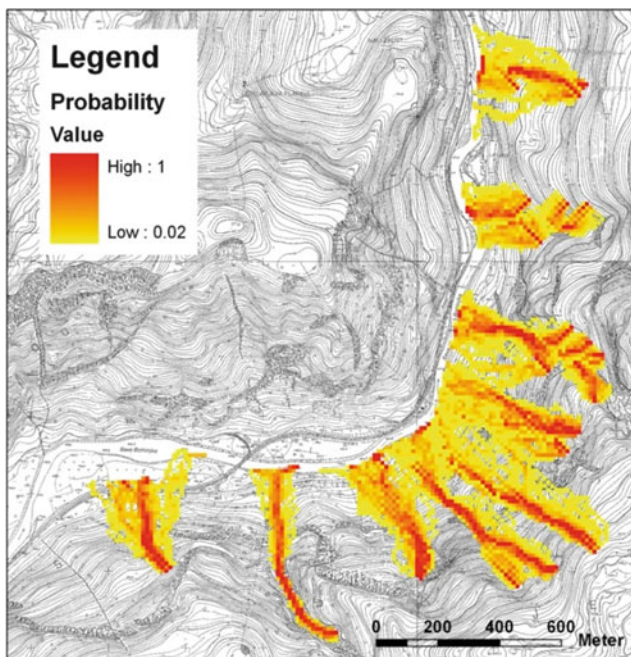
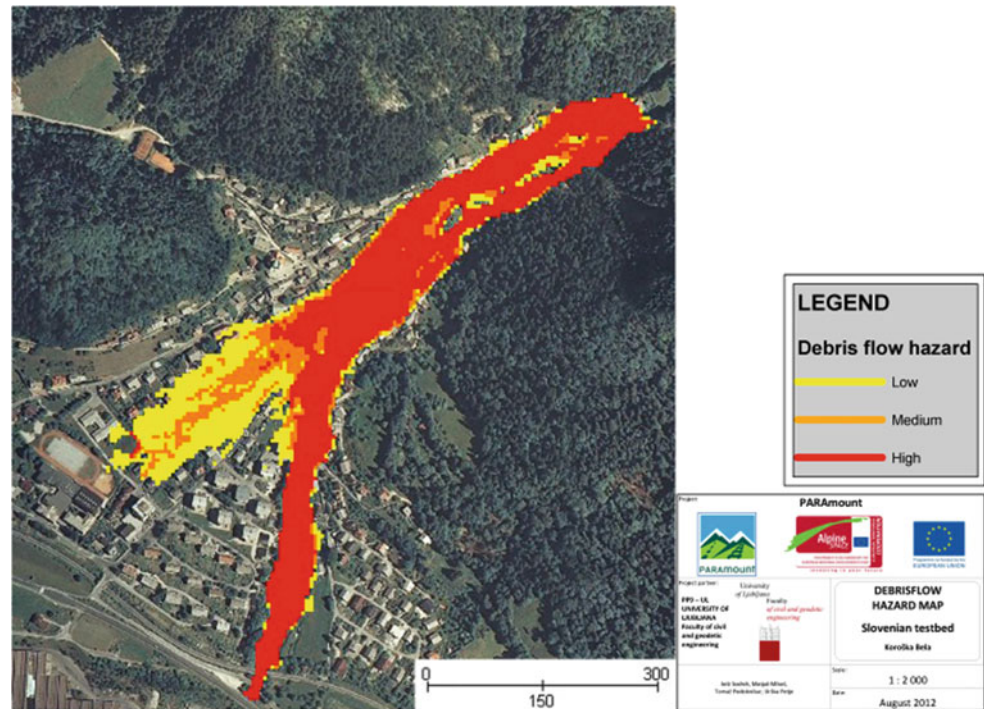


Fig. 3 Preliminary debris-flow hazard map (scale 1:15,000) for the Sava Bohinjka River gorge determined by the TopRunDF model (Fidej 2011)

The aim of the study was to assess the function of beech-dominated forests in protection against debris flows. Forest structure data was obtained from 26 sample plots. A detailed description and delineation of forest stands was performed (method NaiS). The results showed that these forests play an

important role in the protection of infrastructure. Forest protection efficiency can be improved by careful planning of regeneration patches over time and space. Since these forests have not been managed for several decades, natural disturbances (wind throws) are frequent. Research results suggest that assessment and management of these beech-dominated protection forests is necessary, contrary to the current practice of non-management in protection forests in Slovenia.

Acknowledgments The research activities within the framework of the WCoE at UL FGG were supported by the Research Agency of Slovenia (ARRS): research programme P2-0180 “Hydrotechnics, hydraulics and geotechnics” & targeted research project L4-2244 “Protective forests: development principles, risk assessment, coordination of silviculture and utilization technologies”. The Ministry of Defence of the Republic of Slovenia financed the research project “Earth- and concrete dams of the strategic importance in the Republic of Slovenia (2011–2012)”.

Furthermore, the UL FGG staff collaborated in two projects of the EU Alpine Space programme: project PARAMount (“imProved Accessibility: Reliability and security of Alpine transport infrastructure related to mountainous hazards in a changing climate”; 2009–2012) and project SedAlp (“Sediment management in Alpine basins: integrating sediment continuum, risk mitigation and hydropower”; 2012–2015).

References

- Askarinejad A, Leu P, Maček M, Petkovšek A, Springman S (2013a) Prediction of the run out extents of the Slano Blato landslide for future debris flow events. *Geophys Res Abstr* 15: EGU2013-12360-1
- Askarinejad A, Molinari O, Maček M, Petkovšek A, Springman S (2013b) Drainage efficiency of large dowels as a stabilising

- measure, case study of Slano Blato (Slovenia). *Geophys Res Abstr* 15:EGU2013-12302-1
- Askarinejad A, Secchi B, Maček M, Petkovšek A, Springman S (2013c) Effect of unstable layer depth on the pore pressure distribution, case study of the Slano Blato landslide (Slovenia). *Geophys Res Abstr* 15: EGU2013-12249-3
- Fidej G (2011) Assessment of protective effect of forest against debris flows along Sava Bohinjka in Soteska gorge. Graduation thesis, University of Ljubljana BF, Ljubljana, Slovenia. http://www.digitalna-knjiznica.bf.uni-lj.si/dn_fidej_gal.pdf Last Accessed 12 Jul 2013
- Maček M (2012) Vpliv matrične sukcije na pomike plazu Slano blato – The influence of matrix suction on the movements of Slano blato landslide. PhD thesis, University of Ljubljana FGG, Ljubljana, Slovenia. http://drugg.fgg.uni-lj.si/3994/1/GRD226_Macek.pdf. Last Accessed: 12 Jul 2013
- Maček M, Majes B, Petkovšek A (2012a) Gibanje vode v plazu Slano blato = Movement of water in Slano blato landslide. In: Proceedings of the 6th Symposium of the Slovenian geotechnical society, 14–15 June, 2012, Lipica, Slovenia. pp 249–262
- Maček M, Mikoš M, Petkovšek A, Majes B (2012b) Influence of soil suction on stability of landslide. In: Zbornik radova XIV. simpozijuma iz inženjerske geologije i geotehnike sa međunarodnim učešćem, 27–28 September 2012. Beograd, Serbia, pp 479–488
- Mihalić Arbanas S, Arbanas Ž, Mikoš M, Abolmasov (2012a) The ICL Adriatic-Balkan Network: scientific background, opportunities and challenges for regional cooperation. In: Proceedings IPL symposium Kyoto, 20 January 2012. Kyoto, Japan, pp 27–37
- Mihalić Arbanas S, Arbanas Ž, Abolmasov B, Mikoš M, Komac M (2012b) Regional cooperation in the frame of the ICL Adriatic - Balkan network. In: Zbornik radova XIV. simpozijuma iz inženjerske geologije i geotehnike sa međunarodnim učešćem, 27–28 September 2012. Beograd, Serbia, pp 43–52
- Mihalić Arbanas S, Arbanas Ž, Abolmasov B, Mikoš M, Komac M (2013) The ICL Adriatic-Balkan Network: analysis of current state and planned activities. *Landslides* 10(1): 103–109. doi: [10.1007/s10346-012-0364-2](https://doi.org/10.1007/s10346-012-0364-2), [10.1007/s10346-012-0364-2#doi](https://doi.org/10.1007/s10346-012-0364-2#doi)
- Mikoš M (2011a) Public perception and stakeholder involvement in the crisis management of sediment-related disasters and their mitigation: the case of the Stože debris flow in NW Slovenia. *Integr Environ Assess Manage* 7(2):216–227. doi:[10.1002/ieam.140](https://doi.org/10.1002/ieam.140)
- Mikoš M (2011b) Landslides: a state-of-the art on the current position in the landslide research community. *Landslides* 8(4): 451–551. doi: [10.1007/s10346-011-0297-1](https://doi.org/10.1007/s10346-011-0297-1), [10.1007/s10346-011-0297-1#doi](https://doi.org/10.1007/s10346-011-0297-1#doi)
- Mikoš M (2012) The ICL landslide monitoring and warning thematic network. *Landslides* 9(4): 565–569. doi: [10.1007/s10346-012-0359-z](https://doi.org/10.1007/s10346-012-0359-z), [10.1007/s10346-012-0359-z#doi](https://doi.org/10.1007/s10346-012-0359-z#doi)
- Mikoš M, Kryžanowski A (2011) Debris-flow breakers as an unconventional dam type. In: Proceedings of the international symposium Dams – recent experiences on research, design, construction and service, 17–18 November 2011. Skopje, Macedonia, pp 63–70
- Mikoš M, Petkovšek A, Majes B (2009) Mechanisms of landslides in over-consolidated clays and flysch: Activity scale and targeted region: national. *Landslides* 6(4): 367–371. doi: [10.1007/s10346-009-0171-6](https://doi.org/10.1007/s10346-009-0171-6), [10.1007/s10346-009-0171-6#doi](https://doi.org/10.1007/s10346-009-0171-6#doi)
- Mikoš M, Jemec Auflič M, Ribičič M, Čarman M, Komac M (2012a) Earthquake-induced landslides in Slovenia: historical evidence and present analyses. In: Ugai K, Yagi H, Wakai A (eds) Earthquake-induced landslides. Springer, Berlin, pp 225–233, 996 p. ISBN: 978-3-642-32237-2
- Mikoš M, Sodnik J, Podobnikar T, Fidej G, Bavec M, Celarc B, Jež J, Rak G, Papež J (2012b) PARAMount – European research project on transport infrastructure safety in the Alps. In: Proceedings of the IPL symposium Kyoto, 20 January 2012. Kyoto, Japan, pp 111–118
- Mikoš M, Bavec M, Celarc B, Fidej G, Jež J, Podobnikar T, Sodnik J (2012c) Debris-flow impacts on roads – results of the European research project PARAMount. In: Proceedings of the 11th Slovenian road and Transport Congress, 24–25 October 2012. Portorož, Slovenia, pp 1–8
- Petkovšek A (2006) Vpliv matrične sukcije na trdnostno deformacijske lastnosti zemljin = The influence of matrix suction on strength and stiffness of soils. PhD thesis, University of Ljubljana FGG, Ljubljana, Slovenia
- Petkovšek A, Maček M, Kočevar M, Benko I, Majes B (2009) Soil matrix suction as an indicator of the mud flow occurrence. In: 17th International conference on soil mechanics and geotechnical engineering, vol 3, Alexandria, Egypt, pp 1855–1860
- Petkovšek A, Fazarinc R, Kočevar M, Maček M, Majes B, Mikoš M (2011) The Stogovce landslide in SW Slovenia triggered during the September 2010 extreme rainfall event. *Landslides* 8(4): 499–506. doi: [10.1007/s10346-011-0270-z](https://doi.org/10.1007/s10346-011-0270-z), [10.1007/s10346-011-0270-z#doi](https://doi.org/10.1007/s10346-011-0270-z#doi)
- Petkovšek A, Maček M, Mikoš M, Majes B (2013) Mechanisms of active landslides in flysch. In: Sassa K, Briceño S, McSaveney M, He B, Rouhban B (eds) Landslides: global risk preparedness. Springer, Berlin, pp 149–164
- Pulko B, Majes B, Mikoš M (2013) Reinforced concrete shafts for the structural mitigation of large deep-seated landslides: an experience from the Maccesnik and the Slano blato landslides (Slovenia). Landslides (published on web): 1–11. doi: [10.1007/s10346-012-0372-2](https://doi.org/10.1007/s10346-012-0372-2), [10.1007/s10346-012-0372-2#doi](https://doi.org/10.1007/s10346-012-0372-2#doi)
- Sassa K (2012) ICL strategic plan 2012–2021 – To create a safer geo-environment. *Landslides* 9(2):155–164. doi:[10.1007/s10346-012-0334-8](https://doi.org/10.1007/s10346-012-0334-8)
- Sodnik J, Mikoš M (2012a) Koroška Bela: presentation of torrential testbed and debris flow phenomena research. Paramount Post Graduate Course, Innsbruck, 23–25 October, 2012. Innsbruck, Austria, 20 p. <http://paramount-project.eu/downloads/Session8.pdf> Last Accessed 12 Jul 2013
- Sodnik J, Mikoš M (2012b) Natural hazards in Slovenia: regional settings, legislation, hazard assessment and prevention. Paramount Post Graduate Course, 23–25 October, 2012. Innsbruck, Austria, 30 p. <http://paramount-project.eu/downloads/Session8.pdf>. Last Accessed 12 Jul 2013
- Sodnik J, Mikoš M (2012c) Recent developments in assessing debris-flow hazard in Slovenia. In: Proceedings of the 2nd project workshop of the Croatia – Japan project on risk identification and land-use planning for disaster mitigation of landslides and floods in Croatia, 15–17 December 2011. Rijeka, Croatia, pp 159–162
- Sodnik J, Podobnikar T, Petje U, Mikoš M (2011) Topographic data and numerical debris-flow modeling. Book of abstracts of the 2nd World Landslide Forum, 3–9 October, 2011. Rome, Italy, p 151
- Sodnik J, Podobnikar T, Mikoš M (2012a) Using lidar data for debris flow modelling. In: Proceedings of the 12th Congress Interpraevent, 23–26 April 2012. Grenoble, France, pp 573–583
- Sodnik J, Vrečko A, Podobnikar T, Mikoš M (2012b) Digital terrain models and mathematical modelling of debris flows. *Geodetski vestnik* 56(4): 826–837. http://www.geodetski-vestnik.com/56/4/gv56-4_826-837.pdf. Last Accessed 12 Jul 2013



Slope Data Acquisition Along Highways in Sabah State for Hazard Assessment and Mapping

Shabri Shaharom, Che Hassandi Abdullah, and Roslan Majid

Abstract

The need of expenditure for remedial works for slope failures due to landslides in Malaysia have been increasing. The increase number of slope failures is related to heavy rain and rapid development in Malaysia. In 2011, an estimated USD 65 million was needed to repair slopes along highways across the country. Out of the total requirement, only USD 20 million a year were provided to repair these slopes. To fit to this situation, prioritization of slope repairs according to scale of damage and public safety, is being implemented. Looking at this scenario into the future, it is time to divert the slope maintenance to a more systematic method by emphasizing landslide prevention. Slope data acquisition is a first step to ensure success in the Malaysian highway slope maintenance program. Slope data collection in Sabah is the first phase towards a full systematic slope maintenance program in 2013. A few of the obstacles faced during the implementation of this project are heavy rainfall, lack of knowledge on the database needed and differences of management between agencies.

Keywords

Sabah • Slope maintenance • Slope data acquisition

Introduction

Malaysia is a country located in Southeast of Asia, occupying about 330,200 km². Malaysia is divided into two main regions; Peninsular Malaysia and East Malaysia. Peninsular Malaysia lies just south of Thailand and north of Singapore; East Malaysia consisting of Sabah and Sarawak is the northern one-third of the island of Borneo bordering Indonesia and Brunei (Fig. 1).

With a population of about 28.3 million (updated by the Department of Statistics Malaysia on 5th August 2011), the country has a multiracial society with a racial composition consisting of Malay, Bumiputera Sabah Sarawak, Chinese,

Indian and others at a proportion of 50 %, 17.4 %, 24.6 %, 7.3 % and 0.7 %, respectively.

Sabah is a state located in East Malaysia. The western part of Sabah is generally mountainous, containing the three highest mountains in Malaysia. The most prominent range is the Crocker Range with several mountains with heights from about 1,000 m to 4,000 m. At the height of 4,095 m, Mount Kinabalu is the highest mountain in Malaysia and the 10th highest mountain in Southeast Asia. Roads have to be built across these mountainous areas, exposing users to landslide risk. Figure 2 shows the terrain map of Sabah.

Slope Maintenance Management in Sabah

Current Situation

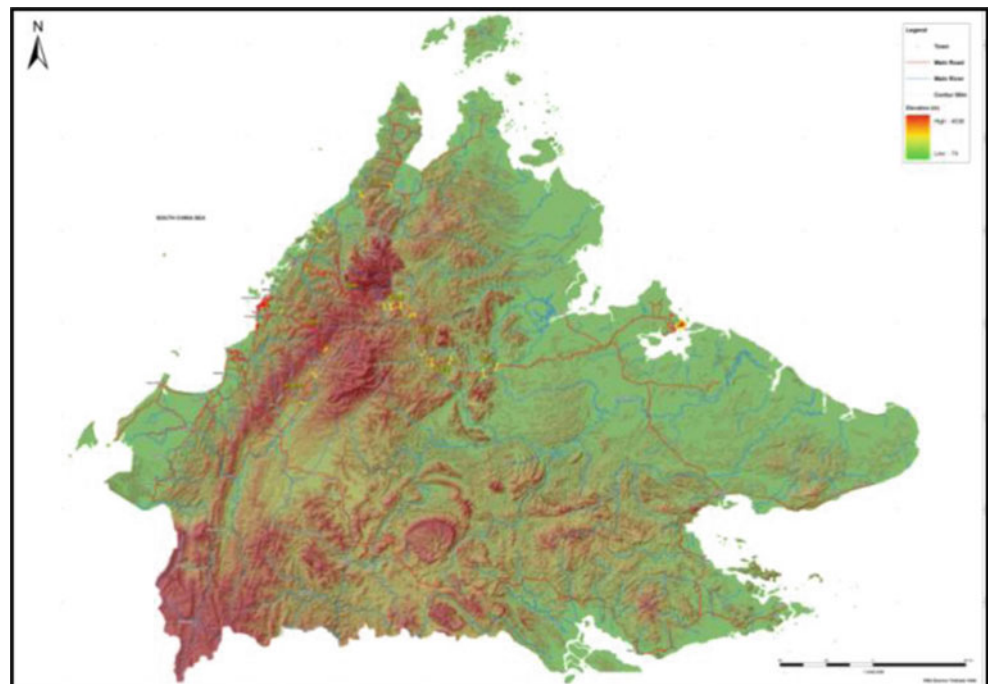
At present, the maintenance of slopes in the state of Sabah is implemented partly upon inspection when signs of distress occur on the slope surface and partly on an ad-hoc basis

S. Shaharom (✉) • C.H. Abdullah • R. Majid
Slope Engineering Branch, Public Works Department (Jabatan Kerja Raya Malaysia), Ministry of Works, Jalan Sultan Salahuddin, 50582 Wilayah Persekutuan Kuala Lumpur, Malaysia
e-mail: Shabri@jkr.gov.my; Hassandi@jkr.gov.my; Roslanm@jkr.gov.my

Fig. 1 Geographical map of East Malaysia



Fig. 2 Terrain level map of Sabah



when failure has already occurred. Maintenance is mostly focused on treating the failed slopes where remedial works are limited to a certain scale of damage and cost of remedial work to less than USD 150 thousand per site.

By implementing this approach the department manage to remediate 37 slopes along highways of Sabah in 2012 to a total cost of USD 3.3 million per year. For slope failures that exceed the limit of damage and cost, a special fund is used.

In 2009, Slopes Engineering Branch, Public Works Department put all the effort to record approximately 4,000 slopes along Sabah Highway. The data were collected by ground survey and airborne LiDAR survey.

Slope Maintenance Programmes Along Highways in State of Sabah

In 2011, a Slope Maintenance Program in Highways in Sabah was being developed and was planned to be launched in mid 2012. This program will be implemented in two phase. Phase I is the Slope Data Acquisition which will be implemented in a period of 6 months. Followed by Phase II that is the maintenance and the inspection works on all 4,000 slopes in the state of Sabah for the time frame of 5 years.

Slope Data Acquisition Along Highways in the States of Sabah

Slope Data Acquisition along highways of Sabah includes data collection for approximately 4,000 slopes for a total cost of USD 10 million. These slopes are located along 22 Federal Roads in the state of Sabah which total up to 1,520 km.

Global Positioning System (GPS) and mobile Geographical Information System (GIS) technology and airborne LiDAR are applied at the fullest for this purpose.

Along with this data collection task, a system will be developed to facilitate storage, retrieval, manipulation and analysis of the data. It will also facilitate the integration of ground and airborne data. The development of the system will be based on GIS format using the Windows platform. All the data will be geo-referenced according to the local coordinate system. The formula used for the assessment of slope hazard will be customized in the system. It will then be able to analyze the slope data to produce hazard maps. These maps will be disseminated to the end-users via internet.

Objectives of Slope Data Acquisition

The project consists of four main objectives [3, 4, 5]. These objectives are set as guidelines throughout the implementation of the projects. The objectives are:

1. to establish spatial and non-spatial databases for slope assessment and mapping;
2. to produce hazard and risk maps;
3. to provide a 'decision-support system' for the slope maintenance program;
4. to identify potential problem areas;
5. to monitor and control the slope maintenance program and work

Resources Necessary for the Project

Rugged terrain in Sabah make it impossible to climb some hills or to descend into some ravines to check the slope condition. To overcome this access problem, a special team equipped with special gadgets and technology needs to be formed to collect the aforesaid data. With proper and reliable data, a proper slope maintenance program should be planned ahead thus reducing the impact and vulnerability caused by landslide incidents. About 140 workers are deployed to

Table 1 Stages of work plan for slopes data acquisition along highways in the state of Sabah

Stage	Activities
1	Field data collection works—raw data
2	Airborne laser scanning (LiDAR) and aerial photo imaging—raw point cloud data
3	GIS data integration—database
4	Data extraction (quantity) for maintenance contract purpose
5	Slope hazard and risk assessment and mapping—hazard and risk map
6	System development—integrated slope maintenance system

complete the job in 6 months. This team will be divided into sub-units and each sub-unit will consist of Climbing Specialist, Senior Engineer, Geologist, Civil Engineer, and General Workers. For the system-development team there are IT Personnel, GIS Personnel, System Analyst etc.

Work Plan

The implementation of this project will be subdivided into six stages. The stages are designed to ensure a smooth program that covers all the components needed. These stages of the projects are shown in Table 1.

Stage I is the field data Collection Works. This stage fits the data collection for non mountainous road. Data collection will be done through walking and on site assessment. Ground data collection for these projects are mainly conducted in town area where the ground is flat and access to slope is easy. These town area are identified as Kota Kinabalu, Sandakan to Lahad Datu, Pandewan to Pensiangan.

A specific type of form named the JKR Primary Data Capture proforma are to be filled and completed. General information of slopes such as location and GPS coordinate are taken. The forms also includes other important information of slopes such as feature type of slopes, such as height, slope angle, slope shape, slope cross-section, plan profile, cutting-topography relationship, feature aspect, structures present, upslope/and downslope geometry and geological feature. Facilities surround the slopes are also taken to complete the survey proforma.

Stage 2 involves the Airborne Laser Scanning by Light Detection and Ranging (LiDAR) and Aerial photo on the ground surface. This method is done to cover all mountainous roads and slopes that have limited accessibility on the ground. LiDAR onboard equipment is set up on a fixed-wing aircraft for endurance and clear imagery. Flight and route of flying are planned to the very detail to ensure maintenance of accuracy.

Data from these two methods are then collected and integrated into a database system. This is the stage where information is massaged, and stitched together and missing elements are spotted and rectified.

Stage 4 is the data extraction from the raw data collected from site for contract purposes. These data will mainly be used for the second phase of the maintenance programmes.

The next stage will involve Slope Hazard Assessment and Map production. This stage will evaluate each slope according to the attributes taken from the previous stages and categorize it to a certain hazard rating. Hazard rating implemented by Slope Engineering Branch, Public Works Department is shown in Table 2 [1, 2, 3, 4, 5].

The concept of LiDAR—satellite positioning technology determines the location of the aircraft with respect to the terrain as shown in Fig. 3.

Hazard Mapping are then plotted to be analysed and applied for the second phase of the maintenance project. The map will have the function to identify areas of either existing or potential slope instability thus leading to designed maintenance needed for a specific slope. Figure 4 shows example of hazard mapping along highways.

The last stage, is the stage that will be develop along the implementation even from the first stage. Database containing data of each and every slope and the slopes properties are compiled and recorded into a system that will ease retrieval of information. This system will also provide information on what each slope needs for maintenance and upgrades.

Deliverables

Output produced from this project are:

1. Slope Hazard and Risk Map
2. Other GIS Thematic map such as contour map, hillshade, landcover, Flow accumulation and orthophoto
3. Slope Information System containing database of every slopes
4. Street-view map
5. Fly-through map

Table 2 Hazard rating and definition

Hazard rating	Definition of landslide likelihood
Very high	Certain to occur during a very adverse event; almost certain to occur during an adverse event
High	Almost certain during a very adverse event; might occur under an adverse event
Moderate	Might occur under very adverse conditions
Low	Conceivable, but only during an exceptional event
Very low	Not conceivable under almost all conditions

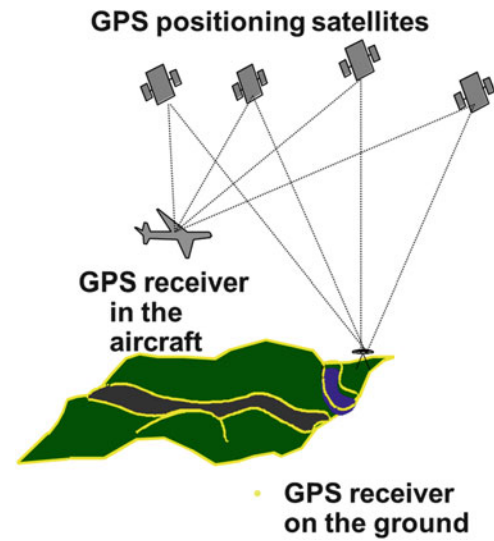


Fig. 3 Airborne LiDAR

Expected Problems Encountered

One of the keys to ensuring success in this project is the availability of landslide specialists to carry out the work. An understanding of landslide mechanisms and the characteristics of soil and rocks in tropical areas is crucial in landslide hazard formulation.

Financial allocation for this project might be limited. Priority is given to the development of infrastructure, and the landslide budget is mainly spent on repair work and only occasionally for slope upgrading work.

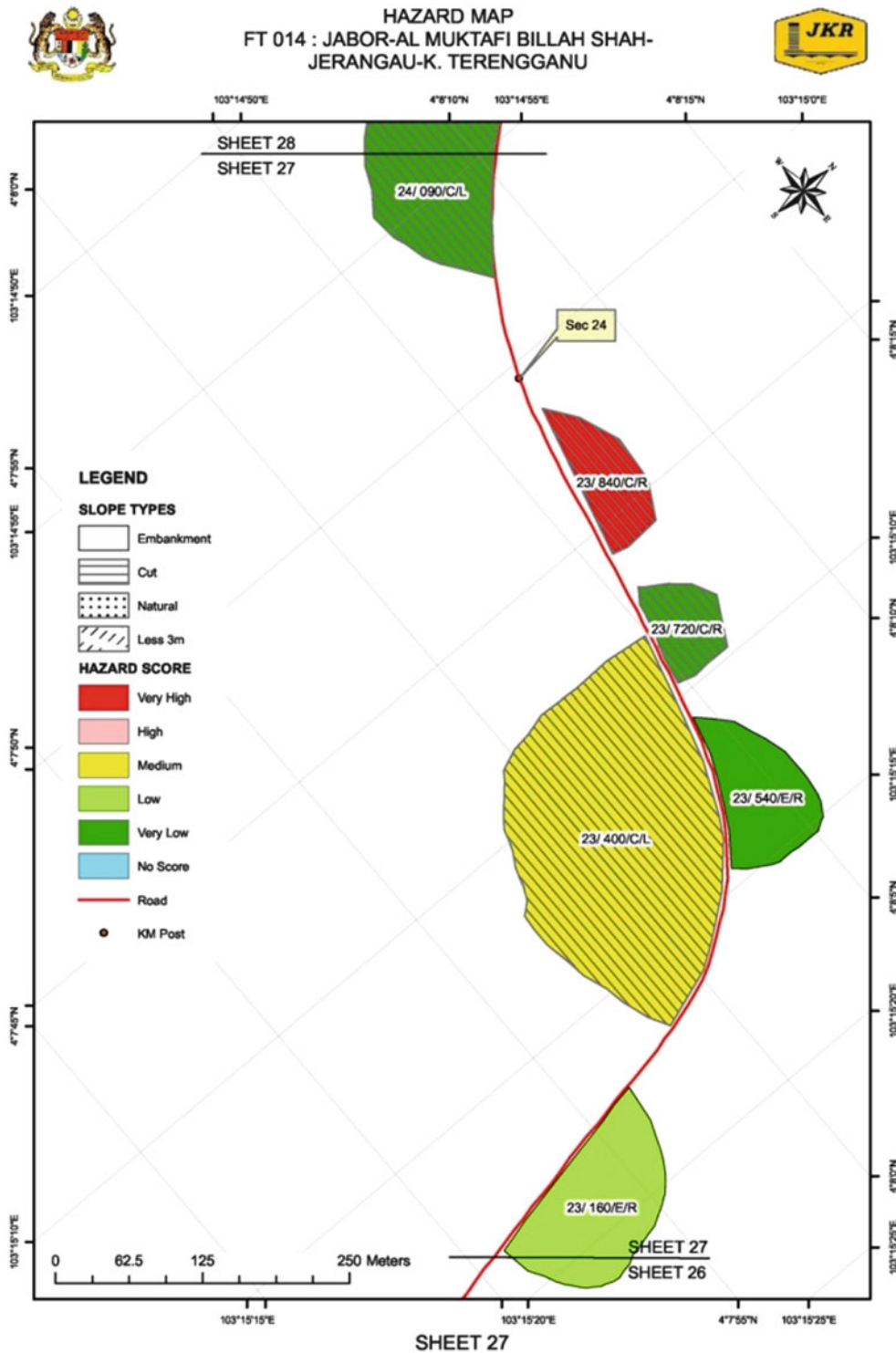


Fig. 4 Hazard Map plotted from data collected on site

References

- Othman MA (1989) "Highway cut slope instability problems in West Malaysia". Ph.D. thesis, University of Bristol, UK
- Othman MA, Llyod D, Majid R (2004) Project report on " Slope protection Study for Federal Route 22 in Sabah, East Malaysia". Public Works Department, Kuala Lumpur, Malasia
- Shaharom S, Baba F (2008) Project report on "Ulu Klang Slope Hazard Assessment Study". Public Works Department, Kuala Lumpur, Malaysia
- Shaharom S, Majid R (2011a) Project report on " Spatial data acquisition by Lidar on road slope, Peninsula Malaysia". Public Works Department, Kuala Lumpur, Malaysia
- Shaharom S (2010) Project report on "Penang Island slope hazard assessment study". Public Works Department, Kuala Lumpur, Malaysia
- Shaharom S, Majid R (2011b) Project report on " Spatial data acquisition by Lidar on road slope". Public Works Department, Kuala Lumpur, Malaysia



Climate-Change Impacts on Embankments and Slope Stability in Permafrost Regions of Bei'an-Heihe Highway

Wei Shan, Ying Guo, Chengcheng Zhang, Zhaoguang Hu, Hua Jiang, and Chunjiao Wang

Abstract

China's Bei'an to Heihe Expressway is located on the southern boundary of high-latitude permafrost, and intersects the north section of the Lesser Khingan Mountain. The geological conditions are extremely complex. In recent years, in this section, roadbed settlement, dribbling icing of roads and cut-slope landslides are increasing, threatening subgrade stability and operational safety. The mechanisms, morphological characteristics and movement of the above phenomena are very different from that in un-frozen areas. These problems are common in highway construction in high-latitude permafrost regions of Northeast China, relevant research has been included in the key research programs of China Communications Construction and international landslide programs (IPL) "Landslides Mechanism and the Subgrade Stability Controlling Measures in Island Permafrost Area (IPL-167)". Using annual average temperature data from 1954 to 2011 in Sunwu County, the relationship between annual average temperature change and permafrost distribution are analyzed. Based on the data of ground temperature, moisture, surface and landslide deformation monitoring data from 2009 to 2012 in Bei'an to Heihe Expressway K161 + 860 to K178 + 530 section which traverses the north section of the Lesser Khingan Mountain, mountain body landslide and dribbling flow ice on the road area caused by freeze-thaw, as well as landslide mechanism and motion characteristics are analyzed. Results show that: in the past 50 years, the annual average temperature in Sunwu region show a clear upward trend, permafrost degradation has accelerated. Affected by atmospheric precipitation, melting permafrost, seepage water, air temperature, geological condition and human activity, landslides and dribbling flow ice on the road area often occur. These geological problems are controlled by seasonal temperature change, affected by slope water content change, related to geological condition, and have the characteristics of low angle, intermittent, creeping.

Keywords

Climate change • Permafrost • Creeping • Landslide • Expressway

Introduction

The northeast of China is the only high-latitude permafrost region of China, in this region, snow, vegetation, water, topography, atmospheric inversion and other local factors cause local temperature variability, thus forming Khingan-Baikal type permafrost which is very different from the permafrost in polar and high-altitude regions (He et al.

W. Shan (✉) • Y. Guo • C. Zhang • Z. Hu • H. Jiang • C. Wang
Northeast Forestry University, Harbin, China
e-mail: shanwei456@163.com

2013). In recent years, affected by climate change, the southern boundary of high-latitude permafrost in Northeast China has moved north, the permafrost near the southern boundary is discontinuous, distributed as permafrost “islands” and undergoing accelerated degradation (Lin et al. 1995; Shi et al. 1995; Zhou et al. 2000; Ren et al. 2005; Ding et al. 2006).

Frozen soil is a soil medium containing ice, and is extremely sensitive to temperature change. Frozen soil has characteristic rheological properties—its long-term strength is much lower than its instantaneous strength. Precisely because of these characteristics, engineering structures in permafrost face the danger of frost heave and thaw settlement leading to uneven deformation of the roadbed and slopes, and even instability slumps.

Landsliding is a natural geological phenomenon, its occurrence mechanisms and evolution laws are closely related to the geological conditions and environmental factors, and it is controlled by the factors of geological force, lithology and landform. It also is affected by environmental changes in land cover, rainfall and human activity, and has the characteristics of uncertainty, continuity and irreversibility in space and time. Landsliding is caused by changing geological environmental conditions, it also violently changes the geological environmental condition. Because of the complexity of landslide formation and evolution and the seriousness with which landslides influence human survival and activities, people are paying more and more attention to research on landslides, getting many valuable research results. Northeast China is China’s cryopedology cradle and one of the early intensive study areas, but after thirty years of studying global climate change in this area, we only see the study of permafrost degradation affecting engineering structures in airports, roads and pipelines. There is no systematic study of climate-change influences on permafrost change in northeast high-latitude permafrost regions (Wei et al. 2010; Chang et al. 2013). In permafrost regions, study of the occurrence mechanism, movement characteristics, and disaster laws of landslides caused by permafrost melting due to climate change, extreme climate phenomena and geological condition of landslide, also is basically blank.

Herein we examine the Bei’an to Heihe Expressway in China which traverses the Lesser Khingan Mountain, and in particular, the uneven settlement of the roadbed, dribbling flow ice on cut slopes, and landslides in the road area of the K162 + 860 and K178 + 530 sections. We apply weather monitoring data from the Sunwu County meteorological station, landslide engineering geological surveys and monitoring data, to analyze the formation mechanisms and movement laws of roadbed uneven settlement, dribbling flow ice and landslides.

Study-Area Natural Condition

The study area (K153 + 440 – K184 + 100) is in the northwest section of the Lesser Khingan Mountain (N49°27′–N49°45′ and E127°12′–E127°33′). Ground elevation is 210–330 m and the relief, about 120 m, in undulating terrain. Slope is steep in some areas, and vegetation flourishes.

The basement bedrock is upper Jurassic Shenshu formation and lower Cretaceous Guanghua formation volcanic and late Indosinian granite, the covering layer is the upper Cretaceous Nenjiang formation and Tertiary Pliocene series Sunwu Formation River and Lake Facies deposition. Neotectonic movement in this area is mainly vertical movement of fault blocks, the new rift zone decreased firstly and then increased, the Tertiary Pliocene series Sunwu formation which mainly consists of coarse sand or sand conglomerate overlaps the tops of the mountain and hills. This rock has no cementation, and is in a loose state. The upper Cretaceous Nenjiang formation is exposed in the lower parts of the mountains or hills. Its lithology is mudstone, alternating fine sandstone and fine sandstone, with weak cementation, the weathering depth is large, and the near-surface portion substantially weathered. Holocene (modern) river alluvium and stack layers are distributed in the low-lying valleys.

Climate Change and Permafrost

Asymmetry of mountain distribution, slope directions and hilly areas, and wide and stable persistence of inversion layer in winter, have important impacts on the permafrost distribution, permafrost development and change processes, and permafrost features. However, the covering layer which is composed of forest, shrub, grass, moss also plays an important role in the development and protection of permafrost. Affected by inversion phenomenon, loose covering layer thickness differences, vegetation, slope direction, surface water, geological structure and other natural factors, permafrost distribution and degree of development of different geomorphologic positions in this region are obviously different. This region has mainly developed “Khingian-Baikal type” discontinuous permafrost, its main distribution characteristics are that permafrost is well developed in the relatively low-lying areas and has greater thickness. The degradation process occurs first on sunny slopes and then on shady slopes, first on high and then on low, first on mountain and then in valley.

For Fig. 1, we employed the May 3, 2011 and October 10, 2011 Landsat ETM + images, extracted thermal infrared band data, through data fusion, overlaid the June 15, 2004



Fig. 1 The permafrost distribution map of high upper limit. (Based on Landsat ETM + images)

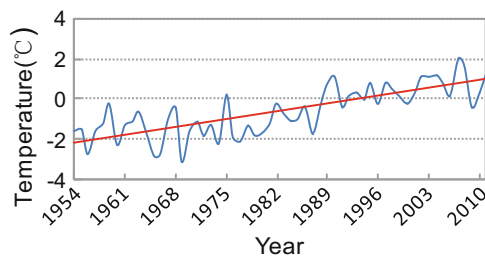


Fig. 2 Annual average temperature curve (1954–2011, Sunwu)

satellite photo of study area (from Google earth) to obtain the high upper limit of permafrost distribution map in study area. It has good agreement with survey results. The inversion results show that in the study area, the permafrost distribution has obvious “Khangai-Baikal type” discontinuous permafrost characteristics.

In the past 100 years, the global climate system has changed, from 1906 to 2005, global surface temperature has increased by $+0.74\text{ }^{\circ}\text{C}$. In China, the most significant warming region is north China, east Inner Mongolia and northeast China over the last 50 years, and the highest heating rate has been $+0.8\text{ }^{\circ}\text{C}/\text{decade}$. Our study area is located in the Sun Wu-Heihe district which has one of the highest warming rates in nearly 50 years, according to the meteorological data of Sun Wu weather station from 1954 to 2011, Sun Wu annual average temperature has risen from $-1.6\text{ }^{\circ}\text{C}$ in 1954 to $1.2\text{ }^{\circ}\text{C}$ in 2011, warming by $2.8\text{ }^{\circ}\text{C}$ (see Fig. 2).

In this study, the effect of climate change is not only reflected in the annual average temperature, but also is reflected in changes in extreme maxima and minima temperature, according to 1954–2011 monthly extreme maximum temperature (Max.T), minimum temperature, average air temperature data of Sunwu weather station (Fig. 3). Each monthly extreme maximum temperature, extreme minimum temperature, and average temperature has generally trended

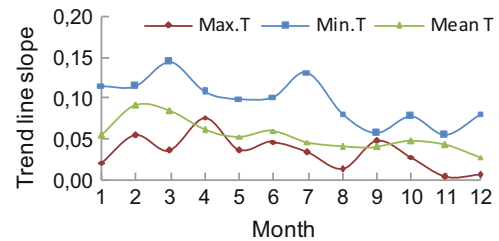


Fig. 3 Trend line slope of monthly temperature (1954–2011, Sunwu)



Fig. 4 Creeping surfaces and the distribution of melting permafrost in study area

upward in this area, the extreme minimum temperature has risen fastest, except for September, the extreme minimum temperature increase is two times the extreme maximum temperature increase, September is the month when seasonal frozen soil thawing depth is the largest in this region, from another point of view demonstrating the relationship between permafrost degradation, distribution and climate change.

Impact of Seasonal Freeze–Thaw and Permafrost Degradation

In the study area, 80 % surface is covered by larch, oak, poplar, linden, birch, coniferous and broad-leaved mixed forest, hill slopes are between $10\text{--}35^{\circ}$, slope creep surfaces are active, and the geological condition is very unstable. Carex tato, fish-scale turf, drunken forest, curved trees and other permafrost geomorphic features distribute on the slopes (Fig. 4). Figure 4 is the June 15, 2004 satellite photo of study area (from Google Earth), there are local surface folds and multi-level surfaces distributed in the area. In the photo, the red-line marked part is the geologically unstable region judged from geomorphology, the blue-line marked part is permafrost thawing water surface exposed region. C1 is the slope heading west permafrost melting area, melt water flows into the seasonal river. C2 is the cultivated land surface shallow permafrost melting area. C3 is the

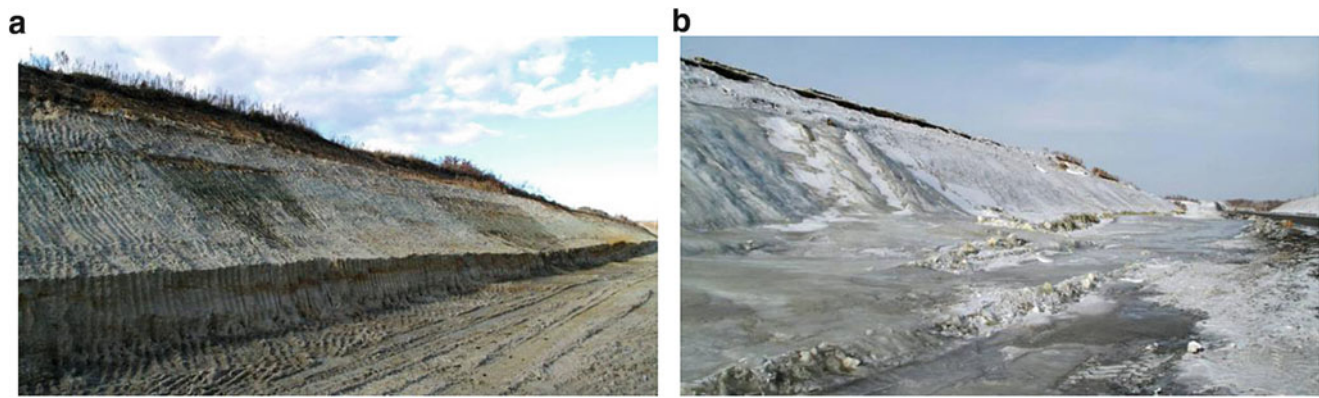


Fig. 5 Cutting slope taken in K161 + 860 section of Bei'an to Heihe Expressway (a: October 6, 2009; b: Dribbling flow ice taken on March 15, 2010)

ridge permafrost melting water exposed area, on the right side of C3 is an abandoned road where a landslide occurred during the subgrade construction in 2000, on the left side of C3 is the ridge changed section. C4 is the landslide creeping surface margin permafrost melting water exposed area. Combining with Fig. 1, the permafrost distribution map of high upper limit, it can be seen that the permafrost distribution has good agreement with regions of unstable geological conditions, so the multi-level surfaces in the study area are the result of permafrost successive degrading and surface creeping. With evolution of the climate change process, low-lying areas and deep permafrost will gradually degrade, repeated freeze-thaw and atmospheric precipitation, melting permafrost will further weaken the strength of shallow soil bodies, and promote the development of surface creeping, then lead to surface-creeping potential energy and increased landslide risk.

Mechanism and Evolution of Roadbed Uneven Settlement, Seasonal Dribbling Ice and Landslides

Soil moisture has an important impact on soil physical and mechanical properties. In permafrost regions, affected by air-temperature change, the soil body experiences freeze-thaw cycles, alternating between a three-phase and four-phase system, which drastically changes the engineering properties of the soil. The change in soil engineering properties with soil temperature is non-linear, and in permafrost regions, the engineering geological conditions are bound to change as environmental conditions change.

Seasonal dribbling ice flow is a unique geological phenomenon in very cold regions. Its occurrence is related with slope position and topography, vegetation distribution and coverage conditions, moisture and temperature in slope shallow layer, as

well as the impact of engineering structures, and has seasonal, occasional, positional uncertainty characteristics. Repeated occurrence of ice dribbles can change moisture and temperature in shallow layer of the slope, weakening soil strength, and increasing the risk of shallow landslides.

Figure 5a shows a new cut slope in the K161 + 860 section of Bei'an to Heihe Expressway. The photo was taken in the autumn, and Fig. 5b is the same place in March, after dribbling ice flow has occurred. Figure 6 is the relationship curve between soil temperatures, pore-water pressure in different depth and time (the second step of cut slope in K161 + 860 section, 1.5 m depth). In Fig. 6, as freezing progresses from the surface to deeper, the groundwater in the shallow layer undergoes increasing pressure caused by upper freezing front moving down and lower impermeable layer, this interlayer water changes from non-pressure into pressure water gradually, soil pore-water pressure increases rapidly, and reaches a peak value in early February. Soil pore-water pressure will decrease rapidly if there is a weak point somewhere on the slope that will let unfrozen confined water outflow, otherwise, the soil pore-water pressure will remain near the peak value, until the frozen layer melts in spring, when it will decrease rapidly. In summer, the soil moisture at the former position of dribbling flow ice will still be saturated or near saturation with increased landslide risk.

Because there is unfrozen water in winter, the position where dribbling flow ice often takes place has a shallower freezing depth, smaller than the average freezing depth, and there must be permafrost under this shallow groundwater layer.

In permafrost areas, due to the role of freeze-thaw and impact of permafrost on the mechanism and movement law of the landslides there are also distinctive features (Figs. 7 and 8). In Figs. 7 and 8, the slope angle of K178 + 530 section is 8.14° . Atmospheric precipitation and shallow groundwater outcropping in trailing edge provides adequate

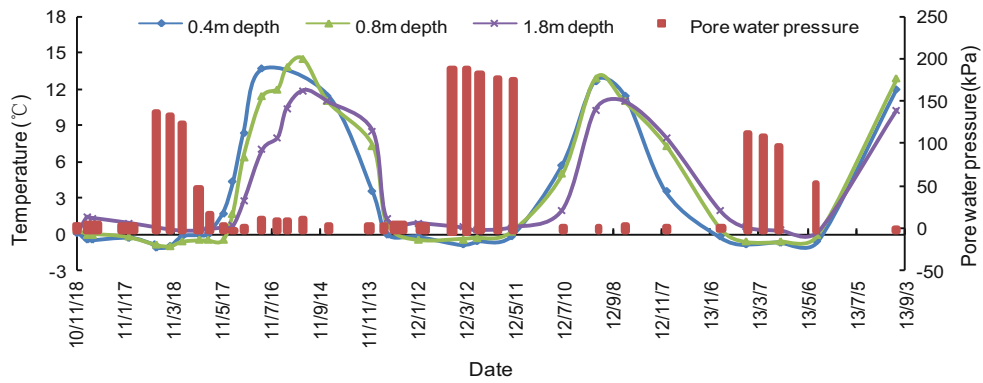


Fig. 6 Relationship curve between soil temperature, soil pore-water pressure and time in K161 + 860 section

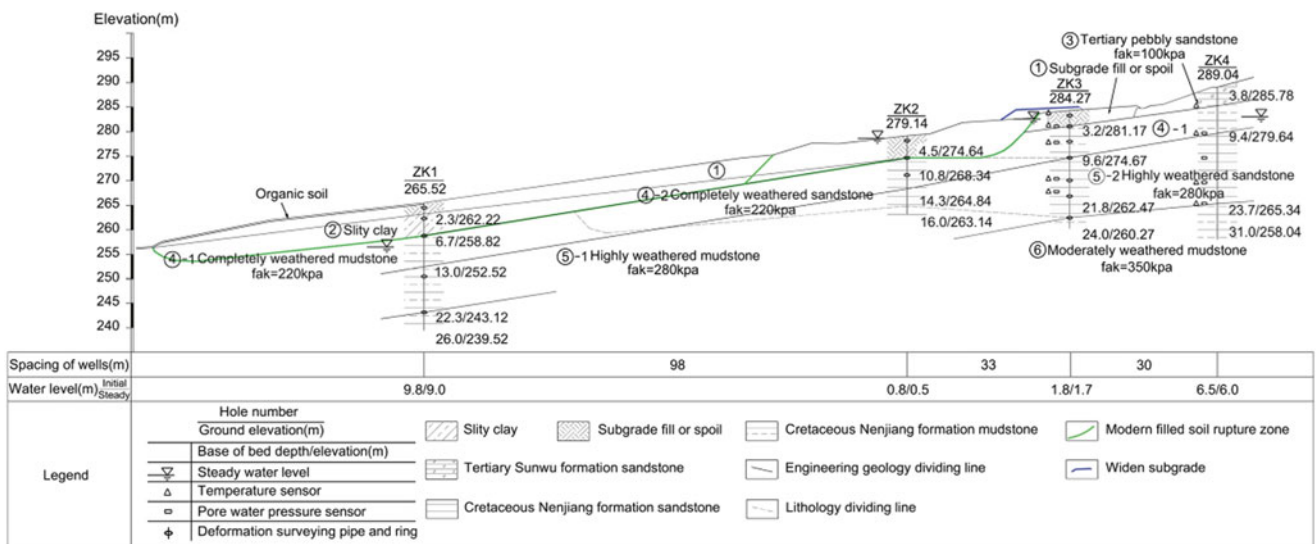


Fig. 7 Landslide geological profile and arrangement diagram of monitoring equipment (K178 + 530 section)

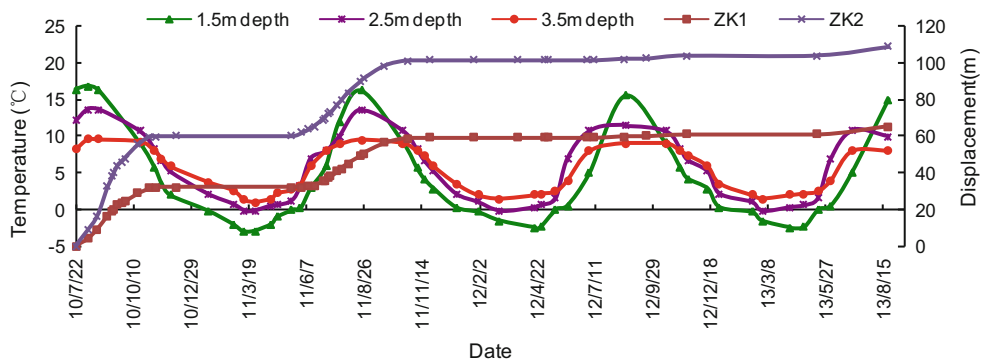


Fig. 8 Time evolution of soil temperature (1.5 m,2m,3.5 m depth) and surface displacement (ZK1, ZK2) in K178 + 530 section: ZK1 (from road shoulder 131 m), ZK2 (from road shoulder 33 m)

water to the shallow slope layer. Above a lower confining layer, the water content in a shallow layer may rise too high, leading to the sloping soil sliding along the top of the impermeable layer. The slide begins in the spring thawing period and stops after the autumn rainfall period. The slip rate in the rear is much higher than the front. Whole landslides have a low angle, intermittent motion feature.

Conclusions

Through IPL-167 project, the following conclusions were drawn:

1. Topography in high-latitude permafrost regions of Northeast China determines permafrost distribution in this area. With the accelerated process of global climate change, road area of Bei'an to Heihe Expressway through Lesser Khingan Mountain has warming trend. The annual average temperature rise in the region, not only is the reason for permafrost degradation, but also is the result of permafrost degradation.
2. Permafrost degradation in high-latitude permafrost regions of Northeast China, change the regional geological environment, and change the engineering geological conditions, which can lead to engineering geological disasters.
3. Repeated seasonal dribbling flow ice on slopes in Bei'an to Heihe Expressway through Lesser Khingan Mountain is one important cause of slope landslides. Seasonal dribbling flow ice in the road area and shallow-layer landslides are not only caused by the geological structure in this region, but also caused by the changes in geological conditions. So changes in the geological environment is the main reason for engineering geological problems.
4. The landslides in area are closely related to seasonal thawing of permafrost and seasonal frozen soil, as well as to the precipitation. They feature a characteristic low angle, intermittent motion.

The social impact of IPL-167 project achieved is:

1. Through systematic measurement of geological conditions, weather conditions and climate change in Bei'an-Heihe highway (which is near the southern boundary of high latitude permafrost and Lesser Khingan Mountain) the formation mechanism, morphological characteristics and motion of the landslides are studied to reveal the evolution of regional environmental geological conditions and enrich the understanding of cold-regions landslides.
2. In a study section, soil temperature, soil moisture and soil pore-water pressure were monitored at depth by sensors. Shallow soil body deformation also was monitored by deformation monitoring tubes, settlement gauges and inclinometers. The deformation of slope surface was measured by GPS through the

monitoring points on the slope. Geological survey was conducted by geological drilling, ground-penetrating radar and high-density electrical resistivity survey. The regional permafrost distribution was obtained by comprehensive analysis of meteorological data, geological data and remote-sensing satellite data. The slope safety factor under varying conditions was calculated by finite element analysis of laboratory-test data and field-monitoring data. Finally, slope reinforcement measures of gravel piles, antifreeze seepage blind ditches and friction piles were adopted.

Through this project, monitoring methods of cold-region landslides has been further enriched. Because of the good results of engineering reinforcement measures, much practical experience of highway construction in high-latitude permafrost regions has been accumulated.

3. Through this project, 12 papers have been published, 4 doctors and 7 masters have been trained. Five international and domestic academic conferences were organized and participated in. So personnel training and academic exchanging have achieve excellent results.

Acknowledgments This work was financially supported by the key science and technology project of Heilongjiang Communications Department "Study on Subgrade Stability Controlling Technology of Freeway Expansion Project Permafrost Melt and Landslides Sections" (2011318223630).

References

- Chang XL, Jin HJ, He RX (2013) Review of permafrost monitoring in the northern Da Hinggan Mountains, Northeast China. *J Glaciol Geocryol* 35(1):93–100
- Ding YH, Ren GY, Shi GY, Gong P, Zheng XH, Zhai PM, Zhang DE, Zhao ZC, Wang SW, Wang HJ, Luo Y, Chen DL, Gao XJ, Dai XS (2006) China's national assessment report of climate change (I): climate change in China and the future trend. *Adv Clim Change Res* 2(1):3–8
- He W, Bu RC, Xiong ZP, Hu YM (2013) Characteristics of temperature and precipitation in Northeastern China from 1961 to. *Acta Ecol Sinica* 33(2):519–531
- Lin XC, Yu SQ, Tang GL (1995) Series of average air temperature over China for the last 100-years period. *Sci Atmos Sinica* 19(5):525–534
- Ren GY, Guo J, Xu MZ, Chu ZY, Zhang L, Zou XK, Li QX, Liu XN (2005) Climate changes of China's mainland over the past half century. *Acta Meteorol Sinica* 63(6):942–956
- Shi N, Chen JQ, Tu QP (1995) 4-phase climate change features in the last 100 years over China. *Acta Meteorol Sinica* 53(4):431–439
- Wei Z, Jin HJ, Zhang JM (2010) Prediction of permafrost changes in Northeastern China under a changing climate. *Sci Chin Earth Sci*. doi:10.1007/s11430-010-4109-6
- Zhou YW, Guo DX, Qiu GQ (2000) *Geocryology in China*. Science Press, Beijing, pp 171–423
- Zuo HC, Lü SH, Hu YQ (2004) Variations trend of yearly mean air temperature and precipitation in China in the last 50 years. *Plateau Meteorol* 23(2):238–244



International Summer School on Rockslides and Related Phenomena in the Kokomeren River Valley, Tien Shan, Kyrgyzstan: IPL-106-2 Project and WCoE

Alexander Strom and Kanatbek Abdrakhmatov

Abstract

The International Summer School on Rockslides and Related Phenomena in the Kokomeren River valley, Tien Shan, Kyrgyzstan is the annual field training course focused on identification and study of large-scale bedrock landslides. These phenomena pose a threat to communities living in mountainous regions all over the world and are characterised by the enormous amount of material involved, and its high mobility and ability to create natural dams. Since 2006 more than 50 students and young landslide researchers from 17 countries have been introduced to rockslides and rock avalanches of different morphological types, some of which have formed deeply eroded rockslide dams that allow study of their internal structure, as well as evidence of inundation and of catastrophic outburst floods, and impressive manifestations of recent tectonic phenomena.

Keywords

Rockslide • Rock avalanche • Natural dam • Outburst flood

Introduction

Rockslides (bedrock landslides) pose a threat to vast areas due to the enormous amount of material involved (sometimes up to billions of cubic meters), and their high mobility and ability to create large natural dams, which result in inundation of the valleys upstream and catastrophic outburst floods downstream. Fortunately such large-scale rock slope failures occur rarely in comparison with landslides in non-lithified soils. At the same time, the uniqueness and relative rareness of such phenomena require that more attention be paid to prehistoric events to better understand the motion

mechanism(s) of highly mobile rock avalanches, and large rockslide dams behaviour.

It is critically important for researchers working in this field, especially for those who are starting their professional career, to visit as many bedrock landslides of different types as possible. The best are those in arid climatic zones where there is a lack of vegetation and good outcrops, and where details of rockslide morphology and internal structure can be observed.

Excellent examples of long runout rock avalanches, of intact and deeply eroded rockslide dams, of lacustrine sediments that accumulated in the landslide-dammed lakes and of catastrophic outburst flood traces can be found in the Kokomeren River basin (Central Tien Shan, Kyrgyzstan). There are many sites within a limited area of about 30×80 km (Fig. 1) located at a 1-day trip distance from the city of Bishkek, the capital of Kyrgyzstan. Most of these sites can be easily reached by car or require few hours of hiking (Strom and Abdrakhmatov 2009).

This region was selected for a field training course due to the unique concentration of rockslides and rock avalanches of different morphological types combined with impressive neotectonic structure and evidence of the active tectonic

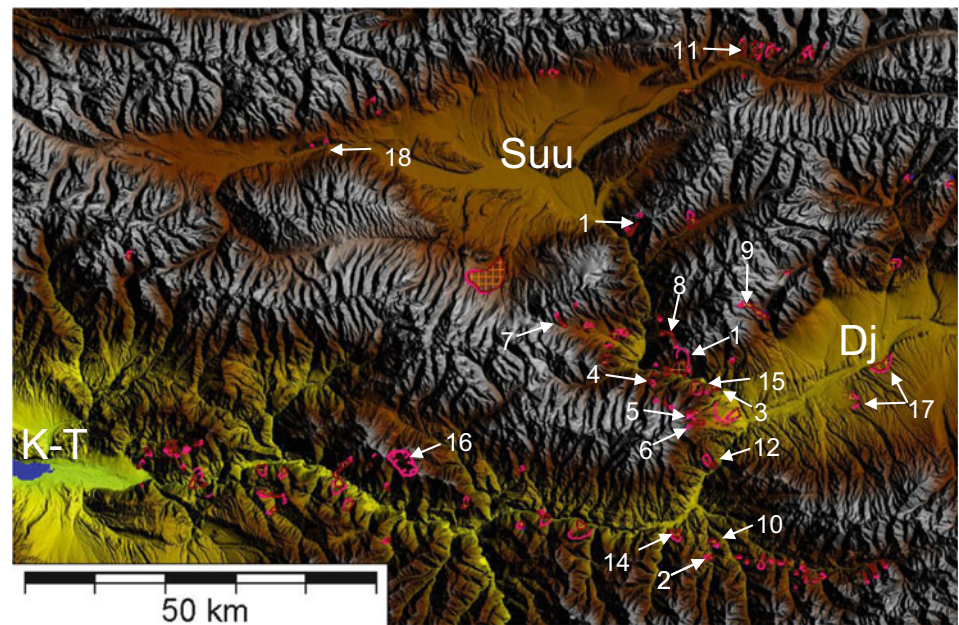
A. Strom (✉)

Geodynamics Research Centre – Branch of JSC “Hydroproject Institute”, Volokolamskoe Shosse 2, 125993 Moscow, Russia
e-mail: strom.alexandr@yandex.ru

K. Abdrakhmatov

Kyrgyz Institute of Seismology, Asanbay 52/1, Bishkek 720060, Kyrgyzstan
e-mail: kanab53@yandex.com

Fig. 1 Large-scale landslides, rock avalanches and caldera-like collapses in the Kokomeren River basin and adjacent part of the Naryn River basin. Suu, Dj and K-T—the Suusamy, the Djungal and the Ketmen-Tiube intermountain depressions. Case studies described in the Summer School Guidebook: 1—Seit; 2—Ak-Kiol; 3—Mini-Köfels; 4—Kashkasu; 5—Northern Karakungey; 6—Southern Karakungey; 7—Chongsu; 8—Sarysu; 9—Ming-Teke; 10—Lower Ak-Kiol; 11—Snake-Head; 12—Lower-Aral; 13—Kokomeren; 14—Ornok; 15—Displaced Peneplain; 16—Kyzylkiol; 17—Chaek; 18—1992 Suusamy



processes that are considered to be one of the main triggering factors of large-scale bedrock slope failures.

All these features have been examined by the participants of the International Summer School on Rockslides and Related Phenomena, an annual field training course that had started in 2006, and was supported by the IPL-M-111 Project. Since 2008 it has been supported by the IPL-106-2 Project.

During these years more than 50 participants from 17 countries—Argentina, Austria, Belgium, China and Hong Kong, Czech Republic, France, Germany, Great Britain, Italy, Kyrgyzstan, New Zealand, Russia, Switzerland, Spain, Tajikistan and USA—participated in the ICL Summer School.

The field training course is the main activity of the WCoE of the Kyrgyz Institute of Seismology (KIS) and Institute of the Geospheres Dynamics of Russian Academy of Sciences (IDG), an ICL member. Since 2011 the latter was replaced by the Geodynamics Research Center, a branch of JSC “Hydroproject Institute” (GRC).

Participants are provided with a detailed full-colour Guidebook containing more than 130 photographs, maps and schemes that describes all features investigated during the field trips. The Guidebook is updated regularly being complemented by new data, obtained during previous training courses. At the end of the training course all participants receive special Certificates (Fig. 2).

Rockslide and Rock Avalanche Morphology

An abundance of rockslides that occurred on slopes of different height and steepness and moved either across prominent topographic lows or directly down-valley produced bodies of



Fig. 2 Participants of the 2012 Summer School with certificates on the last day of this training course

different morphological types, allowing a classification based on the longitudinal debris distribution and selection of rockslide types irrespective of the terrain topography. It is proposed that such debris distribution reflect the peculiarities of the motion mechanism, allowing a better understanding of the latter (Strom 1996, 2006). Features of all these types are described in the guidebook and are visited during field trips.

We start by examining the morphological peculiarities of bedrock landslides from the case studies of the most “simple”—Primary—type, which are characterized by distal debris accumulation. An excellent example of this type is the 3.2 km long Seit rock avalanche (1 on Fig. 1). The same debris distribution is typical of several rockslides that had moved across relatively narrow valleys and formed compact dams with distinct proximal lowering—the Ak-Kiol (2 on Fig. 1) and Mini-Köfels rockslides (3 on Fig. 1).

All rockslides of the Primary type are characterized by distal debris accumulation along with the practical absence of debris within the headscarp area (Strom 2013c).

The participants' attention is drawn to the presence of trimlines much above the top of the deposits showing that rock avalanche debris had moved initially as a thick body and later flowed out like a liquid (Strom 2013c).

Rock avalanches of the second morphological type—Jumping—occur when the sliding surface at the source zone comes out on the slope well above its foot. They are exemplified by the Kashkasu (4 on Fig. 1) and Norther Karakungey (5 on Fig. 1) rockslides that have compact proximal and avalanche-like (mobile) distal parts. It is hypothesized that the mobile part of such rockslide could be formed by squeezing of the rockslide frontal part out from under the following sliding mass that collapses from the upper part of the source zone (Strom 2006, 2013c). A similar longitudinal debris distribution can be observed at the famous Elm rock avalanche caused by artificial slope undercutting at a slate quarry (Heim 1882; Hsü 1975).

It is assumed that Jumping rockslides on natural slopes could be triggered by seismic shaking, considering the well-known effect of strong motion amplification at the upper parts of topographic irregularities (Meunier et al. 2008; Huang 2013).

Rock avalanches of the last—Secondary—morphological type are exemplified by the Southern Karakungey (6 on Fig. 1), the Chongsu (7 on Fig. 1), the Sarysu (8 on Fig. 1), the Ming-Teke (9 on Fig. 1) and, likely, by the Lower Ak-Kiol (10 on Fig. 1) rockslides. All these case studies are ascribed to the “Classical” subtype of this morphological type (Strom 2010). They form when rapidly moving debris hits either the opposite slope of the valley at an angle that differs from the perpendicular to the valley trend, or, sometimes, when it hits the valley bottom (Strom 2006, 2010). One case study—the Snake-Head rock avalanche (11 on Fig. 1)—is ascribed to the “Bottleneck” subtype, which originates when a rockslide body passes through a sharp narrowing on its way (Strom 2010).

Mobile “avalanche-like” parts of Secondary rock avalanches often move in similar way to Primary rock avalanches, forming debris accumulations at their distal parts and leaving trimlines on slopes.

Internal Structure of Rockslide Bodies

Considerable attention during the training courses is paid to the internal structure of large-scale rockslide bodies, especially the Kokomerren (13 on Fig. 1) and the Ornok (14 on Fig. 1) rockslides, which had occurred on slopes composed



Fig. 3 Participants of the 2007 Summer School on top of the coarse carapace of the Kokomerren rockslide



Fig. 4 Participants of the 2011 Summer School performing an in-situ permeability test at the comminuted lower part of the Kokomerren rockslide deposits. Plastic bottles were used to bring sufficient water to the site, which is about 150 m above the river

of variable and multi-colour lithologies (Strom 1994; Abdrakhmatov and Strom 2006). Both were deeply dissected by erosion providing excellent outcrops. It was found out that debris, originating from different parts of the source zone does not mix during the emplacement and forms pseudo-stratified bodies preserving the succession of rock types typical of the headscarp area.

Better understanding of the internal structure and grain-size composition of rockslide bodies is critically important for assessing the stability of rockslide dams and predicting their breach mode (Dunning and Armitage 2011). Besides visual inspection of the relationships between debris units originating from different lithologies (Fig. 3) some engineering-geological tests have been performed to measure grain-size composition and permeability of the comminuted lower part of the Kokomerren rockslide body (Fig. 4).



Fig. 5 Participants of the 2008 Summer School in front of the headscarp of the Pleistocene Displaced Peneplain rockslide

Peculiarities of the internal structure of large-scale rockslide deposits (the above-mentioned “stratification” and intensive crushing of the internal/lower units contrasting to the coarse outer carapace) allow confident identification of old rockslides, which have bodies that are so strongly reworked by erosion that they can be hardly recognised morphologically. In the study region it is exemplified by the gigantic Displaced Peneplain rockslide (15 on Fig. 1), about 0.5 km^3 , if not larger, in volume (Fig. 5).

This Pleistocene rockslide had blocked the Kokomeren River and forced it to cut a new bypass section through the left bank bedrock massif (Fig. 6). This case study is very instructive and we always spend 1–2 days demonstrating how to use structural peculiarities and the grain-size composition of the rockslide deposits to distinguish them from material of other origin.

Evidence of River Damming and Outburst Floods

Many rockslides in the Kokomeren River basin had dammed rivers and formed temporary or long-lived lakes. Most of them have been breached, though the lake dammed by the abovementioned Kashkasu Jumping rockslide was silted up completely forming an unusual forested planar area surrounded by steep rocky cliffs.

The breach of some of the rockslide dames that had stored a large amount of water was catastrophic and participants of the Summer School are acquainted with impressive evidence of powerful outburst floods allowing reconstruction of the

dam breach process and peak discharge assessment (Strom 2013a; Strom and Zhirkevich 2013).

Study of Paleoseismic Evidence

The study area provides impressive manifestations of Quaternary tectonics and paleoseismic features. Surface ruptures indicating recurrent Late Pleistocene and Holocene faulting events associated with large earthquakes as well as the 1992 M7.3 Suusamyр earthquake surface rupture are shown to the Summer School participants.

In 2012 the world-leading expert in paleoseismology, Prof. James McCalpin, author of the famous “Paleoseismology” text (McCalpin 2009) visited our training course (Fig. 7) and demonstrated some methods for identifying and dating past surface ruptures.

In addition to surface ruptures, attention is paid to the methods to prove the seismic origin of rockslides. An approach based on joint analyses of indirect evidence allow a well grounded assumption of seismic triggering of bedrock slope failure and is exemplified by the Kokomeren and Lower-Aral case studies (13 and 12 on Fig. 1). Indirect evidence of rockslide seismic triggering are those indicating slope failures within the area surrounding the rockslide in question and closely timed to its formation. They could be best identified at the outcrops of lacustrine sediments accumulated in the lake dammed by the study rockslide (Fig. 8), which accumulation starts from the first days to a few years after the river damming event (Strom 2013b).

Some rockslides with seismic origin that can be neither proved nor disproved at the present-day level of knowledge are visited as well. One of them is the gigantic Late Pleistocene Aksu rockslide (Fig. 9) located north from the area shown on Fig. 1. Usually we visited it on the way back from the Kokomeren valley to Bishkek, at the end of the training course.

Along with “typical” paleoseismic features there is an unusual recent structure located west of the Kokomeren River basin on top of the Santash Ridge, which forms the right bank of the Naryn River valley. It is a unique Holocene (?) caldera-like depression $3 \times 2 \text{ km}$ in size and up to 700 m deep—the so called Kyzylkiol cavity (16 on Fig. 1). Its formation was associated with the disappearance of about 3 km^3 of rocks in the ridge’s interior. Strom and Groshev (2009) hypothesized that this very mysterious feature could reflect the final stage of evolution of a neotectonic detachment anticline. As this site is rather distant from the main Summer School area we did not visit it during past training courses but its detailed description is included in the Guidebook.

Fig. 6 Participants of the 2008 Summer School at the “entrance” of the abandoned valley on the right bank of the Kokomeren River immediately upstream from the section that had been blocked by the Displaced Peneplain rockslide. The present-day stream passes in front of this outcrop from right to left



Fig. 7 Prof. James McCalpin (in the centre) with the 2012 Summer School participants at a surface rupture outcrop north from the Chaek town



Fig. 8 Participants of the 2006 Summer School studying an outcrop of an active fault that displaced lacustrine sediments of the Kokomeren rockslide-dammed lake



Fig. 9 Participants of the 2009 Summer School at the foot of ca. 1.5 km^3 Aksu rockslide headscarp

Conclusions

A field training course in the Kokomeren River valley has proved its efficacy and has been carried out annually since 2006 (except in 2010, when it had to be cancelled due to political crisis in Kyrgyzstan), attracting attention of landslide researchers from different countries.

WCoE of KIS and GRC plan to run the Kokomeren Summer School in the future as well. In addition, there are plans to arrange similar field training courses in the Alps, where numerous classical rockslides cited in most textbooks are located, to help researchers outside of Alpine countries to learn more about these case studies and to compare them with bedrock landslides in their own regions.

Acknowledgments We want to express sincere gratitude to Executive director of ICL Prof. Kyoji Sassa for his permanent support of our activities, and to his secretary Mie Ueda for continuous help and to Eileen McSaveney for thorough check of the manuscript.

References

- Abdrakhmatov K, Strom A (2006) Dissected rockslide and rock avalanche deposits; Tien Shan Kyrgyzstan. In: Evans SG, Scarascia Mugnozza G, Strom A, Hermanns RL (eds) Landslides from

- massive rock slope failure. NATO science series IV: Earth and environmental sciences, vol 49. Springer, Dordrecht, pp 551–572. ISBN: 10 1-4020-4036-9
- Dunning SA, Armitage PJ (2011) The grain-size distribution of rock-avalanche deposits: implications for natural dam stability. In: Evans SG, Hermanns R, Strom AL, Scarascia-Mugnozza G (eds) Natural and artificial rockslide dams, vol 133, Lecture notes in earth sciences. Springer, Heidelberg, pp 479–598
- Heim A (1882) Der Bergsturz von Elm. *Deutsch. Geol Gesell Zeitschr* 34: 74–115
- Hsü KJ (1975) Catastrophic debris streams (sturzstroms) generated by rock falls. *Geol Soc Am Bull* 86:129–140
- Huang R (2013) Slope motion response and failure under strong earthquakes: recording, monitoring and modeling. In: Ugai K, Yagi H, Wakai A (eds) Earthquake-induced landslides. Springer, Heidelberg, pp 59–73. ISBN: 978-3-642-32237-2
- McCalpin JP (2009) *Paleoseismology*, 2nd edn. Elsevier, Amsterdam. 613 p & CD ROM. ISBN: 978-0-12-373576-8
- Meunier P, Hovious N, Haines JA (2008) Topographic site effects and the location of earthquake induced landslides. *Earth Planet Sci Lett* 275:221–232
- Strom AL (1994) Mechanism of stratification and abnormal crushing of rockslide deposits. In: Oliveira R, Rodrigues LF, Coelho A, Cunha AP (eds) Proceedings of the 7th international IAEG congress, vol 3. Balkema, Rotterdam, pp 1287–1295. ISBN: 90-5410-506-2
- Strom AL (1996) Some morphological types of long-runout rockslides: effect of the relief on their mechanism and on the rockslide deposits distribution. In: Senneset K (ed) Landslides. Proceedings of the 7th international symposium on landslides. Balkema, Rotterdam, pp 1977–1982
- Strom AL (2006) Morphology and internal structure of rockslides and rock avalanches: grounds and constraints for their modelling. In: Evans SG, Scarascia Mugnozza G, Strom A, Hermanns RL (eds) Landslides from massive rock slope failure. NATO science series IV: Earth and environmental Sciences, vol 49. Springer, Dordrecht, pp 305–328. ISBN: 10 1-4020-4036-9
- Strom AL (2010) Evidence of momentum transfer during large-scale rockslides' motion. In: Williams AL, Pinches GM, Chin CY, McMorran TG, Massei CI (eds) Geologically active. Proceedings of the 11th IAEG Congress, Auckland, New Zealand, 5–10 September 2010. Taylor & Francis Group, London, pp 73–86. ISBN: 978-0-415-60034-7
- Strom A (2013a) Geological prerequisites for landslide Dams' disaster assessment and mitigation in Central Asia. In: Wang F, Miyajima M, Li T, Fathani TF (eds) Progress of geo-disaster mitigation technology in Asia. Springer, Berlin, pp 17–53. ISBN: 978-3-642-29106-7
- Strom A (2013b) Use of indirect evidence for the prehistoric earthquake-induced landslide identification. In: Ugai K, Yagi H, Wakai A (eds) Earthquake-induced landslides. Springer, Heidelberg, pp 21–30. ISBN: 978-3-642-32237-2
- Strom A (2013c) Rockslides and rock Avalanches in the Kokomeren River Valley (Kyrgyz Tien Shan). In: Arbanas Z, Arbanas S (eds) Proceedings of the 1st regional symposium on landslides in the Adriatic-Balkan Region, Zagreb, Croatia, 7–9 March 2013
- Strom AL, Abdrakhmatov KE (2009) International summer school on rockslides and related phenomena in the Kokomeren River valley, Tien Shan, Kyrgyzstan. In: Sassa K, Canuti P (eds) Landslides – disaster risk reduction. Springer, Heidelberg, pp 223–227. ISBN: 978-3-540-69970-5
- Strom A, Groshev M (2009) Mysteries of rock massifs destruction. In: Abbie M, Bedford JS (eds) Rock mechanics: new research. Nova Science Publishers, New York, pp 211–231. ISBN: 978-1-60692-459-4
- Strom A, Zhirkevich A (2013) “Remote” landslide-related hazards and their consideration for the hydraulic schemes design. In: Proceedings of the International Conference “Vajont, 1963–2013: thoughts and analyses after 50 years since the catastrophic landslide”, Padua, Italy, 8–10 October 2013



Rainfall Intensity and Duration for Debris Flow Triggering in Peninsular Malaysia

Suhaimi Jamaludin, Che Hassandi Abdullah, and Norhidayu Kasim

Abstract

In response to the rising problems of debris flow events in Malaysia, the Public Works Department of Malaysia (PWD), through the Slope Engineering Division, has decided to carry out a study to comprehend the characteristics of debris flows in Peninsular Malaysia. The relationship between rainfall patterns characterized by intensity and duration, and the occurrence of debris flows, was analyzed. In this paper, four debris-flow events in Peninsular Malaysia are presented. The results indicate that the debris-flow events bear similar characteristics to those discussed by other researchers throughout the world.

Keywords

Debris flow • Rainfall • Intensity • Duration • Mechanism

Introduction

A debris flow is a fast-moving mass of unconsolidated, saturated debris that can carry clasts ranging in size from clay particles to boulders, and also often contains a large amount of woody debris. It is normally triggered by high-intensity rain. The speed of a debris flow varies depending on the materials, steepness and travel distance of the flow. The debris flow generally forms when unconsolidated material becomes saturated and unstable. It is extremely destructive to life and property due to its rate of movement.

In Peninsular Malaysia at least eight significant debris-flow occurrences have been reported (Table 1). The locations of these debris-flow events are shown in Fig. 1.

In this paper only four of the occurrences will be discussed; i.e. Lentang in Pahang (at km 52.4 of the Kuala

Lumpur—Karak Highway), Genting Sempah in Selangor (at km 38.6 of the Kuala Lumpur—Karak Highway), Fraser's Hill in Pahang (from km 4 to km 5 of Gap-Fraser's Hill Road) and Gunung Pulai in Johor.

Description of Four Selected Debris-Flow Occurrences in Peninsular Malaysia

Characteristics of the four debris flow are as follows:

Debris Flow at Lentang

The debris-flow event occurred on November 2, 2004, resulting in the temporary closure of the Kuala Lumpur—Karak Highway. The Malaysian Highway Authorities (MHA) took a few days to clean all the mud, rocks, and timber from the site. This incident occurred at km 52.4 from Kuala Lumpur. The estimated losses due to this incident were about RM 11.86 million. The flow initiated upstream, then flowed down the channel and onto the road.

S. Jamaludin (✉) • C.H. Abdullah • N. Kasim
Public Works Department, Slope Engineering Section, 50582 Kuala Lumpur, Malaysia
e-mail: suhaimij@jkr.gov.my; Hassandi@jkr.gov.my; Norhidayu@jkr.gov.my

Table 1 Eight significant debris flow occurrences in Peninsular Malaysia

Date of occurrence	Location
30-June-95	km 38.6, Kuala Lumpur-Karak Highway, Selangor (Genting Sempah)
28-Dec.-01	Gunung Pulai, Kulai, Johor (Gunung Pulai)
10-Nov.-03	Section 23.3 to 24.10, Kuala Kubu Baru—Gap Road, Selangor (Kuala Kubu—Gap)
10-Nov.-04	km 302, North South Expressway, Perak (Gunung Tempurung)
2-Nov.-04	km 52.4, Kuala Lumpur-Karak Highway, Pahang (Lentang)
12-Apr.-06	km 33, Simpang Pulai—Cameron Highland Road, Perak (Simpang Pulai)
15-Nov.-07	km 4 to 5, Gap-Fraser's Hill Road, Pahang (Fraser's Hill)
3 Jan.-09	Section 62.4, Lojing-Gua Musang Road, Kelantan (Lojing)

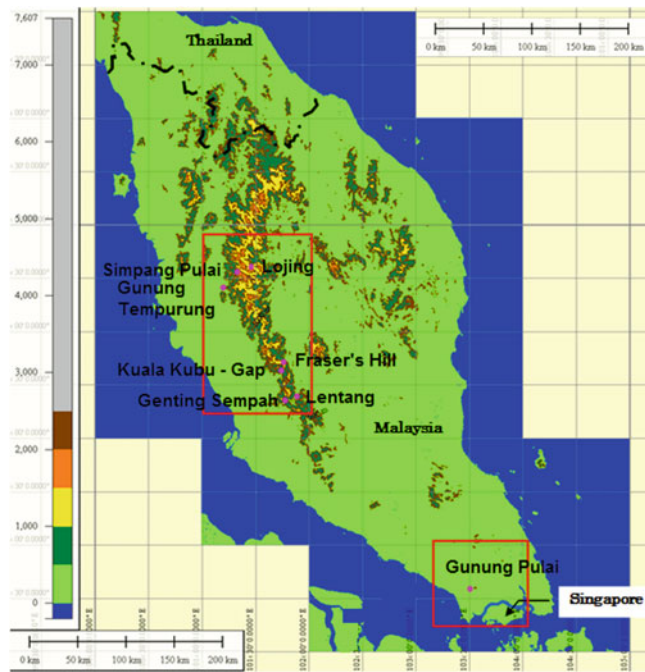


Fig. 1 Locations of the eight significant debris-flow occurrences in Peninsular Malaysia

The type of outcrop exposed at the site is deeply weathered fine to medium grained granite. This site is located within the main range granite of Peninsular Malaysia.

Photos taken after the debris flow indicate that the debris contained mostly wood, mud and gravels, with a few boulders (as shown in Figs. 2 and 3).

The mechanisms of the debris flow, based on the findings, are as follows:

- (a) The part of the alluvial cone near the exit of the channel may have been the source of debris that was washed out to the road.



Fig. 2 General view of the debris flow at Lentang



Fig. 3 The debris, consisting of wood, mud, and gravels without large boulders, was removed to the opposite side of the highway (Lentang event)

- (b) The debris flow mainly consisted of water and gravels without many large boulders, since there was no damage to trees in the channel.
- (c) A 'flash flood' type of flow may have occurred in the upper stream, washing out the fan deposits in the area from the first Sabo dam to the end of the channel.
- (d) Eventually, the debris flow spilled out to the highway with wood and gravel (as illustrated in Fig. 4).

Debris Flow at Gunung Pulai

This debris flow occurred on December 28, 2001, and claimed the lives of five residents during a tropical storm that passed through Johor Bharu from 14:00 pm on December 27 to 2:00 am. The two-day cumulative rainfall prior to the date of debris flow was 15 mm, and the total rain on

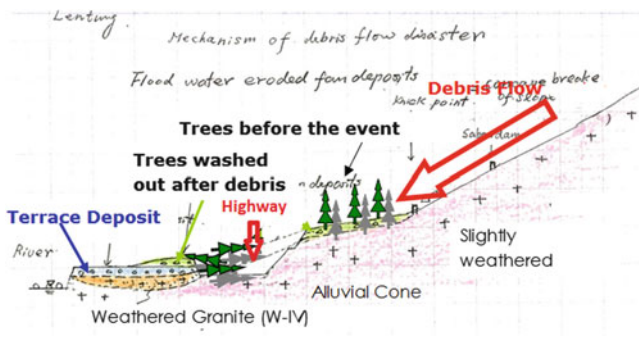


Fig. 4 Illustration of the Lentang event

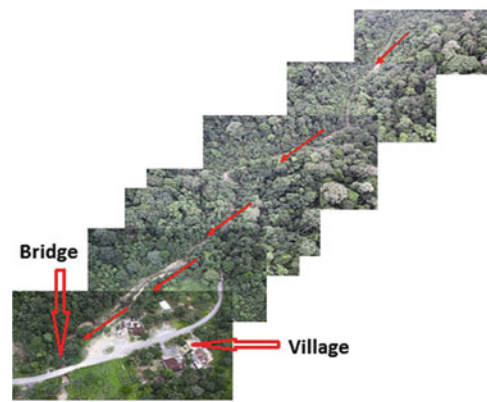


Fig. 6 Aerial view shows the course of the debris flow into the village at Gunung Pulai, Kulai, Johor



Fig. 5 General view of the debris flow somewhere near to the bridge at Gunung Pulai, Kulai, Johor



Fig. 7 Aerial view of the road at FT 148 and FT 55, the impact of a debris flow in February 2009

December 28 was 90 mm. It has been suggested that strong wind caused trees on the river banks to fall into the river to form a natural dam, which breached, causing the debris flow. The debris was composed of soil, mud, boulders and timber, as shown in Fig. 5. The local rock was weathered granite of Grades V and IV. Landslides occurred both in manmade and natural slopes.

The increased in the water level of the river caused by substances such as woody debris, boulders and soil, blocked the bridge near houses. As a result of this phenomenon, several houses were damaged and destroyed.

These areas are generally covered by granite, volcanic, metamorphic and sedimentary rocks. The boundary between granite rocks and volcanic rocks could be seen at the waterfall. The slope angle where the failures occur is between 50° to 70°.

The probable mechanism of the debris flow is as follows:

(a) Shallow failures scars are quite frequent in the initiation area of the debris flow. Shallow failures of the weathered granite slopes may have been the source of the relatively large volume of sediment.

- (b) It is unlikely that the large boulders had travelled downstream when the debris flow occurred on December 28, 2001, since the downstream gradient is less than 2°. Hence, the damage in 2001 may be regarded as a result of flooding due to the timber that clogged the bridge (refer Fig. 6).
- (c) It is to be noted that the same thing can happen again in a similar storm.

Debris Flow at Fraser’s Hill

The debris flows at the Fraser’s Hill site are complex because they occurred repeatedly. They were initiated by retrogressive collapse of a slope at Section 5 (or 5 km) of the FT 148 (Gap—Fraser’s Hill road) as shown in Figs. 7 and 8. Debris flowed down a channel at high speed and severely damaged the road at FT 55 (Gap-Raub), which lies



Fig. 8 The damage at FT 55 from Gap to Raub on 6 February 2009

approximately 300 m below the debris-flow source. Debris flows occurred three times between November 2007 and end of January 2009.

Fraser's Hill is located in a large enclave of meta-sedimentary rocks that was formed within the Main Range granite (Roe 1951). The Main Range is a range of highlands that divides the east and west of Peninsular Malaysia down its centreline. The rocks are of shale, schist, phyllite and chert, with layers of metaquartzite and schistose coarse sandstone. The rock exposed at the site is granite. Based on observation of granite samples, it was observed that quartz grains are round, which may indicate that the rocks have experienced tectonic activities such as faults or shears.

At the initiation area, the grade of weathering varies from Grades III to VI. These areas have undergone severe physical weathering.

The mechanism of the debris flow is described below. This mechanism is partially based on the aerial photographs taken after the occurrence of a debris flow.

- (a) Little sediment was found in the channel with slightly weathered outcrop. The gradient is high, allowing the debris to flow down to the deposition area near FT55 which is located downstream, without leaving sediment in the channel.
- (b) The debris flow occurred as intermittent multiple events. In some cases slope failures may turn into debris flows, while in some other cases, debris flows may occur as a result of erosion of sediment in the channel.

Debris Flow at Genting Sempah

The debris-flow occurrence at Genting Sempah on June 30, 1995, resulted in 20 deaths, 22 people injured and some vehicles damaged. Figure 9 shows an aerial photograph taken after the event.



Fig. 9 General view of debris flow at Genting Sempah

Intense, heavy rain saturated the residual soil, triggering at least two major landslides upstream of one of the tributaries of the Gombak River. The landslide material entered the stream, forming a debris flow which subsequently scoured top soil and boulders in its path as it moved downstream. Gravity increased the momentum of the debris flow, thereby increasing the power to scour the soil. The debris flow from the elevation of 800 m to 570 m covers a length of approximately one kilometer, moving about 3,000 m³ of debris.

This site is also located in the Main Range of the Peninsular Malaysia. Two types of rock are found at the sites, namely volcanics and metasediments. The metasediments are composed of highly fractured, massive and fine-grained metasandstone, while the volcanic rocks comprise mainly foliated rhyolite with phenocrysts of quartz and feldspar. Observations along the stream indicate that the soil cover is mainly of Silty to Clayey Sand with boulders of rock.

Rainfall Intensity and Duration Correlations for Debris Flows in Peninsular Malaysia and Comparison with Other Countries

In this study, rainfall data from four debris-flow occurrences in Malaysia; i.e. Lentang, Genting Sempah, Fraser Hills and Gunung Pulai were studied.

Comparison Between Worldwide Threshold Data (Jakob et al. 2005) and Peninsular Malaysian Data

Figure 10 indicates worldwide rainfall thresholds compiled by Jakob et al. (2005) using the method established by Caine (1980). The intensity; I is the maximum hourly rainfall

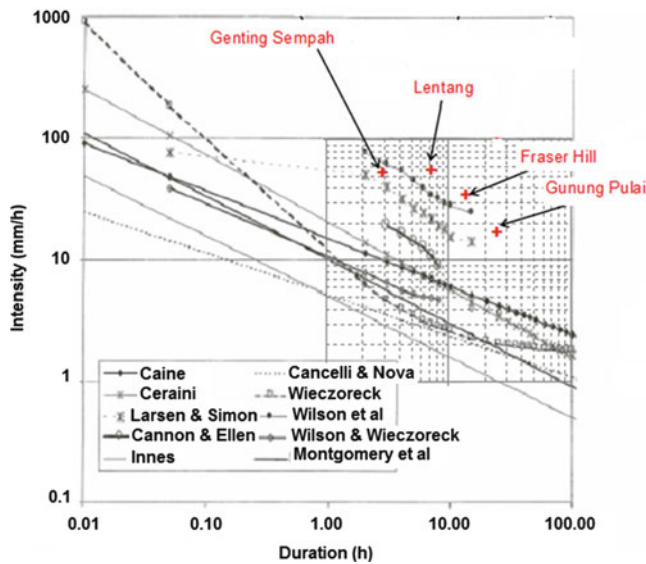


Fig. 10 Intensity-duration plots (Jakob et al. 2005) with rainfall data for debris-flow sites in Malaysia

Table 2 Calculated and recorded critical intensity for a given duration

Location	Duration (h)	Critical intensity (mm)	
		Calculated	Recorded
Gunung Pulai	24	18	20
Genting Sempah	3	62	55

(mm/h) that triggered failure, whereas D is the duration of rainfall in hours.

The threshold by Caine (1980), Cancelli and Nova (1985) and Ceriani et al. (1992) are global (i.e., they were prepared using all worldwide data available at the time) (Caine 1980; Innes 1983) or, for large areas with different soils, morphology and rainfall characteristics (Ceriani et al. 1992). Local or regional thresholds are from Larsen and Simon (1993), Cannon and Ellen (1985), Wieczorek (1987), Wilson and Wieczorek (1995) and Montgomery et al. (2000).

The maximum hourly rainfall depths and durations that are correlated with the debris flows in Peninsular Malaysia are plotted together with the intensity-against-duration criteria to see which criterion can approximate the threshold of failure events in Peninsular Malaysia (Fig. 10). These four events shown in Fig. 10 were selected because hourly rainfall data on the dates of the debris-flow events were available. It shows that the series of points, given by Wilson et al. (1992) are close to those of the four events in Malaysia.

The equation that represents the Wilson et al. (1992) data point is expressed as:

$$I_p = 121.4 \times D^{-0.602} \quad (1)$$

where I_p : Highest rainfall intensity during the rainfall event, and D: Duration of the rain in hours.

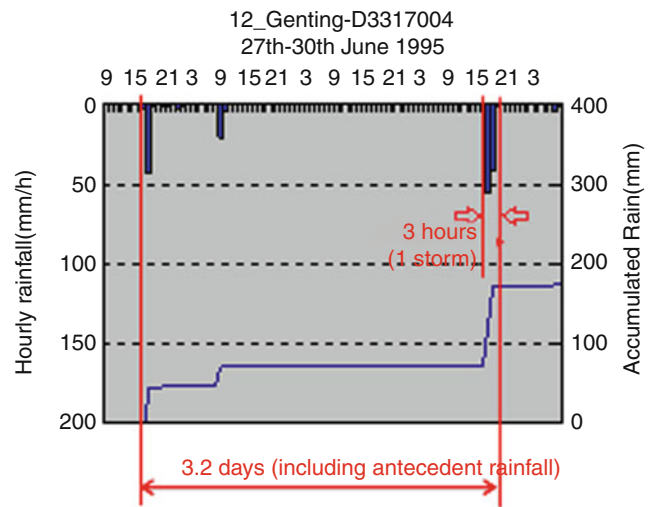


Fig. 11 Duration of rainfall and accumulated rainfall depth of Genting Sempah

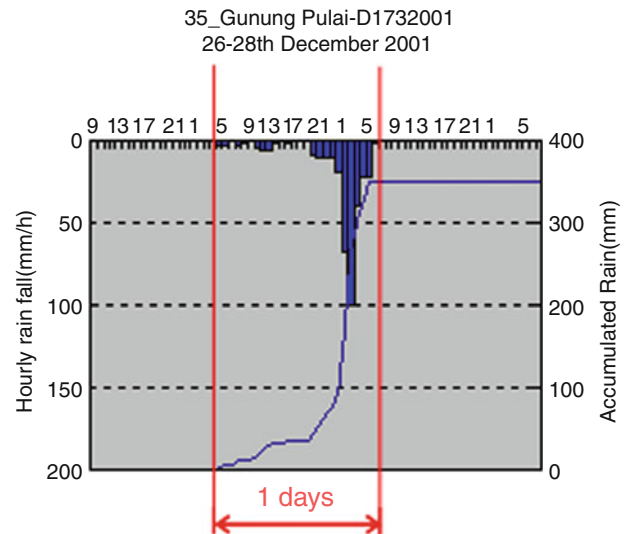


Fig. 12 Duration of rainfall and accumulated rainfall depth of Gunung Pulai

As an example, the critical intensities are calculated for the two sites using (1) as shown in Table 2. The corresponding hourly rainfall curves for these two sites are given in Figs. 11 and 12.

Comparison of Rainfall Intensity-Duration Thresholds for Debris Flows in Europe and in Malaysia

Jakob and Hungr (2005) used data collected from the Alps, the Pre-Alps and the Sarno region of Italy in the development of thresholds. The intensity; I is the highest rainfall intensity during the series of rainfall. Data points are

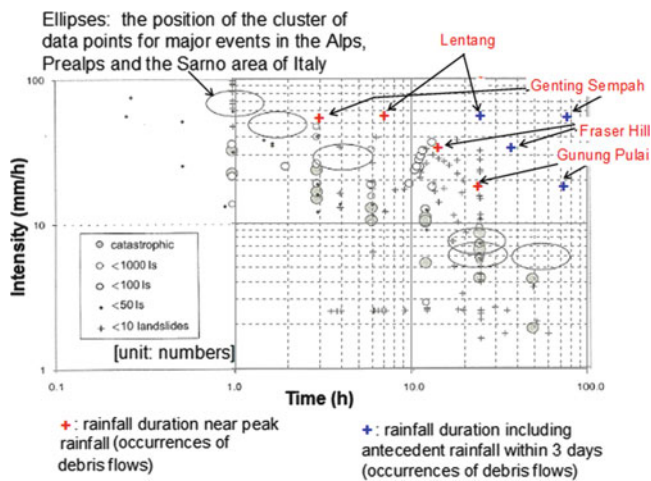


Fig. 13 Comparison between plots by Jakob and Hungr (2005) and rainfall data of four (4) sites in Peninsular Malaysia

differentiated with respect to number or density of landslides.

Rainfall intensity-duration data that triggered sediment-related disasters (landslides, debris flows, etc.) in Peninsular Malaysia are compared with the rainfall intensity-duration threshold in Europe.

Data were compared either for: (1) the rainfall intensity-duration relationship in a series of rainfall events; or (2) the rainfall intensity-duration relationship for about three days including antecedent rainfall. Figure 13 shows European data (from the disasters occurring in the Alps and in Sarno in Italy) and Peninsular Malaysian data for comparison. Data based on (1) are shown in red, whereas those based on (2) in blue. As shown in the figure, Malaysian threshold values generally lie at the upper limits of European threshold values.

Conclusions

The studies carried out at the four locations indicate that initiation sites were located in the residual soils of igneous rock (granitic or rhyolite) formations or at the boundary with a meta-sedimentary formation.

Comparison between worldwide threshold data compiled by Jakob et al. (2005) and Peninsular Malaysian

data shows that the trigger thresholds are generally higher for Malaysia.

Comparison of rainfall intensity-duration threshold for debris flow in Europe based on works by Jakob and Hungr (2005) and four sites in Peninsular Malaysia shows that Malaysian data plot around the threshold at the upper limits of the European data.

References

- Caine N (1980) The rainfall intensity – duration control of shallow landslides and debris flows. *Geogr Ann, Phys Geogr* 62A:23–27
- Cancelli A, Nova R (1985) Landslides in soil debris cover triggered by rainstorms in Valtellina (central Alps, Italy). In: *Proceedings of 4th international conference on landslides*. Japanese Landslide Society, pp 267–272
- Cannon SH, Ellen S (1985) Rainfall conditions for abundant debris avalanches in the San Francisco Bay region, California. *Calif Geol* 38(12):267–272
- Ceriani M, Lauzi S, Padovan N (1992) Rainfalls and landslides in the Alpine area of Lombardia Region, Central Alps Italy. In: *Proceedings of the international symposium “Interpraevent”*, vol 2, pp 9–20
- Innes J (1983) Debris flows. *Progr Phys Geogr* 7:469–501
- Jakob M, Hungr O (2005) *Debris-flow hazards and related phenomena*. Springer, Heidelberg
- Jakob M, Bovis M, Oden M (2005) The significance of channel recharge rates for estimating debris flow magnitude and frequency. *Earth Surf Process Landf* 30:755–766
- Larsen MC, Simon A (1993) A rainfall-intensity duration threshold for landslides in a humid-tropical environment, Puerto Rico. *Geogr Ann* 75A(1/2):13–23
- Montgomery DR, Schmidt KM, Greenberg HM, Dietrich WE (2000) Forest clearing and regional landsliding. *Geology* 28(4):311–314
- Roe FW (1951) “The geology and mineral resources of Fraser’s Hill area Selangor, Perak, Pahang, Federation of Malaya, with an account of mineral resources”, *Memoir No. 5*, Geology Survey Department, Federation of Malaya
- Wieczorek GF (1987). Effect of rainfall intensity and duration on debris flows in central Santa Cruz Mountains, California. In: Costa JE, Wieczorek GF (eds) *Debris flows/avalanches: process, recognition and mitigation (Reviews in Engineering Geology No. 7: 93–104)*. Geological Society of America, Boulder, CO
- Wilson RC, Wieczorek GF (1995) Rainfall thresholds for the initiation of debris flows at La Honda, California. *Environ Eng Geosci* 1 (1):11–27
- Wilson RC, Torikai JD, Ellen SD (1992). Development of rainfall warning thresholds for debris flows in the Honolulu District, Oahu (USGS Open-File Report 92-521, 45 pp). US Geological Surveys, Reston, VA

Thematic and Regional Networks on Landslides



Introduction: Thematic and Regional Networks on Landslides

Snježana Mihalić Arbanas, Kaoru Takara, N.M.S.I. Arambepola, and Renato Eugenio de Lima

Abstract

This is a short introduction to Part II of this volume which includes background information about establishment of regional and thematic networks by the International Consortium on Landslides (ICL) and summarized overview of nine ICL networks established in the period 2012–2013, as well as contributions from WLF3 Session A2. Papers included in this part of the volume represent the most important activities of the following networks: ICL Latin America Network (ICLLAN), South-East Asian Network for Landslide Risk Management, ICL Adriatic-Balkan Network (ICL ABN) and ICL thematic network on Landslide Monitoring and Warning (ICL LaMaWaTheN).

Keywords

WLF3 • ICL regional networks • ICL thematic networks • ICLLAN • ICL ABN • ICL LaMaWaTheN

Background

International Consortium on Landslides (ICL) decided to establish thematic and regional networks at the 10th Session of Board of Representatives of ICL held in Rome (Italy) on 5

S. Mihalić Arbanas (✉)

Faculty of Mining, Geology and Petroleum Engineering, University of Zagreb, Zagreb 10000, Croatia
e-mail: smihalic@rgn.hr

K. Takara

Disaster Prevention Research Institute (DPRI), Kyoto University, Uji, Kyoto 611-0011, Japan

N.M.S.I. Arambepola

Asian Disaster Preparedness Center (ADPC), Bangkok 10400, Thailand

R.E. de Lima

Center for Scientific Support in Disasters (CENACID), Federal University of Paraná (UFPR), Caixa, Curitiba 19023, Brazil

October 2011. The main goal was to intensify collaboration within ICL members and cooperation with non-ICL organizations, as well as to enhance thematic and regional activities of the ICL. First eight network proposals had been approved at the 10th ICL anniversary meeting held on 17–20 January 2012 in Kyoto. ICL networks are considered to have one of the key functions in the development of ICL in the next decade, according to “ICL Strategic Plan 2012–2021—To create a safer geo-environment”.

In the period 2012–2014 nine ICL networks have been established, listed in Tables 1 and 2. Four regional networks include 27 ICL members (5 World Centers of Excellence, WCoE 2011–2014) from 17 countries: Albania, Brazil, China, Chinese Taipei, Columbia, Croatia, Honduras, Indonesia, Japan, Korea, Malaysia, Mexico, Peru, Serbia, Slovenia and Thailand. Five thematic networks include 22 ICL members (10 WCoE 2011–2014) from 16 countries. They cooperate with 12 non-ICL members, i.e., institutions and organizations from academic, governmental and the private sector, on the subjects related to research on targeted

Table 1 Regional ICL networks established in the period 2012–2013

ICL network title	Network coordinator
Adriatic-Balkan Network	Co-coordinator(s)/Deputy coordinator(s)
	Coordinator: Snježana Mihalić Arbanas Co-coordinators: Željko Arbanas, Biljana Abolmasov
Latin America Network	Coordinator: Irasema Alcántara-Ayala Deputy coordinator: Renato Eugenio de Lima
	Coordinator: Kaoru Takara Deputy coordinators: Sangjun Im, Xiaochun Li
South-East Asian Network for Landslide Risk Management	Coordinator: N.M.S.I. Arambepola Deputy Coordinator: Ko-Fei Liu

Table 2 Thematic ICL networks established in the period 2012–2013

Network on Landslide Risk Management	Coordinator: Surya Parkash Deputy coordinator: Dwikorita Karnawati
	Coordinator: Dwikorita Karnawati Deputy coordinators: Yin Yueping, Irasema Alcántara-Ayala
Landslides in Cold Regions Network	Coordinator: Wei Shan Deputy coordinators: Alexander Strom, Hideaki Marui
	Coordinator: Claudio Margottini Co-coordinator: Vit Vilimek
Landslide Monitoring and Warning Network	Coordinator: Matjaž Mikoš Deputy coordinators: Hirotaka Ochiai, Željko Arbanas

landslides (landslides in the cold regions and in cultural or natural heritage environments); landslide monitoring; landslide risk management; and capacity development.

Overview of ICL Networks

A comprehensive overview of nine ICL regional and thematic networks is given below, according to data from networks' proposals and annual reports for 2012.

Adriatic-Balkan Network

Coordinator: Snježana Mihalić Arbanas

Co-coordinators: Željko Arbanas, Biljana Abolmasov

ICL Member Organizations involved in the Network: Faculty of Civil Engineering, University of Rijeka, Rijeka, Croatia; Faculty of Mining, Geology and Petroleum Engineering, University of Zagreb, Zagreb, Croatia; Faculty of Civil and Geodetic Engineering, Ljubljana, University of Ljubljana, Ljubljana, Slovenia (WCoE 2011–2014); Faculty Mining and Geology University of Belgrade, Belgrade, Serbia; Geological Survey of Slovenia, Ljubljana, Slovenia; Albanian Geological Survey; Emergency Management Office, City of Zagreb, Zagreb, Croatia.

Objectives for the initial 3 years: The general objective is advancing landslide science and its practical application in the region for the benefit of society and the environment. Specific objectives are (1) to set up scientific and legislative background for regional cooperation; (2) regional unification of information about landslides and landslide research at national levels; and (3) development of landslide science by capacity building at regional level and practical applications of outcomes to societies in the region.

Latin America Network

Coordinator: Irasema Alcántara-Ayala

Deputy coordinator: Renato Eugenio de Lima

ICL Member Organizations involved in the Network: Institute of Geography, National Autonomous University of Mexico (UNAM), Mexico City, Mexico (WCoE 2011–2014); Center for Scientific Support in Disasters, Federal University of Paraná (UFPR), Curitiba, Brazil; GRUDEC AYAR, Cusco, Peru; Universidad Politécnica de Ingeniería (UPI), Tegucigalpa, Honduras; Universidad Nacional de Colombia, Bogotá, Colombia.

Objectives for the initial 3 years: (a) Setting up a database of experts of landslides in the region; (b) Identifying the areas of landslide expertise of the participants; (c)

Establishing a programme of necessities and priorities to be addressed; (d) Organizing a summer/winter school of landslides for young students/researchers, and landslide workshops; (e) Strengthening activities associated to landslide capacity building within Universities and governmental institutions; (f) To facilitate scientific support during and after landslide disasters.

North-East Asian Network

Coordinator: Kaoru Takara

Deputy coordinators: Sangjun Im, Xiaochun Li

ICL Member Organizations involved in the Network:

Korea Institute of Geoscience and Mineral Resources (KIGAM); Korean Society of Forest Engineering; China Geological Survey; Northeast Forestry University; Bureau of Land and Resources of Xi'an; Institute of Mountain Hazards and Environment, Chinese Academy of Sciences; Japan Landslide Society (WCoE 2011–2014); University of Tokyo, Geotechnical Engineering Group, Civil engineering; Niigata University, Research Institute for Natural Hazards and Disaster Recovery (WCoE 2011–2014); Forestry and Forest Product Research Institute; Disaster Prevention Research Institute (DPRI), Kyoto University, Japan; Department of Forest Sciences, College of Agriculture and Life Sciences, Seoul National University, Korea.

Objectives for the initial 3 years: The general objective is to promote the research on landslides triggered by earthquake, rainfall and their combination. Specific objectives are (1) promote international cooperation on landslide research triggered by earthquake, rainfall and their combination. (2) supply training course for landslide disaster mitigation. (3) Capacity building for areas and regions facing landslide problems.

South-East Asian Network for Landslide Risk Management

Coordinator: N.M.S.I. Arambepola

Deputy coordinator: Ko-Fei Liu

ICL Member Organizations involved in the Network:

National Taiwan University; Gadjah Mada University, Indonesia (WCoE 2011–2014); Asian Disaster Preparedness Center, Thailand (WCoE 2011–2014); Slope Engineering Branch, Public Works Department Headquarters, Malaysia.

Objectives for the initial 3 years: Long term goal of the network is to contribute to the Hyogo Framework for Action (HFA) by sharing experience, knowledge and expertise through networking in the area of landslide risk management technology applications for disaster risk management and

sustainable development in mountainous areas of South-East Asia. The international exchange and collaboration in landslide risk management practice and applied research is of utmost importance for meeting the future national, regional and global environmental challenges and their consequences. South-East Asian Network for Landslide Risk Management promotes and facilitates regional collaboration for applied research, exchange of experiences, knowledge sharing and initiate interventions for capacity building through active involvement of landslide risk management practitioners in South-East Asia to support effective implementation of the Hyogo Framework for Action.

Network on Landslide Risk Management

Coordinator: Surya Parkash

Deputy coordinator: Dwikorita Karnawati

ICL Member Organizations involved in the Network:

National Institute of Disaster Management, New Delhi, India (WCoE 2011–2014); Gadjah Mada University, Indonesia (WCoE 2011–2014); Geological Survey of Canada (WCoE 2011–2014); Institute of the Geospheres Dynamics, Russian Academy of Sciences, Russia (WCoE 2011–2014); University of Florence, Italy (WCoE 2011–2014); Building and Housing Research Centre, Iran; Institute of Geography, UNAM, Mexico (WCoE 2011–2014).

Objectives for the initial 3 years: (1) To invite participation and contribution on landslide risk management from different stakeholders in various sectors/entities throughout the world; (2) To create a thematic network of people, organizations, institutes, governments, societies etc. with a view to coordinate and integrate their efforts towards landslide risk reduction; (3) To collect, compile and disseminate information, knowledge, ideas, innovations and experiences related to landslides risk management for socio-economic and environmental safety as well as development; (4) To facilitate sharing, exchange and transfer of socio-cultural, scientific, technological, administrative, legal practices for promoting good practices and discouraging the bad practices; (5) To document all the activities done by the network.

Capacity Development Network

Coordinator: Dwikorita Karnawati

Deputy coordinator: Yin Yueping, Irasema Alcántara-Ayala

ICL Member Organizations involved in the Network: Gadjah Mada University, Indonesia (WCoE 2011–2014);

Institute of Geography at the National Autonomous University of Mexico (UNAM) (WCoE 2011–2014); China Institute of Geo-environmental Monitoring (Center of Geohazards Emergency, MLR); National Institute of Disaster Management, New Delhi, India (WCoE 2011–2014); Disaster Prevention Research Institute (DPRI), Kyoto University, Japan; Geodynamic Research Center, JSC “Hydroproject Institute”, Russia; International Institute of Earthquake Engineering and Seismology (IIEES), Iran; Central Engineering Consultancy Bureau (CECB), Sri Lanka.

Objectives for the initial 3 years: (a) Capacity development with respect to landslide risk reduction such as through courses/training, summer camp, expert and student exchanges; (b) Establishment of knowledge management system to support the capacity development program in landslide risk reduction, such as via the E-learning system.

Landslides in Cold Regions Network

Coordinator: Wei Shan

Deputy coordinators: Alexander Strom, Hideaki Marui

ICL Member Organizations involved in the Network: Northeast Forestry University, China; JSC “Hydroproject Institute”, Russia; Research Institute for Natural Hazards and Disaster Recovery, Niigata University, Japan (WCoE 2011–2014); Geological Survey of Canada (WCoE 2011–2014); Department of Earth Sciences, University of Florence, Italy (WCoE 2011–2014); Department of Geosciences, Shimane University, Japan; College of Construction Engineering, Jilin University, China; College of Geology Engineering and Geomatics, Chang’an University, China; Department of Geography, University of Zurich, Switzerland; Ministry of Forests, Lands and Natural Resource Operations, Canada; Earth Cryosphere Institute SB RAS, Russia; Georadar Division, IDS Ingegneria Dei Sistemi S.p.A. Italy.

Objectives for the initial 3 years: (1) To establish specialized agency under ICL; (2) Relying on financial support from both IPL project and government, corporate project, to convene regular meetings, to organize on-site visits, to exchange research results, and to train relevant persons; (3) To establish more landslide project in cold regions, and to enrich the cold regions landslide research results further.

Landslides and Cultural and Natural Heritage Network

Coordinator: Claudio Margottini

Co-coordinator: Vit Vilimek

ICL Member Organizations involved in the Network: ISPRA Geological Survey of Italy; Charles University in

Prague, Faculty of Science, Department of Physical Geography and Geoecology (WCoE 2011–2014); Bratislava University, Slovak Republic; Cairo University, Egypt; Gadjah Mada University, Indonesia (WCoE 2011–2014); University of Florence, Italy (WCoE 2011–2014); Geological Survey of Canada (WCoE 2011–2014); National Agency for Cultural Heritage Preservation of Georgia, Georgia; University of Capetown, Institute of Geomatic, South Africa.

Objectives for the initial 3 years: (1) To develop an emergency intervention group for the safeguard of natural and cultural heritage at risk in different part of the world; (2) To promote a culture of resilience for the protection of natural and cultural heritage from landslide hazard; (3) To develop low environmental impact approach, monitoring and solutions for safeguard of natural and cultural heritage from landslide hazards.

Landslide Monitoring and Warning Network

Coordinator: Matjaž Mikoš

Deputy coordinators: Željko Arbanas, Hirotaka Ochiai

ICL Member Organizations involved in the Network: Charles University, Faculty of Science, Department of Physical Geography and Geoecology, Czech Republic (WCoE 2011–2014); Comenius University, Faculty of Natural Sciences, Department of Engineering Geology, Bratislava, Slovakia; Croatian Landslide Group from Faculty of Civil Engineering, University of Rijeka, Croatia & Faculty of Mining, Geology and Petroleum Engineering, University of Zagreb, Croatia; Forestry and Forest Product Research Institute, Tsukuba, Japan; Gadjah Mada University, Faculty of Engineering, Department of Civil and Environmental Engineering, Yogyakarta, Indonesia (WCoE 2011–2014); Geological Survey of Slovenia, Ljubljana, Slovenia; Geo-Tools, NGO, Zdiby, Czech Republic; Kokusai Kogyo Co., Ltd., Tokyo, Japan; Public Works Department of Malaysia, Slope Engineering Branch, Kuala Lumpur, Malaysia; University of Florence, Department of Earth Sciences, Italy (WCoE 2011–2014); University of Ljubljana, Faculty of Civil and Geodetic Engineering, Ljubljana, Slovenia (WCoE 2011–2014); University of Niigata, Research Center for Natural Hazards & Disaster Recovery, Niigata, Japan (WCoE 2011–2014).

Objectives for the initial 3 years: The general objective is to compare experiences in the field of landslide monitoring and installed early warning systems for active landslides in different regions of the world. This objective is to be achieved by: (1) setting up of a dedicated web page (within IPL web pages) showing advanced landslide monitoring techniques and by giving a short overview of selected installed monitoring systems for active landslides in the world; and (2) preparing a series of review papers for the

journal *Landslides* covering the themes of the network and being prepared jointly by the members of the network (strong international cooperation).

Overview of WLF3 Session A2

ICL Regional Networks

(Alcántara-Ayala et al. 2014) present an overview of the two main activities of the ICL Latin America Network (ICLLAN) in 2013: First Central American and Caribbean Congress on Landslides held in Tegucigalpa, Honduras on March 20–22, 2013; the International Course-Workshop FORIN-Forensic Investigations of Disasters associated with landslides held in Tuxtla Gutiérrez Chiapas, Mexico on June 24–July 5, 2013. The First Central American and Caribbean Congress on Landslides was hosted by the Engineering Polytechnic University (UPI) together with the pre-congress seminar “Introduction to Landslide Identification, Assessment and Mitigation Measures” (16–19, March, 2013) which was attended by 33 professionals and engineering students. The FORIN Course-Workshop was hosted by Universidad de Ciencias y Artes de Chiapas (24–25, June 2013) and it was attended by 25 young scientists from seven Latin-America countries: Argentina, Brazil, Colombia, Guatemala, Mexico, Panama and Venezuela. ICCLAN is currently committed to strengthening collaboration among Latin American countries by reinforcing capacity building and promoting integrated disaster risk research on landslides. The paper also briefly introduces landslide hazard and risk evaluation in several municipalities of Colombia, using a deterministic approach.

(Arambepola 2014) provides a short overview of network objectives, past collaborative efforts of the network members, and expected results, as well as current and planned activities of the South-East Asian Network for Landslide Risk Management. The paper describes in more detail a summer training course on “Slope and Landslide Disaster Reduction” hosted by National Taiwan University in Taipei, Taiwan, held on August 4–16, 2013. The course was attended by around 35 participants from Afghanistan, Bangladesh, Bhutan, China, India, Indonesia, Iraq, Japan, South Korea, Lao PDR, Madagascar, Nepal, Nigeria, Sri Lanka, Thailand, and Vietnam. There were three field visits organized during summer training course: (1) Xiaolin village landslide in Kaohsiung County, Taiwan; (2) 921 Earthquake Museum of Taiwan; and (3) Chiu-fen-erh-shan landslide (located 12 km to the north of the 921 earthquake epicentre). Taiwan National University, by organizing the summer school, has created a unique opportunity for sharing experience and knowledge in landslide risk management with landslide practitioners from Asia. It will also provide

assistance to the ICL South-East Asian Network in organizing other planned symposia, workshops and network meetings in 2015/2016.

(Arbanas et al. 2014) briefly present an overview of the main ICL Adriatic-Balkan Network (ICL ABN) activities in the period from the beginning of 2012 till the end of 2013. One of the main ICL ABN activities was launching regional thematic conferences on landslides by organizing the 1st Regional Symposium on Landslides in the Adriatic-Balkan Region (1st ReSyLAB) in Zagreb (Croatia) on March 6–9, 2013. More than 110 participants from 12 countries (regional countries: Albania, Bosnia and Herzegovina, Bulgaria, Croatia, Kosovo, Macedonia, Slovenia, Serbia, Romania; and Japan, Russia, Vietnam) presented 77 scientific and professional papers. This paper describes in more detail the symposium technical sessions and side events (field trip to the Kostanjek landslide, two round tables, photo exhibition ‘Living with landslides’ and book promotion) of the 1st ReSyLAB, which were hosted by the University of Zagreb and the City of Zagreb. The social and technical program of the symposium enabled to the participants from nine regional countries to share their experiences about local landslide research at the regional level and enhanced establishment of relations between scientist in the region, which are important for future cooperative research and capacity building. The paper also shortly introduces the Croatian Landslide Portal (CLP), which has been available at the web address <http://www.klizista-hr.com> from July 2013; it will serve for dissemination of information on regional collaboration.

ICL Thematic Network

(Maček et al. 2014) present basic information about the ICL thematic network on Landslide Monitoring and Warning (ICL LaMaWaTheN), together with a description of the concept of a landslide monitoring database. One of the planned activities of the ICL LaMaWaTheN is to establish a web-based database entitled the World Report on Landslide Monitoring Sites (WRLMS), presenting the installed monitoring systems on landslides around the world, with links to web pages presenting the active monitoring of landslides. The paper describes in more detail terminology for landslide description and the description of the landslide monitoring techniques which will be used for database development. Data collection is planned through a questionnaire available at the official IPL web server. This landslide monitoring database is assumed to be a companion database to the already established World Report on Landslides (WRL; available at: <http://iplhq.org/category/iplhq/world-report-on-landslides/>). The specific objective of this ICL LaMaWaTheN activity is to establish a framework which

will enable people to gain a broader knowledge of the expertise on the topic of landslide monitoring available in the world.

Acknowledgments The conveners of the A2 Session would like to thank all the reviewers who have reviewed the papers submitted to this Session. The papers in the Session are significantly improved through mindful editing conducted by Eileen McSaveney, Lynn Highland and Mauri McSaveney. Their editorial work is highly appreciated.

References

- Alcántara-Ayala I, Carreño R, Ávila G, Godoy A (2014) The ICL Latin American Network (ICLLAN): past activities and challenges ahead. In: Sassa K et al (eds) *Landslide science for a safer geoenvironment*, Vol 1. Springer, Heidelberg, pp 181–185
- Arambepola NMSI (2014) A South-East Asian Network for landslide risk management for regional collaboration. In: Sassa K et al (eds) *Landslide science for a safer geoenvironment*, Vol 1. Springer, Heidelberg, pp 187–191
- Arbanas Ž, Mihalić Arbanas S, Vivoda M, Martinović K, Bernat S (2014) Landslide knowledge exchange through the regional cooperation in the Adriatic-Balkan region. In: Sassa K et al (eds) *Landslide science for a safer geoenvironment*, Vol 1. Springer, Heidelberg, pp 199–205
- Maček M, Petkovšek A, Majes B, Mikoš M (2014) Landslide monitoring techniques database. In: Sassa K et al (eds) *Landslide science for a safer geoenvironment*, Vol 1. Springer, Heidelberg, pp 193–197



The ICL Latin American Network: Past Activities and Challenges Ahead

Irasema Alcántara-Ayala, Raúl Carreño, Guillermo Ávila, and Aníbal Godoy

Abstract

Landslide disasters have major impact in developing countries due to the social vulnerability of communities and the lack of integrated risk research. In the last decades landslide disasters in Latin America triggered by precipitation, earthquakes volcanic eruptions and the built environment, have increased considerably. Therefore, scientific contributions towards reducing vulnerability of exposed communities to landsliding are quite urgent. The International Consortium of Landslides Latin American Network (ICCLAN) is currently under the commitment of strengthening collaboration among Latin American countries in the field of integrated disaster risk research on landslides through a multi and trans-disciplinary approach. Aiming at achieving such commitment, the organisation of two main activities has taken place in 2013. First of all, the First Central American and Caribbean Congress on Landslides was held in Tegucigalpa, Honduras. Secondly, an International Workshop on Forensic Investigations of Disasters (FORIN) associated with Landslides was also organised (Tuxtla Gutiérrez, Chiapas, México). Additional activities carried out in Colombia were included.

The objectives of ICL Latin American network (ICCLAN) include (a) Setting up a database of experts on landslides in the region; (b) Identifying the areas of landslide expertise of the participants; (c) Establishing a programme of necessities and priorities to be addressed; (d) Organizing a summer/winter school of landslides for young students/researchers, and landslide workshops; (e) Strengthening activities associated with landslide capacity building within Universities and governmental institutions; and (f) Facilitation of scientific support during and after landslide disasters.

Keywords

Landslide disasters • Risk assessment • Latin America • Caribbean region

I. Alcántara-Ayala (✉)
Instituto de Geografía, Universidad Nacional Autónoma de México,
Circuito Exterior s/n, México, México
e-mail: irasema@igg.unam.mx

R. Carreño
Grudec Ayar, Cusco, Peru
e-mail: raulcarreno@ayar.org.pe

G. Ávila
Universidad Nacional de Colombia, Bogotá, Colombia
e-mail: geavilaa@unal.edu.co

A. Godoy
Universidad Politécnica de Ingeniería, Tegucigalpa, Honduras
e-mail: agodoyv2003@yahoo.com

Introduction

Landslide disasters in Latin America have increased during the last decades. Examples include the consequences of hurricane Mitch in 1998, which were devastating in Central America, and particularly in Nicaragua and also in Honduras, a country that has been considered by the United Nations as the third most vulnerable, world-wide.

In almost all the Latin American region, landslide disasters are increasing as result of unsustainable development policies. Most of the cities do not have risk maps and

also there is a lack of expertise in many areas to assess and to evaluate mass movement potential zones. There is a clear need to share capacity and experiences to improve the Latin America programmes for landslide disasters reduction.

First Central American and Caribbean Congress on Landslides

The Congress

The First Central American and Caribbean Congress on Landslides took place in Tegucigalpa, Honduras, from March 20 to March 22, 2013. It was hosted by the Engineering Polytechnic University (UPI-Universidad Politécnica de Ingeniería). Support for the organisation was kindly provided by the Japan International Cooperation Agency (JICA), the International Consortium of Landslides (ICL), Honduran Civil Engineering Association (CICH), and some others institutions including the PanAmerican Union of Engineering Organizations (UPADI), the Federation of Engineering Organizations of Central America and Panama (FOICAP), Honduran Geoscience Institute, and the Center for Disaster Management Information Research of Ehime University in Japan (Figs. 1, 2 and 3).

The objectives of the Congress were: (1) Strengthening and promoting the study of landslides in Honduras and the whole Central American and Caribbean Region; (2) Sharing state-of-the-art landslide knowledge, including strengths and weaknesses; (3) Experience exchange; (4) Commitment and organization of future landslide events for Latin America and the Caribbean region.

Topics considered included: landslide typology, case studies, landslides disasters, urban landslides, human-made landslides, landslides and mining, landslide mapping and GIS, landslides and infrastructure, mitigation measures, landslides and planning, and landslides and watershed management.

The Seminar “Introduction to Landslide Identification, Assessment and Mitigation Measures”

From 16 to 19, March, 2013, as the main pre-activity to the First Central American and Caribbean Congress on Landslides, the ICL Latin American network (ICLLAN) organised the Seminar, *Introduction to landslide identification, assessment and mitigation measures*. The seminar took place in the Polytechnic University of Engineering—UPI, and was attended by 33 professionals and engineering students.



Fig. 1 Opening ceremony of the First Central American and Caribbean Congress (from Facebook-Congress page)



Fig. 2 Certificates were provided to participants by ICLLAN members (from Facebook-Congress page)



Fig. 3 Activities during the Seminar and Congress included landslide information dissemination through different media (from Facebook-Congress page)

The ICLLAN seminar comprised different topics as follows (1) Introduction to Disaster Risk Reduction associated with slope instability; (2) Hillslope instability: causes and mechanisms involved; (3) Landslide taxonomy; (4) Landslides in Honduras; (5) Mitigation measures; and (6) Landslide identification, mapping and monitoring.

At the end of the seminar, on March 18, 2013, a field trip to El Playon at Ajuterique, Comayagua was organised. In that area it was possible to observe and discuss the occurrence of a large landslide.

Forensic Investigations of Disasters Associated with Landslides

Introduction

The International Course-Workshop on Forensic Investigations of Disasters (FORIN) associated with landslides took place at Universidad de Ciencias y Artes de Chiapas, Tuxtla Gutiérrez Chiapas, Mexico during June 24–July 5, 2013 (Fig. 4). The main objective of the workshop was to share FORIN, a methodology proposed by the program on Integrated Research on Disaster Risk (IRDR), in order to understand the complex and underlying causes of disasters (Burton, 2010; IRDR 2011, 2013). The course was directed to young scientists and students from all disciplines related to the field of disaster risk reduction. Participants are expected to apply the FORIN methodology through study cases in different Latin-American countries (Fig. 5) (Alcántara-Ayala and Oliver-Smith 2014).

The workshop was sponsored by the International Council of Science (ICSU) and the International Geographical Union (UGI). It was supported by the ICSU program on Integrated Research on Disaster Risk (IRDR), the ICSU Regional Office for Latin America and the Caribbean (ICSU-ROLAC), the Mexican Academy of Sciences, the International Consortium on Landslides (ICL), the National Autonomous University of Mexico, the University of Sciences and Art of Chiapas, and the National Center for Disaster Prevention (CENAPRED) (Alcántara-Ayala and Oliver-Smith 2014).

Twenty five young scientists from different countries of Latin-America participated in the workshop. They included Argentina, Brazil, Colombia, Guatemala, Mexico, Panama and Venezuela. Scientific backgrounds of participants were variable. They comprised fields in both natural and social sciences, such as Geological Engineering, Geophysics, Geography, Anthropology, Politics Sciences, Architecture, Sustainable development, planning and environmental sciences. There was a gender balance since participants were 13 males and 12 females (Fig. 6).



Fig. 4 Conference on Integrated Research for Disaster Risk applied to landslides



Fig. 5 FORIN workshop activities



Fig. 6 Participants of the FORIN Workshop

Workshop activities included a series of lectures, presentations of individual projects, working groups, interviews with local media, fieldwork in a local community threatened by landslides (Fig. 7), and final project proposals.



Fig. 7 Fieldtrip to Las Cuevas del Jaguar landslide

Study cases incorporated the disasters of Yungay, Perú, 1970; hurricane Mitch in Honduras, 1998; hurricane Katrina, New Orleans, 2005; and the earthquake of Haiti, 2010, and others. Particular attention was paid to different aspects of the theory associated with the social construction of disasters, vulnerability analysis, landslide hazard assessment, field evaluation of landslides and mapping, displacement and resettlements, risk reduction and integrated research on disaster risk (Alcántara-Ayala and Oliver-Smith 2014).

Landslide Assessment in Colombia

Landslide hazard and risk evaluation has taken place in several municipalities of Colombia. It involved the multi-disciplinary work of engineers, geologists, social workers and GIS experts. Physical or structural vulnerability, as well as social vulnerability has been evaluated by considering surveys and detailed interviews of a certain number of families and houses that provide a representative sample.

Landslide hazard has been evaluated deterministically, that is to say, factors of safety of the slopes and a risk matrix that can be related to vulnerability and hazard. Direct communication with communities and local authorities has been very useful in these studies since a true representation of the results can be easily noticed. The produced risk maps will serve as tools to elaborate on the plans of expansion and land-use planning.

One of the studied municipalities, Guayabetal, is situated in a seismically active region about 80 km south of Bogotá (Fig. 8). The urban area is topographically constrained by a deep river channel and very steep slopes.



Fig. 8 Guayabetal municipality: unstable vegetated slopes



Fig. 9 Rock-fall at Guayabetal municipality

Precarious housing is located on unstable escarpments, where rainfall is higher than 4,000 mm per year. In July, 2013 a landslide and rock-fall (Fig. 9) occurred affecting approximately 20 houses, and fortunately there were no casualties. Risk analysis carried out for this area suggested that mitigation works would be more expensive than relocation of affected families.

Conclusions

Landslide disaster risk reduction focuses on the necessity to develop and implement integrated landslide research for disaster risk from a multi- and trans-disciplinary scheme to support and help societies. Understanding risk and investigating both natural and social spheres of disasters are essential practices for disaster risk reduction. Integrated risk research should be therefore viewed as a

key element for sustainable development, principally in vulnerable communities that have been frequently exposed to several hazards.

Consequently, reinforcing capacity building and promoting integrated disaster risk research on landslides would be the major challenge to be faced by our network as it could help to reduce vulnerability in the Latin-American region.

Acknowledgments We are most grateful to the International Council of Science (ICSU) and the International Geographical Union (UGI). Thanks are also due to CONACYT (Consejo Nacional de Ciencia y Tecnología, México) for financial support for the Project 156242: MISTLI (Monitoreo, Instrumentación y Sistematización Temprana de Laderas Inestables).

References

- Alcántara-Ayala I, Oliver-Smith A (2014) ICL Latin-American network: on the road to landslide reduction capacity building. *Landslides*
- Burton I (2010) Forensic disaster investigations in depth: a new case study model. *Environment* 52(5):36–41
- IRD (2011) Forensic investigations of disasters, FORIN-Report. <http://www.irdrinternational.org/>. Last Accessed 16 Sept 2013
- IRD (2013) Integrated research on disaster risk, strategic plan 2013-2017. <http://www.irdrinternational.org/2013/04/15/irdr-strategic-plan-2013-2017/>. Last Accessed 16 Sept 2013



A South-East Asian Network for Landslide Risk Management for Regional Collaboration

N.M.S.I. Arambepola

Abstract

Increasing landslide disaster risk is a global concern, but in South East Asia the situation is pressing. South East Asia is receiving a disproportionately large share of landslide disasters within Asia. It is therefore important to bring the regional landslide risk management community together to collaborate with other stakeholders, allowing everyone to profit from each other's knowledge and experiences for mutual benefit.

The mountainous areas in South East Asia are undergoing rapid change due to development interventions; as a result, human habitat, infrastructure, and lifeline facilities are becoming more vulnerable to landslides. There are other factors responsible for increasing vulnerability of hill slopes such as variability and extent of precipitation events, environmental degradation, urbanization and depletion of natural resources. It is likely that more frequent and more severe landslide disaster events will occur in the future, a trend that disaster statistics also support. To prevent and mitigate landslide disasters, reliable and up-to-date information on climate forecasts, geo-technical characteristics of slopes, sub-surface geological deposits, land-use changes etc. must be available to disaster managers and decision makers. Such information will allow them to make appropriate decisions and take timely actions to manage landslide risk. It is mutually useful if landslide practitioners share the experience in innovative and cost effective landslide risk reduction measures, strategies, methods, and applications to use them in their own countries and elsewhere.

The South-East Asian Network for Landslide Risk Management expects to promote and facilitate regional collaboration for applied research, exchange of experiences, knowledge sharing and to initiate interventions for capacity building through active involvement of landslide risk management practitioners within the sub-region. The ultimate aim is to support effective implementation of the Hyogo Framework for Action. This paper presents the planned interventions by the South-East Asian Network for Landslide Risk Management for the purpose of providing an opportunity to share some of the sound practices for landslide risk management, allowing network members to learn from other regional networks and to promote regional cooperation and collaborations among practitioners to effectively build safer and more resilient mountain settlements within South-East Asia.

Keywords

Experience sharing • Knowledge management • Collaboration

N.M.S.I. Arambepola (✉)
Asian Disaster Preparedness Center (ADPC), SM Tower, 24th Floor,
979/69, Paholyothin Road, Samsen Nai, Bangkok 10400, Thailand
e-mail: arambepola@adpc.net

Introduction

The mountainous areas within South-East Asia are undergoing rapid changes through development efforts of respective governments. As a result, built-up areas, infrastructure, lifeline facilities etc. are increasingly exposed to extreme events. The global factors (urbanization, depletion of natural resources, etc. combined with continuing economic development) invariably lead to adjustments in land use, human settlements, farming and agricultural practices etc. within mountainous areas. Such changes also increase the vulnerability of communities to hydro-meteorological and geo-hazards to which they are often exposed. Among them, landslides appear to be more frequent and more widespread phenomena within the mountainous areas of the South-East Asian region. It is likely that South-East Asian countries may experience more frequent and severe landslide disasters in the future. To prevent and mitigate future potential landslide disasters within the mountainous areas, more innovative and cost-effective measures are needed. It is useful for landslide practitioners to share the strategies, methods, and applications for mutual benefit and to build resilient communities. It is important to have more collaboration in the region for landslide risk management, in order to share knowledge, experiences and to combine efforts to overcome challenges and difficulties.

Objective of the Network

The long term goal of the South-East Asian Network for Landslide Risk Management is to effectively contribute to the Hyogo Framework for Action (HFA). The network will achieve this by sharing experience, knowledge and expertise through networking in the area of landslide risk management technology applications for disaster risk management and sustainable development of mountainous areas of South-East Asia.

International exchange and collaboration in landslide risk management practice and applied research is of the utmost importance for meeting future national, regional and global environmental challenges and their consequences. The South-East Asian Network for Landslide Risk Management promotes and facilitates regional collaboration for applied research, exchange of experiences, knowledge sharing and initiates capacity building through active involvement of landslide risk management practitioners in South-East Asia. Ultimately such efforts are expected to support effective implementation of the Hyogo Framework for Action by countries in the sub-region.

Past Collaborative Efforts of the Network Members

The network started its operations and activities in 2012. But there were several previous initiatives undertaken by members of the ICL, which prompted some active members to realize the usefulness of more collaborative effort. Some of such activities are:

- (a) ICL headquarter and Gadj Mada University, AIT, China Geological Survey have conducted the Asian Joint project on Early Warning of Landslides (IPL105) since 2008.
- (b) The Institute of Transport Science and Technology (ITST) in Vietnam, the ICL-Headquarter, the Forestry and Forest Product Research Institute of Japan, and the Japan Landslide Society have started a joint project with the financial assistance of the government of Japan in June 2011. The project will continue until March 2017 largely due to strong commitment and cooperation between ITST and two Japanese ICL members since 2010.
- (c) ICL headquarters, the Forestry and Forest Product Research Institute of Japan, the Japan Landslide Society, Gadj Mada University (Indonesia),
- (d) National Taiwan University, Asian Disaster Preparedness Center (ADPC) and others began collaboration to develop Landslide Teaching tools in April 2012.
- (e) ADPC in partnership with Norwegian Geotechnical Institute (NGI) has organized several Regional Workshops on Landslide-risk management for target countries of the Asian Program for Regional Capacity Enhancement for Landslide Impact Mitigation (RECLAIM) such as Bangladesh, Bhutan, China, India, Indonesia, Myanmar, Nepal, Pakistan, Philippines, Sri Lanka, Thailand and Vietnam. In the meeting organized in Yangon, Myanmar during 24-27 January 2012 which was attended by around 12 countries have emphasized the importance of having a Regional network for Landslide risk management.

Realizing the importance of establishing a network within South-East Asia, some of the active members of the ICL in landslide risk management in the sub-region such as the Gadj Mada University (Indonesia), National Taiwan University, Asian Disaster Preparedness Center (ADPC), Slope Engineering Branch, Public Works Department Malaysia jointly submitted a proposal to establish the South-East Asian Network for Landslide Risk Management (Arambepola 2012a) to ICL headquarters. Approval to establish the network under the auspices of ICL was granted in 2012.

Expected Results

Proposed interventions of the South-East Asian Network for Landslide Risk Management will be expected to achieve following results but not limited to:

- Build a strong regional network on landslide disaster mitigation for advancement of landslide science.
- Promote international exchange and collaboration in landslide-risk management practice through organizing networking events.
- Contribute through joint applied research in landslide-risk management, for meeting the future national, regional and global environmental challenges and their consequences.
- Initiate capacity-building interventions in partnership with partner institutions and make contributions in developing Landslide Teaching tools.
- Assist in documenting and disseminating sound practices.
- Policy advocacy and enhancement of public awareness.

Overview of Current Activities

Summer Training Course on “Slope and Landslide Disaster Reduction”

One of the active network members, the National Taiwan University in collaboration with the South-East Asian Network for Landslide Risk Management has organized a summer training course on “Slope & Landslide Disaster Reduction” (Arambepola 2012b). The course was held in Taipei, Taiwan during August 4–16, 2013. This course received Sponsorship from the National Science Council of Taiwan, Taiwan International Consortium on Geo-Disaster Reduction, Taiwan Intelligent Ironman Creativity Contest Association (National Taiwan University 2013). Landslide-related disasters are becoming more and more frequent in Taiwan owing to global warming. The objectives of the summer training course were to promote capacity building as a tool in landslide risk management and to share the efforts of the Taiwan Government in undertaking effective interventions for reducing the loss due to landslide disasters. This course was one of the first activities towards achieving the objectives of the South-East Asian Network for Landslide Risk Management. The course was attended by around 35 participants from Afghanistan, Bangladesh, Bhutan, China, India, Indonesia, Iraq, Japan, South Korea, Lao PDR, Madagascar, Nepal, Nigeria, Sri Lanka, Thailand, and Vietnam. A Group Photo of the Participants of the summer training course on “Slope & Landslide Disaster Reduction” is given below in Fig. 1.

Several faculty members from Taiwan National University headed by the course Director Prof. Ko-Fei Liu and representatives from other institutions shared the Taiwan



Fig. 1 Participants of the summer training course on “Slope and Landslide Disaster Reduction”

experience in dealing with Slope land Disaster Risk reduction. Taiwan has all types of slope land hazards and has many important research applications, sound practices as well as experience in legal enforcement at a local level. Therefore, Taiwan National University by organizing the summer school has created a unique opportunity for sharing experience and knowledge in landslide risk management with landslide practitioners from Asia. As a member of the landslide society, the National Science Council in Taiwan provided financial support for participants of this training course by way of full fellowships as a token in fulfilling the responsibility towards building a safer world. Many experts who had provided resource inputs to the course have covered the content integrating the experience and practitioners’ perspectives in applications bringing examples of various scenarios, contributing not only in providing knowledge but also in providing new ideas and techniques.

Field Visits Organized During Summer Training Course

For the benefit of course participants the course also arranged field visits to several geo-hazard locations to share experience. Some of the mobile facilities used by agencies also were demonstrated during the course (Fig. 2).

Xiaolin Village Landslide and Risk Reduction Measures

The participants had an opportunity to see the Xiaolin village landslide in Kaohsiung County, Taiwan. During typhoon Morakot, a deep-seated, dip-slope landslide with an area of 2.5 km² occurred and killed more than 400 people. It occurred



Fig. 2 Demonstration of the mobile facility used for debris-flow monitoring in Taiwan



Fig. 4 Participants visit to 921 Earthquake Museum of Taiwan



Fig. 3 Participants during the field visit to Xiaolin village landslide

on August 9, 2009 due to heavy rainfall. The mean depth of Xiaolin landslide was 44.6 m. The main sediment slid through an original valley, dammed the Chishan River, and buried a part of Xiaolin village. Dam-breaking occurred shortly after and buried the remaining part of the village. It was the most devastating disaster that had occurred since the typhoon warning system was established in Taiwan in 1992.

During the visit, participants (Fig. 3) learned how several mitigation and preparedness measures were being undertaken and saw the context of the disaster site.

Visit to 921 Earthquake Museum of Taiwan

At 01:47 AM on September 21, 1999, the central part of Taiwan was struck by an earthquake that registered 7.3 on the Richter scale. The resultant loss of life and damage to

property put it among the worst natural disasters of the past century in Taiwan. In the wake of the 921 disaster, the local government decided to preserve some of the phenomena related to the earthquake such as slip on the fault line, collapsed schools, raised river beds and other selected locations, to remind the public of the need to prepare for such disasters and to be ready to provide emergency rescue services.

The 921 Earthquake Museum of Taiwan combines an Exhibition Building with the geological changes and destroyed structures in one place to present a clear impression of the damage that was caused by the earthquake. The structures serve as pointers to the fault lines hidden under the earth and make the earthquake more real to visitors. Chelungpu Fault Gallery is located next to the oval track that was sharply displaced during the earthquake, showing very distinctly how the fault line moved. Figure 4 shows the visit of course participants to 921 Earthquake Museum of Taiwan).

Visit to Chiu-fen-erh-shan Landslide

The Chiu-fen-erh-shan landslide took place about 12 km to the north of the 921 earthquake epicenter. The area of the landslide was more than 200 ha and the volume moved was about 30 million m^3 . The slide moved more than two kilometres and 20 households were destroyed. The slide is located in the Inner Western Foothill zone and affected middle to late Miocene sandstones with inter-bedded shale layers. The average thickness of the deposit is 60–80 m. It consists of a chaotic mixture of small rock fragments and jointed blocks. The slide is one of the largest in Taiwan's history. A Memorial park was established to preserve the entire original phenomenon. A comprehensive monitoring system has been constructed here by the Bureau of Water and Soil Conservation.

Contributions to Landslide Teaching Tools

Network members made significant contributions to the ICL project on development of Landslide Teaching tools. Among them were National Taiwan University, Forestry and Forest Product Research Institute of Japan, the Japan Landslide Society, Gadjadara University (Indonesia), the National Taiwan University, and Asian Disaster Preparedness Center (ADPC).

Planned Future Activities

The Network is in the process of mobilizing funding to organize several activities in the future. It expects to organize another summer training course on “Slope & Landslide Disaster Reduction” with the generous assistance of network member National Taiwan University. Other planned activities are:

1. Symposium/workshop/network meeting on landslides in South East Asia in 2015/2016 within the area.
2. A network meeting during World Landslide Forum 3 in Beijing, 2014.
3. The network will continue contributing to the development and improvement of landslide teaching tools.

Conclusion

Landslide risk management can provide significant contributions to overall risk reduction, loss minimization and sustainable development in disaster affected countries in SEA. The South-East Asian Network for Landslide Risk

Management has made useful contributions during its initial year in enhancing the capacity of landslide professionals and sharing knowledge and experience in landslide risk management practice. However there is a long way to go to achieve its objectives fully and the results will largely depend on the participation of present network members and also if it can be extended to obtain the support of more agencies and individuals engaged in landslide risk management within South-East Asia.

Acknowledgment The network wish to thankfully acknowledge the support, guidance and help extended by Prof. Kyoji Sassa and the ICL management team in its initial year operations. The network also wish to thank Prof. Ko-Fei Liu and National Taiwan University for extending support in organizing the 1st summer training course on “Slope & Landslide Disaster Reduction” and all other network members in collaborating and extending support in organizing events of the network.

References

- Arambepola NMSI (2012a) Proposal of ICL South-East Asian network for landslide risk management. <http://iplhq.org/icl/wp-content/uploads/2013/02/SEA-Network-proposal.12.pdf>. Last Accessed 15 Sep 2013
- Arambepola NMSI (2012b) Progress report on the activities of the South-East Asian network for landslide risk management. http://iplhq.org/icl/wp-content/uploads/2013/11/Progress-Report-2012_SEA_Arambepola.pdf. Last Accessed 15 Sep 2013
- National Taiwan University (2013) Final report on the summer training course on “Slope & Landslide Disaster Reduction”. <http://2013sldr.weebly.com/download.html>. Last Accessed 15 Sep 2013



Landslide Monitoring Techniques Database

Matej Maček, Ana Petkovšek, Bojan Majes, and Matjaž Mikoš

Abstract

An ICL thematic network Landslide Monitoring and Warning Thematic Network (LaMaWa TheN) was established in 2011 and includes ten ICL member organizations and two ICL supporters from eight countries. Of the different proposed activities of this ICL thematic network, we at the University of Ljubljana, Faculty of Civil and Geodetic Engineering (UL FGG) have started to set up web pages showing advanced landslide monitoring techniques and giving case examples of landslide monitoring and early warning systems. In the first phase, we started to put together a literature review on landslide monitoring systems with the description of landslides—a landslide monitoring database. The database will later be used as a base for formulating a web questionnaire to be filled by landslide experts worldwide to gain a broader knowledge on the expertise available in the world on the topic of landslide monitoring.

Keywords

Web applications • Landslides • Database • Landslide monitoring

Introduction

In recent years, the monitoring of landslides has improved by the development of new monitoring equipment, automatic measurements done by computerized equipment and a decrease in equipment costs. However, together with these newly developed techniques, old techniques still remain in everyday use by geotechnical engineers. Thus, results of both new and old techniques for landslide monitoring are reported in the literature.

The techniques used for landslide monitoring depend on the type and size of a landslide, as well as the risks involved from its movements. There are also differences between countries, due to their gross domestic product, past experiences with landslide monitoring and other factors.

The main aim of the newly established ICL thematic network is to critically compare different monitoring techniques and early warning systems (EWS) from an international point of view, together with the possible transfer of technologies and experiences using them.

To achieve the objectives of the thematic network, a web page will be set up showing selected but advanced landslide monitoring techniques and providing a short but comprehensive overview of installed monitoring systems on active landslides around the world and to prepare review papers covering different landslide monitoring techniques and early warning systems.

The ICL LaMaWa TheN: A Thematic Network on Landslide Monitoring and Warning

The International Consortium on Landslides (ICL) was established in 2002, and during ICL's 10th anniversary (Kyoto, January 2012), a strategic document for the next decade with the motto "to create a safer geoenvironment"

M. Maček • A. Petkovšek • B. Majes • M. Mikoš (✉)
Faculty of Civil and Geodetic Engineering, University of Ljubljana,
Jamova c. 2, 1000 Ljubljana, Slovenia
e-mail: matej.macek@fgg.uni-lj.si; ana.petkovsek@fgg.uni-lj.si;
bojan.majes@fgg.uni-lj.si; matjaz.mikos@fgg.uni-lj.si

was adopted, recognizing thematic and regional networks for landslide risk reduction to be an important form of ICL activity in the next decade.

One of them is the Landslide Monitoring and Warning Thematic Network (LaMaWa TheN), which was proposed during the 10th session of the Board of Representatives of ICL in October 2011, at FAO (Mikoš 2012), with the objectives of setting up web pages showing advanced landslide monitoring techniques and to prepare review papers covering landslide monitoring techniques and early warning systems.

The LaMaWa TheN is a joint effort of 10 ICL member organizations and 2 ICL supporters from 8 countries: Croatia, Czech Republic, Indonesia, Italia, Japan, Malaysia, Slovakia and Slovenia. All of the network members have different and extensive experiences with landslide monitoring, landslide mitigation, landslide risk reduction and EWS (Mikoš 2012).

Monitoring of Landslides

Monitoring of landslides presents a challenge for geotechnical engineers, in part due to a lack of definition and due to their usually large scale (Mikkelsen 1996). Before the monitoring of a landslide is executed, careful plans should be made that consider topography, geology, ground water levels, material properties, possible mass movements, and reasons for monitoring. Typical monitoring tasks include determination of the slip surface, rate of movements, monitoring of marginally stable slopes before, during and after new construction, and evaluation of the effectiveness of mitigation works and EWS. The most important parameters for successful description of the landsliding should be recognized during planning, as well as the precision needed and time scale of the measurements. Usually the most important parameters are also the ones which will change significantly during the possible mass movement event. The selected parameters are thus problem dependent and in general depend on landslide types and reasons for landslide observation. The quality and the quantity of measurements are also dependent on economic constraints, which are dependent on the risk imposed by possible landslide movement. In the case of historic sites, the monitoring system is more comprehensive and innovative (e.g. Vlcko 2004; Chelli et al. 2006; Greif et al. 2006; Coppola et al. 2006).

The distinction should also be made between landslide monitoring and landslide survey. Landslide survey is done by surface survey and subsurface exploration (boreholes, geologic mapping, Fig. 1) and the landslide monitoring is carried out at regular time intervals by different measurement techniques, such as piezometers, inclinometers and extensometers.



Fig. 1 Drilling work for a borehole (piezometer) above the scarp of the Stože Landslide in NW Slovenia

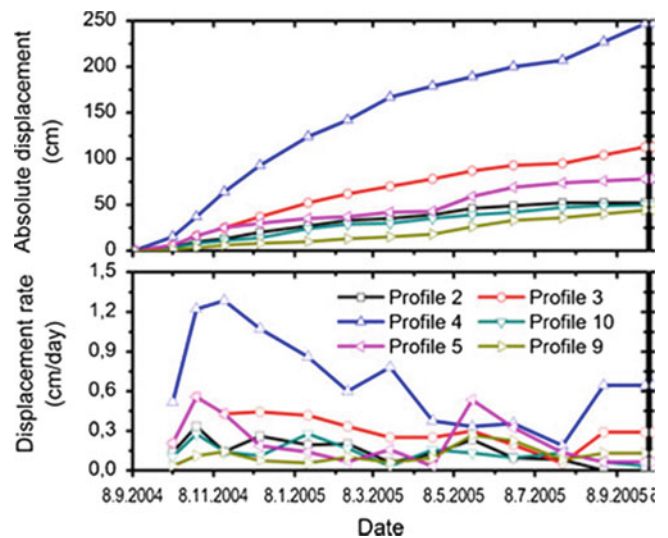


Fig. 2 Absolute displacements and displacement rates in six measuring cross sections on the Macesnik landslide (N Slovenia) (Pulko et al. 2013)

However, there are known examples of using landslide surface surveys (e.g. Fig. 2) and subsurface exploration techniques for landslide monitoring, as in case of the Slano Blato landslide (Logar et al. 2005; Pulko et al. 2013; Fig. 3).

The equipment used for landslide monitoring should also be reliable, being capable of functioning for long periods of time without maintenance or replacement. The response time should be short, and the sensitivity should be high enough for the given problem.

Landslide Monitoring Database

In 2013, we at UL FGG started to put together a database on different techniques used for landslide monitoring in 2013. The database will consist of case studies with descriptions

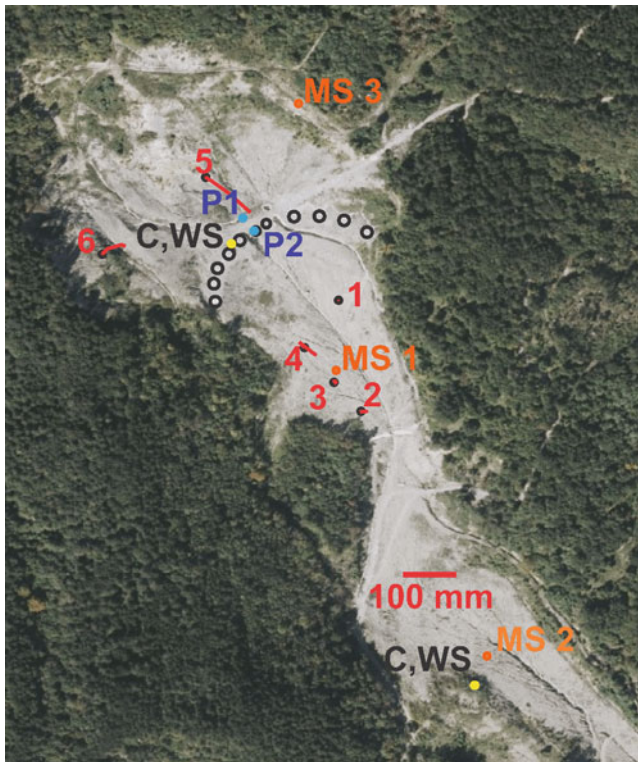


Fig. 3 Elements of the monitoring system on the Slano Blato Landslide (W Slovenia): *C* video camera, *WS* weather station, *MS* 1, 2 & 3 monitoring of soil suction, *P1* and *P2* piezometers 1 to 6 geodetic points (Petkovšek et al. 2013)

of landslides based on the Cruden and Varnes (1996) landslide classification system. The Cruden and Varnes (1996) landslide classification system uses long descriptions of the landslides with given activity, distribution and style, together with descriptions of first and second movement types. In complex landslides there could be additional movement types and for the database the relevant ones will be given in the landslide description. Figure 4 gives guidelines for forming names of landslides.

After the landslide description the task of landslide monitoring should be stated and the landslide monitoring techniques used should be given. For the database it would be a benefit to have some classification of the landslide monitoring techniques. These classifications could be found in the literature. Based on Mikkelsen (1996) the landslide monitoring techniques are divided into monitoring of surface movements, monitoring of pore water pressure inside the landslide, monitoring of ground displacements and others (Table 1). The equipment could be further divided based on how the measurements are performed. The measurements could be manual, as in case of probe inclinometers, or automatic by sampling in regular time intervals with electronic data loggers. The measurements collected by data logger could be collected manually or could be transferred automatically via internet, radio or

Activity			
State	Distribution	Style	
Active	Advancing	Complex	
Reactivated	Retrogressive	Composite	
Suspended	Widening	Multiple	
Inactive	Enlarging	Successive	
	Confined	Single	
	Diminished		
	Moving		
Description of movement			
Rate	Water content	Material	Type
Extremely rapid	Dry	Rock	Fall
Very rapid	Moist	Soil	Topple
Vapid	Wet	Earth	Slide
Moderate	Very wet	Debris	Spread
Slow			Flow
Very slow			
Extremely slow			

Fig. 4 Glossary for forming names of landslides (Cruden and Varnes 1996)

Table 1 Division of landslide monitoring methods by Mikkelsen (1996)

Surface movements measurements
Conventional equipment (optical instruments survey, tape/electronic distance measurements, total stations)
Tiltmeters
Differential global positioning system
Ground displacements measurements
Inclinometers (probe inclinometer, in-place inclinometer)
Extensometers (rod and wire extensometers, slope extensometers)
Groundwater monitoring
Open standpipe piezometer
Pressure sensor piezometer

mobile phones. The division made by Mikkelsen (1996) should be supplemented by newer techniques found in the literature.

In the recent years the project SafeLand: Living with landslide risk in Europe: Assessment, effects of global change, and risk management strategies (SafeLand 2012a) produced several reports dealing with landslide detection, fast characterisation, rapid mapping, monitoring and early warning systems. In these reports a slightly different division of landslide monitoring techniques is given (Table 2).

The division of landslide monitoring techniques is more based on who performs the tests and not the physical quantity. Report D4.4 of the SafeLand project (SafeLand 2012b) gives a comprehensive review of remote sensing techniques and also guidelines for their selection for long-term landslide monitoring, based on landslide rate, movement type, and for different phases of the risk management cycle. Report D4.5 (SafeLand 2012c) describes some new methods for landslide monitoring. The results of these two reports should be included in the database.

Table 2 Classification of methods for landslide detection, fast characterisation, rapid mapping and long-term monitoring (SafeLand 2012a)

Remote sensing
Passive optical sensors (ground based photography, aerial imagery, satellite imaging)
Active optical sensors (aerial laser scanner, terrestrial laser scanner, electronic distance meters)
Active microwave sensors (InSAR, DInSAR, PSI, GBinSAR, polarimetry for soil moisture estimation)
Geophysics
Ground-based (electricity, electromagnetic, micro-seismicity, ground penetrating radar, gravimetry, borehole geophysics)
Offshore (multi-faisseau, 2D, 3D seismic, sonar)
Airborne
Geotechnique
Inclinometers (probe, in place)
Extensometers (wire, probe extensometers, fixed)
Other (piezometers, contact earth pressure cells)
Other
GNSS
Core logging

Table 3 Division of landslide monitoring methods by ClimChAlp project (2008)

Geodetic surveying
Tacheometry
Terrestrial laser scanning
Precise levelling
Global positioning system
Geotechnical monitoring
Crack monitoring
Tiltmeters extensometers
Borehole inclinometers
Borehole extensometers
Piezometers
Time domain reflectometry
Fibre optics
Geophysical methods
Direct current geoelectric
Microseismic monitoring
Remote sensing
Photogrammetry
Airborne laser scanning
Satellite-born radar interferometry
Ground-based radar interferometry

Similar to the SafeLand project the ClimChAlp project (ClimChAlp—Climate Change, Impacts and adaptation strategies in the Alpine Space) divides monitoring methods into four main categories: geodetic, geotechnical, geophysical and remote sensing (Table 3).

As seen from Tables 1, 2 and 3, there are different divisions of landslide observation techniques and a combination of these should be used.

Discussion and Conclusion

It is important to note that usually only one part of a landslide monitoring system is described in a publication (e.g. a journal paper), and it is thus problematic to get an integrated picture of the whole landslide monitoring system. Publications mainly describe new measurement equipment, compare two different measurements (e.g. water level and landslide movements), or compare measured and predicted data.

To obtain a better understanding of which field measurements are important for a specific type of landslide and if there are differences between landslide monitoring techniques in different countries, a web questionnaire will be prepared to be filled in on-line by landslide experts. In the first phase, only members of the LaMaWaTheN network will be asked to participate. The results of the survey will be discussed, and the questionnaire may be modified if needed. In the second phase, the questionnaire will be opened to other professionals in the field.

The place for such a web questionnaire can be the official IPL web server. Using the results of the web survey, we may establish a web-based database named the World Report on Landslide Monitoring Sites (WRLMS), presenting the installed monitoring systems on landslides around the world, with links to web pages presenting the active monitoring of landslides. It can be a companion database to the already existing World Report on Landslides (WRL; available at: <http://iplhq.org/category/iplhq/world-report-on-landslides/>).

References

- Chelli A, Mandrone G, Truffelli G (2006) Field investigations and monitoring as tools for modelling the Rossena castle landslide (Northern Appennines, Italy). *Landslides* 3(3):252–259. doi:10.1007/s10346-006-0046-z
- ClimChAlp (2008) Slope monitoring methods, a state of the art report, p 179. http://www.lfu.bayern.de/geologie/massenbewegungen/projekte/climchalp/doc/engl_report_6.pdf. Last Accessed 30 Aug 2013
- Coppola L, Nardone R, Rescio P, Bromhead E (2006) Reconstruction of the conditions that initiate landslide movement in weathered silty clay terrain: effects on the historic and architectural heritage of Pietrapertosa, Basilicata, Italy. *Landslides* 3(4):349–359. doi:10.1007/s10346-006-0064-x
- Cruden DM, Varnes DJ (1996) Landslide types and processes. In: Turner AK, Schuster RL (eds) *Landslides investigation and mitigation; Special report 247*. National Academy Press, Washington, DC, pp 36–75
- Greif V, Sassa K, Fukuoka H (2006) Failure mechanism in an extremely slow rock slide at Bitchu-Matsuyama castle site (Japan). *Landslides* 3(1):22–38. doi:10.1007/s10346-005-0013-0
- Logar J, Fifer Bizjak K, Kočevar M, Mikoš M, Ribičič M, Majes B (2005) History and present state of the Slano Blato landslide. *Nat Hazards Earth Syst Sci* 5:1–11

- Mikkelsen PE (1996) Filed Instrumentation. In: Turner AK, Schuster RL (eds) Landslides investigation and mitigation; Special report 247. National Academy Press, Washington, DC, pp 278–316
- Mikoš M (2012) The ICL landslide monitoring and warning thematic network. *Landslides* 9(4):565–569. doi:10.1007/s10346-012-0359-z, 10.1007/s10346-012-0359-z#doi
- Petkovšek A, Maček M, Majes B (2013) Lessons learned from the 6 years matrix suction monitoring on the Slano Blato landslide (Slovenia). Mediterranean Workshop on Landslides. Napoli, 2013, pp 1–4. <http://www.mwl.unina2.it/Download/Petkovsek%20et%20al.pdf>. Last Accessed 15 Sep 2013
- Pulko B, Majes B, Mikoš M (2013) Reinforced concrete shafts for the structural mitigation of large deep-seated landslides: an experience from the Macesnik and the Slano blato landslides (Slovenia). *Landslides* 11(1):81–91. doi:10.1007/s10346-012-0372-2
- SafeLand (2012a) SafeLand–FP7, Deliverable 4.1, Review of techniques for landslide detection, fast characterization, rapid mapping and long-term monitoring, 401 p. <http://www.safeland-fp7.eu/results/Pages/wa4.aspx>. Last Accessed 30 Aug 2013
- SafeLand (2012b) SafeLand–FP7, Deliverable 4.4, guidelines for the selection of appropriate remote sensing technologies for monitoring different types of landslides, 91 p. <http://www.safeland-fp7.eu/results/Pages/wa4.aspx>. Last Accessed 30 Aug 2013
- SafeLand (2012c) SafeLand–FP7, Deliverable 4.5, Evaluation report on innovative monitoring and remote sensing methods and future technology, 280 p. <http://www.safeland-fp7.eu/results/Pages/wa4.aspx>. Last Accessed 30 Aug 2013
- Vlcko J (2004) Extremely slow slope movements influencing the stability of Spis Castle, UNESCO site. *Landslides* 1(1):67–71. doi:10.1007/s10346-003-0007-8



Landslide Knowledge Exchange Through the Regional Cooperation in the Adriatic-Balkan Region

Željko Arbanas, Snježana Mihalić Arbanas, Martina Vivoda, Kristina Martinović, and Sanja Bernat

Abstract

Regional cooperation among ICL members in the Adriatic-Balkan region has been initiated at the beginning of 2012 by establishing the ICL Adriatic-Balkan Network on Landslides which encompasses seven institutions from four regional countries, Albania, Croatia, Serbia and Slovenia. The objectives of regional cooperation are to conduct regional cooperative research and capacity building in landslide study and related risk prevention and mitigation for the benefit of society and the environment. This paper presents an overview of the main ICL ABN activities in the period from the beginning of 2012 to the end of 2013. One of the main activities was launching regional thematic conferences on landslides by organizing the 1st Regional Symposium on Landslides in the Adriatic-Balkan Region (1st RegSyLAB) in Zagreb, Croatia in March 2013. The social and technical program of the symposium enabled the participants from nine regional countries to share their experiences about local landslide research at the regional level and enhance the establishment of relations between scientist in the region which are important for future cooperative research and capacity building. This paper describes in more detail the technical sessions and side events of the 1st RegSyLAB, so as report symposium's outcomes as they relate to the promotion of landslide science.

Keywords

Adriatic-Balkan Network • ICL • Regional cooperation • Regional symposium on landslides

Ž. Arbanas (✉) • M. Vivoda
Faculty of Civil Engineering, University of Rijeka, Radmile Matejčić 3,
Rijeka 51000, Croatia
e-mail: zeljko.arbanas@gradri.uniri.hr; martina.vivoda@gradri.uniri.hr

S. Mihalić Arbanas • S. Bernat
Faculty of Mining, Geology and Petroleum Engineering, University of
Zagreb, Zagreb 10000, Croatia
e-mail: smihalic@rgn.hr; sanja.bernat@rgn.hr

K. Martinović
City of Zagreb, Emergency Management Office, Zagreb 10000, Croatia
e-mail: kristina.martinovic@zagreb.hr

Introduction

The ICL Adriatic-Balkan Network (ICL ABN) was established in January 2012 as one of eight regional and thematic networks of the International Consortium on Landslides (ICL) in order to promote its own activities as well as activities of the International Programme on Landslides (IPL). Figure 1 presents the logo of the ICL ABN. The network encompasses seven institutions (four universities, two national geological surveys and one governmental office) from Albania, Croatia, Serbia and Slovenia. The common interests for the establishment of this regional network on landslides are outlined in Mihalić et al. (2012a) and are as follows: (1) alignment of professional and scientific resources at the regional level by initiating and implementing joint bilateral or multilateral projects with participants from



Fig. 1 Logo of the ICL Adriatic-Balkan Network

the region; (2) sharing of information and knowledge; (3) enhancing education and training by exchanging scientists and professionals between regional institutions, establishing courses and schools on landslides for young researchers, and educating the public and local administrations; and (4) development of regionally harmonized strategies for landslide hazard/risk prevention and mitigation.

ICL ABN joint activities began in early 2012 by the preparation of a review of a wide range of subjects relevant for landslide research and mitigation in Croatia, Serbia and Slovenia. The review encompasses all issues which are considered as important for better understanding of the current state in the region at that time and presents background for further activities. The preliminary overview was presented at one regional conference (Mihalić Arbanas et al. 2012b) and the final one is published as ICL/IPL Activities in the Landslides Journal (Mihalić Arbanas et al. 2012c).

The official adoption and signing of the documents which confirm establishment of the ICL ABN was on 28 September 2012, during the first meeting of the Adriatic-Balkan Network in Belgrade, Serbia. The documents of the ICL ABN are, a Letter of Intent and Declaration of the Regional Cooperation and International Consortium on Landslides' Adriatic—Balkan Network Constitution. During the regional conference in Belgrade in September 2012 (14th Serbian Symposium of Engineering Geology and Geotechnics), regional ICL board members and coordinators of ICL ABN made two public presentations important for dissemination of information to non-ICL members. The first presentation, in the form of an oral presentation and brochure, was about the crucial documents, i.e., 2006 Tokyo Action Plan toward a Dynamic Global Network of IPL and ICL Strategic Plan 2012–2021 to create a Safer Geo-environment (ICL 2012). The second presentation was about the abovementioned review of the current state of landslide science, practice and management in Croatia, Slovenia, and Serbia, followed by information from Albania.

Discussion and endorsement in the course of the ICL ABN activities was performed in the format of the 1st ICL ABN Round Table which was held in March 2013 in Zagreb, Croatia, during the 1st Regional Symposium on Landslides in the Adriatic-Balkan Region. The resulting action plan of the Adriatic-Balkan Network is aligned with the following: (1) five priorities for action of the Hyogo Framework for Action, (2) the Action plan of the ICL for the next decade (published in ICL Leaflet 2012 in the frame of the ICL

Strategic Plan 2012–2021), (3) the ongoing current state of the region as it relates to landslide professional, scientific, educational, and management issues (Mihalić Arbanas et al. 2012b).

In the following paragraphs two main activities of the ICL ABN in the 2-year period 2012–2013, are described in more detail. The 1st Regional Symposium on Landslides in the Adriatic-Balkan Region presents implementation of ICL ABN activity in 2013 primarily aimed at the exchange of knowledge at the regional level. It was organized as a conference with more than 100 participants and a series of side events: a landslide photo exhibition; technical tour to the Kostanjek Landslide (Mihalić Arbanas et al. 2013); two round tables; and promotion of the book by Sassa et al. (2013). The second ICL ABN activity implemented in 2013 is related to the unified collection of data about landslides, where the Croatian Landslide Group initiated systematic collection of landslide data on the national level through the development of the Croatian Landslide Portal.

1st Regional Symposium on Landslides in the Adriatic-Balkan Region

The 1st Regional Symposium on Landslides in the Adriatic-Balkan Region entitled “Landslide and Flood Hazard Assessment” was held in March 2013 in Zagreb (Croatia) together with the 3rd Workshop of the Croatian Japanese SATREPS FY2008 Project on “Risk Identification and Land Use Planning for Disaster Mitigation of Landslides and Floods in Croatia”. More than 110 participants (Fig. 2) from 12 countries (Albania, Bosnia and Herzegovina, Bulgaria, Croatia, Japan, Kosovo, Macedonia, Slovenia, Serbia, Romania, Russia, and Vietnam) presented 77 scientific and professional papers about landslides and floods hazard assessment as well as other topics related to landslide science and practice. All paper abstracts are published in the proceedings by Mihalić Arbanas and Arbanas (2013), as shown in Fig. 3. Technical sessions were accompanied by a series of side events: a field trip, round tables, photo exhibition and book promotion.

All symposium activities were organized as a four-day program. The symposium started on Wednesday 6 March with the welcome reception at the Faculty of Mining, Geology and Petroleum Engineering. The first part of the technical program (oral presentations) was held in the City Assembly Hall on Thursday 7 March. A guided sightseeing tour in the Upper Town was held during the lunch-break. Thursday night was reserved for the cocktail reception by the Mayor of the City of Zagreb, in the Dverce Palace. The second part of the technical program (oral and poster presentations) was held in the University Rectorate on Friday 8 March. Two round tables were organized at the end of

Fig. 2 Participants of the 1st Regional Symposium on landslides in Adriatic-Balkan Region entitled “Landslide and Flood Hazard Assessment” in the front of the building of the University Rectorate (Zagreb, 8 March 2013)



Fig. 3 Front cover of the 1st RegSyLAB Abstract proceedings with 77 abstracts

the technical sessions on 7 and 8 March. The symposium closing was held in the ZgForum followed by the opening of the landslide photo exhibition “Living with Landslides” and, finally, the promotion of the book “Landslides: Global Risk Preparedness” (Sassa et al. 2013). Saturday 9 March was reserved for a technical tour to the Kostanjek Landslide Field Observatory for landslide monitoring situated in the City of Zagreb.

Technical Program of the 1st RegSyLAB

All symposium paper presentations were grouped in three thematic sessions which reflects the structure of the working groups of the Croatian-Japanese SATREPS FY2008 project. The session entitled “Landslides” encompassed presentations about landslide investigations, landslide monitoring, numerical modeling and landslide remediation. The session entitled “Flash-Floods and Debris Flow” was aimed at presentations about observations of meteorological and hydrological parameters in the analyzed catchment areas, numerical and hydrological analysis of the measured parameters and the development of simulation models of floods and debris flows, as well as establishing of early warning systems of these phenomena. The session entitled “Hazard Mapping” encompassed presentations about landslide inventories, and landslide susceptibility, hazard and risk assessment and zonation.

The first symposium day was reserved for presentation of activities and results of the Croatian-Japanese five-year

bilateral project (2009–2014) “Risk Identification and Land-Use Planning for Disaster Mitigation of Landslides and Floods in Croatia” (Mihalić and Arbanas 2013). It was the 3rd Project Workshop, after the 1st Workshop held in Dubrovnik in 2010 and the 2nd Workshop held in Rijeka in 2011. The aim of the Workshop was to present recent results of the 4-year joint research performed at all project pilot areas in the City of Zagreb, Primorsko-Goranska County and Splitsko-Dalmatinska County. Researchers from Croatia and Japan presented scientific papers with results for the following investigations and analyses: aerial photo and satellite image interpretation, geodetic and geotechnical monitoring of landslides, continuous monitoring of sediment flows in torrents, advanced investigation of physical and mechanical properties of soils and rocks, landslide susceptibility and hazard zonation, establishment of early warning systems, and risk mitigation through the system of urban planning and civil protection. More than 60 Croatian and Japanese scientists from University of Rijeka, University of Zagreb, University of Split, Croatian Geological Survey, Niigata University, Kyoto University and International Consortium on Landslides presented 31 scientific papers.

The second symposium day was reserved for oral and poster presentations of 44 papers prepared by scientists and experts from nine countries in the region, and from Japan, Russia and Vietnam. Papers provided insight into regional and international research focused on landslide and flood characterization, modeling, monitoring, mapping and remediation. Regional and international guest landslide scientists and experts came from 12 universities, 8 institutes and 8 companies.

Field Trip: The Kostanjek Landslide Observatory for Landslide Monitoring

A field trip to the Kostanjek Landslide, the largest landslide in Croatia (Mihalić Arbanas et al. 2013) was organized for the last day of the symposium. The objective of the field trip was to present the general design of a comprehensive automated monitoring system of the Kostanjek landslide to the symposium participants.

The monitoring system of the Kostanjek Landslide was designed to include a number of different types of sensors communicating in near-real time to a data acquisition processing centre located at the Faculty of Mining, Geology and Petroleum Engineering, University of Zagreb. It is equipped within the framework of the Croatian-Japanese SATREPS FY2008 project. An integrated monitoring system will finally consist of approximately 40 sensors for geodetic and geotechnical monitoring of landslide movement and landslide triggering factors (rain and earthquake):

15 precise GNSS rovers, 9 long-span and short-span extensometers, 4 vertical extensometers, 1 inclinometer, 3 pore pressure gauges in boreholes, 3 water level gauges in wells, rain gauge, weather station and 7 accelerometers. The installation of the system started in November 2011 and will be nearly finished in 2013. The system is meant to improve and contribute to public safety, public education, scientific research, and university education.

Round Tables

The first Round table entitled “Application of Croatian-Japanese Project Results in the Systems of Land-Use Planning, Construction and Civil Protection in Croatia” was held on 7 March 2013 in the City Hall. It was an exceptional opportunity to gather the representatives of local and national government of the Republic of Croatia and the scientists involved in landslide and flood research. Round table discussion was organized in collaboration with the City of Zagreb and Primorsko-Goranska County. The aim of the round table discussion was to debate, with a wide audience, the future practical application of scientific results in the Croatian system of land-use planning, construction and civil protection. Core topics of the discussion were landslide maps (landslide inventory maps and landslide hazard and risk prognostic maps), flood maps (hazard and risk prognostic maps), landslide and flash flood monitoring and early warning systems, landslide modeling and flash flood propagation with different hazardous test scenarios.

The second Round table entitled “Discussion and Endorsement in the Course of the ICL Adriatic-Balkan Network Activities” was held on 8 March 2013 at the University of Zagreb. The main topic of this round table was how to plan and deliver activities of the ICL ABN successfully, which is one of the greatest challenges of the regional network. Landslide scientists from Croatia, Slovenia, Serbia, Macedonia and Albania were involved in the discussion. Strengths, weaknesses, opportunities, and challenges of the current status of landslide research and landslide risk management in the Adriatic-Balkan region were discussed as a basis for further development of the ICL ABN action plan. One of the main conclusions of this round table was the organization of regional symposia every two years. 2nd ReSyLAB will be held in Belgrade in 2015.

ICL ABN Photo Exhibition “Living with Landslides”

A photo exhibition “Living with Landslides” was organized with the cooperation of Croatian ICL members (two faculties from Zagreb and Rijeka and the Emergency Management



Fig. 4 Landslide photographs and brochures (Fig. 5) of the photo exhibition ‘Living with Landslides’ in ZgForum gallery (Zagreb, 8–15 March 2013)



Fig. 5 Front cover of the photo exhibition brochure



Fig. 6 The photo which was awarded first prize entitled ‘The Siriu Landslide’ (author Teodor Burilescu, Romania)

Office from Zagreb) with Office of the Strategic Planning and Development of the City of Zagreb. Photos showing different landslide scenarios were presented in the ZgForum (Fig. 4), gallery and multimedia center located in the downtown area of the Zagreb city. The photo exhibition ceremony opened on 8 March by the Vice Mayor of Zagreb, and was also open for the public until 15 March 2013.

The 35 exhibited photos were taken by 24 photographers from 8 countries, most of them participants of the symposium (Fig. 5). Every photo was accompanied by a short landslide story. Photo exhibition jury selected the best three photos as follows: 1st prize—Teodor Burilescu for the photo “Landslide Siriu” taken in Romania (Fig. 6); 2nd prize—Toni Nikolić for the photo “The Floating houses”

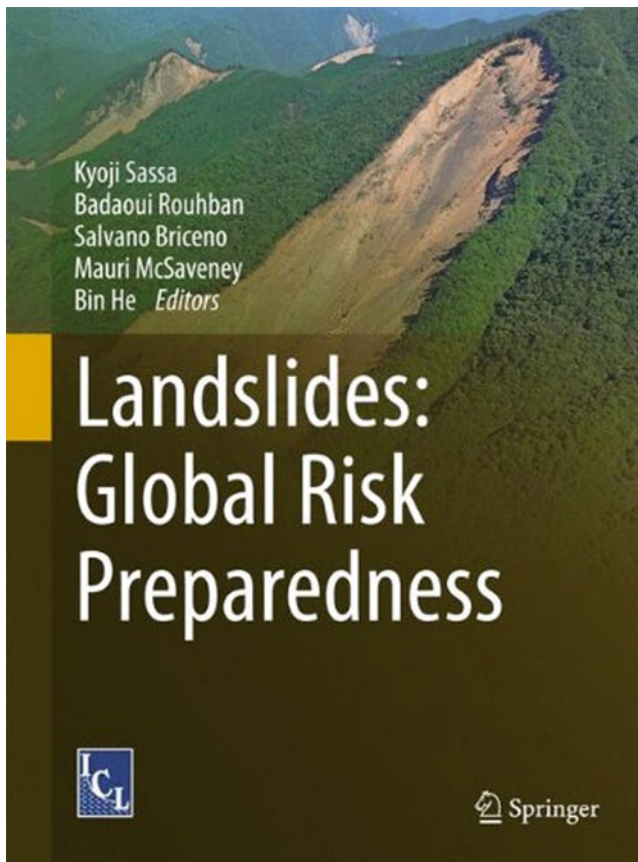


Fig. 7 Front cover of the book “Landslides: Global Risk Preparedness” (Sassa et al. 2013)

taken in Bosnia and Herzegovina, presenting Maglaj landslide that completely destroyed 7 and damaged 10 houses; 3rd prize—Željko Arbanas for photo “The road” taken in Croatia, presenting a damaged local road one day after activation of the Brus landslide in Istria.

Book Promotion

During the opening ceremony of the photo exhibition “Living with Landslides”, the ZgForum gallery also hosted the

promotion of the book “Landslides: Global Risk Preparedness” edited by distinguished Professor Kyoji Sassa and co-editors Dr. Badaoui Rouhban, Dr. Salvano Briceño, Dr. Mauri McSaveney and Dr. Bin He (Fig. 7). This book presents the global landslide risk preparedness implemented through the International Programme on Landslides (IPL). The 26 book chapters are organized into four main parts: Outline of the International Programme on Landslides and IPL Global Promotion Committee; Achievements of major IPL projects in research and capacity building; World Centres of Excellence on Landslide Risk Reduction (WCoEs) and Landslide School Network; Key documents of IPL and ICL including Tokyo Action Plan, Application of ICL, IPL Projects, WCoEs and Landslide School Network.

Croatian Landslide Portal

The Croatian Landslide Portal (CLP) has been available at the web address <http://www.klizista-hr.com> from July 2013. It has been established and maintained by members of the Croatian Landslide Group from the Faculty of Civil Engineering (University of Rijeka) and Faculty of Mining, Geology and Petroleum Engineering (University of Zagreb). The CLP is developed as a web interface for: (i) announcing news about landslide events from Croatia and from around world (Fig. 8); (ii) promotion of landslide science by publishing information about scientific projects, pilot areas and scientific conferences; (iii) promotion of the education about landslides by publishing information about educational institutions, landslide courses, teaching tools, etc. (iv) making public the Croatian Landslide Catalog (CLC), data base which is under development, by collecting and archiving data about approximately 900 landslide events reactivated in 2013. Portal visitors can also submit landslide occurrence information for the CLC using a simple on-line form. Scientists from faculties in Zagreb and Rijeka are cooperating with the Croatian National Protection and Rescue Directorate in maintenance of the Croatian landslide data base.

Fig. 8 Web interface of the Croatian Landslide Portal (<http://www.klizista-hr.com>) with landslide news

The screenshot shows the web interface of the Croatian Landslide Portal (KLIZISTA-hr). At the top, there is a navigation menu with links for HOME, ORGANIZATION, DATA BASE, and CONFERENCES. The main header features the KLIZISTA-hr logo and the text 'CROATIAN LANDSLIDE PORTAL'. Below this is a large banner image showing a landslide site with several people standing on a concrete structure. The banner text reads: 'WHERE AND WHEN DO LANDSLIDES OCCUR? Read in our news from around Croatia and world'. Below the banner, there are three columns of news items:

- NEWS HR:** 15/11/2013 **Rockfall buried railway near the City of Buzet**. The rockfall from the, so called, Raspadalica Cliff in the Čičarija Massif buried the railway at the section from the Buzet Rail Station to the Roč Village in Istria.
- NEWS WORLD:** 28/12/2013 **Section of Tijuana-Ensenada Scenic Highway Collapses**. A section of the toll road leading from Tijuana to Ensenada collapsed more than 300 feet toward the ocean early. The collapse happened at kilometer 93 just south of Salsipuedes following a magnitude 4.6 earthquake on December 20.
- INFORMATION:** 18/12/2013 **Japan tsunami exacerbated by landslide**. The 2011 Japan tsunami, which killed up to 20,000 people and caused the partial meltdown of the Fukushima nuclear plant, was made worse by an underwater landslide, according to scientists.

On the right side, there is a sidebar with logos for the University of Rijeka Faculty of Civil Engineering and the International Consortium on Landslides. Below the logos is a red cover of the journal 'Landslides'.

References

- ICL (2012) Leaflet of the International Consortium on Landslides. ICL, Kyoto, 60 p
- Mihalić Arbanas S, Arbanas Ž (eds) (2013) Landslide and flood hazard assessment. In: Abstract Proceedings of 1st regional symposium in the Adriatic-Balkan region with the 3rd Workshop of the Japanese-Croatian Project. Emergency Management Office, Zagreb, 85 p. ISBN: 978-953-7479-28-2
- Mihalić Arbanas S, Arbanas Ž, Abolmasov B, Mikoš M, Komac M (2012a) Regional cooperation in the frame of the ICL Adriatic-Balkan network. In: Sunarić D, Jevremović D (eds) Proceedings of 14th symposium on engineering geology and geotechnics, 27–28 September 2012, Belgrade, Serbia, pp 43–56 (in Serbian)
- Mihalić Arbanas S, Arbanas Ž, Abolmasov B, Mikoš M, Komac M (2012b) The ICL Adriatic-Balkan Network: analysis of current state and planned activities. *Landslides* 10(2):103–111
- Mihalić S, Arbanas Ž, Mikoš M, Abolmasov B (2012c) The ICL Adriatic-Balkan network: scientific background, opportunities and challenges for regional cooperation. In: Sassa K, Takara K, He B (eds) Proceedings of IPL symposium, 20 January 2012, Kyoto, Japan, pp 27–37
- Mihalić Arbanas S, Arbanas Ž, Krkač M (2013) TXT-tool 2.385-1.2 A comprehensive landslide monitoring system: The Kostanjek landslide, Croatia. In: Sassa K et al (eds) ICL landslide teaching tool. ICL, Kyoto, Japan, pp 158–168. ISBN 978-4-9903382-2-0
- Mihalić S, Arbanas Ž (2013) The Croatian–Japanese joint research project on landslides: activities and public benefits. In: Sassa K et al (eds) *Landslides: global risk preparedness*. Springer, Berlin, pp 333–349. ISBN 978-3642220869
- Sassa K, Rouhban B, Briceño S, McSaveney M, He B (eds) (2013) *Landslides: global risk preparedness*. Springer, Berlin, 370 p. ISBN 978-3642220869

Policy, Legislation and Guidelines on Landslides



Introduction: Policy, Legislation and Guidelines on Landslides

Salvano Briceno

Keywords

Risk management • Risk governance • Disaster risk reduction • Landslide risk reduction • Policy • Legislation • Organizational arrangements • Institutional arrangements

The institutional requirements for managing risk related to landslides—also known as governance of landslide risk reduction—comprise a number of elements, which include policy, legislation, organizational arrangements as well as a number of ethical, educational, awareness, training, research, scientific and technological capacities.

Managing the risk associated with landslides is part of wider disaster risk reduction governance, which often requires a multi-hazard approach as an essential condition for effectiveness; hence, specialists on governance are not necessarily specialists in landslide studies but they need to address landslides as a key hazard, related equally amongst hydro-meteorological, geophysical and geological hazards.

Managing the risk of landslides includes various strategies and measures of prevention, mitigation and preparedness for such hazards, which in turn need to be integrated into other policy sectors, such as land-use and urban planning, environment, agriculture, health, education, transport, tourism, infrastructure besides disaster or emergency management.

Overall guidance for risk management related to natural phenomena is still effectively provided by the *Hyogo Framework for Action (2005–2015): Building the resilience of*

nations and communities to disasters. The policy guidelines contained in the Hyogo Framework are being currently reviewed with the intent to update and enhance the content for adoption at the upcoming Third World Conference for Disaster Risk Reduction, planned for Sendai, Japan from 14–18 March 2015. The contents of this publication (as currently revised) as well as the discussions pending at the Third World Landslide Forum (Beijing, 2–6 June 2014) represent a substantive contribution by experts from the technical, scientific, engineering and other practitioners communities that work on landslides, to the benefit of a wider disaster risk management community who will meet at Sendai in 2015.

The rapid increase in urban vulnerability, due to urban population growth and poverty but also to the increasing effect and impacts of climate variability and climate change, makes risk management and wider risk governance a much higher priority for governments. Risks associated with landslides have the terribly damaging potential to contribute to loss of lives as well as the reduction of development gains; hence the need for appropriate disaster risk governance to be placed close to the highest authority levels in government (local, national, regional to international levels). A number of countries have advanced in this regard and are showing the way for many other countries that have not as yet addressed the full range of requirements of risk governance.

The development of risk governance, also recognized as the institutional requirements for managing risk needs to be addressed by governments jointly or in close collaboration with the academic and scientific institutions that specialize

S. Briceno (✉)
Science Committee, Integrated Research on Disaster Risk (ICSU/ISSC/
UNISDR), Haidian District, Beijing, China
e-mail: salvanob@gmail.com

in various hazards and the vulnerability components of risk; including also experts from civil society organizations and the private sector.

The Third World Landslide Forum provides a valuable opportunity to policy-makers to enhance their understanding of risk related to landslides that are increasingly causing losses and damages to exposed populations, societal

infrastructure and for promoting a team effort amongst policy-makers, experts and practitioners from all sectors.

The papers in this session provide examples of some of the relevant elements and considerations in this field of consideration. Other examples are scattered within the many other sessions at the Third World Landslide Forum.



Disaster Risk Reduction and Sustainable Development

Mark Pelling, Reid Basher, Joern Birkmann, Susan Cutter, Bina Desai, S.H.M. Fakhruddin, Ferruccio Ferrugini, Tom Mitchell, Tony Oliver-Smith, John Rees, and Kuniyoshi Takeuchi

Abstract

Scientific research and practitioner experience have revealed that disasters, development and poverty are intimately linked. Destruction of assets and livelihoods in disasters set back hard-won development gains and worsen poverty, often for extended periods of years. Progress in ending extreme poverty may be reversed in the face of a disaster event and poverty re-entrenched. Disaster impacts are growing, amplified by rapid growth and unsustainable development practices that increase the exposure and vulnerabilities of communities and capital assets. Governments increasingly recognise that the reduction of disaster risks is a foundation for successful sustainable development, and that disaster risk is a crosscutting issue, requiring action across multiple sectors.

Keywords

Sustainable Development Goals • Poverty • Risk drivers

Introduction

The discussion set out in this paper was prepared by experts associated with the Integrated Research on Disaster Risk (IRDR) programme for the Seventh Session of the UN General Assembly Open Working Group on Sustainable Development Goals, New York, 6–10 January 2014. For further information see <http://www.irdrinternational.org>. The IRDR is jointly sponsored by the International Council for Science (ICSU), the International Social Science Council (ISSC) and the UN Secretariat of the International Strategy for Disaster Reduction (UNISDR). The paper was supported by the British Geological Survey and followed extensive discussion within the wider membership of the IRDR community, Reid Basher acting as the expert author and Mark Pelling as overall project coordinator and editor.

M. Pelling (✉) • R. Basher • J. Birkmann • S. Cutter • B. Desai • S.H.M. Fakhruddin • F. Ferrugini • T. Mitchell • T. Oliver-Smith • J. Rees • K. Takeuchi
e-mail: mark.pelling@kcl.ac.uk

Overview

Increasing Disaster Impacts and the Downward Spiral
Globally, the impacts of disasters have risen rapidly over recent decades, affecting almost all sectors and rich countries and poor countries alike (UNESCAP 2010, 2012; UNISDR 2013a; World Bank 2013). Several hundred million people are affected annually and losses reached a record US\$ 371 billion in 2011 (CRED 2012). This figure may underreport the true losses by 50 % or more (UNISDR 2013b). It does not incorporate knock-on impacts across economies and it undervalues the relative economic impacts on individual and particularly poor households. In some regions numerous smaller-scale and unreported events are a major source of aggregate loss, especially in developing countries and poor communities (Bull-Kamanga et al. 2003; UNISDR 2013b). A particular concern is that disaster-damaged livelihoods and economies can set the preconditions for further rounds of excessive exposure, susceptibility and loss, blocked escapes from poverty and negative spirals of development failure. This may occur at any level, from household to state.

Underlying Risk Factors The United Nations-sponsored Hyogo Framework for Action 2005–2015 (UN 2005), which seeks to build the resilience of nations and communities to disasters, includes the integration of disaster risk considerations into sustainable development processes as a key strategy. One of its five priorities is the reduction of underlying risk factors, involving environmental, social and economic actions, but it is here that least progress has been achieved according to reporting by Governments (see <http://www.preventionweb.net/english/hyogo/progress>).

Explicit recognition of disaster risk reduction in the Sustainable Development Goals will provide critical weight to help drive the substantive work on underlying disaster risk in the parallel post-2015 framework planned to succeed the Hyogo Framework for Action.

The Disaster Risk Process and Risk Management

Disasters can be considered an outcome of an ongoing “risk process”, in which the prevailing circumstances of hazards, exposure and vulnerabilities combine to generate disaster risk. The risk may grow and accumulate over time, becoming evident as greater losses only when a hazard event strikes. This is a radical shift from earlier ideas of disasters as acts of God or as natural events. A geophysical hazard event may be natural but its impacts depend on the circumstances of people, households and societies, which in turn arise from diverse micro- to macro-level political, social, economic and environmental processes. Knowledge of the driving factors in disaster risk is the essential basis for pre-emptive policy and action to reduce the risks. Integrated approaches will improve outcomes and opportunities for both disaster risk reduction and sustainable development. A basic requirement in both cases is to systematically monitor disaster risk.

Linkages with Climate Change It is well accepted that disaster risk reduction measures will play an important role in responding to the projected increases in weather- and climate-related hazards including sea-level rise (IPCC 2012). Good management of today’s existing risks is clearly the starting point for facing tomorrow’s changed risks, whether from climate change, globalization or development. These three policy arenas share interests in monitoring changing risks, reducing exposure and vulnerability and advancing the transformation to resilience and sustainability.

Targets and Indicators High-level meetings have identified the need to address resilience and disaster risk reduction in the Sustainable Development Goals (UN 2012, 2013). Targets and indicators work can draw on the experience gained in monitoring progress on the Hyogo Framework

for Action. Various global and national databases are available for natural hazards, exposure and disaster losses, and research is advancing on measures of vulnerability and resilience (see final section).

Disasters and Sustainable Development

Disaster Events Undermine Poverty Eradication The livelihoods, productive economic activity and public capacities that keep poverty at bay are compromised when the underpinning assets and resources of households and countries are destroyed in disasters (Shepherd et al. 2013). This can generate new poor as well as deepening existing poverty. For example, a study of 2,454 municipalities for a 5-year period showed significant impacts from disasters, with a 0.8 % decrease in the Human Development Index in affected areas, similar to a 2-year setback, and a 3.6 % increase in extreme food poverty (Rodriguez-Oreggia et al. 2010).

Disaster Linked to Unsustainable Growth In 1998, Central America suffered massive losses associated with Hurricane Mitch, with thousands of deaths, millions of displaced people and estimated losses of about US\$6 billion. Studies (Ensor 2009) show that the impacts were particularly severe where the development model sought agricultural diversification and export-led growth but at the expense of floodplain exploitation, deforestation and soil degradation and reduced opportunities for small farmers. The social and economic processes involved rendered the environment, infrastructure and population exceptionally vulnerable to the hurricane. In this way, disaster risk was actively created through human action. Similar lessons have been learned in developed countries, for example as a result of major flood loss events in Europe and North America over recent decades.

Disasters and Inequality On average, disasters disproportionately affect women, children, the aged and disabled (Enarson 2012). For example, a study of villages affected by the 2004 Indian Ocean tsunami (Guha-Sapir et al. 2006) showed that the death rate was highest for young children and the elderly and was 40 % higher for women than for men. These patterns are related to the prevailing social roles and expectations. Disadvantaged groups also are often excluded or not catered for in disaster response and recovery stages (IFRC 2007). While disasters can thus amplify social exclusion, economic inequality and poverty, they also provide an opportunity, through risk reduction action and post-disaster recovery, to address such issues as part of the promotion of resilience and sustainable development.

Magnified Impacts for Small Developing Countries The greatest absolute losses occur in larger and richer countries, but the greatest relative losses occur in small countries and particularly small island countries. In some years, the disaster losses can exceed the annual GDP. One study showed that 26 countries have an average annual economic impact of more than 1 % of GDP, with seven countries above 2 % GDP (World Bank 2011). Most of these countries are small-island developing states or small coastal countries. Such high average impacts represent a serious drag on long-term development. The problem arises partly because hazard events such as a storm or earthquake may cover most of a small country leaving the remaining unaffected parts unable to internally fund the recovery.

Disaster Impacts on Cities Cities are engines of economic development. Large cities exposed to cyclones and earthquakes will more than double their population by 2050 (from 680 million in 2000 to 1.5 billion in 2050). The resulting growth in exposure will need to be matched by substantial reductions in urban vulnerability if disaster losses are to be restrained in these cities as they grow. Cities struck by major hazards can take years to recover. An economics study of the 1995 Kobe earthquake (DuPont and Noy 2012) showed that in 2008, 13 years after the event, the city's per capita GDP was lower by 12 %. This impact is persistent, clearly observable, and attributable to the earthquake, and it occurred despite the relative wealth of the country and the considerable recovery support provided to the city. Another study (Hallegate et al. 2013) has estimated a ninefold increase in the global risk of floods in large port cities between now and 2050, as a result of rapid population increases, economic growth, land subsidence and climate change, with a similar increase in losses, rising to US\$ 52 billion. The cost of required flood management for the 136 cities studied is estimated at around US\$ 50 billion per year.

Globalisation and Cascading Risk Globalised systems involving highly interactive and optimised production give rise to large-scale vulnerabilities. In some countries, electricity failures arising from minor technical problems have cascaded to affect millions of people for several days. Imbalances in global grain supply and demand in 2008, precipitated by poor harvests in major grain production countries and market speculation led to a severe spike in food prices, with wheat prices rising to more than double the price of the previous 5 years. The impacts were mainly felt elsewhere, in poorer countries and communities, leading to food crises and urban food riots. The 2011 Tohoku earthquake and tsunami led to a cascade of power outages, radioactive pollution, closure of nuclear plants, reactivation of fossil fuel plants, and disruption of global industrial supply chains.

Disaster Impacts Extend Widely Disasters bring a range of indirect and secondary impacts in addition to the direct losses (mortality, injury, physical damage and economic loss). Individuals may suffer long term disability, psychological harm, degraded living circumstances, interrupted education, increased disease occurrence, loss of employment and relocation. Prolonged drought can lead to reduced nutrition and stunting. Expertise, skills and resources will be diverted from growth activities to recovery activities. Businesses and investment may fail and sectors may not reach their production targets and development targets. Government finances are often severely disrupted. A key lesson is that disaster risk is a systemic issue and must be managed on a system-wide basis.

Economic Impacts and Hazard and Development Status A review of econometric literature (Benson 2012) has shown that: (1) disasters have larger relative impacts on developing, than developed, countries; (2) the nature of impact varies between types of hazard; (3) climatological hazards have negative long-term economic impacts, particularly in lower-income countries; (4) earthquakes may have positive long-term macroeconomic consequences for middle- and upper-income countries but negative consequences for lower-income states; and (5) severe disaster events do not have positive economic impacts under any circumstances. Indirect losses and secondary effects can increase sharply if post-disaster contraction and reallocation of government resources delay reconstruction and dampen the pace of capital accumulation. An alternative countercyclical response may be more cost-effective, by spurring recovery and reconstruction, and “building back better”, with reduced risk and future losses.

Development Opportunities Involve Risks Taking on risks and proactively managing them is a natural element of development. This includes disaster risk, which is often associated with favourable economic assets such as fertile floodplains and volcanic soils and coastal zones. A key need is for shared action on risks which individuals or enterprises cannot handle alone. Governments have a critical role in managing systemic risks, providing an enabling environment, and channelling support to vulnerable groups. Measures to reduce damages from earthquakes, floods and tropical storms can have median benefit-cost ratios of 2–5, while the provision of earlier warnings of disasters in developing countries could yield estimated benefit-cost ratios of 4–36. By way of example, a national system that provides flood warnings up to 10 days ahead to millions of Bangladesh villagers and supports community-level planning and household action to preserve assets and livelihoods generates 10-year savings of US\$ 40 for each dollar invested, according to one study.

Private Sector Roles The private sector is responsible for 70–85 % of all investment worldwide in new buildings, industry and small- to medium-size enterprises (UNISDR 2013b). The pursuit of short-term gains can be a major factor in disaster risk generation, for example through inappropriate land use or building construction practices. Private sector enterprises are vulnerable to disasters not only through direct effects on plant, equipment and personnel but also through disruption of supporting infrastructure for inputs such as water and electricity and transportation to maintain supply chains and product distribution. When these lifelines are cut, costs rise, competitiveness and reputation suffer, and businesses may close or move elsewhere. The business sector is an important partner in systematic risk reduction action, alongside community and government sectors.

Broad Economic Policy Can Reduce Disaster Risks One economics study (DuPont and Noy 2012) suggests that substantial reductions in risk could be achieved through relatively inexpensive interventions in broader policy settings, particularly in respect to information availability, the functioning of markets, the role of public infrastructure and the effectiveness of public institutions. Adequate funding of infrastructure, data gathering, basic services, early warning and evacuation systems will have high payoffs.

Humanitarian Intervention and Resilience Large sums are expended on international emergency assistance, approaching US\$ 12.4 billion in 2010. This is in effect a risk transfer mechanism, as it helps in smoothing the economic impacts on the affected communities, albeit at a very basic level. Only about 4.2 % of official humanitarian aid was invested in disaster risk reduction between 2006 and 2010. However, more timely interventions and sustained multi-year support to risk management and resilience building can pay handsomely. In one case studied, resilience building activities over 20 years cost US\$21 billion less than the more common late humanitarian response. Good linkages between humanitarian relief, rehabilitation and reconstruction can lead to more sustainable, resilient and adaptive outcomes and avoid the common trap of re-creating the original risk profile (Venton 2012).

Status of Disaster-Related Goals, Targets and Indicators

Existing Capabilities The risk process described in the Overview provides the basis for disaster-related goals, targets and indicators. The key elements are: (1) the hazard profile; (2) the exposure (of people and assets); (3) the vulnerability of people and assets to hazards (including

community and institutional capacities and the related concept of resilience); and (4) the losses that occur, such as mortality, morbidity, livelihood and asset loss, social and macroeconomic impact, etc. The field relies on the physical, environmental and social sciences and relevant sector expertise.

Links to the UN Disaster Reduction Strategy The Hyogo Framework for Action has stimulated the development of reporting and databases. A process of national self-reporting has been put in place to monitor progress against measures of national achievement on the priorities and tasks.¹ Most of the measures address inputs and processes, rather than outcomes. The experience to date provides a valuable foundation for the consideration of disaster-related goals and targets in the Sustainable Development Goals process. A post-2015 successor arrangement to the Framework is being developed, in parallel with the Sustainable Development Goals process. Many United Nations member states have called for stronger targets and upgraded accountability in the new framework (UNISDR 2013c).

Expert Workshop A meeting of experts on disaster targets and indicators in July 2013 reviewed options for supporting the Sustainable Development Goals process (UNDP 2013). The meeting welcomed the target proposed by the High-Level Panel (UN 2013) to “build resilience and reduce deaths from natural disasters by x%” and its positioning within the goal to “end poverty.” It also welcomed several other Panel-proposed targets that aim at increased resilience. The group reviewed a number of disaster-related indicators, and concluded that a range of indicator types should be pursued, including outcome indicators where possible, but also process indicators and input indicators.

Hazards, Exposure and Losses Data gathering, historical databases and data modelling for hazards, exposure and losses are relatively well developed (see <http://www.preventionweb.net/english/hyogo/gar/2013/en/home/data-platform.html>) and can readily support indicator development, although the spatial scale rarely reaches down to community level. Hazard modelling is most developed and can be combined with population and asset data to form maps and indexes of exposure. However, disaster loss databases lack consistency in what they measure and in their geographic

¹The term “risk management” refers to the systematic approach and practice to minimise potential harm and loss, whereas “disaster risk reduction” may be seen as a policy objective, one that depends heavily on the tools of risk management. For further definitions see 2009 UNISDR terminology on disaster risk reduction, available at <http://www.unisdr.org/we/inform/publications/7817>, and the glossary of IPCC, 2012.

coverage. Consideration could be given to more informative indicators of disaster loss, such as working days lost, days of school closure, price of seasonal produce, etc.

Vulnerability and Resilience Vulnerability and resilience are widely used concept, albeit with varied interpretations and with limited systematic collection of data. However, with improved data systems at local and national levels there is good scope to generate data sets and indicators, and to measure long-term changes (Birkmann 2013). Both can be represented by surrogates such as household income or community-level capacities. The establishment of vulnerability lines alongside poverty lines is a possibility. Observation and indexing of vulnerability (and associated capacity) is most developed at the community level, but there also exist a number of national and global tools, as well as some common frameworks. Indexes of relative vulnerability, expressed as the proportion of people or assets exposed to hazard types that suffer harm from events (e.g. mortality, homelessness, livelihood loss), or that benefit from protective capacities (e.g. early warnings, building codes, insurance), are simple to generate and communicate (UNDP 2004). Specific targets for vulnerability reduction and adaptation to extreme events also need to be defined to monitor progress.

Risk Measures Are Least Developed Risk requires the integration of hazard, exposure, vulnerability and capacity, and while this is difficult, models do exist. Risk management capability is also captured in some models but this relies on self-reporting by country officials. Comparative analysis and analyses of over time within a single unit are possible. Progress in the management and reduction of risk can only be demonstrated from data and longitudinal studies that span a decade or more.

Indicators of Disaster Risk Reduction Action These include measures of public commitment, such as the availability and effective application of legislation, the level or proportion of annual government spending allocated to disaster risk reduction, and the integration of disaster risk assessment into private sector development projects. Though simple in concept, their implementation requires considerable effort and cooperation among countries and between different administrative levels.

Uncertainty of Loss Events A particular challenge for the application and communication of disaster-related indicators lies in the high variability of many hazards. In particular, the losses during a year may be substantial, despite major risk reduction efforts, or conversely may be minimal despite high risks and small efforts. This means that monitoring progress on disaster risk reduction cannot rely solely on direct disaster loss information, and that a variety of indicators

are necessary to track exposure, vulnerability, risk and risk reduction actions.

References

- Benson C (2012) Indirect economic impacts of disasters. Commissioned review, foresight, Government Office for Science, UK. Accessed from <http://www.bis.gov.uk/foresight/our-work/policy-futures/disasters>
- Birkmann J (2013) Measuring vulnerability to natural hazards—towards disaster resilient societies, 2nd edn. UNU Press, Tokyo, 460 p. ISBN 10: 9280812025
- Bull-Kamanga L et al (2003) From everyday hazards to disasters: the accumulation of risk in urban areas. *Environ Urban* 15(1):193–203
- CRED (2012) Annual disaster statistical review 2012: the numbers and trends. Centre for Research on the Epidemiology of Disasters, University of Louvain, Brussels
- DuPont W, Noy I (2012) What happened to Kobe? A reassessment of the impact of the 1995 earthquake in Japan. University of Hawaii working paper, submitted to Economic Development and Cultural Change. Accessed from <http://www.cirje.e.u-tokyo.ac.jp/research/workshops/twid/twid2012/twid0116.pdf>
- Enarson E (2012) Women confronting natural disaster: from vulnerability to resilience. Lynne Rienner, London, 250 p. ISBN 10: 1588268314
- Ensr MJ (ed) (2009) The legacy of Mitch: lessons from post-disaster reconstruction in Honduras. University of Arizona Press, Arizona, 240 p. ISBN 10: 0816527849
- Guha-Sapir D et al (2006) Risk factors for mortality and injury: post-tsunami epidemiological findings from Tamil Nadu. Centre for Research on the Epidemiology of Disasters (CRED), Brussels
- Hallegatte S et al (2013) Future flood losses in major coastal cities. *Nat Clim Chang* 3:802–806
- IFRC (2007) World disasters report: focus on discrimination. International Federation of Red Cross and Red Crescent Societies. Accessed from <http://www.ifrc.org/PageFiles/89755/2007/WDR2007-English.pdf>
- IPCC (2012) Managing the risks of extreme events and disasters to advance climate change adaptation. Special report of the Intergovernmental Panel on Climate Change. Cambridge University Press, New York, 594 p
- Rodriguez-Oreggia E et al (2010) The impact of natural disasters on human development and poverty at the municipal level in Mexico. Working paper 43, Center for International Development, Harvard University
- Shepherd A et al (2013) The geography of poverty, disasters and climate extremes in 2030. ODI, London. Accessed from <http://www.odi.org.uk/sites/odi.org.uk/files/odi-assets/publications-opinion-files/8633.pdf>
- UNDP (2004) Disaster risk—a challenge for development. UNDP, New York
- UNDP (2013) Targets and indicators for addressing disaster risk management in the post 2015 Development Agenda. Meeting of experts, New York, 18–19 July 2013. Meeting report (Draft 26 August 2013) UNDP, New York
- UNESCAP (2010) Asia Pacific disaster report 2010: protecting development gains. UN Economic and Social Commission for Asia and the Pacific, Bangkok
- UNESCAP (2012) Asia Pacific disaster report 2012: reducing vulnerability and exposure to disasters. UN Economic and Social Commission for Asia and the Pacific, Bangkok
- UNISDR (2013a) Global assessment report on disaster risk reduction 2013. Accessed from <http://www.unisdr.org/we/inform/publications/33013>
- UNISDR (2013b) Disaster statistics. Accessed from <http://www.unisdr.org/we/inform/disaster-statistics>

- UNISDR (2013c) Synthesis report: consultations on a post-2015 framework on disaster risk reduction (HFA2). Accessed from http://www.unisdr.org/files/32535_hfasynthesisreportfinal.pdf
- United Nations (2005) Hyogo framework for action 2005-2015: building the resilience of nations and communities to disasters. Accessed from <http://www.unisdr.org/we/inform/publications/1037>
- United Nations (2012) Resolution adopted by the general assembly on 27 July 2012, A/RES/66/288. The future we want. See para. 186–189 on disaster risk reduction
- United Nations (2013) A new global partnership: Eradicate poverty and transform economies through sustainable development. The report of the High-Level Panel of Eminent Persons on the Post-2015 Development Agenda
- Venton C (2012) The economics of early response and disaster resilience: lessons from Kenya and Ethiopia. Department for International Development, London
- World Bank (2011) Natural hazards, unnatural disasters: the economics of effective prevention. World Bank, Washington DC, 280 p. Accessed from <https://www.gfdrr.org/gfdrr/node/281>
- World Bank (2013) Risk and opportunity, managing risk for development. World Development Report 2014, 60 p



Economic Impact Assessment of Landslide Events

Mike G. Winter, Derek Palmer, Jonathan Sharpe, Barbara Shearer, Clare Harmer, David Peeling, and Trevor Bradbury

Abstract

The economic impacts of landslide events can be classified into those that are direct, direct consequential and indirect consequential. In this paper we present data from a set of four landslide events/groups of events, that occurred in Scotland in 2004 and 2007, on the first two impact types and indicate progress on work to develop the methodology for and data gathering on the third type. The data presented here relates to events that occurred in a road environment and for which there were no casualties. Direct costs range between approximately £300 k and £1,400 k whereas direct consequential costs range between around £100 k and £1,000 k. The latter costs are largely dependent upon the amount of traffic that uses the road and the duration of the disruption that is caused by the landslide event(s).

Keywords

Landslides • Debris flow • Economic impacts • Assessment

Introduction

Rainfall-induced debris flows are a common occurrence in Scotland and in 2004 a series of such events was associated with monthly average rainfall substantially in excess of the norm.

Critically, some of the resulting landslides affected important parts of the trunk (strategic) road network, linking not only cities but also smaller, remote communities. Notable events occurred at the A83 between Glen Kinglas and to the north of Cairndow (9 August), the A9 to the north of Dunkeld (11 August), and the A85 at Glen Ogle (18 August). While there were no major injuries, the most dramatic events

occurred at the A85 Glen Ogle, where 57 people had to be airlifted to safety when they became trapped between two major debris flows.

The A83 Rest and be Thankful site, in particular, has been extremely active in recent years with multiple debris flow events and associated closures and events in 2007, 2008 and 2009 had an adverse effect on the travelling public; subsequent events in 2011 and 2012 have continued this trend. This has meant that the area has become the focus of not only concern but also extensive landslide management and mitigation activity. This culminated in a study being commissioned to assess and make recommendations on potential landslide remediation actions (Anonymous 2013; Winter and Corby 2012).

Such landslides have significant socio-economic impacts even in the, perhaps fortuitous, absence of serious injuries and fatalities to those involved. However, the real impacts of these events were economic and social. Such impacts include the cost of delays and diversion on transport networks and the severance of access to and from relatively remote communities for services and markets for goods; employment, health and educational opportunities; and social activities.

M.G. Winter (✉) • B. Shearer
Transport Research Laboratory (TRL), 13/109 Swanston Road,
Edinburgh EH10 7DS, UK
e-mail: mwinter@trl.co.uk

D. Palmer • J. Sharpe • C. Harmer • D. Peeling • T. Bradbury
Transport Research Laboratory (TRL), Crowthorne House, Nine Mile
Ride, Wokingham RG40 3GA, UK



Fig. 1 View of the 28 October 2007 debris flows at the A83 Rest and be Thankful

The A83 (Fig. 1), carrying up to 5,000 vehicles per day (all vehicles two-way, 24 h annual average daily traffic, AADT) was closed for slightly in excess of a day, the A9 (carrying 13,500 vehicles per day) was closed for 2 days prior to reopening, initially with single lane working under convoy, and the A85 (carrying 5,600 vehicles per day) was closed for 4 days. The traffic flow figures are for the most highly trafficked month of the year (July or August). Minimum flows occur in either January or February and are roughly half those of the maxima reflecting the importance of tourism and related seasonal industries to Scotland's economy. Substantial disruption was thus experienced by local and tourist traffic, and goods vehicles.

This paper describes part of a study to assess the economic impacts of selected debris flow events in Scotland, based on the scheme set-out by Winter and Bromhead (2012).

Economic Impacts

Due to the major contribution that tourism makes to Scotland's economy the impacts of such events can be particularly serious during the summer months, during which period debris flows usually occur in July and August. Nevertheless, the impacts of any debris flow event occurring during the winter months, during which debris flow usually occurs between October/November and January, should not be underestimated. Not surprisingly, the debris flow events described created a high level of interest in the media in addition to being seen as a key issue by politicians at both the local and national level. Indeed, the effects of such small events which may, at most, affect directly a few tens of metres of road cast a considerably broader vulnerability shadow (Winter and Bromhead 2012).

The qualitative economic impacts of such landslide events include:

- The loss of utility of parts of the road network,
- The need to make often extensive detours in order to reach a destination, and
- The severance of access to and from relatively remote communities for services and markets for goods; employment, health and educational opportunities; and social activities.

The economic impacts of a landslide event and its associated vulnerability shadow that closes a road, or other form of linear infrastructure were summarized by Winter and Bromhead (2012), in three categories, as follows:

- Direct economic impacts.
- Direct consequential economic impacts.
- Indirect consequential economic impacts.

Direct economic impacts: The direct costs of clean-up and repair/replacement of lost/damaged infrastructure in the broadest sense and the costs of search and rescue. These should be relatively easy to obtain or estimate for any given event.

Direct consequential economic impacts: These generally relate to 'disruption to infrastructure' and are really about loss of utility. For example, the costs of closing a road (or implementing single-lane working with traffic lights) for a given period with a given diversion, are relatively simple to estimate using well-established models. The costs of fatal/non-fatal injuries may also be included here and may be taken (on a societal basis) directly from published figures. While these are set out for the costs of road traffic accidents,

or indeed rail accidents, there seems to be no particular reason why they should be radically different to those related to a landslide as both are likely to include the recovery of casualties from vehicles. Indeed, for events in which large numbers of casualties may be expected to occur, data relating to railway accidents may be more appropriate.

Indirect consequential economic impacts: Often landslide events affect access to remote rural areas with economies that are based upon transport-dependent activities, and thus the vulnerability can be extensive and is determined by the transport network rather than the event itself. If a given route is closed for a long period then how does that affect confidence in, and the ongoing viability of, local businesses. Manufacturing and agriculture (e.g. forestry in western Scotland and coffee production in Jamaica) are a concern as access to markets is constrained, the costs of access are increased and business profits are affected and short-term to long-term viability may be adversely affected. Perhaps of even more concern are the impacts on tourist (and other service economy) businesses. It is important to understand how the reluctance of visitors to travel to and within ‘landslide areas’ is affected after an event that has received publicity and/or caused casualties and how a period of inaccessibility (reduced or complete) affects the short- and long-term travel patterns to an area for tourist services. Such costs form a fundamental element of the overall economic impact on society of such events. They are thus important to governments as they should affect the case for the assignation of budgets to landslide risk mitigation and remediation activities. However, these are also the most difficult costs to determine as they are generally widely dispersed both geographically and socially. Additionally, in an environment in which compensation might be anticipated, albeit often erroneously, those that have the best data, the businesses affected by such events, are also those that anticipate such compensatory events.

The vulnerability shadow (Winter and Bromhead 2012) cast can be extensive and its geographical extent can be determined by the transport network rather than the relatively small footprint of the event itself. In this particular case the event itself was of the order of around 400 m³ (Winter, in press) with a footprint that closed a few tens of metres of the road; the vulnerability shadow can be estimated to be of the order of 3,500 km² [albeit including a significant area of sea (Fig. 2)].

The economic impacts and the vulnerability shadows are concepts that apply equally to other discrete climate driven events that have the potential to close parts of the road network such as flood events. Like landslides, flood events are generally thought to be likely to increase in frequency as a result of climate change (Galbraith et al. 2005; Anonymous 2011; Winter et al. 2010; Winter and Shearer 2013).

The work of Schuster (1996), Highland (2006) and Schuster and Highland (2007) have been especially

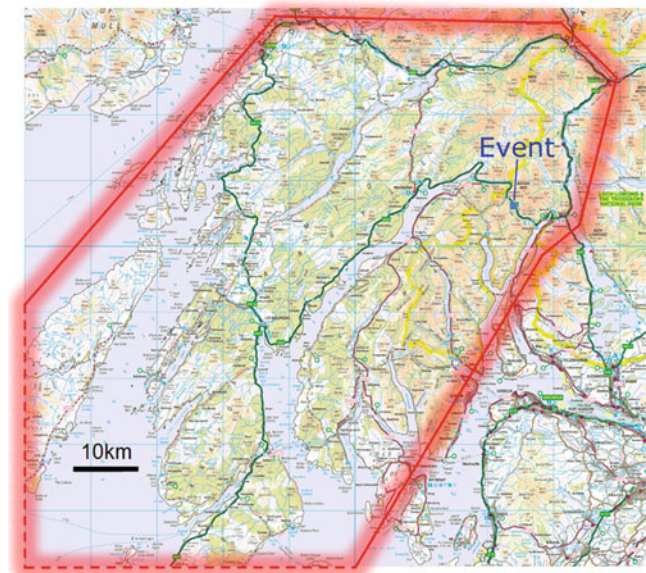


Fig. 2 A relatively small debris flow event closed the A83 at the Rest and be Thankful in October 2007; the vulnerability shadow that was cast (bounded in red) was extensive (Winter, in press)

informative and helpful in determining the approach to this work. Ongoing work is targeted at broadening the data set available for direct and direct consequential economic impact and further refining the methodology and gathering data for the indirect consequential economic impacts.

Direct Economic Impacts

Direct economic impacts include:

1. The direct costs of clean-up and the costs of search and rescue.
2. The repair/replacement of lost/damaged infrastructure in the broadest sense.

These might otherwise be described as ‘emergency response’ and ‘remedial works’, respectively and should be relatively easy to obtain or estimate for any given event. It was intended that the Direct Economic Impacts of four events would be determined as follows:

- August 2004 A85 Glen Ogle landslides.
- October 2007 A83 Rest and be Thankful landslide.
- January 2011 A8 Inverclyde flooding.
- January 2012 A78 Largs to Skelmorlie coastal flooding.

Direct economic impacts should be the most straightforward to determine. Indeed this has generally proved to be the case with relatively recent events that occurred within the currency of existing Operating Company (OC) contracts. Thus, data relating to the 2007 A83 Rest and be Thankful event was readily available from Scotland TranServ who were the OC for the north-west at the time of enquiry.

Table 1 Direct economic impacts

Event	Emergency response	Remedial works	Total
August 2004: A83 Glen Kinglas to Cairndow	£300 k		£300 k
August 2004: A9 N of Dunkeld	£700 k		£700 k
August 2004: A85 Glen Ogle	£500 k		£500 k
October 2007: A83 Rest and be Thankful	£270 k	£1,156 k	£1,426 k

Data from less recent events such as the landslide events of 2004 (Winter et al. 2005, 2006, 2009) proved more difficult to obtain largely as both the operators and auditors had changed since the events occurred. This has limited the resolution and reliability of the data that can be obtained for these events. What data have been obtained has been derived from high level reporting documents to Scottish Ministers and Senior Civil Servants and covers all three of the event groups from August 2004 (A83, A9 and A85). These data have been interpreted and broken down to the best of the ability of the original authors and editors of the Scottish Road Network Landslide Study reports (Winter et al. 2005, 2009). The available data are given in Table 1.

Direct Consequential Economic Impacts

Direct consequential economic impacts are those that relate to ‘disruption to infrastructure’ and are really about loss of utility. For example, the costs of closing a road (or implementing single-lane working with traffic lights) for a given period with a given diversion, are relatively simple to estimate using well-established models. The costs of fatal/non-fatal injuries may also be included here and may be taken (on a societal basis) directly from published figures. Whereas these are set out for the costs of road traffic accidents, or indeed rail accidents, there seems to be no particular reason why they should be radically different to those related to a landslide as both are likely to include the recovery of casualties from vehicles. Indeed, for events in which large numbers of casualties may be expected to occur, data relating to railway accidents may be more appropriate.

For example, if a road is closed, either fully or partially, some or all of the users of that route will have to take an alternative, diversionary route, which may be significantly longer than the primary route. Even if no diversion is necessary, reduction in the road capacity (e.g. through a lane closure or the imposition of a speed limit) may mean that queues form, particularly at peak times, slowing the traffic

flow. These effects can significantly increase road users’ journey times.

The QUADRO (QUEues And Delays at Roadworks) model provides a method for assessing the costs imposed on road users while roadworks are being carried out, considering:

- Delays to road users: the change in road users’ journey times, priced using the value of their time (e.g. cost to their employer’s business of the time spent travelling during the working day) based on the type of vehicle, its occupants and trip purpose.
- Fuel carbon emissions: the change in carbon emissions due to vehicle fuel consumption, based on average figures per litre of fuel burnt and costed using estimated abatement costs (see STAG: Anonymous 2012a/WebTAG: Anonymous 2012b).
- Accident costs: the change in the occurrence of accidents, in terms of the additional delay caused and the direct costs (e.g. property damage, police time and insurance administration).

The program contains a model for allocating traffic to the diversion route if the site becomes overloaded, representing both the road users that queue through the site and those that take an alternate route. The details of QUADRO, including all assumptions made in its calculations, are provided in the manual (DMRB 14: Anonymous 2006).

In order to carry out modelling of a road closure in QUADRO, a diversionary route needs to be defined. The QDIV (QUADRO Diversion) tool was used to define these routes.

QDIV requires each diversionary route to be defined in terms of a set of links (each defined as rural, urban, sub-urban or small town) that can be combined in series and parallel to build up a network. For each event, a simplified diversionary network schematic was developed and Google Maps was used to measure the length of each link. Traffic data, represented as annual average daily traffic (AADT), were sourced using data from the relevant Road Administrations.

Where information was not available (e.g. lane and verge widths), the default values suggested in the QUADRO manual were adopted. Classified (i.e. split into different vehicle types) traffic counts, and therefore the proportion of heavy vehicles, were only available for some links; either the proportion from the closest link or a nominal 10 % HGVs was assumed. The site data are given in Table 2.

It was assumed that all of the roads affected were rural all-purpose single carriageways with a speed limit of 96 km/h (60 mph), reduced to 48 km/h (30 mph) where part of the road remained open following the landslide, and that the length of the affected site in each case was 100 m.

QUADRO calculates the costs of user delays, carbon emissions from vehicles and accidents associated with the

Table 2 Site parameters for the direct consequential economic impacts analysis

Parameter	August 2004: A83 Glen Kinglas to Cairndow	August 2004: A9 N of Dunkeld	August 2004: A85 Glen Ogle	October 2007: A83 Rest and be Thankful
Traffic flow (AADT) (vehicles per day)	5,554	13,864	4,403	5,748
HGVs (%)	9	18	10	10
Junction length (km)	20	18	26	20
Closure type(s)	Full closure	Full closure then shuttle working with convoy	Full closure	Full closure then single lane with traffic light control
Closure duration	2 days	2 days (full) 6 days convoy	4 days	15 days (full) 27 days (single lane) ^a

^aThis figure represents the duration of the closure due to the instability and the immediate engineering works required to allow the reopening of the road. It is acknowledged that the road was subsequently subject to single lane working with traffic light control for a significantly longer period due to engineering works necessitated by the combination of this and subsequent events in the immediate vicinity

Table 3 QUADRO results, daily closure-related costs for each site: direct consequential economic impacts analysis

Cost (£)	August 2004: A83 Glen Kinglas to Cairndow	August 2004: A9 N of Dunkeld (full/single lane closure)	August 2004: A85 Glen Ogle	October 2007: A83 Rest and be Thankful (full/single lane closure)
Delay cost	46,813.86	150,739.14/75,286.29	39,937.00	49,091.57/256.43
Carbon cost	3,527.57	10,290.14/5,145.14	3,662.43	3,642.43/3.71
Accident cost	-2,630.86	-6,790.71/-3,395.29	-2,722.71	-2,722.71/478.29

Table 4 QUADRO results, total closure-related costs for each site: direct consequential economic impacts analysis

Cost (£)	August 2004: A83 Glen Kinglas to Cairndow	August 2004: A9 N of Dunkeld	August 2004: A85 Glen Ogle	October 2007: A83 Rest and be Thankful
Delay cost	93,627.72	753,196.02	159,748.00	743,297.16
Carbon cost	7,055.14	51,451.12	14,649.72	54,736.62
Accident cost	-5,261.72	-33,953.16	-10,845.16	27,926.82

road works, reporting the costs on the basis of an average day over a whole week. The results of the QUADRO analyses are shown in Table 3, with the totals for each site summarised in Table 4.

Careful consideration of the relative traffic levels, and closure type and duration (Table 1), reveals patterns that are broadly consistent with those that might be that might be inferred intuitively, as follows:

- The costs of similar closures depend on traffic levels and with costs being higher where traffic is higher (A83 2004 compared to A9).
- Doubling the duration incurs higher costs, but may be reduced if the traffic levels are lower (A83 2004 compared to A85).
- A much longer duration increases the costs significantly (A83 2007).

Of particular interest are the negative costs (i.e. cost reductions) for accident cost that suggest a decrease in accident/accident severity as a result of the diversions. This seems most likely to be as a result of reduced traffic speeds.

Indirect Consequential Economic Impacts

There is a wide range of possible approaches to estimating the indirect consequential economic impacts of landslides. These include the following:

- Cost-benefit analysis.
- Cost-effectiveness analysis.
- Willingness to pay.
- Multi-criteria analysis.
- Methods based upon Transport Appraisal.

In addition there are bespoke methods designed to address a particular set of circumstances (e.g. MacLeod et al. 2005; Anonymous 2013).

A survey of businesses has been undertaken in the area of the 2004 A85 event. This is part of a first phase of work to ascertain the availability and reliability of data that would be required in order to identify, and to develop, a measurement methodology of the indirect consequential economic impacts of landslides in Scotland.

Summary and Conclusions

This paper presents the initial results of a study to develop methods of obtaining data on the economic impacts of landslides and to obtain such data. The economic impacts of landslides are considered in three categories: direct economic impacts, direct consequential economic impacts, and indirect consequential economic impacts. This approach is applicable to other events that reflect relatively discrete closures due to climate driven events such as flooding.

The work presented herein includes data for four landslide events/groups of events that occurred in Scotland in 2004 and 2007. Direct costs range between approximately £300 k and £1,400 k while direct consequential costs range between around £100 k and £1,000 k. The latter are largely dependent upon the amount of traffic that uses the road and the duration of the disruption. Work is ongoing to define the indirect consequential costs of such events.

Acknowledgments Transport Scotland's funding of this work is gratefully acknowledged.

References

- Anonymous (2006) Design manual for roads and bridges (DMRB): volume 14: economic assessment of road maintenance—QUADRO4 user manual, June. <http://www.dft.gov.uk/ha/standards/dmrb/>
- Anonymous (2011) Scottish road network climate change study: UKCP09 update. Report by Jacobs for Transport Scotland. <http://www.transportscotland.gov.uk/>
- Anonymous (2012a) Scottish transport appraisal guidance. Transport Scotland, Edinburgh. <http://www.transportscotland.gov.uk/stag/home>
- Anonymous (2012b) TAG UNIT 3.3.5: the greenhouse gases sub-objective, August. Department for Transport, London. <http://www.dft.gov.uk/webtag>
- Anonymous (2013) A83 trunk road route study: part A—A83 Rest and be Thankful. Final report. Report prepared by Jacobs for Transport Scotland, 212 p. <http://www.transportscotland.gov.uk/road/maintenance/landslides>
- Galbraith RM, Price DJ, Shackman L (eds) (2005) Scottish road network climate change study. Scottish Executive, Edinburgh, 100 p
- Highland LM (2006) Estimating landslide losses—preliminary results of a seven-state pilot project. US Geological Survey Open File Report 2006-1032. USGS, Reston, VA
- MacLeod A, Hofmeister RJ, Wang Y, Burns S (2005) Landslide indirect losses: methods and case studies from Oregon. State of Oregon, Department of Geology and Mineral Industries Open File Report O-05-X. Portland, OR
- Schuster RL (1996) Socioeconomic significance of landslides. In: Turner AK and Schuster RL (eds) Landslides—investigation and mitigation, National Research Council, Transportation Research Board Special Report 247, Washington, DC, pp 36–75
- Schuster RL, Highland LM (2007) The third Hans Cloos lecture. Urban landslides: socioeconomic impacts and overview of mitigative strategies. *Bull Eng Geol Environ* 66:1–27
- Winter MG (2013) A classification scheme for landslide management and mitigation. *Int J Landslide Environ* 1(1):123–124
- Winter MG, Bromhead EN (2012) Landslide risk: some issues that determine societal acceptance. *Nat Hazards* 62(2):169–187
- Winter MG, Corby A (2012) A83 Rest and be Thankful: ecological and related landslide mitigation options. Published project report PPR 636. Transport Research Laboratory, Wokingham
- Winter MG, Shearer B (2013) Climate change and landslide hazard and risk—a Scottish perspective. Published project report PPR 650, Transport Research Laboratory, Wokingham
- Winter MG, Macgregor F, Shackman L (eds) (2005) Scottish road network landslides study. The Scottish Executive, Edinburgh, 119 p
- Winter MG, Heald A, Parsons J, Shackman L, Macgregor F (2006) Scottish debris flow events of August 2004. *Q J Eng Geol Hydrogeol* 39(1):73–78
- Winter MG, Macgregor F, Shackman L (eds) (2009) Scottish road network landslides study: implementation. Transport Scotland, Edinburgh, 278 p
- Winter MG, Dent J, Macgregor F, Dempsey P, Motion A, Shackman L (2010) Debris flow, rainfall and climate change in Scotland. *Q J Eng Geol Hydrogeol* 43(4):429–446



A Safety Guideline for Hill-Site Development of Penang, Malaysia: Challenges and a Way Forward

See-Sew Gue

Abstract

A safety guideline for hillside developments of a state government has been developed with the aim of mitigating landslides and saving lives. Landslides often occur in areas with steep hills especially hills with activities such as developments for residents and commercial or agricultural purposes. The risk to lives and properties is higher in hillside developments for residents and commercial purposes. This paper describes the initiatives taken by a state government in Malaysia to improve the practice of engineering on slopes for new developments. This safety guideline was developed for a more transparent and clearer practice on what needs to be done by main stakeholders, namely developers and their consultants, contractors and the local authority. The Guideline starts with a simple slope classification based on gradient for planning approval. The design requirements for a hillside development are based on the hazard levels. The required expertise to ensure safety of slopes with gradient steeper than 25° and above is specified. It also requires an independent audit of the design and regular inspection of the site to check the compliance of construction. The qualifications of submission engineers for a proposed development and its independent checker on slopes greater than 25° are specified to ensure competent geotechnical engineers with relevant experience to undertake the design and supervision and independent checking works. The Guideline also details the submission requirements needed for a proposed development including the formats of geotechnical design and independent checker reports.

Keywords

Hill-site • Safety • Policy • Guideline • Planning • Slope

Introduction

A clear and transparent Guideline for hillside development is very important to ensure safety. A local Government or authority needs to spell out systematic ways for developers to submit their proposal of a hillside development from planning to design, construction and maintenance.

S.-S. Gue (✉)
G&P Professionals Sdn Bhd, Kuala Lumpur, Malaysia
e-mail: ssgue@gnpgroup.com.my

Objectives

The objectives of the Guideline are to improve safety and environment of hillside developments. It provides clear and consistent application procedures together with a transparent approving mechanism for Governmental Approval and control during construction and maintenance.

The Guideline, among others:

- Has made clearer classification of slopes for ease of implementation at planning stage.
- Has stated the duties and responsibilities of Engineers and Independent Auditors during design and construction stages.

- Requires Independent Auditors to visit project sites during constructions and report any non-compliance directly to the local authority for prompt enforcement.
- Has better defined the qualification and experience of key personnel (geotechnical engineer and independent checkers) to ensure quality of works for hillside developments during the design and construction stages.
- Has made it mandatory for developers to engage qualified engineers and independent checkers—having the required expertise and experience on hillside developments and sufficient capacity to design and supervise the constructions.
- Requires contractors to comply with the design drawings and specifications for the slope works.
- Has reduced the requirement for plinth area (maximum allowable hard surface footprint) for buildings on Class 3 and Class 4 hillside lands, with the intention of preserving more natural green areas.
- Requires engineered slopes including earth retaining systems to incorporate green features to enhance Penang's natural environment.

Towards a Safe and Green Penang

The Guideline addresses and upgrades existing safety measures and outlines better project implementation procedures and effective enforcement. It strives to inculcate good slope design, construction and maintenance culture. With its proper implementation, the Guideline will inspire confidence in the safety of hillside developments in Penang.

The advisory panel, which drew up the Guideline, will continue to assist the authorities to effectively implement and enforce it. This is to ensure that developers, engineers, contractors and property owners in hillside areas comply with good engineering practices relating to the stability of hill slopes.

Still lingering in the Malaysian public's consciousness are the many hill land failures which caused tragedies over the past 20 years.

The major causes of slope failures can be summarised as follows:

- **Design**—inadequate ground investigation, lack of understanding of engineering analysis and design.
- **Construction**—lack of quality assurance and quality control by contractors and lack of proper site supervision by engineers.
- **Maintenance**—lack of slope maintenance culture is prevalent in both the public and private sectors.
- **Communication**—lack of communication amongst various parties involved in construction.

The resulting loss of lives, destruction to public and private properties as well as the ensuing legal tangles that may be still ongoing have triggered various reactions; there had been conferences, seminars, dialogues, more stringent rules and regulations and better practices for hillside development.

This Guideline makes a concerted attempt to incorporate all the lessons learnt.

Major Considerations

Numerous guidelines for hillside developments from various agencies have been produced after the collapse of Block 1 of Highland Towers in 1993. This Guideline aims to simplify existing procedures and to improve the safety of hillside developments.

To further improve the safety of slopes and earth retaining systems, this Guideline has some major considerations that include:

- Slope classification for planning approval has been simplified for clarity and consistency.
- Design requirements of slope have been strengthened through clearer definitions.
- The required qualifications of engineers including geotechnical engineers needed for different terrain classification of slopes are established.
- The requirement and need for independent auditors is not better defined and the input is extended beyond design to include inspection during construction.
- Maintenance of slope needs proper input by the Engineers which includes the need to produce maintenance manuals so that owners know their responsibilities and what entails in the maintenance of slopes.
- The maximum allowable hard surface footprint has been intentionally reduced by more than 5 % for Class 3A and 3B and about 20 % for Class 4A and 4B slopes. This will improve safety and enhance the preservation of the green environment.
- Geotechnical engineers shall provide solution for localised Class 3 and 4 slopes within the proposed development.
- Proposed development on flat land adjacent to potentially unstable slope, as shown in Fig. 1 which could not be strengthened for any reason including its inaccessibility due to trespass and/or land issues, will require a suitable buffer zone. The width of the buffer zone should be at least the height of the slope.
- Proposed development on potentially unstable slope as shown in Fig. 2, which could not be strengthened due to inaccessibility and/or land issues, shall not be allowed.

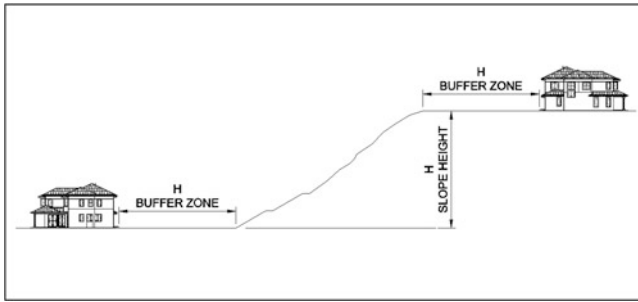


Fig. 1 Buffer zone

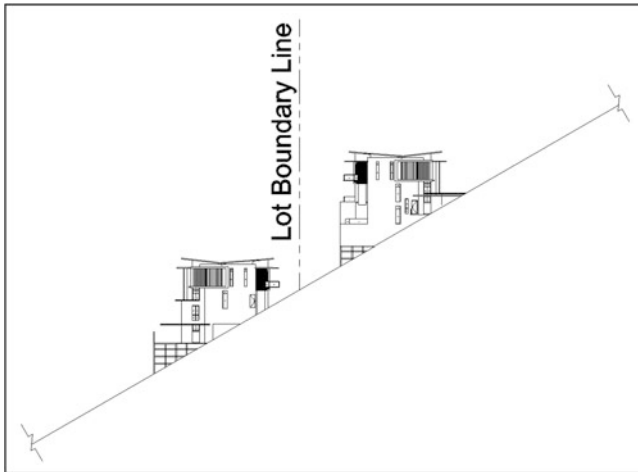


Fig. 2 Development on slope

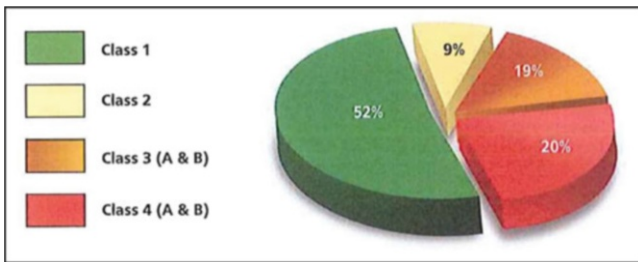


Fig. 3 Penang Island's hill land distribution

Classifications of Slopes

Slopes are classified according to slope gradient and type (Fig. 3).

The slope gradient, in degrees, is measured from the horizontal plane. Sufficient survey points shall be obtained to produce accurate contour lines at 5 m intervals. More survey points shall be obtained at localized areas such as existing slip, man-made slopes/structures, etc. The extent of survey shall include an area beyond the land boundary not less than 20 m.

The type of slopes is divided into natural or man-made slopes. Man-made slopes are further divided into cut or fill slope. Higher risk is associated with fill slopes.

Table 1 shows the Slope Classification for Design Purposes. The table also shows the associated risk and the maximum allowable hard surface footprint. The maximum allowable hard surface footprints for Class 3A, 3B, 4A and 4B are reduced in this guideline as compared to the previous guidelines. This is to preserve green areas and to allow easy maintenance and strengthening of slopes.

The maximum allowable hard surface in Table 1 below is applicable to all allowable developments. Nonetheless, the state's planning policy at the material time, including any height restriction shall take precedence.

Table 2 shows the submission requirements for all the classes of slopes by submission engineers. The qualifications of the submission engineers are stated in Table 3. Table 4 states the responsible party for the appointment of Geotechnical Design Engineer and Independent Checkers.

Please take note of the following:

- The Civil Engineer and Geotechnical Engineer for a particular project can be the same or different engineer.
- The Geotechnical Engineer and Independent Auditor for a particular project must be different engineers. They must also not be from the same firm.

During construction, proper and adequate supervision are important. Table 5 states the construction supervision requirement.

Submission Requirements

Pre-submission Consultation

Submitting Person (SP)—be it the Planner, Architect, Engineer, Geotechnical Engineer or Surveyor—shall engage in pre-submission consultation with the relevant departments prior to submission of Layout Plan and Geotechnical Report for all hillside development projects.

The submitting person shall compile or make available some basic documents and/or information for discussion during the pre-submission consultation with the relevant authorities. For example land classification, land suitability, preliminary proposed Layout Plan, Land Survey plan and Terrain Mapping.

Preparation of Final Layout Plan and Geotechnical Report

The SP shall ensure that there will be no more changes made to the Layout Plan and shall order the Final Geotechnical

Table 1 Slope classification for design purposes

Class	Slope gradient	Associated risk			Maximum allowable hard surface footprint
		Natural slope	MAN-made slope		
			Cut	Fill	
1	0°–15°	Low	Low	Low	Refer to current policy
2	>15°–25°	Low	Low	Low	
3A	>25°–35°	Medium	Medium	Not applicable	35 %
3B	>25°–35°	Not applicable	Not applicable	High	35 %
4A	>35°	High	High	Not applicable	30 %
4B	>35°	Not applicable	Not applicable	Very high	30 %

Table 2 Submission requirements

Class	Submission requirements
1 (Low risk)	Slope stability analysis by Civil Engineer
2 (Low risk)	Geotechnical design report by Geotechnical Design Engineer
3A (Medium risk), 3B, 4A (high risk), 4B (very high risk)	Geotechnical design report by Geotechnical Design Engineer and Geotechnical review report by Independent Checker

Table 3 Qualifications of engineers

Submission engineer	Qualifications
Civil Engineer	1. Meets relevant Local Authority's requirements 2. Registered Professional Engineers with Board of Engineers, Malaysia (BEM)
Geotechnical Design Engineer	1. Meets relevant local authority's requirements 2. Registered Professional Engineers with BEM with minimum 3 years practical geotechnical experience and 1 year gained in Malaysia
Independent Checker	1. Meets relevant local authority's requirements 2. Registered Professional Engineers with BEM with (a) At least 10 years relevant practical experience in the design or construction of buildings and, during the period 7 years immediately preceding the current appointment, has been engaged in geotechnical design after registration as a professional engineer with at least 1 year of such practical experience gained in Malaysia (b) At least 3 years relevant practical experience in slope engineering with at least 1 year of such practical experience gained in Malaysia OR Registered Accredited Checkers (Geotechnical) with BEM

Table 4 Appointment of Geotechnical Engineer and Independent Checker

Class	Appointment
1 (Low risk)	Geotechnical Design Engineer is not required
2 (Low risk)	Appointment of Geotechnical Design Engineer by Developer
3A (Medium risk), 3B and 4A (high risk)	Appointment of Geotechnical Design Engineer and Independent Checker by Developer
4B (Very high risk)	Appointment of Geotechnical Design Engineer and Independent Checker by Developer and concurred by Local Authority

Table 5 Construction supervision requirements

Class	Supervision requirements
1 and 2 (Low risk)	No changes to existing requirements as stipulated in UBBL Sections 5 and 7
3A (Medium risk), 3B and 4A (high risk)	Additional audit via site visits shall be carried out by Independent Checker Minimum frequency of site visits shall be once a month
4B (Very high risk)	Additional audit via site visits shall be carried out by Independent Checker Minimum frequency of site visits shall be once every fortnightly Instrumentation monitoring shall be carried out to monitor conditions of slopes

Report to be prepared for concurrent submission to One-Stop Centre (OSC) of the authority.

Changes made during the delivery process may result in re-submission of Layout Plan and Geotechnical Report for approval.

Figure 4 shows the colours to use in preparing terrain map and submission flow chart with timeline for approval was also included to ensure effective implementation.

Notes to the submission flow chart

1. Pre-Submission Consultation
2. Preparation of final Layout Plan and Geotechnical Report for Submission

Fig. 4 Colour code for terrain mapping

Slope Classification	Colour	Decimal RGB Codes			Equivalent AutoCAD Colour Index #
		Red	Green	Blue	
Class 1	Light Green	212	255	170	71
Class 2	Beige	255	255	170	51
Class 3A	Brown	255	234	170	41
Class 3B	Orange	255	170	170	11
Class 4A	Light Red	255	63	0	20
Class 4B	Red	255	0	0	1

3. Submission to One-Stop Centre
4. Submission of Geotechnical Report to JKR (Malaysian Public Works Department)
5. Comments and Requirements by Geotechnical Engineer
6. Compliance of Requirements by Geotechnical Engineer
7. Approval of Geotechnical Report

Appointment of Competent Engineers

The Guideline also includes the method and procedure of selecting engineers by ability shall be as follows:

- Technical competence
- Managerial ability
- Availability of Resources
- Professional Independence and Integrity
- Fairness of Fee
- Quality Assurance System

These are very important criteria to be considered in selecting a competent engineer.

The other considerations are the engineer's personal attributes such as having good commitment towards projects, communication skills and engineering judgement, and these should be well augmented with their experience in the industry.

Maintenance Inspection

The maintenance of slopes and earth retaining walls should generally follow the specific guidelines with a maintenance manual prepared by the Consulting Engineer.

A Way Forward

This Guideline needs the commitment of all the stakeholders to improve safety of hillside development and enhance the environment. To succeed, it demands:

- Developers must engage their competent engineers and contractors with capability and capacity.
- Engineers must exercise due skill and care when performing their duties in planning, analysis, design and supervision, and must complement these duties with a regiment of quality checking and review. Their service must include the preparation of maintenance manuals and the duty of adequate post-construction inspections.
- Contractors must have trained personnel and proper and adequate plant and equipment to meet the design and specification requirements of the works. The importance of implementing temporary works for safety, site control and erosion protection must be instilled in the workers and implemented at the construction site.
- Approving authorities must have experienced engineers in their geotechnical units to facilitate and enforce compliance with the Guideline.

When hard surfaces such as earth retaining systems and reinforced slopes have to be constructed to enhance or achieve safety, all stakeholders must be committed to the green initiative to incorporate planting provisions on these facilities to achieve a friendlier environment.

Acknowledgments Penang State Government for establishing the clear and transparent Guidelines. The Advisory Panel Committee for the Guideline, Penang State Government's Agencies and Guideline Secretariat (Penang Island Municipal Council). Please see <http://www.mppp.gov.my/en> for the Guideline in detail.



Guidelines and Initiatives in the Aftermath of Highland Towers Landmark Landslide

Abdullah Che Hassandi

Abstract

After the 1993 Highland Towers landslide, the Government of Malaysia drafted several new guidelines to control development on hillsides and hilly terrain. Some initiatives, such as carrying out a national slope master plan study, landslide public awareness and education programs and amendments to relevant legislation to incorporate landslide elements, have been introduced to reduce the risks. Some of the initiatives from the state governments were triggered by the actions taken by the federal government. This paper discusses the effectiveness of these measures and other initiatives that are currently under consideration.

Keywords

Development • Guidelines • Slope master plan • Legislation • Initiatives • Malaysia

Introduction

Based on the National Slope Master Plan study it has been estimated that approximately USD one billion has been lost due to landslides in Malaysia. The number of deaths due to landslides from 1973 to 2013 is approximately 613 (including deaths due to debris flow). The first recorded landslide incident, which is still quoted as a landmark event in Malaysia, occurred on December 11, 1993 when one of three condominium blocks toppled over. As a result of the incident, 48 people were killed in one block and the residents of the other two apartment blocks were asked to vacate when the government declared the still standing blocks to be unsafe. Before this, no landslide had killed so many people. The fact that the incident—which came to be known as the Highland Towers landslide—happened so near the capital city of Kuala Lumpur resulted in a much-publicised search and rescue operation and extensive and lengthy media attention. The litigation that ensued only came to closure in 2006.

Figure 1 shows the apartment block that collapsed and the two remaining blocks, now abandoned.

Initiatives for Slope Management After 1993

Some initiatives were carried out by the Malaysian government to address the issues on landslide risks and losses. Some of the initiatives were independent of the federal government initiatives, but were spun off from the government-initiated programs. Some of the initiatives were taken by the state governments, local authorities and NGOs. The initiatives that unfolded in the aftermath of the disaster are presented in the following sections.

Establishment of Special Malaysia Disaster Assistance and Rescue

During the rescue operations of the Highland Towers landslide, the government immediately realised the inadequacy of the Fire and Rescue Department team at that time to carry out search and rescue operations such as this one. External assistance from Japan, United Kingdom and even as far away as United States arrived days later to search for

A.C. Hassandi (✉)
Public Works Department, Jalan Sultan Salahuddin,
50582 Kuala Lumpur Malaysia
e-mail: Hassandi@jkr.gov.my



Fig. 1 The collapsed apartment building with the abandoned ones in the background

survivors. Only three people were rescued alive, although one of them later succumbed to injuries. As a result of this experience, the Special Malaysia Disaster Assistance and Rescue Team (SMART) was then established in 1995. The department specializes in search and rescue operations during disasters such as landslides. Recently, however, there have been questions about the need of having SMART when there is already in existence the Fire and Rescue department and Civil Defence Department that are doing almost the same thing.

Guidelines for Development on Hillsides

Malaysia's economic development began in earnest in the late 1980s from an agricultural economy to a manufacturing one. The economy grew approximately 9 % from 1987 to 1997 (The Encyclopedia of Nations). With the economic boom, physical development grew dramatically in major cities such as the capital city of Kuala Lumpur and Penang Island. Development began to encroach onto hilly terrain areas surrounding the cities, and new roads were built traversing through mountain ranges. As a result of the rapid developments, the frequency of landslides and associated fatalities also increased. This phenomenon is in agreement with the observations made by Remendo et al. (2005) with regards to the relationship between frequency of landslides and human activity.

However, it is important to note that not all landslides are due to development; others may be due to extreme weather conditions and natural causes.

The findings from the Highland Towers disaster indicate that the following were lacking or inadequate:

- The local authority did not have the capacity and capability to approve developments on hillsides,

- There were guidelines on development on hillsides for developers and local authorities,
- Planning, design and construction processes lacked adequate standards for development that carries higher risks,
- Maintenance of man-made slopes was not carried out, and there were no provisions for the authorities to take any actions against the guilty parties unless there were signs of impending danger to the public.

In 1997, a set of guidelines titled 'Development Guidelines in Hilly Terrain Areas,' were prepared by the Ministry of Housing and Local Authority. Risk was associated with how steep the natural slope was before development. Slopes that are more than 25° are considered high risk and slopes that are less than 25° are considered low to medium risk. The guidelines were vague; slope features regarding buffer zones, height of hills or mountains where developments were allowed and not allowed were not specified. Lack of clarity and difficulty in enforcement resulted in complete abandonment of the guidelines. Nobody remembers ever abiding by these first guidelines.

Subsequently, in 2005, new guidelines were drafted by the Ministry of Natural Resources and Environment. Input from various agencies such as the Public Works Department and the Department of Minerals and Geosciences were sought during the drafting of the guidelines. This time, the guidelines were more specific; for example, natural slopes were divided into four categories based on slope gradients from 15° to 35° and geological conditions of the slope, i.e., whether the slopes in the area are prone to instability or excessive erosion. For slope gradients greater than 35° no development was allowed. But again, buffer zones were not mentioned in the guidelines, and the density of build-up areas was also not specified. Although better than the one in 1997, the revised guidelines were still inadequate, with loopholes that developers could manipulate to their advantage.

The years 1993–2008 saw an increasing number of landslides and fatalities due to landslides (Fig. 2). During this period there were more than ten major landslides that cost more than USD 500 million in losses (Slope Engineering Branch). In 2008, there was a major landslide at Bukit Antarabangsa near Kuala Lumpur that killed five people and destroyed 14 houses. More than 5,000 people in the neighbourhood were directly affected by the landslides because the road leading to their houses was completely cut off and basic facilities such as water and electricity supplies were disrupted for more than 3 days. Having another major landslide only 1.4 km away from Highland Towers caused a huge public outcry. People started to compare the two landslides and at the same time lamenting that the government had not done anything since the Highland Towers disaster.

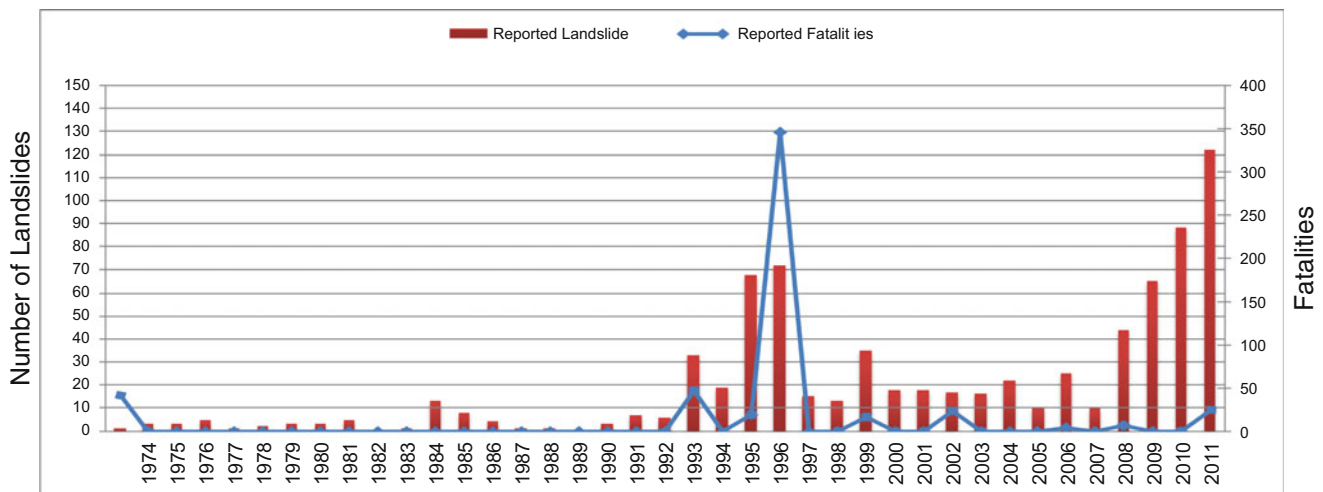


Fig. 2 Increase in the number of landslides and landslide fatalities between 1973 and 2011

In Malaysia, especially in the cities, the public always blame the government for any disasters that occur. Questions such as:

- Why did the government approve the development to be carried out when it knows that the areas are risky?
- Why wasn't there any enforcement and monitoring done on works by errant developers?
- Has the government learnt nothing from the previous landslide incidents?

These are some of the questions raised in the media after a major landslide such as the recent Bukit Antarabangsa landslide. Usually, it is the local authorities that bear the brunt of this public anger. Sensing the need for stringent controls on developments on hillsides, the federal government in 2008 instructed the Ministry of Housing and Local Authority to draft new guidelines that were more comprehensive and less ambiguous to replace the 2005 guidelines. The guidelines were approved by the Cabinet in 2009 and came into effect immediately after it was approved by the Prime Minister and chief ministers of various states during the 62nd National Assembly for Local Authority. After that they were published by the Ministry of Housing and Local Authority.

New additions to the guidelines were specific and clear:

- Buffer zones for buildings to be included in the development plan
- Maximum height of man-made slope cannot exceed 42 m
- Maximum building footprints for hilly and mountainous areas are specified
- Procedures for approval and time allocations for these approvals are indicated
- On hazardous slopes, independent checker has to be appointed by developer and approved by the local authority
- References are made to technical guidelines or manuals produced by relevant technical agencies that are related to slopes

- Areas where no development is allowed are also specified.
- No developments are allowed if the average slope angle is more than 35°

After the federal guidelines were published, some states and a federal territory have come up with their own guidelines for hillside developments. These states are generally more affluent. The states that published their own guidelines are Kuala Lumpur City, Selangor and Pulau Pinang. The state guidelines were published and came into force from 2010 to 2012. Some of these guidelines are more stringent than the federal guidelines whereas others are more accommodating to development. Many developers were not happy with the guidelines because of the restraints imposed on the land use especially where lands are a scarce commodity. However, from the standpoint of the government, the existence of guidelines ensured that developers, planners, designers, landowners, and local authorities carry out their roles and responsibilities. The guidelines also serve to clarify the role and scope of the government in slope matters and services. It is not uncommon for private landowners to report abnormal conditions that may or may not be related to slope instability to the Slope Engineering Branch of the Public Works Department or local authorities instead of retaining the services of private geotechnical engineers or geologists. Most of the public believes that this is completely legitimate since they pay taxes.

The government also set up a clearinghouse for development orders in the form of a 'One Stop Centre', which comprises relevant technical agencies that review development applications, particularly those on hillsides. While the idea for this procedure is sound, in reality some of these agencies do not have the technical capability at district and state levels to provide advice to the local authorities.

The guidelines and legislation relating to slope development and management have been used to good effect by

some local authorities, especially those in and around Kuala Lumpur. However, some local councils are still oblivious to the guidelines and the relevant legislation. These guidelines are not applicable to designated agricultural areas such as Cameron Highlands, a well-known agriculture and highland resort area. There are also areas outside the local authority that are under the district land office where the guidelines are not enforced.

Although quite stringent, the 2009 guidelines provide greater power to the local authorities to exercise control over development on hillsides, especially in the cities where the public are more educated and vocal. However, the guidelines have to be revised from time to time to meet the demands for affordable housing whilst at the same time not putting the population at unnecessary risks.

Establishment of the Slope Engineering Branch and Its Activities

In October 2003 a rockslide at Bukit Lanjan near Kuala Lumpur caused a toll expressway to be closed for more than 6 months. The expressway was one of the busiest expressways in Malaysia. The rockslide caused massive congestion in the capital as traffic was diverted to other roads that do not have the capacity to bear additional traffic load. As a result of this landslide, on February 2, 2004 the Malaysian Cabinet instructed the Public Works Department to establish a dedicated slope engineering division to reduce risks and losses due to landslides.

The National Slope Master Plan

In the same year the Cabinet instructed the Slope Engineering Branch to carry out a National Slope Master Plan (NSMP) study. The NSMP study was approved by the Cabinet in August 2009. The NSMP Terms of Reference was partly based on USGS Circular 1244 (Spiker and Gori 2003) and works by the Committee on the Review of the National Landslide Hazards Mitigation Strategy Board of the United States National Research Council (2004). In USGS Circular 1244 there are nine components that form the mainstay of the NSMP study; the component Policy and Institutional Framework was added in the Malaysian study. Thus, the NSMP consists of ten components. The components are:

1. Policy and Institutional Framework
2. Hazard Mapping and Assessments
3. Early Warning System and Real Time Monitoring
4. Loss Assessment
5. Information Collection, Interpretation, Dissemination and Archiving

6. Public Awareness and Education
7. Loss Reduction Measures
8. Training
9. Emergency Preparedness, Response and Recovery
10. Research and Development.

One of the recommendations in the NSMP is the setting up of a dedicated agency to oversee slope management throughout the country. In theory this seems to be a step forward; however, in Malaysia, land and water affairs are completely under the jurisdiction of the state. Federal government and agencies exercise little or no control over these matters. Thus, the agency has yet to be set up, although some quarters are pushing for its establishment.

Hazard and Risk Assessment

The NSMP implementation plans fell behind schedule due to many constraints, funding and human resource being a few of them. However, for the hazard and risk mapping component, considerable progress has been made, especially mapping in landslide-prone areas such as Ampang Jaya (where many of the landslides had occurred including the Highland Towers landslide), Penang Island and Canada Hills in Miri, Sarawak. The hazard and risk maps were given to local authorities for their planning, inspection and maintenance programmes. Some of the authorities have made good use of the information given to them, whereas others have had difficulty in making use of the information due to inadequate technical capability and funding. One of the issues is that local authorities do not possess the GIS-based software used for displaying the maps. The Slope Engineering Branch is currently working on putting the map online for usage by the local authorities. The access has to be through a secure website since the maps are not made public. More hazard and risk mapping works are in the pipeline. The Slope Engineering Branch will continue to collaborate very closely with the local authorities to update information and ensuring that the data produced is fully utilised.

Public Awareness and Education

Another component where considerable progress has been made is public awareness and education. The programmes started before the completion of the of the NSMP study. The programme consisted of campaign activities for various target groups. One of the most important groups is the communities in at-risk areas because of the obvious risk to life and property. The assumption at the outset of the programme was that public awareness to this group would yield the best results among all the target groups because of the immediate safety concern to themselves (Motoyama and Abdullah 2011). As a result of the campaign, an NGO that teaches communities on recognising and reporting signs of



Fig. 3 Exhibition carried out in a mall

landslides was established in Bukit Antarabangsa, the location where a major landslide occurred in 2008.

Other awareness activities consist of roadshows to the general public via exhibitions in malls; giving out brochures on landslide pertaining to signs; community-based slope inspection and maintenance; and advertorials in newspapers and on television. The campaigns seem to be working based on the increased number of complaints received by the Slope Engineering Branch and feedbacks from the public. Figures 3 and 4 show one of the exhibitions carried out in a mall and newspaper advertorial in four different languages representing the four major ethnic groups in Peninsular Malaysia. In Sabah and Sarawak, the languages used by the communities are different from Peninsular Malaysia but all of them understand Malay or English.

The authorities are the only government body with the charter to enforce safety guidelines and by-laws and engage in maintenance measures. Because they are the first line of contact with the residents, it is crucial that the engineering departments of the authorities are well trained and well equipped. Several training programmes were carried out in collaboration between the Slope Engineering Branch and the Ministry of Housing and Local Authority. Training modules usually cover good construction practices, inspection and maintenance. But most importantly, local authorities are taught to recognise and prioritise signs of landslides. Prioritisation helps in allocating resources and funds in order of urgency. A lot more has to be done to ensure that the capacity and capabilities of the local authorities can cater to the increasing issues and demands posed by the public, especially those living in landslide-prone areas. A few local authorities have shown marked improvement in handling and acting on complaints from the public.

Early Warning System and Real Time Monitoring

An initial study for an area-based warning system was conducted for a mountainous road connecting Tapah, a small town at the foothills, to Cameron Highlands, an agricultural and tourist centre situated in the middle of the mountain range that divides Peninsular Malaysia into east and west. The study tried to correlate rainfall patterns with landslides in the area. Additional studies are currently underway to provide a higher confidence level such that early warnings can be provided to the motorists and members of the public living in the highlands. The study is expected to be completed within 5 years, culminating in a warning system that can inform motorists of the danger level during rainy seasons or when the antecedent and intensity rainfall exceeds a threshold limit.

A localised landslide monitoring system has been set up at two locations along the Simpang Pulai-Cameron Highlands Road, which is an alternative road to Cameron Highlands. The system used for this site is an automatic total station that sends data every three hours to the Slope Engineering Branch in Kuala Lumpur via GSM networks. In the event where the network is not available, communication is done via satellite. This kind of monitoring system is installed only in situations where slope strengthening works are too costly. The localised monitoring system is used on a case-by-case basis. Figure 5 shows a slope that has slipped by more than 30 m at the crest, and Fig. 6 depicts a graph displaying the movements that have been monitored and measured at one of the locations on the surface of the slope since 2003.

Information Collection, Interpretation and Sharing

The information collection, interpretation, dissemination and archiving component started with the formation of the Slope Engineering Branch in 2006. The GIS-based system known as the *Integrated Slope Information System* gathers and disseminates information for use within the division, although there are plans to extend the service to relevant agencies and local authorities. Information sharing among the relevant agencies is under discussion with the formation of the Interagency Committee on Slope Management. The committee is chaired by the National Security Council with the Slope Engineering Branch playing the role of the secretariat. One of the key information that can be shared is rainfall data, which is collected by three organisations: the Slope Engineering Branch and expressway concession companies, which requires the data for landslide warning system; and Drainage and Irrigation Department, which requires the data for flood forecasting and warning.

Other data that can be shared are aerial photographs, satellite images and LiDAR data that some of the agencies have produced at one time or the other for their study or investigation. Data sharing can reduce redundancies in data collection and generation.

Fig. 4 Newspaper advertorial in four languages

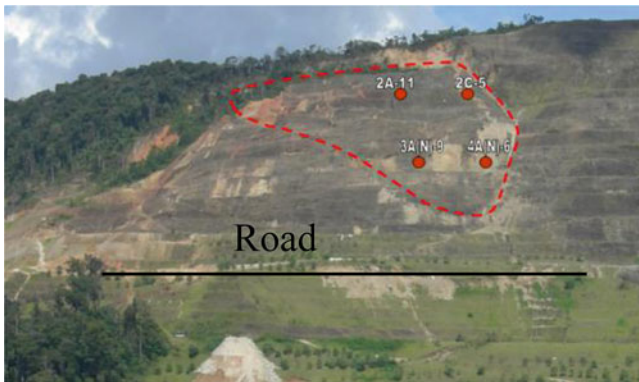


Fig. 5 Landslip at the crest of the mountain and some markers installed on the slope for real time monitoring

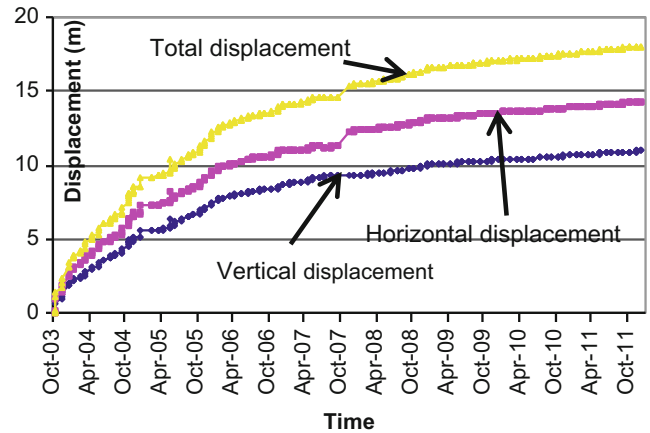


Fig. 6 Displacements at marker 2A-11

Conclusions

Various initiatives to reduce the risk of landslides, especially on man-made slopes, commenced after the Highland Towers disaster in 1993. The first was the setting up of the SMART rescue unit that specialises in search and rescue operations during disasters such as landslides. This initiative was spurred by a series of other landslides after the Highland Towers incident including the Bukit Lanjan and Bukit Antarabangsa landslide in 2008. Another was the creation of guidelines for development on slopes and hilly terrains, which have gone through

several changes since the first release in 1997. Due to pressure from the public the guidelines have become stricter. The latest was published in 2009 by the Ministry of Housing and Local Authority. After the establishment of the Slope Engineering Branch more initiatives were formulated. In 2009 the NSMP was published to steer the course for better slope management throughout the country. Some of the components in the NSMP have made reasonable progress such as hazard and risk mapping; public awareness and education; warning systems; and information collection, dissemination and sharing. However, others have not progressed as planned. To ensure

that the other initiatives are eventually carried out and the government maintains its commitment towards slope safety, public awareness and pressure must be continued and sustained.

References

- Motoyama E, Abdullah CH (2011) Landslide public awareness and education programs in Malaysia. In: Proceedings of the second World Landslide Forum, 3–7 October 2011, Rome
- National Research Council (2004) Partnerships for reducing landslide risk—assessment of the national landslide hazards mitigation strategy. National Academies Press, Washington, DC
- Remendo J, Soto J, Gonzalez-Diaz A, de Teran JRD, Cendrero A (2005) Human impact on geomorphic processes and hazards in mountain areas in northern Spain. *Geomorphology* 66:69–84
- Slope Engineering Branch (2009) National slope master plan. Public Works Department, Malaysia
- Spiker EC, Gori PL (2003) National landslide hazards mitigation strategy—a framework for loss reduction, Circular 1244, United States Geological Survey
- The Encyclopedia of the Nations, Malaysia—Economy. <http://www.nationsencyclopedia.com/Asia-and-Oceania/Malaysia-ECONOMY.html>. 13 Sept 2013

Climate and Land-Use Change Impacts on Landslides



Introduction: Climate and Land-Use Change Impacts on Landslides

Vít Vilímek and Mike Winter

Abstract

Landslides may be triggered by a variety of factors and processes. Amongst the most important and common of these is rainfall whether in the form of high-intensity short-duration storms, lower intensity higher-duration antecedent events or a combination of both. Nevertheless we have to consider carefully all of the meteorological factors as triggers with respect to the complexity of the natural environment. This is especially important during times of rapid climate change and associated land-use change. The total annual amount of precipitation, the distribution of precipitation through the year, and the frequency and magnitude of extreme rainfall events are all important factors. Regional variations are extremely important and the handling of uncertainties in the climate change predictions is very important.

Keywords

Climate change • Land-use • Rainfall • Mountain environment

Climate and land use changes can significantly affect slope instability and landslide evolution, both positively and negatively, and alter the magnitude and/or frequency of such events. The impacts of climate and land use changes may be especially significant in sensitive mountain environments.

The scope of the papers that follow this short introduction encompasses the impact of these changes on landslide triggers (e.g. rainfall, flood, freeze-thaw), landslide frequency and magnitude, and the associated changes to geographical and temporal patterns of landslide hazard and risk. In terms of the timescales over which climate change, in particular, are viewed it is recognized that demographic change, including factors such as changing population

distributions and travel patterns, are an important consideration in the evolution of patterns of risk.

Landslides of different types and within different climatic zones and geomorphological settings are described within the papers. There is a focus on improving the understanding of the impacts on triggering factors, and the distribution of hazard and risk in order to increase the effectiveness of landslide risk reduction.

Slope deformations are influenced by a wide range of factors including the geological and geomorphological settings, water, vegetation, anthropogenic activity as well as meteorological events such as intense and/or lengthy rainfall events. Climate is the long-term manifestation of meteorological patterns and has a clear influence on slope movements albeit that it is not a straightforward matter to assess the influence of such changes on instability. Whether the cause of climate change is natural or anthropogenic, and there is both a significant body of evidence and a strong consensus of opinion that point towards anthropogenic activity as the cause, the meteorological manifestations of such change will have an effect on various types of slope deformation. Climatic factors influence the origin as well as the

V. Vilímek (✉)

Faculty of Science, Department of Physical Geography and
Geocology, Charles University in Prague, Albertov 6, 128 43
Prague 2, Czech Republic
e-mail: vit.vilimek@natur.cuni.cz

M. Winter

Transport Research Laboratory (TRL), 13/109 Swanston Road,
Edinburgh EH10 7DS, UK

development of the deformation, which means that changes in meteorological factors over the period during which some large landslides are active can induce a corresponding change in the development of slope movements. As a result it is important that the individual meteorological parameters are considered, although it is not easy to evaluate the impact for each parameter (e.g. total precipitation, temperature changes, etc.).

Scale is also a very important consideration. Patterns that are both clear and important at the large-scale can very easily mask important details at the small-scale and a clear understanding of the boundaries, limitations and the scale of any data set, and the associated analysis and conclusions, is vital. The forecast climate changes vary from region-to-region and the papers should be seen in this context: that is, as region-specific analyses of the actual and/or potential effects of climate change on slope movement patterns for one or more specific landslide type.

No thematic set of papers on climate change, let alone one that considers its effects on landslides, would be complete without considering uncertainty. In terms of the potential variability in climate changes, and the subsequent impacts, the statement widely attributed to Donald Rumsfeld, the former US Secretary of Defence at a Defence Department briefing in 2002, is pertinent:

“There are known knowns. There are things we know that we know. There are known unknowns. That is to say, there are things that we now know we don’t know. But there are also unknown unknowns. There are things we do not know we don’t know.”

This may be framed as follows (Winter et al. 2010):

Known knowns: These include historic and recent climate trends, their relation to current patterns and the fact of climate change (the sequence of emissions, global warming, and climate change and instability).

Known unknowns: The precise degree and nature of climate change and some of its impacts, particularly in the light of the variability in climate change forecasts and likely instability in year-on-year climate patterns. These impacts might, for example, include the reaction of vulnerable human populations to both climate change and instability.

Unknown unknowns: The nature of some other impacts of climate change, although as these are genuinely unknown unknowns these will really have to wait until our knowledge is more complete—that these are unknowns is after all the point. Possibly the real value of this element of the framework is as a reminder that there will always be issues that arrive unexpectedly out of the leftfield.

This emphasises the need for effective and ongoing communication both within and between the professions. If we are to thrive in an uncertain future, we must be able to bring to bear the talents and resources of a suitably broad range of people to provide effective solutions to the problems that will face society as a result of global change.

Reference

- Winter MG, Dixon N, Wasowski J, Dijkstra T (2010) Introduction to land use and climate change impacts on landslides. *Q J Eng Geol Hydrogeol* 43(4):367–370



Modelling the Influence of Tree Removal on Embankment Slope Hydrology

Kevin Briggs, Joel Smethurst, and William Powrie

Abstract

Trees cover the slopes of many railway earthworks supporting the United Kingdom's transport network. Root water uptake by trees can cause seasonal shrinkage and swelling of the embankment soil, affecting the line and level of the railway track. This requires continual maintenance to maintain the serviceability of the track and reduce train speed restrictions. However, the removal of trees from railway embankment slopes and the loss of soil suctions generated by root water uptake may negatively impact embankment stability, particularly during periods of wet weather. An improved understanding of the influence of tree removal on embankment hydrology is required so that infrastructure owners can develop a managed system of vegetation clearance.

Hydrological field monitoring data from an instrumented railway embankment are presented and compared with a finite element model of root water uptake incorporating daily weather data. It is shown that trees maintain persistent suctions within their root zone which are unaffected by seasonal wetting and drying at the soil surface. However, the removal of trees from the embankment slope causes wetting of the soil from the soil surface as persistent soil suctions within the root zone are lost.

Keywords

Tree removal • Hydrological modelling • Transport infrastructure

Introduction

Trees cover the slopes of many earthworks supporting the United Kingdom's railway network. Many of these trees are deciduous, transpiring and removing water from the soil during the summer months. Deciduous trees remain dormant in the winter and cease to remove water from the soil, during which time rainfall rehydrates the soil from the surface. This

seasonal pattern of soil wetting and drying causes volume change in high plasticity clays. For tree-covered railway embankment slopes in areas of high plasticity clay, such as the London Clay basin, seasonal volume change of the soil can affect the line and level of the railway track. However, trees can provide a beneficial contribution to slope stability, through mechanical root reinforcement and the generation of soil suctions within the tree root zone. Railway infrastructure owners require a better understanding of tree influence on pore water pressure variation within slopes, to assess the impact of tree removal on railway embankment hydrology, deformation and hence stability.

Trees draw water from their root zone, which typically extends to about 2–3 m depth (Biddle 1998). In addition to seasonally wetting and drying the soil, mature trees have been shown to develop persistent suctions within their root zone that help to maintain the stability of railway

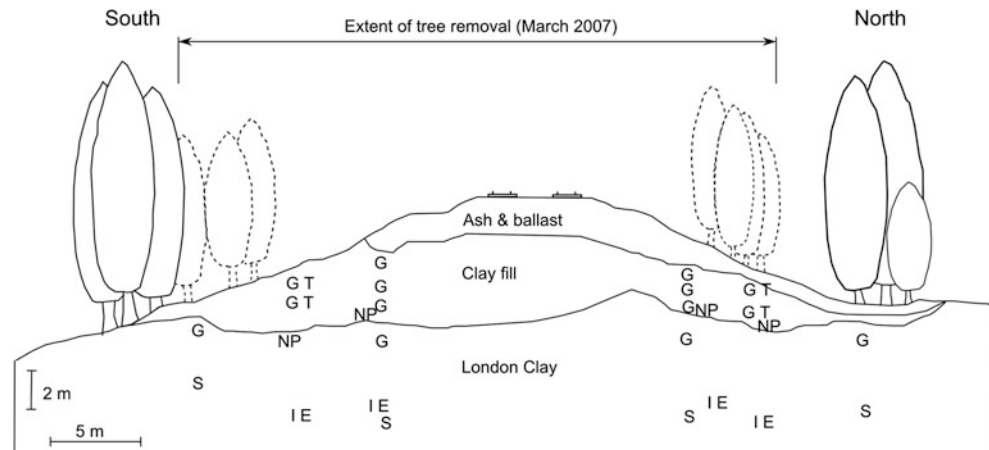
K. Briggs (✉)

Department of Architecture and Civil Engineering, University of Bath,
Bath BA2 7AY, UK
e-mail: k.m.briggs@bath.ac.uk

J. Smethurst • W. Powrie

Faculty of Engineering and the Environment, University of
Southampton, Southampton SO17 1BJ, UK
e-mail: jas@soton.ac.uk; wp@soton.ac.uk

Fig. 1 A cross section of the instrumented embankment showing the location of geopiezometers (G), standpipe piezometers (S), inclinometers (I), extensometers (E), neutron probe (NP) and TDR theta probes (T)



embankment slopes (O'Brien 2007; Glendinning et al. 2009). In some railway embankments constructed of low permeability clay fill, surface water is unable to infiltrate to greater than 1–2 m depth during the winter months. This allows zones of persistent suction to develop below 1–2 m depth on tree-covered slopes. In over-steep embankments, or where the clay fill has reduced strength due to strain softening of the clay, these persistent suctions may be crucial in preventing deep-seated instability of the embankment slopes (Scott 2006). Removal of mature trees from railway embankment slopes may negatively impact their stability, particularly during periods of wet winter weather.

Railway infrastructure owners, such as Network Rail, have been removing vegetation from the upper part of railway embankment slopes to reduce localised movements affecting the line and level of the railway track. Observations of changes in pore water pressure and soil moisture content in response to tree removal are required. This will allow railway infrastructure owners to assess the impact of tree removal on railway embankment hydrology, so that a managed system of vegetation clearance may develop.

This paper presents monitoring data from an instrumented railway embankment with mature tree cover and a history of seasonal railway track movement. Trees were removed from the embankment slope after 1 year and the mechanical and hydrological response of the slope was measured for an additional two and a half years. A hydrological model incorporating a climate boundary condition is used to understand the influence of tree root water uptake on slope hydrology, for comparison with the field measurements from the embankment slope.

Field Measurements

Site Description and Instrumentation

The instrumented embankment is situated on the Shenfield-Southend Victoria line in the south east of England. The

embankment is 5.5 m high, with typical slope angles of 23° on the north side and 20° on the south side. The embankment is constructed of intermediate to very high plasticity clay fill, excavated from a local cutting during construction in the 1800s. The embankment is founded on London clay and has a layer of granular ash covering the upper slope (Briggs 2011). Prior to vegetation clearance the embankment was vegetated with mature and semi-mature trees covering the north and south slopes. In March 2007 trees were removed from the upper two-thirds of both slopes. The extent of the tree clearance is shown in Fig. 1.

Instrumentation was installed at the site during March 2006 by Smethurst (2010). Instrumentation was installed on both the north and the south slopes of the embankment (Fig. 1), with groups of instruments located at the crest, mid slope and the toe. A neutron probe with access tubes installed in the embankment slope and TDR ThetaProbes were used to measure soil moisture content. Pore water pressure was measured using GeO-flushable piezometers capable of measuring suctions of up to 90 kPa (Ridley et al. 2003) and conventional standpipe piezometers. Lateral and vertical movement of the embankment was measured using inclinometers and extensometers. Rainfall was measured using a tipping bucket rain gauge installed on the embankment slope. The instrumentation of the embankment is described by Briggs (2011).

Monitoring Results

Removal of trees from the embankment slope caused the embankment soil to swell, pore water pressures within the embankment to increase and volumetric water content to increase from a persistently dry profile to a saturated condition.

Vertical displacement measured at the crest of the north slope of the embankment showed downward movement (settlement) of the embankment during the summer of 2006 followed by upward movement (heave) during the

Fig. 2 Indicative pore water pressures at 2.8 m, 3.7 m and 5.8 m depth, measured at the North crest by Briggs (2011)

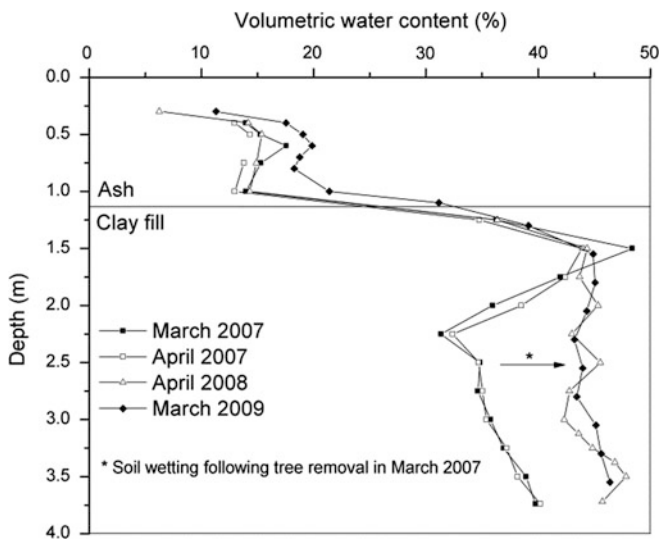
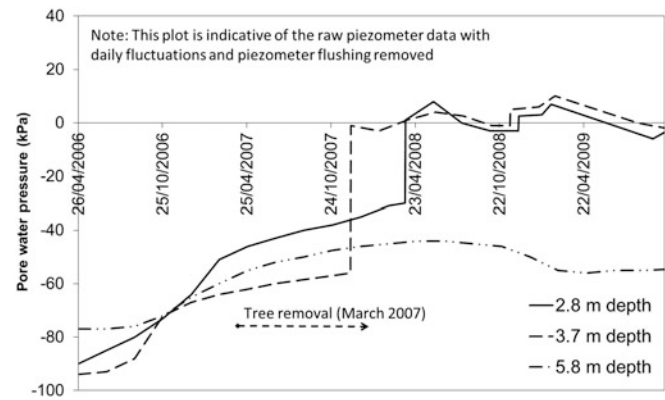


Fig. 3 End of winter (March/April) volumetric water content at the crest of the north slope before and after tree removal in March 2007

winter of 2006/2007. Following tree removal in 2007 the seasonal movement of the slope ceased and the crest of the embankment continuously moved upward as the clay swelled. The swelling extended to approximately 3 m below the ground surface (Briggs 2011).

Indicative piezometer data from the north crest of the embankment shows a condition of pore water suction (50–80 kPa), immediately prior to tree removal (Fig. 2). Pore water pressure increased towards 0 kPa following tree removal in March 2007. One year later, between March 2008 and September 2009, a pattern of seasonal pore water pressure variation close to 0 kPa was measured as light shrub vegetation became established on the embankment slope. A pore water pressure increase was measured at 5.8 m depth, but negative pore water pressure was maintained.

Figure 3 shows profiles of volumetric water content with depth measured at the crest of the north embankment slope. Measurements of the wet, end-of-winter condition (March/April) are shown for 2007–2009. Figure 3 shows a dry profile within the clay fill below 2 m depth before tree

removal. Following tree removal in March 2007 the soil progressively rewet towards saturation in April 2008 and the persistently dry profile was lost.

Finite Element Modelling

Finite element analysis using the software Vadose/w was used to examine the influence of tree root depth and tree removal on embankment hydrology, for comparison with the monitoring data.

Vadose/w calculates saturated and unsaturated water and heat flow in response to applied boundary conditions (GeoSlope 2007). Most notably, a climate boundary can be applied; this uses daily climate data to calculate water infiltration and water removal from the surface of the soil and from a defined rooting zone. This enables variations in pore water pressure and volumetric water content with time, in response to changes in weather conditions or changes in vegetation cover, to be investigated.

Mesh Geometry

A one-dimensional soil column was used to calculate vertical water flow in response to a climate boundary condition. This soil column represented a borehole at the crest of the north embankment slope.

The model explores the extent to which a one-dimensional soil column with a climate boundary condition and root water uptake function can provide useful comparisons with the field measurements. The soil column considers changes in pore water pressure and volumetric water content in response to transient pressure gradients applied at the upper surface boundary and within the vegetation root zone of the column. A fine mesh of 0.1 m elements was used in the surface zone of the soil column, where high pressure gradients were likely to occur, while a mesh of 0.5 m elements was used in the remainder of the soil column.

Table 1 Summary of soil properties used in the finite element model [From Briggs et al. (2013)]

Soil type	Permeability (ms^{-1})	Van Genuchten constants				
		AEV	θ_s	θ_r	m	n
Ash and ballast	4×10^{-5}	2	0.45	0.1	0.5	2
Clay fill	5×10^{-8}	30.3	0.47	0.1	0.13	1.15
London Clay	5×10^{-9}	125	0.47	0.1	0.15	1.18

Where AEV = air entry value, θ_s = saturated water content, θ_r = residual water content, m and n = constants

Table 2 Summary of the climate boundary condition applied to the finite element model

Model stage	Vegetation cover	Weather data	Root depth
Initial condition	Mature tree cover	01/01/2001–31/12/2005	3 m
Before tree removal	Mature tree cover	01/01/2006–31/03/2007	3 m
Immediately after tree removal	Very light vegetation	01/04/2007–31/08/2007	0.05 m
After tree removal	Newly established shrubs	01/09/2007–01/09/2009	0.2 m

Material Properties

The soil column is representative of the borehole at the crest of the north embankment slope, which consists of 1.1 m of ash and ballast overlying 3 m of clay fill, with a London clay foundation extending for 13 m below.

The hydrological soil properties used in the one-dimensional soil column are shown in Table 1. These are consistent with those used by Loveridge et al. (2010) and Briggs et al. (2013) to model railway embankment hydrology. The saturated permeability of the clay fill was based on the results of permeability testing by O'Brien et al. (2004), while the London clay underlying the embankment was assigned a saturated permeability consistent with the range measured by Chandler et al. (1990). The ash and the ballast soil layer was assigned a saturated permeability consistent with a sandy gravel, as in situ permeability data was unavailable.

As the soil becomes unsaturated, both its water content and its hydraulic conductivity decrease. Unsaturated soil properties describing the reduction in soil water content and hydraulic conductivity for the clay fill and the London clay were based on a modified version of the Croney (1977) soil water retention curve for London clay (Briggs et al. 2013). The soil water retention curve for the ash and ballast was based on the curve for a coarse granular material. The soil water retention curves were used to define the reduction of soil hydraulic conductivity and water content with increasing soil suction using the Mualem (1976) method with van Genuchten (1980) constants and saturated permeability. Table 1 summarises the van Genuchten (1980) constants and soil properties used in the soil column. The lower limit of hydraulic conductivity for the ash and ballast layer was limited to $1 \times 10^{-8} \text{ ms}^{-1}$, to facilitate rainfall infiltration into soil in the dry condition. The hysteretic wetting and drying of the granular soil with large voids

was not well represented by the continuum assumed in the finite element model.

Boundary Conditions

A climate boundary condition using daily weather data (solar radiation, relative humidity, temperature, rainfall and wind speed) was used to calculate the water flux at the soil surface. A root water uptake function was used to model water removal at depth due to transpiration. Three slope vegetation conditions were applied to the surface of the soil column, to represent the stages of tree removal at the instrumented embankment; mature tree cover, tree clearance (i.e. very light vegetation) and newly established shrubs (Table 2).

The Vadose/w climate boundary condition calculates evaporation from an unsaturated soil using the Penman-Wilson equation (Wilson et al. 1994). A proportion of the potential evaporative surface flux is removed as transpiration. This proportion is defined using a Leaf Area Index (Ritchie 1972). As soil dries and soil water is not readily available, plants close stomata on their leaves to reduce their transpiration rate and reduce water loss. The reduction of transpiration due to plant stress was modelled using the Feddes et al. (1978) relationship, with transpiration reducing linearly between 100 kPa soil suction and the plant wilting point at 1,500 kPa soil suction.

Within Vadose/w, evaporated water is removed from the soil surface while transpired water is removed from the soil at depth using a root water uptake function (Tratch et al. 1995). The depth of root water uptake was used to differentiate between vegetation types on the instrumented embankment slope (Table 2).

A summary of the climate boundary condition applied to the soil column is shown in Table 2. The depth of root water

uptake was varied to simulate the mature tree cover and tree clearance at the instrumented slope.

Slope vegetation cover of mature tree cover (3 m root depth) was applied to the soil column prior to tree removal in March 2007. Very light vegetation cover (0.05 m root depth) was applied to the soil column for 3 months following tree removal (April 2007 to September 2007). Newly established shrub cover (0.2 m root depth) was applied to the soil column after September 2007, to model the growth of vegetation observed on the slopes of the instrumented embankment during this period.

Daily weather data was obtained from a weather station at Shoeburyness, 11 km from the instrumented embankment and applied to the soil column. The weather data showed that the years preceding the monitoring period (2003 and 2005) were drier than the long-term average for the south east of England, while the summers of 2007 and 2008 (immediately after tree felling) were wetter than average (Briggs 2011). An initial condition of hydrostatic pressure above and below a zero pressure line at 8 m depth was applied to the soil column. Five years of weather data recorded prior to the monitoring period was then applied to the soil column to establish an initial distribution of pore water pressure. This was followed by nearly 4 years of weather data corresponding to the monitoring period (Table 2). Sensitivity analysis showed that after less than 2 years of applied climate data the pore water pressure distribution within the soil column was independent of the initial condition.

Modelling Results

Altering the depth of root water uptake influenced pore water pressure and volumetric water content within the soil column. Figure 4 shows pore water pressure calculated at locations between 2 and 5.8 m depth below the surface of the soil column from January 2001 to October 2009. Pore water pressure calculated before tree removal shows seasonal pore water pressure variation, influenced by root water uptake. Before tree removal, soil suctions increased during the summer months due to water uptake within the tree root zone and evaporation from the soil surface. During the winter months soil suctions decreased as root water uptake and evaporation from the soil surface was reduced, allowing rainfall to infiltrate the soil. The highest pore water pressure (lowest suction) occurred at the end of winter, in March of each year.

The model showed a pore water pressure increase from soil suction towards 0 kPa in the 4 months immediately after tree removal, when the depth of root water uptake was reduced (Table 2). During this period surface water was able to infiltrate below the plant root zone and rewet the soil. After September 2007 the model showed seasonal pore water pressure variation close to 0 kPa. This is in qualitative

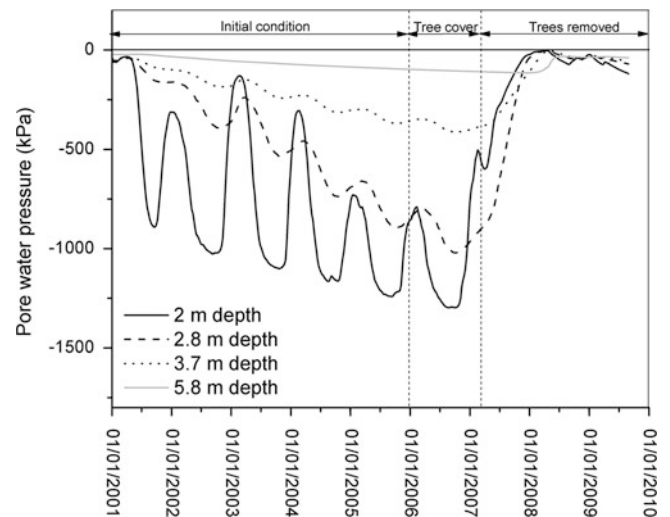


Fig. 4 Finite element calculations of pore water pressure for the crest of the north embankment slope

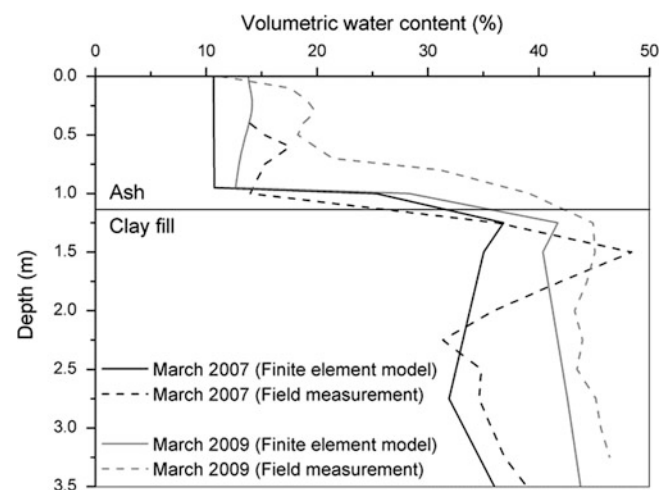


Fig. 5 Comparison of finite element calculations and field measurements of volumetric water content before and after tree removal at the crest of the north embankment slope

agreement with piezometer data from the north crest of the instrumented embankment (Fig. 2).

Figure 5 shows the volumetric water content with depth within the soil column for an end of winter (March) condition, before and after tree removal. This is compared with the field monitoring data for the same period (March 2007 and March 2009). The model shows that a persistently dry profile is maintained within the tree root zone, below 1.5 m depth, following the winter weather in 2007. During this period surface water was unable to infiltrate the soil and rewet the tree root zone before root water uptake commenced in the summer. However, after tree removal the persistently dry profile was lost and volumetric water content increased

towards a saturated profile within the model. Figure 5 shows that this is in agreement with the field measurements.

Comment and Conclusions

A finite element model incorporating a climate boundary condition and root water uptake was compared with hydrological measurements from an instrumented embankment following tree clearance from the embankment slopes.

The field measurements and model results showed that pore water pressure and soil displacement within an embankment are influenced by mature trees on the embankment slopes. The finite element model showed that the magnitude of pore water pressure variation within an embankment slope is influenced by the depth of the plant root zone.

The following conclusions can be drawn:

1. Mature trees are able to maintain a persistent water deficit within their root zone. Surface water is unable to infiltrate the soil and saturate the soil profile during the winter before root water uptake resumes in the summer months. This aids embankment slope stability during wet winter weather.
2. Root water uptake at depth ceases following tree removal and is not re-established by light, shallow rooted vegetation. This causes the embankment to rewet, pore water pressures to increase and the persistent soil water deficit and soil suctions to be lost. This reduces the resilience of the embankment to pore water pressure increases at depth during wet winter weather, potentially reducing the stability of the embankment slope.

Acknowledgments The installation of instrumentation and monitoring of the embankment was funded by Network Rail. The work was carried out at the University of Southampton Industry Doctoral Training Centre (IDTC) in Transport and the Environment, supported by EPSRC and Mott MacDonald.

References

Biddle PG (1998) Tree root damage to buildings. Willowmead Publishing, Wantage

- Briggs KM (2011) Impacts of climate and vegetation on railway embankment hydrology. EngD thesis, University of Southampton, Southampton, UK
- Briggs KM, Smethurst JA, Powrie W, O'Brien AS (2013) Wet winter pore pressures in railway embankments. *Proc ICE Geotech Eng* 166 (5):451–465
- Chandler RJ, Leroueil S, Trenter NA (1990) Measurements of the permeability of London Clay using a self-boring permeameter. *Geotechnique* 40(1):113–124
- Cronley D (1977) The design and performance of road pavements. Her Majesty's Stationery Office, London
- Feddes RA, Kowalik PJ, Zaradny H (1978) Simulation of field water use and crop yield. Wiley, Toronto, ON
- Geo-Slope (2007) Vadose zone modeling with Vadose/w 2007. Geo-Slope International, Calgary, AB
- Glendinning S, Loveridge FA, Starr-Kedde RE, Bransby MF, Hughes PN (2009) Role of vegetation in sustainability of infrastructure slopes. *Proc ICE Eng Sust* 162(ES2):101–110
- Loveridge FA, Spink TW, O'Brien AS, Briggs KM, Butcher D (2010) The impact of climate and climate change on UK infrastructure slopes. *Q J Eng Geol Hydrogeol* 43(4):461–472
- Mualem Y (1976) A new model for predicting the hydraulic conductivity of unsaturated porous media. *Water Resour Res* 12:513–522
- O'Brien AS (2007) Rehabilitation of urban railway—investigation, analysis, and stabilisation. In: Cuellar V, Dapena E et al (eds) Proceedings of the 14th international conference on soil mechanics and geotechnical engineering, madrid, vol 1. Millpress Science Publishers, Rotterdam, pp 125–143
- O'Brien AS, Ellis EA, Russell D (2004) Old railway embankment fill—laboratory experiments, numerical modelling and field behaviour. In: Advances in geotechnical engineering: proceedings of the Skempton conference, vol 2. Thomas Telford, London, pp 911–921
- Ridley AM, Dineen K, Burland JB, Vaughan PR (2003) Soil matrix suction: some examples of its measurement and application in geotechnical engineering. *Géotechnique* 53:241–253
- Ritchie JT (1972) Model for predicting evaporation from a row crop with incomplete cover. *Water Resour Res* 8(5):1204–1212
- Scott JM (2006) Influence of vegetation on the performance of railway embankments. In: Szavits-Nossan V (ed) Proceedings of the 17th European, young geotechnical engineers conference, Zagreb, 2006. Croatian Geotechnical Society, Velika Gorica, Croatia, pp 101–112
- Smethurst JA (2010) Tracking changes. *Ground Eng*, July 2010, pp 12–14
- Tratch DJ, Wilson GW, Fredlund DG (1995) An introduction to analytical modelling of plant transpiration for geotechnical engineers. In: 48th Canadian geotechnical conference, Vancouver, Canada, pp 771–780
- Van Genuchten MT (1980) A closed-form equation for predicting the hydraulic conductivity of unsaturated soils. *Soil Soc Am* 44:892–898
- Wilson G, Fredlund D, Barbour S (1994) Coupled soil-atmosphere modeling for soil evaporation. *Can Geotech J* 31:151–161



Age and Reactivations of Catastrophic Complex Flow-Like Landslides in the Flysch Carpathians (Czech Republic/Slovakia)

Tomáš Pánek, Veronika Smolková, Jan Hradecký, Ivo Baroň, and Karel Šilhán

Abstract

Catastrophic complex flow-like landslides (CFLLs) are characterised by a deep-seated retrogressive landslide of structurally unfavourably oriented rocks and earthflows that occupy the lower slope positions and originate due to the liquefaction of material accumulated on the upper slopes. These landslides are locally important geomorphic agents of Late Quaternary mountain evolution in the Flysch Belt of the Outer Western Carpathians (Czech Republic/Slovakia). Most of the CFLLs dammed and steepened adjacent valleys. Radiocarbon dating suggests that a majority of them moved repeatedly throughout the Holocene, namely approx. every 1–2 ka. Dated events occurred during humid phases of the Younger Dryas/Holocene transition (11.5–9.4 cal ka BP), Atlantic chronozone (7.4–6.6 cal ka BP), the beginning of the Subboreal chronozone (ca. 4.6 cal ka BP) and, primarily, within the Subatlantic chronozone at ca. 2–0.8 cal ka BP (>50 % of all events). Our study suggests that slopes based on an unfavourable structural setting and affected by long-term deep-seated gravitational deformations may produce CFLLs, even if they are located in medium-high mountains. Although our chronological dataset is influenced by the erosion of older landforms, most of the dated reactivations correlate with regional increase in precipitation identified by previous palaeoenvironmental studies.

Keywords

Complex flow-like landslides • Radiocarbon dating • Holocene • Flysch Carpathians • Czech Republic • Slovakia

Introduction

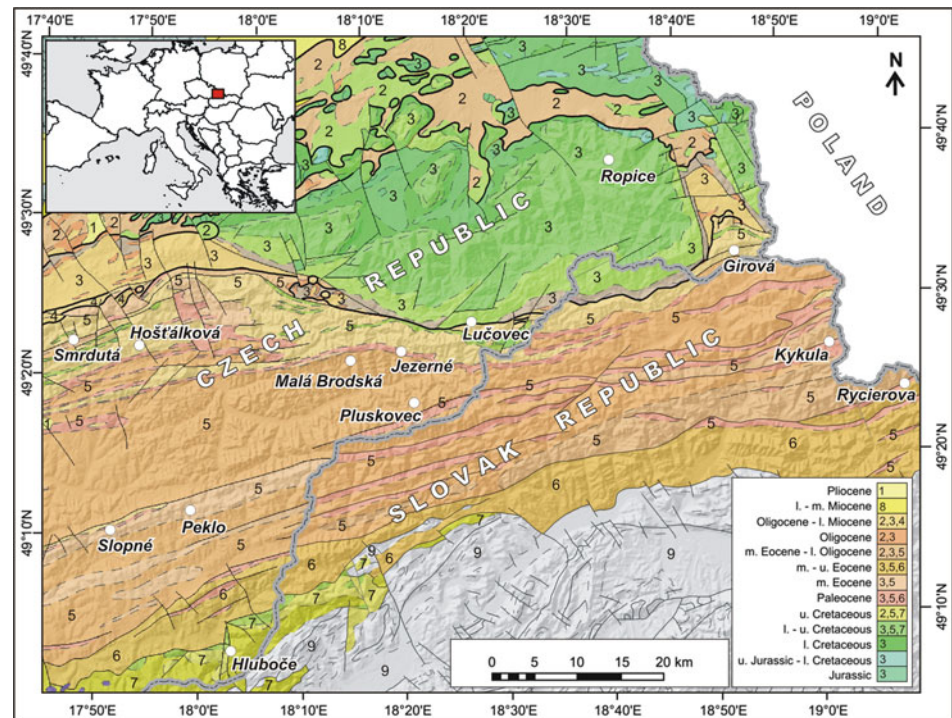
Investigation and dating of preserved deposits of ancient long-runout landslides in mountainous terrains are useful both for the elimination of landslide hazards and for the understanding of late Quaternary history. Recent field

investigations in the Flysch Belt of the Outer Western Carpathians led to the discovery of several large rotational-translational slope failures that had transformed into shallow earthflows at their frontal parts due to substrate liquefaction (Baroň et al. 2004, 2011; Pánek et al. 2013). Herein, we call such failures *complex flow-like landslides* (CFLLs) (Pánek et al. 2013). These failures correspond to complex landslides of Cruden and Varnes (1996), but using this new term we put stress on the role of flow-type behaviour during landslide emplacement. The basal sliding zone of CFLLs crops out in the upper/middle parts of deformed slopes, while in their lower positions the sliding material liquefies and evolves into earthflows. Some of these failures progressed catastrophically during heavy rainfall and snowmelt periods in 1919, 1997, 2006 and 2010 and they therefore pose a significant

T. Pánek (✉) • V. Smolková • J. Hradecký • K. Šilhán
Department of Physical Geography and Geoecology, University of
Ostrava, Ostrava 71000, Czech Republic
e-mail: tomas.panek@osu.cz; veronika.smolkova@osu.cz;
jan.hradecky@osu.cz; karel.silhan@osu.cz

I. Baroň
Geological Survey of Austria, Neulinggasse 38, Vienna 1030, Austria
e-mail: IvoBaron@seznam.cz

Fig. 1 Geology of the study area with locations of the studied CFLLs. Reprinted from Quaternary Research, 80, Pánek T et al., Holocene reactivations of catastrophic complex flow-like landslides in Flysch Carpathians (Czech Republic/Slovakia), p. 34, Copyright (2013), with permission from Elsevier



hazard in the study region (Baroň et al. 2004; Pánek et al. 2013).

The aims of our study are (1) to provide the evaluation of CFLLs in Flysch Carpathians together with the discussion of their imprint in geomorphic evolution of this region, (2) to determine Holocene history and recurrence of most pronounced failures and (3) to correlate the studied events with regional Holocene palaeoenvironmental and palaeoclimatological proxies. To answer such questions, a detailed study was performed of thirteen most pronounced examples of CFLLs in the study region (Fig. 1).

Regional Settings

The study area involves the western part of Flysch Carpathians situated along the border between the Czech Republic and Slovakia (Fig. 1). Flysch Carpathians comprise a fold-and-thrust belt consisting of shales, claystones and sandstones of Mesozoic and Tertiary age which were thrust onto the Northern European platform and part of its foredeep during the Palaeogene and Neogene. Anisotropic flysch strata are highly prone to landsliding, especially due to elevated pore-water pressures during extreme hydro-meteorological events such as heavy rainfall and rapid snow-melt (Margielewski 2006a). To date, more than 10,500 landslides have been documented within the region (Pánek et al. 2013).

Materials and Methods

Emphasis of this paper is on the geomorphic and chronological aspects of CFLLs with a special attention to possible recurrence. Geomorphic analyses involved the mapping of landslide deposits by means of field methods and aerial photographs. Structural conditions were evaluated in the vicinity of landslides (especially in the headscarp areas) via measurements of main discontinuity sets whose interplay with slope geometry was analyzed as well as possible kinematics of landslide movements (Margielewski 2006b).

The age of landslides was constrained by radiocarbon dating of organic material obtained either from the landslide debris (natural outcrops) or sediments connected with the evolution of landslides (i.e. deposits of dammed lakes or peat bogs on the surface of the landslides). Our strategy of landslide dating brings some uncertainties connected with both over- and underestimation of the timing of landslides. The age of organic material incorporated in landslide debris could be older than a particular landslide due to possible multiple re-deposition. Conversely, the ages of sediments trapped in dammed lakes and landslide peat bogs are younger than a particular slope failure. A total of 25 radiocarbon dates (mainly AMS) define the origin or reactivation of individual landslides (Pánek et al. 2013). Radiocarbon dates were converted into calendar ages using IntCal 09 calibration curve in OxCal v 4.1.7 software.

Results

CFLLs in the study area comprise various slope failures extending over relatively long distances (470–2,950 m) and are characterised by high mobility (10^{-1} – 10^2 m/day as stated for recent events), high volumes (0.1 – 12×10^6 m³) and significant liquefaction of displaced material in their middle to lower portions (Pánek et al. 2013). The largest group of CFLLs includes older failures (Kykula, Peklo, Slopné, Lučovec, Pluskovec) and recent catastrophic failures (January 1919 Hošťálková, July 1997 Malá Brodská, April 2006 Hluboče and May 2010 Girová landslides), which originated mainly within rock massifs containing a significant fraction of weak claystone/mudstone-dominated flysch (Fig. 2a). Failures in this group are rotational-translational or purely translational landslides combined with distal earthflows. Another group of CFLLs (Smrdutá, Ropice, Rycierova, and Jezerné) is characterised by rockslides affecting predominantly competent sandstone beds. These failures have distal, up to 1 km long tongues bearing pronounced stony accumulations with metre-scale sandstone blocks (Fig. 2b). Most of the CFLLs are spatially related to deep-seated gravitational slope deformations (DSGSDs) found along tectonic discontinuities and tectonically weakened (mainly wedge-type) zones in flysch rock masses (Pánek et al. 2013).

The ages of CFLLs in our dataset span the entire Holocene period with a strong bias towards the youngest, Subatlantic chronozone (Pánek et al. 2013). The oldest landslide (Kykula) originated in the Younger Dryas/Holocene transition (11.5–9.4 cal ka BP), while the youngest reactivation (excluding modern catastrophic failures) was identified within the Little Ice Age period (Smrdutá landslide, ca. 0.3 cal ka BP). One of the largest CFLLs (Girová landslide) originated during the extreme rainfall event of May 2010. Most of the dated landslides (75 %) have originated in the last 2,000 years, with a pronounced cluster between ca. 1.7 and 1 cal ka BP (34 % of all dated activations). Some individual events were dated to the Atlantic chronozone (7.4–6.6 cal ka BP; Girová and Peklo landslides) and the beginning of the Subboreal chronozone (ca 4.6 cal ka BP; Smrdutá and Peklo landslides) (Pánek et al. 2013).

One of the most important findings of this study is that most CFLLs are recurrent phenomena (Table 1). For instance, the Peklo landslide contains four scarps characterised by different degrees of denudation suggesting multistage evolution. This is supported by four generations of fluvio-lacustrine sediments in the adjacent dammed palaeolake dated to 7.2, 6.4, 4.5 and 0.6 cal ka BP. Generally, we can identify two chronological types of recurrences – successive major activations separated by

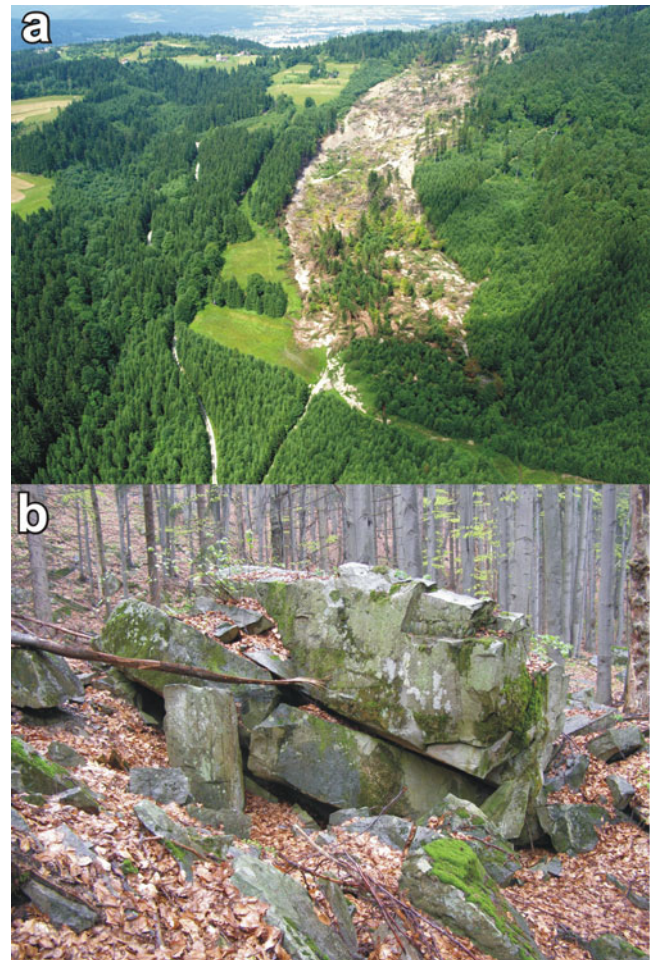


Fig. 2 Examples of CFLLs. (a) The May 2010 Girová landslide originated in the slope section with preceding landslide activity dated to 7.5, 1.5 and 0.6 cal ka BP. (b) Large sandstone blocks within the accumulation of the Rycierova rockslide (dated to ca. 1.0 cal ka BP)

short chronological intervals (up to several centuries; e.g. Kykula or Lučovec; Fig. 3), and repeated major movements after relatively long periods spanning more than one millennium (e.g. Malá Brodská landslide). Some failures from the latter group were reactivated several times throughout the Holocene (e.g. Peklo and Girová landslides). Liquefied and relatively long-runout slope failures reached valley floors and affected the geomorphic regime of mountain rivers. Except for two cases, all landslides in our dataset blocked valley floors and influenced the steepness parameters of river profiles. Sedimentological and pollen indices show that the longevity of landslide-dammed lakes before the breaching of dams spanned a variety of timescales including >2 ka for the Kykula landslide (Pánek et al. 2010), 10^2 years for the Smrdutá, Peklo and Pluskovec landslides, and 10^{-1} – 10^2 years for the Lučovec landslide (Pánek et al. 2013).

Table 1 Timing and recurrence intervals for selected CFLs [Partly reprinted from Quaternary Research, 80, Pánek T et al., Holocene reactivations of catastrophic complex flow-like landslides in Flysch Carpathians (Czech Republic/Slovakia), p. 43, Copyright (2013), with permission from Elsevier.]

Landslide	Available period (cal ka BP)	Number of dated events	Average rec. interval (ka)
Kykula	~11.5–9.4	2	2.1
Peklo	~7.2–0.6	4	2.2
Girová	~7.4–AD2010	4	2.5
Smrduť	~4.6–0.3	3	2.2
Lučovec	~1.7–0.8	3	0.4
Hošťálková	~1.4–AD1919	2	1.4
Ropice	~1.4–0.4	2	1
Hluboče	~1.3–AD2006	2	1.3
M. Brodská	~1.1–AD1997	2	1.1
Jezerné	~1.0–0.8	2	0.3

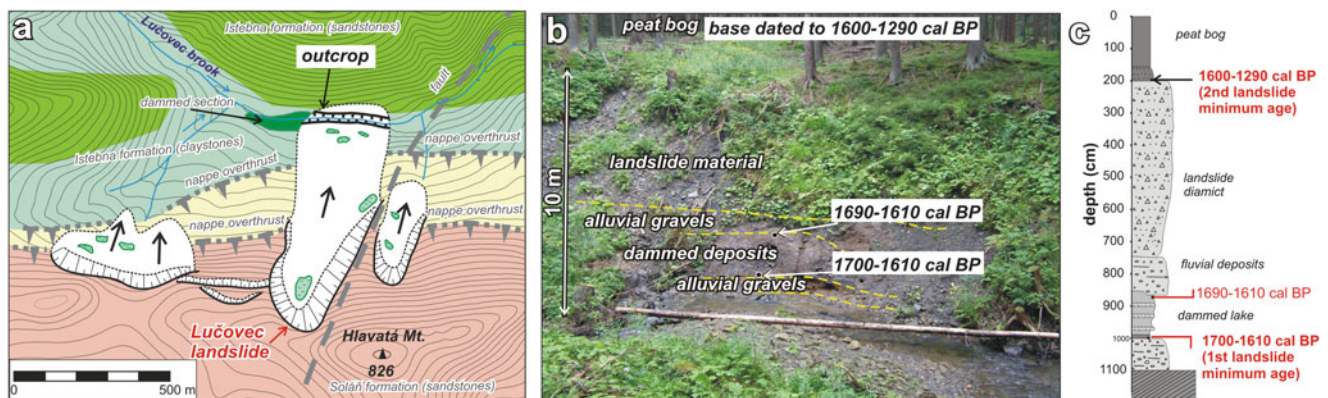


Fig. 3 A recurrent landslide in the Lučovec valley. (a) Geomorphic sketch of landslide blocking valley floor. (b) Exposure evidencing two generations of successive landslides which took place during a short

time interval between ca 1.3–1.7 cal ka BP. A possible younger retrogressive shift of headscarp took place ca 0.7 cal ka BP. (c) Interpreted stratigraphic log of the exposure

Discussion and Conclusion

A majority of CFLs in the study region fall within the Holocene period with most ages spanning to the Subatlantic chronozone (>50 % of all events) (Pánek et al. 2013). The analysis of the history of individual instabilities reveals that a majority of landslides are recurrent features with a time interval between two successive major events being in the orders of 10^1 – 10^3 years. An important issue for hazard planning is that released debris from some of recurrent catastrophic long-runout landslides has nearly reached the same position as during previous events, for example, Malá Brodská, Girová or Smrdutá landslides. As a result, some slope and valley-floor sections are particularly dangerous for human activities (Pánek et al. 2013; Fig. 2a). Factors that affect the time span between CFLs reactivations include (1) frequency of extreme hydrometeorological events (e.g. heavy rainfalls and rapid snowmelt) and (2) progressive strength degradation along major discontinuity sets

(Kemeny 2003). While hydrometeorological extremes are immediate triggers of stability changes within rock massifs, strength degradation seems to be the most important for the time span between CFLs reactivations in connection with the fact that some major failures (e.g. May 2010 Girová landslide which is one of the largest Holocene failures) originated during rather moderate hydrometeorological events (Pánek et al. 2011). The pre-failure behaviour of catastrophic landslides is often characterised by creep movements within weakened bedrock. Three major recent catastrophic events of our dataset (January 1919 Hošťálková, March 2006 Hluboče and May 2010 Girová landslides) were preceded by several years of minor instability (Pánek et al. 2013).

Our dataset (25 dated landslide events) is also limited for chronological determinations, but it shows a possible correlation with other Central European palaeoclimatological proxy records including lake-level highstands (Magny 2004), $\delta^{18}\text{O}$ speleotheme records (Niggemann et al. 2003), Alpine glacial advances (various authors in Starkel et al. 2006), palaeofloods (Starkel

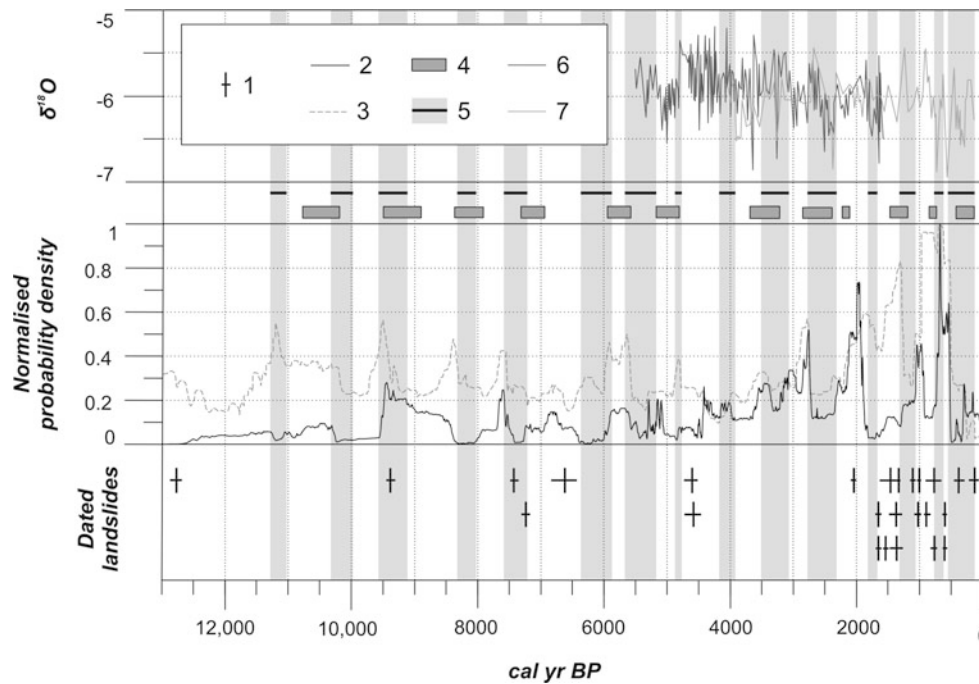


Fig. 4 Dating of individual CFFLs and their reactivations compared to the probability density curve of the Holocene dated landslide events in the Czech and Polish part of the Outer Western Carpathians and other central-European palaeoclimatological proxy records: (1) single dates of studied CFFLs (median $\pm 1\sigma$), 25 dates (Baroň 2007; Baroň et al. 2011; Pánek et al. 2009a, b, 2010, 2011, 2013); (2) normalised probability density curve of the Czech and Polish landslide events, 85 dates (Alexandrowicz 1993; Alexandrowicz and Alexandrowicz 1999; Margielewski 1997, 1998, 2001, 2003, 2006a; Margielewski and Kovalyukh 2003; Baroň 2007; Margielewski et al. 2010, 2011) and

unpublished ages of 5 landslides from the Czech part of the Outer Western Carpathians (3) normalised probability density curve of the hydrological events in Polish rivers, 331 dates (Starkel et al. 2006); (4) advances of Alpine glaciers (by various authors in Starkel et al. 2006); (5) mid-European higher lake-level phases (Magny 2004); (6) $\delta^{18}\text{O}$ record from stalagmites AH-1 and (7) B7-7 in Sauerland/Germany (Niggemann et al. 2003). Reprinted from Quaternary Research, 80, Pánek T et al., Holocene reactivations of catastrophic complex flow-like landslides in the Flysch Carpathians (Czech Republic/Slovakia), p. 44, Copyright (2013), with permission from Elsevier

et al. 2006), and timing of other landslides from the Czech and Polish Flysch Carpathians (Baroň et al. 2004; Margielewski 2006a; Margielewski et al. 2011) (Fig. 4). Highly skewed temporal distribution of CFFLs biased to the Subatlantic chronozone is most likely determined by erosion of older landslides and/or burial of ancient accumulations by debris coming from the latest stages of mass movement activity. Bias in our dataset is partly caused by types of the studied landslides, i.e. highly mobile failures with large erosive potential. In contrast to our study, a large number of predominantly short-displacement rotational bedrock landslides were dated in the Czech Carpathians by Baroň et al. (2004) and in the Polish Carpathians by Margielewski (2006a) to earlier stages of the Holocene.

To sum it up, the dating of individual CFFLs and their reactivations indicates that these mass movements originated throughout the Holocene period (Pánek et al. 2013). The largest landslides originated both at the beginning and end of the observed time period. This pattern suggests that gross conditions influencing slope stability and activation of CFFLs are relatively similar throughout

the Holocene and future sporadic large liquefied slope failures with a relatively long run-out can be expected in this region.

Acknowledgments This research was supported by the Czech Science Foundation project GAP209/10/0309: “The effect of historical climatic and hydrometeorological extremes on slope and fluvial processes in the Western Beskydy Mts and their forefield” and by the Czech Geological Survey project 215124-2: “Investigation and monitoring of slope failures on territory of the Czech Republic—ISPROFIN”.

References

- Alexandrowicz SW (1993) Late Quaternary landslides at eastern periphery of the National Park of the Pieniny Mountains, Carpathians, Poland. *Stud Geol Pol* 192:209–225
- Alexandrowicz SW, Alexandrowicz Z (1999) Recurrent Holocene landslides: a case study of the Krynica landslide in the Polish Carpathians. *The Holocene* 9:91–99
- Baroň I (2007) Results of radiocarbon dating of deep-seated landslides in the area of Vsetín and Frýdek-Místek districts. *Geologické výzkumy na Moravě a ve Slezsku* 14:10–12
- Baroň I, Cílek V, Krejčí O, Melichar R, Hubatka F (2004) Structure and dynamics of deep-seated slope failures in the Magura Flysch Nappe,

- Outer Western Carpathians (Czech Republic). *Nat Hazards Earth Syst Sci* 4:549–562
- Baroň I, Řehánek T, Vošmík J, Musel V, Kondrová L (2011) Report on a recent deep-seated landslide at Gírová Mt., Czech Republic, triggered by a heavy rainfall: the Gírová Mt., Outer West Carpathians; Czech Republic. *Landslides* 8:355–361
- Cruden DM, Varnes DJ (1996) Landslide types and processes. In: Turner AK, Shuster RL (eds) *Landslides: investigation and mitigation*. Transportation Research Board, Washington, DC, pp 36–75
- Kemeny J (2003) The time-dependent reduction of sliding cohesion due to rock bridges along discontinuities: a fracture mechanics approach. *Rock Mech Rock Eng* 36:27–38
- Magny M (2004) Holocene climate variability as reflected by mid-European lake-level fluctuations and its probable impact on prehistoric human settlements. *Quat Int* 113:65–79
- Margielewski W (1997) Dated landslides of the Jaworzyna Krynicka Range (Outer Carpathians) and their relation to climatic phases of the Holocene. *Ann Soc Geol Pol* 67:83–92
- Margielewski W (1998) Landslide phases in the Polish Outer Carpathians, and their relation to climatic changes in the Late Glacial and the Holocene. *Quatern Stud Pol* 15:37–53
- Margielewski W (2001) Late Glacial and Holocene climatic changes registered in forms and deposits of the Klakłowo landslide (Beskid Średni Range, Outer Carpathians). *Studia Geomorphologica Carpatho-Balcanica* 35:63–79
- Margielewski W (2003) Late Glacial-Holocene palaeoenvironmental changes in the Western Carpathians: case studies of landslide forms and deposits. *Folia Quaternaria* 74:1–96
- Margielewski W (2006a) Records of the Late Glacial–Holocene palaeoenvironmental changes in landslide forms and deposits of the Beskid Makowski and Beskid Wyspowy Mts. Area (Polish Outer Carpathians). *Folia Quaternaria* 76:1–149
- Margielewski W (2006b) Structural control and types of movements of rock mass in anisotropic rocks: case studies in the Polish Flysch Carpathians. *Geomorphology* 77:47–68
- Margielewski W, Kovalyukh NN (2003) Neoholocene climatic changes recorded in landslide's peat bog on Mount Ćwilin (Beskid Wyspowy Range, Outer Carpathians). *Studia Geomorphologica Carpatho-Balcanica* 37:59–76
- Margielewski W, Krąpiec M, Valde-Nowak P, Zernitskaya V (2010) A Neolithic yew bow in the Polish Carpathians: evidence of the impact of human activity on mountainous palaeoenvironment from the Kamiennik landslide peat bog. *Catena* 80:141–153
- Margielewski W, Kołaczek P, Michczyński A, Obidowicz A, Pazdur A (2011) Record of the meso- and neoholocene palaeoenvironmental changes in the Jesionowa landslide peat bog (Beskid Sądecki Mts. Polish Outer Carpathians). *Geochronometria* 38:138–154
- Niggemann S, Mangini A, Mudelsee M, Richter DK, Wurth G (2003) Sub-Milankovitch climatic cycles in Holocene stalagmites from Sauerland, Germany. *Earth Planet Sci Lett* 216:539–547
- Pánek T, Smolková V, Hradecký J, Šilhán K (2009a) Late Holocene evolution of landslides in the frontal part of the Magura Nappe: Hlavatá Ridge, Moravian-Silesian Beskids (Czech Republic). *Moravian Geogr Rep* 17:2–11
- Pánek T, Hradecký J, Minár J, Hungr O, Dušek R (2009b) Late Holocene catastrophic slope collapse affected by deep-seated gravitational deformation in flysch: Ropice Mountain, Czech Republic. *Geomorphology* 103:414–429
- Pánek T, Hradecký J, Smolková V, Šilhán K, Minár J, Zernitskaya V (2010) The largest prehistoric landslide in northwestern Slovakia: chronological constraints of the Kykula flow-like landslide and related dammed lakes. *Geomorphology* 120:233–247
- Pánek T, Šilhán K, Tábořík P, Hradecký J, Smolková V, Lenart J, Brázdil R, Kašičková L, Pazdur A (2011) Catastrophic slope failure and its origins: case of the May 2010 Gírová Mountain flow-like rockslide (Czech Republic). *Geomorphology* 130:352–364
- Pánek T, Smolková V, Hradecký J, Baroň I, Šilhán K (2013) Holocene reactivations of catastrophic complex flow-like landslides in the Flysch Carpathians (Czech Republic/Slovakia). *Quat Res* 80:33–46
- Starkel L, Soja R, Michczyńska DJ (2006) Past hydrological events reflected in Holocene history of Polish rivers. *Catena* 66:24–33



Antecedent Precipitation as a Potential Proxy for Landslide Incidence in South West United Kingdom

Catherine Pennington, Tom Dijkstra, Murray Lark, Claire Dashwood, Anna Harrison, and Katy Freeborough

Abstract

This paper considers the effects of antecedent precipitation on landslide incidence in the United Kingdom. During 2012–2013 an extraordinary amount of precipitation resulted in an increase in the number of landslides reported in the UK, highlighting the importance of hydrogeological triggering. Slope failures (landslides on engineered slopes) in particular caused widespread disruption to transport services and damage to property. SW England and S Wales were most affected. Easy-to-use and accessible indicators of potential landslide activity are required for planning, preparedness and response and therefore analyses have been carried out to determine whether antecedent effective precipitation can be used as a proxy for landslide incidence. It is shown that for all landslides long-term antecedent precipitation provides an important preparatory factor and that relatively small landslides, such as slope failures, occur within a short period of time following subsequent heavy precipitation. Deep-seated, rotational landslides have a longer response time, as their pathway to instability follows a much more complex hydrogeological response. Statistical analyses of the British Geological Survey landslide database and of weather records have enabled determination of the probability of at least one landslide occurring based on antecedent precipitation signals for SW England and S Wales. This ongoing research is of part of a suite of analyses to provide tools to identify the likelihood of regional landslide occurrence in the United Kingdom.

Keywords

Antecedent • Rainfall • Regional • National • Landslide • Slope failure • UK

Introduction

Large parts of the United Kingdom (UK) experienced several months of above-average precipitation from April to December 2012, making it one of the wettest periods of time for the country since meteorological records began. Throughout this period and into early 2013, a marked increase in the number of landslides was widely reported

and captured in the National Landslide Database (NLD) of the British Geological Survey (BGS) (Figs. 1 and 2; Pennington and Harrison 2013). Tragically, four people were killed and at least six people were injured. The dominant type of reported landslide is slope failure, often a relatively small landslide occurring on engineered slopes and capable of disrupting transport services and causing damage to property, infrastructure and businesses. While these slope failures are, by far, the most frequent landslide type in the data, their impacts therefore tend to be minor and remediated within a few days. This is in contrast to less frequently reported larger landslides on natural slopes that take many more resources and time to remediate.

C. Pennington (✉) • T. Dijkstra • M. Lark • C. Dashwood •
A. Harrison • K. Freeborough
British Geological Survey, Kingsley Dunham Centre, Nicker Hill,
Keyworth, Nottinghamshire NG12 5GG, UK
e-mail: cpoulton@bgs.ac.uk

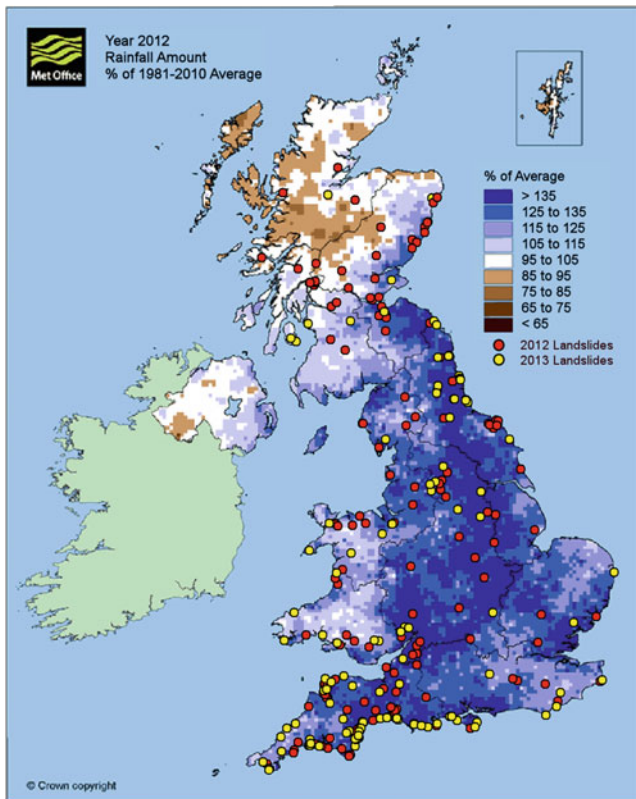


Fig. 1 Landslides reported in Great Britain in 2012 (red) and Jan–Jul 2013 (yellow) and the precipitation amount as a percentage of the long-term average (source: MetOffice)

Landscapes evolve over time, continuously adjusting to achieve equilibrium conditions of stability and responding to influences in a highly complex system; active slope instability is a highly visible outcome of this process (Dijkstra and Dixon 2010). Precipitation provides a spatially distributed trigger mechanism capable of driving these adjustments and the ability to quantify relevant thresholds is of great practical value in enhancing the planning, preparedness and response modes to these disrupting phenomena. Its potential use has been demonstrated around the world on the site- and catchment-specific scales through the long-term instrumentation and monitoring of slopes (e.g. Baum and Godt 2009; Crozier 1999; Minder et al. 2009; Prokešová et al. 2013; Rutter and Green 2011). Regional thresholds defined for areas with similar meteorological, climatic, physiographic and soil characteristics are potentially suited for landslide warning systems based on quantitative spatial precipitation forecasts, estimates, or measurements (Guzzetti et al. 2008). These thresholds are dependent on a range of reliable data gathered systematically over a long period of time, e.g. reporting research on UK field study sites including the Mam Tor landslide, Derbyshire (Dixon and Brook 2007; Rutter and Green 2011) and BGS-managed field sites of natural slopes at Hollin Hill and Aldbrough in Yorkshire

(Gunn et al. 2013; Chambers et al. 2010) and engineered slopes such as the Victorian railway embankment at East Leake (Gunn et al. 2011).

This paper discusses preliminary investigations into the empirical relationship between landslide occurrence and antecedent precipitation in the meteorological region of SW England and S Wales. The paper focuses on the period from January 2006 to July 2013, with special attention to the peak in reported landslide events during a very wet period from November 2012 to January 2013 (Fig. 2). It identifies antecedent precipitation as a potential proxy to communicate the likelihood of landslide incidence through, for example, the Natural Hazards Partnership (NHP) where the BGS issues a daily landslide hazard warning using a traffic-light^{plus} system (green, yellow, amber, red) (British Geological Survey 2013).

British Geological Survey National Landslide Database (UK)

The Landslides Team at the British Geological Survey (BGS) catalogue landslide information in the National Landslide Database NLD. It is used for a wide range of applications including their national landslide susceptibility map GeoSure (e.g. Booth et al. 2010; Foster et al. 2011; Pennington et al. 2009). The BGS National Landslide Database is the most comprehensive source of information on landslides in Great Britain and currently holds records of over 17,000 landslide events that are continually updated and added to as information is reported (Foster et al. 2012). Each of the landslide event records can hold information on over 35 attributes including location, dimensions, landslide type, trigger mechanism, damage caused, slope aspect, material, movement date, vegetation, hydrogeology, age, development and a full bibliographic reference. The information within the database is corporately maintained and held in a digital format that can be adapted and updated. For information on the history of the National Landslide Database see Foster et al. (2012).

Information Sources

As well as routinely collecting data from ongoing regional geological surveys (e.g. Evans et al. 2013) and the published scientific literature, the online press has been monitored for information about landslides through various Internet search engines since 2006.

In August 2012, social media were incorporated into this search. Twitter, a popular micro-blogging tool where real-time observations are published to the web, has proved to be the most prolific source of information, as it has for

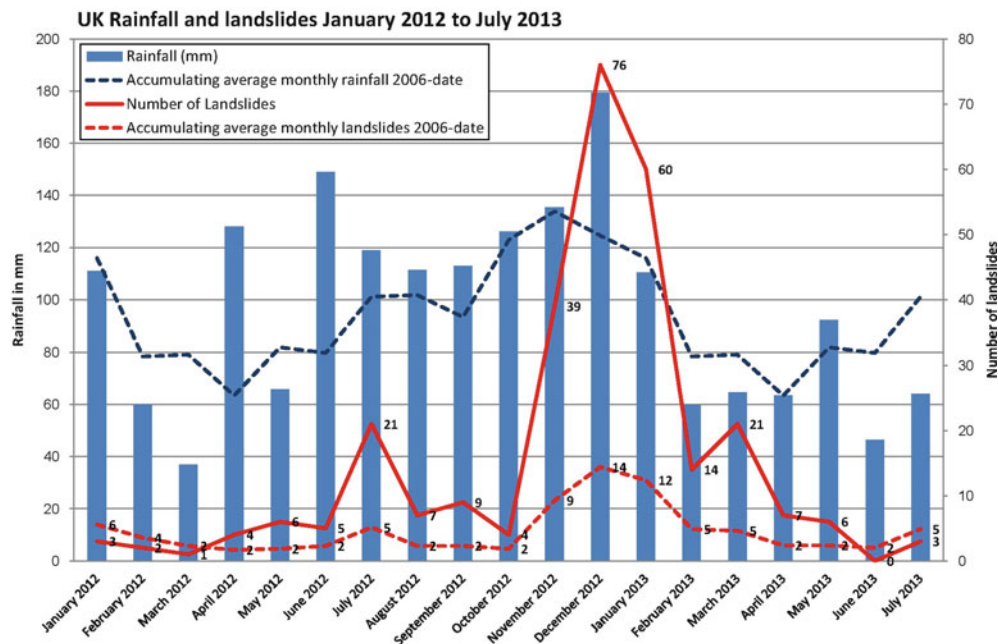


Fig. 2 Precipitation (source. MetOffice) and landslide incidence (source. BGS) in the UK from January 2012 to July 2013

other geohazards such as earthquakes and tsunamis (e.g. Earle et al. 2011; Doan et al. 2012; Stollberg and de Groeve 2012). This instantaneous reporting ('tweeting') mainly is a response to events that have an immediate impact on society such as travel disruption and it has resulted in small slope failures being captured in the National Landslide Database. Previously, these small events would not be as visible in the regional and national media and would thus have a much lower likelihood of being recorded in the National Landslide Database.

Antecedent Precipitation and Landslide Incidence

SW England and S Wales were most affected by excessive precipitation and reported landslides (Figs. 1 and 3). SW England has a number of areas of concentrated landsliding, mainly associated with outcrops of Jurassic or Cretaceous formations such as the East Devon Upper Greensand upland slopes which have undergone large-scale landsliding and the West Dorset Jurassic clays. The more stable slopes in the west underlain by Carboniferous and Devonian rocks are less likely to fail, but there are a number of shallow planar failures in this region, mainly associated with changes in ground water and failure occurring within a drape of superficial materials. Particularly active areas of coastal landsliding can be found along the south coast from Lyme Bay to Poole Bay, as well as the Devonian cliffs of north and south Devon. The valleys of the South Wales Coalfield

have a long history of landslide activity, mostly associated with the Carboniferous Coal Measures, which has led to damage to residential and industrial property and the disruption of roads and services in a populous industrialised area (Conway et al. 1980).

To achieve an insight into the significance of antecedent precipitation for the triggering of landslides a number of analyses have been performed on the landslide dataset for SW England and S Wales. One set of analyses was performed using information from the very wet period from 01/11/2012 until 31/01/2013 when landslides were in the news frequently. Data captured over a longer period, March 2006 until August 2013, was used to evaluate long-term antecedent signals in the triggering of landslides. A large proportion of these landslides (43 %) took place on man-made slopes such as road and railway embankments and cuttings. These slope failures are usually small-scale slumps or flows. Reported observations have shown that these are generally triggered by heavy precipitation and occur within a short period of time after prolonged heavy rain.

Winter 2012/2013 Antecedent Precipitation Signal

The short period from November 2012 until January 2013 fell at the end of a very wet summer and autumn and a continuous period of above-average precipitation, which resulted in further incidents of unstable slopes (Fig. 2).

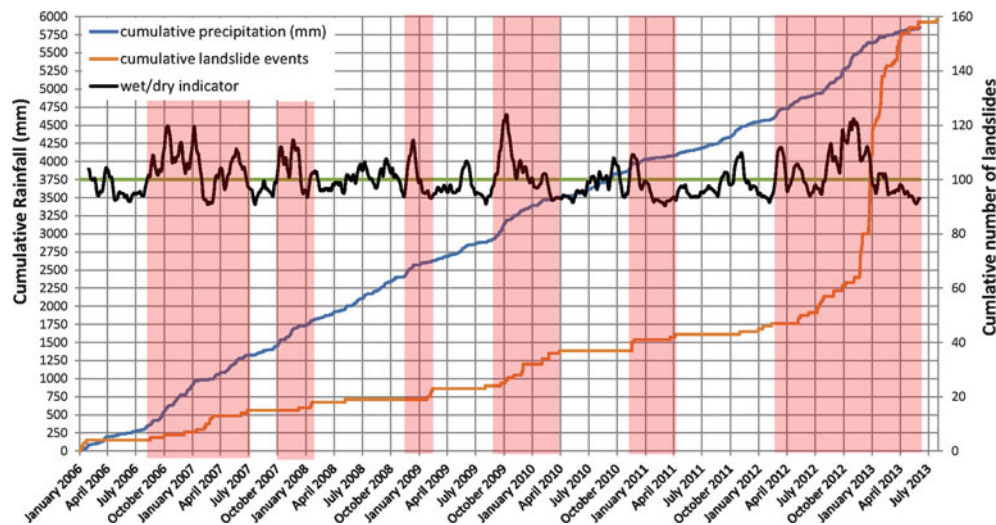


Fig. 3 Landslides and precipitation correlation (*pink*) in SW England/S Wales highlighted using a wet/dry indicator (proportional difference between actual and long-term average precipitation where 100 represents

equality and values >100 show actual conditions wetter than the long-term average). (Landslide information from BGS National Landslide Database; weather data from MetOffice and Wunderground.com)

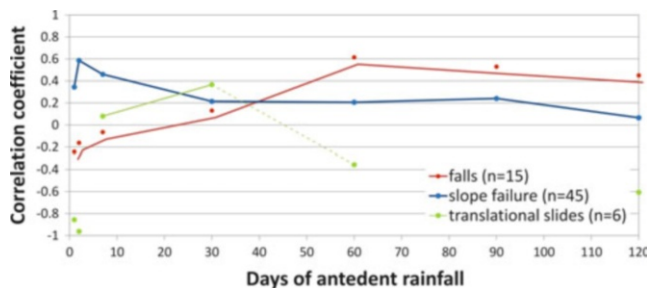


Fig. 4 Correlation coefficients for antecedent precipitation and landslide type for events between 01/11/2012 and 03/01/2013 in SW England and S Wales

Low temperatures and frequent precipitation justified the use of unadjusted ‘total’ precipitation to analyse landslide response to antecedent precipitation. For three types of landslides (falls, slope failures and translational slides) a series of correlation coefficients were determined relating landslide type to antecedent precipitation period (1, 2, 7, 30, 60, 90 and 120 days; Fig. 4). Slope failures correlate most closely with short duration antecedent precipitation (1, 2 and 7 days), followed by translational slides (7 and 30 days) and then falls (60 days). However, the outcomes are not very robust, as the number of observations is low. The observations do enable investigation of the antecedent precipitation signal and this, in turn, can be used to increase our understanding of the types of triggering precipitation over longer time periods. The antecedent precipitation signature required to trigger landslides was analysed against the number of observations per day (Fig. 5). The majority of events involved single events per day, but there were several days where a larger number of landslides were reported.

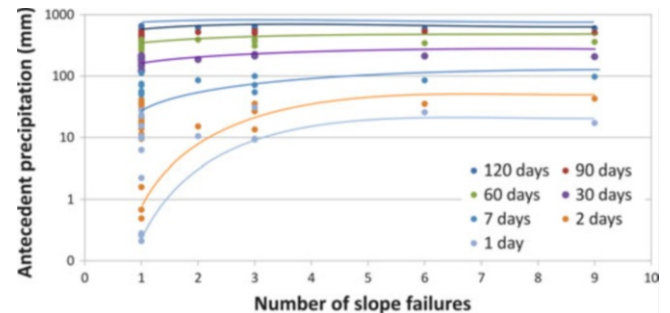


Fig. 5 Antecedent precipitation and number of slope failures per day. At six and nine events per day the antecedent precipitation signal appears more consistent

In Fig. 5 lines are drawn linking the lowest recorded antecedent precipitation signals. It appears that when six or more landslides are recorded per day in the study region, a steady signal becomes more apparent, as a spatially distributed trigger mechanism is required to drive these larger numbers of failures. Clearly, when fewer landslides occur per day the spatial relevance of the triggering mechanism diminishes and specific local conditions start to overshadow the antecedent precipitation signal. To inform the threshold model of how much precipitation is required to result in widespread unstable slopes, the antecedent precipitation sequence of the nine landslides per day event has been selected (Fig. 6). The antecedent signal clearly follows two trends—a steep section of conditions up to 7-days and a long-term, less intense accumulation from 7 to 90-days. This may suggest that a long period of precipitation is required to prepare the landscape for instability and that a final period of more intense precipitation is necessary to

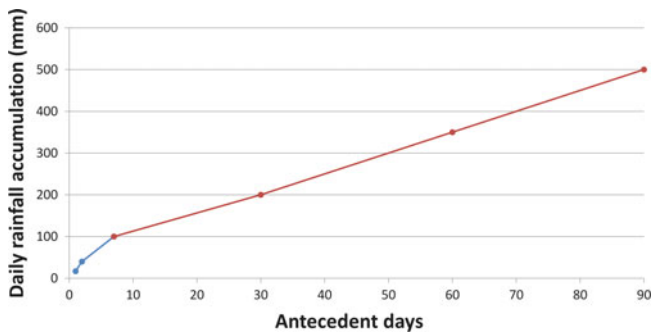


Fig. 6 Antecedent precipitation 'winter' threshold envelope for slope failure for SW England and S Wales. Event sequences plotting above the lines represent 'wetter than usual' conditions that can lead to multiple landslides

trigger landslides as has been clearly articulated by others in the UK context (e.g. Dixon and Brook 2007; Collison et al. 2000; Dijkstra and Dixon 2010).

It appears that the trends of Fig. 6 fit very well with the long-term average antecedent conditions. Further investigation of multiple events triggered per day during the same period of the year show that all fall on, or slightly above this trend. The trends could therefore be interpreted as a threshold envelope where antecedent precipitation plotting above the envelope is a signature for conditions 'wetter than usual' that can lead to multiple landslide events, and that signatures plotting below this trend represent conditions 'drier than normal', which would not result in precipitation-triggered landslides.

To extend these observations to a longer time period (years, rather than months), it is necessary to estimate the proportion of total precipitation that can reach the ground surface once account has been taken of seasonal variations in evapotranspiration. This variation is quite considerable, and in summer months it will be rare if conditions persist that result in widespread slope instability. As discussed by Pennington and Harrison (2013) these conditions existed in 2012, leading to a record year for landsliding in Britain.

Probability of Landslide Occurrence

For the determination of a probability of landslide occurrence the database from 01/01/2006 until 31/07/2013 (2,710 records) was used. For each date, information was available on numbers of landslides and seasonally adjusted antecedent effective precipitation for 1, 2, 7, 30, 60 and 90 days. A generalised linear model was fitted to the data for the prediction of landslide events from antecedent precipitation over 1, 2, 7, 30, 60 or 90 days. The model was fitted using the generalised linear model procedure in the MASS package for the R platform (Venables and Ripley 2002). A Poisson link function was used, after exploratory analysis

of a quasi-Poisson model. A subset of predictors was then selected using the stepAIC procedure in the MASS package, which uses stepwise backward predictor selection according to the Akaike Information Criterion. By this procedure the selected predictors for all landslides were antecedent precipitation over 1, 7 and 90 days. For slope failures/planar slides the selected predictors were antecedent precipitation over 1, 2, 7, 30 and 90 days. It must be noted that the records are affected by a perceived lower landslide capture success rate, particularly in the period before April 2012 (Pennington and Harrison 2013) and that this database contains zeros that do not always reliably indicate a non-occurrence of landslides, but rather that landslides were not recorded or reported. This is a reason for caution about interpretation of the fitted models. Nonetheless, these do provide evidence that long-term antecedent precipitation is an important factor in determining landslides occurrence. The fitted values of the generalised linear model are the expected number of landslides according to the model on any data. Treating this as the parameter of a Poisson variable, one may compute the probability of at least one landslide occurring for (a) the full landslides dataset and (b) slope failures and planar slides. These probabilities are plotted along with the observed number of landslides on each day (Fig. 7a) and a subset including only slope failures and planar slides (Fig. 7b).

It is evident from these analyses that single landslide occurrence per date does not correspond well with the probability distribution. When several landslides occur per date there is a much better correspondence. The probability distribution for slope failures and planar slides results in a lower temporal dispersion when compared to the undifferentiated landslides probability distribution, suggesting a possible way forward for fine-tuning an antecedent precipitation signal dependent upon landslide type. Further analyses of longer periods are currently being investigated. Some landslide events appear not to be represented by an elevated probability of occurrence (e.g. 12/2010)—this may be caused by local triggering precipitation not represented by the regional record used. Once a general model is better established, routes towards local differentiation and greater spatial relevance will be evaluated.

For a regional model intending to provide indicators of changes in the susceptibility of a landscape to generate landslides, this approach appears adequate. It provides a mechanism that can be tested against the 'expert-based' landslide hazard assessments that are carried out on a daily basis for the Natural Hazards Partnership (NHP). In the current situation, antecedent conditions are included in the reasoning to determine a regionally specific landslide hazard warning (following the traffic-light^{plus} communication, discussed above). The statistical model will now run alongside this assessment to test its performance and evaluate its potential as an objective method of determining landslide

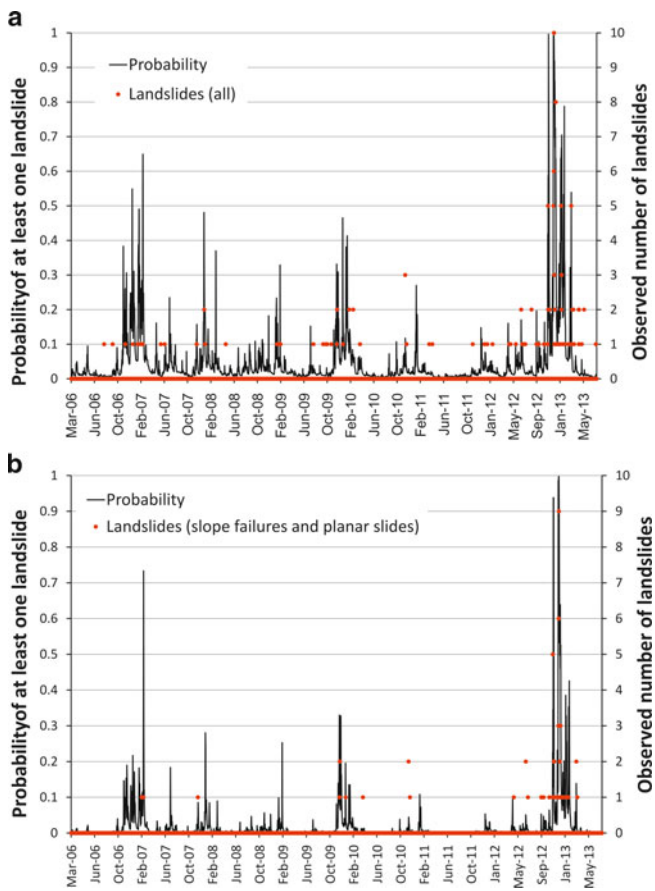


Fig. 7 The probability of at least one occurrence of any type of landslide (a) and slope failures/planar slides (b) on a given date taking into account antecedent precipitation conditions

hazard warning status. This approach is part of a suite of tools in development at the BGS that includes developing the use of models that analyse temporal fluctuations in soil moisture and groundwater levels in the landscape veneer on a more detailed, slope-specific scale.

Conclusions

The weather information is based on generalised regional precipitation data. Finer spatial resolutions will enable determination of antecedent precipitation patterns of greater relevance to individual landslide occurrences. Conversion factors for the determination of effective precipitation provide an initial approximation of the amount of water reaching the top of the soil column. Further work is progressing using water balance models to determine how much water is available to affect effective stress changes at critical depths. Without exception, all the landslides reported in 2012–2013 have been described in the media and social media because they have had an impact on society such as road diversions, rail delays, homes being demolished or the closure of coastal footpaths. While these are valid reports, the

following scenarios must be considered to fully appraise the rise in landslides over the winter of 2012/2013 period:

- The data represent an accurate picture of the true number of landslides occurring;
- The data are artificially high due to a heightened awareness of landslides through added media attention following four fatalities in SW England by three separate landslide events in 2012–2013;
- The data give a false impression of more landslides occurring when there were just fewer reported prior to August 2012 due to the timing of the inclusion of social media information sources, also coincident with the rise in precipitation and landslide reports;
- The data under-report the true number of landslides occurring as the social impacts were insufficient to warrant reporting. This may be especially true for those larger and older landslides which may have started to reactivate but have no immediate impact for the public.

Once the reliability of these models has been evaluated they provide an opportunity to forecast changes in landscape instability based on weather forecasts and an analysis of the results in the context of long-term forecasted changes in weather event sequences, such as those derived from UKCP09.

Acknowledgments The authors would like to thank BGS staff: H Reeves, V Banks, H Jordan, D Boon, P Hobbs, M Kirkham & G Jenkins; the Met Office. The authors publish with the permission of the Executive Director of the BGS (NERC).

References

- Baum RL, Godt JW (2009) Early warning of rainfall-induced shallow landslides and debris flows in the USA. *Landslides* 7:259–272
- Booth KA, Diaz Doce D, Harrison M, Wildman G (2010) User guide for the British Geological Survey GeoSure dataset. BGS Open Report OR/10/066
- British Geological Survey (2013) Natural hazards partnership. British Geological Survey, Nottingham. <http://bgs.ac.uk/research/naturalHazardsPartnership.html>
- Chambers JE, Hobbs P, Pennington CVL, Jones L, Dixon N, Spriggs M, Haslam E, Meldrum P, Foster C, Jenkins G (2010) Integrated LiDAR, geophysical and geotechnical monitoring of an active inland landslide. *EGU* 12:5244
- Collison A, Wade S, Griffiths J, Dehn M (2000) Modelling the impact of predicted climate change on landslide frequency and magnitude in SE England. *Eng Geol* 55(3):205–218
- Conway BW, Forster A, Northmore KJ, Barclay WJ (1980) South Wales Coalfield landslip survey. Institute of Geological Sciences, Special Surveys Division Engineering Geology Unit, Report EG 80/4
- Crozier M (1999) Prediction of rainfall-triggered landslides: a test of the antecedent water status model. *Earth Surf Process Landf* 24:825–833
- Dijkstra TA, Dixon N (2010) Climate change and slope stability in the UK: challenges and approaches. *Q J Eng Geol Hydrogeol* 43(4):371–385

- Dixon N, Brook E (2007) Impact of predicted climate change on landslide reactivation: case study of Mam Tor, UK in *Landslides*. *J Int Consort Landslides* 4(2):137–147
- Doan S, Vo B-K H, Collier N (2012) An analysis of Twitter messages in the 2011 Tohoku Earthquake. *Soc Inform Telecommun Eng* 91:58–66
- Earle PS, Bowden DC, Guy M (2011) Twitter earthquake detection: earthquake monitoring in a social world. *Ann Geophys* 54(6):708–715
- Evans HM, Pennington CVL, Jordan C, Foster C (2013) Mapping a nation's landslides: a novel multi-stage methodology. *Landslide Sci Pract* 1:21–27
- Foster C, Harrison M, Reeves HJ (2011) Standards and methods of hazard assessment for mass-movements in Great Britain. *J Torrent Avalanche Landslide Rock Eng* 166:156–163
- Foster C, Pennington CVL, Culshaw MG, Lawrie K (2012) The national landslide database of Great Britain: development, evolution and applications. *Environ Earth Sci* 66(3):941–953
- Gunn DA, Chambers JE, Meldrum PI, Ogilvy RD, Wilkinson PB, Haslam E, Holyoake S, Wragg J (2011) Volumetric monitoring of dynamic moisture distribution in an aged railway embankment. In: 17th Near Surface 2011, Leicester, UK, 12–14 Sept 2011
- Gunn DA, Chambers JE, Hobbs PRN, Ford JR, Wilkinson PB, Jenkins GO, Merritt A (2013) Rapid observations to guide the design of systems for long-term monitoring of a complex landslide in the Upper Lias clays of North Yorkshire, UK. *Q J Eng Geol Hydrogeol* 46(3):323–336
- Guzzetti F, Peruccacci S, Rossi M, Stark CP (2008) The rainfall intensity–duration control of shallow landslides and debris flows: an update. *Landslides* 5:3–17
- Minder JR, Roe GH, Montgomery DR (2009) Spatial patterns of rainfall and shallow landslide susceptibility. *Water Resour Res* 45(4):W04419
- Pennington CVL, Harrison AM (2013) 2012 landslide year? *Geoscientist Geol Soc London* 23(5):10–15
- Pennington CVL, Foster C, Chambers J, Jenkins GO (2009) Landslide research at the British Geological Survey: capture, storage and interpretation on a national and site-specific scale. *Acta Geol Sin* 83(6):801–840
- Prokešová R, Medvedová A, Tábořík P, Snopková Z (2013) Towards hydrological triggering mechanisms of large deep-seated landslides. *Landslides* 10:239–254
- Rutter EH, Green S (2011) Quantifying creep behaviour of clay-bearing rocks below the critical stress state for rapid failure: Mam Tor landslide, Derbyshire, England. *J Geol Soc* 168:359–371
- Stollberg B, de Groeve T (2012) The use of social media within the global disaster alert and coordination system (GDACS). In: Proceedings of the 21st international conference companion on World Wide Web, pp 703–706
- Venables WN, Ripley BD (2002) *Modern applied statistics with S*, 4th edn. Springer, New York



Natural Hazards in the Cordillera Blanca of Peru During the Time of Global Climate Change

Vít Vilímeck, Jan Klimeš, Adam Emmer, and Jan Novotný

Abstract

The Cordillera Blanca (Ancash region, Peru) is the most heavily glacierized tropical range in the world. Due to the global climate change, the retreat and thinning of most of the glaciers has recently increased. Rapid geomorphic changes, especially direct and indirect slope movements, are closely connected with the changing environment. Glacier retreat also leads to the formation and development of all types of potentially hazardous glacial lakes. A sudden water release from a glacial lake irrespective of its cause is called a glacial lake outburst flood (GLOF). The hazard of GLOF is strongly connected with dynamic slope movements (ice- and rock-falls; landslides of steep moraine slopes). About 80 % of the GLOFs in the Cordillera Blanca since the end of the Little Ice Age were caused by dynamic slope movements into the lake. The released water has a high erosion and sediment transport potential and can easily transform into various types of flow movements (e.g. debris or mud flows). These are highly hazardous and significant landscaping processes, by which the high mountainous environment evolves. Using the DesInventar database for the period from 1971 to 2009, debris flows (locally known as aluvión) have been evaluated as the most frequent type of natural hazard in the Ancash region. Several valleys in the Cordillera Blanca are currently being studied, using flood modelling, geomorphological mapping and calculation of slope stability in moraines. Conditions leading to slope movements on moraines include not only moraine properties, such as grain size and sediment structure, but also water infiltration from adjacent slopes.

Keywords

Natural hazards • Slope movements • Climate change • Cordillera Blanca • Peru

V. Vilímeck (✉) • A. Emmer
Faculty of Science, Department of Physical Geography and
Geoecology, Charles University in Prague, Albertov 6, 128 43
Prague 2, Czech Republic
e-mail: vit.vilimeck@natur.cuni.cz; aemmer@seznam.cz

J. Klimeš
Institute of Rock Structure and Mechanics, Academy of Sciences
of the Czech Republic, V Holešovičkách 41, 182 09 Prague 8,
Czech Republic
e-mail: klimes@irms.cas.cz

J. Novotný
ARCADIS Geotechnika, Geologická 4, 152 00 Prague,
Czech Republic
e-mail: novotny@arcadisgt.cz

Introduction

The question whether climate changes could really lead to an increase in natural hazards in general is out of the scope of this paper, nevertheless we have to analyze the weather extremes and the way in which they influence natural hazards including landslides in the Cordillera Blanca (Ancash region). The whole Cordillera Blanca range has been influenced by natural hazards for a very long time. The most important reasons behind this are the orogenetic activity of the area and climate change.

High mountain glaciers and permafrost areas are one of the most sensitive indicators of global climate change

(e.g. Clague et al. 2012). Most of the glaciers respond by retreating and thinning and permafrost responds by its degradation (melting). This scenario can be seen also in the most heavily glacierized tropical range in the world—the Cordillera Blanca in the Ancash region of Peru (Georges 2004). Retreat of the glacier and permafrost degradation is closely tied with significant geomorphical and landscape changes (e.g. Evans and Clague 1994) including dynamic processes, which are characterised as natural hazards.

From the perspective of natural hazards the most important changes occur through the mass movements of great volumes of material. These are not only direct (e.g. ice-falls) and indirect slope movements (e.g. landslides on exposed moraines) in deglaciated areas, but also aluvións (debris flows) and a specific phenomenon called “glacial lake outburst flood” (GLOF) following sudden water release from any type of glacial lake irrespective of its cause. GLOF in the Cordillera Blanca is most frequently caused by dynamic slope movement into the lake and thanks to the high erosion and transport potential may easily transform into flow movement. As glacier retreat continues, leading to the formation and development of new potentially hazardous glacial lakes, new opportunities for GLOFs are provided and thus the overall threat is increased.

Data and Methods

Data

We analysed DesInventar data focusing on the period from 1971 to 2009 (DesInventar 2013). In the analysis that follows we consider natural hazards to be events caused by endogenous or exogenous processes that result in damage to the population (according to DesInventar—deaths, injuries, missing persons, evacuations, migrations) or damage to private or public property (according to DesInventar—destroyed and damaged human dwellings, industrial and agricultural buildings and equipment, or technical, transport and public infrastructure).

Various types of natural hazards are often compared in terms of their threat or frequency of recurrence. Such analyses are, among other things, influenced by the character and quality of the database used. The DesInventar database is homogenous and, thus, serves as a useful tool for describing the significance of landslides.

Repeated remotely sensed photos were used for identification of newly forming potentially hazardous glacial lakes and for an assessment of the dynamics of their evolution. Three sets of aerial photos (1948–1950, 1962–1963 and 1970) from the archive of Autoridad Nacional del Agua and three sets of satellite images (1970, 2003–2005 and

2011–2012) from Google Earth Digital Globe 2013 were used for this purpose.

Methods

To reveal the possible influence of climate change on natural hazards in the Cordillera Blanca we used the work by Vuille and Bradley (2000), who analyzed 268 stations from the period 1959–1998 in the central part of the Andes between 1° n.l. and 23° s.l.

Stability of the youngest terminal moraine slopes was evaluated using granulometric information about 33 disturbed soil samples originating from moraine slopes. Their shear strength was assessed using expert knowledge and the results of direct shear tests on similar materials (Bolton 1986; Simoni and Houlby 2006).

Results

Climate Change and Extreme Weather Conditions

The rate of warming in Central Andes calculated from the period 1959–1998 is on average 0.2 °C/10 years (Vuille and Bradley 2000). The value of warming decreases with increasing altitude—i.e. 0.16 °C at an altitude of between 4,000 and 5,000 m. The glacial retreat is significant in several valleys and leads to dynamic environmental changes and various types of natural hazards (e.g. Vilímek et al. 2005).

The warmest years in the period 1939–1998 were identified as being: 1941, 1944, 1953, 1957, 1969, 1972, 1983, 1987, 1991, and 1997/1998 (Vuille and Bradley 2000). The same years were identified as years with El Niño (with the exception of 1944 and 1969). The most important manifestations of El Niño (since the middle of the nineteenth century) were adopted from Kuroiwa (2004). All of the warmest years fit with the strongest El Niño conditions (extreme, very strong, strong). On the other hand there are some El Niño conditions (mean and feeble) which are not among the “warmest years”. Rather inexplicable are the 1960s when there was no El-Niño during the warmest year (1969) and several El Niño conditions (feeble and mean) during 1960, 1963 and 1964–1965 are not registered as warm years. The opposite situation La Niña manifests itself as a cold period.

The rate of hazards caused by El Niño on the overall number of hazards conditioned by extraordinary meteorological conditions is clear from Fig. 1 which shows an increased number of recorded natural hazards in the Ancash region in years with higher variance of sea surface

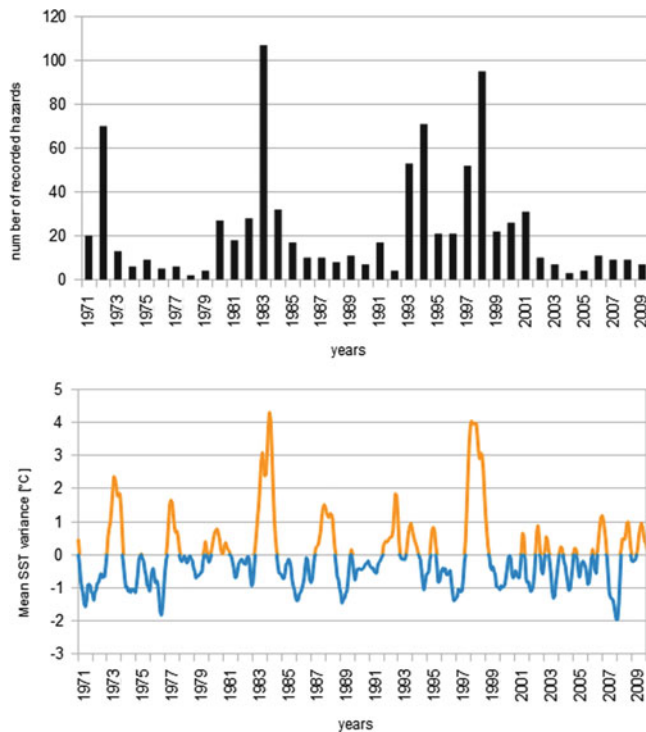


Fig. 1 Number of natural hazards in the Ancash region of Peru and ENSO phases represented by variance of sea surface temperature (SST). Data sources: DesInventar; CPC—NOAA (2011)

temperature (SST), which is commonly used for ENSO quantification. The most visible correlation is in the years 1983 and 1998.

There are no significant differences in total precipitation in the Cordillera Blanca from a longer perspective. There are only local changes at the level of the microclimate. From the 42 analyzed meteorological stations in the period 1950–1994 (Vuille et al. 2008) only five station revealed higher precipitation and two of them lower precipitation (both with a 95 % statistical level of significance).

Share of Slope Movements on Natural Hazards in the Cordillera Blanca

During the nearly 40-year period between January 1971 and December 2009, 914 natural hazards occurred in the Ancash region (Table 1), which translates to an average of two events per month.

During the analysed period, from 1971 to 2009, the most frequent type of natural hazard in the Ancash region was *aluvión* (a local term for debris flow). This was followed by flooding, extreme rainfall and landslides (see Table 1). Altogether, these phenomena represented almost 80 % of all naturally conditioned catastrophic events. If we combine the various forms of mass movement (*aluvións*, landslides)

Table 1 Frequency of natural hazard occurrence in the Ancash region during the period from 1971 to 2009 (prepared on the basis of DesInventar data, own calculations)

Type of natural hazard in the Ancash region	Absolute frequency	Relative frequency (%)
Slope movements	399	43.65
Aluvións	262	28.67
Landslides	107	11.71
Avalanches (snow avalanches and rockfalls)	30	3.28
Flood events	226	24.73
Floods	212	23.19
Flash floods	14	1.53
Earthquakes	31	3.39
Extreme meteorological events	120	13.13
Draught	31	3.39
Storms with dangerous associated phenomena	29	3.17
Extremely low temperatures	21	2.30
Strong wind (storm)	19	2.08
Hailstorms	12	1.31
Snowstorms	5	0.55
Extremely high temperatures	3	0.33
Extreme rainfall (torrential, long-lasting)	107	11.71
Strong swell (huge waves)	31	3.39
In total	914	100.00

they clearly comprise a dominant portion of natural hazards in the given region and during the given period (Vilímek et al. 2013). However, we should recognise the interconnection of various natural processes in the sense of a cause-effect relationship, wherein hydro-meteorological events or earthquakes could be the primary cause and different forms of mass movement are merely a subsequent effect.

Deglaciation, Lake Formation, Development and Threat of GLOFs

Significant deglaciation has been recorded in this region since the end of the Little Ice Age, whose second phase culminated here (according to lichenometry and ice-core dating) at the end of the nineteenth century (Thompson et al. 2000; Solomina et al. 2007). This intense deglaciation led to the formation and development of new, potentially dangerous glacial lakes mostly at elevations of above 4,600 m a.s.l. (Emmer et al. 2014) (Figs. 2 and 3).

The overall number of glacial lakes within the Cordillera Blanca is increasing rapidly with continuing deglaciation (Emmer and Vilímek 2013) and the question of its potential hazardousness is highly topical. It is thought that higher overall number of glacial lakes should naturally lead to the



Fig. 2 An example of a new unnamed rapidly growing bedrock-dammed lake in direct contact with the glacier beneath the Chopicalqui massif (6,354 m a.s.l.) at an elevation of 4,630 m a.s.l. (see also Fig. 3)

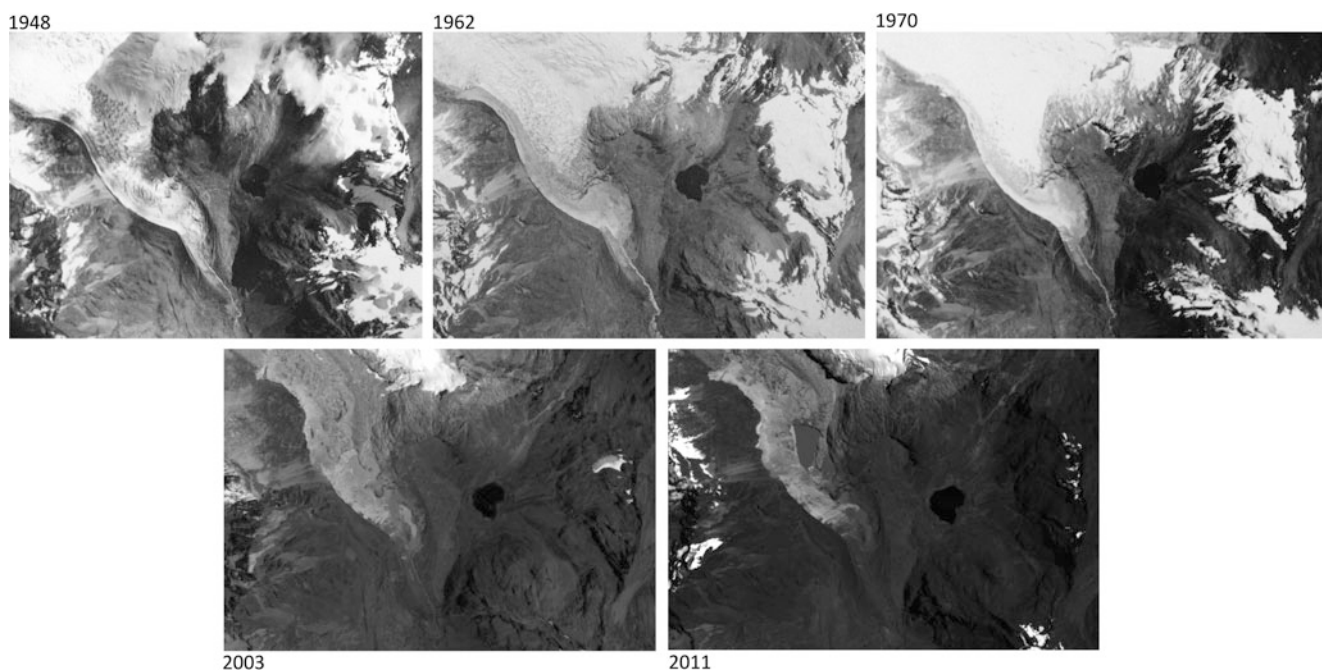


Fig. 3 Example of glacier retreat in the head of the Cancahua Valley, which leads into the Ulta Valley (Central Cordillera Blanca, Peru) between 1948 and 2011. The area shown covers approximately $2 \times 3 \text{ km}^2$. Note the formation and rapid evolution of a new bedrock-

dammed lake replacing the retreating terminus of the glacier tongue on the eastern side of the Chopicalqui massif (see also Fig. 2). Data sources: Archive of Autoridad Nacional del Agua, Huaráz, Peru; Google Earth Digital Globe 2013

higher number of GLOFs. This is confirmed by several GLOFs, which occurred in last decade within the study area of the Cordillera Blanca (Emmer et al. 2014). According to Costa and Schuster (1988), Clague and Evans (2000) and Richardson and Reynolds (2000), young glacial lakes are generally considered to be hazardous because: (1) they are often in direct contact with glaciers, exposed to the direct slope movements associated with deglaciation, such as ice-falls or ice avalanches, into the lake, followed by displacement wave

(s), which may overflow or rupture the lake dam; (2) their young dams (in the case of ice-dammed or moraine-dammed lakes) are not stable and thus they are prone to the spontaneous failure without any evident dynamic initializing event (so-called “dam self-destruction”; Yamada 1998); and (3) they are often rapidly growing; the surface area and related overall volume of accumulated water are increasing, thus there is a higher potential to cause significant damage in the case of a GLOF from the given lake.



Fig. 4 A steep lateral moraine surrounding Lake Palcacocha beneath the Pucaranra massif (6,156 m a.s.l.). A landslide of part of the lateral moraine into the lake caused a GLOF in Cojup Valley in 2003

There are a number of new glacial lakes within the Cordillera Blanca that meet some or all of the above mentioned criteria of preliminary hazard identification and thus represent a serious threat for the inhabitants of the valley areas. Identification and understanding of regional specifics is an important step in effective hazard assessment and therefore we established the GLOFs database. The preliminary results showed that about 80 % of the GLOFs from moraine-dammed lakes, which occurred within the region of Cordillera Blanca, were caused by both direct (45 %) and indirect (35 %) dynamic slope movements into the lake (Fig. 4). Other recorded causes were earthquakes and dam overtopping or rupture by the flood wave from a lake situated upstream (Emmer and Cochachin 2013). For a precise hazard assessment and subsequent implementation of the optimal mitigation measures, field study is still necessary, despite the contemporary progress in remotely-sensed data sources and GIS.

Stability of LIA Moraine Slopes

Slope movements from inner parts of moraines are one of the most important triggers of GLOFs (apart from rockfalls and icefalls). Therefore, the stability analysis of these slopes is of high importance.

The estimated peak strength of the analysed moraine material ranged from 40° to 48° depending on the considered stresses and assuming a constant volume friction angle of $\phi'_{cv} = 35^\circ\text{--}36^\circ$. Nevertheless, in many cases the moraine slopes (especially those facing the glacial lakes) maintain slope angles exceeding the peak strength friction angle by up to 20° for long periods of time. It is therefore clear that the temporal stability of these slopes is an additional factor for

increasing slope stability. Another factor is the internal structure of the moraines where large blocks can be found wedged into each another or slab-like blocks laid perpendicular to the potential failure surfaces. Further more secondary cementation was observed in some of the moraine sediments.

Discussion and Conclusions

Natural hazards in the Cordillera Blanca are closely connected with weather extremes irrespective of the cause—extreme precipitation during El Niño episodes or during ordinary rainy periods. Most of the events happened during El Niño periods. Nevertheless trends in precipitation changes are not convincing and if they are, they are site dependent. Both variant increase and decrease were identified. Climate change in the Central Andes is evident considering the increase in air temperatures. Warming occurs slightly less at higher altitudes compared to the foothill (on the Pacific Ocean side). The most important influence of climate change in the Cordillera Blanca is on deglaciation which is rather strong and well documented.

Deglaciation is connected with the formation of new lakes as well as with instability problems of young moraines. The main triggers of GLOFs are dynamic slope movements into the lakes, earthquakes and flood waves from lakes situated upstream. Therefore the GLOF phenomenon should be studied properly in future, because of its rising importance.

Despite several landslides from lateral moraines most of them have maintained slope angles exceeding the peak strength friction angle by up to 20° for decades. The internal structure of the moraines seems to be a very important factor for slope stability.

However, regarding the database statistics (from DesInventar) we must take into consideration the fact that truly extreme catastrophic events can, at least partially, distort the above statistics—e.g. the earthquake of May 31, 1970 which triggered hundreds of landslides in the Cordillera Blanca (Plafker et al. 1971). Five important El Niño episodes, which occurred in 1972/1973, 1982/1983, 1986/1987, 1991/1992 and 1997/1998, are the direct reason of nearly half (41 %) of the catastrophes caused by extreme weather in the given region and during the observed period. Therefore, monitoring a longer time series in the future should have an even greater informative value, as it will be possible to eliminate the impact of any one extreme event on the statistical average (like the strong earthquake of 1970).

Acknowledgments The authors would like to thank Marco L. Zapata, Alejo Cochachin and the staff of Autoridad Nacional del Agua (Huaráz, Peru) for their kind scientific and logistical support, and also projects from the Grant Agency of Czech Republic (P 209/11/1000)

and Grant Agency of Charles University (Project GAUK No. 70 413) which provided financial support.

References

- Bolton MD (1986) The strength and dilatancy of sands. *Geotechnique* 36:65–78
- Clague JJ, Evans SG (2000) A review of catastrophic drainage of moraine-dammed lakes in British Columbia. *Quat Sci Rev* 19: 1763–1783
- Clague JJ, Huggel C, Korup O, McGuire B (2012) Climate change and hazardous processes in high mountains. *Rev Asoc Geol Argent* 69(3):328–338
- Costa JE, Schuster RL (1988) The formation and failure of natural dams. *Geol Soc Am Bull* 100:1054–1068
- DesInventar (2013) Disasters inventory system, version 2011.056 online. <http://online.desinventar.org>. Last accessed 12 Sept 2013
- Emmer A, Cochachin A (2013) Causes and mechanisms of moraine-dammed lake failures in the Cordillera Blanca, North American Cordillera and Himalaya. *AUC Geogr* 48(2):5–15
- Emmer A, Vilímek V (2013) Review article: lake and breach hazard assessment for moraine-dammed lakes: an example from Cordillera Blanca (Peru). *Nat Hazards Earth Syst Sci* 13:1551–1565
- Emmer A, Vilímek V, Klimeš J, Cochachin A (2014) Glacier retreat, lakes development and associated natural hazards in Cordillera Blanca, Peru. In: Shan W et al (eds) *Landslides in cold regions in the context of climate change*. Springer, Switzerland. ISBN 978-3-319-00866-0
- Evans SG, Clague JJ (1994) Recent climatic change and catastrophic geomorphic processes in mountain environments. *Geomorphology* 10:107–128
- Georges C (2004) The 20th century glacier fluctuations in the tropical Cordillera Blanca, Peru. *Arctic Antarctic Alpine Res* 36:100–107
- Kuroiwa J (2004) Disaster reduction. living in harmony with nature. Quebecor World Peru S.A., Lima, 496 p. ISBN:9972-9999-0-4
- Plafker G, Ericksen GE, Concha JF (1971) Geological aspects of the May 31, 1970, Perú earthquake. *Bull Seismol Soc Am* 61:543–578
- Richardson SD, Reynolds JM (2000) An overview of glacial hazards in the Himalayas. *Quat Int* 65(66):31–47
- Simoni A, Houlby GT (2006) The direct shear strength and dilatancy of sand-gravel mixtures. *Geotech Geol Eng* 24:523–549
- Solomina O, Jomelli V, Kaser G, Ames A, Berger B, Pouyaud B (2007) Lichenometry in the Cordillera Blanca, Peru: “Little Ice Age” moraine chronology. *Glob Planet Chang* 59:225–235
- Thompson L, Mosley-Thompson E, Henderson K (2000) Ice-core paleoclimate records in tropical South America since the last glacial maximum. *J Quat Sci* 15:377–394
- Vilímek V, Zapata ML, Klimeš J, Patzelt Z, Santillán N (2005) Influence of glacial retreat on natural hazards of the Palcacocha Lake area. *Peru Landslides* 2:107–115
- Vilímek V, Hanzlík J, Sládek I, Šandová M, Santillán N (2013) The share of landslides in the occurrence of natural hazards and the significance of El Niño in the Cordillera Blanca and Cordillera Negra Mountains, Peru. In: Sassa K, Rouhban B, Briceno S, McSaveney M, He B (eds) *Landslides: global risk preparedness*. Springer, Heidelberg, 385 p. ISBN:978-3-642-22086-9
- Vuille M, Bradley RS (2000) Mean annual temperature trends and their vertical structure in the tropical Andes. *Geophys Res Lett* 27(23):3885–3888
- Vuille M, Francou B, Wagnon P, Juen I, Kaser G, Mark BG, Bradley RS (2008) Climate change and tropical Andean glaciers: past, present and future. *Earth Sci Rev* 89:79–96
- Yamada T (1998) Glacier Lake and its outburst flood in the Nepal Himalaya. Japanese Society of Snow and Ice, Tokyo, 96 p. ISSN:1344 – 1205



Land-Use Change and Shallow Landsliding: A Case History from the Apennine Mountains, Italy

Janusz Wasowski, Marina Dipalma Lagreca, and Caterina Lamanna

Abstract

We investigate temporal variations in land use and landsliding in a small catchment characterized by the predominance of clay-rich materials and known to be prone to shallow slope failures. The results demonstrate a pronounced change from land use dominated by grassland pasture (~53 % in 1955) to wheat-based agriculture (~74 % in 2011). The temporal series of landslide inventories also indicate significant variations in landslide activity in the same period. In particular, the highest susceptibility to landsliding has been registered in recent years on the sown fields which had initially (1955) been used for pasture and grazing. The data also reveal that with time the steeper and apparently more landslide-prone slopes with grassland-pasture have been given over to new wheat cultivation. The introduction of ploughing for the new wheat cultivation on the often steep slopes that had originally been covered by grass is considered to be a significant factor in the increased susceptibility to landsliding. The negative impact on slope stability can be related to the decrease in effective strengths of soil resulting from modification of the existing cover from grass that is present all year to wheat characterized by a few month growth period per year, which implies increase in groundwater levels, and mechanical disturbance of soil caused by tillage. Finally, for the studied period (1955–2011) the local precipitation data indicated high inter-annual variability without the presence of any statistically significant trends.

Keywords

Land use change • Wheat cultivation • Landslide activity • Apennines • Italy

Introduction

This work follows up our earlier studies on the relative impacts of land-use change and climate on landslide activity in the municipality of Rocchetta Sant'Antonio (the

Apennine Mountains) in the period 1976–2006 (Wasowski et al. 2007, 2010; Lamanna et al. 2009). Here, we focus on a small catchment (15.6 km²) and extend the observation period of land-use changes and variations in landslide activity by examining historical air photos from 1955 and recent (2011) orthophotos. Furthermore, with respect to the previous studies, the investigation of land-use change is more detailed, thanks to the inclusion of an additional class, i.e. grassland-pasture. For the entire period (1955–2011) precipitation data from a local weather station are also used to assess rainfall temporal variability and identify possible long-term trends.

The main objective of this work is to draw attention to anthropogenic pressures that can have considerable influence

J. Wasowski (✉) • C. Lamanna
CNR – IRPI, National Research Council, Institute of Geo-Hydrological Protection, Bari 70126, Italy
e-mail: j.wasowski@ba.irpi.cnr.it; cate.lama@tiscali.it

M.D. Lagreca
Department of Earth and Geo-Environmental Sciences, University of Bari, Bari 70125, Italy
e-mail: marina.dipalmalagreca@uniba.it

on local slope stability (e.g. DeGraff and Canuti 1988; Sidle and Ochiai 2006). By using the example of this study we argue that a detailed assessment of historical to recent land-use changes is needed to avoid potentially misleading interpretations and conclusions regarding impacts of climate change and variability on landslide activity.

Environmental Setting of the Study Area

General

The study catchment is in the southern part of the Apennine Mountains, often called the Daunia Apennines. The area studied is characterized by moderate relief topography, with elevations below 800 m above sea level and modest slope inclinations ($\sim 10^\circ$ on average).

Today the land use and vegetation cover is dominated by agricultural activity (mainly cereals). Grassland-pasture and trees are only locally significant. Barren land is very limited, corresponding to flysch, limestone and clay outcrops. Similarly, developed land (e.g. rural settlements, roads) accounts for a small portion of the territory.

The area is characterized by a Mediterranean sub-humid (sub-Apennine) climate, with annual rainfall values that show large variations, from about 400 to nearly 1,000 mm (Fig. 1). Fall and winter months have similar precipitation, which together on average accounts for about 60 % of the annual total. The winter season is relatively mild, with a modest amount of snow precipitation. Summers are typically dry and hot.

Geology

The geologic units cropping out in the study area belong to tectonically deformed flysch successions of Late Cretaceous-Miocene age. They can be divided into three main categories, each dominated by one specific lithology. These include: clays-clay shales (76.5 % of the overall area), sandstones (18 %) and limestones (5.5 %). The predominance of sheared, scaly clays (Fig. 2) with weak geotechnical properties (Φ'_r varying from 6.9° to 16.5°) and the presence of poorly drained slopes are considered the underlying causes of landsliding (Wasowski et al. 2010, 2012).

Landslides

The Daunia Apennines are well known for recurrent landslide problems (e.g. Zezza et al. 1994; Magliulo et al. 2008). In a study of the area (132 km^2) neighbouring to the north-west of the territory of Rocchetta Sant'Antonio, Mossa et al. (2005) reported a frequency of landslides exceeding 20 %.

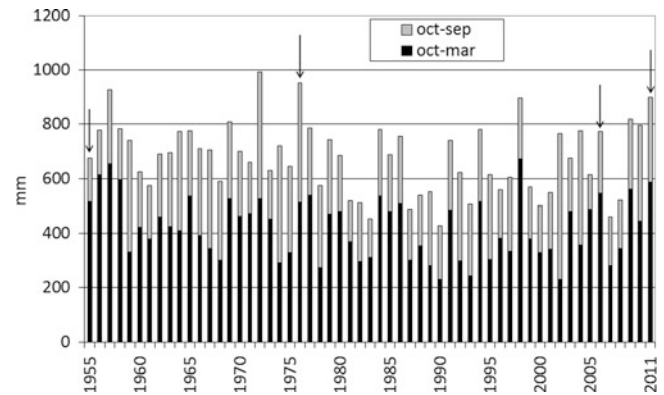


Fig. 1 Time series of hydrological year (October–September) and 6 month groundwater recharge period (October–March) precipitation registered in Rocchetta Sant'Antonio; note the large inter-annual variability. Arrows indicate the 4 years for which land use maps and landslide inventories were compiled

They also showed that the landslide frequency is the highest in the $10\text{--}15^\circ$ slope class, followed by the $5\text{--}10$ and $15\text{--}20$ slope classes.

For the municipal territory of Rocchetta Sant'Antonio (72 km^2), the landslide inventories compiled by Lamanna et al. (2009) revealed the impact of slope failures, with areal frequency of active landslides amounting to 2.0 % and 5.2 %, respectively in 1976 and 2006. Most of these landslides were relatively small, with resulting densities (number per km^2) ranging from about 6 (in 1976) to 34 (in 2006).

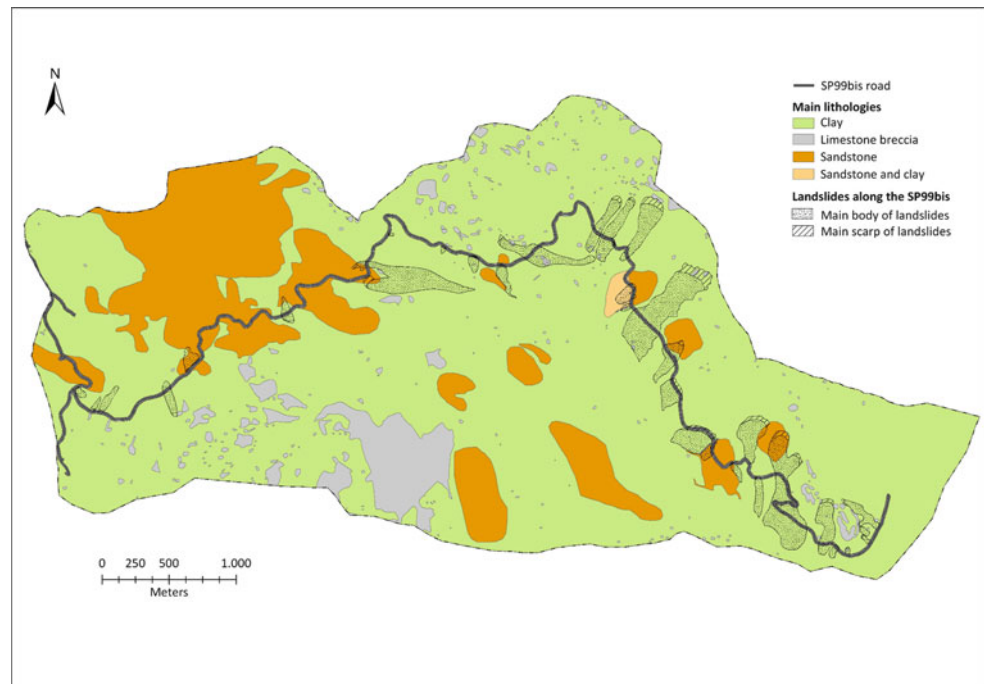
Subsequent studies within the municipality of Rocchetta Sant'Antonio focused on the 15.6 km^2 catchment traversed by SP99bis road. The road was damaged by series of landslides in the period 2003–2005 (Fig. 2) and this prompted detailed subsurface geotechnical investigation, as well as piezometer and inclinometer borehole monitoring. The outcomes of the investigation demonstrated the link between the presence of high piezometric levels in winter and early spring months and the occurrence of predominantly shallow slope failures (Wasowski et al. 2010, 2012).

Data and Methods

The information and datasets used in this work included:

- Topographic base map at 1:5,000 scale, from 2002, and the derived digital elevation model (DEM);
- Slope map obtained from the DEM;
- Inventory map of 30 landslides that damaged the road in the catchment in the period 2003–2005 (from Wasowski et al. 2010);
- Inventory maps of active landslides derived from 1976 black and white air photos (1:25,000 scale) and high resolution (1 m panchromatic) 2006 IKONOS-2 multispectral imagery (from Wasowski et al. 2010);

Fig. 2 Distribution of main lithologic units in the study area and locations of 30 landslides, mapped in 2005, which damaged different portions of the SP99bis road



- Inventory maps of active landslides derived from 1955 black and white air photos (1:33,000 scale) and 2011 multispectral orthophotos (0.5 m resolution);
- Land-use maps derived from the same 1976 air photos and 2006 orthophotos (updated after Wasowski et al. 2010);
- Land-use maps derived from the same 1955 air photos and 2011 orthophotos;
- Daily rainfall data (1955–2011) from the pluviometric station in Rocchetta Sant’Antonio.

This work also relied on frequent in situ inspections conducted in the study area since 2005. All the datasets were collated and analyzed using commercial Geographic Information Systems (GIS) and remote sensing software.

Landslide Inventories

To assess the differences between historical (1955, 1976) and recent (2006, 2011) landsliding, four temporally distinct landslide activity maps were considered. In this effort we closely followed our earlier work and the generally accepted landslide mapping criteria (cf. Wasowski et al. 2010).

In addition to the already available 1976 and 2006 datasets, a historical landslide inventory was obtained through a stereoscopic interpretation of 1955 air photos. Furthermore, a recent landslide inventory was produced from high resolution multispectral orthophotos acquired in late winter of 2011.

Land-Use Maps

To estimate the differences between historical (1955, 1976) and recent (2006, 2011) land use, four temporally distinct maps were compiled from the same air photos and multispectral imagery used for landslide mapping. Only two of them (for 1955 and 2011) are shown here (Fig. 3).

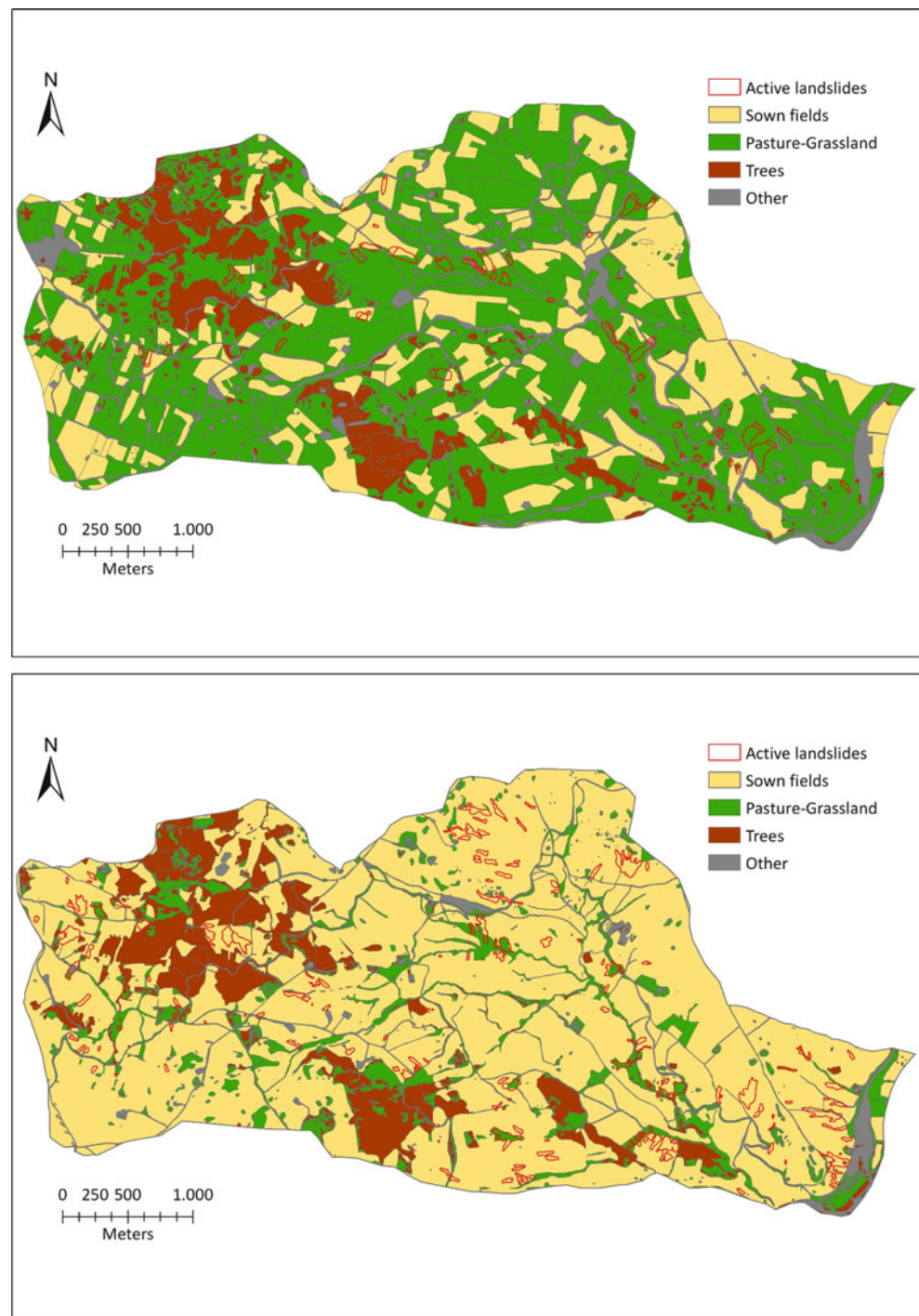
We followed the approach described in our earlier work (Wasowski et al. 2010, 2012). In particular, through image interpretation four major land-use classes were distinguished: (i) agricultural land (sown fields with mainly cereal cultivation); (ii) grassland-pasture; (iii) trees, including dense shrub; (iv) other (including uncultivated and barren land and man-made structures). We will show that these four classes of land cover and land use can have different impacts on the susceptibility of slopes to shallow landsliding.

Results

Variation in Landslide Activity

Table 1 shows a summary of landslide statistics for the four inventories: 1955, 1976, 2006 and 2011. The results, presented in terms of areal frequency of landslides (in percent of total land area) and their density (number per km²), reveal the presence of substantial variations over time.

Fig. 3 Land use and distribution of active landslides in 1955 (*upper*) and in 2011 (*lower*). A comparison of the two maps reveals pronounced change from grass-pasture land use to sown field-based agriculture. There are more active landslides in 2011 and they involve mainly the sown fields. See Fig. 4 for land-use statistics for 1955 and 2011, as well as for the intermediate years 1976 and 2006



In particular, there is an increase over time in areal frequency, from about 1.5 % in 1955 (2.49 % in 1976), to 5.6 % in 2006 (2.73 % in 2011). The lower frequency of landslides in 2011 could be in part due to the early acquisition date of the orthophotos with respect to the imagery used to produce the other three inventories (respectively before and after the spring seasons).

Historical and Recent Land Use Versus Landslide Activity

The land-use maps in Fig. 3 illustrate the changes that occurred between 1955 and 2011. Whereas in 1955 the major part of the land has been used as pasture and grass, by 2011 sown fields are predominant.

Table 1 Variation of landslide activity with time in terms of areal frequency (%) and density per km²

Year	Active landslides	
	Area (%)	Number (km ²)
1955	1.5	3.3
1976	2.5	6.3
2006	5.6	60.3
2011	2.7	12.7

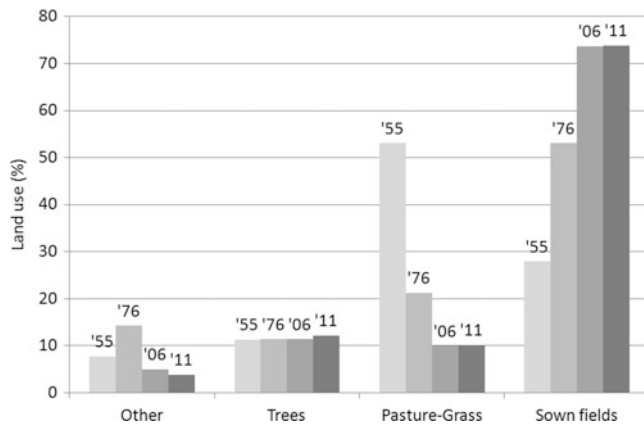


Fig. 4 Statistics of lands use in 1955, 1976, 2006 and 2011. Note the remarkable change from the grassland-pasture in 1955 (53 % of the total area) to agriculture with the predominance of the sown fields (74 %)

The temporal variations in land use are further detailed in Fig. 4 in terms of areal frequency of the four land-use classes: sown fields, grass-pasture, trees and other. This quantification reveals that the increase in sown fields from 28 % in 1955 to 74 % in 2011 originated from the concomitant reduction of the land used for pasture and grazing (from 53 % to 10 %).

Furthermore, already by 1976 the portion of the land used as sown fields had nearly doubled with respect to 1955, exceeding 50 %. During the entire period considered the remaining two land-use classes have undergone relatively minor changes (Fig. 4).

The influence of land-use changes on slope instability appears evident when considering the distributions of active landslides in 1955 and 2011 versus land cover in the same years (Fig. 3). The maps indicate that the portions of the grassland-pasture that have been changed to sown fields agriculture are today (2011) most prone to failure. This is consistent with the findings of Wasowski et al. (2010), who compared land use and landslide activity in 1976 and 2006.

Further details on the influence of land-use changes on slope instability, and in particular on the role of conversions to sown fields are presented in Fig. 5. It is shown that the areas with sown fields, which in 1955 had been used for pasture and grazing, today (2011) exhibit the highest frequency of active landslides (nearly 4 %). Indeed, before the conversion

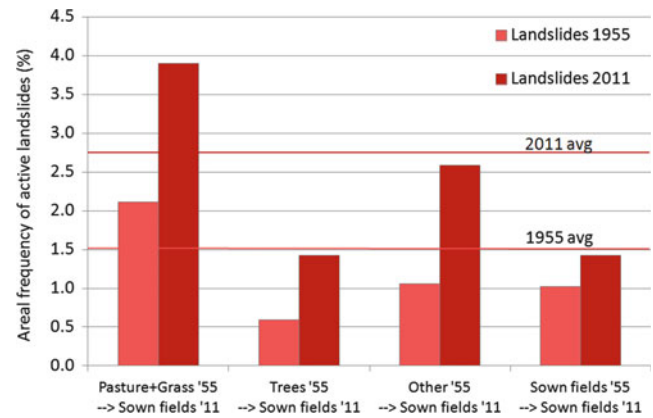


Fig. 5 Areal frequency of active landslides in 1955 and 2011 for fields that have already been sown in 1955 (“old” sown), and for the remaining three land-use classes (grass-pasture, trees and other) that have become sown after 1955. The two lines mark the average areal frequency of landslides in 1955 and 2011. At present (2011), the highest frequency to landsliding is observed on the sown fields which had initially (1955) been used for pasture and grazing

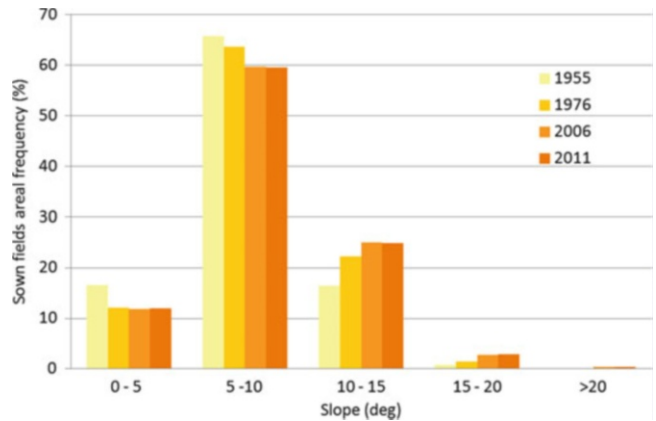


Fig. 6 Areal frequency of fields sown in 1955, 1976, 2006 and 2011 for different slope classes. Note the trend over time towards cultivation of steeper slopes

this land-use class had already been the most landslide-prone. Figure 5 also indicates that the conversion to sown fields resulted in an additional increase in susceptibility to slope failure.

The increased susceptibility to landsliding is further investigated by considering variations of slope inclinations of the sown fields. Figure 6 shows that during the entire period (1955–2011) the majority of the sown fields were within the same slope interval of 5–10°. Nevertheless, the data revealed also a clear trend towards the cultivation of steeper slopes. In particular, in the periods 1955–1976 and 1976–2006 the percentage of sown fields significantly increased for the slope classes 10–15° and 15–20°. It is likely that the expansion of cultivation onto steeper and presumably less stable slopes also contributed to the observed increases in frequency of active landslides.

Discussion and Conclusion

Even though the comparison of the historical (1955, 1976) and recent (2006, 2011) inventories demonstrated a significant increase over time in landslide activity in the investigated catchment, the data available for the same period from the local weather station did not reveal any clear temporal trends in precipitation. In fact, the climatic data indicated significant variations in the annual rainfall, which are even more marked if the October–March (groundwater recharge periods) are considered (Wasowski et al. 2010).

Instead, the recent increases in the frequency of active landsliding coincided with significant change in land use over time. In particular, the areal extent of sown fields (used mainly for wheat cultivation) grew from about 28 % (of the total catchment area) in 1955 to about 74 % in 2011. Furthermore, a comparative analysis of the land-use maps and landslide inventories demonstrated that the highest areal frequency of failures is recently being registered on the slopes which had initially been used for pasture and grazing. The negative impact of the conversion to wheat cultivation on slope stability can be related to the decrease in effective strengths of soil resulting from (i) modification of the existing cover from grass that is present all year to wheat characterized by a few month growth period per year, which implies increase in groundwater levels and (ii) mechanical disturbance of soil caused by tillage.

Acknowledgments We thank the Prefettura di Foggia, Rocchetta Sant'Antonio administration and Eng. G. Amoruso (Regione Puglia) for their support. This work benefited from the review by Jerome DeGraff.

References

- DeGraff JV, Canuti P (1988) Using isopleths mapping to evaluate landslide activity in relation to agricultural practices. *Bull Int Assoc Eng Geol* 38:61–71
- Lamanna C, Casarano D, Wasowski J (2009) Cambiamenti dell'uso del suolo e aumento dell'attività franosa nel territorio di Rocchetta Sant'Antonio (Appennino dauno) Il quaternario. *Ital J Quat Sci* 22 (2):139–156
- Magliulo P, Di Lisio A, Russo F, Zelano A (2008) Geomorphology and landslide susceptibility assessment using GIS and bivariate statistics: a case study in southern Italy. *Nat Hazards* 47:411–435
- Mossa S, Capolongo D, Pennetta L, Wasowski J (2005) A GIS-based assessment of landsliding in the Daunia Apennines, southern Italy. In: *Proceedings of the international conference "Mass movement hazard in various environments"* 20–21 October 2005, Cracow, Poland, pp 86–91
- Slide RC, Ochiai H, (2006), *Landslides: processes, prediction and land use*. American Geophysical Union, Water Resources Monograph 18
- Wasowski J, Casarano D, Lamanna C (2007) Is the current landslide activity in the Daunia region (Italy) controlled by climate or land use change? In: *Proceedings of the international conference on landslides and climate change*, Ventor, Isle of Wight, UK, 21–24 May 2007, pp 41–49
- Wasowski J, Lamanna C, Casarano D (2010) Influence of land-use change and precipitation patterns on landslide activity in the Daunia Apennines Italy. *Quart J Eng Geol Hydrogeol* 43: 1–17
- Wasowski J, Lamanna C, Gigante G, Casarano D (2012) High resolution satellite imagery analysis for inferring surface-subsurface water relationships in unstable slopes. *Remote Sens Environ* 124:135–148
- Zeza F, Merenda L, Bruno G, Crescenzi E, Iovine G (1994) Condizioni di instabilità e rischio da frana nei comuni dell'Appennino Dauno Pugliese. *Geologia Applicata e Idrogeologia* 29:77–141



Applicability of Relative Weights Derived for Nuwara Eliya and Badulla Regions to the Areas with Different Terrain and Climatological Characteristics

Kumari M. Weerasinghe, P.H.E. Dulanjalee, H.K.D.W.M.I.U.K. Hapuhinna, and Hasali Hemasinghe

Abstract

Landslides affect the life and economy of Sri Lanka frequently. The National Building Research Organisation (NBRO), Sri Lanka, has identified factors (i) bedrock geology, (ii) hydrology and drainage, (iii) surface overburden, (iv) slope angle range, (v) land use, and (vi) land forms as the major causative factors of Sri Lankan landslides. As these factors contribute in different degrees to initiate a landslide, they have been assigned subjective severity levels based on the characteristics of studied landslides.

The numerical evaluation system, presently used by NBRO to assess the overall landslide hazard of a given site, has been derived through studying 1,076 landslides in Nuwara Eliya and Badulla districts. As NBRO has extended its landslide hazard mapping programme into other districts, verification of the applicability of weights derived through Nuwara Eliya–Badulla study to the other districts with different terrain and climatological characteristics has become a timely requirement.

The researchers have selected the districts of Galle, Kalutara and Kegalle for this verification. Galle and Kalutara districts have gentler terrains than those in Nuwara Eliya and Kegalle which have similar rugged terrains. The Galle, Kalutara and Kegalle districts have higher soil moisture content than those in Nuwara Eliya and Badulla. The geology of all districts belong to the highland series, with differences in rock constituents and the structure. Similar to Nuwara Eliya, tea plantation is the major land use in Galle and Kegalle districts. The land use in Kalutara, is rapidly changing from rubber plantation to other commercial crops. All these regions have a recorded history of landsliding. These highlands are becoming rapidly populated and inappropriate land use practices also have contributed to the increasing frequency of landslides. Therefore, accurate mapping of landslide potential is essential for ensuring the safety of the people and to delineate the suitable land for development.

Keywords

Landslides • Hazard mapping • Causative factors • Relative weights

Introduction

Landslides and other forms of slope failures often affect the life, property and economy in the hilly and mountainous region of Sri Lanka. Water infiltration due to excessive or prolonged rainfall, weathering of bedrock and water intrusions through geologically weak strata are the most common natural conditions which influence the stability of

K.M. Weerasinghe (✉) • P.H.E. Dulanjalee • H.K.D.W.M.I.U.K. Hapuhinna • H. Hemasinghe
Landslide Research and Risk Management Division, National Building Research Organisation, 99/1, Jawatta Road, Colombo 005, Sri Lanka
e-mail: kmweera@yahoo.com; eranga.dulanjalee@yahoo.com; imalihapuhinna@gmail.com; hasali.hemasinghe@gmail.com

Sri Lankan landslides. Non-engineered slope modifications for construction and other development, removal of plant cover and root structure leading to excessive surface erosion, and construction of water retaining structures upstream of a slope are the man-induced conditions that frequently affect slope's natural equilibrium.

Several efforts have been taken by the experts to accurately map the distribution of severity in landslide potential in the central highlands in Sri Lanka and to develop guidelines and construction methods for appropriate land utilisation in that region. The outcomes of the landslide hazard zonation mapping programme (LHMP) implemented by the National Building Research Organisation (NBRO) in 1990 identifies the factors; bedrock geology, surface overburden, slope angle range, hydrology and drainage, land use, and land forms as the major causative factors of Sri Lankan landslides (NBRO 1995). Those factors contribute in different degrees to initiate landslides. Since the impacts of those identified factors are compounded (Bhandari and Weerasinghe 1996), the integration of their impacts to evaluate the overall landslide potential depends on reasonable and accurate appraisal of their independent contribution.

At present, NBRO applies numerical severity levels to interpret the relative contribution of causative factors (mapping attributes); however, NBRO's rating criteria consist a subjective severity levels as well (NBRO 1995).

Physical Characteristics of the Selected Study Areas

The researchers have selected three study areas within the districts of Nuwara Eliya, Galle, and Kegalle for this verification (Fig. 1). Nuwara Eliya is located in the center of the central highlands where the elevation ranges from 100 m to 2,524 m above MSL and carries the highest peaks and plateaus of several mountain ranges some of which having relief upto 700 m. A part of the southern border of the highlands are located in the Galle district where the elevation ranges from 100 m to 800 MSL. Kegalle district is located in the western part of the central highlands and the elevation of the mountainous areas in Kegalle ranges from 250 m to 1,800 m MSL. Both in Nuwara Eliya and Kegalle districts, the mountains are complex and corrugated, where as in Galle district, undulating to rolling hills and monadnock can be observed.

The geology of all districts belong to the highland series, with differences in rock constituents and the structure. Charnockitic Gneiss and Granulitic Gneiss are the predominant lithology observed in the study area of Nuwara Eliya. Charnockite is the most abundant rock type in the study area of the Kegalle district. The study area of the Galle district is mostly underlain by Charnokitic Gneiss and Khondalite (Fig. 2).



Fig. 1 Locations of selected study areas marked on a relief map of Sri Lanka (source: <http://www.ourlanka.com>)

The Galle, and Kegalle districts have higher soil moisture contents than those in Nuwara Eliya. Tea plantation and forest plantations are the major land use practiced in Nuwara Eliya with minor extents of sparsely used croplands, scrubs, and homesteads. Hilly terrains in Kegalle district are widely utilized for rubber plantations along with lower extents of mixed tree crops, and homesteads. The highlands in Galle district is mostly covered by Forests and scrublands. Mixed agroforestry homesteads, rubber plantations and terraced paddy cultivations are also present but are fewer in extent (Fig. 3). All these regions are becoming rapidly populated and inappropriate land management has also contributed to the increasing frequency of landslides.

The study areas commonly experience heavy rain during the monsoon period and the landslides recorded within these three districts are triggered by the high intensity rainfall.

Criteria for Relative Ranking of Mapping Attributes

For landslide hazard zonation mapping, the mapping attributes or the causative factors and the sub factor attributes within a factor need to be ranked or assigned

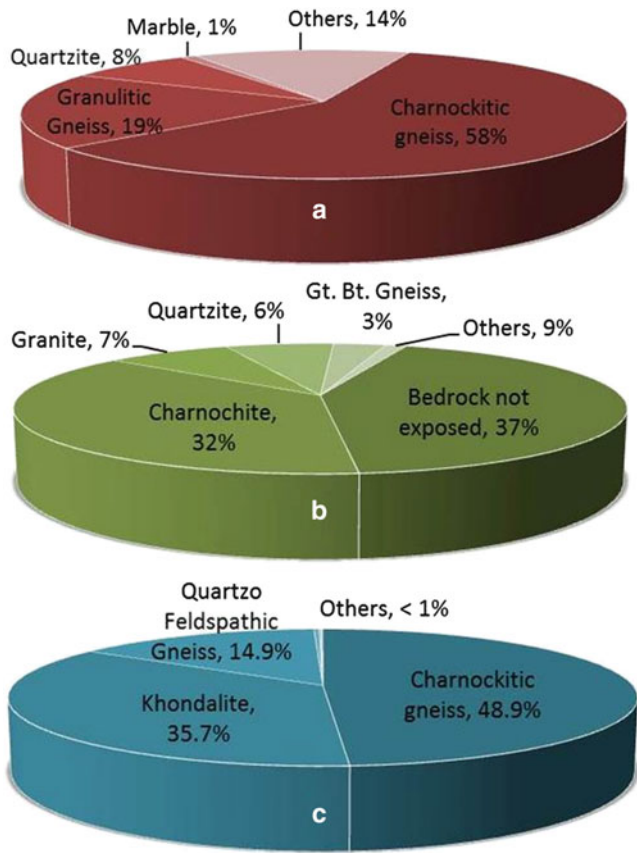


Fig. 2 Distribution of predominant rock types within (a) Nuwara Eliya (Wijewickrama et al. 1994), (b) Kegalle (Weerasinghe 2001) and (c) Galle

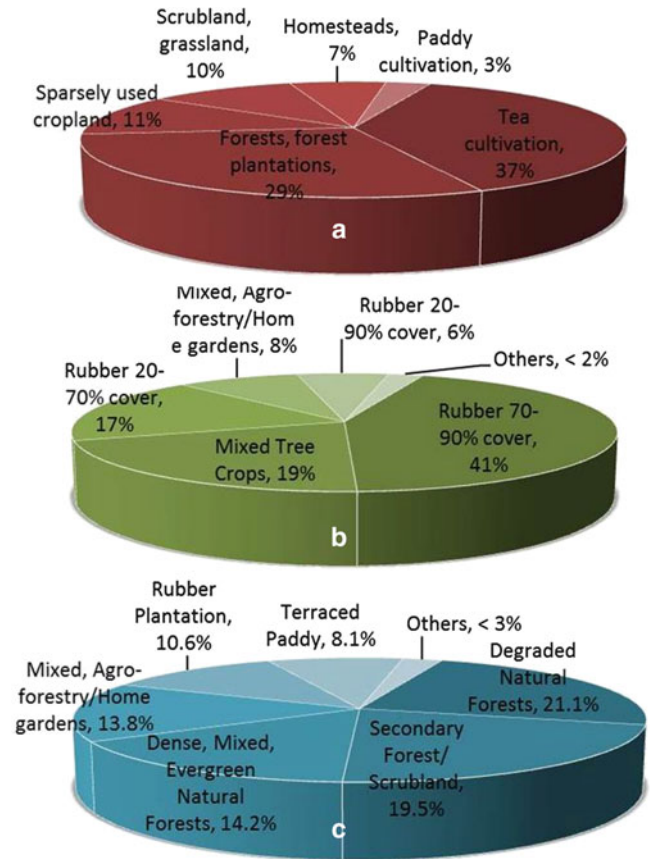


Fig. 3 Distribution of land use practices within (a) Nuwara Eliya (NBRO 1988), (b) Kegalle (Weerasinghe 2001) and (c) Galle

weights based on their relative contribution towards causing a landslide. The basis of assigning weights to mapping attributes and sub factor attributes completely depends on the interrelationship between the observed landslides read from a landslide inventory map and the mapping attributes read from different factor maps, However, within NBRO’s mapping methodology, assigning severity levels based only on the frequency of landslides observed within a mapping unit is highly discouraged, since that would unacceptably favour to the map units with the larger areas (NBRO 1995). For example, NBRO’s studies based on 863 landslide sites in Nuwara Eliya and 213 landslide sites in Badulla reflects the fact that majority of the landslides have been associated with slope angle range of 17–31° which is also the most abundant slope angle range present in the investigated regions. The landslide hazard zonation maps prepared by assigning highest weightings to this slope angle range indicated a poor relationship between the inferred hazard and the observed hazard (Bhandari and Weerasinghe 1996).

NBRO’s methodology suggests the following six criteria C1 to C6 for studying the relationship between the mapping attributes and observed landslides (NBRO 1995).

$$C_1 = \frac{N_u}{A_u} \tag{1}$$

$$C_2 = \frac{A_{lu}}{A_u} \tag{2}$$

$$C_3 = \frac{N_u}{\sum_{u=1}^{u=n} \frac{N_u}{A_u}} \tag{3}$$

$$C_4 = \frac{A_{lu}}{\sum_{u=1}^{u=n} \frac{A_{lu}}{A_u}} \tag{4}$$

$$C_5 = \frac{N_u}{\frac{N_t}{A_t}} \tag{5}$$

$$C_6 = \frac{1}{2} + \left[\frac{A_{lu}}{A_t} + \frac{N_u}{N_t} \right] \frac{A_t}{A_u} \quad (6)$$

Within the above six criteria, N_u is the total number of landslides observed within mapping unit, A_u is the land extent of that mapping unit, A_{lu} is the total area of a mapping unit, which has been affected by landslides, A_t is the total area mapped, N_t is the total number of landslides observed within the mapped area, A_{lt} is the total land extent affected by landslides within the mapped area.

In defining the six criteria, C1–C6, suggested within NBRO's hazard mapping methodology experts has given due consideration not only to the percentage of landslides observed within a mapping unit or attribute, but also to the area covered by landslides within a map unit, because the significance of a number of smaller area landslides is not similar to the significance of a single landslide with equivalent total area.

The present numerical rating system has been derived by application of above (1), (2), (3), (4), (5), (6) on the information gathered on landslides in Nuwara Eliya and Badulla districts (NBRO 1995). The interrelation between mapping attributes of each of the six causative factors and the landslides observed within the study area of Kegalle district had been studied against the same six criteria in the year 2001 (Weerasinghe 2001). Within this research the interrelation between the mapping attributes and the landslides observed in the study area of Galle district was studied against the above described six criteria. The results of this research along with the results obtained for Kegalle district in 2001 will then be compared with the severity levels derived in 1995 (Tables 1, 2, and 3) to investigate the rationale of utilizing the relative weights derived by using the Nuwara Eliya data for the relative ranking of same mapping attributes in other areas with different terrain characteristics, different climatological conditions, different lithological attributes and land use patterns. The research is on going and this paper focusses only on the the analysis of mapping attributes of three causative factors; (i) Landforms, (ii) Land use and management, and (iii) the attributes of geological subfactor, lithology.

Landslides Observed Within Different Mapping Units

Kegalle District

For the Kegalle study performed in 2001, 156 landslides observed within about 220 sq. km of land area had been evaluated against the mapping attributes. Figure 4 interprets frequency of landslides observed within the mapping attributes of lithology, land use, and landforms. The abbreviations used for landforms attributes (Hettige et al. 1994) are explained in the Table 4.

Table 1 Weights assigned for lithology attribute

Lithological map unit	Numerical rating	Qualitative rating
Quartzite	08	Very high
Charnockite, Granulite or bedrock not exposed	05	High
Granite, Garnet Biotite Gneiss, and all other rock types	03	Medium
Weathered rock	01	Low
Marble	00	Very low

Table 2 Weights assigned for land use and land management attribute

Land use mapping attribute	Numerical rating	Qualitative rating
Chena and other annual crops, Grasslands, Open Country/ miscellaneous Uses, Water bodies	15	Very high
Poorly managed tea estate, Rubber estate, Poorly managed forest plantation, Terraced paddy, Agro forestry/Home gardens, Market gardens and small holder tea cultivation, Degraded forests, Secondary forests, scrublands, wastelands, non-agricultural land and rural settlements	8	Medium
Well managed tea estate, Coconut estate, Farms and commercial enterprise, Well managed forest plantations, Urban settlements	3	Very low

Table 3 Weights assigned for Landforms attribute

Landforms mapping attribute	Numerical rating	Qualitative rating
Colluvial benches, Talus/screen slopes, landslide scars, dissected gullied surfaces, fault fracture zones, River/stream capture zones	10	Very high
Mountain slopes with relief above 200 m (except terraced slopes), sink holes, waterfalls	5	High
Hill slopes with 100–200 m relief (except terraced slopes), terraced slopes with relief above 200 m	3	Medium
Plateau, Hillocks and ridges with relief below 100 m, terraced hill slope with relief 100–200 m, Alluvial systems, water bodies	1	Very low

Galle District

For the Galle study 568 landslides observed within about 240 sq. km of land area had been evaluated against the mapping attributes. Figure 5 interprets frequency of landslides observed within the same three mapping attributes.

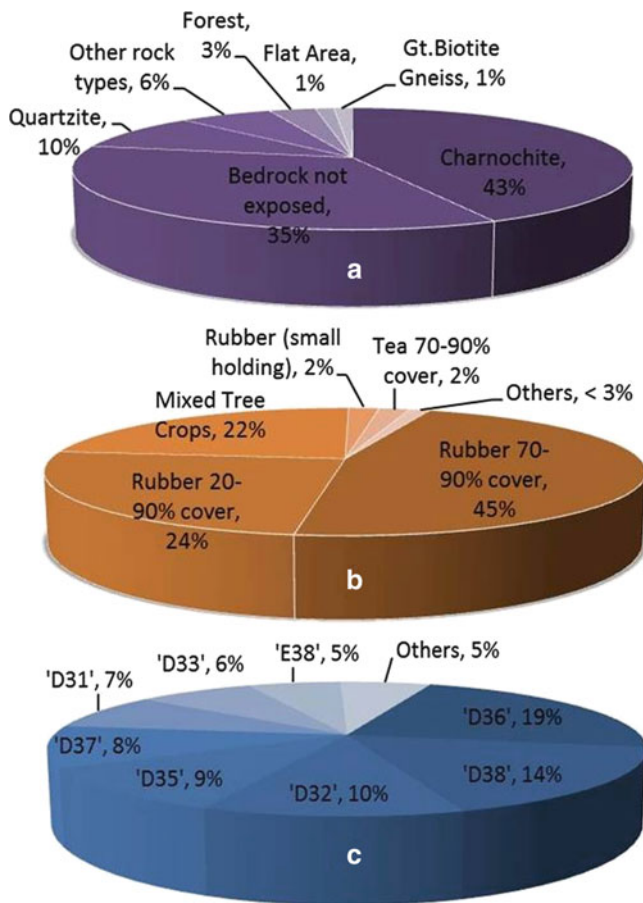


Fig. 4 Distribution of landslide frequency, in Kegalle district, within (a) different lithological attributes, (b) different land use attributes, and (c) different landforms attributes (Weerasinghe 2001)

Evaluation of Severity Levels of Mapping Attributes

The results obtained by application of criteria C1–C6 were first normalized for the ease of comparison and plotted as illustrated in Figs. 6, 7, 8, 9, 10, and 11. While the criteria C1, C3 and C5 investigates the impacts of mapping attributes by looking at the landslide density within a mapping attribute, criteria C2 and C4 investigates the impacts of mapping attributes by looking at the area affected by landslides within a single mapping unit. The criterion 6 evaluates the severity levels by reviewing both the number of landslides observed within a mapping unit and the landslide affected land extent of a mapping unit.

Even though the results shown in Figs. 6, 7, 8, 9, 10, and 11 are sorted based on the normalized value of C1, in defining severity levels, the normalized values obtained for any of the (1), (2), (3), (4), (5), (6) were considered in assigning subjective and numerical weights to the mapping attributes.

Table 4 Description of landforms interpreted by different codes (Hettige et al. 1994)

Major landform category	Tertiary landform category	Code	
Hill slope 50–350 m MSL (plateau)	Undulating land	D11	
	Undulating to rolling	D12	
	Isolated hillocks	D21	
	Undulating land + hillocks	D22	
Hill slope 50–350 m MSL (summits or crest lines)	Rolling land with hillocks and ridges	D23	
	Rolling hillocks an minihills (dissected plateau)	D24	
	Hill slope 50–350 m MSL (relief below 100 m)	Straight slopes (no variation of slope)	D31
		Complex slope	D32
Corrugated slope (straight longitudinally, rolling later		D33	
Hilly and mountainous (elevation 300–1,200 m)	Corrugated and complex	D35	
	Complex hill	E32	
	Dissected hill slope	E34	
	Complex corrugated and dissected	E38	
Hilly and mountainous and plateau (elevation > 1,200 m)	Straight mountain slope	E41	
	Mountain slopes (Relief > 200 m) straight	F51	

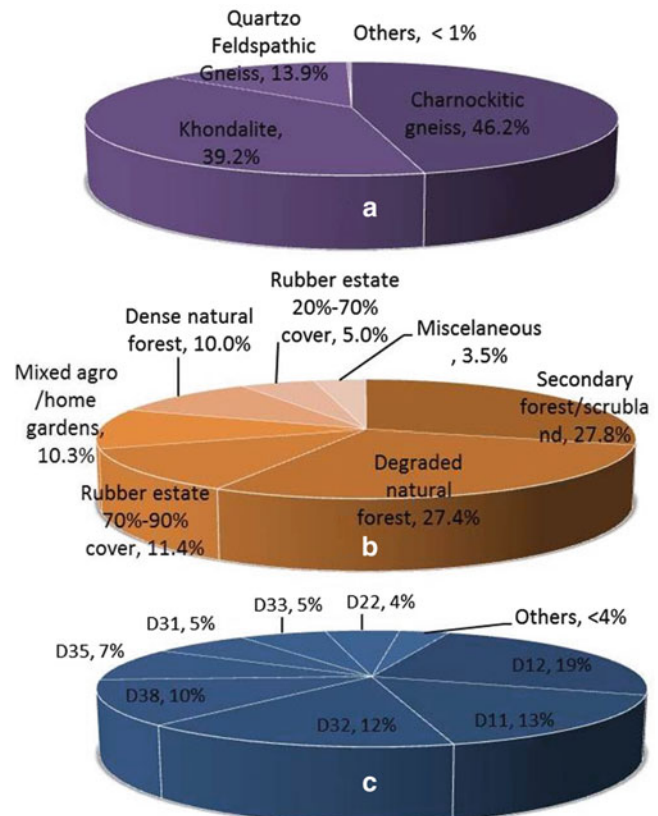


Fig. 5 Distribution of landslide frequency, in Galle district, within (a) different lithological attributes, (b) different land use attributes, and (c) different landforms attributes

Fig. 6 Relative ranking of landforms mapping units in Kegalle district according to the six criteria

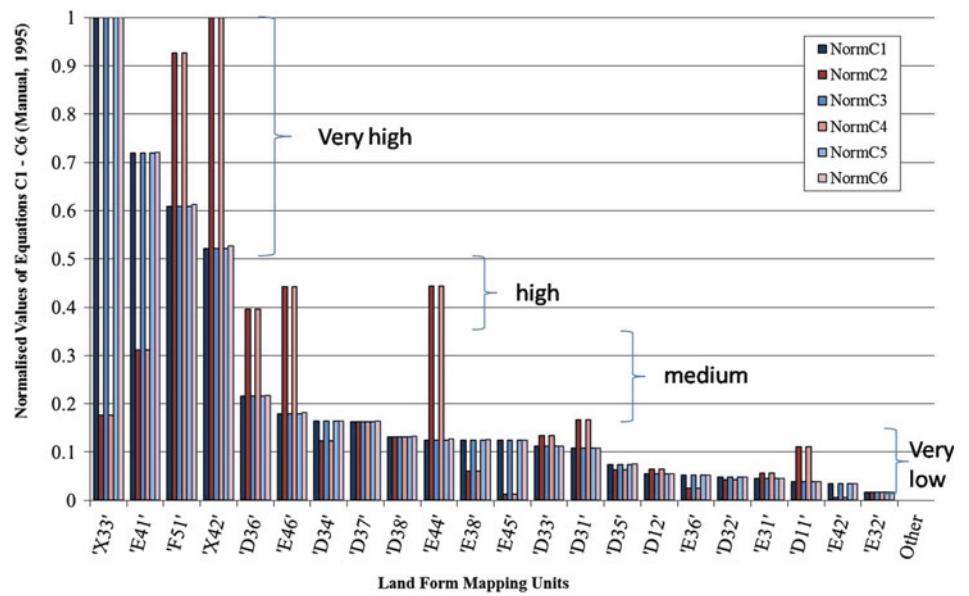


Fig. 7 Relative ranking of landforms mapping units in Galle district according to the six criteria

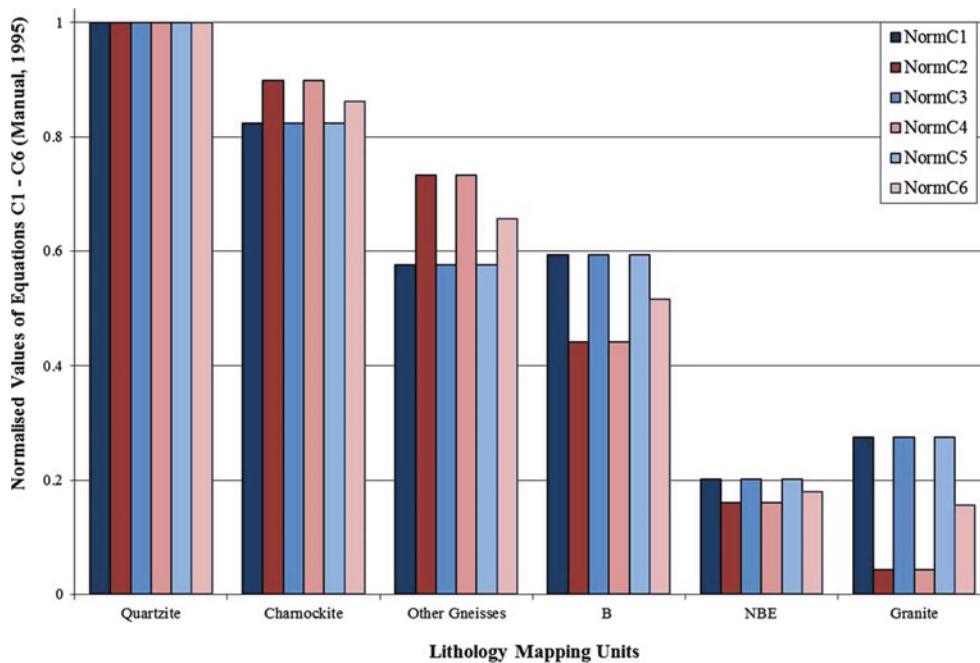
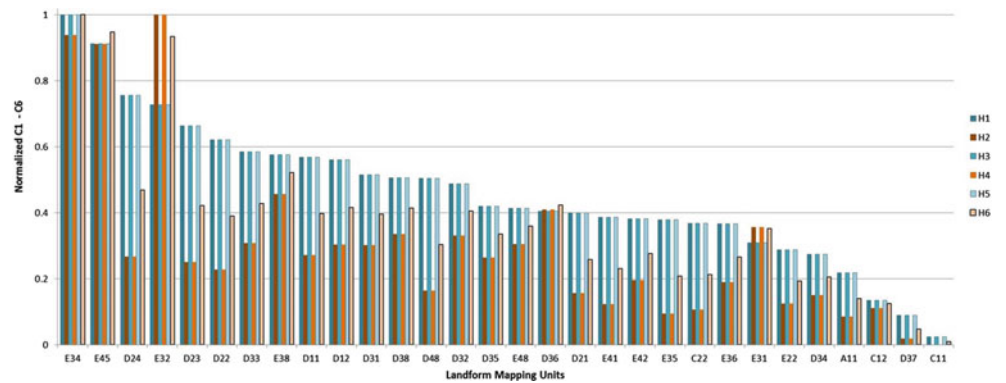


Fig. 8 Relative ranking of Lithological mapping units in Kegalle district according to the six criteria

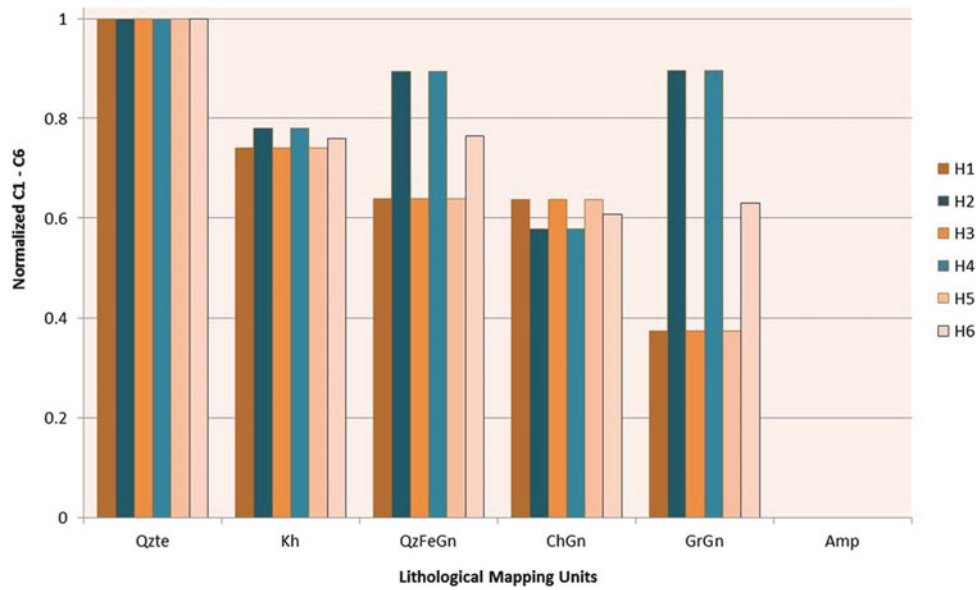


Fig. 9 Relative ranking of lithological mapping units in Galle district according to the six criteria

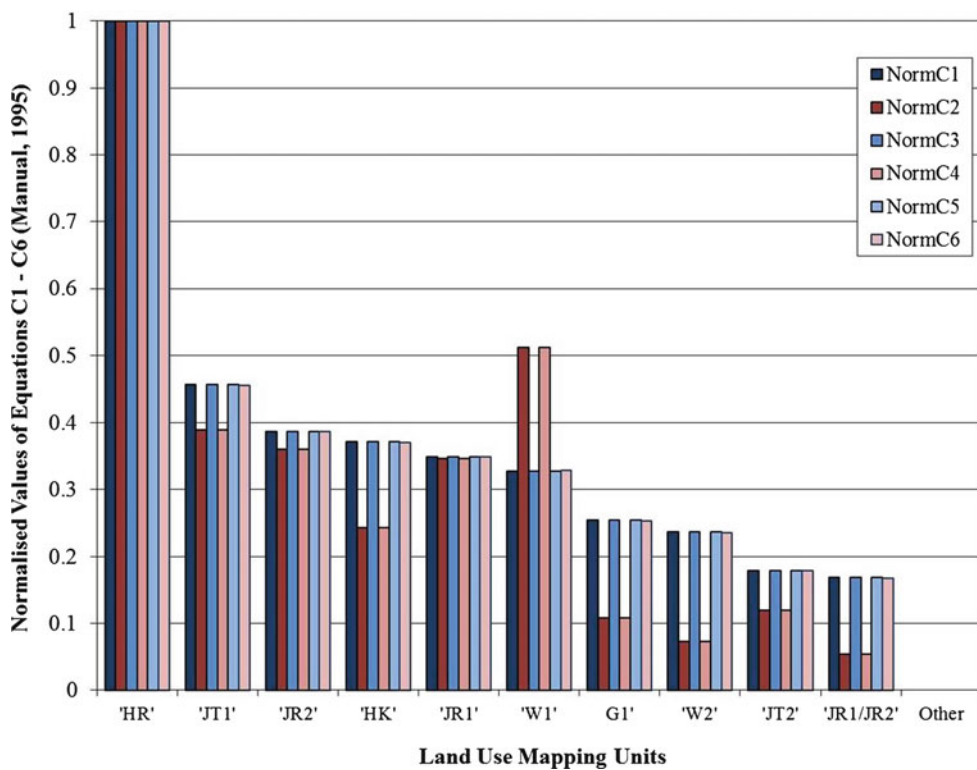


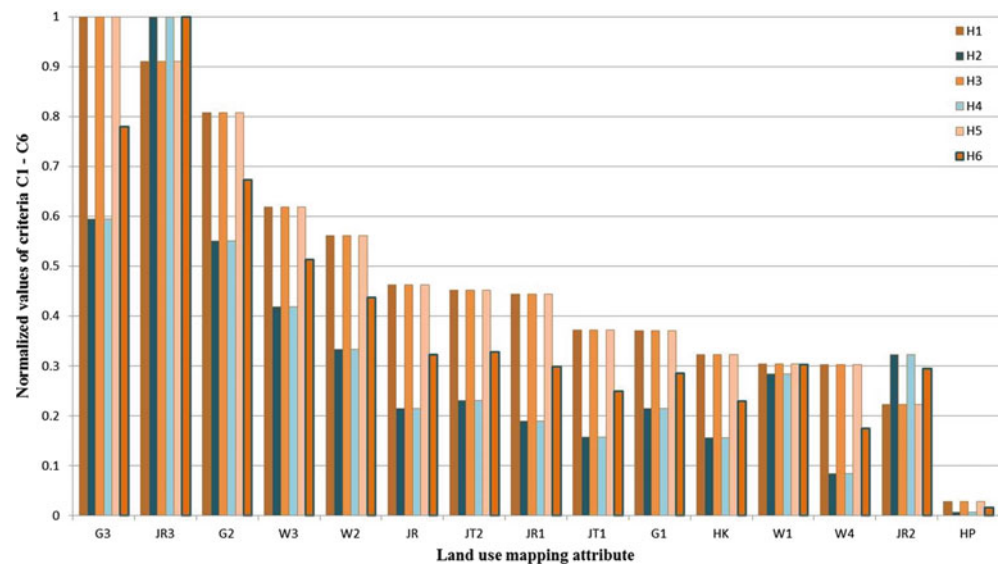
Fig. 10 Relative ranking of land use mapping units in Kegalle district according to the six criteria

As shown in Fig. 6, for Kegalle district, the landforms attributes X33, E41, F51 and X42 shows very high severity level. Similarly, the landform attributes D36, E46, D34, D37, D38 and E44 show high severity level. The attributes E38, E45, D33, and S31 show medium severity level,

whereas the attributes D35, D12, E36, D32, E31, D11, E42, E32 show very low severity level.

According to the Fig. 7, for Galle district, the landforms attributes E34, E45, D24, E32, D23, D22, D33, E38, D11, D12, D31, D38, D48 show very high severity level. while the

Fig. 11 Relative ranking of land use mapping units in Galle district according to the six criteria



landform attributes D32, D35, D36, D21, E48, E41, E42, E35, C22, E36, E31 show high severity level. Landform attributes E22, E34, A11 show medium severity level while the attributes C12, D37, C11 show very low severity levels. The severity levels for remaining two attributes can also be defined in the same manner.

As evident by Figs. 8 and 9, the severity levels derived for lithological attribute quartzite seems to have the highest severity level both in Kegalle and Galle districts also. The attributes, Charnockite, Khondalite, Charnockitic gneiss, granulitic gneiss and Quartzofeldspathic gneiss also seems to have high severity levels. In general, for the lithological attributes, the same severity levels are applicable in all three districts.

Further evaluation of the Figs. 10 and 11 indicates that the normalized values of criteria C1–C6 calculated for land use and land management attribute also show different trends for the two districts of Kegalle and Galle and the severity levels of these attributes seems to be different from those observed in Nuwara Eliya district.

Conclusion

The results of this research indicate that the severity levels of the mapping attributes of causative factors Landforms and Land Use show different trends depending on the geographical region which can be related to the terrain characteristics and land use practices of the region. Even though the severity levels assigned for the lithological mapping attributes can be considered as common to all three regions considered within this research, such outcome may have been caused by the fact that all three regions belong to the highland series

and share somewhat similar geological characteristics. Therefore, it is advisable to execute the relative ranking criteria, whenever a new region with different characteristics is mapped and assign the severity levels to the mapping attributes, based on the outcome of such evaluation. This is an ongoing research and evaluation of severity levels for the remaining three causative factors should be appraised before arriving at a final conclusion.

Acknowledgments The authors of this paper acknowledge the contribution of Dr. R.K. Bhandari, Mr. Piyasiri Hettige, Mr. K.S. Senanayake and all other pioneers of the Landslide Hazard Mapping Project at NBRO. They also acknowledge the support provided by the present management of NBRO in executing this research.

References

- Bhandari RK, Weerasinghe KM (1996) Pitfalls in subrogating slope maps for landslide hazard maps. In: Proceedings of 17th Asian conference on remote sensing, 4–8 November 1996, Colombo, Sri Lanka, pp C3-1–C3-5
- Hettige PML, Jinadasa LD, Jayaweera S (1994) Categorization of landform map units, according to their stability attributes. In: Proceedings of the conference on landslides, Colombo
- NBRO (1988) Proposal for landslide hazard mapping in Badulla and Nuwara Eliya Districts, p II.2
- NBRO (1995) User manual on landslide hazard zonation mapping. National Building Research Organisation, Colombo
- Weerasinghe KM (2001) Application of fuzzy sets and other statistical techniques in landslide hazard zonation mapping. MEng thesis, University of Moratuwa, Moratuwa, Sri Lanka
- Wijewickrama MIDH, Kotuwegoda WPPK, Wickramathanthri NC, Karunaratne RAP, De AM (1994) Landslides in Nuwara Eliya District. In: Proceedings of the conference on Landslides, Colombo



Landslide Hazard and Risk in a Changing Climate

Mike G. Winter and Barbara Shearer

Abstract

Although the UK is a relatively low-risk environment where landslides are concerned such events do have important socio-economic impacts and fatalities do occur. This report considers the potential for landslide events in Scotland in the light of future climate change. In particular, the UKCIP02 (deterministic) and UKCP09 (probabilistic) climate change forecasts, current climate data and historic trends in Scotland's climate are discussed to obtain a clear picture of recent, current and likely future trends. The outcomes from this analysis are then reconciled with a view of likely future landslide hazard trends and a picture of potential future landslide risk in Scotland is presented.

Keywords

Landslides • Debris flow • Climate change • Rainfall

Introduction

The causal link between anthropogenic emissions of greenhouse gases, increases in the global temperature anomaly and climate change, which may or may not manifest as higher temperatures at any given location, are now well-established and have become part of the body of mainstream thinking (e.g. Hill et al. 2007). Climate change is thus increasingly seen as a scientific fact; occasionally a dissenting voice may be heard but such disputes are increasingly focused upon the scale of such changes and on the most appropriate actions to be taken in terms of mitigation and adaptation (e.g. Bellamy and Barrett 2007).

There is perhaps a tendency to focus upon the future climate change issues at the expense of the wealth of information captured within current weather patterns and recent climate trends. In this paper these three closely related threads of information—recent trends/current climate, historical trends and future change (UKCIP02 and UKCP09)—

are brought together to provide a more holistic view of climate patterns as they relate to landslides.

Scotland's Rainfall Climate

The climate of Scotland in terms of its rainfall may be very broadly divided into the relatively dry east and the relatively wet west (Fig. 1), where almost twice as much rain falls, on average, each year. Figure 1 shows data for the United Kingdom in its entirety. The trend towards greater rainfall in the more westerly parts is broadly maintained throughout. However, it is also clear that the areas subject to high rainfall are much smaller in the southern part of Great Britain (England and Wales) than in Scotland in the north.

The data (Anonymous 1989) indicate that, in the lowland regions in the east of Scotland, overall annual rainfall levels are relatively low, being broadly comparable with drier parts of England. While rainfall generally peaks in the summer months of July and August in the east, the monthly average rainfall data for Edinburgh (Figs. 2 and 3), which is broadly representative of the east and one of the driest locations in Scotland, indicates that in the main the monthly variations in rainfall are relatively slight.

M.G. Winter (✉) • B. Shearer
Transport Research Laboratory (TRL), 13/109 Swanston Road,
Edinburgh EH10 7DS, UK
e-mail: mwinter@trl.co.uk

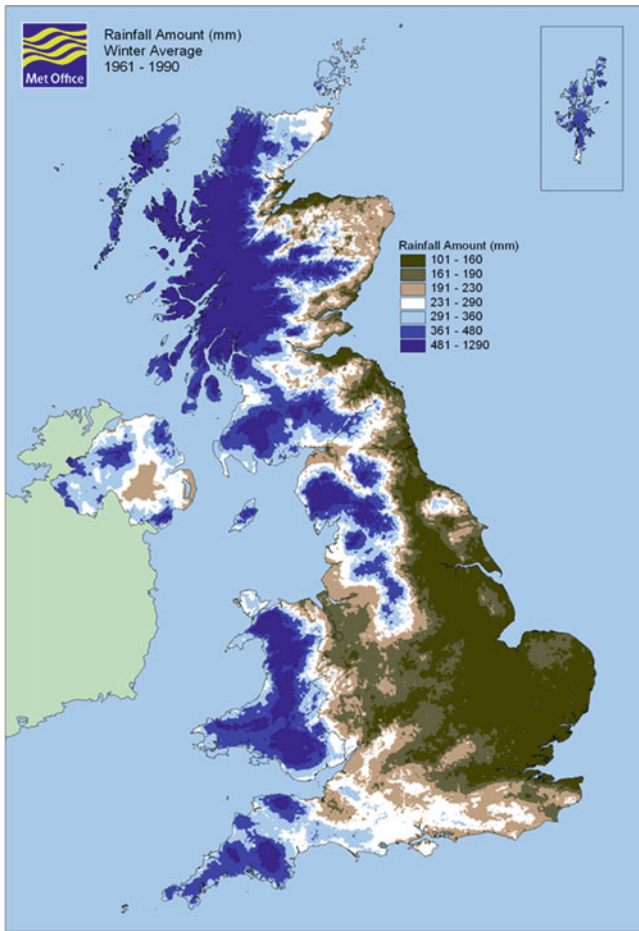


Fig. 1 UK Met Office 30-year monthly average rainfall data (1961–1990) for winter; *blue* indicates high and *brown* low rainfall (the pattern is similar for other seasons albeit the numbers vary) (images courtesy of the Met Office)

In the wetter west, maximum rainfall levels are reached during the period September to January (e.g. Tiree, Fig. 2). Perhaps most marked is the variation in the monthly averages with the driest month of May receiving around half of the rainfall experienced in the wettest month of October.

Although rainfall levels in the west are relatively low in August, they do increase from a low point in May. It is worth noting that while Tiree shows rainfall levels significantly in excess of those for Edinburgh and Pitlochry (1,106 mm on average per annum compared to 626 mm and 824 mm respectively) other locations in the west of Scotland experience significantly more rainfall: e.g. Inveraray Castle with around 2,036 mm of rainfall on average per annum (Fig. 2).

The central area, as represented by Pitlochry (Fig. 2), has what might best be described as a mix of the rainfall characteristics of the ‘east’ and the ‘west’. The rainfall peak is both lower and shorter (December and January) than in the west, but there are also small sub-peaks in August and October.

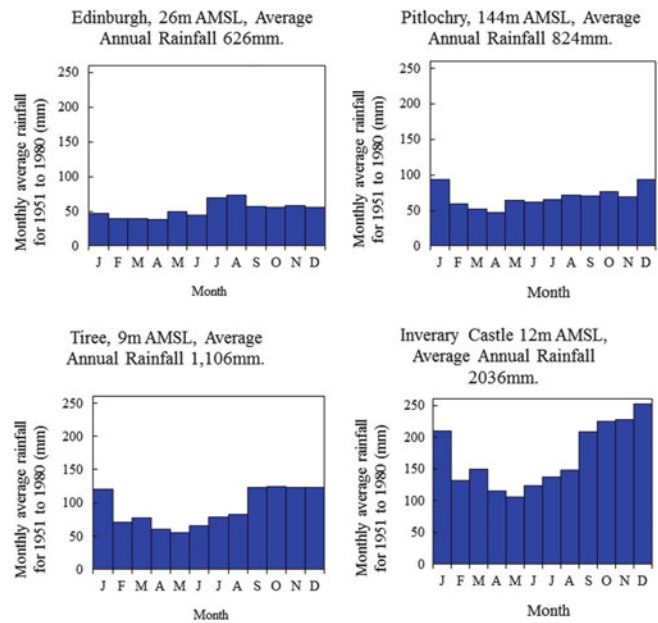


Fig. 2 Average rainfall patterns for selected locations in Scotland, based upon 30-year 1951–1980 averages from Anonymous (1989)



Fig. 3 Map showing locations in Fig. 2. Reproduced by permission of Ordnance Survey, on behalf of HMSO, © Crown copyright and database rights, 2014. All rights reserved. Ordnance Survey Licence number 100046668

Such average values mask large annual variations. Data presented by Barnett et al. (2006a, b) indicate that the annual average rainfall for the west of Scotland varies between around 1,200 and 2,100 mm for the period 1914–2004, equivalent figures for the east of Scotland indicate an equivalent range of between around 770 and 1,450 mm. Such figures themselves can, of course, mask significant areal variations.

Additionally, the majority of weather monitoring stations, including rainfall gauges, is located in more accessible low-lying areas. While developments in remote sensing have seen an increase in the number of observing sites in the more remote areas it remains the case that the station network is sparser in mountainous areas (McGregor and MacDougall 2009). It is also the case that the network of observation stations is designed to meet general uses and climate (synoptic) monitoring requirements.

Rainfall amounts in the higher elevation, mountain areas are usually greater due to orographic effects, albeit that the accumulations are likely to be generally higher on the westward-facing, windward, side of Scottish mountain ranges than on the eastward-facing, leeward, side where rain shadow effects may come into play. In broad terms these orographic effects are borne out at the macro scale for Scotland, and the UK as a whole, in Fig. 1. However, scenarios in both the west and the east indicate that the soil may be undergoing a transition from a dry to a wetter state at or around August and that in the period October/November to January the soil is likely to be in a wet, if not saturated, state and that rainfall continues to be at relatively high levels. This indicates an increased potential for debris flow and other forms of shallow landslide activity during these periods.

Clearly, the soil water conditions necessary for debris flows may be generated by long periods of rainfall or by shorter intense storms. It is however widely accepted that Scottish debris flow events are usually preceded by both extended periods of (antecedent) rainfall and intense storms (Winter et al. 2009) and it should be acknowledged that two landslide seasons are typically considered to prevail in Scotland: Summer, July and August; and Winter, (October) November to January (Winter et al. 2005).

Historical Trends

The observed trends in the climate of the recent past are relevant as well as the forecasts for future climate change. Work by Barnett et al. (2006a, b) describes trends in climate across Scotland during the last century. The annual average rainfall figures presented (for 1914–2004) indicate a broad, but small, increase in the running annual average rainfall for the north and, particularly, the west of Scotland while figures

for the east of Scotland are broadly stable. Barnett et al. (2006a, b) consider two time periods: 1914–2004 and 1961–2004.

The data from the shorter (1961–2004) period, which is affected by a dip in the overall average rainfall levels in the 1960s and 1970s, shows a clear upward trend in both winter and annual precipitation while there is no clear trend for the spring, summer and autumn periods. For the longer period the statistical certainty inherent in the data is less and only two clear trends are apparent: a reduction in summer precipitation in east Scotland and an increase in spring precipitation in west Scotland.

Notwithstanding those trends that can be supported at the 95 % statistical confidence level, the data more generally point to increases in precipitation in the winter and in annual precipitation levels, particularly in the north and west of Scotland. Changes in summer precipitation show no clear trend in the 1961–2004 period but show a likely reduction for the longer 1914–2004 period. Certainly if a single long-term summary point is sought it would be that the trend in annual precipitation is either to remain roughly constant or to increase slightly while the changes within the annual period are generally reflective of increased winter precipitation, particularly in the west and north, and decreased summer precipitation, particularly in the north and east.

Potential Climate Change: UKCIP02

The deterministically-based UKCIP02 (UK Climate Impacts Programme) report considered three periods: the 2020s, the 2050s and the 2080s and four alternative emissions scenarios namely Low Emissions, Medium-Low Emissions, Medium-High Emissions and High Emissions (Hulme et al. 2002).

The scenarios for Scotland show little predicted change in annual mean precipitation over the next few decades, with change being within the range attributable to natural variability. However, Galbraith et al. (2005) discerned a distinct seasonal pattern by the 2020s and in the low emissions scenario. While little significant change was predicted for the spring or autumn precipitation, changes were found to be likely for the winter and summer. Winter precipitation increases were between 10 and 15 % for the Low and High emissions scenarios in the eastern regions, with changes elsewhere being within the range of that which can be accounted for by natural variability.

In the summer, decreases in the average precipitation are predicted to be widespread with only the far northwest seeing little change. By the 2020s Galbraith et al. (2005) indicate that the High emissions scenario implies that decreases are likely to be greatest in the south east of Scotland and could be as much as 20 % less than present day modelled levels. Year-on-year, or inter-annual,

variability in precipitation is also predicted to change (Galbraith et al. 2005).

Potential Climate Change UKCP09

UKCP09 gives climate change projections for a number of climate variables over seven 30-year overlapping time periods, at a resolution of 25 km (for administrative regions and river basins) (Jenkins et al. 2009). This is the first UK set of predictions to attach probabilities to different levels of future climate change. These probabilities represent the relative degree to which each climate outcome is supported by the evidence currently available (Anonymous 2011a). While UKCIP02 considered four scenarios UKCP09 considers three scenarios (High, Medium and Low).

The three emissions scenarios presented broadly similar results up until the 2050s, before starting to diverge as the 2080s were approached (Anonymous 2011b). Accordingly they designated the 2050s as the central point and structured the relationship between emissions scenarios and predicted climate change as follows:

- Lower limit: 10 % probability with low emissions scenario
- Central estimate: 50 % probability with medium emissions scenario
- Upper limit: 90 % probability with high emissions scenario

This simplification makes extensive and complex data sets manageable while retaining their meaning and breadth (Winter and Shearer 2013). The data presented by both Anonymous (2011a) and Anonymous (2011b) broadly confirm the likelihood of decreased summer precipitation and increased winter precipitation, although it is perhaps more difficult to assign specific regional differences. Additionally, the data suggests approximately unchanged annual precipitation although the lower limit estimate implies decreases and the upper limit estimate implies increases in the annual average, most markedly in the west of Scotland.

Precipitation intensity is considered by the proxy of wettest day in winter and summer (Anonymous 2011b). In the winter for the lower limit and central estimate the change is less than ± 10 % across most of the country. However, for the upper limit the increase is of the order of 30–40 % in coastal areas. In the summer the change could range from 10 to 20 % less in the lower limit prediction to 10–20 % greater in the upper limit prediction.

The various data sets present a consistent picture and a number of clear themes emerge:

- Spring and autumn rainfall is broadly unchanged or slightly reduced as is the annual total.
- Winter precipitation is increased.
- Summer precipitation is decreased.

- Across the seasons storm rainfall events are expected to become more intense and more frequent. (This is, however, perhaps one of the facets that climate models are least well-suited to determining.)

Changing Hazard and Risk

The soils and weathering mantle that form the slopes subject to debris flow comprise a wide range of materials, albeit that periglacial, glacial, and post-glacial (including paraglacial) processes dominate their formation and subsequent modification. The particle size composition of debris flow materials includes sizes ranging from coarse granular (including boulders) to fine cohesive with most sizes between potentially represented (e.g. McMillan et al. 2005); observations of the characteristics of the materials involved in the August 2004 landslide events in Scotland indicate such a diverse composition (Winter et al. 2006). Both Winter et al. (2010a) and Milne et al. (2009) acknowledge the importance of water-bearing soils, particularly peat, located on high, relatively flat ground as trigger materials for gully-constrained debris flows. The materials that are later eroded, entrained and transported in the body of the flow may be of entirely different characteristics; often coarser-grained materials from morainic and related features are critical to the development of such flows.

Increased rainfall during the winter months seems likely to increase the prevalence of landsliding in Scotland. This is particularly so when considered in the context of the likelihood of more intense rainfall events. The reduced soil moisture, as a result of both predicted temperature increases and rainfall decreases, during the summer and autumn may mean that the short-term stability of some slopes, particularly those formed from granular materials, may be enhanced by the suction pressures that may develop in such conditions. However, the available evidence for climate change does point to an increase in short duration, high intensity rainfall events, including in summer. Soils under high levels of suction are vulnerable to rapid inundation (Toll 2001), and a consequent reduction in the stabilising suction pressures.

In addition, non-granular soils may form low permeability crusts during extended dry periods as a result of desiccation. If these do not experience excessive cracking due to shrinkage, then runoff to areas of vulnerable granular deposits may be increased. However, the formation of drying cracks could lead to the rapid development of instabilities in soil deposits, potentially creating conditions for the formation of debris flows. It is thus clear that there is a number of potential failure mechanisms that may lead to the initiation of a debris flow.



Fig. 4 Urban landslide at Bervie Braes, Stonehaven, on the north-east coast of Scotland (February 2010). The landslides at Bervie Braes occur on a raised sea cliff

Vegetation will also be affected by climate change. Extended periods of dry weather leading to wildfires and associated debris flow seem less likely to be a major factor in the relatively wet climate of Scotland; it seems more likely that an extension to the growing season will predominate in terms of the effects of vegetation—a factor that is most likely to have a positive effect upon instability. However, the possibility of vegetation desiccation cannot be dismissed during prolonged summer dry spells.

The available climate change forecasts thus present a picture that tends to suggest that landslide hazard frequency and magnitude may well increase in Scotland, at least in the winter months. A rather more complex picture emerges for the summer months but one possible outcome is that the frequency of events may decrease but that the magnitude of those that do occur may increase.

The primary landslide risks relate to transport infrastructure, albeit not exclusively (Fig. 4). Increases in the elements at risk and the associated vulnerability (both the infrastructure and road traffic/users) seem likely in line with road traffic and rail passenger growth.

Set against this are major activities such as the planned upgrade of the A9 strategic road to dual-carriageway and major studies to identify and examine options to reduce landslide risk. Indeed, it is worth considering that should traffic levels grow substantially then the infrastructure will cease to be viable in its current form. If limits on access to the network are not to be introduced, then major upgrades will become necessary affording the opportunity to address landslide hazards and risks from the outset.

However, the approach of infrastructure upgrade does seem to be unlikely to be viable across the network and certainly is unlikely to be so much beyond the strategic road network for example. In such cases localised hazard mitigation schemes and route-based exposure management schemes will be necessary.

In addition the complex interplay between changing land use and the effects of emerging technology on work patterns will change the way in which society addresses such infrastructure and may also introduce new infrastructure that may itself be at risk from landslide hazards (Winter and Shearer 2013).

Conclusions

Rainfall-induced debris flow events are a relatively common occurrence in Scotland. In broad terms the available climate change forecasts present a picture that suggests that landslide hazard frequency and magnitude will increase in Scotland in the future, at least in the winter months when rainfall is expected to increase. The picture for the summer months is considerably more complex, but one likely outcome is that while the frequency of events may decrease their magnitude, when they do occur, may increase.

The primary landslide risks relate to transport infrastructure, albeit by no means exclusively. It seems clear that the effects of climate change is most likely to increase the hazard and also that increases in the elements at risk and their vulnerability are likely to increase in line with traffic growth. Landslide risk is thus likely to increase as a result of these factors.

Against this must be set planned network upgrades that may minimize such hazards and risks at the outset, albeit this will not be a universal panacea and exposure management and hazard mitigation schemes will be necessary. The complex interplay between changing land use and the effects of emerging technology on work patterns will change the way in which society addresses such infrastructure and may also introduce new infrastructure that may itself be at risk from landslide hazards.

While we are still asked, as scientists, whether we “believe in climate change” (Pope 2009), the question

has long since ceased to have meaning; we do not drive our cars in a manner so as to avoid impacts with other vehicles and pedestrians because we ‘believe’ in Newton’s Laws, the scientific evidence for the existence and veracity of which in a terrestrial environment is overwhelming. The scientific evidence for climate change is also overwhelming; belief simply does not come into the equation. There remains, of course, significant uncertainty surrounding those changes and Winter et al. (2010b) summarised these with reference to Donald Rumsfeld, the former US Secretary of Defence as follows, there are:

- *Known knowns*: Including past climate trends, their relation to current patterns and the fact of climate change and instability.
- *Known unknowns*: The degree and nature of climate change and its impacts, particularly in the light of the variability in climate change forecasts and instability in year-on-year climate patterns. The impacts might, for example, include the responses of vulnerable human populations to climate change and instability.
- *Unknown unknowns*: The nature of some other impacts of climate change, although as these are genuinely unknown unknowns these really will have to wait until our knowledge is more complete—they are after all unknown. Possibly the real value of this point is to serve as a reminder that there will always be issues that arrive unexpectedly out of the leftfield.

Acknowledgments The work described in this paper was supported by the European Commission through the project SafeLand “Living with landslide risk in Europe: assessment, effects of global change, and risk management strategies” under Grant Agreement No. 226479 in the 7th Framework Programme of the European Commission. This support is gratefully acknowledged. Additional funding from Transport Scotland is also gratefully acknowledged.

References

- Anonymous (1989) The climate of Scotland—some facts and figures. The Stationery Office, London
- Anonymous (2011a) Scottish road network climate change study: UKCP09 update. Report by Jacobs for Transport Scotland. <http://www.transportscotland.gov.uk/>
- Anonymous (2011b) Paths and climate change—an investigation into the potential impacts of climate change on the planning, design, construction and management of paths in Scotland. Commissioned Report No 436 by Walking-the-Talk. Scottish Natural Heritage, Inverness
- Barnett C, Perry M, Hossell J, Hughes G, Procter C (2006a) A handbook of climate trends across Scotland; presenting changes in the climate across Scotland over the last century, Project CC03. Sniffer, Edinburgh, 62 p
- Barnett C, Perry M, Hossell J, Hughes G, Procter C (2006b) Patterns of climate change across Scotland: technical report, Project CC03. Sniffer, Edinburgh, 102 p
- Bellamy D, Barrett J (2007) Climate stability: an inconvenient proof. *Proc ICE Civil Eng* 160(2):66–72
- Galbraith RM, Price DJ, Shackman L (eds) (2005) Scottish road network climate change study. Scottish Executive, Edinburgh, 100 p
- Hill D, Winter MG, McCrae IS (2007) Opportunities for offsetting carbon emissions on the Scottish trunk road network: overview report. Transport Scotland, Edinburgh
- Hulme M, Jenkins GJ, Lu X, Turnpenny JR, Mitchell TD, Jones RG, Lowe J, Murphy JM, Hassell D, Boorman P, MacDonald R, Hill S (2002) Climate changes scenarios for the United Kingdom: the UKCIP02 scientific report. Tyndall Centre for Climate Change research, University of East Anglia, Norwich, 120 p
- Jenkins GJ, Perry MC, Prior MJO (2009) The climate of the United Kingdom and recent trends. Met Office Hadley Centre, Exeter
- McGregor P, MacDougall K (2009) A review of the Scottish rain-gauge network. *Proc ICE Water Manage* 162(2):137–146
- McMillan P, Brown DJ, Forster A, Winter MG (2005) Debris flow information sources. In: Winter MG, Macgregor F, Shackman L (eds) Scottish road network landslides study. The Scottish Executive, Edinburgh, pp 25–44
- Milne FD, Werritty A, Davies MCR, Browne MJ (2009) A recent debris flow event and implications for hazard management. *Q J Eng Geol Hydrogeol* 42(1):51–60
- Pope V (2009) Stop misleading climate claims. 11 February. Met Office, Exeter
- Toll DG (2001) Rainfall-induced landslides in Singapore. *Proc ICE Geotech Eng* 149(4):211–216
- Winter MG, Shearer B (2013) Climate change and landslide hazard and risk—a Scottish perspective. Published Project Report PPR 650, Transport Research Laboratory, Wokingham
- Winter MG, Macgregor F, Shackman L (eds) (2005) Scottish road network landslides study. The Scottish Executive, Edinburgh, 119 p
- Winter MG, Heald A, Parsons J, Shackman L, Macgregor F (2006) Scottish debris flow events of August 2004. *Q J Eng Geol Hydrogeol* 39(1):73–78
- Winter MG, Macgregor F, Shackman L (eds) (2009) Scottish road network landslides study: implementation. Transport Scotland, Edinburgh, 278 p
- Winter MG, Dent J, Macgregor F, Dempsey P, Motion A, Shackman L (2010a) Debris flow, rainfall and climate change in Scotland. *Q J Eng Geol Hydrogeol* 43(4):429–446
- Winter MG, Dixon N, Wasowski J, Dijkstra T (2010b) Introduction to land use and climate change impacts on landslides. *Q J Eng Geol Hydrogeol* 43(4):367–370



Validation of a Simulation Chain to Assess Climate Change Impact on Precipitation Induced Landslides

Alessandra L. Zollo, Guido Rianna, Paola Mercogliano, Paolo Tommasi, and Luca Comegna

Abstract

Since prehistoric times, the clayey slopes of Orvieto (Central Italy) have been affected by slow movements directly related to soil–atmosphere interaction. Understanding how climate changes could affect future evolutions of such movements is a challenging issue; to this aim, a simulation chain is set up: General Circulation model (GCM) outputs are dynamically downscaled through regional climate models (RCMs); rainfall values are then subjected to techniques to correct biases; so obtained rainfall time series can be adopted as input for tools evaluating slope stability conditions. Three bias correction techniques (BCT) have been applied: linear-scaling, quantile mapping and Analogs method. This work analyses their strength and limitations as well as their capability for outperforming the uncalibrated RCM outputs under current climate conditions (1981–2010) for the Orvieto case study. These results suggest that the BCT may be very useful tools for climate change impact studies where users require high resolution data and systematic errors to be minimized.

Keywords

Over consolidated clay • Climate change • Climate model • Bias correction • Rainfall thresholds

A.L. Zollo (✉) • G. Rianna

Impacts on Soil and Coasts Division, Centro Euro-Mediterraneo sui Cambiamenti Climatici (CMCC), via Maiorise s.n.c., Capua (CE) 81043, Italy
e-mail: a.zollo@cira.it; g.rianna@cira.it

P. Mercogliano

Impacts on Soil and Coasts Division, Centro Euro-Mediterraneo sui Cambiamenti Climatici (CMCC), via Maiorise s.n.c., Capua (CE) 81043, Italy

Meteo System and Instrumentation Laboratory, Italian Aerospace Research Center (CIRA), via Maiorise s.n.c., Capua (CE) 81043, Italy
e-mail: p.mercogliano@cira.it

P. Tommasi

National Research Council, Institute for Environmental Geology and Geo-Engineering c/o Engineering Faculty – Sapienza University of Rome, Rome, Italy
e-mail: paolo.tommasi@uniroma1.it

L. Comegna

DICDEA – Department of Civil Engineering, Design, Construction Industry and Environment, Second University of Naples, Naples, Italy
e-mail: luca.comegna@unina2.it

Introduction

In recent years, the variation in magnitude and frequency of landslide events induced by changing rainfall patterns caused by climate changes (CC) is an issue that is widely debated in the literature (Coe and Godt 2012; Crozier 2010; Sidle and Ochiai 2006).

Evaluations of future evolutions of slope stability conditions are often carried out through prospective approaches based on the commonly adopted hydrologic-slope stability models where upper boundary conditions are the forcing obtained from climate projections (Dixon and Brook 2007; Dehn et al. 2000; Collison et al. 2000).

Accordingly, in order to obtain data at temporal and spatial scales suitable for hydrological impact studies, General Circulation Model (GCM) outputs (maximum resolution 50 km) can be downscaled through dynamical approaches which nest regional climate models (RCMs) on the GCMs for the area of interest.

In order to investigate the effect of CC on landslides though GCM + RCM simulation chain, two important constraints have been taken into account:

- (i) it returns reliable outputs until daily scale (Maraun et al. 2010); for this reason, until now, researches have been focused on landslide phenomena induced by effective precipitations over not less than 1 month (Collison et al. 2000; Dehn et al. 2000; Dixon and Brook 2007), while few attempts are conducted to investigate the effect of CC on shallow landslides controlled by heavy hourly precipitations;
- (ii) the comparisons between observations and RCM outputs (both precipitation and temperature) show bias regardless the used RCM and the investigated areas (Christensen et al. 2007; Maraun et al. 2010; Gudmundsson et al. 2012; Lafon et al. 2013); thus, RCM output cannot be directly used as input for impact models (Gutjahr and Heinemann 2013).

To reduce the bias in climate data, many investigators have adopted stochastic weather generator techniques (Kilsby et al. 2007) or bias correction techniques (BCTs) (Lafon et al. 2013; Themeßl et al. 2010). In particular, the different BCTs, developed in recent years, differ from each other depending on the features of the impact study for which are to be used (e.g. need to correct only the mean value or the entire probability distribution) and the amount of observed data required for a proper calibration.

In the present work, three bias correction methods with increasing complexity have been considered in cascade to RCM: linear-scaling, quantile mapping and analogs method. Since a realistic representation of precipitation fields is crucial for impact assessment, their performances are tested in reproducing the current climate (1981–2010).

This work is then aimed to display, for Orvieto (central Italy) landslide case-history, what is the benefit of implementing bias correction techniques, the effectiveness of the widely used approaches in removing precipitation bias and how they obtained data result in different estimates of slope stability conditions.

Orvieto Case-History

Orvieto is an historical town of Central Italy raising on top of a 50-m-thick tuff slab (about $700 \times 1,500$ m) delimited by subvertical cliffs; the slab overlies an half cone formed by overconsolidated clays; between the slab and the clay substratum, a sequence of coarse-grained (Albornoz) fluvial-lacustrine sediments (variable thickness 3–15 m) is interposed.

The clay formations present the following succession of materials (from bottom to top): at depth, clay is stiff and intact; in the central part, the fissures appear and gradually

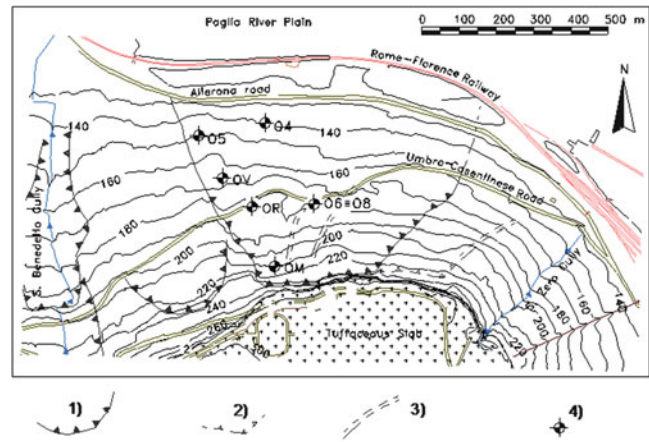


Fig. 1 Map of the northern slope of Orvieto hill; (1) slide scarp, (2) limit of the area affected by 1900 Porta Cassia Slide, (3) limit of independent portions inside the 1900 Porta Cassia slide, (4) instrumented boreholes (modified by Tommasi et al. 2012)

increase upward; in the shallower part, the clay formation shows fissures and joints (opened at the top) and clear signs of oxidation.

The clayey slopes are blanketed by an irregular cover of talus and slide debris. Talus debris originate from the disruption of volcanic and Albornoz materials while landslide debris are caused by landslide movements (Tommasi et al. 2006, 2012).

Oedometer compression tests and, in situ, falling head tests in Casagrande piezometers provided permeability values of the magnitude of 10^{-11} , 10^{-10} , and 10^{-9} m/s for the stiff clay, softened clay, and slide debris, respectively.

However, bulk hydraulic permeability of the softened clay and the shallow debris could be significantly higher due to the presence of vertical fissures and joints.

Since prehistoric times, failures and slow movements have been affected the Orvieto slopes (Lembo Fazio et al. 1984): the two historically failures events (Porta Cassia, on northern slope, 1900 and Cannicella, on southern slope, 1979) were induced by man-made changes to slope geometry or hydraulic conditions; ongoing slow movements (translational) are directly related to soil-atmosphere interaction. Deep movements occur along pre-existing slip surfaces located within the softened part of clay formation (displacement rates from 2 to 6 mm/years) while, shallow movements, superimposed to the deep ones, involve the debris cover and show higher displacement rate (displacements between 7 and 12 mm/month).

For this reason, since 1982 the northern slope (Fig. 1) has been monitored; for each of seven monitoring stations, instrumented boreholes provide displacements values (through the inclinometers) and piezometric levels (Casagrande piezometers) at several depths within the soil.

The contemporary presence of weather data and of displacement measures has allowed to check, in previous researches (Tommasi et al. 2006, 2012), how the cumulative precipitation of 120 days P_{120} exhibits a very good correlation with activity of deep movements; a value of such parameter ranging from 400 mm and 500 mm, appears as a reasonable threshold beyond which sliding re-activate or sharply accelerates.

The P_{120} frequency distribution over the 30-years monitoring period is approximated through the Generalized Extreme Value (GEV) model (continuous black line in Fig. 3), the recurrence period T_r for the values corresponding to the extremes of the “threshold” interval defined above, ranges from 1.5 and 3 years, close to the mean value calculated for observed period of landslide reactivation.

Data and Methods

Observed Data

Daily temperature and precipitation data for Orvieto site are available since 1921 thanks to a meteorological station of the Hydrological Office of Regione Umbria located on top of slab (315 m a.s.l.), very close to the investigated slope. The daily data cover the time window 1921–2010; the rainfall values time series result quite complete; major gaps concern the period 1943–1946 (reliable observations are not available even for neighboring stations) and the data related to years 1966, 1979 and 1980; for these 3 years, data are replaced by measurements at Acquapendente station (425 m a.s.l.; about 20 km away from the case study site). This choice was dictated by the good agreement between cumulated precipitation values of Orvieto and Acquapendente station on seasonal and annual scale during regular working periods.

COSMO-CLM Regional Climate Model

In this study, COSMO-CLM regional climate model is considered to perform dynamical downscaling (Rockel et al. 2008).

In order to test the capabilities of the regional model in reproducing the present climate, two simulations have been performed for the control period 1981–2010: one forced by ERA-Interim Reanalysis (Dee et al. 2011) allowing a characterization of the error related only to the regional climate model COSMO-CLM and one driven by CMCC-CM global climate model (Scoccimarro et al. 2011) in order to test the predictive capabilities of GCM + RCM simulation chain.

The two COSMO-CLM simulations adopted in this work have been performed over Italy (3–20°E/36–50°N) at a

horizontal resolution of 0.0715° (about 8 km), 40 vertical levels and seven soil levels.

Bias Correction Techniques

The aim of this work is to investigate what is the benefit of implementing bias correction techniques in order to reduce the bias of climate models. The three considered bias correction methods are: (i) linear-scaling (LS), (ii) quantile mapping (QM), and (iii) MOS Analog method.

Linear scaling is the simplest approach: it consists in scaling the model data using a corrective factor calculated as the ratio of observed and simulated monthly mean precipitations:

$$P^*(d) = P(d) \frac{\mu_m(P_{obs}(d))}{\mu_m(P_{rcm}(d))} \quad (1)$$

where, for the day d of the month m , $P^*(d)$ is the corrected value, $P(d)$ is the original daily precipitation from the RCM, $\mu_m(P_{obs}(d))$ and $\mu_m(P_{rcm}(d))$ are respectively the observed and simulated monthly average precipitation for the month m .

The quantile mapping correction, instead, tries to adjust all the moments of the probability distribution function (PDF) of the precipitation field. It estimates P^* as a function of the original variable P using a transfer function calculated forcing the equality between the CDF (cumulative distribution function) of the observed and simulated variables (Piani et al. 2010):

$$F_{rcm}(P_{rcm}) = F_{obs}(P_{obs}) \quad (2)$$

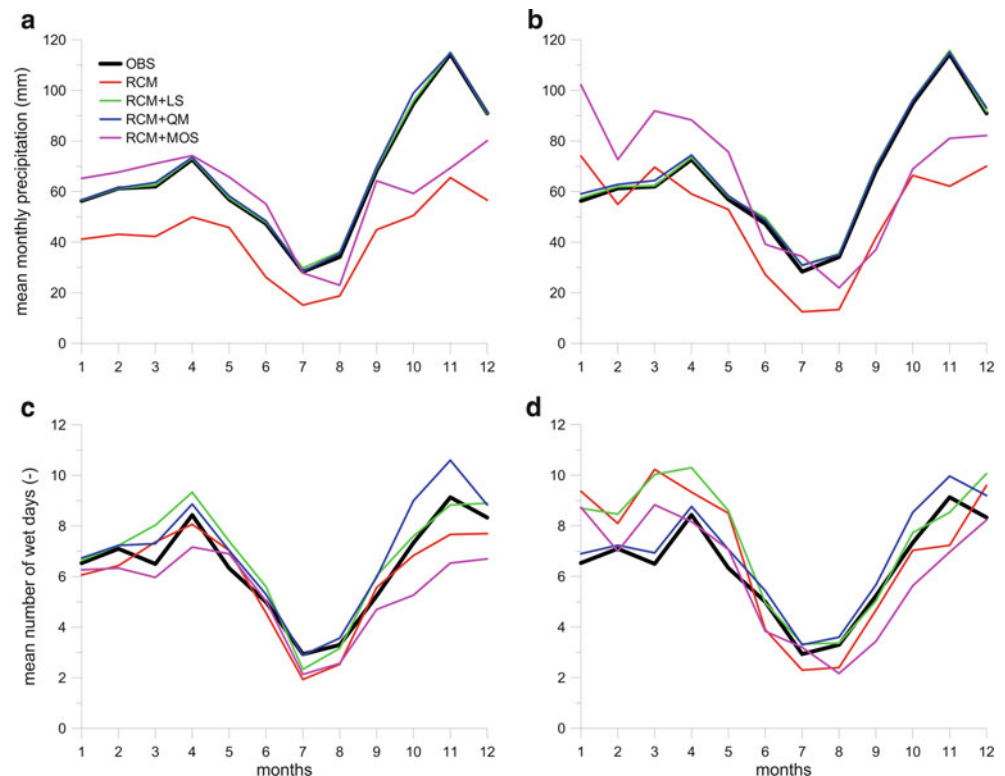
where F_{rcm} and F_{obs} are, respectively, the CDF of the simulated and observed precipitation. So the corrected precipitation is obtained using the following equation:

$$P^*(d) = F_{obs}^{-1}(F_{rcm}(P_{rcm}(d))) \quad (3)$$

The most commonly used distribution for representing the PDF of precipitation is the Gamma distribution, dependent only on two parameters. Several studies have proved that it is effective for modeling rainfall data (see e.g. Gutjahr and Heinemann 2013; Teutschbein and Seibert 2012). In this study we use this distribution to approximate both observed and simulated monthly data.

The last considered bias correction technique is the MOS analog method. The original idea of this method (Lorenz 1969) is based on the comparison between large-scale weather patterns and observational record: a simulated large-scale atmospheric situation (predictor) is compared to each one of the historical observations and the most similar,

Fig. 2 Mean monthly precipitation (a), (b) and mean number of wet days (c), (d) for observed data (OBS), original simulation (RCM) and corrected simulations using linear scaling (RCM + LS), quantile mapping (RCM + QM) and MOS analog (RCM + MOS) methods. Plots are relative to the simulations forced by ERA-Interim (a)–(c), and by the GCM, CMCC-CM (b)–(d)



according to Euclidean distance, is chosen as its analog. The corresponding local-scale observation (predict and) is then associated to the simulated large-scale pattern. This procedure is repeated for each day to be downscaled. Here a new implementation of the standard analogs method is considered, that has been positively tested over Spain by Turco et al. (2011), in which the predictor is the daily RCM precipitation.

Results

Mean monthly precipitation (Fig. 2a, b) and mean number of wet days $\mu_m(n_{wd}(d))$ (Fig. 2c, d) are displayed for the observed data (black line) and for the COSMO-CLM model forced by ERA-Interim reanalysis data (left side), and by the GCM, CMCC-CM (right side) respectively under uncorrected or bias-corrected configurations.

For estimating the landslide activity of the Orvieto slope, sensitive to cumulative rainfall over very long periods, both $\mu_m(P_{obs}(d))$, and $\mu_m(n_{wd}(d))$ play a significant role.

The configuration, with “perfect” boundary conditions allows to isolate the uncertainties related only to RCM (+BCT), while GCM + RCM(+BCT) enables to evaluate the uncertainties of the entire simulation chain.

To increase the signal to noise ratio (Maraun et al. 2010; Fowler and Ekström 2009), results are not calculated for the grid point nearest to the slope but for a 5×5 grid point box

having the investigated area as midpoint. This procedure considers the spatial scale on which RCM has provided, for this test, the higher predictability.

Observed data show a rainfall pattern typical of Central Italy characterized by two peaks: the first one between March and April and the second one, much sharper, between October and November.

All approaches reproduce the actual pattern of mean precipitation (Fig. 2a, b); nonetheless, for both forcing configurations, COSMO-CLM values show a significant underestimation during the entire year; the bias is comparable to that shown by other RCMs (Frei et al. 2006; Christensen et al. 2007). The model dramatically underestimates the marked rainfall peak in the fall season (on average, of 40 mm/month) while in the other seasons the bias is less pronounced, but still significant. Of course, such data are not suitable for impact studies. Regardless of how regional model is driven, linear scaling and quantile mapping allow to nullify the bias. LS approach, acting on the monthly average values of RCM precipitation distribution, essentially moves upward the initial RCM trend, while QM, trying to reproduce the entire distribution as well as possible, completely removes the error associated to the mean value, reduces greatly the error related to standard deviation and, at lesser extent, the error for the other statistical moments (further results not shown).

On the other hand, the MOS analog approach, although markedly improves the RCM estimates, does not reach the

same results, probably, because it is more affected by the intrinsic difficulty of relating a model to a single station point.

Indeed it should be noted that the model output is not a point value but an average value over a grid which is reliable at the scale of a few grid cells (Maraun et al. 2010). In Fig. 2c, d, the seasonal cycles of the mean number of wet days (e.g. daily rainfall higher than 1 mm) for both forcing configurations are displayed. COSMO-CLM forced by re-analysis data captures the observed cycle during the winter and spring seasons but it underestimates the number of rainy days during the summer and fall seasons (probably due to a poor estimation of convective events); instead, COSMO-CLM forced by GCM CMCC-CM probably reproduces too many drizzle days in winter and spring, overestimating the mean number of wet days in these seasons.

Following Maraun (2013), it could be attributable more than to deficiencies of the RCM but mostly to scale mismatch between rain gauge point and area average simulations. Regarding the BCTs, the MOS analog approach again does not properly correct the RCM outputs and exasperates its underestimation during the summer and fall; LS approach allows a better estimate mainly for ERA-Interim driven configuration. QM technique, working on the entire probability distribution, change heavily the RCM values; for ERA-Interim driven configuration, it involves an overestimation of actual number of wet days during the fall and early winter season while, for GCM driven configuration, it allows to get an excellent estimate of measured values (bias much lower than 1 day during the entire year).

Finally, the poor performance of the MOS analog approach (in the last column) points out how it is not a suitable tool to remove bias to the slope station scale.

The described results lead to the estimates of activity of deeper movements reported in Fig. 3. The estimates, using GEV model, of the recurrence period T_r of P_{120} values (observed or simulated according the four approaches) are reported.

Under both configurations (ERA driven and GCM-driven), uncorrected RCM approach returns values of the “threshold” interval which are significantly underestimated. The MOS analog approach partly improves them despite, for the upper extreme of the range, estimates a value three times higher and thus a consistent underestimation of the landslide body movements.

LS and QM approaches are able to fit the GEV based on observed data regardless of forcing adopted for the regional model; in particular, the QM technique only slight deviates from the observed values, at very high P_{120} when ERA-Interim data is adopted to force RCM.

The approach carried out, in this case, to estimate landslide activity, requires as input only the maximum yearly cumulative precipitation and it is completely insensitive about the distribution of the precipitation over the seasons;

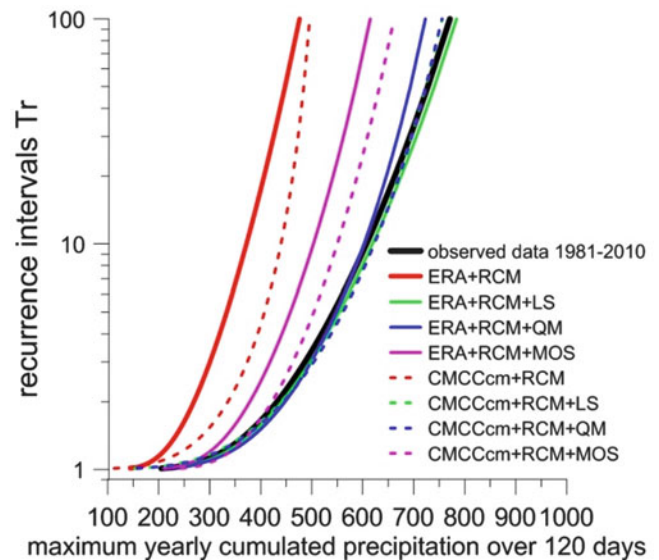


Fig. 3 Estimate of the recurrence period of P_{120} according to GEV model on 1981–2010 observed dataset (black line); continuous and dashed lines are, respectively, adopted for ERA-Interim and CMCC-CM driven configurations for uncorrected outputs (red) or corrected according quantile mapping (blue), linear scaling (green) or MOS analog (magenta) approaches

under such hypotheses, LM and QM return nearly the same results.

Conclusions

As already found in other impact studies about the effect of climate changes conducted with GCM/RCM simulations, the outputs of these climate models are not directly suitable also for landslides.

The choice of the proper bias correction technique is a function of the analysis scale and of the tool used for estimating slope stability.

In this respect, this work proves that, at the slope scale, MOS analog technique is not applicable.

Moreover if the estimate of landslide activity is only based on the average precipitation values, LS and QM return similar performances. Conversely, if the slope hydrologic balance is carried out through more sophisticated tools, the daily variability can be significant and BCTs, able to correct the entire distribution, have to be adopted.

In the specific for QM, the γ -distribution-based correction method performs well in reducing RCM output errors, but is only applicable if observed and simulated precipitation follow a γ -distribution. A possible alternative is the use of nonparametric methods. In the literature, other QM approaches using empirical distribution functions exist and have the advantage of being used without specific assumptions about rainfall frequency distribution (Lafon et al. 2013; Gudmundsson et al. 2012). These methods have proven to return excellent performances but they

have many degrees of freedom and therefore they are more sensitive to the choice of time period and to possible overfitting (Gutjahr and Heinemann 2013). Moreover the application of this method for future periods is more problematic due to the likely presence of unprecedented values in future scenarios (Berg et al. 2012).

Furthermore, the need of implementing stochastic bias correction approaches to properly address the scale mismatch between point observation and area-averaged simulations (Maraun 2013) will be examined.

Acknowledgments The authors Rianna and Zollo have developed this work within the framework of GEMINA and NextData projects, funded by the Italian Ministry of Education, University and Research and the Italian Ministry of Environment, Land and Sea.

References

- Berg P, Feldmann H, Panitz HJ (2012) Bias correction of high resolution regional climate model data. *J Hydrol* 448–449:80–92
- Christensen JH, Hewitson B, Busuioc A, Chen A, Gao X, Held I, Jones R, Koli RK, Kwon W-T, Laprise R, Rueda VM, Mearns L, Menéndez CG, Räisänen J, Rinke A, Sarr A, Whetton P (2007) Regional climate projections. In: Solomon S, Qin D, Manning M, Chen Z, Marquis M, Averyt KB, Tignor M, Miller HL (eds) *Climate change, the physical science basis. Contribution of working group I to the fourth assessment report of the Intergovernmental Panel on Climate Change*, Cambridge University Press, Cambridge, pp 847–940
- Coe JA, Godt JW (2012) Review of approaches for assessing the impact of climate change on landslide hazards. In: Eberhardt E, Froese C, Turner AK, Leroueil S (eds) *Landslides and engineered slopes, protecting society through improved understanding*, vol 1. Proceedings of the 11th international and 2nd North American symposium on landslides and engineered slopes, Banff, Canada, 3–8 June 2012. Taylor & Francis Group, London, pp 371–377
- Collison A, Wade S, Griffiths J, Dehn M (2000) Modelling the impact of predicted climate change on landslide frequency and magnitude in SE England. *Eng Geol* 55:205–218
- Crozier MJ (2010) Deciphering the effect of climate change on landslide activity: A review. *Geomorphology* 124:260–267
- Dee DP, Uppala SM, Simmons AJ, Berrisford P et al (2011) The ERA-Interim reanalysis: configuration and performance of the data assimilation system. *Q J R Meteorol Soc* 137(656):553–597
- Dehn M, Burger G, Buma J, Gasparetto P (2000) Impact of climate change on slope stability. *Eng Geol* 55:193–204
- Dixon N, Brook E (2007) Impact of predicted climate change on landslide reactivation: case study of Mam Tor, UK in Landslides. *J Int Consort Landslides* v 4(2):137–147
- Fowler HJ, Ekström M (2009) Multi-model ensemble estimates of climate change impacts on UK seasonal precipitation extremes. *Int J Climatol* 29(3):385–416
- Frei C, Schöll R, Fukutome S, Schmidli J, Vidale PL (2006) Future change of precipitation extremes in Europe: intercomparison of scenarios from regional climate models. *J Geophys Res* 111, D06105. doi:10.1029/2005JD005965
- Gudmundsson L, Bremnes JB, Haugen JE, Engen Skaugen T (2012) Technical note: downscaling RCM precipitation to the station scale using statistical transformations – a comparison of methods. *Hydrol Earth Syst Sci* 2012(9):6185–6201. doi:10.5194/hess-16-3383-2012
- Gutjahr O, Heinemann G (2013) Comparing precipitation bias correction methods for high-resolution regional climate simulations using COSMO-CLM. *Theor Appl Climatol*: 1–19
- Kilsby CG, Jones P, Burton A, Ford A, Fowler H, Harpham C, James P, Smith A, Wilby R (2007) A daily weather generator for use in climate change studies. *Environ Model Softw* 22:1705–1719
- Lafon T, Dadson S, Buys G, Prudhomme C (2013) Bias correction of daily precipitation simulated by a regional climate model: a comparison of methods. *Int J Climatol* 33(6): 1367–1381. doi: 10.1002/joc.3518, 10.1002/joc.3518#_blank
- Lembo Fazio A, Manfredini M, Ribacchi R, Sciotti M (1984) Slope failure and cliff instability in the Orvieto hill. In: 4th international symposium on landslides, vol 2. Toronto, pp 115–120
- Lorenz E (1969) Atmospheric predictability as revealed by naturally occurring analogues. *J Atmos Sci* 26(4):636–646
- Maraun D, Wetterhall F, Ireson AM, Chandler RE, Kendon EJ, Widmann M, Brienen S, Rust HW, Sauter T, Themessl M, Venema VKC, Chun KP, Goodess CM, Jones RG, Onof C, Vrac M, Thiele-Eich I (2010) Precipitation downscaling under climate change. Recent developments to bridge the gap between dynamical models and the end user. *Rev Geophys* 48: RG3003. doi: 10.1029/2009RG000314
- Maraun D (2013) Bias correction, quantile mapping and downscaling. Revisiting the inflation issue. *J Clim* 26:2137–2143
- Piani C, Weedon GP, Best M, Gomes SM, Viterbo P, Hagemann S, Haerter JO (2010) Statistical bias correction of global simulated daily precipitation and temperature for the application of hydrological models. *J Hydrol* 395(3–4):199–215
- Rockel B, Will A, Hense A (2008) The regional climate model COSMO-CLM (CCLM). *Meteorol Z* 17(4):347–348
- Scoccimarro E, Gualdi S, Bellucci A, Sanna A, Fogli PG, Manzini E, Vichi M, Oddo P, Navarra A (2011) Effects of tropical cyclones on ocean heat transport in a high-resolution coupled general circulation model. *J Clim* 24:4368–4384
- Sidle RC, Ochiai H (2006) Landslides: processes, prediction, and land use. *Water Resour Monogr Ser* 18:312 (AGU, Washington, DC). doi:10.1029/WM018
- ThemeBl MJ, Gobiet A, Heinrich G (2010) Empirical-statistical downscaling and error correction of daily precipitation from regional climate models. *Int J Climatol* 31:1530–1544. doi:10.1002/joc.2168
- Teutschbein C, Seibert J (2012) Bias correction of regional climate model simulations for hydrological climate change impact studies: Review and evaluation of different methods. *J Hydrol* 456–457:12–29
- Tommasi P, Pellegrini P, Boldini D, Ribacchi R (2006) Influence of rainfall regime on hydraulic conditions and movement rates in the overconsolidated clayey slope of the Orvieto hill (Central Italy). *Can Geotech J* 43:70–86
- Tommasi P, Boldini D, Caldaroni G, Coli N (2012) Influence of infiltration on the periodic re-activation of slow movements in an overconsolidated clay slope. *Can Geotechn J* 2013 50(1):54–67. doi:10.1139/cgj-2012-0121
- Turco M, Quintana-Seguì P, Llasat MC, Herrera S, Gutiérrez JM (2011) Testing MOS precipitation downscaling for ENSEMBLES regional climate models over Spain. *J Geophys Res* 116(D18):1–14

Recognition and Mechanics of Landslides



Introduction: Recognition and Mechanics of Landslides

L. Picarelli and B. Abolmasov

Abstract

Landslides are complex geologic events whose movement patterns (mechanisms) are strongly related to the mechanical processes that take place in the soil/rock mass from the pre-failure to the post-failure stage. Only a clear understanding of the relations between mechanisms and mechanics can support landslide analysis and mitigation.

Keywords

Landslide mechanisms • Mechanics • Classification

A landslide is the last stage of a failure process, started some time ago somewhere in the slope, which can be considered fully accomplished only when both edges of an often thin persistent zone of rupture, spreading into the outcrop (typically a shear or a tensile zone depending on material), eventually reach the ground surface. At that time no further reserve of strength is available and conventionally infinite strains can eventually take place within the zone of rupture.

The mechanics of the failure process is always complex, being affected by a number of factors, as the slope geometry, the outcrop lithology and/or structure, the initial conditions (both state of stress and pore pressures), the boundary conditions (or triggering factors, according to a simplified view of the problem), the rate of stress change and the soil properties. With a few exceptions, slope failure is then a progressive process which can follow variable mechanisms and rates revealed by the landslide type, that is roughly categorized through classic landslide classifications [see Varnes (1978), or the more recent update by Hungr et al. (2013)].

An important feature which still more contributes to landslide classification is the mechanism of post-failure movements, which can be by fall, topple, slide, flow, spread, or by a combination of these styles. Again, different factors contribute to the movement pattern: slope geometry, geological settings, rock and soil properties, failure mechanism, pore pressure regime and potential changes induced by the failure itself or by subsequent movement. It is well known and widely recognized that the post-failure pattern is a key aspect which affects the landslide intensity, thus the hazard and risk and both the procedures to adopt and the resources to provide for risk mitigation.

Therefore, a landslide has always to be viewed as the result of a mechanical process covering the pre-failure, the failure and the post-failure stage (Leroueil et al. 1996). Mechanism (or pattern) and mechanics of the entire process cannot be separated (Picarelli 2000). Without a clear view of this close relationship any landslide cannot be completely understood and its potential consequences mitigated. This should be a major aim of investigations, including site surveys, site investigations, laboratory testing, monitoring results, numerical experiments and analyses.

These were excellent reasons to organize a session on “Recognition and Mechanics of Landslides”, well aware that useful data and considerations on landslide mechanisms and mechanics can be found in any paper, whatever is the session to which it belongs, provided it deeply grounds its roots in the domain of the Soil or Rock Mechanics.

L. Picarelli (✉)
Department of Civil Engineering, Design, Home Building and Environment, Seconda Università di Napoli, Aversa, Italy
e-mail: luciano.picarelli@unina2.it

B. Abolmasov
Faculty of Mining and Geology, University of Belgrade, Belgrade, Serbia

References

- Hungr O, Leroueil S, Picarelli L. (2013) Varnes classification of landslide types, an update. *Landslides*. ISSN:612-510X, doi:[10.1007/s10346-013-0436-y](https://doi.org/10.1007/s10346-013-0436-y)
- Leroueil S, Vaunat J, Picarelli L, Locat J, Lee H, Faure R (1996) Geotechnical characterization of slope movements. In: Senneset K (ed) Special lecture, landslides, 7th international symposium on landslides, Trondheim, vol 1. A.A. Balkema, Rotterdam, pp 53–74. ISBN:90 5410 818 5
- Picarelli L (2000) Mechanisms and rates of slope movements in fine grained soils. In: Issue paper, international conference on geotechnical and geological engineering GeoEng2000, Melbourne, vol 1. pp 1618–1670
- Varnes DJ (1978) Slope movement types and processes. In: Schuster RL, Krizek RJ (eds) *Landslides, analysis and control*, special report 176: Transportation Research Board, National Academy of Sciences, Washington, DC, pp 11–33



Mechanism and Dynamics of Umka Landslide, Belgrade, Serbia

Biljana Abolmasov, Svetozar Milenković, Branko Jelisavac, Uroš Đurić, and Miloš Marjanović

Abstract

Landslide development along the valley banks of the Sava and Danube rivers is linked to the theory of river channel evolution, which encompasses the synchronous evolution of erosion and accumulation processes within the river channels and their impact on the morphological modeling of river banks. Within this process, the evolution of each part of the river valley is carried out regularly, with the development of characteristic relief forms on one hand and adequate accumulation products on the other. One of the largest landslides in Serbia, Umka, is formed on the right bank of the river Sava. The physical and mechanical properties of the colluvium vary over a wide range due to the complex composition and susceptibility to external impacts. By analyzing all the available data in the light of monitoring results, it may be possible to come to a rational explanation of the landslide's origin, properties and their mechanism and dynamics, position and features of landslide zones and dependable definition of landslip maximum depth with a realistic forecast of further development.

Keywords

Landslide origin • Mechanism • Monitoring • Dynamics

Introduction

Slopes instabilities in the areas on the edges of the Pannonia basin, as well as in the wider vicinity of Belgrade, i.e. the slopes of the right banks of Sava and Danube, are well known in the literature. They were reported in the past by Luković (1951), Perić (1970), Vujanić et al. (1981) and

Lokin et al. (1988). The basic cause of these instabilities is the complexity of geological and morphological evolution of the terrain during the Tertiary and Quaternary, related to the synchronised fluvial erosion of the right banks of the Sava and Danube and accumulation on the left bank (Rokić 1997; Rokić et al. 1998; Rokić and Vujanić 2002). Intensive human activities, especially during the twentieth century, reactivated many fossil landslides of the right banks of Sava and Danube, and activated numerous new ones.

Landslide Umka is located 25 km south-west of Belgrade, Serbia (Fig. 1), and has been investigated in detail over the past 30 years, which provides extensive geotechnical documentation, as well as a great number of published papers: Vujanić et al. (1981, 1984, 1995), Čorić et al. (1994, 1996), Dangić et al. (1997), Hadžiniković (1998) and Jelisavac et al. (2006). The last phase of investigations for the Preliminary Design of the E-763 motorway was completed in 2005, and no further investigation has been conducted since then. No remedial measures were implemented, and the motorway

B. Abolmasov (✉) • U. Đurić • M. Marjanović
Faculty of Mining and Geology, University of Belgrade, Đušina 7,
11000 Belgrade, Serbia
e-mail: biljana@rgf.bg.ac.rs; djuric@rgf.bg.ac.rs; milos.marjanovic@rgf.rs

S. Milenković
Geomonitoring Team, Juriša Gagarina 111, 11070 Belgrade, Serbia
e-mail: tozony@gmail.com

B. Jelisavac
The Highway Institute, Kumodraška 257, 11000 Belgrade, Serbia
e-mail: jelisavac.branko@gmail.com

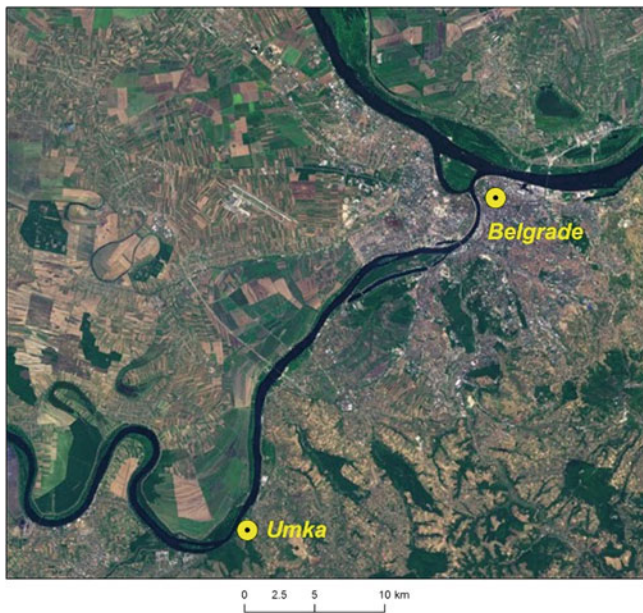


Fig. 1 Geographical location of the study area

was not built. Conventional monitoring of the Umka landslide lasted during the financing period of the investigations in 1992 and 2005, but after the completion of the last phase in 2005 this was also stopped. Automated GNSS monitoring was established in March 2010 in the body of the Umka landslide as part of a project supported by the Ministry of Education, Science and Technological Development of the Republic of Serbia TR 36009 (Abolmasov et al. 2012). Since November 2012, research and monitoring of the Umka landslide are supported as project No 181 ICL/IPL.

This paper presents the results of investigations undertaken until now, as well as the results of the landslide monitoring. The analysis of all currently available results of investigations and monitoring of the landslides allowed remedial measures to be proposed. These proposed remedial measures are the result of combined knowledge and understanding of the causes, mechanisms and dynamics of the landslide of Umka near Belgrade.

Materials and Methods

Detailed geotechnical investigations of the Umka and Duboko landslide localities have been conducted to prepare technical documentation for different phases of planning and design of the E-76 (renamed to E-763) highway, which transects both landslides. Smaller scale investigations have been undertaken for urban development of the Umka settlement. The first phase of investigations began in 1979 by the Highway Institute Belgrade; however, this documentation was not available. Results of this phase of investigations

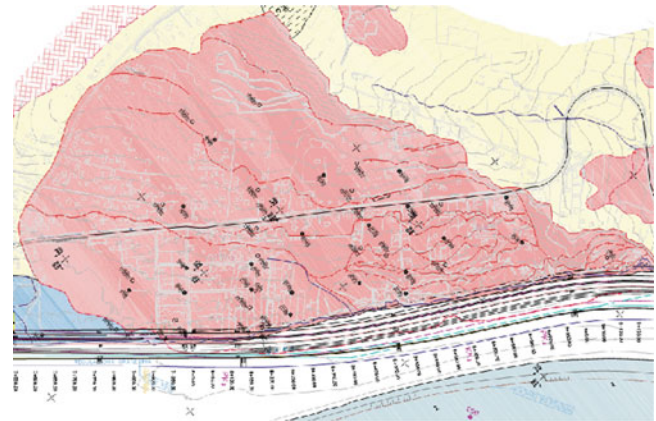


Fig. 2 Engineering geological map of Umka landslide

were published by Vujanić et al. (1981, 1984). The following and most extensive phase of was completed in 1992, and the documentation was available in analogue format, as were the published reports and papers Ćorić et al. (1994, 1996), Dangić et al. (1997), Hadžiniković (1998) and Jelisavac et al. (2006). Apart from extensive geotechnical investigations, various paleontological, mineralogical, geochemical, chemical, hydrological and other investigations were conducted during this phase. Large number of samples from the landslide body, sliding surface and bedrock taken from boreholes, shafts and pits were tested in the laboratory in order to establish their physical and mechanical characteristics (determination-classification and stress-strain tests). Conventional monitoring of the landslide included monitoring in 10 inclinometer constructions and 65 geodetic reference points that were recorded by tachymetry. In addition, the inhabitants of the Umka settlement have been interviewed and an inventory of types and level of damage to the housing structures was carried out. The last phase of investigations was completed in the period 2005–2006, and during this phase the accent was on landslide monitoring and definition of the exact depth to the sliding surface.

During the investigations conducted in 2005, intensive secondary movements within the body of the Umka landslide occurred, so the most of inclinometer constructions were stopped after 3–4 months. At the same time, the recorded levels of river Sava were very high, as were the levels of underground waters after the period of rapid thaw during the early spring (Abolmasov et al. 2012).

Following 2005 there was no landslide monitoring or investigations conducted until automated GNSS monitoring of the Umka landslide was established in 2010 (Abolmasov et al. 2012, 2013). Since then, the movements and fluctuations of the levels of the Sava, as well as hydro-meteorological parameters (type and amount of precipitation, temperature regime, etc.), have been followed daily.

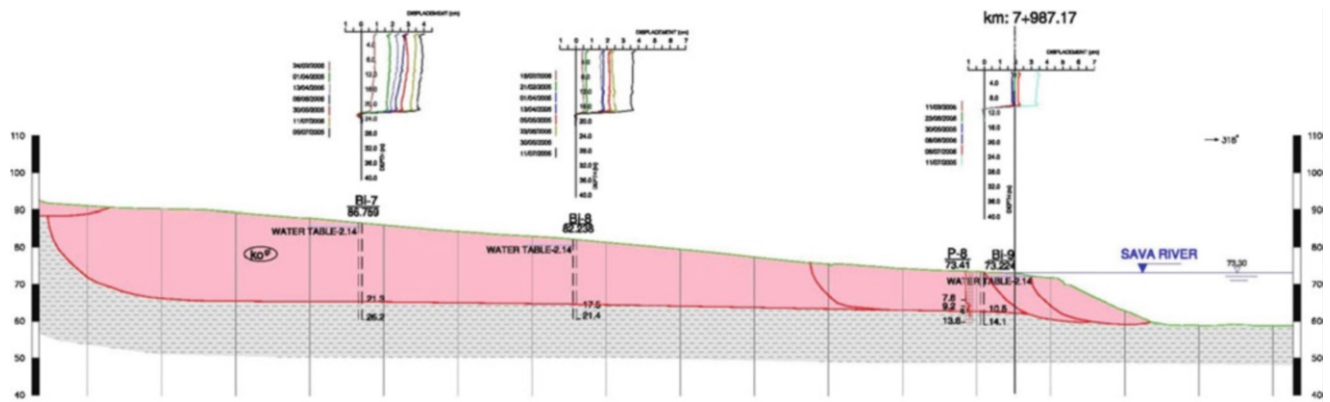


Fig. 3 Engineering geological cross section km 7 + 987.17 (lower part of landslide), block A

Study Area

Landslide Umka is located on the right bank of the river Sava in the crook of the large right meander before its confluence with Danube (Fig. 1). In that section, the river bed narrows and the river main stream directly erodes the right bank. The height difference between the frontal scarp below the elevation of the Rucka hill (187 m a.s.l.) and the river Sava (54 m a.s.l.) is 130 m. The total length of the landslide is approximately 1,450 m and its width is around 900 m. The average inclination of the slope is 9° , apart from the main scarp zone and numerous minor scarps within the landslide body where it is steeper (15° – 30°), or closer to the bank where it is much gentler, up to 6° .

Geological setting of the terrain comprises Neogene—Miocene (Pannonian) grey marls over 200 m in thickness. They are intensively degraded by weathering, so that the thickness of the weathering crust is in places over 26 m. Quaternary sediments—loess—is found only in non-displaced sections of the terrain, outside of the body of the landslide.

Based on the results of geotechnical investigations of the terrain (1980, 1992, and 2005) and on the results of conventional monitoring during 1992 and 2005, the engineering geological composition of the terrain has been defined, with precise dimensions as well as the depth of the sliding surface (Figs. 2 and 3). The landslide covers the area of approximately 1.8 km^2 , and is in the shape of a wide fan, with a volume of around $14,000,000 \text{ m}^3$.

The landslide has been divided into three blocks (A, B, C), based on all of the investigations conducted to date, and depending on the depth of the sliding surface, speed of the displacement and characteristics of the colluvial material (Fig. 4). During the monitoring in 2005, the deepest sliding surface was determined in block A, 26 m, while in the blocks B and C it was between 5 m and 15 m. However, the most intensive secondary displacement was noted in the B block in the embankment area.

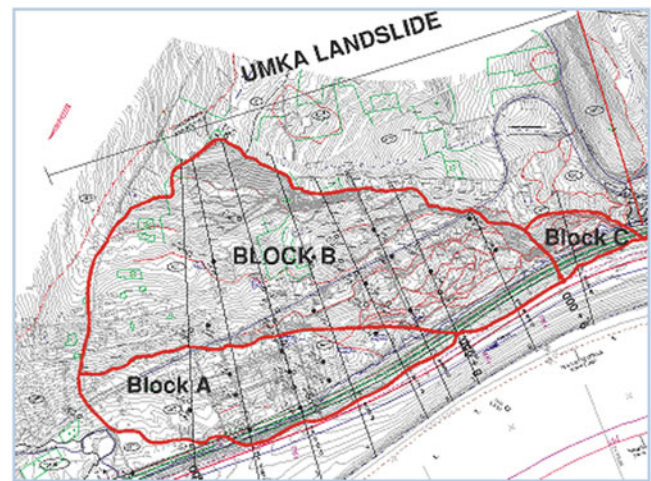


Fig. 4 Zoning of Umka landslide based on sliding mechanism and dynamics



Fig. 5 Deformation on road M-19

Table 1 Shear strength parameters—colluvium, active sliding planes and bedrock (Jelisavac et al. 2006)

Material	ϕ_r' (°)	C_r' (kPa)	$I_c; w$
Sliding planes	7–13	0	$I_c \leq 0.5; w \text{ 30–45 \%}$
Colluvium-weathered marly clays	7–22	15–30	$I_c \text{ 0.5–1.2}; w \text{ 20–45 \%}$
Bedrock-marls	18–28	50–200	$I_c \gg 1; w \leq 30 \%$

Urbanisation of the area began during the early twentieth century, so the Umka landslide is populated with over 500 habitation structures, 80 % of which are damaged. Regional road M 19 Beograd-Šabac, with a daily traffic volume of approximately 10,000 vehicles, transects the landslide. Deformation of the dwellings, as well as the M 19 roadway (Fig. 5), are noticeable.

Results and Discussion

Umka landslide is an old-fossil landslide whose activity started during Pleistocene, due to migration of the Sava’s riverbed and synchronised erosion of the right river bank, coupled with neo-tectonic activity and accumulation of material on the left alluvial plateau.

In the geological history of the terrain, a thick crust of weathered Neogene-Pannonian marls formed during the Pleistocene, leading to the present situation where the colluvial material (weathered brown soft clay marls) are clearly separate from the bedrock (grey hard marls). As a rule, the border of the weathering zone is most often the depth of the deepest sliding surface.

The causes of landslide re-activation are the erosion of the right bank of the Sava river at the landslide toe, combined with prolonged weathering, followed by uncontrolled and continuous urbanisation of the landslide area from the beginning of the twentieth century. Triggers of the intensive activity phase of the landslide are the cumulative precipitation regime or a sudden thaw, in combination with an increase or sudden decrease of the river Sava levels.

Analysis of numerous laboratory results of testing of samples taken from the colluvium, sliding planes and bedrock, defined the parameters and their mechanical characteristics (Table 1).

Data analysis from inclinometer monitoring during 2005, type and amount of precipitation, temperature regime, observation of the levels of underground waters in piezometers, as well as the measuring of the levels of the Sava, indicated that the intensifying of activity was caused by a sudden increase in Sava levels and a sudden thaw (30 cm of snow melted in 24 h), followed by a quick drop in Sava level (Figs. 6, 7 and 8).

After the automated GNSS monitoring in the last 3 years, a similar pattern was observed, and more intense speed of the movement was registered when the aforementioned conditions were present (Abolmasov et al. 2012). During the dry periods and periods of low water levels of the

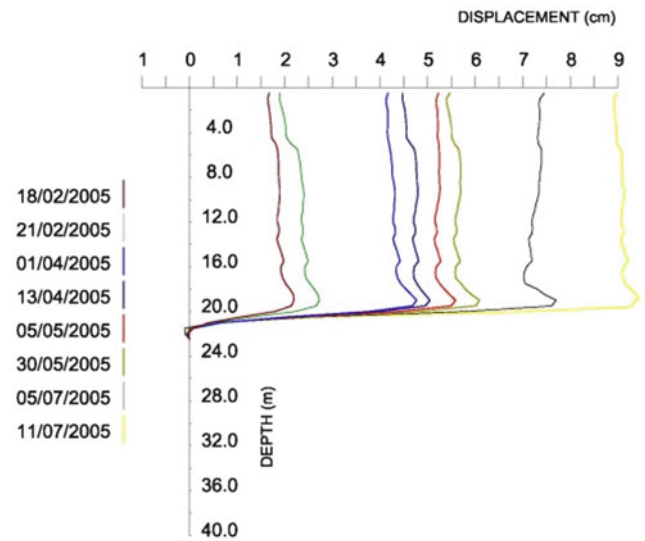


Fig. 6 Data plot from inclinometer BI-11 during 2005 monitoring (block A)

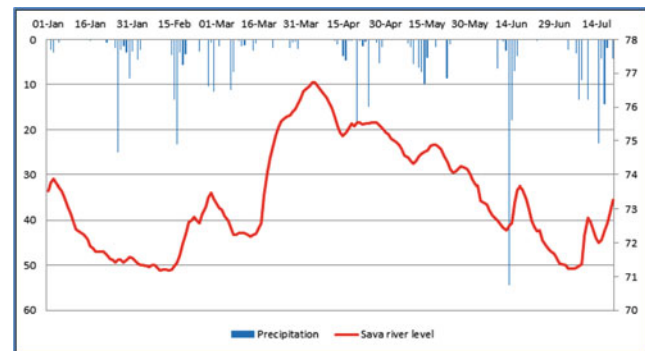


Fig. 7 Average daily precipitation and Sava river level (January–July 2005)

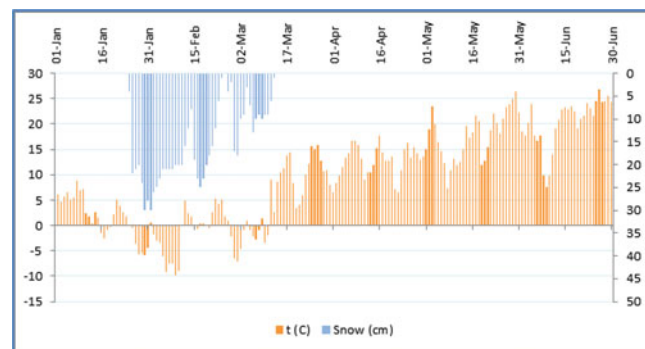


Fig. 8 Average daily temperature and snow amount (January–June 2005)

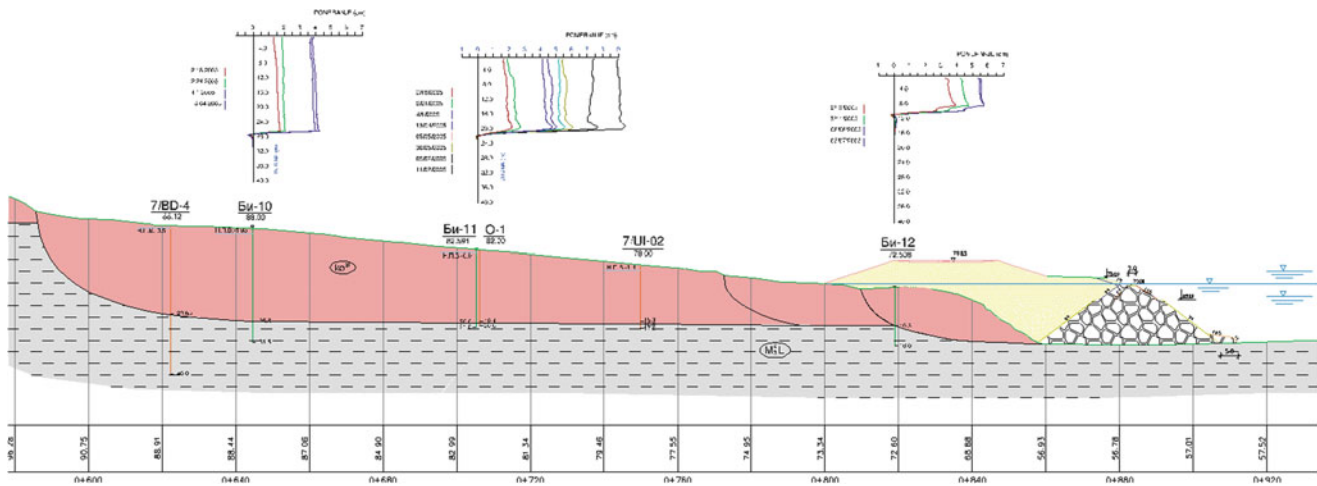


Fig. 9 Engineering geological cross section km 8 + 151 with retaining structure, Block A

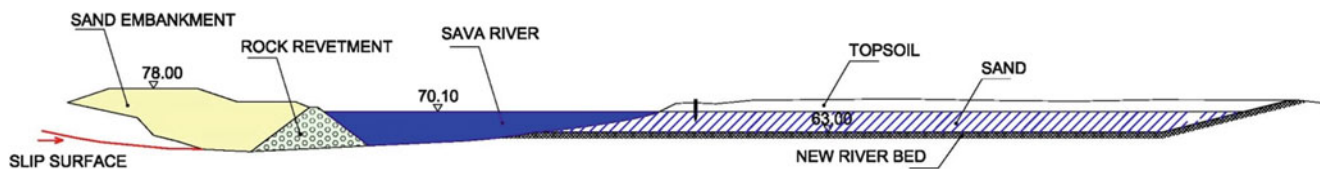


Fig. 10 Schematic model of Sava river channel regulation

Sava, the landslide had a low speed and even a slow-down (i.e. the landslide was becoming a very slow landslide instead of a slow landslide). Umka landslide is a typical slow to very slow landslide, with phases of intensive and slower movements directly triggered by the precipitation regime and fluctuation of the Sava levels.

Based on analyses and a series of iterative procedures, decisions for the design of remedial measures has been made as follows: to widen the river channel of Sava on the left bank, to build a parallel protective retaining and training structure made of crushed stone on the right bank, and to set the motorway road base on a high embankment (made of dredged sand) behind the mentioned structure. In addition, it has been envisioned to carry out the work of drainage, leveling and afforestation of unstable terrains (Figs. 9 and 10).

Conclusion

Umka landslide is the largest active landslide in Serbia. During the last 30 years, extensive investigations were carried out in order to prepare data for designing the E763 highway which transects the landslide. Analysis of the investigation results led the conclusion that the landslide was formed in the Neogene-Pannonian marls which are weathered in the superficial layers, placing the deepest sliding surfaces in the contacts between the weathered-

clayey marls and “fresh” marls as bedrock. Basic causes of the landslide emergence are the prolonged erosion of the right bank of the Sava River in the area of the landslide toe, as well as the specific morphological and hydrogeological characteristics of the terrain, i.e. the physical-mechanical characteristics of the landslide body, sliding surface and bedrock. Unregulated urbanisation of the landslide area also had significant influence.

Umka landslide is complex bloc landslide whose activity intensifies in the periods of saturation by precipitation as well as during sudden changes in the water levels of the river Sava. The course, direction and speed of displacement have been analysed based on inclinometer measurements and automated GNSS monitoring of the landslide. Based on the results, Umka landslide is classified as complex, active, slow to very slow landslide.

Suggested remedial measures during the Preliminary Design phase have emanated from the analysis and synthesis of the results of the investigation conducted during the last 30 years on the Umka landslide, as well as from conditions required by the project design of the E763 motorway.

Acknowledgments The research was supported by the Ministry of Education, Science and Technology of the Republic of Serbia Project No TR 36009 and ICL/IPL Project No 181. The research would have

not been possible without support from Republic Geodetic Authority and Republic Hydrometeorological Service of Serbia.

References

- Abolmasov B, Milenković S, Jelisavac B, Vujanić V, Pejić M, Pejović M (2012) Using GNSS sensors in real time monitoring of slow moving landslides—a case study. In: Eberhardt E, Froese C, Turner K, Leroueil S (eds) Proceedings of the 11th international and 2nd American symposium on landslides and engineered slopes, Banff, Canada, 3–8 June 2012, vol 2. Taylor & Francis Group, London, pp 1381–1385
- Abolmasov B, Milenković S, Jelisavac B, Vujanić V (2013) Landslide Umka: the first automated monitoring project in Serbia. In: Margottini C, Canuti P, Sassa K (eds) Landslide science and practice, vol 2, Early warning, instrumentation and monitoring. Springer, Berlin, pp 339–346, <http://www.springer.com/978-3-642-31444-5>
- Ćorić S, Božinović D, Vujanić V, Jotić M, Jelisavac B (1994) Slope instability analysis in Neogene clays and marls. In: Oliveira R, Rodrigues LF, Coelho AG, Cunha AP (eds) Proceedings of 7th international IAEG congress, Lisboa Portugal, 5–9 September 1994, vol 3. Balkema, Rotterdam, pp 1759–1770
- Ćorić S, Božinović D, Vujanić V, Jotić M, Jelisavac B (1996) Geotechnical characteristics of old landslides in Belgrade area. In: Senneset K (ed) Proceedings of the 7th international symposium on landslides, Trondheim, Norway, 17–21 June 1996, vol 2. Balkema, Rotterdam, pp 689–694
- Dangić A, Vujanić V, Josipović J, Jotić M, Jelisavac B (1997) Geochemical and geotechnical study of complex landslide in vicinity of Belgrade, Yugoslavia. In: Marinos P, Koukis GC, Tsiambaos GC, Stoumbaras GC (eds) Proceedings of the international symposium on engineering geology and environment, Athens, Greece, 23–27 June 1997, vol 1. Balkema, Rotterdam, pp 581–566
- Hadžiniković G (1998) Slope stability analysis in complex geotechnical conditions. In: Moore D, Hungr O (eds) Proceedings of 8th international IAEG congress, Vancouver, Canada, 21–25 September 1998, vol 3. Balkema, Rotterdam, pp 11523–11529
- Jelisavac B, Milenković S, Vujanić V, Mitrović P (2006) Geotechnical investigations and repair of the landslide Umka—Duboko on the route of motorway E-763 Belgrade–South Adriatic. International workshop-Prague geotechnical days, Prague, 2006
- Lokin P, Sunarić D, Cvetković T (1988) Landslides in Neogene sediments on the right Danube bank, Yugoslavia. In: Senneset K (ed) Proceedings of the 5th international symposium on landslides, Trondheim, Norway, 17–21 June 1996, vol 2. Balkema, Rotterdam, pp 213–217
- Luković MT (1951) Važniji tipovi naših klizišta i mogućnosti njihovog saniranja. Geološki Vesnik Savezne uprave za geološka istraživanja, Knjiga IX. Beograd, pp 275–310 (on Serbian)
- Perić J (1970) Hipoteza o uzrocima nastanka klizišta u padini duž desne obale Dunava od Vinče do Grocke. Zbornik radova Rudarsko-geološkog fakulteta, Univerzitet u Beogradu, Sveska 13. Beograd, pp 213–226 (on Serbian)
- Rokić LJ (1997) Origin of landslides on the right bank of Danube river near Novi Sad. In: Marinos P, Koukis GC, Tsiambaos GC, Stoumbaras GC (eds) Proceedings of the international symposium on engineering geology and environment, Athens, Greece, 23–27 June 1997, vol 1. Balkema, Rotterdam, pp 1003–1008
- Rokić LJ, Vujanić V (2002) A contribution to the study of landslide origins in Neogene sediments of Danube river coastal area. In: Rybar J, Stemberk J, Wagner P (eds) Proceedings of the 1st European conference on landslides, Prague, Czech Republic, June 24–26 2002. Balkema Publishers, pp 291–298
- Rokić LJ, Vujanić V, Jotić M (1998) Forecast of the landslide development processes based on the study of erosion processes of rivers in the plains. In: Moore D, Hungr O (eds) Proceedings of 8th international IAEG congress, Vancouver, Canada, 21–25 September 1998, vol 3. Balkema, Rotterdam, pp 1485–1491
- Vujanić V, Livada N, Jotić M, Gojković S, Ivković J, Božinović D, Sunarić D, Šutić J (1981) Klizište “Duboko” na Savi kod Beograda. In: Zbornik radova Simpozijuma istraživanje i sanacija klizišta, Bled 1981, Knjiga 1. pp 119–134 (in Serbian)
- Vujanić V, Livada N, Božinović D (1984) On an old landslide in Neogene Clays on the right bank of the Sava near Belgrade. In: Proceedings of 4th international symposium on landslides, Toronto, Canada, 1984, vol 2. pp 227–233
- Vujanić V, Jotić M, Jelisavac B, Božinović D, Ćorić S (1995) Sinteza rezultata geotehničkih istraživanja klizišta na Savi: Umka I Duboko. In: Zbornik radova Drugog simpozijuma Istraživanje I sanacija klizišta, 6–9 juni 1995, Donji Milanovac, pp 335–351 (on Serbian)



Shear Strength Recovery of Clayey Soils Following Discontinuation of Shear at a Residual State

Deepak R. Bhat, Netra P. Bhandary, and Ryuichi Yatabe

Abstract

Residual shear strength is generally used for design and repairs on slopes containing pre-existing shear surfaces in large-scale landslides. Some recent research works suggest that the pre-existing shear surface of a large-scale landslide can regain strength with the passage of time, which should be considered in designing the slope stability measures. In this study, three landslide soils were tested in a ring shear apparatus with rest periods between shear of 1, 3, 7, 15, and 30 days, with the following main objectives (1) to understand the strength recovery behavior of landslide soils in residual state of shear after as long as 30 days of rest between shearing, (2) to understand the comparative pattern of strength recovery in highly plastic and less plastic soils, and (3) to understand the mechanism involved in strength recovery at residual state of shear. The obtained experimental results indicate that the recovery of shear strength in the residual state started to appear slightly after shear was discontinued for 3 days, and was lost immediately after a very small shear displacement. On the other hand, as understood from the experimental work in this study, the trend of strength recovery, is somewhat in increasing order with prolongation of the period that shear is discontinued.

Keywords

Landslide soils • Residual strength • Strength recovery • Ring shear test

Introduction

Based on the back-analysis of an ancient landslide in cohesive colluvial soil in West Virginia, D'Appolonia et al. (1967) reported that the mobilized shear strength is greater than the drained residual strength of the slip surface material. Direct shear tests on undisturbed specimens containing the

pre-existing shear surface, obtained from shallow portions of the slip surface, show peak strengths greater than drained residual strengths. Researchers have suggested that the shear surface in the cohesive colluvial soil underwent “recovery/healing”, which caused an increase in shear strength beyond the drained residual value. Ramiah et al. (1973) investigated the strength gain in remolded and normally consolidated kaolinite and bentonite in reversal direct shear tests, using rest periods of up to 4 days. Ramiah et al. (1973) found that the strength gain for high plasticity soil (bentonite) is higher, even with a short rest period. Using the Bromhead (1979) ring shear apparatus, the shearing occurs at the top of the specimen, at the soil-to-top bronze porous stone interface. Angeli et al. (1996) used a Bromhead (1979) ring shear tests to study the strength gain mechanism in different clays, including London clay. Tests were performed on normally consolidated specimens. Angeli et al. (1996,

D.R. Bhat (✉)

Geo-Disaster Research Laboratory, Graduate school of Science and Engineering, Ehime University, 3 Bunkyo-Cho, Matsuyama 790-8577, Japan

e-mail: deepakrajbhat@gmail.com

N.P. Bhandary • R. Yatabe

Graduate school of Science and Engineering, Ehime University, 3 Bunkyo-Cho, Matsuyama 790-8577, Japan

e-mail: netra@ehime-u.ac.jp; yatabe@cee.ehime-u.ac.jp

2004) concluded that there is an increase in the recovered shear strength with time during these direct and ring shear tests. Gibo et al. (2002) used a Bishop et al. (1971) type ring shear apparatus and concluded that a silt- and sand-dominated sample recovered its strength; however, the smectite-dominated sample did not recover its strength. Stark et al. (2005) presented Bromhead (1979) type ring shear test laboratory results for two soils of different plasticity for rest periods up to 230 days. Stark et al. (2005) observed that the magnitude of recovered shear strength increases with increasing soil plasticity, but the recovered strength was lost with small shear displacement. Carrubba and Del Fabbro (2008) conducted Bromhead (1979) ring shear tests, similar to those performed by Stark et al. (2005), for rest times of up to 30 days and found more strength gain in Montona flysch than in Rosazzo flysch. Nakamura et al. (2010) and Stark and Hussain (2010) discussed the application of recovered strength in the stability analysis of reactivated landslides.

For the design and repair of slopes containing pre-existing shear surfaces in large-scale landslides, the selection of shear strength parameters is important (Bhat et al. 2011, 2012, 2013b, d). The basic design principle based on the lab-determined drained residual shear strength is consistent with the back-calculated drained residual shear strength for a landslide slip surface. If a preexisting shear surface recovers its residual strength in a short period of time, that recovered strength may be used as a remedial measure for the problematic layer. The recovered strength is greater than the residual strength, which increases the resisting force. Thus, the factor of safety increases, which reduces the cost of remedial measures (Bhat et al. 2013c, 2014). The study of the strength recovery from a residual state of shear is extremely important.

The Bishop et al. (1971) type ring shear apparatus is best suited for investigating the strength recovery in the laboratory because the shear is confined and occurs at a soil-to-soil interface, which may represent the field condition of slip surfaces under slow-moving large-scale landslides (Bhat et al. 2013c, 2014). Gibo et al. (2002) used a Bishop et al. (1971) type ring shear device to first observe the strength recovery effect on soil samples obtained from two different reactivated landslides. They concluded that the strength recovery effect should be considered in the stability analysis of a reactivated landslide dominated by silt and sand particles at an effective normal stress of less than 100 kN/m². However, the use of normally consolidated specimens and the short test duration (i.e. 2 days) may not be sufficient to reach this conclusion. The strength recovery observed for a normally consolidated Xuechengzhen specimen (i.e. silt and sand dominate) may have been caused by the presence of silt or sand particles along the shear surface; these particles may have penetrated the shear surface or zone

during secondary compression of the ring shear specimen and provided some additional shear resistance. However, Gibo et al. (2002) concluded that the Kamenose specimen (i.e., smectite-dominated) did not exhibit any strength recovery. This result contradicts the findings of Ramiah et al. (1973), which indicated that bentonitic soils exhibit higher strength gain. The Xuechengzhen specimen strength gain may have been more pronounced if Gibo et al. (2002) had used a longer rest period. The residual shear strength in pre-existing landslides is more common in overconsolidated soil, and rest periods longer than 2 days are necessary to simulate field conditions.

In this study, three clayey soils collected from large-scale landslide sites in Nepal and Japan are tested using the Bishop et al. (1971) type ring shear apparatus for rest (discontinued shear) periods of 1, 3, 7, 15, and 30 days. This paper describes the ring shear strength recovery laboratory test procedure and the observed strength recovery behaviors of three soil samples. The main objectives of this study are as follows (1) to test the soil strength recovery from the residual state of shear during the long rest period (i.e. up to 30 days) by using the Bishop et al. (1971) type ring shear apparatus, (2) to compare the strength recovery of high plasticity soils and low plasticity soils, and (3) to understand the strength recovery mechanisms at the residual state of shear.

Materials and Method

In this study, three landslide soils were obtained from the large-scale landslide areas in Japan and Nepal. The soil samples were from the Shikoku and the Toyooka-kita landslide areas of Japan, and from the Krishnabhir landslide area of Nepal. The physical properties of the tested samples are shown in Table 1. The solid densities of the Shikoku landslide and the Krishnabhir landslide samples are higher than the solid density of the Toyooka-kita landslide (Table 1). The plasticity index of the Krishnabhir landslide is lower than the Shikoku landslide and the Toyooka-kita landslide.

The torsional ring shear apparatus (based on the concept reported by Bishop et al. 1971) was used in this study. In this apparatus, the specimen container has inner and outer diameters of approximately 8 cm and 12 cm, respectively, and an average thickness of 3.2 cm. The specimen is sheared through a level of 0.7 cm above the base of the lower plate. The ratio of the outer to inner ring diameters is 1.5. In this study, all tests are conducted in a drained condition. The excess pore water pressure is assumed to dissipate and to have no influence on the normal stress in the drained condition. Thus, the effect of pore water pressure is negligible.

There are two main steps in the strength recovery test. (1) The ring shear test: This test is performed to obtain the residual state of the shear of specimens in the fully saturated

Table 1 Physical properties of tested samples

Sample type	Solid density	Plasticity index (%)	Grain size classification (%)		
			Clay	Silt	Sand
Krishna-bhir landslide	2.74	13.41	21.0	59.7	19.3
Shikoku landslide	2.75	16.26	20.0	68.1	11.9
Toyooka-kita landslide	2.65	37.50	24.0	55.1	20.9

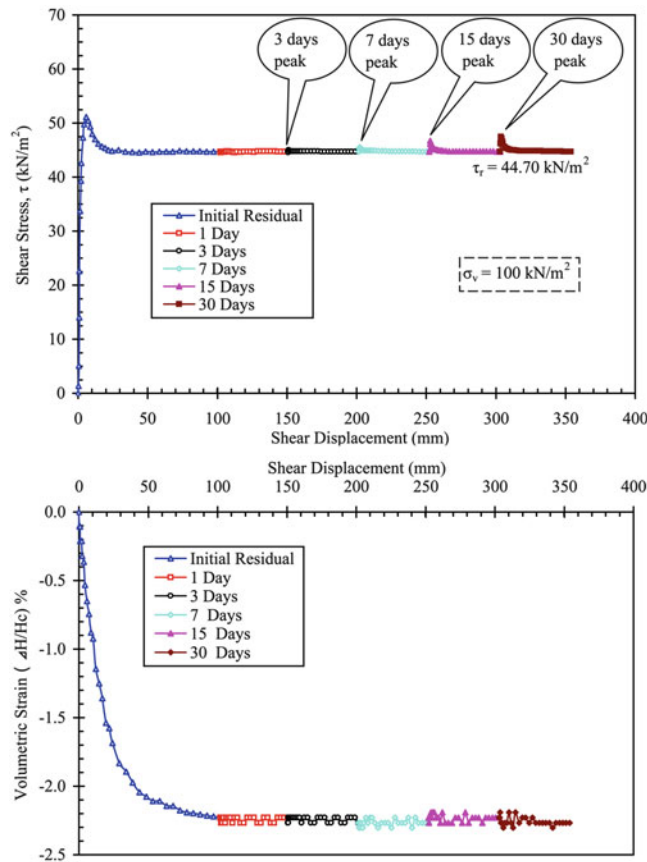


Fig. 1 Typical results of ring shear tests and strength recovery tests (on Krishnabhir landslide)

state. This residual state is confirmed when the shearing has reached the value of minimum shear, as indicated by constant values for both the load-cell and dial gauge readings after a large displacement. The specimen is then ready for the strength recovery test. (2) The strength recovery test: when the specimen reaches the residual state of shear, the strength recovery test will begin. In the strength recovery test, shearing is stopped after the residual state of shear is achieved, and the specimen is allowed to rest in the ring shear apparatus. The specimen is subjected to the applied effective normal stress and the measured residual shear stress for the duration of the rest period. The shear force applied at the end of the residual strength test is maintained throughout the rest period to simulate field conditions because the sliding mass in the field remains subject to a shear stress after movement. The motor used to rotate the lower part of the

ring shear specimen container remains engaged and prevents any reduction in the shear force during the rest period. Therefore, the specimen remains subject to the residual shear and normal stress during the rest period. The effective normal stress applied during the tests is 100 kN/m².

After a rest period of 1 day, shearing is restarted with a shear and effective normal stress corresponding to the initial drained residual condition. The shearing rate of the specimen is fixed at 0.16 mm/min (Bhat et al. 2013a), and the maximum strength after recovery/healing (which may or may not be greater than the residual value) is measured. Shearing is continued until the residual state of shear is achieved again. After the residual state of shear is achieved again with additional shear displacement, shearing is stopped and the specimen is allowed to rest under the imposed shear and effective normal stress for the next rest period. The recovered shear strength for the other rest periods, i.e. 3, 7, 15, and 30 days, is measured after repeating the 1-day rest period procedure.

Results and Discussion

In the strength recovery test, the ring shear test was initially performed to obtain the residual state of shear. The results of the ring shear tests and the strength recovery tests are presented in terms of shear stress variation and specimen depth with respect to shear displacement. The residual state of shear is obtained after 10.0 cm of shear displacement in the initial condition. The ring shear test results indicate that the peak strength and the residual strength of soil samples from the Krishnabhir landslide are the highest, followed by the Shikoku landslide, and then the Toyooka-kita landslide. However, the difference between the peak strength and the residual strength of the Krishnabhir landslide is the lowest, followed by the Shikoku landslide and then the Toyooka-kita landslide. It is observed that the Krishnabhir landslide is the strongest and that the Toyooka-kita landslide is the weakest. The Toyooka-kita landslide and the Shikoku landslide demonstrate the high plasticity in the soil's nature. Similarly, the Krishnabhir landslide demonstrates a low plasticity in its soil.

Typical results of ring shear tests and strength recovery tests of the Krishnabhir landslide are presented in terms of variation of shear stress and specimen depth with the shear

Table 2 Summary of strength recovery in terms of internal frictional angles

Sample type	Residual frictional angles	Increase in internal frictional angles (deg) ($\Delta\phi_r = \phi_{Rec} - \phi_r$)				
	(ϕ_r , deg)	1 Day	3 Days	7 Days	15 Days	30 Days
Krishnabhir landslide	24.50	0.00	0.13	0.40	0.96	1.33
Shikoku landslide	13.82	0.00	0.25	0.49	1.14	1.65
Toyooka-kita landslide	5.16	0.00	0.38	0.65	1.25	1.96

Table 3 Summary of shear displacements during strength recovery tests

Sample type	Shear displacement upon recovered strength (mm)					
	Initial	1 Day	3 Days	7 Days	15 Days	30 Days
Krishnabhir landslide	5.83	0.00	0.48	0.73	0.73	0.97
Shikoku landslide	4.37	0.00	0.48	0.73	0.97	1.46
Toyooka-kita landslide	2.43	0.00	0.73	0.97	1.46	1.46

displacement (Fig. 1). The value of the residual friction angle (ϕ_r) and the difference between the drained recovered friction angle (ϕ_{Rec}) and residual friction angle (ϕ_r) (i.e., increase in the frictional angle, $\Delta\phi_r = \phi_{Rec} - \phi_r$) of the Krishnabhir, Shikoku, and the Toyooka-kita landslide soils are summarized in Table 2. For identical rest periods, the friction angle increase is slightly greater in the case of the Toyooka-kita landslide, followed by the Shikoku landslide and then the Krishnabhir landslide (Table 2). There are no frictional angle increases for the 3 days rest periods, but the frictional angles increase by only one degree or so for the rest periods of 30 days.

The shear displacement during the strength recovery test results are summarized in Table 3. The peak strength (i.e. 51.09 kN/m²) was obtained after the initial shear displacement of 5.83 mm in the case of the Krishnabhir landslide. After the rest period of 1-day, the maximum value of the shear strength was identical to the residual strength (i.e. 44.86 kN/m²). Thus, the recovered strength was not observed after the 1-day rest period. After the 3 days rest period, the maximum shear strength value of 44.98 kN/m² was achieved, after the shear displacement of 0.48 mm, which was slightly greater than the residual strength. Similarly, little increase in shear strength from the residual shear strength was recorded (Table 2) after the small shear displacements of 0.73 mm, 0.73 mm, and 0.97 mm for the rest periods of 7, 15, and 30 days, respectively (Table 3). The small increase in shear strength from the residual shear strength indicates that the shear strength was recovered from the residual state of shear after the 3 days rest periods, but the shear displacement up to the recovered strength was small compared to the initial shear displacement (i.e. 5.83 mm) up to the peak strength (Table 3). The recovered strength was lost after shear displacements of 0.73 mm and 0.97 mm for the 15 days rest period in the case of the Krishnabhir landslide and the Shikoku landslide, but the shear displacement in which the recovered strength was lost was slightly greater (i.e. 1.46 mm) for the Toyooka-

kita landslide (Table 3). At the rest period of 30 days, the recovered strength was lost after the 1.46 mm of shear displacement in the case of the Shikoku and Toyooka-kita landslides. The recovered strength of the Krishnabhir landslide reached a residual state of shear after a small shear displacement compared with the other landslides (Table 3).

The test results indicate that the measured recovered strength (τ_{Rec}) up to the rest time of 3 days is negligible (Table 2). After a rest time of 3 days, there was a minimal increase in the strength from the residual state of shear with respect to the increase in rest time (Table 2). The value of recovered strength is small and may not be used for back analysis of the reactivated landslides; relying on such recovered strength was judged to be unrealistic for design purposes. The recovered strength is not expected to exceed the critical state (i.e. fully softened shear strength) in the laboratory or field because of the presence of a pre-existing shear surface and the alignment of clay particles along the shear surface parallel to the direction of shear. If the strength recovery test will be conducted for a long rest period, the value of the frictional angle may increase up to the critical state. However, the experimental results indicated that the recovered strength of the residual state of shear gradually started to appear after a shear rest period of 3 days and was lost immediately after a small shear displacement. Hence, the use of a recovered strength for the design and repair of slopes containing pre-existing shear surfaces is not recommended in this study. However, the strength recovery phenomenon may be useful to understand the creeping behaviors of landslides or slope stability prior to reactivation as suggested by D'Appolonia et al. (1967). Therefore, Skempton's method (1964, 1985) should still be followed for remediation of reactivated landslides and for comparison with back-calculated shear strength parameters.

The ratio between the recovered shear strength and the initial residual shear strength as a function of rest time is shown in Fig. 2. The strength ratio of the Toyooka-kita landslide is the highest, followed by the Shikoku landslide

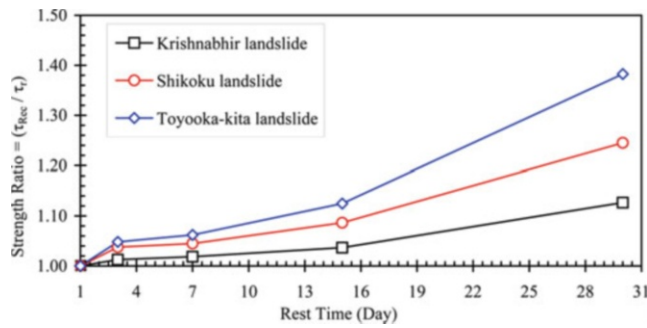


Fig. 2 Strength ratio versus rest time

and then the Krishnabhir landslide (Fig. 2). The strength ratio versus rest time curves of the Krishnabhir, the Shikoku, and the Toyooka-kita landslides are approximately equal, but the strength ratio value of the Toyooka-kita landslide is slightly greater than for the Shikoku and the Krishnabhir landslides (Fig. 2). For example, the strength ratio values at rest times of 15 days for the Krishnabhir, the Shikoku, and the Toyooka-kita landslides were found to be 1.03, 1.08, and 1.12, respectively. The differences between the peak strength and the residual strength of the Krishnabhir, the Shikoku, and the Toyooka-kita landslides were 6.30 kN/m², 19.57 kN/m², and 32.19 kN/m², respectively. The Toyooka-kita landslide demonstrates a highly plastic soil nature compared with the Shikoku and the Krishnabhir landslides. From Fig. 2, it can be concluded that the soil with the smaller difference between the peak strength and the residual strength shows a lower value of recovered strength when compared with the soil with a larger difference between the peak strength and the residual strength. Thus, the recovered strength from the residual state of shear will be higher in high plasticity soils when compared with low plasticity soils.

Although some researchers have recognized that strength recovery above the residual value occurs over time, the actual mechanisms that cause this phenomenon remain unknown. However, a few hypotheses are proposed for the mechanisms of strength recovery. Primary and secondary compression has a role in strength recovery (Gibo et al. 2002). Under the application of normal stress, secondary compression will occur even if no significant primary consolidation occurs (Mesri and Castro 1987). In secondary compression, the strength will increase due to decrease in void ratio, micro-interlocking, and inter-particle contacts (Schmertmann 1991). If so, at a higher effective normal stresses, the amount of secondary compression should be greater than at lower effective normal stress and the strength recovery should be higher at higher effective normal stresses. However, Stark and Hussain (2010) reported that strength recovery is minimal at a low effective stress of less

than 100 kN/m² and that the strength recovery effect is negligible at an effective stress greater than 100 kN/m². These results suggest that the effect of primary and secondary compression of the slip surface soil on strength recovery may not be considerable. In an overconsolidated specimen, the magnitude of secondary compression will be reduced during the rest period; thus, the strength recovery may not be the cause of primary and secondary compression.

A smooth, shiny slickensided surface exhibits more van der Waals attraction than the rough particle surfaces (Czarnecki and Dabros 1980). It is assumed that oriented clay particles with smooth platy and shiny surfaces have greater van der Waals attraction than randomly arranged clay particles. Thus, the strength recovery mechanism may be the cause of van der Waals attraction between soil particles. Mitchell and Soga (2005) reported that clay particles absorb cations under the given environmental conditions (pressure, temperature, chemical and biological composition of the water). The net negative charge on the surface of soil particles is neutralized by cations in water (Terzaghi et al. 1996). The exchange reaction generally depends upon the electrovalence of the cations and the relative concentration of cations in the water. The physical and physicochemical properties of the soil may be changed during the exchange reaction, but the clay particle structures are not ordinarily affected (Mitchell and Soga 2005). The strength recovery along the failure surface may also be the cause of cation exchange. Most soils contain cementing agents, such as free carbonates, iron oxides, alumina, and organic matter, which may precipitate at inter-particle contacts (Mitchell and Soga 2005). Cementation may be a strength recovery mechanism of an ancient landslide (D'Appolonia et al. 1967). For the cementation process to occur, sufficient time would be required, hence the remolded specimen in the laboratory may not have experienced cementation because of insufficient time. The bond formed by cementation tends to be brittle and can be destroyed by a small shear displacement. External agents (i.e. admixture) would thus be required for cementation to occur; however, cementing agents were not added during this test. Moreover, all test conditions, e.g. application of effective normal stress, room temperature, etc., were kept constant during the experiments. Hence, the recovery of strength in this study may not be a result of cementation.

Conclusions

In this study, three soil samples collected from three different large-scale landslides in Nepal and Japan were tested using the Bishop et al. (1971) type ring shear apparatus. The test rest periods were 1, 3, 7, 15, and 30 days. The main findings of this study are summarized below:

1. Soil strength recovery at an effective normal stress of 100 kN/m^2 in a torsional ring shear test was minimal after a rest period of 3 days.
2. The present study re-establishes that the strength recovery from the residual value would be greater in high plasticity soils, with a large difference between the peak strength and the residual strength, than in low plasticity soils at an effective normal stress of 100 kN/m^2 . However, the strength recovery was lost after the specimen undergoes a small shear displacement.
3. Strength recovery from the residual state of shear may be the result of rebounding or reorienting of clay particles that are already oriented parallel to the direction of shear. However, the reason why the residual strength increases with the increase in duration of discontinued shear needs further investigation.

Acknowledgements The first author would like to acknowledge the Special Graduate Course on Disaster Mitigation Study for Asian Students, Graduate School of Science and Engineering at Ehime University, Japan for funding the project.

References

- Angeli MG, Gasparetto P, Menotti RM, Pasuto A, Silvano S (1996) A visco-plastic model for slope analysis applied to a mudslide in Cortina d'Ampezzo. *Q J Eng Geol* 29:233–240
- Angeli MG, Gasparetto P, Bromhead N (2004) Strength-regain mechanisms in intermittently moving slides. In: Proceedings of the IXth international symposium on landslides, Rio de Janeiro 1. Taylor and Francis, London, pp 689–696
- Bhat DR, Bhandari NP, Yatabe R, Tiwari RC (2011) Residual-state creep test in modified torsional ring shear machine: methods and implications. *Int J Geomate* 1(1):39–43
- Bhat DR, Bhandari NP, Yatabe R, Tiwari RC (2012) A new concept of residual-state creep test to understand the creeping behavior of clayey soils. *Geocongress 2012*:683–692. doi:10.1061/9780784412121.071
- Bhat DR, Bhandari NP, Yatabe R (2013a) Effect of shearing rate on residual strength of Kaolin Clay. *Electron J Geotech Eng* 18 (G):1387–1396
- Bhat DR, Bhandari NP, Yatabe R (2013b) Residual-state creep behavior of typical clayey soils. *Nat Hazards* 69:2161–2178. doi:10.1007/s11069-013-0799-3
- Bhat DR, Bhandari NP, Yatabe R (2013c) Study of preexisting shear surfaces of reactivated landslides from a strength recovery perspective. *J Asian Earth Sci* 77:243–253. <http://dx.doi.org/10.1016/j.jseaes.2013.08.023>
- Bhat DR, Bhandari NP, Yatabe R (2013d) Method of residual-state creep test to understand the creeping behaviour of landslide soils. *Landslide Sci Pract* 2:635–642. doi:10.1007/978-3-642-31445-2_83
- Bhat DR, Bhandari NP, Yatabe R (2014) Strength recovery from residual-state of shear on soils. *Indian Geotech J* 44:94–100. doi:10.1007/s40098-013-0066-2
- Bishop AW, Green E, Garge VK, Andresen A, Brown JD (1971) A new ring shear apparatus and its application to the measurement of residual strength. *Geotechnique* 21(4):273–328
- Bromhead EN (1979) A simple ring shear apparatus. *Ground Eng* 12 (5):40–44
- Carrubba P, Del Fabbro M (2008) Laboratory investigation on reactivated residual strength. *J Geotech Geoenviron* 134 (3):302–315
- Czarnecki J, Dabros T (1980) Attenuation of the van der Waals attraction energy in the particle/semi-infinite medium system due to the roughness of the particle surface. *J Colloid Interface Sci* 78 (1):25–30
- D'Appolonia E, Alperstein R, D'Appolonia DJ (1967) Behavior of a colluvial slope. *J Soil Mech Found Div* 93(4):447–473
- Gibo S, Egashira K, Ohtsubo M, Nakamura S (2002) Strength recovery from residual state in reactivated landslides. *Geotechnique* 52 (9):683–686
- Mesri G, Castro A (1987) C_a/C_c concept and K_0 during secondary compression. *J Geotech Eng* 113(3):230–247
- Mitchell JK, Soga K (2005) *Fundamentals of soil behavior*, 3rd edn. Wiley, New York
- Nakamura S, Gibo S, Yasumoto J, Kimura S, Vithana S (2010) Application of recovered strength in stability analysis of reactivated landslide, Xuechengzhen, China. *GeoFlorida 2010*:3149–3154
- Ramiah BK, Purushothamaraj P, Tavane NG (1973) Thixotropic effects on residual strength of remoulded clays. *Indian Geotech J* 3 (3):189–197
- Schmertmann JH (1991) The mechanical ageing of soils. *J Geotech Eng* 117(12):1288–1330
- Skempton A (1964) Fourth rankine lecture: long term stability of clay slopes. *Geotechnique* 14(2):77–101
- Skempton AW (1985) Residual strength of clays in landslides, folded strata and the laboratory. *Geotechnique* 35(1):3–18
- Stark TD, Hussain M (2010) Shear strength in preexisting landslides. *J Geotech Geoenviron* 136(7):957–962
- Stark TD, Choi H, McCone S (2005) Drained shear strength parameters for analysis of landslides. *J Geotech Geoenviron* 131(5):575–588
- Terzaghi K, Peak RB, Mesri G (1996) *Soil mechanics in engineering practice*, 3rd edn. Wiley, New York



Landslides on a Cretaceous Fluvial Sediment

Peter Redshaw, Max Barton, and Caroline Stuver

Abstract

This paper reviews the landslides developed in the coastal outcrop of the Wessex Formation, Isle of Wight, UK. The Wessex Formation (Lower Cretaceous) is the product of fluvial deposition on a distal plain meander belt. The outcrop stretches for approximately 7 km and lies on the northern flank of the asymmetric Brighstone Anticline axis.

The Wessex Formation has a varied lithology, ranging from massive red mudstones, to variously coloured mudstones with pseudo-anticlines, thin extensive splay sandstones, sand and pebble point bars, and some plant debris beds.

The coastal landslides are typically large isolated rock falls from thick channel sandstone units or mudslides within mudstone units. The Roughlands Landslide is the only current example of an active compound coastal landslide, comprising a series of degrading slumped blocks moving seaward above a persistent and slickensided basal shear surface. This poses the problem as to how a large complex landslide can be accommodated in a fluvial formation which, unlike marine sediments, is without well-formed bedding planes able to provide the basal translational shear plane associated with compound slides.

Whilst landslides continue to form a major feature on the southwest coast of the Isle of Wight, the longevity of each slide is likely to be short-lived; a trait illustrated by a small but significant 'disappearing landslide' towards the northwest edge of the outcrop.

Keywords

Cretaceous • Fluvial • Mudslide • Shear-surface

Location

The Isle of Wight sits just offshore from the southern coastline of mainland United Kingdom (Fig. 1) and has been the focus of many key studies into the mechanics and recognition of coastal landslides (perhaps the most well-known of these incorporated into the area known as The Undercliff, near Ventnor).

P. Redshaw (✉) • M. Barton • C. Stuver
Faculty of Engineering and the Environment, University of
Southampton, Highfield, Southampton SO17 1BJ, UK
e-mail: pgr1c11@soton.ac.uk; M.E.Barton@soton.ac.uk;
css1g09@soton.ac.uk

Geology

The Cretaceous (Barremian) Wessex Fm. represents the oldest of the strata seen on the Isle of Wight. Of a total estimated thickness of 580 m only the top ~ 150 m are exposed on the SW coastline, brought to exposure in the centre of the Brighstone Anticline (Hopson 2011).

The result of fluvial deposition on a frequently flooded meander-plain, the Wessex Formation consists of mudstones (clays and silty clays), sandstones and interbeds of the two, organized into complex bedforms of lens, channel and sheet-shaped units. Whilst many sub-horizontal (stratigraphically) erosional or gradational contacts between units can be seen, the term 'bedding' or 'bedding plane' may be misleading. Where it is the norm when examining coastal exposures in

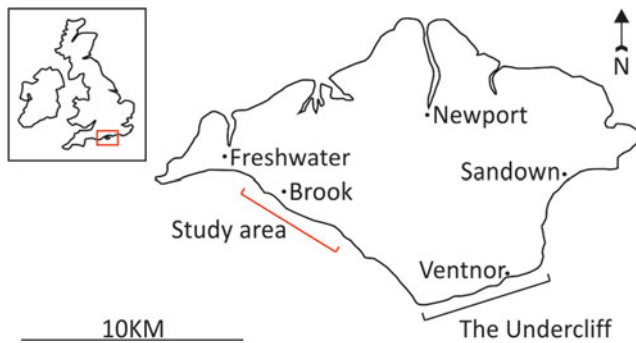


Fig. 1 Isle of Wight location map

marine deposits to log cliff stratigraphy and extrapolate back into the cliff based upon dip to solve engineering problems, such an approach is not feasible within the Wessex Fm (J. Radley, personal communication, 24.07.2012). ‘Bedding planes’ are sub-horizontal at best and in some cases persist for very short distances before truncation by the non-horizontal erosion surface of a separate mudstone or sandstone unit (with the exception of the *plant debris clay beds*).

Existing literature sub-divides the Wessex Fm. according to palaeoenvironment. While many early studies offered conflicting accounts (no doubt arising from the often confusing stratigraphy of ancient fluvial systems), clarity was first offered by Stewart (1978). Stewart’s account offers subdivisions such as ‘overbank mudstones’, ‘channel sandstones’, ‘abandoned channel sandstones’ and ‘flash-flood plant debris beds’. These form the basis of the simplified sub-division to be used by this study (Redshaw et al. 2013).

Varicoloured Mottled Mudstones

The mudstones (clays and silty clays) of the Wessex Fm. are the result of overbank sedimentation from a meandering river channel (Radley and Allen 2012). Post-depositional pedogenesis and sub-aerial weathering generates spectacular blue, green, grey, purple, red and yellow mottles which reflect subtle changes in geochemistry.

Geotechnically the clays are stiff, with low void ratios resulting from consolidation to an estimated pre-consolidation pressure of 10.2–11.9 MPa. Curiously, the varicoloured clays exhibit a low plasticity index (PI = 14.4 %, PL = 20.8 %, LL = 35.2 %) and a low clay fraction when determined by the pipette method (34.0 %), the hydrometer method (45.0 %) and by laser diffraction (26.4 %), yet residual shear strength testing using a Bromhead-type apparatus (Bromhead 1979) reveals low shear strengths which are typically associated with high plasticity, high clay fraction soils (Fig. 2). This issue is readily resolved with reference to clay particle aggregation;

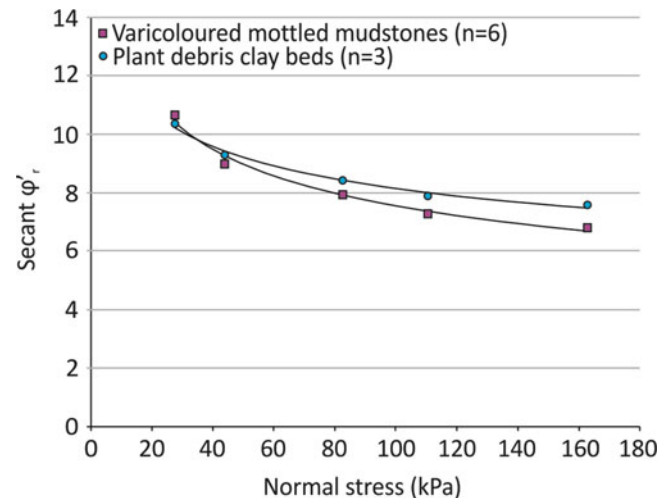


Fig. 2 Residual shear strength behaviour of Wessex Fm. clay facies (n = number of tests conducted)

the process by which clay minerals are rolled together to form silt-sized particles (Bell 1981). During shearing, and as part of the process of clay mineral re-alignment, these clay aggregates are mechanically broken down to reach a low residual shear strength.

Plant Debris Clay Beds

The plant debris beds of the Wessex Fm. are flash flood deposits, representing periods of widespread flood water inundation onto the Cretaceous meander-plain (Insole and Hutt 1994). As the flood-waters spread across the meander-plain they filled hollows (creating what are seen today as 0.5–3 m thick dark greenish grey clay deposits—type 1) and formed widespread interconnecting sheets (which are seen today as thinner, debris-starved, dark greenish grey clay units—type 2) (Stewart 1978).

Whilst the residual shear strength of the plant debris beds is similar to that of the varicoloured mottled mudstones (Fig. 2), Plasticity Index (PI), Plastic Limit (PL) and Liquid Limit (LL) are increased (17.9 %, 21.0 % and 38.9 %, respectively), although how much this is a function of aggregation remains to be investigated. Estimates of clay fraction are also in reasonable agreement with those of the varicoloured mottled mudstones (23.1 % by laser diffraction method—pipette and hydrometer methods not tested).

Sandstones

The sandstone facies of the Wessex Fm. represent meandering Cretaceous river-channels, the best example of which being the Sudmoor Sandstone between Sudmoor



Fig. 3 Persistent and active shear surface underlying the Roughlands Landslide. (a) colluvium, (b) shear surface, (c) in situ varicoloured mottled mudstones, (d) accumulated talus cone of colluvium

Point and Chilton Chine (Figs. 3 and 4). The units are typically formed of multiple lateral accretions of fine- to medium-grained, inter-locked and lightly cemented sandstone, typically with an erosional base, often marked by a thin (<0.5 m thick) conglomerate (Stewart 1978).

Thin interbeds of (commonly red) mudstone and fine sandstone are infrequently encountered, although are of far too limited exposure to be considered relevant to the engineering behaviour of the wider formation. Insole and Hutt (1994), estimate that interbedded mudstones and sandstones comprise <5 % of the total exposure.

Overlying Drift Deposits

Quaternary age sands, gravels and brickearth overlie the Wessex Fm. (Hopson 2011). Seepage erosion from the groundwater outflow at the base of the brickearth leads to much small scale slumping of the cliff top.

Landslides on the Wessex Formation

Compound Landsliding

Recognition: The only example of an active compound landslide seen within the Wessex Fm. is the Roughlands Landslide Complex. This is situated centrally within the outcrop (Fig. 4) and is formed of a series of rapidly degrading slumped blocks moving seawards along what is presumed to be a compound shear surface. The complex incorporates a 600–800 m stretch of coastline with a maximum toe to rear scarp distance of 150 m and reaching a maximum elevation of about 28 m OD. As yet no boreholes have been drilled to determine the form of the bounding shear surface. The only aspect of the latter is seen fronting the eastern side of the landslide, where a persistent and active basal shear surface

formed in the mudstone and surmounted by colluvium, outcrops near the top of a 5 to 7 m high cliff at the back of the beach (Fig. 3). This forms a nearly level surface extending for about 200 m before descending in an arcuate curve towards the central area where it becomes covered by colluvium.

Mechanics: In marine sediments, basal shear surfaces are characteristically formed along bedding planes with a low shearing resistance, referred to as slide-prone horizons by Bromhead (2013). Since the Wessex Fm. is a fluvial sediment without regular well-formed bedding planes in the central part of the outcrop, the problem arises as to what has led to the development of the surface seen in the cliff below the Roughlands Landslide. It does not appear to be the simple result of cliff failure, since the intact mudstone is a strong material and will be subject to more intense shear stress at the base of the Barnes High cliffs, which are much higher than the back scarp at Roughlands (Fig. 4) and where there is no sign of either compound landsliding or exposure of an active shear surface. Two possibilities present themselves for the solution of this problem.

- (i) The plant debris beds which were formed by large scale flooding are described by Stewart (1978) as including widespread sheets (type 2) which connect up the more localised deposits filling up the channels and small hollows (type 1). The widespread sheets would provide the only laterally extensive and persistent bedding feature within the mudstones at the centre of the Wessex Fm. outcrop that could feasibly be re-used to guide a modern shear surface. The cliff line provides only a cross section of the original Barremian flood plain, so direct evidence for the widespread flood deposit is not available, but in view of the conditions known to have existed (Radley and Allen 2012) such deposits seem very probable. Active shearing beneath the Roughlands Landslide would readily remove weak materials so, as with slide prone horizons in general, evidence for the material originally present just above the shear surface is no longer evident.
- (ii) An alternative possibility is the presence of original slope failure surfaces such as may have originated during the cutting of channels; most likely steep-sided, during flood events, across the Barremian flood plain. The existence of deep and wide channels is demonstrated by the existence of the point bars that make up the Sudmoor sandstone (Stewart 1978 having enumerated seven such units at Sudmoor Point). Slope failures in modern river valleys, such as the Mississippi, are a well-known phenomenon of engineering significance. Channel bank failures which occurred during the formation of Pennsylvanian deltas have been found during modern open-cast coal extraction (Laury 1971) so it is well within the bounds of probability that such feature

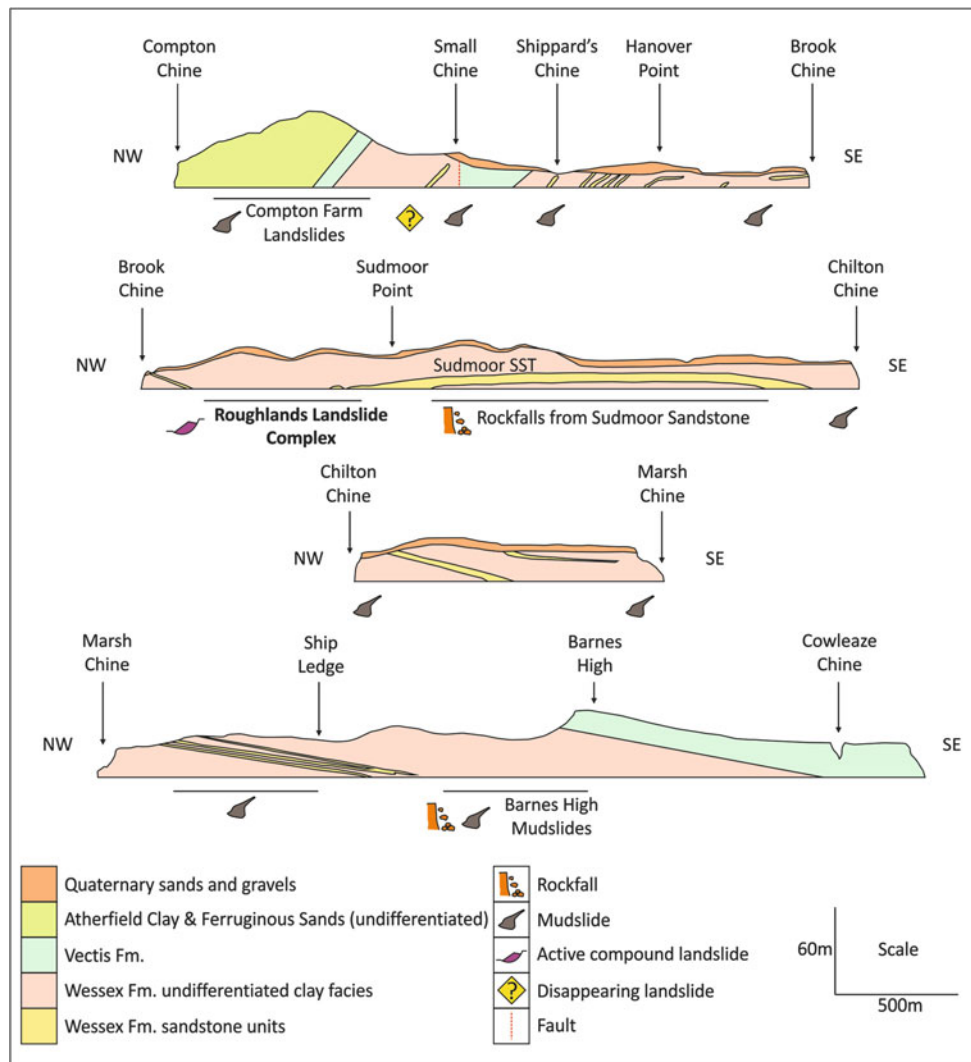


Fig. 4 Landslides of the Wessex Fm. as viewed in cliff section (modified from Insole et al. 1998; Stuiver 2010)

developed in ancient fluvial meander plains could be preserved and exhumed during modern slope instability. The development of clay orientation as a result of ancient shearing as a mechanism by which slide-prone horizons become residual strength surfaces, is implicit in Hutchinson's (1988) study of flexural slip.

Mudslides

Recognition: Lobate mudslides in the typical form as shown and defined by Hutchinson (1988) are characteristically associated with the Wessex Fm. mudstones (Fig. 4). They are well seen as secondary features leading to the degradation of the Roughlands Landslide, with the mudslide tongues extending from the rear of the slide down to the beach. Large examples of lobate mudslides are seen forming a lower

bench within the Wessex Fm. below the Barnes High cliff. Mudslides are also generated by the modern weathering of the mudstones exposed in high level benches developed above the sandstone units and move seaward either through narrow channels or else move in periodic slumps over the sandstone scarp faces. Mudslide tongues which fall over the lower steep cliff at the back of the beach are quickly eliminated by the high rate of wave erosion, the beach volumes being insufficient to protect either mudslide or talus for any length of time.

Mechanics: Observation of the mudslide morphology indicates that these are true slides with bounding lateral and basal shear surfaces. Their high water content is generated by inflow from surface water, outflow of groundwater from the Quaternary terrace sands and gravels and also from the sandstone units were present. Rockfalls onto the mudslides from steep scarp faces, particularly in the case of



Fig. 5 Rockfall from the Sudmoor Sandstone between Sudmoor Point and Chilton Chine: (a) Quaternary sands and gravels, (b) Wessex Fm. mudstones, (c) Wessex Fm. sandstones (Sudmoor Sandstone), (d) large boulders of sandstone, (e) rockfall debris, (f) vegetation indicating excessive seepage

the Barnes High cliff, will generate the phenomenon of undrained loading (Hutchinson and Bhandari 1971). A monitoring programme to determine the rates of movement of both the mudslides and the slump blocks with the Roughlands Landslide is currently underway and has shown that the mudslides are actively moving even during the dry summer of 2013.

Rockfalls

Recognition: The Sudmoor Sandstone is the main source of rockfalls from within the Wessex Fm (Figs. 4 and 5). These usually consist of a number of larger ($\sim 1 \text{ m}^3$) blocks surrounded by increasingly smaller sandstone debris forming a talus cone at the base of the sub-vertical cliff (which reaches 15–20 m in places) (Fig. 5). Large volumes of sand (not sandstone) often accompany the larger blocks—an indication of the weakly cemented nature of the unit.

Mechanics: Rockfalls from the sandstone units of the Wessex Fm. develop along persistent and often dilated joint sets. In stark comparison to the surrounding low-permeability clays, the sandstone units offer a preferential path for groundwater flow (as indicated by abundant vegetation growth at the sandstone-clay boundary, Fig. 5), encouraging the washing-out of fines leading to a loss of strength and subsequent failure. Being weakly cemented, the sandstone units are particularly susceptible to mechanical weathering. Where overlying clays slip over the sandstones, the top edge of the sandstone becomes exposed. This increases both the overturning (seaward) moment and the tendency for cracks to develop and subsequently be exploited by rainwater infiltration and frost shattering. Clays underlying large sandstone bodies are particularly

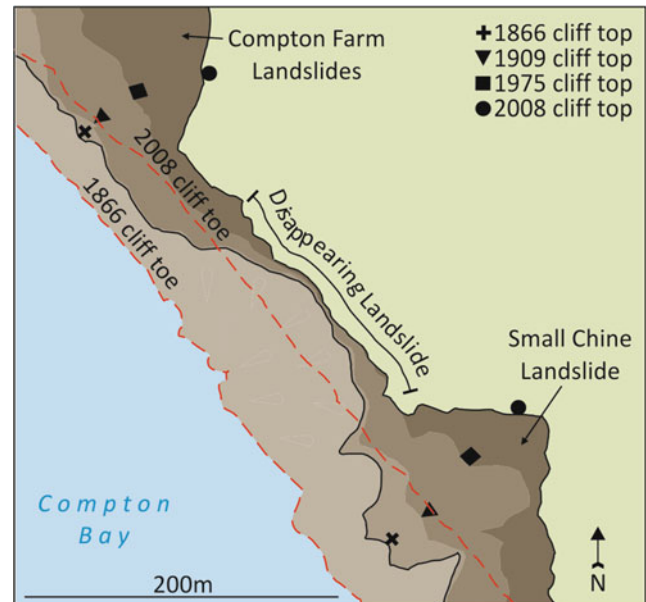


Fig. 6 Historical development of the disappearing landslide between Small Chine and the Compton Farm Landslides (Stuiver 2010)

prone to marine erosion (and hence undercutting of the sandstone) between Sudmoor Point and Chilton Chine (Jenkins et al. 2011).

Previous Landsliding

Recognition: The OS map for 1866 in the north western part of the outcrop shows a concave re-entrant in the cliff line with an extensive area on the seaward side of what appears to be a compound landslide (Fig. 6). Study of subsequent revisions of the historical maps shows that this presumed landslide gradually disappeared; the modern map shows that the cliff now conforms to the characteristic shape with a steep profile between beach and cliff top. The evidence indicates that a former compound landslide has effectively been removed by subsequent cliff recession (Stuiver 2010). At the site of this disappearing landslide, the dip has steepened to about 20° . With a coastal recession rate of approximately 0.5 m/year, combined with the steepness of the dip, indicates that whatever feature was responsible for the compound sliding at this location was effectively removed by coastal erosion during the late nineteenth and twentieth centuries.

Mechanics: The highest part of the Wessex Fm. (north-west from Hanover Point and south east of Marsh Chine, Fig. 4) shows a more regular stratigraphy, with varicoloured mottled mudstone units dissected by sandstones (White 1921); the result of increased dip imposed upon the extremities of the outcrop by the Brighstone Anticline.

With sandstone overlying mudstone this raises the possibility of seepage erosion which would aid shear failure along bedding features during slope failure. In the northwest area, at the site of the disappearing landslide, there is also the possibility of flexural slip along bedding features being induced by the high stresses associated with the monoclinical folding of the Isle of Wight. Sliding along bedding was reported for a site adjacent to Shippards Chine (Fig. 4) by Bromhead et al. (2002) and Rust and Gardener (2002) from an exposure visible in the cliff face at the time of their investigations. No evidence of these features is visible at the present time, the rate of recession having set back the cliff line by over 5 m since these observations were made. Thus in these areas, the form of landsliding may be more akin to the forms seen in other types of sediment, but without the abundance of slide-prone bedding planes which characterise marine sediments and can promote long-term continual landsliding.

Conclusions

The Wessex Fm. is of fluvial origin, being deposited in a distal meander belt floodplain. The central section of the outcrop (the oldest part of the formation) provides evidence of its origin in the form of massive red mudstones with indeterminate bedding, included mottled sections resulting from past pedological processes, large sandstone point bars and plant debris beds arising from flash flooding. A large compound landslide, the Roughlands Landslide, has developed in this central part of the outcrop but the relation of its bounding shear surface to the sedimentary characteristics of the containing sediment remains to be investigated. It is a major puzzle that requires a comprehensive subsurface drilling programme to solve.

The higher parts of the formation show more regular stratification but still without the frequent slide prone bedding planes that characterise marine sediments. There is however evidence that landsliding within the Wessex Fm. has previously taken place in these areas, but with the current high rate of recession, traces of shear surfaces and other lines of evidence are rapidly lost to marine erosion.

References

- Bell FG (1981) *Engineering properties of soils and rocks*. Butterworth-Heinemann, Oxford
- Bromhead EN (1979) A simple ring-shear apparatus. *Ground Eng* 12:40–44
- Bromhead EN (2013) Reflections on the residual strength of clay soils, with special reference to bedding-controlled landslides. *Quart J Eng Geol Hydrogeol* 46:132–155
- Bromhead EN, Ibsen ML, Papanastassiou X (2002) Three-dimensional stability analysis of a coastal landslide at Hanover Point, Isle of Wight. *Quart J Eng Geol Hydrogeol* 35:79–88
- Hopson P (2011) The geological history of the Isle of Wight: an overview of the ‘diamond in Britain’s geological crown’. *Proc Geol Assoc*, 745–763
- Hutchinson JN (1988) General report: morphological and geotechnical parameters of landslides in relation to geology and hydrogeology. In: Bonnard C (ed) *Proceedings of the 5th international symposium on landslides*. A.A. Balkema, Rotterdam, Netherlands, pp 3–35
- Hutchinson JN, Bhandari RK (1971) Undrained loading, a fundamental mechanism of mudflows and other mass movements. *Geotechnique* 1:353–358
- Insole AN, Hutt S (1994) The palaeoecology of the dinosaurs of the Wessex Formation (Wealden Group, Early Cretaceous), Isle of Wight, Southern England. *Zool J Linn Soc* 112:197–215
- Insole A, Daley B, Gale A (1998) *The Isle of Wight: geologists association guide no. 60*. Geologists Association, London
- Jenkins GO, Foster C, Hopson PM (2011) Geology as a control on landslides on the Isle of Wight: an overview. *Proc Geol Assoc* 906–922
- Laury RL (1971) Stream bank failure and rotational slumping: preservation and significance in the geological record. *Geol Soc Am Bull* 82:1251–1266
- Radley JD, Allen P (2012) The Wealden (non-marine Lower Cretaceous) of the Wessex Sub-basin, southern England. *Proc Geol Assoc* 123:319–373
- Redshaw PG, Barton ME, Stuiver CS (2013) Lithofacies variations within the Wessex formation and their influence on coastal stability. In: *Conference programme and abstracts volume, 10th international conference on fluvial sedimentology, July 2013, Leeds, UK*, pp 401–402
- Rust D, Gardener J (2002) Lithological and structural controls on style and rate of coastal slope failure: implications for future planning and remedial engineering measures, SW coast, Isle of Wight. *Instability: planning and management*. Thomas Telford, London
- Stewart DJ (1978) *The sedimentology and palaeo-environment of the Wealden Group of the Isle of Wight, Southern England*. PhD thesis, Portsmouth Polytechnic
- Stuiver C (2010) *The Southwest Coast of the Isle of Wight: influence of geology on coastal morphology and recession rate*. MSc Thesis, University of Southampton
- White HJO (1921) *A short account of the Geology of the Isle of Wight*. Geological Survey Office, London



Prediction Method of the Onset of Landslides Based on the Stress-Dilatancy Relation Against Shallow Landslides

Katsuo Sasahara, Kazuya Itoh, and Naoki Sakai

Abstract

The combination of the monitoring of the surface displacement and the creep theory (strain–time relation) of a soil is adopted in practice to predict the time of onset of a shallow landslide. This method sometimes cannot make good prediction because the creep theory cannot treat the change of stress in the slope. Some variant should be necessary for indicating the stress state. The utility of the ratio of the increase of the compression strain to the increase of the shear strain (strain increment ratio) in the slope and the ratio of the increase of the vertical displacement to the increase of the surface displacement (displacement increment ratio) as the stress parameter were examined in this paper based on analysis of the monitoring data of the deformation of the sandy model slope. As results, the strain increment ratio and the displacement increment ratio at deeper soil layer approaches toward zero with the increase of the shear strain or the surface displacement. It means the soil layer approaches the critical (failure) state. These facts show that the strain increment ratio and the displacement increment ratio can express instability of the slope.

Keywords

Shallow landslide • Early warning • Shear strain • Compression strain • Dilatancy

Introduction

Existing methods for the early warning against rainfall-induced landslides is divided into two kinds. The first is a rainfall threshold (Caine 1980) which is for the time prediction of landslides at an area while the latter is monitoring of soil water or deformation of a slope for a prediction at a specific slope. Only the latter can treat the characteristics of a slope such as geometry, rainfall infiltration characteristics, and mechanical characteristics of the slope.

The sediment-related disaster prevention law (MLIT Japan 2001) was enacted at 2001 in Japan. A sediment-related disaster hazard area should be designated by prefectural governors based on the basic survey. It is defined as the area vulnerable to sediment-related disasters. A warning and evacuation system should be established by municipal governors in the area according to the law. The monitoring of the soil water or the deformation of a slope can be an effective tool for the system.

Basic Concept of Proposed Time Prediction Method

Time prediction methods based on the monitoring of the displacement of a slope have been proposed and been already in practice. Those are usually empirical equations which express the relationship between an elapsed time and a displacement of a slope and express a time-dependent

K. Sasahara (✉)
Kochi University, 200, Monobeotsu, Kochi 783-8502, Japan
e-mail: sasahara@kochi-u.ac.jp

K. Itoh
National Institute of Occupational Safety and Health, Tokyo, Japan

N. Sakai
National Research Institute for Earth Science and Disaster Prevention,
Tsukuba, Ibaraki, Japan

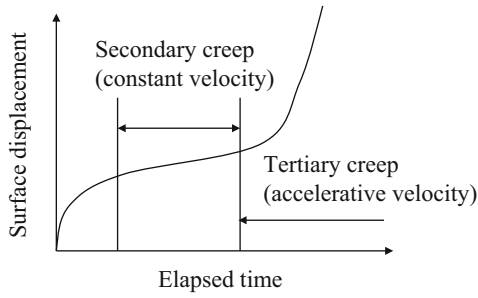


Fig. 1 Creep curve of the soil

relationship (time–strain relationship) of the deformation of the soil. The time-dependent relationship between an elapsed time and a displacement of the soil is called ‘creep’ and has been recognized as Fig. 1.

Fukuzono equation (Fukuzono 1985) is one of the most famous one based on the creep theory as below.

$$\frac{d^2x}{dt^2} = a \left(\frac{dx}{dt} \right)^\alpha \quad (1)$$

Here, x : surface displacement, t : elapsed time, a and α : constants. After the integration of (1); (2), (3), (4) can be derived as follows:

$$0 < \alpha < 1 : \frac{dx}{dt} = \{a(1 - \alpha)\}^{\frac{1}{1-\alpha}} (t_1 + t)^{\frac{1}{1-\alpha}} \quad (2)$$

$$\alpha = 1 : \frac{d\alpha}{dt} \exp\{a(t_2 + t)\} \quad (3)$$

$$\alpha > 1 : \frac{dx}{dt} = \{a(\alpha - 1)\}^{\frac{1}{1-\alpha}} (t_r - t)^{\frac{1}{1-\alpha}} \quad (4)$$

Here, t_1 , t_2 , and t_r : constants for integration. These equations can well simulate the accelerated velocity at the tertiary creep stage (Fig. 1) in some cases. While it failed to predict the time in other cases. The reason for the unsuccessful cases might be the change in the stress condition in the slope due to the change of the rainfall intensity or the slope geometry due to a cutting work or a filling work. The formula cannot describe the deformation due to the change in the stress condition because it only describes the time–strain relation under constant stress conditions in the soil. The stress–strain relation is necessary to describe the change in the stress conditions.

The strain increment ratio which is the relation of the normal strain increment to the shear strain increment (dilatancy) under direct shear condition might be able to be the indicator of the stress in the slope. It is widely recognized that the strain increment ratio is linear to the stress ratio (the ratio of the shear stress to the normal stress) under direct shear condition (Fig. 2). In the case of loose sandy slope,

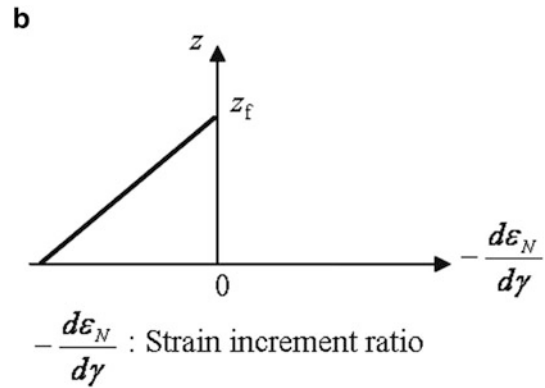
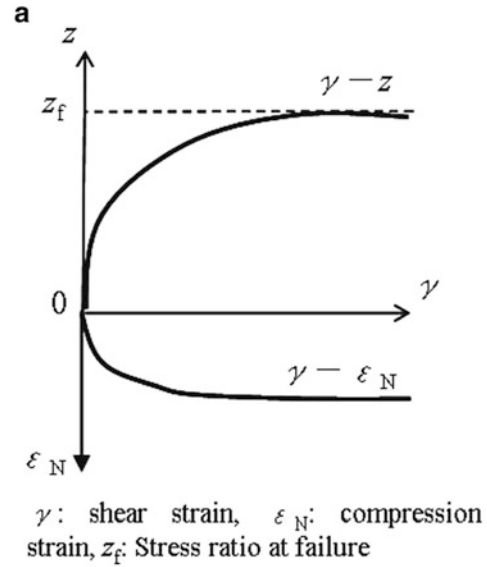


Fig. 2 Shear strain–normal strain of loose sand under direct shear. (a) Shear strain–normal strain, (b) Strain increment ratio–stress ratio

normal strain increases at first and then remains constant with the increase of the shear strain. The ratio of the normal strain increment to the shear strain increment decreases toward zero with the shear strain increase. The normal strain increment reaches zero just before the failure and this is called as the critical state. In this research, the relation between the shear strain and the normal strain in the sandy model slope under artificial rainfall is examined to prove that the relation can be applied to the time prediction of the onset of the rainfall-triggered landslide.

Methodology

Model Slope and Experimental Equipments

Figure 3 shows the longitudinal section of the model slope and the location of the monitoring devices. The scale in the vertical direction is 2.9 times that in the horizontal direction

- Pore pressure gauge (at the base)
- Soil moisture sensor (10, 20, 30, 40, 50cm)
- Tensiometer (5, 15, 25, 35, 45cm)
- ▽ Moving pole of Extensometer
- ▬ Shear strain gauge (4.6, 13.8, 23, 32.2, 41.4, 50.6cm)
- ⊥ Vertical displacement gauge (0, 10, 20, 30, 40, 50cm)

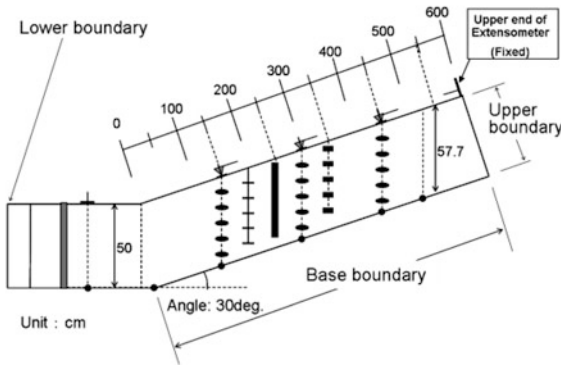
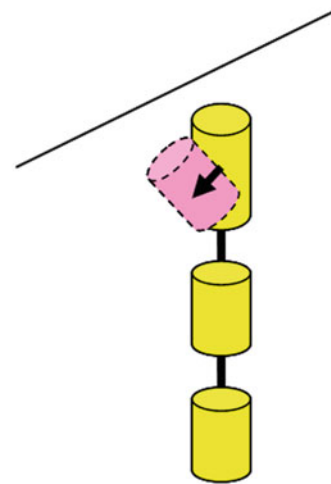


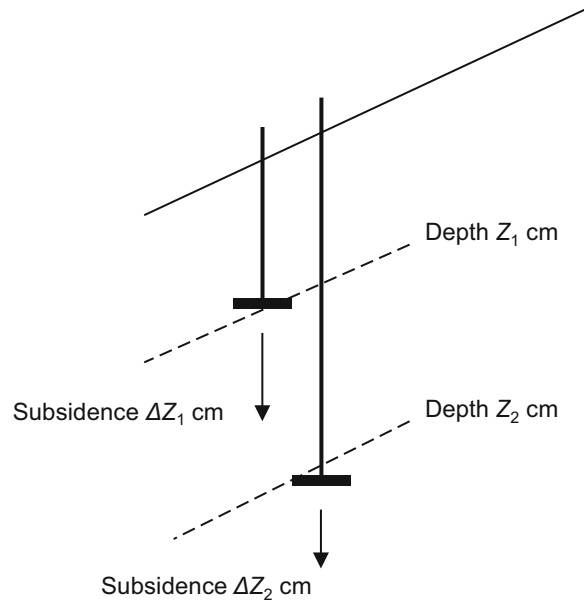
Fig. 3 Geometry of the model slope and the arrangement of the measurement devices

in Fig. 3. The model is 300 cm in length, 150 cm in width, and 50 cm in depth in the gravitational direction at the horizontal section and 600 cm in length, 150 cm in width, and 57.7 cm in depth at the slope section with an inclination of 30°. The model is composed of granite soil ($D_{50} = 1.3$ mm, $U_C = 22.23$, $F_C = 13.2$ %) and was made in a steel flume with vertical blades of 1 cm in height at every 50 cm in the longitudinal direction at the base of the slope to prevent slippage between the base of the model and the flume. The surface of the slope is parallel to the base of the slope. The inclination and the thickness of the model slope are determined based on the fact that most rainfall-induced landslides at the topsoil layer occur on slopes of 30–50° that are 0.5–1.5 m thick in Japan (Osanaï et al. 2009). The soil is compacted horizontally by human stamping at every 20 cm to construct the model slope. The void ratio ranged from 0.65 to 0.68, and the water content of the soil layer was 3.7–4.4 %. The base and upper boundary of the flume were in an undrained condition, while the lower boundary was in a drained condition. It is just like the structure of the slope layers with the top soil layer on the impermeable base rock. The shear strain in the slope was measured by a shear strain gauge, which is a series of tilt meters located vertically every 9.2 cm in depth. The shear strain is defined at the depth of the center of each tilt meter. The shear strain increment at a depth $\Delta\gamma$ is defined as $\tan(\Delta\theta)$, while $\Delta\theta$ is the inclination increment of the tilt meter (Fig. 4). The tilt meters used for the shear strain gauges have a non-linearity of 0.2°, which corresponds to a value of 0.0035 for $\Delta\gamma$. The compression



$\Delta\theta$: Increment of inclination angle of tilt meter
 Shear strain increment $\Delta\gamma = \tan(\Delta\theta)$

Fig. 4 The definition of shear strain



$$\text{Compression strain } \epsilon_{comp..} = (\Delta Z_1 - \Delta Z_2) / (Z_2 - Z_1)$$

Fig. 5 The definition of compression strain

strain at a depth was measured by two vertical displacement gauges and defined as shown in Fig. 5 at the depth $Z_{1.5}$, which is a midpoint between depth Z_1 and depth Z_2 . The vertical displacement gauge is composed of a steel plate that can move with the soil and a linear displacement gauge with an accuracy of 0.2 mm. The vertical displacement of the surface is also measured by the same method. The compression strain was regarded as the normal strain to the slip surface in this

research. The surface displacement was defined as the distance between the upper boundary of the flume and the moving pole at the surface of the slope. The surface displacement was measured by an extensometer with a non-linearity of approximately 0.1 mm which was fixed at the upper boundary of the flume. The groundwater level (hereafter, G.W.L.) at the base of the slope was measured by a water level gauge with an accuracy of 1 cmH₂O. A tensiometer and a soil moisture sensor are installed for the measurement of a suction and a volumetric water content.

Experimental Conditions

To simulate the actual soil–water condition in a natural slope which has experienced many rainfalls, three pre-rainfall events were conducted before the main rainfall event. The pre-rainfall events had the rainfall intensity of 15–30 mm/h and the duration of 100–180 min. The main rainfall had the intensity of 30 mm/h and continued until the onset of the failure of the model slope. The duration of the main rainfall is 240 min. The time interval between each pre-rainfall was 3 days and the interval between the last pre-rainfall and the main rainfall was 9 days. Rainfall intensity was determined on the consideration that the rainfall-induced landslide occurs at the rainfall with the rainfall intensity of more than 30 mm/h in Japan (Osanai et al. 2009). The deformation was video-recorded from the lateral side of the model slope, and no slip on the base of the flume could be observed.

Experimental Results

Figure 6 shows time variation of the surface displacement, the vertical displacement at the surface of the slope, and the groundwater level at the base of the model slope. The groundwater level at 450 cm is zero throughout the experiment; therefore, it is not shown in Fig. 6. The surface displacement at 150 cm and 300 cm shows accelerative increases from 12,000 s. A remarkable increase in the surface displacement at 450 cm starts from 13,000 s, which is slightly later than the increases at 150 cm and 300 cm. The vertical displacements at 300 cm, 150 cm, and 450 cm increase remarkably from 11,000 to 13,000 s. The groundwater level at 150 cm and 300 cm increases significantly from 11,000–13,000 s when the surface and vertical displacements start to increase significantly. These facts suggest that the surface and vertical displacements increase significantly with the generation of pore pressure at the base at the section between 150 cm and 300 cm while they increase without the generation of pore pressure at 450 cm.

Figure 7 shows the time variation of the shear strain and the compression strain in the model slope. The shear strain at each

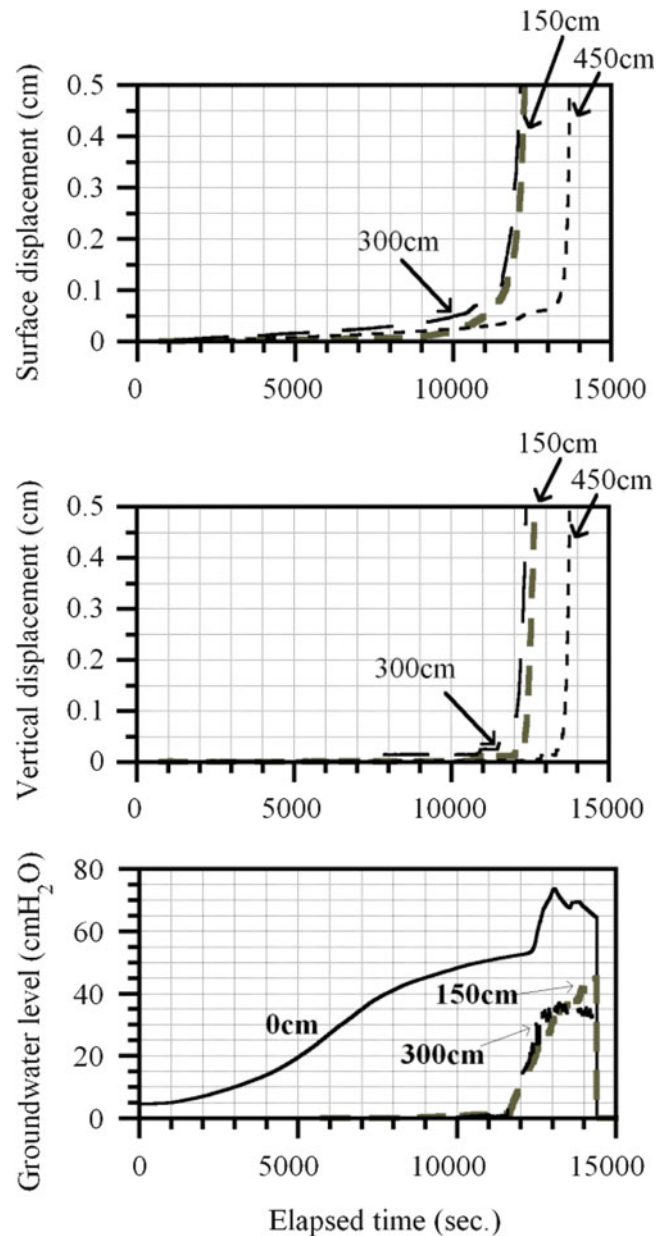


Fig. 6 Time variation of the surface displacement, the vertical displacement and the groundwater level at different distances from the toe of the model slope

depth is small until 12,000 s and then it shows an accelerated increase. The negative value at 13.8 cm may be due to the reaction of the tilt meter at this depth against the large movement of the tilt meters at higher or lower locations. The compression strain above 25 cm in depth is negative which indicates swelling, while the compression strain below 25 cm in depth is positive which indicates compression. The compression strain at each depth is also small before 12,000 s and then it shows significant increases. The time of the start of the large increase of the shear and compression strain is almost same with that of the generation of the G.W.L. according to Fig. 6.

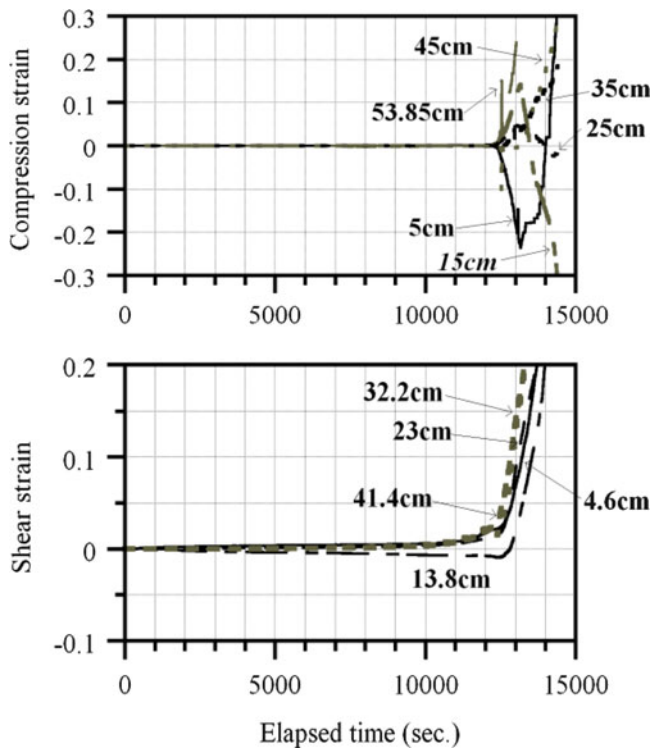


Fig. 7 Time variation of the compression strain and the shear strain in the slope

Discussion

The Relation Between the Shear Strain and the Compression Strain

Now the relationship between the shear strain and the compression strain in the model slope is examined to make confirm the stress-strain relation and the dilatancy characteristics of the soil in the model slope. Figure 8 shows the relationship between the shear strain and the compression strain at different depth in the model slope. The compression strains at 32.2 cm, 41.4 cm, and 50.6 cm are positive (compressive) throughout the experiment while those at 13.8 cm and 23 cm are positive (compressive) at first and then become negative (dilative). It suggests that the deeper soil layer is more compressive. But the compression behavior at 4.6 cm is rather strange because it is dilative at first and then becomes compressive. At the same time, it is also strange that the compression strains at 41.4 cm and 50.6 cm are very small until the shear strain of 0.15 and then increase significantly. More data on the compression deformation are necessary for the examination of these behaviors. The relation throughout the experiment at 4.6 cm and the relation at 41.4 cm and 50.6 cm until the shear strain of 0.15 are neglect in this examination. The compression strain at deeper layers is larger (more compressive) at a shear strain of 0.25, and the ratio of the increase of

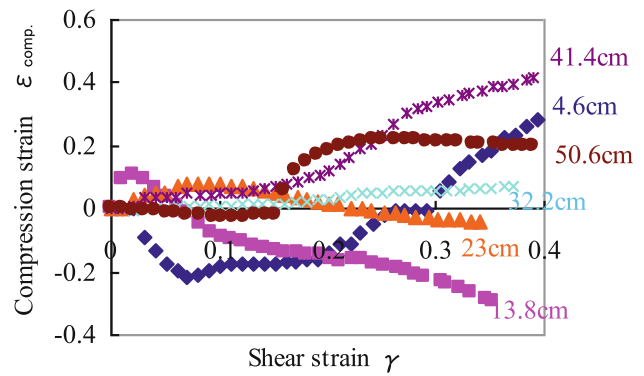


Fig. 8 Relationship between the shear strain and the compression strain at the same depth

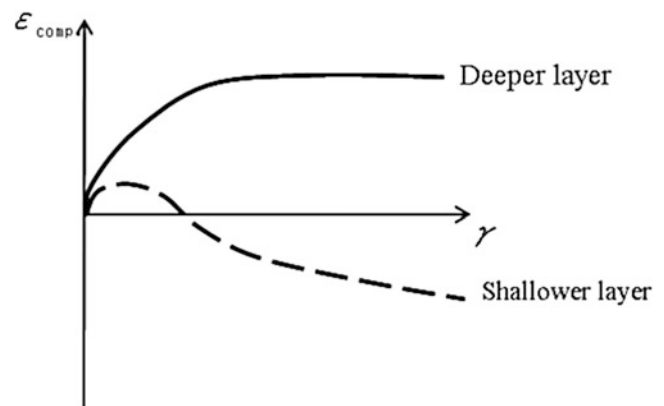


Fig. 9 Modification of the relation between the shear strain and the compression strain. ϵ_{comp} : the compression strain. γ : the shear strain

the compression strain to the increase of the shear strain at deeper layers is smaller at a shear strain of 0.25, which suggests the soil at deeper layer is closer to the critical state. The ratio of the increase of the compression strain to the increase of the shear strain at 50.6 cm becomes almost zero after the shear strain of 0.25, which indicates that the soil is in the critical state. However, the increase of the compression strain at shallow layers (13.8 cm and 23 cm) at final is still large, which means that it is far from the critical state. The characteristics of the relation between the compression strain and the shear strain mentioned above are modified in Fig. 9. These facts suggest that the ratio of the increase of compression strain to the increase of the shear strain might be able to express how far it is from present state to the failure.

The Relation Between the Surface Displacement and the Vertical Displacement

Because the surface displacement and the vertical displacement can be regarded as the sum of the shear strain and the

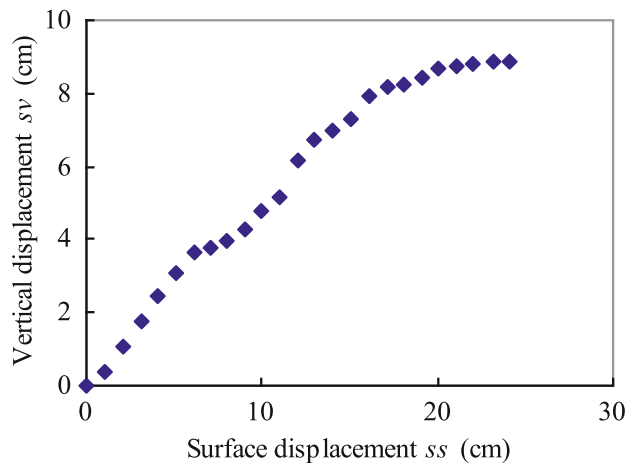


Fig. 10 Relationship between the surface displacement and the vertical displacement at 300 cm from the toe of the slope

compression strain in a cross-section, it is expected that the relation between the surface displacement and the vertical displacement is almost like the relation between the shear strain and the compression strain in the slope. The measurement of the surface displacement and the vertical displacement is much easier and more practical than the measurement of the strain in the slope. Figure 10 shows the relationship between the surface displacement and the vertical displacement at 300 cm on the surface of the model slope. The vertical displacement increases with the increase of the surface displacement at first and then the ratio of the vertical displacement increment to the surface displacement increment (the displacement increment ratio) gradually becomes smaller with the increase of the surface displacement. The vertical displacement increment to the surface displacement increment becomes zero at final. This is the same tendency with the relation between the shear strain and the compression strain in the slope.

Conclusion

Monitoring of the shear and compression deformation in a sandy model slope under artificial rainfall was

performed and the measured data was analyzed. The conclusions were derived as follows:

1. The deformation at shallower layer is dilative while the deformation at deeper layer is compressive during the experiment. The compression strain at deeper layer is larger in general. The ratio of the compression strain increment to the shear strain increment is far from zero at first and then approaches toward zero. The ratio at deeper layer approaches to almost zero which means the layer is at critical state (failure state).
2. The relation between the surface displacement and the vertical displacement on the surface of the slope is also like that between the shear strain and the compression strain. The ratio of vertical displacement increment to the surface displacement increment becomes almost zero at final (failure state).
3. From the facts as above, it can be suggested that the ratio of the compression strain increment to the shear strain increment in the slope might indicate the stress state and show how far it is from the present state to the failure state. The ratio of the vertical displacement increment to the surface displacement increment also might indicate the instability of the slope. The measurement of surface displacement and the vertical displacement is more convenient than that of the deformation in the slope.

References

- Caine N (1980) The rainfall intensity-duration control of shallow landslides and debris flows. *Geograf Ann Ser A Phys Geogr* 62:23–27
- Fukuzono T (1985) A new method for predicting the failure time of a slope. In: *Proceedings of the IVth international conference and field workshop on landslides*, Tokyo, Japan, pp 145–150
- Ministry of Land, Infrastructure, Transport and Tourism of Japanese Government (2001) Establishment of sediment-related disaster prevention law. http://www.mlit.go.jp/river/sabo/panf/j_sabo/english/30-31.pdf. Last Accessed 14 Apr 2013
- Osanai N, Tomita Y, Akiyama K, Matsushita T (2009) Reality of cliff failure disaster. Technical note of National Institute for land and infrastructure management no. 530 (in Japanese)

Part VII

General Landslide Studies



Introduction: General Landslide Studies

Peter Bobrowsky, Yueping Yin, and Alexander Strom

Abstract

Highlights for several papers included in the “general landslide” session for the 3rd World Landslide Forum are presented. Topics range from early warning systems and modelling to geomorphology and solid waste disposal settlements to flow mechanics and landslide susceptibility mapping. All the topics link issues, observations and solutions to slope instability related topics.

Keywords

Landslides • General topics

The World Landslide Forum provides all researchers involved in the study of landslide issues the opportunity to share the results of their research with fellow colleagues in the global community of practitioners. Although the conference organizers have done their best to accommodate the full range and diversity in research topics that individuals may address in their practice by designating key thematic or sectoral or geographic sessions, occasionally some topics are truly unique, specialized or professionally esoteric to the point that they cannot be easily pigeonholed into existing categories.

To ensure that such areas of interest are given equally visibility in the forum, the organizers have grouped the contributions under the category of “General Landslide Studies”. Herein readers will find a collection of interesting but different submissions on a wide range of key issues. In common, of course, is the underlying theme of landslides, but beyond that the aspects covered are deliberately unique.

P. Bobrowsky (✉)
Geological Survey of Canada, Ottawa, Canada
e-mail: Peter.Bobrowsky@nrcan-mrcan.gc.ca

Y. Yin
China Geological Environmental Monitoring Institute, Beijing, China

A. Strom
Geodynamics Research Center, Moscow, Russia

The first contribution in this section is by Emmanuelle Klein and colleagues and is entitled “Early Warning Systems and time series modelling: a new challenge for landslide risk prevention” provides a novel approach to using statistical short-term forecasting capabilities based on an auto-regressive integrated moving average type model as an attempt at early warning. The authors use 3-years worth of data collected at the active landslide of Ruines de Séchilienne in France. The study is based on an integrated technological platform, which combines microseismic, geotechnical, hydrogeological and meteorological measurements, together with three dimensional displacement measurements.

Udeni P. Nawagamuwa and W. Dayarathne’s paper “Slope Stability analysis at Bloemendhal open Dump Site in Sri Lanka” is a study on the properties of solid wastes to predict settlement, slope stability and shear strength parameters from a dump site called Bloemendhal near the Colombo Metropolitan area, Sri Lanka. Resultant data suggests that the internal nature of this and other dumps requires additional scrutiny to avoid slope instability issues.

The third contribution in this section is entitled “Slope Dynamic geomorphology of the Mailuu-Suu area, aspects of long-term prediction” and is authored by Yuri Aleshin and Isakbek Torgoev. The authors focus on the development of a modified model (based on Saito) which integrates a viscose component in their examination of loess based landslides in Kyrgyzstan.

Anja Dufresne examines the relationship between substrate materials and how they influence rock and debris avalanche emplacement in the paper “An overview of rock avalanche-substrate interactions”. The author specifically focuses on runout distance and impediments, material mobility, size of the area of deposition, and flow complexities.

“Landslide Susceptibility of Kavaja, Albania” by Olgert Jaupaj, Olivier Lateltin and Mentor Lamaj is an excellent example of a methodology to produce a landslide susceptibility map for the Kavaja district in central-western Albania. The 1:25,000 scaled product was produced using a bivariate approach to ranking parameters in each of the various subclasses.

Sun-Gon Lee and Stephen Hencher analyze landslides that occurred in 2011 in South Korea as part of their critical assessment of the characteristics of the failures and the effectiveness of the response in their work “Recent extreme rainfall-induced landslides and government countermeasures in Korea”. They conclude that a management agency akin to GEO in Hong Kong is required to deal with slope stability issues in this country.

The next contribution in this section is by Wei Meng, Thom Bogaard and Rens van Beek and is entitled “How the stabilizing effect of vegetation on a slope changes over time: a review”. These authors provide a review of the changing (de-)stabilizing effect of forest stands on potentially unstable slopes. They focus primarily on the combined hydrological and mechanical effects as a function of temporal forest stand dynamics.

Do Minh Duc and colleagues provide a detailed analysis of the factors that contributed to the Vietnamese April 2012 disaster in their contribution “Analysis of a Deep-seated landslide in the Phan Me Coal Mining Dump Site, Thai Nguyen Province, Vietnam”. They propose that the two key contributors to the disaster were the water storage nature of the waste dump materials as well as the overloading of the waste dump deposits at the top of the slope.

“Geological Complexities of Rawana landslide, Sirmaur District, Himachal” by D.K. Chadha provides a summary of his studies to understand the nature and characteristics of the Rawana landslide in the outer Himalayas. The author proposes a number of mitigation measures that can be applied to this particular failure.

“Highways vs. Landslides and their Consequences in Himalaya” by Kishor Kumar, Lalita Jangpangi and S. Gangopadhyay summarizes the researchers work into better understanding the relationship between landslides in the Himalayas that impact roads and related infrastructure as a function of cloudburts and earthquake triggers. Finally they propose a new hazard management system applicable to this situation.

Y. Yin, Sianguang Qin and Wuji Zhao give an excellent report on the use of different high resolution remote sensing data to assess landslides along the upper reaches of the Yellow River in the northeastern Tibetan Plateau of China in their contribution “Characteristics of landslides from Sigou Gorge to Lagan Gorge in the upper reaches of Yellow Zhiqiang”.

Authors Zhang Yong, Shi Sheng-wei, Song Jun and Cheng Ying-jian present the results of their landslide work in another Chinese gorge in their paper called “Evaluation on effect for the prevention and control against the landslide disasters in the Three Gorges Reservoir area”. These authors review 72 engineering projects related to slope instability. They propose a hazard prevention and control efficiency evaluation model based on an integrated fuzzy hierarchy process theory.

The final paper in this series is entitled “Fiber optic strain monitoring and evaluation of a slow-moving landslide near Ashcroft, British Columbia, Canada” and is written by David Huntley and colleagues. They examine the effectiveness of this real time monitoring technique in relation to other traditional monitoring tools such as remote sensing, piezometer, inclinometers, etc.

Papers submitted to this special session were reviewed multiple times by various reviewers. Although reviewed, the contributions did not receive the same “English” scrutiny that would be accorded to a journal article; as such some minor errors may still be recognized. The primary concern for reviewers was originality and technical quality of the submissions with an aim to provide publication opportunities for all participants and especially those from less developed nations. We thank all of the contributors and reviewers for their kind efforts.



Early Warning Systems and Time Series Modelling: A New Challenge for Landslide Risk Prevention

Emmanuelle Klein, Cristina Occhiena, Alicia Durenne, Yves Gueniffey, and Marina Pirulli

Abstract

This paper deals with the application of statistical methods for the analysis of a multi-parameter data set recorded at an active landslide, the Ruines de Séchilienne (France). Here a monitoring system was set up on the western edge of the existing large active zone. It is based on an integrated technological platform, which combines microseismic, geotechnical, hydrogeological and meteorological measurements, together with three-dimensional displacement measurements. The work, still in progress, illustrates difficulties in modelling the times series due to the ongoing self-accelerating deformation processes of the landslide. In-depth processing and analysis of multi-parameter time series remains a tricky task when using only data-based statistical methods. Additional investigations are being made to set-up statistical analysis methods suitable for automated use on a routine basis.

Keywords

Time series • Microseismicity • Rainfall • 3D displacements • Early warning systems

Introduction

The pervasive nature of landslides and unstable rock slopes creates numerous situations rated as risks across the world. When public safety is at stake early warning systems can offer a temporary robust strategy for mitigating the hazard prior to more definitive remediation or vulnerability reduction works. These warning systems are set up as reliable alarms for appropriate decision making and timely action and for planning important investments. Because

landslides can be triggered by external natural factors (such as rainfalls or earthquakes), multi-parameter monitoring is now recognized as essential (e.g. Bigarré et al. 2011). Early-warning systems can produce numerous and varied times series using a range of disciplines (geophysics, geotechnics, hydrology etc.) that call for the use of advanced data processing techniques as well as proven statistical analysis methods. To develop warning systems, the following objectives must be met: (1) analyse and understand the evolution of the different variables in space and time to detect any significant abnormal change and (2) identify and quantify causal inferences and time delays between those variables. The final aim is to determine probabilistic laws for occurrences of the hazard phenomena or at least to help in the production of reliable alarms based on statistical short-term forecasting capabilities.

This paper illustrates these issues using as an example the deep-seated Séchilienne landslide (France). It first describes briefly the site and the multi-parameter monitoring system, as well as the data collected between November 2009 and June 2013. It then attempts to characterize the relationships between rainfall, microseismicity and surface displacements

E. Klein (✉) • A. Durenne
INERIS, Campus ARTEM, CS 14234, 54042 Nancy, Cedex, France
e-mail: emmanuelle.klein@ineris.fr; alicia.durenne@ineris.fr

C. Occhiena • M. Pirulli
Department Of Structural Geotechnical and Building Engineering,
Politecnico di Torino, Turin, Italy
e-mail: cristina.occhiena@polito.it; marina.pirulli@polito.it

Y. Gueniffey
Laboratoire Georessources, Ecole des Mines, Campus ARTEM, CS
14234, 54042 Nancy, Cedex, France
e-mail: yves.gueniffey@mines.inpl-nancy.fr

and detect situations presenting a risk. Finally, the relevance of statistical short-term forecasting capabilities based on an automated analysis is discussed.

Case Study: Séchilienne Landslide

Description of the Site

The deep-seated Séchilienne landslide is located in the French Alps, at the southwest tip of the crystalline massif of Belledonne. The movement involves a surface area of around 70 ha with a potential volume of several million cubic metres. It lies on a SSE-facing slope that extends from 600 m above sea level (a.s.l.) up to 1,130 m a.s.l. The slope deformation processes appear to be very complex. It is certainly not a true slide in the usual meaning (i.e. with a planar or pseudo-circular failure surface), but instead involves 3D slope deformation processes (Durville et al. 2009). In fact, the deformation mechanism combines a toppling of gneisses and micaschists that creates major discontinuities towards the valley and subsidence of the upper part of the hill. It is an irreversible and self-accelerating process.

Since 1985, this risk management strategy for this landslide has been to rely on a monitoring system (Durville et al. 2009) operated by the Les Centres d'Etudes Techniques de l'Équipement (CETE) and based on rainfall and surface displacements measurements (using extensometers, radar, infrared, camera and video). Since 2009, the French National Institute for Industrial Environment and Risks (INERIS) has been running a multi-parameter observations system placed along the west border of the very active zone of the landslide (Fig. 1) where large cracks regularly open. This system is based on the technology described in Klein et al. (2008). It combines in-depth microseismic, hydrogeological and geotechnical monitoring, as well as meteorological and three-dimensional displacement measurements.

Description of the Monitoring System

This monitoring system comprises (Dünner et al. 2010):

- eight high-resolution microseismic probes, including four three-dimensional probes positioned at depth (in a sub-vertical borehole 80 m deep and in a 240 m sub-horizontal survey gallery), each equipped with a bi-axial inclinometer,
- one piezometer and one conductivity-temperature sensor in a dedicated borehole that is 150 m deep,
- three GPS-RTK stations, including one reference station on the opposite stable slope. The convention is such that an increase in latitude and respectively longitude



Fig. 1 Top view of the site (©Google): seismic sensors in the gallery (red dots), GPS stations (triangles), and boreholes for hydrological (blue diamond) and microseismic (red diamond) measurements

indicates movement towards the North, and toward the West,

- one meteorological station (air and ground temperatures, rainfall) also on the opposite slope.

The microseismic network was calibrated in 2010 when high-resolution seismic profiles were conducted on the north-western edge of the landslide. The calibration data confirmed the proper coupling of probes with the rock mass, as well as their capacity to detect low-energy events at a distance of more than 240 m (Dünner et al. 2010). They also helped to calibrate the processing routines, including the determination of a seismic wave velocity model with high contrasts (travel times indicated 1,400 m/s on the surface and 4,500 m/s beyond 40 m deep) in agreement with geological and geophysical observations.

Main Microseismic Signatures

The microseismic signals show substantial variability in terms of waveforms, frequency content, amplitude and duration due to the complexity of the deformation processes involved. Then, in addition to regional earthquakes and small local roof rockfalls in the sub-horizontal gallery, the monitoring system records three event types (Fig. 2):

- rockfalls and rockslides occurring in the very active zone or its vicinity,
- tremor-type signals with a long-lasting, rhythmic signal whose origin is not well understood,
- microearthquakes corresponding to in-depth rock mass fracturing and movement.

The tremors represent more than 65 % of the recordings. This proportion tends to increase over time.

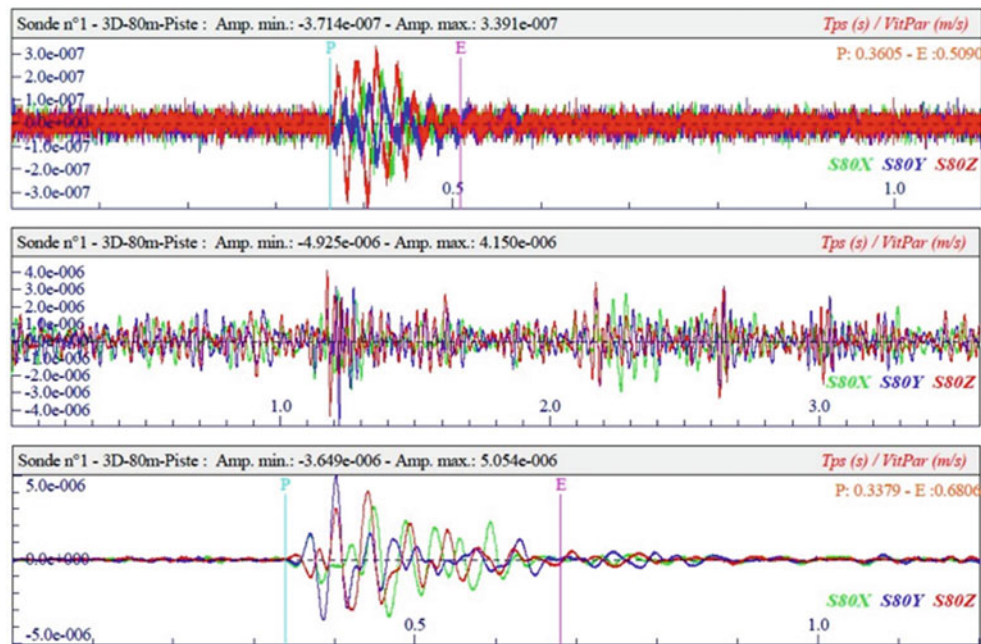


Fig. 2 Seismograms (amplitude in m/s versus time in s) recognized at one 3-component station on Sechilienne landslide: rockfalls (*top*), tremor type event (*middle*), in-depth microearthquake (*bottom*)

Time Series Over the Period

Figure 3 presents the main time series, including the microseismic activity per day, the cumulative displacement recorded by GPS-RTK station No. 2 and the daily rainfall. It shows that the microseismic activity has increased considerably from year to year (+120 % between 2011 and 2012). The movement is also quite rapid, with more than 6 m of total displacements in only 2 years (+100 % from 1 year to another). In addition, there seems to be a coincidence between microseismic surges, acceleration of surface displacement and intense rainfall or snowfall. The major microseismic peak is observed in November 2012, which is the wettest month of the period. It is also at that period that the velocities of surface displacement are larger than ever (up to 3 cm/day on average). Other peaks, although of minor amplitudes, can be seen at the end of July 2011, at the end of December 2011, in the middle of April 2012 and between March and April 2013. In Fig. 4 the superimposition of the cumulative displacements and daily microseismic activity over the daily rainfalls is shown. The rectangles identify, for each of the above-mentioned peaks, a corresponding period of intense rainfalls. A qualitative correspondence between the microseismicity and the displacements is more difficult to see. Only for the major peak of November 2012 ((d) period in Fig. 4) it is possible to see a clear increase of the surface displacements, evidenced by a change in the slope steepness in the cumulative displacement trend. The peak of November, which reaches the peak between 10th and 20th November, occurred at the end of a long period of intense activity: in fact,

the trend of the cumulative daily number of events shows an acceleration since the middle of September, together with an intensification of the rainfalls.

The piezometric time series is not presented here because the dedicated borehole became irretrievably blocked in April 2010 after technical works on site. The period is then too short for piezometric time series modeling, but it was long enough to bring out four major recharge episodes that caused a cumulative increase in the level of groundwater of more than 12 m (Dünner et al. 2010). The time series was typical of a dual permeability aquifer with rapid recharge episodes and slow discharges, with evidence of the participation of various groups of discontinuities in groundwater draining: major fractures on the surface contribute to rapid recharge, whereas fractures at depth with lower permeability slow drainage.

In order to better investigate the effective presence of a possible correlation between microseismicity, displacements and rainfalls, a statistical analysis has been applied, as described in the following.

Statistical Analysis: Overview of the Methodology

Data Preparation

In environmental time series, it is quite common to have complex or messy data. Some samples can be missing and exhibit outliers; the sampling can also differ from one time series to another. The unevenly-spaced microseismic time

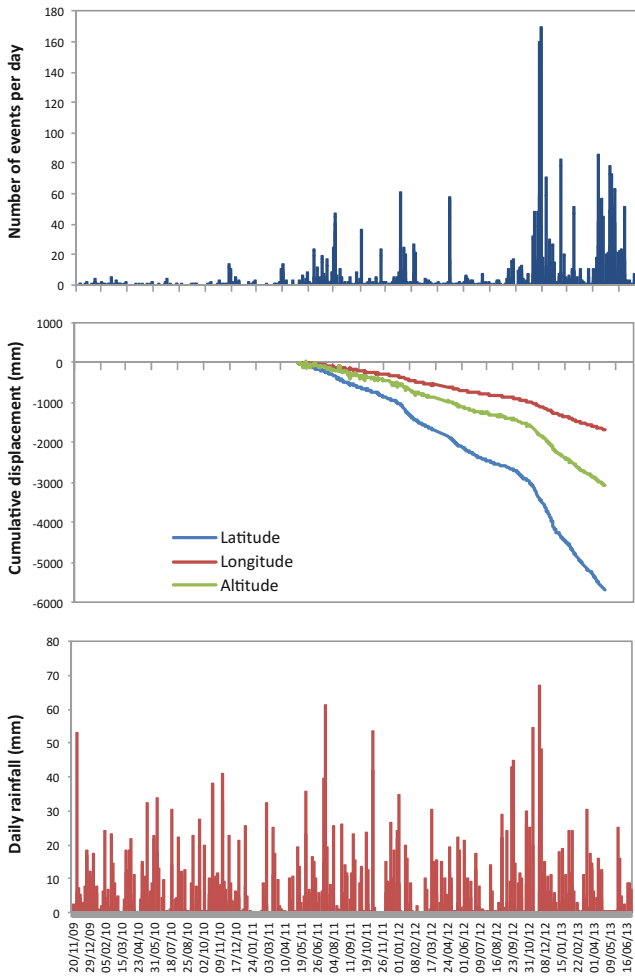


Fig. 3 Number of seismic events (*top*), cumulative displacement (*middle*) and daily rainfall (*bottom*) from November 2009 to June 2013. GPS station was installed in April 2011 and moved to another place in April 2013

series that results from passive listening for rock mass fracturing also strongly depends on the acquisition settings: a change in these settings can lead to an apparent surge or, on the other hand, to an apparent decrease in the activity. In addition, when studying natural hazards on a long-term basis it could be necessary to consider environmental changes such as those induced by climate change, for example.

To obtain statistically meaningful results, it is necessary to prepare and structure the data carefully, taking into account uncertainties and the resolutions of the instrumental techniques.

Here we reduce the sampling frequency for all series to one sample per day. We consider that the microseismic time series is homogeneous: there are no missing data over the period and no artefacts (the in-depth position of the probes efficiently limits artefacts and promotes low seismic noise). In the following, we consider the number of events per day. The displacement series is cleaned of outliers using standard GPS quality factors (e.g. dilution of precision, etc.), missing data are estimated and finally only the maximum value per day is kept. Outliers or missing values in the rainfall series are replaced by measurements provided by Les Centres d’Etudes Techniques de l’Équipement (CETE). The daily value corresponds to cumulative rainfall per day.

Time Series Modelling and Cross-Correlation Analysis

One of the most popular and frequently used methods when considering environmental data was proposed by Hipel and McLeod (1995). It permits the description of the inherent structure of each series using appropriate models, to bring out possible relationships between a set of series and make forecasts.

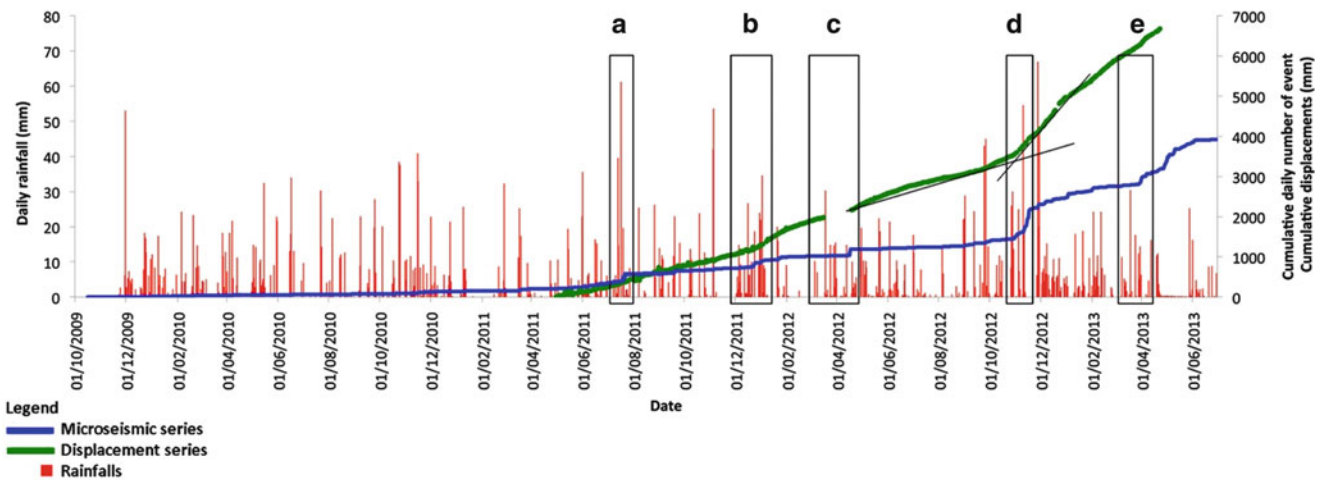


Fig. 4 Cumulative daily number of events, cumulative displacements and daily rainfall series between October 2009 and June 2013: the rectangles highlight the peaks in microseismic activity that occurred

(a) at the end of July 2011, (b) at the end of December 2011; (c) in the middle of April 2012; (d) in the middle of November 2012; and (e) between the end of March 2013 and the beginning of April 2013

Table 1 Results of the correlation study with rainfall using MA2 auto-regressive integrated moving average type model: the lag is mentioned when a correlation is found

	Correlation with rainfall	Correlation factor	5 % level
Microseismicity			
All	Yes, 0 day	0.18	0.05
Rockfalls	No	–	–
Tremors	Yes, 0 day	0.15	0.05
Microearthquakes	Yes, 0 day	0.34	0.05
Cumulative displacement—GPS station no. 2			
Longitude	Yes, 2 days	0.20	0.07
Latitude	No	–	–
Altitude	No	–	–
Total	No	–	–
Daily displacement—GPS station no. 2			
Latitude	Yes, 2 days	0.20	0.07

The level of significance is given by $1.96/\sqrt{n}$ (where n is the number of observations)

Here, to study the impact of a forcing variable or ‘input’ (for example rainfall) on a forced variable denoted ‘output’ (for example displacement) the first step consists of establishing an auto-regressive integrated moving average type model that best fits the input. This is the prewhitening stage. This model is then applied to the output to study the cross-correlation. The goal is to identify the possible delay (first significant correlation) of the action of the input on the output, and the duration of this effect (number of significant contiguous correlations). The same procedure is repeated for each pair of input/output. In the following, data are correlated when the conventional significance level (or p -value) at 5 % is exceeded.

Detection of Structural Changes

In the literature, many techniques exist to detect structural changes in times series. When considering monotonically increasing series such as cumulative displacements or cumulative number of seismic events, one simple and efficient way to detect these structural changes relies on the identification of inflection points: the calculations of the first and second derivatives mark the transition from concavity to convexity (acceleration phases) and vice versa (slowdown phases).

Correlations and Risk

Influence of Rainfall

The main results of the correlation analysis are given in Table 1. Microseismicity is significantly correlated, with no delay, to rainfall, meaning that the water supply triggers immediately seismic events, particularly those related to

in-depth rock mass fracturing (the correlation factor reaches 0.34 for microearthquakes). This result is consistent with those obtained by Helmstetter and Garambois (2010) who analyzed seismic data collected between 2007 and 2009 using a different statistical method.

Regarding cumulative (or relative) displacement the results are as good. There is no relationship between rainfall and movement northward, although it is the main component of displacement. However, a causal inference is apparent in daily displacements northward; the effect is observed with a 2-day lag. It means that water supply tends to accelerate the displacement, but it does not affect significantly the general trend associated with the continuous deformation of the landslide. Some other published studies (e.g. Chanut et al. 2013; Vallet et al. 2013) show correlation factors between rainfall and surface displacements higher than 0.6. These studies are, however, based on a method that is not feasible in many cases because it requires accumulating data over periods of several weeks or months.

Influence of Antecedent Rainfall

To try to improve the previous results and better account for the complex hydro-geological response of Sechilienne landslide to meteorological conditions, we investigated correlations with antecedent rainfall. For that purpose, we used the following formulation that reflects the fact that an old rainfall event may impact the groundwater hydrodynamic due to drainage processes:

$$R_{a0} = R_0 + kR_1 + k^2R_2 + \dots + k^nR_n \quad (1)$$

where R_{a0} is the antecedent rainfall (mm) for the current day, R_0 is the current day rainfall (mm), k is a decay factor, and R_n the daily rainfall (mm) on the n th day before 0.

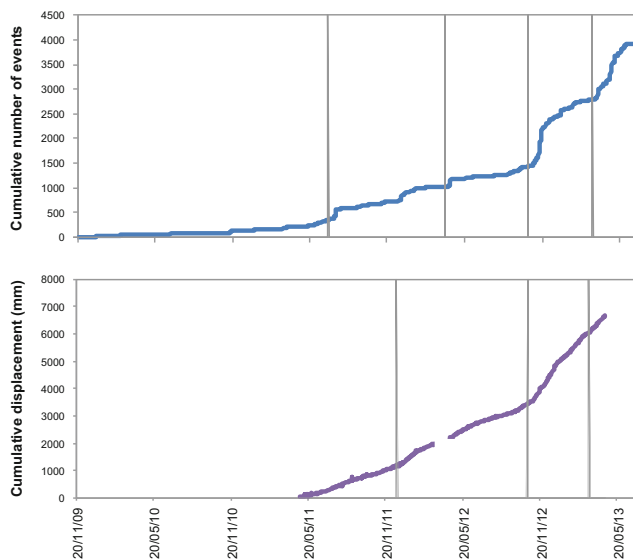


Fig. 5 Structural changes detected in the cumulative microseismic series (*top*) and in the cumulative 3D-displacement series (*bottom*) between November 2009 and June 2013. A GPS station was installed in April 2011 and moved to another place in April 2013.

We then calculated the antecedent rainfall time series, with k ranging from 0.1 to 0.9 (increment 0.05) and n ranging from 1 to 60 (increment 5), trying to identify the set of parameters giving the best correlation. Among all the combinations tested, none improve the correlation with seismic events.

Detection of Potential Risk

Over the period of study, the microseismic series presents four structural changes as defined in the previous section, in May 2011, December 2011, October 2012 and March 2013 (Fig. 5). They mark the onset of the microseismic surges mentioned in Fig. 4. A similar analysis can be carried out for the cumulative 3D-displacement series: it exhibits three acceleration phases—in November 2011, October 2012 and March 2013.

Two structural changes are thus detected quasi simultaneously on both series: mid October 2012 and mid March 2013. These two breakpoints can be seen as markers of potential risk. They should activate more vigilant monitoring of external aggravating or triggering factors such as heavy rainfall or earthquakes.

Discussion

For the Sèchilienne landslide, when applying proper statistical methods and employing quantitative concepts such as confidence, reliability or significance, observations which

seemed to be strongly interrelated (Fig. 4) are in fact weakly correlated (Table 1). Under these circumstances it is not possible to either provide or test a predictive model. Two reasons can explain these results. First, this study covers a short (3 years) period during which the movement and deformation processes are clearly self-accelerating. This complicates the approach, especially because of the data-based nature of the auto-regressive integrated moving average time series models used in this study. Second, these models are usually very efficient when considering systems whose function can be approximated as being linear. Nonlinear relationships that contain a linear component can be missed.

From a more general perspective, it is too early to come to conclusions about the unfeasibility of using statistical short-term forecasting capabilities based on an auto-regressive integrated moving average type model in early warning systems. Here, both the context and the insufficient amount of data do not permit conclusions in that sense. Some practical recommendations can however be enacted to promote the proper use of statistical methods in early warning systems applied to landslide risk management.

First it is important to design multi-parameter monitoring systems that meet the requirements imposed by statistical methods. For example, it is necessary that any intervention in the system that could affect the time series in some way be recorded as well. Also, the concept of significance (in the statistical sense) has to be systematically taken into account to put results, their interpretation and related decisions in perspective. Early-warning systems have to get rid of “significance” in the practical sense.

Second, in situations where time series analysis cannot provide models to forecast future events, simple criteria can be defined to detect potential risk. Here, the approach relies on the detection of acceleration phases simultaneously on multiple cumulative time series.

Acknowledgments This work was supported by the French Ministry in charge of the environment (*CENARIS* project) and the French National Research Agency (*ANR SLAMS* project). Authors wish to thank M.A. Chanut (CETE Lyon) and A. Vallet (Franche Comté University) for their helpful assistance in analysing Sèchilienne data and for sharing displacement and effective rainfall data.

References

- Bigarré P, Klein E, Gueniffey Y, Verdel T (2011) Cloud monitoring: an innovative approach for the prevention of landslide risks. In: The Second World Landslide Forum Rome, 2011, Abstracts Book WLF2, L16, p 475
- Chanut M-A, Dubois L, Duranthon J-P, Durville J-L (2013) Mouvement de versant de Sèchilienne: relations entre précipitations et déplacements. In: Proceedings of the 1st international conference on landslides risk, Tunisie, 14–16 mars 2013

- Dünner C, Klein E, Charmoille A, Bigarré P (2010) Multi-parameter monitoring strategy applied to unstable rock slopes: the example of the Ruines de Séchilienne. In: RSS 2010 Symposium, Paris
- Durville J-L, Kasperski J, Duranthon JP (2009) The Séchilienne landslide: monitoring and kinematics. Rainfall induced landslides. In: 1st Italian Workshop on landslides, Napoli, vol 1, pp 174–180
- Helmstetter A, Garambois S (2010) Seismic monitoring of Séchilienne Rockslide (French Alps): analysis of seismic signals and their correlation with rainfalls. *J Geophys Res* 115: F03016. doi: [10.1029/2009JF001532](https://doi.org/10.1029/2009JF001532)
- Hipel KW, McLeod AI (1995) Time series modelling of water resources and environmental systems. Elsevier, Amsterdam, The Netherlands
- Klein E, Nadim C, Bigarré P, Dünner C (2008) Global monitoring strategy applied to ground failure hazards. In: Proceedings of the 10th international symposium on landslides and engineered slopes, Xi'an, Chine, pp 1925–1931.
- Vallet A, Bertrand C, Mudry J (2013) Effective rainfall: a significant parameter to improve understanding of deep-seated rainfall triggering landslide – a simple computation temperature based method applied to Séchilienne unstable slope (French Alps). *Hydrol Earth Syst Sci Discuss* 10:8945–8991. doi:[10.5194/hessd-10-8945-2013](https://doi.org/10.5194/hessd-10-8945-2013)



Slope Stability Analysis at Bloemendhal Open Dump Site in Sri Lanka

Udeni P. Nawagamuwa and W. H. R. S. Dayarathne

Abstract

Civil engineering construction in the Colombo city area have commenced on lands previously used for the dumping of waste. Construction on covered dump wastes will cause a lot of problems, such as settlement, slope instability, and shear failure. Therefore similar to soil properties, it is important to study the properties of solid wastes to predict settlement, slope stability and shear strength parameters, though there are additional differences due to some chemical reactions occurring in the solid waste with time.

In this research, the geotechnical properties of solid waste from a dump site called Bloemendhal was studied. Several tests were made to identify and classify the so-called soils taken from the this location. Basic tests such as sieve analysis, Proctor compaction, consolidation and direct shear were conducted.

Open dumps are sometimes higher than 10 m. There is a huge risk of slope failures due to any modification of slope geometry or loading above. Therefore, in this research, that aspect was considered as an important issue. Several sections where possible failures could happen were analyzed using Geo-Slope software, using the results obtained from basic tests. Factor of safety values obtained for the existing conditions and with possible loading imposed due to any future constructions are discussed.

Keywords

Slope stability • Open dumps • Geotechnical properties • Bloemendhal

Failures of Waste Fills

A waste slide is an uncontrolled movement of waste down a slope. In developed countries, landfills are not located in an unstable area without a demonstration of stability. There is a good reason for these requirements, the consequences of a slide can be damaging to the adjacent residents and environment. This will become a very serious concern to developing countries like Sri Lanka, because local authorities are the agencies responsible for handling waste. Concerns about the stability and other issues had been neglected when the waste

was dumped. At the moment, Colombo has little suitable land left for new developments and several civil engineering projects have been begun on land previously used for the dumping of waste. There are several locations where these types of dump areas have been used for the construction of buildings. Two such recent examples are Peliyagoda fish market and relocation of underserved settlements at K. Cyril C. Perera Mawatha Colombo-14. Construction on already covered dump wastes will pose many problems such as settlement, slope instability, and shear failure.

Engineering of landfills is not being practiced in Sri Lanka, while developed countries maintain well controlled landfills. However, several failures have been recorded, even at controlled landfills, for various reasons. As mentioned by Boutwell (2004), a municipal soil waste facility in southern US in 1997 had a failure at the waste/soil interface.

U.P. Nawagamuwa (✉) • W.H.R.S. Dayarathne
Department of Civil Engineering, University of Moratuwa, Moratuwa,
Sri Lanka
e-mail: udeni@uom.lk; dayarathne.uom@gmail.com

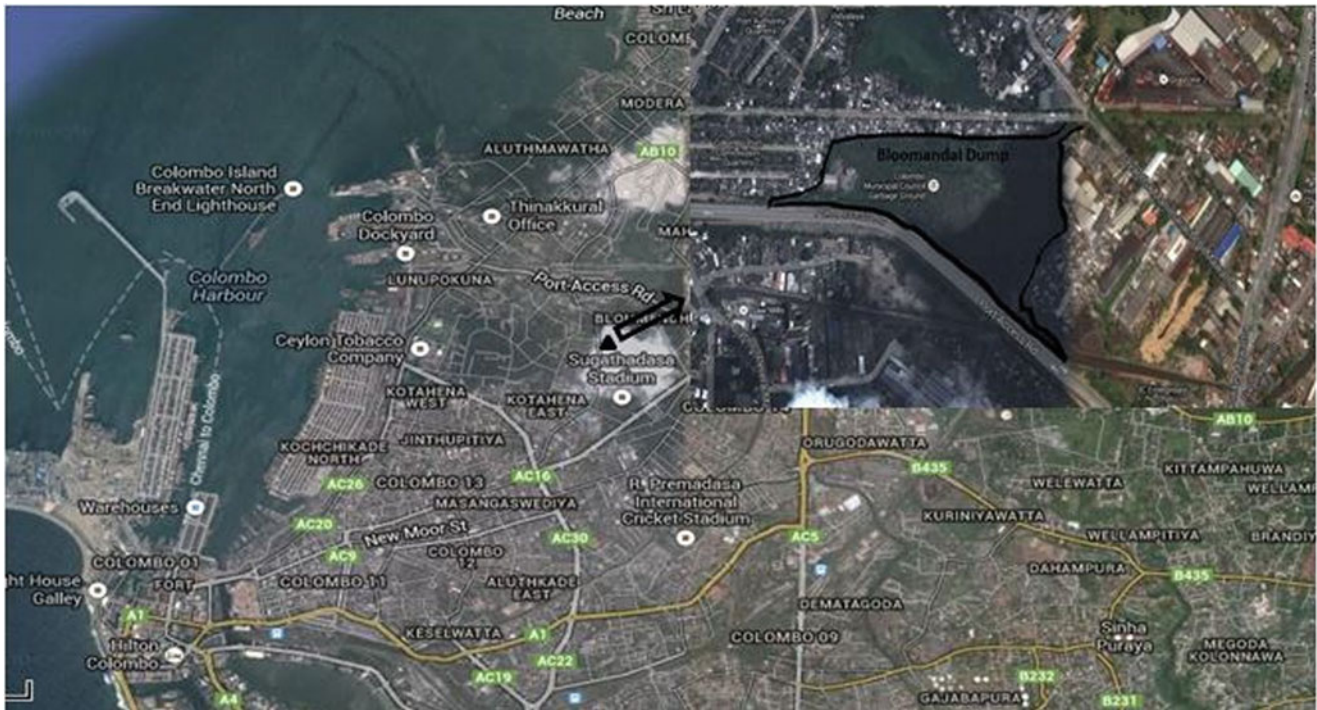


Fig. 1 Bloemendhal dump in Colombo Metropolitan area close to the harbour

The reason recorded was a modification done against the original design recommendations. A non-hazardous industrial waste (NHIW) facility in north-central US in 1997 had a failure within the waste. The reason was found to be placement of waste on a slope steeper and taller than the design.

Boutwell (2004) further reported that a strong MSW failure had occurred in a weak plane in the natural soil (foundation soils) in a MSW facility in midwestern US in 1996. A failure along the interface between a geo-membrane liner and the native soil was recorded at a Hazardous Waste facility in western US in 1988.

Bloemendhal Dump Site

Need for the Study

The study area for this analysis is the Bloemendhal dump (Fig. 1), with 12 acres of land situated just opposite to the Colombo Harbor. This dump has not been in operation since 2006, however, this is a very old dump which was in operation for more than 25 years (Berenger and Fazlulhaq 2009). However, now, with rapid urbanization and population growth, the requirements for new land for construction purposes are increasingly high, though the usable land areas are not readily available. Therefore, previously

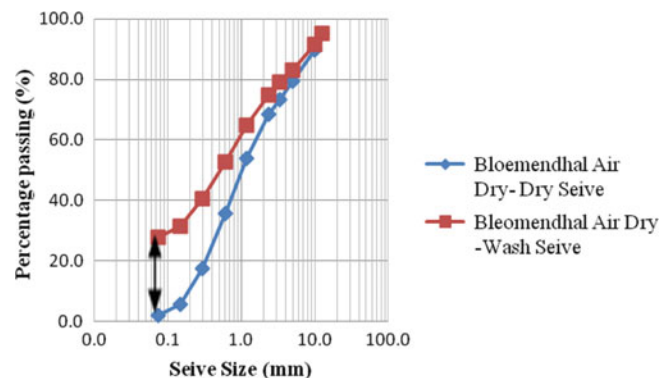


Fig. 2 Grading curves of air dry and wash sieve samples from Bloemendhal dump

rejected lands like dump areas are now being used for construction.

General Geotechnical Properties

Figure 2 gives details of dump sample grading curves obtained from dry and wash sieve methods after air drying. This provides an indication of occurrence of mostly a coarse grained soil in the site. Several samples were collected, such as from the top and bottom of the dump and at locations where burnings were carried out. The results of a standard Proctor compaction are illustrated in Fig. 3 for both bulk and

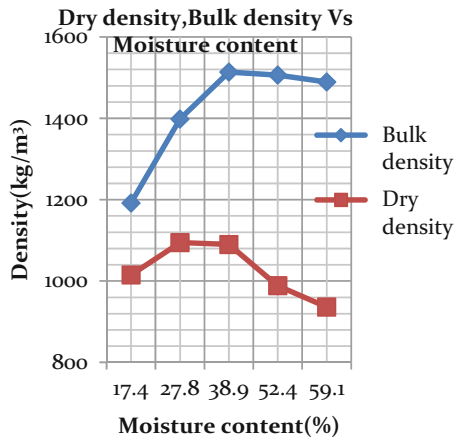


Fig. 3 Dry density and bulk density vs. moisture content

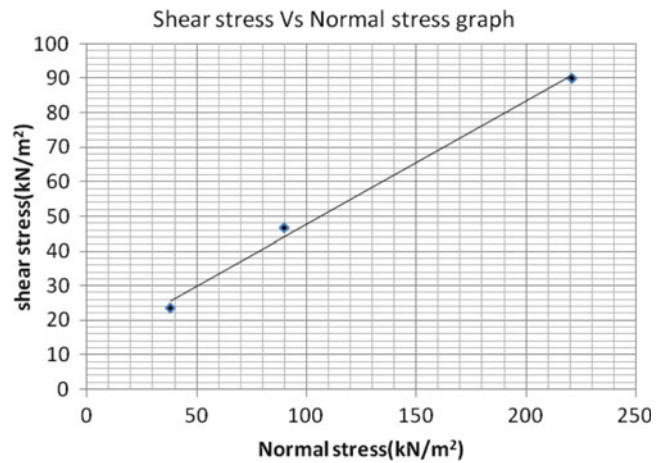


Fig. 5 Shear stress vs. normal stress graph with an OMC 30 %

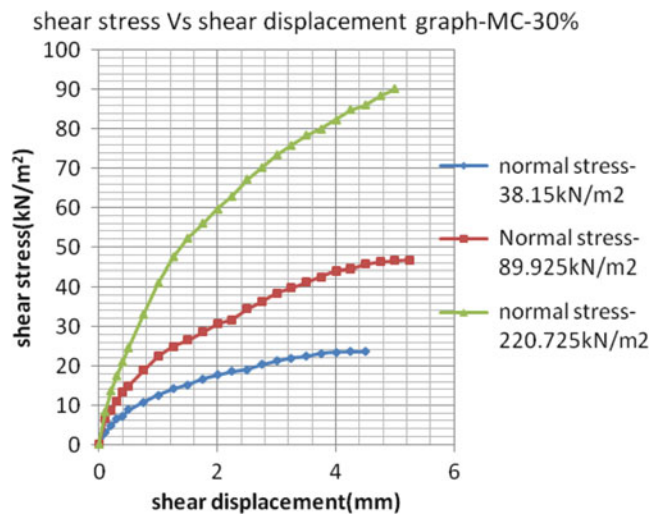


Fig. 4 Shear stress vs. shear displacement graph with an OMC 30 %

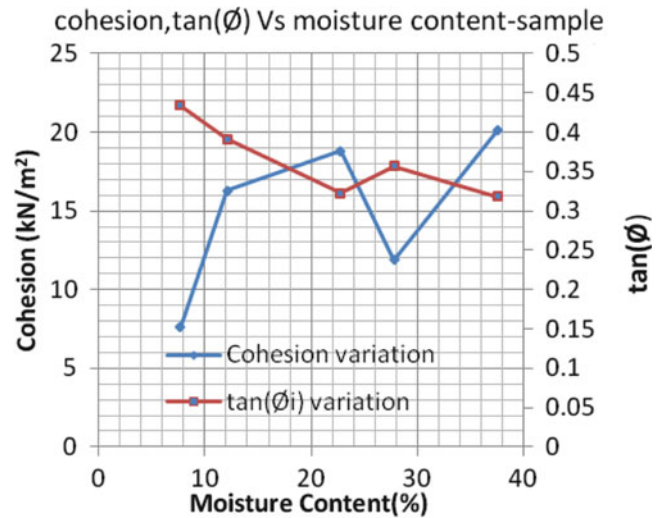


Fig. 6 Variations in shear strength parameters with moisture content (%)

dry densities. It was necessary to compare bulk density as there could be some losses due to the oven-drying process. A number of tests were conducted, with results showing a general bulk density of 1,500 kg/m³ and a dry density in the range of 1,000–1,100 kg/m³, with an optimum moisture content of around 30–32 %.

Further, these samples were tested with direct shear apparatus to obtain shear parameters. The results are shown in Fig. 4. Samples were collected from several locations at the dump; including the top, bottom and some burnt samples. These were tested at each moisture content level during standard Proctor compaction tests. All these tests were done using ASTM D 698. Polythene and other non bio-degradable particles greater than 19 mm were removed before testing.

These results obtained in Fig. 4 can be presented in a typical plot as shown in Fig. 5. Several such tests conducted for different moisture contents are summarized in Fig. 6.

Stability Analysis and Results

Two critical slopes were identified in considering the geometry of slopes. The thickness of the waste layers, their boundaries and the water table location were assumed and varied for the analysis. Finally, the idealized model shown in Fig. 7 was used. Due to the heterogeneous conditions at the site, it was decided to observe the impact of using lower

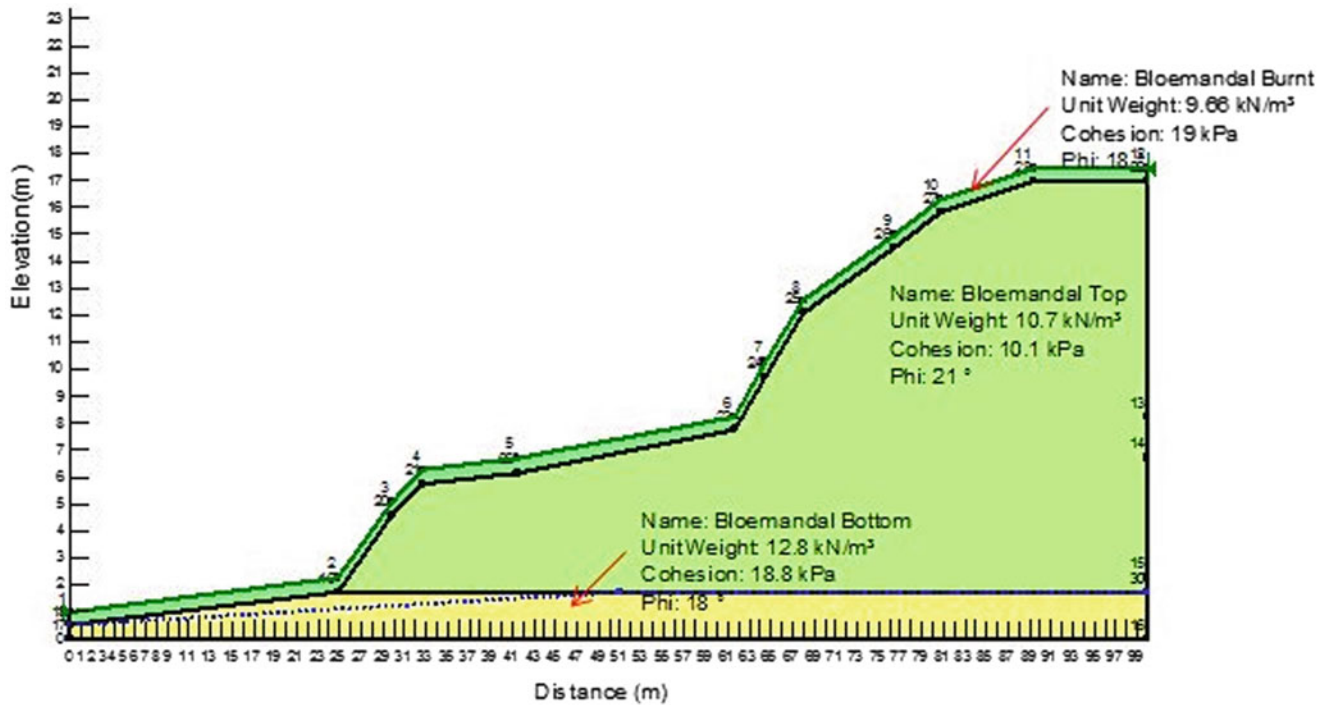


Fig. 7 Idealized model for Bloemendhal dump with different strength properties

Table 1 Variation of cohesion values

Analysis	Soil layer	C (kPa)	ϕ^0	γ (kN/m ³)
1	Top	10.1	21	10.7
	Bottom	18.8	18	12.8
	Burnt	19	18	9.66
2	Top	5	21	10.7
	Bottom	15	18	12.8
	Burnt	19	18	9.66
3	Top	1	21	10.7
	Bottom	10	18	12.8
	Burnt	19	18	9.66
4	Top	0	21	10.7
	Bottom	5	18	12.8
	Burnt	19	18	9.66

Table 2 Variation of values of friction angle

Analysis	Soil layer	C (kPa)	ϕ^0	γ (kN/m ³)
1	Top	10.1	21	10.7
	Bottom	18.8	18	12.8
	Burnt	19	18	9.66
2	Top	10.1	15	10.7
	Bottom	18.8	15	12.8
	Burnt	19	18	9.66
3	Top	10.1	10	10.7
	Bottom	18.8	10	12.8
	Burnt	19	18	9.66
4	Top	10.1	5	10.7
	Bottom	18.8	5	12.8
	Burnt	19	18	9.66
5	Top	10.1	1	10.7
	Bottom	18.8	1	12.8
	Burnt	19	18	9.66

values in addition to the values obtained during the laboratory tests.

Analysis was carried out while varying the shear strength parameters such as cohesion (C) and angle of shearing resistance (ϕ). Different categories of analysis were considered, based on the strength properties. Variation of cohesion and friction angle are described in Tables 1 and 2 respectively. Analysis 1 represents the findings from the laboratory tests.

Stability aspects were considered for the existing conditions and for possible future construction work. Therefore, analysis was done while adding a surcharge, ranging

from lower to higher values, to simulate future construction on this dump area. GeoStudio (2007) was utilized to carry out the analysis. It is extremely difficult to get seasonal variations of water table within a dump due to unavailability of piezometers within the site. So, a possible maximum water table level was assumed for the analysis. Factors of safety for the critical slip surfaces for each case are presented in Tables 3 and 4. Factor of safety values were calculated

Table 3 Factor of safety for the critical failure surface in C reduction analysis

Analysis	Surcharge (KPa)	Factor of safety in critical failure surface			
		Ordinary method	Janbu	Bishop	Spencer
1	0	2.102	2.065	2.229	2.226
	10	2.096	2.059	2.23	2.227
	20	2.064	2.02	2.169	2.167
	30	1.994	1.954	2.096	2.094
	50	1.812	1.772	1.926	1.925
	75	1.627	1.59	1.733	1.731
	100	1.481	1.445	1.568	1.567
2	0	1.717	1.727	1.78	1.778
	10	1.717	1.727	1.78	1.778
	20	1.715	1.71	1.787	1.785
	30	1.701	1.675	1.746	1.745
	50	1.552	1.525	1.606	1.606
	75	1.408	1.384	1.478	1.477
	100	1.285	1.259	1.352	1.353
3	0	1.233	1.255	1.302	1.301
	10	1.212	1.266	1.299	1.299
	20	1.217	1.251	1.294	1.293
	30	1.221	1.255	1.299	1.299
	50	1.227	1.255	1.3	1.299
	75	1.227	1.255	1.3	1.299
	100	1.234	1.26	1.305	1.304
4	0	1.088	1.15	1.183	1.182
	10	N/C	N/C	N/C	N/C
	20	N/C	N/C	N/C	N/C
	30	N/C	N/C	N/C	N/C
	50	1.086	1.16	1.183	1.182
	75	1.112	1.139	1.183	1.182
	100	1.112	1.139	1.183	1.182

N/C not calculated

using different methods such as Janbu, Ordinary, Bishop and Spenser.

Based on the results after varying the cohesion values, it can clearly be summarized that up to analysis 4 in Tables 3 and 4, failure is unlikely to be observed in the site. However, analysis 4 with “no surcharge” also shows a factor of safety of less than 1.3. To get a clear view of the variation, surcharge vs. Factor of Safety, which is obtained by using Spencer method, is plotted for each case. Figures 8 and 9 show that those discussed variations of C and ϕ analysis respectively.

Conclusions

Construction has been carried out on sites previously used for dumping wastes due to rapid urbanization and scarcity of suitable land for construction. Studies of geotechnical properties at those dumps, which are not in operation now, are required to predict their behaviour due to possi-

Table 4 Factor of safety for the critical failure surface in ϕ reduction analysis

Analysis	Surcharge (KPa)	Factor of safety in critical failure surface				
		Ordinary method	Janbu	Bishop	Spencer	
2	0	1.727	1.695	1.824	1.823	
	10	1.709	1.672	1.805	1.803	
	20	1.639	1.594	1.732	1.73	
	30	N/C	N/C	N/C	N/C	
	50	1.415	1.37	1.506	1.504	
	75	N/C	N/C	N/C	N/C	
	100	1.149	1.117	1.228	1.227	
3	0	1.4	1.368	1.475	1.474	
	10	1.381	1.345	1.444	1.443	
	20	1.315	1.272	1.378	1.377	
	50	1.121	1.083	1.18	1.18	
	100	0.887	0.858	0.946	0.945	
	4	0	1.09	1.06	1.124	1.124
		10	1.056	1.02	1.19	1.089
20		0.998	0.957	1.031	1.03	
50		0.825	0.779	0.861	0.86	
100		0.633	0.595	0.671	0.669	
5		0	0.845	0.811	0.853	0.854
		10	0.833	0.776	0.84	0.84
	20	0.793	0.723	0.802	0.802	
	50	0.659	0.581	0.674	0.673	
	100	0.487	0.43	0.509	0.508	

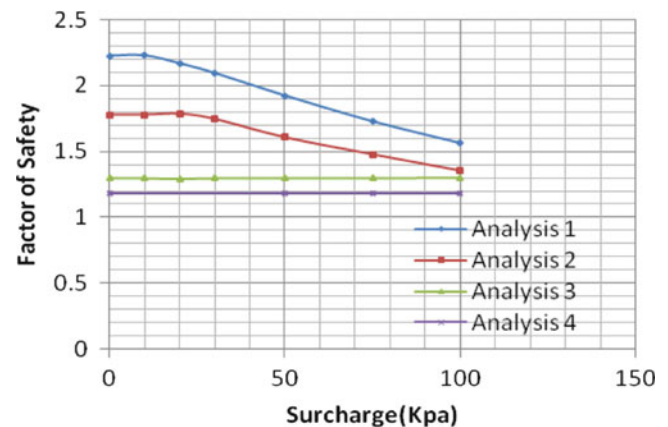


Fig. 8 Factor of safety variation for different cohesion values

ble future construction. Heterogeneity in the waste due to the presence of various types of materials and dumping during different time periods caused very difficult problems for the analysis. However, with several assumptions, it was found that if there are lower values of strength parameters available in different cross-sections, there could be possible failures. Therefore, it is necessary to do a detailed and long-term study at these dumps with proper instrumentation.

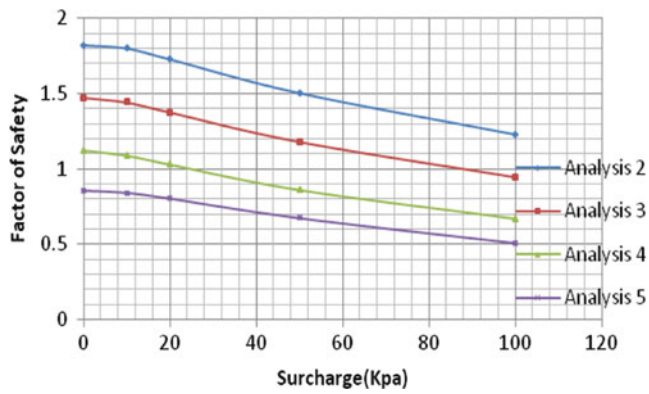


Fig. 9 Factor of safety variation for different friction angle values

Acknowledgments The authors would like to acknowledge the laboratory staff of soil mechanics lab, University of Moratuwa for their continuous help during the testing programme. Further, the officials of Colombo Municipal Council are gratefully remembered for allowing the authors to use Bloemendhal dump site for this study.

References

- Berenger L, Fazlulhaq N (2009) Garbage crisis growing by the day. The Sunday Times, 22 March, viewed 12 Aug 2013. http://WWW.sundaytimes.lk/090322/News/sundaytimesnews_00200903221.html
- Boutwell GP (2004) Slides happen—landfill stability analysis. Presentation, Civil Engineering Department, North Carolina University, Raleigh, NC
- GeoStudio (2007) SLOPE/W software, Version 7.17, Build 4921, copyright 1991–2010. GEOSLOPE International Ltd



Slope Dynamic Geomorphology of the Mailuu-Suu Area, Aspects of Long-Term Prediction

Yuri Aleshin and Isakbek Torgoev

Abstract

Long-term monitoring and the analysis of stability of the slopes subject to landslides on the territory of southwest Tien Shan where loessial soils are common, show almost a constant speed of deformation (secondary creep) and accelerating/decelerating movement of unstable masses due to hydrological changes. Landslides can occur without any previous noticeable warning signs. Slow movement of slope cover in Paleogene-Neogene clays over 10 or more years creates the effect of accustoming local residents to the hazard. Under such circumstances, it is important and critical to rank slopes according to a hazard rating; the estimation of the remaining time to slope failure may serve as a criterion of the hazard. We have applied the Saito model coupled with a viscous model for ranking and classifying slopes of the large landslide-prone area of Mailuu-Suu. More than 200 landslides occurred in this mountain territory (~50 km² in area) over the last 60 years. The reactivation of most paleolandslides is connected with intensive mining activity and urbanization. The proposed model is useful for short, mid and long-term predictions of secondary creep. The main factors in the prediction are slope steepness, steady-state moisture content of clay soils along its contact with the bedrock, a possibility of sudden and fast water table rise, and type of hydrogeological recharge. Thus local site maps were formed as a basis for detailed and systematic study of slopes, starting with the most dangerous ones with the shortest lifetime. It does not matter that long-term predictions remain uncertain due to change of hydrogeological conditions with time and soil degradation. Detailed study of such slopes is carried out for the latter. It is recommended to install automatic extensometers with telemetric transmission of landslide movement data on slopes with predicted life spans of 1–3 years.

Keywords

Creep • Viscosity • Landslide velocity • Failure prediction

Y. Aleshin (✉)
Institute of Geomechanics and subsoil development, National Academy of Sciences of the Kyrgyz Republic, Mederova Street, 98, Bishkek, Kyrgyz Republic
e-mail: Yuri.Aleshin@gmail.com

I. Torgoev
Scientific-Engineering Center “Geopribor”, National Academy of Sciences of the Kyrgyz Republic, Mederova Street, 98, Bishkek, Kyrgyz Republic
e-mail: geopribor@mail.ru

Introduction

The main feature of modern landslides in the Mailuu-Suu River basin is the slope nature of the unstable mass displacements, in which landslides and avalanches different in scale syndynamically reach the base of the slope. Where the boulder-fragment and soil slide masses cease to move, having reached the base of the slope or deposited at the current river terrace, sometimes partially damming the river. Subsequently, there is a gradual dewatering of the

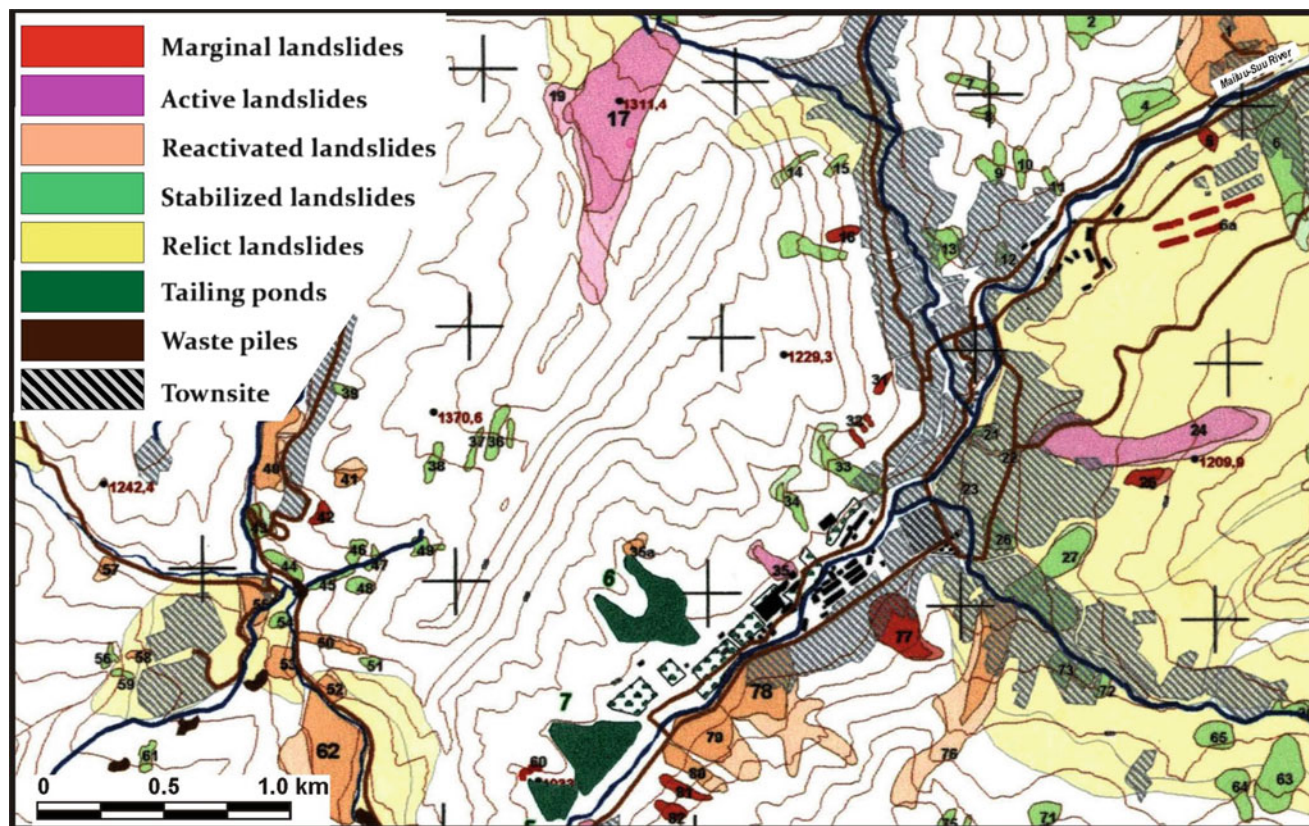


Fig. 1 The landslide incidence in the Mailuu-Suu area

landslide body when water and the most mobile clay fractions of fluid consistence are carried ahead of the landslide limit. There are very few fast syndynamic along-valley “dry” flows with a run-out distances $L > 3l_1$, where l_1 is the landslide body length along the main displacement vector (Aleshin Yu et al. 2006; Torgoev et al. 1997).

Continuous, long-term monitoring of landslide displacements on a series of slopes and analysis of seismic and meteorological factors allow us to establish close but delayed (from a few days to 2 or 3 months) correlations between slow speed landslide displacements and precipitation, groundwater level and seismic activity of the subregion territory. For example, at the: “Izolith” landslide this relationship was explicitly revealed in the spring of 1998, when the time delay of landslide activity in different parts of the landslide body was from a few hours to 3–5 days, depending on the thickness of the unstable blocks. Properties of the clay soils of the unstable cover on the slopes in the Mailuu-Suu River basin (Fig. 1) are such that in a fairly high moisture conditions they remain relatively high values of internal friction angle φ and viscosity factor ζ . However, with a small but the continuous additional moisture, these values are reduced considerably.

These properties determine the features of the development of exogenous geological processes on the territory

described, in particular the long and slow (measured at a rate of $\sim n \times 10$ mm/year) deformation of weak stable slopes, which ultimately determines the even greater fall in clay soils’ strength. In the setting of Mailuu-Suu, the landslide processes themselves can be visually recorded only in the last stage of displacement, the preparation of which may continue for a long time—for many years. This is evidenced by the tension cracks almost universally observed on the slopes and the stream net on the ground surface, which appear long before the catastrophic stage of landslide process, creating an effect for concern to residents and concerns for safety. The catastrophic phase of rapid displacement of landslide masses used to occur unexpectedly without expressive visible symptoms and extreme precipitation factors, as was the case between 2002 and 2006, when similarity between several major landslides were noted, although there was no abnormal precipitation.

Methods and Results

The main characteristic of landslide displacement of unstable slopes under the influence of rheological factors is the rate of landslide displacements. This can be determined

using the Bingham model (Maslov 1982), with the initial ground resistance against the displacement

$$dV_y = \frac{\tau_y - \tau_{lim}}{\zeta} dy \tag{1}$$

where V_y is the velocity of the unstable surface at the level y (in depth from the daylight surface); $\tau_y = \rho_\omega(H - y)\sin\alpha$ is the value of shear stress at the level y ; $\tau_{lim} = \delta \tan \varphi_\omega + C_\omega$ is the creep threshold; ζ_ω is the soil viscosity factor; H is thickness of the unstable cover; α is angle of the slip plane; δ is normal stress by the weight of the earth cover overlying slip plane, φ_ω is the internal friction angle and C_ω is structural strength of soil for in situ conditions. Lower index values emphasize a significant effect of the moisture content ω on the physical and mechanical properties of soils.

Upon integration of (1) we have an opportunity to formulate a necessary condition for the weak stable cover displacement as:

$$\tan \alpha > \tan \varphi_\omega + \frac{C_\omega}{\rho_\omega H \cos \alpha} \tag{2}$$

Finally, having the soil test data and using the relation of their physical and mechanical properties with moisture, we can get the limit equilibrium condition in the slope

$$H \leq H_{lip} = f(\omega^*, \alpha) \tag{3}$$

where $f(\cdot)$ is a complicated function from humidity indicators of the clay layers and/or soil layers, as well as the angle of their incidence towards the valley.

Discussion

Figure 2 graphically presents the relation (3). It follows from these graphs that long-term stability of Cretaceous-Paleogene-Neogene interlaminated structures represented by sandstone, siltstone, clay, gritstone, limestone, with a total thickness of up to 100 m at the slip plane with angles 20–25°, is guaranteed if the clay layers in slip planes are in a semi-solid and low-plastic consistency. Thin beds and Quaternary covers (of ~10 m thickness) lose their stability during the transformation of Paleogene and Upper Cretaceous clay into a state of high plasticity and flowing consistency.

The Tertiary clay in the structures which formed Mailuu-Suu anticlines are characterized in situ by an extremely low index of plasticity (15–20 %) and almost the same average of natural water content both in the primary bedding, as well as in the disrupted beds (in the primary bedding—between 13 and 15 %, in the disrupted bedding—between 17 and 19 %), due to low water conditions of the uppermost areas of anticlines. In primary bedding these clays have a very high

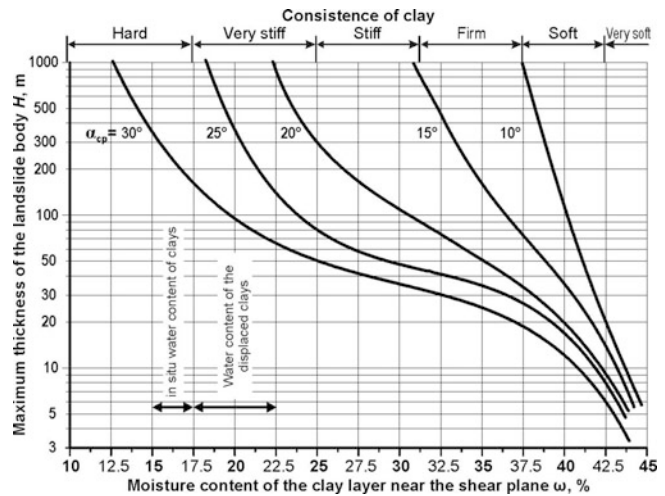


Fig. 2 The relationship of the critical thickness of Cretaceous–Paleogene block from clay layer moisture in the slip plane, in which there is a loss of stability of the slope

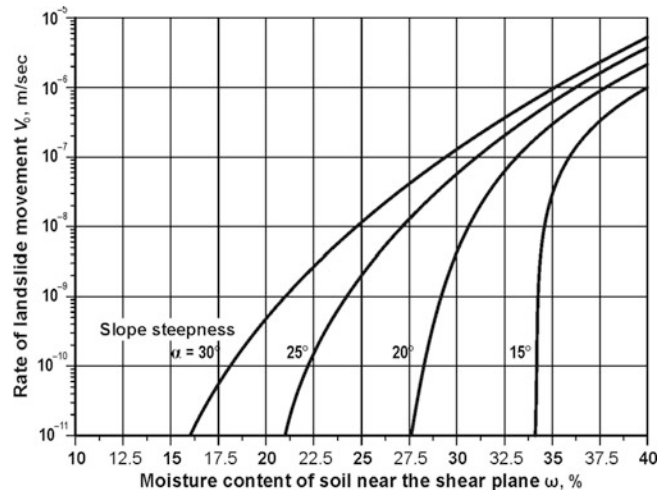


Fig. 3 The relationship between the displacement velocity of the Quaternary cover based on the Cretaceous-Paleogene platform from the Tertiary clays humidity

compactness, as evidenced by their high unit weight and low moisture content—1.5–2 times lower than the plastic limit. Even in the disrupted bedding the moisture content does not exceed this limit. This suggests that the clays are in hard consistency in such masses. The water content is just over the plastic limit only for Cretaceous clay in the disrupted bedding, and only in water-saturated areas of ancient landslides does it reach high values—up to 30–33 %, but these are usually in depression areas of the daylight surface and landslide accumulation zones. For this reason, there is no doubt about the current stability of the Cretaceous deposits.

Another situation arises on the slopes covered with Quaternary deposits, or in areas of ancient landslide deposits of clayey soils. Fig. 3 show graphs of displacement velocity

Table 1 Clayey soil water content ω , % in the slip plane, which provides various stages of loss of stability of the Quaternary cover on the Mailuu-Suu slopes

Stage of creep	Landslide stage (The “lifetime” of the slope)	Predicted parameters for slope angles α (deg)			
		15	20	25	30
Primary stage, of damping	Unconditional stability	≥ 34.5	≥ 27.5	≥ 21.2	≥ 16.5
Secondary stage, of constant displacement rate	Secular stability (of at least 100 years)	35.0 ± 0.2	29.6 ± 1.1	25.0 ± 1.5	21.0 ± 2.0
	Long-time stability (30–100 years)	35.3 ± 0.2	30.7 ± 1.0	26.2 ± 1.2	23.7 ± 2.0
	Practical stability (10–30 years)	35.7 ± 0.3	31.5 ± 1.0	27.2 ± 1.8	25.5 ± 2.5
	Preparation of the displacement (3–10 years)	36.3 ± 0.5	32.6 ± 1.0	30.2 ± 2.2	28.8 ± 1.8
	Significant displacement (1–3 years)	37.1 ± 0.9	33.7 ± 1.3	32.0 ± 2.3	30.7 ± 2.8
Tertiary stage, of accelerating displacement	Emergency evolution (4 months to 1 year)	38.5 ± 1.5	36.5 ± 2.1	35.0 ± 2.5	33.6 ± 2.9
	Before catastrophic collapse (<1 month)	41.0 ± 3.0	40.0 ± 3.0	39.5 ± 3.0	39.0 ± 3.0

**Fig. 4** The upper part of the “Tecktonik” landslide: the formation zone of landslide blocks

of the Quaternary cover (~10 m thick) on thin clay layer of $d \sim 10$ cm against the moisture of this layer, derived from a calculation using the relation (1) and the objective parameters of the physical and mechanical properties of clayey soils of Mailuu-Suu. Going to the rate of deformation of clay layers in the slip plane, and using the Saito equation (Saito 1982) to predict a slope failure time, we can get the calculated (predicted) soil moisture parameters, which are specific for different stages of formation and development of the landslide process (see the Table 1).

The final stage of the landslide process is the most difficult to predict: the moment of fast catastrophic release of landslide masses towards the foot of the slope. This is due largely to the conditions and characteristics of the watering of soils on the slopes of the Mailuu-Suu River basin. There are three sub-zones of moistening: top sub-zone—up to a depth of 2 m in undisturbed cover loamy soils and 4 m in shifted rocks, with a very large range of soil moisture

variation (5–18 %); intermediate sub-zone—with thickness ranging from 4 to 8 m with a relatively constant soil humidity (13–17 %); lower sub-zone—with thickness ranging from 2 to 3 m, where the increase in moisture is due to capillary fringe of constant weak underground stream in contact with the Cretaceous–Paleogene rocks, where moisture of clay soils can reach 25–35 %. The areas of landslides accumulation and shifted loamy soils have a rather high permeability index ($K_{\phi} > 10^{-5}$ m/s), but despite this, in wet years the groundwater supply through the aeration zone is negligible for a thick surface cover even with a possible increase in moisture of the upper sub-zone by 1.5–2 times. During the intense and prolonged precipitation in the spring, when the surface runoff is produced, the moisture penetrates through the numerous cracks on the slopes with an off-surface cover, which causes an increase in the speed rate of displacement, especially the lower part of the unstable surface covers, decompression of soils in the

middle and head parts of landslides, the formation of new cracks with their aperture and increase of soil moisture permeability. Thus there is penetration of atmospheric moisture into the lower sub-zone, a kind of “closure” aquifers; inside of the landslides bodies there are sometimes layers of soils of a fluid-plastic consistency, and landslides in their foot parts are transformed (as in case of the processes at the “Tecktonik” landslide); there is a sharp increase in the landslide mass displacement speed rate in leading blocks, sometimes with release of fluid consistency soils out of the upslope bedding and complete disintegration of the blocks (Fig. 4). In this state, the landslide bodies may be stabilized for many years—as long as they will not be involved in the landslide process of the upslope bedding soils on the slope with a cascade upslope soils development of landslides, so characteristic for the Mailuu-Suu.

The duration of the active phase of the shift increases when groundwater discharge of distant feeding zones, which is done through tectonic faults in the bedrock, is delayed by 1–3 months relative to the period of intense precipitation in April and May of each year. Such conditions are created on the slopes of old-landslide slopes of “Koi-Tash” and “Sary-Bee.” There is almost constant hydrogeological water supply of soil during the year, which determines the implementation of the secondary creep regime of the Quaternary cover and old-landslides deposits with a deformation rate of $de/dt \sim 10^{-a} \text{ s}^{-1}$, where $a = (10 \pm 1)$. For decades, these soils filled the depression in the lower parts of the mountain slopes, where they quickly were released in the form of small landslides with a volume $\sim n \times 10^3 \text{ m}^3$ on the river terrace. Landslide processes in such areas reflect a quasi-periodic nature.

Conclusions

Thus, studies have shown that the special characteristics of the soil and the regime of their moisture on the slopes

of the Mailuu-Suu river basin define complex of landslide developments in the area, a kind of intermittent displacement regime of landslide bodies with temporary stabilization, lasting sometimes for several years, followed by a rapid intensification of the process with a transition to a catastrophic stage. Existing theories of landslide process development fairly well describe the real shifts of the blanket covers of the slopes, which are at the stage of secondary creep, and they can be used for the purpose of long-term forecasting of the landslide situation in Mailuu-Suu by calculating the moment of transition to the active phase of the tertiary creep. The final stages of landslide development are currently difficult to forecast. The problem can be solved radically by equipping the mountain slopes, which are in the stage of tertiary creep, with automated systems of geological control over landslide displacements (Torgoev et al. 1999), and landslide danger early warning systems. A similar system was established with the participation of the authors and that functioned in Mailuu-Suu for 6 years.

References

- Aleshin Yu G, Torgoev IA, Mamyrova RK (2006) Geological and ecological risks in complex mining development. *Vestnik KRSU* 6(7):74–83 (in Russian)
- Maslov NN (1982) The fundamentals of engineering geology and soil mechanics. Vysshaya Shkola, Moscow (in Russian)
- Saito M (1982) Evidential study of forecasting occurrence of slope failure. *Probl Geomech* 8:45–74
- Torgoev IA, Aleshin Yu G, Moldobekov BD, Meleshko AV (1997) Genetic factor of landslide evolution in the Mailuu-Su River basin. In: *Problems of geomechanics and mineral deposits exploitation*. Ilim, Bishkek, pp 76–103 (in Russian). ISBN 5-8355-0946-4
- Torgoev IA, Aleshin Yu G, Moldobaeva BB (1999) *Geoenvironmental safety and risk of natural catastrophes and man-made disasters*. JEKA Ltd, Bishkek, 288 p (in Russian). ISBN 9967-423-14-5



An Overview of Rock Avalanche-Substrate Interactions

Anja Dufresne

Abstract

Large rock or debris avalanches inevitably encounter and interact with a variety of earth materials along their paths. These substrate materials influence rock and debris avalanche emplacement in one or several of the following ways (1) longer runout due to an increase in volume by entrainment on the steep failure slope, (2) higher mobility by reduction in basal frictional resistance (e.g. emplacement over glacier ice), or (3) a larger area of deposition due to transformation into debris flows, contrasted by (4) runout impediment due to interactions along the flatter runout path (e.g. bulldozing of substrate material or entrainment of high-friction debris), and introducing (5) flow complexities resulting from changes in basal mechanical properties and other localized interactions. Additionally, the total area affected by a rock avalanche may extend beyond the deposit margin itself when sediments in front of the rock avalanche are bulldozed or are mobilized and flow independent of the rock avalanche for some further distance.

Keywords

Rock avalanche • Debris avalanche • Runout-path material • Entrainment

Introduction

In 1881, Buss and Heim proposed the idea that liquefied substrates have a major influence on rock avalanche mobility. Over the past few decades, this topic has been widely discussed in the landslide literature, with more and more reports of field and theoretical evidence for the influence of substrate materials on avalanche emplacement (Abele 1974, 1997; Hsü 1975; Sassa 1988; Hungr 1990; Yarnold 1993; Voight and Sousa 1994; Abbot et al. 2002; Legros 2002; Clavero et al. 2004; Hungr and Evans 2004; Abdrakhmatov

and Strom 2006; Hewitt 2006; Crosta et al. 2009; Dufresne et al. 2009; Wang et al. 2012; Xu et al. 2012).

In typical rock avalanche settings, material along the runout path consists of unconsolidated valley-fill sediments of fluvial, glacial, lacustrine or colluvial origin. Surface water in the form of rivers and lakes is present, and in some cases snow and glacier ice as well. In addition, pyroclastic deposits and lava flows are common in volcanic settings.

Only locally are the substrates beneath rock avalanches undisturbed; they almost everywhere are deformed, in some instances to a high degree. Where rock avalanche-substrate interaction features are exposed, they provide evidence for rock avalanche emplacement processes. This contribution presents an overview of features produced by the interaction of rock avalanches with their substrates and of inferred changes in rock avalanche mechanical behaviour, mobility and runout.

A. Dufresne (✉)
Institut für Geo- und Umweltwissenschaften, Geologie, Albert-Ludwigs Universität Freiburg, Albertstr. 23b, 79117 Freiburg, Germany
e-mail: anja.dufresne@geologie.uni-freiburg.de

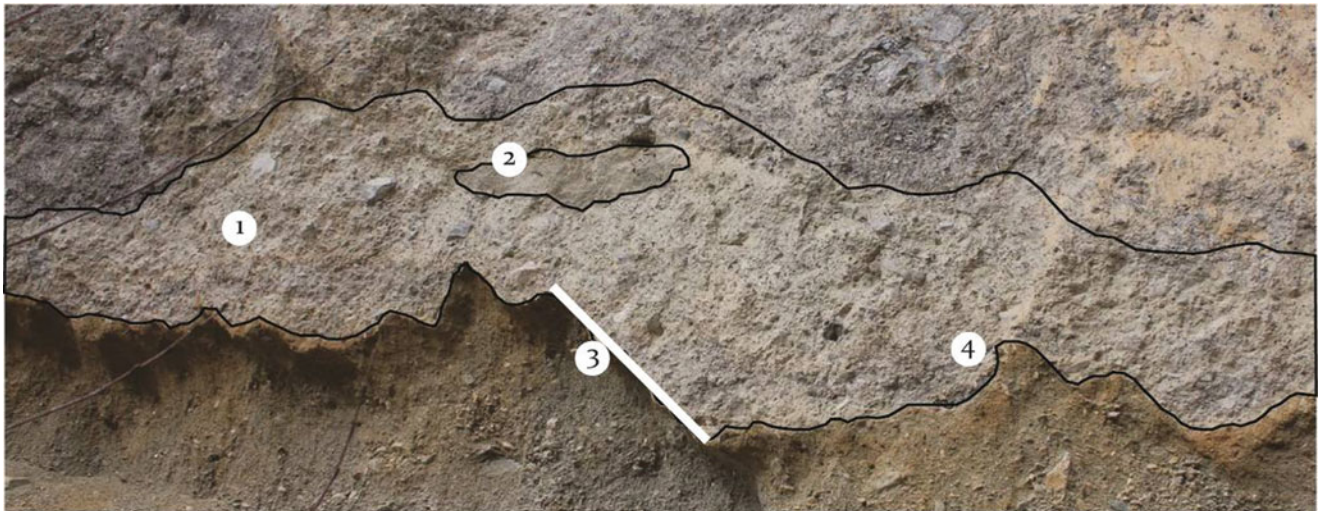


Fig. 1 Example of common features at the contact between a rock avalanche deposit and its substrate: (1) basal mixed zone in which rock avalanche and substrate material are thoroughly mixed; (2) rip-up clast of coarse, unconsolidated alluvial sand; (3) fault offsetting alluvial sand

layers; and (4) ductile deformation. This example is from the Tschirgant rock avalanche, Tyrol, Austria. The section is about 10 m long. Direction of rock avalanche movement is left-to-right

Substrate Erosion and Entrainment

The most extreme effect that sediments and water from the substrate can have on rock avalanches is to completely transform them into highly mobile debris flows. In many cases, there is a volume increase without a flow transformation, with two possible consequences: (1) simple volume increase with the possibility that the rock avalanche will cover a greater area with debris; (2) changes in the composition and mechanical properties of the basal rock avalanche material, which in turn may either impede runout if high friction materials are entrained or enhance runout when frictional resistance is lowered, specifically when sufficient amounts of ice, snow or water are mixed into the base of the landslide.

Basal Mixed Zone and Rip-Up Clasts

Rock avalanche material rarely mixes entirely with entrained sediments. Instead, there is commonly a basal mixed zone that is relatively thin compared to the total thickness of the landslide deposit (example in Fig. 1 is 10 % of the deposit thickness). Mixing in this basal zone can be thorough, and the zone may be sharply bounded by both overlying rock avalanche and underlying disrupted substrate materials. Based on the example in Fig. 1, it is clear that entrainment and mixing of fluvial sand and gravel occurred before overriding and deformation of the *in situ* substrates, which have a different composition than the entrained material. Between these two events, unconsolidated coarse sand was

entrained as coherent clasts, but did not disaggregate and mix with the rock avalanche debris. In this instance, three different processes can be inferred to have occurred in succession along the travel path, with a decreasing degree of interaction: (1) entrainment and mixing, with the formation of a basal mixed zone; (2) breaking of unconsolidated granular substrate material into clasts and their incorporation into the rock avalanche without further mixing; and (3) faulting and folding of the *in situ* substrate, apparently without significant entrainment. In other examples, rip-up clasts are present in otherwise pure rock avalanche material, with no signs of disruption, mixing or incorporation, and leaving no evidence of how they reached their position. Could they have been emplaced by laminar flow and ductile deformation? Or perhaps, they moved upward along temporarily opened faults or shear zones.

Flow Transformation

Rock avalanches transform into debris avalanches when a large volume of substrate material is entrained on the steep slope below the failure surface. Analysis of volumes of source rocks, rock avalanche deposits and entrained substrates suggests that 20–50 % by volume of the final deposit, or at least 30 % of the original source volume (prior to failure and fragmentation) must be entrained to induce flow transformations (Dufresne et al. 2009). These values are in accordance with entrainment ratios (i.e. the ratio of the volume of entrained material to the bulked volume of the initial mass due to fragmentation) greater than 0.25 inferred by Hungr et al. (2001). Such large

entrained volumes on steep slopes add material with significant potential energy to the moving mass and thereby increase total rock avalanche volume and runout potential. In contrast, substrate entrainment on the flatter runout path is more likely to impede runout and induce local complexities in basal composition and mechanical behaviour (Fig. 1).

Further transformation into highly mobile debris flows can occur when sufficient volumes of surface water or saturated sediment are entrained anywhere along the failure slope or runout path. Debris flow mobility commonly exceeds that of comparably sized rock avalanches by 100 % (Iverson 1997).

Substrate Deformation

Any interaction, for example erosion, folding, faulting or shearing, of a mass in motion with stationary material requires the transfer of kinetic energy from the moving mass to the substrate. The result is local runout impedance, flow diversions, and sometimes unique morphological signatures.

Bulldozing

Sediment bulldozing at the termini of rock and debris avalanches has been documented at the volcanic debris avalanche deposits of Parinacota, Chile/Bolivia (Clavero et al. 2002); Shiveluch, Kamchatka (Belousov et al. 1999); and Socompa, Chile (van Wyk de Vries et al. 2001); and the rock avalanche deposits Adair Park Breccia, Arizona (Yarnold and Lombard 1989); Ananievo, Kyrgyzstan (Abdrakhmatov and Strom 2006); Baga Bogd, Mongolia (Philip and Ritz 1999); Blackhawk, California (Johnsons 1978); and Arvel, Switzerland (Choffat 1929 as cited in Crosta et al. 2009). Particularly impressive is the bulldozer facies of the 1964 Shiveluch volcanic debris avalanche deposit, where pyroclastic sediments are folded over an area of 1.5 by 6 km (Belousov et al. 1999). Longitudinal ridges of the Shiveluch debris avalanche appear to terminate well before the front of the deposit (elsewhere they extend to the frontal margin), suggesting feedback from bulldozing onto the debris avalanche. In this case, sediment bulldozing might act similar to topographic obstacles and decrease avalanche runout.

Likewise, localized substrate bulldozing within the boundaries of rock or debris avalanches, such as in front of longitudinal ridges, can impede runout and influence their morphology by preventing the break-up of ridges into distal hummocks. Examples of substrate bulldozing at ridge termini include Altenau, Germany (von Poschinger 1994), Ghoroh I, Pakistan (Hewitt 2006), Round Top, New Zealand (Dufresne et al. 2009) and Artillery Peak, Arizona (Yarnold 1993). Fluvial sediments and peaty-clayey soils were

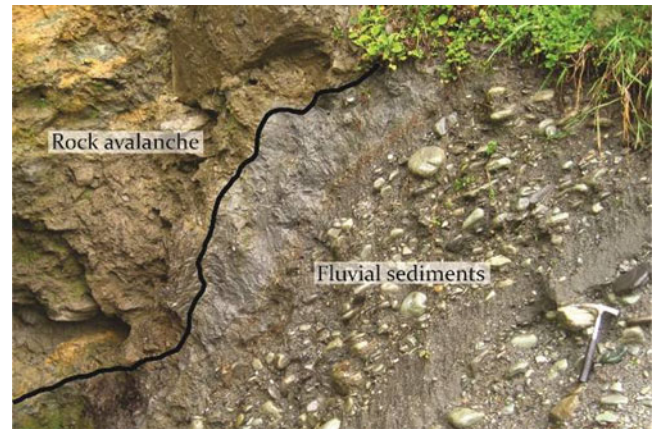


Fig. 2 Section in a longitudinal medial ridge of the Round Top rock avalanche deposit, New Zealand. The flow direction is toward the camera. Fluvial gravel and peaty-clayey soil were detached and bulldozed by the advancing ridge. Hammer for scale

bulldozed in front of a high longitudinal ridge in the medial deposition zone of the Round Top rock avalanche (Fig. 2). The stratigraphy of the bulldozed deposits remained intact, although shear zones are preserved in the topmost soil layers, documenting different stages of disruption and bulldozing. The ridge behind these bulldozed sediments appears shortened, as if its front abruptly decelerated while the still mobile rear part collided into it, creating a steep frontal margin and a pronounced hummocky surface. Other ridges in the same deposit are flatter and longer, with more gentle slopes.

Folding and Faulting

Folds and faults of a wide range of sizes (e.g. Hewitt et al. 2008) are found along the rock avalanches-substrate contact, within the substrate, outside the deposit margins, and throughout the avalanche mass itself. Small-scale faults that developed beneath a rock avalanche probably do not influence the emplacement dynamics, but they attest to the substantial impact of the avalanche on the materials it interacts with. A change in avalanche behaviour could be induced when it encounters weaker substrates, as in the case of the Ollagüe volcanic debris avalanche in Chile (Clavero et al. 2004). Near the distal limit of this deposit, the amplitude of substrate folds increases where the avalanche encountered more ductile sediments. There, isolated hummocks sit atop thickened and folded unconsolidated saline sediments.

Basal Friction and Shear

Shear features form beneath rapidly moving rock avalanches, as they do beneath slowly moving glaciers (Piotrowski et al. 2004). The fact that they are preserved

beneath rock avalanche deposits allows two kinds of inferences. (1) Shearing takes place only during the final stages of movement, and thus is a late-stage phenomenon that does not significantly influence avalanche mobility. (2) Shearing occurs during the high-velocity emplacement phase and has a considerable influence on avalanche mobility. In the second case, preservation of the features requires (2a) constant arising and diminishing and location changes of shear bands, and/or (2b) incremental deposition preventing destruction of the shear bands, and (2c) a lack of substrate erosion to the base of these shear bands.

Shear stresses can be transferred to considerable depth into the substrate without eroding it. At the Gol-Ghone B rock avalanche, Pakistan, sheared substrates are found to 200 m below its base (Hewitt 2006). Erosion versus shearing will depend on substrate and basal avalanche mechanical properties, as well as avalanche velocity.

High basal frictional resistance opposes the forward motion of the rock avalanche and is transferred back into the mass. Consequences might include sudden avalanche deceleration, the generation of a steep frontal margin, or basal deceleration accompanied by the upward migration of a shear zone and, possibly, incremental stacked deposition.

A well-documented example of lowered basal friction is rock avalanche emplacement on glacier ice (Evans and Clague 1998). The low-relief and low-friction surface of a glacier allows rock avalanche material to spread, thin and travel significantly farther than would be the case if it moved over other materials (Evans and Clague 1998; Sosio et al. 2014).

Substrate Mobilization

Fluidization of water-saturated sediments by rock or debris avalanche impact is facilitated by the generation of a pore pressure gradient in the substrate that counteracts the cohesive forces and frictional strength of the materials (Gauer and Issler 2004). Pore fluid pressures temporarily rise to the point that incompressible interstitial fluids carry all the applied stresses, leading to loss of shear resistance. Substrates in a fluidized state pose no resistance to avalanche motion; instead they reduce the basal frictional resistance of the moving mass, which favours enhanced motion. Secondary debris flows can be generated ahead of the avalanche in this manner, enlarging the total area affected. The role of rapid undrained loading in long rock avalanche runout has been discussed since Hutchinson and Bhandari proposed this mechanism in 1971. Although locally important, the existence of dry long-runout rock avalanches shows that it cannot be a universal explanation.

In the case of earthquake-induced landslides, runout path material might liquefy prior to overriding (Wang et al.



Fig. 3 Base of the Perrier volcanic debris avalanche, France. (1) Sharp shear horizon. (2) Larger fractured and (3) partially sheared clasts

2012), making it all the more susceptible to mobilization by the rock avalanche.

Isolated distal hummocks (toma hills), like those of the Ollagüe example mentioned above, have been found at the Fernpass rock avalanche, Austria up to 4 km from the margin of the deposit (Prager et al. 2006). They were produced by mobilization of saturated substrates either during the rock avalanche or due to gravitational spreading shortly afterwards.

Emplacement Mechanism Indicators

Features resulting from rock avalanche-substrate interactions provide important clues about rock avalanche dynamics. The contact between the rock avalanche deposit and its substrate may look sharp and lack evidence of disturbance, in all likelihood, though, it is an erosional surface (Fig. 3); a basal mixed zone should be sought farther downflow. Furthermore, the base of the moving mass might not be the rock avalanche-substrate contact; it could lie well below this contact and within the materials thought to be *in-situ* sediments (e.g. Gol Ghone B; Hewitt 2006).

Flame injections have limited value as kinetic indicators because they may be bent into or toward the direction of flow (Yarnold 1993; Friedmann 1997; Dufresne 2012). Other injections may follow shear planes, thus indicating short-lived brittle faulting or opening of the rock avalanche mass.

Conclusions

Substrate materials along the runout path of rock and debris avalanches introduce many complexities to the emplacement of such landslides. They locally change the mechanical behaviour of the moving mass, impeding or enhancing mobility and spreading. Their specific influence crucially depends on substrate properties and location of encounter, e.g. entrainment on the steep failure slope versus the flatter runout path. Liquefaction of saturated substrates, though not a universal explanation

for the excess runout of rock and debris avalanches, is one of several factors involved in the complex interactions of these landslides with their runout path materials.

Acknowledgements This contribution is based in part on the author's PhD research at the University of Canterbury, Christchurch, New Zealand, which was funded by a 3-year (2006–2009) New Zealand International Doctoral Research Scholarship (NZIDRS) and the University's Mason Trust. Ongoing research at the University of Freiburg is funded by the German Research Foundation (DFG), Project AD-1294/2: "Long-runout landslides: the effect of lithology on comminution, (micro-) structure, morphology and runout". Careful reviews by G.B. Crosta and J.J. Clague have improved this manuscript and are gratefully acknowledged.

References

- Abbot PL, Kerr DR, Borron SE, Washburn JL, Rightmer DA (2002) Neogene sturzstrom deposits, Split Mountain area, Anza-Borrego Desert State Park, California. In: Evans SG, DeGraff JV (eds) *Catastrophic landslides: effects, occurrence, and mechanisms*, vol XV, *Reviews in engineering geology*. Geological Society of America, Boulder, CO, pp 379–400
- Abdrakhmatov K, Strom A (2006) Dissected rockslide and rock avalanche deposits: Tien Shan, Kyrgyzstan. In: Evans SG, Scarascia-Mugnozza G, Strom AL, Hermanns RL (eds) *Landslides from massive rock slope failures*. Springer, Netherlands
- Abele G (1974) Bergstürze in den Alpen. *Wissenschaftliche Vereinshefte* 25: 230 pp
- Abele G (1997) Rockslide movement supported by the mobilization of groundwater-saturated valley floor sediments. *Z Geomorphol* 41 (1):1–20
- Belousov A, Belousova M, Voight B (1999) Multiple edifice failures, debris avalanches and associated eruptions in the Holocene history of Shiveluch volcano, Kamchatka, Russia. *Bull Volcanol* 61 (5):324–342
- Buss E, Heim A (1881) *Der Bersturz von Elm*. Zürich, Worster
- Choffat P (1929) L'écroulement d'Arvel (Villeneuve) de 1922. *Bull Soc Vaud Sci Nat* 57(1):5–28
- Clavero J, Sparks R, Huppert H, Dade W (2002) Geological constraints on the emplacement mechanism of the Parinacota debris avalanche, northern Chile. *Bull Volcanol* 64(1):40–54
- Clavero J, Polanco E, Godoy E, Aguilar G, Sparks RSJ, van Wyk de Vries B, de Arce CP, Matthews S (2004) Substrata influence in the transport and emplacement mechanism of the Ollagüe debris avalanche (northern Chile). *Acta Vulcanologica* 64(1):59–76
- Crosta GB, Imposimato S, Roddemann D (2009) Numerical modeling of entrainment/deposition in rock and debris avalanches. *Eng Geol* 109(1–2):135–145
- Dufresne A (2012) Granular flow experiments on the interaction with stationary runout path materials and comparison to rock avalanche events. *Earth Surf Process Landf* 37:1527–1541
- Dufresne A, Davies TR, McSaveney MJ (2009) Influence of runout-path material on emplacement of the Round Top rock avalanche, New Zealand. *Earth Surf Process Landf* 35:190–201
- Evans SG, Clague JJ (1998) Rock avalanche from Mount Munday, Waddington Ridge, British Columbia, Canada. *Landslide News* 11:23–25
- Friedmann SJ (1997) Rock-avalanche elements of the Shadow Valley basin, eastern Mojave Desert, California: processes and problems. *J Sediment Res* 67(5):792–804
- Gauer P, Issler D (2004) Possible erosion mechanism in snow avalanches. *Ann Glaciol* 38:384–392
- Hewitt K (2006) Rock avalanches with complex run out and emplacement, Karakoram Himalaya, Inner Asia. In: Evans SG, Scarascia-Mugnozza G, Strom AL, Hermanns RL (eds) *Landslides from massive rock slope failures*. Springer, Netherlands
- Hewitt K, Clague JJ, Orwin JF (2008) Legacies of catastrophic rock slope failures in mountain landscapes. *Earth Sci Rev* 87:1–38
- Hsü KJ (1975) Catastrophic debris streams (Sturzstroms) generated by rockfalls. *Geol Soc Am Bull* 86(1):129–140
- Hung O (1990) Mobility of rock avalanches. Reports of the National Research Institute for Earth Sciences and Disaster Prevention, vol 46. Tsukuba, Japan, pp 11–20
- Hung O, Evans SG (2004) Entrainment of debris in rock avalanches: an analysis of a long-runout mechanism. *Geol Soc Am Bull* 116:1240–1252
- Hung O, Evans SG, Bovis M, Hutchinson JN (2001) Review of the classification of landslides of the flow type. *Environ Eng Geosci* 7:221–238
- Hutchinson JN, Bhandari RK (1971) Undrained loading, a fundamental mechanism of mudflows and other mass movements. *Geotechnique* 21:353–358
- Iverson RM (1997) The physics of debris flows. *Rev Geophys* 35 (3):245–296
- Johnsons B (1978) Blackhawk landslide, California. In: Voight B (ed) *Rockslides and avalanches*, vol 1, *Natural phenomena*. Elsevier, Amsterdam, pp 481–504
- Legros F (2002) The mobility of long-runout landslides. *Eng Geol* 63:301–331
- Philip H, Ritz J-F (1999) Gigantic paleolandslide associated with active faulting along the Bogd fault (Gobi-Altay, Mongolia). *Geology* 27 (3):211–214
- Piotrowski JA, Larsen NK, Junge FW (2004) Reflections on soft subglacial beds as a mosaic of deforming and stable spots. *Quat Sci Rev* 23:993–1000
- Prager C, Krainer K, Seidl V, Chwatal W (2006) Spatial features of Holocene sturzstrom-deposits inferred from subsurface investigations (Fernpass rockslide, Tyrol, Austria). *Geo Alp* 3:147–166
- Sassa K (1988) Geotechnical model for the motion of landslides. In: *Proceedings, 5th international symposium on landslides*, vol 1. pp 37–56
- Sosio R, Crosta GB, Chen JH, Hung O (2014) Runout prediction of rock avalanche in volcanic and glacial terrains. In: Margottini C, Canuti P, Sassa K (eds) *Landslide science and practice*, vol 3. Springer, Netherlands
- van Wyk de Vries B, Self S, Francis PW, Keszthelyi L (2001) A gravitational spreading origin for the Socompa debris avalanches. *J Volcanol Geoth Res* 105(3):225–247
- Voight B, Sousa J (1994) Lessons from Ontake-San: a comparative analysis of debris avalanche dynamics. *Eng Geol* 38(3–4):261–297
- von Poschinger A (1994) Some special aspects of "impact" of a landslide on the valley floor. *Landslide News* 8:26–28
- Wang G, Huang R, Chigira M, Wu X, Lourenco SDN (2012) Landslide amplification by liquefaction of runout-path material after the 2008 Wenchuan (M 8.0) earthquake, China. *Earth Surf Process Landf* 38 (3):265–274
- Xu Q, Shang Y, van Asch T, Wang S, Zhang Z, Dong X (2012) Observations from the large, rapid Yigong rock slide—debris avalanche, southeast Tibet. *Can Geotech J* 49:589–606
- Yarnold JC (1993) Rock-avalanche characteristics in dry climates and the effect of flow into lakes: insights from mid-Tertiary sedimentary breccias near Artillery Peak, Arizona. *Geol Soc Am Bull* 105 (3):345–360
- Yarnold JC, Lombard JP (1989) Facies model for the large rock avalanche deposits formed in dry climates. In: Colburn IP, Abbott PL, Minch J (eds) *Field trip guidebook—Pacific section*, Tulsa, Oklahoma. Society of Economic Palaeontologists and Mineralogists, vol 62. pp 9–31



Landslide Susceptibility of Kavaja, Albania

Olgert Jaupaj, Olivier Lateltin, and Mentor Lamaj

Abstract

In this paper, a GIS-based methodology has been used to produce a landslide susceptibility map of Kavaja located in central-western part of Albania. The landslide inventory was compiled at 1:25,000 scale through: field reconnaissance to investigate landslide occurrences, collection of historic information of landslides from the Central Archive of the Albanian Geological Survey and interpretation of landslide occurrences from aerial photographs coupled with field verification. For this study the Bivariate approach was used to obtain the susceptibility map. In order to explain these landslides, six landslide casual factor maps were selected and prepared in GIS: geology, slope, aspect, land-use, distance from stream, and seismicity. The landslide susceptibility map is the combination of all Wij of each factor. The final landslide susceptibility map of the study area indicates that the low, moderate, high classes respectively cover 129.7 km² (84 %), 14.3 km² (9 %), 10.5 km² (7 %) of the study area. The high landslide susceptibility zones are predominantly characterized by: the geological features N₂(h)c, slope angles between 10° and 25° and West facing exposition slope and Northeast facing slope, the land-use features are urban areas and shrubs, distance from stream 0–25 m, and earthquake zone with magnitude M > 3.5 and I > VII.

Keywords

Landslide causative factors • Landslide susceptibility • GIS

Introduction

In natural systems, landslides are often recognized as one of the most significant “natural hazards” in many areas throughout the world (Crozier and Glade 2005). Landslide

is a general term used to describe the mass movement of soil and rock downslope under gravitational influence. Landslides annually destroy or damage industrial or residential developments, forest and agricultural lands. They often cause deaths, injuries and homelessness. They affect settlements, roads and other infrastructures, constituting a major problem worldwide. Humans and nature combine in increasing landslide risk. Climate change has locally increased the intensity of rainfall, raising the frequency of fast moving, shallow landslides. The population growth and the expansion of settlements and lifelines over potentially hazardous areas are increasing the impact of landslides. The GIS technique has been widely used around the world in landslide hazard because of its capability to predict in advance potential landslide-prone areas by applying different models and approaches.

O. Jaupaj (✉) • M. Lamaj (✉)
Department of Engineering Geology, Albanian Geological Survey,
Shërbimi Gjeologjik Shqiptar, Rruga e Kavajës Nr 153, Tiranë, Albania
e-mail: gertjaupaj@gmail.com; olgert.jaupaj@gsa.gov.al;
lamajmentor@yahoo.com; <http://www.gsa.gov.al>

O. Lateltin
Swiss Geological Survey, Federal Office of Topography Swisstopo,
Seftigenstrasse 264, Postfach 3084, Wabern, Switzerland
e-mail: olivier.lateltin@swisstopo.ch, <http://www.swisstopo.ch>

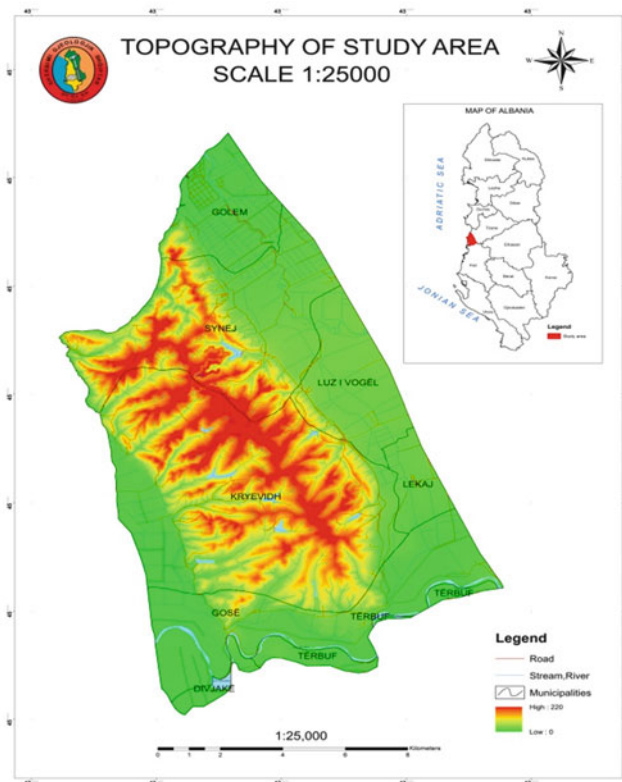


Fig. 1 Topography of the study area

The two main methods that are generally applied to landslide susceptibility assessment are either qualitative methods, which are direct hazard mapping techniques, or quantitative methods, which are indirect mapping techniques. Both qualitative and quantitative approaches are based on the principle that future landslides are more likely to occur under the same conditions. The methodology proposed from literature can be divided in five groups (1) direct geomorphological mapping; (2) analysis of landslide inventories; (3) heuristic approach; (4) statistical approach, and (5) process based conceptual models.

For this study the Bivariate approach was used where ranking values of each parameter sub-class are based on cross tabulation data defining the spatial correlation between the landslide inventory map and causative factors maps.

The Study Area

Geographically, the study area Fig. 1 is located in central-western part of Albania between latitudes $41^{\circ} 12' 56''$ to $41^{\circ} 1' 16''$ North, and longitudes $19^{\circ} 26' 17''$ to $19^{\circ} 36' 34''$ East. The study area is about 155 km^2 and belongs to the Kavaja district. This area is bounded by the Adriatic Sea in the north and west, Lowland Kavaja to the east and alluvial areas of the Shkumbini River. This area intersects seven local

municipalities the most important of which is Kryevidhi Municipality. An estimated 15,000 people live and work in this area. The provincial economy is based on agriculture due to favourable geographic position, field landscape, the mild climate and tourism especially in summer. Beach tourism occurs in the coastal regions of Spille-Karpen. The area is part of the coastal area of the central region of Durrës-Vlore. It is a sandy beach with pine woods extended alongside it by giving it a beautiful view both from the aesthetic aspect and the functional for Macedonia as well as by local people in summer.

Based on morphology features the studied area is divided in two geographic regions: (a) Lowlands's areas are represented by the Adriatic flat plain, (b) Rolling hills representing an anticline structure in the centre of study area. The elevation ranges from 0 to 220 m above sea level. The rivers and streams have short lengths and flow into gentle slopes and flat area. Two major rivers that drain in this area are Shkumbini and Darci River.

Geological Setting

This area, which belongs to a pre-Adriatic depression of Albania geological terrains, consists entirely of molasse formations of Pliocene which extend transgressively upon underlying formations of the Ionian and Kruja zones. There are no outcrops of Messinian deposits in the study area. Transgression starts during the Langhian and continued with some pause cycles until the Pliocene. The Adriatic Lowland built up the western and central area of Tirana–Durrës–Kavaja region. The main geological formations Fig. 2 that crop out in study area are represented by Quaternary deposits as represented by coastal, alluvial, lagoons, swamps deposits and fluvial deposits or by Pliocene deposits which built the Kryevidhi hills. In upper part of lithological profile these rocks consist of claystone of Helmesi formation (N2H) and by the sandstone-conglomerate of Rogozhina formation (N2R) and Messinian molasses, and other rocks.

Landslides of Study Area and Bivariate Approach

The landslide inventory was compiled at a 1:25,000 scale through fieldwork to investigate landslide occurrences. Collection of historic information of landslides from the Central Archive of the Albanian Geological Survey and interpretation of landslide occurrences from aerial photographs were coupled with field verification. In the study area we identified 89 landslides. For each landslide, evaluation

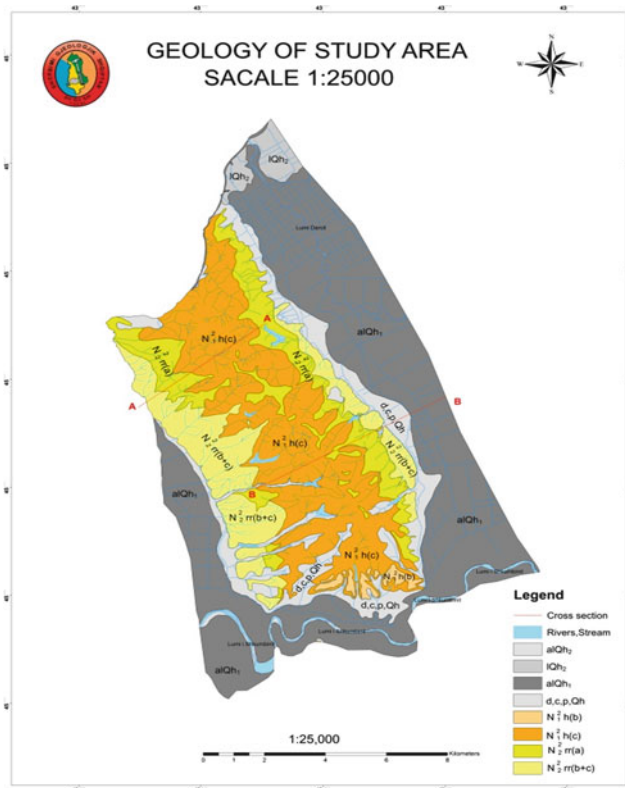


Fig. 2 Geology of study area

during the field surveys involves completion of a data sheet. It is organized into five information levels of increasing detail.

The 1st level contains general information: region, municipality, topographic map and geographical coordinates X, Y. The 2nd level contains data for the geology of the body to move, the plan of slide and the basement that does not move. The 3rd level provides data on morphology (lithology, land-use, erosion, cause of activation). The 4th level contains hydrogeological data (ground water, underground water level, and springs). The 5th level contains geological engineering data (type of movement, state of activity, humidity).

Based on the analysis of the landslide inventory and field work, three major types of slope movements can be identified. The rotational slides occur principally in Q (moraine deposits) and $N_2^1h(c)$. The translational slides occur in the Kryevidhi hills in the $N_2^2rr(a)$ geological formation. Finally the earth flows occur only in $N_2^1h(c)$. The average area of landslides is approximately 1.25 km² and the depths vary from 1.2 to 15 m. Some images of landslides are shown in Fig. 3.

In this study, landslide susceptibility analysis was performed objectively by using a statistical bivariate method, namely the statistical index (W_i) method. This method is based on a statistical correlation of a landslide map with the different parameter maps.



Fig. 3 Landslide pictures of the study area

Weighting values of each parameter sub-class are fundamentally based on cross tabulation data defining the spatial correlation between the landslide inventory map and causative factors maps. To perform this, each thematic map was overlaid and crossed separately with the landslide map using ArcGIS 10.1. Weighting values were generated for each parameter map in based of as the natural logarithm of the landslide density in the class divided by the landslide density in the entire map. This method is based upon the by (1) of Van Westen

$$W_{ij} = \ln \left(\frac{A_{ij}}{A_{ls}} * \frac{B}{ij} \right) \quad (1)$$

Where: W_{ij} —The weight given to a certain class i of parameter j , A_{ij} —area of landslides in a certain class i of parameter j , A_{ls} —total area of landslides in the entire map, B —total area of the entire map B_{ij} —area of a certain class i of parameter j .

Landslide Causative Factors

The causative factors of the landslides are chosen after a careful bibliographical review and field investigations. These factors are as follows: geology, slope angle, aspect, land use, seismicity, and distances from drainages, rainfalls data are not taken in analyses because our study area is very small and rainfall accumulation and intensity is more or less homogeneous.

Table 1 Geology classes, landslides and W_i value

Geology	Area (%)	Landslide area (%)	Statistical index (W_i)
$N_2^{rr}(b+c)$	11	0	-3.65
AlQh ₂	1	0	-1.24
lQh ₂	2	0	0
AlQh ₁	41	0	0
$N_2^{rr}(a)$	10	19	0.67
$N_2^h(dk)$	1	0	0
$N_2^1h(c)$	23	79	1.23
d_c_p_Qh	12	2	-2.04

Table 2 Slope classes, landslides and W_i value

Slope angle	Area (%)	Landslide area (%)	Statistical index (W_i)
0°–10°	76	39	-0.6818
10°–20°	21	57	0.9879
20°–25°	2	4	0.9097
25°–30°	1	0	-0.2027
30°–40°	0	0	-1.3469
>40°	0	0	0
0°–10°	76	39	-0.6818

Geological Factor

Geology is considered as a fundamentally causative factor in this research because strongly influences slope stability. In this study, a digital geology map of the area is prepared based on a combination of six geological sheet maps at 1:25,000 scales. The distribution of landslides occurrence for geology and weight W_{ij} values is shown in Table 1.

From the Table 2 can be noted that the $N_2^1h(c)$ formation ($W_{ij} = 1.23$) and $N_2^{rr}(a)$ formation ($W_{ij} = 0.67$) are more favourable for land sliding compared to the other geological formations.

Slope Factor

The slope is one of the principle factors affecting landslide occurrence. The slope map of the study area is derived from the DEM using Arc_GIS10. DEM is created from izohipse which are extracted from topographic map with scale 1: 10,000. The map of slope classes is generated by separating the slope angles into six different classes (1) 0°–10°, (2) 10°–20°, (3) 20°–25°, (4) 25°–30°, (5) 30°–40°, and (6) >45°. The distribution of landslides occurrence for slope angle and weight W_{ij} values is shown in Table 2.

Analysis shows that slopes from 10° to 25° are more prone to landsliding. It is a fact that fewer landslides occur on mild and steep slope angles.

Table 3 Aspect classes, landslides and W_i value

Aspect	Area (%)	Landslide area (%)	Statistical index (W_i)
Flat	18	0	-4.16
Northeast	9	15	0.54
East	9	9	-0.17
Southeast	11	10	-0.10
South	11	6	-0.66
Southwest	10	14	0.34
West	9	17	0.63
Northwest	15	18	0.22
North	9	12	0.28

Table 4 Distribution of landslides for land-use and W_{ij} values

Land_use	Area (%)	Landslide area (%)	Statistical index (W_i)
Agriculture area	60	17	-1.27
Not forested	21	42	0.69
Urban Area	6	28	1.52
Shrub	6	14	0.81
River	1	0	0
Forest	6	0	-2.94
Agriculture area	60	17	-1.27

Slope Aspect

The slope orientation relative to the movement of the sun, is another factor that can influence slope failure. The difference in the amount of solar radiation received may result in differences in soil temperature, moisture and soil thickness. The aspect map of the study area is derived from the DEM created from contour line which are extracted from topographic map with scale 1: 10,000. The distribution of landslides occurrence for slope aspect and weight W_{ij} values is shown in Table 3.

From the Table 3 can be noted that West facing slope ($W_{ij} = 0.63$) and Northeast facing slope ($W_{ij} = 0.54$) are more favorable for landsliding compared to the other slope aspects.

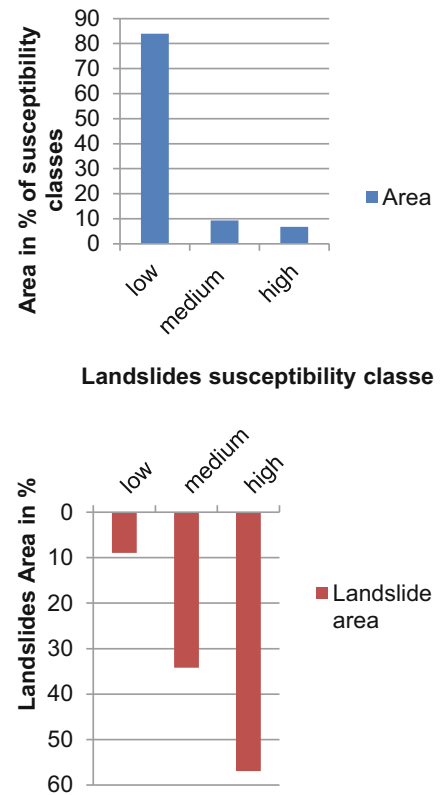
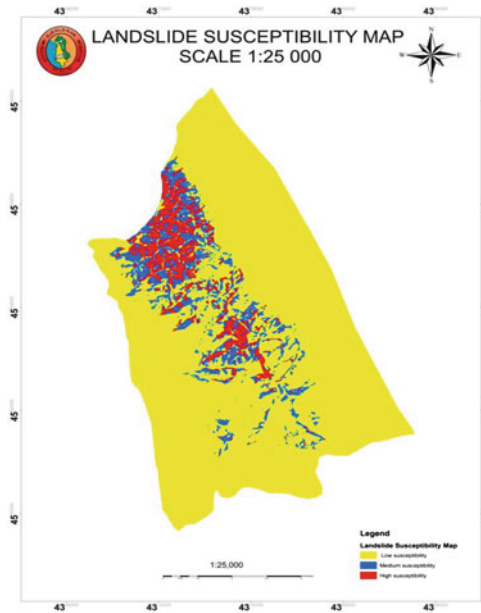
Land-Use Factor

Land-use is the factor related to the effects caused by human activities on landslide occurrence. Excavation of steep slopes for house building, agricultural terraces and deforestation is considered one of the main preparatory factors for landslide occurrence. The land use map is provided from ATTC (Centre for Agricultural Technology Transfer). The distribution of landslides occurrence for land-use and weight W_{ij} values is shown in Table 4. From this table can be noted that urban areas ($W_{ij} = 1.52$) and shrubs ($W_{ij} = 0.81$) are more prone to landsliding compared to the other land-use because human activities and modification of the landscape play an important roles in triggering landslides.

Table 5 Distance from stream classes, landslides and W_i value

Distance	Area (%)	Landslide area (%)	Statistical index(W_i)
0–25 m	15	30	0.71
25–50 m	14	21	0.44
50–100 m	23	22	-0.06
>100 m	48	27	-0.60

Fig. 4 Landslides occurrence in susceptibility classes



Distance from Stream

The distance from streams is important parameter that controls the stability of a slope. Rivers and streams are extracted from topographic maps at scale 1:25,000. Streams may adversely affect stability by eroding the slopes or by saturating the lower part of material until resulting increase in water level. Four different buffer areas are created in the study area to determine the degree to which the streams affected the slopes. The landslide occurrence in each buffer zone and weight W_{ij} is given in Table 5.

Analysis shows that distance from stream 0–25 m ($W_{ij} = 0.71$) and 25–50 m ($W_{ij} = 0.44$) are more prone to landsliding compared to other distances.

Seismicity

The second major factor in the triggering of landslides is seismicity. Landslides occur during earthquakes as a result

of two separate but interconnected processes: seismic shaking and pore water pressure generation. The study area is divided in two parts. The north part has a much higher recurrence level for major earthquakes. The earthquakes of this zone have a magnitude $3 > M > 5$ and an intensity $I > VI$. The southern part is characterized by micro earthquake with very low intensity and with magnitudes $M < 2$.

Landslide Susceptibility Map

All W_{ij} layers for all the causative factors created in Arc_GIS10 (Appendix) are summed by (2) in raster calculator in Arc_GIS 10.1 to obtain landslides susceptibility index map. The preparation of a landslides susceptibility map involves, manipulating, analyzing and presenting these data in GIS

$$LSI = \sum_{j=1}^n W_{ij} \tag{2}$$

Where: LSI: Landslide susceptibility index, W_{ij} - weight of class i in parameter j , n -number of parameters. The W_{ij} maps of each different causative factor are obtained in Arc_GIS 10.1.

The LSI values in the landslide susceptibility map Fig. 4 of the study area obtained using equation III-2 in raster calculator. The landslide susceptibility index values range

from -2.2 to 0.89 . For simplification the map interpretation the LSI values are divided into three different susceptibility classes, which are: low landslide susceptibility $LSI < 0.25$, moderate susceptibility $0.25 > LSI > 0.5$ and high susceptibility $LSI > 0.5$. From the comparison of the landslide inventory map and susceptibility map, the area in the landslide inventory map showing where landslides occurred matched the data on the landslide susceptibility map. The area of each susceptibility classes and landslides occurrence in this susceptibility classes are showed in Fig. 4.

Conclusions

Landslides susceptibility mapping is very necessary due to the strong impact of landslide processes on people and their goods. The landslide susceptibility map is a useful tool in urban planning, specifically for the definition of the land use zones and for the design of future construction projects. The final landslide susceptibility map of the study area indicates that the low, moderate, high classes respectively cover 129.7 km^2 (84 %), 14.3 km^2 (9 %) and 10.5 km^2 (7 %) of the study area. The detected landslide areas in the low, moderate, high and very high landslide susceptibility classes are respectively 0.11 km^2 (9 %), 0.43 km^2 (34 %), and 0.71 km^2 (57 %). The high landslide susceptibility zones are predominantly characterized by the geological formation $N_2^1 h(c)$, slope angles between 10° and 25° and west facing exposure and northeast facing slopes, distance from streams $0\text{--}25 \text{ m}$, and an earthquake zone with magnitude $M > 3.5$ and $I > VII$. This preliminary map should serve as a positive model to be applied in other region with similar geological conditions as Kavaja.

Acknowledgments I would like to thank you CERG-C 2012.

I would like to thank you my colleagues of the Department of Engineering Geology specially Eng. Mimoza JUSUFATI, and Eng. Musli DARDHA for the time, suggestion, assistance and encouragement.

References

- Cepeda J (2011) Risk assessment and mitigation training workshop, GFDRR, pp 3–18
- Crozier MJ, Glade T (2005) Landslide hazard and risk: issues, concepts and approach. In: Glade T, Anderson M, Crozier M (eds) Landslide hazard and risk. Wiley, Chichester, pp 1–40
- Jaiswal P (2011) Landslide risk quantification along transportation corridors based on historical information. Doctoral thesis, University of Twente, 57–60, 92–96, 125–141
- Lateltin O, Bonnard CH, Haemmig CH, Raetzo H (2005) Landslide risk management in Switzerland. *J Int Consort Landslides* 2:313–320. doi:10.1007/s10346-005-0018-8, 313–320
- Mancini F, Ceppi C, Ritrovato G (2010) GIS and statistical analysis for landslide susceptibility mapping in the Daunia area, Italy. *Nat Hazards Earth Syst Sci* 10:1851–1864, 1855–1859
- Muceku Y (2012) The engineering geological mapping on scale 1:10,000 for tourism development in Adriatic Coastal Plain-Divjaka, Albania. *Int J Civil Environ Eng IJCEE-IJENS* 12 (04):33–39
- Naço P (2003) Geological report of Tirana-Durres-Kavaja district. Albanian Geological Survey, Albania, pp 68–74
- Papathoma-Köhle M, Kappes M, Keiler M, Glade T (2011) Physical vulnerability assessment for alpine hazards: state of the art and future needs. *Nat Hazards* 58:645–680. doi:10.1007/s11069-010-9632-4, 648–653
- Reichenbach P, Galli M, Cardinale M, Guzzetti F, Ardizzone F (2000) Geomorphological mapping to assess landslide risk, concepts, methods and applications in Umbria region of central Italy, Chap 15. In: Glade H, Anderson MG, Crozie MJ (eds) Landslide hazard and risk 2000. Wiley, New York
- Rrapo O (2007) The general model of construction of the Albanian earth crust and its seismactive features according to the seismological data. Doctoral thesis, Polytechnic University of Tirana
- Singh RG (2009) Landslide classification, characterization and susceptibility modelling in Kwazulunatal. Degree of Master of Science, University of the Witwatersrand, 27–30, 83–84
- Sulstarova E, Koçiaj S, Aliaj S (1980) Seismic zonation of RPS Albania. Academy of Sciences, Tirana, 297 p
- Sulstarova E, Koçiaj S, Peçi V (1996) Catalogue of Albanian earthquakes for the period 1901–1995. Institute of Seismology, Tirana, 350 p
- Thanh Long N (2008) Landslide susceptibility mapping of the mountainous area in a Luoi district, Thua Thien Hue province, Vietnam. Doctoral thesis, University of Vrije Brussel, 14–15, 79–86
- Thiery Y (2008) Landslide susceptibility assessment by bivariate methods at large scales: application to a complex mountainous environment, Elsevier Editorial System(tm) for Geomorphology, GEOMOR-445R2, 2–6
- Van Westen CJ (2004) Geo-Information tools for landslide risk assessment. An overview of recent developments. In: Proceedings of the 9th international symposium on landslides, June 28–July 2 2004 Rio de Janeiro, Brazil, ISBN: 978-0-415-35665-7, 7-11
- Van Westen CJ, Van Asch TWJ, Soeters R (2006) Landslide hazard and risk zonation—why is it still so difficult? *Bull Eng Geol Env* 65:167–184. doi:10.1007/s10064-005-0023-0, 168–178
- Wati SE, Hastuti T, Widjojo S, Pinem F (2010) Landslide susceptibility mapping with heuristic approach in mountainous area a case study in Tawangmangu sub district, central java, Indonesia. International archives of the photogrammetry, remote sensing and spatial information science, vol XXXVIII. Part 8, Kyoto, Japan, 2010, pp 249–252
- Xhomo A, Kodra A, Xhafa Z, Shallo M (2008) Geology of Albania. Albanian Geological Survey (AGS), 215–222, 226–228
- Zêzere JL, Garcia RAC, Oliveira SC, Reis E (2008) Probabilistic landslide risk analysis considering direct costs in the area north of Lisbon (Portugal). *Geomorphology* 94:467–495, 468, 477–490



Recent Extreme Rainfall-Induced Landslides and Government Countermeasures in Korea

Su-Gon Lee and Stephen R. Hencher

Abstract

This paper describes the characteristics of recent landslides in South Korea. Case examples are used to demonstrate failings in the way that the Korean authorities plan for and react to such disasters. A plan for improved management is presented.

Keywords

South Korea • Rainfall-induced • Mitigation

Introduction

During 2011 many landslides occurred throughout South Korea, triggered by heavy rainfall, and these resulted in more than 60 fatalities, many injuries, damage to property and traffic disruption. Most of the fatal landslides were essentially anthropogenic, related to land development and infrastructure rather than due to natural factors.

Case examples from 2011 serve to illustrate the ineffectiveness of the Korean Government countermeasures with respect to landslides. Generally when a serious event occurs, restoration works are commenced immediately without any attempt to investigate the cause and without any proper design response process. Remediation tends solely to comprise the application of hard-covering to failure surfaces to prevent further erosion, together with the provision of check dams across valleys where debris flows have taken place. These measures are implemented without any input from specialist engineering geologists or geotechnical engineers.

Historically, persons injured or subjected to economic loss as a result of landslides have sometimes taken legal action against the Korean Government. The most usual outcome of such actions is that experts appointed by the courts follow the traditional stance of the Government and simply conclude that landslide disasters are the natural consequence of heavy rainfall. This is despite the huge international literature (including Korean) that shows clearly that many landslides are avoidable or that the risk may be mitigated against in some other way including through good design practice and land planning strategy (e.g. Lee and Jones 2004). As a result claimants have generally lost their cases and received no compensation. Furthermore because of the lack of proper investigations of major incidents few lessons are learned. As Hencher et al. (1985) concluded, detailed study of landslides including back analysis is one of the most fruitful ways of advancing knowledge of landslide mechanisms to allow improved design and land management. This practice of studying serious landslides in depth, as part of a strategy to reduce landslide risk, is now carried out routinely in Hong Kong (e.g. Ho and Lau 2010). To date the Korean Government has resisted setting up a special department tasked with reducing landslide risk despite the apparent effectiveness of so doing in other countries as in the establishment of the Geotechnical Control (now Engineering) Office in Hong Kong in 1979 and GEO-RIO in Brazil.

S.-G. Lee (✉)
Department of Civil Engineering, University of Seoul, Seoul, South Korea
e-mail: sglee@uos.ac.kr

S.R. Hencher
Department of Earth Science, University of Leeds, Leeds, UK

Halcrow China Limited, A CH2MHILL company, Hong Kong, China
e-mail: s.hencher@see.leeds.ac.uk

Korean Conditions

South Korea is a peninsula located in north-eastern Asia and situated between China and Japan, with an area of 99,600 km². The capital is Seoul and the nation population is about 50,000,000. In general, the peninsula is mountainous (about 70 % of the total area), but rarely exceeding 1,200 m in altitude. The mean annual temperature is 10 °C, ranging between −15 °C in winter and 30 °C in summer with four distinct seasons. The average annual rainfall is about 1,200 mm, 60 % of which falls between June and August. Vegetation cover is about 70 % of the total area of Korea.

The geology of the Korean peninsula is varied ranging from Precambrian to Recent. Regardless of rock types however, the depth of residual soils is generally limited to a few metres (Lee and deFreitas 1989). There is no recorded case of slope failure triggered by earthquakes in Korea (Lee 1993).

Characteristics of Slope Failure

In Korea, most landslides are triggered by intense rainfall during typhoons and seasonal rain fronts from June to September. It is evident that risk to life and property is increasing as more development takes place on sites close to steep natural slopes in mountainous areas.

In natural terrain, landslides generally occur on slope sections inclined between 20° and 40°. Most such hill slope failures are relatively small scale with run out lengths of up to 20–30 m, and a width less than 10 m. Failure depth is typically shallow and often less than 1 m and such shallow landslides usually occur during heavy rainfall and are associated with shallow perched water tables and erosion processes (Hencher 2010). For channelized debris flows, run-out lengths typically range from 100 to 500 m. Considerable damage is often associated with erosion caused by debris flows running along watercourses (Lee 1987, 1988, 1994; Lee et al. 2008; Shin 2013).

On average 60 fatalities and damage to property valued at 500–1,000 million US dollars can be attributed to landslides annually in Korea. This is a high proportion of the annual damage from all natural disasters (10–20 %). In addition, traffic disruption is a frequent consequence of debris flows. A high proportion of national roads and national highways are located close to the bottom of main valleys and are particularly vulnerable to the effects of debris flows from side valleys. Despite such damage, disruption and rate of casualties, as noted earlier, no single agency has been set up

in Korea to manage slopes on a par with the Geotechnical Engineering Office (GEO) in Hong Kong (Lee 2002).

Recent Landslide Events

A large number of landslides occurred in South Korea as a result of heavy rainfall (160–300 mm/day) which fell between 29 June and 27 July 2011. From analysis of density of landslides vs. intensity of 24-h rainfall, mostly in Hong Kong, rainfall intensity of about 300 mm per 24 h would be anticipated to result in about 1 incident per square km; 160 mm would relate to a density of landslides about five times less (Hencher et al. 2006). Fifty eight people were killed and 200 injured at 11 locations. Figure 1 shows the 11 locations.

The incidents (Seoul (Mt.Choan), Boeun, Gunsan, Suncheon and Songchi) illustrated in Fig. 1 were associated with damage to road infrastructure; those (Miryang, Daejeon, Suncheon (Dugok), Seocheon, Boseong and Chuncheon) shown in Fig. 1 involved damage to residential buildings and houses.

Among the 11 cases, the Seoul landslides were the most important events and these serve to illustrate some of the current problems with landslide management in South Korea. On 27 July 2011, there were many debris flows that occurred simultaneously at Umyeonsan (Mt.) in downtown Seoul (Fig. 2). The landslides resulted in 18 fatalities and 50 persons were injured.

Firstly it is noted that several major debris flows had occurred on the same mountain on 21st September 2010 but no attempt had been made to carry out studies to identify causes, susceptibility and to initiate and preventive measures.

The immediate response was to carry out restoration works instructed by forestry workers without input from any geotechnical specialists. The restoration works were aimed at reducing erosion by constructing drainage channels with rock revetment (Fig. 3). The works were not designed following any concept of safety protection—i.e. there was no attempt to design works mitigating against further landslides or preventing debris run out impacts. Thirty percent of the planned restoration works had been completed by November 14, 2011 when the Korean Government concluded that the design was inadequate. A 2nd design of restoration works was therefore produced by the end of January 2012, but the concept of the 2nd design was almost the same as the original design.

A safety investigation report was completed at the end of November 2011 by the Korean Geotechnical Society but this simply demonstrated the link to rainfall and presented photographs of the landslides. There was no attempt to

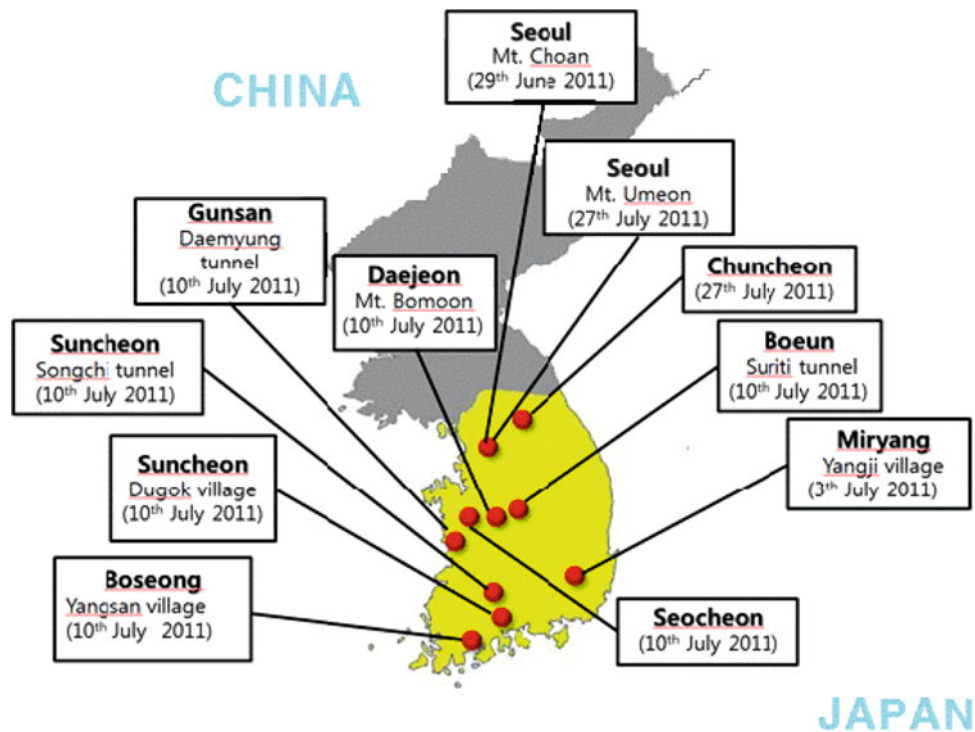


Fig. 1 Locations of fatal landslides that caused 58 deaths and many injuries between 29th June and 27th July 2011



Fig. 2 Twelve large landslides occurred associated with 230 mm rainfall at Mt. Umyeon, Seoul on 27th July 2011. The landslides caused 18 deaths and 51 were injured. The proximity of a military camp at the

top of the mountain and pedestrian roads across the mountains may have led to concentrated flows and been a major contributory cause of the landslides (a). Just after landslides (27th July 2011) (b)

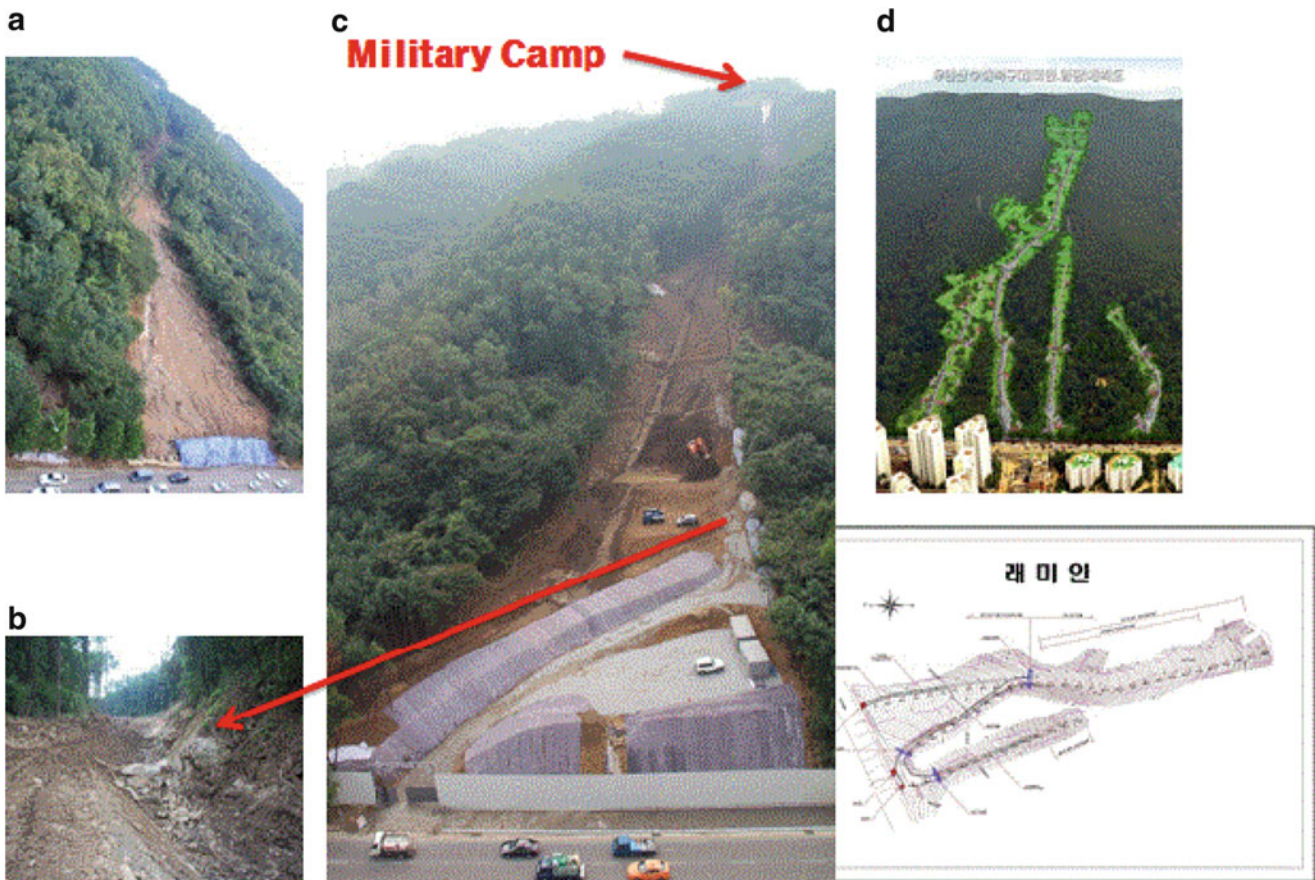


Fig. 3 Remediation works in progress, based on the concept of erosion control rather than landslide prevention (2 million US dollars). (a) Just after landslides (July 27, 2011), (b) restoration works with rock blocks

(Aug 31, 2011), (c) restoration works were started immediately after landslides (photos on Aug 31, 2011), (d) design report was completed on November 14, 2011

examine the causative mechanisms or to model the landslides which might have given some insight into avoiding further occurrences at this location. Furthermore the KGS report failed to consider anthropogenic influences that may have served to concentrate flows and infiltration. In particular the proximity of some of the landslides to a military camp at the top of mountain and to pedestrian roads was ignored.

In this event, the Seoul Government recognized that the safety report was not sufficient so a 2nd safety investigation report was requested and conducted by another organization (Korean Society of Civil Engineers). This investigation was carried out between June and November 2012. By this time the remedial works (designed by forestry workers to reduce erosion only) were almost complete and most of the evidence that might have been used to deduce the cause of landslides had been destroyed. The 2nd safety report was criticized as inadequate by some Korean geotechnical engineers.

As noted earlier, the Government tends to judge the cause of (and responsibility for) landslides on the basis of professional reports. In this case the victims of the Seoul landslides have not been compensated for their losses from the landslides because of the 1st and 2nd safety investigation reports that simply concluded that the Seoul landslides were inevitable natural disasters due to heavy rainfall. The fact that no preventive or other mitigation action was taken following earlier landslides at nearby locations, and the technical inadequacies of the reports themselves, seem to have been ignored. Elsewhere in the world, geotechnical engineers are able to design preventive works to avoid or protect the population from landslides and professionals take responsibility for safety of slopes but in Korea landslides are always treated as natural occurrences over which we have no control at all.

In summary it can be argued that the Government action was too hasty with a wish to do something, however superficial before the next rainy season and without proper

investigation to deal with the landslide risk even at this specific location systematically and effectively.

Conclusions

Recent fatal landslides occurred in 2011 can be attributed at least in part to human activities such as infrastructure development without proper consideration of adjacent slopes. Examples include construction of an army camp, a forest road, cemetery and other tombs and, in one case, development of a vegetable garden and fruit farm. The practical consequences appear to be compounded by a lack of clear responsibilities and an associated lack of willingness to operate in the context of the broader geomorphological and geological setting when planning and designing construction works.

Every year similar events occur through South Korea. Having reviewed many cases, it does seem that many of the landslide problems are exacerbated by a lack of understanding of the hazards and risks associated with landslides by Government authorities and generally throughout the construction industry.

For the last 20 years Korean landslide specialists have urged the Seoul Government of the need to establish landslide prevention and mitigation systems. In the event, whilst the Government is reluctant to spend money for landslide prevention measures before landslide events, they are forced to spend probably comparable amounts of money only after landslide events.

It is concluded that the establishment of a management agency, with some similarities of function with the GEO in Hong Kong, would have some value, particularly in mountainous city areas and areas of intensive development in Korea. Such an organization should inspect and assess existing slopes and take a lead in

standardizing design and construction criteria for new developments in mountainous areas.

References

- Hencher SR (2010) Preferential flow paths through soil and rock and their association with landslides. *Hydrol Process* 24:1610–1630
- Hencher SR, Massey JB, Brand EW (1985) Application of back analysis to some Hong Kong landslides. In: *Proceedings of the 4th international symposium on landslides*, vol 1. Toronto, pp 631–638
- Hencher SR, Anderson MG, Martin RP (2006) Hydrogeology of landslides. In: *Proceedings of international conference on slopes*, Malaysia, pp 463–474
- Ho KKS, Lau JWC (2010) Learning from slope failures to enhance landslide risk management. *Q J Eng Geol Hydrogeol* 43:33–68
- Lee SG (1987) Weathering and geotechnical characterization of Korean granites. Unpublished Ph. D. thesis, Imperial College, University of London, UK
- Lee SG (1988) A study on landslide in Korea, researches on geological hazards. Research report of Korea Institute of Geoscience and Mineral Resources. KR-88-(B)-7, pp 145–148
- Lee SG (1993) A study on slope stability evaluation and control in urban arrears (Part II). Korea Institute of Geoscience and Mineral Resources, Korea, pp 21–36
- Lee SG (1994) Natural hazards in Korea. In: *Proceedings of international forum on natural hazards mapping*, vol 281. Geological Survey of Japan, pp 145–148
- Lee SG (2002) Characteristics and countermeasure to the landslide and cut slope failure by typhoon-Rusa. In: *Proceedings of Korean Society of Civil Engineering (KSCE)*, pp 23–26
- Lee SG, deFreitas MH (1989) A revision of the description and classification of weathered granite and its application to granites in Korea. *Q J Eng Geol* 22(1):31–48
- Lee EM, Jones DKC (2004) *Landslide risk assessment*. Thomas Telford Publishing, London, 454 p
- Lee SG, Lee KS, Park DC, Hencher SR (2008) Characteristics of landslides related to various rock types in Korea. In: Chen Z et al. (ed) *Proceedings of 10th international symposium on landslides and engineered slopes*, 30 June–4 July, Xi'an, China, pp 427–433
- Shin HW (2013) Prediction and characteristics of debris flows in Korea. Ph.D., thesis, University of Seoul, Korea (under preparation)



How the Stabilizing Effect of Vegetation on a Slope Changes Over Time: A Review

Wei Meng, Thom Bogaard, and Rens van Beek

Abstract

The principles of slope stabilization through vegetation are well known but substantial uncertainty remains about its transient effects, for example that of a forest stand throughout its life cycle. This comprises direct impacts but also more indirect ones that influence soil development that can be important but also difficult to observe and quantify. Often these effects are ambiguous, having potentially a stabilizing or destabilizing influence on a slope under particular conditions (e.g., more structured soils leading to both rapid infiltration and drainage).

The overall aim of this research is to review the changing (de-)stabilizing effect of forest stands on potentially unstable slopes. Here we focus on the combined hydrological and mechanical effect as a function of temporal forest stand dynamics. To this end, we reviewed the fragmented literature on the life cycle of stands with respect to their water use, or more specifically their role in the water cycle and with respect to the development of root strength, particularly root density, area and root strength. We highlight that the life cycle of a forest stand has clear influence on the stability of a slope. The review will also identify knowledge gaps and future research needs.

Keywords

Slope stability • Forest stands • Long-term effect

Introduction

Vegetation is used to stabilize shallow landslides for its hydrological and mechanical effects. The role of forest stands in the hydrological cycle consists of the canopy and forest floor intercepting rainfall and roots extracting water from the soil by transpiration. Low soil water content

favours slope stability. In contrast, high soil water content generates positive pore pressures, which reduce the shear strength according to Terzaghi's principle of effective stress. Mechanically, deep rooting of vegetation stabilizes a soil by increased root strength, anchoring and buttressing.

The occurrence of landslides is often related to soil hydrological condition. Rainfall with certain intensity and duration always leads to increased soil pore pressures [positive pressure in the saturated zone or decreased soil suction in the unsaturated zone (Van Asch and Sukmantalya 1993)] and this results in reduced soil strength and possibly to slope failure.

The interaction of the forest on the hydrological cycle has been recognized for a long time. For example, abundant research attention has been dedicated to the effect of forests on floods (Troendle and King 1985). Andréassian (2004) reviewed the hydrological studies on the effect of vegetation

W. Meng • T. Bogaard (✉)
Department of Water Management, Section Water Resources, TU Delft
University of Technology, PO Box 5048, 2600 GA Delft, The
Netherlands
e-mail: w.meng@tudelft.nl; t.a.bogaard@tudelft.nl

R. van Beek
Department of Physical Geography, Utrecht University, PO Box
80115, 3508 TC Utrecht, The Netherlands
e-mail: r.vanbeek@uu.nl

on the hydrological cycle and placed it in a historical context. He demonstrated that previous studies mostly focused on the impact of land-use change on annual flow, flood peaks, low flows and baseflow in a catchment. Those were conducted normally based on reforestation or deforestation actions with a catchment or within catchment comparison studies. However, less studied is the impact of gradual changes of forest growth on the water availability in a catchment or in a soil profile.

The mechanical effect of vegetation relates mainly to root reinforcement. Based on field and laboratory work respectively Wu (1976, 1979) and Waldron (1977) developed a simple root reinforcement model to quantify shear resistance of a rooted soil column. It requires knowledge of the tensile strength of the roots and the cross-sectional area of fibers crossing the shear plane. The Wu and Waldon Model assumes that roots within the soil column reach maximum tensile strength simultaneously. However, this assumption has been challenged as a more progressive failure of roots takes place in reality. The Fiber Bundle Model (Pollen and Simon 2005) was proposed as an upgrade for the Wu and Waldon Model and hypothesized that the roots break progressively during the soil failure process which results in lower estimations of the maximum root reinforcement.

Moreover, the mechanical effect of forest on slope stability also changes due to root evolution. Generally speaking, the decreasing cellulose contents in roots leads to less flexible, more brittle roots. This, and a decreased renewal of roots, could lead to more variable and lower reinforcement in older stands. However, although the development of root tensile strength has been investigated (e.g. Genet et al. 2008) together with the change in spatial distribution of roots, this was done mostly on agriculture crops (Burns 1991; Bouillet et al. 2002). Studies on how root reinforcement in forest stands develops spatially and temporally are rare.

The aim of this paper is to summarize existing but fragmented knowledge on age-dependent characteristics of trees and forest stands in order to show its effect on the long-term slope stability. This comprises the effect of life stages on both water use, root evolution and stand development. As exact characteristics are species dependent, we will focus on similar trends and patterns; several examples will be given where we focus on perennial, woody vegetation.

Age-Related Changes of Individual Trees

General Growth and Development Trends for Tree

Trees grow gradually by assimilating water and carbon dioxide with solar energy and converting this to biomass using nitrogen and minor nutrients. It is well recognized that



Fig. 1 Diagram of typical growth stage for *Eucalyptus* by Woodgate et al. (1996), which is modified from Jacobs (1955), from left to right, there are regeneration, regrowth, younger mature, older mature, senescent (late mature), and senescent (overmature)

growth of trees is strongly dynamic. It fluctuates within seasons, from year-to-year as well as within a life span of maybe a century or more. Although, highly variable growth patterns are attested for different species and at different sites, trees go through expansive, stable, and declining growth phases. Schematically, tree growth follows a clear age-related trend (Fig. 1). Previous studies described this pattern of tree growth based on its morphology and physiology. For example, Jacobs (1955) proposed juvenile sapling, pole, mature (early), mature, mature (late) and overmature for *Eucalyptus maculate*; Woodgate et al. (1996) used regeneration, regrowth, mature and senescing in their studies in New South Wales, Australia for old-growth forest and George et al. (2005) talked about seeding, sapling, pole, mature phases for *Eucalyptus camaldulensis*, also in South Australia.

Summarizing, in young forests, growth accelerates as the canopy closes. It declines after a stable period of maximum canopy as fewer leaves will be present relative to the size of a tree. Studies on tree growth over time have shown clear relationship between age and tree stand characteristics, such as LAI (leaf area index). Since leaf area is a crucial determinant of photosynthesis, allometric relationships are used in forestry and ecology to estimate growth potential of trees through LAI (Barclay 1998). Table 1 gives a review of age-related LAI for different species. As a general trend it can be concluded that LAI reaches a peak at the first few years of the mature stage and then declines. As an example, Watson and Vertessy (1996) proposed the following equation for LAI development of *Eucalyptus regnans*:

$$LAI_{ash} = 11.014A - 1.624(A - 5.04)^{1.180} \times 3.592^{(A-5.04)(-0.319)} \quad (1)$$

where A is the stand age in years. This equation has been demonstrated 10–32 % error in predicting LAI for stands less than 60 years old. Although we focus on the long-term development here, it should be emphasised that the LAI is not constant over the year due to seasonality.

Table 1 Summary of age-related characteristic in stands and transpiration

Stand characteristics										
References	Species	Age (year)	Tree area (ha ⁻¹)	Transpiration (mm year ⁻¹)	LAI [m ² m ⁻²]	Sapwood area [m ² ha ⁻¹]	Basal area [mm ha ⁻¹]	Area/region	Remarks	
Dunn and Connor (1993)	Mountain ash (Eucalyptus regnans F. Muell)	50	176	679		6.7	56.6	Maroondah catchment, Southeast Australia		
		90	106	610		6.1	63.1			
		150	56	365		4.2	73.2			
		230	72	296		4.0	78.6			
Vertessy et al. (2001)	Mountain ash (Eucalyptus regnans F. Muell)	15		733	4.0			Maroondah catchment, southeast Australia	$LAI_{avg} = -11.014A - 1.624(A - 5.04)^{1.120} \times .592^{(-2.04 \times -0.218)}$ Where LAI is LAI of mountain ash overstorey and A is the stand age in years	
		30		590						
		60		450						
		120		310						
		240		249	1.3 (235 years)					
Roberts et al. (2001)	Eucalyptus sieberi	14		2.2	3.6	11.0		Yamulla State Forest, southeastern New South Wales, Australia		
		45		1.4	4	6.5				
		160		0.8	3.4	3.1				
Köstner et al. (2002)	Norway Spruce (Picea abies)	40	1,680	Highest	5.3	20.0		Fichtelgebirge, Germany. Altitude = 750–800m, P = 1000–1200mm year ⁻¹	Ec/LAI decreased with age	
		40 (boggy)			6.5	23.0				
		70			7.9	20.0				
		110			7.8	19				
		140	320	Lowest	6.5	14.0				
		10	1,200	508	344	2.9				Southwestern France. Maritime climate. Altitude = 60 m, P = 977 mm year ⁻¹
		32	600	296	177	2.2				
Delzon and Loustau (2005)	Maritime pine (pinus pinaster Ait.)	54	270	144	1.8			Ballarat, Victoria, Australia. P = 700 mm year ⁻¹	Fast growing stands. Linear relationship between E and LAI. $E = 0.12 + 0.44LAI$ ($R^2 = 0.68, P = 0.028$)	
		91	155	127	1.7					
Forrester et al. (2010)	Eucalyptus globules	2.2	935	1.0	0.4	1.1				
		4.2	1,088	2.7	1.34	6.1				
		9.5	968	2.8	1.64	7.3				
		6.2	1,006	3.7	1.36	11.2				
		7.2	1.86	3.5	1.89	10.6				
8.2	1,001	2.7	1.12	8.9						

Other morphology indices are also used to study tree growth although they are usually correlated with LAI. For example, tree height, DBH and sapwood area. Tree height increases in its young stage rapidly and then slows down or even reaches a plateau (Köstner et al. 2002). Also the increase in DBH slows down with age (Köstner et al. 2002). And lastly, the sapwood area was shown to be linearly correlated with LAI (Forrester et al. 2010). However, Köstner et al. (2002) reported a shift in relationship between sapwood area and LAI between 40 years old and older *Picea abies* stands. In even-aged *Picea pinaster* stands, sapwood area increased in young stages (32 years old) and remained constant at about $20 \text{ m}^2 \text{ ha}^{-1}$ for older stages.

The Explanation of Allometry Growth

The observation of age-related growth relates to the internal physiological dynamics and can be explained by the age effect on mass and energy exchange, particularly of carbon and water (Kowalski et al. 2003; Law et al. 2001, 2003). The decline with age in above-ground productivity has been known from observations of tree morphology. A widely accepted early hypothesis is that growth respiration declines as maintenance respiration increases, and that meanwhile the photosynthesis capacity of the tree reaches a plateau due to the constant leaf area (Kira and Shidei 1967; Yoda et al. 1965; Waring and Schlesinger 1985; Oliver and Larson 1996). This assumption is based on photosynthesis capacity versus growth and maintenance respiration (Yoda et al. 1965; Whittaker and Woodwell 1968). It implies that the supply of resources, acquisition of resources, and efficiency of resource usage remain constant. However, later measurements showed that the increased sapwood respiration (as part of the maintenance respiration) did only account for a small fraction of productivity decrease (Ryan and Waring 1992; Magnani et al. 2000). Even, the total stem respiration was lower in the older than in the younger subalpine lodgepole pine stand. Other possible explanations on the decline of productivity with age were summarized by Ryan et al. (1997): (1) increased hydraulic resistance; (2) decreased nutrient supply; (3) reduced leaf area caused by crown abrasion; (4) increased reproductive effort; and (5) genetic changes with meristem age. In a review, Weiner and Thomas (2001) repeated these hypotheses.

Another point of view is that a larger proportion of the produced biomass is below rather than above ground. This was initially proposed by analysing the simulation results of the G'DAY model, which describes C and N dynamics in an ecosystem (Murty et al. 1996). It demonstrated that declining above ground productivity was related to nutrient availability which was influenced by litter accumulation on the

soil and increasing allocation of below ground biomass. The below/above ground biomass allocation shift was supported by observations (Ryan and Waring 1992; Vanninen et al. 1996) and synthetic results (simulation and observation) from Magnani et al. (2000) for *P. sylvestris* stands. Moreover, it was shown to be consistent with observations for other species (Santantonio 1990).

The age-related decline in tree growth was also partly explained by a shift of root/shoot ratio. However, the most promising idea was that the hydraulic resistance slows down the tree growth because of longer stems and longer branches (Ryan and Yoder 1997; Delzon et al. 2004). Early studies on gas exchange found stomata closure caused by higher hydraulic resistance (Sperry and Pockman 1993; Sperry et al. 1993; Teskey et al. 1983), and it was a result of increased xylem path length (Yoder et al. 1994; Hubbard et al. 1999). This is a 'self-protect' mechanism to prevent trees from xylem cavitations when leaf water potential decreases over a day (Tyree and Sperry 1988; Zimmermann 1983). Ryan et al. (2006) revisited their hydraulic limitation hypothesis and concluded that hydraulic limitation of gas exchange is proven and exists but is not universal. Trees also compensate the effects of increased path length, i.e. physiological changes with tree height.

Moreover, some studies conducted direct measurement on hydraulic resistance for young and older stands. For example, Mencuccini and Grace (1996) showed that the hydraulic conductance in 30 m tall, 270 years old ponderosa pine trees was only half of that in a 10 m tall, 40 years old trees. Later on, quantifying hydraulic response to trees height was based on a simple hydraulic model (see Delzon et al. 2004):

$$E_L = g_s D = K_L \Delta \Psi_{S-L} \quad (2)$$

where E_L is the tree transpiration rate per unit leaf area; g_s is the stomatal conductance per unit leaf area, D is the air water vapour saturation deficit; K_L is the leaf-specific hydraulic conductance between the soil and leaves; and $\Delta \Psi_{S-L}$ is the soil-leaf hydraulic gradient. The equation assumes that leaf temperature equals the air temperature, and stem water storage is negligible.

This equation expresses the demand and supply mechanics in the body of a plant. In the equation, Ψ_S depends on soil properties, and Ψ_L is the hydraulic head in leaves which has a minimum threshold of -2 MPa (Delzon et al. 2004) due to hydraulic homeostasis (Yoder et al. 1994; Hubbard et al. 1999; Ryan et al. 2000; Bond and Kavanagh 1999; Cochard et al. 1996; Saliendra et al. 1995). K_L was observed to decrease with height of trees (Mencuccini and Grace 1996; Hubbard et al. 1999; Ryan et al. 2000; Phillips et al. 2001; McDowell et al. 2002). Finally, E_L declines with increasing tree height.

Some mechanisms adapt and try to offset the decrease in hydraulic conductivity, such as: (1) xylem vessels are developing with increasing permeability (Pothier et al. 1989); (2) decreasing leaf area-xylem area ratio; (3) increasing $\Delta\Psi_{S-L}$ (Hacke et al. 2000). However, these physiological adaptations of trees cannot compensate the declined tree growth. Furthermore, the stand structure dynamics influence the decline in productivities which we will elaborate later.

In all, the decline with age seems associated with height growth, decreased hydraulic conductivity, below ground allocation, nutrient limitation, and declined leaf area, etc. All the effects influence and strengthen on each other.

Evidence of Age-Dependent Water-Use by Individual Trees

Weighing lysimeters, large-tree potometers, ventilated chambers, radioisotopes, stable isotopes and an array of heat balance/heat dissipation methods have been used to provide quantitative estimate of whole-tree water use (Wullschlegel et al. 1998).

Sap flux measurement enables to give us individual tree or stand transpiration (Cohen et al. 1985; Green and Clothier 1988; Hatton and Vertessy 1990). Measurements of sap flow velocities were multiplied by sapwood cross-section area to computer transpiration flux in individual trees (Vertessy et al. 1995). Delzon and Loustau (2005) scaled up mean sap flux density to the overstorey transpiration (E_T) by using:

$$E_T = \overline{Q_S} S^{-1} \sum_{i=1}^n (A_{S,LC,i} C_i) \quad (3)$$

With Q_S is the mean sap flux density under the live crown, S the ground area for the stand, $A_{S,LC,i}$, the sapwood area below the live crown of tree i , n the number of trees per stand and C_i a correction factor for individual tree sapwood area.

The results from the sap flux method are restricted among others by water supply condition, aspect of tree to the solar radiation, other vegetation growth conditions and the depth of sensors to cambium. For example, sap flux density fluctuates during day and night due to radiation changes (Ford et al. 2007), which also explains why sap flux measurement devices give variable results as a consequence of the aspects of a forest to solar radiation (Lu et al. 2000). Moreover, Köstner et al. (1996) showed measured sap flux densities at four depths beneath the cambium with identical diurnal variation pattern but value differences of up to 50%. However, monitoring for longer time periods and statistical analyses will help improving the accuracy of sap flux records.

Forest Stand Development

Forest Stand Development and Gap Features

A stand development is an interaction between individual trees in a population (Hutchings and Budd 1981). A stand starts with relatively small trees without competition for resources. Then, the competitive interaction begins with increment in size. Some trees die in this competition. A stand is at the peak of its tree vigour when the canopy is closed. However, the trees finally get too old to maintain this closed canopy, and gaps in the stand appear. Independent of stand density the canopy will close (Long and Smith 1984). Westoby (1977, 1981) suggests a relationship between tree size and stand density for a stand.

Stand structure development induces heterogeneous dynamics within it. The internal heterogeneity in mature or old-growth forest was known as 'gaps' and 'islands' within closed forest stand. Gaps form when one or a few individual trees die, break or uproot (Yamamoto 1996). The size of gaps is around 30–140 m² in warm-temperate forest and accounts for 5–31 % of the stand area (Yamamoto 1992), around 90–125 m² in tropical forest which accounts for 3–23 % of stand area (Brokaw 1985). Generally there are more small sized gaps than large-sized gaps (Yamamoto 2000). The relationship between gaps size and number is described as negative exponential (Brokaw 1982; Foster and Reiners 1986; Lawton and Putz 1988; Spies et al. 1990; Yamamoto 1997) or lognormal (Naka 1982; Runkle 1982; Spies et al. 1990) in various forest types. Gaps provide a different environment which is important for the regeneration of new trees. The effect of gaps on forest stand ecology are: (1) canopy opening in stand with increase in light and rainfall; (2) root distribution heterogeneity (Mao et al. 2011); (3) regeneration within gaps means young generation complexity (Oliver 1980); and (4) affect understory vegetations (Kato and Yamamoto 2000).

In a self-thinning stand, the most accepted theory describes the stand structure development with a relationship between average size of trees and maximum density (Yoda 1963).

$$Y = K\rho^A \quad (4)$$

Where Y is mean tree size (grams), ρ is the stand density (plants m⁻³), K and A are constant. It was already proven that A is not influenced by site conditions, species or initial density (Yoda 1963; White and Harper 1970; Gorham and Ingersoll 1979). When the mean tree size refers to the weight, and A is taken as 1.5, K varies between 10³ and 10⁴ (g cm⁻³) (White 1981).

The formula not only provides a relation between average tree size and possible maximum density in a self-thinning forest stand (White 1981), but also indicates the upper boundary of the so called ‘full density curve’ (Ando 1968) or ‘maximum size and density’ (Drew and Flewelling 1977).

Instead of average weight of plants, the diameter at breast height can also be taken as proxy for tree size. The size and density relation then becomes (Reineke 1933; Curtis 1970):

$$DBH_Q \propto \rho^{-0.625} \quad (5)$$

where DBH_Q is the quadratic mean diameter at breast height. The size-density line represents both the maximum density according to the diameters and the self thinning trajectory of individual stand (Long and Smith 1984).

The stand self-thinning process and heterogeneity of tree distribution in a forest result in dynamic reinforcement of roots in a soil. In that respect, gaps in forested areas could have higher landslides occurrence. Measurements by Mao et al. (2011) showed approximately three to five times differences in soil cohesion due to root spatial variation in tree islands and gaps. Moreover, Genet et al. (2008) suggested that low root density due to large distance between trees may give rise to the chance of soil failure. However, although the heterogeneity of root reinforcement of soil has been recognized for long time (Roering et al. 2003; Stokes 2007), to our knowledge there are few observations on prevailing occurrence of landslides in forest gaps.

Age-Dependent Water Use on Stand and Catchment Scale

Different methods have been applied to study how water use of an entire forest stand changes in response to vegetation growth, i.e. direct measurements on evaporation with large-scale lysimeters and indirect calculations of evaporation using long-term water balance records on catchment scale.

Lysimeters are devices designed for measuring evaporation and transpiration to study water use by vegetation (Howell et al. 1998). Precision lysimetry directly depends on lysimeter size (area and mass) and type. Many lysimeters have accuracies better than 0.05 mm of water (Howell et al. 1995; Liu et al. 2002). As an example, a ‘natural’ lysimeter, which comprises 26 mature spruce trees, was installed close to the centre of Hafren forest of central Wales to measure the water loss of forest due to transpiration and evaporation of interception water. A time integral of the evaporation vapour flux was given by the 84 m² lysimeter, amounting to twice the open water evaporation (Calder 1977). A 2,600 m³ lysimeter was used to monitor water fluxes in a *Pinus sylvestris* forest since 1974 in Colbitz, Germany. The decline of drainage from

the lysimeter reflected the increased water use accompanying growing vegetation (Struthers et al. 2003).

In contrast to the direct lysimeter measurements, many studies rely on long-term water balance records to extract forest stand evaporation. The vast majority of these studies, based on catchment water balances, studied on the effect of land use change and concluded that deforestation increases outflow of a catchment while afforestation decreases it (Andréassian 2004). However, some of those studies found that after reforestation, the catchment outflow changed with forest growth. Bosch and Hewlett (1982) summarised catchment hydrology data and showed that the effect of vegetation on water yield could be determined with fair accuracy and that it is proportional to the vegetation cover. An interesting, long-term observation stems from monitoring streamflows before and after a large wild fire of Mountain Ash (*Eucalyptus regnans*) in south-eastern Australia (Langford 1976; Kuczera 1985, 1987). Several years after the wildfire, when re-growth of a new generation of forest had started, the streamflow declined below pre-wildfire conditions. The following studies established relationship between catchment discharge and age-related water use by forest. The final results indicated that recovery in streamflow yield should be practically complete by the time the Mountain ash stands reached maturity (Kuczera 1987).

Scott and Prinsloo (2008) performed a quantitative study on the long term effects of afforestation with pine and eucalypt stands on streamflows in South Africa. Plantation of the two species caused large reductions on streamflow, also positively related to available water. 5 year old pine plantation and 3 year-old eucalypt stand reduced the peak of streamflow with 44 mm a⁻¹ and 48 mm a⁻¹ for each 10 % of catchment planted respectively. The reduction decreased progressively and could not be observed anymore after the stands had matured to 30 years old pine and 15 years old eucalypt trees.

Marc and Robinson (2007) reviewed long-term water balance results of Plynlimon catchments in mid-Wales, UK and assessed the impact of logging and land cover change. They evaluated the annual catchment evaporation via P-Q, where P is precipitation and Q is streamflow. The water balances of two subcatchments were compared, that of the Severn with 70 % forest cover and of the Wye with grassland. There was a reduction in ‘excess’ evaporation from 250 mm in 1972 to 150 mm year⁻¹ 1982 (‘excess’ evaporation by forest at Severn compared to grassland at Wye). This reduction in ‘excess’ evaporation in 10 years was explained by the relation between tree age and evaporation rate. Clearly, Marc and Robinson (2007) also admitted there are uncertainties in such a water balance approach which influence the exact quantification of the age-related transpiration.

Delzon and Loustau (2005) employed a water balance calculation. The study was carried out on a chronosequence of four even-aged maritime pine (*P. pinaster* Ait.) stands in southwest France. The results showed drastic decline of overstory transpiration from 508 mm a⁻¹ to 144 mm a⁻¹ from 10 to 54 year old stands. Interestingly, this decline in transpiration from the overstory was (partly) compensated by increase transpiration by the understory following an increase in its leaf area.

Age-Dependent Development of Root Morphology and Root Cohesion

Generally speaking, three factors influence root reinforcement of soils: the mass of roots, its distribution and the tensile strength and these factors all change over the life span of a forest stand. As fine roots (<2 mm; Claus and George 2005) are most important for water and nutrient uptake, eco-engineers and ecologists focus on fine roots when looking at the evolution of stands.

Vogt et al. (1983, 1987) published root biomass data for fifteen Douglas-fir dominated forests aged from 11 to 160 years old. The results showed that root biomass reached a maximum with canopy closure and thereafter either decreased or stabilised in the two studied Douglas-fir stands. Claus and George (2005) investigated fine root biomass and biomass distribution in different age-classes of three European forest chronosequences in mixed stands dominated by *Fagus sylvatica* L., *Picea abies* K., and *Quercus cerris* L. and described root biomass development in three phases: a fast increase in young stand; a peak in adult stands with a slow decline afterwards and lastly a steady-state root biomass in mature stands. Moreover, root development estimation in Japanese cedar (Fujimaki et al. 2007) demonstrated maximum root biomass (639 g m⁻²) appeared in a 15-year old stand, just before canopy closure and showed a fall in root biomass in the 30-year-old stand (422 g m⁻²), where after it remained constant.

In contrast, Finér et al. (2007) compiled a fine root biomass database of three main European species and showed the ambiguity of the relationship between root biomass and age: e.g. fine root biomass of beech stands decreased with age whereas that of pine stands increased with stand age. They also showed that climate was a factor to consider in this relationship. In another review, Finér et al. (2007) showed there is a positive relationship between fine root biomass and above-ground biomass.

According to the literature, most fine roots concentrate in the shallow soil. There is no generic principle on how fine root distribute vertically with regard to forest stand age. Genet et al. (2008) demonstrated that the cumulative root density distribution with regard to depth was approximately

the same in juvenile, intermediate and mature stands, with 50 % of the total fine root density in 0.1–0.2 m below soil surface. However, data from *P. kesiya* forests in India showed in a 6-year old stand, 77 % of total fine roots in 0–20 cm layer. In contrast, in 15- and 23-year old stands more fine roots were present in deeper soil layers (John et al. 2001).

Almost no published data exists on the development of root tensile strength as function of aging forest stands. Genet et al. (2008) showed root tensile strength in three *Cryptomeria japonicas* stands in China aged 9, 20 and 30 years old. Root tensile strength varied from 22.6 to 25.3 MPa and 31.7 MPa respectively. However, root tensile strength is one component determining the soil additional root cohesion. The others are root biomass (root density) and root distribution. Overall the results of Genet et al. (2008) showed that soil additional root cohesion was lower in intermediate aged plantation than in the juvenile and mature plantations.

Although crucial for soil strength, knowledge on the development of roots over the life cycle of woody vegetation in terms of root density, root distribution and especially root tensile strength seems limited. However, it is clear that generic conclusions on age-dependent development of roots are cumbersome as data collection is very time consuming and depending on species, climate and other a-biotic and biotic local conditions.

Summarizing How Vegetation Life Stages Can Affect Slope Stability

The aim of this review is to show the dynamic (de-) stabilizing effects of forest stands on potentially unstable slopes. This review discussed the hydrological and mechanical aspects of vegetation on slope stability by looking at knowledge on the behaviour of individual trees as well as of forest stands over their life cycle. Individual trees show a development over their life span from fast growing to a stable phase with mainly maintenance respiration and finally decay. This is directly related to the water (nutrient) uptake from abundant water use to significantly lower amounts. In forest stands the same type of pattern arises, from many young trees competing for resources to increasing lower stem densities in mature stands with also regular gaps developing. Hydrologically, the transpiration changes over life cycles of forest stands are very well known: trees in mature forest stands have been shown to transpire less water than juvenile forest stands, leaving more water yield in the streams—and thus higher groundwater levels in the catchments. The latter is supported by a long list of scientific literature, both on species as on stand scale. However, there are almost no studies published linking the long-term hydrological effect of vegetation stands on the probability of landslide occurrence with the exception

of landslide occurrence linked to a phase of root decay after wildfire, forest diseases or felling (e.g. Johnson and Wilcock 2002). Meng et al. (2012) presented a proof-of-concept and showed using a theoretical modelling approach that the hydrological effects can significantly influence the probability of slope failure. Of course, depending on the specific conditions and species and not taking into account the mechanical effects of aging forest stands.

In contrast, the knowledge of the mechanical effects of trees via root reinforcement is more constrained to individual species and not yet looked at on stand scale. Clearly, it is very hard to collect that information, especially when both spatial and temporal scales are involved. However, we also identify some lack of empirical information in scientific literature on the (absence of a) relationship of stand development and landslide occurrence. To understand the practically unlimited amount of interactions that act in a forest ecosystem and its influence on slope stability (landslide occurrence?), a combined effort is needed of compiling empirical evidence from existing landslide inventories and forest inventories, which are not always in the public domain, together with detailed process studies and model experiments at the stand and catchment scale. This will help us to understand these interactions and effectively apply forestry as protection measure for slope stability.

References

- Ando T (1968) Ecological studies on the stand density control in even-aged pure stands. *Bull For Prod Res Inst* 210:1–152
- Andréassian V (2004) Waters and forests: from historical controversy to scientific debate. *J Hydrol* 291(1–2):1–27
- Barclay HJ (1998) Conversion of total leaf area to projected leaf area in lodgepole pine and Douglas-fir. *Tree Physiol* 18(3):185–193
- Bond BJ, Kavanagh KL (1999) Stomatal behavior of four woody species in relation to leaf-specific hydraulic conductance and threshold water potential. *Tree Physiol* 19(8):503–510
- Bosch J, Hewlett J (1982) A review of catchment experiments to determine the effect of vegetation changes on water yield and evapotranspiration. *J Hydrol* 55(1–4):3–23
- Bouillet J-P, Laclau J-P, Arnaud M, M'Bou AT, Saint-André L, Jourdan C (2002) Changes with age in the spatial distribution of roots of *Eucalyptus* clone in Congo: impact on water and nutrient uptake. *For Ecol Manag* 171(1):43–57
- Brokaw NV (1982) The definition of treefall gap and its effect on measures of forest dynamics. *Biotropica* 14:158–160
- Brokaw NV (1985) Gap-phase regeneration in a tropical forest. *Ecology* 66(3):682–687
- Burns I (1991) Short-and long-term effects of a change in the spatial distribution of nitrate in the root zone on N uptake, growth and root development of young lettuce plants. *Plant Cell Environ* 14(1):21–33
- Calder I (1977) A model of transpiration and interception loss from a spruce forest in Plynlimon, central Wales. *J Hydrol* 33(3–4):247–265
- Claus A, George E (2005) Effect of stand age on fine-root biomass and biomass distribution in three European forest chronosequences. *Can J For Res* 35(7):1617–1625
- Cochard H, Breda N, Granier A (1996) Whole tree hydraulic conductance and water loss regulation in *Quercus* during drought: evidence for stomatal control of embolism? *Ann Sci Forest* 53(2–3):197–206
- Cohen Y, Kelliher F, Black T (1985) Determination of sap flow in Douglas-fir trees using the heat pulse technique. *Can J For Res* 15(2):422–428
- Curtis RO (1970) Stand density measures: an interpretation. *For Sci* 16(4):403–414
- Delzon S, Loustau D (2005) Age-related decline in stand water use: sap flow and transpiration in a pine forest chronosequence. *Agric For Meteorol* 129(3):105–119
- Delzon S, Sartore M, Burlett R, Dewar R, Loustau D (2004) Hydraulic responses to height growth in maritime pine trees. *Plant Cell Environ* 27(9):1077–1087
- Drew TJ, Flewelling JW (1977) Some recent Japanese theories of yield-density relationships and their application to Monterey pine plantations. *For Sci* 23(4):517–534
- Dunn G, Connor D (1993) An analysis of sap flow in mountain ash (*Eucalyptus regnans*) forests of different age. *Tree Physiol* 13(4):321
- Finér L, Helmissaari HS, Löhmus K, Majdi H, Brunner I, Børja I, Eldhuset T, Godbold D, Grebenc T, Konôpka B, Kraigher H, Möttönen MR, Ohashi M, Oleksyn J, Ostonen I, Uri V, Vanguelova E (2007) Variation in fine root biomass of three European tree species: Beech (*Fagus sylvatica* L.), Norway spruce (*Picea abies* L. Karst.), and Scots pine (*Pinus sylvestris* L.). *Plant Biosyst* 141(3):394–405
- Ford CR, Hubbard RM, Kloeppel BD, Vose JM (2007) A comparison of sap flux-based evapotranspiration estimates with catchment-scale water balance. *Agric For Meteorol* 145(3):176–185
- Forrester DI, Collopy JJ, Morris JD (2010) Transpiration along an age series of *Eucalyptus globulus* plantations in southeastern Australia. *For Ecol Manag* 259(9):1754–1760
- Foster JR, Reiners WA (1986) Size distribution and expansion of canopy gaps in a northern Appalachian spruce-fir forest. *Vegetatio* 68(2):109–114
- Fujimaki R, Tateno R, Tokuchi N (2007) Root development across a chronosequence in a Japanese cedar (*Cryptomeria japonica* D. Don) plantation. *J For Res* 12(2):96–102
- Genet M, Kokutse N, Stokes A, Fourcaud T, Cai X, Ji J, Mickovski S (2008) Root reinforcement in plantations of *Cryptomeria japonica* D. Don: effect of tree age and stand structure on slope stability. *For Ecol Manag* 256(8):1517–1526
- George AK, Walker KF, Lewis MM (2005) Population status of eucalypt trees on the River Murray floodplain, South Australia. *River Res Appl* 21(2–3):271–282
- Gorham TW, Ingersoll RV (1979) Evolution of the Eocene Galisteo basin, north-central New Mexico. In: *New Mexico Geological Society, Guidebook, Santa Fe country, vol 30*. pp 219–224
- Green S, Clothier B (1988) Water use of kiwifruit vines and apple trees by the heat-pulse technique. *J Exp Bot* 39(1):115–123
- Hacke U, Sperry J, Ewers B, Ellsworth D, Schäfer K, Oren R (2000) Influence of soil porosity on water use in *Pinus taeda*. *Oecologia* 124(4):495–505
- Hatton TJ, Vertessy RA (1990) Transpiration of plantation *Pinus radiata* estimated by the heat pulse method and the Bowen ratio. *Hydrol Process* 4(3):289–298
- Howell T, Schneider A, Dusek D, Marek T, Steiner J (1995) Calibration and scale performance of Bushland weighing lysimeters. *Trans ASAE* 38(4):1019–1024
- Howell TA, Tolk JA, Schneider AD, Evett SR (1998) Evapotranspiration, yield, and water use efficiency of corn hybrids differing in maturity. *Agron J* 90(1):3–9
- Hubbard RM, Bond BJ, Ryan MG (1999) Evidence that hydraulic conductance limits photosynthesis in old *Pinus ponderosa* trees. *Tree Physiol* 19(3):165–172

- Hutchings MJ, Budd CS (1981) Plant competition and its course through time. *Bioscience* 31:640–645
- Jacobs M (1955) Growth habits of the eucalypts. Forestry and Timber Bureau, Canberra, 262 pp
- John B, Pandey HN, Tripathi RS (2001) Vertical distribution and seasonal changes of fine and coarse root mass in *Pinus kesiya* Royle Ex. Gordon forest of three different ages. *Acta Oecol* 22(5):293–300
- Johnson AC, Wilcock P (2002) Association between cedar decline and hillslope stability in mountainous regions of southeast Alaska. *Geomorphology* 46:129–142
- Kato K, Yamamoto S-I (2000) Effects of canopy on the sapling composition and structure in a subalpine old-growth forest, central Japan. *Ecoscience* 7(2):237–242
- Kira T, Shidei T (1967) Primary production and turnover of organic matter in different forest ecosystems of the western Pacific. *Jpn J Ecol* 17(2):70–87
- Köstner B, Biron P, Siegwolf R, Granier A (1996) Estimates of water vapor flux and canopy conductance of Scots pine at the tree level utilizing different xylem sap flow methods. *Theor Appl Climatol* 53(1–3):105–113
- Köstner B, Falge E, Tenhunen J (2002) Age-related effects on leaf area/sapwood area relationships, canopy transpiration and carbon gain of Norway spruce stands (*Picea abies*) in the Fichtelgebirge, Germany. *Tree Physiol* 22(8):567–574
- Kowalski S, Sartore M, Burrell R, Berbigier P, Loustau D (2003) The annual carbon budget of a French pine forest (*Pinus pinaster*) following harvest. *Glob Chang Biol* 9(7):1051–1065
- Kuczera G (1985) Prediction of water yield reductions following a bushfire in ash-mixed species eucalypt forest. Melbourne and Metropolitan Board of Works. Water supply catchment hydrology research, Rep No MMBW-W-0014
- Kuczera G (1987) Prediction of water yield reductions following a bushfire in ash-mixed species eucalypt forest. *J Hydrol* 94(3–4):215–236
- Langford K (1976) Change in yield of water following a bushfire in a forest of *Eucalyptus regnans*. *J Hydrol* 29(1–2):87–114
- Law B, Thornton P, Irvine J, Anthoni P, Van Tuyl S (2001) Carbon storage and fluxes in ponderosa pine forests at different developmental stages. *Glob Chang Biol* 7(7):755–777
- Law B, Sun O, Campbell J, Van Tuyl S, Thornton P (2003) Changes in carbon storage and fluxes in a chronosequence of ponderosa pine. *Glob Chang Biol* 9(4):510–524
- Lawton RO, Putz FE (1988) Natural disturbance and gap-phase regeneration in a wind-exposed tropical cloud forest. *Ecology* 69:764–777
- Liu C, Zhang X, Zhang Y (2002) Determination of daily evaporation and evapotranspiration of winter wheat and maize by large-scale weighing lysimeter and micro-lysimeter. *Agric For Meteorol* 111(2):109–120
- Long JN, Smith FW (1984) Relation between size and density in developing stands: a description and possible mechanisms. *For Ecol Manag* 7(3):191–206
- Lu P, Müller WJ, Chacko EK (2000) Spatial variations in xylem sap flux density in the trunk of orchard-grown, mature mango trees under changing soil water conditions. *Tree Physiol* 20(10):683–692
- Magnani F, Mencuccini M, Grace J (2000) Age-related decline in stand productivity: the role of structural acclimation under hydraulic constraints. *Plant Cell Environ* 23(3):251–263
- Mao Z, Saint-André L, Genet M, Mine FX, Jourdan C, Rey H, Courbaud B, Stokes A (2011) Engineering ecological protection against landslides in diverse mountain forests: choosing cohesion models. *Ecol Eng* 45:55–69
- Marc V, Robinson M (2007) The long-term water balance (1972–2004) of upland forestry and grassland at Plynlimon, mid-Wales. *Hydrol Earth Syst Sci* 11(1):44–60
- McDowell N, Barnard H, Bond B, Hinckley T, Hubbard R, Ishii H, Köstner B, Magnani F, Marshall J, Meinzer F (2002) The relationship between tree height and leaf area: sapwood area ratio. *Oecologia* 132(1):12–20
- Mencuccini M, Grace J (1996) Hydraulic conductance, light interception and needle nutrient concentration in Scots pine stands and their relations with net primary productivity. *Tree Physiol* 16(5):459–468
- Meng W, Bogaard TA, van Beek LPH (2012) The long-term hydrological effect of forest stands on the stability of slopes (Proceedings of ISL-NASL conference, Banff, Canada). In: Eberhardt et al (eds) *Landslides and engineered slopes: protecting society through improved understanding*. Taylor & Francis, London, pp 1631–1636. ISBN 978-0-415-62123-6
- Murty D, McMurtrie RE, Ryan MG (1996) Declining forest productivity in aging forest stands: a modeling analysis of alternative hypotheses. *Tree Physiol* 16(1–2):187–200
- Naka K (1982) Community dynamics of evergreen broadleaf forests in southwestern Japan. I. Wind damaged trees and canopy gaps in an evergreen oak forest. *Bot Mag Tokyo* 95(4):385–399
- Oliver RL (1980) A cognitive model of the antecedents and consequences of satisfaction decisions. *J Mark Res* 17:460–469
- Oliver C, Larson B (1996) *Forest stand dynamics*. Wiley, New York
- Phillips N, Bond BJ, Ryan MG (2001) Gas exchange and hydraulic properties in the crowns of two tree species in a Panamanian moist forest. *Trees* 15(2):123–130
- Pollen N, Simon A (2005) Estimating the mechanical effects of riparian vegetation on stream bank stability using a fiber bundle model. *Water Resour Res* 41(7), W07025
- Pothier D, Margolis HA, Poliquin J, Waring RH (1989) Relation between the permeability and the anatomy of jack pine sapwood with stand development. *Can J For Res* 19(12):1564–1570
- Reineke LH (1933) Perfecting a stand-density index for even-aged forests. US Government Printing Office, Washington, DC
- Roberts S, Vertessy R, Grayson R (2001) Transpiration from *Eucalyptus sieberi* (L. Johnson) forests of different age. *For Ecol Manag* 143(1–3):153–161
- Roering JJ, Schmidt KM, Stock JD, Dietrich WE, Montgomery DR (2003) Shallow landsliding, root reinforcement, and the spatial distribution of trees in the Oregon Coast Range. *Can Geotech J* 40(2):237–253
- Runkle JR (1982) Patterns of disturbance in some old-growth mesic forests of eastern North America. *Ecology* 63(5):1533–1546
- Ryan MG, Waring RH (1992) Maintenance respiration and stand development in a subalpine lodgepole pine forest. *Ecology* 73:2100–2108
- Ryan MG, Yoder BJ (1997) Hydraulic limits to tree height and tree growth. *Bioscience* 47(4):235–242
- Ryan MG, Binkley D, Fownes JH (1997) Age-related decline in forest productivity: pattern and process. In: Begon M, Fitter AH (eds) *Advances in ecological research*. Academic, San Diego, CA, pp 213–262
- Ryan MG, Bond BJ, Law BE, Hubbard RM, Woodruff D, Cienciala E, Kucera J (2000) Transpiration and whole-tree conductance in ponderosa pine trees of different heights. *Oecologia* 124(4):553–560
- Ryan MG, Phillips N, Bond BJ (2006) The hydraulic limitation hypothesis revisited. *Plant Cell Environ* 29(3):367–381
- Saliendra NZ, Sperry JS, Comstock JP (1995) Influence of leaf water status on stomatal response to humidity, hydraulic conductance, and soil drought in *Betula occidentalis*. *Planta* 196(2):357–366
- Santantonio D (1990) Modeling growth and production of tree roots. In: Dixon RK, Meldahl RS, Ruark GA, Warren WG (eds) *Process modeling of forest growth responses to environmental stress*. Timber Press Inc, Oregon, pp 124–141
- Scott DF, Prinsloo F (2008) Longer-term effects of pine and eucalypt plantations on streamflow. *Water Resour Res* 44 (7):W00A08

- Sperry J, Pockman W (1993) Limitation of transpiration by hydraulic conductance and xylem cavitation in *Betula occidentalis*. *Plant Cell Environ* 16(3):279–287
- Sperry J, Alder N, Eastlack S (1993) The effect of reduced hydraulic conductance on stomatal conductance and xylem cavitation. *J Exp Bot* 44(6):1075–1082
- Spies T, Bresnahan M, Bahrain S, Arnold D, Blanck G, Mellins E, Pious D, DeMars R (1990) A gene in the human major histocompatibility complex class II region controlling the class I antigen presentation pathway. *Nature (London)* 348:744–747
- Stokes A (2007) Eco-and ground bio-engineering: the use of vegetation to improve slope stability. In: Proceedings of the first international conference on eco-engineering, 13–17 September 2004, vol 103. Springer
- Struthers I, Hinz C, Sivapalan M, Deutschmann G, Beese F, Meissner R (2003) Modelling the water balance of a free-draining lysimeter using the downward approach. *Hydrol Process* 17(11):2151–2169
- Teskey RO, Hinckley TM, Grier CC (1983) Effect of interruption of flow path on stomatal conductance of *Abies amabilis*. *J Exp Bot* 34(10):1251–1259
- Troendle CA, King RM (1985) The effect of timber harvest on the Fool Creek watershed, 30 years later. *Water Resour Res* 21(12):1915–1922
- Tyree MT, Sperry JS (1988) Do woody plants operate near the point of catastrophic xylem dysfunction caused by dynamic water stress? Answers from a model. *Plant Physiol* 88(3):574–580
- Van Asch TW, Sukmantalya I (1993) The modeling of soil slip erosion in the upper Komering area, South Sumatra Province, Indonesia. *Geogr Fis Din Quat* 16:81–86
- Vanninen P, Ylitalo H, Sievänen R, Mäkelä A (1996) Effects of age and site quality on the distribution of biomass in Scots pine (*Pinus sylvestris* L.). *Trees* 10(4):231–238
- Vertessy R, Benyon R, O’Sullivan S, Gribben P (1995) Relationships between stem diameter, sapwood area, leaf area and transpiration in a young mountain ash forest. *Tree Physiol* 15(9):559–567
- Vertessy RA, Watson FGR, O’Sullivan SK (2001) Factors determining relations between stand age and catchment water balance in mountain ash forests. *For Ecol Manag* 143(1–3):13–26
- Vogt KA, Moore EE, Vogt DJ, Redlin MJ, Edmonds RL (1983) Conifer fine root and mycorrhizal root biomass within the forest floors of Douglas-fir stands of different ages and site productivities. *Can J For Res* 13(3):429–437
- Vogt KA, Vogt DJ, Moore EE, Fatuga BA, Redlin MR, Edmonds RL (1987) Conifer and angiosperm fine-root biomass in relation to stand age and site productivity in Douglas-fir forests. *J Ecol* 75:857–870
- Waldron L (1977) The shear resistance of root-permeated homogeneous and stratified soil. *Soil Sci Soc Am J* 41(5):843–849
- Waring RH, Schlesinger WH (1985) Forest ecosystems. Concepts and management. Academic, San Diego, CA
- Watson F, Vertessy R (1996) Estimating leaf area index from stem diameter measurements in Mountain Ash forest. Cooperative Research Centre for Catchment Hydrology. Melbourne. Report 96/7, November 1996, 102 pp
- Weiner J, Thomas SC (2001) The nature of tree growth and the “age-related decline in forest productivity”. *Oikos* 94(2):374–376
- Westoby M (1977) Self-thinning driven by leaf area not by weight. *Nature (London)* 265:330–331
- Westoby M (1981) The place of the self-thinning rule in population dynamics. *Am Nat* 118(4):581–587
- White J (1981) The allometric interpretation of the self-thinning rule. *J Theor Biol* 89(3):475–500
- White J, Harper J (1970) Correlated changes in plant size and number in plant populations. *J Ecol* 58:467–485
- Whittaker RH, Woodwell GM (1968) Dimension and production relations of trees and shrubs in the Brookhaven Forest, New York. *J Ecol* 56:1–25
- Woodgate P, Peel B, Coram J, Farrell S, Ritman K, Lewis A (1996) Old-growth forest studies in Victoria, Australia concepts and principles. *For Ecol Manag* 85(1):79–94
- Wu TH (1976) Investigation on landslides on Prince of Wales Island. Alaska Geotech. Report No 5, Department of Civil Engineering, Ohio State University, Columbus, USA
- Wu TH (1979) Strength of tree roots and landslides on Prince of Wales Island, Alaska. *Can Geotech J* 16:19–33
- Wullschlegel SD, Meinzer F, Vertessy R (1998) A review of whole-plant water use studies in tree. *Tree physiol* 18(8–9):499–512
- Yamamoto S-I (1992) The gap theory in forest dynamics. *Bot Mag Tokyo* 105(2):375–383
- Yamamoto S (1996) Gap regeneration of major tree species in different forest types of Japan. *Vegetatio* 127(2):203–213
- Yamamoto S-I (1997) Gap-disturbance regimes in different forest types of Japan. *J Sustain For* 6(3–4):223–235
- Yamamoto S-I (2000) Forest gap dynamics and tree regeneration. *J For Res* 5(4):223–229
- Yoda K (1963) Self-thinning in over-crowded pure stands under cultivated and natural conditions. (In-traspecific competition among higher plants. XI.). *J Biol Osaka City Univ* 14:107–129
- Yoda K, Shinozaki K, Ogawa H, Hozumi K, Kira T (1965) Estimation of the total amount of respiration in woody organs of trees and forest communities. *J Biol Osaka City Univ* 16:15–26
- Yoder B, Ryan M, Waring R, Schoettle A, Kaufmann M (1994) Evidence of reduced photosynthetic rates in old trees. *For Sci* 40(3):513–527
- Zimmermann M (1983) Ethical guidelines for investigations of experimental pain in conscious animals. *Pain* 16(2):109–110



Analysis of a Deep-Seated Landslide in the Phan Me Coal Mining Dump Site, Thai Nguyen Province, Vietnam

Do Minh Duc, Nguyen Manh Hieu, Kyoji Sassa, Eisaku Hamasaki, Khang Dang, and Toyohiko Miyagi

Abstract

A large landslide occurred at the Pha Me coal mining dump site at 4:20 AM on 15 April 2012, buried a huge area, including tens of houses and seven persons. There was no abnormal weather or seismic activity at the time of the landslide. A joint work between Vietnamese and Japanese experts was carried out to investigate characteristics and reasons of the landslide. The achieved results show that coal mining wastes are disposed of on low hill sites where granitic bedrock was intensively crushed due to tectonic activity. Weathering crusts include rich clays of over 15–20 m in thickness. The landslide has a volume of about 2.5 million m³, with a slip surface cut through weathering soils at a depth of about 10 m. The scarp of the landslide departs at an approximate elevation of 85–100 m. Travel distance is 300–350 m. Sliding materials are primarily mining wastes. However the sliding surface is defined to be situated at the depth of 12–15 m in the residual soils. There are two significant causes of the disaster. Firstly, the waste dump site plays a role as a water-storage layer which keeps residual soils permanently saturated. The second cause of the deep-seated landslide is over-loading of mining wastes. Prior evidences of the landslide such as cracks at the top, heave at the trough of the dump site were recognized a week before, however they were not seriously considered.

Keywords

Deep-seated landslide • Coal waste dump site • Residual soils • Slope stability • Vietnam

D.M. Duc (✉) • N.M. Hieu • K. Dang
VNU University of Science, Vietnam National University, 334 Nguyen
Trai, Thanh Xuan, Hanoi, Vietnam
e-mail: ducdm@vnu.edu.vn; hieugeo@gmail.com; khangdq@gmail.com

K. Sassa
International Consortium on Landslides, UNITWIN Headquarters
Building, Kyoto University Uji-Campus, Uji, Kyoto 611-0011, Japan
e-mail: kyoji.sassa@gmail.com

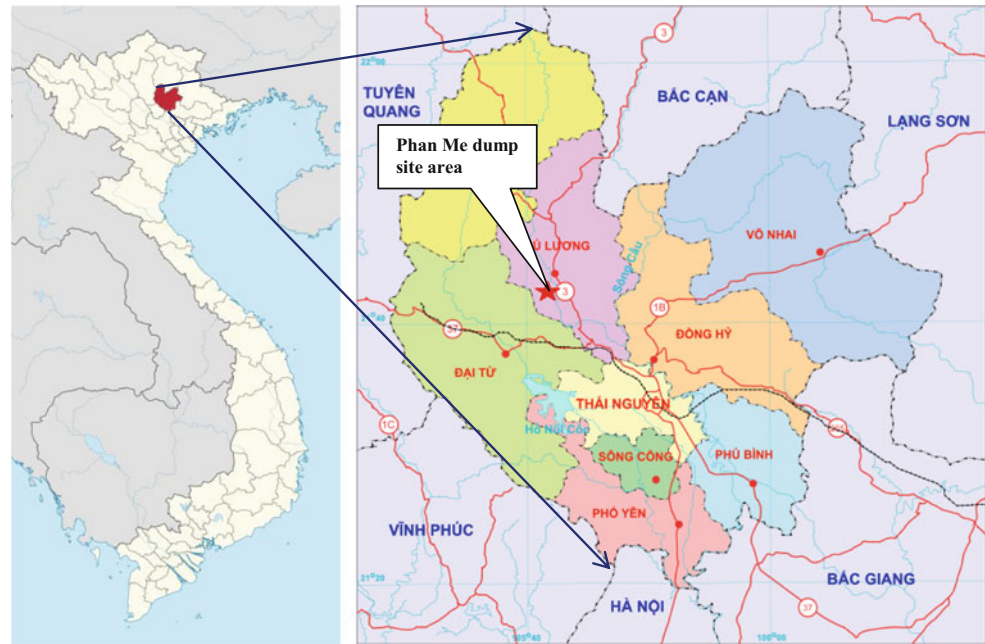
E. Hamasaki
Department of Technology, Advantech Co., Ltd, 1-4-8,
Kakyoin, Sendai 980-0013, Japan
e-mail: hamasaki@advantechology.co.jp

T. Miyagi
Tohoku Gakuin University, 1-13-1 Chuo, Tagajo, Miyagi 985-8537,
Japan
e-mail: miyagi@izcc.tohoku-gakuin.ac.jp

Introduction

In recent years, landslides have occurred in dumps of municipal solid waste (Blightw and Fourie 2005, Yilmaz and Atmaca 2006) and coal mine waste (Geertsema et al. 2006, Steiakakis et al. 2009), which are artificial mountains with heights of nearly a hundred meters. They are not only damaging the environment but are also dangerous to human life and property. For example, the Buffalo Creek disaster in the USA in 1972 that killed 118 people, made 4,000 homeless and destroyed 50 million US dollars worth of property and facilities. The flow slide that occurred in the Umraniye—Hekimbasi refuse dump in Turkey in 1993 killed 39 people (Blightw and Fourie 2005).

Phan Me coal mine is situated in Thai Nguyen province, Northeast Vietnam (Fig. 1). Established in 1960, it had an

Fig. 1 Location of the study area

initial designed capacity of 50,000 t of coal per year. Recently, the mine had two sites of exploitation: North Lang Cam open pit mine with a reserve of 1,560,000 t, designed capacity of 100,000 t per year and South Lang Cam pit mine with usable reserves of 1,640,000 t, designed capacity of 30,000 t per year. The mine has three waste dump sites which are about 2–3 km away from the open pit.

A large landslide occurred at a dump site of Phan Me coal mining at 4:20 AM on 15 April 2012, buried a huge area, including tens of houses and seven persons. There was no abnormal weather or seismic activity at the time of landslide. The achieved results show that coal mining wastes that were disposed of on low hill sites where bedrock is intensively crushed due to tectonic activities. This paper aims to define characteristics and causes of the landslide, including slope stability analysis of the Phan Me coal mining waste dump site using SLOPE/W software.

Study Methods

Site Investigation

After the landslide occurred, a research group investigated the boundary of the landslide by using a GPS Garmin 72 with an accuracy of ± 5 m. Boundary of the landslide was marked on the topography map, at a scale 1/10,000 and a Google Earth image. In-situ density of coal mining wastes and clay layers were also determined by digging holes and taking undisturbed samples, respectively (Fig. 2).

Waste materials mainly include sand, gravel and boulders. In order to determine the average internal friction

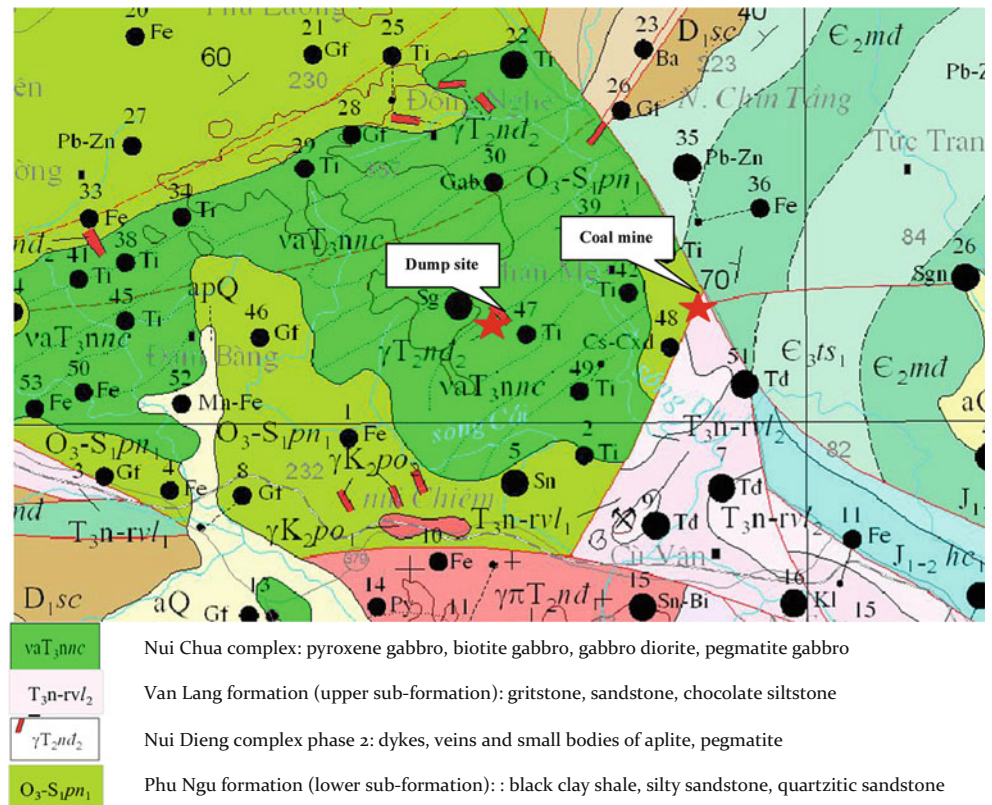
**Fig. 2** Determine in-situ density of waste materials by digging hole

angle of the waste materials, the internal friction angle of each kind of material was measured after landslide event. In-situ samples included waste materials and weathered clay and were retrieved to determine physical and mechanical parameters that were used for stability analysis as density, effective cohesion, and effective internal friction angle.

Laboratory Tests

Undisturbed samples and disturbed samples were taken from the site including weathered clayey soil and material from the dump site for laboratory tests. Tests were performed according to the specifications of ASTM (American Society

Fig. 3 Geological settings in Phan Me area



for Testing and Materials 2001). Grain size analysis was conducted by the wet sieve method with sieve sizes of 20, 10, 5, 2.5, 1, 0.5, 0.25, 0.10, and 0.05 mm, respectively. Effective internal friction angle and cohesion of residual soils were determined by direct shear test (ASTM 2001 D3080). Density of soils was determined in both natural condition and saturated condition.

The other data used in the study includes topographic and geological maps at a scale of 1: 50,000 and data on the exploitation activities at the Phan Me coal mine.

Results and Discussion

Topography and Geological Settings

The Phan Me community belongs to the Phu Luong district. It is located at tanhe elevation of 150–200 m. Slope angle of the terrain ranges between 5 deg and 20 deg. The dump site was located on hills with a natural slope angle of 15–20°.

A large area of the Phan Me community lies on the Nui Chua complex (vaT_3nnc) including pyroxene gabbro, biotite gabbro, gabbro diorite, pegmatite gabbro. The Coal mine is exploiting the Van Lang formation (T_3n-rvl) (Fig. 3). Coal mining waste was subsequently dumped on a hilly site which is a weathering crust of the Nui Dieng complex phase

2 (γT_2nd_2). Residual soils are rich clays of 15–20 m thickness. Composition of the Nui Dieng complex phase 2 includes dykes, veins and small bodies of aplite, and pegmatite. The area is characterized by a complex system of faults. Especially, the mine is in the area of interference between three faults.

Characteristics of the Landslide

The dump site was 90 m high, including two steps in front of the landslide. The lower step was 35 m in height and the upper part was 55 m in height. Average slope angle was 34°. Prior to the landslide, there were some cracks at the top of the dumpsite. The trough heaved up to 0.5 m in some places (per communication with local people). However, these signs were not taken into account as early warnings of a landslide by both managers of the mine and local people.

The landslide occurred at 4:20 AM on 15 April 2012. There was no abnormal weather or seismic activity before or after the time of landslide. The scarp departed at an approximate elevation of 85–100 m. Landslide debris run out was up to 300–350 m (Fig. 4), buried ten houses (two houses were only 30 m away from the dump site). Rice fields were affected and seven people were killed (Figs. 5 and 6). Rice fields at the outer side of landslide debris were pushed up several meters (Fig. 7) and displaced 20–30 m westwards.

Fig. 4 Boundary of the landslide before and after event



Fig. 5 Dump site area after the landslide



Fig. 7 Rice field was pushed up by the landslide debris



Fig. 6 A house was completely destroyed

The landslide has a volume of about 2.5 million m³ with the slip surface cut through weathering soils at the depth of about 15 m.

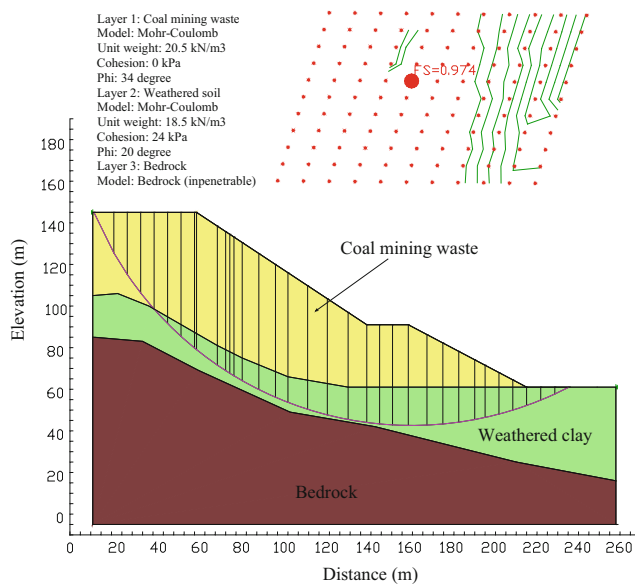
Soil Characteristics and Slope Stability Analysis

Slope stability analysis have been carried out at several waste dump sites (Chaulya et al. 1999, Omraci et al. 2003, Nyssen and Vermeersch 2010, Wang et al. 2011, Pinto 2009). In order to analyze the stability of the Phan Me coal dump site, we used input data for the model as geometry measured on site, characteristics of soil layers determined by field and laboratory tests. Factor of safety of the dump site was calculated by (GEO-SLOPE International Ltd. 2004) software using the Bishop simplified method.

The deep-seated landslide in Phan Me coal mine occurred in the weathering crust. Residual soils are rich clays with a

Table 1 Geotechnical properties of coal mining waste and residual soil

Soil	Grain size (mm) (%)						Bulk density (kN/m ³)	Effective cohesion (kPa)	Effective internal friction angle (degree)
	>20	10–20	5–10	0.1–5	0.05–0.10	<0.05			
Coal mining waste	40.1	12.2	6.7	29.8	11.2	0	20.5	0	34
Residual soil	0	0	21.7	26.1	15.7	36.5	18.5	24	20

**Fig. 8** Result of slope stability analysis using SLOPE/W

thickness of 15–20 m. Geotechnical properties of the soils and waste materials are shown in Table 1. After the landslide, the slope angle of the sand and gravel material was 32–33°; slope angle of the material containing boulders was 35°. An average value of 34° was used for stability analysis of the waste dump site. In terms of geometry, the dump site has two steps, the first step is 30 m high and the second step is 55 m high.

Results of slope stability analysis (Fig. 8) shows that the overburden load of mining wastes was above shear strength of the residual soils. Slip surface is about 35 m below the terrain and cut 14 m into the weathering crust.

Conclusion

In spite of prior evidences of a large landslide at the Phan Me coal mine, waste materials were still disposed at the dump site. The deep-seated landslide occurred at 4:20 AM on 15 April 2012 without any abnormal weather or

seismic activity. There are two main causes of the disaster. Firstly, the waste dump site plays a role as a water-storage layer which keeps residual soils permanently saturated. The second cause of the deep-seated landslide is over-loading of mining wastes. The landslide once again raises the awareness and serious warning of disaster risk management in mining areas in Vietnam and many other developing countries.

References

- ASTM (2001) D3080 Test method for direct shear test of soils under consolidated drained conditions. ASTM Standards on Disc CD 1, volume 04.08, Soil and Rock (I): D420–D5779
- Blightw GE, Fourie AB (2005) Catastrophe revisited—disastrous flow failures of mine and municipal solid waste. *Geotech Geol Eng* 23:219–248
- Chaulya SK, Singh RS, Chakraborty MK, Dhar BB (1999) Numerical modeling of biostabilisation for a coal mine overburden dump slope. *Ecol Model* 114(1999):275–286
- Geertsema M, Clague JJ, Schwab JW, Evans SG (2006) An overview of recent large catastrophic landslides in northern British Columbia, Canada. *Eng Geol* 83:120–143
- GEO-SLOPE International Ltd (2004) Stability modeling with SLOPE/W—an engineering methodology. Calgary, Alberta, Canada
- Nyssen J, Vermeersch D (2010) Slope aspect affects geomorphic dynamics of coal mining spoil heaps in Belgium. *Geomorphology* 123:109–121
- Omraci K, Merrien-Soukatchoff V, Tisot JP, Piguat JP, Le Nickel SLN (2003) Stability analysis of lateritic waste deposits. *Eng Geol* 68:189–199
- Pinto PSS (2009) Static and seismic analysis of solid waste landfills. In: Proceedings of international symposium on geoenvironmental engineering, ISGE2009, 8–10 September 2009, Hangzhou, China
- Steiakakis E, Kavouridis K, Monopolis D (2009) Large scale failure of the external waste dump at the South field lignite mine Northern Greece. *Eng Geol* 104:269–279
- Wang G, Kong X, Gu Y, Yang C (2011) Research on slope stability analysis of super-high dumping site based on cellular automaton. *Procedia Eng* 12:248–253
- Yilmaz A, Atmaca E (2006) Environmental geological assessment of a solid waste disposal site: a case study in Sivas, Turkey. *Environ Geol* 50:677–689. doi:10.1007/s00254-006-0241-1



Geological Complexities of Rawana Landslide, Sirmaur District, Himachal

D.K. Chadha

Abstract

The Rawana Landslide is unique as it is dynamic in nature, associated with emission of hot water vapors (Temp 45–60 °C), change in chemical quality and a foul smell emitting from some of the vents. The active landslide area is increasing in its aerial extent as observed from LISS III, the present dimension shows a length of 420 m and variable width ranging 190–270 m. The toe of the landslide is in the Giri River Channel and continuous erosion by the river is leading to reactivation of the slide. Geologically, the landslide material is composed of carbonaceous shale/slatey shale with nodules of pyrite minerals, occurrence of quartzite of Infra-Krols and carbonate rocks of Upper Krols formation. Thus the landslide is in a geologically complex area where lithology, structural features, seepage from springs and so on are contributing to the recurrence of landslide activity. This activity is associated with the NW-SE trending linear Giri Thrust, and is marked by a prominent fault trending NNW-SSE. The other prominent structural feature is the presence of a NE-SW trending planar lineament, orthogonal to the Giri Thrust, which dissects the landslide mass on its SE extreme and rendering the western portion to move down compared with the eastern part. This has resulted in the formation of a prominent scarp on the western side facilitating the slide. The landslide area has a close network of drainage pattern and presence of two springs which continuously drain through the landslide, producing an exothermic reaction converting seepage water into acidic water with low pH (2.4) and high salinity at EC 6320 mhos. These chemical reactions have altered the basic composition of rock producing new mineral assemblages.

Based on the study of various parameter for Landslide Hazard Evaluation Factor (LHEF) rating, the total estimated hazard value is 7.75 which shows the landslide falls under Zone IV of the Hazards Zone i.e. High Hazard Zone. Although it is difficult to tackle the complex nature of the landslide by any known engineering methods and based on the detail study of the landslide, it is suggested that a toe wall, preferably of flexible type, may be constructed at the base of the slide and properly anchored to the bed rock and providing other solutions to deal with the water problem.

Keywords

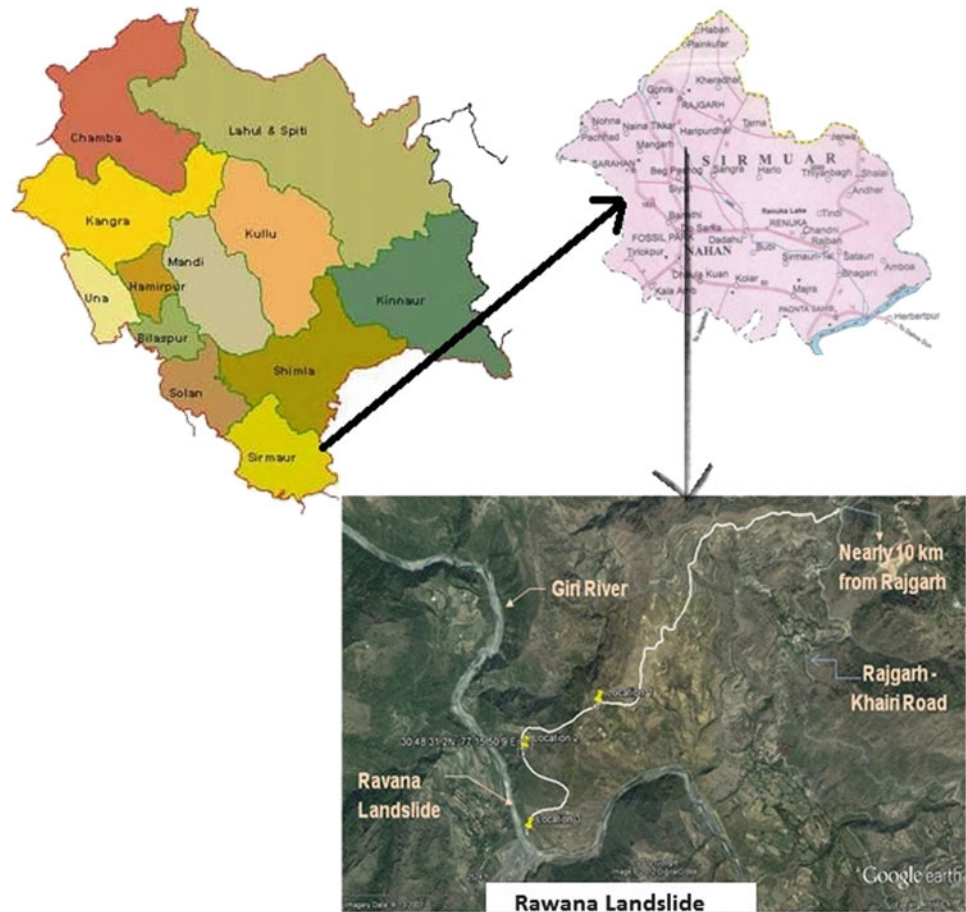
Giri Thrust • Infra Krol • Carbonaceous shale • LHEF • Scarp

Introduction

The landslide is located in the steep rugged mountain terrain of outer Himalayas near Rawana Village (30° 48' 25" N: 77° 15' 30" E), Himachal Pradesh and it distinguishes itself from

D.K. Chadha (✉)
Global Hydrogeological Solutions, Vikaspuri, New Delhi 110018,
India
e-mail: dkchadha27@gmail.com

Fig. 1 Location map of the project area



other landslides because of the emission of hot vapours with a pungent smell, geological complexities and changes in hydrochemistry of water (Fig. 1). The occurrence of landslides is a common phenomenon in the Himalayas and yet the causes and mechanism remain poorly understood for different landslides. The initiation and occurrence of most of the landslides in the Himalayas can be attributed to slope morphology, local geology and tectonics, lithology, weathering and influence of natural (rainfall) and anthropogenic activities.

The attention to the Rawana landslide was drawn in 2005 when some hot gases were noticed emitting from the surface near the left bank of the Giri River. During November 2005, an expert team from the Geological Survey of India (GSI) visited the site and they reported that the surface oozing hot water mixed gas was confined to a near circular area of 5 m diameter and the temperature varied between 60° and 100°. Since the area lacked any indication of present day volcanic activity it was inferred that the phenomenon may be related either to reactivated geothermal activity subsequent to the 8th October 2005, Muzaffarabad earthquake (Intensity 7.6, distance 863 km from landslide) or to some exothermal chemical reaction, localized within the sulfurous formation of infra krols.

Another expert team constituted by the Department of Science and Technology (DST), Government of India,



Fig. 2 Field photograph showing the view of the Rawana landslide and the area of hot gas emanations in 2005

visited in August 2006 and opined two possible explanations for the cause of emission of the heat and gas: (1) Localized burning of partially burned charcoal pockets in the carbonaceous slate at shallow depths and, (2) The heat and gas are being transmitted through a channel along the Giri Thrust or its branching fault from a geothermal source at depth which lies in the close proximity of the landslide (Fig. 2).



Fig. 3 Google snapshot of the study area showing 30 other landslides along the Giri River

The landslide being located in a remote area and not causing any disruption of the vehicular traffic so no special attention was given to study the landslide in detail. The only impact seen is the subsidence of agriculture and pasture land besides some cracks in the nearby building. But the landslide being a singular case amongst the 30 landslides (Fig. 3) in its vicinity which show unusual characterization like high temperature, emission of hot vapours, etc., the Department of Science and Technology, Govt. of India supported the study of the landslide, and the present paper is the outcome of this study.

Dynamic Nature of Landslide

It is observed that Rawana Landslide is an old slide whose downstream part culminates in Giri River is essentially a toe driven slide and its main causative factor is the continuous erosion of its toe by the Giri River which runs along a regional thrust. As a result its slope has continuously been disturbed and further aided by the structural set up, weak lithology mainly weathered shale, and seepage from the springs etc increasing its mobility. Likewise, the crown region got disturbed and lost its equilibrium and get destabilized. In year 2002, the slide covered an area of 8,490 m² which increased to 49,440 m², 58,828 m² and 86,021 m² in the years 2006, 2007 and 2012 respectively. The slope angle of the slide is nearly 45° from crown to mid-level, which steepens to 70° between middle part and its toe.

The slide zone has been advancing laterally and also towards the crown front, as a result of which it has engulfed the fields and houses of the Upper Rawana village and endangering the adjacent fields. The dimension of the slide as observed during different years since 2002–2012 is given

Table 1 Areal extent of landslide (2002–2012)

Year	Area (m ²)
2002	8,490
2006	49,440
2007	58,828
2012	86,021



Fig. 4 Google snapshot of year 2002 and field photograph of 2012 to show the dynamic nature of the landslide

in Table 1 and comparative dimension of 2002 and 2012 is shown in Fig. 4.

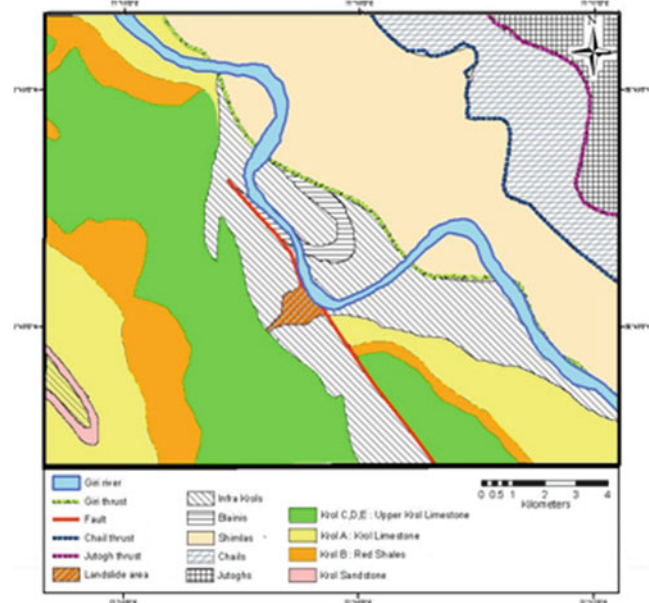
Geology

Regional Geology

Geologically, the area shows the signatures of Himalayan tectonism and uplift, which caused strong erosional flux and produced the present day landforms and instability zones. The Jutogh and Chail Formations are low to medium grade metamorphic rocks of Precambrian age, which are thrust (Jutogh/Chail thrusts) over the rocks of Simla and Jaunsar Groups of Precambrian age. The latter do not show signs of metamorphism except its incipient effects at places (e.g. slaty shale), and are faulted/thrust over a group of sedimentary sequences consisting of Blaini, Infra-Krol and Krol formations, which in turn overlies the Lower Tertiary

Table 2 Regional Litho-tectonic units around the study area

Litho-unit	Lithology
Subathu formation	Greenish grey to grey mudstone and shale with thin layers of nummulitic limestone
<i>Krol Thrust (Main Boundary Thrust)</i>	
Krol E	Light coloured limestone with thin shale
Krol D	Cherty limestone and shale
Krol C	Dark blue, grey limestone with algal structures
Krol B	Red and purple shale with minor limestone
Krol A	Calcareous shale and thin layers of limestone
Krol sandstone	Sandstone, orthoquartzite and sand
Infra-Krol	Black pyritiferous shale and quartzite bands
<i>Unconformity/Giri Thrust</i>	
Simla/Jaunsar group	Quartzite, grits, thin slaty bands
Nagthat formation	
Chandpur formation	Slates, phyllites, thin bedded limestone
Mandhali formation	Slates, quartzite, boulder bed, limestone

**Fig. 6** Geological map of the Rawana landslide zone vicinity

Local Geology

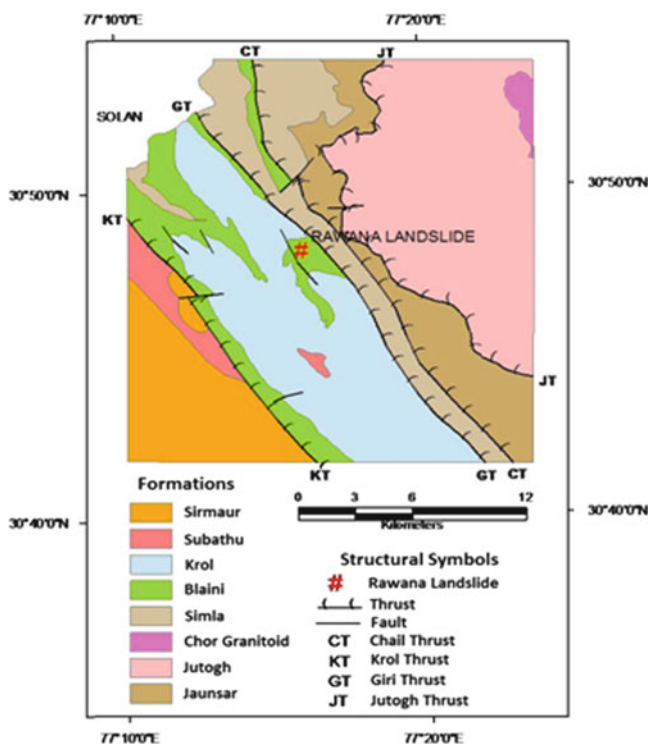
The Rawana Landslide is located in geologically complex area where both, the lithology and structural features, have contributed to the landslide activity. The geological setting of the landslide zone and its surroundings is shown in the Fig. 6.

The Rawana Landslide is essentially a debris slide composed mainly of carbonaceous shale/slaty shale and minor quartzite of Infra-Krols, and carbonate rocks of Upper Krols. The Infra-Krols dip 30°–60° south-westerly into the hill. The crown of the slide has touched the Upper Krol limestone where its fragments and debris are observed. Farther up, the limestone is exposed in weathered blocks. In the intervening area are fields and a dwelling house.

Lithology

The landslide zone is confined to the lower parts of the Krol Belt consisting of Blaini, Infra-Krol and Krol-A, the description of different rock formations near to the slide zone is given below:

Infra-Krols: These mainly consist of dark shale and slate, closely inter-bedded buff weathering bands of impure slaty quartzite. Towards the top of Infra-Krols (below the Krol sandstone and limestone) black carbonaceous shale or slate occurs without the thin bands of slaty quartzite. The banded facies of dark shale and paler impure quartzite weathers to a very characteristic association of thin, shiny gritty, greenish clay-slate and ring bleached slate. The later are ramified with irregular joints, marked by ridges as a result of liberation of iron and its precipitation as ferric

**Fig. 5** Regional geological map showing Rawana landslide and location of thrust faults

formations (Subathu, Dagshai, Kasauli) along the Krol Thrust (Auden 1934).

The regional litho-tectonic units around the study area have been given in Table 2 and are shown in the geological map (Fig. 5).

Table 3 Constituent analysis of the slide mass in the samples from pits

S. no	Pit no.	Sample at depth (m)	Mechanical analysis			Plastic limit (%)	Silt factor
			Gravel (%)	Sand (%)	Silt (%)		
1	1	1.00	35	45	20	N.P.	3.18
2		2.00	43	40	17	N.P.	3.46
3	2	1.00	38	42	20	N.P.	3.31
4		2.00	44	38	18	N.P.	3.53
5	3	1.00	18	37	45	N.P.	2.41
6		2.00	30	41	29	N.P.	3.03
7	4	1.00	32	48	20	N.P.	3.14
8		2.00	48	38	19	N.P.	3.64

hydroxide cement. The commonness of iron in Infra-Krols is seen in the universal seepage of ferric hydroxide and white encrustations of ferric sulphate and chloride, which covers the surfaces of these rocks. The parent mineral is pyrite.

Krol Sandstone: is generally soft, without bedding, and stained an orange colour with iron. In its southern extension it becomes hard and is well bedded. It has the presence of bands containing disc like fragments of black shale, about 2 mm thick and 5 mm long; and farther southeast, these bands change into pebbly beds.

Krol A (Lower Krol Limestone): consists of dolomitised limestone and shale in beds from 2 to 10 cm thick. The rock is bluish on a fresh surface while weathered surfaces show grey-green tints. Fracture cleavage is conspicuous. The outcrop thickness of this unit varies from 30 to 700 m, which may be due to thrust elimination or multiplication, while the actual thickness may vary between 100 and 200 m.

Krol B (Red Shale): is characterized by soft, finely laminated or massive purple red shale with blotches and intercalations of green shale. At the top it becomes shaley limestone similar to Lower Krol Limestone (Krol A). At many places it is sheared along which the development of chlorite may be seen. The maximum thickness of the unit is 100 m.

Krol C: is a massive, dark blue, crystalline limestone, which stinks on fracturing and weathers to black surfaces and is dolomitised. The unit is 100 m thick.

Krol D: Has alterations of cherty limestone and shale, the latter being predominate. The limestone is pale or dark in 3–10 m thick beds. At places it occurs as penecontemporaneous breccia. Shale is of different colours, mainly black, red, green and orange. The darker varieties often bleach in a manner similar to those of the Infra-Krols. The maximum thickness is about 200 m.

Krol E: constitutes banded grey and pale cream-white microcrystalline limestone, which occurs at higher altitudes above 1,200 m. Fresh surface of paler varieties are white and porcelain. Thin crinkled veins of calcite are common. The thickness of the unit is 150 m.

Slide Debris Mass: Debris material is fully decomposed of the carbonaceous/slate. In order to understand the composition of the debris, 4 pits were excavated up to a depth of 2 m and samples of the slides mass were collected from 1 m interval for grain size analysis to get the percentage of gravel, sand and silt. The result of the same is presented in Table 3.

The gravel content in the pits invariably exhibited an increase with depth ranging from 8 to 16 %. The sand content usually decreased with depth from 10 to 4 %, except in Pit-3 where it increased by 4 %. The silt content showed marginal decrease with depth within the range of 1 % and 3 %, except in Pit-3 where it decreased by 16 %. These values indicate, in general, the composition of the slide mass which is essentially decomposed material of carbonaceous shale. The silt factor ranges from 2.41 to 3.64 %.

Structure and Tectonics

The slide zone has become highly complicated as it is influenced by different fault plain/thrust. From the map it is apparent that the thrust between the Krol belt and the Shimla/Jaunsar groups viz, the Giri Thrust and the thrust between the Jaunsar group and the Chail metamorphic come very near to each other near the slide zone. Bhargava (1976) reported that the Chail thrust overlaps the Giri Thrust. Due to this, the Infra Krols and the Krol A, which are dominantly grey and black shales are crushed and break into small fragments.

A prominent fault trending NNW-SSE, with down throw towards the NNE, pass through the Giri River channel near the sharp bend close to the toe of the slide. It follows the Jabyana nala and appears to be sympathetic to the Giri Thrust. This fault has been named here as 'Rawana Fault'. The Infra Krols in the western block along this fault abut against Krol A, B and C. The rocks are highly folded and jointed. Because of thrust and fault planes, the lithological units have been sheared, fractured and pulverized, as a result the rocks of the Infra Krols and Krol-A, which are dominantly grey and black shale, are crushed into small fragments

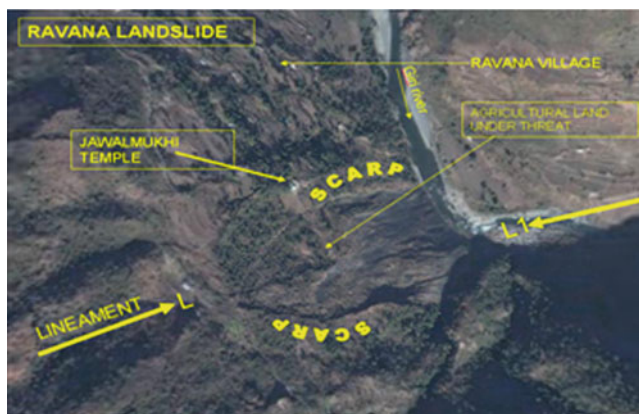


Fig. 7 Google Image showing conspicuous scarp developed on western and eastern flanks of the landslide

that easily slide down, which during the rainy season becomes saturated and flows as mud flow.

In order to gather more information on the structures and tectonics, LISS-III images and High resolution images of Google dated 2010–2011 were studied to capture the regional disposition of the major tectonic features, the inferences drawn are briefly described below:

1. The Rawana Landslide is closely associated with NW-SE trending linear Giri Thrust, a major tectonic feature that dominates the geological disposition of the area. A prominent fault trending NNW-SSE, with down throw towards the NNE, pass through the Giri River channel near the sharp bend close to the toe of the slide. It follows the Jabyana Nala and appears to be sympathetic to the Giri Thrust. This fault has been named here as 'Rawana Fault'. The location of oozing of hot water is close to the proximity of foot-wall side of the Rawana Fault.
2. Presence of a NE-SW trending planar lineament, orthogonal to the Giri Thrust, which dissects the landslide mass on its SE extreme and rendering the western portion to go down compared with the eastern part, and resulting in the formation of a prominent scarp on the western side facilitating the slide (Fig. 7). A trace of a scarp noticeable on the eastern side coupled with the western one form a concentric shape defining the upper limit of the slide zone. It thus, forms a micro-zone of disturbance across the Giri Thrust lineament.
3. The course of Giri River is controlled by the lineament of Giri Thrust, and its tributaries by the lithology and local structure.
4. The emanation of gas/heat/water/vapours in the landslide mass may be attributed to the lineaments, viz., the Giri Thrust and the NNW-SSE trending fault in the slide zone. The morphotectonic features of Rawana Landslide can be summarized as follows:
 - The NW limit of the landslide zone is marked by morphotectonic features that are transverse to the valley.

Graben like landform is seen on the NW boundary of the slide zone. A fissure having an opening of 10 cm can be traced in the NE-SW direction along the slope at about the middle of the graben like feature.

- The slide zone is truncated in the NW and SE by relatively straight line that is apparently marked by an escarpment face that reaches up to about 30 m to a maximum in the middle part of the slide zone. The escarpment line trends parallel to the slope and at right angles to the southeasterly flowing Giri River.
- The river takes a sharp transverse bend downstream at a point close to the foot of the escarpment. The river valley regains its NW-SW trend after about 100 m long transverse valley. The sharp bend in the Giri River can also be linked to geomorphic feature defining a lineament on the satellite imagery.

Drainage

Drainage is an important geo-system controlling the landslide since its densities denote the nature of the soil and its geotechnical properties. The drainage pattern of the area was digitized using GIS software and analyzed. Giri River is the major river draining through the region and is fed by various tributaries which can be classified as first, second, third and fourth order tributaries as shown in the drainage map (Fig. 8). Near the south-eastern part of the toe of Rawana Landslide, the Giri River takes an abrupt turn of about 90° angle, which may be due to the presence of a transverse fault.

The seepage from the springs is one of the main factors for mobility of landslide.

Chemical Characteristics of the Surface Water

In order to comprehend the changes in water quality which drains through the landslides and discharge into the Giri River, 14 water samples were collected from different places as shown in Fig. 9. The chemical analysis of the water samples were carried out and only the water samples which gave abnormal values is presented in the Table 4.

The analysis shows that the surface water oozing out from the landslide area has low pH values, about 2.40, 5.80, 2.58, 3.16, at certain places, and high pH values, about 7.03 to 7.79, at most of the places. The low values indicate acidic and high values indicate alkaline nature of the water. Similarly, high values of sulphide and iron are also observed, which indicate that high mineralization has been taken place due to low pH. Interestingly, the two samples DK-8 and DK-11 show high sulphate, Ca, Mg and Fe concentration.

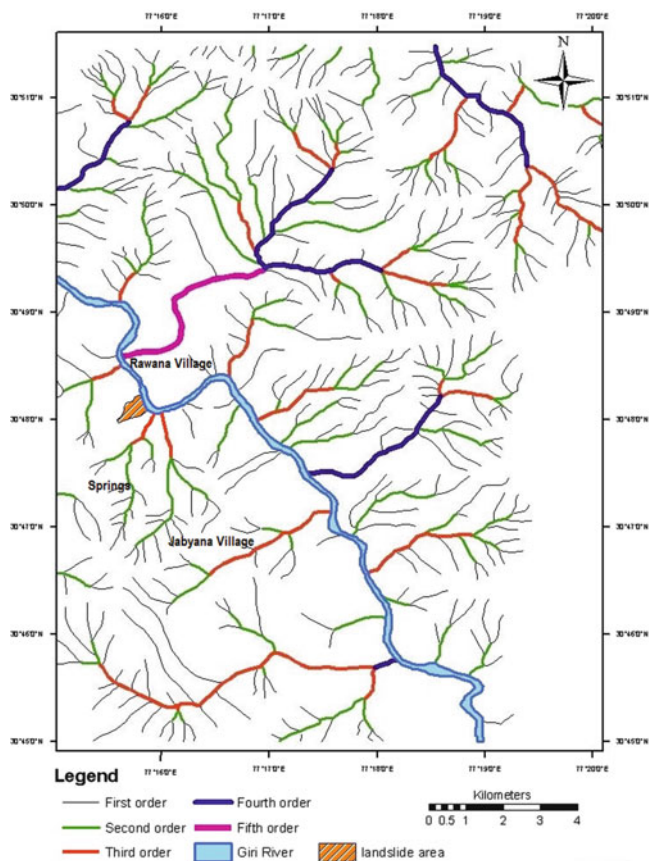


Fig. 8 Drainage map of the study area



Fig. 9 Photograph of the landslide area showing locations of the water samples for chemical analysis

Source of Sulphate (SO₄): Pyrite crystals often occur in sedimentary rock and constitute a source of both ferrous ion and sulphate in spring ground water. Pyrite is particularly commonly associated with biogenic deposits under strongly reducing conditions.

Other source is sulphur, when dissolved in water it generally occurs in fully oxidized (S+6) state complexed with

Table 4 The chemical analysis of the water samples which gives abnormal values

S. no	Parameter (mg/l)	DK-8	DK-9	DK-11	DK-12
1	pH	2.4	5.8	2.58	3.16
2	EC	3,980	500	6,320	1,180
3	Dissolved solid	2,510	310	4,000	730
4	Alkalinity (as CaCO ₃)	–	24	–	–
5	Chloride (Cl)	31	14	28	17
6	Sulphate (SO ₄)	2,803	235	3,655	628
7	Nitrate (NO ₃)	ND	1	ND	4
8	Fluoride (F)	ND	ND	ND	–
9	Calcium (Ca)	353	51	335	84
10	Magnesium (Mg)	238	29	631	76
11	Total hardness (as CaCO ₃)	1,861	245	3,433	525
12	Sodium (Na)	11	14	27	15
13	Potassium (K)	3	3	6	3
14	Iron (Fe)	129 with dilution 100 times	0.522	406 with dilution 100 times	ND

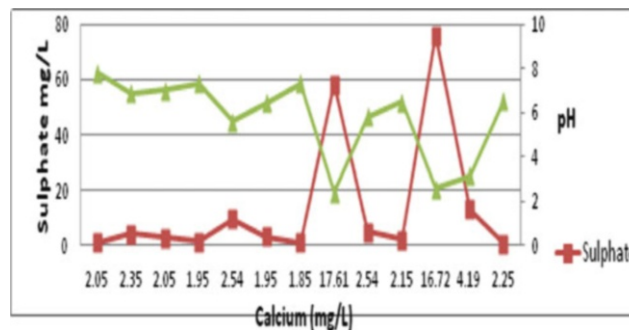


Fig. 10 Relationship of pH with sulphate and calcium

oxygen as the anion sulphate S₀₄-2. The reduced forms S₋₂ are sometimes found as the HS⁻ ion or as dissolved undissociated H₂S. Conversion of oxidized to reduced species of vice versa often is associated with biochemical processes. Foul smell of H₂S is observed in the study area, which indicates that the sulphur is more common in pyrite (FeS₂), where the sulphur is present as S⁻². Free sulphur, HS⁻, H₂S (aq.), and S₋₂ occur only at very high pH. It is observed that where the pH is between 7.03 and 7.79, sulphate is low and it is possible that sulphate might be reduced to HS⁻, H₂S and S₋₂, it is evident from foul smell of H₂S.

It is significant to note that with the decrease in pH the concentration of sulphate increases due to the formation of H₂S gas, as shown in Fig. 10 representing all the 13 analyzed samples.

Table 5 Details of LHEF rating of Rawana landslide

Causative factor	Max. LHEF rating
1. Lithology—(Local geology—black carbonaceous shales and minor quartzites of Infra-Krols, Dolomitic L.stone of Krols, weathered rockmass)	1.9
2. Structure—(Rawana lies in a structurally disturbed area to close proximity of Giri Fault, a major tectonic junction between the Infra-Krol-Krol sequence and the Shimla Group, and a transverse fault)	1.5
3. Slope Morphometry—(The crown of the landslide is located near the steeply dipping (60°–70°) Krol Limestone. The average slope of the slide is 35° from crown to mid-level, middle part the slope is 45° thereafter up to its toe)	1.5
4. Land use/land cover—(Agricultural land, populated flat land, also considering the assumed depth of soil/debris cover)	0.65
5. Relative relief—(200–300 m, relative class—high, relative relief 200–300 m)	0.8
6. Hydrogeological conditions—flowing	0.8
Sum of LHEF rating	7.15
Correction due to external factor (a) seismicity	0.4
(b) Rainfall (To be added separately to the total LHEF)	0.2
Total estimated hazard (TEHD)	7.75

Landslide Hazard Evaluation Factor (LHEF Rating)

The sum of LHEF ratings of the causative factors that affect the Rawana landslide have been deduced based on the various inputs collected during investigation. While doing so, care has also been taken of the other and external factors which includes seismicity, which is quite high in the project and surrounding areas (seismic zone IV) and rainfall (more than 1,200 mm per annum). The sum of the Total Landslide Hazard Evaluation Factor Rating (THEF) comes to 7.75 which are called the Total Estimated Hazard (TEHD), as shown in Table 5.

In this case it falls under the zone of high hazard (HH) Zone (After Anbalagan et al. 2008) with TEHD falling under $6.5 < \text{TEHD} \leq 8.0$.

Mitigation Measures

The upper land surface of the landslide is of the high temperature and also landslide not been located cutting across a highway as such the possible mitigation measures can be:

1. The construction of the toe wall preferably of the flexible type anchor to the bed rock;

2. The well designed network of surface drainage to prevent incursion of water into the slide body from the springs.
3. The slope to be graded with provision of berms
4. To provide vegetation cover over the treated slopes to protect the slide mass from direct impact of precipitation and to increase shear strength of the surface material.

Conclusions

Rawana landslide is the singular case of the many landslides, in the Shimla Himalayas, having complex geological and structural setup, dynamic in nature, having exothermic reaction bringing change in hydrochemistry, emission of hot water vapour with foul smell etc. The landslide is dynamic in nature and the effective area of the landslide is increasing over the years from 8,490 m² in 2002 to 86,021 m² in 2012. The main reasons attributed are the continuous toe erosion, seepage from the springs, Rawana fault underlying the landslide transverse to Giri Thrust. The emission of water vapour/gases with pungent smell are related to deep tectonic fracture, presence of pyrite mineral in Infra Krol shale leading to exothermic reaction. The Landslide Hazard Evaluation Factor (LHEF) rating of different causative factors shows that the total Estimated Hazard is 7.75 which shows that the landslide is under High Hazard zone. The landslide needs to be further investigated for the change in the petrology of the parent rock, hydrochemistry and the reasons for the exothermic reaction.

Acknowledgments The present paper is the outcome of the research project supported by Department of Science and Technology, Govt. of India. The technical discussion and support by Dr. Bhoop Singh, Dr. V. C. Thakur, Dr. R.K. Sood, Prof. Ramesh Kakkar, Dr. M.S. Virdi is thankfully acknowledged. Thanks are also due to Ms Nidhi Jha, Dr. RajKumar and Mr. Avinash Chandra.

References

- Anbalagan R, Singh B (2006) Landslide hazard zonation mapping—a need for sustainable development of Utranchal with special references to route locations. *J Eng Geol (ISEG)* XXXII:13–22
- Anbalagan R, Chakraborty D, Kohli A (2008) Landslide hazard zonation (LHZ) mapping on meso-scale for systematic town planning in mountainous terrain. *J Sci Ind Res* 67:486–497
- Auden JB (1934) Geology of the Krol belt. *Rec Geol Surv India* 67 (4):357–454
- Avasthy RK, Singh B, Sivakumar R (eds) (2006) Landslides: perception and initiatives of DST. Indian Society of Engineering Geology, Department of Science and Technology, Government of India, Lucknow
- Bhargava ON (1976) Geology of the Krol belt and associated formations: a reappraisal. *Mem Geol Surv India* 106(I):167–234
- Champati Ray PK, Irashad P, Lakhera RC (2008) Seismically triggered landslide and associated hazard assessment in Kashmir Himalaya. *Indian Landslides* 1:1–10

- Gansser A (1964) *Geology of the Himalaya*. Interscience, New York, 289 pp
- Pilgrim GE, West WD (1928) The structure and correlation of the Simla rocks. *Mem Geol Surv India* 53: 140 pp
- Thakur VC (2006) Seismotectonics and earthquake geology aspects of Northwestern Himalaya. *Geol Surv India Spec Publ* 85:61–71
- Virdi NS, Mazari RK, Philip G (2003) Environmental geomorphology and active fault tectonics of Paonta Sahib-Sataun-Renuka area, Distt. Sirmaur, Himachal Pradesh. *Bull Indian Geol Assoc* 35 (2):91–106
- Yeats RS, Thakur VC (1998) Reassessment of earthquake hazard based on a fault-bend fold model of the Himalayan plate -boundary fault. *Curr Sci* 74(3):230–233



Highways Vs. Landslides and Their Consequences in Himalaya

Kishor Kumar, Lalita Jangpangi, and S. Gangopadhyay

Abstract

Landslides are considered a part of normal processes of landscape forming. All these processes have been occurring since the emergence of the earth and shall continue to occur as a dynamic earth process system. But, such a statement should be understood in a sense of naturally occurring landslide processes without human intervention. The same processes however raise greater concern when they cause loss of life and/or property of a bigger magnitude. The highways/roads constructed across the hills and mountains of Himalayan terrain face severe landslide problems. The frequency of their recurrence/occurrence is so high that the states generally find themselves helpless in properly addressing restoration issues, as well as rehabilitation and short term/long term mitigation and management issues. The most disturbing fact is that the phenomenon is repetitive every year and the costs, only on restoration works increase exorbitantly. Even the best constructed highways suffer from repeated onslaught of landslide and similar processes. The Himalaya, which are considered as a dynamic chain of the hills and mountains with fragile geological formations, youthful river systems, steep slopes, heavy rainfall and so on are cut across for construction of highways with minimal understanding of their fragile geo-environmental setup. In spite of the modern technology of the highest level the highways continue to suffer. In this paper, we address some of the important issues and gaps pertaining to planning, construction and maintenance of highways/roads in Himalaya.

Keywords

Himalayas • Highways • Landslides • Issues • Consequences

Introduction

The socio-economic and cultural health of any country depends upon its communication potential which includes the surface transport such as rail and road network (Gangopadhyay and Kumar 2012). It is not merely the connectivity per-se but the quality, efficiency, durability and the safe road network and its infrastructure which matters. Indian highways in the mountainous terrain of Himalayas

suffer due to frequent landslides of various kinds. In one estimate, 15 % of the Indian landmass or 0.49 million sq km area is prone to landslide hazard of which 0.392 million sq km is part of the Himalayan region. Himalaya's dynamic nature including its geological setup, narrow and deep gorges, meandering rivers, snow clad bodies, climatic diversities, sudden and heavy downpour including cloudbursts, flash floods, earthquakes etc., have always been considered as part of its natural developmental processes. Landslide and other mass movements have also been part of landscape formation. The scenario however has changed completely and the rare incidences or events of landslides, floods and so on have increased significantly compared to the last few decades (Kumar et al. 2011) due to unparallel influence of

K. Kumar (✉) • L. Jangpangi • S. Gangopadhyay
Central Road Research Institute, New Delhi 110025, India
e-mail: kishornhrm@gmail.com; Lalita157@gmail.com; Sgp.
crri@nic.in

human interference. Indian highways in hilly areas have been experiencing horrific landslide incidences. The Darjeeling floods of 1968 destroyed vast areas of Sikkim and West Bengal. The 60 km mountain highway to Darjeeling was severed at 92 places resulting in the loss of lives and total disruption of the communication system. The Malpa rock avalanche tragedy of 18 August 1998 killed 220 people and wiped-out the entire village of Malpa on the right bank of river Kali with the tracking route, in the Kumaun Himalaya of the state of Uttarakhand. In the same year and month, Madhmaheswar valley, in Okhimath District of Uttarakhand state witnessed a devastating landslide affecting 9000 plus people in 29 villages. More than 100 fatalities were reported. A cloudburst followed by heavy landslide had completely wiped out three hamlets in Munsiyari sub-division of Pithoragarh district, Uttarakhand, killing 43 people and more than 100 cattle on 8th August 2009.

Recently during 16th–18th June 2013 an unprecedented rainfall followed by flash flood in different parts of hilly areas of the country caused havoc. Over 2,000 landslides were reported and over 5,000 people had been killed. In several hundred places the roads were washed out due to high magnitude flash flood or blocked due to landslides. Due to the poor condition of the highways the rescue and rehabilitation work has got hampered very badly.

A huge amount of revenue spent only on restoration of highways from repeatedly recurring landslides not only exceeds the cost of the construction of road but also misbalances the annual maintenance budget which unfortunately does not include the prevention/mitigation of landslides, as a result of which most of the highways are found under maintained. The hills and mountains of complex geological conditions and fragile rock formations make the slopes sensitive to failure in case of sudden external triggering forces like unprecedented rainfall and earthquake tremors. But, not all the slopes behave identically and only a few slopes experience failure. In the majority of instances the slopes failure/landslides are caused, more because of man made mistakes than natural causes. In each case hundreds of new landslides of various shapes and size have been generated. Contrary to this, most of them are linked to the difficult terrain characteristics, adverse climatic conditions etc. but not often to the ill planned developmental activities which are conspicuously more responsible to such happenings.

Himalayan Highways and Landslides

As population increases and our society becomes ever more complex, the economic and societal costs of landslides and other ground failures will continue to rise. Out of all known natural hazards landslides have become the most significant

hazards because they are most frequent and widespread in developed areas of every hilly terrain of our country, particularly in the fragile Himalayan regions along highways.

It is therefore important that road/highway infrastructure building also includes slopes/landslides as an inclusive element of road development policy. In spite of loss of unprecedented amounts of funds and human lives and increasing danger on highways, there is still no workable and inclusive policy in place.

Different Facets of Landslides in Himalaya

Landslide Vs. Cloudburst

Cloudburst, a geo-hydrological hazard also known as rain gush or rain gust has attracted the interest of many researchers in recent years. It is a phenomenon of heavy precipitation (equal to or greater than 100 mm rainfall in an hour). It is one of the biggest trigger of a series of landslides in mountainous valleys particularly on the highways. An examination of available data of cloudbursts in the Himalayan region clearly indicates that the number of incidences of cloudbursts has increased with time. On dividing the time period in two, before 2,000 and after 2,000, as per the records available from various resources, it was concluded that before 2,000 only 29 events of cloudburst have occurred while the numbers have increased after 2,000 to 50 incidences (Fig. 1). Cloudbursts are more common in the region of glacial lakes. The moraine dams are comparatively weak and can breach suddenly, leading to the discharge of huge volumes of water and debris (Eriksson et al. 2009). Extreme rainfall within short time period in the form of cloud burst in such regions can increase multi-fold the mayhem by breaching such dams, e.g. Gaunatal (5 Aug 1894), Birahi valley where 40 thousands million cubic water washed away major towns of the Garhwal Himalaya, or the July 1970 flashflood in Alaknanda river in Patalganga basin gulping Belakuchi settlement with several busses, pilgrims and local life, and most recently the event of a cloudburst in Kedarnath valley of Uttarakhand. The cloud bursts in the month of June 2013 devastated the valley by stranding and further impacting thousands of tourist and local people. Such incidences were also reported in 2012 in the mountain valleys of the Himalayan state. Three major cloud bursts were reported from Uttarakhand in 2012 and two from Himachal that year (Chauhan 2013).

Landslide Vs. Landslide Dams

One of the major problems in the Himalayan valley is formation of landslide dams across rivers. The lifespan of

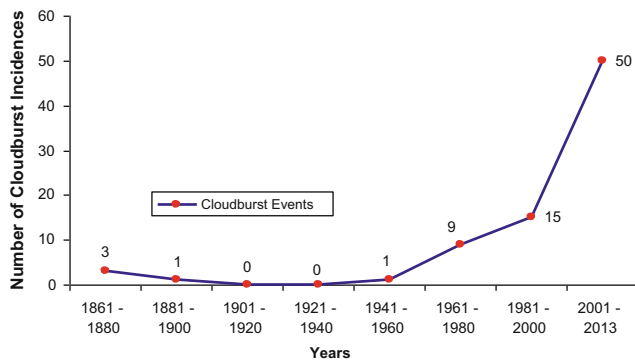


Fig. 1 Frequency of cloudburst from year 1860 to year 2013

this type of dam is very much dependent upon the occurrence of extreme weather conditions. It can burst in short time interval under the influence of heavy precipitation or cloudburst. Such an incidence occurred on 20th July 1970 in Patalganga Basin where a naturally formed dam due to cloudburst breached under the pressure of extreme precipitation. The flash flood of July 1970 in the Alaknanda, which brought loss of life and property damage of an unprecedented magnitude, was a rare catastrophe for the Himalayan region. Belakuchi hamlet, which happened to be the centre for regulating the one-way traffic for the Joshimath-Niti and Badrinath bound vehicles, was completely washed away, wherein about 15 vehicles and 35 lives were taken, on the fateful night of 20th July, also added to the loss. Nearly 15 km of Joshimath-Rishikesh road between Pipalkoti and Langsi was also breached, resulting in de-linking the life-line of the highlanders including the large defence outposts located in the boarder areas of district Chamoli. The impact of this event was experienced from Badrinath to Haridwar, approximately 310 km stretch (Kumar and Sati 2005). Large numbers of landslides along the river bank as well as on above and below the road have developed. The consequences of which we are still facing and shall be doing so for many years to come due to recurring landslides developed during 1970 flash flood.

Earthquake Induced Landslides

In the seismically very active Himalayan region earthquake induced landslides are one of the most damaging hazards and contribute mayhem to the population and transport infrastructure. They cause considerable damage to highways/roads and in turn put a break in rescue work. In Sikkim on 18th Sept. 2011 an earthquake triggered several new and some old landslides along the road network of the

region making the circumstances even worse for the people. Along 12 different roads stretches of Darjeeling-Sikkim Himalayas a total of 210 landslides were recorded. Amongst the 210 landslides: 195 were new and 15 reactivated ones. The number of debris slides (114) is slightly higher than rock slides (77) and rock fall (8) (Chakraborty et al. 2011).

A few decades ago no one could foresee the intense development the Himalayan hills would undergo and over the years we have also failed to foresee the serious consequences of such a development in multi-hazard prone regions. The seismogenic landslides which are otherwise known as dynamic landslides are one of the most damaging collateral hazards associated with earthquakes. During the past century this region has experienced four major earthquakes measuring magnitude above 8 with several others of lesser magnitude. Each time such earthquake happened, huge number of landslide are generated which could be noticed on the ground but the real challenge lies in accounting for the carryover effects of the history of past disastrous events in the area, especially on the consequences. In the context of the carry forward effect of the past events in the valley, it is important to recall the number of earthquakes occurred during the last century and the imparting fear of the high magnitude earthquake expected any time from now.

Highways Vs. Landslides

This is normal to think that network of roads in hill areas is less safe than the plain area roads because of many inherent topographic, geological and geomorphological conditions and external influences due to extreme meteorological and seismic events which differ from the plain areas to a great extent. But, there are a few questions, the unclear answers of which complicate the task of landslides management to these regions. Firstly, do we have adequate knowledge about the above stated inherent conditions? Secondly, do we follow proper sequence of survey-mapping-investigation-construction aspect using modern techniques and methods? Thirdly, do we consider landslide and related disasters as part of inclusive road development policy in hilly areas? Fourthly, do we classified/divide the terrain based on its susceptibility to fail and follow it as a guiding factor during or after construction? In other words are the hazards prone areas identified before the actual construction of the roads. Lastly, is there any landslide hazard mitigation and management system on Indian highways in place? To be honest the answers of all these questions by any responsible organisation would be unsatisfactory because of lack of enforcement of the guidelines on the ground.

Landslide Hazard Mitigation and Management System

Despite the decades of research and development on the diverse aspects of mitigation and management of natural disasters in India, the following questions continue to defy neat and practical answers (Gangopadhyay and Kumar 2009).

- What are the predicted most likely natural disaster scenarios that must be taken into account in planning, design, construction and management of the roads and highways in India?
- What methodology needs to be followed in the risk assessment of roads and road networks, given the single and large scale hazard maps?
- How can the science and art of landslide instrumentation and monitoring be improved to a level that delivers effective and reliable and cost effective early warning systems against landslides.
- How should technology packages for landslide remediation and control be designed to meet situation specific requirements with fullest consideration of the landslide history of the area, ongoing development programmes, environmental imperatives and climate change?
- How can the local communities could be made aware of landslide hazards in their respective areas, and trained in the management of landslides to avert disasters?
- How can the Landslide Knowledge Networks be further developed and linked with allied global networks to serve all the various stakeholders and landslide management agencies?

A workable Landslide Hazard Management System which would help us to understand the issues pertaining to landslides and their management concerning particularly to the highways should be developed with the following objectives:

1. To ensure that the safety of the hazardous slopes along the highways is adequately managed and their stability maintained.
2. To ensure that the inhabitants of landslide hazard and risk prone areas as well as the concerned agencies are kept informed about the risk during the recurrence period of such disasters so that they can take appropriate steps to avoid loss of life.
3. To provide background data and guidelines on acceptable limits of risks such as—to accept the risk, to avoid the risk, to reduce the likelihood of the risk, reduction of consequences of risk, Monitoring of risk and transfer of risk.
4. Ensure, risk free, year round operability of highway network which have strong bearing on the socio-economic development of the region and also on strategic needs in the border areas through online forecasting system of the critical disastrous areas.

The Proposed Hazard Management System

The proposed hazard management system on Highway and roads of the country has been presented before the council of Indian Roads Congress in 2012 at New Delhi. A brief of the proposed management system is described in Fig. 2 by highlighting a few of the components of the system.

Inventory and Database of Highway Network and Landslides (INDA)

The digital inventory of highways along with existing landslides is one of the primary requirements of the management plan. The database and inventory of landslides prior to any mitigation and management planning and construction of any highway infrastructure is prerequisite because the area under consideration can be said to be susceptible to landslides, when the terrain conditions are comparable to those where a slide has occurred. Moreover, the database could be of immense help to get useful indicators for landslide hazard assessment such as the frequency of landslides, runout distance, velocity, etc. Therefore the first step of the management plan is to prepare an inventory of the landslides along with the network of the highways.

Highway Slope Information System

It includes details about the road cuttings and associated details. The planning of hill roads, unlike that of the plan area roads, should be considered in the back ground of a number of unforeseen factors and problems, which may generally arise during actual construction and even during maintenance periods. Road cuts made during construction, left untreated even those requiring preventive measures may generate slides during rains, destabilize hill or strata. Hill side erosion may start soon after cutting or even after lapse of some years after construction of a road, resulting in damage to hill face, landslides or some other complex problem. There are plenty of such examples where a small erosional patch of slope left untreated got, over the time, transformed into a major landslide needing huge sum of public money to be spent only for restoration of traffic by minor preventive work during every monsoon. All these chronic landslide areas not only damage the road and other property but also threaten the life of people. The frequent and long term damage of highways also creates social unrest in the region. Road cuts may be located in thick forests, steep hill face with heavy undulations requiring excessive cross drainages etc, may be with frequent alternation of different lithologies. Besides other considerations such as that to

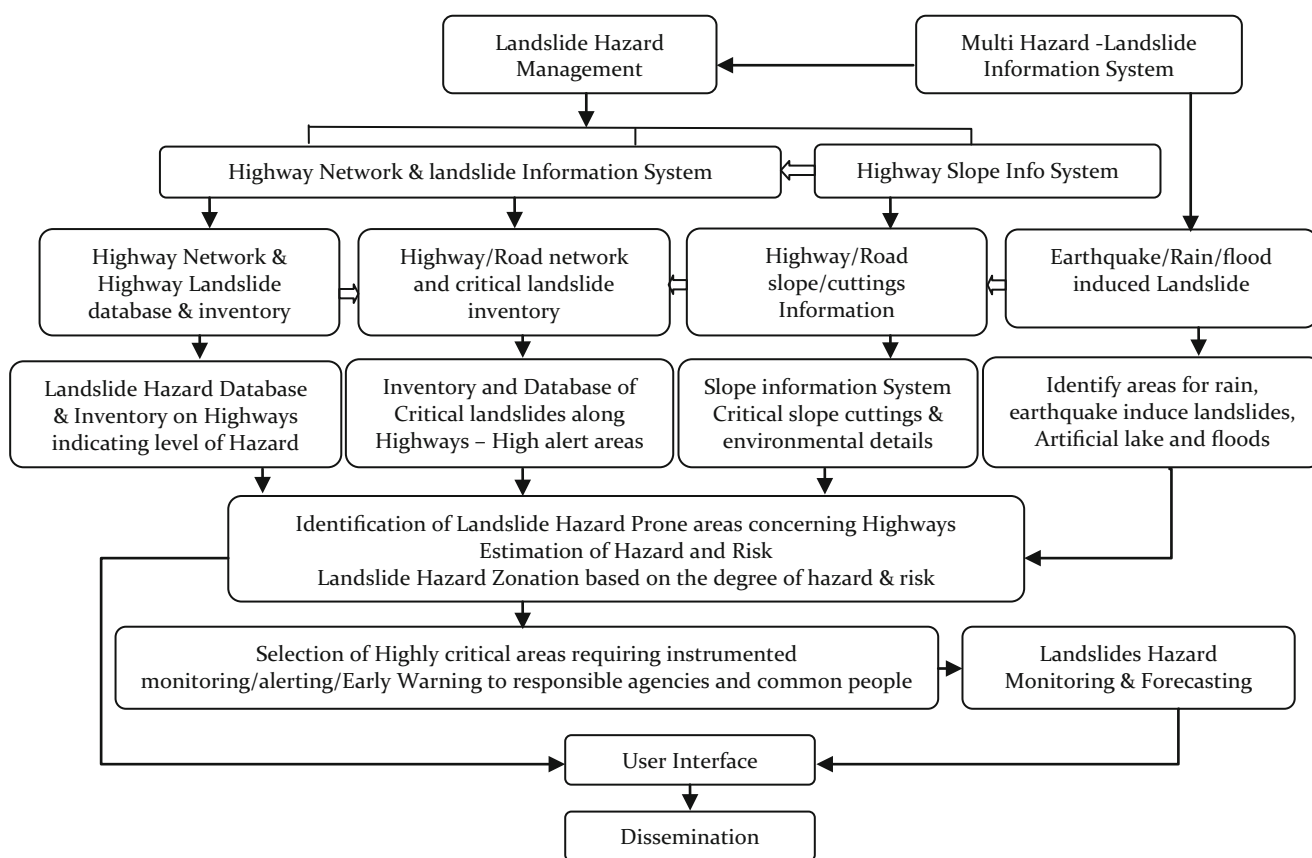


Fig. 2 Landslide hazard management plan

maintain the aesthetics of the hill road, the need to classify the cuts based on their vulnerability is of paramount requirement so as to avoid further development of slides for the benefit of a smooth functioning road. The safety of the roads therefore cannot be ensured until the information about the cuts and associated feature of the slope, particularly in critical areas are known.

Landslides Hazard Monitoring and Forecasting

There are various major landslides along the Highway which are critical in nature and recurring every year. These landslides cause huge amount of revenue loss every year on account of restoration and repair works and detouring of the traffic during the landslide events. There are hundreds of such chronic landslides on various highways of the regions. For example, a landslide called Kaliasaur on one of the national highway of the north western Himalaya has been active since 1920 and is still in an active state. Recently CRRI has done a study on economic loss due to detouring for 45 days of blockage during 2010. It was estimated that only for the duration of blockage, 180 million Indian rupees have

been spent only on detouring. If we calculate for all the years since 1940, the sum will be exorbitantly high of tax payer's money. Had, in the first instance, some long term measures been designed and implemented instead of repeated repair and restoration works a large sum of tax payer's money could have been saved. It is required to scientifically study those landslides as pace setter examples and state of the art work involving every step right from reconnaissance survey, large scale mapping, geotechnical, geomorphological, geological investigations, instrumented monitoring, risk analysis, forecasting and remedial actions.

The information about forecasting would be disseminated on line through a web based system so that anyone can have forehand information to avoid the risk and danger and possible damage.

Multi Hazard Information

Landslides often occurs as elements of interrelated multiple hazard processes in which an initial event triggers secondary events or in which two or more natural hazard processes occur at the same time. They commonly occur in conjunction with

other major natural disasters, such as earthquakes, volcanic activity and floods caused by heavy rainfall etc. The resulting multiple hazard problems require a shift in perspective from study of individual landslide hazard, to a broader systems framework that takes in to account the impact of the all process involved. One of the examples of such multiple hazard problems is formation of landslide dams. Such a phenomenon involves chocking of the stream flowing at the toe or bottom of landslide in question by its debris in narrow parts of the valley thereby creating a temporary dam which breaks on exceeding its capacity to hold the enormous amount of the water. Finally bursting of such a dam on its own develops devastating flood which inundates the downstream areas and cause heavy destruction to highways and creates more landslides along the valley. Famous Gohana Tal Lake, Ukhimath Tragedy, and Alaknanda tragedy in Uttarakhand state are some of the case examples involving landslides created by the Lake Phenomenon. Often such possibilities of creation of landslide dams are overlooked while preparing landslide hazard maps. It is required that the potential places for creation of such dams are demarcated. Similarly there are instances, when large number of landslides has occurred after the earthquakes as “carry forward effect”. Each type of earthquake-induced landslide occurs in various geological environments, ranging from steep rock slopes to gentle slopes, with unconsolidated sediments.

Landslide Hazard Zonation and Risk Estimation

Hazard may be expressed as the frequency of a particular type of landslide of a certain volume or landslides of a particular type (rock fall, debris flow, debris slide etc), volume and velocity (which may vary with distance from the landslide source) or, in some cases, as the frequency of landslides; i.e. number of landslide of certain characteristics that may occur in the study area in a given span of time with a particular intensity i.e. damaging capability of the landslide (AGS 2007). The hazard analysis will follow the estimation of risk which combines the probability information from a landslide hazard map with an analysis of all possible consequences of an event (property damage, casualties, and loss of service) (Spiker and Gori 2000). The consequences includes: extent of damage to highway/road and its infrastructure, probability of damage to the vehicles, number of deaths etc. It is not always possible to foresee the exact time of the event, if a proper database is not maintained. A scenario, in which the database of landslide lacks information about the frequency, runout and velocity etc., the hazard situation, can not be foretold, simply because the hazard pertains mainly to temporality of the foreseen or predicted event. In such cases, as already

followed, instead of cooking information which might give wrong predictions, professionals should concentrate on susceptibility zonation which in anyway are prepared but without the element of temporality.

Conclusions

When planning a new road, the alignments of the route should be carefully determined considering the probability of landslides during and after the construction. Without which the roads are likely to face unexpected problems of slope stability as noticed in most of the Himalayan roads.

The increasing trend of the landslides incidences and recurrences along the highways is quite alarming and raise concerns regarding the stability of landslide areas along these highways and their potential impact to the safety of the traveling public, infrastructure and their property. Hundreds of landslides which recur during every year are required to be studied scientifically involving large scale mapping, geotechnical, geomorphological, geological investigations, instrumented monitoring, risk analysis, forecasting followed by permanent stabilization and not only short term repair. This way the problems generally keep on multiplying and reach to the point of no remedy.

Landslides should not be viewed as an isolated phenomena but in conjunction with other events such as floods, earthquakes, cloudbursts etc. For example, a number of seismogenic landslides developed during the major earthquake events continue to reactivate during monsoon rains and cause substantial damage to highway and other infrastructure. It is therefore require to identify the areas prone to such kind of landslides incase an earthquake event happens anytime from now. Similarly, floods which are common phenomena in the region create hundreds of landslides along the banks of rivers/major streams. Some of the narrow gorges on the rivers/streams get blocked due to generation of excessive slided debris thereby creating artificial dams, on breaching of which huge destruction is caused downstream up to hundreds of kilometers.

References

- AGS (2007) Guideline for landslide susceptibility, hazard and risk zoning for land use planning. J News Aust Geomech Soc 42(1). ISSN: 0818-9110
- Chakraborty I, Ghosh S, Bhattacharya D, Bora A (2011) Earthquake induced landslides in the Sikkim-Darjeeling Himalayas – An aftermath of the 18th September 2011 Sikkim earthquake. Geological Survey of India, Kolkata

- Chauhan C (2013) Cloudbursts go up, but no system for forecast. Hindustan Times Post. <http://www.hindustantimes.com/India-news/NorthIndiaRainFury2013/Cloudbursts-go-up-but-no-system-for-forecast/Article1-1083525.aspx>. 27 Jun 2013
- Eriksson M, Jianchu X, Shrestha AB, Vaidya RA, Nepal S, Sandström K (2009) The changing Himalayas – Impact of climate change on water resources and livelihoods in the Greater Himalayas. International Centre for Integrated Mountain Development (ICIMOD), 9p
- Gangopadhyay S, Kumar K (2009) A cover article on theme “safety and efficient management of road network in landslide prone areas. J Sci Cult Ind Sci News Assoc Kolkata 75(11–12):380–388
- Gangopadhyay S, Kumar K (2012) Hill road and highways vs. landslides hazards. Seminar on recent trends in highways development,, 10–11 Oct 2012. IRC, New Delhi, pp 155–165
- Kumar K, Sati D (2005) Exploring the history of Alaknanda – Patalganga tragedy of 1970 & possibility of its recurrence and impacts on Patalganga basin – A GIS and remote sensing based study. In: Proceedings of 8th annual conference and exhibition in the field of GIS, GPS, Aerial photography and remote sensing, 7–9 Feb 2005. Map India and Geomatics, New Delhi
- Kumar K, Prasad P.S., Kathiat A, Negi I S, Mathur S (2011) Landslide hazard management on mountainous highways of India – A critical need. In: 12th ESRI India user conference, Noida (NCR), 7–8 December
- Spiker EC, Gori PL (2000) National landslide hazards strategy, a framework for loss reduction. US geological survey, Open-file report 00-450



Characteristics of Landslides from Sigou Gorge to Lagan Gorge in the Upper Reaches of Yellow River

Zhiqiang Yin, Xiaoguang Qin, and Wuji Zhao

Abstract

The upper reaches of the Yellow River on the northeastern Tibetan Plateau (TP) in western China, is a zone highly prone to geological disasters. Giant landslides in this region are notable for their scale, complex formation mechanism, and for their ability to cause serious destruction. In this study, several different high resolution remote sensing data, such as QuickBird (QB), GeoEye, ZY-3, ZY-1 02C, and Google Earth were used as source data. These were combined with various field survey techniques to determine the spatial flat forms of landslides and their distribution characteristics. Remote sensing images of these characteristics can be clearly seen in 508 landslides in the study area, many of which are distributed in the Qunke-Jianzha basin. The spatial morphological flat pattern distribution of landslides can be divided into eight categories as follows: round-backed armchair-like and semi-elliptical pattern, dustpan pattern, dumbbell pattern, tongue pattern (including long tongue, rectangular, mat, stepped shape), saddle pattern, long-arc pattern and triangular pattern. The rock and soil types of landslides can be divided into four categories: loess, mudstone, semi consolidated digenetic, and rock, with a prevalence of mudstone landslides. The length and breadth of landslides masses are mainly concentrated between 550–1,500 m and 600–1,500 m, and are polarized in different directions. The average elevation of landslides is mainly between 2,400–2,800 m, and the relative elevation differences of the front sheer opening and back trailing edges are concentrated at around 150–400 m and at around 750 m. There is a good linear relationship between the average slope angle, relative elevation difference, and length of the landslides mass. The results of our research provide evidence for use in serious geological disasters prevention and environment protection within the study area.

Keywords

Remote sensing • Upper reaches of Yellow River • Landslides • Developmental characteristics

Introduction

In mountain areas where intense rainfall occurs, and large differences in altitude exist, landslides and debris flows frequently occur and represent a major geological hazard (Qiao and Li 2000; Yan et al. 2000; Antony et al. 2003; Shang et al. 2003; Bijan and Nicholas 2004; Onder et al. 2004; Armelle and Thorsteinn 2006; Oliver et al. 2007; Stephen et al. 2009). Such events occur in the north-eastern

Z. Yin (✉) • X. Qin
Institute of Geology and Geophysics, Chinese Academy of Sciences,
No. 19 Beitucheng West Road, Beijing 100029, China
e-mail: yinzq@mail.cigem.gov.cn; xiaoguangqin@mail.igcas.ac.cn

W. Zhao
The College of Earth Sciences and Resources, China University of
Geosciences (Beijing), Beijing 100083, China
e-mail: 715161752@qq.com

areas surrounding the Tibetan Plateau, from the Sigou gorge to the Lagan gorge in the upper reaches of the Yellow River, where there is a transition zone between the Tibetan Plateau and the Loess Plateau in China, and between the southern Qilian mountains and the western Qinling mountains (Li et al. 2011). Changes in tectonic deformation intensity and in the regional climate contribute to the frequent occurrence of landslides, debris flow, and other geological disasters (Zhang et al. 2000; Yin et al. 2010). In addition to large and deep-seated landslides, this region has recently experienced large and deep-seated landslides, which are recognized by their size, wide distribution, large-scale disasters-causing capability, dynamic mechanism complexity, and extreme destructivity, and thus represent a significant hazard to mountain communities, frequently causing loss of life and damage to infrastructure (Huang 2003, 2007; Qin and Yin 2012).

We used remote sensing in observing landslide areas because of its high resolution and ability to cover a wide region (Franco and Robert 1996; Hou et al. 2000; Zhao and Liu 2000; Wang 2007; Liu et al. 2007; Qin and Yin 2012), and have been used in numerous studies. Franco and Robert (1996) carried out the detection and classification of landslides using imagery on different scales; Wang (2007) studied the Yigong landslide of the Tibet Autonomous Region, and the Tiantai landslide of Sichuan province using remote sensing data, and developed landslide hazard maps by analyzing the landslide development environment, sliding direction and distance, slope angle changes, and the impact of large-scale construction, thereby evaluating slope stability. Shi and Wu (2008) used remote sensing in their study of landslide hazards; and Qin and Yin 2012 used remote sensing analysis to discuss giant landslides in unconsolidated sediment triggered by earthquakes and local rainfall along the upper Yellow River. Liu and Lu (2007) analyzed typical landslides interpreted using remote sensing imagery from ETM+, IRS-P6, and QuickBird (QB). Yin et al (2010) carried out a geological hazards field survey, and researched the main stream on both sides of the upper reaches of Yellow River. They found that landslides have been widely developed since the late Pleistocene, where they developed predominantly in the loess L₁₋₂ weak warm phase. Since that time they have been widely distributed in the Qunke-Jianzha basin. Furthermore, landslides throughout the ages have devastated the geological environment of the Yellow River, resulting in large numbers of casualties and property loss. Some have even blocked the Yellow River, destroyed farmlands and changed the watercourse. From such a history, it is evident that there is significant scientific value and a strong practical significant in carrying out research work in this area in relation to landslides hazards.

In this paper high resolution remote sensing images such as QuickBird (QB), GeoEye, Resources satellite III (ZY-3),

Resources satellite 02C Star (ZY-1 02C) and Google Earth, were interpreted for use in our landslide investigation. In addition we used field surveys and remote sensing field validation for the exploration of spatial flat forms, spreading and distribution characteristics, and the possible factors influencing landslides in the region. The aim of this study is to provide technical information for use in the prediction of landslides in the region, and for the prevention of impacts related to geological disasters.

Developmental Characteristics of Landslides Interpreted from Remote Sensing Imagery

From the topographical variation and landslide deposition overlying terrain, as seen from high-resolution remote sensing satellite images, the micro-geomorphologic features of landslides in this region can be generally expressed as being shaped like a round-backed armchair. The images also show that some giant landslides have blocked the Yellow River to form a huge barrier lake (for example the Gelongbu landslide located in the Jishixia valley). A significant amount of back trailing of landslides can be seen, together with landslide dislocation platforms, closed low-lying lands, transverse ridge-like distributions, horizontal arc tensional fissures and across-river accumulation deposits. The front sheering opening of landslides can be seen as having radial tongues related to the longitudinal development of fissures after occurrence.

On the basis of pre-processing with geometric correction, and using image fusion from remote sensing (RS) QB, GeoEye, ZY-3, ZY-1 02C (Table 1) in the region, the authors interpreted landslides from RS images and noted 508 landslides of various types (this figure includes 116 landslides noted in field surveys between 2008 and 2012), of which there were 24 super-large landslides and 92 giant landslides (Fig. 1). The RS images can be interpreted to show the morphological spatial distribution of landslides, the length and width of the landslide mass, back trailing edge, and front shear opening elevation of the landslide, and the slope angle and other aspects of the landslide mass. However, it is not possible to obtain information related to thickness using RS directly, and requires both engineering geological drilling and field surveys. The authors therefore obtained thickness information relating to 116 landslides from geological drilling and field surveys.

RS images and field surveys show that the major distribution zone of landslides is in the Qunke-Jianzha basin, accounting for 29.3 % of the total number, followed by (in order) the Xunhua Basin, Gonghe Basin, Guanting Basin, Guide Basin, Laxiwa gorge, Lijixia gorge, Jishixia gorge and Gongboxia gorge (Fig. 2). From an analysis of the number of landslides occurring, and the amount of residual

Table 1 Satellite data characteristics of remote sensing for landslides interpretation

Types of remote sense	Spectral characteristics	Spatial resolutions	Received date
QuickBird	Visible to near-infrared has 4 bands and panchromatic has 1 band	Panchromatic 0.61 m, multispectral 2.4 m	2006.8
GeoEye	Multispectral blue, green, red and near-infrared bands, panchromatic 1 and	Panchromatic 0.41 m, multispectral 1.65 m	2007.5 2009.92012.3
ZY-3	Multispectral 4 bands, panchromatic 1 band	Panchromatic 2.1 m, multispectral 6 m	2012.5
ZY-1 02C	Multispectral 3 bands, panchromatic 1 band	Panchromatic 2.36 m, multispectral 10 m	2012.4

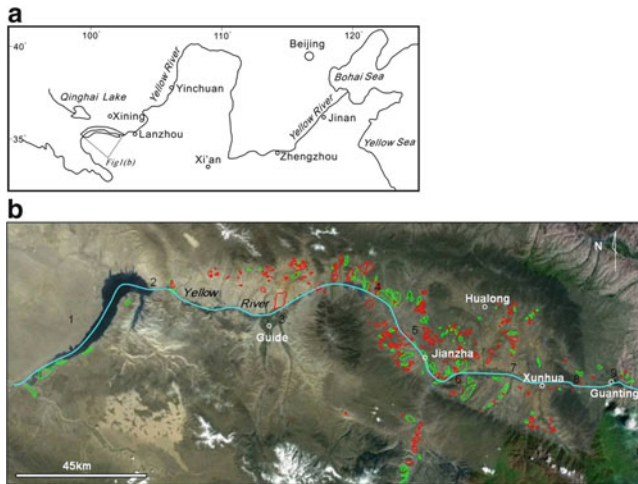


Fig. 1 Location of the study area and distribution map of landslides. (a) Location of the study area in the Yellow River. (b) Distribution map of landslides (red lines represent the locations of landslide masses with a length greater than the width and the green lines represents landslides with opposite features. (1) Gonghe basin, (2) Laxiwa gorge, (3) Guide basin, (4) Liji Xia gorge, (5) Qunke-jianzha basin, (6) Gongboxia gorge, (7) Xunhua basin, (8) Jishixia gorge, (9) Guanting basin (the remotely sensed image is from Google Earth)

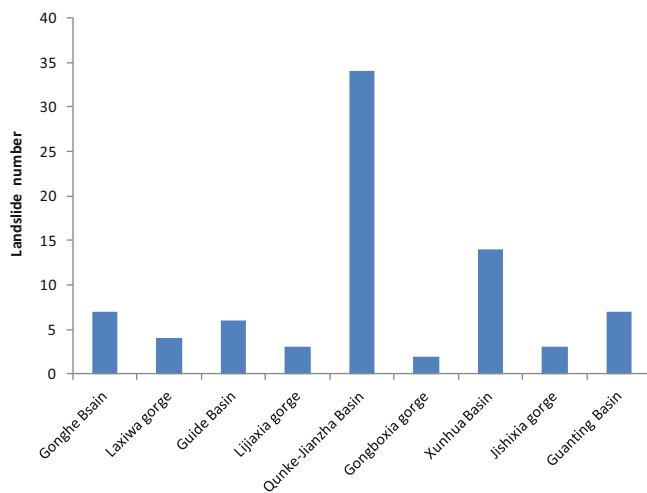


Fig. 2 Spatial distribution characteristics of landslides in the study area

volume, it is evident that there is high-intensity development on the south bank of the Yellow River in the Guide basin, and the Qunke-Jianzha basin, in comparison with the north side, and this includes evidence of the occurrence of huge landslides, giant landslides, and super-large landslides on a large-scale. The spatial distribution of landslide characteristics is closely linked to the topography, active tectonics, regional climate change, and other factors within the studied area (Yin et al. 2010; Li et al. 2011).

The standard types of material composition of landslides in the study area are as follows: loess, mudstone, semi-consolidated materials, and rock (Fig. 3). The largest number of landslides in the area contain tertiary mudstone (accounting for 75 % of the total number), such as the Xiazangtan landslide (first phase) and the Lannitan (LNT) landslide. This is then followed by rock landslides, such as the Suozi rock landslide on the north bank of the Yellow River in the Qunke-Jiazha basin, and the landslide mass of Permian gneiss which crossed and covered the tertiary red clay on the other side of Yellow River (Fig. 4).

Spatial Morphological Features of Landslides

Many landslide patterns are represented in the upper reaches of the Yellow River, including a variety of flat landslide patterns. Some landslides, such as the Xiazangtan landslide, have standard landslide morphology, but some are triangular, inverted triangular, tongue-shaped, or rectangular. In some cases landslides have developed on a slope in a step-like series, and in other cases they have developed in a row on a slope. Some giant landslides consisting of unconsolidated sediments have developed on a mild slope, and these need only slip a short distance to leave a scarp behind the landslide body, such as the Xiaqiongsi landslide. The variety of patterns within the region necessitates summarization (Qin and Yin 2012).

In the north-eastern Tibetan Plateau, the morphological characteristics of landslides are very evident and easy to identify, whether using field surveys or remote sensing images. The back-trailing edge-shape of landslides is

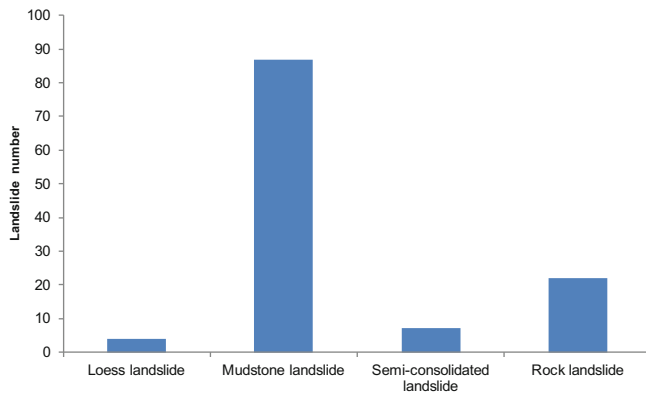


Fig. 3 The rock and loose soil types distribution characteristics of landslides in the study area



Fig. 4 Image of the Suozi landslide mass on the right bank of Yellow River (Photo on May 17, 2012)

typically armchair-shaped, and generally the steepest angles of slope are between 50° and 70° . Some that have a front shear opening also have a tongue, or long-tongue shape. However, some ancient examples of this type have been extensively eroded by the Yellow River, preserving only the round-back of the armchair-like morphology or the trailing edge of the steeper slope relating to residual erosion. The flat morphological characteristics of landslides in the study area can be mainly divided into seven categories of shapes: round-backed armchair-like (including semi-elliptical-shaped, dustpan-shaped, dumbbell-shaped, tongue-shaped (including long tongue, rectangular, mat, and stepped shape), saddle-shaped, long-arc-shaped, and triangular (for the flat patterns of representative landslide remote sensing images and more detailed information please see Fig. 5 and Table 2).

Length, Width and Thickness Characteristics of Landslides

After remote sensing image interpretation and field surveys the authors conducted a statistical analysis in relation to the length, width, slope angle, and area of 508 landslides, and the thickness of 116 landslides. The residual volume above 116 landslides was then calculated. Using these statistics, the distribution characteristics of the length, width, thickness, area, and volume of landslides were obtained. The results are as follows:

Length (L): there is a large range of landslide lengths. The minimum and maximum lengths are 120 m and 6,500 m, respectively, with most of the range fitting between 500 m and 2,200 m. 76.4 % of landslides have a length of between 550 and 1,500 m, (165 in total), accounting for 32.5 % of all landslides (Table 3).

Width (W): the length range of the span of the mass of landslides is also large. The minimum width is 90 m and the maximum 7,200 m. Most lie between 560 m and 2,500 m, and the majority are concentrated in the range 600 m to 1,500 m, (405, accounting for 79.7 % of the total numbers) (Table 4).

The relationship between L and W: 303 landslides have a length greater than the width; on the contrary, the numbers are 205 of all 508 landslides in the study area. There is a certain relationship between the L and W of the landslide mass (Fig. 6): when L and W are less than 1,500 m, the ratio of W to L is close to 1, (accounting for 20 % of all landslides in the study area); but when L and W of the landslide mass are greater than 1,500 m the linear relationship shifts and is polarized, although the overall growth rate of the length is greater than the width, the peak ratio is 2:3.2, which means that the length of the landslide being 2–3 times greater than its width (Fig. 7).

The statistics show that most of the landslides with lengths greater than widths are mainly distributed in the Qunke-Jianzha basin (such as the Xiazangtan landslide, Kangyang landslide, Lannitan landslide, Shengguotan landslide, Suozi landslide). In addition, according to their residual volume, the material of which they are composed, and the type and shape, they can be attributed to the following types of landslide: super-large landslides, mudstone landslides, round-backed armchair-like, long tongue-shaped, and dumbbell-shaped, respectively, which implies that the sliding distance and speed were longer and



Fig. 5 Remote sensing of landslides with representative flat shapes. (a) The ZY-1 02C image of the Xiazangtan landslide and the front edge of two sub-scale landslides (Kangyang landslide and Lannitan landslide) (LNT). The flat pattern of the Xiazangtan landslide and Kangyang landslide have an *armchair-* and *semi-elliptical-shape*, and

their patterns are thus defined as “round-backed armchair-shaped and semi-elliptical”, respectively. (b) GeoEye-2 remote sensing of the Lannitan landslide and ZY-3 of the Xijitan landslide, with evident characteristic of length of landslide mass far longer than width. Their patterns are thus defined as “*long-tongue* or *rectangle shaped*”.

Table 2 Distribution of representative landslides locations and types of image

No.	Flat pattern	Representative landslide	Longitude (E) and latitude (N)	Types of RS
a	Round-backed armchair-like	Xiazangtan landslide I	101°59',35°58'	ZY-1 02C
b	Long tongue or Rectangle	Lannitan landslide and Xijitan landslide	101°58',35°59' and 100°29',35°49'	GE and ZY-3
c	Dustpan	Baicitan landslide	100°29',35°49'	QB
d	Dumbbell	Geza landslide	101°36',36°08'	GE
e	Saddle	Landslide of Mangla River(MR) estuary	100°24',35°45'	
f	Long-arc	Landslides of left bank of MR	100°26',35°43'	
g	Triangular	Mengdaxiang landslide	102°38',35°49'	

RS Remote Sensing, QB QuickBird, GE GeoEye

Table 3 Table of length statistics of landslides mass

Length of interval/m	≤550	551–970	971–1,400	1,401–2,670	2,671–4,800	>4,801
Numbers	111	165	113	92	22	5
Proportion/%	21.9	32.5	22.2	18.1	4.3	1.0

Table 4 Table of width statistics of landslides mass

Width of interval/m	≤560	561–1,040	1,041–1,510	1,501–2,930	2,931–5,300	>5,301
Numbers	175	144	89	71	23	6
Proportion/%	34.5	28.3	17.5	14.1	4.5	1.1

faster, thus being typical types of high-speed remote landslides (Zhang and Yin 2010). Some landslides, such as the Suozi rock landslide and the Gelongbu landslide, have caused partial blocking of the Yellow River, forming a huge barrier lake and leaving the landslide mass opposite the Yellow River. Another type of landslide in the basin belongs to a type known as a creeper deformation which has a short sliding distance and a slow speed (for example the Shange landslide in the GongboXia gorge).

Landslides in the Gonghe Basin mainly have a width greater than the length, (such as the Bancitan landslide, the left bank of the Mangla river landslide, and the Mangla river estuary landslide), and belong to the category of semi-consolidated diagenetic landslides according to their material composition. They are mainly rendered as having flat morphology and semi-elliptical, dustpan, saddle and long-arc

shapes. The sliding distances of such landslides are shorter, and the posterior edge is preserved intact and steeply upright. Therefore, these two types of landslides are obvious differences whether the flat shapes or materially composition.

Thickness: The minimum and maximum thicknesses of 116 landslides as obtained by field survey in the study area are 15 m and 135 m, respectively (with an average thickness of 39.6 m). Based on criteria used to classify the thickness of landslide mass (Yin 2008), the authors found that the thickness of landslides in the region is mainly concentrated in the region of 30–50 m, and consist of deep-seated landslides, (accounting for 67.2 % of the total number in the survey). In addition, there were 25 ultra-thick landslides (more than 50 m), and these belonged mainly to the super-large landslide category (accounting for 21.6 % of the total number—for detailed information please see Table 5 and Fig. 8).

Fig. 5 (continued) (c) QuickBird image of the Baicitan landslide. The back trailing edge is very steep and the landslide mass relatively flat. The entire mass looks like a *dustpan* and is thus called a “dustpan shape”. (d) GeoEye image of the Geza landslide. The front sheer opening of the landslide mass rushed to the Yellow River and covered the flood plain. The sliding distance is very long, and the mass looks like a *dumbbell*. It is thus defined as having a “dumbbell shape”. (e) GeoEye image from Google Earth of the Mangla River estuary landslide. The back trailing edge is centrally concave on both sides of a convex shape, and looks like a horse saddle. It is thus defined as being a

“saddle-shape”. (f) GeoEye image from Google Earth of the landslide located on the right bank of the Mangla River. The whole boundary of the landslide mass seems to be shaped as a *long-arc*, and is thus defined as a “long-arc flat shape”. (g) GeoEye image from Google Earth of Mengdaxiang landslide. The landslide mass rushed to the opposite bank of the Yellow River and blocked it for short time. The whole boundary of the mass has a *triangular form*, and is thus defined as having a “triangular shape”. In all images the *red lines* and *arrows* show the boundary and sliding direction of the landslides; the *blue arrow* shows the flow of the Yellow River

Table 5 Table of thickness statistics of landslides mass

Types	Numbers	Average thickness/m	The depth grading of landslide /m			
			Shallow	Middle	Deep	Ultra-deep
			<10	10–25	25–50	>50
Numbers	116	39.6	0	13	78	25
Proportion/%			0	11.2	67.2	21.6

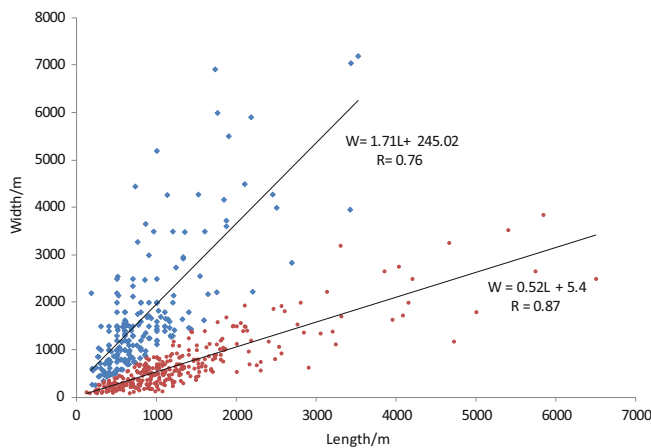


Fig. 6 Linear relationship of length (L) and width (W) of landslides mass

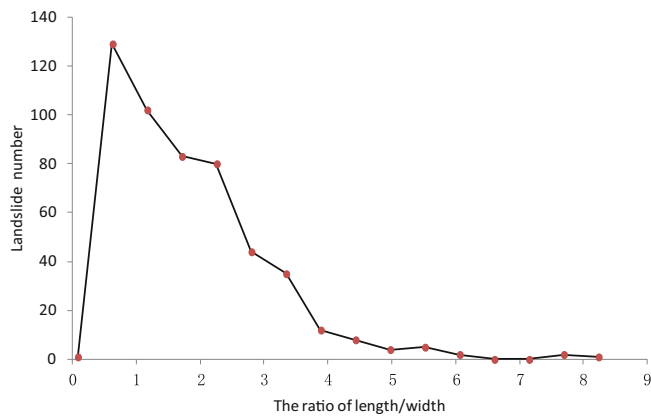


Fig. 7 Ratio of length (L) to width (W) of landslides mass

Characteristics of Area and Volume of Landslides

Area: Out of 508 landslides in the region, the minimum and maximum areas covered are 0.01 km² and 16.26 km², with the main distribution in the range of 0.01–4.00 km². 319 landslides have an approximate area of 1 km², and this accounts for the vast majority (Fig. 9). There are very few

landslides with areas of more than 10 km², (such as the first phase of the Xiazangtan landslide (I), which covered an area of 14.12 km²).

Volumes: The total residual volume of the mass of 116 landslides equates to approximately 98.35 × 10⁸ m³, and the average is 0.85 × 10⁸ m³. The peak values of the residual volume are mainly concentrated in four ranges: 0.5–4 × 10⁸ m³, 6–8 × 10⁸ m³, 10–12 × 10⁸ m³ and 15–17 × 10⁸ m³ (Fig. 10), the categories either side of these ranges belong to giant landslides and super-large landslides, and the residual volume of super-large landslides is more than 15 × 10⁸ m³ (these develop in the multiple mudstone strata in the study area; and are represented by the first phase of the Xiazangtan landslide which is located on the right bank of the Yellow River in the Qunke-Jianzha basin, and the Xijitan landslide located on the left bank of the Yellow River in the Guide basin).

Slope Angle of Landslide Mass

Angle: the average slope angle of landslide deposits is small in the study area, and most landslides are small-angled; statistics show the angle to be mainly between 15–40° and mostly in the region of 15–20° and 35–40° developmental quantity maximum (Fig. 11). Field surveys show that the landslide slope angle of 15–20° is seen to be stable, and is unlikely to cause an event such as in the Xiazangtan landslide’s first phase, which slippery mass slow down steep inclination of 8° in the middle and back trailing edge, central of deposits had water into a landslide lake and disappeared later owing to gullies cutting; the front edge opening dues to the occurrence of secondary disintegration landslide, thus front edge opening steeper and reaching at 31°, the current landslide in a stable state as a whole. The other group of landslides with slope angles of between 35 and 40° are unstable, with the possibility of recurrence in heavy and sustained rainfall, such as the Cambra Park landslide located on the right bank of the Liji Xia roadside, where the back trailing edge of the landslide appears in various tensile cracks under the action of precipitation, making it very unstable and likely to fall onto the Guide to Kanbula road and onto the front edge of the reservoir.

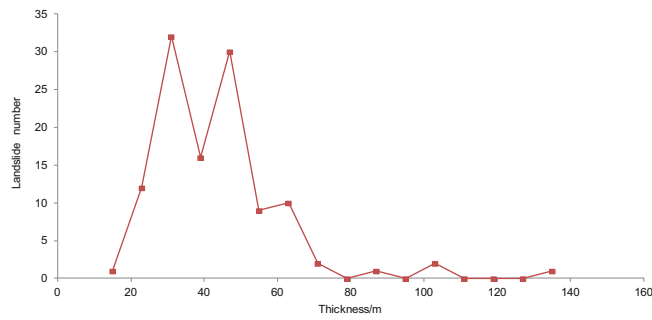


Fig. 8 Thickness distribution characteristics of landslides masses in the study area

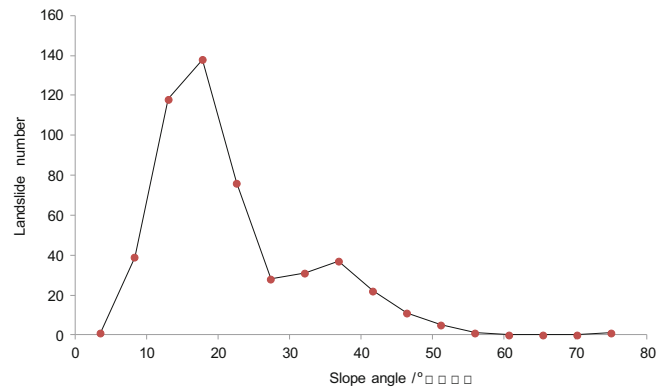


Fig. 11 Slope angle distribution characteristics of landslides mass in the study area

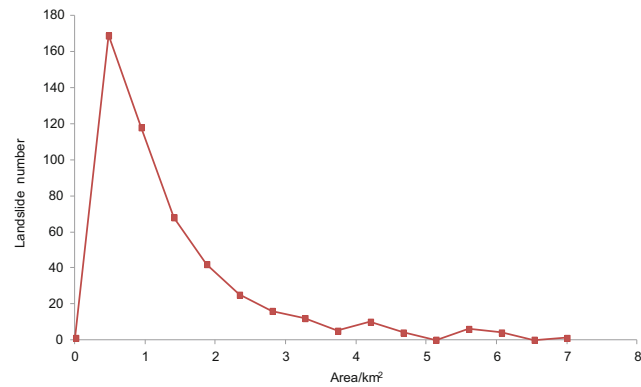


Fig. 9 Area distribution characteristics of landslides mass in the study area

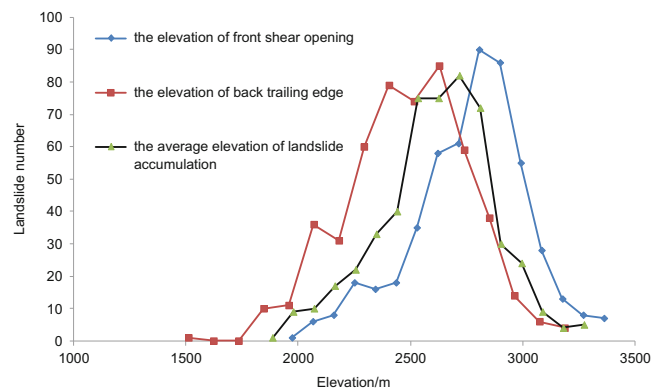


Fig. 12 Evaluation distribution histogram of landslides

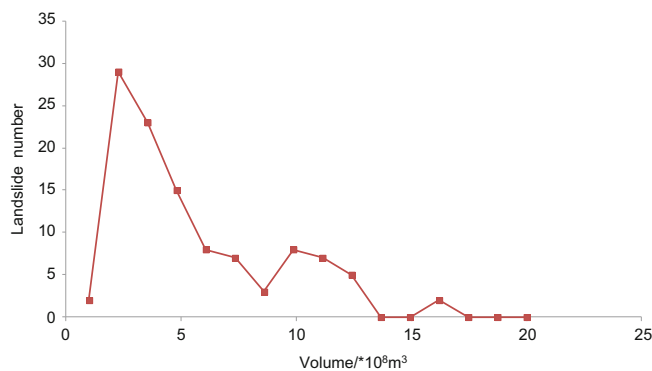


Fig. 10 Volume distribution characteristics of landslides mass in the study area

Elevation Distribution Characteristics of Landslides

The minimum and maximum elevation values of the front shear openings were 1,510 m and 3,187 m, respectively, as shown by remote sensing image statistics in the study area. The elevation minimum and maximum values of the back

trailing edge of the landslides were 1,972 m and 3,363 m, respectively. The average minimum and maximum elevations of the landslides were 1,885 m and 3,274 m, and the landslide developmental elevation values were mainly concentrated between 2,000–2,800 m, particularly between 2,400–2,800 m (Fig. 12). Most of the landslides were ancient or old landslides, with later weathering and erosion reworking limited because of their huge volume, and most of them therefore retain the basic characteristics of the landslide, such as the slippery stepped terrain, or imbricate obvious, the back trailing edge upright, central fracture development, and are therefore easily recognizable with use of high-resolution remote sensing images.

Centralized values of the main relative elevation differences between the front shear opening and the back trailing edge of the landslides masses are between 150 m and 400 m, and present two main centralized peaks [the largest number are between 200 m and 300 m, and the maximum elevation difference is 875 m (Fig. 13)]. The erosion landform height difference of the Yellow River is consistent and the authors considered that the steep slope of the Yellow

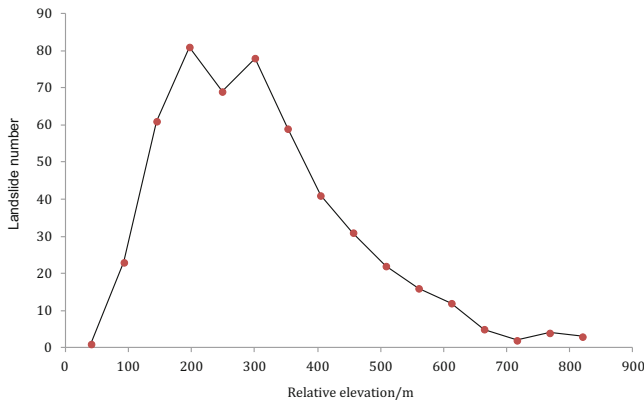


Fig. 13 Relative evaluation distribution of landslides

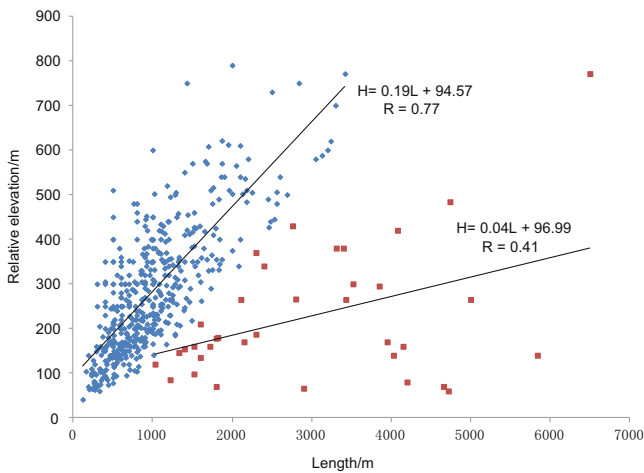


Fig. 14 Relationship between relative evaluation and length of landslides

River for landslides development providing adequate spacing conditions, centralized development phases of landslides in the role of tectonic activity or heavy precipitation.

In addition, statistical analysis reveals a good linear relationship between the relative elevation difference and the length of landslides mass (the greater the relative difference, the longer the length of the landslide mass). Landslides are divided into two categories according to their relationship between the relative elevation and the length. The first category has an excellent correlation with a coefficient of 0.77, and usually occurs in a region of slope with a high steep elevation difference, and fully reflects the dominant background factors of the landslides in the topography. The second category usually occurs in the smaller slope region of the main stream and tributaries, and is often expressed as being a creep, low angle landslide (Fig. 14).

Conclusions

For our data source we used QB, GeoEye, ZY-3ZY-1 02C, and Google Earth images of the upper reaches of the Yellow River region, combined with the results of field surveys and remote sensing validation to examine the spatial shape and distribution characteristics of landslides. Our conclusions are as follows:

1. The characteristics of landslide images are evident and significant in the upper reaches of the Yellow River. The authors found 508 landslides, of which 24 were super-large, and 92 were giant, and that the largest numbers of landslides were distributed in the Qunke-Jianzha basin.” Please ensure that this information matches that presented in your statistics.
2. The spatial distribution of landslide mass morphology can be divided into types: round-backed armchair-shaped and semi-elliptical, dustpan-shaped, dumbbell-shaped, long tongue-shaped (rectangular), saddle-shaped, half-curved, and irregular. Types of rocks and soil can also be divided into four categories: loess landslides, mudstone landslides, semi-consolidated diagenetic landslides, and rock landslides (with most landslides belonging to the mudstone landslide category).
3. The length and mass of the landslides (width) are mainly concentrated between 550–1,500 m and 600–1,500 m, the depth of most of the landslides’ mass is >50 m, but the area of landslide distribution is uneven, and the volumes of 116 landslides equates to $98.35 \times 10^8 \text{ m}^3$.
4. The average elevation of landslide mass is between 2,000 m and 2,800 m, and the majority are between 2,400 m and 2,800 m. The average slope-angle of landslide mass is mostly concentrated between 15° and 20° . There is a good linear relationship between the average slope, relative elevation difference, and the length of landslides mass.

We consider that this research provides technical knowledge in relation to the prevention of serious geological disasters and for geological environment protection.

Acknowledgements This research was funded by the National Nature Science Foundation of China under Grant Nos. 40802089, 41172158, and funded by the China Geological Survey under Grant No. 1212011220123. This financial support is gratefully acknowledged.

References

Antony J, David N, William M (2003) Down-slope variation in geotechnical parameters and pore fluid control on a large-scale Alpine landslide. *Geomorphology* 54:49–62
 Armelle D, Thorsteinn S (2006) Geomorphic evidence for present-day snow-avalanche and debris-flow impact in the Icelandic Westfjords. *Geomorphology* 80:80–93

- Bijan K, Nicholas S (2004) Evaluation of factors controlling earthquake-induced landslides caused by Chi-Chi earthquake and comparison with the Northridge and Loma Prieta events. *Eng Geol* 71:79–95
- Franco M, Robert S (1996) Remote sensing techniques for landslide studies and hazard zonation in Europe. *Geomorphology* 15:213–225
- Hou G, Qian X, Wang S, Sun J (2000) Possibility of the application of the ultra-long electromagnetic wave remote sensor to marine geological exploration. *Acta Geol Sin* 74(2):391–393
- Huang R (2003) Mechanism of large scale landslides in western China. *Quat Sci* 23(6):641–646 (in Chinese with English Abstract)
- Huang R (2007) Large-scale landslides and their sliding mechanisms in China since the 20th century. *Chin J Rock Mech Eng* 26(3):433–445 (in Chinese with English Abstract)
- Li X, Guo X, Li W (2011) Mechanism of giant landslides from Longyangxia valley to Liujiaxia valley along upper Yellow River. *J Eng Geol* 19(4):516–530 (in Chinese with English Abstract)
- Liu S, Lu K (2007) The application of huge landslides survey by Quick Bird remote sensing data—for Shengguotan landslides of Longyang valley to Sigou valley of the Yellow River. The homeland economic strategy of Qinghai 4: 38–39 (in Chinese with English Abstract)
- Oliver K, John J, Reginald L, Kenneth H, Alexander L (2007) Giant landslides, topography, and erosion. *Earth Planet Sci Lett* 261:578–589
- Onder K, Isik N, Unutmaz B (2004) Seismically induced landslide at Degirmendere Nose, Izmit Bay during Kocaeli (Izmit)-Turkey earthquake. *Soil Dynam Earthq Eng* 24:189–197
- Qiao Y, Li M (2000) Application of the Landsat-5 TM image data in the feasibility study of mudflow hazards in the southern Taihang Mountains. *Acta Geol Sin* 74(2):334–338
- Qin X, Yin Z (2012) Earthquake and local rainfall triggered giant landslides in the unconsolidated sediment distribution region along the upper yellow river-remote sense analysis of geological disasters. *J Geophys Remote Sensing* 1:e105. doi:10.4172/2169-0049.1000e105
- Shang Y, Yang Z, Li L (2003) A super-large landslide in Tibet in 2000: background, occurrence, disaster, and origin. *Geomorphology* 54:225–243
- Shi J, Wu S (2008) Remote sensing for landslide study: an overview. *Geol Rev* 54(4):505–509 (in Chinese with English Abstract)
- Stephen G, Nicholas J, Anatoli I, Keith B, Galina S, Galina S, Olga T (2009) Landslides triggered by the 1949 Khait earthquake, Tajikistan, and associated loss of life. *Eng Geol* 109:195–212
- Wang Z (2007) The remote sensing and its new progress for landslides in China. *Remote Sens Land Resour* 19(4):7–10 (in Chinese with English Abstract)
- Yan C, Sun Y, Tang H (2000) Surface micro textures of slipping zone soil of some landslides in the three gorges reservoir district and their significance. *Acta Geol Sin* 74(2):349–352
- Yin Y (2008) Specification of geological survey for landslide on the scale of 1:50000. *Chin Geol Surv*: 6–9 (in Chinese with English summary)
- Yin Z, Cheng G, Hu GaWG, Wei G (2010) Preliminary study on characteristic and mechanism of super large landslides in the upper Yellow River since late Pleistocene. *J Eng Geol* 18(1):41–52 (in Chinese with English Abstract)
- Zhang M, Yin Y (2010) Development status and prospects of studies on kinematics of long run out rock avalanches. *J Eng Geol* 18(6):805–813 (in Chinese with English Abstract)
- Zhang C, Zhang Y, Hu J (2000) Spatial and temporal distribution characteristics and forming conditions of Chinese geological disasters. *Quat Sci* 20(6):559–564 (in Chinese with English Abstract)
- Zhao Y, Liu D (2000) Research on the application of the light-energy spectrum fusion technique to land and resources survey. *Acta Geol Sin* 74(2):381–383



Evaluation on Effect for the Prevention and Control Against the Landslide Disasters in the Three Gorges Reservoir Area

Yong Zhang, Sheng-wei Shi, Jun Song, and Ying-jian Cheng

Abstract

This paper takes the landslide disasters in Three Gorges Reservoir Region as object of study, and then summarizes and analyzes totally 72 control engineering projects that used for the disasters. It sums up the characteristics of prevention technology for landslide disasters in the area. Based on the analysis of the fundamental type and hazard prevention features for the Three Gorges Reservoir Area Landslide Hazard Prevention Project, it has identified the prevention and control efficiency evaluation index, and established the evaluation index system involving up to 11 impact factors and the corresponding prevention and control efficiency grading standards. The landslide hazard prevention and control efficiency evaluation model based on an integrated fuzzy hierarchy process theory was utilized to perform prevention and control efficiency evaluation on the typical project cases, and the evaluation results was excellent in consistent with the judgment result of field geological survey.

Keywords

Landslide • The Three Gorges Reservoir area • Effects of the control engineering • Evaluation index system • Hierarchy-fuzzy comprehensive evaluation method

Introduction

China is characterized by extremely complex and specific geological environment, and the Three Gorges Reservoir Area is featured by enormous quantity, particularly wide and great variety of geological hazards, which result in serious threat to the life and property safety of immigrants in the reservoir area. The state has attached great importance to the prevention and control of geological hazards in the Three Gorges Reservoir Area. Since the implementation of geological hazard prevention and control work within Three

Gorges Reservoir Area in 2001, a total of 452 landslides have been subject to the engineering governance, accounting more than 80 % of the geological hazard prevention projects within the Three Gorges Reservoir Area and invested more than RMB ten billion. The governance project for the landslide hazard in the Three Gorges Reservoir Area fundamentally covers the currently commonly-used landslide prevention project measures. The large number of landslide prevention projects in Three Gorges Reservoir Area has constituted huge information and data.

In 2009, after basically completed the landslide prevention projects in Three Gorges Reservoir Area, there are a number of problems to be solved for the prevention and control of landslides in Three Gorges Reservoir Area, e.g., how to summarize the gains and losses of the landslide prevention project, how to establish a landslide prevention project evaluation system, how to scientifically evaluate the operating conditions, prevention and control efficiency of

Y. Zhang • S.-w. Shi • J. Song • Y.-j. Cheng (✉)
Technical Center for Geological Hazard Prevention and Control, CGS,
Chengdu 611734, China

Institute of Exploration Technology, CAGS, Chengdu 611734, China
e-mail: 16536763@qq.com; 519903933@qq.com; 545539905@qq.com; cyjiet@163.com

Table 1 The domestic and international representative researches on the evaluation of landslide prevention and control efficiency

Author	Major contents
Findlay and Fell (1977)	In accordance with the long-term treatment experience of landslides and rockfalls in North America, it is indicated that landslide prevention project is a systematic project, and the evaluation of prevention and control efficiency should comply with the "Geology-Project" integration concept
Helwany (2001)	Based on the stress test analysis of various indoor retaining walls and slide-resistant piles, this paper has discussed the possible stress changes that may be caused by design differences of varied dimensions and conducted field tests to verify the reinforcement effect
Hu (2006)	His paper has investigated the landslide sliding-resistance engineering effects of Three Gorges Reservoir under water level fluctuations by finite element numerical analysis method, and studies have shown that seepage slides are largely affected by reservoir water level, thus it should appropriately increase the safety reserves
Feng et al. (2006)	From the prospective of safety whole process for landslide prevention project: this paper has summarized the problems prone to appear in the investigation, design and construction quality stage, and strengthened the important role in monitoring and evaluation
Huang et al. (2012)	Based on the whole process of landslide governance project, effectiveness evaluation is classified into a multi-level, multi-index system, and AEI method is applied to establish the evaluation model, which is also verified by examples
Zheng Ming-xin	This paper, from the landslide project geological point of view, has comprehensively expounded the principles, contents and standards on the evaluation of landslide prevention and control efficiency. In addition, it has established a total of 11 factor evaluation models based on fuzzy theory and which have been verified by examples

the completed prevention projects, and so forth. Thus, focusing on the landslide hazard prevention project in Three Gorges Reservoir Area, this paper has summarized and analyzed a total of 72 landslide hazard prevention projects in Three Gorges Reservoir Area, and concluded the landslide hazard prevention technical characteristics in Three Gorges Reservoir Area; On this basis, it has established the Three Gorges Reservoir Area Landslide Hazard Prevention Project Evaluation Index System involving four major categories and eleven impact factors, and has developed the landslide prevention and control efficiency grading standard to evaluate the prevention and control efficiency of typical landslide cases. The implementation of landslide hazard prevention and control efficiency evaluation work for the Three Gorges Reservoir Area is designated to enhance the scientific level of investment decision-making on the landslide prevention project, so as to finally accomplish safe, economical and reasonable landslide prevention project.

Certain Research Contents on Evaluation of Landslide Prevention and Control Efficiency

At present, no uniform standard has been proposed on the evaluation of landslide prevention and control efficiency. European and American geologists generally considered that: it should at least survey the landslide for more than 20 years in order to understand the prevention and control efficiency of a landslide. However, the majority of codes and studies on landslide prevention and control focus on the design and construction contents of landslide prevention project, while the evaluation on landslide prevention project is to inspect the quality of prevention project during the intermediate inspection and completion acceptance.

In contrast, it has paid little attention on the research of the suitability, adequacy, and effectiveness, etc., of the prevention project after landslide governance.

The existing domestic and international studies (Table 1) have offered a useful exploration in the evaluation of landslide prevention and control efficiency from the following four aspects principally: ① to analyze the stress and deformation characteristics of supporting structure by embedding monitoring instruments on-site; ② to research through indoor dimensions scaling physical simulation test; ③ to conduct post-evaluation on the efficiency of landslide prevention project by operational research and mathematical methods; and ④ to invert the prevention and control efficiency via numerical simulation and calculation method. Although starting from a different angles, they have concluded a common understanding that the landslide prevention and control is a systematic project, and the evaluation on the efficiency of landslide governance project is a more comprehensive integrated analysis process.

Technical Characteristics of Landslide Prevention and Control for the Three Gorges Reservoir Area

The commonly-used prevention project measures used for landslide hazard in Three Gorges Reservoir Area can be divided into six categories in accordance with different purposes of prevention and control, the majority of which are designated for fundamental large-scale landslide preventive measures. In particular, the distinctive one is directing at the impact of impoundment in Three Gorges Reservoir. In general, the wading landslide hazard should be provided with the bank protection and slope protection measures. In addition, the application of slope cutting, back-pressure and

Table 2 Commonly used control engineering of the landslide

Program	Prevention purposes	Method	Engineering measures
1	Bypassing or handling	Bypassing	Diversion of lines and buildings, avoided with tunnels or open cut tunnels, bridging across the landslide and so on
2	Eliminate or reduce a variety of formation factors	Surface water discharge	Intercepting drains, drainage ditches, and dredge natural ditches
		Groundwater discharge	Blind ditches, blind holes, supporting blind ditches, sewers, vertical drilling groups, horizontal drilling groups, and drainage galleries
		Prevent water erosion	Anti-scour retention walls, pitched works, riprap revetment and "spur" dike project
		Slope surface remediation	Cutting slopes, slope protection, leveling, stair steps, infill cracks, etc
3	Change the internal mechanical equilibrium of slope mass	Weight reduction	Cutting and load shedding at the rear part of the landslide
		Back pressure	Preloading at the sliding-resistant section in front of the landslide
4	Directly prevent the development of landslide	Set various sliding engineering works	Sliding-resistant retaining wall, pre-stressed anchorage, pre-stressed anchorage sliding-resistant retaining wall, slide-resistant piles, pre-stressed anchoring slide-resistant piles, steel frame slide-resistant piles, sliding-resistant open cut tunnels, slab-pile wall, etc
5	Change the properties of slip band soil	Sliding-resistant key replacement	Excavate the will slip band, replacement of reinforced concrete sliding-resistant key
6	Prediction and forecasting of landslide deformation damage	Landslide monitoring	Landslide stress, displacement, rainfall, groundwater monitoring, etc

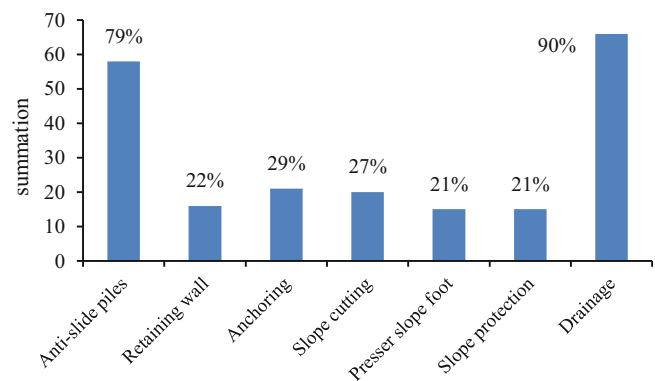
Table 3 Statistical table of the control engineering

Engineering measures	Slide-resistant piles	Retaining wall	Anchoring	Slope cutting	Presser foot	Slope protection	Drainage
Quantity	58	16	21	20	15	15	66
Proportion	79 %	22 %	29 %	27 %	21 %	21 %	90 %

other engineering measures so as to take full advantage of landslide mass to perform resettlement of inhabitant, town construction and so on, which are relatively rare in the landslide projects of other regions. The commonly-used prevention and control engineering measures are shown in Table 2.

In accordance with the site survey and data analysis of landslides in Three Gorges Reservoir Area, it has carried out the investigation and statistical work of totally 72 landslide hazard prevention projects in Three Gorges Reservoir Area. The statistical results for the utilization rate of various prevention engineering measures in the landslide hazard are shown in Table 3 and Fig. 1, indicating that:

1. The landslide hazard prevention projects in Three Gorges Reservoir Area cover almost all commonly-used landslide prevention and control technologies and methods;
2. For the landslide hazard prevention projects in Three Gorges Reservoir Area, slide-resistant pile and drainage project is the highest utilization rate of engineering measures;
3. The retaining work is almost a hundred percent utilization rate;
4. In respect of the landslide hazard in Three Gorges Reservoir Area, the relatively distinctive one is the prevention

**Fig. 1** The percentage of different control engineering

- and control concept adapted to local conditions. Among them, slope cutting and presser foot and slope protection revetment are the relatively less used landslide prevention and control measures adopted in other areas, however, which are more common in the landslide prevention and control measures adopted in Three Gorges Reservoir Area;
5. In addition, monitoring is a necessary means for all landslide hazard prevention projects, including deformation, stress and groundwater monitoring, etc.

Establishment of Landslide Hazard Prevention and Control Efficiency Evaluation Index System in the Three Gorges Reservoir

The landslides in Three Gorges Reservoir Area are characterized by great distribution and scale, and the relocation towns of certain migrants are located directly on the landslide. Thus, the damage or failure of the landslide prevention project will result in immeasurable loss; however, if the design of the prevention project is too conservative, it will lead to excessive workload of engineering prevention and control, thereby affecting the project construction period or the size of funds in most cases. Therefore, it shall carry out the re-evaluation of the prevention project after the landslide governance and timely feedback the efficiency of landslide prevention project so as to provide basis for decision making to the engineering department and to further improve the design theory of landslide prevention project.

Selection Principle of Evaluation Indexes

With regard to the evaluation and inspection of landslide prevention and control efficiency, it shall select the evaluation indexes of prevention and control measures at first, which should focus on reflecting the changes of landslide's stability before and after governance, reasonability of prevention and control program, monitoring after landslide governance, hazard prevention benefits and so on. The selection of the evaluation indexes of landslide prevention and control efficiency should comply with the following principles:

1. Objective principle

Principally, the evaluation indexes should be real and objective, and it should select the factors that earnestly play key influence on the prevention and control of landslide hazard.

2. Universal principle

The occurrence of landslide hazard is subject to various and complex influence factors, which may have certain correlation. For the landslide hazards in different regions or with different types in Three Gorges Reservoir Area, the influence degree of various influence factors is varied. Therefore, the selection of evaluation indexes should not only consider those differences, but also need to consider its universality and suitability characteristics.

3. Hierarchical principle

The evaluation index system should be established in a explicit hierarchy manner in order to comprehensively reflect the control factors that affect the landslide prevention and control efficiency.

4. Concise and operable principle

Emphasizing on the simplicity and operability of indexes is especially important to promote the evaluation system. Simplicity means that the evaluation indexes should be as simple and clear as possible, which are representative; Operability means that the contents of evaluation indexes can be relatively accessed or implemented easily by actual work.

Selection of Evaluation Indexes

The selection of evaluation indexes are required that, individual index should not only be able to accurately reflect the objectives and requirements of landslide hazard prevention and control efficiency, but also should be subject to mutual correlation among various indexes to meet the demands of system construction. In this paper, based on the Analytic Hierarchy Process (AHP), it has selected "Fundamental Landslide Elements", "Governance Design", "Construction Organization," "Stability Condition" and "Governance benefit" as the evaluation objectives, and then select the individual evaluation factors in accordance with the evaluation objectives, and select the landslide prevention and control efficiency evaluation indexes. Taking the "Fundamental Landslide Elements" as an example, it shall select the indexes that can reflect the features of landslide and affect the landslide stability. In accordance with the statistical analysis results of landslide hazard lithology, slope structure and so on in Three Gorges Reservoir Area, such as lithology elements, the landslides in Three Gorges Reservoir Area are mostly occurred in hard and soft interlayered rock mass, while the slope structures are mostly comprised by bedding structure with the sliding surface slope angle of 15–35°. Hydrogeological condition is an important factors affecting the landslide stability, and deformation failure characteristics can reflect the current signs of landslide deformation and future trends.

In accordance with the selection principles of landslide evaluation indexes, and the requirements of various evaluation objectives and contents, a total of 5 aspects and 11 specific influence factors have been selected as the evaluation indexes involving the entire process such as landslide investigation, design, construction, operation and post-effectiveness, etc.

Establishment of Evaluation Index System

In accordance with the field investigation and data collection of multiple landslide hazard prevention projects, the evaluation indexes that are both universal and accessible, but also can effectively reflect the prevention and control efficiency in the prevention projects are selected to primarily establish

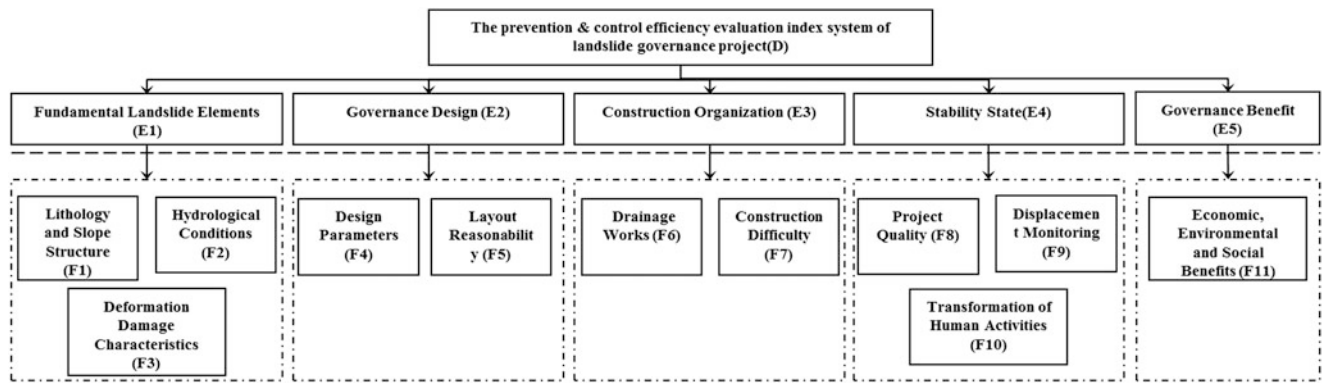


Fig. 2 Evaluation index system of the landslide control in the Three Gorges Reservoir area (target layer (D), criterion level (E), program layer (F))

the landslide hazard prevention and control measure evaluation system of the Three Gorges Reservoir area (Fig. 2).

Grading Standards of Landslide Hazard Prevention and Control Efficiency in the Three Gorges Reservoir Area

In accordance with the established evaluation system for landslide hazard prevention and control measures in Three Gorges Reservoir Area landslide hazard, the various factor indexes reflecting the landslide prevention and control efficiency should be evaluated one by one, so as to propose a comprehensive judgment or evaluation result. The evaluation results can be divided into four grades in accordance with the prevention and control efficiency, including Excellent, Good, Ordinary and Poor, respectively, which is comprehensively evaluated on the landslide prevention and control efficiency according to the corresponding evaluation index. The grading results of landslide prevention and control efficiency are summarized in Table 4. The grading standard of landslide hazard prevention and control efficiency is identified in line with the evaluation index combined by qualitative and quantitative indexes to provide an important reference and basis for subsequent evaluation of prevention and control efficiency.

Landslide Prevention and Control Efficiency Evaluation Model and Engineering Applications

Establishment of Fuzzy Hierarchy Process Comprehensive Evaluation Theory and Evaluation Model

After establishing the landslide prevention and control efficiency evaluation index system and grading standard, it has evaluated a variety of qualitative and quantitative indexes

reflecting the landslide prevention and control efficiency, and comprehensively evaluated the landslide prevention and control efficiency by referring to the grading standard. The entire evaluation process requires the application of uncertainty mathematical method to express the language, quantitative indexes and evaluation procedures for the evaluation of landslide prevention and control measures in the form of mathematical symbols and mathematical formulas, and deriving the final comprehensive evaluation results. In this paper, a landslide hazard prevention and control efficiency evaluation model, based on Fuzzy Hierarchy Process Comprehensive Evaluation Theory has been established to evaluate the prevention and control of typical landslides. In addition, the evaluation results are compared with the on-site geological survey results to verify the reliability of this model (Table 5).

Firstly, the analytic hierarchy process is used to establish the following forms of comparison and judgment matrix.

The elements in the comparison and judgment matrix should satisfy the following properties.

$$b_{ij} > 0, b_{ij} = 1/b_{ji}, b_{ii} = 1 \tag{1}$$

Where, b_{ij} stands for the importance relative to its associated upper level element A , element B_i and element B_j .

The commonly-used eigenvalue method is used to calculate the weight of influence factor ω_i . Supposing the largest eigenvalue of the judgment matrix is λ_{max} , and the corresponding eigenvector is ω , then the weight ω_i of influence factor i and the calculation formula of judgment matrix λ_{max} is expressed as follows, and should perform conformance test.

$$\omega_i = \left(\prod_{j=1}^n b_{ij} \right)^{1/n}, \omega_i^0 = \frac{\omega_i}{\sum_{i=1}^n \omega_i} \quad (\text{vector normalization}) \tag{2}$$

$$\lambda_{max} = \sum_{i=1}^n \frac{(A - B_i \cdot \omega)_i}{n \cdot \omega_i} \tag{3}$$

Table 4 Classification of the effects on the landslide control in the Three Gorges Reservoir area

Grading	Characteristics of landslide prevention and control efficiency
Excellent	Landslide is stable (comprehensively determined by the macroscopic geological surveys and deformation monitoring, the prevention and control measures are reasonable and economical ① The landslide is stable after prevention and control; ② The displacement monitoring of landslides and sliding-resistant structure is within the allowable range; ③ The layout of governance works is reasonable, effective drainage; ④ The prevention project is in compliance with the engineering design life; ⑤ Human engineering activities have no effect on the prevention project; ⑥ Landslide prevention benefits are remarkable.
Good	Landslide is stable, the prevention and control measures are basically reasonable ① The landslide is stable after prevention and control; ② The displacement monitoring of landslides and sliding-resistant structure is within the allowable range; ③ The layout of governance works is relatively reasonable, and it is able to fundamentally drain the groundwater, surface water; ④ The prevention project is in compliance with the engineering design life; ⑤ Human engineering activities have certain impact on the prevention project but do not affect the stability; ⑥ Landslide prevention benefits are ordinary.
Ordinary	The prevention and control measures have a certain effect, but which are not reasonable, or the landslides still reserve some threats ① The stability of landslide is in compliance with the initial requirements after prevention and control; ② The displacement monitoring of landslides and sliding-resistant structure is within the allowable range; ③ The layout of governance works is not reasonable, and the drainage efficiency is ordinary; ④ The prevention project is basically in compliance with the engineering design life; ⑤ Human engineering activities have certain impact on the prevention project but do not affect the stability of the landslide; ⑥ The cost performance of landslide prevention and control efficiency is not high.
Poor	Landslide is not completely eliminated, reserving greater threat, or the quantity of prevention project is huge, too conservative ① The stability of landslide is not in compliance with the requirements after prevention and control; ② The displacement monitoring of landslides and sliding-resistant structure exceeds the allowable range; ③ The layout of governance works is not reasonable, and the drainage is impeded; ④ The prevention project is not in compliance with the engineering design life; ⑤ Human engineering activities have certain impact on the prevention project but do not affect the overall stability of the landslide; ⑥ The cost performance of landslide prevention and control efficiency is low.

Table 5 Combined weights of analytical hierarchy process

A-Bi	Major factor				Total ranking weight
B_1	b_{11}	b_{12}	\cdots	b_{1n}	$\sum_{j=1}^n a_j b_{1j}$
B_2	b_{21}	b_{22}	\cdots	b_{2n}	$\sum_{j=1}^n a_j b_{2j}$
\vdots	\vdots	\vdots	\vdots	\vdots	\vdots
B_n	b_{n1}	b_{n2}	\cdots	b_{nn}	$\sum_{j=1}^n a_j b_{nj}$

Fuzzy Comprehensive Identification should firstly establish the fuzzy set and membership function content for the evaluation of landslide prevention and control efficiency:

1. Supposing The Evaluation Set (Prevention and Control Efficiency Level) Is,

$$V = \{V_1, V_2, V_3, V_4\} = \{I, II, III, IV\} \quad (4)$$

Where, V_1 —Excellent; V_2 —Good; V_3 —Ordinary; V_4 —Poor.

2. Determining Involved Element (Evaluation Index) Set,

$$U = \{U_1, U_2, U_3, U_4, U_5\} \quad (5)$$

Where, U_1 —Fundamental Landslide Elements; U_2 —Governance Design; U_3 —Construction Organization; U_4 —Stability Condition; and U_5 - Governance Benefit.

3. Selecting Involved Element’s Evaluation Factor Set

$$\begin{cases} C(u_1) = \{F_1, F_2, F_3\} \\ C(u_2) = \{F_4, F_5, F_6\} \\ C(u_3) = \{F_7, F_8\} \\ C(u_4) = \{F_9, F_{10}\} \\ C(u_5) = \{F_{11}\} \end{cases} \quad (6)$$

Where, F_1 —lithology and slope structure; F_2 —hydrogeological conditions; F_3 —deformation failure characteristics; F_4 —design parameters; F_5 — engineering layout reasonability; F_6 —drainage works; F_7 —construction difficulty; F_8 —project quality; F_9 —displacement monitoring; F_{10} — transformation of human activities; and F_{11} — economic, environmental and social benefits.

Supposing a_1, a_2, \dots, a_m is the weight of evaluation factor u_1, u_2, \dots, u_m , respectively, and , if $A=(a_1, a_2, \dots, a_m)$, then A is the fuzzy set (i.e. weight vector) reflecting the factor weight.

The integrated membership degree B is obtained by the “integration” of weight vector and fuzzy matrix. Namely, by virtue of fuzzy operation $B = A \cdot R$, it will derive the fuzzy set $B=(b_1, b_2, \dots, b_m)$ ($0 \leq b_j \leq 1$), where

$b_j = \sum_{i=1}^m a_i r_{ij} (M(\bullet, +))$, “(•,+)” is the weighted average compositional operations. This model adopts the weighted average method, equivalent to multiplication of two matrixes, namely, $B = A \cdot R$.

Where, $b_j = \sum_{i=1}^m a_i r_{ij}$; j is the column number of the R and B , m is the number of evaluation factors.

Finally, in accordance with the maximum membership degree criteria, the corresponding grading of $b_{i0} = \max_{1 \leq j \leq n} \{b_j\}$

is the landslide prevention and control efficiency level i_0 .

Based on the Fuzzy Hierarchy Process Comprehensive Evaluation Theory, the weights of various impact factors in the landslide prevention and control efficiency evaluation system are calculated as vector A ,

$$A = (0.043, 0.043, 0.085, 0.065, 0.029, 0.075, 0.063, 0.127, 0.275, 0.135, 0.060) \quad (7)$$

Engineering Application Example

Taking the governed and representative Liujiabao Landslide in Three Gorges Reservoir Area for example, the evaluation model proposed in this paper is applied to conduct evaluation and compare with the results by traditional qualitative determination on site in order to verify whether this model is reliable.

Liujiabao Landslide is a non-wading accumulative landslide in the Three Gorges Reservoir Area, which is located on the right bank, Lijia Ditch, Sanmasan Community, Fengjie County, north-south trending. This landslide covers an area of about $6.5 \times 10^4 \text{ m}^2$ with a size of approximately $235 \times 10^4 \text{ m}^3$. As this landslide is situated in the resettlement key area and is close to the Transportation Bureau, Sanitation Bureau, Bureau of Retired Veteran Cadres and other government agencies, its hazard is prominent. The governance project of Liujiabao Landslide had been completed in early 2007.

In order to conform to urban development, this landslide prevention project adopts the “slope cutting and backfill + multi-level slope protection works + surface drainage system” prevention and control program adhering to the design concept of “transforming slope into terrace”: the front edge of the slope is compacted and backfilled in layered manner by earth-borrow at the slope gradient of 1: 2; the middle and upper surfaces of the slope are leveled according to the slope ratio of 1.75, each 10 m elevation difference is classified as a level of banquette, a total of seven levels. A 2 m wide bridleway is constructed between the banquettes. Upon completion of backfilling earthwork, the slope surface is

constructed with the slope protection and surface interception and drainage system by stone blocks with cement mortar. In accordance with the analysis and calculation of visit surveys and abundant investigation design data, the layout of landslide prevention projects is relatively reasonable, coordinating with the urban construction (not affecting the lower traffic roads and real estate development), the main structures of project (slope protection lattice and drainage system) are intact and non-destructed, while only the trailing edge of the landslide and the damp surface of side ditch concrete beams on both sides have been slightly corroded. Nowadays, the upper part of slopes are constructed with roads and building (trailing edge loading), and human engineering activities are frequent, but there is no abnormality in displacement monitoring (within the reasonable fluctuation range). In addition, there is no obvious signs of deformation on the slope surface after landslide hazard governance. Accordingly, the qualitative judgment deems that the landslide prevention and control efficiency is excellent.

The Comprehensive Analytic Hierarchy Fuzzy Theory was used to evaluate the prevention and control efficiency of Liujiabao Landslide. After completing the field geological survey and the collection of design and construction data, monitoring displacement data, this evaluation model was used to grade the Liujiabao Landslide in line with the prevention and control efficiency grading standard as follows:

I	0	0	1	0	0	0	0	0	1	0	1
II	0	1	0	0	1	1	1	1	0	0	0
III	0	0	0	1	0	0	0	0	0	1	0
IV	1	0	0	0	0	0	0	0	0	0	0
	F_1	F_2	F_3	F_4	F_5	F_6	F_7	F_8	F_9	F_{10}	F_{11}

Accordingly, it can derive R (the fuzzy subset on $U \times V$).

$$R = (r_{ij})_{m \times n} = \begin{bmatrix} 0 & 0 & 1 & 0 & 0 & 0 & 0 & 0 & 1 & 0 & 1 \\ 0 & 1 & 0 & 0 & 1 & 1 & 1 & 1 & 0 & 0 & 0 \\ 0 & 0 & 0 & 1 & 0 & 0 & 0 & 0 & 0 & 1 & 0 \\ 1 & 0 & 0 & 0 & 0 & 0 & 0 & 0 & 0 & 0 & 0 \\ 1 & 0 & 0 & 0 & 0 & 0 & 0 & 0 & 0 & 0 & 0 \end{bmatrix}^T \quad (8)$$

The weight vector of those 11 evaluation factors in the landslide hazard prevention and control efficiency evaluation is vector A :

Thus,

$$B = A \bullet R = (0.430, 0.340, 0.210, 0.043)$$

In accordance with the principle of fuzzy judgment maximum membership degree, the prevention project prevention and control efficiency of Liujiabao Landslide is excellent, and this evaluation result is in consistent with the qualitative

judgment result on site, indicating that this model has good applicability, and providing a reference for the prevention and control efficiency evaluation of similar landslide hazards in Three Gorges Reservoir Area.

Conclusions

The landslide hazard prevention project in Three Gorges Reservoir Area is characterized by various types and great scale. The implementation of landslide prevention and control efficiency evaluation has great significance on improving landslide project design and safeguarding people's life and property safety.

In this paper, in accordance with the summary of landslide hazard prevention and control technologies in Three Gorges Reservoir Area, it has primarily established landslide hazard prevention and control measure evaluation system in Three Gorges Reservoir Area. In addition, it has also developed the prevention and control efficiency evaluation criteria and established the prevention and control efficiency evaluation model, based on fuzzy analytic hierarchy theory. The engineering examples verified the reliability and practicability of this model.

The research contents will have important theoretical and practical significance on achieving effective feedback for landslide prevention and control efficiency, and providing reference and basis for the landslide prevention project design and engineering decision-making departments. The subsequent activities will further improve the prevention and control efficiency grading standard and make in-depth discussion on the value of factor weight for this evaluation model.

Acknowledgments This paper is a partial interim research achievements of the "Three Gorges Reservoir Area Landslide Hazard Prevention Technology and Demonstration", a special subject in the "Twelfth Five-Year" National Science and Technology Support Program "Landslide Hazard Prevention Technology Research and Demonstration In Major Engineering Disturbed Zone". Hereby, I'm most

grateful for the guidance and advice from Wu Shu-ren, the researcher of the research group on the contents of this special subject and paper.

References

- Chang Zhong-hua, Wu Xiao-liu, Wu Fa-quan (2008) Main types and protective measures of engineering slopes in the Three Gorges Reservoir areas. *J Eng Geol* (S1):245–250
- Ding S-c, Zhang Q-l, Chen H-y (2007) The distribution of landslides in the Three-Gorge reservoir region and their prevention and control. *Resour Environ Eng* 21(3):265–268
- Hu X-l (2006) Numerical simulation of effectiveness of anti-slide piles construction for landslide in Three Gorges Reservoir area under water-level fluctuation. *Rock Soil Mech* 27(12):2234–2238
- Huang J, Ju N-p (2012) Evaluation approach of countermeasure efficiency for landslide hazards. *J Eng Geol* 20(2):189–194
- Kepaptsoglou K, Karlaftis MG, Gkoutis J (2013) A fuzzy AHP model for assessing the condition of metro stations. *J Civil Eng* 17(5):1109–1116
- Lan J-b, Xu Y, Huo L-a et al (2006) Research on the priorities of fuzzy analytical hierarchy process. *Syst Eng-Theory Pract* 9:741–756
- Helwany MB (2001) Seismic analysis of segmental retaining walls (model verification, effects of facing details). *J Geotechn Geoenviron ASCE* 127(9):741–756
- Ghafoori M, Lashkaripour GR, Moghaddas NH et al (2013) Landslide susceptibility mapping for Yadak-Tevil Watershed (Northeast Iran), Using AHP Method. *Landslide Sci Pract* (1):567–572.
- Feng W-k et al (2006) Safety evaluation of landslide preventive measures-illustrated with case study. *J Eng Geol* 14(5):670–676
- Findlay PJ, Fell R (1997) Landslides risk perception and acceptance. *Geotechn J Can* 34(2):169–188
- Su A-j, Gao Y (2005) Some issues in the design of landslide control works in the Three Gorges reservoir area. *Yangtze River* 36(3):7–9
- Tong G-q, Wang X-j, Shi G (2011) Analysis and strategies on prevention measures of geological disasters in the Three Gorges Reservoir area. *Yangtze River* 42(22):20–22
- Wu S-r, Shi J-s, Zhang Y-s et al (2006) Landslide mechanisms-a case study of the Yangtze Three Gorges reservoir area. *Geol Bull Chin* 25(7):874–879
- Wang Gong-xian (2006) Choice and optimization of landslide control plan. *Chin J Rock Mech Eng* (S2): 3867–3873
- Xie Q-m, Xia Y-y (2003) Fuzzy hierarchy analysis on decision making of rockmass slope treatment based on entropy weight. *J Rock Mech Eng* 22(7):1117–1120



Fiber Optic Strain Monitoring and Evaluation of a Slow-Moving Landslide Near Ashcroft, British Columbia, Canada

David Huntley, Peter Bobrowsky, Zhang Qing, Wendy Sladen, Chris Bunce, Tom Edwards, Michael Hendry, Derek Martin, and Eddie Choi

Abstract

Landslides in British Columbia are costly geological hazards that have challenged the major rail companies for over 120 years. Presented here are preliminary results and analyses of fiber Bragg grating and Brillouin optical time domain reflectometry monitoring of a deforming trackside lock-block retaining wall on the Ripley Slide in the Thompson River valley south of Ashcroft, British Columbia. Fiber optic strain data are evaluated in the context of results from global positioning system monitoring, field mapping and electrical resistivity tomographic survey across the landslide. This research aims to reduce the economic, environmental, health and public safety risks that landslides pose to the railway network operating in Canada and elsewhere.

Keywords

Railways • Ripley Slide • British Columbia fiber Bragg grating • Brillouin optical time domain reflectometry • Global positioning system • Electrical resistivity tomography

D. Huntley (✉)
NRCan, Geological Survey of Canada, 1500-605 Robson Street,
Vancouver, Canada V6B 5J3
e-mail: david.huntley@nrcan.gc.ca

P. Bobrowsky • W. Sladen
NRCan, Geological Survey of Canada, 601 Booth Street, Ottawa,
Canada K1A 0E8

Z. Qing
Centre for Hydrogeology and Environmental Geology, China
Geological Survey, Hebei, China

C. Bunce • E. Choi
Canadian Pacific Railway, 7550 Ogden Dale Road, SE, Calgary,
Canada T2C 4X4

T. Edwards
Canadian National Railway, 10229-127th Avenue, Edmonton, Canada
T5E 0B9

M. Hendry • D. Martin
Civil and Environmental Engineering, University of Alberta,
Edmonton, Canada T6G 2W2

Introduction

The Thompson River valley south of Ashcroft, British Columbia, Canada is a unique area where complex glacial geology, active geomorphic processes and critical transportation infrastructure (both major national rail lines—CN and CPR) intersect with, and are affected by a long history of slope instability. Well-documented landslides along a >10 km stretch of the valley have been impacting infrastructure since the nineteenth century (Fig. 1). Because the economic, environmental and public safety repercussions of severing both railways in this area would be pronounced, a multi-year collaborative study has been undertaken to investigate and monitor landslide activity in this vital transportation corridor (Bunce and Chadwick 2012; Bobrowsky et al. 2014; Huntley and Bobrowsky 2014).

Landslide Activity in the Thompson River Valley

Large rotational and retrogressive translational landslides were initially triggered through deep incision of Pleistocene

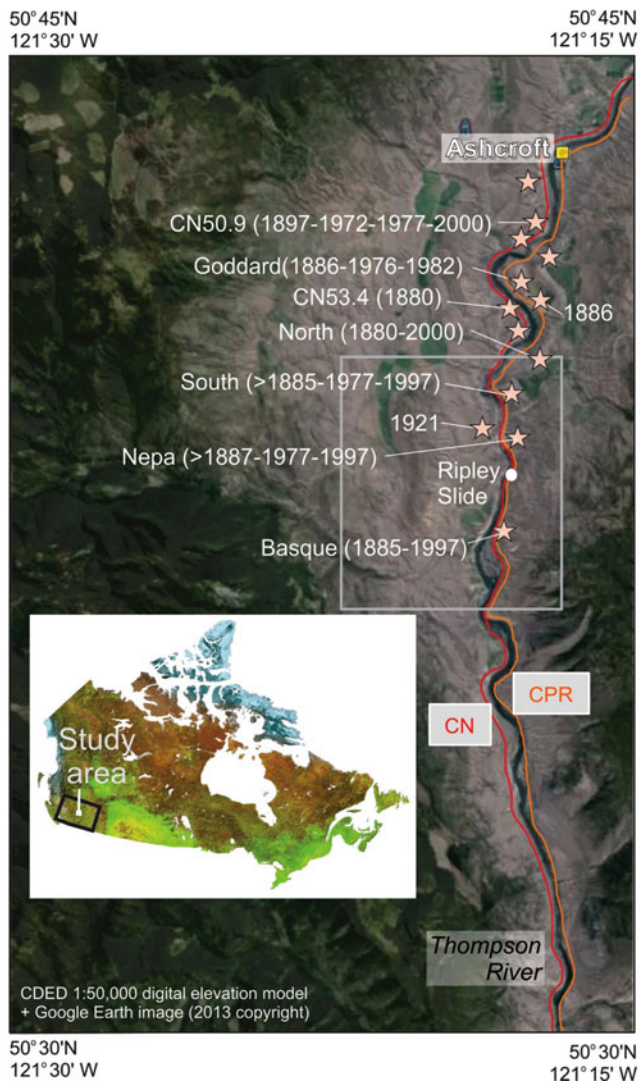


Fig. 1 Significant landslides along Thompson River south of Ashcroft with approximate dates of activity

sediments by post-glacial Thompson River. Pleistocene deposits infill a deeply incised Paleogene landscape consisting of topographic uplands and remnant sections of paleochannels with moderate to steep slopes. This valley fill includes multiple glaciolacustrine clay-rich units separated by tills and outwash gravel related to least three Pleistocene glaciations (Ryder et al. 1991; Clague and Evans 2003; Johnsen and Brennand 2004; Tribe 2005).

Although some landslides failed and moved rapidly in prehistoric times; today and in the recent past, all are slow-moving reactivated compound features (Porter et al. 2002; Clague and Evans 2003; Bishop et al. 2008; Eshraghian et al. 2008; Bunce and Chadwick 2012). For most, movement occurs along weak, sub-horizontal glaciolacustrine zones confined between overlying till and underlying gravel deposits and bedrock. This movement is accommodated by one or more of three failure mechanisms: (1) slow-moving

(2–10 cm/year) rotational failures with large back-tilted blocks; (2) slow-moving (2–10 cm/year) retrogressive translational slides with little rotation; and (3) rapid debris slumps involving flowage and sliding of landslide material (Clague and Evans 2003). At present, Thompson River affects landslide stability by changing: (1) the pore water pressure in the slope mass and in particular in relation to rupture surfaces; (2) the supporting force on landslide toes; and (3) through cutbank erosion, thereby affecting the geometry of the landslide (Clague and Evans 2003; Eshraghian et al. 2008).

Ripley Slide

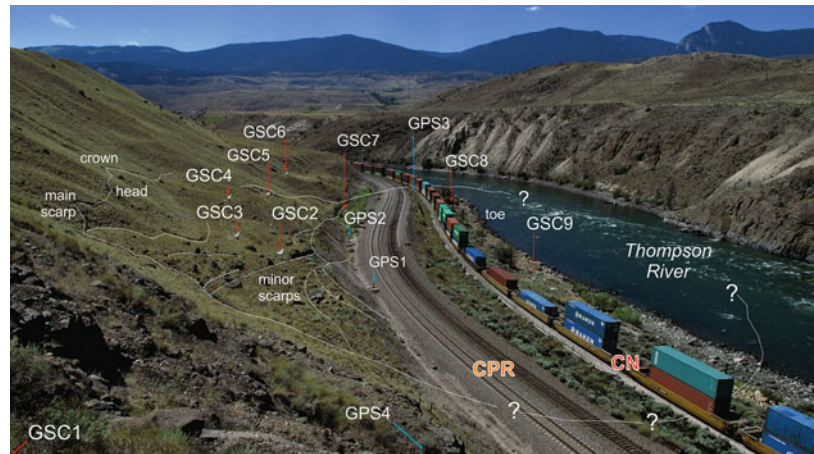
The Ripley Slide is a small (area ca. 220 m × 150 m, volume 400,000 m³), slow-moving retrogressive translational landslide (Fig. 2). Fieldwork was undertaken in the spring, summer and autumn of 2013 to address significant gaps in our knowledge of the nature of surficial earth materials, their stratigraphic relationships, and in the controls on the style of mass wasting at this site. Ten surficial geology units are defined on the basis of facies and landform associations, texture, sorting, colour, sedimentary structures, degree of consolidation, and stratigraphic contact relationships (Huntley and Bobrowsky 2014). From oldest to youngest, the mapped earth materials include: Mesozoic bedrock; Pleistocene colluvium, glaciolacustrine sediments, till, glaciofluvial sediments; in addition to Holocene colluvial deposits, alluvial sediments and anthropogenic fill (e.g., railway ballast, culverts).

Preliminary results from a global positioning system (GPS) indicate that the Ripley Slide is in a continual cycle of stability and instability (Bunce and Chadwick 2012). The landslide experiences small increments of movement over time, with documented cumulative horizontal movement rates ranging from 2.55 mm/year at GPS1, to 36.5 mm/year at GPS2 and 54.75 mm/year at GPS3 that are consistently to the WNW (Bunce and Chadwick 2012; Fig. 4). Peak movement rates occur from autumn to winter as river and groundwater reach minimum levels. Peak river flows, bank erosion, bed scour, and highest differential between river and groundwater levels occur from spring to summer (cf. Eshraghian et al. 2008; Bunce and Chadwick 2012).

Infrastructure at Risk

The Ripley Slide is known to have been active since 1951; and although movement was slow in the late twentieth century, cumulatively it was sufficient to open numerous tension cracks in the main body of the landslide and cause a visible displacement in the fence line east of the CPR track by the early 2000s (Bunce and Chadwick 2012). In 2005, a

Fig. 2 Overview of the Ripley Slide highlighting the location of GPS monitoring stations (GPS1-4) and InSAR corner reflectors (GSC1-9); fiber optic monitoring systems are installed along the retaining wall separating the CPR and CN tracks; maximum displacement of the landslide occurs at GPS3; view to south



rail siding was extended across the landslide that required upslope cuts and embankment widening, including the construction of a lock-block retaining wall between the CN and CPR tracks at the southwest limit of the toe slope, and in the vicinity of GPS3 (Fig. 2). During the autumn of 2006 and spring of 2007, track lifting between 10 and 20 mm as often as every 3–6 weeks was required; and a back scarp of a 40,000 m³ portion of the landslide became visible in the excavated cut slope east of GPS1 (Fig. 2). A noticeable depression in the retaining wall coincides with the maximum detectable surface displacement of GPS3 (Fig. 3).

The Ripley Slide currently poses a significant hazard to the onsite infrastructure since both the CN and CPR tracks run adjacent to each other along the entire breadth of unstable terrain. On average some 80 trains per 24 h period travel through the area and therefore cross this particular landslide. Locomotives traverse the landslide at a precautionary maximum speed of 30 km/h; so in the event of a derailment, the potential is low for injury and death of engineers, conductors, passengers and other individuals.

Potential environmental damage to Thompson River and groundwater by spilled dangerous goods is also minimized at this speed (Bunce and Chadwick 2012). Unfortunately, as the magnitude and frequency of landslide activity increases, the frequency of track maintenance and operation costs rise. Consequently, the economic repercussions of a severed railway here remain pronounced.

There are three strategies for railways to reduce the risks associated with landslides in the Thompson River valley: (1) avoid landslide-prone terrain—not possible at the Ripley Slide and surrounding area; (2) stabilize the landslide—an unresolved and prohibitively costly geotechnical problem at this and other landslides in the Thompson River valley; and (3) monitor for unsafe ground movement—the most cost effective risk management approach for this landslide (Bunce and Chadwick 2012).

Landslide Monitoring

A large consortium of research partners has embarked upon a detailed multi-year study to investigate the Ripley Slide (Bobrowsky et al. 2014). The objective of this collective effort is to better understand and manage the Ripley Slide, and by extension other landslide hazards in Canada and elsewhere.

An extensive array of monitoring technology has been installed that includes traditional applications including permanent monitoring using GPS stations and piezometers; as well as subsurface investigations involving drilling and borehole logging, electrical resistivity tomography (ERT), electromagnetic (EM), ground penetrating radar (GPR), seismic reflection and refraction surveys. In addition, our work involves the application of fiber Bragg grating (FBG) and Brillouin optical time domain reflectometry (BOTDR) and subsurface inclinometry using ShapeAccelArray (SAA), the installation of corner reflectors for satellite based (RADARSAT-2) interferometry and the deployment of ground-based SAR and LiDAR for ongoing quantitative assessment (Bobrowsky et al. 2014). The focus of this paper is the installation, preliminary results and interpretation of fiber optic monitoring systems; and comparison with GPS and ERT data.

Fiber Optic Monitoring

Conventional vibrating wire piezometers, inclinometers, strain gauges, accelerometers and geophones require a large number of cables per installation, experience electromagnetic interference and signal degradation with long distance transmission, and generally have low long-term reliability. In contrast, sensors systems using optical glass fiber cable do not have these limitations, making them

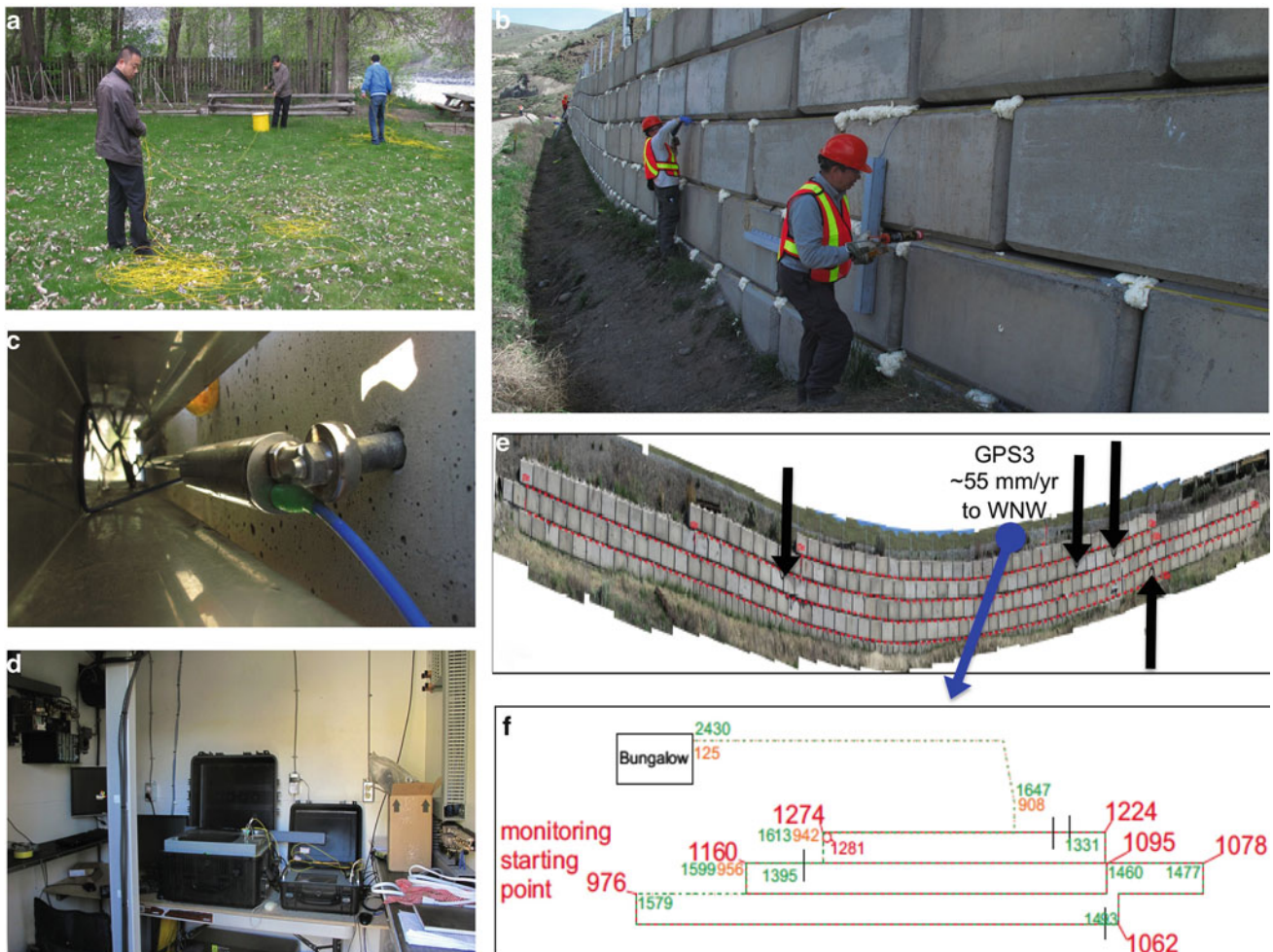
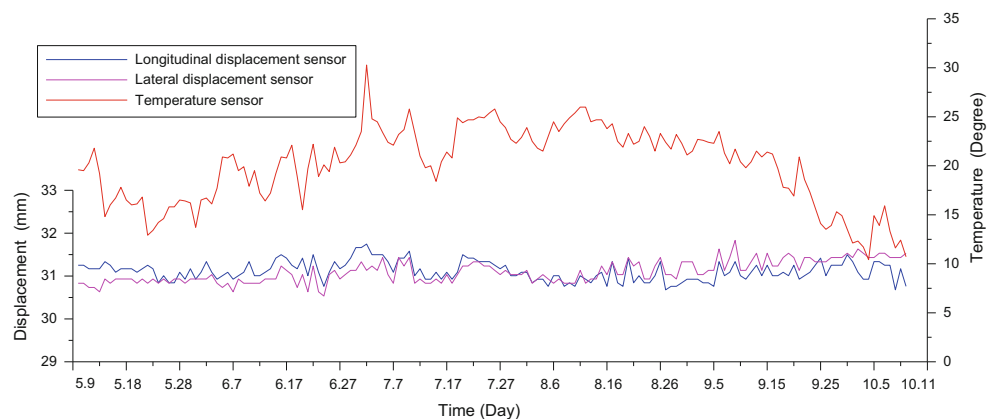


Fig. 3 Installation, monitoring, data telemetry and analysis: (a) measuring out and calibrating fiber optic cables; (b) bonding of cable network to lock-block retaining wall; (c) displacement sensing strain gauges bolted to the retaining wall block; (d) bungalow housing data acquisition and transfer modules; (e) panorama of retaining wall

showing movement of GPS3 (blue arrow) and location of strain indicated by BOTDR (black arrows); (f) plan of FBG and BOTDR cables on retaining wall, strain locations indicated (thin black vertical bars)

Fig. 4 FBG displacement monitoring curves for May 2013



reliable for monitoring strain and pore water pressure in landslides. In addition to being more cost effective, fiber optic systems also have performance advantages including higher data resolution and faster sampling rates (e.g., Huang

et al. 2002; Yoshida et al. 2002; Yong et al. 2005; Laudati et al. 2007; Xu et al. 2007; Huafu et al. 2011).

For this study, strain (and temperature) in the lock-block retaining wall was monitored by a combination of FBG and

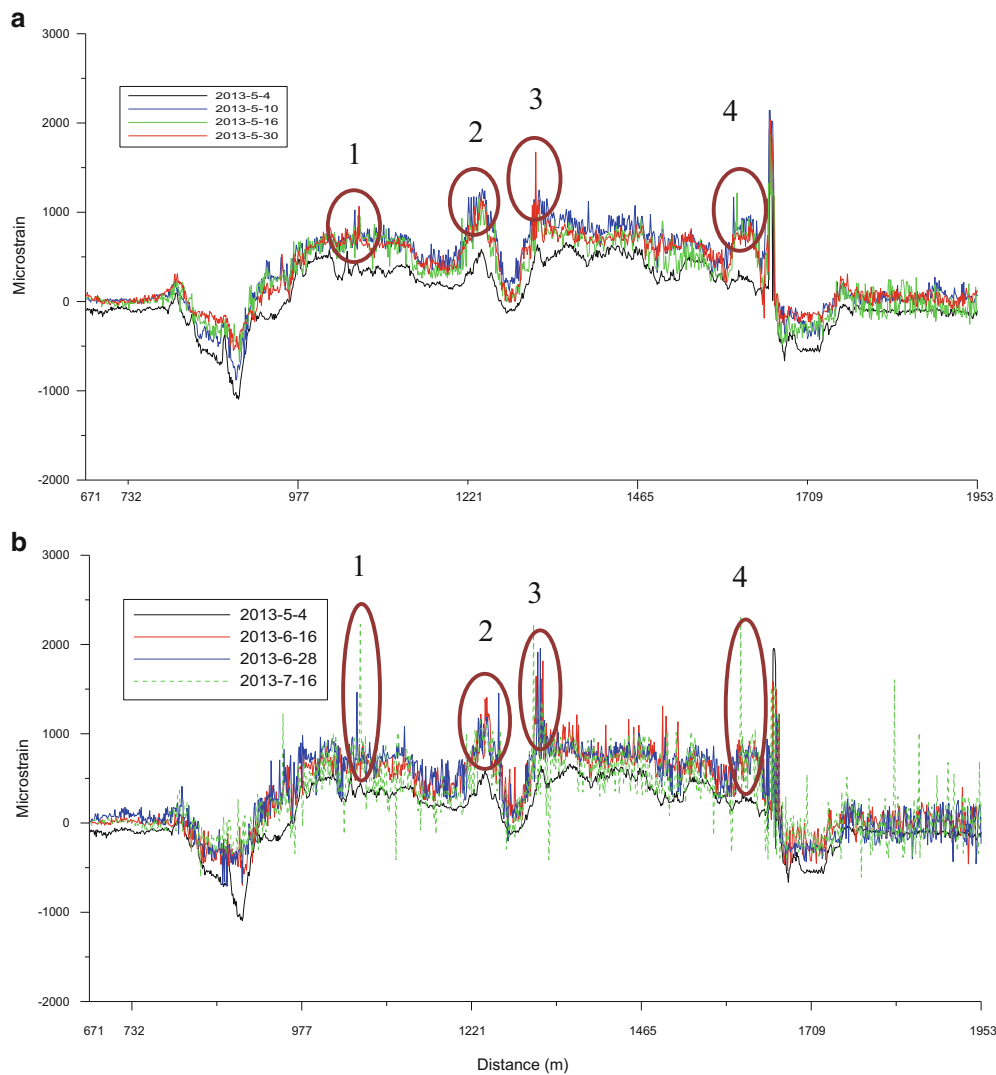


Fig. 5 BOTDR monitoring curves: (a) May 2013; (b) June and July 2013; ellipses correspond to strain locations at 1,060 m (1), 1,230 m (2), 1,320 m (3) and 1,610 m (4)

BOTDR. Installation was undertaken in late April to early May 2013 and overseen by the Geological Survey of China (CGS) and Geological Survey of Canada (GSC). Following calibration (Fig. 3a), a combination of household epoxy resins, caulking products and foam fillers were used to glue fiber optic cables and sensors to the concrete blocks (Fig. 3b). Linear displacement between monitoring and fixed points was recorded by angular displacement sensors and converted into corresponding electrical signals (Fig. 3c). These data processed on site (Fig. 3d) then accessed by wireless transmitter from remote terminals at the CGS and GSC offices where information is analyzed through monitoring software (Fig. 3e, f).

Preliminary Results

The two FBG displacement sensors detected no obvious displacement following equipment installation on May 9

2013. FBG sensor measurement results are influenced by temperature (Fig. 4). BOTDR monitoring curves for May, June and July 2013 are presented in Fig. 5. These curves have a relative shift compared to the initial curve following installation on May 4 2013. Four places with obvious strain are recognized at 1,060 m, 1,230 m, 1,320 m and 1,610 m (Figs. 3e, f and 5a, b). Strain is also detected in other places along the array (Fig. 5a, b).

Analysis and Evaluation with Other Techniques

Initial shifts in FBG and BOTDR curves are probably attributed to strain in the optical fiber produced by the process of glue solidification (Figs. 4 and 5). The four strain locations identified using BOTDR (Figs. 3e, f and 5a, b) bracket the area of maximum displacement captured by GPS3 and likely represent hinge lines developing in the sagging retaining wall (Fig. 3b).

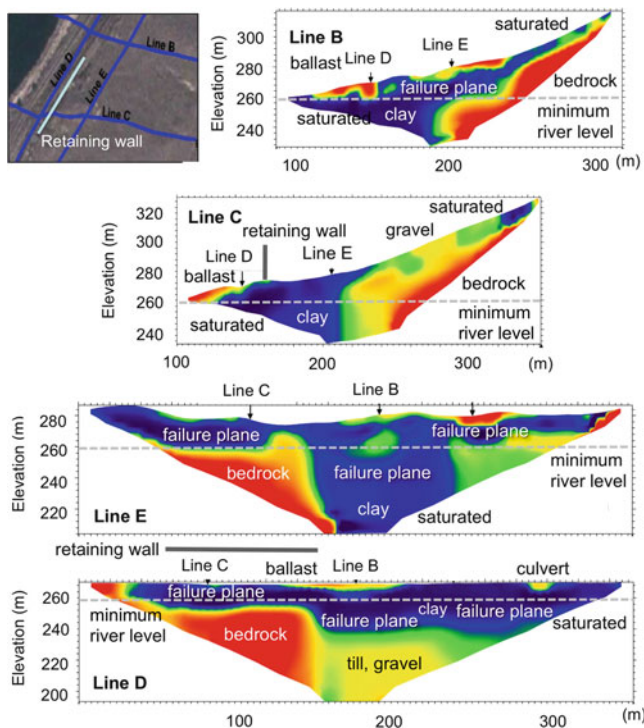


Fig. 6 ERT transects (B, C, D and E) with provisional interpretation of sub-surface geology, groundwater conditions and landslide structures in the vicinity of the retaining wall

Geophysical data provide insight into potential sub-surface structures that are manifesting as sources of strain in the retaining wall. ERT results reveal a high relief bedrock surface overlain by a 10–60 m + thick package of clay, till and groundwater-rich gravel (Fig. 6). Discrete curvilinear ERT features are distinguishable along Lines B, C, D and E that are interpreted as failure planes in clay beds beneath the rail ballast and retaining wall (Fig. 6).

Conclusions

This paper is a collective effort to better understand and manage the Ripley Slide, and by extension other landslide hazards in Canada and elsewhere. We demonstrate that distributed fiber optic strain monitoring yields meaningful results, especially when considered in the context of other geological and geophysical information.

For the duration of monitoring (~3 months), FBG sensors detected no displacement of blocks. BOTDR detected strain corresponding to the zone of broad downwarping in the lock-block retaining wall, and maximum horizontal displacement of GPS (Figs. 3e, f and 5a, b). Field observations and preliminary ERT data reveal the presence of thick accumulations of clay and other glacial deposits, groundwater, and listric (curvilinear) landslide failure planes beneath CN and CPR tracks,

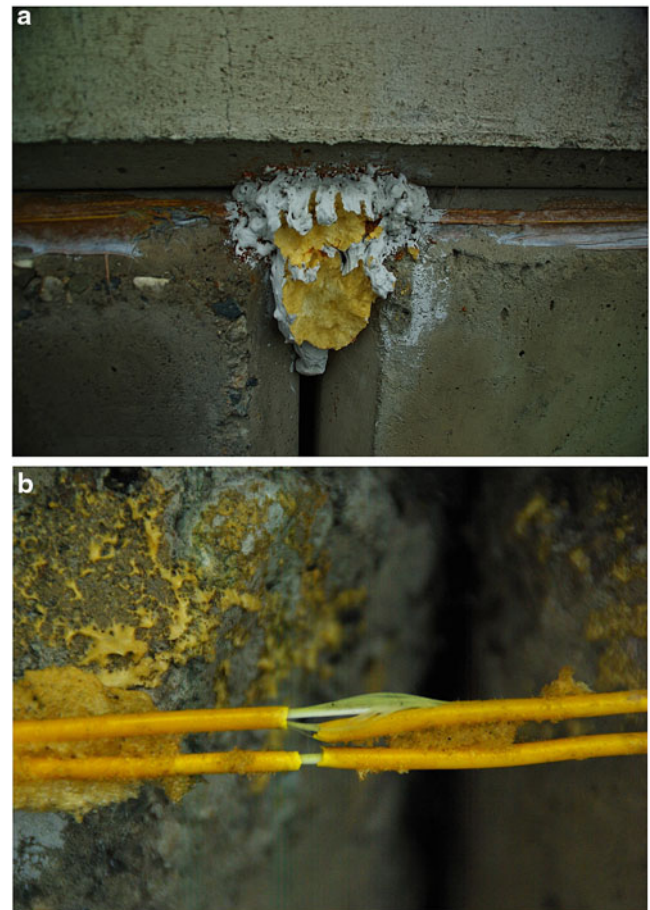


Fig. 7 (a) Bear claw marks on foam infill; (b) damaged cable coatings and exposed optical fibers

retaining wall, and extending upslope above the railway right-of-way (Fig. 6).

Three months of FBG and BOTDR data were collected for the Ripley Slide before the installation was damaged by black bear activity (Fig. 7a, b). In addition, epoxy resin and caulking products failed during prolonged intervals of sub-zero temperatures, so that cables are no longer attached to the retaining wall in many places. Periodic on-site visits were also required to trouble-shoot hardware, software and telemetry issues. Despite these apparent setbacks, the real-time monitoring possibilities warrant continued application of FBG and BOTDR monitoring at the Ripley Slide. To address these problems, solutions will be developed during pre-fieldwork technical workshops at CGS and GSC offices.

Acknowledgements The project has benefited from management by Carmel Lowe, Adrienne Jones and Philip Hill (GSC Sidney, British Columbia); and Merrina Zhang (Transport Canada, Ottawa, Ontario). ERT, EM, GPR, seismic surveys and geophysical data modelling was

completed by Neil Parry, Megan Caston, Cassandra Budd and Gordon Brasnett (EBA-Tetrattech, Edmonton, Alberta). The following colleagues contributed on site and in the office: Lionel Jackson (GSC Vancouver, British Columbia); Renato Macciotta and Hengxing Lan (University of Alberta, Civil and Environmental Engineering, Edmonton, Alberta); and Ian Chadwick (ERD Consulting Ltd., Kamloops, British Columbia). Field safety was ensured by Gary Maximiuk and Roy Olsen (CPR) and Jennifer Kutchner and Mark McKay (CN).

References

- Bishop N, Evans S, Petley D, Unger A (2008) The geotechnics of glaciolacustrine sediments and associated landslides near Ashcroft (British Columbia) and the Grand Coulee Dam (Washington). In: Proceedings of the 4th Canadian conference on geohazards: from causes to management
- Bobrowsky P, Sladen W, Huntley D, Qing Z, Bunce C, Edwards T, Hendry M, Martin D, Choi E (2014) Multi-parameter monitoring of a slow-moving landslide: Ripley landslide, British Columbia, Canada. In: Proceedings of the international association of engineering geologists, Turin, Italy
- Bunce C, Chadwick I (2012) GPS monitoring of a landslide for railways. In: Eberhardt E et al (eds) Landslides and engineered slopes: protecting society through improved understanding. CRC, London, pp 1373–1379
- Clague J, Evans S (2003) Geologic framework for large historic landslides in Thompson River valley, British Columbia. *Environ Eng Geosci* IX:201–212
- Eshraghian A, Martin D, Morgenstern N (2008) Movement triggers and mechanisms of two earth slides in the Thompson River Valley, British Columbia, Canada. *Can Geotech J* 45:1189–1209
- Huafu P, Peng C, Jianhua Y, Honghu Z, Xiaoqing C, Laizheng P, Dongsheng X (2011) Monitoring and warning of landslides and debris flows using an optical fiber sensor technology. *J Mt Sci* 8(5):728–738
- Huang C-J, Chu C-R, Tien TM, Yin HY, Chen P-S (2002) Calibration and deployment of a fiber-optic sensing system for monitoring debris flows. *Sensors* 12:5835–5849
- Huntley D, Bobrowsky P (2014) Surficial geology and monitoring of the Ripley Slide, near Ashcroft, British Columbia, Canada. *Geol Surv Can Open File* 7531: 21 p
- Johnsen TF, Brennand TA (2004) Late-glacial lakes in the Thompson Basin, British Columbia: paleogeography and evolution. *Can J Earth Sci* 41:1367–1383
- Laudati A, Mennella F, Esposito M, Cusano A, Giordano M, Breglio G, Sorge S, Calisti Tassini C, Torre A, D'Altrui G, Cutolo A (2007) A fiber optic Bragg grating seismic sensor. In: SPIE proceedings on optical fibre sensors, vol 6619
- Porter MJ, Savigny KW, Keegan TR, Bunce CM, MacKay C (2002) Controls on stability of the Thompson River landslides. In: Proceedings of the 55th Canadian geotechnical conference: ground and water—theory to practice, Canadian Geotechnical Society, pp 1393–1400
- Ryder JM, Fulton RJ, Clague JJ (1991) The Cordilleran Ice Sheet and the glacial geomorphology of southern and central British Columbia. *Geogr Phys Quatern* 45:365–377
- Tribe S (2005) Eocene paleo-physiography and drainage directions, southern Interior Plateau, British Columbia. *Can J Earth Sci* 42:215–230
- Xu L, Li S, Liu X, Feng C (2007) Application of real-time telemetry technology to landslide in Tianchi Fengjie of three Gorges Reservoir region. *Chin J Rock Mech Eng* 26:4477–4483
- Yong D, Bin S, He-liang C, Wen-bin S, Jie L (2005) A fiber optic sensing net applied in slope monitoring based on Brillouin scattering. *Chin J Geotech Eng* 27:338–342
- Yoshida Y, Kashiwai Y, Murikami E, Ishida S, Hashiguchi N (2002) Development of the monitoring system for slope deformations with fiber Bragg grating arrays. In: SPIE proceedings 4694, smart structures and materials 2002: smart sensor technology and measurement systems, p 296



Landslides Susceptibility of Chittagong City, Bangladesh and Development of Landslides Early Warning System

Reshad Md. Ekram Ali, Lloyd Warren Tunbridge, Rajinder Kumar Bhasin, Salma Akter, Md. Mahmood Hossain Khan, and Mohammad Zohir Uddin

Abstract

Chittagong, the second largest city of Bangladesh is mostly developed on the hilly areas. Hills are mostly covered with loose and weathered Tertiary sedimentary rocks susceptible to landslides. Deforestation and hill cutting are also accelerating the destructive process of landslides considerably. Generally, due to heavy rainfall, within a short period of time, water easily infiltrates into the loose rocks and soils which increase the pore water pressure and finally exceeds the shear strength of the materials to initiate landslides under the influence of gravity. On the basis of landslides history, slope characteristics, geology and geotechnical properties Chittagong City and surroundings have been divided into four landslide hazard zones. East of Chittagong City, zone-I is most susceptible to landslides and the city is progressively less susceptible further westward up to zone IV. Batali hill, Bayjeed Bostami, Chittagong Cantonment, Chittagong University Campus and their surrounding areas have been identified as most susceptible areas to landslides. Prevention of landslides in most cases requires costly engineering solutions. Therefore, mitigation through timely evacuation of people from landslides susceptible areas is the best solution to combat landslides. Two automated rain gauges installed in high risk zone with built-in rainfall threshold values. Threshold values for early warning of landslides are 100 mm in 3 h, 200 mm in 24 h and 350 mm in 72 h. These rain gauges send real time early warning to the registered mobile phones so that first responding organizations can take action straight away before landslides happen.

Keywords

Landslides • Tertiary sedimentary rocks • Hazard zoning • Rainfall threshold values • Landslides early warning

Introduction

In the southeast of the country, Chittagong City has developed partly in hilly area and rest on the coastal plain. The area is bounded by longitudes $91^{\circ} 46'$ to $91^{\circ} 50'$ and latitudes $22^{\circ} 22'$ to $22^{\circ} 29'$ (Fig. 1). Hills are mostly composed of loose and weathered Tertiary (65 m.y.–1.8 m.y.) sedimentary rocks prone to landslides. In and around Chittagong City more than 200 people killed due to landslides between the years 2006 and 2013. Rainfall induced landslides are common here like in other tropical mountainous regions of Southeast Asia (Brand et al. 1984; Guidicini and Iwasa 1977; Lumb 1975).

R.M.E. Ali (✉) • S. Akter • M.M.H. Khan • M.Z. Uddin
Geological Survey of Bangladesh (GSB), 153 Pioneer Road,
Segunbagicha, Dhaka 1000, Bangladesh
e-mail: reshadekram@gmail.com; salma.akter_gsb@yahoo.com;
apu.gsbdu@gmail.com; zohir.uddin@gmail.com

L.W. Tunbridge • R.K. Bhasin
Norwegian Geotechnical Institute (NGI), P.O. Box 3930, Ullevaal
Stadion, 0806 Oslo, Norway
e-mail: Lloyd.Tunbridge@ngi.no; Rajinder.Kumar.Bhasin@ngi.no

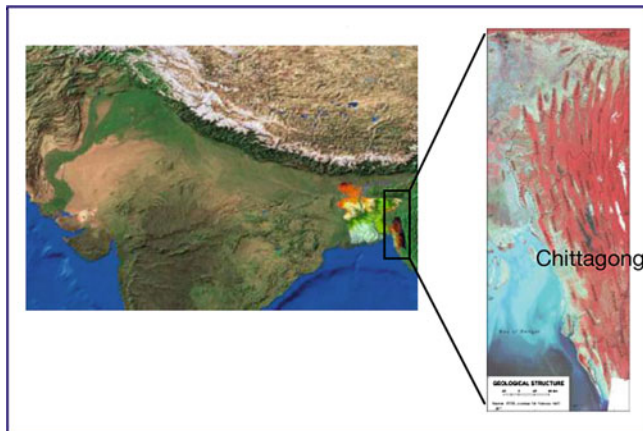


Fig. 1 Location map of Chittagong area

The purpose of the investigation is to find out the causes of landslides, landslides hazard zoning and to establish a landslides early warning system to save lives and properties. Study includes development of a landslides zoning map of Chittagong City and establish a network of automatic rain gauges for landslides early warning. Moreover, the scope of the study is to help the policy makers, engineers, town planners and geologists to build a reasonably geo-hazards free safe hilly city.

The climate of the area falls under tropical monsoon climate. The mean monthly maximum and minimum temperature ranges between 78.76 to 90.44 °F and 55.88 to 77.38 °F. The monthly average minimum and maximum rainfall is 0.66 mm (January) and 74.70 mm (July) respectively. The yearly average rainfall is about 279.65 mm (Anonymous 2010). The northwester and monsoon are mainly responsible for the rainfall in the area. About 90 % of yearly rainfall occur between the months of June and October.

The geological and geotechnical behavior of the landslide materials and nature of failures have been studied in detail. Landslide areas have been plotted on the geological map of the area and correlated with the regional geology and geological structure of the area. The geological structures, rock types, nature of weathering, groundwater condition of the area have also been studied for landslide hazard zoning of the area.

Most of the landslides are triggered by rainfall. Event based rainfall data of the area has been collected and analyzed to determine the threshold values of rainfall to trigger landslides. Accordingly an automated rain gauge network has been installed in the area to warn people via mobile phone to local administration and first responding organizations to take necessary steps to save lives and properties from potential landslide hazard.

Geomorphology and Geology of the Area

Tectonically Chittagong area is along the western edge of the tectonically active Tripura-Chittagong Folded Belt (Guha 1978). The folds are mostly tight, plunging and faulted in

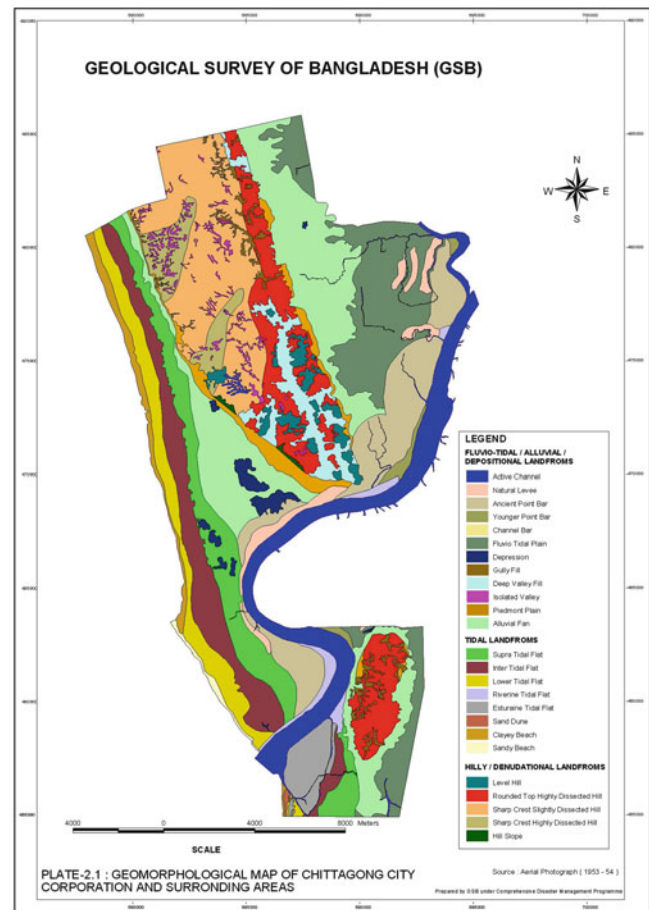


Fig. 2 Geomorphological map of Chittagong city and its environs

nature with NNW-SSE alignment (Karim et al. 1990). Chittagong City can be divided into three broad distinct geomorphological divisions: (1) hilly area (2) fluvio-tidal plain and (3) tidal plain (Fig. 2). For landslides investigation only hilly areas have been considered. Chittagong City is located in the southern plunging part of the Sitakund Anticline. The anticline is asymmetrical and has steeper western (faulted) flank and gently sloping eastern flank. The folded sediments are highly twisted and distorted in the plunge area around the city (Muminullah 1978; Hasan 1981).

Around Chittagong City, from east to west, exposed geological formations are Dihing Formation, Dupi Tila Formation, Tipam Sandstone and Bokabil Formation (Alam et al. 1990). Under different environments, these formations (Fig. 3) were deposited in Mio-Pliocene time (25 m.y.–2 m.y.). As a result their rock types as well as their geotechnical properties are different. Moreover, since its deposition, the rocks have experienced different climatic changes as well as tectonic activities, which ultimately influenced the geotechnical properties of the rocks. Locations of landslides on landslide hazard zoning map of Chittagong city indicate that most of the landslides occurred in sandstone of Dupi Tila Formation of zone II (Fig. 4).

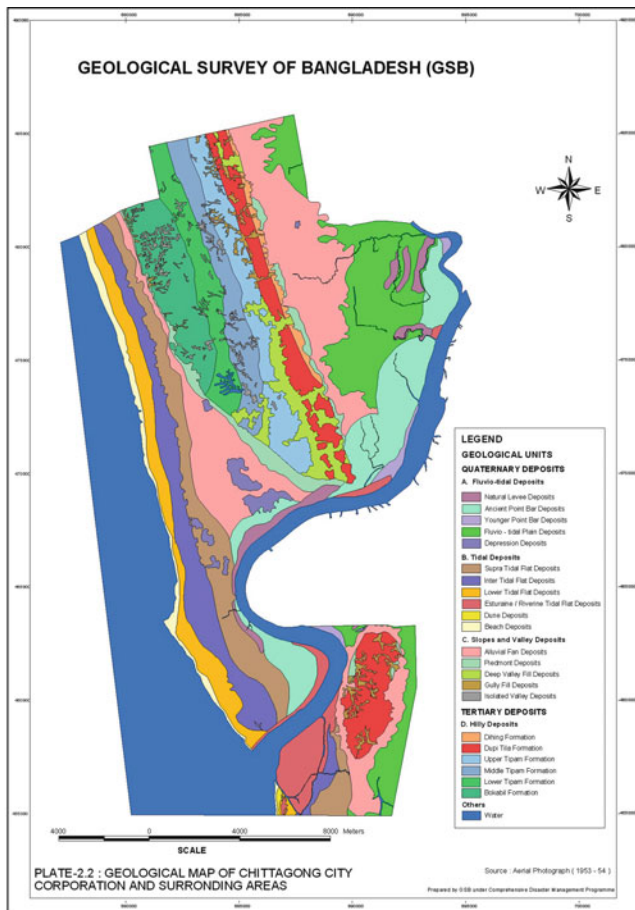


Fig. 3 Geological map of Chittagong City and its environs

The hills of Dupi Tila Formation have a rugged topography formed of numerous ridges and valleys. The hills are dome shaped with flat top having an average elevation of about 30 m from the ground. The lengths of the hill slopes are very short (15–50 m) and their gradient varies from 10° to 40° . The profile of the slopes is concave to convex and finally fairly regular. Two types of valleys developed here. V-shaped valleys having higher gradient in the eastern side than the western. Valleys across the strike are symmetrical, shallow, U-shaped, open and smooth. The hills are rolling type with sub dendritic medium dense drainage system (Karim et al. 1990).

Description of Landslides

Most of the landslides are small in size but there are number of slides at each location. Repeated landslides one after another at some locations might be the main cause of high death toll. In most cases once a landslide happened, people start rescue operation but subsequently another landslide buried even the rescuers.

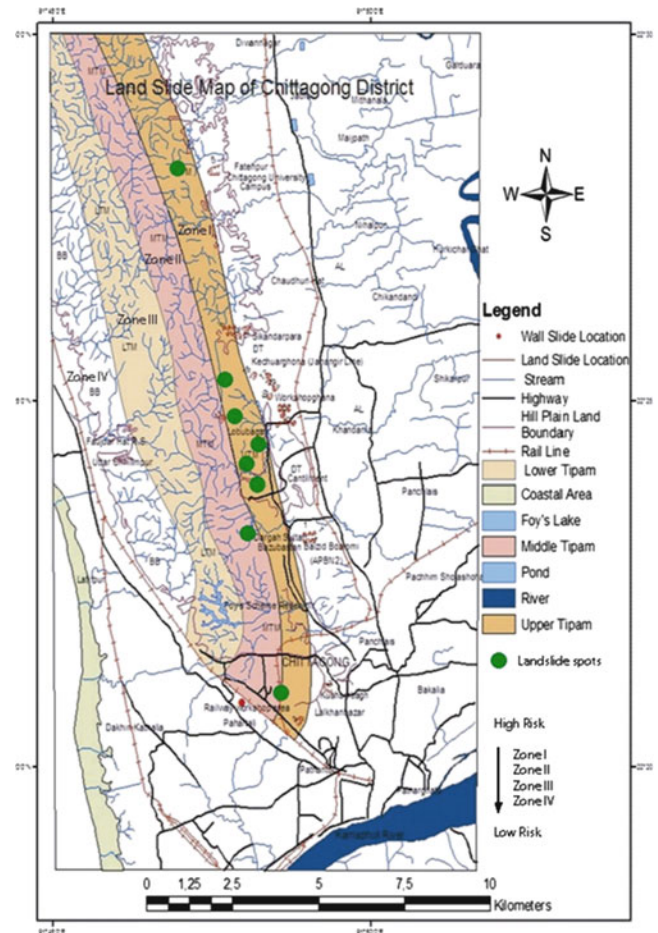


Fig. 4 Landslide hazard zoning map of Chittagong City and its surroundings

Most of the landslides were initially slide type but finally terminated as dry flow, only exception was some rock falls in some places. In many places around the city slopes were almost 90° due to hill cutting and a combination of slide and fall and finally flow have occurred over the adjacent area.

Each landslide has well-developed main scarp and surface of rupture. The slope materials are loose sandstone with little or no silty shale or shale. High permeability of slope materials allows rainwater to infiltrate easily. Most of the hill slopes were barren except small bushes and grass cover sparsely. The heights of main scarps are about 1 m or less. In some places above the main scarps, lunar cracks developed in the crown of the landslides. At these lunar cracks rainwater infiltrated more and more to initiate the surface of rupture. The main bodies of the landslides are generally free from minor scarp and debris. Sediments slide with extraordinary rapid movement under the influence of gravity rolled over the hill slopes and started to flow over the gentle part of the slopes.

Causes of Landslides

The causes of landslides mostly related to the change in hillside equilibrium. The three factors that influence stability of hill slopes are (Coates 1981).

Internal Properties of the Earth Materials

Landslides have mostly occurred along N-S alignment in the eastern part of the city. Around Chittagong City Dupi Tila, Tipam and Bokabil formations are exposed. But landslides occurred mostly in sandstone of Dupi Tila Formation. Sandstone consists of 52–74 % medium to coarse sand, 28–45 % fine sand and only 2–4 % silt. Field investigation and laboratory tests indicate landslides happened in sandstone that consists of very little or without silt and clay. Sands are medium to coarse grained, poorly sorted, moderately weathered, loose with no cementing materials, highly porous and permeable and easily powdered between the fingers indicates little bond strength between individual particles. It is massive, joints and fractures are not common but occasionally with inter-bedded iron bands. Unconfined compressive strength, cohesion and angle of internal friction of sandstones ranges from 1.2 to 1.8 kgf/cm², 0.0459 to 0.0801 kg/cm² and 32.3° to 34.3° respectively. Hezen's uniformity coefficient is less than 2. Specific gravity ranges from 2.39 to 2.57 and permeability ranges from 0.2116 to 0.5184 cm/s.

Geomorphic Setting and Environment

The area is characterized by low dome like hills with flat top. The flanks of the hills are very short in length (15–50 m). Natural slope angle of landslide areas varies from 34° to 84° but most of the slopes are more than 40° which is greater than the average values of angle of internal friction of slope materials (26°–34°). Therefore, under natural condition slopes were unstable. The profile of the slopes is concave at the top, convex at the middle and fairly regular at the bottom. The valleys and gullies, which follow the east-west direction are shallow U-shaped, open and smooth. The valleys trending north-south are relatively deeper and V-shaped, elongated and parallel to the strike of the bedding. The hills are rolling type with sub-dendritic and medium dense drainage. The hill slopes are devoid of large trees and covered with grass and shrub type vegetation.

Independent External Factors

External factors are triggering factors those cause landslides. The three most common triggering mechanisms of landslides

are excessive precipitation, human activities, and earthquakes. There is no record of earthquakes on or close to the day of landslides. Human activities like hill slope cutting and deforestation are common. Chittagong city is familiar with excessive precipitation within a short period of time, the important triggering factor for landslides impact.

The magnitude, intensity and duration of the rainstorm play a role in determining whether a hill slope will fail or not. Rainfall lubricates and increases the weight of slope materials. Excessive rainfall weakens earth materials by displacing air and increasing the pore water pressure along shear surfaces. Conditions that enhance ultimate failure occur when surface materials are porous and permeable and are underlain by materials of low permeability. Absence of inadequate drainage of rainwater also causes more infiltration into the ground.

Mechanism of Landslides

The slopes were almost barren, rainwater easily infiltrated into the slope materials that ultimately increased the pore water pressure. As a result, crown cracks developed on top of hills, cracks allow more and more water to infiltrate into the materials. Continuous heavy rainfall resulting pore water pressure exceeded the shear resistance of the slope materials. Landslides began to start when this shear resistance threshold is exceeded by pore water pressure.

The pore water pressure normally developed in the convex part of the slope. As the pore water pressure exceeded the resistance of the materials, the slope materials started to move. Initially, the convex parts of the slope materials with huge volume of water began to slide and jumped over the concave part and eventually on fairly regular part (settlement areas) of the slope. Sediments slide with extraordinary rapid movement, destroyed and buried people and houses and finally the slide terminated as dry flow due to non-cohesive nature of slope materials. The stages of development of landslides can be summarized as below:

- Due to heavy rainfall, rainwater easily infiltrated into the slope materials that increased pore water pressure.
- Crown cracks developed on top of hills, cracks allow more and more water to infiltrate into the materials.
- Resulting pore water pressure exceeded the shear resistance of the slope materials.
- Landslides began to start when this shear resistance threshold is exceeded by pore water pressure.

Landslides Prevention and Control

Choice of landslides prevention and control measures depend upon the geological condition, physiography, available technology and above all the socioeconomic condition

of the people. According to Donald R. Coates (1981), important methods of landslides prevention and controls are:

Avoid Method: If slope is really dangerous and landslides control measures are costly, the only viable solution is complete avoidance of the area.

Water Control Method: Normally rainwater infiltrates into the soil materials of slopes and make them vulnerable to landslides. Proper drainage of rainwater from the slope instead of infiltration into the soil can reduce considerable landslide vulnerability. This can be achieved easily by afforestation and construction of appropriate drainage structures.

Excavation Method: The main objective of excavation method is to make slope stable by modifying the slope angle so that angle of internal friction of the slope materials is higher than the slope angle.

Retaining Structure: Important structures for slope stability are by buttresses, shear keys, retaining walls, guide walls etc.

Miscellaneous: These are the special methods for slope stability normally used for specific cases which include grouting, electro-osmosis, temperature changes, etc.

Best prevention method for Chittagong area will be complete avoidance of dangerous slopes. Second option will be excavation method that suggests reshaping the slope so that the slope angle is less than the angle of friction of slope materials. Thirdly retaining structures like retaining wall, guide walls or buttresses can be constructed here to protect the slopes from further landslides. Above all to develop real time landslides early warning should be the best option to save lives.

Landslides Susceptibility Zoning and Early Warning

On the basis of rock types, their geotechnical properties and locations of past landslides, hilly part of Chittagong City and its surrounding areas have been classified into four zones. These zones are very closely correlated with the geology of the area. Depending on past landslides data, Zone I is most dangerous and Zone IV is comparatively less dangerous for landslides hazard. In Zone I rock type is mostly loose, highly weathered sandstone and Zone IV is mostly compacted shale. Considering the age of the rock types, Zone I is younger than Zone IV (Fig. 4).

Under present situation, it is most important to save people and properties from the potential hazard of landslides. To this purpose the Geological Survey of Bangladesh (GSB) and the Norwegian Geotechnical Institute (NGI) are working together to reduce the risks from landslides in Chittagong City. Rainfall induced landslides are common phenomenon in Chittagong and in adjoining areas where scores of people are being killed each year due

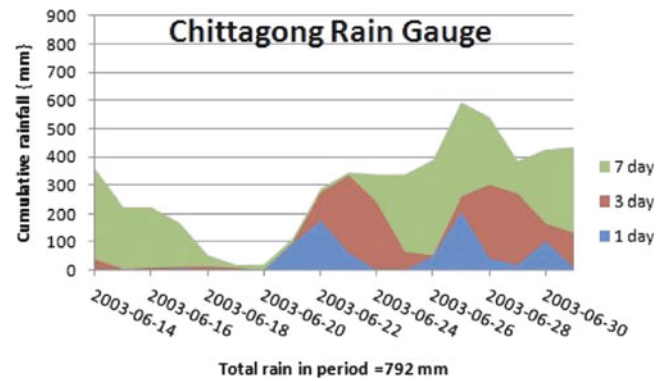


Fig. 5 Statistical analysis of rainfall data

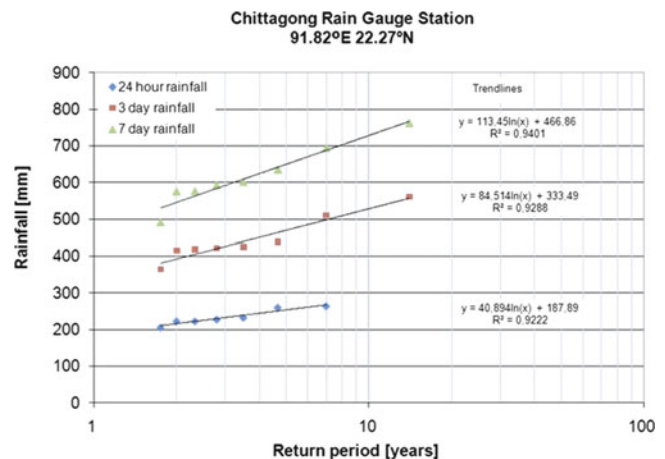


Fig. 6 Return periods analysis of extreme rainfall events

to landslides. The co-operating partners have developed an early warning system to forecast rainfall induced landslides in Chittagong so that people can be aware of impending landslides beforehand.

Event based rainfall data are statistically analyzed (Figs. 5 and 6) to determine the Rainfall Threshold Values for landslides (Table 1)

Automatic rain gauges for Landslides Early Warning have been installed in Chittagong City Corporation and Chittagong University Campus which record rainfall data every 15 min and send it to an online system. In addition, the rain gauges have been programmed to send SMS messages to registered mobile phones of ten organizations/personnel as soon as the rainfall thresholds, which have been set-up in the system are exceeded.

Rainfall Threshold Values for Chittagong City are:

3 h: 100 mm

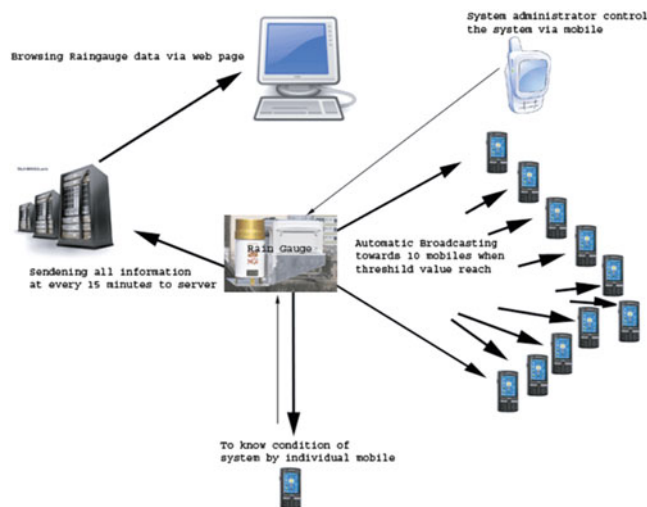
24 h: 200 mm

3 Day: 350 mm

These rain gauges send real time early warning to the registered mobile phones so that first responding organizations can take action straight away before landslides

Table 1 Results of statistical analysis of rainfall data

Chittagong Rainfall (mm)				
	Return Period (years)			
Period	1	2	3	4
7 Day	467	545	591	624
3 Day	333	392	426	451
1 Day	188	216	233	245

**Fig. 7** Schematic diagram for landslide early warning system

happen. This is intended to facilitate the evacuation of the people residing close to landslides prone areas. The automatic rain gauges installed in Chittagong are receiving power from a solar panel to charge the batteries and requires only mobile telephone coverage at the installed location. The stations work with standard mobile telephone SIM cards and do not require any special infrastructure from the local mobile telephone operator (Fig. 7).

Conclusions

Heavy rainfall in short span of time is the main cause of landslides in and around Chittagong City. At the same time, the geotechnical properties of the slope materials (loose, well-graded sand, low internal friction angle, high permeability and porosity, and weathering characteristics) are also responsible. In some cases, hill cutting accelerates the process of landslides but was not the main cause of landslides.

Depending on geology, geotechnical properties of rocks and locations of landslides in Chittagong City and its surroundings, the area have been classified into four landslide hazard zones. Of these, Zone I is more

susceptible to landslides and Zone II, III and IV are comparatively less susceptible progressively.

Rainfall is the main triggering factor of landslides and it is statistically calculated that 100 mm rainfall in 3 h, 200 mm in 24 h and 350 mm in 72 h can be the thresholds values of rainfall to warn the people before landslides happen.

Accordingly two automated rain gauges have been installed in and around Chittagong City. If threshold values exceed, the system automatically send landslide early warning to ten selected mobiles of local administration and first responding organizations so that they can alert people in advance before landslides. The ultimate goal is to save the people from landslide disaster and build a landslide resilience community.

Acknowledgement Authors are indebted to Ms. Moonira Akhter Chowdhury, Director General, GSB for her kind permission to present and publish the paper. Thanks to Government of Bangladesh and Norwegian Ministry of Foreign Affairs to provide fund to establish and run the Landslides Early Warning in Bangladesh. Thanks to Ms. Shahtaj Karim, Assistant Director, GSB for her support to prepare the paper.

References

- Alam MK, Hasan AKM, Khan MR, Whitney JW (1990) Geological map of Bangladesh. Geological Survey of Bangladesh, Dhaka
- Anonymous (2010) Statistical yearbook of Bangladesh, Bangladesh Bureau of Statistics, Dhaka
- Brand EW, Premchitt J, Phillipson HB (1984) Relationship between rainfall and landslides in Hong Kong. In: Proceedings of the IV international symposium on landslides, vol 1. Toronto, pp 377–384
- Coates DR (1981) Environmental geology. Wiley, New York
- Guha DK (1978) Tectonic framework and oil and gas prospects of Bangladesh. In: Proceedings of the 4th annual conference, Bangladesh Geological Society, pp 65–75
- Guidicini G, Iwasa OY (1977) Tentative correlation between rainfall and landslides in a humid tropical environment. Bull Int Assoc Eng Geol 16:13–20
- Hasan AKMS (1981) Slope instability and construction damages at Mercantile Marine Academy Chittagong District, Bangladesh. Records of the Geological Survey of Bangladesh, vol 3. part-1, Dhaka
- Karim MF, Ahmed S, Olsen HW (1990) Engineering geology of Chittagong City, Bangladesh (Unpublished Report). Geological Survey of Bangladesh, GSB/DATA/UR No.-408
- Lumb P (1975) Slope failure in Hong Kong. Q J Eng Geol Hydrogeol 8:31–65
- Muminullah M (1978) Geology of Northern part of Chittagong District Bangladesh. Records of the Geological Survey of Bangladesh, vol 2. Part-3, Dhaka

Part VIII

Side Events



Introduction: Session D1-D4—Side Events of World Landslide Forum

Bin He and Kyoji Sassa

Abstract

The session of Side Events is a first try in WLF3. Totally, there are five side events in WLF3: Student Session; Landslide Teaching Tools; Dialogues on Country Landslide Issues; SATREPS Project “Development of Landslide Risk Assessment Technology in Vietnam”; Inter-graduate School Program for Sustainable Development and Survivable Society (GSS), Kyoto University. For the session D1-D4, 32 abstracts are submitted and 18 full papers are contributed by landslide researchers from different parts of the world. This introductory paper provides a brief overview on the D section of the WLF3 volume.

Keywords

Landslides • Forum • Side events • D session

Introduction of Session D

Student Session

Conveners: Bin He, Hongjian Liao, Sangjun Im, Oleg Zerkal, Chunjiao Wang, Dwikorita Karnawati.

In the student session, professors are invited to participate and the students are encouraged to build networks among their peers to discuss their research and findings. The students will have an opportunity to give a technical oral presentation on their research which will facilitate cooperation within the landslide research. An award will be given to the best oral presentation in this student session.

B. He (✉)

Key Laboratory of Watershed Geographic Sciences, Nanjing Institute of Geography and Limnology, Chinese Academy of Sciences, Nanjing 21008, China
e-mail: hebin@niglas.ac.cn

K. Sassa

International Consortium on Landslides, Kyoto 606-8226, Japan

Landslide Teaching Tools

Conveners: Kyoji Sassa, Ko-Fei Liu, Nmsi Arambepola, Fausto Guzzetti, Osamu Nagai, Bin He.

ICL is developing Landslide Teaching Tools to facilitate landslide education. The Teaching Toolbox contains five parts: (1). Mapping and Site Prediction, (2). Monitoring and Early warning, (3). Testing and Numerical Simulation, (4). Risk Management and Others, (5). Country Practices and Case Studies. The Teaching Toolbox contains three types of tools.

- TXT-tools consisting of original texts with figures
- PDF-tools consisting of already published reference papers, manuals, guidelines, and others
- PPT-tools consisting of PowerPoint® files made for lectures.

The initial TXT tools was published as a full color booklet in 405 pages. PDF tools and PPT tools are contained in DVD. Each tool has its own Identifiers consisting of country number, organization number and tool number. The contributing organization maintains a copyright of its teaching tool and shall update and improve the content periodically. New members can contribute their teaching tools with their own identifier number. The ICL teaching tools will be enhanced and improved as the effective and practical tools.

Dialogues on Country Landslide Issues

Conveners: Srikantha Herath, Hiromitsu Yamagishi, Luis Eveline, Pavle Kalinić, Saowanee Prachansri, Dangsheng Tian, Adil Neziraj, Mohd Jamaludin Md. Noor, Madhav Karki, S. Diop.

The WLF3 is not only about the presentation of research papers. This session is planned to give an opportunity for open discussion on a country's landslide issues and exchange experiences between different countries. Practitioners, government officers, community leaders, and individuals tackling landslide disasters as well as landslide experts who have completed investigations in other countries and cooperated for landslide disaster reduction are invited to present and exchange their experiences with other participants. Please be free to contact with "ICL-Network" < icl-network@iclhq.org > as well as D3 conveners.

SATREPS Project "Development of Landslide Risk Assessment Technology in Vietnam"

Conveners: Kyoji Sassa, Van Tien Dinh, Toyohiko Miyagi, Hirotsuka Ochiai, Do Minh Duc.

The Government of Japan founded a new SATREPS (Science and Technology Research Partnership for Sustainable Development) programme to cooperate with developing countries to solve global issues including disaster reduction. One of the ongoing projects is "Development of Landslide risk assessment technology in Viet Nam". The Vietnam project includes four groups of mapping, testing, monitoring and integration and teaching aspects. The project plans to develop new technology and equipment which can be practically used in the cooperation between countries through technological development, education, and donation of equipment. Those who are interested in this project are invited to participate in this session.

Inter-graduate School Program for Sustainable Development and Survivable Society (GSS), Kyoto University

Conveners: Hiroshi Fukuoka, Kaoru Takara.

This session introduces an interdisciplinary 5-year graduate school program, which Kyoto University has launched in cooperation with nine graduate schools (Education, Economics, Medicine, Science, Engineering, Agriculture, Asia and African Area Studies, Informatics, and Global Environmental Studies) and three research institutes (Disaster Prevention, Sustainable Humansphere, and Southeast Asian Studies) of the university. This GSS (Global Survivability Studies, for short) program intends to produce excellent global leaders in safety and security areas, providing

graduate students with various opportunities such as field exercise, internship training, interdisciplinary seminars, international school programs, university-industry projects, and international cooperation projects in four major areas of interest in the framework of GSS: natural hazards and disasters, man-made disasters and accidents, regional environmental degradation, and food security, which we are facing as global/regional threats in the world. Higher education matters are also discussed in this session.

Compendium of Seven Papers Contributed to D Section of WLF3 Volume

Detection of Active Landslide Zone from Aerial Photograph Interpretation and Field Survey in Central Provinces of Vietnam

Field survey activities are very important to verify the characteristics of the landslides. Through such activity researchers can evaluate probability of landslide occurrence, recognize active zones, and the type, size and main factors contributing to landslides. This paper (Luong et al., 2014) has attempted to explore the distribution of landslides along Ho Chi Minh road and how the distribution relates to these controls. With regard to most of the landslides in the study area, the authors recognized the presence of coal layers within a landslide left exposed on slopes after landslides occurred. The slip surface of the landslide has the tendency to parallel the bedding plane with thin beds or lenses of coal shale. From aerial photographs, 28 landslides were recognized and the initial characteristics of landslides were analyzed.

Numerical Assessment of Shallow Landslide Using the Distributed Hydrological-Geotechnical Model in a Large Scale

A hydrological-geotechnical modelling system was applied in Kyushu (Japan) using observed rainfall for a regional shallow landslide prediction system (Luo et al., 2014). The physically based distributed landslide model has been developed by integrating a grid-based distributed kinematic wave rainfall-runoff model with an infinite slope stability approach. The resulting time-invariant landslide susceptibility map shows good agreement with the spatial patterns of observed landslides in Kyushu region. Application of the model to calculate the shallow landslides shows that the model can successfully simulate the effect of rainfall movement and intensity on the spatiotemporal dynamic of hydrological variables that trigger shallow landslides. The result of this study can be used to develop the potential applicability of the modelling system for shallow landslide disaster predictions and warnings.

Simulation of a Rapid and Long-Travelling Landslide Using 2D-RAPID and LS-RAPID 3D Models

Two process-based computer numerical models for simulating the generation and propagation of landslide are developed by integrating the initiation process triggered by rainfalls and/or earthquakes and the development process to a rapid motion due to strength reduction and the entrainment of deposits in the runout path (He et al., 2014). They were applied in a rapid and long-traveling landslide, which occurred on 17 February 2006 in the southern part of Leyte Island, Philippines. As simulation results, the application of these two simulation models could reproduce well the initiation and the rapid long runout motion of the Leyte landslide. However, for the deposition area, the 2D landslide model resulted in a higher and narrower mass volume than the 3D landslide model. The distributional information of soil parameter can be set and the 3D view of the calculated landslide initiation and runout can be successfully achieved in LS-RAPID 3D Model. Each of these different dimensional landslide models has its respective advantages and disadvantages depending on the target study area and the type of the area.

The Influence of Countermeasure on Debris Flow Hazards with Numerical Simulation

The numerical simulation of the influence of countermeasures on debris flow hazards was demonstrated with a case study of the Taipei DF024 potential debris flow torrent (Wu and Liu, 2014). This torrent would be considered as straight in many simulations. However, unlike the one-dimensional model reported in previous literatures, the two-dimensional debris flow model, Debris2D, is applied for simulation. Two simulation conditions, with and without countermeasure, are compared. Comparing the results of two simulation conditions, we find Debris2D is able to reflect the variation of local topography. In 2D simulation, some locations identified to be safe by the 1D simulation, were identified as disaster potential areas. This means a 2D model is required for debris flow hazards simulation for evaluation of the countermeasure design efficiency, even for a straight channel.

Study on Strength and Deformation Behavior of Loess Slope Supported by Micropiles

Based on the practice of application of micropiles in slope support engineering and a large-scale field experiment, some factors influencing the reinforcing effect of micropiles in step-shaped slope were studied with FLAC software, using

finite difference method (Tian et al., 2014). Firstly, referring to the scale of the large-scale field experiment, a numerical model was established and calculations were performed to study the effect of slope angle, slope height and load position on the slip surface in order to determine the location of slip surface based on the loads applied on the top of the slope. Then, micropiles were arranged on the step-shaped slope based on the critical slip surface, and the ultimate bearing capacities of the slope with or without micropiles and with different numbers of micropiles were calculated, and the failure modes of step-shaped slope were analyzed. The reinforcing effect of micropiles with the variation of soil cohesion and internal friction angle was also studied.

The Simulation of a Deep Large-Scale Landslide Near Aratozawa Dam Using a 3.0 MPa Undrained Dynamic Loading Ring Shear Apparatus

The mechanism of the deep and large-scale landslide near Aratozawa dam (Japan) was analyzed through a physical laboratory experiment (Setiawan et al., 2014). Deep landslide simulation is conducted by applying high normal stress to address the assumed slip surface of 150 m depth in the Aratozawa case. The 3.0 MPa undrained dynamic loading ring shear apparatus with the high pore-water pressure controlled is used to meet the criteria of deep-seated landslide of Aratozawa. The effect of groundwater fluctuation and the inter-linkage with the reservoir in the Aratozawa dam was found to be the main concern besides the peak ground acceleration based on the 2008 landslide event. Results also show that there was no significant deformation in the Aratozawa dam area when the large Tohoku earthquake, magnitude 9.0, in 2011. Indication is, that the slide blocks, ridges and mass depression due to the 2008 event are already stable. However, the slope and soil mass movement are still possible in the future.

Stability Analysis of a High Slope Along a Loess Plateau Based on Field Investigation and Numerical Analysis

A landslide along a high loess plateau is studied by the method of field investigation, laboratory test and numerical analysis (Ma et al., 2014). Based on the information from field investigation and the results of laboratory test, three-dimensional stability analysis of the high loess slope is analyzed using the FLAC3D code and UST model. The influence of the ground water level variation and the seepage flow on the slope stability is analyzed. The calculation results of the ground water level variation suggest that the

slope reaches an equilibrium state after a certain amount of deformation is yielded. However, the displacement increased significantly and the failure of the high loess slope occurred suddenly when the seepage flow is taken into account. The analysis results of this paper indicated that it is necessary to reduce the reclamation and irrigation along the boundary of the loess plateau, and the stability of the high loess slope along the loess plateau could be ensured.

References

- He B, Sassa K, Nagai O, Takara K (2014) Simulation of a rapid and long-travelling landslide using 2D-RAPID and LS-RAPID 3D models. In: Sassa K (ed) *Landslide science for a safer geo-environment: Vol. 1: International program on landslides*. Springer, Heidelberg
- Luo P, Apip, Takara K, He B, Duan W, Hu M (2014) Numerical assessment of shallow landslide using the distributed hydrological-geotechnical model in a large scale. In: Sassa K (ed) *Landslide science for a safer geo-environment: Vol. 1: International program on landslides*, Springer, Heidelberg
- Luong LH, Miyagi T, Abe S, Hamasaki E, Tien DV (2014) Detection of active landslide zone from aerial photograph interpretation and field survey in central provinces of Vietnam. In: Sassa K (ed) *Landslide science for a safer geo-environment: Vol. 1: International program on landslides*. Springer, Heidelberg
- Ma Z, Liao H, Ning C, Feng Z (2014) Stability analysis of a high slope along a loess plateau based on field investigation and numerical analysis. In: Sassa K (ed) *Landslide science for a safer geo-environment: Vol. 1: International program on landslides*. Springer, Heidelberg
- Setiawan H, Sassa K, Takara K, Miyagi T, Fukuoka H, He B (2014) The simulation of a deep large-scale landslide near Aratozawa dam using a 3.0 MPa undrained dynamic loading ring shear apparatus. In: Sassa K (ed) *Landslide science for a safer geo-environment: Vol. 1: International program on landslides*. Springer, Heidelberg
- Tian C, Liao H, Peng Y, Hao D, Peng J (2014) Study on strength and deformation behavior of loess slope supported by micropiles. In: Sassa K (ed) *Landslide science for a safer geo-environment: Vol. 1: International program on landslides*. Springer, Heidelberg
- Wu Y, Liu K (2014) The influence of countermeasure on debris flow hazards with numerical simulation. In: Sassa K (ed) *Landslide science for a safer geo-environment: Vol. 1: International program on landslides*. Springer, Heidelberg



Detection of Active Landslide Zone from Aerial Photograph Interpretation and Field Survey in Central Provinces of Vietnam

Hong Luong Le, Toyohiko Miyagi, Shinro Abe, Eisaku Hamasaki, and Van Tien Dinh

Abstract

Landslides are destructive and an annually recurring phenomena which cause disruption of traffic and fatalities along transport arteries in Vietnam, especially in central provinces of Vietnam. These landslides are caused by deep weathering processes, high precipitation and cut slopes. This paper presents a summary of our findings on some landslides in central provinces of Vietnam based on aerial photography interpretation and field surveys. It covers: (1) landform deformation features, (2) types, sizes and dynamic characteristics of moving masses, (3) geologic structure, (4) active zonation.

Keywords

Central Vietnam • Landslide mapping • Risk evaluation • Deep weathering • Geologic structures

Introduction

Landslides in mountainous areas and along transport arteries are a serious hazard. They seriously affect living conditions, resulting in loss of human life, substantial property damage and possible disruption of vital transport and communication links.

In central provinces of Vietnam, along the Ho Chi Minh road, landslides occur frequently. According to the Ho Chi

Minh project management unit's report, there are 1,600 landslides and slope failures which account for a total length of 146 km out of the 2,499 km-long Ho Chi Minh road. These are mostly concentrated along the 1,200 km from Quang Binh to Daklak province (central provinces of Vietnam). Many landslides result from the reactivity of aged landslides after slopes were cut for road construction. Most of them occur in the rainy season.

The area studied is located on the 35 km-long Ho Chi Minh road, between Prao and Thach My towns in the central provinces of Vietnam (Fig. 1). The area has a tropical monsoon climate with two seasons: a typhoon and high rainfall season lasting from September through March and a dry season lasting from April through August. The study area has an annual average temperature of 25.6 °C and receives an average rainfall of 2,300–2,800 mm. Rainfall is typically highest between October and November and lowest between January and April.

Geologically, the study area is situated at the edge of a Paleozoic fold belt known as the Truong Son Orogenic Zone, where the main deformation occurred during the early Carboniferous period. The geological structure has one complex and five formations: the Dai Loc complex, the A Vuong formation, Nong Son formation, Huu Chanh

H.L. Le (✉) • T. Miyagi
Tohoku Gakuin University, Izumi Campus/2-1-1 Tenjinzawa,
Izumi-ku, Sendai 0081, Japan
e-mail: lehongluong@gmail.com; miyagi@izcc.tohoku-gakuin.ac.jp

S. Abe
Okuyama-Boring Co. Ltd, 10-39, Shinmei-Cho, Yokote-Shi,
Akita-Ken 0081, Japan
e-mail: abe@okuyama.co.jp

E. Hamasaki
Advantech Co. Ltd, Aoba-ku, Sendai 0081, Japan
e-mail: hamasaki@advantech.co.jp

V.T. Dinh
Institute of Transport, Science and Technology, 1253 Lang road,
Dongda, Hanoi 084, Vietnam
e-mail: dvtien.gbn@gmail.com



Fig. 1 Location map of study area

formation, Khe Ren formation, Ban Co formation. These consist of gneiss/granit, siltstone, sandstone, mudstone, conglomerate and thin beds or lenses of coaly shale.

The high precipitation and fractured, weathered sedimentary rocks in this area make it extremely prone to landslides.

Identify Landslide by Aerial Photo Interpretation

100 black and white aerial photographs were used for interpretation and analysis of the area. They are named D2-99 and were taken in 1999. With this approach, landslides can be easily recognized. Geomorphological features associated with mass movements such as scarps, landslide bodies, gullies, trenches, debris flows and rockfalls can also be mapped. All the landslides could be distinguished as slides, flows or slope deformations. The state of activity of the landslides is classified as either active, inactive or dormant.

28 landslides were recognized as shown on Fig. 2. These were assigned numbers from 1 to 28. Some landslides were easy to recognize; landslide No. 18 for example has a very clear main scarp and side scarp. There is no talus deposit and no weathering shape modifications at the boundary scarp and the landslide body. The lower part is divided into three to four sub landslides and slide type changed into that of a debris flow. The upper half is a typical block, so the body has low levels of disturbance. In the case of landslide No. 1,

half of the scarp is very clear, and the remaining crown scarp is dissected. With others landslides, most crown scarps are dissected. Landslides No. 2, 3, 5 to 17 and from No. 19 to No. 28 are examples of this. A detailed map of the landslides in the study are presented in Fig. 2.

Inspection Sheet for Risk Evaluation

An inspection sheet (Fig. 3) was used for risk evaluation of potential reactivation based on an AHP approach, which involves the geomorphic factors within and outside of landslides. On the inspection sheet, some items, as key to the evaluation of the probability of landslide occurrence, were categorized as follows. The large categories of classification contains: (I) The micro landforms of the landslide body as an aspect of the characteristics of movement, (II) The boundary of major landslide landform components as an aspect of the time process, (III) The landslide topography and the adjoining environment as an index of geomorphic setting. They each have the medium classifications of nine categories; A: manner of movement, B: degree of sharpness C: degree of instability of landslide body, D: probability of direct feature of landslide action E: between the top edge of main scarp and the upper slope F: between the main scarp and the body, G: between the landslide body and the frontal slope, H: the toe part of landslide body, I: the lower part of landslide body. The items of the medium classifications further divided into small categories, which were checked indexes in the inspection sheet. Each classification was compared as a pair of items based on AHP. For convenience, the categories as shown on the inspection sheet are arranged from the left to the right. The detailed description of this inspection sheet can be seen in *Landslide Risk Evaluation and Mapping—Manual of Aerial Photo Interpretation for Landslide Topography and Risk Management* (Miyagi et al. 2004). The inspection sheet is basically used by highly-skilled engineers. In the case of landslide No. 18 (as mentioned in Fig. 3) the scores are a result of discussion by many engineers. The other landslides not yet discussed, so scores cannot be put into Table 1. The results show that landslide No. 18, has a high possibility of reactivation.

Field Work Surveys

Field work activities on the Ho Chi Minh road involved verifying the landslides that had been identified during preliminary aerial photo interpretation. Probability of landslide occurrence was evaluated, and geological structure was observed. The length, width, and depth of these landslides were inspected and recorded.

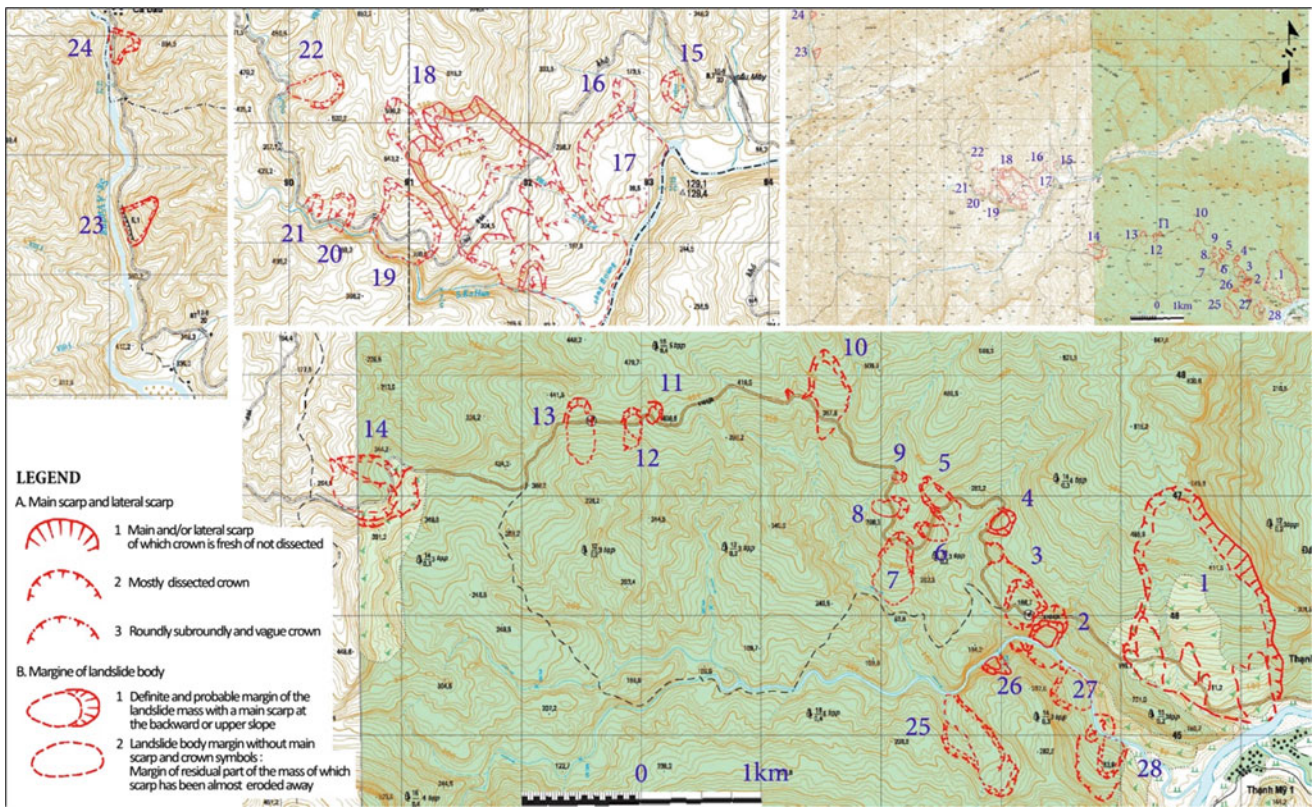


Fig. 2 Landslide distribution map along the Ho Chi Minh road

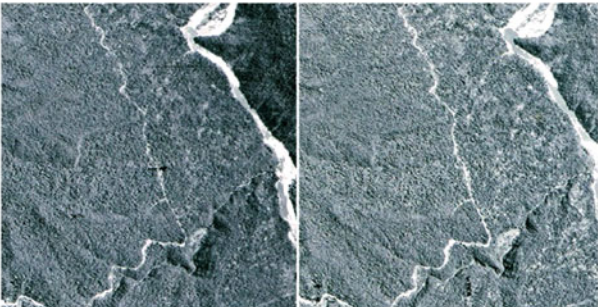
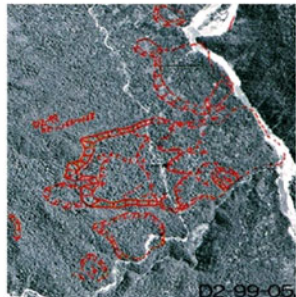
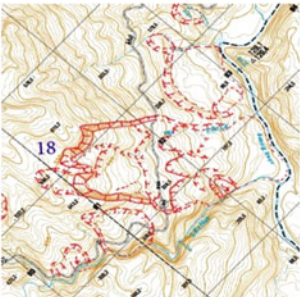
Inspection sheet		Inspection record sheet for landslide risk evaluation						LS No: 18		
LS No: 18 Aerial photo No: D2-99-05 (167-168) Date of aerial photo taken: 1999 Name of topographic map: Thon A So Topographic map scale: 1/25000		Major division	Main factor	Observation theme	Unstable factor			Remarks	AHP score	
 <p>Stereo pair aerial photograph</p>  <p>Aerial photo for making</p>  <p>Topographic map</p>		Micro landform features in landslide body	Characteristics of active landslide	A: Type of movement	Flow mound Pressure ridge 12,1	Minor scarp 4,9	Separation scarp Depression trench 2,0		8,5	
				B: Level of clearness and micro landform components within LS body	Huge no. of deformed blocks and clear micro topographic boundary 19,5	Clear micro-topography smooth boundary 12,5	Unlear blocks deformed block 6,0	Smooth boundary 5,5		15
				C: Level of stable	Head block separate from lower part 13,9	Gullies development 3,6	Linear erosion Development 1,5			10
				D: Direct features of movement	Cracks and scarlet 18,8	Tree crown deformation 6,3				16
				Other minor features	(Causes: Swamped land, Pond, Deformed, Crack, change?) surface development					
		Level of after moving deformation at major boundaries	Age distribution	E: Top edge main scarp	3,8	3,2	1,8	1,5	1,3	3,5
				F: Boundary of the main scarp and the body	3,1	1,8	1,1	0,6		2,5
				G: Boundary of landslide body and the front slope	1,0	0,5	0,4	0,3		0,5
		Landslide and adjacent environment	Geomorphic setting	H: Landslide body toe	8,6	4,4	1,6			4,4
				I: Change of the potential of instability at lower half of body	19,2	9,2	2,7			6
Particularly removable deformed block in landslide		Yes			Non (Total No. small blocks)					
Un-disintegrable meters Unaffected landform of landslide					Total points of AHP assessment			No. 66,4		
Risk of landslide occurrence base on your experience		Large → Middle → Small			Score by own inspector			No. 70,0		
Comment and view of each selection										

Fig. 3 Inspection sheet of risk evaluation based on an AHP approach to landslides on the Ho Chi Minh road

Table 1 Characteristics of landslide unit

LS No	Size (m)	Landslide type	Depth of slip (m)	Land cover	AHP score
01	1,000 × 2,000	Rotational rock slide	70–100	Degraded forest	
18	1,500 × 2,000	Rotational slide	70–150	Forest	70
19	260 × 260	Rotational slide	20–35	Forest	
20	100 × 250	Translational rock slide	3–15	Forest	
21	80 × 125	Translational rock slide	3–15	Forest	
23	250 × 350	Rotational rock slide	5–25	Shrubs and grass	

6 landslides (No. 1, 18, 19, 20, 21, 23) within 23 landslide points were observed in the field. Landslide No. 1, No. 19, No. 20, No. 23 are likely to be a rockslide (rotational-translational slide) formed by fractures and displacement of sedimentary rocks over a weaker layer (e.g. mudstone or coal layer). There is no other evidence of recent movement—trees on the landslide backwall are straight and not distorted, nor are there cracks in the ground. Thus, these landslides are classified as inactive.

In the case of landslide No. 21, no deformation or subsidence is present on the road and foot slope (Fig. 4) but there are some cracks (Fig. 5) on the crest slope. These cracks broke the concrete U-ditch along the crest slope and water effused from the landslide body was observed. Thus, the authors have assumed that though a small part of the upper side slope may be classified as active, it is nonetheless a shallow landslide and the overall landslide is inactive.

In the case of landslide No. 18, there is some evidence that can be observed on the western half of the field. These include, for example: the tilting retaining wall, some dislocations which appear at a certain part of the landslide body, some tilting trees and a considerable volume of water effusing from the middle part of the landslide body. The aerial photo shows that this landslide occurred once, a relatively long time ago, and was followed in 2007 by a reactivation landslide which damaged the road. After that, a retaining wall was put in place as a countermeasure, and concrete was used to strengthen the existing road. The countermeasures were, however, ineffective. The retaining wall was observed to be tilting, with a displacement of about 5–10 cm, and there were many cracks on the road and concrete pavement.

This evidence was observed to be distributed only upon the western half of the landslide area. This landslide is very large, about 1.5 km in width and 2 km in length. It may be the case, however, that all its parts may be inactive at present. Finally, the authors formed the conclusion that the western half of the landslide area must be more active than the eastern half (Fig. 6).

Based on field surveys, the authors agreed that the type of landslide in the study area is a translational-rotational slide. The size and type thereof were recorded and shown in Table 1.

**Fig. 4** No deformation or cracks on the road at landslide No. 21**Fig. 5** Cracks on top of slope and concrete ditch at landslide No. 21

Identifying Geological Structure and Making Observations on the Slip Surface

Geologically, (Fig. 7) the study area is mostly composed of Jura and Trias sedimentary rocks. The strata exposed in this area are the Nong Son formation and Ban Co formation. The

Fig. 6 Some evidence of landsliding was observed at a part of landslide No. 18

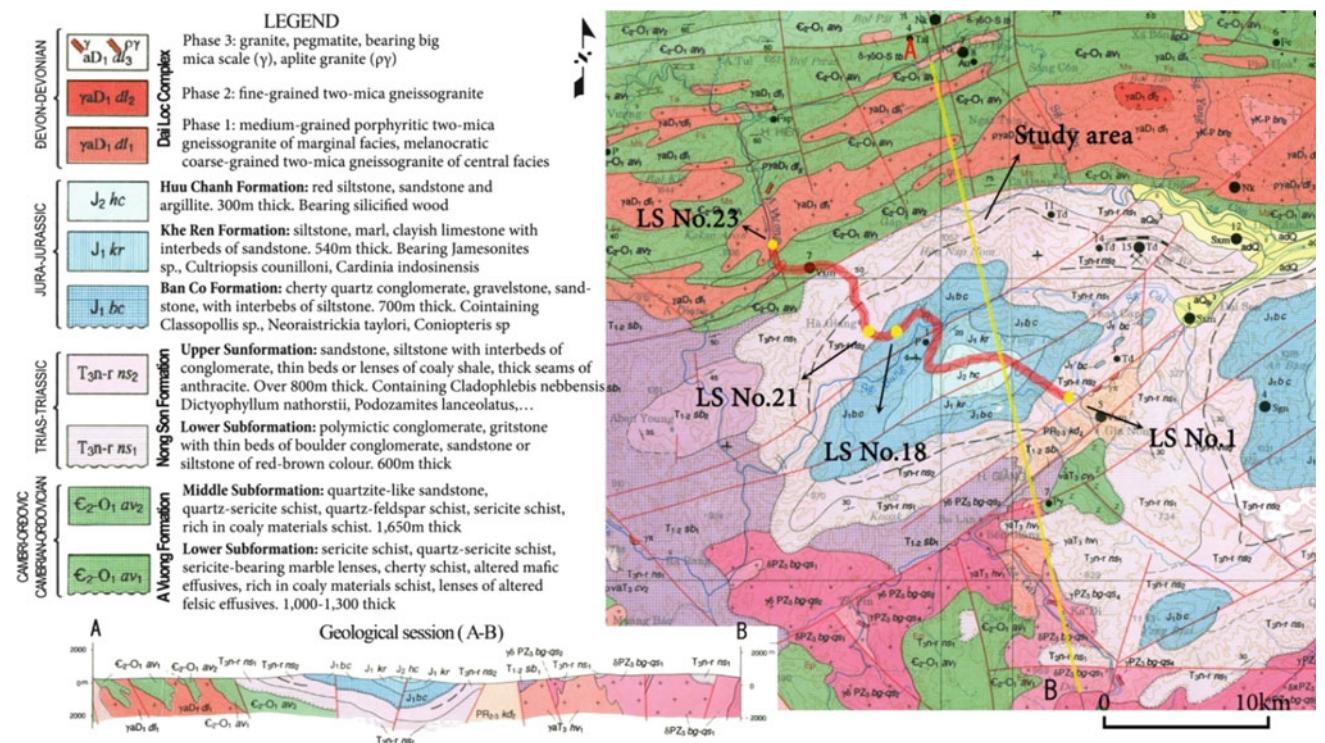


Fig. 7 Geological map of the study area (red colour line: Ho Chi Minh road, LS No. 1, etc: landslide location)



Fig. 8 Coal layer and fractured rock consisting of sandstone, mudstone and conglomerate on landslide No. 18

Nong Son upper formation consists mainly of sandstone and siltstone with interbeds of conglomerate, a thin bed of lenses of coaly shale, thick seams of anthracite; containing *Cladophlebis nebbensis*, *Dictyophyllum nathorstii* and *Podozamites lanceolatus*. The Ban Co formation consists of cherty quartz conglomerate, gravelstone, and sandstone, with interbeds of siltstone; containing *Classopollis*, *Neoraistrickia taylori*, *Coniopteris* (Geological and mineral resources map of Viet Nam 1995). This formation is easily traced in the field as shown in Figs. 8, 9 and 10. It is necessary to understand the bedding plane in order to understand the patterns and distribution of landslides within the study area.

Field observation shows that below the weathering crust about 1–5 m thick, on the upper sedimentary rocks layer, there are a lot of vertical joints (fractures). These fractures allow water and surface moisture to penetrate the rock and weaken mudstone, siltstone and the coal layer, causing an increase in weight, reducing the bonding strength between two layers and thus promoting failure. With regard to most of the landslides observed, the authors recognized that landslides extended into sedimentary rock and were a rotational or translational type of slide, formed by displacement of sedimentary rocks over a weaker layer (e.g. mudstone or coal layer). Of particular importance was the presence of coal layers, shale and mudstone within a slope/landslide between sedimentary rocks (sandstone, siltstone) as shown in Figs. 8, 9 and 10. The authors all assume this is a controlling factor causing landslides in the study area.

In the cases of most of the landslides observed in this study, the slip surface had been covered by debris, but it was exposed in landslide No. 20 and 21 (Fig. 9). In these cases,

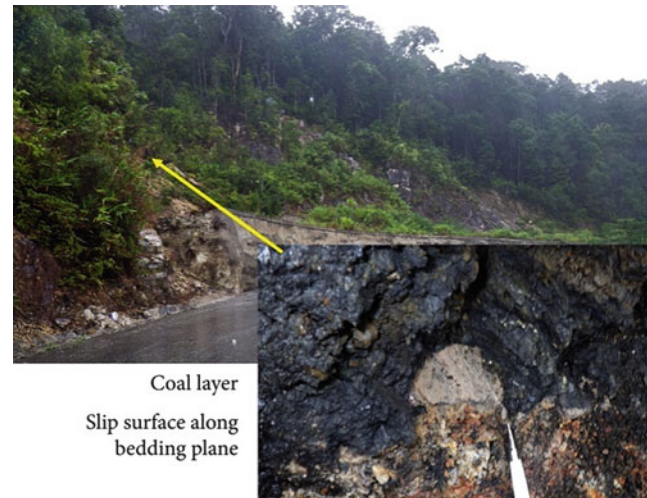


Fig. 9 Coal layer, landslide No. 20



Fig. 10 Coal layer, landslide No. 21

the slip surface is smooth and parallel to the bedding plane, and the strike and dip are $N45^{\circ}E$ and $15^{\circ}SE$. If this bedding plane is a keybed and controls landslides No. 15–21, we can calculate the depth of slip surfaces. For example: the depth of slip surface of landslide No. 15 is 109 m, landslide No. 16 45 m, landslide No. 17 104 m, and landslide No. 18 has a slip surface of 162 m. These results are not in accord with field observation and aerial photo interpretation, where the depth of slip surface often ranges from 1/10 to 1/7 as large as the width of a landslide. Thus, there may be at least two coal layers in this study area. This problem will be investigated during the next survey.

Conclusion and Discussion

From aerial photographs, the authors recognized 28 landslides along the Ho Chi Minh road and have formed initial characteristics of landslides: landform deformation features, types, sizes and dynamic characteristics of movement.

Field survey activities are very important to verify the characteristics of the landslides. Through such activity we can evaluate probability of landslide occurrence, recognize active zones, and the type, size and main factors contributing to landslides.

All landslides in the study area occur as translational-rotational slides of well-bedded sedimentary rocks such as mudstone, sandstone, siltstone and schist. The landslides reflect the controlling factors of bedding plane and weathering. This paper has attempted to explore the distribution of landslides in the study area and how the distribution relates to these controls.

With regard to most of the landslides in the study area, the authors recognized the presence of coal layers within a landslide left exposed on slopes after landslides

occurred. The authors assumed that this coal layer is a main factor in controlling and causing landslides.

The strata in the studied area are mainly bedded sandstone and siltstone. The slip surface of the landslide has the tendency to parallel the bedding plane with thin beds or lenses of coal shale.

References

- Geological and mineral resources map of Vietnam on 1:200,000 (1995)
General department of geology and minerals of Vietnam
- Miyagi T, Prasad GB, Tanavud C, Potichan A, Hamasaki E (2004)
Landslide risk evaluation and mapping—manual of aerial photo interpretation for landslide topography and risk management.
Report of the National Research Institute for Earth Science and Disaster Prevention



Numerical Assessment of Shallow Landslide Using the Distributed Hydrological–Geotechnical Model in a Large Scale

Pingping Luo, Apip, Kaoru Takara, Bin He, Weili Duan, and Maochuan Hu

Abstract

Kyushu is the third largest island of Japan. The natural hazards accompanied with geomorphic changes like landslides and debris flows occur at many places in Kyushu region. In this study, a hydrological–geotechnical modelling system was applied in Kyushu using observed rainfall for a regional shallow landslide prediction system. The physically based distributed landslide model has been developed by integrating a grid-based distributed kinematic wave rainfall-runoff model with an infinite slope stability approach. The resulting time-invariant landslide susceptibility map shows good agreement with the spatial patterns of observed landslides in Kyushu region. Application of the model to calculate the shallow landslides shows that the model can successfully simulate the effect of rainfall movement and intensity on the spatiotemporal dynamic of hydrological variables that trigger shallow landslides. The results of this study can be used to develop the potential applicability of the modelling system for shallow landslide disaster predictions and warnings.

Keywords

Numerical assessment • Kyushu • Large scale • Distributed hydrological–geotechnical model • Shallow landslide

P. Luo (✉) • K. Takara
Disaster Prevention Research Institute (DPRI), Kyoto University,
Gokasho, Uji City, Kyoto 611-0011, Japan
e-mail: luoping198121@gmail.com; takara.kaoru.7v@kyoto-u.ac.jp

Apip
Research Center for Limnology, Indonesian Institute of Sciences
(LIPI), Bogor, Indonesia
e-mail: apipkazumi@gmail.com

B. He (✉)
Key Laboratory of Watershed Geographic Sciences, Nanjing Institute
of Geography and Limnology, Chinese Academy of Sciences, Nanjing
21008, China
e-mail: hebin@niglas.ac.cn

W. Duan (✉) • M. Hu
Department of Civil and Earth Resources Engineering, Graduate
School of Engineering, Kyoto University, Kyoto, Japan
e-mail: duan.scut.cn@gmail.com; hu-maochuan@163.com

Introduction

Shallow landslides are one of the most dangerous hazards, occurring frequently with the conditions of heavy rainfall, steep slope, and unstable soil. Due to the increase of extreme rainfall under climate change, the shallow landslides are happening frequently. In previous studies, shallow landslides have been studied using many methods and assessed in many countries. Most methods for studying shallow landslides are divided into categories of statistical analysis, geophysical mapping, and modelling. Statistical analysis has been used for assessing shallow landslide susceptibility in Italy (Piacentini et al. 2012). For geophysical mapping, the Geographic Information system (GIS) is used for constructing the landslide inventory map and the spatial database in Korea (Park et al. 2013) and a demonstration of mapping regional, rainfall-triggered landslide susceptibility using a stress transfer mechanism in Taiwan (Liu and Wu

2008). For modelling methods, the application of radar data for modelling shallow landslides has been studied in Taiwan (Chiang and Chang 2009), the location of shallow landslides and their effects on landscape dynamics has been modelled and analysed in Northern New Zealand (Claessens et al. 2007), and a three-dimensional deterministic model has been applied in a mountainous area of Japan (Jia et al. 2012). The physically-based shallow landslides model is tested for its performance in a high resolution small-scale landscape in New Zealand (De Sy et al. 2013).

In this study, we use the distributed hydrological–geotechnical model to identify the location and deposition of the shallow landslide occurrences in Kyushu Island, Japan. In addition, the shallow landslides hazard/risk map that indicates Spatial Dynamic and Time-Variance of Potential Slope Instability Map and Shallow Landslide Probability Occurrence are assessed and presented by using the results from the modelling simulation and ArcGIS. The results of this research can provide scientific information for the policy makers and researchers on shallow landslides predictions and warnings.

Study Site and Data

Study Site

Kyushu Island is the southwest island of Japan. It is connected with the mainland and close to Shikoku Island. It is the third largest island in Japan. Kyushu Mountains are aligned in a north–south direction in the centre island and comprise the topography of Kyushu Island. At Kyushu Island, there are four large calderas which are called Aso, Aira, Ata, and Kikai calderas. The spatial distribution of rainfall in Kyushu Island is higher than for other regions in Japan. The Digital Elevation Model and the 120 selected Amedas rainfall stations are presented in Fig. 1a). There are stations at St. 82306 (KURUME), St.83431 (UME) and St.87426 (MIYAKONOJO) that are marked with red circles that are chosen to identify the trend of average daily rainfall from 2000 to 2008 (Fig. 3). The trend of average daily rainfall from 2000 to 2008 indicates that the most extreme rainfall is in July, August and September. During the summer season (July, August and September), the shallow landslides are frequently occurred due to the rainfall storms and typhoon events (Duan et al. 2014).

Data

The original Digital Elevation Model (DEM) and 100 m mesh land use data are obtained from the Ministry of Land, Infrastructure, Transport and Tourism (MLIT), Japan. The

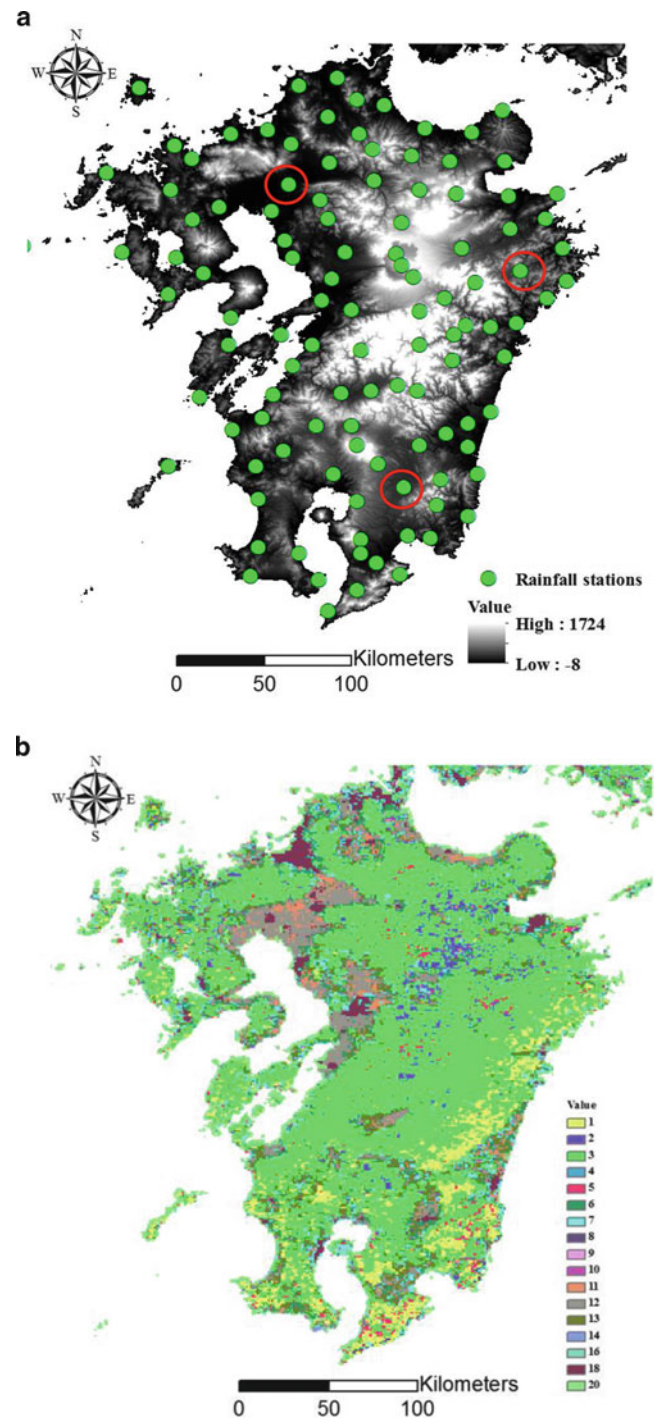


Fig. 1 (a) Digital elevation model and location of Amedas rainfall stations, (b) Land use map of Kyushu island

500 m resolution DEM and land use maps (Fig. 1b) which is resampled from the original DEM and 100 m mesh land use data are used in this study. The years of observed rainfall data from 2000 to 2008 of 120 selected Amedas rainfall stations is from the data provided by the Japan Meteorology Agency (JMA). The deposition of landslides map (Fig. 2) is

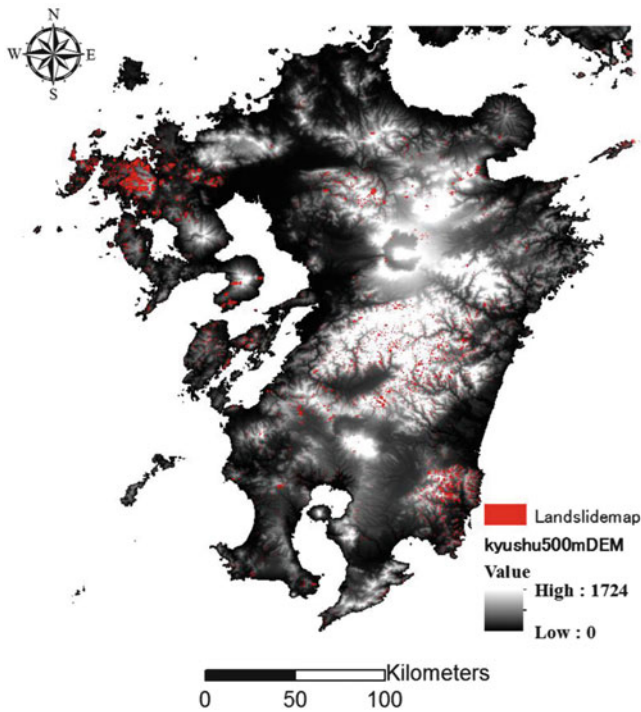


Fig. 2 Observed landslide deposition map

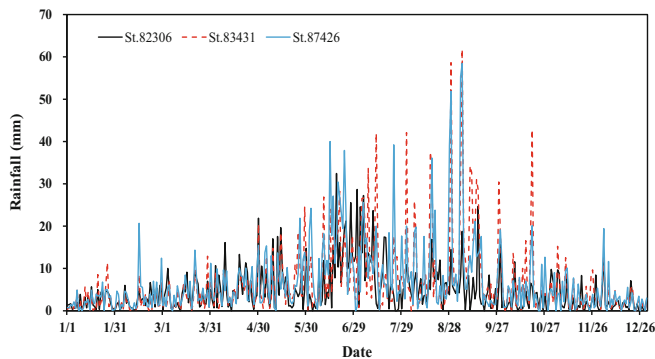


Fig. 3 Average daily rainfall at St. 82306 (KURUME), St.83431 (UME) and St.87426 (MIYAKONOJO) from 2000 to 2008

downloaded from the website of Landslides Distribution Maps database published by National Research Institute for Earth Science and Disaster Prevention (NIED 2013).

Methodology

Framework of the Modelling System

This study has developed the framework for the shallow landslide modelling system referred to as debris flows and characterized by rapidly moving flows of mixed soil and rock. These shallow landslides often occur on saturated hillslopes due to heavy or extreme rainfall. The purpose of

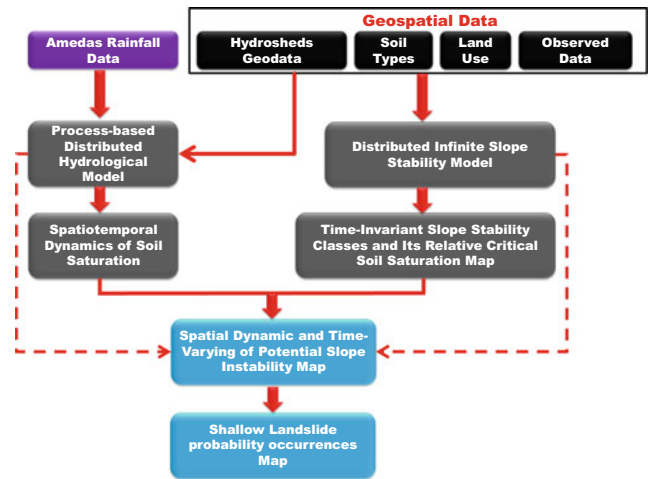


Fig. 4 Process of shallow landslide occurrences, probability mapping system

this Modelling System is to examine them by mapping areas of potential slope instability over the river catchment. The modelling system is designed for assessing the shallow landslides using a hazard/risk map that induces Spatial Dynamic and Time-Varying of Potential Slope Instability Map and Shallow Landslide Probability Occurrence. The Amedas observed rainfall data has been used for the shallow landslides hazard/risk mapping.

The framework of the modelling system (Fig. 4) is to identify where the shallow landslides have occurred, and “where” shallow landslides may occur in the largerscale region. The detailed description of the process is given below:

1. The geospatial data and Amedas rainfall data are collected for this study. The geospatial data includes hydro-sheds geo-data, soil types, land use, and other observed data. The hydro-sheds geo-data which includes flow direction and flow accumulation is made from ArcGIS 10 from the DEM. The distribution of 120 Amedas rainfall stations in Kyushu Island are interpolated in ArcGIS 10.
2. The Geospatial data is as the input into the distributed infinite slope stability model to derive a time-invariant spatial distribution map of the areas susceptible to slope instability. The catchment area is characterized by stability classes according to critical relative soil saturation. The effect of quasi-static land surface variables such as geometric characteristics of the slope, geotechnical properties, and strength parameters of the soil on slope instability is described in the time-invariant spatial distribution map.
3. The process-based hydrological model which is described in next session is calculated by using the observed Amedas rainfall data and Geospatial data from step 1.
4. Evaluation of the hydrological model performance through calibration of a hydrological response was

carried out by the spatiotemporal dynamics of soil saturation and the observed stream flow discharge from observed data.

5. Based on the calibrated spatiotemporal dynamics of soil saturation and the evaluated time-invariant slope stability spatial distribution map, the long-term spatial dynamic and time-varying of potential slope instability map can be drawn out. The hydrological model predicts the dynamic of soil saturation in each grid element, which is then used to update the state of relative soil saturation and to assess local slope instability for whole areas predefined as potentially stable/unstable.
6. The shallow landslide occurrences probability map of shallow landslides is calculated from the spatial dynamic and time-varying of potential slope instability map. The critical relative saturation level of shallow landslides was compared with the spatial information found in the landslide inventory from the observed data (NIED 2013).

Physically Based Distributed Hydrological Model

In this study, a distributed hydrological–geotechnical model was applied for the assessment of shallow landslide risk. The model links the hydrological model and a slope stability model. The grid-Cell Distributed Rainfall Runoff Model Version 3 (CDRMV3) solves the Kinematic wave equation using the Lax Wendroff scheme at every node of each cell (Kojima et al. 1997). A Monte Carlo simulation was added for the evaluation of model performance and uncertainty analysis of the linked CDRMV3 and Sediment Transport model (Apip et al. 2010). In addition, a lumped sediment-runoff model has been developed and applied by Apip et al. (2012) based on the CDRMV3 model structure using a steady state assumption. In this modelling framework, catchment topography is represented based on digital elevation model (DEM) which is divided into an orthogonal matrix of square grid-cells. A square area on a node point of a DEM is considered as a sub-catchment, which is called a grid-cell. The river catchment is modeled as a network of grid-cells. Each grid-cell receives flows from upper grid-cells and rainfall on it. These grid-cells are connected to each other with a drainage path defined by the steepest of eight directions. Discharge and water depth diffuse to the next grid-cell according to predefined eight-directional flow map and routine order determined in accordance with DEM and river channel network data. The hillslopes flow is routed and integrated into the river flow routing model; then the river flow is routed to the outlet.

CDRMV3 provides the surface and subsurface hydrological processes in each grid cell based on the kinematic wave

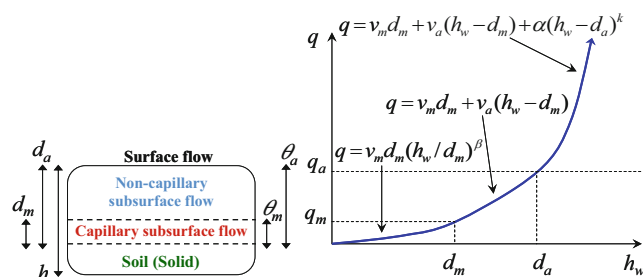


Fig. 5 Schematic diagram of soil model structure and stage-discharge relationship in each particular grid-cell (Apip et al. 2010)

method. The model simulates three lateral flow mechanisms including (1) subsurface flow through capillary pores, (2) subsurface flow through non-capillary pores and (3) surface flow on the soil layer. At each grid-cell, when the water depth is lower than the equivalent water depth for unsaturated flow ($0 \leq h \leq d_m$), flow is simulated by Darcy's law with an unsaturated hydraulic conductivity k_m . The model includes a stage-discharge, q - h relationship for both surface and subsurface runoff processes [(1), Fig. 5] (Luo et al. 2013 and 2014):

$$q = \begin{cases} v_m d_m \left(\frac{h}{d_m} \right)^\theta, & 0 \leq h \leq d_m \\ v_m d_m + v_a (h - d_m), & d_m < h \leq d_a \\ v_m d_m + v_a (h - d_m) + \frac{\sqrt{i}}{n}, (h - d_a)^m, & d_a < h \end{cases} \quad (1)$$

$$v_m = k_m i, v_a = k_a i, k_m = \frac{k_a}{\theta}$$

$$d_m = D\theta_m, d_a = D\theta_a$$

where q is the discharge per unit width, h (mm) is the water depth, i is the slope gradient, k_m (mm/s) is the saturated hydraulic conductivity of the capillary soil layer, k_a (mm/s) is the hydraulic conductivity of the non-capillary soil layer (saturated), d_m (mm) is the depth of the capillary soil layer (unsaturated), d_a (mm) is the depth of the capillary and non-capillary soil layer, v_m and v_a are the flow velocities of unsaturated and saturated subsurface flows respectively, θ is a non-dimensional parameter for unsaturated flow, θ_a is the effective porosity of the soil layer (D), θ_m is the effective porosity of the unsaturated layer, and n ($m^{-1/3}$ s) is the Manning's roughness coefficient based on the land cover classes. Initial conditions at each grid-cell were assumed to be in steady-state. Given the observed discharge at the catchment outlet, the discharge from every grid-cell was assigned in proportion to each of the grid-cells upstream to it, and the assigned discharge in each grid-cell was converted to the value of the water depth according to the stage-discharge relationship Equation (1).

Slope Stability Model

The slope stability model is developed based on the concept of the infinite slope model, using the factor of safety (FS) that considers a failure surface. The following are assumed: (i) failure is the result of translational sliding, (ii) the failure plane and water table are parallel to the ground surface, (iii) failure occurs as a single layer, (iv) the failure plane is of infinite length, and (v) the impacts of adjacent factors are not taken into account (Apip et al. 2010). For hillslopes, the safety factor generally is represented as the ratio of the available resisting force (shear strength) to the driving force (shear stress). Instability occurs when the shear strength of a soil layer becomes smaller than the shear stress acting on the soil. The governing equation of the safety factor used in this study is based on a Mohr–Coulomb failure law.

Figure 6 illustrates the forces acting on a point along a slope with potential for failure. The resisting force of a soil layer is the shear strength (s) as a combination of forces, including the normal stress (σ), pore pressure (u) within the soil material, cohesion factors (c), and the effective angle of internal friction in degrees (ϕ). The resultant force between normal stress and pore pressure is the effective normal stress. The resultant force between normal stress and pore pressure is the effective normal stress. Shear strength based on the Mohr–Coulomb law can be expressed as follows:

$$s = c + (\sigma - u) \tan \phi \quad (2)$$

Normal stress is the vertical component of gravity that resists downslope movement as follows:

$$\sigma = \rho_s g h \cos \theta \quad (3)$$

where ρ_s is the wet soil density (kg/m^3), g is the gravitational acceleration ($= 9.81 \text{ m/s}^2$), h is the vertical soil depth perpendicular to the slope (m), and θ is the slope angle (deg). The unit weight of soil material and the resisting and driving forces are increased with the soil moisture. Soil moisture brings about the pore pressure, which sags the effective normal stress and shear strength. A large temporal variation is existed in the pore pressure with the slope differs among sites. These values and the parameters in this model are very difficult to estimate at a large scale catchment. Therefore, the condition of pore pressure in the slope has been simplified by assuming that the pore pressure in the slope is always in the static state condition (Apip et al. 2010). To assume no excess pore water pressure, the pore pressure is quantified by the following equation:

$$u = \rho_w g h_w \cos \theta, \quad (4)$$

where ρ_w is the density of water ($= 1,000 \text{ kg/m}^3$) and h_w is the height of the water depth perpendicular to the slope (m).

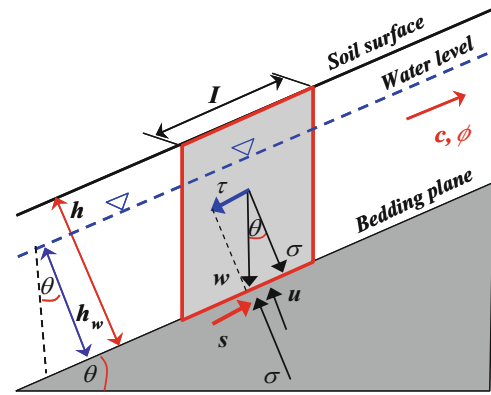


Fig. 6 Forces diagram on a slice of an infinite slope

This assumption gives greater pore water pressure in the rising process of the subsurface water and smaller pore water pressure in the descending process of the subsurface water.

The shear stress as driving force, defined by the down-slope parallel component of gravity, can be expressed as follows:

$$\tau = \rho_s g h \sin \theta \quad (5)$$

By substituting the formula for shear strength and shear stress, the factor of safety without considering root cohesion and vegetative surcharge equals

$$FS = \frac{c^* + \cos \theta [1 - r_u] \tan \phi}{\sin \theta}; \quad \begin{cases} c^* = \frac{c}{\rho_s g h} \\ r_u = \frac{h_w \rho_w}{h \rho_s} \end{cases} \quad (6)$$

The dimensionless form of Equation (6) was used to analyse the stability of shallow soil using digital terrain models (Montgomery and Dietrich 1994; Wu and Siddle 1995; Casadei et al. 2003).

Based on the Equation (6), most of the variables could be considered as spatially distributed, but h_w is the time-varying parameter. The water depth (h_w) is determined by the flux of subsurface water flow which is calculated from the hydrological model (see Equation 1). The ratio ($m^c = h_w/h$) presents that the relative saturated depth is time-dependent (range between 0.0 and 1.0). The driving forces prevail, and the potential for failure is high whenever $FS < 1.0$. With an inversion of the standard factor of safety (Equation 6), the fixed time-invariant critical relative soil saturation (m^c) triggering slope instability (i.e., relative soil saturation that yields $FS = 1.0$) of each grid element could be estimated as the following Equation (7):

$$m^c = \left(\frac{h_w}{h} \right)^c = \frac{\rho_s}{\rho_w} \left(1 - \frac{\tan \theta}{\tan \phi} \right) + \frac{c}{h \rho_w g \cos \theta \tan \phi} \quad (7)$$

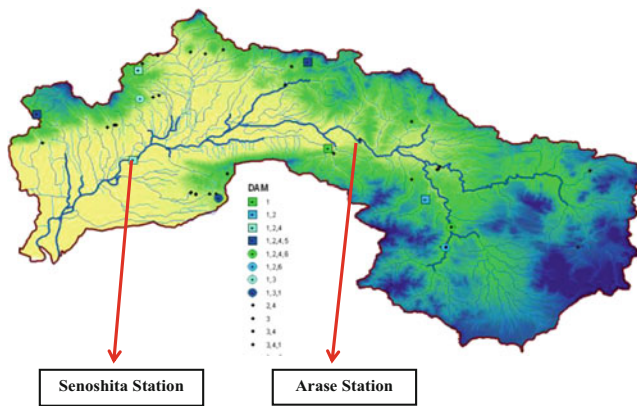


Fig. 7 Observed discharge stations in Chikugo River

The detail description of the hydrological–geotechnical model used in this study can be found in the paper of Apip et al. (2010).

Results and Discussion

Model Performance

Evaluation of the hydrological model performance through calibration of a hydrological response was carried out at the Senoshita and Arase Stations of the Chikugo River (Fig. 7). The calibration result at Arase Station (Fig. 8a) presents the simulated discharge as matching the observed discharge very well with the Nash-Sutcliffe (NS) coefficient of 0.93. The simulated peak discharge is similar with the observed peak discharge. The trend of simulated discharge is also bracketed well with the observed discharge. The simulated discharge at Senoshita Station is very similar to the observed discharge with the Nash-Sutcliffe (NS) coefficient of 0.86. However, the simulated peak discharge is a little over estimated when compared with the observed discharge. The simulated discharge from the 22nd hour to the 36th h and from the 57th h to 82nd h is under-estimated.

Slope Stability Model

Simulated hydrologic response to heavy rainfall generally leads to saturation of the entire catchment. As a result, the slope stability model may represent all potential shallow slope failures at each grid element. However, real landslides generally occur in instances where the suggested threshold for shallow landslides is exceeded. In order to avoid overestimation of landslide occurrence, critical relative soil saturation values were used to subdivide the catchment area into three slope stability classes according to Equation (7). Shallow landslide potential was only defined for stable/unstable grids

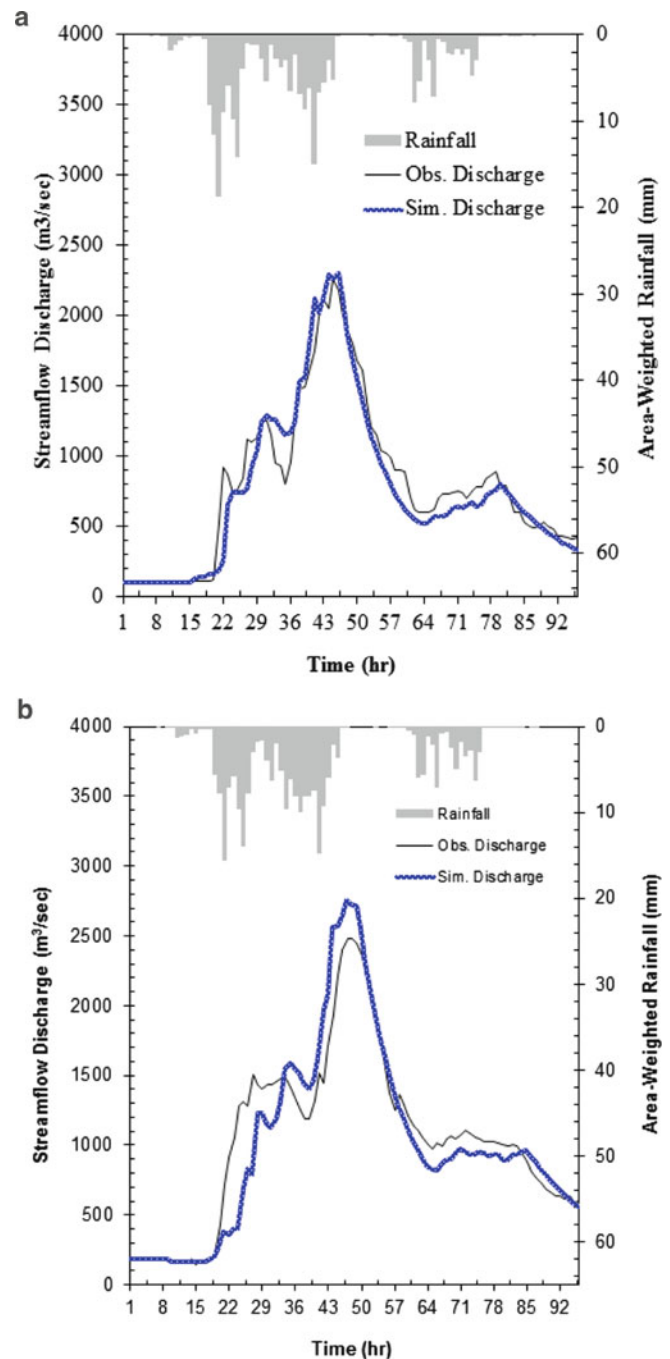


Fig. 8 Calibration result of hourly discharge at (a) Arase Station and (b) Senoshita Station (Luo et al. 2014)

where the critical relative soil saturated depth values ranged from 0 to 1. Geotechnical parameter calibration was conducted by mapping slope stability model with predicted critical relative saturated depths and comparing these to locations of observed landslides and quantifying the proportion of catchment area placed in the various critical relative saturated depths ranges (the zone of potential instability) with the corresponding fraction of the observed landslide grids.

Slope Stability Model

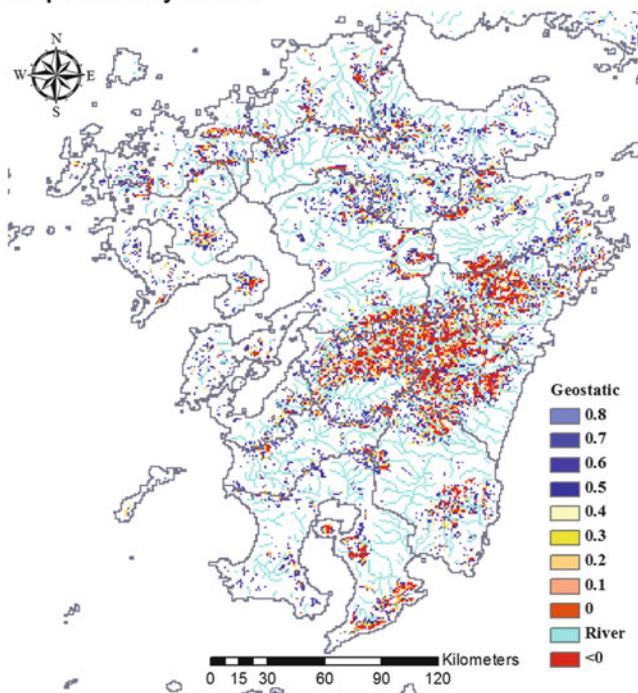


Fig. 9 Critical relative saturation level map (the detail description of critical relative saturation level is in introduction of m_c at the slope stability model section)

Figure 9 shows the critical relative saturation level map. The red colour area with value equal or less than 0 is present as the highest potential area where the shallow landslides are likely to occur. The area with the critical relative saturation level of 0.8 is the most stable area where the shallow landslides are not susceptible. The highest potential area of the shallow landslides occurrences is quite fixed with the observed location map of landslides occurrences (Fig. 10). However, this observed location map includes all the types of landslides.

Discussion

The results of this study presented the critical relative saturation level map which provided the landslide-prone area and location, with scientific information for the shallow landslide management. The critical relative saturation level map can be used to identify where the most dangerous area for shallow landslides is located and will inform the local residents to be aware of the potential for shallow landslides during the extreme rainfall events. The next step for this study is to provide the shallow landslide occurrences probability map.

The limitation of this study is the lack of a detailed deposition map for shallow landslides. In this study, we only obtained the deposition map of all types of landslides

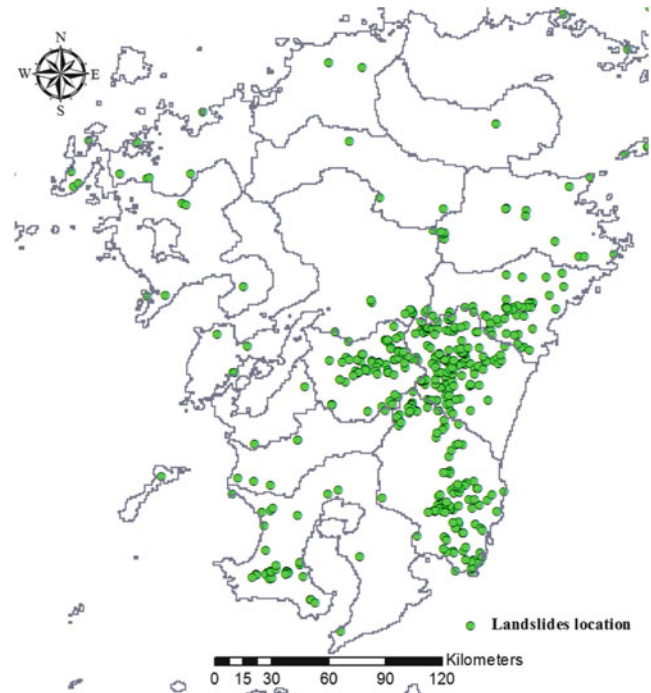


Fig. 10 Location of landslides occurrences (NIED 2013)

and it is difficult to identify shallow landslides; most landslides that have occurred in Japan are shallow landslides. The resolution in the numerical simulation of shallow landslides in Kyushu Island is 500 m mesh which will be improved in the future study. The land use type also take an important role, and affect the occurrence of shallow landslides. In future research, we would like to use the 100 m mesh land-use data as the input data.

Conclusion

In this study, we can conclude the following:

1. The framework for numerical assessment of shallow landslide using the distributed hydrological–geotechnical model in a large scale has been developed.
2. The calibration of a hydrological response for the model performance evaluation at the Senoshita and Arase Stations of Chikugo River concludes that the simulated discharge matched very well with the observed discharge.
3. The Critical relative saturation level map simulated from the slope stability model is shown to have a good relationship with the observed landslides location map.

Acknowledgments The authors thanks the supports from the Japan Society for the Promotion of Science (JSPS) KAKENHI Grant Number 24-02055, the Kyoto University Global COE program on “Sustainability/Survivability Science for a Resilient Society Adaptable to Extreme Weather Conditions”, and Inter-Graduate School Program for Sustainable Development and Survivable Societies (GSS), MEXT Program for Leading Graduate Schools 2011-2018, Designing Local Frameworks for Integrated Water Resources Management at the Research Institute for Humanity and Nature (RIHN), JSPS Grant-in-Aid for Scientific Research(A) Grant Number 24248041.

References

- Apip, Takara K, Yamashiki Y, Sassa K, Ibrahim AB, Fukuoka H (2010) A distributed hydrological–geotechnical model using satellite-derived rainfall estimates for shallow landslide prediction system at a catchment scale. *Landslides* 7(3):237–258
- Apip, Sayama T, Tachikawa Y, Takara K (2012) Spatial lumping of a distributed rainfall sediment runoff model and effective lumping scale. *Hydrol Process* 26(6):855–871
- Casadei M, Dietrich WE, Miller NL (2003) Testing a model for predicting the timing and location of shallow landslide initiation in soil-mantled landscapes. *Earth Surf Process Landforms* 28:925–950
- Chiang S-H, Chang K-T (2009) Application of radar data to modeling rainfall-induced landslides. *Geomorphology* 103(3):299–309
- Claessens L, Schoorl JM, Veldkamp A (2007) Modelling the location of shallow landslides and their effects on landscape dynamics in large watersheds: an application for Northern New Zealand. *Geomorphology* 87(1–2):16–27
- De Sy V, Schoorl JM, Keesstra SD, Jones KE, Claessens L (2013) Landslide model performance in a high resolution small-scale landscape. *Geomorphology* 190:73–81
- Duan W, He B, Takara K, Luo P, Nover D, Yamashiki Y, Huang W (2014) Anomalous atmospheric events leading to Kyushu's flash floods, July 11–14, 2012. *Nat Hazards*. doi:10.1007/s11069-014-1134-3
- Jia N, Mitani Y, Xie M, Djameluddin I (2012) Shallow landslide hazard assessment using a three-dimensional deterministic model in a mountainous area. *Comput Geotech* 45:1–10
- Kojima T (1997) Application of remote sensing and GIS to hydrological analysis. Doctorate of Engineering Dissertation, Kyoto University, Japan (in Japanese)
- Liu C-N, Wu C-C (2008) Integrating GIS and stress transfer mechanism in mapping rainfall-triggered landslide susceptibility. *Eng Geol* 101(1–2):60–74
- Luo P, Takara K, Apip, He B, Nover D (2013) Palaeoflood simulation of the Kamo River basin using a grid-cell distributed rainfall run-off model. *J Flood Risk Manage*. doi: 10.1111/jfr3.12038
- Luo P, Apip, Takara K, He B, Nover D, Duan W, Hu M (2014) Monthly assessment of shallow landslide risk in Kyushu Island, Japan. *Nat Geosci*. In submission
- Montgomery DR, Dietrich WE (1994) A physically based model for the topographic control on shallow landsliding. *Water Resour Res* 30(4):1153–1171
- NIED National Research Institute for Earth Science and Disaster Prevention (2013) Landslides distribution maps database published. <http://lsweb1.ess.bosai.go.jp/>. Last Accessed 24 Aug 2013.
- Park HJ, Lee JH, Woo I (2013) Assessment of rainfall-induced shallow landslide susceptibility using a GIS-based probabilistic approach. *Eng Geol* 161:1–15
- Piacentini D, Troiani F, Soldati M, Notarnicola C, Savelli D, Schneiderbauer S, Strada C (2012) Statistical analysis for assessing shallow-landslide susceptibility in South Tyrol (south-eastern Alps, Italy). *Geomorphology* 151–152:196–206
- Wu W, Sidle RC (1995) A distributed slope stability model for steep forested basins. *Water Resour Res* 31(8):2097–2110



Stability Analysis of a High Slope Along a Loess Plateau Based on Field Investigation and Numerical Analysis

Zongyuan Ma, Hongjian Liao, Chunming Ning, and Zhigang Feng

Abstract

In this paper, a landslide along a high loess plateau is studied by the method of field investigation, laboratory test and numerical analysis. First, the environmental factors that induce the landslide of the high loess slope are investigated. Second, an elastoplastic constitutive model based on the unified strength theory (UST) was established and implemented in a three-dimensional finite difference code FLAC3D. Based on the information from field investigation and the results of laboratory test, three-dimensional stability analysis of the high loess slope is analyzed using the FLAC3D code and UST model. The influence of the ground water level variation and the seepage flow on the slope stability is analyzed. The calculation results of the ground water level variation suggest that the slope reaches an equilibrium state after a certain amount of deformation is yielded. However, the displacement increased significantly and the failure of the high loess slope occurred suddenly when the seepage flow is taken into account. The analysis results of this paper indicated that it is necessary to reduce the reclamation and irrigation along the boundary of the loess plateau, and the stability of the high loess slope along the loess plateau could be ensured.

Keywords

High loess slope • Slope stability analysis • Seepage flow • Testing study • Numerical analysis

Z. Ma (✉)

School of Civil Engineering and Architecture, Xi'an University of Technology, Xi'an 710048, China
e-mail: mzy_gogo@hotmail.com

H. Liao • Z. Feng

Department of Civil Engineering, Xi'an Jiaotong University, Xi'an 710049, China
e-mail: hjliao@mail.xjtu.edu.cn; hjliao@mail.xjtu.edu.cn

C. Ning

Department of Capital Construction, Xi'an Jiaotong University, Xi'an 710049, China
e-mail: cmning@mail.xjtu.edu.cn

Introduction

High loess slopes are widely distributed in northwestern China, and usually formed along the boundary of the loess plateaus. These high slopes have several common features, e.g., large height difference, steep slope and complex geologic origin. The urban area of the town is encroaching on the loess plateau during the urbanization acceleration process. The arid climate of the loess area often causes a significant rise of the ground water level due to the large scale irrigation and seasonal raining. In recent years, the stability of the loess plateau boundary is influenced significantly by the climatic and anthropogenic factors, moreover, the disasters of the landslides in the loess plateau caused by the variations of ground water level have become more and more serious (Lei 1995). Figures 1 and 2 show the mean

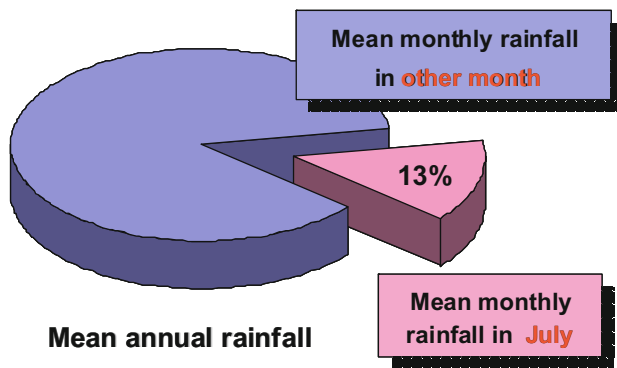


Fig. 1 Comparison the mean annual rainfall

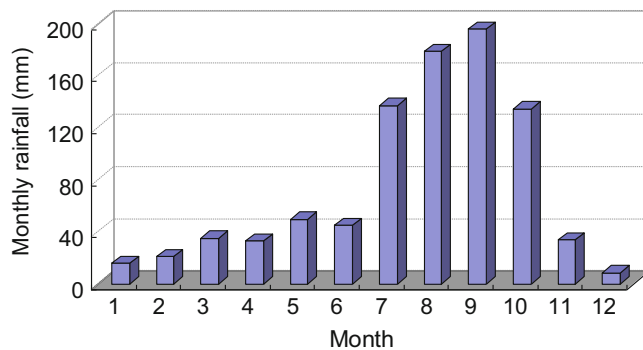


Fig. 2 Mean monthly rainfall for each month in 2003

annual rainfall comparison of July to other months and monthly rainfall in 2003, respectively. The slope failure caused by ground water and seepage flow is investigated by many researchers. The soil slope failure caused by seepage flow has been simulated via two-dimensional finite element method (Sanavia 2009). The soil slope failure caused by raining and infiltration has been analyzed by Rahimi et al. (2010) and Chen et al. (2009). A large-scale slope model subjected to rising and lowering water levels has been studied by Jia et al. (2009).

The high loess slope is situated along the northern boundary of a loess plateau close to the Jingyang town, ShaanXi province, China (Liao et al. 2008, 2011). Figure 3 shows the large landslide on a high loess slope at Jingyang town. The distance from the high loess slope to the urban district of Xi'an city is about 25 km. The Jinghe river flows beside the northern boundary of the loess plateau (Fig. 3). Many high loess slopes along the boundary of northern loess plateau became unstable due to the erosion of the Jinghe river. The boundary of the northern loess plateau is about 30 km long, with an elevation of 30–90 m above the Jinghe river; the slope angle is about 45–80°. Several landslide events have taken place along the boundary of the northern loess plateau in recent years, and four villages near to the boundary have



Fig. 3 Location of the study landslide. (a) Mapping, (b) Google Earth@ image 2003

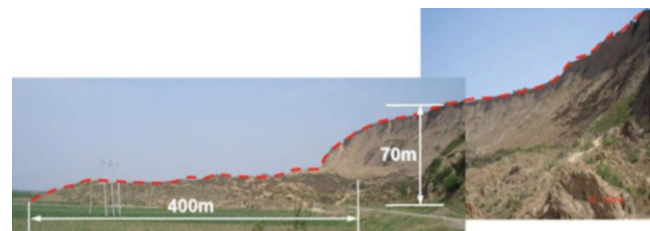


Fig. 4 Field photo of Jingyang landslide (2003)

been affected by those landslide events. The landslide case study is located in the southern bank of the Jinghe river and occurred in July, 2003. According to the statistics, the rainfall at Xi'an city fluctuates seasonally, and the most rainfall occurs during the months of July to September. The mean monthly rainfall in July is about 13 % of mean annual rainfall. For example, the rainfall from July to October 2003 is more than 70 % of the annual rainfall. Irrigation in summer also leads to a rapid rise of ground water level on the top of the loess plateau. Thus, it is necessary to analyze the stability of high loess slope effects due to seepage flow caused by rainfall and irrigation. The field photos of the study landslide are shown in Fig. 4 (Liao et al. 2008). The cross section sketch of the landslide is shown in Fig. 5. According to the results of the field investigation, more than 100,000 m³ of loess slid from the high slope. The length and width of the landslide mass is about 400 and 410 m, respectively, and the slope angle is about 45–55°. Ground water in the Jingyang loess plateau is stored within the

Fig. 5 Cross Section of the landslide

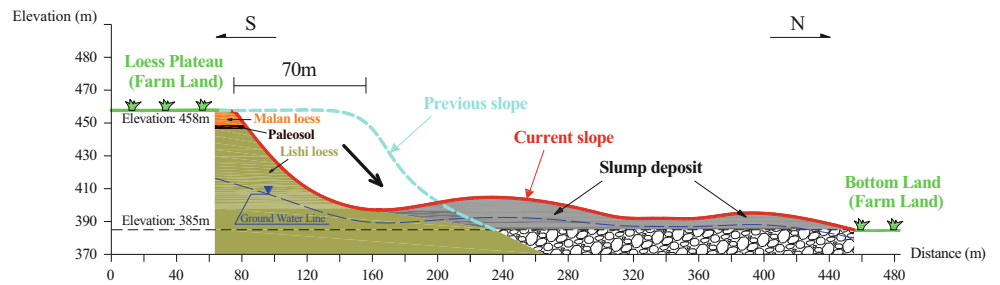


Table 1 Statistics of previous landslides along the Jingyang loess plateau

Location	Height	Slope angle	Size of landslide: Length (L), Width (W), Thickness (T), Volume (V)	Loss
To the west of Jinyu village, Gaozhuang town	24 m	40°	L 38 m, W 330 m, T 4.0 m, V $5 \times 10^4 \text{ m}^3$	Families: 28, population: 110, Houses: 112
To the east of Jinyu village, Gaozhuang town	21 m	65°	L 23 m, W 330 m, T 2.5 m, V $1.9 \times 10^4 \text{ m}^3$	Families: 6, population: 23, houses: 20, threatens a highway
Group 9 of Fuxia village, Gaozhuang town	25 m	30°	L 50 m, W 85 m, T 3.0 m, V $1.3 \times 10^4 \text{ m}^3$	Farmland: $0.67 \times 10^4 \text{ m}^2$
Jiangliu village, Jiangliu town	53 m	70°	L 56 m, W 320 m, T 12 m, V $18.8 \times 10^4 \text{ m}^3$	Farmland: $3.33 \times 10^4 \text{ m}^2$, garden: $4.67 \times 10^4 \text{ m}^2$, threatens a private road of a company
To the north of the Dabuzi primary school in Jiangliu town	49 m	65°	L 52 m, W 720 m, T 30 m, V $35 \times 10^4 \text{ m}^3$	Families 3, population: 15, houses: 12, school teachers and students: 196
Group 6 of Dongfeng village, Jiangliu town	77 m	68°	L 82 m, W 200 m, T 10 m, V $12.6 \times 10^4 \text{ m}^3$	Farmland: $3.3 \times 10^4 \text{ m}^2$
Fujia village, Jiangliu town	81 m	73°	L 260 m, W 360 m, T 43 m, V $110 \times 10^4 \text{ m}^3$	Damage to pond for sewage, Xihang sewage treatment plant
Miao village, Taiping town	63 m	68°	L 1,000 m, W 1,000 m, T 15 m, V $94.5 \times 10^4 \text{ m}^3$	Farmland: $4.0 \times 10^4 \text{ m}^2$
Zhaitou village, Taiping town	54 m	70°	L 2,000 m, W 2,000 m, T 17.5m, V $189 \times 10^4 \text{ m}^3$	Farmland: $35 \times 10^4 \text{ m}^2$

phreatic aquifer. In 1976, the ground water level kept equal to the water surface of the Jinghe river (elevation is 380 m). However, a distinct rise in ground water level was induced by the large scale irrigation and rainfall. In 1992, the depth of ground water under the loess plateau was about 37 m (elevation is 425 m). Since 1976, landslides in this area have occurred over 40 times, and the economic development of the local area has been affected (Lei 1995). Statistics for previous landslides along the Jingyang loess plateau are shown in Table 1.

Testing Results

Soil samples were taken from four exploratory holes in the field around the study landslide as shown in Fig. 6a. In order to understand the mechanical and physical characteristics of the soil samples which are excavated, a series of laboratory tests, including particle-size analysis test and consolidated

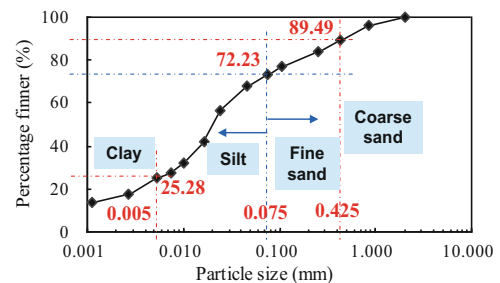
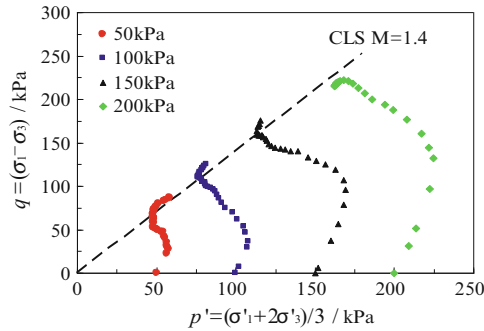


Fig. 6 Particle size distribution

undrained (CU) triaxial test were conducted. The physical properties of the landslide soil are shown in Table 2. The particle size distribution results for the loess are shown in Fig. 6 (Liao et al. 2008). The result of particle-size analysis test shows that the percent of particles with diameters greater than 0.075 mm is 27.8 %, which is less than 50 %. The percent of particles with diameters less than 0.005 mm is greater than 10 %. The plasticity index I_p ranges from 3 to

Table 2 Physical properties of the landslide soil

Density ρ (kg/m ³)	Specific gravity d_s	Natural water content w_n (%)	Void ratio e	Plasticity index I_p	Young's modulus E (MPa)	Poisson's ratio ν
1,540	2.72	17.8	1.08	8.6	5.0	0.33

**Fig. 7** Effective stress path of loess for landslide

10. Therefore the soil can be classified as loess-like clayey silt. Figure 7 shows the effective stress path of the disturbed loess excavated from the study landslide, and little volume dilation was observed in CU triaxial test. The stress-strain relationships from CU triaxial test for undisturbed and disturbed loess under natural water content (unsaturated) and saturated condition are shown in Fig. 8 (Liao et al. 2008). The stress-strain relationship of undisturbed loess shows a slight strain softening characteristic, and the strain hardening characteristic of the disturbed loess have appeared both in saturated or unsaturated (natural water content) situation.

The cohesion and the friction angle of the loess samples obtained from CU triaxial test under the different confining pressures are shown in Table 3. The numerical values of cohesion and friction angle varied with the state of the loess samples changed. The friction angle of the disturbed loess sample (natural water content or saturated) is higher than the undisturbed loess sample (natural water content). However, the cohesion of the disturbed loess sample (natural water content or saturated) is lower than the undisturbed loess sample (natural water content). The reason for this phenomenon is that the undisturbed loess has a marked soil structure characteristic, and the cohesive strength between the soil granules (cohesion) will be enhanced by the natural structure of loess under the undisturbed state. However, the natural structure of loess could be destroyed by seepage flow or dip in water, and this characteristic is called loess collapsibility (Zhang and Sassa 1996). For disturbed state, the friction between the soil granules (friction angle) will be increased with the natural structure of loess destroyed, and the cohesive strength between the soil granules (cohesion) will be decreased. In this paper, the natural structure and collapsibility of loess is not taken into account in the slope stability analysis.

Numerical Simulation

In this paper, numerical computations using finite difference method are reported in order to analyze the high loess slope stability problem using the unified strength theory. The unified strength theory (UST) for geomaterials was proposed by Yu (2004). The principal stress form of UST can be written as:

$$\begin{cases} f = \frac{b\sigma_2 + \sigma_3}{(1+b)N_\varphi} - \sigma_1 + \frac{2c}{\sqrt{N_\varphi}}, & \text{when } \sigma_2 \leq \frac{1+\sin\varphi}{2}\sigma_1 + \frac{1-\sin\varphi}{2}\sigma_3 \\ f' = \frac{\sigma_3}{N_\varphi} - \frac{\sigma_1 + b\sigma_2}{1+b} + \frac{2c}{\sqrt{N_\varphi}}, & \text{when } \sigma_2 \geq \frac{1+\sin\varphi}{2}\sigma_1 + \frac{1-\sin\varphi}{2}\sigma_3 \end{cases} \quad (1)$$

where c and φ are the cohesion and friction angle for geomaterials, and $N_\varphi = (1 + \sin\varphi)/(1 - \sin\varphi)$. The order of the three principal stresses follows $\sigma_1 \geq \sigma_2 \geq \sigma_3$. For the non-associated flow rule (Zienkiewicz et al. 1975), the plastic potential function g can be written as follows:

$$\begin{cases} g = \frac{b\sigma_2 + \sigma_3}{(1+b)N_\psi} - \sigma_1, & \text{when } \sigma_2 \leq \frac{1+\sin\varphi}{2}\sigma_1 + \frac{1-\sin\varphi}{2}\sigma_3 \\ g' = \frac{\sigma_3}{N_\psi} - \frac{\sigma_1 + b\sigma_2}{1+b}, & \text{when } \sigma_2 \geq \frac{1+\sin\varphi}{2}\sigma_1 + \frac{1-\sin\varphi}{2}\sigma_3 \end{cases} \quad (2)$$

where $N_\psi = (1 + \sin\psi)/(1 - \sin\psi)$ and ψ is the dilation angle for geomaterials. If $\psi < \varphi$, then the plastic flow rule is non-associated, while for the associated flow rule, $\psi = \varphi$. Direct comparisons with the analytical method can be made when the associated flow rule is used in numerical methods. The limit loci of UST on the deviatoric plane and principal stress space are shown in Fig. 9, where θ_b is the stress angle for the junction of two yield surfaces and depends only on the friction angle. UST takes the influence of intermediate principal stress into account with a bilinear yield surface, and the different effect of the intermediate principal stress for different materials can be reflected by the coefficient b of UST. FLAC^{3D} is a three-dimensional finite difference code, and an explicit Lagrangian computation scheme is used in this code (Itasca Consulting Group 2005). The elastoplastic model following UST is loaded into FLAC^{3D} with a dynamic link library file (DLL) written by C++ (Ma et al. 2013). The unbalanced force rate is used in FLAC^{3D} to control the convergence. The unbalanced force rate can be defined as the maximum unbalanced force magnitude for all

Fig. 8 Stress-stain relationship of loess for landslide. (a) Disturbed loess in natural water content, (b) disturbed loess in saturated condition

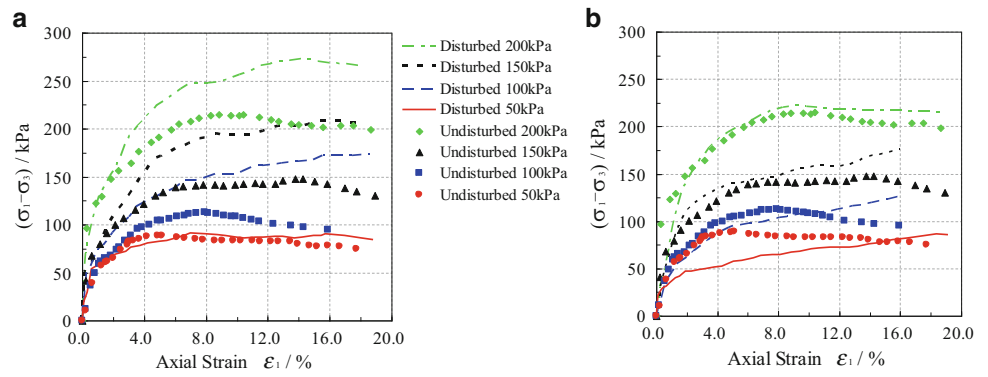


Table 3 Cohesion and friction angle for loess sample from CU triaxial test

Loess samples	Water content <i>w</i> (%)	Cohesion <i>c</i> (kPa)	Friction angle φ (°)
Undisturbed loess sample	Natural water content	13.2	17.2
Disturbed loess sample	Natural water content	12.9	21.6
Disturbed loess sample	Saturated	9.6	19.1

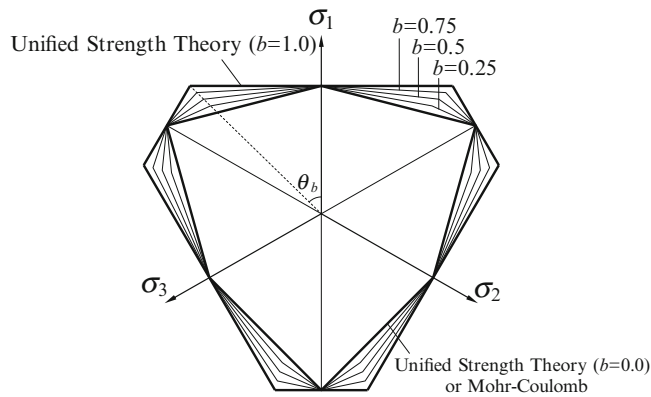


Fig. 9 Limit loci of the unified strength theory

nodes divided by the average applied force magnitude for all the nodes. By default, the ratio limit for convergence is 1.0×10^{-5} .

The relationship between the limit equilibrium and finite element method in slope stability analysis is discussed by Zienkiewicz et al. (1975), Duncan (1996) and Griffiths and Lane (1999) using the Strength Reduction Method (SRM) to analysis the slope stability problem with associated and non-associated flow rule. The Factor of Safety (FOS) of slope is calculated via SRM, and the original shear strength parameters are divided by Strength Reduction Factor (SRF) in order to bring the slope to the point of failure. The strength parameters of soil mass are decreased gradually by SRF until the slope becomes unstable, and the values of elastic parameters (Young’s modulus *E* and Poisson’s ratio *v*) have no effect on the value of FOS (Griffiths and Lane

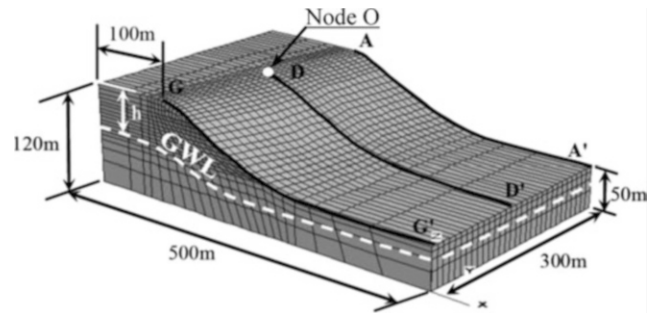


Fig. 10 Meshing model and ground water level variation for slope stability analysis

1999; Cheng et al. 2007; Swan and Seo 1999). In this paper, the same factor SRF is applied to both of two strength parameters *c* and φ . The non-convergence option is taken as being an indicator of failure for FOS determination. The parameters c_f and φ_f are given by

$$c_f = \frac{c}{SRF}, \quad \varphi_f = \arctan\left(\frac{\tan \varphi}{SRF}\right) \quad (3)$$

The three-dimensional model for the high loess slope prior to the landslide event is created based on the terrain information from field investigation. The dimension and meshing of the model for numerical simulation are shown in Fig. 10. The dashed line represents ground water level and *h* is the depth of ground water. The cohesion and the friction angle of the undisturbed loess obtained from CU triaxial test are used, and the dilation angle ψ is set to zero throughout the whole calculation process. In order to compare the slope stability

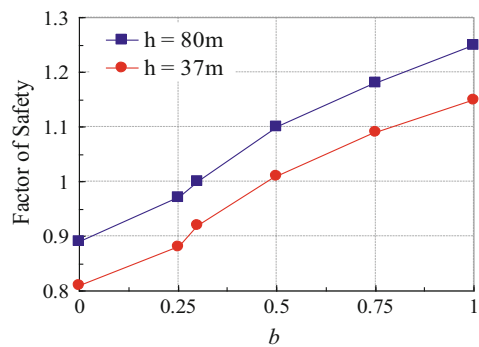


Fig. 11 Relationship between FOS and values of parameter b

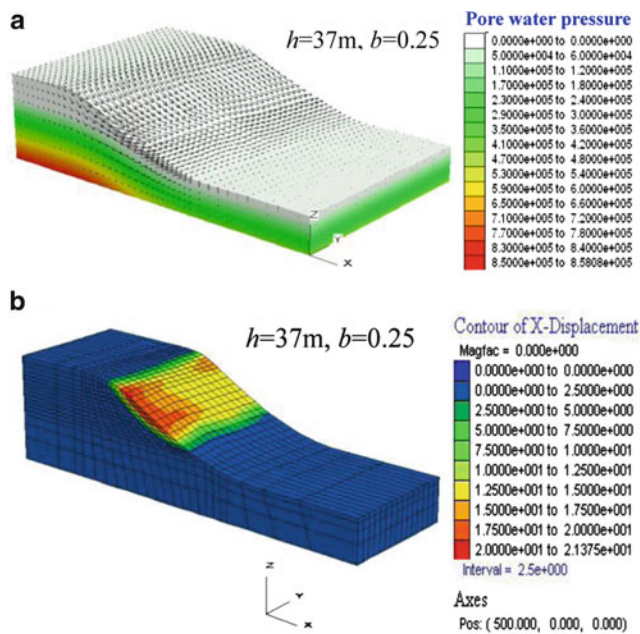


Fig. 12 Results plots under $\text{SRF} = \text{FOS} = 0.88$, $h = 37$ and $b = 0.25$, (a) pore-water pressure and displacement vector, (b) horizontal displacement contour

under the different ground water levels, the calculations are performed under the ground water level in 1976 ($h = 80$ m) and 1992 ($h = 37$ m), respectively. The relationship between FOS and the magnitude of b underground water level in 1976 and 1992 is shown in Fig. 11. The slope changes towards instability with the decrease of parameter b , and the slope failure occurs when the magnitude of b decreased below a certain value. Because the high loess slope was stable before 1976, the stability analysis taking the influences of the

intermediate principal stress into account can reflect the actual situation more accurately. Figure 12 shows the pore-water pressure, displacement vector and horizontal displacement contours of slope under $h = 37$ m and UST ($b = 0.25$). The results of Fig. 12 suggest that the high loess slope can't remain stable if the ground water level $h = 37$ m and $b = 0.25$. In order to analyze the stability of the high loess slope during the process of rise in ground water level caused by fall and irrigation, analysis is performed with different depth ($h = 35$ – 50 m) of ground water level under the loess plateau. Because the rise velocity of the ground water level is very low, the seepage of ground water is not taken into account and the soil under the ground water level is saturated. Figure 13a shows the relationship between displacement of node O in the x -direction and calculation steps under different depth of ground water level when the parameter $b = 0.5$. According to the statistics, landslides which are induced by the distinct change of ground water level in loess area occurred frequently from the short-time rainfall during the rainy season. The rainfall in Xi'an fluctuates seasonally, and the most rainfall is yielded during the months from July to September; the time of rainfall is very short. The mean monthly rainfall of July to September is about 12.5–16.4 % of mean annual rainfall. For example, the total rainfall for 2003 is 898.7 mm, and the total rainfall for July in 2003 is close to 140 mm, which is about 15 % of total rainfall in 2003 (Song et al. 2002). The high loess slope in the southern bank of the Jinghe river slid in July of 2003. Thus, it is necessary to analyze the influence of a distinct rise of the ground water level and seepage flow on the stability of high loess slope. The parameters of the soil are the same as the calculation of no seepage flow, and the soil permeability is 0.1 m/d (Liao et al. 2008, 2011). The calculations of seepage flow and stress field are parallel and the stress field of slope is influenced by pore-water pressure changes. The calculation of seepage flow is performed in four steps: the ground water level $h = 30$ m, 35 m, 40 m, 45 m under the loess plateau. Figure 13b shows the relationship between x -displacement of node O and flow times when the parameter of UST $b = 0.5$. The results suggest that the x -displacement of node O is significantly increased with the increase of h , and the x -displacement is increased rapidly when $h = 45$ m. Compared with the numerical results of the no seepage case (as shown in Fig. 13), the results of the seepage flow case show that the displacement of node O in the x -direction increases significantly when the unbalanced force rate is close to the target of convergence and the slope failure occurs suddenly when h reaches a certain value. However, the results of no seepage calculation show that the slope

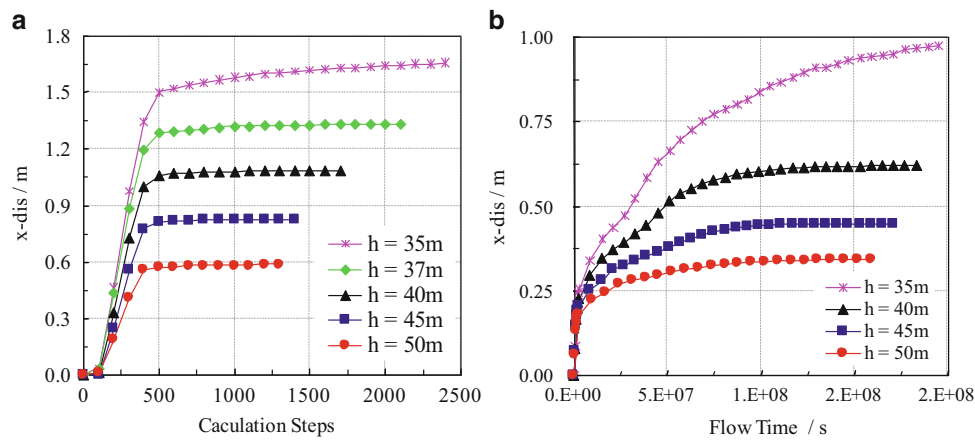


Fig. 13 Relationship between x-displacement of node O. (a) No seepage flow (b) seepage flow

reaches a static state when the unbalanced force rate is decreased. On the other hand, the x-displacement at node O from the seepage calculation is less than the case of no seepage calculation. This phenomenon suggests that the deformation of loess slope is too limited to absorb the overload of seepage flow completely, thus, the sudden failure of loess slope may occur more easily during the process of seepage flow.

Conclusion

The landslide groups along the Jingyang loess plateau were induced by both internal and external factors. The internal factors include new tectonic movement, topography and geography, and underground hydrology conditions. The external factors include irrigation, excavation, and rainfall. The soil of the study slope can be classified as loess-like clayey silt, the friction between the soil granules of disturbed loess will increase with the natural structure of loess destroyed. Meanwhile, the cohesion between the soil granules will be decreased under the disturbed state. The result of slope stability analysis which takes the influence of intermediate principal stress into account is more close to the actual conditions. Result of no seepage calculation suggests that the slope reaches an equilibrium state after a certain amount of deformation occurred. The displacement of the slope from the seepage calculation is less than the case of no seepage calculation, but the displacement increased significantly and the sudden failure occurred more easily during the process of seepage flow. The large-scale irrigation and seasonal rainfall often causes the ground water level to rise significantly. According to the analysis results of this paper, it is necessary to reduce the reclamation and irrigation of the farmland along the boundary of the loess plateau, so that the stability of the high loess slope can be ensured.

Acknowledgments The research is funded by the National Nature Science Foundation of China (41172276, 51279155), and central financial funds for the development of characteristic key disciplines in local universities (No. 106-00X101, 106-5X1205). The authors would like to acknowledge the “FY2011 JSPS Invitation Fellowship Program for Research in Japan” for its support.

References

- Chen RH, Chen HP, Chen KS et al (2009) Simulation of a slope failure induced by rainfall infiltration. *Environ Geol* 58(5):943–952
- Cheng YM, Lansivaara T, Wei WB (2007) Two-dimensional slope stability analysis by limit equilibrium and strength reduction methods. *Comput Geotech* 34:137–150
- Duncan JM (1996) State of the art: limit equilibrium and finite-element analysis of slopes. *J Geotech Eng Div ASCE* 122(7):577–596
- Griffiths DV, Lane PA (1999) Slope stability analysis by finite elements. *Geotechnique* 49(3):387–403
- Itasca Consulting Group (2005) *FLAC-Fast Lagrangian analysis of Continua*. Itasca Consulting Group, Minneapolis, MN
- Jia GW, Tony LT, Chen YM et al (2009) Performance of a large-scale slope model subjected to rising and lowering water levels. *Eng Geol* 106:92–103
- Lei XY (1995) The hazards of loess landslides in the southern tableland of Jingyang county, Shaanxi and their relationship with the channel water into fields. *J Eng Geol* 3(1):56–64 (In Chinese)
- Liao HJ, Su LJ, Li ZD et al (2008) Testing study on the strength and deformation characteristics of soil in loess landslides. In: *Proceedings of 10th international symposium on landslides and engineered slopes*, vol 2, pp 443–447
- Liao HJ, Li T, Peng JB (2011) Study of strength characteristics of high and steep slope landslide mass loess. *Rock Soil Mech* 32(7):1939–1944 (In Chinese)
- Ma ZY, Liao HJ, Dang FN (2013) Unified elastoplastic finite difference and its application. *Appl Math Mech* 34(4):457–474
- Rahimi A, Rahardjo H, Leong EC (2010) Effect of hydraulic properties of soil on rainfall-induced slope failure. *Eng Geol* 106:135–143
- Sanavia L (2009) Numerical modelling of a slope stability test by means of porous media mechanics. *Int J Comput Aided Eng Softw* 26(3):245–266

- Song JX, Li HE, Wang BD et al (2002) Approach on urban rainfall resources and its utilization in Xi'an city. *J Soil Water Conserv* 16 (3):102–105 (In Chinese)
- Swan CC, Seo YK (1999) Limit state analysis of earthen slopes using dual continuum/FEM approaches. *Int J Numer Anal Methods Geomech* 23:1359–1371
- Yu MH (2004) *Unified strength theory and its applications*. Springer, Berlin
- Zhang D, Sassa K (1996) A study of the apparent friction angle after failure during undrained shear of loess soils. *Jpn Soc Erosion Control Eng* 49(3):20–27
- Zienkiewicz OC, Humpheson C, Lewis RW (1975) Associated and non-associated visco-plasticity and plasticity in soil mechanics. *Geotechnique* 25(4):671–689



The Simulation of a Deep Large-Scale Landslide Near Aratozawa Dam Using a 3.0 MPa Undrained Dynamic Loading Ring Shear Apparatus

Hendy Setiawan, Kyoji Sassa, Kaoru Takara, Toyohiko Miyagi, Hiroshi Fukuoka, and Bin He

Abstract

The translational block glide of deep and large-scale landslide near the Aratozawa dam that occurred in the middle of 2008 is of great importance for detailed study. Aratozawa landslide had resulted from landform deformation and the subsequent change of watershed geomorphology at the upstream part of the Aratozawa reservoir. The evidence of this phenomena was revealed during a site investigation in November 2012, as several natural reservoirs (lakes) formed in the cavities between ridges and the depression zone in main block slide. Aratozawa landslide located in the Ohu Mountains basically was triggered by the earthquake which had a peak ground acceleration of more than 1,000 gal. In addition, the possibility of reactivated landslides in surrounding terrains near Aratozawa dam has resulted in the hypothesis that the 2008 event was one sequence of the dynamic-geomorphological activity in this mountainous area within a period of hundred years. In this paper, the mechanism of the deep and large-scale landslide near Aratozawa dam is analysed through a physical laboratory experiment. Deep landslide simulation is conducted by applying high normal stress to address the assumed slip surface of 150 m depth in the Aratozawa case. The 3.0 MPa undrained dynamic loading ring shear apparatus with the high pore-water pressure controlled is used to meet the criteria of deep-seated landslide of Aratozawa. The effect of groundwater fluctuation and the inter-linkage with the reservoir in the Aratozawa dam was found to be the main concern besides the peak ground acceleration

H. Setiawan (✉)
Department of Civil and Earth Resources Engineering, Kyoto
University, Kyoto 615-8540, Japan
e-mail: hendy@flood.dpri.kyoto-u.ac.jp

K. Sassa
International Consortium on Landslides, Kyoto 606-8226, Japan
e-mail: sassa@iclhq.org

K. Takara • H. Fukuoka
Disaster Prevention Research Institute (DPRI), Kyoto University, Uji
611-0011, Japan
e-mail: takara.kaoru.7v@kyoto-u.ac.jp; fukuoka@landslide.dpri.kyoto-u.ac.jp

T. Miyagi
Tohoku-Gakuin University, Sendai, Miyagi 981-3193, Japan
e-mail: miyagi@izcc.tohoku-gakuin.ac.jp

B. He
Key Laboratory of Watershed Geographic Sciences, Nanjing Institute
of Geography and Limnology, Chinese Academy of Sciences, Nanjing
21008, China
e-mail: hebin@niglas.ac.cn

based on the 2008 landslide event. Results also show that there was no significant deformation in the Aratozawa dam area when the large Tohoku earthquake, magnitude 9.0, in 2011. Indication is, that the slide blocks, ridges and mass depression due to the 2008 event are already stable. However, the slope and soil mass movement are still possible in the future.

Keywords

Deep large-scale landslide • High normal stress • Groundwater effect • Ring shear tests • Simulation

Introduction

The Aratozawa dam is located southeast of Mount Kurikoma in the Miyagi-Iwate Prefecture of Japan. The height of Aratozawa dam is 74.4 m with the geographical position at $38^{\circ}53'4.98''$ of north latitude and $140^{\circ}51'42.93''$ of east longitude. The Kitakami rivers and Nihasamagawa are the main discharge river basins for the Aratozawa reservoir. The catchment area of the Aratozawa reservoir is approximately 20.4 km^2 with the total water storage capacity design of about 14,130 thousand m^3 . The main purposes of the Aratozawa dam and reservoir are flood control and irrigation.

The location of the Aratozawa Dam is in line with the Ohu Mountains that extend from Tohoku district. The Iwate-Miyagi Nairiku inland earthquake of magnitude 7.2 occurred on June 14 2008. The peak ground acceleration from the inland earthquake at the Ohu Mountains caused thousands of landslides and slope failures including the large-scale deep landslide at the upper stream area of the Aratozawa reservoir (Fig. 1).

As reported by Miyagi et.al. (2008, 2011), the landslide near Aratozawa dam was stated to be the largest catastrophic landslide in the last 100 years in Japan. Moreover, this large-scale landslide event has some unique characteristics that are important to study further. Previous research, investigations and analysis indicated that the slicken-sided slip surface of the Aratozawa landslide has a gradient of about $2\text{--}4^{\circ}$ at a depth of 70–150 m, and resulted in the movement of massive blocks of 1,300 m in length and 900 m wide with a sediment volume of more than 67 million cubic meters (Miyagi et al. 2011; Gratchev and Towhata 2010). The complexity of the Aratozawa landslide that consists of massive blocks, ridges and depression zones generally are identified as the translational block glide of a deep slide.

Site Investigations

The Aratozawa landslide resulted in landform deformation and the resultant change of watershed geomorphology at the upstream part of the Aratozawa reservoir. The evidence of

this phenomena was revealed during a site investigation in autumn of November 2012 and the summer of June 2013, whereby several natural reservoirs (lakes) formed in the cavities between ridges and a depression zone in main block slide were observed (Fig. 2).

Aratozawa landslide was triggered by an earthquake with the peak ground acceleration more than 1,000 gal. In addition, the possibility of reactivated landslides in surrounding terrains near Aratozawa dam has brought about the hypothesis that the 2008 event was one sequence of the dynamic-geomorphological movement in this mountainous area within a period of a hundred years.

The mechanism of the deep and large-scale landslide near Aratozawa dam is analysed through physical laboratory experiment using the undrained dynamic loading ring shear apparatus ICL2.

Materials and Methods

Undrained Dynamic Loading Ring Shear Apparatus ICL2

The development of ring shear apparatus has been conducted since 1984 in order to address the needs of undrained shear tests with pore pressures monitoring and sliding surface observation at large shear displacement (Sassa et al. 2004). The ring shear apparatus developed by Sassa and colleagues has been used to study and analyse the initiation of soil failure, residual shear resistance as well as post-failure motion and deformation characteristic in large displacement (Sassa et al. 2007, 2010).

The latest version of this apparatus is called the undrained dynamic loading ring shear apparatus ICL-2 and was developed by the International Consortium on Landslides as a part of SATREPS-Vietnam project in 2012 (Fig. 3).

The ICL2 has high performances (Table 1) which can give and maintain the stress-pressure up to 3 MPa in the scope of drained-undrained consolidation, shear stress and speed controlled, pore pressure fluctuation controlled, stress dynamic and earthquake wave tests. With such features and



Fig. 1 Landslide near the Aratozawa reservoir



Fig. 2 Natural reservoirs in the cavity of the lower depression



Fig. 3 The overview of the undrained dynamic loading ring shear apparatus ICL2

Table 1 Features of the undrained dynamic loading ring shear apparatus ICL2

ICL 2 (Sassa et al. 2012)	
Inner diameter (cm)	10
Outer diameter (cm)	14.2
Max. height of sample (cm)	5.2
Shear area (cm ²)	79.79
Max. Normal stress (kPa)	3,000
Max. Shear speed (cm/s)	50
Max. Pore-water pressure (kPa)	3,000

performances, ICL2 could represent the simulation and reproduction of deep landslide tests that need high stress and pressures.

Samples Near Aratozawa Dam

Samples from Aratozawa landslide were taken during site investigations. The detailed locations that were observed during investigations are the open crack above the main scarp, top of main scarp, lower ridge, exposed wall on the upper depression, upper ridge, mound secondary collapse zone, small depression at toe part, disturbance zone at toe part, deformation near reservoir, huge landslide block with deformed and translated road network and debris bordered area at the secondary collapse zone (Fig. 4). Three samples locations were chosen for the test: a small depression at toe part, secondary collapse zone and mound at flank side of collapse zone.

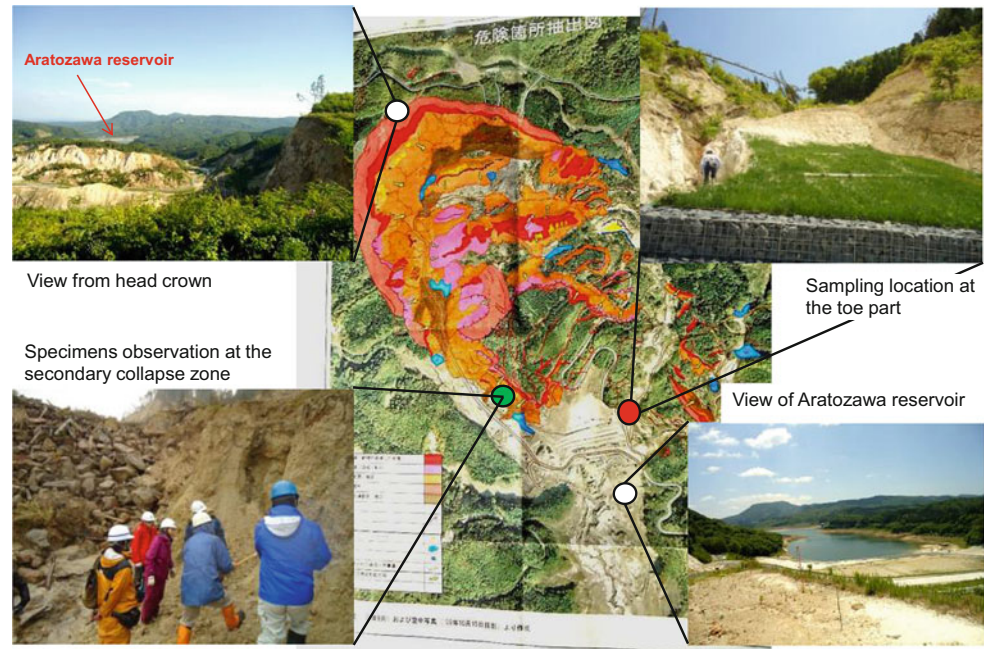
Test Procedures

All the Aratozawa samples were prepared carefully in fully saturated conditions through immersion in de-aired water and then left in a vacuum tank (Ostric et al. 2012). The gap adjustment in the apparatus was conducted to avoid water leakage during the high stress of tests while minimizing the rubber-edge friction between inner and outer ring shear box and rubber edges at the lower part of the apparatus. The gap value is kept constant during the test to ensure the stress given to the samples and the data acquisition can be monitored.

When the shear box was installed, the CO₂ and de-aired water circulation were carried out before pouring the saturated samples to avoid the entrapped air inside the shear box. The degree of saturation was checked by measuring BD value in undrained condition (Sassa 1988) which is defined as the pore pressure parameter in the direct shear state (Vankov and Sassa 1998) and formulated as $BD = \Delta u / \Delta \sigma$.

The samples then consolidated in drained conditions under normal stress and static shear stress. The values of the stresses were decided based on the pre-assumed landslide geometry (depth, slope angle) and soil properties (unit

Fig. 4 Sampling and site investigation at the Aratozawa landslide



weight). The deep landslide reproduction using ICL2 is conducted by giving a high normal stress in order to address the assumed slip surface of 150 m depth (in the Aratozawa case). Then the cyclic, speed control and earthquake tests are conducted in the 2.0 and 3.0 MPa range of normal stress. The maximum 2.0 and 3.0 MPa tests using undrained dynamic loading ring shear apparatus ICL2 with the high pore-water pressure controlled is used to meet the criteria of deep-seated landslide near Aratozawa reservoir.

Results

Rubber-Edge Friction Measurement

The test of rubber-edge friction against shear displacement has been carried out carefully to avoid the excess friction between rubber edges and the shear box without any water leakage occurred. As seen in Fig. 5 below, the rubber-edge friction of ICL2 was obtained with the condition of 1 MPa normal stress and 10 m shear displacement.

Undrained Speed Control Tests

A speed control test in the undrained condition was conducted under constant shear speed of 1 cm/s. The aims of this test are to obtain the values of residual shear resistance at steady state condition. In addition, the peak, mobilized and apparent friction angle were also obtained (Figs. 6 and 7).

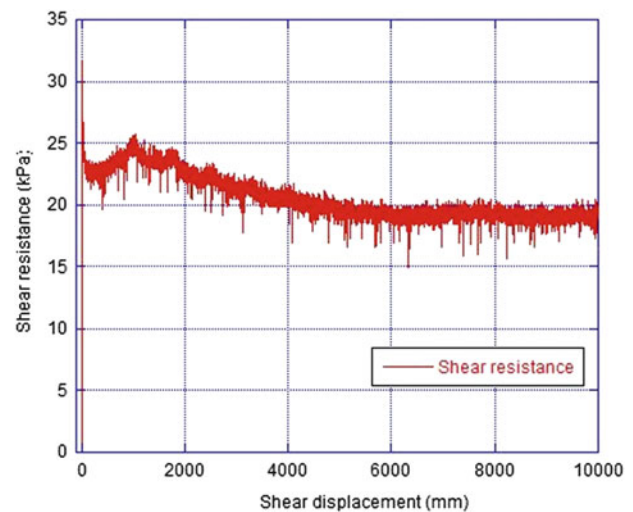


Fig. 5 Rubber-edge friction against shear displacement

Cyclic Shear Tests

A cyclic shear test in undrained condition was conducted in order to observe the pore pressure generation and initiation of failure motion due to the cyclic shear load. The cyclic shear test for Aratozawa samples from the secondary collapse zone was obtained as seen in Figs. 8 and 9.

Earthquake Wave Tests

The simulation tests for Aratozawa landslide using ICL2 also conducted the earthquake wave test. The earthquake

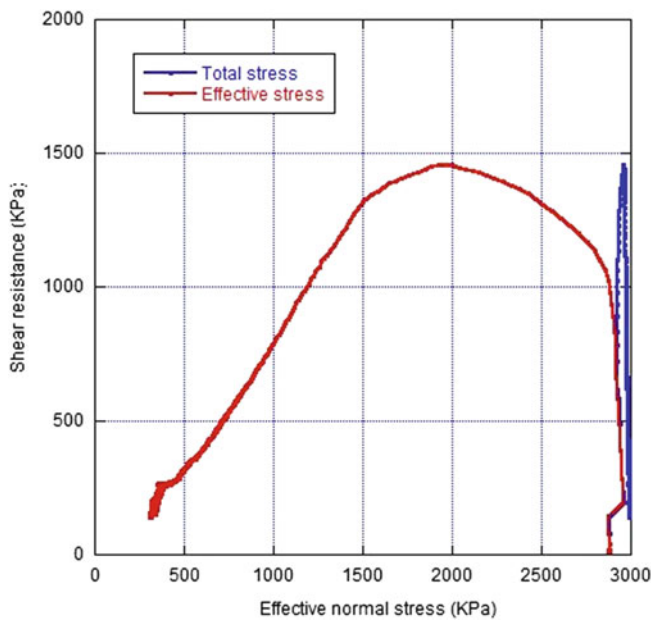


Fig. 6 The undrained speed control test for mound at flank side of collapse zone

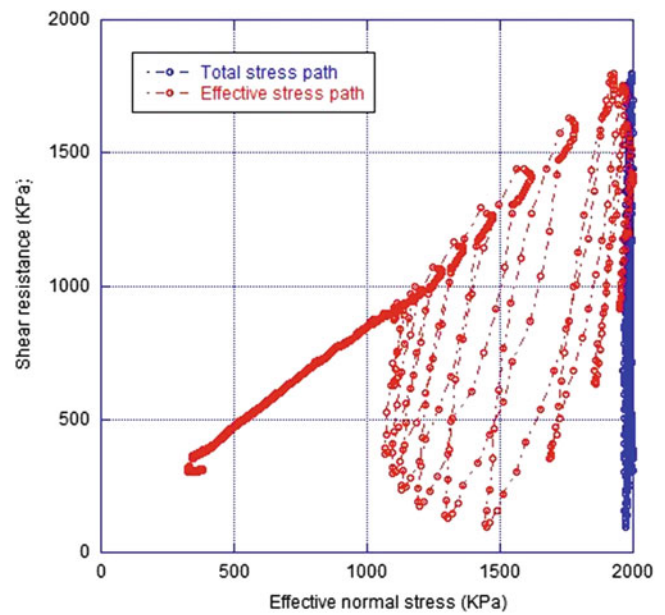


Fig. 8 Effective stress path of cyclic shear test for the secondary collapse zone of Aratozawa landslide ($\sigma = 2 \text{ MPa}$, $\tau = 1.2 \text{ MPa}$)

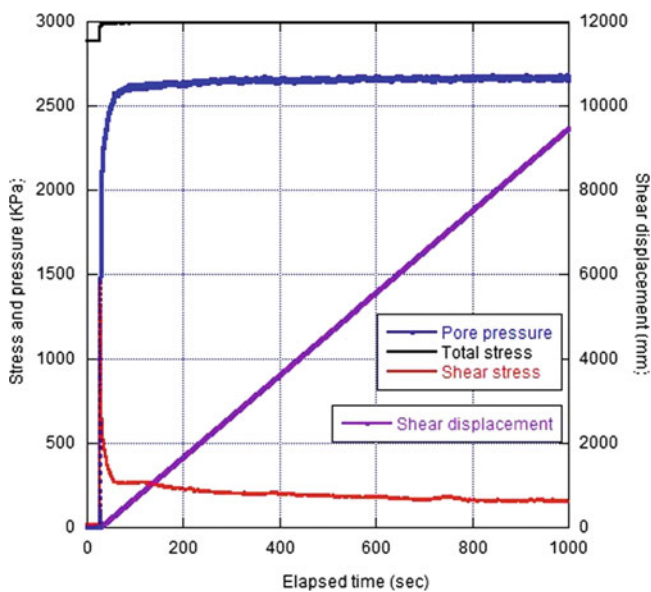


Fig. 7 Time-series data for stress, pressures and shear displacement of undrained speed control test for mound at flank side of collapse zone

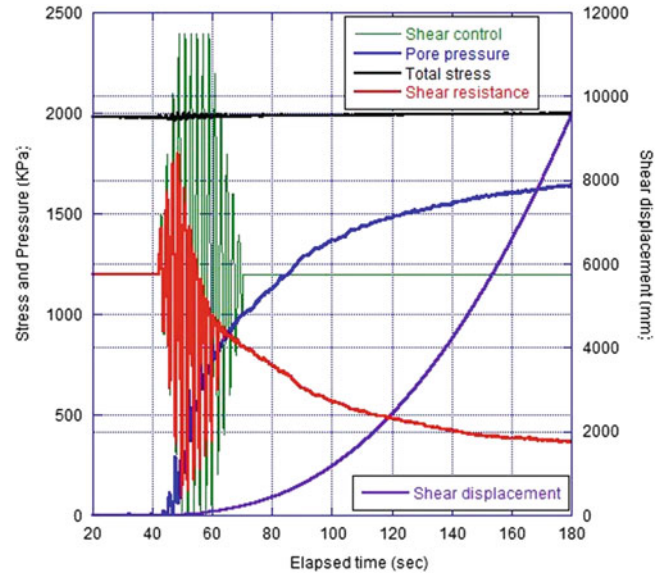


Fig. 9 Time series data for stress, pressures and shear displacement of cyclic shear test for secondary collapse zone of Aratozawa landslide

wave has taken from the Iwate-Miyagi Nairiku inland earthquake record wave which occurred on June 14 2008. The interim result indicated that in 2 MPa normal stress and 1.5 MPa static shear stress, the earthquake wave load did not trigger the failure in any significant way because only small pore pressure was generated, as seen in Fig. 10. There should be another trigger factor which would stimulate the acceleration and excess pore-water pressure generation.

Discussion

The objective of this paper is to study the mechanism of deep and large-scale landslide near Aratozawa dam through a physical laboratory experiment. Three samples from small depressions at the toe part, secondary collapse zone and mound at flank side of collapse zone of Aratozawa landslide area were taken from the sites and tested in the laboratory

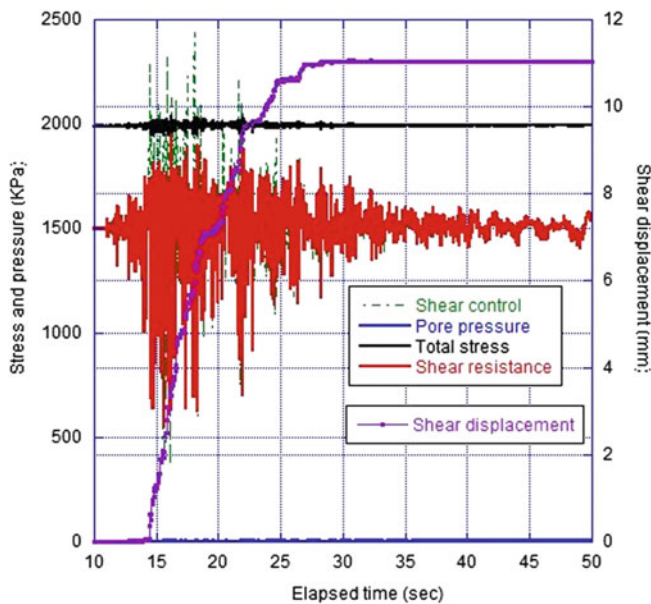


Fig. 10 Earthquake wave test for mound at flank side of collapse zone of Aratozawa landslide

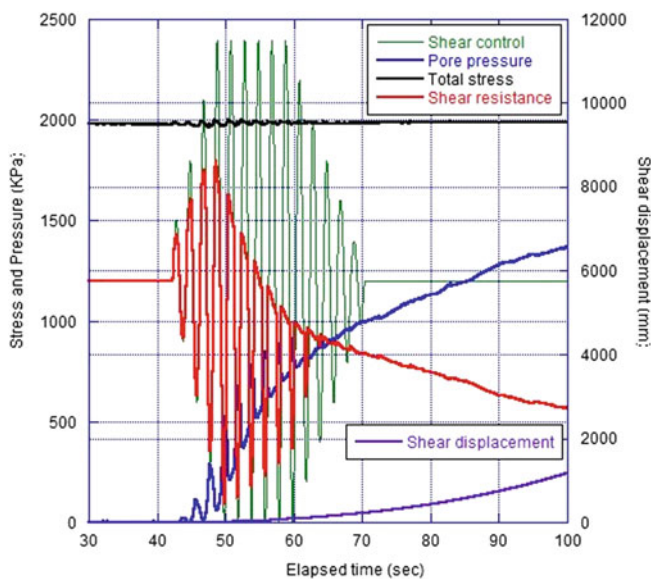


Fig. 11 Enlargement of Fig. 9 that shows the pore pressure generation and the initiation of failure motion

using ICL2. The undrained speed control test was conducted for all three samples to obtain the residual shear resistance at a steady state condition with high normal stress of 3 MPa.

Based on data from the cyclic test, the pore pressure generation reached 1.0 MPa before the initiation of failure motion. The large increment of pore pressure has followed the acceleration motion in a post-failure condition and caused the enlargement of shear displacement (Fig. 9 in Fig. 11).

The result shown in Fig. 11 has strengthened the previous research result that the samples had a high potential for generation of excess pore-water pressures, and liquefaction might have occurred during the 2008 earthquake (Gratchev and Towhata 2010).

From the earthquake wave test for mound samples at flank side of collapse zone of Aratozawa landslide, the test result (Fig. 10) has shown that the 2008 Iwate-Miyagi Nairiku earthquake might not have fully triggered the pore pressure generation and even the shear displacement was increased but it was very small and not significant. This interim result raises questions that there might be other factors that combined with the earthquake which caused the large-scale and deep landslide near the Aratozawa reservoir.

Conclusions

Several ring shear tests using ICL2 for Aratozawa samples has been carried out, consisting of undrained speed control tests, cyclic shear tests and earthquake wave tests. As shown in the result and discussion parts of this paper, the effect of groundwater fluctuation and the inter-linkage with the Aratozawa reservoir might be the main causes of the landslide in addition to the peak ground acceleration of the 2008 earthquake.

This paper described the interim results of the Aratozawa landslide research through ring shear apparatus. Further, other factors such as rainfall analysis and groundwater fluctuation analysis should be investigated.

From the site observation and monitoring from the Japan Forestry Agency, there is no significant deformation in the Aratozawa dam area when the big 9.0-magnitude Tohoku earthquake occurred in 2011. The indication is, that the slide blocks, ridges and mass depression due to the 2008 event are already stable.

However, several cracks at the upper part of the headscarp were found. In order to prevent further collapse, the headscarp of the Aratozawa landslide was reconstructed by the authorities since the slope and soil mass movement near Aratozawa dam and reservoir can still possibly occur in the future.

Acknowledgments The assistance from Japan Conservation Engineering and Japan Forestry Agency is gratefully acknowledged. The author would like to thank Dang Quang Khang, doctoral student of Kyoto University for helping the tests and thanks to Kawanami Akiko from Ministry of Agriculture, Forestry and Fisheries of Japan who in charge of the recovery works of Aratozawa dam and reservoir area for her kind assistance during site investigations. The ICL2 is developed by the International Consortium on Landslides as a part of SATREPS-Vietnam project in 2012–2017.

References

- Gratchev I, Towhata I (2010) Geotechnical characteristics of volcanic soil from seismically induced Aratozawa landslide, Japan. *Landslides* 7:503–510
- Miyagi T, Kasai F, Yamashina S (2008) Huge landslide triggered by earthquake at the Aratozawa Dam Area, Tohoku, Japan. In: *Proceedings of the first world landslide forum*. ICL, ISDR, Tokyo, pp 421–424
- Miyagi T, Yamashina S, Esaka F, Abe S (2011) Massive landslide triggered by 2008 Iwate-Miyagi inland earthquake in the Aratozawa Dam area, Tohoku, Japan. *Landslides* 8:99–108
- Ostic M, Ljutic K, Krkac M, Setiawan H, He B, Sassa K (2012) Undrained ring shear tests performed on samples from Kostanjek and Grohovo landslide. In: *Proceedings of the 10th anniversary of ICL*, Kyoto, January 2012
- Sassa K (1988) Geotechnical model for the motion of landslides. In: *Proceedings of the 5th international symposium on landslides, "Landslides"*, vol 1. Balkema, Rotterdam, pp 37–56
- Sassa K, He B, Miyagi T, Strasser M, Konagai K, Ostic M, Setiawan H, Takara K, Nagai O, Yamashiki Y, Tutumi S (2012) A hypothesis of the Senoumi submarine megaslide in Suruga Bay in Japan-based on the undrained dynamic-loading ring shear tests and computer simulation. *Landslides* 9:439–455
- Sassa K, Nagai O, Solidum R, Yamazaki Y, Ohta H (2010) An integrated model simulating the initiation and motion of earthquake and rain induced rapid landslides and its application to the 2006 Leyte landslide. *Landslide* 7:219–236
- Sassa K, Fukuoka H, Wang GH, Wang FW (2007) Undrained stress-controlled dynamic-loading ring-shear test to simulate initiation and post-failure motion of landslide. In: *Progress in landslide science*, Chap 6. Springer, Heidelberg, pp 79–98
- Sassa K, Fukuoka H, Wang G, Ishikawa N (2004) Undrained dynamic-loading ring-shear apparatus and its application to landslide dynamics. *Landslides* 1(1):7–19
- Vankov DA, Sassa K (1998) Dynamic testing of soils by the ring-shear apparatus. In: *The 8th international IAEG congress*, Balkema, Rotterdam



Study on Strength and Deformation Behavior of Loess Slope Supported by Micropiles

Chenglin Tian, Hongjian Liao, Yonggang Peng, Dongrui Hao, and Jianbing Peng

Abstract

Based on the practice of application of micropiles in slope support engineering and a large-scale field experiment, some factors influencing the reinforcing effect of micropiles in step-shaped slope were studied with FLAC software, using finite difference method. Firstly, referring to the scale of the large-scale field experiment, a numerical model was established and calculations were performed to study the effect of slope angle, slope height and load position on the slip surface in order to determine the location of slip surface based on the loads applied on the top of the slope. Then, micropiles were arranged on the step-shaped slope based on the critical slip surface, and the ultimate bearing capacities of the slope with or without micropiles and with different numbers of micropiles were calculated, and the failure modes of step-shaped slope were analyzed. The reinforcing effect of micropiles with the variation of soil cohesion and internal friction angle was also studied.

Keywords

Slope • Micropile • Strength parameter • Bearing capacity • FLAC

Introduction

Slope support engineering is utilized to strengthen a slope in order to ensure the safety of the slope. Micropiles have many advantages, such as no need for excavation, small disturbance to the slope, applicable to the narrow construction work area, flexible layout, applicability in different soils

C. Tian (✉) • H. Liao (✉) • Y. Peng • D. Hao
Department of Civil Engineering, Xi'an Jiaotong University, Xi'an
710049, China
e-mail: chenglin_tian@163.com; hjliao@mail.xjtu.edu.cn;
790042306@qq.com; 781162342@qq.com

J. Peng
Key Laboratory of Western Mineral Resources and Geological
Engineering of Ministry of Education, Chang'an University, Xi'an
710054, China
e-mail: dicexy_1@chd.edu.cn

and low construction noise. In recent years, micropiles are widely used for slope reinforcement. Bruce et al. (2004) applied the Lagrangian finite difference method in FLAC to analyze the stability of retaining walls reinforced by micropiles and the spacing and depth of micropiles are optimized. Zhou et al. (2009) proposed that the slide resistance mechanism of micropiles is different from general piles because the landslide thrust is resisted by micropiles through tensile strength and pile-foundation bearing capacity. Ho (1997) carried out model tests on stability of sandy slope strengthened by different rows and different angle of micropiles. The slope is strengthened mostly when the micropiles are vertical to the slip surface. Feng (2005) proposed the shear strength formula for micropiles reinforcing bedding rock slope. Micropiles and rocks formed a rock-pile composite structure. There are also many practical examples of micropiles application in slope reinforcement (Wu et al. 2005; Zhu et al. 2006; Yan 2010).

As a result of the complex geological conditions in loess region, the position of slip surface is greatly influenced by many factors, such as shape of the slope, soil parameters and loading on the top of slope. Therefore, it's of great importance to study the relationship between these factors.

The Field Test

Figure 1 shows a large scale model test carried out in loess slope, and the sketch map of the field test is shown in Fig. 2. Seven micropiles were arranged in the middle of the step and the load was applied on the top of the slope. The slip surface was preinstalled by using double layer plastic film. The micropiles were made of precast reinforced concrete piles, and the strength grade of concrete is C25. The pile length and diameter in the model test are 4 m and 60 mm, respectively, which simulates the pile whose length and diameter are 12 m and 180 mm respectively in the field. There are two kinds of pile reinforcements. When the flexural behavior was mainly concerned, the pile was reinforced by main reinforcement of 4 Φ 8 and stirrup of Φ 4@200. When the shear behavior was mainly concerned, the pile was reinforced by main reinforcement of 1 Φ 16. The pile space was 0.48 m.

Density of the soil, ρ , was 1,900 kg/m³, soil cohesion, c , was 30 kPa, soil internal friction angle, φ , was 20°, soil shear modulus, G , was 8.333 MPa and soil bulk modulus, K , was 3.409 MPa. The geometry of the slope model is shown in Fig. 3. The slope boundary conditions are given as vertical rollers on the left and right boundary, and fully fixity at the base. The self-weight of soils is considered. The soils are modeled as linearly elastic-perfectly plastic materials with Mohr-Coulomb failure criterion.

Effect of Slope Height on Slip Surface

In order to discuss the effect of ratio of step height on the location of slip surface, the geometry properties are listed here. Height of the slope below the step, h_2 , was 2 m, distance between load and the free surface, s , was 0, inclination of the slope above the step, α , was 58°. Height of the slope above the step, h_1 , was 1 m, 2 m, 3 m and 4 m, respectively, resulting in the ratios of step height ($\beta = h_1/h_2$) as 1/2, 1, 1.5 and 2, respectively.

The load on the top of the slope increases until slope failure is reached. The maximum shear strain contours for different slope heights are shown in Fig. 4. The slip surface extends from the toe below the step to the top of slope with $h_1 = 1$ m, i.e., $\beta = 0.5$. So the slope will be reinforced **effectively** if micropiles are installed in the step. The slip surface extends from the toe above the step to the top of slope with $h_1 = 2$ m, 3 m and 4 m, respectively, i.e., $\beta = 1$,

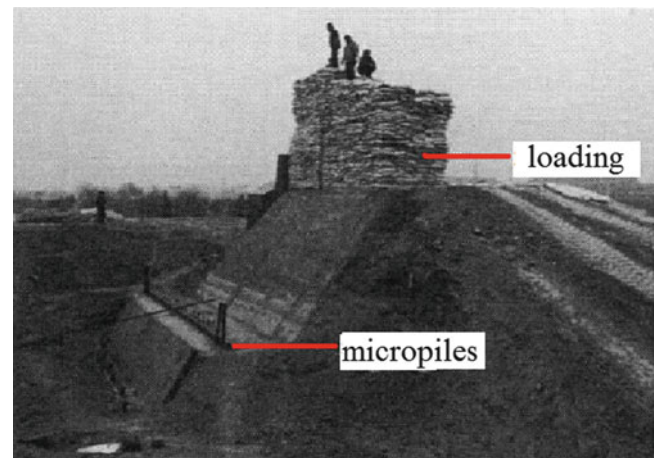


Fig. 1 Field test of micropiles, Yan (2010)

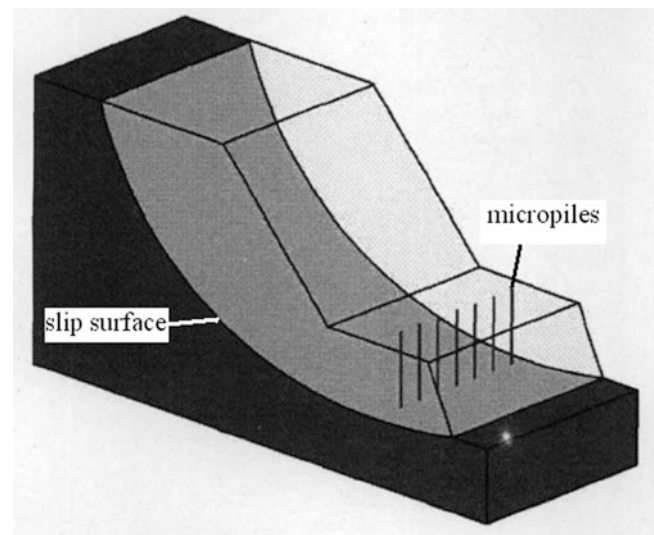


Fig. 2 Sketch map of field test

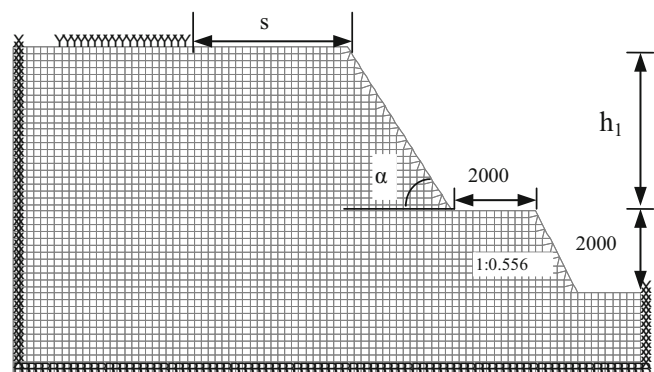


Fig. 3 Geometry of the slope model

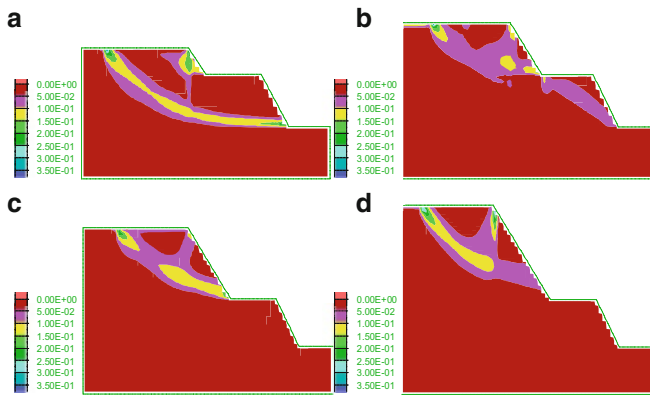


Fig. 4 Maximum shear strain contours for different slope heights. (a) $h_1 = 1$ m, (b) $h_1 = 2$ m, (c) $h_1 = 3$ m, (d) $h_1 = 4$ m

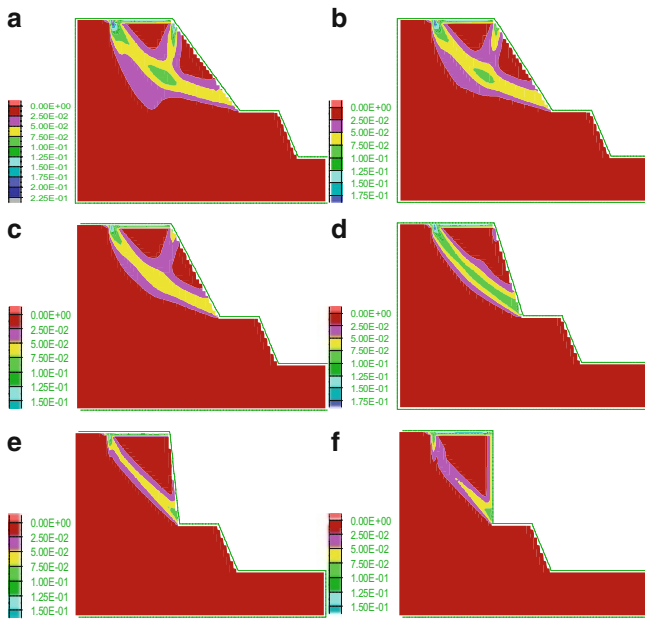


Fig. 5 Maximum shear strain contours for different slope angles. (a) $\alpha = 49^\circ$, (b) $\alpha = 53^\circ$, (c) $\alpha = 58^\circ$, (d) $\alpha = 69^\circ$, (e) $\alpha = 83^\circ$, (f) $\alpha = 90^\circ$

1.5 and 2, respectively. Then micropiles should be installed in the slope above the step in order to strengthen the slope effectively. In this study, when ratio of step height is larger than 1, the slip surface extends from the toe above the step to the top of slope with little effect on slope below the step.

Effect of Slope Inclination on Slip Surface

The slope geometry is same as that in the large scale model test. Height of the slope above the step, h_1 , was 4 m, height

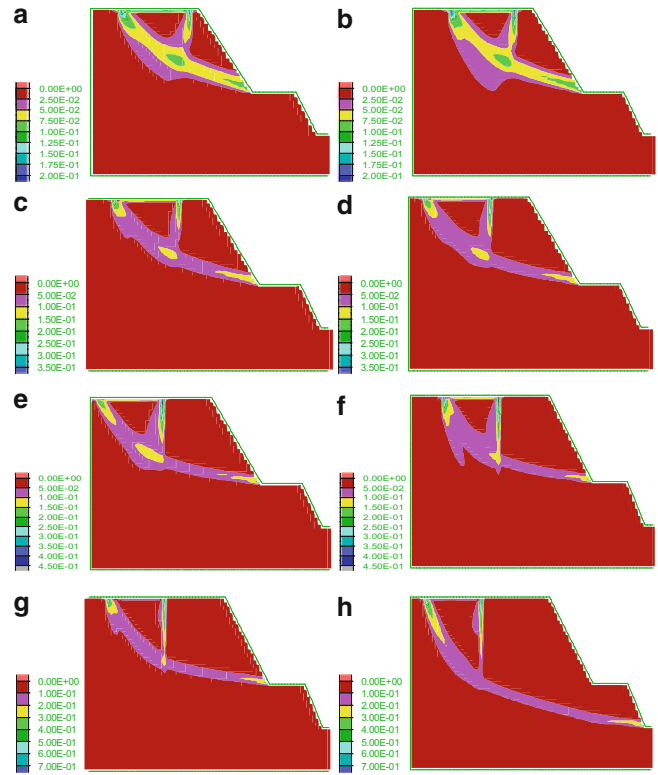


Fig. 6 Maximum shear strain contours for different load positions. (a) $s = 0.5$ m, (b) $s = 1$ m, (c) $s = 1.5$ m, (d) $s = 2$ m, (e) $s = 2.5$ m, (f) $s = 3$ m, (g) $s = 3.5$ m, (h) $s = 4$ m

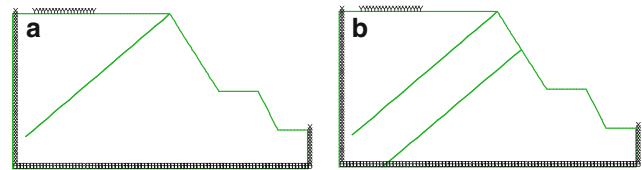


Fig. 7 Layout of the micropiles. (a) single-row micropile, (b) double-row micropiles

of the slope below the step, h_2 , was 2 m, i.e., $\beta = 2$, distance between load and the free surface, s , was 0, inclination of the slope above the step, α , were 49° , 53° , 58° , 69° , 83° and 90° , respectively. The maximum shear strain contours for different slope inclinations are shown in Fig. 5. The results indicate that the slip surface extends from the toe above the step to the top of slope for all the slope inclinations, and the arc-shaped slip surface tend to be linear. Then micropiles should be installed in the slope above the step to reinforce the slope effectively.

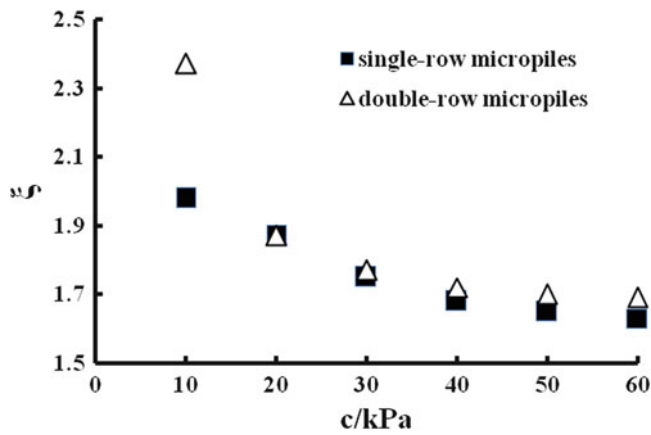


Fig. 8 Relationship of ξ and c

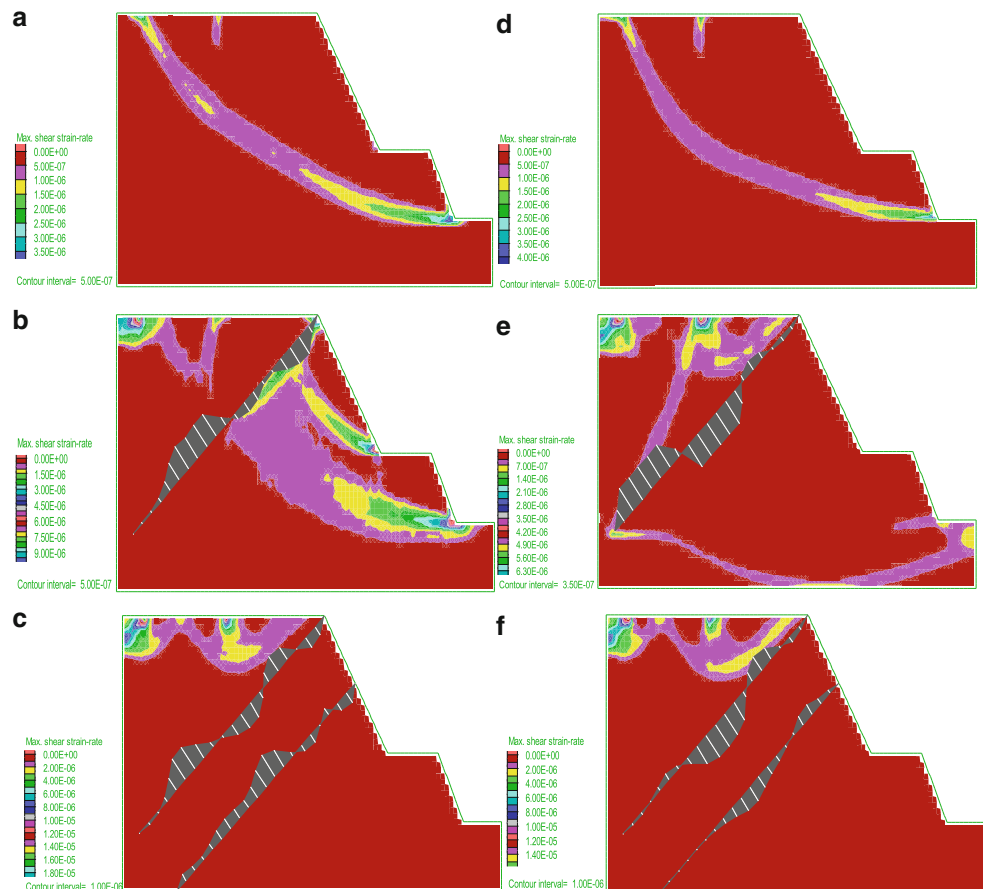
Effect of the Location of Load on Slip Surface

The slope geometry is same as that in the large scale model test. Height of the slope above the step, h_1 , was 4 m, height

of the slope below the step, h_2 , was 2 m, i.e., $\beta = 2$, inclination of the slope above the step, α , was 58° , distances between load and the free surface, s , were 0.5 m, 1 m, 1.5 m, 2 m, 2.5 m, 3 m, 3.5 m and 4 m, respectively. The maximum shear strain contours for different load locations are shown in Fig. 6. The slip surface extends from the toe above the step to the top of slope when s is smaller than 4 m, therefore micropiles should be installed in the slope above the step. The slip surface extends from the toe below the step to the top of slope with $s = 4$ m, which is similar to the large scale model test. Then micropiles should be installed in the step. γ is a new parameter defined in this paper, and $\gamma = s/h_1$. Values of γ were 1/8, 2/8, 3/8, 4/8, 5/8, 6/8, 7/8 and 1 respectively. The slip surface extends from the toe above the step to the top of slope when γ is smaller than 1, and the slip surface extends from the toe below the step to the top of slope with $\gamma = 1$.

After calculation, it could be obtained that the slip surface extended from the toe below the step to the top of slope with $s = 4$ m, $h_1 = 4$ m, $\alpha = 58^\circ$, and these values were chosen

Fig. 9 Maximum shear strain contours and moment of the piles. (a) $c = 10$ kPa, no micropiles, (b) $c = 10$ kPa, $M_{max} = -7 \times 10^3$ N m, (c) $c = 10$ kPa, $M_{max} = -2 \times 10^3$ N m, (d) $c = 30$ kPa, no micropiles, (e) $c = 30$ kPa, $M_{max} = -7 \times 10^3$ N m, (f) $c = 30$ kPa, $M_{max} = 6 \times 10^3$ N m



for the subsequent study. The layout of the micropiles is shown in Fig. 7. Pile radius, Young’s modulus, pile stiffness, pile internal friction angle and pile plastic moment are

0.06 m, 36,100 MPa, 1×10^{10} N/m/m, 50° and 7,000 N m, respectively.

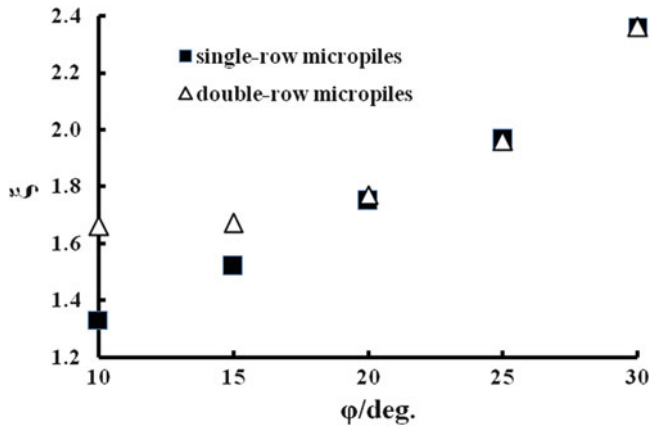


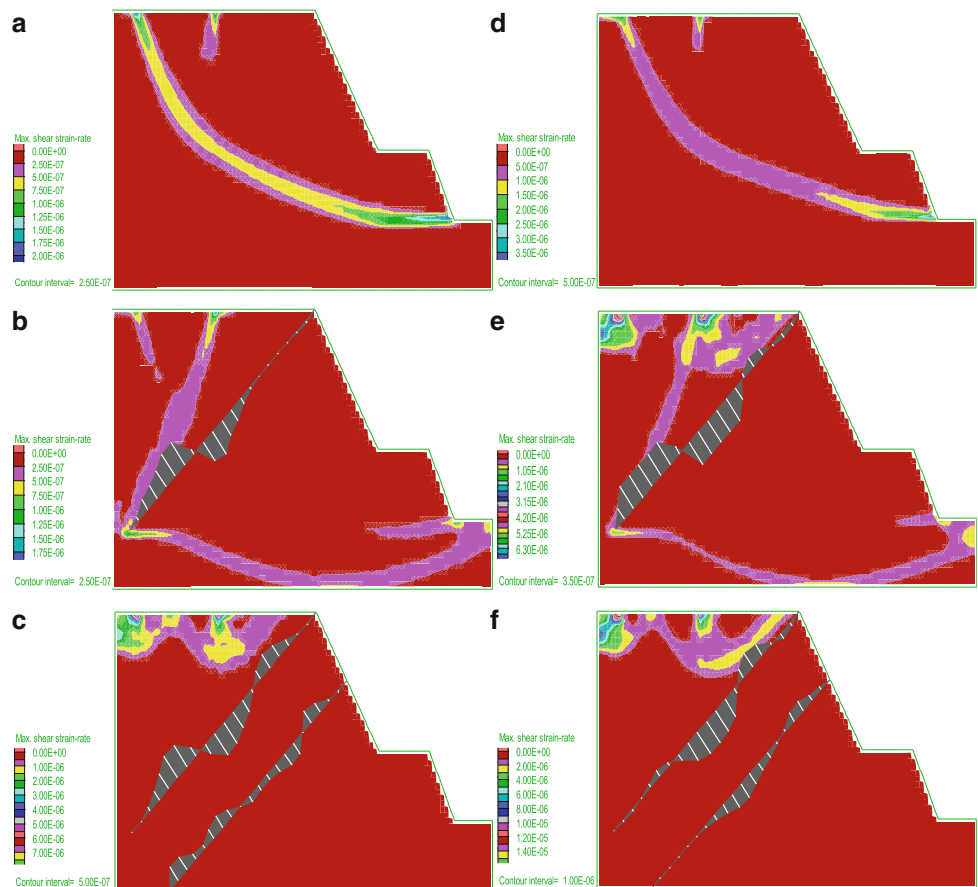
Fig. 10 Relationship of ξ and ϕ

Effect of Soil Cohesion on Micropiles Reinforcement

The material properties are—internal friction angle $\phi = 20^\circ$, cohesion $c = 10$ kPa, 20 kPa, 30 kPa, 40 kPa, 50 kPa and 60 kPa, respectively. Numerical analysis was carried out for three scenarios, i.e., slope without micropiles, slope with single-row of micropiles and slope with double-rows of micropiles. When slope failure is reached, the corresponding load is defined as P_u . P_{u0} is defined for slope without micropiles; P_{u1} is defined for slope with micropiles. Ratio of load $\xi = P_{u1}/P_{u0}$. The relationship of ξ and cohesion for single-row and double-row micropiles is shown in Fig. 8.

The results indicate that P_u of slope reinforced by micropiles is greater than that of slope without micropiles.

Fig. 11 Graph of maximum shear strain contours and moment of the piles. (a) $\phi = 10^\circ$, no micropiles, (b) $\phi = 10^\circ$, $M_{max} = -7 \times 10^3$ N m, (c) $\phi = 10$, $M_{max} = -3 \times 10^3$ N m, (d) $\phi = 20^\circ$, no micropiles, (e) $\phi = 20^\circ$, $M_{max} = -7 \times 10^3$ N m, (f) $\phi = 20$, $M_{max} = 6 \times 10^3$ N m



P_u increases with increasing soil cohesion, which is more obvious for slope reinforced by micropiles. ξ_{double} is greater than ξ_{single} , which indicates that the slope can be reinforced more obviously with more micropiles. ξ will be smaller with increasing soil cohesion.

The maximum shear strain contours and moment of micropiles for $c = 10$ kPa and $c = 30$ kPa are shown in Fig. 9. It can be seen that the shear band will not form completely when slope is reinforced by micropiles, and the failure mode on the top of the slope is similar to ground failure mode, which is more obvious for slope with double-rows of micropiles. The maximum moment of micropiles is smaller than yield moment of micropiles (7×10^3 N m).

Effect of Soil Internal Friction Angle on Micropiles Reinforcement

The material properties are—cohesion $c = 30$ kPa, internal friction angle $\varphi = 10^\circ, 15^\circ, 20^\circ, 25^\circ$ and 30° respectively. Numerical analysis was carried out for three scenarios, i.e., slope without micropiles, slope with single-row of micropiles and slope with double-rows of micropiles. The relationship of ξ and internal friction angle is shown in Fig. 10.

The results indicate that ξ_{double} is larger than ξ_{single} , which indicates that the slope can be reinforced more obviously with more micropiles. ξ increases with increasing internal friction angle. P_u increases with increasing internal friction angle and P_u of slope reinforced by micropiles is greater than that of slope without micropiles. ξ_{double} is greater than ξ_{single} when internal friction angle is smaller than 20° , but ξ_{double} almost equals to ξ_{single} for larger internal friction angles. The effect of micropiles reinforcement is more obvious for larger internal friction angle.

The maximum shear strain contours and moment of micropiles for $\varphi = 10^\circ$ and $\varphi = 20^\circ$ are shown in Fig. 11. It can be seen that the shear band will not form completely when slope is reinforced by micropiles, and the failure mode on the top of the slope is similar to ground failure mode, which is more obvious for slope with double-rows of micropiles. The maximum moment of micropiles is smaller than yield moment of micropiles (7×10^3 N m).

Conclusions

Some conclusions can be made, which are as follows:

1. The slip surface extends from the toe below the step to the top of slope for small ratio of step height, i.e., $\beta = 0.5$. In general, the slip surface extends from the toe above the step to the top of slope.
2. The slip surface extends from the toe above the step to the top of slope for all the slope inclinations, and the arc-shaped slip surface tend to be linear.
3. The slip surface extends from the toe above the step to the top of slope when γ is smaller than 1, and the slip surface extends from the toe below the step to the top of slope when $\gamma = 1$.
4. The shear band will not form completely when slope is reinforced by micropiles, and the failure mode on the top of the slope is similar to ground failure mode. The ratio of load ξ will be larger with increasing internal friction angle and smaller with increasing soil cohesion.

Acknowledgments The research is funded by the National Nature Science Foundation of China (41172276, 51279155) and Opening Research Foundation of Key Laboratory of Western Mineral Resources and Geological Engineering Ministry of Education (CHD2010JC143). The authors would like to acknowledge the "FY2011 JSPS Invitation Fellowship Program for Research in Japan" for its support.

References

- Bruce J, Ruel M, Ansari N (2004) Design and construction of a micropile wall to stabilize a railway embankment. In: Deep foundations institute annual conference on deep foundations. Emerging Technologies, Vancouver
- Feng J (2005) Study on stability and support of consequent bedding rock slope. Chengdu, Southwest JiaoTong University
- Ho CL (1997) Model tests of micropile networks applied to slope stabilization. In: Proceedings of the 14th international conference on soil mechanics and foundation engineering, vol 2, 9. A.A. Balkema, pp 1223–1226
- Wu SC, Gao YT, Jin AB (2005) Study on reinforcement of micro-pile and rockbolt for an unstable high-steep road cut slope. Chin J Rock Mech Eng 24:3954–3958
- Yan JK (2010) Model test study on micropiles in landslide reinforcement. Chang'an University, Xi'an, .
- Zhou DP, Wang HL, Sun HW (2009) Micro-pile composite structure and its design theory. Chin J Rock Mech Eng 28:1353–1362
- Zhu BL, Hu HT, Zhang YF, Chen Q, Zhang SW (2006) Application of steel-tube bored grouting anti-sliding retaining wall to treatment of landslide K108 in Beijing-Zhuhai expressway. Chin J Rock Mech Eng 25:399–406



The Influence of Countermeasure on Debris Flow Hazards with Numerical Simulation

Ying-Hsin Wu and Ko-Fei Liu

Abstract

We present the numerical simulation of the influence of countermeasures on debris flow hazards, supported with a case study. The Taipei DF024 potential debris flow torrent in Taiwan is used for demonstration. This torrent would be considered as straight in many simulations. However, unlike the one-dimensional model reported in previous literatures, the two-dimensional debris flow model, Debris2D, is applied for simulation. Two simulation conditions, with and without countermeasure, are compared. Comparing the results of two simulation conditions, we find Debris2D is able to reflect the variation of local topography. In 2D simulation, some locations identified to be safe by the 1D simulation, were identified as disaster potential areas. This means a 2D model is required for debris flow hazards simulation for evaluation of the countermeasure design efficiency, even for a straight channel.

Keywords

Countermeasure • Numerical simulation • Debris flow hazards • Check dam • Debris 2D

Introduction

In Taiwan, debris flows occur frequently in mountain areas during heavy rainfalls or typhoons. Debris flow hazards often cause serious damages of infrastructure and loss of property as well as human lives. They are severe threats to people who live near the debris flow torrent. The most used countermeasures in potential debris flow torrents is to build one or a series of check dams (also called sabo dam) (Takahashi 2007).

Y.-H. Wu

Department of Civil Engineering, National Taiwan University, Taipei 10617, Taiwan
e-mail: wu.ahsin@gmail.com

K.-F. Liu (✉)

Department of Civil Engineering, National Taiwan University, Taipei 10617, Taiwan

Hydrotech Research Institute, National Taiwan University, Taipei 10617, Taiwan
e-mail: kfliu@ntu.edu.tw

For decades, researchers have studied the efficiency and design criterion for check dams in different aspects such as types, size, numbers and locations. There are many theoretical, experimental and field studies in this area. As numerical simulation technique improves, numerical simulation becomes the most convenient method to evaluate the effect of check dams. A brief literature review for numerical simulation for the effect of check dams is given as follows. Busneli et al. (2001) conducted numerical modeling and experiments to study the erosion and deposition patterns on sediment transport through a slit-check dam. Armanini and Larcher (2001) theoretically derived a relationship among opening width, river topography, sediment characteristics, and water and sediment discharges for designing a slit-check dam. Then, Catella et al. (2005) applied the above model to analyze the efficiency of slit-check dam. The result agreed with the field evidences collected from 2-years monitoring activities. Remaître et al. (2008) applied numerical model to evaluate the influence of number and location of check dams on the reduction of debris flow run-out intensity, in terms of flow thickness, velocity and volume. The result suggests that

check dams located near the potential source areas could be very efficient for controlling the debris flow run-out intensity. Osti and Egashira (2008) also proposed a methodology for designing a series of check dam against debris flow hazards. Their results show that effective control of debris flow can be achieved not only by increasing the number and size of check dams but also by selecting appropriate locations.

However, many details such as topography, grain mixing and bed erosion effects must be evaluated before performing a realistic simulation. This paper will concentrate on the effect of topography. All the above mentioned literatures used one-dimensional (1D) numerical program. But in real condition, the debris flow motion may be irregular along transverse cross-section, and 1D model cannot give a correct assessment. Therefore, two-dimensional (2D) debris flow model may be required for more precise evaluation of check-dam design. To show the effect, we adopt the Debris2D (Liu and Huang 2006), a 2D debris-flow model, to assess the influence of check-dam in a close to 1D debris flow stream. In Taiwan, Debris2D is widely applied for debris flow assessment and proven to be a practical and reliable simulation tool, as will be mentioned in next section. In this study, a case of Taipei DF024 potential debris flow torrent is presented for studying the influence of counter-measure on debris flow hazards.

Introduction to Debris-2D Simulation Program

In this section we briefly introduce the two-dimensional debris flow simulation model, Debris2D, with respect to governing equations, computation algorithm, input and output, and verification of the program.

Governing Equations and Computation Algorithm

In Debris2D, the theory of viscoplastic fluid, a branch of non-Newtonian fluid mechanics, is applied for debris flow motion. The bulk of debris flow is treated as a continuum. The governing equations are mass and momentum conservation equations with shallow water assumption. The coordinate system is the Cartesian coordinate with the average bed elevation as x -axis. The adopted constitutive relation is the three-dimensional generalized one proposed by Julien and Lan (1991) as follows.

$$\tau_{ij} = \left(\frac{\tau_0}{\varepsilon_{II}} + \mu_d + \mu_c \varepsilon_{II} \right) \varepsilon_{ij}, \quad \text{for } \tau_{II} \geq \tau_0, \quad (1)$$

$$\varepsilon_{II} = 0, \quad \text{for } \tau_{II} < \tau_0, \quad (2)$$

where $(i, j) = \{x, y, z\}$;

$$\varepsilon_{II} = \left(\frac{1}{2} \varepsilon_{ij} \varepsilon_{ij} \right)^{1/2} \quad \text{and} \quad \tau_{II} = \left(\frac{1}{2} \tau_{ij} \tau_{ij} \right)^{1/2}. \quad (3)$$

$\varepsilon_{ij} = \frac{1}{2} \left(\frac{\partial u_i}{\partial x_j} + \frac{\partial u_j}{\partial x_i} \right)$ denotes strain-rate tensor; τ_0 is yield stress; μ_d and μ_c are dynamic viscosity and turbulent-dispersive coefficient, respectively. Equation (1) denotes the constitutive relation in the region where the shear stress is greater than yield stress; (2) is for the region with shear stress less than yield stress.

From the analysis of field data, Liu and Huang (2006) found that shear layer thickness is less than 10 % of total flow depth. So, the shear layer can be ignored to the leading order. After simplification and rearrangement, the resulting governing equations in conservative form are conservation of mass

$$\frac{\partial H}{\partial t} + \frac{\partial(uH)}{\partial x} + \frac{\partial(vH)}{\partial y} = 0, \quad (4)$$

and conservation of momentum in x and y directions

$$\begin{aligned} \frac{\partial(uH)}{\partial t} + \frac{\partial(u^2H)}{\partial x} + \frac{\partial(uvH)}{\partial y} = \\ -gH \cos \theta \left(\frac{\partial B}{\partial x} + \frac{\partial H}{\partial x} \right) + gH \sin \theta - \frac{1}{\rho} \frac{\tau_0 u}{\sqrt{u^2 + v^2}}, \end{aligned} \quad (5)$$

$$\begin{aligned} \frac{\partial(vH)}{\partial t} + \frac{\partial(uvH)}{\partial x} + \frac{\partial(v^2H)}{\partial y} = \\ -gH \cos \theta \left(\frac{\partial B}{\partial y} + \frac{\partial H}{\partial y} \right) - \frac{1}{\rho} \frac{\tau_0 v}{\sqrt{u^2 + v^2}}, \end{aligned} \quad (6)$$

where $H(x, y, t)$ is flow depth; $B(x, y, t)$ is the bed topography; $u(x, y, t)$ and $v(x, y, t)$ are depth-averaged velocities in x - and y -direction respectively; $\tan \theta$ is the bottom bed slope; τ_0 and ρ are debris-flow yield stress and density, which are all assumed to be constant here; g is the gravitational acceleration. Since the bottom shear layer is ignored, the yield stress becomes the dominant bottom stress.

With nonlinear treatment, the initiation criterion for any originally stationary debris pile is derived as

$$\begin{aligned} \left(\frac{\partial B}{\partial x} + \frac{\partial H}{\partial x} - \tan \theta \right)^2 + \left(\frac{\partial B}{\partial y} + \frac{\partial H}{\partial y} \right)^2 \\ > \left(\frac{\tau_0}{\rho g \cos \theta H} \right)^2. \end{aligned} \quad (7)$$

The derivatives of B and H represent pressure effect and $\tan \theta$ is the gravitational effect. The right hand side is the

resistance from yield stress. According to (7), debris flow can start to move only if pressure and gravitational effects exceed the yield stress effects.

Debris2D uses finite difference method for the governing equations (4), (5) and (6). In spatial discretization, the first-order Upwind method is applied to discretize convective term and central difference method is used for the remaining terms. The explicit third-order Adams-Bashforth method is used for time advancing. During computation the time step Δt is fixed and holds the Courant-Friedrichs-Lewy condition, and the volume of debris flow bulk is conserved.

For start of computation, Debris2D uses (7) to determine where debris flow can be initialized. If (7) is not satisfied, the mass stays stationary with zero velocities and unchanged flow depth. During computation, if the maximum velocity in the whole computational domain is less than numerical error, the computation terminates automatically.

Input and Output for Simulation

The main inputs include topography, initial debris source distribution, and material property of debris flow. For Debris2D the digital elevation model (DEM) of topography must be in rectangular grids. Man-made structures, e.g., check dam, can be included and modified into DEM for precise simulation.

The debris source distribution can be determined through field survey, aerial or satellite photos or other methods. From field survey or satellite photo analysis, one can find the dry debris volumes V_d and its corresponding triggering locations. Referring to Takahashi (2007), the equilibrium solid volume concentration C_v of a flowing debris flow can be expressed as

$$C_v = \frac{\rho_w \tan \theta}{(\sigma - \rho_w)(\tan \varphi - \tan \theta)}, \quad (8)$$

where ρ_w is water density; σ is the density of dry debris (around 2.65 g/cm³); φ is internal friction angle (about 37°); θ is average bottom slope angle in the field. The maximum value of C_v cannot exceed 0.603 (Liu and Huang 2006), and also $C_v = 0.603$ if $\theta \geq \varphi$. With C_v obtained from (8), the debris flow density is $\rho = \sigma C_v + \rho_w(1 - C_v)$. Also, using C_v the debris flow volume V can be determined using the formula as follows:

$$V = \min\left(\frac{V_d}{C_v}, \frac{V_w}{1 - C_v}\right), \quad (9)$$

where $\min(\cdot)$ is an operational function for returning the minimum value, i.e., $x = \min(x, y)$ if $x \leq y$; V_d represents dry debris volume due to field survey, or other

investigations; V_w is total volume of water for triggering debris flow in the simulation, and it can be obtained using a rainfall-runoff model, or other hydrological analysis methods. But we don't focus on the details of hydrological analysis here. In (9), if water input is sufficient to transform all mass into debris flow, the input volume of debris flow is determined using $V = V_d/C_v$; otherwise, $V = V_w/(1 - C_v)$ is applied for the condition that water is insufficient and only part of total mass volume forms debris flow. These source volumes and their locations can be inputted through graphical user interface of Debris2D program.

The final input is the material property of debris flow. The only rheological parameter needed for input is the yield stress τ_0 . The accurate value for yield stress can be measured and calibrated from samples using the method proposed by Liu and Huang (2006), and Liu and Mei (1989). For a rough estimation the yield stress varies with respect to solid size and composition in the field, and it usually ranges from 10^2 – 10^4 Pa for debris flows with large granular materials. The larger the averaged grain diameter, the higher the yield stress. For mud flows, the yield stress is usually less than 100 Pa.

The outputs of Debris2D include temporal variation of flow depth, depth-averaged (x, y) velocities for the whole domain, final affected area, and the maximum flow depth and velocities variation at each output time. The output time interval of Debris2D can be in seconds. Also, Debris2D can also calculate impact force (Liu and Lee 1997) at specified locations. This impact force information can be a practical reference for design of any control engineering.

Verification and Application

Debris2D program was verified by analytical solution and flume test with error under 0.2 % for predicting front location (Liu and Huang 2006). Also, Liu and Huang (2006) used this program to simulate the debris flow hazard in Nantou County, Taiwan. Compared with the field measurements, the simulation results had less than 5 % error in affected area as well as the final deposition depth. Thereafter, in Taiwan Debris2D has been widely applied for mitigation of debris flow hazards in many aspects, including vulnerability risk assessment (e.g., Liu and Li 2007), and design of evacuation map (e.g., Liu et al. 2009), and potential hazard map (e.g., Liu et al. 2013). It was also proven to be suitable to assess granular debris flow hazards (Wu et al. 2013). As all input parameters are determined by physical procedures, no calibration or back-calculation is needed for Debris2D simulation. There are several successful predictions by Debris2D. For example, Debris2D was applied to assess the debris flow affected area in Daniao tribe, in southeast Taiwan, in 2006 and the predicted result agrees very well with the real event

occurred in 2009 (Tsai et al. 2011). Not only in Taiwan, Debris2D is also successfully applied in other countries, e.g., South Korea (Liu and Wu 2010). From above literatures, Debris2D is proven to be a practical and reliable tool for assessment of debris flow hazards.

Case Study of Taipei DF024

The Taipei DF024 potential debris flow torrent (Taipei DF024) is located at north east part of Taipei city. Figure 1 shows the aerial photo of the whole watershed of Taipei DF024. There are three tributaries in this torrent with average length of 950 m and average slope of 36 %. The total watershed area is 31 ha, and the average accumulated rainfall in this watershed is 3,163 mm.

From field survey results (Liu et al. 2013), three potential masses are distributed along the midstream in Tributary 2, as shown in Fig. 1. The volumes and locations for all initial masses are listed in Table 1. Due to abundant rainfall in this watershed, all masses are assumed to be transformed into debris flow in our case. Using (8) the equilibrium concentration of debris flow is 0.603 in this torrent. So the total volume of debris flow is 5,406 m³. The calibrated yield stress for in-situ material is 750 Pa. Besides, according to field survey, the sediment layer on the surface of riverbed is very thin, and most channel bed is bedrock. So the erosion effect in this torrent can be negligible. Therefore, topography for simulation is assumed to be fixed, i.e., $B(x, y)$ in (4)–(7). Moreover, the sinuosity of tributary 2 is 1.029. It means the flowing condition of debris flow in tributary can be considered as one-dimensional.

The protected targets are two residential houses and a county road near the conjunction of three upstream tributaries. We first examined the hazard area without countermeasure by using original field topography for simulation. The simulated result is shown in Fig. 2b. The result indicates that two residential houses and county roads are covered by debris flow. In order to protect the houses we designed two closed-type check-dams downside the three masses. The detailed information of locations and dimensions for designed check-dams is listed in Table 2. The designed storage capacity of Dam 1 and 2 are 3,900 and 11,125 m³, respectively. The storage capacity of both dams is three times more than the possible total mass from upstream. As considering the designed storage capacity of check dams, if using a 1D program, one would obtain a result showing the area to be completely safe. However, the simulation using Debris-2D gives different result. As is shown in Fig. 2d the simulated result shows that the Dam 1 blocked all debris flow (i.e., 1,968.2 m³ in volume) from its upstream. But for Mass 3, only 75.2 % of total volume (i.e., 2,585.6 m³) is stopped by Dam 2. The county road is covered by debris

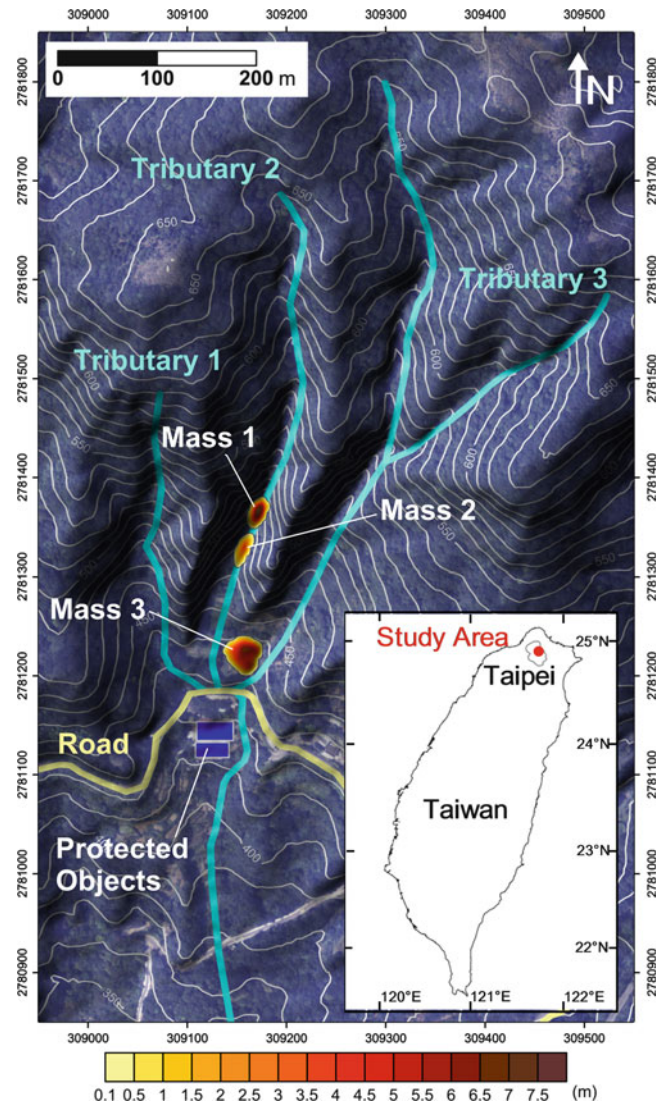


Fig. 1 Aerial photo of Taipei DF024 watershed. There are three tributaries of which average length is 950 m. The protected objects (blue rectangles) are residential houses and county road (chalk yellow line). The sinuosity of Tributary 2 is 1.029. The volumes and locations of three masses (i.e., Mass 1 – 3) are tabulated in Table 1. The coordinate system is Tw97 (modified from figure of S.C. Wei)

Table 1 Information of initial mass distribution (see Figs. 1 and 2 for locations)

No.	Location of mass center ^a (m)		Debris flow volume (m ³)
	E	N	
1	309172	2781367	1,432.8
2	309157	2781330	535.4
3	309158	2781225	3,437.8

^aThe coordinate is TW97

flow. For this case, even the storage capacity of Dam 2 (i.e., 11,125 m³) is three times greater than the total volume of Mass 3 (i.e., 3,437.8 m³), debris flow still flows over the Dam from boundary because of the curving effect from

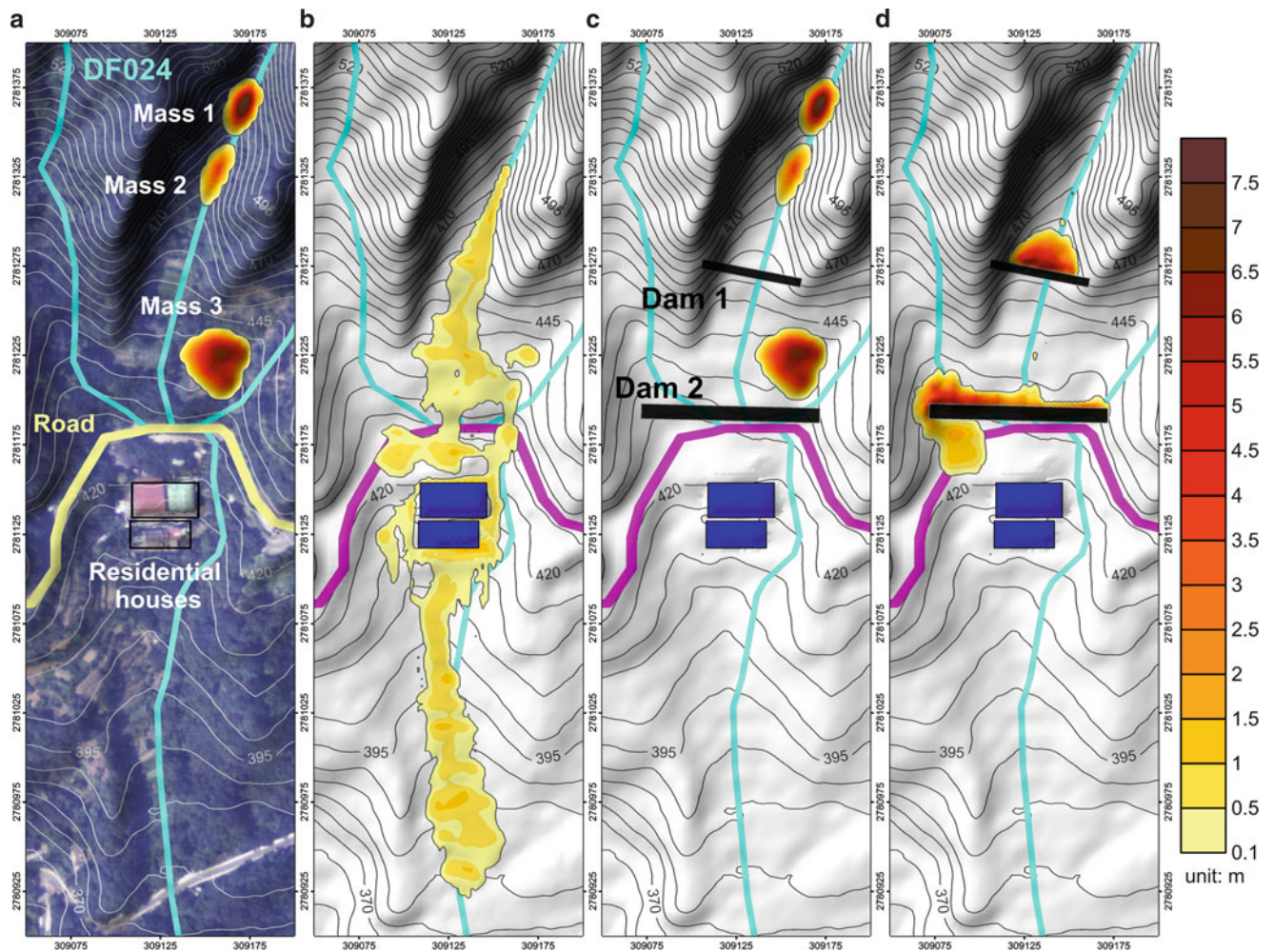


Fig. 2 (a) Aerial photo of Taipei DF024 with initial mass distribution, the volumes and locations are listed in Table 1; (b) final deposition (at 593 s) without countermeasure; (c) locations of two check dams (see Table 2 for details); (d) final deposition (at 288 s) with two check dams. *Blue rectangles indicate houses; Pink line is county road; Light blue line is center line of Taipei DF024. The upper part is the upstream of the debris flows*

Table 2 Information of the designed check dams in case study

No.	Location of mass center ^a (m)		Dimension (m)			Storage capacity (m ³)
	E	N	Length	Width	Height	
1	309135	2781271	50.0	5.0	8.0	3,900
2	309125	2781192	100.0	7.0	8.0	11,125

The locations of two check dams are illustrated in Fig. 2c

^aThe coordinate system is TW97

topography. Even the tributary can be considered as 1D, the flowing condition of debris flow still has 2D feature due to topography effect. Therefore, 2D simulation model is required for the evaluation of efficiency for countermeasure design.

Case presented above shows that using Debris2D we can evaluate the efficiency and capability of the two designed check-dam against debris flow hazards. The topography effect can also be considered in the evaluation. The two-

dimensional distribution of simulated mass gives more information and better assessment.

Concluding Remarks

We presented the numerical simulation for the influence of closed check-dam on debris flow hazard using a case study. The Taipei DF024 potential debris flow torrent in Taiwan was our target of case study. We considered two conditions of topography with or without countermeasures.

In our study, the countermeasures are close-type check-dams. The simulated result for no check-dam situation indicates that two residential houses and county road will be damaged and influenced by debris flow hazards. Then, we used two designed closed-type check-dams at down-side as protection measures. The simulation result shows that residential houses are safe, but county road is covered by debris flow. This overflow is due to topography and cannot be obtained from a 1D model.

In this study, we found that even if the tributaries can be regarded as 1D, the flowing condition of debris flow still has 2D flowing characteristics. Therefore, in order to obtain more accurate simulation result, the evaluation of countermeasure should also consider the topography effect by using 2D simulation model.

We used the Debris2D to simulate the influence of countermeasures on debris flow hazards. From the case study of Taipei DF024, the result shows that this two-dimensional debris flow simulation model is suitable for evaluating the efficiency and capability of countermeasures.

Acknowledgments We would like to thank the financial support from Water Resources Agency, Ministry of Economic Affairs, Taiwan. Preparation of partial data from S.C. Wei is also acknowledged.

References

- Armanini A, Larcher M (2001) Rational criterion for designing openings of slit-check dam. *J Hydraul Eng ASCE* 127(2):94–104
- Busneli MM, Stelling GS, Larcher M (2001) Numerical morphological modeling of open-check dams. *J Hydraul Eng ASCE* 127(2):105–114
- Catella M, Paris E, Solari L (2005) Case study: efficiency of silt-check dams in the mountain region of versilia basin. *J Hydraul Eng ASCE* 131(3):145–152
- Julien PY, Lan Y (1991) Rheology of hyperconcentrations. *J Hydraul Eng ASCE* 117(3):346–353
- Liu KF, Huang MC (2006) Numerical simulation of debris flow with application on hazard area mapping. *Comput Geosci* 10(2):221–240
- Liu KF, Lee FC (1997) Experimental analysis on impact mechanism of granular flow. *Chin J Mech* 13(1):87–100
- Liu KF, Li HC (2007) The assessment of debris flow emergency measures. *City Plann* 34(1):57–73
- Liu KF, Li HC, Hsu YC (2009) Debris flow hazard assessment with numerical simulation. *Nat Hazards* 49:137–161
- Liu KF, Mei CC (1989) Slow spreading of a sheet of Bingham fluid on an inclined plane. *J Fluid Mech* 207:505–529
- Liu KF, Wei SC, Li PC (2013) The influence of accumulated precipitation on debris flow hazard area. *J Chin Soil Water Conserv* 44(3):225–233
- Liu KF, Wu YH (2010) The assessment of debris flow hazard in Korea using Debris2D. In: INTERPRAEVENT 2010-international symposium in Pacific Rim, Taipei, Taiwan. pp 820–827
- Osti R, Egashira S (2008) Method to improve the mitigative effectiveness of a series of check dam against debris flows. *Hydrol Process* 22:4986–4996
- Remaître A, van Asch Th WJ, Malet J-P, Maquaire O (2008) Influence of check dams on debris-flow run-out intensity. *Nat Hazards Earth Syst Sci* 8:1403–1416
- Takahashi T (2007) Debris flow: mechanics, prediction and countermeasures. Taylor & Francis, New York, NY, p 448
- Tsai MP, Hsu YC, Li HC, Liu KF (2011) Application of simulation technique on debris flow hazard zone delineation: a case study in the Daniao tribe, Eastern Taiwan. *Nat Hazards Earth Syst Sci* 11:3053–3062
- Wu YH, Liu KF, Chen YC (2013) Comparison between FLO-2D and Debris-2D on the application of assessment of granular debris flow hazards with case study. *J Mount Sci* 10(2):293–304



Simulation of a Rapid and Long-Travelling Landslide Using 2D-RAPID and LS-RAPID 3D Models

Bin He, Kyoji Sassa, Osamu Nagai, and Kaoru Takara

Abstract

In this study, two process-based computer numerical models for simulating the generation and propagation of landslide are developed by integrating the initiation process triggered by rainfalls and/or earthquakes and the development process to a rapid motion due to strength reduction and the entrainment of deposits in the runout path. Among them, the 2D-RAPID model is a two dimensional model and LS-RAPID 3D Model is a three dimensional model. Both of them were developed from the geotechnical model for the motion of landslides and its improved simulation model and new knowledge obtained from a new dynamic loading ring shear apparatus. The aim of this study is to validate and compare these two models. For this purpose, the two models were applied in a rapid and long-traveling landslide, which occurred on 17 February 2006 in the southern part of Leyte Island, Philippines and caused 154 confirmed fatalities, and with an additional 990 people missing in the debris. For comparison, all the parameters used in the 2D landslide model are using the same values used in the 3D landslide model. As simulation results, the application of these two simulation models could reproduce well the initiation and the rapid long runout motion of the Leyte landslide. However, for the deposition area, the 2D landslide model resulted in a higher and narrower mass volume than the 3D landslide model. Moreover, the 2D-RAPID shows a simple process to handle the input and output database, which is easily understood and can be used in engineering application. In addition, the LS-RAPID 3D Model shows an excellent interface for rainfall or/and earthquake induced landslide with spatially distributed complex topographic data. The distributional information of soil parameter can be set and the 3D view of the calculated landslide initiation and runout can be

B. He (✉)

Key Laboratory of Watershed Geographic Sciences, Nanjing Institute of Geography and Limnology, Chinese Academy of Sciences, Nanjing 21008, China
e-mail: hebin@niglas.ac.cn

K. Sassa • O. Nagai
International Consortium on Landslides, Gokasho, Uji, Kyoto, Japan
e-mail: sassa@iclhq.org

K. Takara
Disaster Prevention Research Institute (DPRI), Kyoto University,
Gokasho, Uji City, Kyoto 611-0011, Japan
e-mail: takara.kaoru.7v@kyoto-u.ac.jp

successfully achieved in LS-RAPID 3D Model. Thus, each of these different dimensional landslide models has its respective advantages and disadvantages depending on the target study area and the type of the area.

Keywords

Landslide • Simulation, LS-RAPID model • 2D-RAPID model • Rainfall • Earthquake • Leyte

Introduction

Landslide is one of the most costly and damaging natural hazards of the world. In the recent decades, it has been increased rapidly all over the world due to severe rainfall by the global climate change. Thus, it is important to understand the process and mechanisms driving the instability, especially, the rapid and long-travelling landslide (Claessens et al. 2007; Sassa et al. 2004). So far, the landslides have been studied by many methods such as statistical analysis, geophysical mapping, and numerical modelling. The characteristics of landslide disasters present the necessity of a new and advanced modelling technology for disaster risk preparedness which simulates its initiation and motion.

Many numerical landslide models are available, with each of these methods having its respective advantages and disadvantages depending on the target study area and the type of the area (Jia et al. 2012; Liu and Wu 2008). From the viewpoint of dimension, a vast range of slope stability analysis tools exist for both 2D and 3D landslide models. The conventional 2D numerical landslide models are simple, fast, inexpensive, and relatively accurate. Due to the rapid development of computing efficiency, several numerical 3D methods are gaining increasing popularity in slope stability engineering. The ability to manage and process fully three-dimensional information has only recently been made available for a few Geographical Information Systems (GIS). An increasing number of investigators are now using 3D numerical calculations for estimating slope stability (Dawson and Roth 1999; Zettler et al. 1999; Hürlimann et al. 2002; Konietzky et al. 2004; Yu et al. 2005). Thus, knowledge of these different methods is essential in view of the potential variation in the input parameters required and in the subsequent interpretation of the generated results. In complex cases, the required analysis methodology may not involve the use of a single technique, but may require the integrated use of several conventional and numerical methods (Eberhardt et al. 2002).

This paper presents the considerable differences between 2D and 3D models, giving 2D-RAPID and LS-RAPID 3D Models as examples. The results of this research can provide scientific information for the researchers on simulation of a rapid and long-travelling landslide using 2D and 3D models.

Study Site

In this study, the Leyte Landslide was used as a working example. A rapid and long-traveling landslide occurred on 17 February 2006 in the southern part of Leyte Island, Philippines (Fig. 1). The landslide caused 154 confirmed fatalities and 990 people missing in the debris. The International Consortium on Landslides (ICL) and the Philippine Institute of Volcanology and Seismology (PHIVOLCS) organized a joint Japanese and Philippine team of 22 scientists and engineers. The team investigated the landslide from the ground and from a chartered helicopter. The investigation was reported at the International Conference Workshop “Guinsaugon 2008-Living with landslides” (Sassa et al. 2008). The results were presented as a part of the paper on the combined effect of earthquake and rainfalls (Sassa et al. 2007). The estimated landslide volume was 20 million m³ (Catane et al. 2007) and 16–30 million m³ (Araiba et al. 2008). The geospatial data includes digital elevation data, soil types, land use, field survey data, etc.

Methodology

This study has developed the simulation framework for the rapid and long-travelling landslide modelling system characterized by rapidly moving flows of mixed soil and rock. These landslides are often occurred on saturated hill slopes due to extreme rainfall or earthquakes. The framework of the modelling system is to identify “from where” the landslides have been initiated, and “until where” landslides may occur in the large scale region.

In this study, the 3D and 2D landslide models were used to emphasize on how the advantages of the different modelling tools can be maximized to provide optimal results with respect to visualization and comprehension of the processes and mechanisms contributing to instability. The current work is basically an extension to the model developed by Sassa et al. (2010). The repeatability of experiments is first investigated by using 3D LS-RAPID model. Then the same parameters are applied in 2D-RAPID model. The detail description of the process is given as below.

Fig. 1 Air photo and the result of computer simulation of the Leyte landslide. Air photo taken from the chartered helicopter by a member of Japan–Philippines investigation team (K. Araiba). The travel distance and the major part of landslide distribution were well reproduced. The secondary debris flow and muddy water spreads to the leftward in the photo and field observation

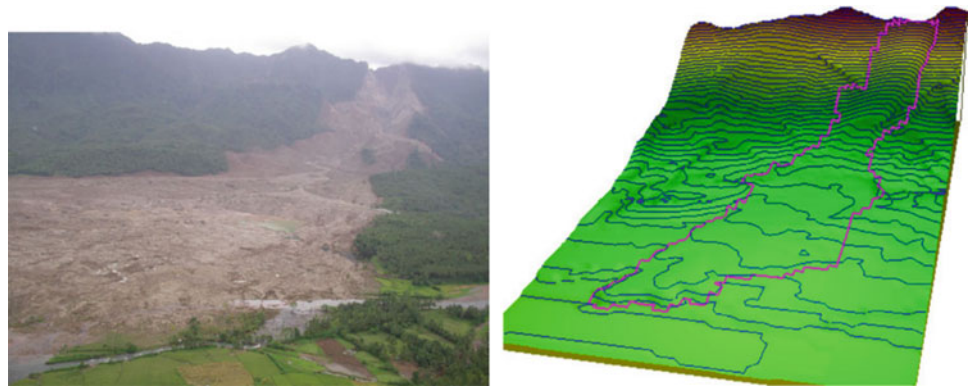
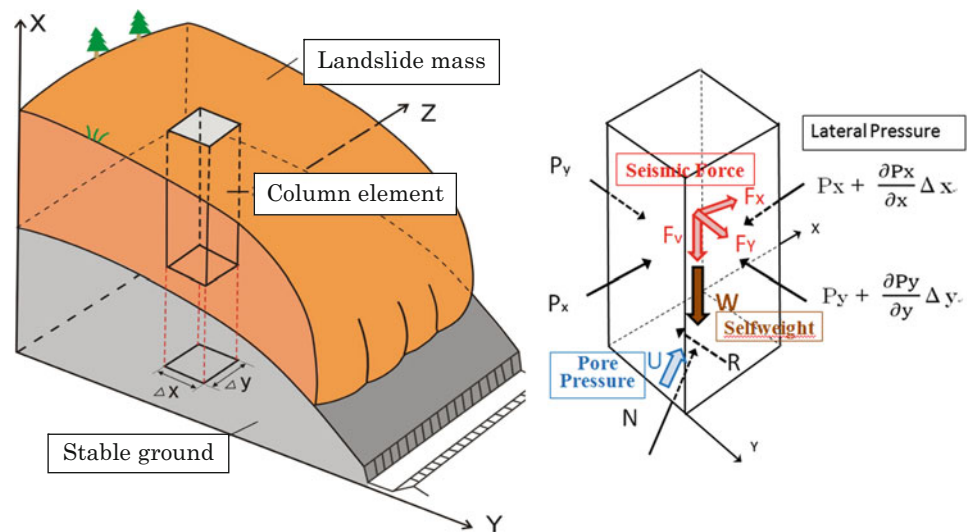


Fig. 2 Geotechnical model for landslide motion (left) and forces acting on a sliding mass column (right). The mesh size at x - y plane is $\Delta x \times \Delta y$. The forces include gravity W , supporting force N , shear resisting force R , and earth pressures P_x and P_y



The 3D Landslide Simulation Model

In this study, a distributed geotechnical 3D landslide simulation model (LS-RAPID) was applied for the assessment of risk of the rapid and long-travelling landslide (Fig. 2). In this modelling framework, catchment topography is represented based on digital elevation model (DEM) which is divided into an orthogonal matrix of square grid-cells. Basic concept of the landslide simulation model is shown in Fig. 1 (Sassa et al. 2004). A vertical imaginary column is considered within a moving landslide mass. The forces acting on the column are (1) self-weight of column (W), (2) lateral pressure acting on the side walls (P), (3) shear resistance acting on the bottom in the upward direction of the maximum slope line (before motion) or in the opposite direction of landslide movement (during motion) (R), and (4) the normal stress acting on the bottom (N) given from the stable ground as a reaction of normal component of the self-weight (Wn). The sum of three forces of (1) (2) (3) will cause the motion of landslides, namely the component of the self-weight parallel

to the slope (Wp), and the sum of the balance of lateral pressures in the directions of X and Y and Shear resistance (R). The landslide mass (m) will be accelerated by an acceleration (a) given by the sum of these three forces.

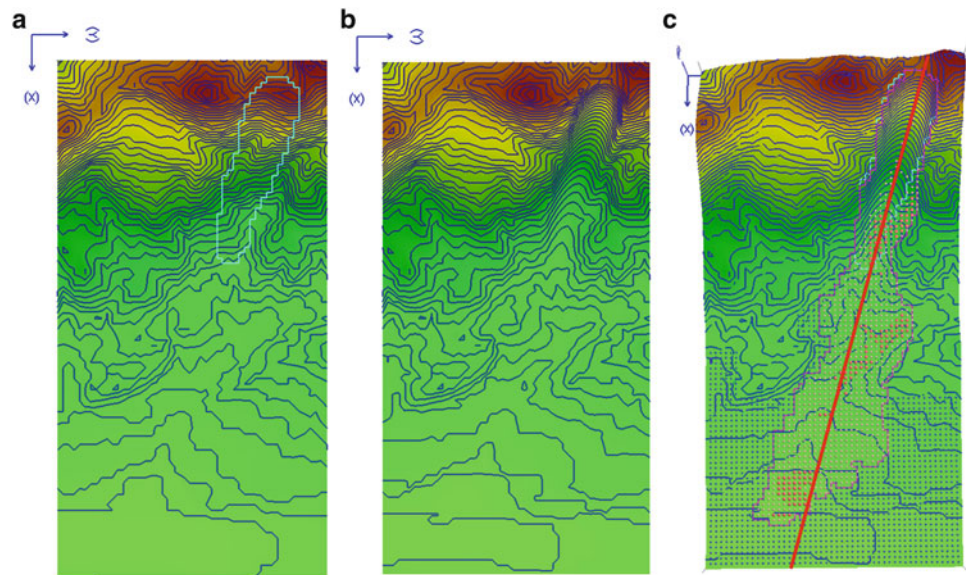
$$am = W_p + \left(\frac{\partial P_x}{\partial x} \cdot \Delta x + \frac{\partial P_y}{\partial y} \cdot \Delta y \right) + R \quad (1)$$

$$W_p = W + F_v + F_x + F_y$$

where, W : self weight, F_v, F_x, F_y : seismic force.

The angle of slope is different in the position of column within landslide mass. All stresses and displacements are projected to the horizontal plane and calculated on the horizontal plane. This simulation model can express the landslide initiation by the combined effects of pore water pressure and seismic shaking and post-failure motion until the deposition. Landslides can be triggered by seismic loading either using real seismic records or simple cyclic waves under a certain pore water pressure (pore pressure ratio) within LS-RAPID. The effect of seismic force is much

Fig. 3 Simulation area in the 3D landslide model. (a) Shows the outline of the unstable mass. (b) Shows the sliding surface created by ellipsoid method. The red line in (c) shows the location of cross section for 2D model



affected by frequency of shear wave and the wave form. It is quite different in the case of static, low frequency, high frequency and the magnitude of peak acceleration.

As for the parameters necessary for the computer simulation, most of soil parameters can be decided from the test on drilled sample by undrained cyclic loading ring shear test, namely the steady state shear resistance, the friction angle at peak, and the friction angle during motion, the shear displacement at the start of strength reduction (DL), the shear displacement at the end of strength reduction (DU). Cohesion is regarded to be small (10 kPa) assuming the shear surface was formed in a not over-consolidated sand layer like the drilled core. Some other parameters such as the lateral pressure ratio and parameters for non-frictional energy consumption are not decided by the ring shear tests (Sassa et al. 2010).

The 2D Landslide Simulation Model

The 2D landslide simulation model (2D-RAPID) is the two-dimensional version of the above developed 3D model. Since it is 2D version, the Y direction will not be considered in (1). Thus, the (1) will be:

$$am = W_p + \left(\frac{\partial p_x}{\partial x} \cdot \Delta x\right) + R \quad (2)$$

$$W_p = W + F_v + F_x$$

Accordingly, the effects of triggering factors of earthquake and pore water pressure will be considered in 2D as below:

$$\frac{\partial h}{\partial t} + \frac{\partial M}{\partial x} = 0 \quad (3)$$

Where, h is the height of the soil mass column in each mesh; M is the soil mass discharge per unit width in X direction; t is time.

From the geometric relation, the horizontal component of gravity plus seismic coefficient to X direction is $g \cdot \tan \alpha / (q + 1) \cdot (1 + K_v)$. Here, g is the gravity (acceleration), α is the angle of the ground surface to x-z plain; k is the lateral pressure ratio (ratio of lateral pressure and vertical pressure); K_v is the seismic coefficient to the vertical direction.

Results and Discussion

Results

The 3D simulation of landslide was firstly run by the LS-RAPID model and the results were published in Sassa et al. (2010). It shows that the 3D landslide model can represent well the slope failures at each grid element from initiation to long way runoff. The computer simulation reproduced a rapid landslide with a similar travel distance and distribution area which was triggered by a pore water pressure ratio of 0.15 and a small seismic shaking of $K_{EW} = 0.12$ and K_{NS} and $K_{UD} = 0.061$ using the seismic wave forms recorded at the Maasin observatory. The simulation result almost corresponded that the rapid landslide triggered by a small nearby earthquake of $M_s = 2.6$ in 5 days after the consecutives heavy rains for 3 days intensity of over 100 mm/day.

To compare the results obtained by the 2D and 3D models, the red line in Fig. 3 showing the location of the cross section has been selected for 2D landslide model. All the parameters used in 2D landslide model are using the same values which were used in 3D landslide model.

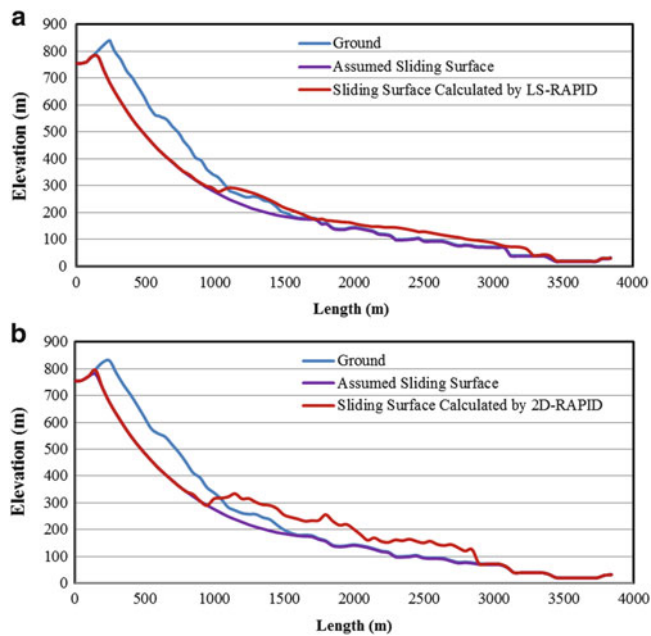


Fig. 4 Cross-section showing the ground surface before and after failure using 2D and 3D landslide models. The assumed sliding surface was decided by using the field survey data

While the 3D landslide model needs a lot of parameters, the 2D landslide model only needs several parameters such as soil unit weight, peak friction coefficient at sliding surface, peak cohesion at sliding surface, friction coefficient during motion at sliding surface, friction coefficient inside landslide mass, lateral pressure ratio, steady state shear resistance at sliding surface.

Figure 4 shows the cross-section of the ground surface before and after failure using 2D and 3D landslide models, respectively. From Fig. 4a, b, it can be clearly found that the sliding surface calculated by LS-RAPID 3D model is more close to the ground surface and the assumed sliding surface. As for the initiation area, the results are almost same for 2D and 3D models. However, for the deposition area, the 2D landslide model has higher and narrow mass volume than the 3D landslide model. This is because the soil mass can move in both X and Y direction when using 3D landslide model. However, the soil mass can only move along X direction when using 2D landslide model.

Discussion

Three-dimensional analyses of slope stability are not often used in practical applications as they are more elaborate than plane-strain analyses, and no convenient methods have been developed for performing such analyses. A two-dimensional (2D) plane strain analysis also can be regarded as

conservative in cases where 3D failure should be expected, and it is often preferred in design (Cornforth 2005). In spite of the fact that most landslides display not cylindrical but spatial slip surfaces, 2D slope stability analysis are widely used. Application of 2D modeling sometimes forces the user to consider the simplification of the real problem. The complexity of the slide geometry presents significant limitations with respect to the applicability of 2D solutions and uncertainty with regards to the underlying failure mechanism requires consideration of both continuum and discontinuum techniques (Cala et al. 2006; Konietzky et al. 2004).

However, in some cases 3D calculations are necessary in order to take the complexity of geology under consideration. As shown in this study, the 3D simulation of Leyte Landslide can give a 3D view of the landslide initiation and deposition area. In addition, the application of 2D models, for certain cases, may lead to a very conservative approach. In case of the limited width of soft subsoil layer, Factor of Safety (FS) obtained from 2D calculations may be seriously underestimated. The results from the 2D-Rapid model shows the deposition area is smaller than that obtained from the 3D LS-RAPID model. It seems that there is a widespread opinion that considering problem in 2D is always conservative and that engineering design doesn't need the third dimension (Cala et al. 2006).

Conclusion

In this study, we can conclude with the following:

1. The framework for numerical assessment of a rapid and long run-out landslide using the distributed 2D and 3D landslide model has been developed.
2. The cross section simulated from the 2D and 3D landslide model shows the good relationship with the observed landslides cross section.
3. The 2D and 3D numerical modelling slope analysis techniques have their own advantages and disadvantages inherent in their respective methodologies.
4. The limitations of existing 2D and 3D landslide models should be recognized by the engineers. In complex cases, the required analysis methodology may not involve the use of a single technique, but may require the integrated use of several conventional and numerical methods. The model and analysis will depend on the site conditions and the potential mode of failure identified through the field survey.
5. The availability of such program developed in this study is very useful in evaluating the safety and for remediation of rainfall/earthquake triggered landslides in different areas, including cut slopes and earth fill embankments in urban areas and along major highways. Moreover, they will be very useful for land use planning.

Acknowledgments This work is funded by “One Hundred Talents Program” of Chinese Academy of Sciences. The authors also thank the support by the JSPS Grant-in-Aid.

References

- Araiba K, Nagura H, Jeong B, Koarai M, Sato H, Osanai N, Itoh H, Sassa K (2008) Topography of failed and deposited areas of the large collapse in Southern Leyte, Philippines occurred on 17 February 2006. In: Proceedings of the international conference on management of landslide hazard in the Asia-Pacific Region (Satellite symposium on the First World Landslide Forum). pp 434–443
- Catane SG, Cabria HB, Tomarong CP, Saturay RM, Zarco MA, Pioquinto WC (2007) Catastrophic rockslide-debris avalanche at St. Bernard, Southern Leyte, Philippines. *Landslides* 4(1):85–90
- Cala M, Flisiak J, Tajdus A (2006) Slope stability analysis with FLAC in 2D and 3D. In: Proceedings of the 4th international FLAC symposium on numerical modeling in the geomechanics, Madrid, Paper (01-02)
- Claessens L, Schoorl J, Veldkamp A (2007) Modeling the location of shallow landslides & their effects on landscape dynamics in large watersheds: application for Northern New Zealand. *Geomorphology* 87(1–2):16–27
- Cornforth D (2005) Landslides in practice: Investigation, analysis, and remedial/preventative options in soils. Wiley, Hoboken, NJ
- Dawson E, Roth W (1999) Slope stability analysis with FLAC. In: Detournay C, Hart R (eds) *FLAC and numerical modeling in geomechanics*. Proceedings of the international symposium, Minneapolis, MN, USA, 1–3 September. Balkema, Rotterdam, pp 3–9
- Eberhardt E, Stead D, Coggan J, Willenberg H (2002) An integrated numerical analysis approach applied to the Randa rockslide. In: Proceedings of 1st European conference on landslides, 24–26 June 2002, Prague, Czech Republic, pp. 355–362
- Hürlimann M, Ledesma A, Marti J (2002) Geotechnical analysis of large volcanic landslides. The La Orotava events on Tenerife, Canary Islands. In: Rybar J, Stemberek J, Wagner P (eds) *Landslides*. Swets & Zeitlinger, Lisse, pp 571–577
- Jia N, Mitani Y, Xie M, Djameluddin I (2012) Shallow landslide hazard assessment using a three-dimensional deterministic model in a mountainous area. *Comput Geotech* 45:1–10
- Konietzky H, Lorenz K, Witter W (2004) Complex 3D landslide simulation. In: Lacerda WA, Ehrlich M, Fontoura AB, Sayao A (eds) *Landslides: evaluation and stabilization*. Taylor & Francis, London, pp 1053–1059
- Liu CN, Wu CC (2008) Integrating GIS and stress transfer mechanism in mapping rainfall-triggered landslide susceptibility. *Eng Geol* 101(1–2):60–74
- Sassa K, Wang G, Fukuoka H, Wang W, Ochiai T, Sugiyama M, Sekiguchi T (2004) Landslide risk evaluation and hazard zoning for rapid and long-travel landslide in urban development areas. *Landslides* 1(3):221–235
- Sassa K, Fukuoka H, Wang FW, Wang GH (2007) Landslides induced by a combined effects of earthquake and rainfall. In: Sassa K, Fukuoka H, Wang F, Wang G (eds) *Progress in landslide science*. Springer, Berlin, pp 311–325
- Sassa K, Fukuoka H, Solidum R, Wang G, Marui H, Furumura T, Wang F (2008) Mechanism of the initiation and motion of the 2006 Leyte landslide, Philippines. In: Proceedings of the international conference-workshop “Guinsaugon 2008 – Living with Landslides (in CD)
- Sassa K, Nagai O, Solidum R, Yamazaki Y, Ohta H (2010) An integrated model simulating initiation & motion of earthquake-rain induced rapid landslides & its application to 2006 Leyte landslide. *Landslides* 7–3:219–236
- Yu Y, Xie L, Zhang B (2005) Stability of earth-rockfill dams: influence of geometry on the three-dimensional effect. *Comput Geotech* 32:326–339
- Zettler AH, Poisel R, Roth W, Preh A (1999) Slope stability based on the shear reduction technique in 3D. In: Detournay C, Hart R (eds) *Proceedings of FLAC and numerical modeling in geomechanics symposium*, Minneapolis, MN, USA, 1–3 September. pp 11–16

Landslide Technology and Engineering in Support of Landslide Science

Kyoji Sassa

The World Landslide Forum (WLF) is the triennial conference of the International Consortium on Landslides (ICL) and the International Programme on Landslides (IPL). The IPL is a programme of the International Consortium on Landslides, managed by ICL and its supporting organizations: UNESCO, WMO, FAO, UNISDR, UNU, ICSU, WFEO and IUGS. IPL and WLF contribute to the United Nations International Strategy for Disaster Reduction.

The World Landslide Forum provides an information and academic-exchange platform for landslide researchers and practitioners. It creates a triennial opportunity to promote worldwide cooperation and share new theories, technologies and methods in the fields of landslide survey/investigation, monitoring, early warning, prevention, and emergency management. The forum's purpose is to present achievements of landslide-risk reduction in promoting the sustainable development of society.

Advancements in landslide science and disaster-risk reduction are supported by developments in landslide technology and engineering. Here we invited ICL supporters who support the publication of the international full-color journal "Landslides: Journal of the International Consortium on Landslides", the companies advertising in the seven volumes of "Landslide Science and Practice: Proceedings of the Second World Landslide Forum 2011" and the companies exhibiting at the Third World Landslide Forum 2014 to introduce their landslide technology and engineering. Six companies applied to exhibit in this book: their names, addresses, contact information and a brief introduction are given below (in the order of receipt of application):

1. MARUI & Co. Ltd.

1-9-17 Goryo, Daito City, Osaka 574-0064, Japan
URL: <http://marui-group.co.jp/en/index.html>

Contact: hp-mail@marui-group.co.jp

MARUI & Co. Ltd is the leading manufacturing and sales company in Japan since 1920 of material testing machines for soil, rock, concrete, cement and asphalt. Marui engineers built and assisted in development of the series of stress and speed control ring-shear apparatus by DPRI and ICL to study landslides since 1982.

2. OSASI Technos, Inc.

65-3 Hongu-cho, Kochi City, Kochi 780-0945, Japan

URL: <http://www.osasi.co.jp/en/>

Contact: info-tokyo@osasi.co.jp

OSASI Technos, Inc. develops and markets the slope-disaster monitoring system called OSASI Network System (OSNET). The monitoring devices use a built-in lithium battery and operate without external electricity supply in mountainous areas. The system enables a network of up to 64 units with up to 1 km distance between units. OSNET is suitable for quickly establishing monitoring systems on landslides in emergencies.

3. Okuyama Boring Co., Ltd.

10-39 Shimei-cho, Yokote City, Akita 013-0046, Japan

URL: <http://www.okuyama.co.jp/>

Contact: info@okuyama.co.jp

The Okuyama Boring Company Ltd specializes in landslide investigation, analysis of landslide mechanisms, and design of landslide remedial measures. The company uses its own software to analyze the initiation and motion of landslides, including the tsunami generated by landslides into reservoirs.

4. Japan Conservation Engineers & Co., Ltd.

3-18-5 Toranomon, Minato-ku, Tokyo 105-0001, Japan

URL: <http://www.jce.co.jp>

Contact: hasegawa@jce.co.jp

Japan Conservation Engineers & Co, Ltd develops landslide-simulation software and shear-testing apparatus, including slip-surface direct-shear apparatus and ring-shear apparatus to measure the shear strength mobilized on the sliding surface of landslides. Japan Conservation Engineers is a consulting company for

K. Sassa (✉)

International Consortium on Landslides, Kyoto, Japan
e-mail: sassa@iclhq.org

landslide investigation, reliable monitoring, data analysis and the design of landslide-risk reduction works.

5. KOKUSAI KOGYO Co., Ltd.

2 Rokuban-cho, Chiyoda-ku, Tokyo 102-0085, Japan

URL: <http://www.kk-grp.jp/english/>

Contact: overseas@kk-grp.jp

Kokusai Kogyo has undertaken aerial surveys, infrastructure development projects for road and harbor facilities, and landslide-disaster prevention and mitigation works since its foundation in 1947. The company has recently developed remote-sensing technology using the laser profiler, satellite synthetic aperture radar, and a new monitoring system called <Shamen-net> integrating GPS and other monitoring devices, all of which contribute to landslide-disaster prevention and mitigation.

6. C.S.G. S.r.l. Centro Servizi di Geingegneria

Via Cazzolini, 15A - 15010 Ricaldone (AL), Italy

URL: <http://www.csgrl.eu>

Contact: csg@csgrl.eu

C.S.G. S.r.l. Centro Servizi di Geingegneria is a leader in the production of multi-parametric in-place borehole monitoring columns called DMS (patents). DMS columns have been installed in a number of important international sites, where continuous monitoring for Early Warning, both in shallow landslides and deep-seated rockslides

requires instrumentation with high-precision, accuracy and reliability. CSG pursues a high quality standard through rigorous laboratory calibration tests, and long-term stability and alignment tests within temperature-controlled vertical and inclined boreholes in field.

Full-color presentations from these six exhibitors focusing on their landslide technology are shown in the following pages.

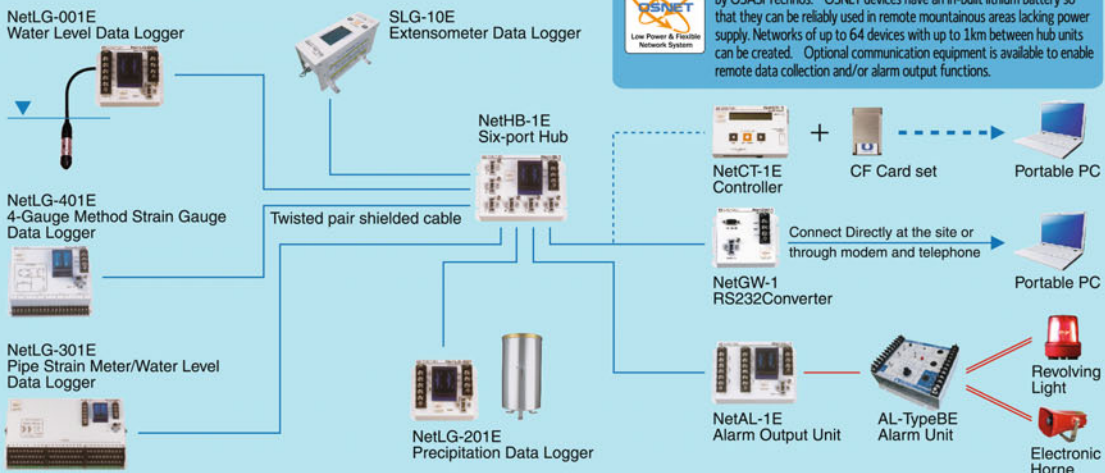
The progress of landslide science is supported by advances in landslide technology. The success of landslide risk-reduction measures needs effective landslide engineering. The International Consortium on Landslides seeks expressions of interest in contributing to “Landslide Technology and Engineering to Support Landslide Science” at the Fourth World Landslide Forum to be held on May 29–June 2, 2017, in Ljubljana, Slovenia. We may call for presentations on landslide technology and engineering in the proceedings, as well as through exhibitions at the site. Those interested in this initiative are requested to contact the Secretariat of the International Consortium on Landslides <secretariat@iclhq.org>. We will send invitations to interested applicants when further details become available.



Web site : <http://www.marui-group.co.jp/en/>
E-mail : hp-mail@marui-group.co.jp
Address : 1-9-17 Goryo, Daito City, Osaka Prefecture,
574-0064, Japan
Phone : 81-72-869-3201 Fax : 81-72-869-3205



EXAMPLE SETUP 2



OSNET is a network solution for disaster prevention monitoring developed by OSASI Technos. OSNET devices have an in-built lithium battery so that they can be reliably used in remote mountainous areas lacking power supply. Networks of up to 64 devices with up to 1km between hub units can be created. Optional communication equipment is available to enable remote data collection and/or alarm output functions.

OSASI
OSASI TECHNOS INC.
We pass on voices of the earth.
OSASI Technos, Inc.



Corporate Headquarters / 65-3 Hongu-cho, Kochi-shi, Kochi 780-0945, JAPAN
Tel: +81-88-850-0535 Fax: +81-88-850-0530

Tokyo Headquarters / Sumitomoseimei Building 4F 1-10-2 nishishinbashi, minato-ku, Tokyo 105-0003, JAPAN
Tel: +81-3-5510-1391 Fax: +81-3-5510-1393

Kyushu Branch Office / Iwaho Building Ekiminami 4F 4-1-17 Hkaka Eki Minami, Hakata-ku, Fukuokashi, Fukuoka 812-0016, JAPAN
Tel: +81-92-434-9200 Fax: +81-92-434-9201

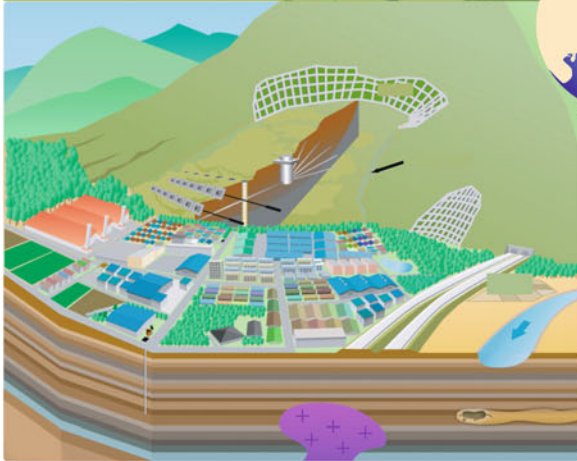
* Please note that specifications for the equipment are subject to change without notice.
* For further detailed specifications, please visit our homepage at <http://www.osasi.co.jp/en/>

We keep a clean nature for the future.

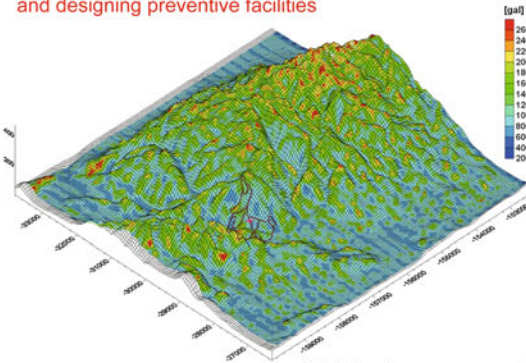
Okuyama Boring Co., Ltd.



<http://www.okuyama.co.jp/>
 E-mail info@okuyama.co.jp



Landslide research, analysis
and designing preventive facilities



Landslide countermeasure works



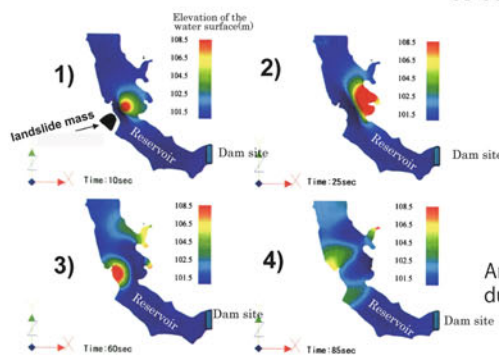
Ground anchor



Water catchment well

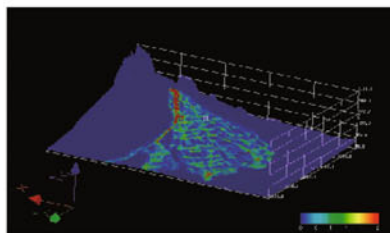


Water catchment boring

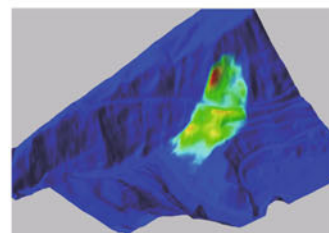


3D Seismic response analysis

Analysis of water waves due to landslide

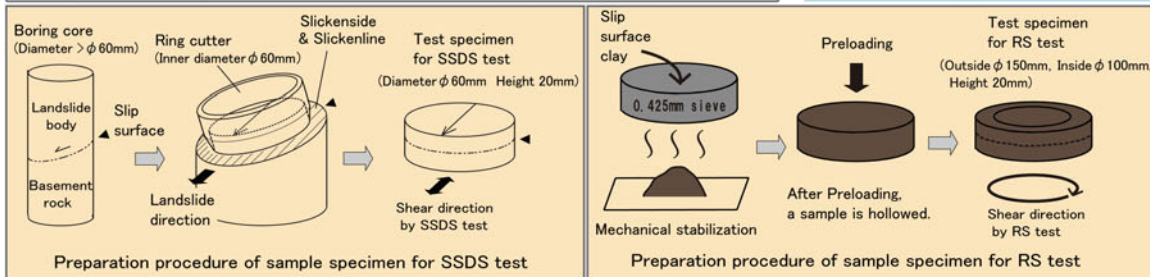
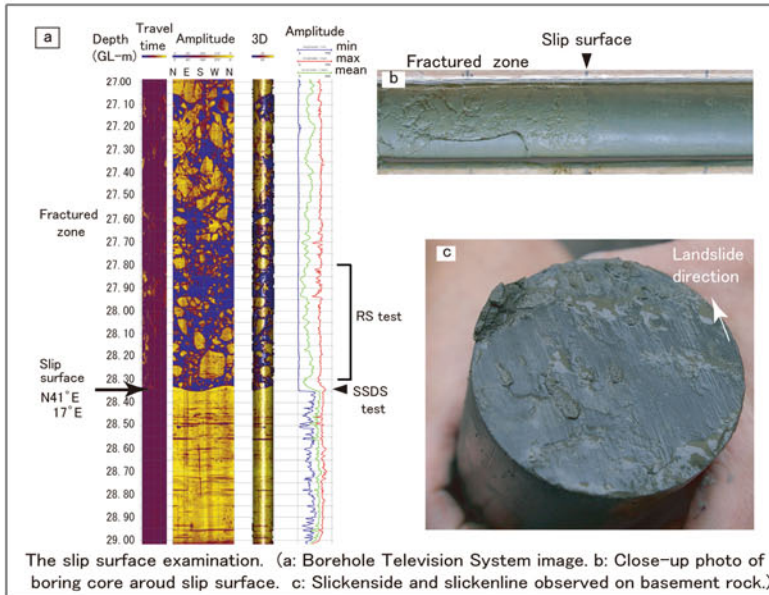


Flooding analysis in area with steep slope



Analysis of grain-fluid flow due to landslide

As for Landslide survey, we have various technologies for the slip surface examination. Slip Surface Direct Shear (SSDS) apparatus we have developed is the repeating one surface shearing testing apparatus which aims to measure the shear strength. This apparatus can exactly examine to the shear strength of the slip surface that will be demonstrated in the site. Ring Shear (RS) test is large displacement test which can obtain the fully softened strength and residual strength of the cohesive soil which constitutes a slip surface.

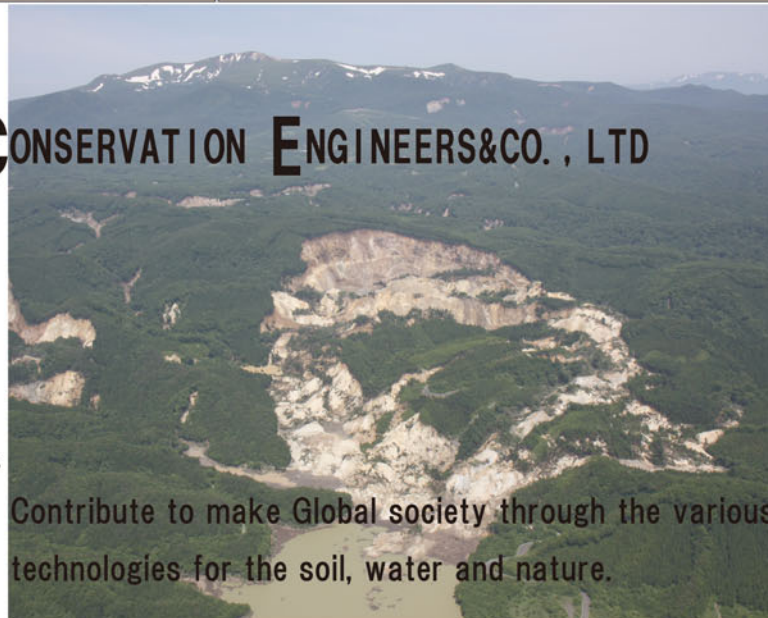


JAPAN CONSERVATION ENGINEERS&CO., LTD

URL:<http://www.jce.co.jp/>

HEAD OFFICE
3-18-5, TORANOMON, MINATO-KU,
TOKYO 105-0001, JAPAN
TEL:+81.3.3436.3673
FAX:+81.3.3432.3787

LABORATORY
34-12, SHIMIZUMAE, MINAMIYANOME,
FUKUSHIMA-SHI, FUKUSHIMA
960-0112, JAPAN
TEL:+81.24.555.0255
FAX:+81.24.557.3966



Contribute to make Global society through the various technologies for the soil, water and nature.



Building sustainable cities of the future
Green communities

Geospatial advantage green communities

We have geospatial technology to create ever more accurate maps, essential for developing social infrastructure and nation building—the backbone of economic growth. We are providing total solutions that merge our geospatial and urban planning technologies with renewable energy sources and to create safer, disaster-resistant communities of the future.

Environment/energy



*Disaster prevention/
risk reduction*



Supporting government



Social infrastructure



Business Solutions



Our Major Fields for international development



Disaster Prevention



Solid Waste Management



Water resource development



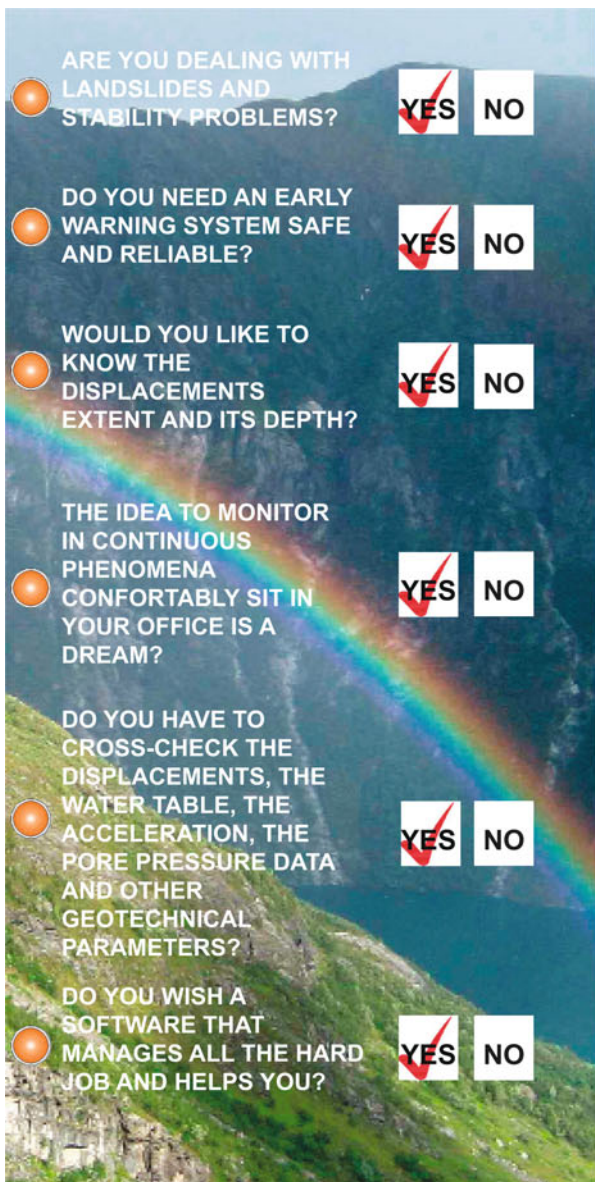
Survey and Mapping



KOKUSAI KOGYO CO.,LTD.

2 Rokubancho,Chiyoda-ku,Tokyo,Japan 102-0085

URL <http://www.kk-grp.jp/english> E-mail info_overseas@kk-grp.jp



ARE YOU DEALING WITH LANDSLIDES AND STABILITY PROBLEMS? **YES** **NO**

DO YOU NEED AN EARLY WARNING SYSTEM SAFE AND RELIABLE? **YES** **NO**

WOULD YOU LIKE TO KNOW THE DISPLACEMENTS EXTENT AND ITS DEPTH? **YES** **NO**

THE IDEA TO MONITOR IN CONTINUOUS PHENOMENA CONFORTABLY SIT IN YOUR OFFICE IS A DREAM? **YES** **NO**

DO YOU HAVE TO CROSS-CHECK THE DISPLACEMENTS, THE WATER TABLE, THE ACCELERATION, THE PORE PRESSURE DATA AND OTHER GEOTECHNICAL PARAMETERS? **YES** **NO**

DO YOU WISH A SOFTWARE THAT MANAGES ALL THE HARD JOB AND HELPS YOU? **YES** **NO**

The multiparametric column allows the measurement of the main geotechnical and mechanical parameters of soil and 2/3D structures, besides water table, temperature and acceleration in the same borehole. The column has digital sensors that transfer data to the control unit, placed on surface, which transmits data in real time to the final user and to the monitoring room.



Via Cazzulini, 15/A
 15010 RICALDONE (AL) ITALY
 Tel. +39 0144 74277
 Fax +39 0144 745914
 www.csgsrl.eu
 csg@csgsrl.eu

GEOTECHNICAL MULTIPARAMETRIC MONITORING COLUMNS

DMS column is like a "spiral cord", to be installed in place inside the borehole, composed by a sequence of hard tubular modules connected each other by special flexible joints having 2 or 3 freedom degrees that make possible to copy any deformation. These joints allow each module to perfectly fit the drilling hole and soil movements, maintaining the azimuthal direction.




**So...
 What you need is DMS**

- Continuous and multi-parametric data in the same borehole
- Fast and easy start up of the monitoring system
- Modular and retrievable system
- Advanced selection procedures
- High mechanical quality
- Advanced data processing software and graphical elaboration
- System developed for deep seated landslides and early warning
- Technical support and remote diagnostic
- After sale support and hire service
- Results and cost reduction

DMS



International Consortium on Landslides

An international non-government and non-profit scientific organization
promoting landslide research and capacity building for the benefit of society and the environment

President: Paolo Canuti (Prof. Emeritus, University of Firenze, Italy)

**Vice Presidents: Kaoru Takara (Kyoto University, Japan)/Yueping Yin (China Geological Survey)/
Claudio Margottini (National Institute for the Protection and Environmental Research (ISPRA), Italy)/
Irasema Alcantara-Ayara, (UNAM), Mexico**

Executive Director: Kyoji Sassa (Prof. Emeritus, Kyoto University, Japan)

ICL Supporting Organizations:

The United Nations Educational, Scientific and Cultural Organization (UNESCO) / The World Meteorological Organization (WMO) / The Food and Agriculture Organization of the United Nations (FAO) / The United Nations International Strategy for Disaster Reduction Secretariat (UNISDR) / The United Nations University (UNU) / International Council for Science (ICSU) / World Federation of Engineering Organizations (WFEO) / International Union of Geological Sciences (IUGS) / Government of Japan

ICL Members:

Albania Geological Survey / Federal University of Parana, CENACID-UPFR, Brazil/ Geological Survey of Canada / Chinese Academy of Sciences, Institute of Mountain Hazards and Environment / Northeast Forestry University, China / Bureau of Land and Resources of Xi'an, China / China Geological Survey / Nanjing Institute of Geography and Limnology, Chinese Academy of Sciences / Universidad Nacional de Columbia, Columbia / City of Zagreb, Emergency Management Office, Croatia /Croatian Landslide Group (Faculty of Civil Engineering, University of Rijeka and Faculty of Mining, Geology and Petroleum Engineering, University of Zagreb) / Charles University, Faculty of Science, Czech Republic / Institute of Rock Structure and Mechanics, Department of Engineering Geology, Czech Republic / Joint Research Centre (JRC), European Commission /Technische Universität Darmstadt, Institute and Laboratory of Geotechnics, Germany / Universidad Politecnica de Ingenieria, UPI, Honduras / National Institute of Disaster Management, India / University of Gadjah Mada, Indonesia / Agricultural Research and Education organization (AREO), Iran / Building & Housing Research Center, Iran / International Institute of Earthquake Engineering and Seismology (IIEES), Iran / University of Firenze, Earth Sciences Department, Italy / Italian Institute for Environmental Protection and Research (ISPRA) - Dept. Geological Survey, Italy / Forestry and Forest Product Research Institute, Japan / Japan Landslide Society / Kyoto University, Disaster Prevention Research Institute, Japan / Niigata University, Research Institute for Natural Hazards and Disaster Recovery, Japan / University of Tokyo (Institute of Industrial Science and Department of Civil Engineering, Geotechnical Engineering Group), Japan / Korea Forest Research Institute, Korea / Korea Infrastructure Safety & Technology Corporation, Korea /Korea Institute of Geoscience and Mineral Resources (KIGAM) /Korean Society of Forest Engineering / Mara University of Technology, Malaysia / Slope Engineering Branch, Public Works Department of Malaysia / Institute of Geography, National Autonomous University of Mexico (UNAM) / International Centre for Integrated Mountain Development (ICIMOD), Nepal / University of Nigeria, Department of Geology, Nigeria / International Centre for Geohazards (ICG) in Oslo, Norway /Grudec Ayar, Peru/ Moscow State University, Department of Engineering and Ecological Geology, Russia / Russian Academy of Sciences, Sergeev Institute of Environmental Geoscience (IEG RAS) / JSC "Hydroproject Institute", Russia / University of Belgrade, Faculty of Mining and Geology, Serbia / Comenius University, Faculty of Natural Sciences, Department of Engineering Geology, Slovakia / University of Ljubljana, Faculty of Civil and Geodetic Engineering (UL FGG), Slovenia / Geological Survey of Slovenia / Engineering Geoscience Unit, Council for Geoscience, South Africa / Central Engineering Consultancy Bureau (CECB), Sri Lanka / National Building Research National Organization, Sri Lanka / Taiwan University, Department of Civil Engineering, Chinese Taipei / Asian Disaster Preparedness Center, Thailand / Ministry of Agriculture and Cooperative, Land Development Department, Thailand / Institute of Telecommunication and Global Information Space, Ukraine / Institute Hydroingeo, State Committee of Geology of Uzbekistan / Institute of Transport Science and Technology, Vietnam

ICL Supporters:

Kawasaki Geological Engineering Co., Ltd., Tokyo, Japan / Marui & Co., Ltd., Osaka, Japan / Okuyama Boring Co., Ltd., Yokote, Japan / GODAI Development Corp., Kanazawa, Japan / Japan Conservation Engineers & Co., Ltd, Tokyo / Kokusai Kogyo Co., Ltd., Tokyo, Japan / Nippon Koei Co., Ltd., Tokyo, Japan / Ohta Geo-Research Co., Ltd., Nishinomiya, Japan / OSASI Technos Inc., Kochi, Japan / OYO Corporation, Tokyo, Japan / Sabo Technical Center, Tokyo, Japan / Sakata Denki Co., Ltd., Tokyo, Japan

Contact:

International Consortium on Landslides, 138-1 Tanaka Asukai-cho, Sakyo-ku, Kyoto 606-8226, Japan

Web: <http://icl.iplhq.org/>, E-mail: secretariat@iclhq.org

Tel: +81-774-38-4834, +81-75-723-0640, Fax: +81-774-38-4019, +81-75-950-0910